Smart Materials for Tissue Engineering
Applications

Edited by

Qun Wang
Iowa State University, Ames, USA
Email: qunwang@iastate.edu

Smart Materials No. 25

Print ISBN: 978-1-78262-484-4
PDF eISBN: 978-1-78801-054-2
EPUB eISBN: 978-1-78801-130-3
ISSN: 2046-0066

A catalogue record for this book is available from the British Library

The Royal Society of Chemistry is a charity, registered in England and Wales, Number 207890, and a company incorporated in England by Royal Charter (Registered No. RC000524), registered office: Burlington House, Piccadilly, London W1J 0BA, UK, Telephone: +44 (0) 207 4378 6556.

For further information see our web site at www.rsc.org

Printed in the United Kingdom by CPI Group (UK) Ltd, Croydon, CR0 4YY, UK

Foreword

In the last few decades, research in the area of tissue engineering has witnessed tremendous progress. The field seeks to replace or facilitate the regeneration of damaged or diseased cells, tissues or organs by applying a biomaterial support system, and/or a combination of cells and bioactive molecules. Meanwhile, advances in new materials provide opportunities to fabricate, characterize and utilize materials systematically to control cell behavior and tissue formation by biomimetic topography which closely replicates the natural extracellular matrix. Tissue morphogenesis is highly dependent on the interaction of cells with the extracellular matrix. Also important are developments of smart materials which can mimic complex interactions between cells and the extracellular matrix will promote functional tissue regeneration.

As an emerging area in materials science, smart materials have achieved extraordinary developments in recent years. Smart materials are materials that respond to small changes in physical or chemical conditions with relatively large property changes. Smart materials for tissue engineering are produced by modifying the physicochemical and biological properties of the scaffolds with response to external stimuli to enhance tissue regeneration. The functions of living cells are regulated by smart materials which respond to changes in the surrounding microenvironment. Smart materials which can respond to external signals and further adapt to their environment are based on various formulas from hard to soft materials. The morphology is from macroscopic to nanoscale dimensions in the form of gels, fibers, particles, colloids, or membranes. All these materials can be smartly designed to respond to specific signals, which range from pH, temperature, light, electrons, magnetism, and enzymes. There are many opportunities for smart materials to aid tissue engineering. Numerous tissue engineering scaffolds

Smart Materials No. 25
Smart Materials for Tissue Engineering: Applications
Edited by Qun Wang

Published by the Royal Society of Chemistry, www.rsc.org

with advanced properties based on smart materials have been developed in recent years, including new discoveries in the field of stem cells.

Fundamental principles and applications are two areas to study smart materials for tissue engineering. The first approach is mostly in the hands of chemists and physicists, the second one is more in the hands of engineers and biologists. The present book tries to bridge the vital gap between these scientific communities. Leading experts in multidisciplinary fields contributing to this book illustrate the fundamentals of smart materials, and their present stage in tissue engineering applications. Applications of a wide range of materials with diverse structures, different processing protocols, and responsiveness to physiological variables are discussed in the current book. An effort has been made to prioritize the concepts that are behind the design and application of smart tissue engineering materials.

The large variety of different smart materials and the large application areas make it difficult to systematically put them together in a single book. This book covers a unique aspect of materials science in tissue engineering, especially the applications of smart materials for tissue engineering. Working in the interface between smart materials and tissue engineering is a long adventure. The editor of this book, Professor Qun Wang of Iowa State University, wants to cover top-down applications. The vision is that there is a need for comprehensive knowledge on different types of smart materials fabrication and their corresponding tissue engineering applications. This book aims to fill this gap and tries to introduce new tissue engineering smart materials to a wide audience, from scientific communities and educational organizations to industrial manufacturers. The book will provide both an introduction to key research areas for new investigators in this highly interdisciplinary field, and a resource for those already working on fundamental materials research for tissue engineering applications. This is an authoritative book in the most recent developments in the area, as well as a valuable reference for anyone contemplating working in the field.

Robert S. Langer
Massachusetts Institute of Technology, United States

Preface

As an emerging area in materials science, smart materials have achieved tremendous success in developments in recent years. However, there is no book to summarize the research of smart materials in tissue engineering. It's difficult to know where to learn about this exciting topic. This book is an attempt to document the recent advancements for applications of smart materials in tissue engineering. Bringing together scientists and engineers that work in different fields of chemistry, physics, biology, materials science, pharmaceutics, medicine, and in clinics, this book has a broad focus on applications of smart materials in tissue engineering. By uniting these diverse areas, fresh prospects are opened up and fill the gap between fundamental research and application-originated technology and products. This book tries to introduce the practice of new tissue engineering smart materials to a wide range of audiences, from scientific communities to industrial organizations. The chapters are comprehensively covered from material manufacturers to clinical applications.

This book has been written by a prestigious group of authors worldwide with international reputations, including a foreword from the founder of tissue engineering in regenerative medicine, Prof. Robert S. Langer, Massachusetts Institute of Technology, United States. All chapters were written by experts in their field. In order to provide a favor to the less-informed readers, it is necessary to summarize in a few lines the essential contents of each chapter. Although all these chapters cover a broad range of topics, occasionally there is overlap between each contribution. Chapter 1 discusses the applications of multifunctional scaffolds in tissue engineering. Chapter 2 illustrates translational smart materials. Chapter 3 contains information about injectable smart materials. Chapter 4 and Chapter 5 highlight recent advancements in silicon and conductive materials for tissue engineering. Chapter 6 discusses cell encapsulation materials. Chapter 7 deals with smart materials for bone tissue engineering, while Chapter 8 discusses smart materials for cartilage

Smart Materials No. 25
Smart Materials for Tissue Engineering: Applications
Edited by Qun Wang

Published by the Royal Society of Chemistry, www.rsc.org

tissue engineering. Chapter 9 and Chapter 10 are devoted to smart materials for cardiovascular tissue engineering and wound healing. Chapter 11 demonstrates the use of magnetic-responsive materials for cardiovascular tissue engineering. Chapter 12 shows how intestinal stem cells are used for intestinal tissue engineering. Chapter 13 and Chapter 14 deal with smart-tissue-engineering-scaffold-originated materials for diabetes treatments and nerve regeneration. From Chapter 15 to Chapter 17, smart cell culture materials, flexible micro- and nanoelectronics, and smart materials that are responsive to different external stimuli to regulate the fate of stem cells are introduced. Chapter 18 and Chapter 19 discuss the principles of drug delivery and cell delivery for tissue engineering. From Chapter 20 to Chapter 23, some new technologies for developing smart tissue engineering scaffolds are introduced, such as multifunctional scaffolds, microfluidic systems, and 3D printing. I hope that this summary will be helpful in encouraging readers to take a closer look at the various chapters.

Different from other books about tissue engineering, this book covers the most recent advancements in smart tissue engineering materials, which are not described in other books, such as multifunctional smart materials and 3D printing materials. It combines different approaches to utilizing smart materials as a substrate for tissue engineering, from drug and cell delivery to stem cell control. It also documents broad topics on smart materials for tissue engineering, from basic designation to clinical applications. This book will have a broad audience at different levels. It could be used by graduate students as a textbook for material science and engineering and biomedical engineering. It could also be used by undergraduates as a supplementary textbook for biological engineering courses, materials engineering courses and chemical engineering courses. It could be a good resource for industry and medical professionals to learn about the recent products of smart materials in tissue engineering, as well as applications of smart materials in clinics.

I am grateful to all contributors for their consistent cooperation, but I take the responsibility for possible shortcomings. I was fortunate to convince these leading experts from different fields to share their views and visions in the book. I thank all of them for their efforts in writing comprehensively, as well as covering each assigned topic in detail. They deserve the merit of the book. My acknowledgement also goes to my mentor, Prof. Robert S. Langer, for his kind foreword and continuous encouragement. I want to acknowledge the indispensable support from the Royal Society of Chemistry staff, particularly Lindsay McGregor for providing invaluable help with editing aspects. I also would like to thank the readers, from whom I will be very humble to receive comments and feedback. The acknowledgements could never be complete without expressing my sincere gratitude to these individuals. I hope that the book will stimulate junior and senior scientists and engineers to explore the intriguing possibilities of using smart materials for applications in the biomedical field, particularly in tissue engineering.

Qun Wang
Iowa State University, United States

Contents

Chapter 1 Applications of Smart Multifunctional Tissue Engineering Scaffolds **1**
M. Kaliva, M. Chatzinikolaidou and M. Vamvakaki

1.1 Introduction 1
1.2 Applications of Multifunctional Scaffolds in Tissue Engineering 2
1.2.1 Bone and Cartilage 2
1.2.2 Muscle 15
1.2.3 Skin Tissue Engineering 17
1.2.4 Cardiovascular 21
1.2.5 Neural Tissue Engineering 25
1.3 Clinical Potential and Applications of Multifunctional Scaffolds in Tissue Engineering 26
1.4 Conclusions 29
References 29

Chapter 2 Translational Smart Materials in Tissue Engineering **39**
C. Pineda Molina and S. F. Badylak

2.1 Introduction 39
2.2 Considerations of Smart Materials in Tissue Engineering 40
2.2.1 Biocompatibility 40
2.2.2 Structure 40
2.3 Classification of Smart Materials in Tissue Engineering 41
2.3.1 Synthetic Materials 41

Smart Materials No. 25
Smart Materials for Tissue Engineering: Applications
Edited by Qun Wang

Published by the Royal Society of Chemistry, www.rsc.org

2.3.2 Biosynthetic Materials 45
2.3.3 Biologic Materials 48
2.4 Clinical Translation of Smart Material for Tissue Engineering 58
2.5 Future Challenges for Translation of Smart Biomaterials in Tissue Engineering 59
References 60

Chapter 3 Applications of Injectable Smart Materials in Tissue Engineering 67
Qiang Zhao

3.1 Introduction 67
3.2 Stimuli-Responsive Injectable Polymeric Hydrogels 68
3.2.1 Temperature-Responsive Injectable Hydrogels 68
3.2.2 pH-Responsive Injectable Hydrogels 69
3.2.3 Enzyme-Responsive Injectable Hydrogels 70
3.3 Injectable Supramolecular Hydrogels 71
3.4 Application of Injectable Smart Materials for Tissue Repair and Regeneration 73
3.4.1 Bone 73
3.4.2 Cartilage 75
3.4.3 Skin 78
3.4.4 Cardiovascular 80
3.4.5 Skeletal Muscle and Tendon 82
3.5 Conclusion and Perspective 82
References 83

Chapter 4 Advances in Silicon Smart Materials for Tissue Engineering 90
Nelli K. Bodiford and Jeffery L. Coffer

4.1 Introduction 90
4.2 Fundamentals of Porous Silicon (pSi) 91
4.2.1 Porous Silicon (pSi) Can Be Processed into a Variety of Shapes and Forms 91
4.2.2 Control Over Pore Structure 95
4.2.3 Surface Chemistry 95
4.2.4 Cell Attachment and Differentiation on Porous Silicon 97
4.2.5 Advantages of pSi/Polymer Composites as Implants for Tissue Engineering 97
4.3 Porous Silicon as a “Smart” Biomaterial 101
4.4 Porous Silicon/Polymer as a “Smart” Tissue-Engineering Scaffold 101
4.5 Clinical Potential 103

4.6 Summary and Future Opportunities 105
Acknowledgements 105
References 105

Chapter 5 Applications of Conductive Materials for Tissue Engineering 110
L. Wang, X. Li, Y. H. Tsou and X. Y. Xu

5.1 Introduction 110
5.2 Conductive Materials 111
5.2.1 Conductive Polymers 112
5.2.2 Piezoelectric Polymeric Materials 113
5.2.3 Other Novel Conductive Nanomaterials 114
5.2.4 Self-Assembled Conductive Hydrogels 115
5.3 Biocompatibility and Biodegradation of Conductive Materials 115
5.3.1 Biocompatibility 115
5.3.2 Biodegradability 116
5.4 Modification of Conductive Materials 117
5.4.1 Bioactive Molecules 117
5.4.2 Biocompatible Polymers 117
5.4.3 Topography Modification of Conductive Materials 118
5.5 Applications of Conductive Materials for Tissue Engineering 118
5.5.1 Applications for Nerve Tissue Engineering 118
5.5.2 Applications for Bone Tissue Engineering 124
5.5.3 Applications for Muscle Tissue Engineering 127
5.5.4 Applications for Cardiac Tissue Engineering 129
5.6 Conclusions and Perspectives 132
References 134

Chapter 6 Smart Biomaterials for Cell Encapsulation 144
Hui Zhu and Zhiqiang Cao

6.1 Introduction 144
6.2 Recent Advances of Smart Biomaterials 145
6.2.1 Smart Biomaterials that Mimic the Native Microenvironment 145
6.2.2 Smart Biomaterials that Overcome Suffocation 148
6.2.3 Smart Biomaterials that Promote Vascularization 150
6.2.4 Smart Biomaterials that Overcome a Foreign Body Reaction 152
6.2.5 Smart Biomaterials that Direct Cell Phenotype 155

6.2.6 Injectable Smart Biomaterials 160
6.2.7 Smart Biomaterials that Remember Shapes 162
6.3 Conclusion and Perspective 163
Acknowledgements 163
References 163

Chapter 7 Multi-Functional Biomaterials for Bone Tissue Engineering 169
Christian Wiraja, Mark S. K. Chong, Yanwan Liao, Sharon W. T. Chew and Chenjie Xu

7.1 Introduction 169
7.2 Multi-Functional Biomaterials for Bone Tissue Engineering 170
7.2.1 Passive Biomaterials for Mechanical Support 170
7.2.2 Active Scaffolds 173
7.2.3 Future Perspectives—Clinical Applications of Multi-Functional Biomaterials for Bone Tissue Engineering 184
7.3 Conclusions 185
Acknowledgements 186
References 186

Chapter 8 Smart Biomaterials for Tissue Engineering of Cartilage 194
Mina D. Fahmy, Brinda Shah, Mehdi Razavi, Hossein Jazayeri, Farahnaz Fahimipour, Joshua White, Radi Masri and Lobat Tayebi

8.1 Introduction 194
8.2 Required Biomaterial Properties for Cartilage Repair 196
8.3 Natural Polymers 198
8.3.1 Collagen 198
8.3.2 Hyaluronic Acid 198
8.3.3 Chitosan 199
8.3.4 Fibronectin 200
8.3.5 Alginate 201
8.4 Synthetic Polymers 201
8.4.1 Polyurethane, Polytetrafluoroethylene, Poly Butyric Acid 201
8.5 Smart Matrices (Scaffolds) 202
8.5.1 Thermo-Responsive Matrices 202
8.5.2 pH-Responsive Systems 204
8.5.3 Self-Assembling Matrices 207
8.5.4 Bioactive-Agent-Releasing Matrices 209
8.6 Response to Dynamic Loading 211
8.7 Matrix Metalloproteinase Response 213

8.8 Shape-Memory Systems 213
8.9 Future Prospects 216
8.10 Concluding Remarks 218
References 218

Chapter 9 Smart Biomaterials for Cardiovascular Tissue Engineering 230
Shinka Miyamoto, Toshihiro Shoji, Hideki Miyachi and Toshiharu Shinoka

9.1 Introduction—Clinical Motivation 230
9.2 Considerations for Vascular Neotissue Formation and TEVG Remodeling 231
9.3 Smart Materials for Cardiovascular Tissue Engineering 234
9.3.1 Decellularized Vascular Scaffolds 235
9.3.2 Natural Polymeric Biomaterials 236
9.3.3 Polymeric Scaffold 239
9.4 Myocardial Tissue Engineering 243
9.4.1 Injectable Biomaterials 244
9.4.2 Patch-Forming Scaffolds 245
9.5 Heart Valve Tissue Engineering 245
9.5.1 Biological-Based Scaffold 246
9.5.2 Degradable Synthetic Scaffolds 247
9.6 The Clinical Potentials and Applications of Smart Materials in Cardiovascular Disease 248
References 249

Chapter 10 Advances of Smart Materials for Wound Healing 258
Junjie Deng, Peter Y. Li and Hao Cheng

10.1 Introduction 258
10.2 Overview of Wound Healing Stages 259
10.2.1 Wounds 259
10.2.2 Phases of Wound Healing 259
10.3 Current Methods and Material Applications in Wound Healing 262
10.3.1 Wound Dressings 262
10.3.2 Delivery Systems for Controlled Release of Growth Factors and Other Biomolecules 262
10.3.3 Stem Cell Therapy in Wound Repair 263
10.4 Stimuli-Responsive Materials for Wound Healing 263
10.4.1 Reactive Oxygen Species (ROS)-Responsive Materials for Inflammation Treatment 263
10.4.2 Temperature-Responsive Materials for Wound Healing 270

10.4.3 pH-Responsive Materials for Wound Healing 272
10.4.4 Enzyme-Responsive Materials in Wound Healing 273
10.4.5 Activated Platelet-Responsive Materials in Wound Healing 279
10.5 Recent Advances in Wound Healing and Future Directions 280
10.5.1 Gene Therapy in Biomaterials 280
10.5.2 Stem Cell Delivery 281
10.5.3 Advances in Immunotherapy 282
10.6 Conclusion 282
References 283

Chapter 11 Applications of Magnetic-Responsive Materials for Cardiovascular Tissue Engineering 290
Lindsay Steele, Gal Margolis, Smadar Cohen and Boris Polyak

11.1 Introduction 290
11.2 Application of Mechanical Cues *via* Magnetic Force 292
11.2.1 Magneto-Mechanical Cues Applied *via* Magnetic Particles 292
11.2.2 Magneto-Mechanical Cues Applied Through Magnetic Scaffolds 300
11.2.3 Cellular Response to Mechanical Stress 302
11.3 Vascularization Challenge and Current Studies 305
11.3.1 Vessel Structure Formation 305
11.3.2 Induction of Vessel Structure Organization 305
11.4 Generation of Functional Cardiac Tissue 309
11.4.1 Effects of Magneto-Mechanical Stimuli on Maturation of Cardiomyocytes 312
11.5 Magnetic Cell Targeting 314
11.5.1 Magnetic Cell Therapy for Heart Regeneration 315
11.5.2 Magnetic Cell Therapy for Blood Vessel Regeneration 316
11.6 Effects of Electro-Magnetic Fields on Cells 317
11.7 Magnetic Methods for Preparation of Specially Designed Tissue Scaffolds 318
11.7.1 Anisotropic Morphology/Topography 318
11.7.2 Remote Controlled Release Scaffold 319
11.8 Concluding Remarks 320
Acknowledgements 321
References 321

Chapter 12 Intestinal Tissue Engineering with Intestinal Stem Cells 329
Zahra Davoudi and Qun Wang

12.1 Introduction 329
12.2 Tissue-Engineered Intestine Components 332
12.2.1 Cells 332
12.2.2 Intestinal Stem Cells 334
12.3 Environmental Factors 340
12.3.1 Mechanical Environment 340
12.3.2 Chemical Environment 345
12.4 Conclusions and Future Perspectives 349
Acknowledgements 353
References 353

Chapter 13 Smart Materials and Systems as Artificial Pancreas for Diabetes Treatment 358
Yuqi Zhang, Mengzhe Wang, Jicheng Yu and Zhen Gu

13.1 Introduction 358
13.2 Smart Synthetic Systems as an Artificial Pancreas 359
13.2.1 GOx-Mediated Systems 359
13.2.2 Phenylboronic Acid (PBA)-Modified Systems 364
13.2.3 Glucose Binding Protein (GBP)-Modified Systems 369
13.2.4 Insulin Modification 371
13.3 Pancreatic Cell-Based Systems as an Artificial Pancreas 372
13.4 Emerging Translation to Clinical Practice 373
13.5 Conclusions 377
References 377

Chapter 14 Smart Materials for Nerve Regeneration and Neural Tissue Engineering 382
Metin Uz and Surya K. Mallapragada

14.1 Introduction 382
14.2 Stimuli-Responsive Biomaterials for Neural Tissue Engineering and Nerve Regeneration 383
14.2.1 Temperature-Responsive Biomaterials 384
14.2.2 pH-Responsive Biomaterials 390
14.2.3 Self-Assembling Biomaterials 391
14.2.4 Photo-Responsive Biomaterials 392
14.2.5 Enzyme-Responsive Biomaterials 393
14.2.6 Conductive, Electrical-Stimuli-Responsive Biomaterials 394

14.3 Functional Delivery Systems for the BBB 399
14.4 Clinical Potential and Applications of Smart Materials in Neural Tissue Engineering 400
14.5 Conclusions and Future Outlook 401
Acknowledgements 401
References 401

Chapter 15 Smart Cell Culture for Tissue Engineering 409
Yehudah Pardo and Minglin Ma

15.1 Introduction 409
15.2 Materials for Modulating Cell Adhesion and Detachment 411
15.2.1 Poly(*N*-Isopropyl Acrylamide), a Material Worth Noting 412
15.2.2 Alternatives to PNIPAAm 414
15.2.3 Beyond Thermo-Responsive Materials 417
15.3 Modulation of the Culture Environment 422
15.3.1 Microfluidic-Based Cell Culture 422
15.3.2 Mechanical Actuation 424
15.3.3 Repositioning of Cells 426
15.4 Applications of Smart Cell Culture and Clinical Perspectives 428
15.4.1 Cell-Sheet Engineering 428
15.4.2 3D Culture 430
15.4.3 Cell Segregation 432
15.4.4 Clinical Perspectives 433
15.5 Conclusion 433
References 434

Chapter 16 Flexible Micro- and Nanoelectronics for Tissue Engineering 439
H. Acarón Ledesma, K. Koehler and B. Tian

16.1 Introduction 439
16.2 Material Building Blocks and Their Interfaces with Cells and Tissues 441
16.2.1 Inorganic Semiconductors 442
16.2.2 Carbon-Based Materials 446
16.2.3 Nanostructured Polymers 451
16.3 Flexible Micro- and Nanoelectronics for Monitoring Biological Activity 454
16.3.1 Nanoscale Electronics Based on Field-Effect Transistor Technology 455
16.3.2 Implantable Devices for *In vivo* Recordings 458

16.3.3 Bioresorbable Electronics 459
16.4 Flexible Electronics for the Stimulation of Excitable Tissues 462
16.5 Clinical Applications of Smart Materials in Tissue Engineering 465
16.6 Conclusions and Outlook 466
References 467

Chapter 17 Smart Materials to Regulate the Fate of Stem Cells 473
Jiabin Zhang, Hu Zhang and Xia Xu

17.1 Introduction 473
17.2 Thermosensitive Materials 475
17.2.1 Facilitating Cell Differentiation by *in vivo* Gelation 476
17.2.2 Determining Cell Differentiation by Gel Modification 477
17.3 Electroactive/Conductive Materials 484
17.3.1 Electrochemical Materials 484
17.3.2 Piezoelectric Materials 485
17.4 Photo-Responsive Materials 486
17.4.1 Photo-Activatable Materials 487
17.4.2 Photo-Cleavable Materials 492
17.4.3 Reversible Isomers 493
17.5 Thixotropic Materials 494
17.5.1 Stiffness-Induced Cell Differentiation 495
17.5.2 Stress Stiffening/Relaxation-Induced Cell Differentiation 495
17.6 pH-Sensitive Materials 498
17.7 Smart Materials in Clinical Applications 499
17.8 Conclusions and Perspectives 500
Acknowledgements 500
References 501

Chapter 18 Smart Drug Delivery Systems for Tissue Engineering 505
Muhanad Ali, Fang Yang and John Jansen

18.1 Introduction 505
18.2 Smart Drug Delivery Vehicles 507
18.2.1 Polymersomes 508
18.2.2 Liposomes 509
18.2.3 Hydrogels 510
18.2.4 Dendrimers 511
18.2.5 Other Delivery Vehicles 511

18.3 Self-Regulated Smart Drug Delivery Systems and Their Applications 512
18.3.1 pH-Responsive 512
18.3.2 Temperature-Responsive 515
18.3.3 Glucose-Responsive 517
18.3.4 Multiple-Responsive Drug Delivery Systems 519
18.4 Externally Regulated Smart Drug Delivery Systems and Their Applications 520
18.4.1 Magnetic-Field-Responsive 520
18.4.2 Light-Responsive 521
18.4.3 Electric-Field-Responsive 523
18.5 Conclusion and Future Perspective 525
References 526

Chapter 19 Smart Materials for Central Nervous System Cell Delivery and Tissue Engineering 529
Timothy M. O'Shea, Alexander L. Wollenberg, Alexander M. Bernstein, Darren B. Sarte, Timothy J. Deming and Michael V. Sofroniew

19.1 Introduction 529
19.2 A Brief History of CNS Cell Transplantation 530
19.3 Objectives and Challenges for Modern CNS Cell Transplantation 531
19.4 The Development of Biomaterials for CNS Cell Transplantation 535
19.5 Emerging Smart Biomaterials for CNS-Based Cell Delivery Applications 542
19.5.1 Protecting Cells during CNS Cell Transplantation 542
19.5.2 Localizing Transplanted Cells to CNS Injuries and Preventing Migration 545
19.5.3 Regulating Grafted Cell Differentiation *In vivo* 545
19.5.4 Promoting Optimal Cell Graft–Host Integration through Modulation of the Biomaterial Host Interface 546
19.5.5 Stimulating Transplanted Neural Cells with Smart Biomaterials 547
19.5.6 Clinical Potential and Applications of Smart Materials for Central Nervous System Tissue Engineering 548
19.6 Conclusions and Future Directions 548
Acknowledgements 549
References 549

Chapter 20 Smart Multifunctional Tissue Engineering Scaffolds 558
Qilong Zhao and Min Wang

20.1 Introduction 558
20.2 Materials and Fabrication Techniques for Tissue Engineering Scaffolds 559
20.2.1 Tissue Engineering Strategies 559
20.2.2 Materials for Tissue Engineering Scaffolds 562
20.2.3 Technologies for Scaffold Manufacture 563
20.3 Design and Manufacture of Multifunctional Tissue Engineering Scaffolds 568
20.3.1 Complexity in Native Tissue Regeneration Process 568
20.3.2 Requirements for Multiple Functions of Scaffolds in Tissue Regeneration 569
20.3.3 Composite or Hybridization Approaches in Developing Multifunctional Tissue Engineering Scaffolds 571
20.4 Fabrication, Properties and Biological Evaluation of Multifunctional Tissue Engineering Scaffolds—Case Studies 573
20.4.1 Selective Laser Sintered Multifunctional Scaffolds for Bone Tissue Regeneration 574
20.4.2 Electrospun Multicomponent Scaffolds for Bone Tissue Regeneration 577
20.4.3 Nanofibrous Cell-Laden Scaffolds for the Regeneration of Complex Body Tissues 582
20.4.4 Theranostic-Embedded Scaffolds for Cancer Patients 587
20.5 Concluding Remarks 589
Acknowledgements 590
References 590

Chapter 21 Applications of Smart Microfluidic Systems in Tissue Engineering 596
Yin Chen, Lu Huang, Kangning Ren, Xuetao Shi and Hongkai Wu

21.1 Introduction 596
21.2 Thermo-Responsive Microfluidic System 597
21.3 pH-Sensitive Microfluidic System 599
21.4 Electro-Active Microfluidic System 600
21.5 Light-Responsive Microfluidic System 604
21.6 Magneto-Responsive Microfluidic System 607

21.7 Enzymatically Degradable Microfluidic System 608
21.8 Conclusion and Outlook 610
Acknowledgements 610
References 610

Chapter 22 Smart 3D Printing Materials for Tissue Engineering 615
Shan-hui Hsu, Kun-Che Hung and Cheng-Wei Chen

22.1 Introduction 615
22.2 Smart Materials 616
22.2.1 Smart Polymers 616
22.3 The Introduction of Hydrogels 616
22.3.1 Environment-Responsive Hydrogels 618
22.3.2 Environment-Responsive Hydrogels in 3D Printing 619
22.3.3 Self-Healing Hydrogels 622
22.3.4 Self-Healing Hydrogels in 3D Printing 623
22.4 Shape-Memory Materials 625
22.4.1 Shape-Memory Materials for Biological Applications 626
22.4.2 Applications of Thermo-Responsive Shape-Memory Materials 627
22.4.3 Applications of Photo-Responsive Shape-Memory Materials 628
22.4.4 Applications of Other Shape-Memory Materials Such as pH-Sensitive Polymers 628
22.4.5 Applications of Shape-Memory Polymers in 3D Printing 629
22.5 Conductive Polymers Combined with 3D Printing Techniques for Applications in Tissue Engineering 630
22.5.1 Applications of Conductive Polymers in Tissue Engineering 631
22.5.2 3D Printing of Conductive Polymers for Applications in Tissue Engineering 632
22.5.3 Piezoelectric Materials for Applications in Tissue Engineering 633
22.5.4 3D Printing of Piezoelectric Materials for Applications in Tissue Engineering 635
22.6 Potential Clinical Applications of Smart Materials Combined with 3D Printing Techniques 635
22.7 Conclusion 636
References 636

Chapter 23 Smart Materials-Originated Microfluidic Systems for Tissue Engineering 642
Ashlyn T. Young and Michael A. Daniele

23.1 Introduction 642
23.2 Chemically-Reactive Smart Materials in Microfluidics for Tissue Engineering 643
23.2.1 Microfiber Fabrication Using Chemically-Responsive Smart Materials 643
23.2.2 Microvessel Network Fabrication and Application Using Chemically-Responsive Smart Materials 648
23.2.3 Microsphere Fabrication in a Microfluidic Device Using Chemically-Responsive Materials 650
23.3 Photo-Responsive Smart Materials in Microfluidics for Tissue Engineering 652
23.3.1 Microfiber Fabrication and Applications Using Photo-Responsive Smart Materials 652
23.3.2 Microvessel Network Fabrication and Application Using Photo-Responsive Smart Materials 653
23.3.3 Microparticle Fabrication in a Microfluidic Device Using Photo-Responsive Smart Materials 655
23.4 Thermo-Responsive Smart Materials in Microfluidics for Tissue Engineering 659
23.4.1 Microchannels Utilizing Thermally-Responsive Smart Materials 660
23.4.2 Thermo-Responsive Microdroplet Fabrication in a Microfluidic Device 662
23.4.3 Thermo-Responsive Microvalves and Pumps in Microfluidic Devices 664
23.5 Conclusions 666
23.5.1 Clinical Potential and Applications 667
References 668

Subject Index 671

CHAPTER 1

Applications of Smart Multifunctional Tissue Engineering Scaffolds

M. KALIVA[a,b], M. CHATZINIKOLAIDOU[a,b] AND M. VAMVAKAKI*[a,b]

[a]Department of Materials Science and Technology, University of Crete, P.O. Box 2208, 710 03, Heraklion, Crete, Greece; [b]Institute of Electronic Structure and Laser, Foundation for Research and Technology-Hellas, P.O. Box 1527, 711 10, Heraklion, Crete, Greece
*E-mail: vamvakak@iesl.forth.gr

1.1 Introduction

Tissue engineering is an attractive approach to restore and replace diseased or defective tissue offering an alternative to other clinical methods such as organ replacement. Conventional tissue engineering approaches involve the use of a scaffold mainly as a structural element with defined physicochemical, mechanical and biological properties and appropriate architecture and porosity to support cell metabolism. However, recent approaches in tissue regeneration combine three key elements: a scaffold as a micro-environment to promote cell adhesion for tissue development, an appropriate cell type, and biomolecules and drugs to guide cell response and function.[1–3] There has been enormous interest lately in the growth of different types of tissues using multifunctional scaffolds that can actively participate in the process to

Smart Materials No. 25
Smart Materials for Tissue Engineering: Applications
Edited by Qun Wang

Published by the Royal Society of Chemistry, www.rsc.org

provide the biological signals that guide and direct cell function (proliferation, growth and differentiation). Such scaffolds are derived from novel functional and smart materials that allow tuning of the properties and behavior of the scaffolds and can perform multiple crucial tasks simultaneously *i.e.* deliver bioactive and pharmaceutical molecules, direct cell growth and differentiation, and control stem cell behavior.[4]

Organic, inorganic and hybrid (organic–inorganic) materials have all been explored in the development of multifunctional scaffolds. Basic material requirements for use in tissue engineering include biocompatibility, histocompatibility, non-toxicity and the ability to engineer an appropriate scaffold with the required functionalities.

Multifunctional scaffolds based on smart materials have been applied in different tissue engineering fields. The most frequently studied areas in the literature include the use of multifunctional scaffolds in bone, cartilage and muscle formation, in cardiovascular and endothelium tissue engineering, in the growth of skin and in neural regeneration. Other applications include their use in dental, corneal and retina tissue engineering as well as in wound healing. This chapter will focus on the most extensively studied tissues of which the understanding and knowledge have matured the most. Although multifunctional materials and stimuli-sensitive nanoparticulate drug delivery systems have also shown great therapeutic potential for various cardiovascular and infectious diseases and cancer,[5] this application will not be discussed here. In the following, the sections are divided based on the respective tissue of interest, for which the material characteristics and the multifunctionality of materials and scaffolds are discussed (Figure 1.1). The potential clinical applications of the multifunctional scaffolds are also considered.

1.2 Applications of Multifunctional Scaffolds in Tissue Engineering

1.2.1 Bone and Cartilage

Bone is a remarkably organized, hierarchical connective and vascularized tissue that provides mechanical support and serves various biological functions. Degenerative diseases, cancer or injury can cause bone defects. Despite the impressive ability of bone to heal spontaneously after trauma or fractures, a significant need still exists to develop strategies that promote the healing of non-spontaneously healed defects as a result of sufficiently large fractures or diseases with poor healing ability (*i.e.* osteoporosis, cancer). Bone tissue regeneration is a physiological and complex procedure that involves a well-orchestrated participation of various bioactive molecules. Bone extracellular matrix (ECM) comprises different proteins such as collagen fibronectin (FN), osteocalcin (OC), osteopontin (OPN), and bone sialoprotein (BSP). Different bone morphogenetic proteins (BMPs) and growth factors, like transforming growth factor-beta (TGF-β), insulin-like growth factor (IGF), platelet-derived

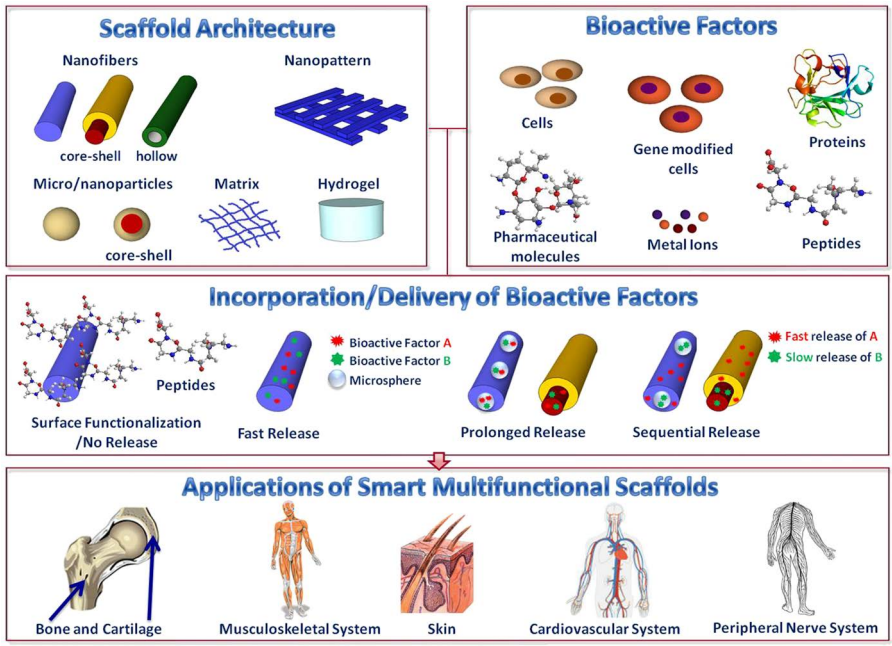

Figure 1.1 Multifunctional materials and strategies for applications in tissue engineering.

growth factor (PDGF), fibroblast growth factor (FGF), and vascular endothelial growth factor (VEGF), are actively involved in the process of bone regeneration, in a spatiotemporal and concentration-controlled manner.[6–8] Multifunctional scaffolds, based on smart materials, are capable of promoting new bone formation, and have received particular attention in the field of bone tissue engineering lately. These scaffolds must indulge a series of different requirements such as bioactivity, biocompatibility, controllable biodegradability, appropriate mechanical strength, architecture and porosity, sustained delivery of chemical and biological cues (growth factors, genes, peptides, small bioactive molecules and ions) to eliminate infection from pathogens and reduce immune response, while promoting cell attachment and growth and stimulating osteo-differentiation and angiogenesis.[9–12]

1.2.1.1 Natural Polymers

Natural polymers have been extensively employed as multifunctional materials in bone and cartilage tissue engineering. This is driven by their superior biological response and their behavior that closely mimics tissue replacement, as well as the inherent non-toxicity and biodegradability of these materials, which renders them particularly attractive for use in biomedical applications. Silk possesses good mechanical properties that can

be combined with the adhesive properties of the tripeptide Arg-Gly-Asp (RGD) for the development of robust multifunctional scaffolds exhibiting good cell adhesive properties, high wettability and enhanced biodegradability supporting the attachment, proliferation, and spreading of MC3T3-E1 cells.[13]

Enormous effort has been focused on the potential of cells and stem cells to differentiate because it allows the growth of tissues *in vitro* before their implantation *in vivo* using a variety of available cells. The design of the scaffold microenvironment, along with the presentation of appropriate cues to induce the differentiation of stem cells, is a highly promising strategy in tissue engineering. The surface functionalization of biomaterial scaffolds with biomimetic proteins is commonly employed in this direction. Collagen is the most frequently used matrix as it is found in the extracellular matrix and provides mechanical strength and supports bone formation. Collagen-based scaffolds have been shown to increase the adhesion, growth, and differentiation of osteoblastic cells and promote tissue formation *in vivo*. On the other hand, adhesive molecules such as FN can regulate cellular recognition of the scaffold through integrin signaling. OC, a non-collagenous protein with a high affinity for mineral crystals, promotes the biomineralization process and has been reported as the key factor during the late phase of osteoblasts and stem cell differentiation. In a novel strategy, OC-FN possessing a collagen binding domain has been integrated in a collagen fibrillar network to provide multifunctional and highly stable scaffolds.[14] The FN active sites enhance the attachment of mesenchymal stem cells (MSC) onto the hybrid matrix, whereas a rapid cell confluence and differentiation to a mature and osteogenic phenotype is driven by OC, leading to significantly improved *in vivo* bone formation in calvarial defects.

BMPs are an important protein family used extensively for the differentiation of pre-osteoblasts and MSCs into osteogenic and chondrogenic cells in bone and cartilage tissue engineering. Among them, BMP-2 exhibits high osteoinductive capacity.[15] However, the delivery mode of BMP-2 from the carrier affects the efficacy of bone regeneration. A sustained *in vivo* delivery of BMP-2 has been shown to favour bone formation compared to the burst release of the protein.[16,17] Site specific binding and regulated delivery of BMP-2 can prolong its delivery and maintain a higher local concentration at the bone injury site. Vehicles based on different biomaterials have been used to tackle this challenge, among which, demineralized bone matrix collagen, derived from cancellous bone tissues, is particularly attractive because it resembles the human bone structure and composition. The specific conjugation of a monoclonal antibody containing six histidine tags on the collagen scaffold followed by BMP-2 binding using orthogonal chemistries increases the loading capacity of the scaffold for BMP-2 and its ability to control the release *in vitro*.[18] The multifunctional scaffolds show increased osteogenic differentiation due to the presence of BMP-2 and more ectopic bone formation. Another strategy employs multifunctional porous or nanoparticulate materials that can deliver single or multiple growth factors in a controllable manner. Alginate is a particularly attractive matrix due to its inertness and lack of interference in

the signaling molecules–cells interactions. Macro-porous alginate scaffolds functionalized with both the TGF-β1 chondrogenic-inducing factor and the RGD peptide strongly affect the MSC morphology, viability and proliferation as well as cell differentiation and the appearance of committed chondrocytes, leading to more effective chondrogenesis compared to the scaffolds functionalized solely with TGF-β1.[19] This is attributed to the effective cell–matrix interactions promoted by the immobilized RGD peptide, which result in a better cell accessibility to the TG-Fβ1 inducer. The regulatory role of TGF-β1 in the osteogenic activity of BMP-2 has been further confirmed in collagen sponge scaffolds. Regulation of the osteoblast and osteoclast generation in the early stages of bone formation induce a five-fold greater bone volume upon the co-delivery of the two growth factors, compared to that induced by BMP-2 alone.[20] Moreover, gelatin sponges comprising a biodegradable three-dimensional hydrogel porous structure, and incorporating both BMP-2 and Wnt1 inducible signaling pathway protein 1 (WISP1), exhibit a higher bone formation capacity for mice with reduced ability to regenerate bone compared to the scaffolds incorporating BMP-2 or WISP1 alone.[21] This indicates that WISP1 enhances the BMP-2-induced osteogenesis and leads to an increased expression of the osteopontin gene *in vivo*, facilitating human bone marrow stromal cell migration to the defective zone. Similar gelatin scaffolds allow the controlled and sustained delivery of a stromal cell-derived factor-1 (SDF-1) and BMP-2 and promote angiogenesis and bone regeneration *in vivo* compared to the release of either of the two proteins alone.[22] The synergistic effect of SDF-1, which induces stem cell migration and inflammatory cell and stem cell recruitment,[23,24] and BMP-2 is attributed to the enhanced expression level of the CXC chemokine cell-surface receptor-4 (Cxcr4), Runt-related transcription factor 2 (RUNX2), and OC genes activating the process of cell recruitment, angiogenesis, and osteogenesis. Apart from porous scaffolds, nanoparticulate carriers have several advantages in terms of prolonging the release of actives. Nanoparticles based on chitosan and chondroitin sulfate are used to deliver proteins, growth factors and platelet lysates to cells.[25] The nanoparticles exhibit high encapsulation efficiencies due to the interactions of the proteins with the polysaccharides and control the release of their cargo for over one month. The platelet-loaded nanoparticles enhance the osteogenic differentiation of human adipose-derived stem cells *in vitro* and exhibit an increased level of mineralization. An interesting approach employs genetically modified plant virus particles as multivalent, low cost and low toxicity nanosized carriers for the presentation of the RGD sequence to enhance bone differentiation of stem cells in osteogenic media containing xenogeneic proteins and growth factors.[26] The virus particles with the RGD peptide extended from the carboxy end of the tobacco mosaic virus coat protein are immobilized onto glass slides pre-treated with two polyelectrolytes, polyallylamine and poly(styrene sulfonate), to form a stable layer-by-layer (LbL) assembly on the substrate. These surfaces induce the rapid onset of several bone differentiation markers, OC, BMP-2 and calcium, in bone-marrow-derived MSC culture, leading to rapid bone replacement.

Finally, self-assembling peptides have lately appeared as a particularly attractive system to replicate the regulatory role of the extracellular matrix and facilitate osteogenic cell differentiation and bone deposition. Bioactive peptide nanofibers presenting histidine moieties on the fiber periphery exhibit multifunctional matrix-regulatory and catalytic properties supporting osteogenesis.[27] This is enabled by the alkaline phosphatase-like behaviour of the imidazole-functionalized peptide fibers that is involved in controlling phosphate homeostasis and in promoting the formation of hydroxyapatite (HA) by the nonspecific cleavage of phosphate esters on the fiber surface. Similar, multifunctional, amphiphilic peptides containing a carboxyl-rich peptide domain and a peptide sequence with binding affinity for BMP-2 are co-assembled with negatively charged spacer molecules into a scaffold exhibiting improved osteogenic efficacy in a rat model (Figure 1.2). A 10-fold decrease of the BMP-2 dose and a 100% and 42% spinal fusion rate in the presence of exogenous and endogenous BMP-2 is recorded.[28]

A very important feature of a functional scaffold is its ability to induce vascularization of the tissue following implantation. This is supported by the porosity of the scaffold as well as its spatiotemporally controlled bioactive release properties. Polysaccharide hydrogel bead scaffolds based on κ-carrageenan can incorporate the PDGF, which induces the production of VEGF and FGF by smooth muscle cells, and support angiogenesis.[29] The great encapsulation efficiency and the sustained release kinetics of PDGF lead to the formation of a highly functional vascular network, whereas the temperature-induced gelling of κ-carrageenan renders these materials attractive for use in injectable systems, requiring minimally invasive procedures.

1.2.1.2 Synthetic Polymers

Synthetic polymers can be appropriately designed to incorporate multiple osteoinductive agents and are very effective in inducing bone formation. Functionalized synthetic micro/nanoparticles and fibers carrying reactive groups and possessing large surface areas for grafting multiple BMPs have been extensively employed to prolong the release of the proteins, reduce their diffusion away from the injury site and maintain sufficient protein concentration for cell differentiation in bone tissue engineering. BMP-7 coupled with BMP-2 in 3-D scaffolds replicates the *in vivo* bone regeneration conditions. The controlled and sequential release of BMP-2 and BMP-7 from nanoparticles incorporated in poly(ε-caprolactone) (PCL) 3-D scaffolds increase the osteoinductive properties of the multifunctional construct compared to the release of BMP-2 alone or the simultaneous delivery of the two growth factors.[30] Electrospun PCL nanofibers have also been employed for the covalent immobilization of liposomes loaded with RUNX2 acting simultaneously as a gene delivery platform and tissue engineering scaffold and supporting the osteogenic differentiation of bone marrow mesenchymal stem cells (BMSCs).[31] The high contact area of the cells with the liposomes facilitates the internalization of the latter by the cells, thus maximizing the

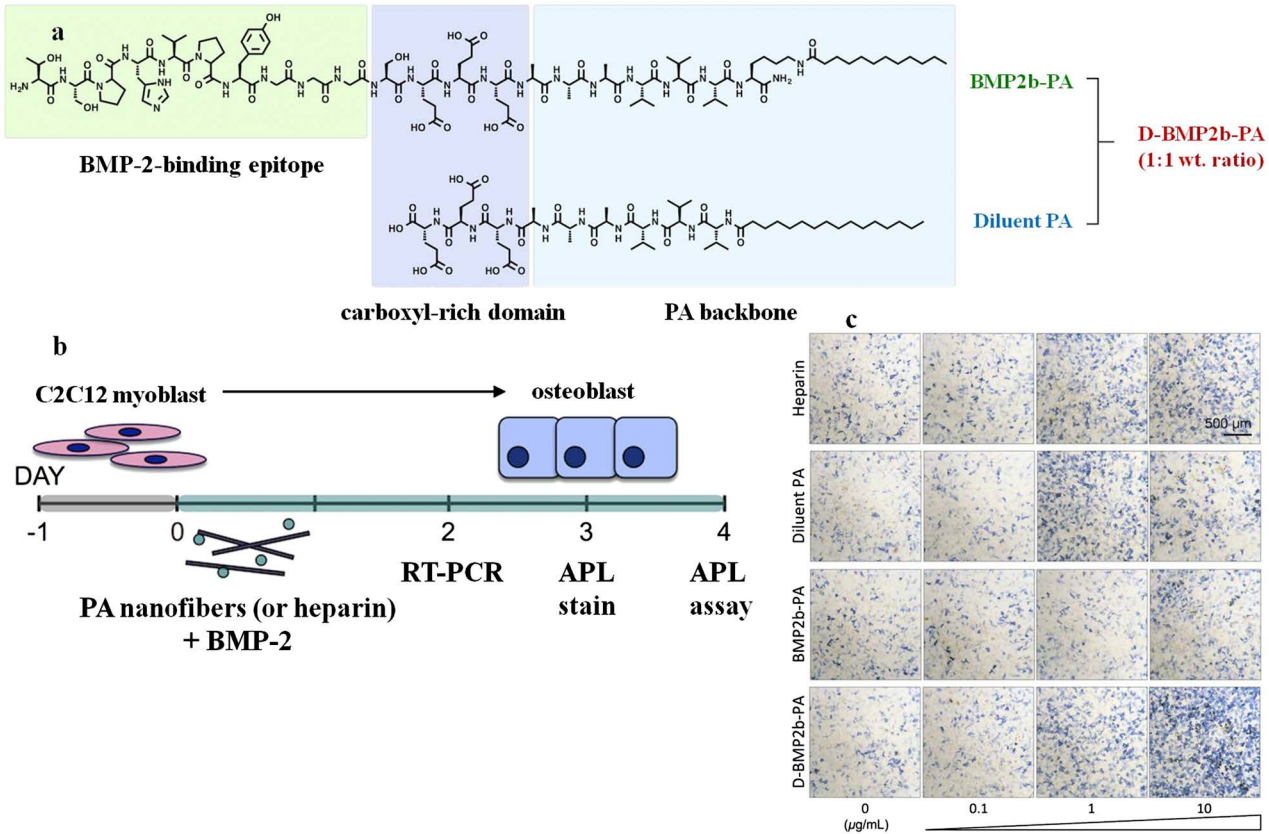

Figure 1.2 (a) Chemical structures of the bone morphogenetic protein 2 (BMP-2)-binding peptide amphiphile (BMP-2b-PA) and the diluent (peptide amphiphile) PA, which are mixed in the BMP-2-binding PA system (D-BMP-2b-PA). (b) Schematic representation of the BMP-2-induced osteoblast differentiation by the PA nanofibers in C2C12 cell cultures. (c) ALP detected in the cells after 3 d. A representative scale bar is displayed. From S. S. Lee, *et al.*, Advanced Healthcare Materials, Copyright © 2015, by John Wiley & Sons, Inc. Reprinted by permission of John Wiley & Sons, Inc.

delivery of the gene and leading to a long-term gene expression and an early onset of other osteoblastic marker expressions relevant for bone homeostasis.

Multilayer films are also attractive for the efficient loading and controlled release of multiple biological cues. Recombinant human (rh) BMP-2, and an angiogenic growth factor, rhVEGF165, have been incorporated in a polyelectrolyte multilayer film. The degradable LbL assembly induces a dosage correlation effect on the differentiation of MC3T3-E1S4 pre-osteoblasts and increases human umbilical vein endothelial cells' (HUVECs) proliferation leading to a 33% higher bone density compared to the BMP-2 alone.[32] Preorganization of the interactions between multivalent scaffolds bearing immobilized cues is nowadays an attractive means to amplify the signaling pathways and control the cell fate. The spatially controlled activation of TGF-β by a self-assembled monolayer displaying peptide ligands to TGF-β receptors, allows the sensitization of the adhered cells to very low amounts of endogenous TGF-β and can serve as a platform for controlling cell decisions.[33] Fibrous materials bearing appropriate functionalities (propargyl, alkene, alkoxyamine, and ketone groups) of controlled surface density enable the use of orthogonal bioconjugation chemistries to prepare multifunctional fibers. Multifunctional coextruded fibers have been modified using a photochemical process to incorporate the functional groups, and then decorated with cell-responsive peptides of spatially controlled surface density.[34] The combined cellular response to two synergistic peptides, the RGD sequence and the osteogenic growth peptide (OGP) sequence induces increased adhesion and differentiation of pre-osteoblast cells on the scaffolds.

Another important family of smart polymers used in tissue engineering is that of electroactive polymers, which allow the stimulation of cell adhesion, proliferation, and differentiation by an electrical stimulus (ES). The incorporation of aniline moieties in polymeric materials can provide scaffolds with electroactive properties. LbL films based on a poly(L-glutamic acid)-*graft*-tetraaniline/poly(L-lysine)-*graft*-tetreaniline assembly can serve as scaffolds of high stiffness, roughness and electroactivity.[35] These characteristics favour the growth and differentiation of pre-osteoblast MC3T3-E1 cells into maturing osteoblasts when applying the ES, presenting a novel approach to improve osteogenesis.

Shape memory materials have also been employed as a novel class of stimuli-responsive materials with great potential for the realization of smart tissue engineering constructs using minimal invasive implantation. Their intrinsic shape recovery properties enable the delivery of a bulky device in a small sized shape through a narrow passage in the body, and the recovery of its original shape when actuated by an external stimulus such as temperature, ultrasound, *etc*. The use of such materials to enhance the efficacy in repairing bone defects has been demonstrated. In one example, rat calvarial osteoblasts were cultured on thermo-responsive and biodegradable poly(D,L-lactide-*co*-trimethylene carbonate) fibrous scaffolds fabricated by electrospinning.[36] The fibers exhibit biomimicking properties and excellent shape memory properties thus enhancing bone tissue repair with minimal

invasive implantation. However, despite their great advantages and potential, injectable, dual-purpose grafts are still limited in the literature.

Nowadays, much research effort has been focused on dual purpose bone grafts delivering locally an antibiotic to prevent bacterial biofilm formation and a growth factor to induce vascularization and bone healing at biologically relevant timescales.[37] Hybrid scaffolds comprising poly(lactic-*co*-glycolic acid) (PLGA) microspheres, containing BMP-2, in poly(β-amino ester) (PBAE) hydrogel particles loaded with ketoprofen, a pharmaceutical molecule, have been developed.[38] The fast-degradation of the PBAE particles induces a rapid drug release over the first 12 h, while at the same time these particles act as a porogen to the PLGA scaffold producing a porous microarchitecture which sustains the BMP-2 release. Another dual growth factor delivery system combing a viscoelastic gellan xanthan gel with bFGF- and BMP-7-loaded antibacterial chitosan nanoparticles has been employed to induce the differentiation of human fetal osteoblasts.[39] The injectable biomaterial with *in situ* ionic- and temperature-induced gelation exhibits enhanced cell growth and differentiation attributed to the prolonged delivery of the two growth factors as well as powerful antimicrobial properties against the most common pathogens in implant infections, and is proposed for minimally invasive bone regeneration. An interesting approach employs a programmable dual therapy multilayer implant coating for single-stage revision in orthopedic applications based on a LbL film (Figure 1.3).[40] The self-assembled, hydrolytically degradable multilayers enable the time-dependent co-delivery of the antibiotic gentamicin and BMP-2 in an independently controlled fashion leading to more effective bacteria-free and rapid bone healing. Other studies have also shown the dual-purpose sustained release of BMP-2 and vancomycin,[41] gentamicin,[42] or nanosilver[43] to control infection and promote bone formation. In all these cases, understanding the molecular interactions of bacteria and cells with the scaffolds in the presence of drugs is essential in the design of the optimal strategy for open fracture healing. The selection of appropriate antibiotics, the tuning of the release kinetics of both pharmaceuticals, as well as more challenging preclinical studies in larger animals, will advance the application of this concept at a clinical level.

1.2.1.3 Inorganic Materials

Inorganic scaffolds for bone tissue engineering are mainly based on bioactive calcium phosphates and bioactive glasses. Biocompatible and osteoconductive tricalcium phosphate (TCP) and HA are typical forms of bioactive calcium phosphates with a chemical composition close to that of the inorganic component of the native bone tissue.[9] Bioactive glasses (BG) include calcium containing silica glasses which upon contact with the body fluids develop a hydroxycarbonated apatite surface deposit. This surface layer induces bone formation and binds strongly to the surrounding tissues and vessels *in vivo*. BG can also stimulate the secretion of angiogenic growth factors *in vitro*.[6,10]

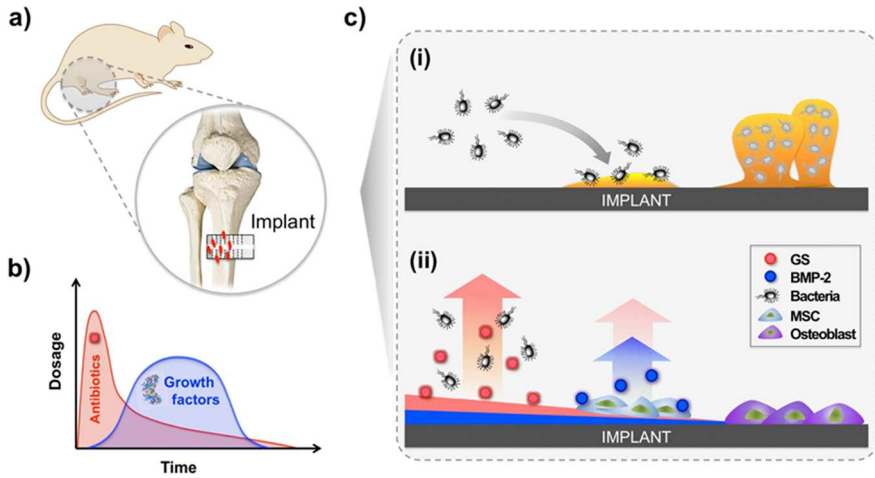

Figure 1.3 Programmed sequential dual therapy delivery strategy. (a) Schematic of a rat tibia model with induced osteomyelitis. (b) Desired release profile of an antibiotic and a growth factor upon degradation of the layer-by-layer (LbL) coating on an orthopedic implant. (c) Possible scenarios following *in vivo* application (i) in an uncoated implant, the residual bacteria in the defect and avascular tissue act as foreign bodies and can cause infection and biofilm formation (represented by the yellow area), (ii) in the dual therapy LbL coating, local delivery of an antibiotic gentamicin (GS) (red dots) controls infection until the implant is vascularized and immune-competent. The subsequent release of BMP-2 (blue dots) induces the osteogenic differentiation of endogenous precursor bone marrow stem cells, resulting in optimal bone healing and implant integrity. Reprinted with permission from ref. 40. Copyright (2016) American Chemical Society.

Multifunctional scaffolds based on these inorganic materials have been developed by the incorporation of growth factors, small drugs, ions (such as copper and cobalt), stem cells or a combination of these bioactive cues. Porous scaffolds, functionalized with such signaling molecules and cells, display the inherent osteoconductivity of the inorganic material in addition to enhanced angiogenic capacity, osteostimulation and antibacterial properties. Several studies have reported the combination of growth factors with metal ions or cells or two different protein growth factors for the development of multifunctional scaffolds in tissue engineering. Specific ions (Li^{+}, Sr^{2+}, Mg^{2+}, Zn^{2+}, Cu^{2+}, Co^{2+}) enhance bone regeneration by stimulating osteogenic differentiation; others ($Cu^{2+}$and Co^{2+}) promote vascularization and some (Cu^{2+}, Ce^{3+} and Ga^{3+}) exhibit antibacterial properties.[44,45] These cations are often loaded in HA or bioactive glasses during synthesis to enhance and ameliorate their ability for bone regeneration. A hierarchically macro/mesoporous biodegradable silica doped with calcium/magnesium and loaded with BMP-2 enhances osteogenesis and bone growth both *in vitro* and *in vivo*.[46] BMP-2 has also been combined with bone marrow stromal cells (BMSCs) in a mesoporous $CaO–P_2O_5$ silica scaffold.[47] The combination of BMP-2 and BMSCs increases new bone formation significantly

compared to the scaffold alone or the scaffold containing only BMP-2. FGF, a mitotic growth factor that stimulates cellular growth and promotes angiogenesis and wound healing, has been combined with mesenchymal stem cells (MSCs) in mesoporous calcium containing silica-based microparticles.[48] The particles exhibit enhanced *in vitro* formation of HA due to the calcium doping and improved adhesion and proliferation of the MSCs induced by the FGF.

An alternative strategy to enhance bone regeneration is by the sequential release of two growth factors with different binding affinities for the scaffold. Porous β-TCP coated with a thin nanoporous mineral layer has been loaded with a mineral-binding version of BMP-2 and VEGF.[49] The higher mineral binding affinity of BMP-2 retards its release compared to VEGF and increases blood vessel density tissue infiltration to the scaffold, however, the low concentration of BMP-2 does not induce ectopic bone formation. Small pharmaceutical drugs have been used extensively to enhance the angiogenic and osteogenic properties of the inorganic scaffolds. By incorporating dimethyloxallyl glycine (DMOG), a small pharmaceutical molecule that inhibits the hypoxia-inducible factor 1a, in a mesoporous bioactive glass (MBG) scaffold, the angiogenic capacity and osteogenic differentiation of human bone marrow stromal cells (hBMSC) have been enhanced.[50] Magnetite nanoparticle decorated HA containing clodronate (CL), a drug for the treatment of osteoporosis that inhibits osteoclast activity, has been shown to possess improved osteoconductivity function and bone formation arising from the HA and CL, while the magnetic nanoparticles are believed to contribute to the rate of bone cell proliferation and differentiation.[51,52]

An attractive platform lately combines scaffolds with antimicrobial properties and high angiogenic and osteogenic differentiation capacity. The former is induced by the incorporation of antibiotics in scaffolds charged with metal ions that promote angiogenesis and bone formation. Levofloxacin has been loaded in Sr doped HA/β-TCP porous granules to enhance pro-osteoblastic proliferation and osteoblastic differentiation of MG63 cells.[53] Multifunctional scaffolds with high angiogenic and antibacterial capacity and antimicrobial properties are also obtained by incorporating cobalt (Co^{2+}) or copper (Cu^{2+}) ions and antibiotics, ampicillin or ibuprofen, in hierarchical mesoporous bioactive glasses (MBG).[54,55] The increased osteogenesis and angiogenesis is attributed to the hypoxia function of the scaffolds induced by the metal ions, whereas the sustained release of the antibiotics and the presence of Cu^{2+} reduces bacterial survival significantly. Moreover, the incorporation of Si and Zn elements, in the form of silica dioxide and zinc oxide, in 3-D printed β-TCP scaffolds has been shown to enhance bone and blood vessel formation and a more vascular branching morphogenesis compared to the undoped scaffolds.[56]

1.2.1.4 Hybrid Polymer/Inorganic Materials

Bone tissue itself is a nanocomposite material consisting of an organic and an inorganic component. The organic phase is mainly based on collagen I, while the inorganic phase is nanocrystalline HA. Therefore, organic–inorganic

hybrid materials, comprising a soft polymer and a hard inorganic component, can better mimic the structure and chemical composition of bone and are particularly advantageous in bone tissue engineering.

Multifunctional hybrid scaffolds comprising a bioactive inorganic material combined with two sequentially delivered growth factors resemble more closely the physiological ECM cues in natural bone tissue regeneration. The sequential delivery of the therapeutic growth factors FGF2 and FGF18 from core PEO-shell PCL hollow fibrous scaffolds increases considerably osteogenesis and new bone formation with 35% new bone volume.[57] Control over the release profile of the growth factors can be achieved by the incorporation of FGF2 in the core of the fibers (fast release) and encapsulation of FGF18 within the MBG also loaded in the core (slow release). Similar behavior is observed for a chitosan sponge loaded with both PDGF, that is released quickly and acts during the first phase of bone regeneration, and VEGF-containing alginate microspheres, which exhibit a slow release of their cargo and are involved in the latter stages of bone formation.[58]

Therapeutic small molecules with controlled release profiles have been extensively incorporated in multifunctional hybrid scaffolds to enhance bone tissue formation. Dexamethasone (DEX), an osteogenic agent, has been loaded in PLGA microspheres immobilized on the surface of a porous HA scaffold to ameliorate both bone volume and quality and a similar effect has been reported for alendronate-containing HA microspheres cross-linked in a chitosan matrix.[59,60] Porous PLGA/TCP scaffolds containing icaritin, a phytoestrogenic molecule from the herb *Epimedium*, can also stimulate both osteogenesis and angiogenesis, leading to an enhanced ALP activity and increased osteogenic marker expression *in vitro* and increase bone formation and vascularization *in vivo*.[61] The combination of osteoconductive and antibacterial properties in a hybrid scaffold requires, as mentioned above for the other types of materials, a scaffold that promotes bone formation and the use of drugs with anti-inflammatory properties. Multifunctional hybrid poly(3-hydroxybutyrate)/bioglass scaffolds with gentamicin, an aminoglycoside antibiotic,[62] and Sr-loaded calcium polyphosphate scaffolds containing erythromycin as the antibiotic and coated with poly(vinyl alcohol) (PVA) have been shown to inhibit bacterial growth both *in vivo* and *in vitro*.[63] On the other hand, the combination of drugs and protein growth factors provides scaffolds with novel properties. A porous collagen-HA scaffold with BMP-2 and zoledronic acid (ZA) exhibits both anabolic (bone forming) and anti-catabolic (minimal bone-resorbing) behavior and a significantly increased bone volume in rats, compared to the scaffold with the BMP-2 alone.[64]

An indirect way to deliver growth factors and favor bone formation involves the incorporation of genes, capable of expressing the growth factors, in the scaffolds. Such a gene therapy approach for the sustained release of growth factors can employ mesoporous bioglass/silk fibrin scaffolds, containing adenovirus for both PDGF-b and BMP-7, which leads to effective treatment of osteoporotic fractures.[65] Often the combined delivery of growth factors and cells is advantageous in bone reformation and vascularization.

Multifunctional nanocomposite scaffolds of PLGA/PCL/HA loaded with vascular stents of PLCL/Col/HA, as a carrier for bone marrow mesenchymal stem cells (BMSCs), and a sodium alginate hydrogel to deliver two growth factors, BMP-2 and the bFGF, increase the ALP activity and the vascularized bone formation significantly.[66] Core–shell fibrous scaffolds consisting of MSCs entrapped in a collagen core and an alginate hydrogel encapsulating BG enriched with Ca and Si ions in the shell enhances the osteogenic differentiation of the MSCs significantly and promotes cellular invasion around the scaffold due to the release of Ca and Si, which act as cues for the surrounding and encapsulated cells.[67]

Triple functional scaffolds displaying three different functions are particularly attractive since they can combine cell adhesion, osteoconductive and osteoinductive properties.[68] Cell adhesion RGD moieties and osteoinductive BMP-2, immobilized on a porous hybrid scaffold based on PLGA and HA, exhibit high density new bone formation when combined with MSCs encapsulated within collagen hydrogels.[69] Modern approaches in bone tissue engineering employ hybrid shape memory scaffolds based on chemically cross-linked PCL and HA particles, with a shape transition from a deformed shape to a recovered shape at body temperature, combined with the BMP-2 growth factor to promote new bone formation under minimally invasive surgery.[70]

However, despite the enormous work involving growth factors for bone formation, their use is still controversial, and thus great attention has been paid lately to growth-factor-free approaches, which employ dynamic and bioactive hybrid materials in bone tissue engineering. The hybrid scaffolds combine enhanced stiffness, enzymatic stability, porosity, injectability and good cell adhesion in the presence of RGD domains, with high osteogenic differentiation of pre-osteoblast cells, in the absence of any osteoinductive factor, driven by the inorganic component.[71]

1.2.1.5 Hybrid Synthetic/Natural Polymers

Another family of hybrid scaffolds is that based on synthetic/natural polymers, which aim to better mimic the natural bone environment. Synthetic/natural polymer scaffolds with multifunctional properties include those used for the delivery of two growth factors or a combination of a drug and a growth factor. Hybrid scaffolds comprising pullulan nanogels as the natural polymer and four-arm thiol-functionalized polyethylene glycol as the synthetic component have been applied for the combined release of FGF18 and BMP-2 and exhibit almost perfect healing, much higher than the scaffolds with only one of the two growth factors (Figure 1.4).[72] DEX and BMP-2 have been combined in core–shell microcapsules comprising a synthetic PLGA core and a natural alginate shell.[73] The controlled release of the two active molecules can be tuned by varying their position in the core or the shell of the capsule, however, the osteogenic activity of rat BMSCs increases in all cases. In a related work, multifunctional hybrid scaffolds based on poly (L-lactide-*co*-ε-caprolactone)/collagen nanofibers have been loaded with bovine

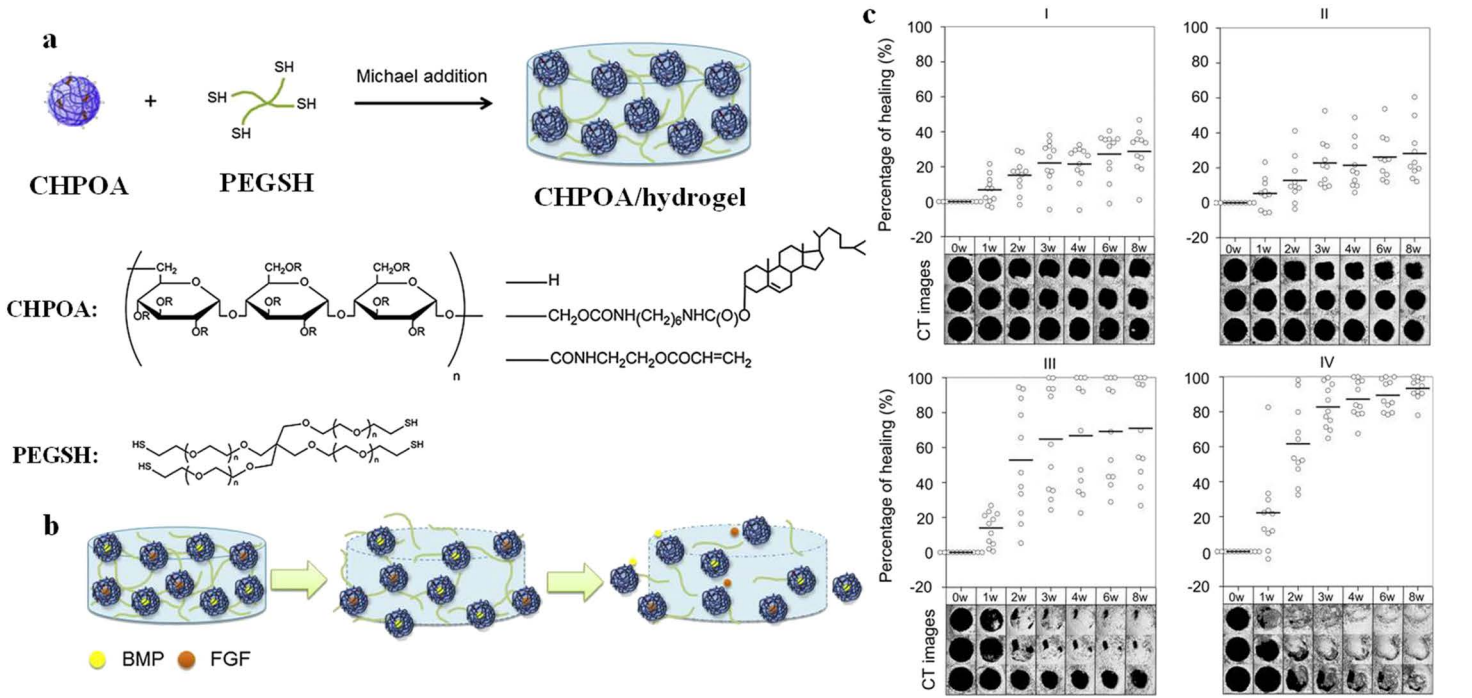

Figure 1.4 (a) Synthetic approach for the preparation of the cross-linked pullulan nanogels *via* Michael addition of the acryloyl-modified pullulan (CHPOA) nanogels with four-arm thiol-functionalized polyethylene glycol (PEGSH). (b) Schematic representation of the fibroblast growth factor 18 (FGF18)- and the BMP-2-release from the nanogels after disintegration. (c) Degree of bone healing *in vivo* at 0, 1, 2, 4, 6, and 8 weeks after implantation: (I) of the FGF18- and BMP-2-containing nanogel/hydrogel pellets, (II) FGF18 only, (III) BMP-2 only, (IV) FGF18 and BMP-2. Scatter spots display data for all specimens, while bars demonstrate the average of each phase. Three representative images of μCT are shown at the bottom of each graph. Reprinted from Biomaterials, 33, M. Fujioka-Kobayashi, *et al.* Cholesteryl group- and acryloyl group-bearing pullulan nanogel to deliver BMP-2 and FGF18 for bone tissue engineering, 7613, Copyright (2012), with permission from Elsevier.

serum albumin (BSA)-stabilized BMP-2 and DEX.[74] The scaffold with both bioactive agents in the core and the shell of the fibers shows the highest ALP activity compared to that incorporating BMP-2 in the core, suggesting that the osteogenic activity is regulated by the concentration of BMP-2 in the cell culture. In order to further control the release of BMP-2 in the medium, electrospun nanofibers based on poly(ε-caprolactone)-*co*-poly(ethylene glycol) (PCL-*co*-PEG) and loaded with DEX and chitosan-stabilized BSA nanoparticles containing BMP-2 (BNPs) have been developed.[75] The sustained delivery of BMP-2 from the BNPs improves further the ALP activity and supports *in vivo* osteogenesis in calvarial bone defects.

Finally, growth-factor-free approaches have employed semipermeable capsules based on a LbL coating of polylysine, alginate, chitosan and alginate, to encapsulate poly(L-lactide) (PLLA) microparticles functionalized with collagen I and a co-culture of adipose stem cells (ASCs) and endothelial cells (ECs). These microcapsules increase the ALP activity and the surface mineralization and enhance the BMP-2, RUNX2 and BSP markers.[76] The observed self-regulation and differentiation of the cells without the need of growth factors is attributed to the liquefied environment of the capsules, which allows the transfer of nutrients, and the spatial coexistence of the cells, which can communicate and self-organize within the capsule.

1.2.2 Muscle

Skeletal muscle tissue engineering employs different cell sources and bioactive molecules to activate skeletal muscle regeneration and can be applied as a promising therapeutic tool to treat patients with large-scale muscle atrophy. Biomaterial scaffolds have been shown in animal models to play a key role in increasing the therapeutic potential of the cells and growth factors. The function of the biomaterial is to serve as a matrix providing a suitable micro-environment for the cells, to guide tissue reorganization and to deliver and release bioactive factors. Biomaterials in different forms, ranging from porous three-dimensional scaffolds to patterned surfaces, have been employed in muscle tissue engineering to induce, among others, vascularization, innervation, and contractility. Multifunctional and hybrid biomaterials that enhance muscle regeneration have attracted particular attention. Such materials can release multiple bioactive molecules and provide surface signals to activate, recruit and rearrange the cell populations (Figure 1.5).[4] The sustained co-delivery of VEGF, to promote angiogenesis, and IGF-1, to directly stimulate muscle regeneration, from an injectable and biodegradable alginate gel has been investigated.[77] The combined release of VEGF and IGF-1 leads concurrently to angiogenesis, reinnervation, and myogenesis in ischemic hindlimbs of mice models. Moreover, appropriate functionalization of the above macroporous alginate scaffold with the cell adhesion oligopeptide G4RGDSP prevents apoptosis of the cells upon transplantation and promotes their proliferation and differentiation to myoblasts, resulting in increased muscle mass and contraction function.[78]

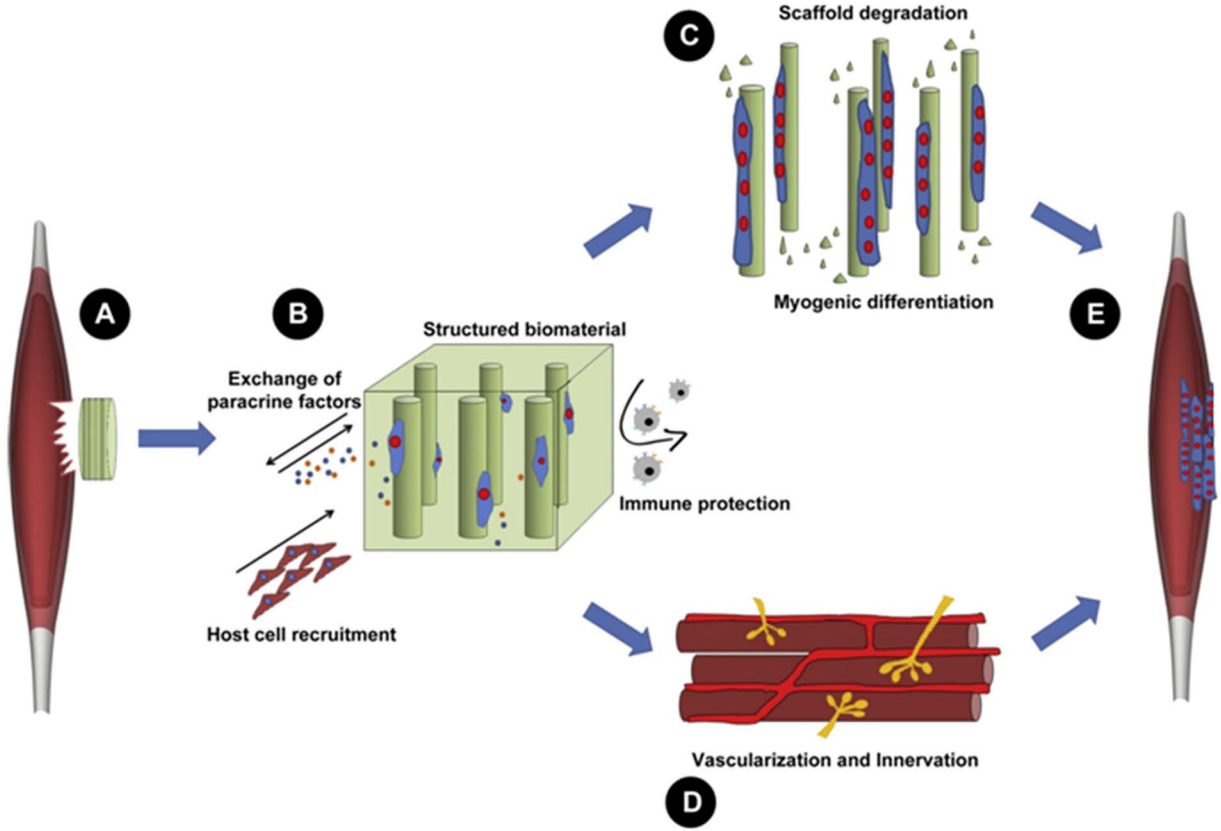

Figure 1.5 Schematic representation of multifunctional scaffolds that stimulate the endogenous mechanism of muscle regeneration. (A) Multifunctional 3-D scaffold combined with cells transferred at the muscle defect site. (B) The hybrid biomaterial characteristics provide immune protection of incorporated cells and at the same time allow them to secrete the paracrine factors, which are involved in recruiting host cell populations. (C) The degradation of the biomaterial over time releases the cells and next *via* the biomaterial scaffold guidance the cell alignment and myoblast differentiation is stimulated. (D) Paracrine cues stimulate vascularization and innervation, (E) and support the multifunctional approach for successful muscle regeneration. Reprinted from Biomaterials, 53, T. H. Qazi, *et al.*, Biomaterials based strategies for skeletal muscle tissue engineering: Existing technologies and future trends, 502, Copyright (2015), with permission from Elsevier.

Electroactive shape memory polymers are particularly attractive in muscle regeneration. Shape memory polymer networks comprising a six-arm polylactide (PLA) star and amino-capped aniline trimers as the electroactive functionalities have been developed and used for the enhanced proliferation and differentiation of C2C12 myoblast cells.[79] The scaffolds displayed good mechanical properties at body temperature, biocompatibility, degradability and excellent shape memory properties with a recovery time of a few seconds, recovery ratio >94%, and fixity ratio ~100%, characteristics that render them excellent candidates in muscle tissue engineering.

A unique tissue interface and a highly specialized region in the muscle–tendon unit, is the muscle–tendon junction (MTJ). Tailor-made materials to support composite MTJ tissue engineering are employed in the fabrication of scaffolds that exhibit different mechanical profiles at different parts of the scaffold mimicking the strain profiles of the native MTJ. Such a mandrel-shaped scaffold, comprising co-electrospun PCL/collagen and PLLA/collagen fibers at the two opposite ends, formed a continuous scaffold with high stiffness/low compliance at one end and low stiffness/high compliance in the other.[80] This scaffold supports both tendon tissue, at the PLLA end, due to its high stiffness and low ductility, and skeletal muscle at the end of electrospun PCL, where the scaffold is less stiff, but has a greater ductility. Another interesting approach in muscle tissue engineering has been introduced based on a soft cell-culture-platform comprising a biocompatible low-modulus polydimethylsiloxane substrate onto which ultrathin stretchable gold nanomembrane sensors and patterned graphene nanoribbons were deposited.[81] The modulus of the system has been designed to match that of muscle tissue and the device has been employed for the unidirectional orientation of C2C12 myoblasts. The platform presents various functions such as enhanced cell proliferation and differentiation and alignment of the cells on the patterned graphene nanoribbons, mimicking the structure of the native muscle tissue.

Finally, an essential aspect for proper *in vivo* skeletal muscle development is the electrical stimulation of the tissue-engineered constructs to mimic the electrical impulses of the muscles from the central nervous system. Although this field is still in its infancy, the pioneering work of Ito *et al.* shows that optimization of the electrical pulse stimulation during myogenic differentiation can lead to functional skeletal muscle tissues.[82]

1.2.3 Skin Tissue Engineering

Skin is the largest human tissue, which consists of three layers—epidermis, dermis and hypodermis—with a complex network of vessels and nerves that under physiological conditions are inherently self-renewable. Skin possesses multiple functions as a physical barrier that protects the host from bacteria and infections and from mechanical or chemical damage. Skin has the ability to regenerate when the injury affects the epidermal layer and the top

layer of the dermis. However, skin regeneration and healing of massive and deep dermal loss due to acute injuries and chronic diseases is still a challenge today. There are several treatments to repair skin trauma including autografts, allografts and xenografts. However, these methods have several downsides such as immune rejections, donor limitations and scarring.[83–86] An alternative approach for skin replacement is skin tissue engineering, which focuses on promoting the regeneration of lost skin by stimulating the ability of the skin to self-regenerate.

Wound healing is an intricate process that consists of three overlapping phases: initial inflammation, proliferation and tissue remodeling. There are numerous protein growth factors (epidermal growth factor, (EGF), PDGF, TGF-β and FGF), cells (fibroblasts, keratinocytes and leukocytes) and cytokines that are involved in the cascade processes of skin regeneration and healing. Current efforts in skin tissue engineering are aimed at the successful development of smart multifunctional scaffolds with the ability to simulate the ECM micro-environment of native skin and to promote the right cues that can direct and promote cell proliferation, differentiation, migration and organization leading to skin regeneration, recovery of its full function and at the same time prevent scars. Bioactive elements that can be embedded within the scaffolds to induce skin regeneration are protein growth factors, cells, or therapeutic molecules with antibacterial and anti-inflammatory properties. These signaling molecules can be incorporated directly within the scaffold or they can be first introduced in polymeric vesicles to control their delivery.[85,86]

The materials used to fabricate scaffolds for skin tissue engineering should be biocompatible, non-cytotoxic, biodegradable, possess appropriate mechanical and physical properties, and promote favorable cell interactions. Natural and synthetic polymers and hybrid materials have all been used for skin regeneration. Natural materials include collagen, gelatin, fibrin, hyaluronic acid, alginate and chitosan (CS), whereas synthetic analogues are PCL, PLGA, PEO and PLA.[85–88] There are several examples of scaffolds incorporating two or more growth factors to enhance their skin regeneration capacity. Electrospun CS/PEO nanofibers containing fast-released VEGF and PDGF-containing PLGA nanoparticles to slow down the release of PDGF, can stimulate angiogenesis, increase re-epithelialization and control granulation tissue formation (Figure 1.6).[89] Similar biological functions are attained by EGF- and VEGF-loaded chitosan microparticles embedded within a dextran hydrogel,[90] while PEO/PLGA nanofibers containing rhEGF- and recombinant human basic fibroblast growth factor (rhbFGF)-loaded PLGA microspheres enhance the proliferation rate of human skin fibroblasts due to the synergistic effect of the two growth factors.[91] Enormous progress has also been made in the simultaneous incorporation of multiple growth factors—VEGF, PDGF, bFGF and EGF—in collagen/hyaluronic acid nanofibers.[92] Control over the sequential release of bFGF and EGF at the first stages of healing to increase epithelialization and vasculature spouting, followed by the slow release of VEGF and

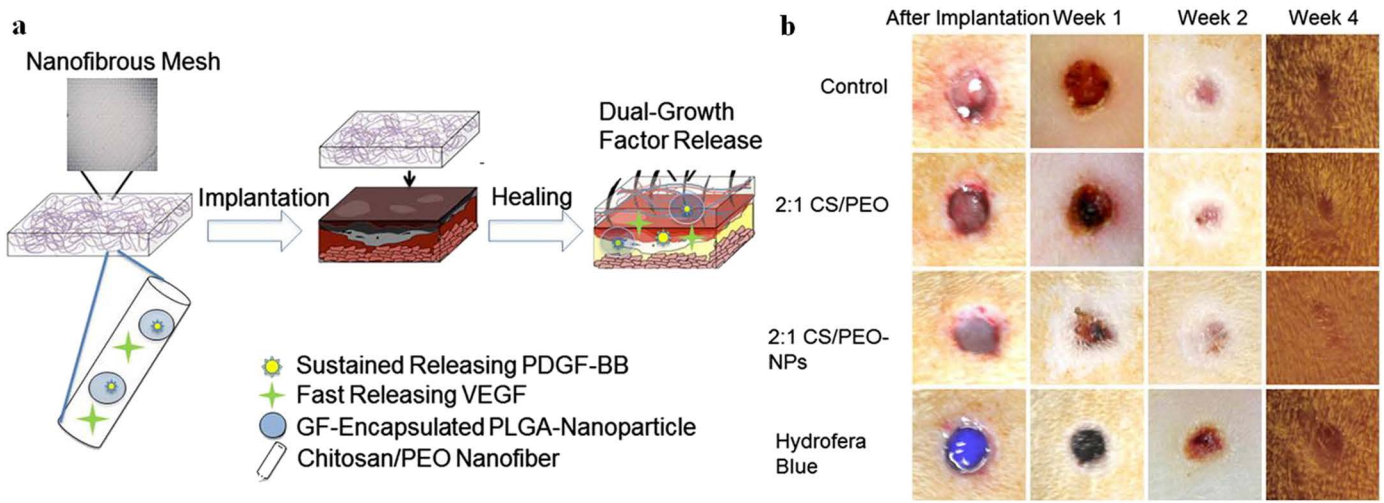

Figure 1.6 (a) Schematic representation of nanoparticle-containing electrospun chitosan/PEO nanofibers carrying two growth factors: VEGF (fast release) and PDGF-BB (slow release). Following scaffold implantation on the skin wound site, tissue regeneration and healing are promoted by releasing the bioactive molecules at different healing phases. (b) Wound healing ability of the nanofibers evaluated using a full skin rat wound model 0, 1, 2, and 4 weeks after curing. Controls are 2 : 1 CS–PEO, 2 : 1 CS–PEO-NPs, and Hydrofera Blue. Reprinted from Acta Biomaterialia, 9, Z. Xie, *et al.* Dual growth factor releasing multi-functional nanofibers for wound healing, 9351, Copyright (2013), with permission from Elsevier.

PDGF, pre-loaded within gelatin nanoparticles, to induce blood vessel maturation, increases the proliferation rate of endothelial cells and results in a better network formation, enhanced wound healing rates, increased collagen deposition and improved vessel maturation upon implantation in diabetic rats.

The combination of the artificial dermal matrix Integra® with hMSCs and platelet-derived rich plasma (PRP) in multifunctional scaffolds offers additional advantages in skin regeneration due to the high plasticity of the hMSCs, which can differentiate into other cell linkages, and the wound healing properties of PRP, by the release of PDGF, TGF-β, EGF, IGF-1, IGF-2 and VEGF.[93] Bioactive molecules, such as vitamins C and D, the steroid hormone hydrocortisone, the peptide hormone insulin, the thyroid hormone triiodothyronine, retinoic acid and EGF, incorporated within collagen/PLGA or core–shell nanofibers consisting of gelatin/poly(L-lactic acid)-*co*-poly(ε-caprolactone) enhance human dermal fibroblast and keratinocyte proliferation as well as ADSCs proliferation and differentiation to epidermal lineages.[94,95] Antibiotics are also important to prevent wound infection. An interesting approach involves the use of collagen-coated poly(3-hydroxybutyric acid)/gelatin nanofibers containing a bioactive extract from the *Coccinia grandis* plant to increase the antibacterial activity of the scaffold against both Gram positive and Gram negative bacteria, as well as the adhesion of both NIH 3T3 fibroblasts and human keratinocytes.[96] Gentamicin- and rhVEGF-containing PLGA microparticles have also been incorporated within collagen/chitosan porous scaffolds to sustain their release and thus promote the antibacterial and angiogenic properties of the scaffold.[97]

Multifunctional, composite, electrospun nanofiber scaffolds comprising cationic gelatin/hyaluronan/chondroitin sulfate with incorporated sericin, an antioxidant, antibacterial, and anticancer factor, and glycosaminoglycans, have been fabricated.[98] The presence of sericin increases the proliferation of human foreskin fibroblasts, human keratinocytes and hMSC and stimulates the hMSCs' epithelial differentiation when co-cultivated with keratinocytes. Gene therapy approaches have been extensively used to induce the local release of growth factors during skin regeneration and to enhance their regenerative potential *in vivo*. Polyethylenimine-coated plasmids coding for VEGF, introduced in a FDA-approved collagen scaffold, increase the release of VEGF and the non-adherent cells significantly, especially erythrocytes, presenting a novel method for scaffold bioactivation.[99] In a similar approach, polyethylenimine polyplexes of a basic fibroblast growth factor-encoding plasmid (pbFGF) incorporated in core–shell PLA–PEG increases skin healing, vascularization and collagen deposition significantly.[100] A novel strategy towards the development of a multifunctional scaffold combines a trimethyl chitosan/siRNA complex in a porous membrane bilayer dermal analogue comprising collagen–chitosan and silicone. The complex architecture promotes skin regeneration in the porous collagen–chitosan scaffold with silicon acting as a temporal epidermis to prevent infections, while the trimethyl chitosan/siRNA complex interrupts the TGF-β1 signaling pathway leading to scar-free new skin formation.[101]

1.2.4 Cardiovascular

The number of patients with cardiovascular diseases (CVDs) has risen worldwide and these diseases are the main cause of mortality.[102] Typical CVDs include coronary artery disease, and the malfunction of myocardium or heart valves. Healthy autologous vascular grafts, which could be a therapeutic approach in clinical use, have the limitation of a shortfall in demand.[103] Potential solutions to overcome existing challenges caused by autologous grafts are based on the development of synthetic materials for vascular and myocardium tissue replacement. Although synthetic polymeric and metallic vascular grafts have a broad clinical use, there are certain limitations introduced by the material's thrombogenic ability, caused due to protein adsorption and platelet adhesion and activation on the surface of the grafts.[104,105]

While the implantation of stents is the major therapeutic approach to cure coronary artery malfunctions,[106] it can give rise to cellular and biochemical actions inducing pathological diseases.[107,108] The series of actions involves inflammation and smooth muscle hyperplasia that can lead to thrombosis upon further inflammation or rupture of the plaque. If the thrombotic event does not occlude the artery, the cycle occurs again.[109–111] The thickening of the artery wall may be due to poor re-endothelialization on the stents.[107] Thrombosis and restenosis are two serious challenges to control as they are major obstacles for commercially available vascular stents.[112] The physiological vascular endothelium comprises a monolayer of endothelial cells (ECs) acting as the natural anticoagulant of the artery wall.[112] This structure is essential to preserve vascular homeostasis and adjust the growth of smooth muscle cells (SMCs). Seeding of endothelial cells (ECs) onto the stent surface has been investigated as a means to avoid direct contact of the blood with the synthetic material producing thrombosis,[113] and to regulate the phenotype and proliferation of the SMCs.[107]

Numerous studies have reported the delayed or absent endothelialization in late stent thrombosis (LST).[114] The bare stent surface is a risk for the formation of LST.[112] Drug-eluting stents (DES) are important tools to treat CVDs as they decrease the restenosis rate significantly.[108,115,116] Current drug-eluting stents aim to prevent the proliferation of vascular SMCs, though they simultaneously inhibit the growth of ECs, resulting in a delayed endothelialization.[117] Thus, using effective techniques for the endothelialization of vascular grafts is of paramount importance in the inhibition of restenosis and the long-term efficacy of the grafts.[106,113]

The inflammatory response is another important issue in the endovascular implantation that is often disregarded.[118] Particularly, the response of SMCs and macrophages to vascular injury and endothelial cell death is critical for the ECs' malfunctions, thrombosis and inflammation.[119] In recent years, there has been a need to develop physical or chemical methods that enable the introduction of multifunctional cues on the materials' surfaces that can simultaneously function as inductive material substrates for increased endothelialization, inhibition of SMCs' hyperplasia, and possess anti-coagulant, anti-restenotic, anti-inflammatory and antibacterial action.

1.2.4.1 Surface Coatings to Enhance Endothelialization

Various multifunctional approaches to enhance endothelialization, a major strategy for the improvement of vascular biocompatibility, will be described in this subsection. As mentioned previously, a vascular stent is important to selectively increase the proliferation of ECs, reduce the growth of SMCs and simultaneously suppress blood coagulation. Research effort has[120] focused recently on the importance of the competitive growth of ECs *versus* SMCs for the development of a functional endothelium on a stent.[120–122] These strategies employ the binding of bioactive peptides and gene engineering,[123] ECM proteins or catechols with EC selectivity, and TiO_2 nanotube coatings as promising platforms to enhance the selectivity of the stents for ECs,[124,125] however, these surfaces still lack effective anticoagulant properties.

To overcome these limitations, the development of TiO_2 nanotube arrays modified by a mussel-inspired polydopamine ad-layer for the controlled loading of the thrombin inhibitor, bivalirudin (BVLD), which was chosen as an eluted anticoagulant and provided multiple functions, such as enhanced hemocompatibility and selectivity for ECs in a competitive growth with SMCs, has been proposed.[126] Similarly, the development of a multifunctional surface comprising hyaluronic acid and dopamine *via* conjugation onto 316L stainless steel led to better hemocompatibility compared to the bare material controls (Figure 1.7),[127] while an electropolymerized polydopamine coating on the surface of complex-shaped cardiovascular stents facilitates the immobilization of vascular endothelial growth factor, enhancing the desired cellular response of ECs and preventing neointima formation after stent implantation.[128] Moreover, co-immobilization of serum albumin and peptide aptamer, with specific activity for endothelial progenitor cells (EPCs) and anti-platelet adhesion, on a polydopamine-coated titanium surface enhances *in situ* self-endothelialization.[129]

Recent advances in vascular tissue engineering apply multifunctional nanotechnology strategies to promote better endothelialization and microvessel regeneration (Figure 1.8).[130] A biodegradable urethane-loaded polyester multifunctional nanoparticulate scaffold has been developed with two ligands,

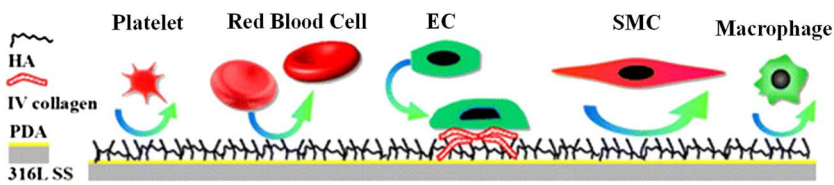

Figure 1.7 Chemically conjugated multicoatings of hyaluronic acid (HA) and dopamine (PDA) on stainless steel. The coatings exhibit improved hemocompatibility, inhibit the growth of muscle cells and the binding/activation of macrophages while they favor endothelialization, and thus could serve as coatings on cardiovascular implanted devices. Reprinted with permission from ref. 127. Copyright (2016) American Chemical Society.

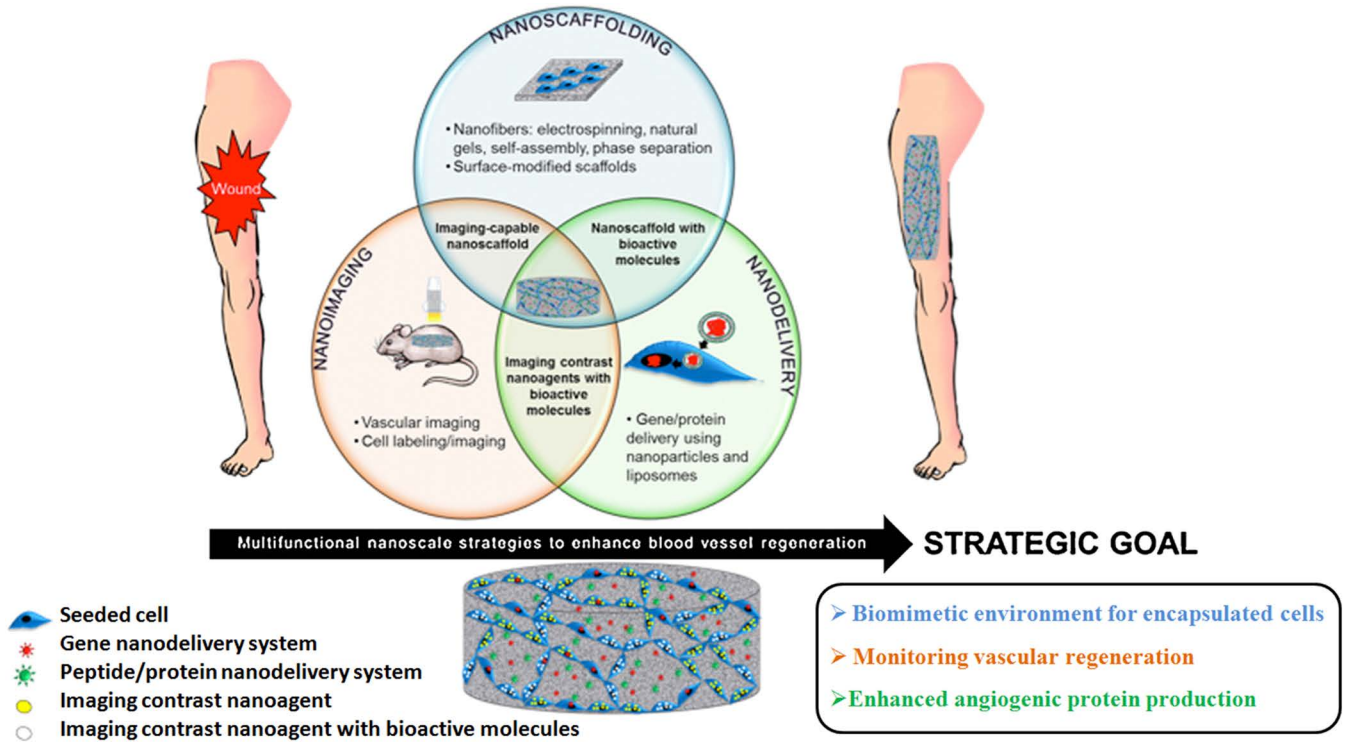

Figure 1.8 Multifunctional nanoscale approaches for vascular tissue engineering include scaffolding, imaging, and delivery of bioactive factors, and can be employed to promote blood vessel regeneration. The combination of nanoscaffolding, nanoimaging, and nanodelivery creates a biomimetic environment for effective cell delivery, allows monitoring of the vascular regeneration process *in vivo*, and increases angiogenesis by delivering bioactive molecules. Seeded cells (blue) loaded with contrast agents (yellow) alone and with bioactive molecules (white). The contrast agents with a gene (red) or protein (green) nanocarrier can be loaded in a 3-D matrix. Reprinted from Nano Today, 7, E. Chung, *et al.*, Multifunctional nanoscale strategies for enhancing and monitoring blood vessel regeneration, 514, Copyright (2012), with permission of Elsevier.

one for glycoprotein 1b to target the damaged arterial endothelium and the second for anti-CD34 antibodies to trap endothelial progenitor cells for endothelium regeneration.[131] Among the synthetic polymeric vascular scaffolds, PCL has been used for the conjugation of the multifunctional REDV short peptide to zwitterionic polycarboxybetaines exhibiting increased antibacterial activity, anti-thrombogenic capacity and endothelial cell growth,[103] while co-immobilization of adhesive peptides and VEGF on a vinylsulfone-modified dextran matrix proved to be selective to ECs over SMCs.[132] Since the mechanical properties of the polymer should match the elasticity of blood vessels, soft poly(*n*-butyl acrylate) networks with tunable mechanical properties can be utilized to angiogenically stimulate intermediate CD163+ monocytes/macrophages as a cellular cytokine delivery system to accomplish functional endothelialization,[133] whereas metallic cardiovascular stents with elastic degradable co-polyetheresterurethane can increase endothelial cell adhesion.[134] Another efficient strategy involves the modification of the titanium surface by forming an endothelial coating on a hyaluronic acid micropattern.[106] A multifunctional ligand comprising a cyclic RGD peptide, a tetraethylene glycol spacer, and a gallate group is used to regulate the adhesion of human ECs and serum proteins to bioceramics.[135]

Moreover, natural biomaterial matrices have been applied as the basis for multifunctionality to enhance angiogenesis and selective endothelialization, as exemplified in the use of porous biodegradable adhesives made with hexanoyl group-modified gelatin,[136] silk heparin biomaterials,[137] and resilin-based hybrid hydrogels.[138] Using biomimicking nanofilaments and microstructured scaffolds, multi-scaled and multifunctional hybrid MSC constructs are produced, which enable vascularized adipose tissue engineering.[139] Another concept, based on a nitric oxide catalytic bioactive coating, which mimics the endothelium function, has been employed in multifunctional vascular stents to promote re-endothelialization and reduce restenosis of stents,[140] while an endothelium-mimicking matrix comprising peptide amphiphiles increases endothelialization, prevents inflammatory responses and promotes vasodilation.[141]

1.2.4.2 Tissue Engineered Cardiovascular Devices

Tissue engineered approaches for efficient cardiovascular devices such as heart valves and cardiac patches using multifunctional materials have been reported recently. Despite the recent advances in the development of functional living heart valves, a clinically viable product does not exist yet. The next step in engineering living heart valves requires a better insight into how natural multi-scale structural and biological heterogeneity ensures their function.[142] A blend of collagen (Type I), silk fibroin and the synthetic polymer poly(glycerol-sebacate) has been used to create multifunctional electrospun nanofibrous materials tailored for heart valve replacement.[128]

Embryonic stem cells have been extensively investigated in the production of human cardiomyocytes (CMs). Important recent advances for the clinical translation of this approach have pursued the cardiac differentiation of

the stem cells at high yield without any genetic modifications. Functional, mature cardiomyocytes that are able to support fast action, conduction and high contractile stresses have been developed. As an example, a tissue engineered cardiac patch that can induce the functional maturation of human ESC-derived cardiomyocytes has been described.[143] Moreover, functional cardiac patches have been engineered from carbon-nanotube-embedded photo-cross-linkable gelatin methacrylate sheets,[144] or collagen covalently linked with VEGF,[145] while Thai silk fibroin and gelatin hydrogels functionalized with simvastatin have been used for a vascular patch.[146] Integration of soft and rigid components such as PEG diacrylate and PCL by a novel bioprinting method has shown great potential for the formation of functional hybrid tissue engineering constructs.[147]

1.2.5 Neural Tissue Engineering

Neural tissue engineering is an emerging field for the treatment of various disorders of the central nervous system (CNS), which includes the brain and the spinal cord, degenerative diseases, and traumatic injuries of the peripheral nerves. Due to the limited regenerative potential of the CNS, there is an unmet need for efficient strategies to replace the damaged neural tissues. To this end, reliable methodologies and systems with multifunctional capabilities that control the guidance of neural tissue formation, the efficient delivery of soluble molecules and the differentiation of neural stem cells are essential (Figure 1.9).[148,149]

Stem-cell-based approaches have shown great promise towards the repair of destroyed neural tissue. Nanoparticulate carriers allow the effective release of biochemical cues to regulate neural differentiation, and offer multifunctional capabilities for delivery, imaging and therapy,[150] while a multifunctional nanocomplex has been reported that simultaneously induces the self-activation of the mRNA sequential expression and allows spatiotemporal imaging of the differentiation of the neural stem cells.[151]

Patterning of multifunctional biomaterials to direct neural precursor cells in a tunable system can provide a unique tool for the investigation of cells in niche-like environments. In this direction, hydrogel-based scaffolds such as heparin and PEG-peptide conjugates,[152] alginate constructs for growth factor delivery,[153] injectable PNIPAAm-PEG for the release of neurotrophins,[154] a poly(ethyl acrylate-*co*-2-hydroxyethyl acrylate) copolymer combined with an injectable self-assembling polypeptide (RAD16-I),[155] multifunctional conducting polymer nanoparticles,[156] elastin-like protein hydrogels,[157] colloidal particles formed by a 'click' reaction of bisepoxide and polyetheramine comonomers,[158] offer useful platforms that can act as guidance conduits and promote neurostimulation. Additionally, thiol-functionalized reduced graphene oxide with poly(methacrylic acid) microcapsules integrate surface topography and electrical stimulation for 3-D neuron-like cell growth,[159] whereas nanoporous gold can affect the surface topography and achieve close physical coupling of the neurons.[160] For the sustained delivery of biochemical cues, electrospun biodegradable PCL-*co*-poly(ethyl ethylene phosphate) copolymer

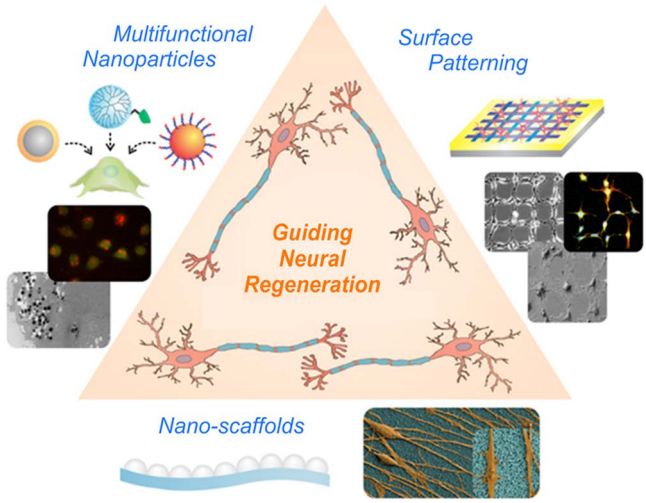

Figure 1.9 Nanotechnology-based approaches to direct stem-cell-based neural regeneration: multifunctional nanoparticles deliver bioactive molecules that promote cell differentiation, patterned surfaces with immobilized extracellular matrix (ECM) proteins and/or nanomaterials direct neuronal growth and polarization and 3-D nanoscaffolds support gene delivery, axonal alignment, and cell differentiation. Adapted with permission from ref. 149. Copyright (2016) American Chemical Society.

fibers[161] to mediate the release of retinoic acid and brain-derived neurotrophic factor[162] have been reported. Moreover, carbon nanotube composites[163] have been employed as multifunctional substrates for the differentiation of human neural stem cells, and soft carbon nanotube fiber microelectrodes for the safe stimulation and recording of neural activity.[164]

Multifunctional fibers enabling the simultaneous optical, electrical and chemical stimulation of neural circuits have been developed using a thermal drawing process,[165] and were assembled into synthetic nerve guidance scaffolds that can replace nerve autografts to repair damaged tissue following peripheral nerve injury.[166] Fiber reinforced conductive polymer composites,[167] as well as lysinated molecular organic semiconductors, are innovative materials offering optoelectronic functionalities with improved biocompatibility and bidirectional communication of neural cells.[168] Finally, scaffolds with metal-ion binding agents can provide multiple targets as therapeutic agents in neurodegenerative diseases.[169]

1.3 Clinical Potential and Applications of Multifunctional Scaffolds in Tissue Engineering

Over the last few years, increased research effort has been undertaken to develop multifunctional smart 3-D biomaterial scaffolds, containing signaling elements and active molecules for tissue engineering applications.

The ability of these scaffolds to promote tissue growth and regeneration has been investigated mainly *in vitro* and *in vivo* using different animal models. The translation of the developed technology and acquired knowledge to clinical trials in human patients is not straightforward and requires the appropriate regulation of numerous issues that will guarantee the safe and efficient application of the technology in humans.[170,171]

The use of multifunctional engineered constructs in clinical trials in humans is still in its infancy and studies demonstrating the potential of these scaffolds in this area are scarce. Current clinical studies use biomaterial scaffolds mainly in the fields of skin, blood vessel, cardiac, bone, cartilage and dental regeneration and in tracheal reconstruction.[170] Clinical applications for some bio-based tissue engineering scaffolds, bioactive proteins, and a reservoir of various growth factors (*i.e.* rhBMP-2, rhBMP-7, PRP) as well as drugs (*i.e.* gentamicin) and various cell types have been approved.[87,172–176]

Most of the clinical trials in bone and cartilage tissue engineering utilize a bio-based scaffold combined with an appropriate cell type. For example, a HA scaffold seeded with MSCs has been used to fill human bone defects,[177] whereas hyaluronan, collagen and alginate scaffolds combined with autologous chondrocytes have been applied for the treatment of chondral injury.[172,178] There are also very few studies reporting the use of growth factors on an engineered construct to produce a functional scaffold. These mainly involve the incorporation of rhBMP-2 in β-TCP granular scaffolds seeded with ASCs for the reconstruction of maxillary and mandibular bone[179–182] and the combination of β-TCP granular scaffolds with BMSCs and a PRP gel for the treatment of an anterior mandibular defect and alveolar bone atrophy.[183] Furthermore, BMP-2 and BMP-7 have been introduced in collagen sponges for the treatment of multiple bone defects,[184] β-TCP particles containing PDGF-BB have been applied for the therapy of bone defects caused by periodontal diseases[185] and PDFG/IGF combined with a methylcellulose gel vehicle has been employed for periodontal regeneration.[186] In other related studies, an injectable gel of thrombin-calcium chloride with BMSCs and PRP has promoted bone regeneration in dental implants,[187] and a microscaffold consisting of calcium phosphate cement (CPC) and rhBMP-2 has induced bone regeneration.[188]

Clinical trials in skin tissue engineering use different cell types with engineered constructs. For example, a collagen sponge scaffold combined with ASCs covered by an artificial dermis can be used to treat knee injuries[179] and an engineered construct consisting of a layer of keratinocytes and a layer of collagen-containing fibroblast is employed in the treatment of foot and venous leg ulcers.[170] Functionalized scaffolds are also used in the treatment of skin injuries. Multi-layers of electrospun fibers serve as patches that are able to control the release of nitric oxide in the treatment of the foot ulcers of diabetes patients and for the therapy of cutaneous leishmaniasis.[189–191] Furthermore, clinical studies have shown an enhancement of the wound healing rate of burn wounds and diabetes ulcers using bFGF, keratinocyte growth factor (KGF) and PDGF.[86,87,192–194]

In cardiovascular interventions, the need to treat restenosis following stent implantation has led to the use of drug-eluting stents (DES) made of metallic or biodegradable polymeric materials[195] coated with anti-proliferative and anti-inflammatory agents that are eluted slowly and reduce neointimal formation.[108] Although preliminary studies in humans applying two anti-proliferative agents, paclitaxel[196] and sirolimus (rapamycin) that inhibit SMCs growth,[197] have been reported with promising results, recent studies have shown that DES can lead to late stent thrombosis and thus result in long-term failure. This has occurred when stenting complex lesions, due to localized allergic reactions at the vessel wall that led to chronic inflammation.[198] An additional deterioration can occur by the release of the anti-proliferative drugs sirolimus and paclitaxel, which not only effect SMCs, but also ECs, and in this way impair the wound healing process.[199] The use of covered stents as a treatment option in various vascular complications, as well as the design and materials employed in the stents' manufacturing process, including nanotechnology approaches, have recently been reviewed.[199] Recent developments in vascular conduits based on the advances in tissue engineering, which are expected to function like real blood vessels with an intact endothelial layer and respond to endogenous vasoactive signals when implanted in clinical applications, are gaining increasing interest for vascular regeneration.[200]

Peripheral nerve reconstruction of gaps in clinical applications utilizes nerve autografts as the gold standard, although they do possess many shortcomings. To improve the outcome, various strategies using collagen, poly(glycolic acid), poly (DL-lactide-ε-caprolactone) and decellularized nerve allografts have been reported in several clinical studies and were reviewed recently by Gerth *et al.*[201] Advances in multifunctional approaches, employing conduits seeded with stem cells and providing local delivery of growth factors and neurotropic factors into the lumen of the engineered conduits, have been described to improve nerve regeneration in several recent reports.[202–205] Moreover, a recent multicenter clinical study using a human acellular nerve graft as an alternative to an autogenous nerve has reported on its safety and efficacy for the repair of nerve defects between 1 and 5 cm in size.[206]

Advances in biology related to the understanding of the fundamental mechanisms underlying the regeneration of different tissues has instructed the choice of cell types and their combination in a tissue engineered approach. On the other hand, great progress has been made in the field of 3-D scaffold fabrication and the methodologies for their surface chemical modification enabling the incorporation of appropriate signaling and pharmaceutical molecules and their controlled release as well as the expression of specific markers to elicit favorable cell responses leading to tissue repair. The combination of the above knowledge and expertise is expected to dramatically change clinical therapies in human patients in the upcoming years.

1.4 Conclusions

Progress in the applications of smart materials and multifunctional scaffolds in tissue engineering has been great over the last decade. The sustained, sequential and controlled release of multiple chemical and biochemical cues have been tackled and surface engineering in terms of physicochemical properties and topography has been addressed. However, there are still critical aspects and challenges to be overcome before the above results can be transferred to the clinic.

In bone tissue engineering, the challenge is to develop smart multifunctional scaffolds presenting multiple cues and mimicking the functions of the natural ECM environment of bone to promote therapeutic drug delivery and vascularized bone tissue regeneration. Muscle tissue engineering is still in its infancy, due to the peculiar organization of the skeletal muscle, which requires smart scaffolds with multiple functions that will provide the appropriate mechanical and bioactive cues for the cells to adhere, proliferate, form networks and replace the dysfunctional tissue. Electrical stimulation of the scaffolds, in a manner to replicate the natural impulses of the muscles from the neural system, needs particular consideration.

In skin tissue engineering, multicomponent structured materials that can regenerate the complex and hierarchical three-layered structure of skin are important. A key factor in achieving a fully functional skin is to establish constructs that will restore its normal connections with the surrounding nerve and muscle tissues once transplanted into living organisms. In cardiac tissue engineering, the development of multifunctional scaffolds with micro-environmental cues can promote the functional maturity of cardiomyocytes, while appropriate multifunctional materials and approaches that eliminate the inflammation and thrombogenicity of intravascular implants are essential. In neural tissue engineering, multifunctional materials are needed for the sustained delivery of biochemical cues, the synergistic topographical signaling and the design of nerve guidance channels with the capability to stimulate topographic, chemotactic and haptotactic signals that will induce functional nerve regeneration, and increase the axon growth rate.

References

1. F. Relaix and P. S. Zammit, *Development*, 2012, **139**, 2845.
2. A. S. Brack and T. A. Rando, *Cell Stem Cell*, 2012, **10**, 504.
3. S. Kuang, M. A. Gillespie and M. A. Rudnicki, *Cell Stem Cell*, 2008, **2**, 22.
4. T. H. Qazi, D. J. Mooney, M. Pumberger, S. Geißler and G. N. Duda, *Biomaterials*, 2015, **53**, 502.
5. V. P. Torchilin, *Nat. Rev. Drug Discovery*, 2014, **13**, 813.
6. A. J. Salinas, P. Esbrit and M. Vallet-Regi, *Biomater. Sci.*, 2013, **1**, 40.
7. T. A. Einhorn and L. C. Gerstenfeld, *Nat. Rev. Rheumatol.*, 2015, **11**, 45.
8. C. Maes, G. Carmeliet and E. Schipani, *Nat. Rev. Rheumatol.*, 2012, **8**, 358.

9. M. A. Fernandez-Yague, S. A. Abbah, L. McNamara, D. I. Zeugolis, A. Pandit and M. J. Biggs, *Adv. Drug Delivery Rev.*, 2015, **84**, 1.
10. M. M. Stevens, *Mater. Today*, 2008, **11**, 18.
11. J. E. Samorezov and E. Alsberg, *Adv. Drug Delivery Rev.*, 2015, **84**, 45.
12. Y.-H. Kim and Y. Tabata, *Adv. Drug Delivery Rev.*, 2015, **94**, 28.
13. Y. J. Yang, Y. Kwon, B.-H. Choi, D. Jung, J. H. Seo, K. H. Lee and H. J. Cha, *Biomacromolecules*, 2014, **15**, 1390.
14. J.-E. Won, Y.-R. Yun, J.-H. Jang, S.-H. Yang, J.-H. Kim, W. Chrzanowski, I. B. Wall, J. C. Knowles and H.-W. Kim, *Biomaterials*, 2015, **56**, 46.
15. Y. Robinson, C. E. Heyde, S. K. Tschöke, M. A. Mont, T. M. Seyler and S. D. Ulrich, *Expert Rev. Med. Devices*, 2008, **5**, 75.
16. O. Jeon, S. J. Song, H. S. Yang, S.-H. Bhang, S.-W. Kang, M. A. Sung, J. H. Lee and B.-S. Kim, *Biochem. Biophys. Res. Commun.*, 2008, **369**, 774.
17. A. E. Mercado, J. Ma, X. He and E. Jabbari, *J. Controlled Release*, 2009, **140**, 148.
18. Y. Zhao, J. Zhang, X. Wang, B. Chen, Z. Xiao, C. Shi, Z. Wei, X. Hou, Q. Wang and J. Dai, *J. Controlled Release*, 2010, **141**, 30.
19. T. Re'em, O. Tsur-Gang and S. Cohen, *Biomaterials*, 2010, **31**, 6746.
20. K. Tachi, M. Takami, H. Sato, A. Mochizuki, B. Zhao, Y. Miyamoto, H. Tsukasaki, T. Inoue, S. Shintani, T. Koike, Y. Honda, O. Suzuki, K. Baba and R. Kamijo, *Tissue Eng., Part A*, 2010, **17**, 597.
21. H. Kohara and Y. Tabata, *Biomaterials*, 2011, **32**, 5726.
22. J. Ratanavaraporn, H. Furuya, H. Kohara and Y. Tabata, *Biomaterials*, 2011, **32**, 2797.
23. V. Sordi, M. L. Malosio, F. Marchesi, A. Mercalli, R. Melzi, T. Giordano, N. Belmonte, G. Ferrari, B. E. Leone, F. Bertuzzi, G. Zerbini, P. Allavena, E. Bonifacio and L. Piemonti, *Blood*, 2005, **106**, 419.
24. A. Peled, I. Petit, O. Kollet, M. Magid, T. Ponomaryov, T. Byk, A. Nagler, H. Ben-Hur, A. Many, L. Shultz, O. Lider, R. Alon, D. Zipori and T. Lapidot, *Science*, 1999, **283**, 845.
25. V. E. Santo, M. E. Gomes, J. F. Mano and R. L. Reis, *J. Tissue Eng. Regener. Med.*, 2012, **6**, s47.
26. L. A. Lee, S. M. Muhammad, Q. L. Nguyen, P. Sitasuwan, G. Horvath and Q. Wang, *Mol. Pharm.*, 2012, **9**, 2121.
27. G. Gulseren, I. C. Yasa, O. Ustahuseyin, E. D. Tekin, A. B. Tekinay and M. O. Guler, *Biomacromolecules*, 2015, **16**, 2198.
28. S. S. Lee, E. L. Hsu, M. Mendoza, J. Ghodasra, M. S. Nickoli, A. Ashtekar, M. Polavarapu, J. Babu, R. M. Riaz, J. D. Nicolas, D. Nelson, S. Z. Hashmi, S. R. Kaltz, J. S. Earhart, B. R. Merk, J. S. McKee, S. F. Bairstow, R. N. Shah, W. K. Hsu and S. I. Stupp, *Adv. Healthcare Mater.*, 2015, **4**, 131.
29. V. E. Santo, A. M. Frias, M. Carida, R. Cancedda, M. E. Gomes, J. F. Mano and R. L. Reis, *Biomacromolecules*, 2009, **10**, 1392.
30. P. Yilgor, R. A. Sousa, R. L. Reis, N. Hasirci and V. Hasirci, *J. Mater. Sci.: Mater. Med.*, 2010, **21**, 2999.
31. N. Monteiro, D. Ribeiro, A. Martins, S. Faria, N. A. Fonseca, J. N. Moreira, R. L. Reis and N. M. Neves, *ACS Nano*, 2014, **8**, 8082.

32. N. J. Shah, M. L. Macdonald, Y. M. Beben, R. F. Padera, R. E. Samuel and P. T. Hammond, *Biomaterials*, 2011, **32**, 6183.
33. L. Li, J. R. Klim, R. Derda, A. H. Courtney and L. L. Kiessling, *Proc. Natl. Acad. Sci.*, 2011, **108**, 11745.
34. S.-E. Kim, J. D. Wallat, E. C. Harker, A. A. Advincula and J. K. Pokorski, *Polym. Chem.*, 2015, **6**, 5683.
35. H. Cui, Y. Wang, L. Cui, P. Zhang, X. Wang, Y. Wei and X. Chen, *Biomacromolecules*, 2014, **15**, 3146.
36. M. Bao, X. Lou, Q. Zhou, W. Dong, H. Yuan and Y. Zhang, *ACS Appl. Mater. Interfaces*, 2014, **6**, 2611.
37. J. C. Wenke and S. A. Guelcher, *Expert Opin. Drug Delivery*, 2011, **8**, 1555.
38. A. Clark, T. A. Milbrandt, J. Z. Hilt and D. A. Puleo, *Acta Biomater.*, 2014, **10**, 2125.
39. D. Dyondi, T. J. Webster and R. Banerjee, *Int. J. Nanomed.*, 2013, **8**, 47.
40. J. Min, K. Y. Choi, E. C. Dreaden, R. F. Padera, R. D. Braatz, M. Spector and P. T. Hammond, *ACS Nano*, 2016, **10**, 4441.
41. S. A. Guelcher, K. V. Brown, B. Li, T. Guda, B.-H. Lee and J. C. Wenke, *J. Orthop. Trauma*, 2011, **25**, 477.
42. R. L. Stewart, J. T. Cox, D. Volgas, J. Stannard, L. Duffy, K. B. Waites and T.-M. Chu, *J. Orthop. Trauma*, 2010, **24**, 587.
43. Z. Zheng, W. Yin, J. N. Zara, W. Li, J. Kwak, R. Mamidi, M. Lee, R. K. Siu, R. Ngo, J. Wang, D. Carpenter, X. Zhang, B. Wu, K. Ting and C. Soo, *Biomaterials*, 2010, **31**, 9293.
44. C. Wu and J. Chang, *J. Controlled Release*, 2014, **193**, 282.
45. A. Hoppe, N. S. Güldal and A. R. Boccaccini, *Biomaterials*, 2011, **32**, 2757.
46. C. Dai, H. Guo, J. Lu, J. Shi, J. Wei and C. Liu, *Biomaterials*, 2011, **32**, 8506.
47. L. Xia, D. Zeng, X. Sun, Y. Xu, L. Xu, D. Ye, X. Zhang, X. Jiang and Z. Zhang, *Microporous Mesoporous Mater.*, 2013, **173**, 155.
48. R. A. Perez, A. El-Fiqi, J. H. Park, T. H. Kim, J. H. Kim and H. W. Kim, *Acta Biomater.*, 2014, **10**, 520.
49. D. Suárez-González, J. S. Lee, A. Diggs, Y. Lu, B. Nemke, M. Markel, S. J. Hollister and W. L. Murphy, *Tissue Eng., Part A*, 2014, **20**, 2077.
50. C. Wu, Y. Zhou, J. Chang and Y. Xiao, *Acta Biomater.*, 2013, **9**, 9159.
51. P. Alessandro, I. Daniela, P. Silvia, M. Monica, T. Anna and G. Signorino, *Nanotechnology*, 2014, **25**, 425701.
52. S. Nomura and T. Takano-Yamamoto, *Matrix Biol.*, 2000, **19**, 91.
53. C. F. Marques, A. Lemos, S. I. Vieira, O. A. B. da Cruz e Silva, A. Bettencourt and J. M. F. Ferreira, *Ceram. Int.*, 2016, **42**, 2706.
54. C. Wu, Y. Zhou, W. Fan, P. Han, J. Chang, J. Yuen, M. Zhang and Y. Xiao, *Biomaterials*, 2012, **33**, 2076.
55. C. Wu, Y. Zhou, M. Xu, P. Han, L. Chen, J. Chang and Y. Xiao, *Biomaterials*, 2013, **34**, 422.
56. G. Fielding and S. Bose, *Acta Biomater.*, 2013, **9**, 9137.
57. M. S. Kang, J.-H. Kim, R. K. Singh, J.-H. Jang and H.-W. Kim, *Acta Biomater.*, 2015, **16**, 103.

58. B. De la Riva, E. Sánchez, A. Hernández, R. Reyes, F. Tamimi, E. López-Cabarcos, A. Delgado and C. Évora, *J. Controlled Release*, 2010, **143**, 45.
59. J. S. Son, M. Appleford, J. L. Ong, J. C. Wenke, J. M. Kim, S. H. Choi and D. S. Oh, *J. Controlled Release*, 2011, **153**, 133.
60. H. Wu, Y. Xu, G. Liu, J. Ling, B. C. Dash, J. Ruan and C. Zhang, *J. Mater. Sci.: Mater. Med.*, 2014, **25**, 2649.
61. X.-L. Wang, X.-H. Xie, G. Zhang, S.-H. Chen, D. Yao, K. He, X.-H. Wang, X.-S. Yao, Y. Leng, K.-P. Fung, K.-S. Leung and L. Qin, *J. Orthop. Res.*, 2013, **31**, 164.
62. L. Francis, D. Meng, J. C. Knowles, I. Roy and A. R. Boccaccini, *Acta Biomater.*, 2010, **6**, 2773.
63. W. Song, W. Ren, C. Wan, A. O. Esquivel, T. Shi, R. Blasier and D. C. Markel, *J. Biomed. Mater. Res., Part A*, 2011, **98A**, 359.
64. C. M. Murphy, A. Schindeler, J. P. Gleeson, N. Y. C. Yu, L. C. Cantrill, K. Mikulec, L. Peacock, F. J. O'Brien and D. G. Little, *Acta Biomater.*, 2014, **10**, 2250.
65. Y. Zhang, N. Cheng, R. Miron, B. Shi and X. Cheng, *Biomaterials*, 2012, **33**, 6698.
66. J. Su, H. Xu, J. Sun, X. Gong and H. Zhao, *Int. J. Mol. Sci.*, 2013, **14**, 12714.
67. J. Olmos Buitrago, R. A. Perez, A. El-Fiqi, R. K. Singh, J.-H. Kim and H.-W. Kim, *Acta Biomater.*, 2015, **28**, 183.
68. H. Pan, Q. Zheng, S. Yang and X. Guo, *J. Biomed. Mater. Res., Part A*, 2014, **102**, 4526.
69. P. Zhang, H. Wu, H. Wu, Z. Lù, C. Deng, Z. Hong, X. Jing and X. Chen, *Biomacromolecules*, 2011, **12**, 2667.
70. X. Liu, K. Zhao, T. Gong, J. Song, C. Bao, E. Luo, J. Weng and S. Zhou, *Biomacromolecules*, 2014, **15**, 1019.
71. J. R. Xavier, T. Thakur, P. Desai, M. K. Jaiswal, N. Sears, E. Cosgriff-Hernandez, R. Kaunas and A. K. Gaharwar, *ACS Nano*, 2015, **9**, 3109.
72. M. Fujioka-Kobayashi, M. S. Ota, A. Shimoda, K.-i. Nakahama, K. Akiyoshi, Y. Miyamoto and S. Iseki, *Biomaterials*, 2012, **33**, 7613.
73. D. H. Choi, C. H. Park, I. H. Kim, H. J. Chun, K. Park and D. K. Han, *J. Controlled Release*, 2010, **147**, 193.
74. Y. Su, Q. Su, W. Liu, M. Lim, J. R. Venugopal, X. Mo, S. Ramakrishna, S. S. Al-Deyab and M. El-Newehy, *Acta Biomater.*, 2012, **8**, 763.
75. L. Li, G. Zhou, Y. Wang, G. Yang, S. Ding and S. Zhou, *Biomaterials*, 2015, **37**, 218.
76. C. R. Correia, R. P. Pirraco, M. T. Cerqueira, A. P. Marques, R. L. Reis and J. F. Mano, *Sci. Rep.*, 2016, **6**, 21883.
77. C. Borselli, H. Storrie, F. Benesch-Lee, D. Shvartsman, C. Cezar, J. W. Lichtman, H. H. Vandenburgh and D. J. Mooney, *Proc. Natl. Acad. Sci.*, 2010, **107**, 3287.
78. C. Borselli, C. A. Cezar, D. Shvartsman, H. H. Vandenburgh and D. J. Mooney, *Biomaterials*, 2011, **32**, 8905.
79. M. Xie, L. Wang, J. Ge, B. Guo and P. X. Ma, *ACS Appl. Mater. Interfaces*, 2015, **7**, 6772.

80. M. R. Ladd, S. J. Lee, J. D. Stitzel, A. Atala and J. J. Yoo, *Biomaterials*, 2011, **32**, 1549.
81. S. J. Kim, H. R. Cho, K. W. Cho, S. Qiao, J. S. Rhim, M. Soh, T. Kim, M. K. Choi, C. Choi, I. Park, N. S. Hwang, T. Hyeon, S. H. Choi, N. Lu and D.-H. Kim, *ACS Nano*, 2015, **9**, 2677.
82. A. Ito, Y. Yamamoto, M. Sato, K. Ikeda, M. Yamamoto, H. Fujita, E. Nagamori, Y. Kawabe and M. Kamihira, *Sci. Rep.*, 2014, **4**, 4781.
83. A. J. Singer and R. A. F. Clark, *N. Engl. J. Med.*, 1999, **341**, 738.
84. P. Martin, *Science*, 1997, **276**, 75.
85. P. S. Korrapati, K. Karthikeyan, A. Satish, V. R. Krishnaswamy, J. R. Venugopal and S. Ramakrishna, *Mater. Sci. Eng., C*, 2016, **67**, 747.
86. L. Yildirimer, N. T. K. Thanh and A. M. Seifalian, *Trends Biotechnol.*, 2012, **30**, 638.
87. G. Gainza, S. Villullas, J. L. Pedraz, R. M. Hernandez and M. Igartua, *Nanomedicine*, 2015, **11**, 1551.
88. S. Huang and X. Fu, *J. Controlled Release*, 2010, **142**, 149.
89. Z. Xie, C. B. Paras, H. Weng, P. Punnakitikashem, L.-C. Su, K. Vu, L. Tang, J. Yang and K. T. Nguyen, *Acta Biomater.*, 2013, **9**, 9351.
90. M. P. Ribeiro, P. I. Morgado, S. P. Miguel, P. Coutinho and I. J. Correia, *Mater. Sci. Eng., C*, 2013, **33**, 2958.
91. O. Mirdailami, M. Soleimani, R. Dinarvand, M. R. Khoshayand, M. Norouzi, A. Hajarizadeh, M. Dodel and F. Atyabi, *J. Biomed. Mater. Res., Part A*, 2015, **103**, 3374.
92. H.-J. Lai, C.-H. Kuan, H.-C. Wu, J.-C. Tsai, T.-M. Chen, D.-J. Hsieh and T.-W. Wang, *Acta Biomater.*, 2014, **10**, 4156.
93. L. Formigli, S. Benvenuti, R. Mercatelli, F. Quercioli, A. Tani, C. Mirabella, A. Dama, R. Saccardi, B. Mazzanti, I. Cellai and S. Zecchi-Orlandini, *J. Tissue Eng. Regener. Med.*, 2012, **6**, 125.
94. P. Peh, N. S. J. Lim, A. Blocki, S. M. L. Chee, H. C. Park, S. Liao, C. Chan and M. Raghunath, *Bioconjugate Chem.*, 2015, **26**, 1348.
95. G. Jin, M. P. Prabhakaran, D. Kai and S. Ramakrishna, *Eur. J. Pharm. Biopharm.*, 2013, **85**, 689.
96. G. Ramanathan, S. Singaravelu, M. D. Raja, N. Nagiah, P. Padmapriya, K. Ruban, K. Kaveri, T. S. Natarajan, U. T. Sivagnanam and P. T. Perumal, *RSC Adv.*, 2016, **6**, 7914.
97. F. Wang, M. Wang, Z. She, K. Fan, C. Xu, B. Chu, C. Chen, S. Shi and R. Tan, *Mater. Sci. Eng., C*, 2015, **52**, 155.
98. S. Bhowmick, D. Scharnweber and V. Koul, *Biomaterials*, 2016, **88**, 83.
99. A. K. Reckhenrich, U. Hopfner, F. Krötz, Z. Zhang, C. Koch, M. Kremer, H.-G. Machens, C. Plank and J. T. Egaña, *Biomaterials*, 2011, **32**, 1996.
100. Y. Yang, T. Xia, F. Chen, W. Wei, C. Liu, S. He and X. Li, *Mol. Pharm.*, 2012, **9**, 48.
101. X. Liu, L. Ma, J. Liang, B. Zhang, J. Teng and C. Gao, *Biomaterials*, 2013, **34**, 2038.
102. K. B. Vartanian, S. J. Kirkpatrick, O. J. T. McCarty, T. Q. Vu, S. R. Hanson and M. T. Hinds, *J. Biomed. Mater. Res., Part A*, 2009, **91A**, 528.

103. S. Yuan, G. Xiong, F. He, W. Jiang, B. Liang and C. Choong, *J. Mater. Chem. B*, 2015, **3**, 8088.
104. M. B. Gorbet and M. V. Sefton, *Biomaterials*, 2004, **25**, 5681.
105. S. Sarkar, T. Schmitz-Rixen, G. Hamilton and A. M. Seifalian, *Med. Biol. Eng. Comput.*, 2007, **45**, 327.
106. J. Li, K. Zhang, J. Wu, L. Zhang, P. Yang, Q. Tu and N. Huang, *Colloids Surf., B*, 2015, **128**, 201.
107. Q. Lin, X. Ding, F. Qiu, X. Song, G. Fu and J. Ji, *Biomaterials*, 2010, **31**, 4017.
108. M. Zilberman and R. C. Eberhart, *Annu. Rev. Biomed. Eng.*, 2006, **8**, 153.
109. T. C. Woods and A. R. Marks, *Annu. Rev. Med.*, 2004, **55**, 169.
110. P. W. Serruys, M. J. B. Kutryk and A. T. L. Ong, *N. Engl. J. Med.*, 2006, **354**, 483.
111. Y. Yuan, C. Liu and M. Yin, *J. Mater. Sci.: Mater. Med.*, 2008, **19**, 2187.
112. Z. Yang, S. Zhong, Y. Yang, M. F. Maitz, X. Li, Q. Tu, P. Qi, H. Zhang, H. Qiu, J. Wang and N. Huang, *J. Mater. Chem. B*, 2014, **2**, 6767.
113. D. W. Losordo, J. M. Isner and L. J. Diaz-Sandoval, *Circulation*, 2003, **107**, 2635.
114. A. V. Finn, M. C. John, H. K. Gold, J. Newell, G. Nakazawa, M. Joner, F. D. Kolodgie and R. Virmani, *Circulation*, 2007, **116**, e550.
115. M. J. Eisenberg and K. J. Konnyu, *Am. J. Cardiol.*, 2006, **98**, 375.
116. N. A. Scott, *Adv. Drug Delivery Rev.*, 2006, **58**, 358.
117. R. Thipparaboina, W. Khan and A. J. Domb, *Int. J. Pharm.*, 2013, **454**, 4.
118. G. Li, P. Yang, X. Guo, N. Huang and R. Shen, *Cytokine*, 2011, **56**, 208.
119. J.-i. Koga and M. Aikawa, *Vasc. Pharmacol.*, 2012, **57**, 24.
120. Z. L. Yang, K. Q. Xiong, P. K. Qi, Y. Yang, Q. F. Tu, J. Wang and N. Huang, *ACS Appl. Mater. Interfaces*, 2014, **6**, 2647.
121. H. Ceylan, A. B. Tekinay and M. O. Guler, *Biomaterials*, 2011, **32**, 8797.
122. Y. Wei, Y. Ji, L. L. Xiao, Q. K. Lin, J. P. Xu, K. F. Ren and J. Ji, *Biomaterials*, 2013, **34**, 2588.
123. X. K. Ren, Y. K. Feng, J. T. Guo, H. X. Wang, Q. Li, J. Yang, X. F. Hao, J. Lv, N. Ma and W. Z. Li, *Chem. Soc. Rev.*, 2015, **44**, 5745.
124. L. Peng, M. L. Eltgroth, T. J. LaTempa, C. A. Grimes and T. A. Desai, *Biomaterials*, 2009, **30**, 1268.
125. L. Peng, A. J. Barczak, R. A. Barbeau, Y. Xiao, T. J. LaTempa, C. A. Grimes and T. A. Desai, *Nano Lett.*, 2010, **10**, 143.
126. Z. L. Yang, S. Zhong, Y. Yang, M. F. Maitz, X. Y. Li, Q. F. Tu, P. K. Qi, H. Zhang, H. Qiu, J. Wang and N. Huang, *J. Mater. Chem. B*, 2014, **2**, 6767.
127. F. Wu, J. Li, K. Zhang, Z. He, P. Yang, D. Zou and N. Huang, *ACS Appl. Mater. Interfaces*, 2016, **8**, 109.
128. J.-l. Wang, B.-c. Li, Z.-j. Li, K.-f. Ren, L.-j. Jin, S.-m. Zhang, H. Chang, Y.-x. Sun and J. Ji, *Biomaterials*, 2014, **35**, 7679.
129. Z. Chen, Q. Li, J. Chen, R. Luo, M. F. Maitz and N. Huang, *Mater. Sci. Eng., C*, 2016, **60**, 219.
130. E. Chung, L. M. Ricles, R. S. Stowers, S. Y. Nam, S. Y. Emelianov and L. J. Suggs, *Nano Today*, 2012, **7**, 514.

131. L.-C. Su, H. Xu, R. T. Tran, Y.-T. Tsai, L. Tang, S. Banerjee, J. Yang and K. T. Nguyen, *ACS Nano*, 2014, **8**, 10826.
132. S. Noel, C. Fortier, F. Murschel, A. Belzil, G. Gaudet, M. Jolicoeur and G. De Crescenzo, *Acta Biomater.*, 2016, **37**, 69.
133. A. Mayer, T. Roch, K. Kratz, A. Lendlein and F. Jung, *Acta Biomater.*, 2012, **8**, 4253.
134. T. Sauter, B. Geiger, K. Kratz and A. Lendlein, *Polym. Adv. Technol.*, 2015, **26**, 1209.
135. F. Borcard, D. Staedler, H. Comas, F. K. Juillerat, P. N. Sturzenegger, R. Heuberger, U. T. Gonzenbach, L. Juillerat-Jeanneret and S. Gerber-Lemaire, *J. Med. Chem.*, 2012, **55**, 7988.
136. K. Yoshizawa, R. Mizuta and T. Taguchi, *Biomaterials*, 2015, **63**, 14.
137. F. P. Seib, M. Herklotz, K. A. Burke, M. F. Maitz, C. Werner and D. L. Kaplan, *Biomaterials*, 2014, **35**, 83.
138. C. L. McGann, E. A. Levenson and K. L. Kiick, *Macromol. Chem. Phys.*, 2013, **214**, 203.
139. T. G. Kirn, S. H. Park, H. J. Chung, D. Y. Yang and T. G. Park, *Adv. Funct. Mater.*, 2010, **20**, 2303.
140. Z. L. Yang, Y. Yang, K. Q. Xiong, X. Y. Li, P. K. Qi, Q. F. Tu, F. J. Jing, Y. J. Weng, J. Wang and N. Huang, *Biomaterials*, 2015, **63**, 80.
141. G. C. Alexander, J. B. Vines, P. Hwang, T. Kim, J. A. Kim, B. C. Brott, Y. S. Yoon and H. W. Jun, *ACS Appl. Mater. Interfaces*, 2016, **8**, 5178.
142. D. Y. Cheung, B. Duan and J. T. Butcher, *Expert Opin. Biol. Ther.*, 2015, **15**, 1155.
143. H. Zhang, X. Jia, F. Han, J. Zhao, Y. Zhao, Y. Fan and X. Yuan, *Biomaterials*, 2013, **34**, 2202.
144. S. R. Shin, S. M. Jung, M. Zalabany, K. Kim, P. Zorlutuna, S. b. Kim, M. Nikkhah, M. Khabiry, M. Azize, J. Kong, K.-t. Wan, T. Palacios, M. R. Dokmeci, H. Bae, X. Tang and A. Khademhosseini, *ACS Nano*, 2013, **7**, 2369.
145. Y. Miyagi, L. L. Y. Chiu, M. Cimini, R. D. Weisel, M. Radisic and R.-K. Li, *Biomaterials*, 2011, **32**, 1280.
146. P. Thitiwuthikiat, M. Ii, T. Saito, M. Asahi, S. Kanokpanont and Y. Tabata, *Tissue Eng., Part A*, 2014, **21**, 1309.
147. Y. Shanjani, C. C. Pan, L. Elomaa and Y. Yang, *Biofabrication*, 2015, **7**, 045008.
148. V. Chiono and C. Tonda-Turo, *Prog. Neurobiol.*, 2015, **131**, 87.
149. S. Shah, A. Solanki and K.-B. Lee, *Acc. Chem. Res.*, 2016, **49**, 17.
150. M. L. Wegscheid, R. A. Morshed, Y. Cheng and M. S. Lesniak, *Expert Opin. Drug Delivery*, 2014, **11**, 957.
151. Z. Wang, R. L. Zhang, Z. L. Wang, H. F. Wang, Y. Wang, J. Zhao, F. Wang, W. T. Li, G. Niu, D. O. Kiesewetter and X. Y. Chen, *ACS Nano*, 2014, **8**, 12386.
152. M. V. Tsurkan, R. Wetzel, H. R. Perez-Hernandez, K. Chwalek, A. Kozlova, U. Freudenberg, G. Kempermann, Y. X. Zhang, A. F. Lasagni and C. Werner, *Adv. Healthcare Mater.*, 2015, **4**, 516.

153. M. S. Shanbhag, J. D. Lathia, M. R. Mughal, N. L. Francis, N. Pashos, M. P. Mattson and M. A. Wheatley, *Biomacromolecules*, 2010, **11**, 2936.
154. N. Comolli, B. Neuhuber, I. Fischer and A. Lowman, *Acta Biomater.*, 2009, **5**, 1046.
155. A. Conejero-Garcia, G. Vilarino-Feltrer, C. Martinez-Ramos, M. M. Pradas and A. Valles-Lluch, *Eur. Polym. J.*, 2015, **70**, 331.
156. D. Ho, J. L. Zou, X. J. Chen, A. Munshi, N. M. Smith, V. Agarwal, S. I. Hodgetts, G. W. Plant, A. J. Bakker, A. R. Harvey, I. Luzinov and K. S. Iyer, *ACS Nano*, 2015, **9**, 1767.
157. K. J. Lampe, A. L. Antaris and S. C. Heilshorn, *Acta Biomater.*, 2013, **9**, 5590.
158. E. A. Morin, S. C. Tang, K. L. Rogers and W. He, *ACS Appl. Mater. Interfaces*, 2016, **8**, 5737.
159. H. W. Liu, W. C. Huang, C. S. Chiang, S. H. Hu, C. H. Liao, Y. Y. Chen and S. Y. Chen, *Adv. Funct. Mater.*, 2014, **24**, 3715.
160. C. A. R. Chapman, H. Chen, M. Stamou, J. Biener, M. M. Biener, P. J. Lein and E. Seker, *ACS Appl. Mater. Interfaces*, 2015, **7**, 7093.
161. S. Y. Chew, J. Wen, E. K. F. Yim and K. W. Leong, *Biomacromolecules*, 2005, **6**, 2017.
162. W. C. Low, P. O. Rujitanaroj, F. Wang, J. Wang and S. Y. Chew, *Drug Delivery Transl. Res.*, 2015, **5**, 89.
163. J. Landers, J. T. Turner, G. Heden, A. L. Carlson, N. K. Bennett, P. V. Moghe and A. V. Neimark, *Adv. Healthcare Mater.*, 2014, **3**, 1745.
164. F. Vitale, S. R. Summerson, B. Aazhang, C. Kemere and M. Pasquali, *ACS Nano*, 2015, **9**, 4465.
165. A. Canales, X. T. Jia, U. P. Froriep, R. A. Koppes, C. M. Tringides, J. Selvidge, C. Lu, C. Hou, L. Wei, Y. Fink and P. Anikeeva, *Nat. Biotechnol.*, 2015, **33**, 277.
166. R. A. Koppes, S. Park, T. Hood, X. T. Jia, N. A. Poorheravi, A. H. Achyuta, Y. Fink and P. Anikeeva, *Biomaterials*, 2016, **81**, 27.
167. F. M. Al-Oqla, S. M. Sapuan, T. Anwer, M. Jawaid and M. E. Hogue, *Synth. Met*, 2015, **206**, 42.
168. S. Bonetti, A. Pistone, M. Brucale, S. Karges, L. Favaretto, M. Zambianchi, T. Posati, A. Sagnella, M. Caprini, S. Toffanin, R. Zamboni, N. Camaioni, M. Muccini, M. Melucci and V. Benfenati, *Adv. Healthcare Mater.*, 2015, **4**, 1190.
169. C. Rodriguez-Rodriguez, M. Telpoukhovskaia and C. Orvig, *Coord. Chem. Rev.*, 2012, **256**, 2308.
170. M. J. Webber, O. F. Khan, S. A. Sydlik, B. C. Tang and R. Langer, *Ann. Biomed. Eng.*, 2015, **43**, 641.
171. F. M. Wood, *Int. J. Biochem. Cell Biol.*, 2014, **56**, 133.
172. S. J. Roberts, D. Howard, L. D. Buttery and K. M. Shakesheff, *Br. Med. Bull.*, 2008, **86**, 7.
173. W. L. Stoppel, C. E. Ghezzi, S. L. McNamara, L. D. Black III and D. L. Kaplan, *Ann. Biomed. Eng.*, 2015, **43**, 657.
174. E. Nyberg, C. Holmes, T. Witham and W. L. Grayson, *Drug Delivery Transl. Res.*, 2016, **6**, 184.

175. B. M. Holzapfel, J. C. Reichert, J.-T. Schantz, U. Gbureck, L. Rackwitz, U. Nöth, F. Jakob, M. Rudert, J. Groll and D. W. Hutmacher, *Adv. Drug Delivery Rev.*, 2013, **65**, 581.
176. S. MacNeil, *Mater. Today*, 2008, **11**, 26.
177. T. Morishita, K. Honoki, H. Ohgushi, N. Kotobuki, A. Matsushima and Y. Takakura, *Artif. Organs*, 2006, **30**, 115.
178. B. J. Huang, J. C. Hu and K. A. Athanasiou, *Biomaterials*, 2016, **98**, 1.
179. Y. He and F. Lu, *Stem Cells Int.*, 2016, **2016**, 5786257.
180. K. Mesimaki, B. Lindroos, J. Tornwall, J. Mauno, C. Lindqvist, R. Kontio, S. Miettinen and R. Suuronen, *Int. J. Oral Maxillofac. Surg.*, 2009, **38**, 201.
181. G. K. B. Sándor, *Ann. Maxillofac. Surg.*, 2012, **2**, 8.
182. G. K. Sandor, V. J. Tuovinen, J. Wolff, M. Patrikoski, J. Jokinen, E. Nieminen, B. Mannerstrom, O. P. Lappalainen, R. Seppanen and S. Miettinen, *J. Oral Maxillofac. Surg.*, 2013, **71**, 938.
183. H. Kagami, H. Agata, M. Inoue, I. Asahina, A. Tojo, N. Yamashita and K. Imai, *Tissue Eng., Part B*, 2014, **20**, 229.
184. K. L. Spiller and G. Vunjak-Novakovic, *Drug Delivery Transl. Res.*, 2015, **5**, 101.
185. M. Nevins, R. T. Kao, M. K. McGuire, P. K. McClain, J. E. Hinrichs, B. S. McAllister, M. S. Reddy, M. L. Nevins, R. J. Genco, S. E. Lynch and W. V. Giannobile, *J. Periodontol.*, 2012, **84**, 456.
186. T. H. Howell, J. P. Fiorellini, D. W. Paquette, S. Offenbacher, W. V. Giannobile and S. E. Lynch, *J. Periodontol.*, 1997, **68**, 1186.
187. Y. Yamada, S. Nakamura, K. Ito, T. Kohgo, H. Hibi, T. Nagasaka and M. Ueda, *Tissue Eng., Part A*, 2008, **14**, 1699.
188. D. Lin, J. Zhang, F. Bai, X. Cao, C. Fan, Y. Yuan, J. Wang, J. Zhang and C. Liu, *Am. J. Transl. Res.*, 2016, **8**, 1379.
189. L. E. Sperling, K. P. Reis, P. Pranke and J. H. Wendorff, *Drug Discovery Today*, 2016, **21**, 1243.
190. S. Y. Silva, L. C. Rueda, M. López, I. D. Vélez, C. F. Rueda-Clausen, D. J. Smith, G. Muñoz, H. Mosquera, F. A. Silva, A. Buitrago, H. Díaz and P. López-Jaramillo, *Trials*, 2006, **7**, 1.
191. S. Y. Silva, L. C. Rueda, G. A. Márquez, M. López, D. J. Smith, C. A. Calderón, J. C. Castillo, J. Matute, C. F. Rueda-Clausen, A. Orduz, F. A. Silva, P. Kampeerapappun, M. Bhide and P. López-Jaramillo, *Trials*, 2007, **8**, 26.
192. S. Akita, K. Akino, T. Imaizumi, K. Tanaka, K. Anraku, H. Yano and A. Hirano, *J. Burn Care Res.*, 2006, **27**, 333.
193. S. Akita, K. Akino, T. Imaizumi and A. Hirano, *Wound Repair Regen.*, 2008, **16**, 635.
194. E. B. Goudie, C. Gendics and J. C. Lantis, *Int. Wound J.*, 2012, **9**, 132.
195. C. V. Bourantas, Y. Onuma, V. Farooq, Y. Zhang, H. M. Garcia-Garcia and P. W. Serruys, *Int. J. Cardiol.*, 2013, **167**, 11.
196. F. Liistro, G. Stankovic, C. Di Mario, T. Takagi, A. Chieffo, S. Moshiri, M. Montorfano, M. Carlino, C. Briguori, P. Pagnotta, R. Albiero, N. Corvaja and A. Colombo, *Circulation*, 2002, **105**, 1883.

197. M. Degertekin, P. W. Serruys, D. P. Foley, K. Tanabe, E. Regar, J. Vos, P. C. Smits, W. J. van der Giessen, M. van den Brand, P. de Feyter and J. J. Popma, *Circulation*, 2002, **106**, 1610.
198. P. S. Teirstein, *Circulation*, 2010, **122**, 5.
199. Y. Farhatnia, A. Tan, A. Motiwala, B. G. Cousins and A. M. Seifalian, *Biotechnol. Adv.*, 2013, **31**, 524.
200. E. Benrashid, C. C. McCoy, L. M. Youngwirth, J. Kim, R. J. Manson, J. C. Otto and J. H. Lawson, *Methods*, 2016, **99**, 13.
201. D. J. Gerth, J. Tashiro and S. R. Thaller, *World J. Clin. Cases*, 2015, **3**, 141.
202. W. C. Chang, E. Hawkes, C. G. Keller and D. W. Sretavan, *Wiley Interdiscip. Rev. Nanomed. Nanobiotechnol.*, 2010, **2**, 151.
203. M. C. O. Rodrigues, A. A. Rodrigues, L. E. Glover, J. Voltarelli and C. V. Borlongan, *Sci. World J.*, 2012, **2012**, 10.
204. W. Daly, L. Yao, D. Zeugolis, A. Windebank and A. Pandit, *J. R. Soc., Interface*, 2012, **9**, 202.
205. S. Sivolella, G. Brunello, N. Ferrarese, A. D. Puppa, D. D'Avella, E. Bressan and B. Zavan, *Int. J. Mol. Sci.*, 2014, **15**, 3088.
206. B. He, Q. Zhu, Y. Chai, X. Ding, J. Tang, L. Gu, J. Xiang, Y. Yang, J. Zhu and X. Liu, *J. Tissue Eng. Regener. Med.*, 2015, **9**, 286.

CHAPTER 2

Translational Smart Materials in Tissue Engineering

C. PINEDA MOLINA[a,b] AND S. F. BADYLAK*[a,b,c]

[a]University of Pittsburgh, McGowan Institute for Regenerative Medicine, 450 Technology Drive, Suite 300, Pittsburgh, 15219, USA; [b]University of Pittsburgh, Department of Bioengineering, 450 Technology Drive, Suite 300, Pittsburgh, 15219, USA; [c]University of Pittsburgh, Department of Surgery, 450 Technology Drive, Suite 300, Pittsburgh, 15219, USA
*E-mail: badylaks@upmc.edu

2.1 Introduction

Tissue engineering/regenerative medicine can be defined as an interdisciplinary approach to the development of functional substitutes for injured or missing tissues and organs.[1] The fundamental building blocks of such efforts include cells, scaffolds/substrates, and cell signaling molecules. The lion's share of attention has been focused upon the use of stem/progenitor cells, but successful examples of scaffold-based approaches and bioactive-molecule-based approaches also exist.[2] Almost uniformly, cell-based approaches, including the use of stem cells, have either failed or provided only incremental advancements in clinical outcomes. The primary reason for these disappointing results has been poor survival of cells following transplantation to the site of interest.[3] The consensus explanation for poor cell survival has been the lack of an appropriate microenvironment for cell

Smart Materials No. 25
Smart Materials for Tissue Engineering: Applications
Edited by Qun Wang

Published by the Royal Society of Chemistry, www.rsc.org

attachment, homeostasis, proliferation, and differentiation. Therefore, the focus of scaffold-based approaches has centered around the development of "cell friendly" biomaterials that can promote appropriate cell behavior, including assembly into functional tissues/organs. To this end, both synthetic and biologic materials have been developed as "smart materials" that attempt to mimic the naturally occurring microenvironmental niche.[4,5] The present chapter provides an overview of attempts to create synthetic and naturally occurring biomaterials, and describes some core concepts around which future attempts may be based.

2.2 Considerations of Smart Materials in Tissue Engineering

2.2.1 Biocompatibility

The ultimate determinant of success (or failure) of a biomaterial is the host response to the material following implantation.[6] The host response is intimately linked to the current understanding/definition of biocompatibility, which can be expressed in terms of tissue-specific functionality and bioactivity.[7,8] Although biocompatibility does not necessarily imply a responsive smart biomaterial as defined in this textbook, smart biomaterials, by definition, focus upon structure–function relationships and would logically be biocompatible.

2.2.2 Structure

The ultrastructure of biomaterials has been a matter of interest and change in the field of tissue engineering. Porous and interconnected structures impart stability and integration with surrounding tissue. Advances in manufacturing techniques have facilitated the production of highly porous materials; *e.g.*, electrospinning, particle leaching, and gas foaming, among others, to produce fibrous and non-fibrous structures that attempt to facilitate the trafficking of cells.[9] Although porosity promotes cell infiltration, additional factors that influence cell behavior must be considered. For example, mechanotransduction signaling pathways are directly related to material stiffness. The combined effects of all structural and material properties influence cell adherence, proliferation, migration, and differentiation. Such factors add to the complexity of smart biomaterials' design and production.[10]

With the understanding that characteristics of materials affect subcellular events, which in turn influence the overall function at the tissue level,[11] new approaches in "hierarchical porosity" are being investigated. Hierarchical porous scaffolds are formed by the combination of pores ranging from nm scale to mm scale.[12] These complex structures provide stability *via* the macroporous component, and unhindered migration and attachment of cells and

biomolecules to the abundant surface area provided by the microporous components. Furthermore, surface modifications at the nanostructure level can imitate active domains of ECM molecules,[5] and facilitate cell–material interactions with subsequent modulation of subcellular components to direct cell fate.[13] Stated differently, although structural considerations are important and useful, they cannot be divorced from non-structural factors such as material composition, surface ligand organization, and material degradation characteristics.

2.3 Classification of Smart Materials in Tissue Engineering

2.3.1 Synthetic Materials

Synthetic materials include metals, alloys, ceramics, and polymers, among others, and have long been of interest in biomaterial sciences. Current manufacturing techniques, and the physico–chemical and mechanical properties of these materials, have been exhaustively described.[14] Synthetic materials can be manufactured with extraordinary reproducibility and typically reasonable manufacturing costs.[15] The in-depth understanding and extensive experience with synthetic materials, as described in subsequent chapters of this text, have provided a solid basis for the creation of next generation smart materials.

Bone tissue engineering has provided a fertile opportunity for smart materials. New metallic biodegradable materials based on magnesium (Mg) and its alloys represent one such example of smart materials for orthopedic applications.[16] Current manufacturing techniques can be applied to generate a macroporous structure, where strength and stiffness of Mg-based materials are comparable with bone. In addition, Mg has the added advantage that it is a natural component of mammalian tissues. Mg-based scaffolds are considered smart materials as they play an important role in bone tissue formation[17] and their degradation can facilitate the healing process, eliminating the need for implant removal.[18]

The degradation rates of Mg-based materials are an active topic of investigation. *In vitro* studies imitating physiological conditions to the greatest extent possible have shown that Mg-based materials corrode very quickly, leading to a rapid change/loss of the mechanical properties.[17] Several Mg-based alloys have been created to decrease the degradation rate.[19] The corrosion of magnesium results in the formation of hydrogen gas (H_2) that, once saturated in the tissue, creates gas cavities and increased mortality in preclinical rodent models.[20] The non-lethal formation of hydrogen gas cavities has been shown in studies by Chaya *et al.* (2015)[21] and by Rössig *et al.* (2015)[22] using pure and Mg-based alloy LAE442, respectively. The results of these studies suggest that such materials still have limitations for effective clinical translation as a smart scaffold material.

Properties such as stiffness and degradation rate of magnesium can be modified by combination with other materials.[4] The generation of surface modifications to the Mg-based materials is being investigated to improve the characteristics and the host response to the implanted scaffold. Mg-based scaffolds coated with polycaprolactone (PCL) and gelatin polymers reduce the degradation rate and control the formation of hydrogen gas. The slower degradation rate of PCL can mitigate the rapid degradation of the Mg-based scaffold when used in combination.[23] Similarly, modifications with octacalcium phosphate (OCP) and hydroxyapatite (HAp) favorably modulate the degradation of Mg-based alloys and facilitate hydroxyapatite deposition.[24] These promising results require further evaluation to determine translatability to clinical approaches.

As with metallic materials, ceramics have been applied to bone tissue engineering applications. The concept of smart ceramic materials, however, has evolved slowly. From the choices of ceramics used in orthopedic restorations, only HAp and calcium metaphosphate (CMP) have been described as smart materials based upon their osteoinductive properties.[25,26] The brittle nature of the HAp limits its use as a material solely to repair hard tissue. Alternative approaches have focused upon the generation of composites with polymeric materials to increase the strength of the scaffolds.[27] Lee *et al.* (2013) showed that HAp coated with type I collagen resulted in a composite material with increased mechanical and structural properties that successfully promoted cell proliferation and osteogenesis when evaluated in a pre-clinical model.[26] Other techniques include the addition of growth factors, mainly bone morphogenetic proteins (BMPs), with an active role in osteogenesis. The use of human recombinant BMP-2 has facilitated the clinical translation of composite scaffold materials for bone tissue engineering applications. Although BMP-2 effectively induces osteogenesis, other tissues, including soft tissues, can be adversely affected by heterotopic osteogenesis. Recent studies have documented the undesirable side effects associated with the high concentrations of BMP-2 administered to patients, raising questions about its safety for selected clinical applications.[28]

Polymeric materials have great potential for the generation of smart materials. The diversity, malleability, and particular properties of synthetic polymers allow applications in tissue engineering ranging from hard to soft tissues. The first success toward the production of polymeric scaffolds is represented by the ability to control the degradation rates of the materials by modifying the molecular weight.[29] Therefore, biodegradable polymers, like those derived from polyesters or α-hydroxyesters, are often preferred over permanent polymers like polypropylene.[30] One advantage of implantable degradable polymers is that the monomeric compounds are often readily recognized by enzymes in the Krebs cycle and can be further metabolized as naturally occurring substrates.[27]

As mentioned previously, the ability of a material to degrade under physiological conditions is not enough to ensure a functional repair of the tissue. It has been found, for example, that hydrophobic polyesters are unable to allow

cell integration.[31] The production of synthetic smart polymers by functionalization steps, by which the surface is modified with antibodies, peptides, or ECM components, is employed to improve their bioactivity.[30] The strategies that are being explored include modifications ranging from complete proteins, usually an integrin ligand to facilitate the cellular attachment, to small peptides, containing only the active domain. Collagen, fibronectin, laminin, and elastin are among the most commonly used proteins for functionalization of synthetic scaffolds.[32] For example, degradable polymeric stents coated with elastin increase endothelial cell adhesion and proliferation.[33] Although ideally the complete protein could provide the cues needed for cell fate regulation, disadvantages associated with the costs of purification, greater control over the functionalization, and biologic variability, have made short peptides, like the Arg-Gly-Asp (RGD) motif, the preferred option.[34]

A critical point during the functionalization of polymeric materials is the attachment of the target molecules to the substrate. Bioactive compounds are organic molecules, highly sensitive to temperature and pH, therefore, functionalization steps should avoid the use of conditions that can affect the structure and activity of these molecules.[35] Physical methods, based on the adsorption and generation of non-covalent interactions, are the less invasive approach to modify the properties of a polymeric material (Figure 2.1(A)).

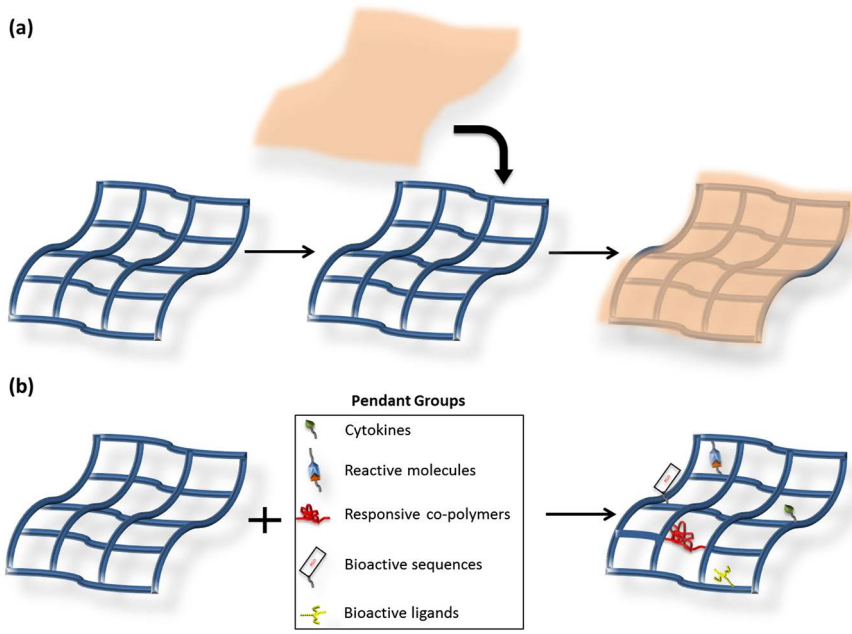

Figure 2.1 Methods of functionalization of polymeric materials. Physical methods of functionalization are based on adsorption and non-covalent binding of the functional groups (a). Chemical methods covalently bind the functional groups (pendant structures) to the polymer (b).

In a study performed by Aguirre *et al.* (2012), composites of polylactic acid (PLA) scaffold polymers coated with calcium phosphate glass provided an active microenvironment that mimicked the mechanotransductory and chemical signals of wound healing, promoting an increased vascularization.[36] In studies conducted by Faulk *et al.* (2014), synthetic non-degradable surgical mesh materials (polypropylene) coated with dermal ECM hydrogel modified the host immune response, the pro-inflammatory response and the amount of fibrous tissue formation.[37]

An alternative method of functionalization of synthetic scaffolds is based on the covalent binding of the active molecule to the polymer (Figure 2.1(B)). With this approach, the risk of delamination that exists with physical methods is eliminated.[38] Recent advances in "click chemistry", a method that utilizes orthogonal modification of materials in a controlled fashion, have provided highly efficient functionalization processes to generate smart synthetic materials. Some derivatives of click chemistry can be made under environmental conditions and without the requirement of toxic catalysts, overcoming the limitations of other traditional chemical methods.[39,40] Biodegradable poly(ester urethane)urea elastomers (PEUUs) have been the target of click chemistry to generate surface-functionalized smart biomaterials for applications in cardiac patches and soft tissue engineering.[41] In particular, the covalent binding of small peptides able to promote endothelial progenitor cell adhesion has been successfully evaluated *in vitro*.[42] Clinical translation of these smart synthetic materials has yet to occur, but the rapid advances of these technologies combined with the use of synthetic materials that are already in the biomedical market will facilitate their use in tissue engineering applications.

An additional surface functionalization method is based on self-assembly techniques to form hydrogels. The classical property associated with hydrogels is their hydrophilic nature, which provides for a viscous, soft material, ideal for soft tissue engineering applications.[43] The specific mechanical, physical, and chemical characteristics of hydrogels can be modulated with the use of different monomers or polymerization methods, like crosslinking modifications.[44] Self-assembled smart hydrogels are generated by mimicking the natural polymerization of the ECM components from a complex of polymeric materials interacting by covalent and non-covalent forces with the active molecules.[45,46] The inclusion of cryptic peptides, zwitterionic molecules and/or growth factors has facilitated the modulation of cell behavior in an ECM-like environment.[47]

Wound healing after burn injuries is a good example of the potential clinical application of a smart hydrogel. Extensive burns are usually associated with high morbidity and increased risk of infection. Tissue engineering approaches in this area are investigating alternatives to reduce the healing time, combined with antimicrobial activities that protect the tissue from infection. For instance, the small peptide sequence (LLKKK18), derived from the antimicrobial peptide (AMP) cathelicidin LL-37, conjugated to dextrin and indirectly linked to Carbopol® hydrogels (based on acrylic acid polymers), is

being investigated for burn treatment.[48] The AMP cathelicidin LL-37 is an active molecule, naturally produced by immune cells[49] such as macrophages, that contributes not only to protection against bacterial infection, but also has chemotactic effects promoting vascularization and the wound healing process.[50] Consistent with the properties attributed to cathelicidin LL-37, preclinical studies using these smart hydrogels showed increased angiogenesis, a shorter healing time, and increased matrix deposition, compared to the non-conjugated hydrogels.[48]

The investigation of non-conventional characteristics of polymers, such as conductive properties, is another area of interest in the development of smart materials. Conductive polymers can be considered a hybrid, as they present mechanical properties of traditional degradable polymers as well as conductive properties of metallic materials.[31,51] Conductive polymers are being widely studied in non-biomedical applications, but the finding that some of these materials have good biocompatibility has raised their biomedical profile. The polymers already investigated for tissue engineering applications belong to a group of polyheterocycles that includes polypyrrole, polyaniline, and polythiophene. The potential use that has been focused upon is the reconstruction of electro-active tissues such as the brain, heart, skeletal muscle, and bone.[52,53] Different molecules carry the charge to be mobilized, tailoring the conductive property of these polymers. Successful approaches involve the use of glycosaminoglycans (GAG) (*e.g.* chondroitin sulfate and hyaluronic acid) as such "doping" molecules, which also can improve cell integration.[31]

Currently, *in vitro* and animal studies have been performed with different modifications of these conductive materials, but to be translated to clinical applications, challenges in the mechanical properties and reproducibility of the manufacturing processes need to be addressed. These materials have been further modified to incorporate specific protein domains to provide cell cues and facilitate cell adhesion and differentiation.[31]

From the review presented herein, it is obvious that synthetic smart materials are rapidly evolving to simulate the regulatory mechanisms that exist within naturally occurring ECM. In the following sections, the analysis of smart biomaterials derived from naturally occurring materials will provide an alternative approach to cell/tissue modulation applicable in tissue engineering approaches.

2.3.2 Biosynthetic Materials

Biosynthetic materials can be defined as polymers produced by microorganisms using natural metabolic pathways, and therefore avoiding the use of potentially toxic chemical catalysts.[54] Polyesters belonging to the group of polyhydroxyalkanoates (PHA), which are formed as energy reserves in bacteria, are the most common examples of biosynthetic materials, with more than a hundred monomeric forms.[55] The biodegradability and biocompatibility of some of these polymers have stimulated interest in their use for

biomedical applications. Their use as homopolymers or co-polymers[56] allows tuning of physical and mechanical properties, which expands the spectrum of potential medical uses for these materials. Table 2.1 lists some of the most common PHAs used in medicine.

The PHAs share several properties with synthetic materials. The biosynthetic polymers can be modified by the same techniques applied to synthetic polymers. For example, Fu *et al.* (2014) explored the use of electrospinning copolymers of P3HB and P4HB (P34HB) to produce scaffolds from unwoven nanofibers, with potential for bone tissue engineering applications;[56] whereas Torun Köse *et al.* (2003) made similar attempts with particle leaching to generate a macroporous structure from PHBHV.[59] The mechanical properties of PHAs have been well studied[62,63] and reported to be analogous to synthetic materials such as polypropylene and polystyrene.[64] If the biodegradability of the PHAs is considered, some advantages for these materials exist when compared to other degradable synthetic polymers. Degradation of PHAs occurs very slowly by hydrolysis and enzymatic methods, which maintains the mechanical properties and provides for a gradual transfer of load to support tissue development. The slow rate hydrolysis also avoids abrupt pH changes in the microenvironment, a situation commonly found in polymers like PGA and which can trigger pro-inflammatory events.

Recent studies have taken advantage of these inherent properties of PHAs. Sun *et al.* (2015) developed laryngeal cartilage using PHBHHx scaffolds by combined methods of casting, compression molding, and leaching. *In vitro* culture of chondrocytes on the scaffold followed by implantation in a rabbit model allowed the formation of mature cartilage, with increased options for functional repair when combined with a myofascial flap.[65]

The generation of smart biosynthetic materials has been achieved by various functionalization methods. One of the most common modifications consists of the addition of pendant functional groups that modify the hydrophobic character of these materials; for example, increased water and protein interactions, as well as swelling of the biosynthetic compounds to form hydrogels.[55] Zhan *et al.* (2015) developed a more complex smart biosynthetic material, able to prevent and control bacterial colonization. In their approach, a self-assembly method was used to generate layers of P34HB interacting

Table 2.1 Polyhydroxyalkanoates used in medical applications.

Name	Abbreviation	Applications	Reference
Poly(3-hydroxybutyrate)	P3HB	Sutures, screws and plates	57
Poly(4-hydroxybutyrate)	P4HB	Heart valves, mesh for hernia repair, sutures	58
Poly(3-hydroxybutyrate-*co*-3-hydroxyvalerate)	PHBHV	Scaffolds for bone tissue engineering	59
Poly(3-hydroxybutyrate-*co*-3-hydroxyhexanoate)	PHBHHx	Tissue adhesion barriers	60
Poly(3-hydroxybutyrate-*co*-3-hydroxyoctanoate)	PHBHO	Drug carrier nanoparticles	61

with a bactericidal agent, poly(amidoamine) dendrimers (PAMAM), and HA as the anti-adhesion agent[66] for potential use in different tissues.

Biosynthetic materials derived from the PHA group have an additional and less explored property. Due to their bacterial origin, these polymers have shown physiological functions that have an effect not only on the bacteria from which they were produced, but on a variety of cells in different tissues and different organisms.[64] The monomeric forms of P3HB and P4HB, 3-hydroxybutyrate (3HB) and 4-hydroxybutyrate (4HB), respectively, are involved in normal physiologic activities and are produced in the body at low concentrations. Specifically, 3HB can serve as a nutritional supplement to increase ketone levels and control metabolic diseases.[67] 4HB is associated with functional activity in the central nervous system (CNS)[68] and has been proposed for neural applications.[64]

More recently, Pineda Molina *et al.* (2017) have shown that scaffolds composed of P4HB were able to resist deliberate *in situ* (1×10^8 CFU) *Staphylococcus aureus* contamination in a rat subcutaneous implantation model.[69] The mechanism of infection resistance appears to be modulation of the host innate immune system rather than direct antimicrobial effects.[70] These results show the potential of PHA-derived scaffolds in contaminated fields (Figure 2.2).

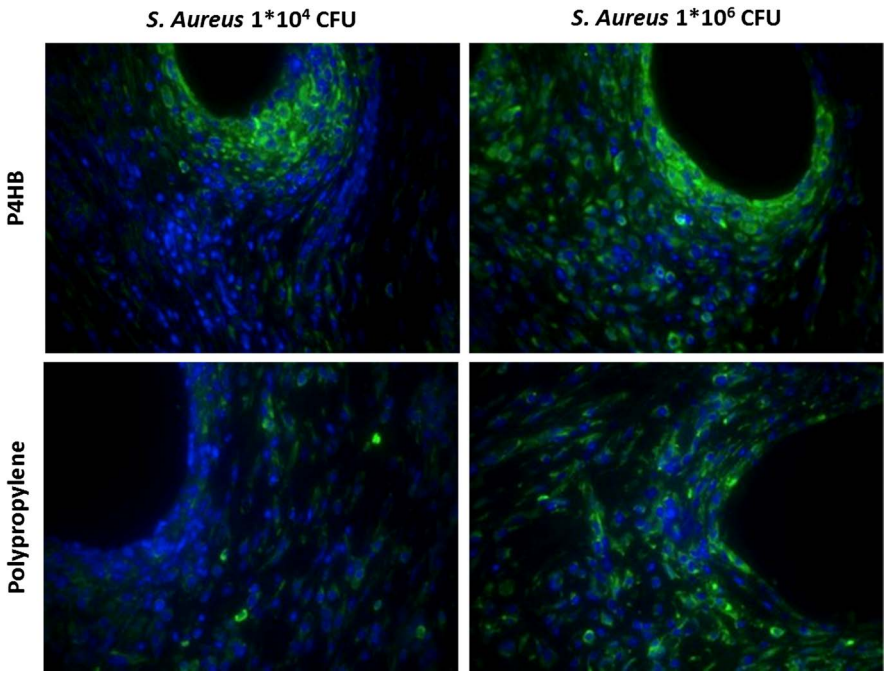

Figure 2.2 Scaffolds composed of P4HB promote the expression of the antimicrobial peptide cathelicidin LL-37 (green) in areas surrounding the mesh fiber material in a rat tissue inoculated with the gram-positive bacteria *Staphylococcus aureus*.

2.3.3 Biologic Materials

Biologic materials include those composed of intact extracellular matrix (ECM), or individual components of the ECM, such as collagen, fibronectin, and glycosaminoglycans, among others.[1,71] Biologic materials possess inherent biologic activity that confers advantages to these materials over their synthetic counterparts,[72] making them an excellent source for the generation of smart materials. The source of biologic materials is not limited to mammalian ECM; naturally occurring materials derived from insects and crustaceans contain structures and ligands that can modulate the mammalian cell response. Specific approaches to smart materials from individual components of the ECM will be discussed first, followed by an overview of intact ECM scaffold materials.

2.3.3.1 Protein-Based Materials

Insects and mammals produce proteins such as silk, collagen, fibronectin, and elastin,[73] among others, that are commonly used in biomedical applications. As was previously discussed, the use of proteins for functionalizing synthetic materials, specifically, their ability to form a tridimensional structure by self-assembly mechanisms and their competence to modulate cell behavior,[74] make them good candidates for smart materials. In the following paragraphs, the specific characteristics of the protein-based scaffold materials, and some attempts of tissue engineering applications will be described.

Silkworms, *Bombyx mori*, are the main producers of silk. The silk fiber is composed of the core protein, or silk fibroin, coated by a second group of proteins, sericins. Applications in tissue engineering require further purification of the silk fibroin proteins, because the sericins negatively affect the biocompatibility of the material.[75] The self-assembly property of the silk fibroin proteins facilitates the formation of diverse structures, such as fibers, sponges, films, hydrogels, and scaffolds, among others. In addition, its amphiphilic character enables the interaction of the silk fibroin with hydrophobic and hydrophilic molecules, as well as facilitation of cell integration.[76] The silk fibroin material has been evaluated in tissue engineering approaches for a wide range of applications, as reviewed by Aguirre *et al.* (2012).[77] *In vitro* studies have shown the ability of silk fibroin to support attachment, proliferation, and differentiation of smooth muscle cells and intestinal epithelial cells, providing potential for tissue engineering applications in the gastrointestinal tract.[78] Furthermore, the ability of the silk fibroin material to degrade slowly *in vivo*, mainly *via* proteinases, has been used in pre-clinical studies investigating its use as a space-filling biomaterial in soft tissue restoration.[79] Other studies have focused on the mechanical properties of the silk fibroin, using it as load-bearing scaffold; for example, Teuschl *et al.* (2016) showed that implanted silk fibroin scaffolds can replace the anterior cruciate ligament, and can reestablish its functionality, allowing cellular infiltration, and new tissue formation.[80]

A second group of protein-based materials is collagen. Collagen fibers represent the main structural compound of the ECM. Fibrillar collagens are the best example of hierarchically structured materials. At the nm scale, these molecules form triple helices of α-chains that self-assemble in the ECM forming an arrangement of microfibrils that are further organized as fibers on the μm scale, providing mechanical strength to the tissues.[74,81,82] The tridimensional organization of the collagen fibers provides also binding sites for cells and ligands, facilitating cell infiltration, platelet adhesion and activation, and regulating access to growth factors and cytokines.[83] The enzymatic degradation of collagen enables the release or exposure of matricryptic peptides, small fragments of peptides with biologic activities such as increased cell mobility, angiogenesis, and ECM deposition, among others.[1,84] For these reasons, this fibrous protein has been investigated as a scaffold material for tissue engineering approaches. Among all the fibrillar collagens, which include type I, II, and III,[85] type I collagen is the most abundant component of almost all tissues, and therefore is the type most explored for use as a scaffold material.

The hierarchical structure of collagen enables a versatile configuration of this material. Hydrogels can be produced by enzymatic solubilization of collagen to produce a biologically active gelatin.[86] Random or highly organized fiber structures can be produced by extrusion, microfluidic channels,[87] and 3D printing techniques.[82] Taking advantage of the inherent properties of collagen fibers and their utility as smart materials, Chan *et al.* (2016) have shown the ability of collagen scaffold materials to promote vascularization in pre-clinical studies, a required event for successful tissue regeneration.[88] Ryan and O'Brien (2015) showed that composites of collagen–elastin accelerate the differentiation of smooth muscle cells, induce their contractility *in vitro*, and improve the mechanical properties by the presence of the elastin molecules in the composite,[89] with potential for use in cardiovascular repair. Levingstone *et al.* (2016) evaluated the osteochondral regenerative potential of a multi-layered scaffold in a pre-clinical model. Three layers of a collagen type I scaffold were differentially conjugated with HAp particles, hyaluronic acid (HA), or collagen type II and HA, and assembled to form the osteogenic, calcified cartilage, and cartilaginous layers, respectively. Complete degradation of the multi-layered scaffold was seen at six months post-implantation and was replaced by new functional tissue produced by the cells that infiltrated the material.[90]

While these investigations using collagen scaffolds as smart materials sound promising in the field of tissue engineering, one of the challenges in the fabrication of collagen scaffolds is the maintenance of adequate site-specific mechanical properties while new tissue is being produced. Different chemical,[91,92] physical,[89] and enzymatic[87] cross-linking agents have been used to modify the final structure of the collagen fibers. Although these methods improve the strength of the collagen scaffold, they negatively affect cytocompatibility and decrease enzymatic access to the collagen, delaying/inhibiting scaffold degradation, affecting the release

of matricryptic peptides, and promoting a foreign body reaction (FBR).[93] Therefore, the smart properties of collagen are quenched by the application of such techniques.

Fibronectin represents the third group of ECM protein-based materials with potential for tissue engineering applications. Fibronectin is a dimeric ECM glycoprotein that polymerizes and becomes functional when forming a fibrillar network around the cells[94] as a consequence of the unfolding of cryptic domains which facilitate interactions with glycosaminoglycans, gelatin, collagen, as well as cell adhesion through integrins.[95] As a result of these interactions and the flexibility of fibronectin fibrils, the fibronectin network regulates the activity of the cells, providing mechanotransductory signals which help regulate ECM deposition.[96] The fabrication of fibronectin scaffolds is challenging, as changes in the tridimensional structure of the glycoproteins are required to form the network. These problems, however, are being addressed with the use of a surface-initiated assembly (SIA) method. Using this technique, the glycoprotein dimers are adsorbed onto a temporary scaffold of polydimethylsiloxane (PDMS), allowing the polymerization of the fibronectin and exposing the cryptic domains.[97] The application of this technique has great potential in the generation of stable structures that trigger the deposition of native ECM in wound repair applications.

From the group of protein-based materials, elastin is the last protein that will be discussed. Elastin forms the second group of fibrillar and structural proteins in the ECM. Being more abundant in tissues like lungs, blood vessels, and the dermis, these proteins provide elasticity to the interstitial matrix structure.[98] The elastic fibers are long-lived proteins assembled during development. Elastin fibers are self-assembled from the tropoelastin precursor, forming a highly hydrophobic protein. The elastin fibers are crosslinked to other glycoproteins or microfibrils that provide the binding domains for interactions with cells and heparin molecules.[95] Elastin fibers are also an excellent source of matrikines, called elastokines, and matricryptic peptides[84] regulating cell behavior and differentiation.[89]

The natural properties and composition of the elastin fibers make them difficult to isolate for biomedical applications; for this reason, more recent approaches make use of recombinant technologies to express structural and functional domains of tropoelastin in bacterial,[99] yeast, or plant settings. The advantages of these genetic engineering approaches include the tailoring of specific properties in the construct by the assembly of hybrid modules of different proteins, as well as the control of the composition of the final product, eliminating the variability between batches.[100] For example, the generation of silk-elastin-like proteins has been investigated to capture in a single construct the elastic properties of elastin and the tensile strength of silk[101,102] while preserving biocompatibility and biodegradability. Likewise, recombinant elastin peptides have been used to improve the biomechanical properties of collagen scaffolds for vascular applications.[103]

2.3.3.2 Polysaccharide-Based Materials

Polysaccharide-based materials used in biomedical applications can be derived from mammalian ECM (*i.e.* hyaluronic acid), algae (*i.e.* alginate), or crustaceans (*i.e.* chitosan). The hydrophilic property of these molecules facilitates their configuration as hydrogels;[5] therefore, they are mainly used as filling/injectable materials for soft tissue engineering applications or as microspheres or nanoparticles for drug delivery. The modification of scaffold materials using controlled drug delivery systems with polysaccharides is being widely studied to make smart composites bearing growth factors, drugs, and antibacterial motifs, among others.[104]

Hyaluronic acid (HA) is a linear high molecular weight non-sulfated GAG responsible for the viscoelastic fraction of the ECM and facilitating cell migration.[10,105] HA accounts for most of the water retention into tissues, allowing transportation and diffusion of molecules throughout the ECM. Biomaterials based on HA are usually extracted from rooster combs and further processed to obtain the final hydrogel, but some other strategies utilize bacterial fermentation to purify the molecule.[106]

Although HA is being used in biomedical applications, mainly as a dermal filler after volumetric loss,[107] it presents some challenges associated with rapid degradation and the lack of mechanical support.[108] Crosslinking strategies have been used to improve the mechanical properties of the HA, but typically, these attempts result in decreased availability of functional groups that actively control the microenvironment once they are implanted.[109] Click chemistry methods are now being used for the modification and crosslinking of HA with peptide amphiphiles,[110] providing a new generation of hierarchical structures non-covalently linked, called supramolecular systems.[111] Supramolecular HA has self-assembly properties that provide versatility and the ability to support structural modifications in response to environmental cues.[112] To maximize the properties of HA and its ability to regulate the storage of molecules, alternative mechanisms are being investigated to generate composites with other biologic and synthetic scaffolds for the production of smart materials.[109,113,114]

Alginate is another polysaccharide being investigated for the generation of smart materials in tissue engineering applications. The material, extracted from brown algae, has FDA approval for selected applications, and is being widely used in dentistry and other biomedical applications. Alginate chains are physically crosslinked with divalent cations, usually calcium (Ca^{2+}), to form a hydrogel. Although the material is non-degradable under physiological conditions, it is subjected to slow erosion by exchanging the Ca^{2+} for sodium ions (Na^{+}) in the milieu. After degradation, alginate molecules less than 50 KDa can be cleared through the urine.[115]

Even though alginate is not a biologically active material, it serves as the platform for the formation of microspheres/nanoparticles carrying heparin-binding proteins, such as cytokines and growth factors. The composite microspheres/nanoparticles are formed through an affinity-binding strategy

using a sulfated form of alginate, which mimics the interactions that naturally occur between the proteins and the sulfated GAGs.[115,116] The affinity-binding approach facilitates the encapsulation of more than one factor at a time and ensures their controlled release over the time. As a consequence, concentrations of specific growth factors required for each step in the tissue reparation process can be predicted and their release can be further programmed. The affinity-binding method also overcomes the problems associated with supra-physiological concentrations of growth factors and cytokines employed in other tissue engineering approaches.[117] Cizkova *et al.* (2015) showed the ability of an affinity-bound system containing epidermal growth factor (EGF) and fibroblast growth factor-2 (bFGF) in an alginate sulfate scaffold to promote the *in vitro* proliferation and differentiation of neural progenitor cells with potential application for spinal cord injury repair.[118] Ruvinov *et al.* (2016) have successfully evaluated this approach in pre-clinical studies for the treatment of hindlimb ischemia and myocardial infarction, for which the implanted nanoparticles loaded with three different growth factors induced angiogenesis and prevented scar tissue formation.[117]

The third polysaccharide of non-mammalian origin with potential application as a smart material is chitosan. Chitosan is a polysaccharide derived from the exoskeleton of arthropods. The structural homology of chitosan with glycosaminoglycans and its hydrophilic surface makes this material suitable for interactions with growth factors, receptors, and adhesion proteins.[119] Tunable characteristics, such as temperature and time to form the hydrogel, have been evaluated by modifying chitosan polymers with β-glycerol phosphate or gelatin.[120] Furthermore, the hemostatic properties and the ability to promote antibacterial activity are being widely explored.[121,122]

2.3.3.3 ECM Materials

The ECM is Mother Nature's version of a smart material. Resident cells of the tissues secrete the ECM components, forming a network of more than 300 molecules, which includes collagens, glycoproteins, glycosaminoglycans, proteoglycans, growth factors, and cryptic peptides, among others,[98] as shown in Figure 2.3. This naturally occurring complex accounts for both the biomechanical (*e.g.* stiffness, elasticity, *etc.*) and biochemical (*e.g.* growth factor and cryptic signaling regulations) properties of the tissue.[123,124] The ECM plays an essential role in cell homeostasis, tissue development, and maintenance of cell and tissue health.[125] The main molecules that constitute the ECM are very well preserved among different species,[1,126] therefore, allogeneic and xenogeneic ECM scaffolds have shown great utility as smart materials for tissue engineering applications.

The manufacture of ECM scaffolds is accomplished through decellularization of a source tissue, and subsequent disinfection and sterilization of the resultant matrix material.[127] Decellularization processes include the use of physical (*e.g.* freeze–thawing cycles, mechanical pressure), chemical (*e.g.* detergents, ionic solutions), and biochemical (*e.g.* enzymes) methods.

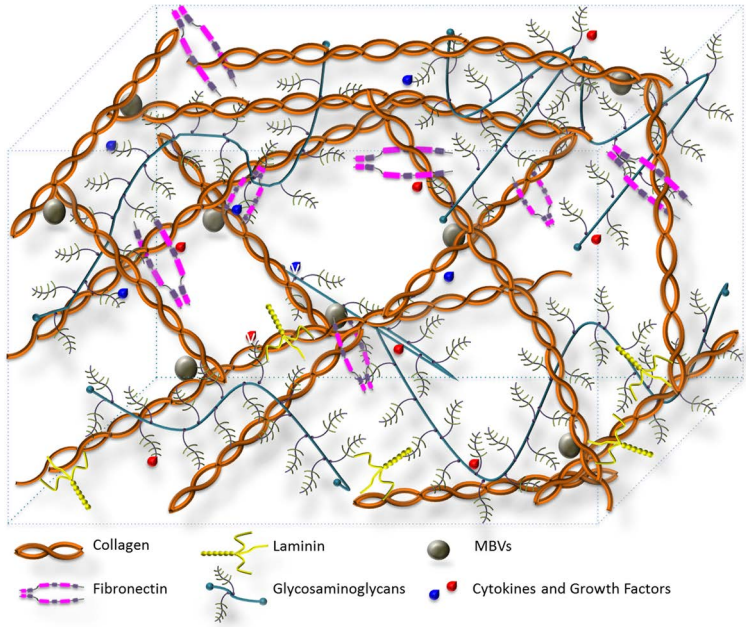

Figure 2.3 Structure of the extracellular matrix (ECM). The ECM is composed of different molecules forming a complex network that provides mechanical and biochemical properties to the tissues. Collagen forms long fibers from which the three-dimensional ECM structure is formed. Glycosaminoglycans store water, growth factors, and cytokines, regulating their availability to the cells. The active binding domains of glycoproteins, such as fibronectin, provide binding sites to connect the ECM components to the cells.

Source tissues vary widely and include the urinary bladder, small intestinal submucosa, dermis, skeletal muscle, esophagus, liver, and heart, among others.[128,129] All methods of tissue decellularization inevitably involve disruption of the matrix relative to its native structure/composition. Failure of adequate decellularization promotes an adverse, pro-inflammatory host response and poor functional outcomes.[130,131] For this reason, a critical balance between decellularization and preservation of native structural and functional compounds of the ECM should be systematically evaluated for each tissue.[132–134] Although there is a lack of consensus regarding metrics to determine sufficient decellularization, criteria have been proposed to guide the threshold above which an ECM scaffold material is prone to promote a pro-inflammatory response.[135]

ECM materials are versatile and can be applied in different configurations (Figure 2.4). These scaffolds have been modified to facilitate their applications in three-dimensional filling spaces. Solubilization of ECM materials into gels is becoming a common practice of the post-processing modifications of these scaffolds. Gels produced from ECM can acquire any desired

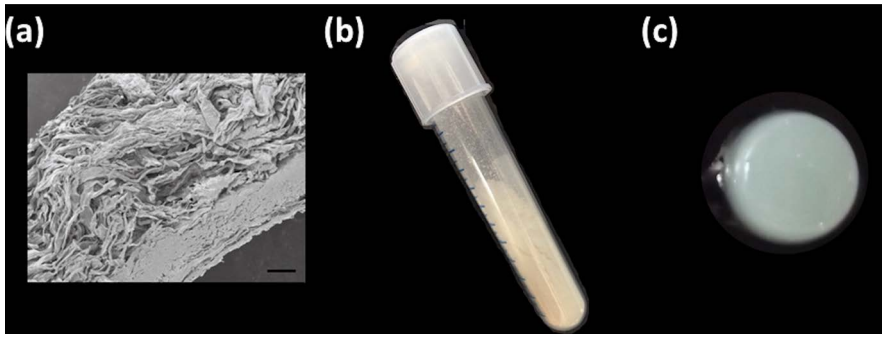

Figure 2.4 Configurations of acellular biomaterials for diverse tissue engineering applications. (a) The immediate product of decellularization is a two-dimensional sheet with defined layers of tissue. SEM image of a vascular ECM scaffold with cross-sections of the abluminal (upper) and luminal sections (lower); scale bar 100 μm. (b) ECM scaffold materials can be further processed by milling the ECM scaffold to generate a powder material for space-filling applications. (c) ECM gels are formed by solubilization of the ECM scaffold; the polymerization process is controlled by temperature, facilitating their use as injectable materials.

three-dimensional structure after physiological temperature-induced polymerization.[136] The self-assembly of the ECM components at physiological conditions provides advantages in the delivery methods for clinical applications, facilitating their use as injectable materials with minimally invasive techniques. ECM gels can be applied as a sole material or conjugated with other polymers to produce surface modifications on them (Figure 2.5).

ECM scaffolds that are properly prepared provide structural and microenvironmental cues that can induce functional repair of the damaged tissue, a process described as "constructive remodeling" and which results in site-appropriate organized tissue deposited at the implanted site.[71,137] The mechanisms by which functional remodeling mediated by ECM scaffolds occur are being increasingly understood, and at least three different mechanisms have been identified (Figure 2.6) and will be discussed below.

2.3.3.3.1 Modulation of the Immune Response. Macrophages play an essential role in tissue remodeling following implantation of an ECM scaffold.[138] Circulating and tissue resident mononuclear cells are recruited to the injured site and differentiate into macrophages within the first 24 to 48 hours. These cells show a predominantly M1-like (pro-inflammatory, cytotoxic) phenotype.[139] The long-term presence of the M1-like macrophage phenotype has been associated with chronic inflammation and FBR, whereas the presence of an M2-like (anti-inflammatory, immuno-regulatory) phenotype of macrophages has been associated with constructive tissue remodeling outcomes.[140] Implanted ECM scaffolds modulate the immune host response by promoting a transition of macrophage phenotype to an M2-like behavior within 3–7 days after implantation.[141] The mechanisms responsible for

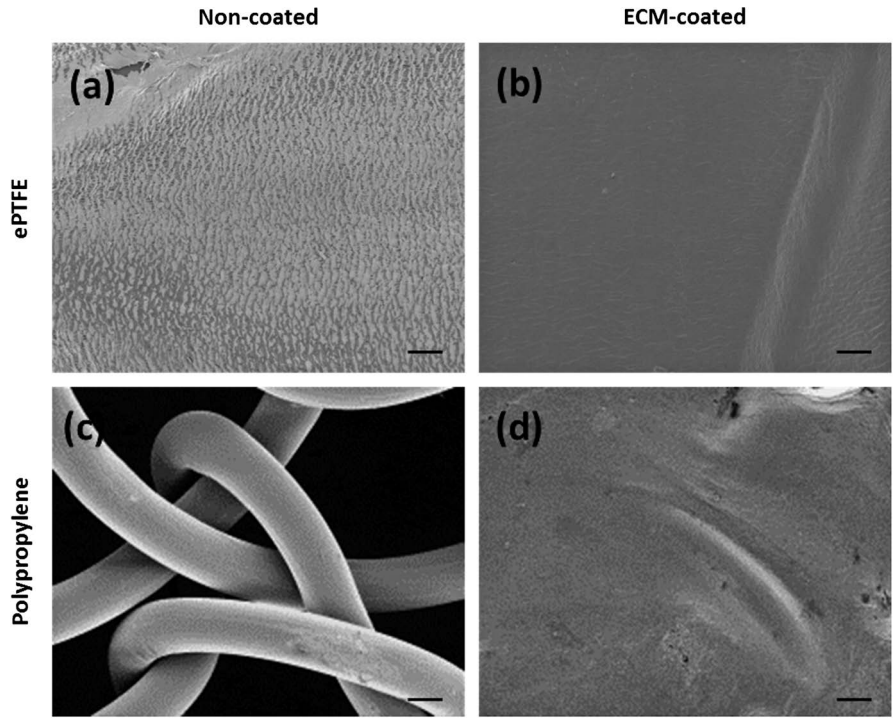

Figure 2.5 Functionalization of synthetic polymer materials with ECM gels. Coating of biomaterials with ECM gels is known to modulate the immune host response. (a) and (c) SEM images showing the topographical structure of non-coated biomaterials used in vascular tissue engineering (ePTFE) and hernial repair applications (polypropylene), respectively. (b) and (d) The same materials were coated with ECM gel, 8%, using a physical method of functionalization. The ECM gel is adsorbed onto the biomaterials modifying the topographical structure. Scale bar 100 μm.

modulating macrophage phenotypes include factors released during the degradation of the scaffold material and the availability and presentation of cryptic peptides to the resident cells.[142,143]

2.3.3.3.2 Degradation of ECM Scaffold Materials. Normal tissue exists in a dynamic state and includes processes of degradation and remodeling of the ECM as mechanisms for development, homeostasis, or response to injury.[144] Such a dynamic environment may be replicated by the implanted ECM scaffold material through mechanisms involving cellular and enzymatic pathways.[137,145] The degradation of the implanted ECM scaffold facilitates the cellular infiltration and the deposition of new site-appropriate tissue. Furthermore, and as previously discussed, the enzymatic degradation of the polymeric components of the ECM scaffold releases and/or exposes peptide motifs, AMPs, growth factors, GAGs, and other bioactive molecules,

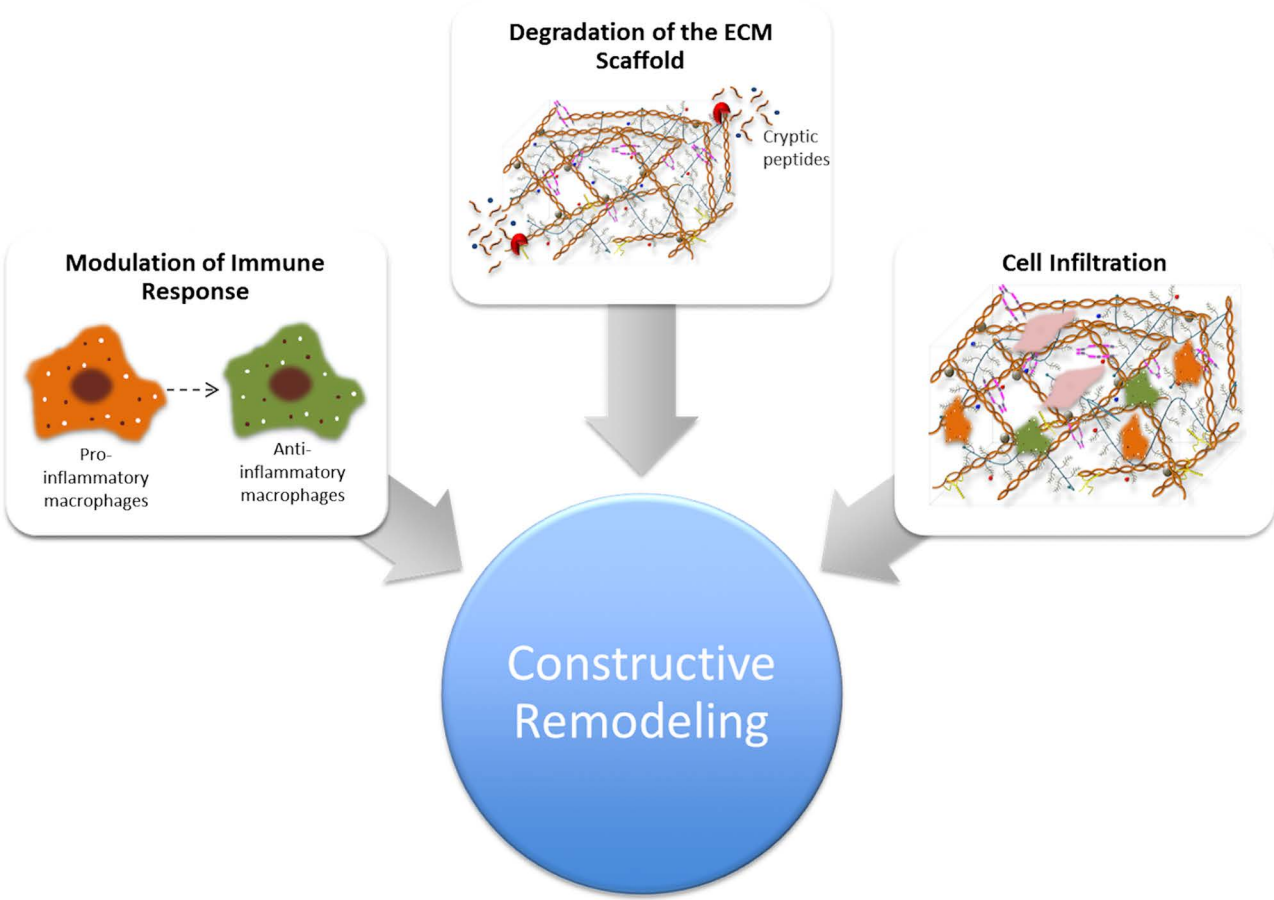

Figure 2.6 Mechanisms involved in constructive remodeling of tissues mediated by ECM scaffolds.

all of which have the potential to regulate cell migration, adhesion, differentiation, and angiogenesis.[146–148]

2.3.3.3.3 Cell Infiltration on ECM Bioscaffolds. The role of the ECM scaffolds and their degradation products is not limited to the immunomodulatory effect upon macrophages at the site of injury. The release of matricryptic peptides from the degraded ECM scaffold also facilitates the recruitment of local and systemic stem/progenitor cells, which in turn participate in the scaffold remodeling process.[149,150]

A large number of pre-clinical and clinical studies have been conducted using ECM scaffold materials for esophageal, musculoskeletal, vascular, and thoracic repair applications, among others. Variability in decellularization and manufacturing methods, and surgical technique, has resulted in disparate clinical outcomes. For example, Sicari *et al.* (2014) successfully showed the implantation of ECM scaffold materials in sites of volumetric muscle loss (VML) in both pre-clinical and clinical studies with resultant constructive remodeling, characterized by cell mobilization and *de novo* skeletal muscle formation.[151] In contrast, Aurora *et al.* (2015) utilized the same ECM scaffold material but did not show the same functional outcome.[152] The studies differ markedly in the associated protocol for post-surgical physical therapy. Whereas the former group initiated the physical/mechanical load of the affected region within 48 hours after implantation of the ECM scaffold, the latter group delayed the initiation of rehabilitation and lacked rigorous control in the rodent model. It is important to emphasize that immediate physical therapy is required to promote cell infiltration and differentiation, align the deposited ECM fibers, and promote angiogenesis, among other factors, which finally have an effect on the final functional outcome.[153,154]

Many studies have shown the potential of using ECM scaffolds derived from non-homologous tissues in a set of clinical applications. Remlinger *et al.* (2013) investigated the role of urinary bladder matrix (UBM) and cardiac ECM scaffolds in the repair of a full thickness defect in the right ventricular outflow tract in rats for the treatment of congenital heart defects. The results showed a robust cell mobilization from the bone marrow, cell infiltration into the ECM scaffold accompanied by site-appropriate tissue remodeling and the presence of cardiomyocytes after 16 weeks of implantation when UBM scaffolds were employed, whereas less degrees of functional outcome were obtained when the cardiac ECM was employed.[155] An additional example of utilization of heterologous ECM scaffolds is the study performed by Nieponice *et al.* (2014). In the pilot clinical study, a commercially available UBM scaffold was employed for the functional repair of damaged esophageal tissue. In all the evaluated cases, the implanted UBM scaffold was replaced by site-appropriate functional tissue with complete epithelialization.[156] Whether or not heterologous tissues can be employed for specific applications is still a topic of discussion and requires further investigation. Factors such as anatomic localization,[157] complexity of the tissue, and mechanical loads, among others, might affect the functionality of the repaired tissue. The large body of studies to date clearly shows the ability

of ECM scaffolds to behave as smart materials, in which common molecules present within tissues regulate events such as cell infiltration, angiogenesis, and functional tissue repair.

2.4 Clinical Translation of Smart Material for Tissue Engineering

Clinical applications of smart materials in tissue engineering are still at incipient stages, especially those of synthetic and biosynthetic origin. Catheters loaded with antibacterial agents for urethral catheterization and bioactive dressings for burn injury treatments[48] are successful examples of the clinical translation of responsive materials for tissue engineering.

The use of ECM-derived scaffolds to repair damaged tissues is common practice in the clinical setting. A partial list of commercially available non-crosslinked ECM scaffold materials is listed in Table 2.2. The Food and Drug Administration (FDA) has regulated these materials as medical devices,[158] facilitating their clinical application. The clinical applications using ECM-derived scaffolds have been focused on hernia repair, musculoskeletal repair, esophageal repair, and breast reconstruction, among others.[159] The potential clinical applications are not limited to these existing approaches, but can be easily expanded to other tissues once further investigated.

Musculoskeletal repair applications have been successfully reported in patients suffering from VML. In the study performed by Sicari *et al.* (2014), five patients with VML received UBM scaffold materials, after poor improvements in muscle volume and function with other techniques. Following the implantation of the acellular bioscaffolds and conjugated with a protocol of physical therapy, the patients showed signs of constructive tissue repair, as specified in the previous section, as well as improvement in muscle strength, re-establishing the quality of life of these patients.[151]

In a more recent study, developed by the same group of researchers, eight patients with VML were treated with ECM scaffolds in the affected area,

Table 2.2 Commercially available non-crosslinked ECM-derived materials.

Specie source	Tissue source	Commercial product
Bovine	Dermis	SurgiMend®, TissueMend® (TEI Biosciences)
Bovine	Pericardium	CopiOs® (Zimmer Biomet)
		Veritas® (Synovis® Surgical Innovations)
Human	Dermis	Alloderm® (LifeCell)
		AlloMax™ (Bard Davol Inc.)
		GraftJacket® (Wright Medical Tech)
Porcine	Dermis	Strattice™ (LifeCell)
		XenMatrix™ (Bard Davol Inc.)
Porcine	Small intestinal submucosa (SIS)	Oasis® (Cook Biotech)
		Restore® (DePuy)
		Surgisis® (Cook Biotech)
Porcine	Urinary bladder matrix (UBM)	MatriStem (ACell Inc.)

increasing the number to thirteen patients in total. Besides the increment in the number of patients, the researchers evaluated the muscle repair and functional outcomes after the implantation of one of three sources of ECM materials: UBM, SIS, and dermis. At a follow-up of six months, the findings of cellular infiltration, and nerve and skeletal muscle fiber formation, confirmed the induced reparative process mediated by the ECM scaffolds. The new therapeutic cases were in agreement with the first patients treated. Advancements in constructive muscle remodeling and positive functional outcomes confirmed the biological activity of these smart materials,[160] and highlighted the importance of the degradation of the scaffold materials and the release of matricryptic peptides to promote the reparative process.

Clinical translation of ECM scaffold materials for esophageal reconstruction represents a significant alternative for a challenging area, in which high morbidity and increased risk of infections are expected after implantation of a pedicled muscle flap or a jejunum interposition. The reconstruction of the esophageal structure in four patients following implantation of UBM scaffold materials has shown promise in the restoration of the esophageal function and the quality of life of the treated patients.[156] The results confirm the potential of ECM materials as mechanical and bioactive structures able to regulate infiltration and ingrowth of epithelial cells and the deposition of native functional ECM.

2.5 Future Challenges for Translation of Smart Biomaterials in Tissue Engineering

Biomaterials science has evolved dramatically during the last 30 years with a significant impact upon clinical outcomes. Materials have transitioned from inert to functional replacements, in which a smart material is intended to mimic the structure–function dynamics of the native tissue.[104] A better understanding of the processes involved in tissue development and repair has facilitated the shift in the targeted clinical utility of biomaterials. The mechanisms of these processes, however, have not been completely elucidated; there are still gaps in the understanding of specific intracellular pathways by which ECM molecules influence cell behavior.

Additional challenges in the generation of smart materials for various clinical applications exist in the context of complex tissue structures. Understanding the dynamic interface between different tissues, gradients of cells and growth factors, and other naturally occurring phenomena may promote the functional repair of tissue junctions such as musculoskeletal interfaces and whole organs.

Despite advances in the generation of smart materials with successful results at the bench, relatively few smart materials have shown successful clinical translation.[161] Different factors can affect the translation of smart materials from the bench to the bedside, including development and manufacturing costs, scalability, use of valid pre-clinical models, regulatory pathways, and determination of long-term safety, among others.[162,163]

As our understanding of the complex mechanisms involved in the micro-environmental niche regulation of cell behavior improves, the design and manufacture of smart materials for a variety of clinical applications will continue to advance based upon concepts described in the following chapters of this textbook.

References

1. R. Londono and S. F. Badylak, *Ann. Biomed. Eng.*, 2014, **43**(3), 577–592.
2. M. M. Martino, P. S. Briquez, K. Maruyama and J. A. Hubbell, *Adv. Drug Delivery Rev.*, 2015, **94**, 41–52.
3. H. Markides, J. McLaren and A. J. Haj, *Int. J. Biochem. Cell Biol.*, 2015, **69**, 162–172.
4. R. A. Perez, J. E. Won, J. C. Knowles and H. W. Kim, *Adv. Drug Delivery Rev.*, 2013, **65**, 471–496.
5. B. M. Holzapfel, J. C. Reichert, J. T. Schantz, U. Gbureck, L. Rackwitz, U. Noth, F. Jakob, M. Rudert, J. Groll and D. W. Hutmacher, *Adv. Drug Delivery Rev.*, 2013, **65**, 581–603.
6. *Host Response to Biomaterials: The Impact of Host Response on Biomaterial Selection*, ed. S. F. Badylak, Academic Press, USA, 2015.
7. B. N. Brown and S. F. Badylak, *Acta Biomater.*, 2013, **9**, 4948–4955.
8. D. F. Williams, *Biomaterials*, 2009, **30**, 5897–5909.
9. L. Moroni, J. R. De Wijn and C. A. Van Blitterswijk, *J. Biomater. Sci., Polym. Ed.*, 2008, **19**, 543–557.
10. N. J. Walters and E. Gentleman, *Acta Biomater.*, 2015, **11**, 3–16.
11. J. A. Stella, A. D'Amore, W. R. Wagner and M. S. Sacks, *Acta Biomater.*, 2010, **6**, 2365–2381.
12. D. Yoo, *Mater. Sci. Eng., C*, 2013, **33**, 1759–1772.
13. J. Kim and R. C. Hayward, *Trends Biotechnol.*, 2012, **30**, 426–439.
14. B. D. Ratner, in *Biomaterials Science: An Introduction to Materials in Medicine*, ed. B. D. Ratner, A. S. Hoffman, F. J. Schoen and J. E. Lemons, Elsevier, USA, 3rd edn, 2013, pp. xli–liii.
15. B. Dhandayuthapani, Y. Yoshida, T. Maekawa and D. S. Kumar, *Int. J. Polym. Sci.*, 2011, **2011**, 1–19.
16. K. F. Farraro, K. E. Kim, S. L. Woo, J. R. Flowers and M. B. McCullough, *J. Biomech.*, 2014, **47**, 1979–1986.
17. K. Lietaert, L. Weber, J. Van Humbeeck, A. Mortensen, J. Luyten and J. Schrooten, *J. Magnesium Alloys*, 2013, **1**, 303–311.
18. H. Windhagen, K. Radtke, A. Weizbauer, J. Diekmann, Y. Noll, U. Kreimeyer, R. Schavan, C. Stukenborg-Colsman and H. Waizy, *Biomed. Eng. Online*, 2013, **12**, 1–10.
19. W. D. Müller, M. L. Nascimento, M. Zeddies, M. Córsico, L. M. Gassa, M. A. Fernández and L. de Mele, *Mater. Res.*, 2007, **10**, 5–10.
20. D. Noviana, D. Paramitha, M. F. Ulum and H. Hermawan, *J. Orthop. Transl.*, 2016, **5**, 9–15.

21. A. Chaya, S. Yoshizawa, K. Verdelis, N. Myers, B. J. Costello, D. T. Chou, S. Pal, S. Maiti, P. N. Kumta and C. Sfeir, *Acta Biomater.*, 2015, **18**, 262–269.
22. C. Rössig, N. Angrisani, P. Helmecke, S. Besdo, J. M. Seitz, B. Welke, N. Fedchenko, H. Kock and J. Reifenrath, *Acta Biomater.*, 2015, **25**, 369–383.
23. M. Yazdimamaghani, M. Razavi, D. Vashaee and L. Tayebi, *Mater. Lett.*, 2014, **132**, 106–110.
24. S. Hiromoto, M. Inoue, T. Taguchi, M. Yamane and N. Ohtsu, *Acta Biomater.*, 2015, **11**, 520–530.
25. B. J. McEntire, B. S. Bal, M. N. Rahaman, J. Chevalier and G. Pezzotti, *J. Eur. Ceram. Soc.*, 2015, **35**, 4327–4369.
26. H. R. Lee, H. J. Kim, J. S. Ko, Y. S. Choi, M. W. Ahn, S. Kim and S. H. Do, *PLoS One*, 2013, **8**, e84272.
27. K. A. Blackwood, N. Bock, T. R. Dargaville and M. Ann Woodruff, *Int. J. Polym. Sci.*, 2012, **2012**, 1–25.
28. D. Gothard, E. L. Smith, J. M. Kanczler, H. Rashidi, O. Qutachi, J. Henstock, M. Rotherham, A. E. Haj, K. Shakesheff and R. O. C. Oreffo, *Eur. Cells Mater.*, 2014, **28**, 166–208.
29. F. J. O'Brien, *Mater. Today*, 2011, **14**, 88–95.
30. M. L. Williams and S. K. Bhatia, *Biotechnol. J.*, 2014, **9**, 337–347.
31. R. Balint, N. J. Cassidy and S. H. Cartmell, *Acta Biomater.*, 2014, **10**, 2341–2353.
32. M. Tallawi, E. Rosellini, N. Barbani, M. G. Cascone, R. Rai, G. Saint-Pierre and A. R. Boccaccini, *J. R. Soc., Interface*, 2015, **12**, 20150254.
33. R. Barenghi, S. Beke, I. Romano, P. Gavazzo, B. Farkas, M. Vassalli, F. Brandi and S. Scaglione, *BioMed Res. Int.*, 2014, **2014**, 624645.
34. M. A. Mateos-Timoneda, R. Levato, X. Puñet, I. Cano, O. Castano and E. Engel, *2015 37th Annual International Conference of the IEEE Engineering in Medicine and Biology Society (EMBC)*, Milan, 2015, pp. 1745–1748.
35. D. Puppi, X. Zhang, L. Yang, F. Chiellini, X. Sun and E. Chiellini, *J. Biomed. Mater. Res., Part B*, 2014, **102**, 1562–1579.
36. A. Aguirre, A. González, M. Navarro, Ó. Castaño, J. A. Planell and E. Engel, *Eur. Cells Mater.*, 2012, **24**, 90–106.
37. D. M. Faulk, R. Londono, M. T. Wolf, C. A. Ranallo, C. A. Carruthers, J. D. Wildemann, C. L. Dearth and S. F. Badylak, *Biomaterials*, 2014, **35**, 8585–8595.
38. P. M. Lopez-Perez, R. M. da Silva, R. A. Sousa, I. Pashkuleva and R. L. Reis, *Acta Biomater.*, 2010, **6**, 3704–3712.
39. K. Fukushima, *Biomater. Sci.*, 2015, **4**, 9–24.
40. C. M. Nimmo and M. S. Shoichet, *Bioconjugate Chem.*, 2011, **22**, 2199–2209.
41. J. Fang, S. H. Ye, V. Shankarraman, Y. Huang, X. Mo and W. R. Wagner, *Acta Biomater.*, 2014, **10**, 4639–4649.
42. J. Fang, S. H. Ye, J. Wang, T. Zhao, X. Mo and W. R. Wagner, *Biomacromolecules*, 2015, **16**, 1622–1633.

43. M. C. Koetting, J. T. Peters, S. D. Steichen and N. A. Peppas, *Mater. Sci. Eng., R*, 2015, **93**, 1–49.
44. D. A. Bichara, X. Zhao, H. Bodugoz-Senturk, F. P. Ballyns, E. Oral, M. A. Randolph, L. J. Bonassar, T. J. Gill and O. K. Muratoglu, *Tissue Eng., Part A*, 2011, **17**, 301–309.
45. M. P. Lutolf and J. A. Hubbell, *Nat. Biotechnol.*, 2005, **23**, 47–55.
46. S. J. Buwalda, K. W. Boere, P. J. Dijkstra, J. Feijen, T. Vermonden and W. E. Hennink, *J. Controlled Release*, 2014, **190**, 254–273.
47. M. Ebara, Y. Kotsuchibashi, K. Uto, T. Aoyagi, Y.-J. Kim, R. Narain, N. Idota and J. M. Hoffman, *Smart Biomaterials*, Springer, Japan, 2014, **2**, pp. 9–65.
48. J. P. Silva, S. Dhall, M. Garcia, A. Chan, C. Costa, M. Gama and M. Martins-Green, *Acta Biomater.*, 2015, **26**, 249–262.
49. A. M. van der Does, P. Bergman, B. Agerberth and L. Lindbom, *J. Leukocyte Biol.*, 2012, **92**, 735–742.
50. M. Schwab, V. Reynders, Y. Shastri, S. Loitsch, J. Stein and O. Schroder, *Mol. Immunol.*, 2007, **44**, 2107–2114.
51. B. Guo and M. Peter, *Sci. China: Chem.*, 2014, **57**, 490–500.
52. B. Guo, L. Glavas and A.-C. Albertsson, *Prog. Polym. Sci.*, 2013, **38**, 1263–1286.
53. C. Vallejo-Giraldo, A. Kelly and M. J. Biggs, *Drug Discovery Today*, 2014, **19**, 88–94.
54. C. W. Pouton and S. Akhtar, *Adv. Drug Delivery Rev.*, 1996, **18**, 133–162.
55. Z. Li and X. J. Loh, *Chem. Soc. Rev.*, 2015, **44**, 2865–2879.
56. N. Fu, S. Deng, Y. Fu, G. Li, X. Cun, L. Hao, X. Wei, X. Cai, Q. Peng and Y. Lin, *Cell Proliferation*, 2014, **47**, 465–475.
57. A. P. Bonartsev, V. L. Myshkina, D. A. Nikolaeva, E. K. Furina, T. A. Makhina, V. A. Livshits, A. P. Boskhomdzhiev, E. A. Ivanov, A. L. Iordanskii and G. A. Bonartseva, in *Communicating Current Research and Educational Topics and Trends in Applied Microbiology*, ed. A. Méndez-Vilas, FORMATEX, 2007, pp. 293–307.
58. S. F. Williams, S. Rizk and D. P. Martin, *Biomed. Tech.*, 2013, **58**, 439–452.
59. G. Torun Köse, H. Kenar, N. Hasirci and V. Hasirci, *Biomaterials*, 2003, **24**, 1949–1958.
60. Z.-W. Dai, X.-H. Zou and G.-Q. Chen, *Biomaterials*, 2009, **30**, 3075–3083.
61. A. Shrivastav, H.-Y. Kim and Y.-R. Kim, *BioMed Res. Int.*, 2013, **2013**, 12.
62. D. P. Martin, A. Badhwar, D. V. Shah, S. Rizk, S. N. Eldridge, D. H. Gagne, A. Ganatra, R. E. Darois, S. F. Williams, H. C. Tai and J. R. Scott, *J. Surg. Res.*, 2013, **184**, 766–773.
63. E. Masaeli, M. Morshed, P. Rasekhian, S. Karbasi, K. Karbalaie, F. Karamali, D. Abedi, S. Razavi, A. Jafarian-Dehkordi, M. H. Nasr-Esfahani and H. Baharvand, *J. Biomed. Mater. Res., Part A*, 2012, **100A**, 1907–1918.
64. G. Q. Chen and Q. Wu, *Biomaterials*, 2005, **26**, 6565–6578.
65. A. Sun, Q. Meng, W. Li, S. Liu and W. Chen, *Exp. Ther. Med.*, 2015, **9**, 1482–1488.
66. J. Zhan, L. Wang, S. Liu, J. Chen, L. Ren and Y. Wang, *ACS Appl. Mater. Interfaces*, 2015, **7**, 13876–13881.

67. N. Boon, T. Defoirdt, W. de Windt, T. Van De Wiele and W. Verstraete, United States Pat. US20100093860 A1, 2007.
68. M. Maitre, *Prog. Neurobiol.*, 1997, **51**, 337–361.
69. D. M. Faulk, R. Londono, C. Pineda-Molina, N. J. Turner, Y. v. d. Merwe, A. E. Loneker, B. M. Sicari and S. F. Badylak, *Abdominal Wall Reconstruction Summit*, 2016.
70. C. Pineda-Molina, B. M. Sicari, R. Londono, R. M. Giglio, D. Wang, R. M. Gandhi, J. Dziki, S. Shaffiey and S. F. Badylak, *2015 4th TERMIS World Congress in Tissue Engineering Part A*, 2015, **21**, S47.
71. N. J. Turner and S. F. Badylak, *Adv. Wound Care*, 2015, **4**, 490–500.
72. S. T. Lopresti and B. N. Brown, in *Host Response to Biomaterials The Impact of Host Response on Biomaterial Selection*, ed. S. F. Badylak, Elsevier, USA, 2015, pp. 53–79.
73. M. S. Desai and S. W. Lee, *Wiley Interdiscip. Rev. Nanomed. Nanobiotechnol.*, 2015, **7**, 69–97.
74. E. Sayin, E. T. r. Baran and V. Hasirci, *Regener. Med.*, 2014, **9**, 687–701.
75. Y. Maghdouri-White, G. L. Bowlin, C. A. Lemmon and D. Dréau, *Mater. Sci. Eng., C*, 2016, **59**, 1168–1180.
76. I. D. Pra, G. Freddi, J. Minic, A. Chiarini and U. Armato, *Biomaterials*, 2005, **26**, 1987–1999.
77. N. Kasoju and U. Bora, *Adv. Healthcare Mater.*, 2012, **1**, 393–412.
78. D. Franck, Y. G. Chung, J. Coburn, D. L. Kaplan, C. R. Estrada Jr and J. R. Mauney, *J. Tissue Eng.*, 2014, **5**, 1–10.
79. E. Bellas, T. J. Lo, E. P. Fournier, J. E. Brown, R. D. Abbott, E. S. Gil, K. G. Marra, J. P. Rubin, G. G. Leisk and D. L. Kaplan, *Adv. Healthcare Mater.*, 2015, **4**, 452–459.
80. A. Teuschl, P. Heimel, S. Nurnberger, M. van Griensven, H. Redl and T. Nau, *Am. J. Sports Med.*, 2016, **44**, 1548–1557.
81. F. Rosso, G. Marino, A. Giordano, M. Barbarisi, D. Parmeggiani and A. Barbarisi, *J. Cell. Physiol.*, 2005, **203**, 465–470.
82. A. Lode, M. Meyer, S. Bruggemeier, B. Paul, H. Baltzer, M. Schropfer, C. Winkelmann, F. Sonntag and M. Gelinsky, *Biofabrication*, 2016, **8**, 015015.
83. J. P. R. O. Orgel, O. Antipova, I. Sagi, A. Bitler, D. Qiu, R. Wang, Y. Xu and J. D. S. Antonio, *Connect. Tissue Res.*, 2011, **52**, 18–24.
84. S. Ricard-Blum and R. Salza, *Exp. Dermatol.*, 2014, **23**, 457–463.
85. B. Alberts, A. Johnson, J. Lewis, M. Raff, K. Roberts and P. Walter, *Molecular Biology of the Cell*, Taylor and Francis CRC, United States, 5th edn, 2012, pp. 1131–1204.
86. X. Zhang, M. R. Battig, N. Chen, E. R. Gaddes, K. L. Duncan and Y. Wang, *Biomacromolecules*, 2016, **17**, 778–787.
87. L. A. Hapach, J. A. VanderBurgh, J. P. Miller and C. A. Reinhart-King, *Phys. Biol.*, 2015, **12**, 1–13.
88. E. C. Chan, S.-M. Kuo, A. M. Kong, W. A. Morrison, G. J. Dusting, G. M. Mitchell, S. Y. Lim and G.-S. Liu, *PLoS One*, 2016, **11**, 1–15.
89. A. J. Ryan and F. J. O'Brien, *Biomaterials*, 2015, **73**, 296–307.
90. T. J. Levingstone, A. Ramesh, R. T. Brady, P. A. Brama, C. Kearney, J. P. Gleeson and F. J. O'Brien, *Biomaterials*, 2016, **87**, 69–81.

91. C. O'Leary, B. Cavanagh, R. E. Unger, C. J. Kirkpatrick, S. O'Dea, F. J. O'Brien and S. A. Cryan, *Biomaterials*, 2016, **85**, 111–127.
92. J. Baek, S. Sovani, N. E. Glembotski, J. Du, S. Jin, S. P. Grogan and D. D. D'Lima, *Tissue Eng., Part A*, 2016, **22**, 436–448.
93. J. M. Aamodt and D. W. Grainger, *Biomaterials*, 2016, **86**, 68–82.
94. K. Wang, B. R. Seo, C. Fischbach and D. Gourdon, *Cell. Mol. Bioeng.*, 2016, **9**, 1–11.
95. A. D. Theocharis, S. S. Skandalis, C. Gialeli and N. K. Karamanos, *Adv. Drug Delivery Rev.*, 2016, **97**, 4–27.
96. H. Bachman, J. Nicosia, M. Dysart and T. H. Barker, *Adv. Wound Care*, 2014, **4**, 501–511.
97. J. M. Szymanski, Q. Jallerat and A. W. Feinberg, *J. Visualized Exp.*, 2014, 1–15.
98. C. Bonnans, J. Chou and Z. Werb, *Nat. Rev. Mol. Cell Biol.*, 2014, **15**, 786–801.
99. B. Aghaei-Ghareh-Bolagh, S. M. Mithieux and A. S. Weiss, *Curr. Opin. Biotechnol.*, 2016, **39**, 56–60.
100. N. Dinjaski and D. L. Kaplan, *Curr. Opin. Biotechnol.*, 2015, **39**, 1–7.
101. X. X. Xia, Q. Xu, X. Hu, G. Qin and D. L. Kaplan, *Biomacromolecules*, 2011, **12**, 3844–3850.
102. R. Machado, A. d. Costa, V. Sencadas, C. Garcia-Arévalo, C. M. Costa, J. Padrão, A. Gomes, S. Lanceros-Méndez, J. C. Rodríguez-Cabello and M. Casal, *Biomed. Mater.*, 2013, **8**, 12.
103. F. Boccafoschi, M. Ramella, T. Sibillano, L. De Caro, C. Giannini, R. Comparelli, A. Bandiera and M. Cannas, *J. Biomed. Mater. Res., Part A*, 2015, **103**, 1218–1230.
104. S. Font Tellado, E. R. Balmayor and M. Van Griensven, *Adv. Drug Delivery Rev.*, 2015, **94**, 126–140.
105. A. Fakhari and C. Berkland, *Acta Biomater.*, 2013, **9**, 7081–7092.
106. J.-F. Kaux, A. Samson and J.-M. Crielaard, *Muscles Ligaments Tendons J.*, 2015, **5**, 264–269.
107. M. Landau and S. Fagien, *Plast. Reconstr. Surg.*, 2015, **136**, 188S–195S.
108. M. N. Collins and C. Birkinshaw, *Carbohydr. Polym.*, 2013, **92**, 1262–1279.
109. H. K. Heris, M. Rahmat and L. Mongeau, *Macromol. Biosci.*, 2012, **12**, 202–210.
110. S. Bou, A. V. Ellis and M. Ebara, *Curr. Opin. Biotechnol.*, 2016, **39**, 113–119.
111. C. B. Highley, G. D. Prestwich and J. A. Burdick, *Curr. Opin. Biotechnol.*, 2016, **40**, 35–40.
112. R. H. Zha, Y. S. Velichko, R. Bitton and S. I. Stupp, *Soft Matter*, 2016, **12**, 1401–1410.
113. V. Vindigni, R. Cortivo, L. Iacobellis, G. Abatangelo and B. Zavan, *Int. J. Mol. Sci.*, 2009, **10**, 2972–2985.
114. H. Tan, X. Gao, J. Sun, C. Xiao and X. Hu, *Chem. Commun.*, 2013, **49**, 11554–11556.
115. E. Ruvinov and S. Cohen, *Adv. Drug Delivery Rev.*, 2016, **96**, 54–76.
116. E. Ruvinov, T. Harel-Adar and S. Cohen, *J. Cardiovasc. Transl. Res.*, 2011, **4**, 559–574.

117. E. Ruvinov, I. Freeman, R. Fredo and S. Cohen, *Nano Lett.*, 2016, **16**, 883–888.
118. D. Cizkova, L. Slovinska, I. Grulova, M. Salzet, S. Cikos, O. Kryukov and S. Cohen, *J. Tissue Eng. Regener. Med.*, 2015, **9**, 918–929.
119. N. R. Blan and R. K. Birla, *J. Biomed. Mater. Res., Part A*, 2008, **86**, 195–208.
120. H. Y. Zhou, L. J. Jiang, P. P. Cao, J. B. Li and X. G. Chen, *Carbohydr. Polym.*, 2015, **117**, 524–536.
121. Y. Chen, Y. Zhang, F. Wang, W. Meng, X. Yang, P. Li, J. Jiang, H. Tan and Y. Zheng, *Mater. Sci. Eng., C*, 2016, **63**, 18–29.
122. E. V. Gladkova, I. V. Babushkina, I. A. Norkin, I. A. Mamonova, D. M. Puchin'yan and E. A. Konyuchenko, *Bull. Exp. Biol. Med.*, 2016, **160**, 715–717.
123. L. L. Ioannides-Demos, L. Piccenna and J. J. McNeil, *J. Obes.*, 2011, **2011**, 179674.
124. A. Naba, K. R. Clauser, H. Ding, C. A. Whittaker, S. A. Carr and R. O. Hynes, *Matrix Biol.*, 2015, **49**, 10–24.
125. M. E. Furth, A. Atala and M. E. Van Dyke, *Biomaterials*, 2007, **28**, 5068–5073.
126. S. Hinderer, S. L. Layland and K. Schenke-Layland, *Adv. Drug Delivery Rev.*, 2016, **97**, 260–269.
127. F. J. Schoen, in *Biomaterials Science: An Introduction to Materials in Medicine*, ed. B. D. Ratner, A. S. Hoffman, F. J. Schoen and J. E. Lemons, Elsevier, USA, 3rd edn, 2013, pp. 452–467.
128. M. Parmaksiz, A. Dogan, S. Odabas, A. E. Elcin and Y. M. Elcin, *Biomed. Mater.*, 2016, **11**, 022003.
129. T. J. Keane, I. T. Swinehart and S. F. Badylak, *Methods*, 2015, **84**, 25–34.
130. T. J. Keane, R. Londono, N. J. Turner and S. F. Badylak, *Biomaterials*, 2012, **33**, 1771–1781.
131. B. N. Brown, J. E. Valentin, A. M. Stewart-Akers, G. P. McCabe and S. F. Badylak, *Biomaterials*, 2009, **30**, 1482–1491.
132. D. M. Faulk, C. A. Carruthers, H. J. Warner, C. R. Kramer, J. E. Reing, L. Zhang, A. D'Amore and S. F. Badylak, *Acta Biomater.*, 2014, **10**, 183–193.
133. J. E. Reing, B. N. Brown, K. A. Daly, J. M. Freund, T. W. Gilbert, S. X. Hsiong, A. Huber, K. E. Kullas, S. Tottey, M. T. Wolf and S. F. Badylak, *Biomaterials*, 2010, **31**, 8626–8633.
134. A. Roosens, P. Somers, F. De Somer, V. Carriel, G. Van Nooten and R. Cornelissen, *Ann. Biomed. Eng.*, 2016, **44**, 2827–2839.
135. P. M. Crapo, T. W. Gilbert and S. F. Badylak, *Biomaterials*, 2011, **32**, 3233–3243.
136. D. O. Freytes, J. Martin, S. S. Velankar, A. S. Lee and S. F. Badylak, *Biomaterials*, 2008, **29**, 1630–1637.
137. I. T. Swinehart and S. F. Badylak, *Dev. Dyn.*, 2016, **245**, 351–360.
138. J. E. Valentin, A. M. Stewart-Akers, T. W. Gilbert and S. F. Badylak, *Tissue Eng., Part A*, 2009, **15**, 1687–1694.
139. B. N. Brown, B. M. Sicari and S. F. Badylak, *Front. Immunol.*, 2014, **5**, 510.
140. J. G. Tidball and S. A. Villalta, *Am. J. Physiol.: Regul., Integr. Comp. Physiol.*, 2010, **298**, R1173–R1187.

141. B. N. Brown, R. Londono, S. Tottey, L. Zhang, K. A. Kukla, M. T. Wolf, K. A. Daly, J. E. Reing and S. F. Badylak, *Acta Biomater.*, 2012, **8**, 978–987.
142. B. M. Sicari, J. L. Dziki, B. F. Siu, C. J. Medberry, C. L. Dearth and S. F. Badylak, *Biomaterials*, 2014, **35**, 8605–8612.
143. B. N. Brown, B. D. Ratner, S. B. Goodman, S. Amar and S. F. Badylak, *Biomaterials*, 2012, **33**, 3792–3802.
144. S. Franz, S. Rammelt, D. Scharnweber and J. C. Simon, *Biomaterials*, 2011, **32**, 6692–6709.
145. R. Xu, A. Boudreau and M. J. Bissell, *Cancer Metastasis Rev.*, 2009, **28**, 167–176.
146. S. F. Badylak, D. O. Freytes and T. W. Gilbert, *Acta Biomater.*, 2015, **23**, S17–S26.
147. A. E. Loneker, D. M. Faulk, G. S. Hussey, A. D'Amore and S. F. Badylak, *J. Biomed. Mater. Res., Part A*, 2016, **104**, 957–965.
148. V. Agrawal, J. Kelly, S. Tottey, K. A. Daly, S. A. Johnson, B. F. Siu, J. Reing and S. F. Badylak, *Tissue Eng., Part A*, 2011, **17**, 3033–3044.
149. A. Nieponice, T. W. Gilbert, S. A. Johnson, N. J. Turner and S. F. Badylak, *J. Surg. Res.*, 2013, **182**, e1–e7.
150. B. M. Sicari, V. Agrawal, B. F. Siu, C. J. Medberry, C. L. Dearth, N. J. Turner and S. F. Badylak, *Tissue Eng., Part A*, 2012, **18**, 1941–1948.
151. B. M. Sicari, J. P. Rubin, C. L. Dearth, M. T. Wolf, F. Ambrosio, M. Boninger, N. J. Turner, D. J. Weber, T. W. Simpson, A. Wyse, E. H. Brown, J. L. Dziki, L. E. Fisher, S. Brown and S. F. Badylak, *Sci. Transl. Med.*, 2014, **6**, 234ra258.
152. A. Aurora, J. L. Roe, B. T. Corona and T. J. Walters, *Biomaterials*, 2015, **67**, 393–407.
153. B. M. Sicari, J. L. Dziki and S. F. Badylak, *Ann. Transl. Med.*, 2015, **3**, 256.
154. N. J. Turner and S. F. Badylak, *Cell Tissue Res.*, 2012, **347**, 759–774.
155. N. T. Remlinger, T. W. Gilbert, M. Yoshida, B. N. Guest, R. Hashizume, M. L. Weaver, W. R. Wagner, B. N. Brown, K. Tobita and P. D. Wearden, *Organogenesis*, 2013, **9**, 149–160.
156. A. Nieponice, F. F. Ciotola, F. Nachman, B. A. Jobe, T. Hoppo, R. Londono, S. Badylak and A. E. Badaloni, *Ann. Thorac. Surg.*, 2014, **97**, 283–288.
157. N. J. Turner, J. S. Badylak, D. J. Weber and S. F. Badylak, *J. Surg. Res.*, 2012, **176**, 490–502.
158. C. L. Dearth, T. J. Keane, C. A. Carruthers, J. E. Reing, L. Huleihel, C. A. Ranallo, E. W. Kollar and S. F. Badylak, *Acta Biomater.*, 2016, **33**, 78–87.
159. S. F. Badylak, *Ann. Biomed. Eng.*, 2014, **42**, 1517–1527.
160. J. Dziki, S. Badylak, M. Yabroudi, B. Sicari, F. Ambrosio, K. Stearns, N. Turner, A. Wyse, M. L. Boninger, E. H. P. Brown and J. P. Rubin, *NPJ Regener. Med.*, 2016, **1**, 16008.
161. M. A. Serban, *Curr. Opin. Biotechnol.*, 2016, **40**, 31–34.
162. E. T. Stace, S. G. Dakin, P. A. Mouthuy and A. J. Carr, *J. Cell. Physiol.*, 2016, **231**, 36–49.
163. G. D. Prestwich, S. Bhatia, C. K. Breuer, S. L. M. Dahl, C. Mason, R. McFarland, D. J. McQuillan, J. Sackner-Bernstein, J. r. Schox, W. E. Tente and A. Trounson, *Sci. Transl. Med.*, 2012, **4**, 160cm114.

CHAPTER 3

Applications of Injectable Smart Materials in Tissue Engineering

QIANG ZHAO[a]

[a]State Key Laboratory of Medicinal Chemistry, Key Laboratory of Bioactive Materials, Ministry of Education, College of Life Sciences, Nankai University, 300071, Tianjin, PR China
*E-mail: qiangzhao@nankai.edu.cn

3.1 Introduction

Tissue engineering, as an interdisciplinary field, combines the principles of life sciences and engineering to develop biological substitutes, which can restore tissue function.[1] A scaffold made from polymers plays a vital role in tissue engineering, because it provides a three-dimensional (3-D) microenvironment that dictates the fate of implanted cells, including adhesion, proliferation, migration, differentiation, and so on.

The properties of smart or stimuli-responsive materials would change in response to external stimuli, including light, temperature, an electric/magnetic field, solvent polarity, ionic strength, and biomolecules. Injectable smart hydrogels that experience sol–gel transitions induced by various stimuli have received increasing attention in tissue engineering because of the easy incorporation of cells or bioactive molecules, simplicity of administration

Smart Materials No. 25
Smart Materials for Tissue Engineering: Applications
Edited by Qun Wang

Published by the Royal Society of Chemistry, www.rsc.org

by injection, and improvement of retention and paracrine of delivered cells.[2] Besides, injectable smart hydrogels are highly desirable clinically because of the minimal invasion after percutaneous or endoscopic procedures.[3,4] In this chapter, different types of injectable smart materials formed due to distinctive mechanisms will be reviewed and their applications in tissue engineering will also be summarized.

3.2 Stimuli-Responsive Injectable Polymeric Hydrogels

3.2.1 Temperature-Responsive Injectable Hydrogels

Poly(*N*-isopropylacrylamide) (PNIPAAm) has received the most attention because of its sharp transition behavior. It shows a well-defined lower critical solution temperature (LCST) around 32–34 °C, which is close to body temperature.[5] Recently, thermosensitive injectable hydrogels based on PNIPAAm and polyethylene glycol (PEG) with different architectures have been developed for tissue engineering applications due to their excellent properties including thermosensitivity, biodegradability, biocompatibility, and easily controlled characteristics.[6]

Wagner *et al.* synthesized types of thermosensitive injectable copolymers by using *N*-isopropylacrylamide (NIPAAM), acrylic acid, *N*-acryloxysuccinimide, and polylactide–hydroxyethyl methacrylate. Collagen I could be further incorporated into this copolymer *via* covalent bonding, which results in enhanced cell adhesion on the hydrogels.[7]

The copolymer of poly(ethylene oxide) and poly(propylene oxide) (with the trade name Pluronic®) in aqueous solutions is another well-known thermosensitive injectable material.[8] It has also been frequently utilized to combine with other biodegradable polymers to provide thermal thermosensitivity. Pluronic has been chemically grafted onto chitosan to obtain a thermosensitive hydrogel, which could serve as an injectable vehicle for cell delivery, thus showing good potential for cartilage regeneration.[9]

In addition to the non-degradability, a major drawback associated with Pluronic is low stability, and the gel persists for only one day after gelation. In order to resolve these problems, PEO–PLLA–PEO was synthesized, in which the central block PPO is replaced by a degradable poly(L-lactic acid) segment, and low-molecular-weight PEO is also utilized (Figure 3.1).[10] Moreover, modification of the hydroxyl terminal group of the copolymer offers an opportunity to modulate the rheology and degradation of the hydrogels.[11] Ding *et al.* systematically investigated the effect of end-groups on the physical gelation of PLGA–PEG–PLGA aqueous solution, and further discussed the sol–gel mechanism of the thermosensitive derivatives.[12]

In general, the majority of temperature-responsive hydrogels do not solidify quickly around body temperature. To address this problem, Wang *et al.* prepared a novel hydrogel by using an ABA block copolymer, poly(ethylene glycol)-*co*-poly(propanol serinate hexamethylene urethane)-*co*-poly(ethylene

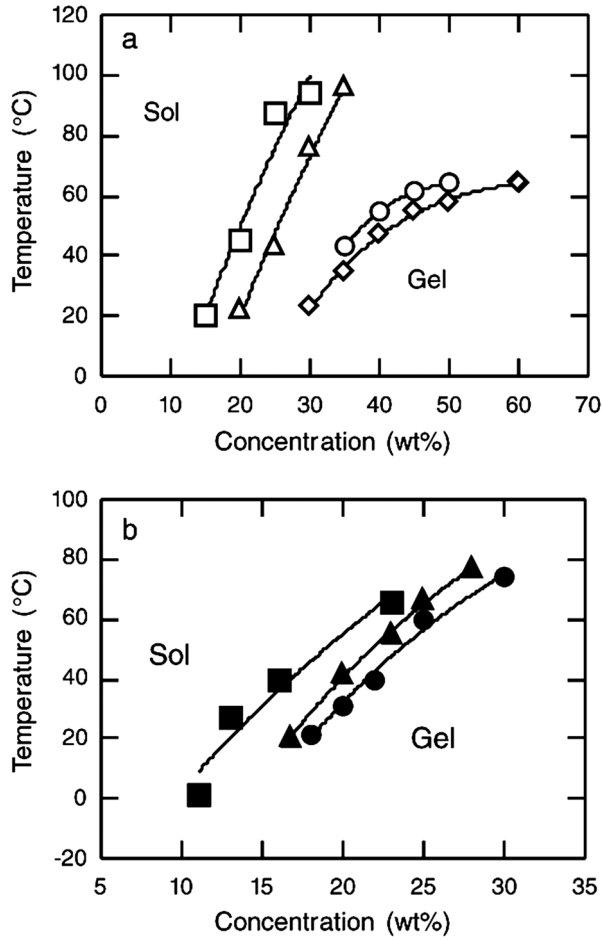

Figure 3.1 Gel–sol transitions of a PEO–PLLA diblock copolymer (a) and PEO–PLLA–PEO triblock copolymer (b). (Reprinted by permission from Macmillan Publishers Ltd: [Nature] (ref. 24), copyright (1997).)

glycol). It took less than a minute to form a gel, which demonstrates promise for internal injection applications.[13]

A thermosensitive hydrogel has also been prepared by combination of natural polymer chitosan with glycerol phosphate (GP),[14] that shows a sol–gel transition at physiological pH *via* electrostatic interactions, hydrogen bonding, and hydrophobic interactions.[15]

3.2.2 pH-Responsive Injectable Hydrogels

Polyacrylic acid (PAAc) is an example of a pH-responsive polymer that responds to the pH of a medium due to the presence of carboxyl groups. Besides, the pH sensitivity of various copolymers is imparted by incorporating carboxylic acid-derived monomers, for example AAc.[16]

Sulfamethazine oligomers (SMOs) with pH sensitivity were coupled to the terminal groups of a thermosensitive poly(ε-caprolactone-*co*-lactide)–poly (ethylene glycol)–poly(ε-caprolactone-*co*-lactide) block copolymer to generate a thermo- and pH- dually sensitive SMO–PCLA–PEG–PCLA–SMO copolymer. Under physiological conditions (37 °C and pH 7.4), the copolymer formed a stable hydrogel rapidly, while it underwent a gel–sol transition at 37 °C and pH 8.0. The hydrogel thus formed holds optimal biocompatibility and demonstrates good promise in bone tissue engineering as an injectable scaffold.[17]

Stayton and co-workers synthesized a pH- and thermo-sensitive hydrogel based on a copolymer of *N*-isopropylacrylamide and propylacrylic acid. The hydrogel could form a hydrogel at acidic pH, which shows promise to deliver drugs to local acidosis environments, including tumors, ischemia, or wound sites.[18]

3.2.3 Enzyme-Responsive Injectable Hydrogels

An enzyme-responsive injectable hydrogel is a novel type of smart material that undergoes macroscopic transitions when triggered by the selective catalysis of certain enzymes.[19] Therefore, the functions of enzymes include catalyzing synthesis and hydrolysis, thus resulting in sol-to-gel and gel-to-sol phase transitions.

3.2.3.1 Sol-to-Gel Transition

Gibson *et al.* synthesized a phosphorylated polymer based on poly(oligoethylene glycol methacrylate), and isothermal transitions could be induced by dephosphorylation mediated by alkaline phosphatase.[20]

3.2.3.2 Gel-to-Sol Transition

Over the past ten years, numerous studies have focused on the employment of matrix metalloproteinase (MMP)-sensitive peptides for the preparation of cell-invasive hydrogels, which could be hydrolyzed by MMP secreted from cells to provide space for cell migration.[21] In addition, thrombin cleavage sites have also been utilized for the construction of enzyme-degradable hydrogels.[22]

CRDTEGE-ARGSVIDRC, a peptide derived from the aggrecanase-degradable segment in aggrecan (a component of cartilage ECM), was introduced into PEG hydrogel. This system enables the encapsulation and delivery of chondrocytes for cartilage repair and regeneration.[23]

Werner *et al.* designed a thrombin-responsive hydrogel to deliver heparin in a controlled manner. The release of heparin was triggered by the level of thrombins, which play an important role in the coagulation cascade and will become inactivated because of the released heparin (Figure 3.2).[24]

Similarly, Burdick *et al.* designed a novel MMP-sensitive polysaccharide-based hydrogel, in which crosslinks could be degraded by active MMPs and encapsulated MMP inhibitors (rTIMP-3) were released locally.

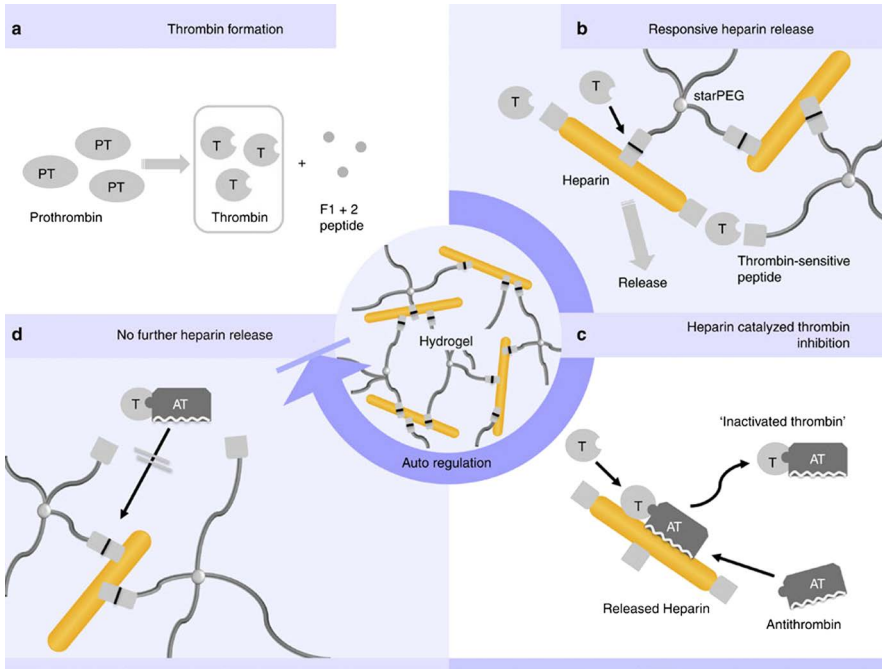

Figure 3.2 Auto-regulation of heparin released from thrombin-responsive star PEG-heparin hydrogel. (a) Thrombin generation from prothrombin. (b) Thrombin, as a selective protease, cleaves the peptide of the linker in the starPEG-heparin hydrogels. Thereafter, heparin releases. (c) Released heparin catalyses the combination of thrombin with its inhibitor, antithrombin, leading to the inactivation of thrombin. (d) Removal of thrombin terminates the degradation of hydrogels and further release of heparin. (Reprinted by permission from Macmillan Publishers Ltd: [Nature Communications] (ref. 24), copyright (2013)).

Hence, on-demand delivery of rTIMP-3 effectively decreased the activity of MMP, and reduced ventricular remodeling of an infarcted heart in a porcine model.[25]

3.3 Injectable Supramolecular Hydrogels

Different from polymer-based hydrogels formed by the covalent crosslinking of random macromolecular chains, supramolecular hydrogels are formed due to self-assembly and noncovalent interactions (hydrogen bonding, π–π stack, and electrostatic interactions), which enables them to respond rapidly to a variety of external stimuli, including temperature, pH, ionic strength, and ligand–receptor interactions.[26] The self-assembly hydrogels have received increasing attention as injectable scaffolds for tissue engineering because of the shear-thinning as well as rapid healing properties.

Due to the high interaction between β-cyclodextrins (β-CD) and adamantane with an association constant of about 3×10^4 M^{-1}, supramolecular

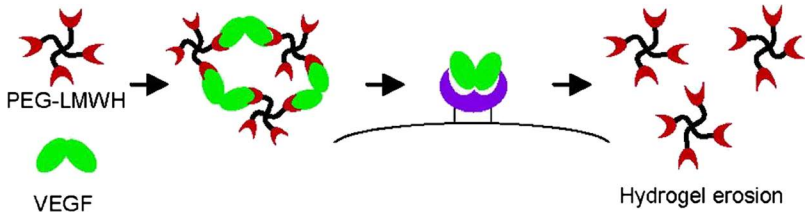

Figure 3.3 Schematic depicting gelation *via* the crosslinking of polysaccharide-based star copolymers by heparin-binding growth factor VEGFs. (Reprinted with permission from ref. 28. Copyright (2007) American Chemical Society.)

hydrogels have been constructed by the host–guest inclusion complexation between adamantyl-containing polymers and CD-dimers or polymers.[27]

The specific molecular recognition between proteins and glycosaminoglycans has been exploited to produce injectable hydrogels that are responsive and reversible. Kiick *et al.* designed a novel supramolecular hydrogel through interactions between a growth factor and a heparin-modified star PEG. This hydrogel provides an opportunity for the controlled delivery of vascular endothelial growth factor, which shows potential for application in vascular tissue engineering[28] (Figure 3.3).

Small molecular hydrogels based on peptides, as a type of supramolecular hydrogels, have been widely investigated and applied in the field of tissue engineering.[29] Xu *et al.* synthesized a novel hydrogelator on the basis of Nap-FFGEY peptide, which shows a reversible sol–gel/gel–sol transition under the catalysis of kinase/phosphatase. Therefore, the supramolecular hydrogel could be formed *in situ* after subcutaneous injection.[30]

Gelain *et al.* designed a class of biotinylated oligopeptides containing a bone marrow homing peptide 1 segment, which could form a self-healing hydrogel *via* self-assembly in β-structured fibers. Since the peptide sequence could provide a functional site for cell adhesion, and further modulate cell proliferation and differentiation, this type of injectable hydrogel provides a wide range of potential applications in tissue engineering.[31]

Yang *et al.* reported a peptide-based hydrogel capped with adamantane groups, which shows a gel–sol phase transition in the presence of β-cyclodextrin (β-CD) derivatives due to the host–guest interaction between β-CD and adamantane. It shows good potential for cell culture with the advantage of rapid recovery of cells from the gels.[32] Inspired by the structure of collagen, they also incorporated a small library of tripeptide sequences into the hydrogels, and evaluated the cell behavior. Results indicate that one peptide hydrogel has properties that are similar to those of collagen for cell culture.[33]

But the main concern about the *in vivo* application of peptide-based hydrogels is the short half-time ($t_{1/2}$ of 2–30 min) because of enzymatic degradation and rapid renal clearance.[34]

3.4 Application of Injectable Smart Materials for Tissue Repair and Regeneration

3.4.1 Bone

As a typical thermosensitive injectable hydrogel, the chitosan/β-glycerol phosphate (β-GP) system has also been intensively investigated in bone tissue engineering.[15,35,36] Liu *et al.* further added Type I collagen into this system, and evaluated the osteogenic properties of bone marrow mesenchymal stem cells (BMSCs) encapsulated in the hydrogel. *In vivo* assay indicates that the osteodifferentiation of BMSCs could be induced solely by this hydrogel without additional supply of osteogenic factors.[37]

Due to the organic/inorganic composition of natural bone, different types of inorganic fillers have been incorporated into chitosan/β-GP in order to provide mechanical reinforcement, and further induce the bone regeneration capability. Borzacchiello *et al.* utilized β-tricalcium phosphate (β-TCP) nanocrystals as an inorganic phase to mimic the chemico–physical composition of natural bone tissue.[38] The influence of β-TCP on bone regeneration was evaluated in an ectopic intramuscular bone formation model of a rat. *In vivo* results showed that mineralized bone formation was significantly enhanced in the group with β-TCP addition in contrast to the control one.[39]

In addition, many types of inorganic fillers, such as bioactive glass[40] and nanohydroxyapatite (nHAp) have been evaluated for the roles they play in promoting bone formation.[41] The results showed that osteoblast differentiation *in vitro* under osteogenic conditions was enhanced due to the addition of nHAp, and bone formation *in vivo* was also improved.[42]

Thermosensitive poly(*N*-isopropylacrylamide) (PNIPAAm) has also been utilized for bone tissue engineering by itself or combined with other natural polymers by co-polymerization. PNIPAAm was grafted onto gelatin to provide an injectable hydrogel that was beneficial for bone defect regeneration. The aforementioned hydrogel showed the ability to promote the regeneration of bone in a cranial model.[43] Chen *et al.* prepared a thermosensitive hyaluronic acid-*g*-chitosan-*g*-poly(*N*-isopropylacrylamide) (HA-CPN) copolymer,[44] and further combined it with biphasic calcium phosphate (BCP) microparticles for application in bone tissue engineering.[45] *In vitro* cell culture assay reflected that HA-CPN/BCP was a better injectable delivery system for bone cells compared to HA-CPN, and the injected cells can form ectopic bone tissue in the hydrogel composite *in vivo*. The potential of other PNIPAAm copolymers, including poly(*N*-isopropylacrylamide-*co*-butyl methylacrylate),[46] and poly(*N*-isopropylacrylamide-*co*-acrylic acid),[47] as bone tissue engineering scaffolds has also been exploited, and they were further combined with inorganic bioactive glass and hydroxyapatite (HA) for the purpose of strengthening mechanical properties and promoting bone formation.

The traditional thermosensitive PEO–PPO–PEO triblock copolymer also finds its application in bone tissue engineering.[48] It could serve as a carrier for simvastatin, and promoted bone regeneration was observed.[49] As an

alternative, triblock copolymers based on degradable polyesters were synthesized by different groups.[50–54] Qian *et al.* evaluated the potential of the PEG–PCL–PEG copolymer to serve as an injectable scaffold in guiding bone regeneration. They further found that the introduction of osteoinductive acellular bone granules into the polymer matrix could enhance bone regeneration guidance in a rabbit cranial defects model.[51] Besides, other copolymers with varied architectures such as PEG-grafted PLGA (PLGA-*g*-PEG)[55] or a methoxy polyethylene glycol–polycaprolactone diblock copolymer (MPEG–PCL)[56] have been developed for bone tissue engineering. Varied structures allow the fine tuning of biodegradability and thermosensitivity.

Mikos *et al.* developed a dual-gelling system that holds both thermal- and chemical-gelation capabilities. The hydrogel demonstrated tunable physiochemical characteristics, biocompatibility *in vivo*, and hydrophobicity-dependent mineralization.[57,58] They further evaluated its osteogenic potential for mesenchymal stem cell transplantation *in vitro* and *in vivo*. The results reveal that this injectable, dual-gelling cell-laden hydrogel could promote bone ingrowth and integration, making it a promising candidate for use in bone tissue engineering (Figure 3.4).[59,60]

Figure 3.4 Histological cross-sections stained by hematoxylin and eosin (H&E), von Kossa, and Goldner's trichrome at different timepoints. Reprinted from Biomaterials, 83, T. N. Vo, S. R. Shah, S. Lu, A. M. Tatara, E. J. Lee, T. T. Roh, Y. Tabata and A. G. Mikos, Injectable dual-gelling cell-laden composite hydrogels for bone tissue engineering, 1–11. Copyright (2016) with permission from Elsevier.

Recently, Song *et al.* reported a novel injectable and degradable thermosensitive poly(organophosphazene) hydrogel. Various substituents could be further introduced into the polymer backbone readily, which provides additional modification of the hydrogel's properties.[61] For example, hydrophobic and ionic interactions were introduced to realize the controlled delivery of bone morphogenetic protein-2. It has been functionalized by a cell binding peptide, GRGDS, and the poly(organophosphazene)–GRGDS conjugate thus prepared shows promise for inducing osteogenesis of MSC to enhance ectopic bone formation.[61,62]

Jeong *et al.* developed a thermogel based on poly(ethylene glycol)–poly(L-alanine-*co*-L-phenyl alanine), in which mesocrystals of calcium phosphate (4–8 μm) were incorporated. The inorganic/organic composite system was effective in enhancing osteogenic differentiation of tonsil-derived mesenchymal stem cells. The possible reason has been explained by the effective surfaces provided by the mesocrystals for protein binding and cell adhesion.[63]

Jabbari *et al.* synthesized an enzymatically degradable hydrogel, that is, poly(lactide-*co*-ethylene oxide-*co*-fumarate) (PLEOF) prepolymer was crosslinked with the MMP-13 cleavable peptide sequence, QPQGLAK. This type of hydrogel holds tunable degradation performance. *In vitro* assays show that bone marrow stromal cells embedded in the hydrogel can differentiate into osteoblasts and produce a mineralized matrix.[64]

A novel type of thermosensitive hydrogel based on glycosyl-nucleosyl-fluorinated compounds was prepared by Chassande and co-workers.[65] The gelation occurs within 25 min through self-assembly of monomers as the temperature decreases. Both *in vitro* and *in vivo* experiments show that this hydrogel can stimulate osteoblast differentiation of adipose-derived stem cells in the absence of osteogenic factors.

Leeuwenburgh *et al.* successfully developed a nanocomposite hydrogel on the basis of reversible bonds between calcium phosphate nanoparticles and bisphosphonate-functionalized hyaluronic acid. This kind of nanocomposite displays a self-healing capacity and good adhesion to mineral surfaces. Most importantly, the composite shows bone-inducing capacity as evidenced by bone ingrowth into the material.[66]

3.4.2 Cartilage

As an avascular and aneural tissue, articular cartilage shows limited self-healing capabilities.[67] In the case of a large-area cartilage defect, there are no effective approaches currently to completely restore injured articular cartilage in terms of morphological, biochemical, and biomechanical characteristics.[68] Currently, a strategy based on tissue engineering offers promise for cartilage repair and regeneration, in which chondrogenic cells are transplanted into a defect site through encapsulating them into an injectable hydrogel (Table 3.1).[3]

Injectable hydrogels also show particular advantages for the treatment of degenerative disc disease, because they could fill a degenerate area perfectly,

Table 3.1 Examples of injectable smart hydrogels used in cartilage tissue engineering.

Materials	Stimuli	Cell type	Application	References
Chitosan/β-glycerophosphate/ hydroxyethyl cellulose	Thermal	Mesenchymal stem cells (MSCs)	The CH–GP–HEC hydrogel provided suitable conditions for chondrogenic differentiation *in vivo*	82
Glycopolypeptide	Enzyme	Rabbit chondrocytes	Cells maintained chondrocyte phenotype and produced the cartilaginous specific matrix in a subcutaneous model of nude mice	83
Chitosan/gelatin/hyaluronic acid (HA)/β-tricalcium Phosphate	Thermal	Cell-free	*In vivo* formed hydrogel induced minimal invasion of inflammatory cells	84
Copolymer of PNIPAAm and PEG	Thermal	Cell-free	It is possible to restore angular stiffness to a cyclically fatigued spinal segment using an injectable hydrogel as a nucleus replacement	85
Poly(*N*-isopropylacrylamide)-*g*-methylcellulose (PNIPAAm-*g*-MC)	Thermal	ATDC5 cells (murine chondrogenic cell line)	PNIPAAm-*g*-MC did not affect the cell viability and proliferation, and synthesis of glycosoaminoglycans was increased	86
Chitosan–Pluronic (CP)	Thermal	Bovine chondrocytes	The proliferation of cells and the amount of synthesized glycosaminoglycan increased for 28 days	9
Pluronic F-127	Thermal	Autologous porcine auricular chondrocytes	Injection of autologous porcine auricular chondrocytes suspended in hydrogel resulted in the formation of cartilage tissue in the approximate size and shape of a human ear helix	87
Poly(*N*-isopropylacrylamide)-*g*-chondroitinsulfate (PNIPAAm-*g*-CS)	Thermal	Cell-free	The mechanical properties, bioadhesive strength, and cytocompatibility satisfy for nucleus pulposus (NP) regeneration	76

Chitosan/β-glycerol phosphate (GP)	Thermal	Primary calfarticular chondrocytes	Hydrogel can support *in vitro* and *in vivo* accumulation of cartilage matrix by primary chondrocytes, while persisting in osteochondral defects *in vivo*	88
Chitosan/β-GP/hydroxyethylcellulose (HEC)	Thermal	—	Chitosan-GP/HEC is suitable for clinical orthopedic applications involving single use treatments that guide acute cartilage repair processes	89
Chitosan/β-GP/hydroxyethylcellulose (HEC)	Thermal	Sheep chondrocytes	The hydrogel could support the matrix accumulation of chondrocytes cultured *in vitro* and could repair sheep cartilage defects in 24 weeks	90
Chitosan/gelatin/β-GP	Thermal	Nucleus pulposus (NP) cells	Gelatin added into β-GP hydrogel significantly shortened the gelation time and improved gel strength without influencing the biocompatibility	91
Chitosan-*graft*-poly(*N*-isopropylacrylamide)	Thermal	Chondrocytes and meniscus cells	The hydrogel preserved the viability and phenotypic morphology of the entrapped cells, and stimulated the initial cell–cell interactions	92
PNIPAAm-*g*-CS (chondroitin sulfate)	Thermal	—	The encapsulation of alginate microparticles within PNIPAAm-*g*-CS gels exhibited increased adhesive strength with tissue, and did not induce cytotoxicity	93
Hyaluronic acid (HA)/Pluronic F127	Thermal	Mesenchymal stromal cells (MSCs)	*In vivo* chondrogenic potential of MSCs could be affected by dexamethasone (Dex) released from microspheres encapsulated in the hydrogel	94
Poly(*N*-substituted α/β-asparagine)	Thermal	Rabbit chondrocytes	The polymers demonstrated a concentration-dependent inhibitory effect on the chondrocytes' survival. Over 70% of the chondrocytes could survive through the physical and/or chemical stress	95

and thus minimize surgical defects. In addition, hydrogels can reduce the risk of implant migration and subsequent loss of height of the intervertebral disc.[69,70] The load-bearing biomechanical function of the intervertebral disc is determined by the composition and organization of the extracellular matrix (ECM) components, collagen and aggrecan. The major role of aggrecan is to maintain tissue hydration, and hence maintain disc height under the high loads imposed by body weight and muscle activity.[71] Due to this important role, glycosaminoglycan from native ECM, including hyaluronic acid (HA)[72] and chondroitin sulfate (CS), has been utilized for the construction of hydrogel systems for nucleus pulposus (NP) regeneration (Table 3.1).[73–81]

In addition to polymers, peptide-based supramolecular hydrogels have also been utilized for cartilage regeneration. An injectable hydrogel based on self-assembling peptide (KLD) was evaluated for its ability to stimulate regeneration of the cartilage in a rabbit model of a full-thickness, critically-sized, cartilage defect. Addition of chondrogenic factors and bone marrow stromal cells remarkably reduced the quality of repair and enhanced osteophyte formation compared to a KLD control after 12 weeks.[96]

Matsuda and Ito reported a novel shear-sensitive hydrogel, which formed by supramolecular self-assembly between PDZ domain-containing fusion protein, and a PDZ domain-recognizable peptide, which was covalently linked to the terminal groups of four-armed poly(ethylene glycol). It demonstrated shear stress-dependent reversible-phase transformation. A spontaneous viscoelastic hydrogel was formed at low shear stress, but it was transformed into a sol at high shear stress. This shear-sensitive hydrogel shows potential for use as an injectable cell delivery system for cartilage repair and regeneration.[97]

Ma *et al.* developed a supramolecular hydrogel with shear-thinning and self-integrating properties, and evaluated the potential for cartilage–bone tissue regeneration in a subcutaneous implantation model of nude mice (Figure 3.5). The regeneration of the cartilage–bone tissue complex was successfully realized by using the self-integrating hydrogel with selected cells and biomolecules.[98]

3.4.3 Skin

In the field of skin tissue engineering, injectable hydrogels have attracted intensive interest because the hydrogels could produce a hydration environment, which is favorable for wound healing. Thermo-sensitive hydrogels that mold into the shape of the wound defect would be more desirable because they are a free-flowing sol at room temperature, and upon direct injection into the injury site, they would fill the wound without wrinkling or fluting. Moreover, owing to the moist environment and porous structure of hydrogels, the encapsulated bioactive substances could be delivered to the wound in a sustained manner.[99]

Injectable hydrogels formed *in situ* by enzyme catalysis have been exploited for use in skin regeneration.[100,101] Park *et al.* utilized an *in situ* gelling system containing rutin and tyramine-modified chitosan for dermal wound healing. Rutin was further added to increase secretion and accumulation of extracellular matrix during the healing process. Results showed that rutin-modified

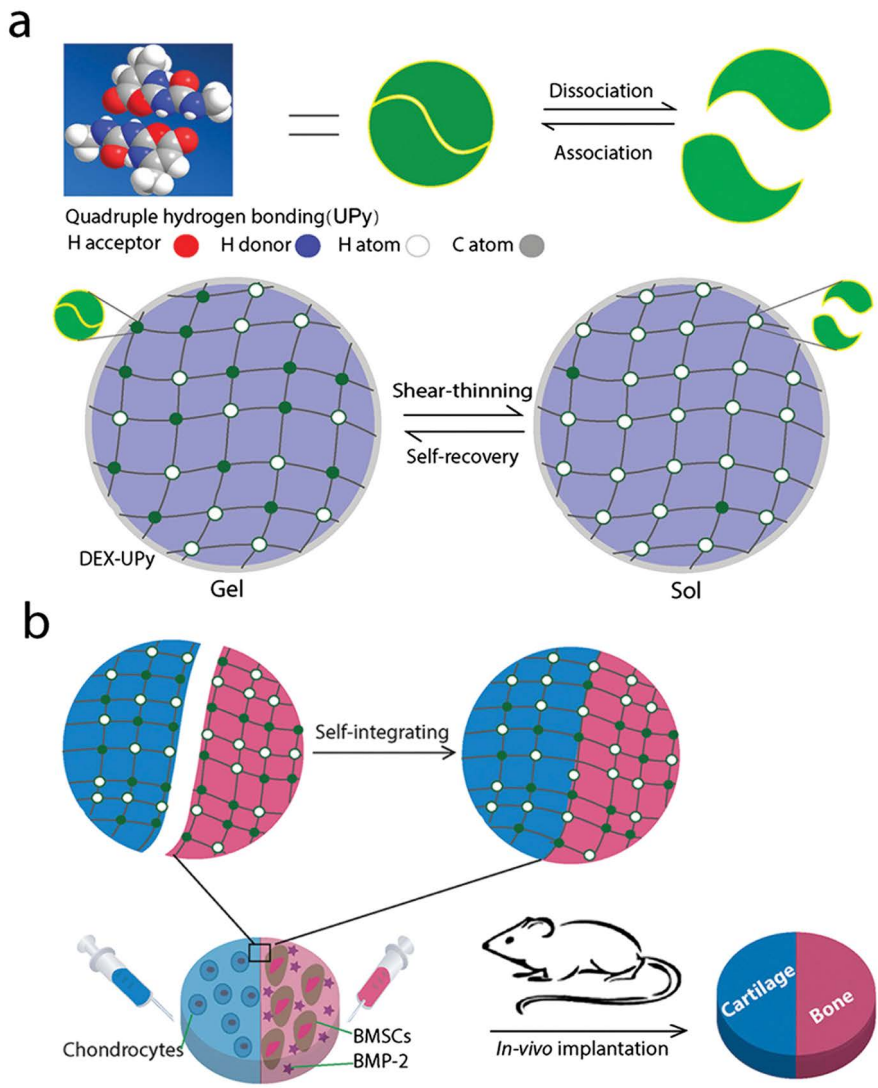

Figure 3.5 Design of a DEX-UPy hydrogel for tissue complex regeneration. a) Scheme depicting the formation of DEX-UPy hydrogel and the mechanisms of the shear-thinning and self-recovery behavior. b) Scheme depicting self-integration and application in cartilage-bone tissue complex regeneration. (From ref. 98. Copyright © 2015 by John Wiley Sons, Inc.)

hydrogels improved tissue regeneration with better defined neo-epithelium formation and thicker granulation, which was closer to the original epithelium.[102]

Our group designed a novel supramolecular hydrogel, which could release nitric oxide in an enzyme-controlled manner.[103] The hydrogel has been utilized for the topical treatment of skin wounds in mice. Controlled release of NO could promote angiogenesis in the wound bed, thus accelerating the wound healing process.

Wang *et al.* prepared an injectable hybrid hydrogel composed of a PEG-based thermosensitive hyperbranched copolymer and thiol-modified hyaluronic acid, which was further combined with adipose-derived stem cells (ADSCs). *In vitro* study showed that this hydrogel dressing system could prevent wound contraction and enhance angiogenesis, demonstrating its potential as a bioactive hydrogel dressing for wound repair.[104]

A thermosensitive hydrogel based on poly(L-lactic acid)-Pluronic L35-poly(L-lactic acid) was synthesized by Guo *et al.*, and human antimicrobial peptides 57 (AP-57)- loaded nanoparticles were further encapsulated in the hydrogel for cutaneous wound repair. In a full-thickness dermal defect model, the developed system could effectively promote cutaneous wound healing.[99]

3.4.4 Cardiovascular

Cardiovascular disease (CVD) is a major cause of mortality, accountable for 30% of global deaths per annum.[105] In recent years, tissue engineering has proved to be an effective strategy that can overcome the problems encountered in interventional therapies and heart transplantation.[106] Injectable biomaterials based on natural or synthetic polymers have been successfully utilized as scaffolds and (or) cell delivery carriers for cardiovascular tissue engineering.[107] Besides, injectable biomaterials, especially injectable smart biomaterials have provided a variety of therapeutic options for myocardial infarction (MI)[108,109] and peripheral artery disease (PAD),[110,111] such as typically thermosensitive Poloxamer 407 and other stimuli-responsive polymers.

Temperature-sensitive hydrogels based on chitosan/β-glycerophosphate (β-GP) have been widely investigated as carriers of stem cells for vascular[112] and myocardium[113] regeneration by different groups. Wang *et al.* have systematically evaluated the therapeutic effects of cell transplantation by chitosan hydrogels on damaged myocardium using different types of stem cells, including embryonic stem cells (ESCs)[114,115] as well as brown adipose derived stem cells (BADSCs).[116] The results indicate that chitosan improved the survival of transplanted BADSCs and effectively increased their differentiation rate into cardiomyocytes *in vivo*. Furthermore, BADSCs delivered by chitosan hydrogel inhibited adverse matrix remodeling, enhanced angiogenesis, and ameliorated heart function. They further modified the chitosan by covalently binding glutathione with the aim of suppressing oxidative stress damage in cardiomyocytes. Results show that the chitosan–glutathione hydrogel can remove excessive intracellular reactive oxygen species (ROS) and suppress oxidative stress damage as well as apoptosis of cardiomyocytes in the presence of high ROS.[117] Similarly, they also modified the chitosan by conjugation of a RoY peptide to enhance angiogenesis at the MI region and improve the cardiac functions.[118]

Poly(*N*-isopropylacrylamide) (PNIPAAm) with thermosensitivity has also been widely employed in cardiovascular tissue engineering.[119] Guan *et al.* prepared a series of thermosensitive hydrogels by copolymerization of *N*-isopropylacrylamide (NIPAAm) with other monomers, including *N*-acryloxysuccinimide, acrylic acid (AAc), 2-hydroxyethyl methacrylate, *etc*., and further

combined them with a natural polymer such as collagen or chondroitin sulfate (CS) to fabricate hydrogel composites.[120] This type of hydrogel demonstrated attractive properties for serving as a 3D scaffold to strengthen the efficacy of cell therapy for heart diseases.[121] They further found that the appropriate gel stiffness could induce the differentiation of mesenchymal stem cells (MSCs) into cardiac cells with high efficiency.[122,123]

Semi-interpenetrating polymer network (sIPN) hydrogels containing dextran-grafted poly(ε-caprolactone)-2-hydroxylethyl methacrylate (PCL-HEMA) and crosslinked poly(*N*-isopropylacrylamide) were utilized alone[122] or combined with cytokines[124] for the therapy of myocardial infarction (MI). The results showed that injection of these hydrogels could attenuate cardiac remodeling and ameliorate heart function after MI.

Cardiac muscle, as an electroactive tissue, is capable of transferring electrical signals, and MI is often associated with abnormal electrical function because of a massive loss of functional cardiomyocytes. Wei and co-workers introduced electroactive tetraaniline (TA) into PNIPAAm-based copolymers. The introduction of tetraaniline endowed the hydrogel with optimal electrical properties and antioxidant activities.[125]

Li *et al.* synthesized a thermosensitive hydrogel based on an aliphatic polyester, poly (δ-valerolactone)-*block*-poly(ethylene glycol)-*block*-poly(δ-valerolactone) (PVL–PEG–PVL), and further conjugated it with vascular endothelial growth factor (VEGF). When injected after MI, this hydrogel alleviated adverse cardiac remodeling and improved ventricular function. These effects could be further augmented when the VEGF was conjugated.[126]

Supramolecular hydrogels have been used in the therapy of infarcted myocardium. A type of injectable hydrogel based on α-cyclodextrin (α-CD) and poly(ethylene glycol)-*b*-polycaprolactone-(dodecanedioic acid)-polycaprolactone-poly(ethylene glycol) has been successfully developed for the therapy of myocardial infarction.[127] This hydrogel could improve the retention of transplanted cells, and prevent cardiac dysfunction.[128,129] Burdick *et al.* designed a supramolecular gel through the pendant modifications of hyaluronic acids separately by the host–guest pairing of β-cyclodextrin and adamantane. It shows shear-thinning and self-healing characteristics, which permit delivery *via* injection within the ischemic myocardium (Figure 3.6).[130] They further introduced secondary covalent crosslinking to regulate the final material's performance. Application of the dual-crosslinking hydrogel in a myocardial infarction model showed improved results compared to supramolecular hydrogel alone.[131]

A supramolecular hydrogel formed due to multiple hydrogen bonds between 2-ureido-4[1*H*]-pyrimidinone (UPy) motifs has also been selected as a delivery system for the controlled release of growth factors, which leads to an improved therapeutic effect in chronic MI.[132]

Injectable hydrogels containing matrix metalloproteinase (MMP)-responsive peptide segments show advantages in cardiac tissue engineering because they can respond to the elevated MMP levels that occur immediately after myocardial infarction.[133] These matrices provide a favorable biomimetic microenvironment to enhance the long-term outcome of cardiac stem cell therapy.[134]

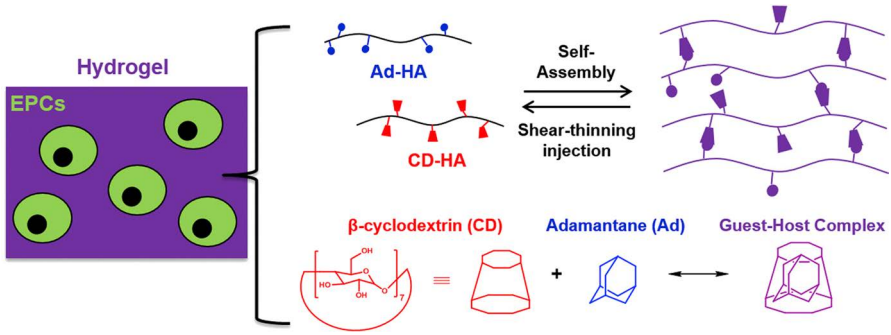

Figure 3.6 Scheme illustrating the formation of a shear-thinning hydrogel (STG) through guest–host inclusion complexation between β-cyclodextrin and adamantane. EPC, endothelial progenitor cell. Reprinted from The Journal of Thoracic and Cardiovascular Surgery, 150 (5), A. C. Gaffey, M. H. Chen, C. M. Venkataraman, A. Trubelja, C. B. Rodell, P. V. Dinh, G. Hung, J. W. MacArthur, R. V. Soopan, J. A. Burdick and P. Atluri, Injectable shear-thinning hydrogels used to deliver endothelial progenitor cells, enhance cell engraftment, and improve ischemic myocardium. 1268–1276. Copyright (2015) with permission from Elsevier.

3.4.5 Skeletal Muscle and Tendon

Xu *et al.* developed an injectable thermosensitive hydrogel through combination of chitosan/β-glycerophosphate with collagen and investigated its potential use as a cell culture substrate. The results indicate that this type of hydrogel is a cytocompatible carrier for the transplantation of skeletal muscle satellite cells (SMSCs) and provides a supportive effect for SMSC plasticity.[135]

Guan *et al.* synthesized a type of thermosensitive hydrogel from *N*-isopropylacrylamide, acrylic acid, and 2-hydroxyethyl methacrylate oligomer with a varied modulus, which plays a vital role in affecting the proliferation and myogenic differentiation of bone marrow mesenchymal stem cells (MSCs) encapsulated in the hydrogel. The injectable hydrogel with an appropriate modulus shows the potential to deliver stem cells into an ischemic limb for improved myogenic differentiation and muscle regeneration.[136] They further incorporated basic fibroblast growth factor (bFGF), a proangiogenic growth factor, into a poly(*N*-isopropylacrylamide)-based system for stem cell delivery. The released bFGF significantly improved the paracrine effects of MSCs *in vitro*. When transplanted into the ischemic limbs, this system dramatically improved MSC retention and differentiation, and a pronounced effect for ischemic limb regeneration has been observed.[137]

3.5 Conclusion and Perspective

In summary, a broad range of injectable smart materials has been successfully employed in the tissue engineering of bone, cartilage, skin, tendon, myocardium and so on. Thanks to the injectability and *in situ* gelling ability

provided by their stimuli-responsive properties, they can also serve as carriers for the delivery of cells and cytokines.

Recently, there is a trend towards *in situ* tissue engineering, in which the tissue microenvironment of the host acts as a bioreactor and the regeneration of targeted tissues is induced by the bioactivity and biofunction of the implanted scaffolds that mimic the native extracellular matrix environment.[138] In this context, the scaffold is required to hold essential physical and mechanical properties to replace the diseased tissues transiently, but also can stimulate the regeneration potential of the host to fulfill the regeneration of targeted tissues. These requirements could be satisfied through careful design and fine tuning of the properties in terms of structure, surface functionalities, degradation rate, and delivery of bioactive molecules. Besides, smart materials that could respond to the stimuli of endogenous signals show their unique advantages in mediating the interaction between the implanted materials and the host, which could further regulate the immunologic response and induce cell ingrowth, thus promoting tissue regeneration and remodeling.

References

1. R. Langer and J. P. Vacanti, *Science*, 1993, **260**, 920.
2. E. J. Kim, J. S. Choi, J. S. Kim, Y. C. Choi and Y. W. Cho, *Biomacromolecules*, 2016, **17**(1), 4.
3. A. A. Amini and L. S. Nair, *Biomed. Mater.*, 2012, **7**(2), 024105.
4. W. E. Hennink and C. F. van Nostrum, *Adv. Drug Delivery Rev.*, 2002, **54**(1), 13.
5. Z. Q. Cao, W. G. Liu, P. Gao, K. D. Yao, H. X. Li and G. C. Wang, *Polymer*, 2005, **46**, 5268.
6. A. Alexander, Ajazuddin, J. Khan, S. Saraf and S. Saraf, *Eur. J. Pharm. Biopharm.*, 2014, **88**(3), 575.
7. J. Guan, Y. Hong, Z. Ma and W. R. Wagner, *Biomacromolecules*, 2008, **9**(4), 1283.
8. R. B. Rutherford, M. Moalli, R. T. Franceschi, D. Wang, K. Gu and P. H. Krebsbach, *Tissue Eng.*, 2002, **8**(3), 441.
9. K. M. Park, S. Y. Lee, Y. K. Joung, J. S. Na, M. C. Lee and K. D. Park, *Acta Biomater.*, 2009, **5**(6), 1956.
10. B. Jeong, Y. H. Bae, D. S. Lee and S. W. Kim, *Nature*, 1997, **388**, 860.
11. M. J. Sandker, A. Petit, E. M. Redout, M. Siebelt, B. Müller, P. Bruin, R. Meyboom, T. Vermonden, W. E. Hennink and H. Weinans, *Biomaterials*, 2013, **34**(32), 8002.
12. L. Yu, H. Zhang and J. Ding, *Angew. Chem., Int. Ed. Engl.*, 2006, **45**(14), 2232.
13. M. K. Sinha, J. Gao, C. E. Stowell and Y. Wang, *Regener. Biomater.*, 2015, **2**(3), 177.
14. Y. Li, J. Rodrigues and H. Tomás, *Chem. Soc. Rev.*, 2012, **41**(6), 2193.
15. R. Ahmadi and J. D. De Bruijn, *J. Biomed. Mater. Res., Part A*, 2008, **86**(3), 824.

16. M. Ebara, Y. Kotsuchibashi, R. Narain, N. Idota, Y. J. Kim, J. M. Hoffman, K. Uto and T. Aoyagi, *Smart Biomaterials*, Springer, Japan, 2014, p. 39.
17. W. S. Shim, J. H. Kim, H. Park, K. Kim, I. K. Chan and D. S. Lee, *Biomaterials*, 2006, **27**(30), 5178.
18. J. C. Garbern, A. S. Hoffman and P. S. Stayton, *Biomacromolecules*, 2010, **11**(7), 1833.
19. R. V. Ulijn, *J. Mater. Chem.*, 2006, **16**, 2217.
20. D. J. Phillips, M. Wilde, F. Greco and M. I. Gibson, *Biomacromolecules*, 2015, **16**(10), 3256.
21. M. P. Lutolf, J. L. Lauer-Fields, H. G. Schmoekel, A. T. Metters, F. E. Weber, G. B. Fields and J. A. Hubbell, *Proc. Natl. Acad. Sci. U. S. A.*, 2003, **100**(9), 5413.
22. N. A. Zehner, S. M. Dietrick, D. A. Tirrell and S. B. Kennedy, *Biomacromolecules*, 2015, **16**(11), 3651.
23. S. C. Skaalure, S. Chu and S. J. Bryant, *Adv. Healthcare Mater.*, 2015, **4**(3), 420.
24. M. F. Maitz, U. Freudenberg, M. V. Tsurkan, M. Fischer, T. Beyrich and C. Werner, *Nat. Commun.*, 2013, **4**, 2168.
25. B. P. Purcell, D. Lobb, M. B. Charati, S. M. Dorsey, R. J. Wade, K. N. Zellars, H. Doviak, S. Pettaway, C. B. Logdon, J. A. Shuman, P. D. Freels, J. H. Gorman, R. C. Gorman, F. G. Spinale and J. A. Burdick, *Nat. Mater.*, 2014, **13**(6), 653.
26. Z. Yang, G. Liang and B. Xu, *Acc. Chem. Res.*, 2008, **41**(2), 315.
27. O. Kretschmann, S. W. Choi, M. Miyauchi, I. Tomatsu, A. Harada and H. Ritter, *Angew. Chem., Int. Ed. Engl.*, 2006, **45**(26), 4361.
28. N. Yamaguchi, L. Zhang, B. S. Chae, C. S. Palla, E. M. Furst and K. L. Kiick, *J. Am. Chem. Soc.*, 2007, **129**(11), 3040.
29. S. Toledano, R. J. Williams, V. Jayawarna and R. V. Ulijn, *J. Am. Chem. Soc.*, 2006, **128**(4), 1070.
30. Z. Yang, G. Liang, L. Wang and B. Xu, *J. Am. Chem. Soc.*, 2006, **128**(9), 3038.
31. D. Silva, A. Natalello, B. Sanii, R. Vasita, G. Saracino, R. N. Zuckermann, S. M. Doglia and F. Gelain, *Nanoscale*, 2013, **5**(2), 704.
32. C. Yang, D. Li, Z. Liu, G. Hong, J. Zhang, D. Kong and Z. Yang, *J. Phys. Chem. B*, 2012, **116**(1), 633.
33. Y. Hu, H. Wang, J. Wang, S. Wang, W. Liao, Y. Yang, Y. Zhang, D. Kong and Z. Yang, *Org. Biomol. Chem.*, 2010, **8**(14), 3267.
34. C. P. Sravan, M. R. Miller, A. Pal, J. Dong, N. R. Madadi, J. H. Xie, H. Joo, J. Tsai, P. Batoon, V. Samoshin, A. Franz, T. Cox, J. Miles, K. C. William, S. P. Miki and M. Alhamadsheh, *Nat. Chem. Biol.*, 2015, **11**, 793.
35. R. Niranjan, C. Koushik, S. Saravanan, A. Moorthi, M. Vairamani and N. Selvamurugan, *Int. J. Biol. Macromol.*, 2013, **54**, 24.
36. J. Lisková, L. Bačaková, A. L. Skwarczyńska, O. Musial, V. Bliznuk, K. D. Schamphelaere, Z. Modrzejewska and T. E. Douglas, *J. Funct. Biomater.*, 2015, **6**(2), 192.

37. B. Sun, W. Ma, F. Su, Y. Wang, J. Liu, D. Wang and H. Liu, *J. Mater. Sci.: Mater. Med.*, 2011, **22**(9), 2111.
38. M. Dessì, A. Borzacchiello, T. H. Mohamed, W. I. Abdel-Fattah and L. Ambrosio, *J. Biomed. Mater. Res., Part A*, 2013, **101**(10), 2984.
39. L. Luca, A. L. Rougemont, B. H. Walpoth, L. Boure, A. Tami, J. M. Anderson, O. Jordan and R. Gurny, *J. Biomed. Mater. Res., Part A*, 2011, **96**(1), 66.
40. D. S. Couto, Z. Hong and J. F. Mano, *Acta Biomater.*, 2009, **5**(1), 115.
41. M. Bongio, J. J. van den Beucken, S. C. Leeuwenburgh and J. A. Jansen, *J. Tissue Eng. Regener. Med.*, 2015, **9**(3), 191.
42. S. Dhivya, S. Saravanan, T. P. Sastry and N. Selvamurugan, *J. Nanobiotechnol.*, 2015, **12**, 13.
43. Z. Ren, Y. Wang, S. Ma, S. Duan, X. Yang, P. Gao, X. Zhang and Q. Cai, *ACS Appl. Mater. Interfaces*, 2015, **7**(34), 19006.
44. H. T. Liao, C. T. Chen and J. P. Chen, *Tissue Eng., Part C*, 2011, **17**(11), 1139.
45. J. P. Chen, M. J. Tsai and H. T. Liao, *Colloids Surf., B*, 2013, **110**, 120.
46. X. Chen, Y. Zhao, S. Geng, R. J. Miron, Q. Zhang, C. Wu and Y. Zhang, *Int. J. Nanomed.*, 2015, **10**, 839.
47. K. Na, S. W. Kim, B. K. Sun, D. G. Woo, H. N. Yang, H. M. Chung and K. H. Park, *Biomaterials*, 2007, **28**(16), 2631.
48. H. W. Huh, L. Zhao and S. Y. Kim, *Carbohydr. Polym.*, 2015, **126**, 130.
49. J. Tan, X. Fu, C. G. Sun, C. Liu, X. H. Zhang, Y. Y. Cui, Q. Guo, T. Ma, H. Wang, G. H. Du, X. Yin, Z. J. Liu, H. J. Leng, Y. S. Xu and C. L. Song, *Osteoporosis Int.*, 2016, **27**(2), 757.
50. S. Fu, P. Ni, B. Wang, B. Chu, L. Zheng, F. Luo, J. Luo and Z. Qian, *Biomaterials*, 2012, **33**(19), 4801.
51. P. Ni, Q. Ding, M. Fan, J. Liao, Z. Qian, J. Luo, X. Li, F. Luo, Z. Yang and Y. Wei, *Biomaterials*, 2014, **35**(1), 236.
52. P. Y. Ni, M. Fan, Z. Y. Qian, J. C. Luo, C. Y. Gong, S. Z. Fu, S. Shi, F. Luo and Z. M. Yang, *J. Biomed. Mater. Res., Part A*, 2012, **100**(1), 171.
53. Q. Yan, L. Q. Xiao, L. Tan, W. Sun, T. Wu, L. W. Chen, Y. Mei and B. Shi, *J. Biomed. Mater. Res., Part A*, 2015, **103**(11), 3580.
54. M. C. Lai, K. C. Chang, S. C. Hsu, M. C. Chou, W. I. Hung, Y. R. Hsiao, H. M. Lee, M. F. Hsieh and J. M. Yeh, *Biomed. Mater.*, 2014, **9**(1), 015011.
55. G. Lin, L. Cosimbescu, N. J. Karin and B. J. Tarasevich, *Biomed. Mater.*, 2012, **7**(2), 024107.
56. J. S. Kwon, S. W. Kim, D. Y. Kwon, S. H. Park, A. R. Son, J. H. Kim and M. S. Kim, *Biomaterials*, 2014, **35**(20), 5337.
57. T. N. Vo, A. K. Ekenseair, P. P. Spicer, B. M. Watson, S. N. Tzouanas, T. T. Roh and A. G. Mikos, *J. Controlled Release*, 2015, **205**, 25.
58. B. M. Watson, F. K. Kasper, P. S. Engel and A. G. Mikos, *Biomacromolecules*, 2014, **15**(5), 1788.
59. T. N. Vo, S. R. Shah, S. Lu, A. M. Tatara, E. J. Lee, T. T. Roh, Y. Tabata and A. G. Mikos, *Biomaterials*, 2016, **83**, 1.

60. B. M. Watson, T. N. Vo, A. M. Tatara, S. R. Shah, D. W. Scott, P. S. Engel and A. G. Mikos, *Biomaterials*, 2015, **67**, 286.
61. C. Chun, H. J. Lim, K. Y. Hong, K. H. Park and S. C. Song, *Biomaterials*, 2009, **30**(31), 6295.
62. B. B. Seo, H. Choi, J. T. Koh and S. C. Song, *J. Controlled Release*, 2015, **209**, 67.
63. H. J. Moon, M. Patel, H. Chung and B. Jeong, *Adv. Healthcare Mater.*, 2016, **5**(3), 353.
64. X. He and E. Jabbari, *Biomacromolecules*, 2007, **8**(3), 780.
65. S. Ziane, S. Schlaubitz, S. Miraux, A. Patwa, C. Lalande, I. Bilem, S. Lepreux, B. Rousseau, J. F. Le Meins, L. Latxague, P. Barthélémy and O. Chassande, *Eur. Cells Mater.*, 2012, **23**, 147.
66. M. R. Nejadnik, X. Yang, M. Bongio, H. S. Alghamdi, J. J. van den Beucken, M. C. Huysmans, J. A. Jansen, J. Hilborn, D. Ossipov and S. C. Leeuwenburgh, *Biomaterials*, 2014, **35**(25), 6918.
67. M. Kim, S. E. Kim, S. S. Kang, Y. H. Kim and G. Tae, *Biomaterials*, 2011, **32**(31), 7883.
68. B. W. Qi, A. X. Yu, S. B. Zhu, M. Zhou and G. Wu, *Exp. Biol. Med.*, 2013, **238**(1), 23.
69. J. Hu, B. Chen, F. Guo, J. Du, P. Gu, X. Lin, W. Yang, H. Zhang, M. Lu, Y. Huang and G. Xu, *J. Mater. Sci.: Mater. Med.*, 2012, **23**(3), 711.
70. M. Likhitpanichkul, M. Dreischarf, S. Illien-Junger, B. A. Walter, T. Nukaga, R. G. Long, D. Sakai, A. C. Hecht and J. C. Iatridis, *Eur. Cells Mater.*, 2014, **28**, 25.
71. S. S. Sivan, S. Roberts, J. P. Urban, J. Menage, J. Bramhill, D. Campbell, V. J. Franklin, F. Lydon, Y. Merkher, A. Maroudas and B. J. Tighe, *Acta Biomater.*, 2014, **10**(3), 1124.
72. G. D. Prestwich, *J. Controlled Release*, 2011, **155**(2), 193.
73. J. E. Frith, A. R. Cameron, D. J. Menzies, P. Ghosh, D. L. Whitehead, S. Gronthos, A. C. Zannettino and J. J. Cooper-White, *Biomaterials*, 2013, **34**(37), 9430.
74. W. Y. Su, Y. C. Chen and F. H. Lin, *Acta Biomater.*, 2010, **6**(8), 3044.
75. E. C. Collin, S. Grad, D. I. Zeugolis, C. S. Vinatier, J. R. Clouet, J. J. Guicheux, P. Weiss, M. Alini and A. S. Pandit, *Biomaterials*, 2011, **32**(11), 2862.
76. C. Wiltsey, P. Kubinski, T. Christiani, K. Toomer, J. Sheehan, A. Branda, J. Kadlowec, C. Iftode and J. Vernengo, *J. Mater. Sci.: Mater. Med.*, 2013, **24**(4), 837.
77. A. Gloria, A. Borzacchiello, F. Causa and L. Ambrosio, *J. Biomater. Appl.*, 2012, **26**(6), 745.
78. J. M. Cloyd, N. R. Malhotra, L. Weng, W. Chen, R. L. Mauck and D. M. Elliott, *Eur. Spine J.*, 2007, **16**(11), 1892.
79. S. Nakashima, Y. Matsuyama, K. Takahashi, T. Satoh, H. Koie, K. Kanayama, T. Tsuji, K. Maruyama, S. Imagama, Y. Sakai and N. Ishiguro, *Biomed. Mater. Eng.*, 2009, **19**(6), 421.

80. Y. C. Chen, W. Y. Su, S. H. Yang, A. Gefen and F. H. Lin, *Acta Biomater.*, 2013, **9**(2), 5181.
81. I. L. Moss, L. Gordon, K. A. Woodhouse, C. M. Whyne and A. J. Yee, *Spine*, 2011, **36**(13), 1022.
82. H. Naderi-Meshkin, K. Andreas, M. M. Matin, M. Sittinger, H. R. Bidkhori, N. Ahmadiankia, A. R. Bahrami and J. Ringe, *Cell Biol. Int.*, 2014, **38**(1), 72.
83. K. Ren, C. He, C. Xiao, G. Li and X. Chen, *Biomaterials*, 2015, **51**, 238.
84. K. J. Walker and S. V. Madihally, *J. Biomed. Mater. Res., Part B*, 2015, **103**(6), 1149.
85. C. Balkovec, J. Vernengo and S. M. McGill, *J. Biomech. Eng.*, 2013, **135**(6), 61004.
86. H. Sá-Lima, K. Tuzlakoglu, J. F. Mano and R. L. Reis, *J. Biomed. Mater. Res., Part A*, 2011, **98**(4), 596.
87. A. B. Saim, Y. Cao, Y. Weng, C. N. Chang, M. A. Vacanti, C. A. Vacanti and R. D. Eavey, *Laryngoscope*, 2000, **110**, 1694.
88. C. D. Hoemann, J. Sun, A. Légaré, M. D. McKee and M. D. Buschmann, *Osteoarthritis Cartilage*, 2005, **13**(4), 318.
89. C. D. Hoemann, A. Chenite, J. Sun, M. Hurtig, A. Serreqi, Z. Lu, E. Rossomacha and M. D. Buschmann, *J. Biomed. Mater. Res., Part A*, 2007, **83**(2), 521.
90. T. Hao, N. Wen, J. K. Cao, H. B. Wang, S. H. Lü, T. Liu, Q. X. Lin, C. M. Duan and C. Y. Wang, *Osteoarthritis Cartilage*, 2010, **18**(2), 257.
91. Y. H. Cheng, S. H. Yang, W. Y. Su, Y. C. Chen, K. C. Yang, W. T. Cheng, S. C. Wu and F. H. Lin, *Tissue Eng., Part A*, 2010, **16**(2), 695.
92. J. P. Chen and T. H. Cheng, *Macromol. Biosci.*, 2006, **6**(12), 1026.
93. C. Wiltsey, T. Christiani, J. Williams, J. Scaramazza, C. Van Sciver, K. Toomer, J. Sheehan, A. Branda, A. Nitzl, E. England, J. Kadlowec, C. Iftode and J. Vernengo, *Acta Biomater.*, 2015, **16**, 71.
94. S. E. Bae, D. H. Choi, D. K. Han and K. Park, *J. Controlled Release*, 2010, **143**(1), 23.
95. S. K. Chueh, Y. Tachibana, H. Uyama, S. Kobayashi and N. Tomita, *Biomed. Mater. Eng.*, 2007, **17**(3), 137.
96. R. E. Miller, A. J. Grodzinsky, E. J. Vanderploeg, C. Lee, D. J. Ferris, M. F. Barrett, J. D. Kisiday and D. D. Frisbie, *Osteoarthritis Cartilage*, 2010, **18**(12), 1608.
97. F. Ito, K. Usui, D. Kawahara, A. Suenaga, T. Maki, S. Kidoaki, H. Suzuki, M. Taiji, M. Itoh, Y. Hayashizaki and T. Matsuda, *Biomaterials*, 2010, **31**(1), 58.
98. S. Hou, X. Wang, S. Park, X. Jin and P. X. Ma, *Adv. Healthcare Mater.*, 2015, **4**(10), 1491.
99. X. Li, R. Fan, A. Tong, M. Yang, J. Deng, L. Zhou, X. Zhang and G. Guo, *Int. J. Pharm.*, 2015, **495**(1), 560.
100. K. M. Park, Y. Lee, J. Y. Son, D. H. Oh, J. S. Lee and K. D. Park, *Biomacromolecules*, 2012, **13**, 604.

101. B. H. Hu and P. B. Messersmith, *Orthod. Craniofac. Res.*, 2005, **8**(3), 145.
102. N. Q. Tran, Y. K. Joung, E. Lih and K. D. Park, *Biomacromolecules*, 2011, **12**(8), 2872.
103. J. Gao, W. Zheng, J. Zhang, D. Guan, Z. Yang, D. Kong and Q. Zhao, *Chem. Commun.*, 2013, **49**(80), 9173.
104. Y. Dong, W. U. Hassan, R. Kennedy, U. Greiser, A. Pandit, Y. Garcia and W. Wang, *Acta Biomater.*, 2014, **10**(5), 2076.
105. Q. Zhao, J. Zhang, L. Song, Q. Ji, Y. Yao, Y. Cui, J. Shen, P. G. Wang and D. Kong, *Biomaterials*, 2013, **34**, 8450.
106. J. Radhakrishnan, U. M. Krishnan and S. Sethuraman, *Biotechnol. Adv.*, 2014, **32**(2), 449.
107. Z. Ye, Y. Zhou, H. Cai and W. Tan, *Adv. Drug Delivery Rev.*, 2011, **63**(8), 688.
108. M. M. Nguyen, N. C. Gianneschi and K. L. Christman, *Curr. Opin. Biotechnol.*, 2015, **34**, 225.
109. T. D. Johnson and K. L. Christman, *Expert Opin. Drug Delivery*, 2013, **10**(1), 59.
110. J. L. Ungerleider and K. L. Christman, *Stem Cells Transl. Med.*, 2014, **3**(9), 1090.
111. M. R. Blatchley and S. Gerecht, *Biomed. Mater.*, 2015, **10**(3), 034001.
112. W. S. Sheridan, O. B. Grant, G. P. Duffy and B. P. Murphy, *J. Biomed. Mater. Res., Part B*, 2014, **102**(8), 1700.
113. D. Zhou, L. Xiong, Q. Wu, R. Guo, Z. Zhou, Q. Zhu, Y. Jiang and J. Huang, *J. Biomed. Mater. Res., Part A*, 2013, **101**(2), 567.
114. W. N. Lu, S. H. Lü, H. B. Wang, D. X. Li, C. M. Duan, Z. Q. Liu, T. Hao, W. J. He, B. Xu, Q. Fu, Y. C. Song, X. H. Xie and C. Y. Wang, *Tissue Eng., Part A*, 2009, **15**(6), 1437.
115. S. Lü, H. Wang, W. Lu, S. Liu, Q. Lin, D. Li, C. Duan, T. Hao, J. Zhou, Y. Wang, S. Gao and C. Wang, *Tissue Eng., Part A*, 2010, **16**(4), 1303.
116. H. Wang, J. Shi, Y. Wang, Y. Yin, L. Wang, J. Liu, Z. Liu, C. Duan, P. Zhu and C. Wang, *Biomaterials*, 2014, **35**(13), 3986.
117. J. Li, Y. Shu, T. Hao, Y. Wang, Y. Qian, C. Duan, H. Sun, Q. Lin and C. Wang, *Biomaterials*, 2013, **34**(36), 9071.
118. Y. Shu, T. Hao, F. Yao, Y. Qian, Y. Wang, B. Yang, J. Li and C. Wang, *ACS Appl. Mater. Interfaces*, 2015, **7**(12), 6505.
119. Y. Xia, K. Zhu, H. Lai, M. Lang, Y. Xiao, S. Lian, C. Guo and C. Wang, *Exp. Biol. Med.*, 2015, **240**(5), 593.
120. F. Wang, Z. Li, M. Khan, K. Tamama, P. Kuppusamy, W. R. Wagner, C. K. Sen and J. Guan, *Acta Biomater.*, 2010, **6**(6), 1978.
121. Z. Li, X. Guo and J. Guan, *Biomaterials*, 2012, **33**(25), 5914.
122. Z. Li, X. Guo, A. F. Palmer, H. Das and J. Guan, *Acta Biomater.*, 2012, **8**(10), 3586.
123. Z. Li, X. Guo, S. Matsushita and J. Guan, *Biomaterials*, 2011, **32**(12), 3220.
124. Y. Y. He, Y. Wen, X. X. Zheng and X. J. Jiang, *J. Cardiovasc. Pharmacol.*, 2013, **61**(4), 283.

125. H. Cui, Y. Liu, Y. Cheng, Z. Zhang, P. Zhang, X. Chen and Y. Wei, *Biomacromolecules*, 2014, **15**(4), 1115.
126. J. Wu, F. Zeng, X. P. Huang, J. C. Chung, F. Konecny, R. D. Weisel and R. K. Li, *Biomaterials*, 2011, **32**(2), 579.
127. X. J. Jiang, T. Wang, X. Y. Li, D. Q. Wu, Z. B. Zheng, J. F. Zhang, J. L. Chen, B. Peng, H. Jiang, C. Huang and X. Z. Zhang, *J. Biomed. Mater. Res., Part A*, 2009, **90**(2), 472.
128. J. Chen, R. Guo, Q. Zhou and T. Wang, *Kaohsiung. J. Med. Sci.*, 2014, **30**(4), 173.
129. T. Wang, X. J. Jiang, Q. Z. Tang, X. Y. Li, T. Lin, D. Q. Wu, X. Z. Zhang and E. Okello, *Acta Biomater.*, 2009, **5**(8), 2939.
130. A. C. Gaffey, M. H. Chen, C. M. Venkataraman, A. Trubelja, C. B. Rodell, P. V. Dinh, G. Hung, J. W. MacArthur, R. V. Soopan, J. A. Burdick and P. Atluri, *J. Thorac. Cardiovasc. Surg.*, 2015, **150**(5), 1268.
131. C. B. Rodell, J. W. MacArthur, S. M. Dorsey, R. J. Wade, Y. J. Woo and J. A. Burdick, *Adv. Funct. Mater.*, 2015, **25**(4), 636.
132. S. Koudstaal, M. M. Bastings, D. A. Feyen, C. D. Waring, F. J. van Slochteren, P. Y. Dankers, D. Torella, J. P. Sluijter, B. Nadal-Ginard, P. A. Doevendans, G. M. Ellison and S. A. Chamuleau, *J. Cardiovasc. Transl. Res.*, 2014, **7**(2), 232.
133. T. P. Kraehenbuehl, L. S. Ferreira, A. M. Hayward, M. Nahrendorf, A. J. van der Vlies, E. Vasile, R. Weissleder, R. Langer and J. A. Hubbell, *Biomaterials*, 2011, **32**(4), 1102.
134. S. T. Wall, C. C. Yeh, R. Y. Tu, M. J. Mann and K. E. Healy, *J. Biomed. Mater. Res., Part A*, 2010, **95**(4), 1055.
135. K. Ding, Z. Yang, Y. L. Zhang and J. Z. Xu, *Cell Biol. Int.*, 2013, **37**(9), 977.
136. Y. Xu, Z. Li, X. Li, Z. Fan, Z. Liu, X. Xie and J. Guan, *Acta Biomater.*, 2015, **26**, 23.
137. Y. Xu, M. Fu, Z. Li, Z. Fan, X. Li, Y. Liu, P. M. Anderson, X. Xie, Z. Liu and J. Guan, *Acta Biomater.*, 2016, **31**, 99.
138. S. Li, D. Sengupta and S. Chien, *Wiley Interdiscip. Rev.: Syst. Biol. Med.*, 2014, **6**, 61.

CHAPTER 4

Advances in Silicon Smart Materials for Tissue Engineering

NELLI K. BODIFORD[a] AND JEFFERY L. COFFER*[a]

[a]Texas Christian University, Department of Chemistry & Biochemistry, 2800 S. University Dr, Fort Worth, 76129, USA
*E-mail: j.coffer@tcu.edu

4.1 Introduction

One of the greatest achievements of the 20th and 21st centuries has been a dramatic increase in average life expectancy, attributed mainly due to the development of successful treatments against numerous infectious and parasitic diseases. As a result, new human pathologies related to aging have emerged—chronic wounds, arthritis, bone disorders, or eye diseases. These new diseases have, in turn, created demands for novel approaches in areas such as regenerative medicine. Within this field, a more recent focus has been on the development of "smart" scaffolds, materials that not only avoid the size limitation of autologous tissue grafts or immune issues associated with transplantation from allogeneic or xenogeneic donors, but also provide a rapid therapeutic response to an onsite-detected medical concern emerging from an integrated sensing component of the structure. At a minimum, several key requirements must be met in order for these synthetic scaffolds to assist in healing and regenerative processes: (i) provide cellular attachment,

Smart Materials No. 25
Smart Materials for Tissue Engineering: Applications
Edited by Qun Wang

Published by the Royal Society of Chemistry, www.rsc.org

proliferation and differentiation, (ii) possess a three-dimensional structure that ensures cell spreading and organization as well as vasculature and neural growth, and (iii) dissolve back into the body after implantation.

While extensive effort has been expended in polymer, ceramic, and metallic-based structures, semiconducting materials have, for the most part, been under-investigated. Of the available options, elemental silicon (Si) is clearly the paradigm, but bulk crystalline silicon commonly used in electronic device platforms is best known as being bioinert. In contrast, the transformation of crystalline Si to a porous morphology known as porous silicon (pSi) has created a material of significant interest for possible use in tissue engineering due to two significant discoveries: (1) in 1990, the report of strong visible photoluminescence from pSi by Canham[1] initiated extensive effort into the use of pSi as a sensing platform and eventual merit as a self-reporting drug delivery device[2] (see Table 4.1); (2) in 1995, mesoporous silicon was shown to be a bioactive material[3] that can induce hydroxyapatite growth (the main constituent of bone), along with its non-toxic degradation into orthosilicic acid.[4] The unique and useful features of this material—a large surface area, controllable pore size, and tunable surface chemistry—not to mention its intrinsic semiconducting character—has opened a wide avenue of opportunities for the use of this material in medical diagnosis and therapy.

Challenges associated with the manipulation of single pSi particles or sharp edge-induced *in vivo* inflammatory response of the as-prepared microparticles can be readily addressed through the use of a combination of biodegradable polymers (or hydrogels) and porous silicon. Some significant advantages are readily envisioned: flexible mechanical properties of the polymer allow for an easy molding into various shapes and forms required for the site of an injury (as the polymer matrix can conform to the specific shape of an actual defect or trauma site); opportunities for the incorporation of sites demonstrating different degradation kinetics (two stage drug delivery vehicles and beyond); more facile incorporation of heterogeneous materials (hard/soft).

In this chapter we will review selected examples illustrating how pSi micro/nanostructures and pSi/polymer composites represent a new class of "smart' materials suitable for tissue engineering.

4.2 Fundamentals of Porous Silicon (pSi)

4.2.1 Porous Silicon (pSi) Can Be Processed into a Variety of Shapes and Forms

In the case of tissue engineering scaffold design, one has to consider the variety of physical forms that a material needs to conform to in order to ensure optimum cellular attachment, differentiation, and proliferation. Multiple particle shapes have been investigated for the possible exploitation of pSi as a theranostic platform, including thin films, as-prepared coarse microparticles, lithographically-designed hemispherical domes,[5] square-shaped

Table 4.1 Key milestones for pSi as a "smart" material.

Milestone	Property evaluated	Reference
pH-Responsive	Thermally hydrocarbonized pSi nanoparticles functionalized with chitosan and coated with a pH-responsive polymer, hydroxyl-propylmethyl cellulose acetate succinate (HPMCAS-MF) for a dual protein-drug (GLP-1 and DPP4) delivery system	[49] (2015)
	PSi loaded with sorafenib and functionalized with a pH-responsive polymer—polyethylene glycol-*block*-poly(L-histidine) and poly(ethylene glycol)-*block*-polylactide methyl ether—for a multi-stage drug delivery system (MDDS)	[50] (2015)
	Thermally hydrocarbonized pSi loaded with atorvastatin followed by encapsulation into the pH-responsive polymer (hypromellose acetate succinate) containing celecoxib to obtain a multi-drug loaded system for combination therapy	[51] (2014)
	The PSi external surface was functionalized with folic acid and fluorescein isothiocyanate for targeting and imaging, respectively. The pore walls were functionalized with carboxyl groups to obtain a higher loading degree of doxorubicin and promote a pH-triggered drug release	[52] (2014)
	Photonic pSi film coated with pH-responsive polymer 2-diethylaminoethyl acrylate (*p*-DEAEA), is used to detect pH changes during acidification of chronic wound fluid as a result of bacterial infection	[53] (2014)
	pSi nanoparticles with a pH-responsive nano valve consisting of an aromatic amino group and a cyclodextrin cap for drug release inside cells	[54] (2011)
	The pore openings of the pSi nanoparticles were grafted with a pH-responsive nano valve of poly(β-amino ester) and the external surface with Pluronic F-127. The drug PTX was encapsulated into the external layer of Pluronic F-127 and DOX was loaded inside the pores thus enabling spatiotemporal drug release	[55] (2015)
	pH-triggered release of the antibiotic vancomycin from porous Si films containing a BSA protein-capping layer	[56] (2008)
	PSi nanoparticles are functionalized with pH-responsive PEGDB polymers. This nanocomposite exhibits improved endosomal escape and thus improved PNA delivery to cytosol where target miRNA are located	[57,58] (2016, 2014)
Temperature-responsive	Thermoresponsive amine-terminated poly(*N*-isopropylacrylamide) brushes are grafted to thin films of freshly-etched porous Si	[59] (2009)
	PSi was loaded with camptothecin and coated with temperature-responsive poly(*N*-isopropylacrylamide-*co*-diethylene glycol divinyl ether) to achieve a sustainable and temperature-dependent drug delivery	[60] (2016)
	PSi films coated with thermoresponsive polymer, poly(*N*-isopropylacrylamide), for a feedback-controlled drug release	[61] (2011)
	PSi nanoparticles were loaded with doxorubicin hydrochloride and trigger the release either under IR or RF irradiation	[62] (2016)

Self-reporting (biosensor)	Psi-based system as a label-free, non-invasive method to continuously monitor cell morphology known as a "smart" petri dish	[63] (2006)
	PSi-optical sensor interfaced with human epithelial cells on the peptide-functionalized regions for detection of cellular responses	[64] (2011)
	PSi-optical sensor coated with an enzymatic degradable polymer, poly(oligoethylene glycol-*co*-acrylic acid)-N_3 to monitor matrix metalloproteinases' enzyme activity	[65] (2014)
	PSi grafted with resazurin as a luminescence-enhancing optical biosensing platform for L-lactate dehydrogenase detection	[66] (2015)
	PSi rugate filter is biocompatible and optically functional *in vitro*, and importantly, in a subcutaneous passive biosensing setting	[67] (2016)
	PSi-optical sensor to monitor the release of bovine serum albumin (BSA), a model protein payload	[68] (2016)
	The incorporation of a chemically-sensitive hydrogel into a 1D photonic pSi transducer is evaluated upon exposure to a target-reducing agent analyte, tris(2-carboxyethyl) phosphine. This sensing system is capable of direct visual color readout	[69] (2010)
	Photonic pSi coated with a pH-responsive polymer can be used to detect pH changes in aqueous media in order to report on acidification of chronic wound fluid through a color change that is visible to the unaided eye	[53] (2014)
	PSi as a label-free sensor that is applicable for rapid detection of cell capture events and identification of microorganisms *e.g.*, bacteria (*E. coli*)	[70] (2014)
	Intravitreal biocompatibility and dissolution of pSi microparticles with the feasibility of pSi as a platform for an intraocular drug-delivery system with a non-invasive remote monitoring of drug release	[71] (2008)
Self-sealing	PSi particles loaded with siRNA act as a self-sealing device through formation of an insoluble salt shell (calcium silicate) inside the pores to protect high concentrations of siRNA	[72,73] (2016, 2010)
Self-assembling	The suitably-modified pSi particles spontaneously align at an organic liquid–water interface, with the hydrophobic side oriented toward the organic phase and the hydrophilic side toward the water. Sensing is accomplished when liquid at the interface infuses into the porous mirrors, inducing predictable shifts in the optical spectra of both mirrors	[2] (2003)
	Thermally hydrocarbonized pSi nanoparticles were modified with a self-assembled coating consisting of fungal hydrophobin (HFBII), which showed an increased accumulation in the liver and spleen compared to the uncoated nanoparticles	[74] (2012)
Electronically-responsive	The controlled release of encapsulated charged species to and from a semi-conducting calcium phosphate/pSi structure was reported, utilizing the electrical conductivity of the material	[75] (2006)

nanoparticles created *via* perforated etching methods,[6] silicon nanotubes,[7] as well as porous machined cubes,[8] and nanoneedles,[9] some of which are illustrated in Figure 4.1. The disc, cube, and related small nanoparticle morphologies of pSi are most commonly investigated with regard to circulatory system-based drug delivery, rather than selected areas of tissue regeneration.

Mesoporous silicon microparticles like those shown in Figure 4.1(E) and (F) have been extensively studied as a drug delivery carrier due to multiple properties (in addition to shape) that are advantageous to drug delivery: tunable pore size and volume; an ability to enhance drug solubility; as well as controlled degradation kinetics either *via* surface modification[11,12] or porosity[4] (*vide infra*). This topic has been reviewed extensively in multiple recent reports.[13–16] Relevant to tissue engineering, pSi can be loaded with various small molecule drugs as well as selected biologics (peptides, enzymes or genes) that can be released afterwards in a sustainable fashion inside a living body to promote tissue healing and regeneration.

One pointed example of this shape-influenced usefulness in therapeutics is the demonstration by Chiappini *et al.* of the successful injection of nucleic acids *via* vertical array of biodegradable porous nanoneedles,[9] which are shown in Figure 4.1(D). The intracellular delivery of nucleic acids enables gene expression regulation thus enabling *in vivo* cellular reprogramming. Consequently, they were able to deliver an angiogenic gene, which triggered

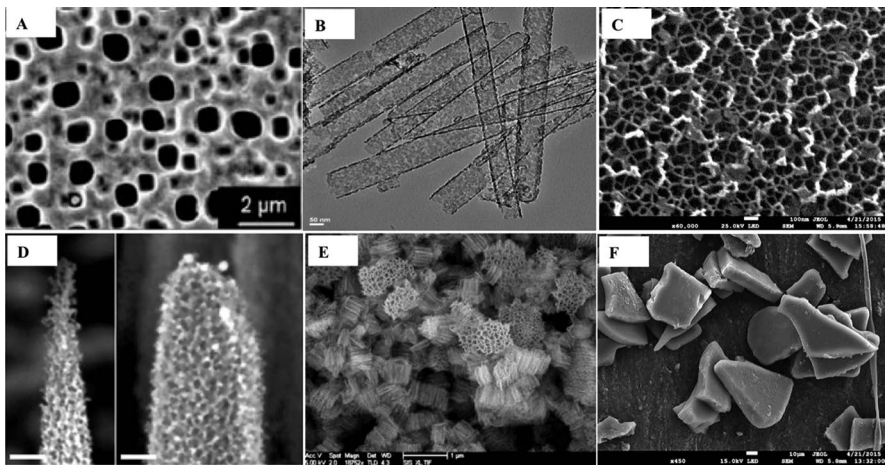

Figure 4.1 Representative shapes and pores of pSi: (A) macroporous Si film, scale bar = 2 μm[10], (B) porous wall silicon nanotubes loaded with cisplatin, scale bar = 50 nm (photo credit: Roberto Gonzalez-Rodriguez, TCU), (C) nanosize pores of microparticles in (F), scale bar = 100 nm, (D) pSi nanoneedles with the tip diameter ranging from less than 100 nm to 400 nm, scale bar = 200 nm (adapted by permission from Macmillan Publishers Ltd: Nature Materials Chiappini *et al.*[9] copyright (2015)), (E) perforated pSi nanostructures, scale bar = 1 μm[6] (photo credit: Chia-Chen Wu, UCSD), (F) free-standing mesoporous Si microparticles, scale bar = 10 μm (photo credit: Nelli Bodiford, TCU).

the patterned formation of new blood vessels within the tissue, thus establishing local control of damaged tissue.

4.2.2 Control Over Pore Structure

The porosification of bulk Si into a porous biocompatible material is most commonly achieved by anodic galvanostatic etching of monocrystalline silicon, using ethanolic hydrofluoric acid (HF) as an electrolyte.[17,18] Pore sizes can range from microporous (less then 2 nm)[19–21] to mesoporous (2–50 nm),[22] to macroporous (>50 nm).[23] An extremely broad range of pore morphologies has been observed, strongly dependent on Si wafer resistivity, magnitude of anodic bias and its duration, electrolyte composition, *etc*.[24] For biomaterial applications, the mesoporous material is most commonly studied, as its window for resorption *in vivo* is most appropriate.[16] Morphologically, this anodically-prepared mesoporous material is often described in terms of a dendritic structure, and also can be created with very high surface areas (in some cases >800 $m^2\ g^{-1}$),[25] which is a key parameter when used to carry useful payloads of drugs, proteins, and peptides. This includes actives relevant to tissue engineering (therapeutic triggers for the enhancement of cell differentiation and/or vascularization). Furthermore, the presence of very small pores in this mesoporous structure (5–50 nm) can influence the crystalline character of solid drugs loaded into the pSi matrix, in some cases inducing amorphization or nanostructuring, that can influence aqueous dissolution behavior and drug release *in vitro/in vivo.*[26]

While pSi prepared by galvanostatic processes certainly dominate the literature, it should be pointed out that additional fabrication options are available, including so-called "open circuit" metal-assisted chemical etching routes,[27] along with eco-friendly methods employing silicon-accumulator plants.[28] Both permit the use of lower cost silicon feedstocks, but produce a rather different morphology than the anodized material.

4.2.3 Surface Chemistry

Surface chemistry plays a critical role in determining whether a designed implant will be accepted or rejected by the host tissue. Especially at the early stages, cell adhesion and cell spreading will be highly dependent on surface chemistry. Porous silicon can be modified with a diverse range of surface chemical moieties to accommodate requirements such as stability in physiological media for a chosen period of time, cell attachment and differentiation, as well as controlled drug delivery.

The surface chemistry of freshly etched, anodized porous silicon is hydride-terminated. Such Si-H_x (x = 1, 2) species are unstable in ambient air and physiological media. In the presence of water, oxidative hydrolysis leads to surface degradation that in turn can impede initial cell attachment. Fortunately, these Si-H_x functionalities can be modified *via* three main routes: thermal oxidation, hydrosilylation and hydrocarbonization.

One of the most commonly used stabilization methods is oxidation of the surface of pSi. In addition to the increased stability, this method also changes the pSi surface from hydrophobic to hydrophilic. The simplest route involves short-term annealing of the pSi in air or oxygen at elevated temperatures (*ca.* 600 °C), but there are multiple oxidation methods as well as other surface functionalization techniques for altering *in vitro/in vivo* degradative stability that have been reviewed elsewhere.[29,30] Besides affecting stability, it is also important to remove all hydride species from the surface of pSi and replace with hydroxyl moieties to facilitate further functionalization with biofunctional compounds using silicon alkoxide derivatives.[31]

If long-term stability of a given pSi surface is desired, hydrosilylation and hydrocarbonization are attractive options. The former involves the use of functionalized alkenes/alkynes, often in the presence of a catalyst at reflux temperatures. The latter involves controlled decomposition of acetylene adsorbed on a freshly prepared pSi surface at elevated temperatures. Both approaches have been described in detail in recent reviews.[11,32]

Many of the above points regarding the influence of surface chemistry on the properties of a given drug loaded into pSi can be illustrated by noting selected highlights of a recent account by Wang *et al.*, who studied the influence of surface chemistry of pSi not only on the dissolution of the carrier itself but also drug loading and consequently its release kinetics.[33] They analyzed three types of porous silicon surfaces with a mesoporous structure: hydrophobic as-prepared (hydrogen-terminated) pSi, hydrophobic octyl-functionalized pSi, and hydrophilic surface oxidized pSi. The observed difference in loading of the antibacterial agent triclosan between as-anodized and oxidized pSi (roughly 8%) was attributed to the reactivity of oxidized surface sites with water molecules leading to additional oxidation. The lower value of 42.1% for the octyl-functionalized pSi is presumably a consequence of a smaller available surface for the drug in the solution (50% water) in the presence of long octyl chains.

A significant difference was observed with regard to the release behavior; with the octyl-functionalized pSi demonstrating the largest per unit time followed by the as-anodized pSi and finally, oxidized pSi. The difference in release kinetics at least for the as-anodized and oxidized pSi was linked to the dissolution rates of these materials.[34] For instance, the rate of dissolution of as-prepared, hydrogen-terminated pSi is about four times higher than that of oxidized material, which explains the difference in drug release. However, the dissolution behavior of the carrier does not explain why octyl-functionalized pSi exhibits much higher release kinetics than that of as-anodized pSi when the dissolution rate of the octyl-functionalized carrier alone is 2.7 times less compared to the as-prepared pSi. Even though alkyl groups suppressed pSi degradation, they provided a hydrophobic interface for the drug (hydrophobic triclosan) that at the end overwhelmed the dissolution rate and resulted in a higher amount of released drug overall. These results clearly show how surface chemistry plays a key role in drug loading and release, by either effecting the dissolution of the carrier alone and/or dissolution from the pores by means of hydrophobic/hydrophilic interactions with the drug molecules.

4.2.4 Cell Attachment and Differentiation on Porous Silicon

Numerous studies have been carried out on various mammalian cells' attachment and differentiation on porous silicon. A very thorough compilation of these studies can be found in the recently published *Handbook of Porous Silicon*,[35,36] covering a broad range of stem, nerve, bone, epithelial, gastric as well as cancer cell interactions with porous silicon. In this section, we will concentrate on some of the latest contributions of pSi in wound healing and how they may play a crucial role in delivering antibacterial drug compounds and growth factors in order to reestablish tissue integrity.

Mori *et al.* reported the preparation of thermally hydrocarbonized porous silicon (THCPSi) microparticles that were covered with well-known biopolymers (chitosan (CHI) and chondroitin sulfate (CS)/hyaluronic acid (HA)).[37] The potent antibacterial drug compounds vancomycin (VCM) and resveratrol (RSV) were subsequently loaded into these modified pSi materials. These biopolymers are well known in pharmaceutics and have been reported to promote tissue repair, *i.e.* fibroblast proliferation.[38–40] As a result, these CHI- or CS/HA-modified pSi microparticles were less toxic compared to the uncoated microparticles as revealed by the high survival of the fibroblast cells. Moreover, the coated particles resulted in controlled release of both VCM and RSV.

In another account, Fontana *et al.* performed studies where hydrocarbonized porous silicon (THCPSi) microparticles were functionalized with platelet lysate (PL) to promote wound healing.[41] PL-loaded porous silicon particles were evaluated for their proliferation effects both *in vitro* in a wound-healing assay and also *ex vivo* over human skin. The *in vitro* wound healing was performed using fibroblast cells to track the wound closure as shown in Figure 4.2.

After 24 hours of incubation, PL-modified THCPSi promoted complete closure of the cell gaps, whereas unmodified pSi microparticles and the controls (positive included) did not reach closure of the gap. Although short lasting, the *ex vivo* assay PL-modified THCPSi showed acidophilia of the collagen fibers, which is a sign of ongoing regeneration. Overall, these results are very promising for the treatment of non-healing wounds using porous silicon.

4.2.5 Advantages of pSi/Polymer Composites as Implants for Tissue Engineering

Polymers (natural and synthetic) have been extensively employed in the field of tissue engineering due to the myriad of useful properties that are important for their use as scaffolds or drug delivery devices. Among these properties are mechanical stiffness, flexibility, and degradability. In addition, polymers can be sculpted into different shapes/forms in order to be used in a wide range of applications. Some common biodegradable synthetic polymers extensively studied and used since the 1930s include poly(lactic acid), PLA, poly(glycolic acid), PGA, poly(ε-caprolactone), PCL.[42] However, there are a few disadvantages to their use. These include: a low drug loading capability, low melting temperatures, insufficient mechanical properties, and lack of optical properties that can be used for label-free sensing.[43] Therefore, there is an emerging interest in

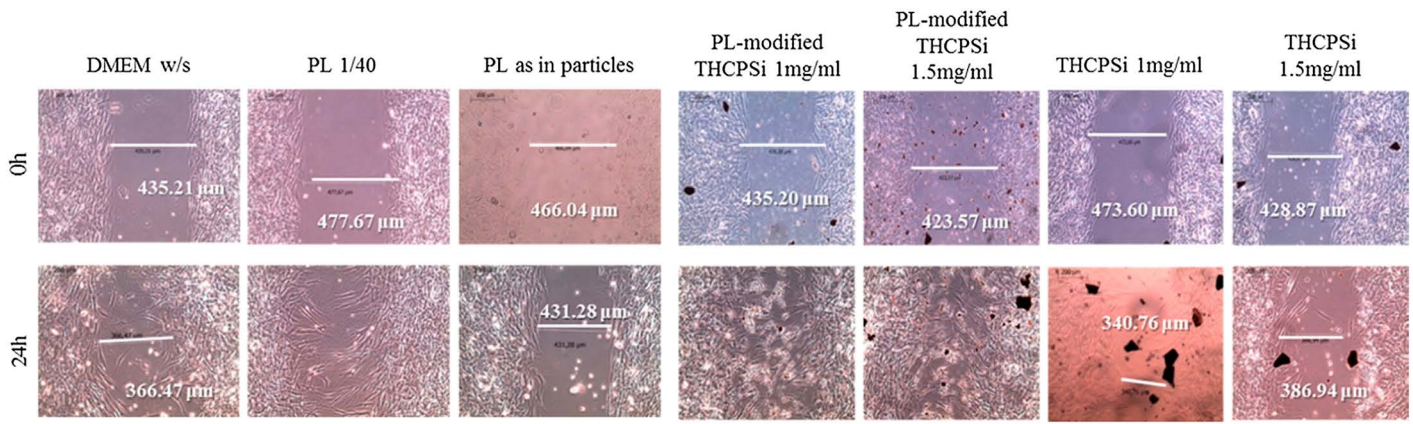

Figure 4.2 Photographs of the cells' gaps at 0 and 24 h after incubation with the samples at 37 °C in 5% CO_2 and 95% relative humidity. The cells were seeded into the two chambers of the inserts and left in the incubator overnight in order to attach to the µ-dish. On the following day, the insert was removed, and the samples were seeded into the appropriate dish. The white lines measure the width of the gaps in µm. Samples: DMEM without serum (M w/s); PL (1 : 40 dilution; PL 1/40); PL "as in particles"; PL-modified THCPSi 1 and 1.5 mg mL^{-1}; and THCPSi 1 and 1.5 mg mL^{-1}. (Reprinted (adapted) with permission from (Fontana *et al.* 'Platelet Lysate-Modified Porous Silicon Microparticles for Enhanced Cell Proliferation in Wound Healing Applications, ACS Appl. Mater. Interfaces, 2016, 8, 988-996 41). Copyright (2016) American Chemical Society.)

the development of composite materials such as pSi/polymers with improved mechanical properties, optical properties for self-reporting, as well as a precisely controlled degradation and drug delivery kinetics for adjuvant therapies.

Given the significance of eye-related diseases in quality-of-life issues, we choose to discuss here an example of the use of pSi/polymer implants for treatment of dysfunctional corneal surfaces that are responsible for painful and blinding diseases such as uveitis. In 2009, Low *et al* used thermally oxidized, aminosilanised porous silicon membranes as a host scaffold for the attachment and growth of human ocular cells. After implantation of the pSi membrane into a rat eye, the seeded cells were viable and moved into ocular tissue causing very little host reaction. The duration of implantation was nine weeks, by the end of which most of the pSi was observed to have been degraded.[44]

These results were very encouraging and prompted further studies that were reported in 2010 by Kashanian *et al.*, who proposed pSi encapsulation in microscale fibers of the biodegradable polymer polycaprolactone (PCL).[45] The introduction of PCL fibers improved the system by providing mechanical flexibility to the construct, removed sharp edges present in pSi microparticles, inhibited a rapid hydrolysis of the pSi, and promoted better human lens epithelial (HLE) cell line proliferation on the fiber template. As the dissolution rate of pSi particles is strongly dependent on pSi surface chemistry, two different types of pSi particle surfaces (hydrogen-terminated and surface-oxidized) were investigated. The rates of dissolution were governed by both the presence of the polymer and the surface chemistry of pSi particles, with the latter turning out to be more dominant. As expected, the hydride-terminated pSi samples had clearly dissolved to a greater extent by the end of a 30-day observation period.

Also in these studies, *in vivo* experiments using a rat eye model showed no evidence of infection around the implant site.[45] A foreign-body response was observed for all pSi/PCL composites, with some histiocyte infiltration at the sites of implantation that were completely resolved over time. Composite fibers containing the surface-oxidized pSi particles demonstrated a superior performance, showing no measurable fibrous capsule. Overall, these results suggested further investigation including incorporation and release of useful therapeutics and transfer of cells.

In 2015, Irani *et al.* extended this work by proposing a new method of fabricating pSi/PCL composites where pSi particles are only partially encapsulated onto PCL fibers, which would allow for a higher drug loading and release.[46] This new type of composite permits drug loading after preparation of the composite, thereby posing a significant advantage over completely encapsulated pSi, as exposure of many drugs to solvents present in PCL during composite fabrication would lead to drug denaturation. In this study, a model drug (fluorescein diacetate (FDA)) and proteins such as insulin, transferrin, and epidermal growth factor (EGF) were successfully loaded into the composites. HLE cell attachment assays were carried out, indicating very successful cell attachment and proliferation on the composites. Lastly, these composites were also tested *in vivo*, with implantation under the rat conjunctiva resulting in no significant inflammation after eight weeks. Figure 4.3 demonstrates the progression of pSi and pSi/PCL implants *in vivo*.

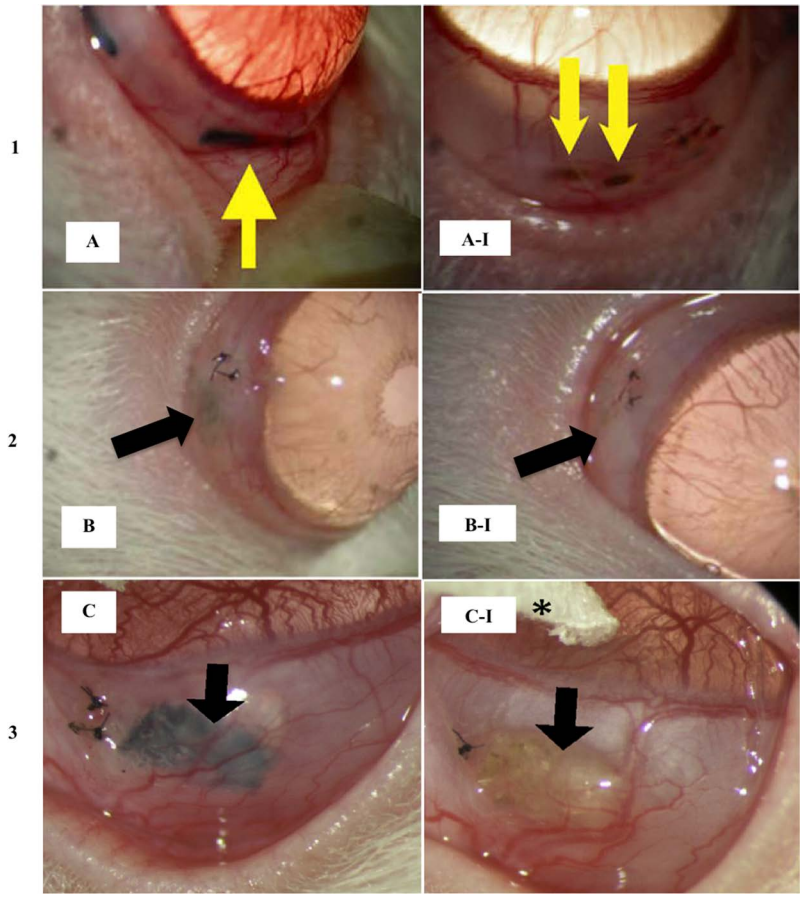

Figure 4.3 (1) Thermally-oxidized, amine-terminated porous silicon membranes implanted under rat conjunctiva, shown immediately after implantation (A) and nine weeks (A-I), (reprinted from The biocompatibility of porous silicon in tissues of the eye, 30, S. P. Low, N. H. Voelcker, L. T. Canham and K. A. Williams, 2873–2880, Copyright (2009), with permission from Elsevier). (2) Oxidized pSi in PCL at one week (B) and eight weeks (B-I) after implantation beneath the conjunctiva, (reprinted from Evaluation of mesoporous silicon/polycaprolactone composites as ophthalmic implants, 6, S. Kashanian, F. Harding, Y. Irani, S. Klebe, K. Marshall, A. Loni, L. Canham, D. M. Fan, K. A. Williams, N. H. Voelcker, J. L. Coffer, 3566–3572, Copyright (2010), with permission from Elsevier). (3) Pressed pSi/PCL composite implanted under the rat conjunctiva, immediately after implantation (C) and eight weeks post implantation (C-I), (reprinted from A novel pressed porous silicon-polycaprolactone composite as a dual-purpose implant for the delivery of cells and drugs to the eye, 139, Y. D. Irani, Y. Tian, M. J. Wang, S. Klebe, S. J. P. McInnes, N. H. Voelcker, J. L. Coffer, K. A. Williams, 123–131, Copyright (2015), with permission from Elsevier). Arrows mark the implants.

In Figure 4.3(1), one can see that pSi membranes at the end of nine weeks showed definite migration from the starting implantation point, which can potentially end up in the vicinity of the visual axis and cause vision impairment. Also, it is highly undesirable to have a rigid material with sharp edges such as pSi move within the tissue, possibly causing any additional inflammatory response. However, when pSi is combined with the polymer, there is no visible pSi particle migration from the site of the implantation as shown in Figure 4.3(2) and (3). Overall, PCL introduces flexibility and provides secure anchoring of pSi particles (or membranes). These pSi/PCL composites demonstrate great potential to be used for ocular surface disease treatment with the ability of high drug/protein load and release and biocompatibility *in vivo.*

4.3 Porous Silicon as a "Smart" Biomaterial

Stimuli-sensitive or "smart" materials are materials that undergo physical or chemical behavior as a response to minor perturbation in the environment. Different stimuli can serve as modulators for the changes within the material. Stimuli may be either physical (temperature, electrical field, mechanical stress or light) or chemical (pH or ionic strength).

In Table 4.1, selected highlights of pSi as a "smart" material are presented along with a brief description of system fabrication and aim for which the system was designed. Typically, pH-sensitive pSi systems have polymer coatings that contain weak acidic or basic groups that act as a proton donor/acceptor in response to changes in environmental pH. In addition, pH-response can be achieved through pSi surface modification (*e.g.* aromatic amino groups).

In order to obtain a temperature-responsive behavior, a well-known polymer, poly(*N*-isopropylacrylamide), should be used in combination with pSi to achieve a sustainable temperature-dependent drug delivery (see Table 4.1). The possibly obtained dual (pH and temperature) response systems are not currently available in the literature for pSi, but would be very useful for sequential release of bioactive agents or cells.

Over the past decade, pSi has been studied as a promising material for label-free optical biosensing applications. Its optical properties, such as photoluminescence and reflectance, are very sensitive to the presence of biomolecules inside the pores.[47,48] Table 4.1 covers some of the most relevant cases to tissue engineering in which pSi was used as an optical sensor for label-free self-reporting properties.

4.4 Porous Silicon/Polymer as a "Smart" Tissue-Engineering Scaffold

In 1995, acellular studies on microporous Si films in simulated body fluids showed an apparent growth of apatite-like phases—a major component of bone—on top of microporous silicon and even on neighboring areas of bulk Si.[3] Since this initial discovery, the use of porous silicon as a bone implantable material has been extensively investigated.

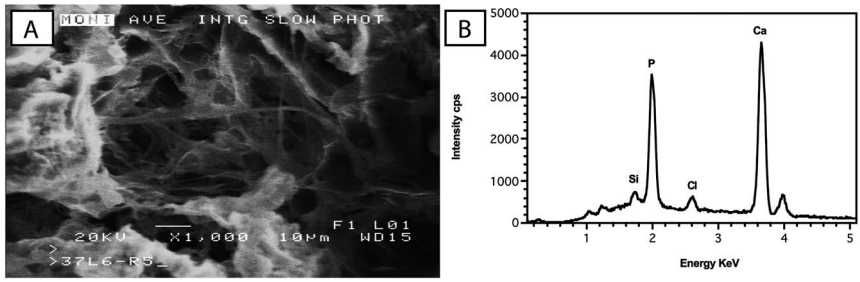

Figure 4.4 (A) SEM image of a porous pSi/PCL composite scaffold (1% pSi). Scale bar = 10 µm. (B) Energy dispersive X-ray spectrum of a mesoporous Si (1%)/PCL scaffold exposed to simulated body fluid (SBF) at 37 °C for 14 days.[76]

In 2005, Coffer *et al.* demonstrated studies on the *in vitro* calcification and proliferation of fibroblasts on the surfaces of pSi/PCL composites.[76] These particular composites were prepared by mixing the mesoporous silicon (67% porosity) in a 1% or 5% (w/w) polymer solution, thereby creating a well-dispersed suspension followed by salt leaching methods resulting in a highly porous composite as shown in Figure 4.4.

Figure 4.4(A) shows the porous morphology of the pSi/PCL material, with micron-sized holes. After two weeks of exposure to an acellular simulated body fluid (SBF) at 37 °C, there were small precipitates about 100 nm in size detected on the surface of the pSi/PCL composites with the confirmed composition of calcium phosphate, Figure 4.4(B). In addition to the performed calcification assays, *in vitro* cell proliferation data for human kidney fibroblasts (HEK293) were acquired, showing cell viability in the presence of the pSi/PCL composites.[76]

A significant advance was reported in 2006, when Batra *et al.* reported the controlled release of compounds from a semiconducting calcium phosphate/pSi structure.[75] This was demonstrated for the reversible adsorption and release of multiple compounds—an anionic salt of fluorescein, ethidium bromide, acridine orange—upon the switching of the direction of bias to the underlying porous Si/Si substrate. For all of these compounds, their delivery/uptake can be mediated in part by the use of a surface layer of the biodegradable polymer poly-(ε-caprolactone) (PCL).

In 2007, the Coffer group continued this work by adding polyaniline (PANi)—an electrically conductive polymer—to pSi/poly(ε-caprolactone) PCL composites.[77] The goal was to fabricate a "smart" conductive scaffold in order to achieve an accelerated formation of calcium phosphate for an increased bone growth rate. Typically, 10% PANi by weight was incorporated into pSi/PCL composites. Figure 4.5 illustrates SEM images of a leached PCL sponge as well as leached PCL sponge with 10% PANi coating with ~1% pSi incorporated into the scaffold.

The resultant PCL/PANi/pSi composite had a very smooth surface coating of PANi and still retained its macroscopic porosity, which is eventually favored for tissue engineering.

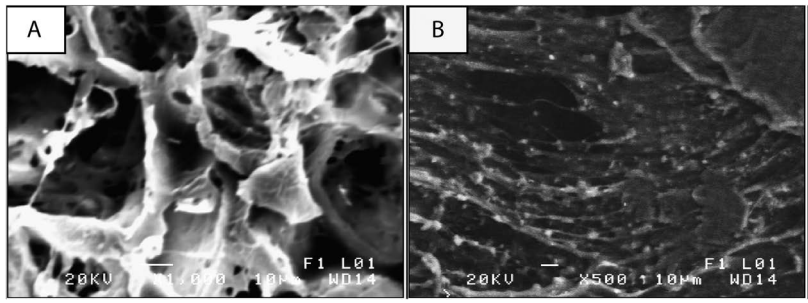

Figure 4.5 (A) SEM images of a leached PCL sponge (90% porosity), (B) a leached PCL sponge with a 10% PANi surface coating and ~1% porous silicon showing the smoother microstructure accompanying the addition of PANi.[77]

In order to assess whether it is possible for the application of electrical bias to influence calcification, a PCL/PANi/pSi composite (1% w/w) at a constant potential of 1.0 V under cathodic conditions was applied to the structure while immersed in SBF for seven hours at room temperature. Calcium phosphate deposits were formed on a pSi-containing sample and were absent on a control sample. Figure 4.6(a) shows SEM images of a PCL/PANi/1% pSi sample after the bias was applied.

The spectrum in Figure 4.6(B) shows that the sponge is phosphate-rich with a P–Ca ratio of ~4.4, but after an additional soaking time in SBF at 37 °C for one week, the calcium-to-phosphate ratio increased to a range of ~1.1–1.7, which is consistent with dicalcium phosphate and hydroxyapatite, respectively. These results clearly demonstrate accelerated calcification of PCL/PANi/pSi composites in SBF when an electrical bias is applied. However, in the absence of bias, calcification is not observed for periods up to a month. These "smart" composites were also tested for cytocompatibility using human kidney fibroblasts (HEK 293) along with more orthopedically relevant mesenchymal stem cells from mouse stroma. In both cases, PCL/PANi/pSi had no toxic effect on cell growth.

With further refinements, these composites can ideally prove to be very beneficial for responsive bone repair, as they are able to promote calcification on demand, and show non-toxic character in the growth and proliferation of cells. With proper tailoring of the polyaniline, it is possible to envision the full degradability of these composites after implantation.

4.5 Clinical Potential

As pointed out above, the fact that porous silicon induces calcification *in vitro* and *in vivo* suggests pragmatic investigation into difficult cases (*e.g.* non-union bone growth) in orthopedics at the clinical level. In addition, the challenges of ocular tissue repair, with a concomitant need for adjuvant drug delivery, also make ophthalmological applications a clear area of promise

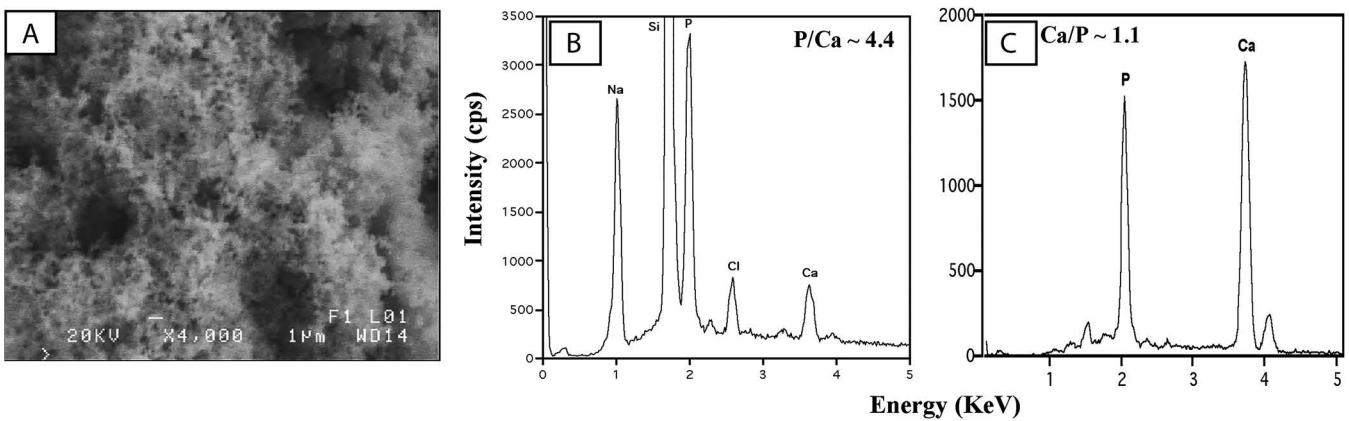

Figure 4.6 (A) SEM image of a leached PCL/PANi/1% pSi sponge after bias was applied showing the presence of CaP. Scale bar is 1 µm. (B) Corresponding EDX of (A). (C) A one-month soak of a similar sample in SBF at 37 °C with zero bias. Calcification occurred only after the sponge was soaked in SBF for one month.

that warrants investment in the near term. In particular, given their favorable properties, pSi/biocompatible polymer composite scaffolds in conjunction with limbal stem cell seeding are appealing candidates for clinical investigations for the possible treatment of chronic eye inflammatory diseases. These fields are ripe for additional discovery and, more importantly, will be of benefit to patients.

4.6 Summary and Future Opportunities

In this chapter we have summarized a number of the key useful properties of porous silicon and associated biocompatible polymer composites that make them relevant candidates for tissue engineering and related applications. While the focus to date has been exclusively at the preclinical level, the demonstrated promise of those studies that center on the evaluation of the perceived "smart" functions of porous silicon—including electrical bias—are just beginning to be realized. With dedicated effort, useful nanostructures based on porous silicon and selected composites should one day be a part of the theranostic toolkit of the clinician.

Acknowledgements

Financial support by the Robert A. Welch Foundation (Grant P-1212) is gratefully acknowledged.

References

1. L. T. Canham, *Appl. Phys. Lett.*, 1990, **57**, 1046–1048.
2. J. R. Link and M. J. Sailor, *Proc. Natl. Acad. Sci. U. S. A.*, 2003, **100**, 10607–10610.
3. L. T. Canham, *Adv. Mater.*, 1995, **7**, 1033–1037.
4. S. H. C. Anderson, H. Elliott, D. J. Wallis, L. T. Canham and J. J. Powell, *Phys. Status Solidi A*, 2003, **197**, 331–335.
5. E. Tasciotti, X. W. Liu, R. Bhavane, K. Plant, A. D. Leonard, B. K. Price, M. M. C. Cheng, P. Decuzzi, J. M. Tour, F. Robertson and M. Ferrari, *Nat. Nanotechnol.*, 2008, **3**, 151–157.
6. Z. T. Qin, J. Joo, L. Gu and M. J. Sailor, *Part. Part. Syst. Charact.*, 2014, **31**, 252–256.
7. X. Z. Huang, R. Gonzalez-Rodriguez, R. Rich, Z. Gryczynski and J. L. Coffer, *Chem. Commun.*, 2013, **49**, 5760–5762.
8. R. Aston and L. T. Canham, US007186267B2, 2001.
9. C. Chiappini, E. De Rosa, J. O. Martinez, X. Liu, J. Steele, M. M. Stevens and E. Tasciotti, *Nat. Mater.*, 2015, **14**, 532–539.
10. W. Sun, J. E. Puzas, T.-J. Sheu and P. M. Fauchet, *Phys. Status Solidi A*, 2007, **204**, 1429–1433.
11. J. M. Buriak, *Chem. Rev.*, 2002, **102**, 1271–1308.

12. M. P. Stewart and J. M. Buriak, *Comments Inorg. Chem.*, 2002, **23**, 179–203.
13. V. P. Lehto and J. Riikonen, in *Porous Silicon for Biomedical Applications*, ed. H. A. Santos, Woodhead Publishing, 2014, ch. 14, pp. 337–350.
14. J. Salonen, in *Handbook of Porous Silicon*, ed. L. T. Canham, Springer, 2014, ch. Part V Applications, pp. 909–916.
15. J. Salonen, A. M. Kaukonen, J. Hirvonen and V. P. Lehto, *J. Pharm. Sci.*, 2008, **97**, 632–653.
16. E. J. Anglin, L. Y. Cheng, W. R. Freeman and M. J. Sailor, *Adv. Drug Delivery Rev.*, 2008, **60**, 1266–1277.
17. A. Halimaoui, in *Properties of Porous Silicon*, ed. L. T. Canham, INSPEC, London, United Kingdom, 1997, ch. 1, pp. 12–22.
18. H. Foll, M. Christophersen, J. Carstensen and G. Hasse, *Mater. Sci. Eng., R*, 2002, **39**, 93–141.
19. N. Koshida, M. Nagasu, K. Echizenya and Y. Kiuchi, *J. Electrochem. Soc.*, 1986, **133**, 2283–2287.
20. L. T. Canham and A. J. Groszek, *J. Appl. Phys.*, 1992, **72**, 1558–1565.
21. M. E. Dudley and K. W. Kolasinski, *Electrochem. Solid-State Lett.*, 2009, **12**, D22–D26.
22. H. Ouyang, M. Christophersen and P. M. Fauchet, *Phys. Status Solidi A*, 2005, **202**, 1396–1401.
23. A. Janshoff, K. P. S. Dancil, C. Steinem, D. P. Greiner, V. S. Y. Lin, C. Gurtner, K. Motesharei, M. J. Sailor and M. R. Ghadiri, *J. Am. Chem. Soc.*, 1998, **120**, 12108–12116.
24. R. L. Smith and S. D. Collins, *J. Appl. Phys.*, 1992, **71**, R1–R22.
25. A. Loni, in *Properties of Porous Silicon*, ed. L. T. Canham, INSPEC, London, United Kingdom, 1997, ch. 1, pp. 51–58.
26. M. J. Wang, J. L. Coffer, K. Dorraj, P. S. Hartman, A. Loni and L. T. Canham, *Mol. Pharmaceutics*, 2010, **7**, 2232–2239.
27. A. Loni, D. Barwick, L. Batchelor, J. Tunbridge, Y. Han, Z. Y. Li and L. T. Canham, *Electrochem. Solid-State Lett.*, 2011, **14**, K25–K27.
28. L. Batchelor, A. Loni, L. T. Canham, M. Hasan and J. L. Coffer, *Silicon*, 2012, **4**, 259–266.
29. J.-N. Chazalviel and F. Ozanam, in *Properties of Porous Silicon*, ed. L. T. Canham, INSPEC, London, United Kingdom, 1997, ch. 1, pp. 59–65.
30. J. Salonen, in *Porous Silicon for Biomedical Applications*, ed. H. A. Santos, Woodhead Publishing, 2014, ch. 2, pp. 21–34.
31. A. M. Tinsley-Bown, L. T. Canham, M. Hollings, M. H. Anderson, C. L. Reeves, T. I. Cox, S. Nicklin, D. J. Squirrell, E. Perkins, A. Hutchinson, M. J. Sailor and A. Wun, *Phys. Status Solidi A*, 2000, **182**, 547–553.
32. J. Salonen, E. Laine and L. Niinisto, *J. Appl. Phys.*, 2002, **91**, 456–461.
33. M. J. Wang, P. S. Hartman, A. Loni, L. T. Canham, N. Bodiford and J. L. Coffer, *Langmuir*, 2015, **31**, 6179–6185.
34. T. Limnell, J. Riikonen, J. Salonen, A. M. Kaukonen, L. Laitinen, J. Hirvonen and V. P. Lehto, *Int. J. Pharm.*, 2007, **343**, 141–147.
35. N. H. Voelcker and S. P. Low, in *Handbook of Porous Silicon*, ed. L. T. Canham, Springer, 2014, ch. Part III Characterization, pp. 481–496.

36. J. L. Coffer, in *Handbook of Porous Silicon*, ed. L. T. Canham, Springer, 2014, ch. Part V Applications, pp. 921–927.
37. M. Mori, P. V. Almeida, M. Cola, G. Anselmi, E. Makila, A. Correia, J. Salonen, J. Hirvonen, C. Caramella and H. A. Santos, *Eur. J. Pharm. Biopharm.*, 2014, **88**, 635–642.
38. W. Y. J. Chen and G. Abatangelo, *Wound Repair Regen.*, 1999, **7**, 79–89.
39. G. Weindl, M. Schaller, M. Schafer-Korting and C. Korting, *Skin Pharmacol. Physiol.*, 2004, **17**, 207–213.
40. T. Chandy and C. P. Sharma, *Biomater., Artif. Cells, Artif. Organs*, 1990, **18**, 1–24.
41. F. Fontana, M. Mori, F. Riva, E. Makila, D. F. Liu, J. Salonen, G. Nicoletti, J. Hirvonen, C. Caramella and H. A. Santos, *ACS Appl. Mater. Interfaces*, 2016, **8**, 988–996.
42. A. Asti and L. Gioglio, *Int. J. Artif. Organs*, 2014, **37**, 187–205.
43. B. Dhandayuthapani, Y. Yoshida, T. Maekawa and D. S. Kumar, *Int. J. Polym. Sci.*, 2011, 1–19.
44. S. P. Low, N. H. Voelcker, L. T. Canham and K. A. Williams, *Biomaterials*, 2009, **30**, 2873–2880.
45. S. Kashanian, F. Harding, Y. Irani, S. Klebe, K. Marshall, A. Loni, L. Canham, D. M. Fan, K. A. Williams, N. H. Voelcker and J. L. Coffer, *Acta Biomater.*, 2010, **6**, 3566–3572.
46. Y. D. Irani, Y. Tian, M. J. Wang, S. Klebe, S. J. P. McInnes, N. H. Voelcker, J. L. Coffer and K. A. Williams, *Exp. Eye Res.*, 2015, **139**, 123–131.
47. A. Jane, R. Dronov, A. Hodges and N. H. Voelcker, *Trends Biotechnol.*, 2009, **27**, 230–239.
48. G. Shtenberg and E. Segal, in *Handbook of Porous Silicon*, ed. L. T. Canham, Springer, 2014, ch. Part V Applications, pp. 857–868.
49. N. Shrestha, M. A. Shahbazi, F. Araujo, E. Makila, J. Raula, E. I. Kauppinen, J. Salonen, B. Sarmento, J. Hirvonen and H. A. Santos, *Biomaterials*, 2015, **68**, 9–20.
50. B. Herranz-Blanco, D. F. Liu, E. Makila, M. A. Shahbazi, E. Ginestar, H. B. Zhang, V. Aseyev, V. Balasubramanian, J. Salonen, J. Hirvonen and H. A. Santos, *Adv. Funct. Mater.*, 2015, **25**, 1488–1497.
51. D. F. Liu, H. B. Zhang, B. Herranz-Blanco, E. Makila, V. P. Lehto, J. Salonen, J. Hirvonen and H. A. Santos, *Small*, 2014, **10**, 2029–2038.
52. W. J. Xu, J. Rytkonen, S. Ronkko, T. Nissinen, T. Kinnunen, M. Suvanto, A. Narvanen and V. P. Lehto, *Chem. Mater.*, 2014, **26**, 6734–6742.
53. S. Pace, R. B. Vasani, W. Zhao, S. Perrier and N. H. Voelcker, *Nanoscale Res. Lett.*, 2014, **9**, 1–7.
54. M. Xue, X. Zhong, Z. Shaposhnik, Y. Q. Qu, F. Tamanoi, X. F. Duan and J. I. Zink, *J. Am. Chem. Soc.*, 2011, **133**, 8798–8801.
55. W. J. Xu, R. Thapa, D. F. Liu, T. Nissinen, S. Granroth, A. Narvanen, M. Suvanto, H. A. Santos and V. P. Lehto, *Mol. Pharmaceutics*, 2015, **12**, 4038–4047.
56. L. A. Perelman, C. Pacholski, Y. Y. Li, M. S. VanNieuvvenhze and M. J. Sailor, *Nanomedicine (London, U. K.)*, 2008, **3**(1), 31–43.

57. K. Beavers, T. Werfel, T. Shen, T. Kavanaugh, K. Kilchrist, J. Mares, J. Fain, C. Wiese, K. Vickers, S. Weiss and C. Duvall, *Presented in Part at the Porous Semiconductors Science and Technology*, Tarragona, Spain, 2016.
58. K. R. Beavers, J. W. Mares, C. M. Swartz, Y. L. Zhao, S. M. Weiss and C. L. Duvall, *Bioconjugate Chem.*, 2014, **25**, 1192–1197.
59. E. Segal, L. A. Perelman, T. Moore, E. Kesselman and M. J. Sailor, *Phys. Status Solidi C*, 2009, **6**(7), 1717–1720.
60. S. J. P. McInnes, E. J. Szili, S. A. Al-Bataineh, R. B. Vasani, J. J. Xu, M. E. Alf, K. K. Gleason, R. D. Short and N. H. Voelcker, *Langmuir*, 2016, **32**, 301–308.
61. R. B. Vasani, S. J. P. McInnes, M. A. Cole, A. M. M. Jani, A. V. Ellis and N. H. Voelcker, *Langmuir*, 2011, **27**, 7843–7853.
62. K. Tamarov, W. Xu, L. Osminkina, V. Timoshenko and V.-P. Lehto, *Presented in Part at the Porous Semiconductors Science and Technology*, Tarragona, Spain, 2016.
63. M. P. Schwartz, A. M. Derfus, S. D. Alvarez, S. N. Bhatia and M. J. Sailor, *Langmuir*, 2006, **22**, 7084–7090.
64. B. S. Flavel, M. J. Sweetman, C. J. Shearer, J. G. Shapter and N. H. Voelcker, *ACS Appl. Mater. Interfaces*, 2011, **3**, 2463–2471.
65. A. H. Soeriyadi, B. Gupta, P. J. Reece and J. J. Gooding, *Polym. Chem.*, 2014, **5**, 2333–2341.
66. S. N. Jenie, B. Prieto-Simon and N. H. Voelcker, *Biosens. Bioelectron.*, 2015, **74**, 637–643.
67. W. Y. Tong, M. J. Sweetman, E. R. Marzouk, C. Fraser, T. Kuchel and N. H. Voelcker, *Biomaterials*, 2016, **74**, 217–230.
68. J. Wang, T. Kumeria, D. Warther, M. T. Bezem and M. J. Sailor, *Presented in Part at the Porous Semiconductors Science and Technology*, Tarragona, Spain, 2016.
69. L. M. Bonanno and L. A. DeLouise, *Adv. Funct. Mater.*, 2010, **20**, 573–578.
70. N. Massad-Ivanir, Y. Mirsky, A. Nahor, E. Edrei, L. M. Bonanno-Young, N. Ben Dov, A. Sa'ar and E. Segal, *Analyst*, 2014, **139**, 3885–3894.
71. L. Cheng, E. Anglin, F. Cunin, D. Kim, M. J. Sailor, I. Falkenstein, A. Tammewar and W. R. Freeman, *Br. J. Ophthalmol.*, 2008, **92**, 705–711.
72. J. Kang and M. J. Sailor, *Presented in Part at the Porous Semiconductors Science and Technology*, Tarragona, Spain, 2016.
73. T. Tanaka, L. S. Mangala, P. E. Vivas-Mejia, R. Nieves-Alicea, A. P. Mann, E. Mora, H. D. Han, M. M. K. Shahzad, X. W. Liu, R. Bhavane, J. H. Gu, J. R. Fakhoury, C. Chiappini, C. H. Lu, K. Matsuo, B. Godin, R. L. Stone, A. M. Nick, G. Lopez-Berestein, A. K. Sood and M. Ferrari, *Cancer Res.*, 2010, **70**, 3687–3696.
74. M. Sarparanta, L. M. Bimbo, J. Rytkonen, E. Makila, T. J. Laaksonen, P. Laaksonen, M. Nyman, J. Salonen, M. B. Linder, J. Hirvonen, H. A. Santos and A. J. Airaksinen, *Mol. Pharmaceutics*, 2012, **9**, 654–663.
75. I. Batra, J. L. Coffer and L. T. Canham, *Biomed. Microdevices*, 2006, **8**, 93–97.

76. J. L. Coffer, M. A. Whitehead, D. K. Nagesha, P. Mukherjee, G. Akkaraju, M. Totolici, R. S. Saffie and L. T. Canham, *Phys. Status Solidi A*, 2005, **202**, 1451–1455.
77. M. A. Whitehead, D. Fan, G. R. Akkaraju, L. T. Canham and J. L. Coffer, *J. Biomed. Mater. Res., Part A*, 2007, **83a**, 225–234.

CHAPTER 5

Applications of Conductive Materials for Tissue Engineering

L. WANG[a,b], X. LI[b], Y. H. TSOU[b] AND X. Y. XU*[b]

[a]College of Chemistry, Chemical Engineering and Materials Science, Soochow University, 199 Ren-Ai Road, Suzhou Industrial Park, Suzhou, Jiangsu 215123, P. R. China; [b]Otto H. York Department of Chemical, Biological and Pharmaceutical Engineering, New Jersey Institute and Technology, University Heights, Newark, NJ 07102, USA
*E-mail: xiaoyang.xu@njit.edu

5.1 Introduction

A major problem in human health care that is both distressing and costly is the depletion or failure of organs or tissues in the body. Tissue engineering is a novel field with promising recoveries by applying the value of engineering with biology to develop functional alternatives for damaged organs and tissues. A major focus in the field of tissue engineering is to use cells, growth factors and biomaterial scaffolds to repair damaged tissues and regenerate lost tissues.[1,2] In order to reinforce cell survival and proliferation in the body, the scaffold must have the same characteristics as the organ it is targeting to replace.

It has been suggested by several studies that cells could respond to many different physicochemical properties of biomaterials, including surface

Smart Materials No. 25
Smart Materials for Tissue Engineering: Applications
Edited by Qun Wang

Published by the Royal Society of Chemistry, www.rsc.org

wettability and morphology,[3] stiffness[4] and elasticity.[5] Particularly, electrical signals have been proven to possess significant effects on cell behaviors, such as proliferation, differentiation and structural reorganization, ultimately affecting several biofunctions of cells and organs in the human body. The influence of electrical stimuli on tissues was first acknowledged in the 1960s after Bassett *et al.* used a low intensity electrical current to effect the bone formation mechanism of adult dogs.[6] During the 18th century it was proven that electrostatic charge could be used for skin lesions.[7] Studies have confirmed that the directional movement and migration of a variety of different cell types, such as keratinocytes[8] and epithelial cells,[9–11] can be influenced by small, applied electric fields. The applied electric fields can also regulate vascular endothelial cell phenotypes,[12,13] regenerate nerve fibers[14] and improve *in vivo* ligament healing used in orthopedic practices.[15] Although the mechanism of electric fields on cell behaviors is still unclear, a direct mechanism and indirect mechanism have been suggested. Electric field effects on cells can not only be directly caused by electrophoretic redistribution of intracellelar components such as adhesion receptors, growth factors or ions,[16–18] but also indirectly caused by conformational change of extracellular proteins or ions.[14,19,20] This area of research is continuously increasingly and advancing in understanding the electrical properties of tissues and cells. Many properties of electrical systems have been proven and shown in living cells.[21,22] Therefore, electrical stimulation is shown to induce beneficial cellular responses of some electrically sensitive tissues such as nerve, bone, muscle and cardiac tissue.

Over the past few decades, electrically conductive materials have drawn great interest in the research field of material science and biomedical engineering. Numerous studies regarding electrical stimuli have shown that the electrical conductivity of materials can affect a variety of cell behaviors, such as cell adhesion, proliferation and differentiation.[23–30] Due to the strong influence of electrical stimulation on cells and tissues, electrically conductive materials such as conductive polymers, piezoelectric polymeric materials and other conductive nanomaterials including carbon nanotubes and graphene have been broadly studied and applied for the advantages of tissue engineering.[31–35]

Based on literature research within the last decade, this present chapter summarizes the most used conductive materials in biomedical applications and common modification strategies for improving their biocompatibility and biodegradability for biomedical applications, as well as their main achievements in nerve, bone, muscle and cardiac tissue engineering.

5.2 Conductive Materials

Conductive materials used for biological applications mainly consist of conductive polymers, piezoelectric polymeric materials, novel conductive nanomaterials including carbon nanotubes and graphene, and self-assembled conductive hydrogels.

5.2.1 Conductive Polymers

Conductive polymers demonstrate outstanding performance for an effective combination of the electrical properties of metals and the physicochemical properties of organic polymers.[36] Normally, conductive polymers are organic polymers composed of high electrical properties with loosely held electrons in their backbones, and doping is an essential process for obtaining high conductivity polymers.[37,38] They have generated extensive significance for many biomedical applications including cell adhesion, proliferation and differentiation regulated by electrical stimulation.[33,39–42] Several different kinds of conductive polymers, such as polypyrrole (PPy), polyaniline (PANI) and polythiophene derivatives, have been developed and investigated for their potential application in the field of tissue engineering.

5.2.1.1 Polypyrrole

Polypyrrole (PPy) (Figure 5.1) is among the top most commonly investigated conductive polymers for electronic devices and chemical sensors because of its unique properties, including high conductivity, good chemical stability and ease of synthesis.[36,43–46]

The immense potential PPy exhibits for biomedical applications is attributed to its excellent properties of biocompatibility *in vitro* and *in vivo*.[19,47–49] It has also been revealed to provide promising reinforcement for the adhesion and growth of various cells.[22,37,50–52] Due to its effect on cell behavior, PPy has been broadly studied in the biomedical and tissue engineering fields.

5.2.1.2 Polyaniline

Polyaniline (PANI) (Figure 5.2) is another common conductive polymer widely studied due to its simplicity of synthesis and good environmental stability.[53,54] Mattioli-Belmonte reported the good biocompatibility of PANI both *in vitro* and *in vivo* for the first time.[55] Since then, numerous studies have

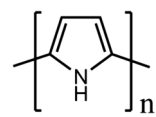

Figure 5.1 Chemical structure of polypyrrole.

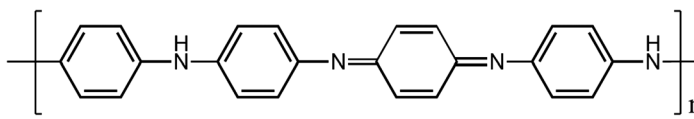

Figure 5.2 Chemical structure of polyaniline.

reported the excellent biocompatibility of PANI and its ability to improve cell growth.[56–58]

Establishing the biocompatibility of PANI both *in vivo* and *in vitro* led to a new research focus on designing materials for tissue engineering applications. Therefore, PANI-based composites were considered, observed and studied in various biomedical applications, particularly for scaffolds in tissue engineering.[59–64]

5.2.1.3 Polythiophene Derivatives

Polythiophene derivatives are another type of electrically conductive polymer investigated in the fields of biomedical and tissue engineering.[65–68] Poly(3,4-ethylenedioxythiophene) (PEDOT) (Figure 5.3) is considered to be the leading type of polythiophene derivative with outstanding conductivity, stability and low redox potentials.[69–71] Two important qualities that make PEDOT excellent for biosensing as well as bioengineering applications are its low inherent cytotoxicity and inflammatory response after implantation[72,73] PEDOT has been explored for use in cochlear implants, vision prosthesis, neural regeneration devices and neural recording electrodes. These studies have led to great discoveries currently being used in bioengineering applications including neural electrodes, nerve grafts and heart muscle patches.[74–76]

5.2.2 Piezoelectric Polymeric Materials

Tissue engineering applications do not only rely on conductive polymers; piezoelectric polymeric materials have also been considered.[34,77,78] The advantage of piezoelectric polymeric materials in biomedical applications is the delivery of an electrical stimulus without the need for an external power source. Under mechanical strain, piezoelectric polymeric materials produce a transient surface charge by mechanical deformations.[14]

The piezoelectricity of poly(vinylidene fluoride) (PVDF) was first discovered by Heiji.[79] Its unique molecular structure led to a transient surface charge produced on the synthetic, semi-crystalline polymer with piezoelectric properties (Figure 5.4). Due to its flexibility and non-toxicity,[80–84] PVDF has been widely studied for many different biomedical applications fields,[85–87] especially in tissue engineering applications, including bone, neural and muscle regeneration.[88–93]

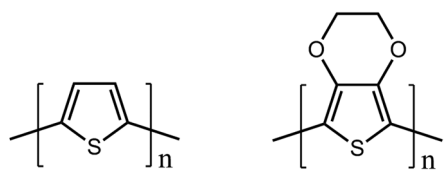

Figure 5.3 Chemical structure of polythiophene and poly(3,4-ethylenedioxythiophene).

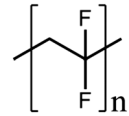

Figure 5.4 Chemical structure of poly(vinylidene fluoride).

5.2.3 Other Novel Conductive Nanomaterials

There has been a shift in research on conductive materials into the nanoscale since nanomaterials were found to have a large specific surface area that can efficiently support electron transfer. In the biomedical and bioengineering fields, conductive nanomaterials have been investigated and employed as biosensors,[94,95] neural probes[96,97] and for tissue engineering.[98,99] Specifically, carbon nanotubes (CNTs) have shown significant capability in guiding the differentiation orientations of stem cells, as well as working as an extracellular matrix to provoke cellular attachment and growth.[100,101] Another conductive nanomaterial is graphene, which has been observed to regenerate electroactive tissues. Graphene exhibits many desirable advantages, such as good biocompatibility and biostability, making it a particularly promising biomaterial.[102]

5.2.3.1 Carbon Nanotubes

Carbon nanotubes (CNTs) have emerged as promising conductive nanomaterials for biomedical applications based on their unique properties.[100,103–107] Specifically, they are conducting fillers integrated into non-conductive polymers. This process provides a material that can be used as a scaffold with structural reinforcement and electrical conductivity to direct cell behaviors and offer favorable conditions to induce proper cellular functions due to its nanoscale cues, texture and roughness. Several studies have shown that CNTs can be excellent substrates for cell attachment and growth.[108–112]

Additionally, bioactive electrically conductive three-dimensional (3D) scaffolds can be prepared for tissue engineering by coating polymers, bioglasses, or collagen with CNTs. CNT coatings have become a promising method and have the potential to develop the upcoming generation of engineered materials for biomedical applications.[113–117]

5.2.3.2 Graphene

Graphene, a two-dimensional monolayer of carbon atoms, is another common type of conductive nanomaterial with intrinsic nanostructure electrical properties. Due to these properties, graphene has been observed being used for various types of applications, including bioanalysis, tumor therapy and stem cell research.[118–123] *In vitro* studies have demonstrated exceptional support of graphene-based nanomaterials for adhesion, proliferation and differentiation behavior for many stem cells.[124,125]

3D graphene foams (3D-GF) are graphene derivatives with 3D porous structures and electrical conductivity,[126] which may help in advancing tissue engineering, specifically for novel scaffolds. 3D-GF can possess topographical as well as chemical and electrical signals in one scaffold. This will help create a steady environment for neural tissue regeneration; of major significance in tissue engineering and biomedical applications.[127]

5.2.4 Self-Assembled Conductive Hydrogels

Self-assembled conductive hydrogels are a type of composite material rapidly emerging in biomedical applications due to their ability to combine the properties and advantages of each constituent, as well as their unique molecular structure.[128] Following the first reported conductive hydrogels by Gong *et al.* in 1991,[129] several studies have been focused on applying conductive hydrogels for biosensors,[130,131] drug delivery[132,133] and tissue engineering.[134–138] A few examples include a poly(2-hydroxyethyl methacrylate) (PHEMA)/PPy hydrogel entrapped with oxidoreductase enzymes designed for glucose oxidase biosensing,[131] PANI-polyacrylamide conductive hydrogels synthesized for the fabrication of controlled drug release devices[133] and CNT-incorporated gelatin methacrylate (GelMA) hydrogels developed for cardiac tissue engineering.[135,137,138]

5.3 Biocompatibility and Biodegradation of Conductive Materials

The best properties for conductive material scaffolds for tissue engineering are good biocompatibility and controlled biodegradability with non-toxic degradation products.

5.3.1 Biocompatibility

Biocompatibility is essential for biomedical applications to be efficient. Fortunately, if a conductive material does not possess biocompatibility, it can be easily repaired through the bonding of biocompatible molecules, segments, or side chains to the conductive polymer material.

The biocompatibility of PPy was previously questioned in some studies and further demonstrated support for adhesion, growth and differentiation of a wide variety of cell types *in vitro* and *in vivo*.[46,50,139–143] Although some studies have contradicted the biocompatibility of PPy, PPy should always be completely biocompatible and show cell adhesion, growth and differentiation as long as the polymer is prepared appropriately with repeated steps of rinsing and extraction.[144] There has been a large contradiction between many studies regarding PANI's biocompatibility. Some previous studies have shown that the conductive polymer can maintain sufficient biocompatibility to support cell growth.[56,145] However, other studies have reported poor cell

adhesion and growth, indicating tissue incompatibility.[39,59] The biocompatibility of PANI can be confirmed using various methods, including additional curing and purification steps, immobilization of bioactive molecules such as specific peptide sequences, and using a medium to pre-soak PANI prior to cell exposure.[58] Unlike other conductive polymers, PEDOT has shown excellent biocompatibility with many cell lines, including neural and neuroblastoma cells, as well as L929 and NIH3T3 fibroblasts.[146–150] Piezoelectric polymer PVDF can also promote cell adhesion and growth, indicating good biocompatibility for many biomedical applications.[85,151,152] As for the biocompatibility of CNTs, there have been studies that claim CNTs are cytotoxic although other studies have demonstrated the exceptional ability of CNTs to be a substrate for cell growth. Due to the contradiction between studies it has been further claimed that CNTs used in suspensions are cytotoxic but are non-toxic when immobilized into a specific polymer.[153] Graphene possess a concern for biomedical applications due to flaws in its biocompatibility. Although cell viability *in vitro* seems not to be affected by graphene materials, their potential cytotoxicity in animal or clinical studies remains unknown. The synthesis technique used to produce graphene has a large influence on its biological effects.[102,118,154]

5.3.2 Biodegradability

Biodegradability is another essential issue for a conductive material to be used in tissue engineering. And this may be the biggest challenge in conductive material scaffolds, which will limit their *in vivo* applications. Tissue engineering materials without the property of biodegradability cannot be used or they may cause chronic inflammation.[155]

Tuning the conductive polymer to become biodegradable can be accomplished by different methods. A solution to this problem is merging conductive materials with suitable biodegradable polymers, resulting in a biodegradable scaffold.[35,156,157] This method allows the positive properties of both components to appear in the composite, which allows the conductivity and degradation rate to be controlled by selecting the appropriate ratio of the two components.[39] Although it seems like a successful method, it does not solve the issue of removing the conductive polymer from the body once the degradable polymer has vanished. Another method is to modify the conductive material itself without compositing it to another polymer. For example, it has been previously reported in multiple studies that the biodegradability properties of PPy can be adjusted by the addition of ionizable or hydrolyzable side groups to the backbone of PPy, specifically butyric acid and butyric ester, respectively.[128,158,159] And the rate of degradation can be corrected depending on the amount of each side group added to the conductive material.

To analyze the toxicity of conductive materials, further research is required on the biocompatibility of the materials. *In vivo* long-term cytotoxicity of these conductive materials should be analyzed. The development of

conductive materials with controlled biodegradability and non-toxic degradation is required for further development.

5.4 Modification of Conductive Materials

The essential properties of conductive materials desired for tissue engineering are electrical conductivity, as well as biostability, biocompatibility, biodegradability, three-dimensional structure and surface topography. In order to obtain these properties, a need to modify the materials to induce special features for further optimization of these materials is required. Conducting materials can be modified to enhance the functionality of the composites, such as improvement of bioactivity, enhancement of cell response and improvement of biodegradation.

There have been many attempts by different researchers to combine the conductivity and biological properties of conductive materials using chemical modification and physical modification. The chemical strategy has been extensively investigated by doping bioactive molecules or biocompatible polymers for improving cell behaviors and functions.[160–163] The physical strategy includes increasing surface roughness and improving surface topography of conductive scaffolds by micropatterning, as well as blending with biological moieties to obtain specific 3D structures.[31,65,147,164–166]

5.4.1 Bioactive Molecules

Scaffolds that are both conductive and bioactive are necessary to increase cell adhesion, proliferation and differentiation. Modification of conductive scaffolds is achieved through incorporating bioactive molecules into conductive scaffolds.[167,168] Doping of conductive materials by the use of bioactive molecules, such as proteins, polysaccharides, collagen, heparin, and growth factors, have been studied and observed for the modification of conductive materials.[49,169–172] Conductive materials doped with biomolecules such as extracellular matrix (ECM) components are becoming more widely evaluated to enhance the compatibility of the materials for biomedical applications.[172,173]

5.4.2 Biocompatible Polymers

The biocompatibility of electrically conductive materials can also be enhanced by the incorporation of natural polymers including chitosan and gelatin, as well as some synthetic biocompatible polymers. For example, chitosan-modified PPy membranes showed good biocompatibility for cell adhesion and proliferation.[174] Electrospun nanofibers with a combination of PANI, poly(ε-caprolactone) (PCL) and gelatin could also support cell growth and proliferation.[175] A 3D nanofibrous scaffold composed of PPy-coated poly(styrene-*b*-isobutylene-*b*-styrene) (SIBS) exhibited excellent performance for the attachment and growth of rat neuronal cells PC12.[176]

5.4.3 Topography Modification of Conductive Materials

The topographical qualities of a conductive scaffold have proven to have a substantial influence on tissue engineering. The conductive materials can be tailored to have fibrous, tubular or porous surface morphologies on a similar scale to that of cells in tissues.[177–181] Studies have shown that the surface roughness and morphology of conductive scaffolds have a significant influence on cell behaviors and functions.[182,183]

Modification and functionalization of conductive materials with different biomolecules have provided us with strategies to functionalize them with biological sensing elements, even to modulate various signaling pathways required for cellular processes. As a result, these modified conductive materials show much better performance in cell attachment, proliferation and differentiation. Therefore, conductive materials offer an excellent opportunity for the design and fabrication of biocompatible, biodegradable and highly specific nanocomposite scaffolds for tissue engineering applications.

5.5 Applications of Conductive Materials for Tissue Engineering

For tissue engineering applications, an active scaffold for supporting cell growth and differentiation is essential for successful regeneration of specific tissues. Tissue functionality in many tissues, including nerve, bone, muscle and cardiac tissues, can be determined through electrical stimulation. Particularly, strong potential has been shown for the usefulness of conductive materials for tissue engineering techniques. Major works using conductive materials for tissue engineering are summarized in Table 5.1.

5.5.1 Applications for Nerve Tissue Engineering

The nervous system is a network of nerves and specialized nerve cells called neurons that transmit signals between parts of the body. Primarily, it is the body's way of communication among the parts of the body. Clearly, the nervous system is of great significance to the body by controlling the interactions in the physiological processes. Harm to any of the nerves may inflict tremendous effects on the body and it is usually very difficult to recover the damaged nerve. It is extremely difficult for a nerve cell or neural tissue to regenerate on its own once neural damage has occurred. Therefore, the need for neural tissue engineering arises as a promising technology to combat the negative effects of disease, aging or injury in the nervous system. The extracellular matrix in the body provides optimal conditions for topographical as well as chemical and electrical signals for the adhesion and growth of neural cells. Therefore, there is a significant need for a synthetic scaffold to play the role of the extracellular matrix, which must be a biocompatible, immunologically inert, infection-resistant and biodegradable biomaterial.[156] Many efforts have been made to design a reasonable scaffold for nerve tissue engineering.

Table 5.1 Summary of conductive materials utilized for tissue engineering application.[a]

Applications	Conductive materials	Scaffolds	Cell type	References
Nerve tissue engineering	PPy	PPy/PDLCL	PC12	52
		PPy/SIBS	PC12	176
		PCL–PPy	DRG	184
		PPy–PLGA	PC12	185 and 186
		PPy–chitosan	Schwann cell	174
		PPy–PLLA	PC12	187
		PPy/PDLLA	PC12	188
		PPy–graphene	RGCs	189
	PANI	PANI/PCL/gelatin	NSCs	175
		PANI–PLCL–SF	PC12	190
		PANI	SH-SY5Y	191
	PEDOT	PEDOT–agarose	Schwann cells	136
	Piezoelectric materials	PVDF	Rat spinal cord neurons	192
		PVDF–TrFE	DRG	193
		PVDF–TrFE	hNSCs	194
	CNTs	CNT rope	NSCs	195
	Graphene	Graphene films	Mouse hippocampal neurons	123 and 154
		Graphene foams	NSCs	127
Bone tissue engineering	PPy	PPy/heparin/PLLA	Osteoblast-like Saos-2 cells	196
	PEDOT	BaG/gelatin/PEDOT:PSS	hMSCs	197
	Piezoelectric materials	PVDF	MC3T3-E1 osteoblast	77 and 198
		PVDF	hMSCs	199
		PVDF	hASCs	200 and 201
		PVDF–TrFE/BT	Human alveolar bone-derived cell	202
		PVDF–TrFE/BT	hPDLF	203
		PVDF–TrFE	NIH3T3	84
	CNTs	PDLA/MWCNTs	Neonatal rat osteoblasts	204
Muscle tissue engineering	PANI	CPSA–PANI/PLCL	Mouse C2C12 myoblasts	205
		PDLA/PANI	Primary rat muscle cells	206
		PCL/PANI	Mouse C2C12 myoblasts	207 and 208
	Piezoelectric materials	PVDF	Mouse C2C12 myoblasts	209
Cardiac tissue engineering	PPy	PPy/PCL/gelatin	Primary cardiomyocytes	210
	PANI	PANI/gelatin	H9c2 rat cardiac myoblasts	211
		PANI–PGS	Mouse C2C12 myoblasts	212

(*continued*)

Table 5.1 (*continued*)

Applications	Conductive materials	Scaffolds	Cell type	References
	Carbon nanomaterials	PLGA–CNF	Human cardiomyocytes	135
		CNT–GelMA	Neonatal rat cardiomyocytes	137
		CNT–hydrogel	Neonatal rat cardiomyocytes	138
		Chitosan/CNF	Neonatal rat cardiomyocytes	213
		CNT–PGS/gelatin	Rat cardiomyocytes	99

[a]PDLCL, poly(D,L-lactide-*co*-ε-caprolactone); SIBS, poly(styrene-β-isobutylene-styrene); PCL, poly(ε-caprolactone); PLGA, poly(lactic-*co*-glycolic acid); PLLA, poly(L-lactic acid) or poly(L-lactide); PDLLA, poly(D,L-lactic acid); PLCL, poly(L-lactide-*co*-ε-caprolactone); SF, silk fibroin; TrFE, trifluoroethylene; BaG, bioactive glass; PSS, poly(4-styrene sulfonate); BT, barium titanate; PDLA, poly(D,L-lactide); MWCNTs, multiwalled carbon nanotubes; CPSA, camphorsulfonic acid; PGS, poly(glycerol-sebacate); CNF, carbon nanofiber; GelMA, gelatin methacrylate. PC12, rat pheochromocytoma 12; DRG, dorsal root ganglion; RGCs, retinal ganglion cells; NSCs, neural stem cells; SH-SY5Y, human neuroblastoma cell; hNSCs, human neural stem cells; hMSCs, human mesenchymal stem cells; hASCs, human adipose stem cells; hPDLF, fibroblasts from human periodontal ligament; NIH3T3, mouse fibroblasts.

A PPy-coated poly(D,L-lactide-*co*-ε-caprolactone) (PDLCL) membrane can support the growth and differentiation of PC12 cells into neuronal phenotypes. Additionally, the implantation of rats with nerve guidance channels constructed of conductive composite materials revealed myelinated axons and Schwann cells comparable to those in the native nerve, indicating sciatic nerve regeneration in rats.[52] Conductive core–sheath nanofibrous scaffolds, PPy–PCL, provide a good model for investigating the synergistic effect of topography and electrical stimulation on neurite outgrowth *in vitro*. A dorsal root ganglion (DRG) displayed good adhesion on the nanofibers and generated neurites across the material surface with nerve growth factor in the medium. Moreover, electrical stimulation was able to further enhance the neurite extension in comparison to non-stimulated nanofibers.[184] Lee *et al.* found that PPy-coated poly(lactic-*co*-glycolic acid) (PPy–PLGA) conductive meshes possessed excellent support for the proliferation and differentiation of embryonic hippocampal neurons and PC12 cells. Furthermore, the electrical stimulation showed positive effects on the neurite formation compared to non-stimulated scaffolds. Stimulated cells on aligned PPy–PLGA nanofibers led to an increase in neurite elongation and proportion of neurite-bearing cells related to cells on random nanofibers. These results indicated that electrical stimulation and topographical guidance show a combined effect on the utilization of these conductive scaffolds for nerve tissue engineering.[185] Also, they chemically immobilized nerve growth factor (NGF) to PPy-coated PLGA fibers. The NGF modified fibers can provide support for PC12 cell growth and neuritogenesis without exogenous NGF in the medium. Moreover, electrical stimulation of PC12 cells through an NGF-modified PPy–PLGA fiber

increased neurite formation and neurite length by 18% and 17%, respectively, in comparison with non-stimulated cells on the fibers. Indications of these results display that the combination of immobilized NGF with electrical stimulation can be used for neural tissue engineering applications.[186]

A PPy/chitosan membrane was found to promote Schwann cell adhesion, spreading and proliferation. More importantly, electrically stimulated cells on the membrane significantly promoted the expression and secretion of NGF and brain-derived neurotrophic factor (BDNF) when measured against cells excluding electrical stimulation. This report was the first to investigate the potentiality of increasing nerve regeneration in conductive scaffolds by means of electrical stimulation-increased neurotrophin secretion.[174] Novel 3D fluffy PPy-coated poly(L-lactic acid) (PLLA) conductive fibrous scaffolds allowed easy cell entrance for a 3D cell culture. The number of rat PC12 cells cultured in the 3D scaffold was much higher than that on conductive fibrous meshes, indicating that the 3D scaffolds supported cell growth and proliferation for a 3D culture.[187]

Xu *et al.* fabricated PPy/poly(D,L-lactic acid) (PDLLA) composite nerve conduits containing various PPy amounts. Electrically stimulated PC12 cells seeded on the conduits showed increased and longer neurites than on PDLLA conduits as the content of PPy increased (Figure 5.5). Interestingly, when using a 5% PPy/PDLLA conduit to reconstruct a rat sciatic nerve defect, the rats displayed functional recovery comparable to that of the gold standard autologous nerve graft, which was enhanced significantly more than that of the PDLLA conduits, indicating great potential for nerve tissue engineering.[188]

Yan *et al.* fabricated PPy-functionalized graphene (PPy-G)-based aligned nanofibers for electrical stimulation and controlled growth of retinal ganglion cells (RGCs). The results showed that the cell viability, neurite outgrowth and antiaging ability of RGCs were significantly increased with electrical stimulation (Figure 5.6). These findings provide the possibility for optic nerve regeneration *via* electrical stimulation on the conductive nanofibers.[189]

Electrospun conductive nanofibrous scaffolds prepared by mixing PANI with PCL/gelatin (PANI/PCL/gelatin) showed significant NSC proliferation and neurite outgrowth in comparison to non-stimulated scaffolds; indicating potential applications for the attachment and proliferation of nerve stem cells.[175] Zhang *et al.* synthesized conductive meshes of PANI and poly(L-lactic acid-*co*-ε-caprolactone)/silk fibroin (PLCL-SF) coated with NGF for the investigation of electrical stimulation and NGF on neuron growth. PC12 cells on the PANI–PLCL–SF scaffolds under electrical stimulation showed more and longer neurites. Furthermore, electrical stimulation was shown to help the NGF release from the conductive core–shell structure nanofiber.[190] The growth and differentiation of several cells, such as human neuroblastoma SH-SY5Y cells, on PANI memristive surfaces were investigated by Juarez-Hernandez *et al.*, and the results showed enhanced growth, proliferation and differentiation of cells seeding on PANI films, demonstrating the suitability of PANI memristors for nerve tissue engineering.[191]

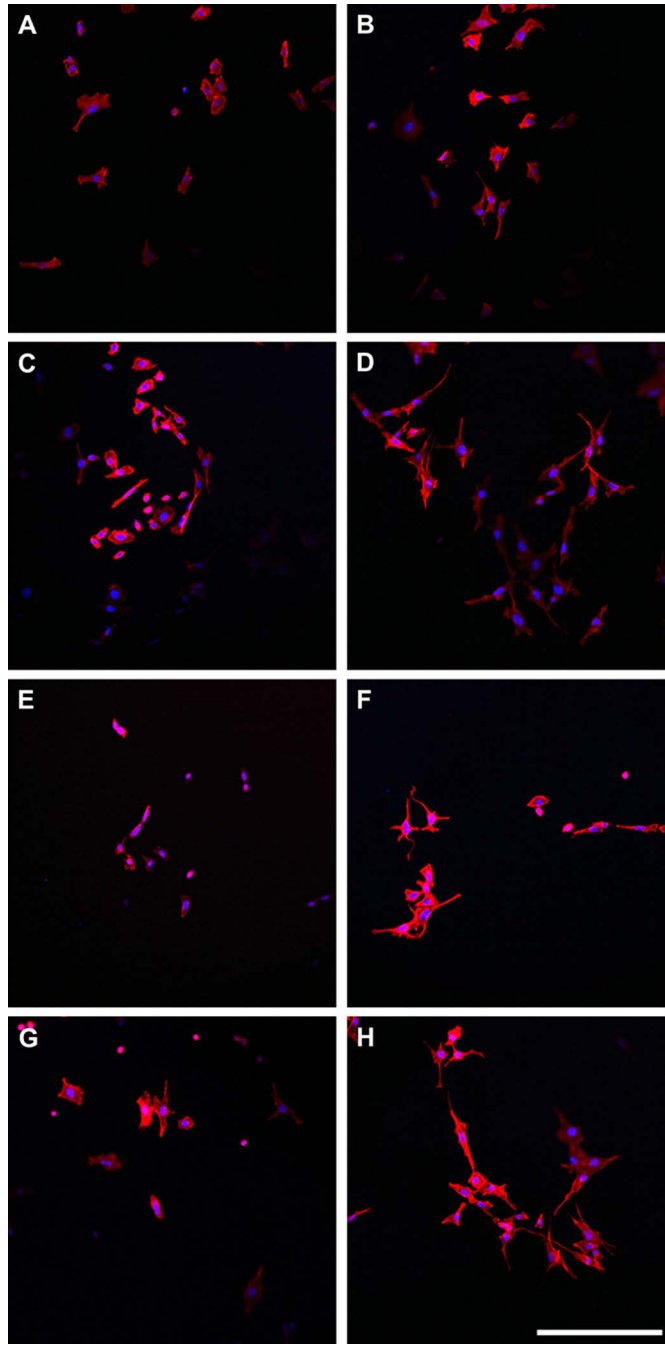

Figure 5.5 Fluorescent images of PC12 cells labeled for actin (red) and nuclei (blue). (A) and (B) PDLLA. (C) and (D) 5% PPy/PDLLA. (E) and (F) 10% PPy/PDLLA. (G) and (H) 15% PPy/PDLLA. (A), (C), (E), and (G) Control cells. (B), (D), (F), and (H) Cells stimulated with 100 mV for 2 h. Scale bar: 200 μm. Reprinted from *Advanced Materials*, **22**, Y. Zhu, S. Murali, W. Cai, X. Li, J. W. Suk, J. R. Potts and R. S. Ruoff, Graphene and graphene oxide: synthesis, properties, and applications, 3906–3924, copyright (2010) with permission from Elsevier.

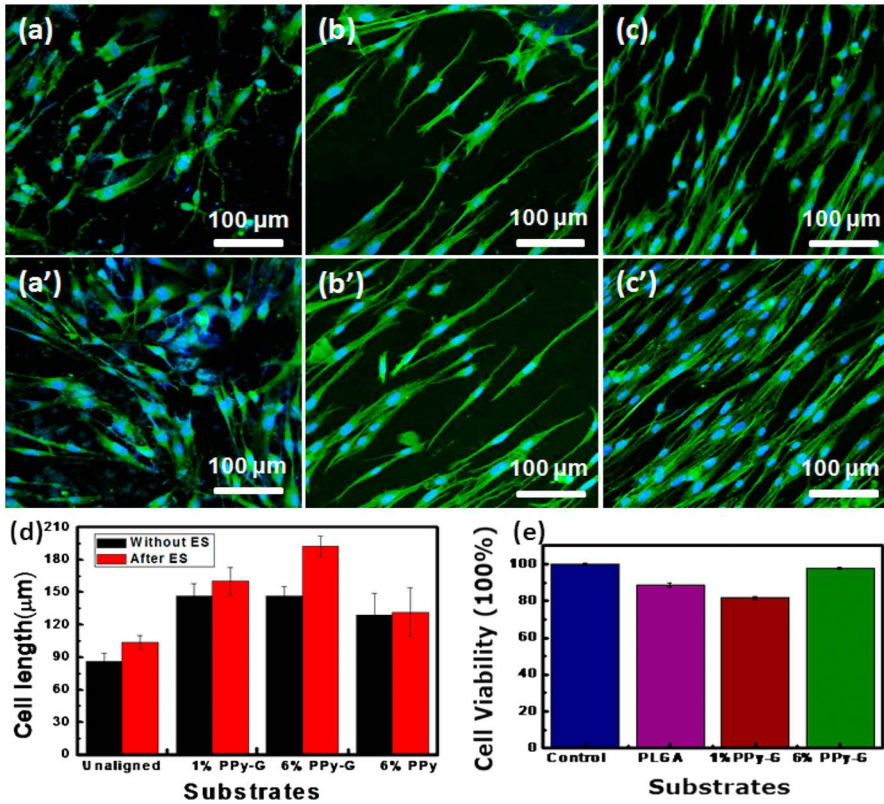

Figure 5.6 Confocal microscopy images of RGC cells seeded on (a) the random PPy-G/PLGA nanofibers without ES and (a′) after ES; (b) the aligned PPy-G/PLGA nanofibers with 1% (w/w) PPy-G without ES and (b′) after ES; (c) the aligned PPy/G-PLGA nanofibers containing 6% (w/w) PPy-G without ES and (c′) after ES. (d) Average cell length of RGCs without and after ES. (e) Cell viability of RGCs cultured on the different substrates. ES conditions: step potential was pulsed between −700 and +700 mV cm^{-1}. ES was performed 1 h every day and lasted for 3 days. Adapted from ref. 189 with permission from the American Chemical Society.

Novel conductive polymer–hydrogel conduits (PEDOT–agarose) for axonal regeneration were synthesized by Abidian *et al.* for the first time. The partially coated PEDOT–agarose conduit showed slightly better performance on supporting axonal growth than the fully coated PEDOT–agarose conduit. This study provided a reasonable design for 3D conductive hydrogel scaffolds for the acceleration, direction and controlling of axonal growth in the peripheral nervous system.[136]

Electrically stimulated rat spinal cord neurons on a PVDF film substrate exhibited an increase in neuronal density and neurite number with over two times more branch points in comparison to those grown on non-stimulated film, which indicates the positive effect of electrical stimulation through the

conductive film on neurite growth and branching.[192] Conductive electrospun random and aligned scaffolds made of copolymer PVDF–trifluoroethylene (PVDF–TrFE) showed good cell adhesion for DRG neurons. However, only aligned scaffolds supported directed neurite outgrowth other than radial extension.[193] Human neural stem cells (hNSCs) cultured on these PVDF–TrFE substrates differentiated towards β-III tubulin-positive cells, indicating neuronal cell differentiation for potential nerve tissue engineering applications.[194]

CNTs possess a unique array property allowing them to interact with neurons at a nanoscale level, and have been utilized in nerve-related research. Huang *et al.* developed a CNT rope substrate to investigate the response of NSCs on the conductive substrate after electrical stimulation. The results show that the orientation of the spiral topography on the CNT rope contributes to neurite extension, and NSCs seeded on CNT rope are differentiated towards neurons when compared with tissue culture plates (TCP). Moreover, electrically stimulated NSCs on the CNT rope showed enhanced neuronal maturity and increased neurite outgrowth speed. Their findings suggest a synergistic effect of the conductive CNT rope substrate and electrical stimulation on promoting neurite extension as well as oriented differentiation of NSCs to mature neuronal cells in the application for nerve tissue engineering.[195]

Park *et al.* reported a graphene substrate that showed a promotional effect on the differentiation of hNSCs into neurons. The graphene substrate was found to be a great cell-adhesion layer for persisting differentiation of hNSCs; also, the hNSCs were more likely to differentiate toward neurons than glial cells (Figure 5.7). Moreover, the differentiated cells showed neural activity with electrical stimulation on the graphene substrate.[123]

Li and group's work demonstrated that graphene films possess excellent biocompatibility for mouse hippocampal neurons. The number and average length of neurites on graphene were significantly enhanced compared to that on TCP; suggesting the potential of graphene as an implanted material for nerve tissue engineering.[154] They further utilized graphene foams to fabricate a novel 3D porous scaffold for NSCs *in vitro*. The 3D graphene foam scaffold not only provides a better support for NSC growth and proliferation than two-dimensional (2D) graphene films, but also promotes the differentiation of NSCs to astrocytes as well as neurons. Moreover, the 3D graphene foams show good electrical coupling with differentiated NSCs for electrical stimulation. These findings indicate that the 3D graphene foams have great potential for nerve tissue engineering.[127]

5.5.2 Applications for Bone Tissue Engineering

External electrical stimulation has a positive effect on bone healing in an injured region.[214–216] Much research has shown that electrical stimulation can significantly influence growth, proliferation, and nodule formation, as well as bone formation gene markers' expression and the protein synthesis

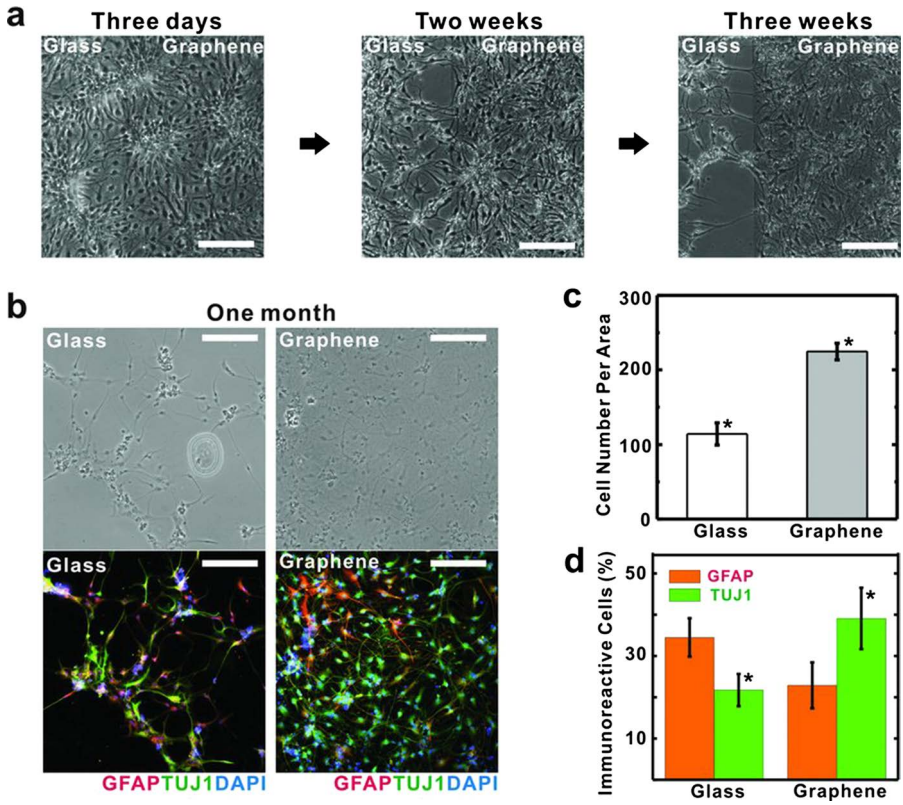

Figure 5.7 Enhanced neural differentiation of hNSCs on graphene films. All scale bars represent 200 μm: (a) bright-field images of the hNSCs differentiated for three days (left), two weeks (middle), and three weeks (right). (b) Bright-field (top row) and fluorescence (bottom row) images of hNSCs differentiated on glass (left) and graphene (right) after one month's differentiation. The differentiated hNSCs were immunostained with GFAP (red) for astroglial cells, TUJ1 (green) for neural cells, and DAPI (blue) for nuclei. (c) Cell counting per area (0.64 mm^2) on graphene and glass regions after one month's differentiation ($n = 5$, $p < 0.001$). (d) Percentage of immunoreactive cells for GFAP (red) and TUJ1 (green) on glass and graphene ($n = 5$, $p < 0.05$). Adapted from ref. 123 with permission from John Wiley & Sons, Inc.

of osteoblasts.[196,217–219] Therefore, a reasonable design and fabrication of 3D conductive scaffolds for bone defects, which can locally transport electrical stimuli, is eminently necessary for the development and clinical applications of bone tissue engineering.

Meng *et al.* synthesized a conductive membrane made of biodegradable PLLA and conductive PPy with heparin (PPy/heparin/PLLA) for the culture of osteoblast-like Saos-2 cells. Electrical stimulation can enhance the adhesion and proliferation of osteoblasts, and obviously increase calcium and phosphate amounts in the mineral deposition of the membranes (Figure 5.8).

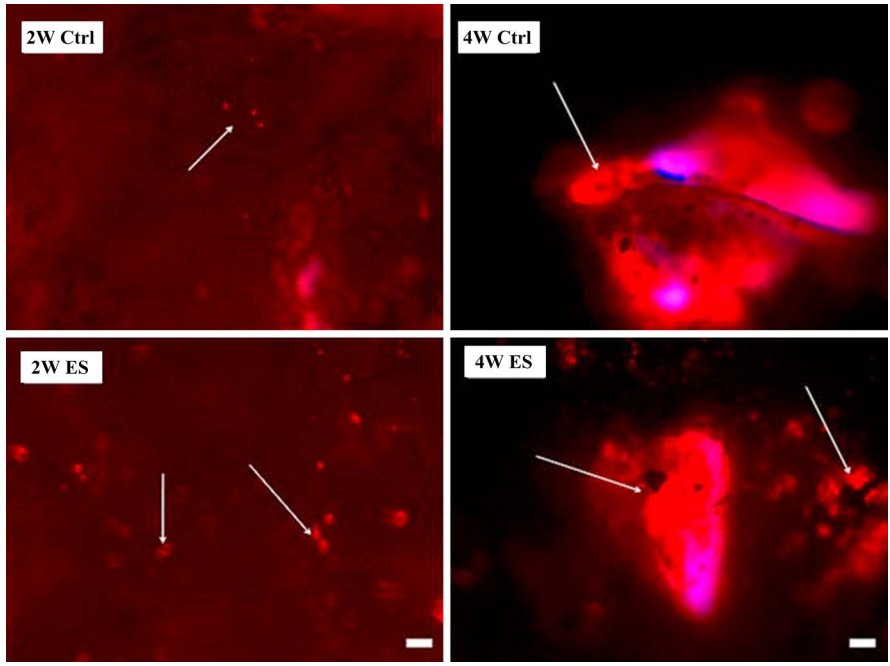

Figure 5.8 Nodule formation under ES. Calcium stained by Alizarin Red S (ARS) shows the formation of the mineralized nodules at week 2 and the significant growth of the nodules at week 4. The controls show fewer and smaller nodules (bar 10 μm). Reprinted from *Journal of Bone and Mineral Metabolism*, Accelerated osteoblast mineralization on a conductive substrate by multiple electrical stimulation, **29**, 2011, 535–544, S. Meng, Z. Zhang and M. Rouabhia, with permission from The Japanese Society for Bone and Mineral Research and Springer.

As well, the expression level of several osteoblast-specific markers was upregulated after electrical stimulation, indicating that an electrical stimulation through a conductive substrate could be applied for bone regeneration.[219] They further investigated the influence of electrical stimulation intensity on the gene activation and protein expression of two essential osteoblast markers, alkaline phosphatase (ALP) and osteocalcin (OC). An electrical stimulation intensity of 200 mV mm^{-1} was found to significantly activate the gene and the relevant protein production. However, electrical stimulation of 400 mV mm^{-1} decreased gene production. These results suggested that specific electrical stimulation parameters, such as intensity through conductive polymer materials, may be utilized to regulate osteoblast markers' production for bone tissue engineering.[196]

Shahini *et al.* fabricated a 3D conductive scaffold by including a biocompatible conductive polymer PEDOT:poly(4-styrene sulfonate) (PSS) in the composition of bioactive glass and gelatin (BaG/gelatin). Incorporation of PEDOT:PSS strengthened the stability of the scaffold, producing enhanced

mechanical properties and biodegradation resistance. Adult human mesenchymal stem cells' (hMSCs) viability was enhanced when increasing the concentration of PEDOT:PSS in the scaffold; indicating that the as-prepared BaG/gelatin/PEDOT:PSS scaffold is not only biocompatible but also can well support the hMSCs' growth.[197]

Another promising scaffold being explored for bone tissue engineering is PVDF due to its electroactivity-confirmed biocompatibility. Positively charged PVDF films coated with a thin titanium layer exhibit higher cell adhesion and proliferation of MC3T3-E1 osteoblasts than uncharged PVDF films; indicating the surface charge could enhance osteoblast growth.[198] hMSCs cultured on electrospun PVDF scaffolds with specific electrical stimulation possess better alkaline phosphatase activity and earlier mineralization in comparison to TCP.[199] Pärssinen *et al.* found that the surface charge of the poled PVDF films could influence the hydrophobicity of the substrates, further inducing the conformation changes of adsorbed extracellular matrix proteins, which finally can be used for the regulation of stem cell adhesion and directionally osteogenic differentiation.[200,201] Human alveolar bone-derived cells cultured on a novel PVDF–TrFE/barium titanate (BT) membrane showed a noticeably higher mRNA expression for all markers compared to those on polytetrafluoroethylene (PTFE), indicating support for the acquisition of the osteoblastic phenotype as well as upregulation of expression of apoptotic markers. These results are obtained *in vitro*, whereas *in vivo* research should be undertaken in the future to prove the promotional effect of PVDF–TrFE/BT membranes on bone formation.[202] PVDF–TrFE blends were subcutaneously implanted into rats, showing normal inflammatory patterns and regression of the chronic inflammatory process over 60 days, which indicate its potential application for bone regeneration.[84]

Random and aligned conductive nanofibers *via* embedding multiwalled carbon nanotubes (MWCNTs) in biodegradable poly(D,L-lactide) (PDLA) were fabricated by Shao *et al.* Non-stimulated neonatal rat osteoblasts on the aligned nanofibers showed enhanced cell extension and better directed cell outgrowth than those on random ones. Electrically stimulated osteoblasts on nanofibers grew along the electrical current route, with no difference between random and aligned fibers (Figure 5.9). These results show the synergistic effect of topography and electrical stimulation of conductive substrates on osteoblast outgrowth for bone tissue engineering.[204]

5.5.3 Applications for Muscle Tissue Engineering

Impairment to skeletal muscle tissue often gives rise to several complications in the human body. Skeletal muscle tissue engineering has been utilized to substitute damaged muscle tissue, which has made great progress in research on musculoskeletal regeneration and orthopaedic surgery.[220–222] Successful matrices for skeletal muscle tissue engineering should not only contribute a suitable surface for cell adhesion, proliferation and differentiation, but also should be nonimmunogenic and biodegradable.

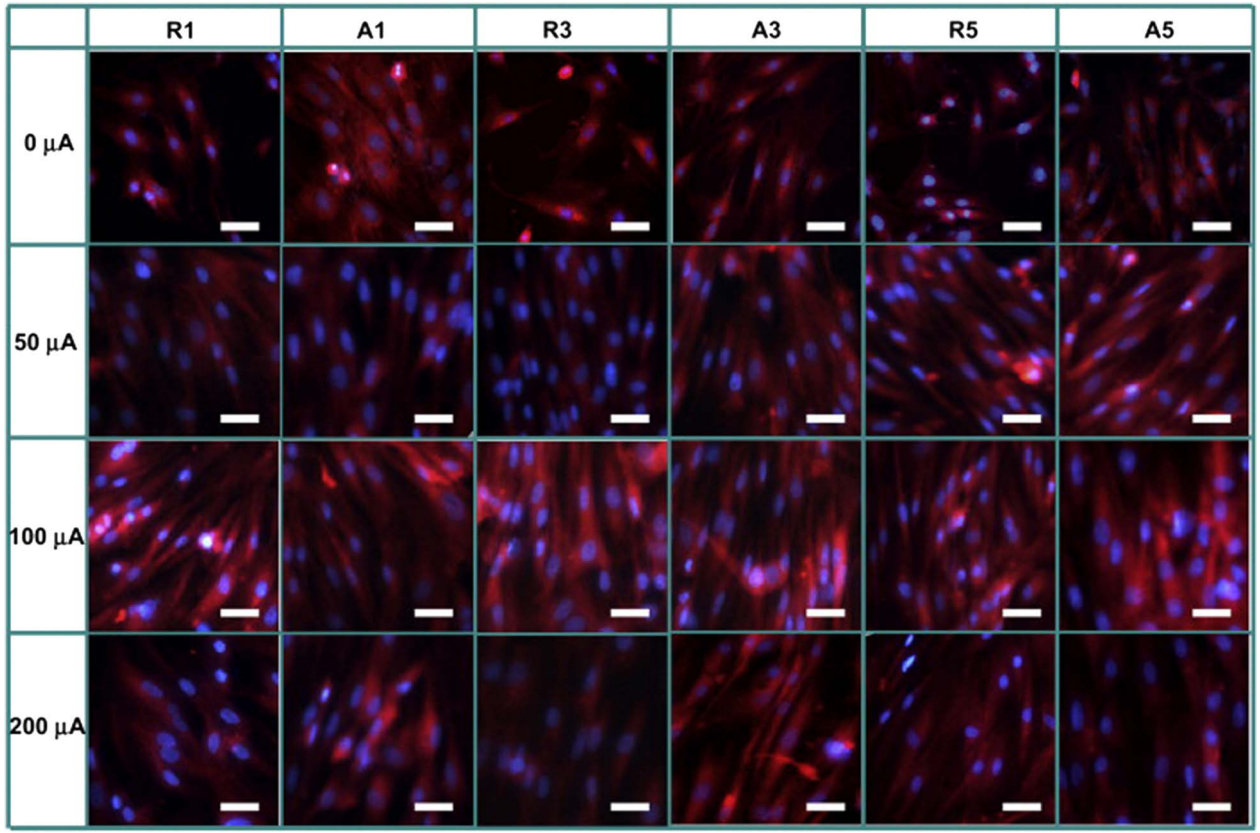

Figure 5.9 Fluorescence microscope images of osteoblasts cultured on R1, R3, R5, and A1, A3, A5 for five days with DC electrical stimulation 0 μA (ES-0), 50 μA (ES-50), 100 μA (ES-100), and 200 μA (ES-200). The nucleus was stained by DAPI (blue) and the cytoplasm was stained by Rhodamine 123 (red). All the scale bars are 50 μm. Reprinted from *Biomaterials*, **32**, Osteoblast function on electrically conductive electrospun PLA/MWCNTs nanofibers, 2821–2833, copyright (2011) with permission from Elsevier.

PANI doped with camphorsulfonic acid (CPSA) was combined with poly (L-lactide-*co*-ε-caprolactone) (PLCL) to fabricate uniform nanofibers by Jeong *et al.* The incorporation of CPSA–PANA showed enhanced mouse C2C12 myoblast adhesion than pure PLCL fibers, indicating the potential application for muscle tissue engineering.[205] A series of PANI and poly(D,L-lactide) (PDLA) mixtures with varying PANI weight percentage were used to prepare electrospun PANI/PDLA scaffolds with conductivity for the adhesion and growth of primary rat muscle cells.[206] Ku *et al.* developed a nanofiber scaffold *via* electrospinning of biodegradable polymer PCL and PANI. Both the alignment and PANI content show a significant influence on the differentiation of mouse C2C12 myoblasts on the PCL/PANI nanofibers, indicating the synergistic effect of topography and electrical stimuli on muscle cell differentiation.[207] Chen's work also shows that aligned PCL/PANI scaffolds can guide C2C12 myoblasts' orientation and promote myotube formation compared with random PCL scaffolds (Figure 5.10). Moreover, electrical stimulation could further promote myotube maturation. These results suggest the potential of aligned PCL/PANI nanofibrous scaffolds for skeletal muscle tissue engineering.[208]

The impact of morphology and polarization of PVDF on the adhesion and morphology of myoblast cells were studied by Martins *et al.*, where the results showed that negatively charged surfaces could encourage the adhesion and proliferation of C2C12 cells. In addition, culturing cells on the aligned fibers can allow for directional growth of myoblast cells.[209]

5.5.4 Applications for Cardiac Tissue Engineering

Cardiac tissue engineering is a potential strategy to regenerate damaged cardiac tissue and reconstruct an infarcted myocardium by using biofunctional scaffolds. The development of biomimetic ECMs, both structurally and functionally, is of immense importance in cardiac tissue engineering.[223,224] In recent years, considerable attention has been dedicated to the design of biomimetic scaffolds for applications in cardiac tissue engineering.

Conductive electrospun PPy/PCL/gelatin nanofibers were fabricated *via* the incorporation of different contents of PPy into PCL/gelatin by Kai *et al.* The scaffold containing 15% PPy showed the most outstanding properties for promoting primary cardiomyocytes' attachment, proliferation and expression levels of cardiac-specific proteins, indicating their great potential application as conductive scaffolds for cardiac tissue engineering.[210]

According to Li's work, electrospun PANI/gelatin nanofibers could reinforce the adhesion and growth of H9c2 rat cardiac myoblast cells to a similar degree as the control TCP, suggesting the conductive nanofibers could be utilized as a suitable scaffold in the cardiac tissue engineering field.[211] PANI doped with camphorsulfonic acid was incorporated into poly(glycerol-sebacate) (PGS) at different contents to fabricate conductive composite cardiac patches for cardiac tissue engineering applications. As shown in Figure 5.11, the PANI–PGS composites exhibited excellent attachment and proliferation

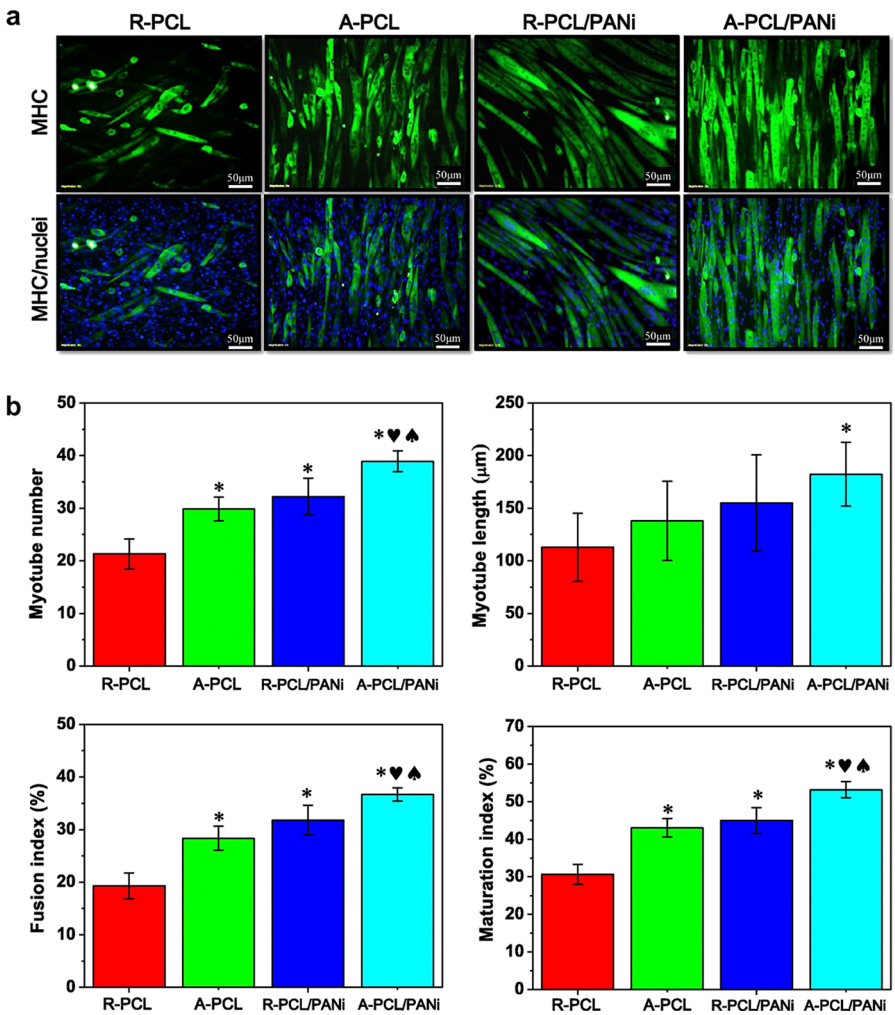

Figure 5.10 (a) Representative immunofluorescent images of myotubes differentiated for five days on random PCL (R-PCL), aligned PCL (A-PCL), random PCL/PANI-3 (R-PCL/PANi) and aligned PCL/PANI-3 (A-PCL/PANI) nanofibers and immunostained for MHC (green) and nucleus (blue). (b) Quantification of the myotube number, myotube length, fusion index, and maturation index of the myotubes formed in (a). *Significantly different in comparison with the R-PCL nanofibers ($P < 0.05$, $n = 5$); ♥ significantly different compared with the A-PCL nanofibers ($P < 0.05$, $n = 5$); ♠ significantly different compared with the R-PCL/PANI nanofibers ($P < 0.05$, $n = 5$). Reprinted from *Acta Biomaterialia*, **9**, M.-C. Chen, Y.-C. Sun and Y.-H. Chen, Electrically conductive nanofibers with highly oriented structures and their potential application in skeletal muscle tissue engineering, 5562–5572, copyright (2013) with permission from Elsevier.

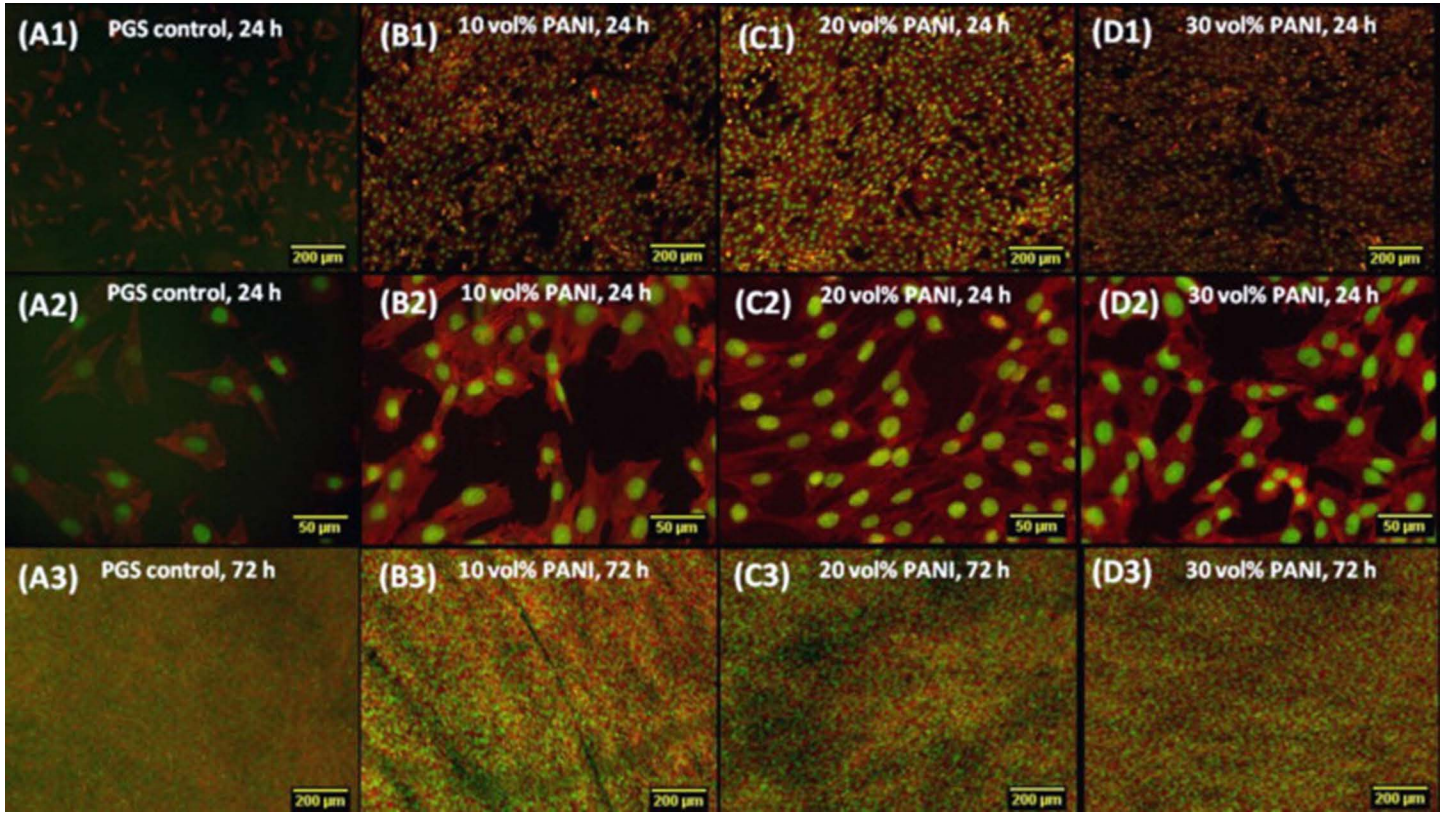

Figure 5.11 Fluorescence images showing Phalloidin-labeled (cytoskeleton; red) and Sytox-labeled (nucleus; green) C2C12 cells grown on PGS control films (A1–A3), 10 vol% PANI–PGS (B1–B3), 20 vol% PANI–PGS (C1–C3) and 30 vol% PANI–PGS (D1–D3). (A–D) 1: C2C12 cells at 24 h (scale bar, 200 µm); (A–D) 2: C2C12 cells at 24 h (scale bar, 50 µm); (A–D) 3: C2C12 cells at 72 h (scale bar, 200 µm). Reprinted from *Acta Biomaterialia*, **10**, T. H. Qazi, R. Rai, D. Dippold, J. E. Roether, D. W. Schubert, E. Rosellini, N. Barbani and A. R. Boccaccini, Development and characterization of novel electrically conductive PANI–PGS composites for cardiac tissue engineering applications, 2434–2345, copyright (2014) with permission from Elsevier.

of C2C12 cells, showing the potential to serve as a carrier of functional cells to myocardial infarctions.[212]

A carbon nanofiber (CNF) was incorporated into PLGA in order to improve the conductivity of unmodified PLGA for myocardial tissue engineering. The PLGA–CNF composites could promote the adhesion and proliferation of human cardiomyocytes and neurons, which are important cells for cardiovascular applications.[135] Shin *et al.* designed novel conductive cardiac constructs by seeding neonatal rat cardiomyocytes on CNT-incorporated GelMA hydrogels with photo-crosslinkage. The CNT–GelMA scaffolds showed improved cell adhesion and organization as well as cell–cell coupling (Figure 5.12). In addition, 3D bioactuators were formed by the release of centimeter-scale patches from glass substrates. This work reported a protective cardiac scaffold for the first time.[137] Also, they embedded aligned CNT microelectrode arrays into biocompatible hydrogels for cell stimulation. Bioactuators were developed by culturing cardiomyocytes on the CNT–hydrogel constructs, showing spontaneous actuation behavior, homogeneous cell organization as well as enhanced cell–cell coupling and maturation. Additionally, the novel constructs can provide an external electrical field for controlling a biohybrid machine.[138]

Martins *et al.* synthesized a porous chitosan/CNF scaffold, and neonatal rat cardiomyocytes grew well in the scaffold pores with higher metabolic activity compared to cells in chitosan scaffolds. Furthermore, the incorporation of carbon nanofibers also resulted in the increase of expression level of cardiac-specific genes.[213] In Kharaziha's work, hybrid scaffolds were developed by the incorporation of CNT into aligned electrospun PGS/gelatin nanofibers. Cardiomyocytes seeded on the CNT–PGS/gelatin scaffolds showed stronger spontaneous and synchronous beating behavior when compared with those cultured on PSG/gelatin scaffolds without CNT, indicating the great potential for generating cardiac tissue constructs.[99]

5.6 Conclusions and Perspectives

The numerous advantages of conductive materials, such as high conductivity, ease of tailoring and vast flexibility, have led to their popularity amongst a large range of biomedical applications. Especially for tissue engineering, conductive materials could direct distinctive cellular behaviors and responses, resulting in the promotion of damaged tissue regeneration, specifically in electrically sensitive tissues such as nerve, bone, muscle and cardiac tissues. The utilization of conductive materials in tissue engineering could effectively introduce electrical stimuli, which provide the possibility to control cell behaviors and further enhance cellular functions.

Great progress has been achieved in the preparation of electrically conductive materials including conducting polymers, piezoelectric polymeric materials, other novel conductive nanomaterials and self-assembled conductive hydrogels with excellent biocompatibility for the adhesion, growth, and differentiation of various stem cells *in vitro*. However, the biocompatibility of

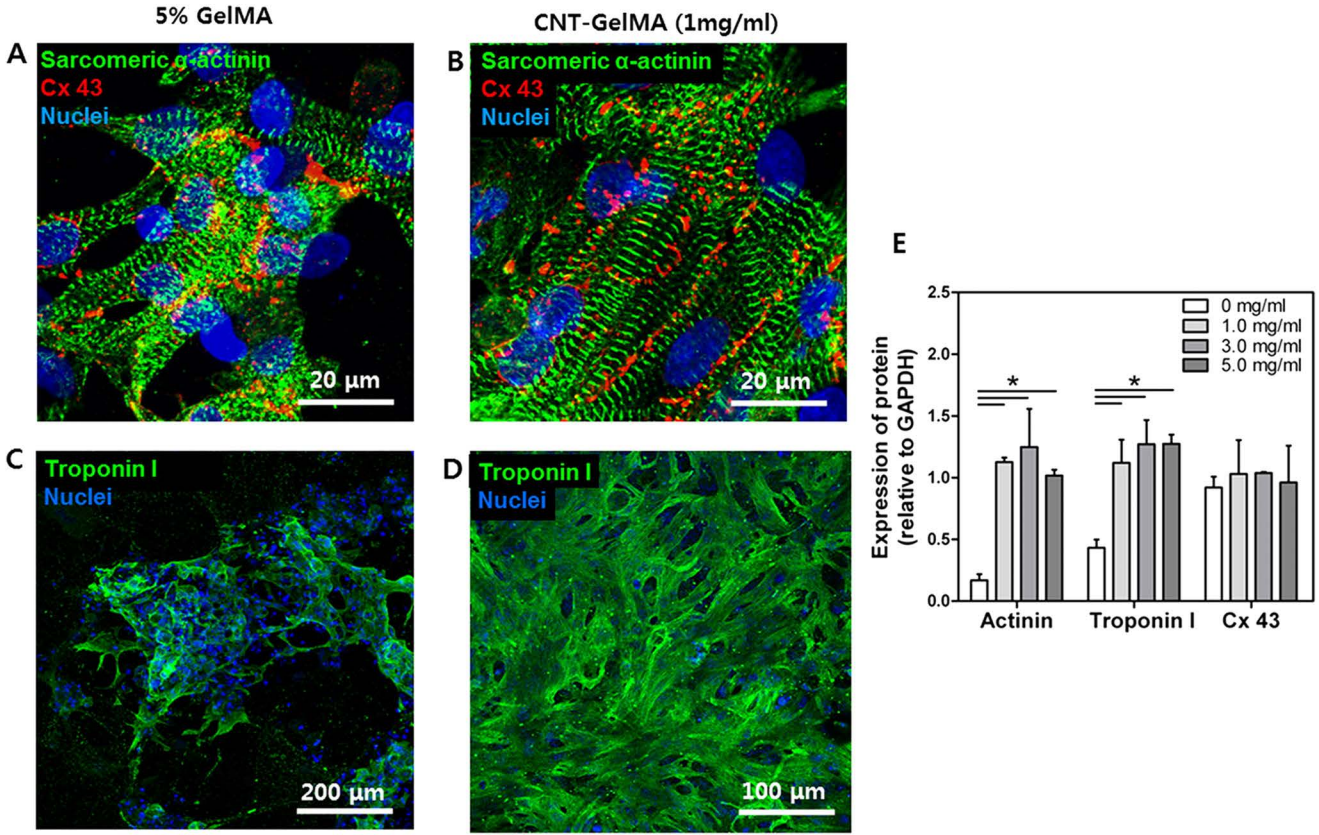

Figure 5.12 Phenotype of cardiac cells on CNT–GelMA hydrogels. Immunostaining of sarcomeric α-actinin (green), nuclei (blue), and Cx-43 (red) revealed that cardiac tissues (eight-day culture) on (A) pristine GelMA and (B) CNT–GelMA were phenotypically different. Partial uniaxial sarcomere alignment and interconnected sarcomeric structure with robust intercellular junctions were observed on CNT–GelMA. Immunostaining of Troponin I (green) and nuclei (blue) showed much less and more aggregated Troponin I presence on (C) pristine GelMA than on (D) CNT–GelMA. (E) Quantification of α-actinin, Cx-43, Troponin I expression by Western blot (*$p < 0.05$). Adapted from ref. 137 with permission from the American Chemical Society.

conductive materials *in vivo* still needs to be identified. Studies on developing conductive materials without cytotoxicity *in vivo* are also necessary.

Fortunately, the easy manufacture of conductive materials provides an additional advantage for improving biocompatibility by modification strategies. Especially, the biocompatibility and biodegradability of conductive materials can be enhanced by the incorporation of bioactive molecules and natural or synthetic biopolymers. Furthermore, the surface properties of biomaterials, such as morphology and topography structure, have been proven to have a crucial influence on cell behaviors. Topography modification strategies for conductive materials offer an opportunity for the design of suitable nanocomposite scaffolds for tissue engineering.

Conductive materials, especially conductive nanomaterials, with improved performance in biocompatibility and biodegradability prove to be a promising and valuable course for future research and the demand for developing novel nanocomposites, such as hydrogels with 3D porous structures or electrospun nanofibers, is also urgent. Additionally, the introduction of other kinds of stimuli besides electrical stimulation should broaden the modulation cues for much more accurate and effective control on cellular behaviors and biofunctions. Therefore, the design for multi-stimuli responsive scaffolds will be another potential direction for future tissue engineering applications. In summary, conductive materials have shown to be an encouraging area of biofunctional materials and tissue engineering, opening up a rich and interesting field for future research with immense promise.

References

1. R. Langer and J. P. Vacanti, *Science*, 1993, **260**, 920.
2. L. G. Griffith and G. Naughton, *Science*, 2002, **295**, 1009.
3. M. M. Stevens and J. H. George, *Science*, 2005, **310**, 1135.
4. D. E. Discher, P. Janmey and Y.-l. Wang, *Science*, 2005, **310**, 1139.
5. A. J. Engler, S. Sen, H. L. Sweeney and D. E. Discher, *Cell*, 2006, **126**, 677.
6. C. A. L. Bassett, R. J. Pawluk and R. O. Becker, *Nature*, 1964, **204**, 652.
7. A. D. Moore, *Med. Instrum.*, 1975, **9**, 274.
8. C. E. Pullar, R. Rivkah Isseroff and R. Nuccitelli, *Cell Motil. Cytoskeleton*, 2001, **50**, 207.
9. M. Zhao, A. Agius-Fernandez, J. V. Forrester and C. D. McCaig, *J. Cell Sci.*, 1996, **109**, 1405.
10. V. A. McBain, J. V. Forrester and C. D. McCaig, *Invest. Ophthalmol. Visual Sci.*, 2003, **44**, 540.
11. E. Wang, M. Zhao, J. V. Forrester and C. D. McCaig, *Exp. Eye Res.*, 2003, **76**, 29.
12. A. Bouaziz, A. Richert and A. Caprani, *Biomaterials*, 1997, **18**, 107.
13. X. Li and J. Kolega, *J. Vasc. Res.*, 2002, **39**, 391.
14. R. F. Valentini, T. G. Vargo, J. A. Gardella and P. Aebischer, *Biomaterials*, 1992, **13**, 183.

15. P.-h. G. Chao, H. H. Lu, C. T. Hung, S. B. Nicoll and J. C. Bulinski, *Connect. Tissue Res.*, 2007, **48**, 188.
16. N. Patel and M. M. Poo, *J. Neurosci.*, 1982, **2**, 483.
17. P. W. Luther, H. B. Peng and J. J.-C. Lin, *Nature*, 1983, **303**, 61.
18. E. K. Onuma and S. W. Hui, *J. Cell Biol.*, 1988, **106**, 2067.
19. C. E. Schmidt, V. R. Shastri, J. P. Vacanti and R. Langer, *Proc. Natl. Acad. Sci.*, 1997, **94**, 8948.
20. T. N. Hieu, W. Claudia, K. C. Jacqueline, N. Lindsey, K. N. Hieu and E. S. Christine, *J. Neural Eng.*, 2013, **10**, 046011.
21. G. G. Matthews, *Cellular Physiology of Nerve and Muscle*, John Wiley & Sons, 2009.
22. L. Ghasemi-Mobarakeh, M. P. Prabhakaran, M. Morshed, M. H. Nasr-Esfahani, H. Baharvand, S. Kiani, S. S. Al-Deyab and S. Ramakrishna, *J. Tissue Eng. Regener. Med.*, 2011, **5**, e17.
23. H. Kaji, T. Ishibashi, K. Nagamine, M. Kanzaki and M. Nishizawa, *Biomaterials*, 2010, **31**, 6981.
24. M. L. P. Langelaan, K. J. M. Boonen, K. Y. Rosaria-Chak, D. W. J. van der Schaft, M. J. Post and F. P. T. Baaijens, *J. Tissue Eng. Regener. Med.*, 2011, **5**, 529.
25. S. J. Hwang, Y. M. Song, T. H. Cho, R. Y. Kim, T. H. Lee, S. J. Kim, Y.-K. Seo and I. S. Kim, *Tissue Eng., Part A*, 2011, **18**, 432.
26. J. S. Park, H. N. Yang, D. G. Woo, S. Y. Jeon, H.-J. Do, S.-H. Huh, N.-H. Kim, J.-H. Kim and K.-H. Park, *Biomaterials*, 2012, **33**, 7300.
27. H. Cui, Y. Wang, L. Cui, P. Zhang, X. Wang, Y. Wei and X. Chen, *Biomacromolecules*, 2014, **15**, 3146.
28. M. Xie, L. Wang, J. Ge, B. Guo and P. X. Ma, *ACS Appl. Mater. Interfaces*, 2015, **7**, 6772.
29. J. G. Hardy, R. C. Sukhavasi, D. Aguilar, M. K. Villancio-Wolter, D. J. Mouser, S. A. Geissler, L. Nguy, J. K. Chow, D. L. Kaplan and C. E. Schmidt, *J. Mater. Chem. B*, 2015, **3**, 8059.
30. C. Ning, P. Yu, Y. Zhu, M. Yao, X. Zhu, X. Wang, Z. Lin, W. Li, S. Wang, G. Tan, Y. Zhang, Y. Wang and C. Mao, *NPG Asia Mater.*, 2016, **8**, e243.
31. N. Gomez, J. Y. Lee, J. D. Nickels and C. E. Schmidt, *Adv. Funct. Mater.*, 2007, **17**, 1645.
32. M. B. Runge, M. Dadsetan, J. Baltrusaitis, T. Ruesink, L. Lu, A. J. Windebank and M. J. Yaszemski, *Biomacromolecules*, 2010, **11**, 2845.
33. S.-C. Luo, *Polym. Rev.*, 2013, **53**, 303.
34. A. H. Rajabi, M. Jaffe and T. L. Arinzeh, *Acta Biomater.*, 2015, **24**, 12.
35. X. Li, T. Zhao, L. Sun, K. E. Aifantis, Y. Fan, Q. Feng, F. Cui and F. Watari, *J. Biomed. Mater. Res., Part A*, 2016, **104**, 322.
36. I. S. Chronakis, S. Grapenson and A. Jakob, *Polymer*, 2006, **47**, 1597.
37. J. Y. Wong, R. Langer and D. E. Ingber, *Proc. Natl. Acad. Sci.*, 1994, **91**, 3201.
38. D. D. Ateh, H. A. Navsaria and P. Vadgama, *J. R. Soc., Interface*, 2006, **3**, 741.

39. N. K. Guimard, N. Gomez and C. E. Schmidt, *Prog. Polym. Sci.*, 2007, **32**, 876.
40. R. A. Green, N. H. Lovell, G. G. Wallace and L. A. Poole-Warren, *Biomaterials*, 2008, **29**, 3393.
41. R. Ravichandran, S. Sundarrajan, J. R. Venugopal, S. Mukherjee and S. Ramakrishna, *J. R. Soc., Interface*, 2010, **7**, S559.
42. J. G. Hardy, J. Y. Lee and C. E. Schmidt, *Curr. Opin. Biotechnol.*, 2013, **24**, 847.
43. X. Zhang and S. K. Manohar, *J. Am. Chem. Soc.*, 2004, **126**, 12714.
44. R. Baumhardt-Neto and M.-A. De Paoli, *Polym. Degrad. Stab.*, 1993, **40**, 59.
45. W. A. Gazotti Jr, V. F. Juliano and M.-A. De Paoli, *Polym. Degrad. Stab.*, 1993, **42**, 317.
46. Z. Wang, C. Roberge, Y. Wan, L. H. Dao, R. Guidoin and Z. Zhang, *J. Biomed. Mater. Res., Part A*, 2003, **66A**, 738.
47. P. M. George, D. A. LaVan, J. A. Burdick, C. Y. Chen, E. Liang and R. Langer, *Adv. Mater.*, 2006, **18**, 577.
48. D. H. Kim, S. M. Richardson-Burns, J. L. Hendricks, C. Sequera and D. C. Martin, *Adv. Funct. Mater.*, 2007, **17**, 79.
49. S. Meng, M. Rouabhia, G. Shi and Z. Zhang, *J. Biomed. Mater. Res., Part A*, 2008, **87A**, 332.
50. P. M. George, A. W. Lyckman, D. A. LaVan, A. Hegde, Y. Leung, R. Avasare, C. Testa, P. M. Alexander, R. Langer and M. Sur, *Biomaterials*, 2005, **26**, 3511.
51. S. Lakard, G. Herlem, N. Valles-Villareal, G. Michel, A. Propper, T. Gharbi and B. Fahys, *Biosens. Bioelectron.*, 2005, **20**, 1946.
52. Z. Zhang, M. Rouabhia, Z. Wang, C. Roberge, G. Shi, P. Roche, J. Li and L. H. Dao, *Artif. Organs*, 2007, **31**, 13.
53. X. Bai, X. Li, N. Li, Y. Zuo, L. Wang, J. Li and S. Qiu, *Mater. Sci. Eng., C*, 2007, **27**, 695.
54. Q. Z. Yu, M. M. Shi, M. Deng, M. Wang and H. Z. Chen, *Mater. Sci. Eng., B*, 2008, **150**, 70.
55. M. Mattioli-Belmonte, G. Giavaresi, G. Biagini, L. Virgili, M. Giacomini, M. Fini, F. Giantomassi, D. Natali, P. Torricelli and R. Giardino, *Int. J. Artif. Organs*, 2003, **26**, 1077.
56. P. R. Bidez, S. Li, A. G. MacDiarmid, E. C. Venancio, Y. Wei and P. I. Lelkes, *J. Biomater. Sci., Polym. Ed.*, 2006, **17**, 199.
57. D.-F. Li, W. Wang, H.-J. Wang, X.-S. Jia and J.-Y. Wang, *Appl. Surf. Sci.*, 2008, **255**, 581.
58. P. Humpolicek, V. Kasparkova, P. Saha and J. Stejskal, *Synth. Met.*, 2012, **162**, 722.
59. D. K. Cullen, A. R. Patel, J. F. Doorish, D. H. Smith and B. J. Pfister, *J. Neural Eng.*, 2008, **5**, 374.
60. N. V. Blinova, J. Stejskal, M. Trchová and J. Prokeš, *Polym. Int.*, 2008, **57**, 66.

61. D. D. Zhou, X. T. Cui, A. Hines and R. J. Greenberg, in *Implantable Neural Prostheses 2: Techniques and Engineering Approaches*, ed. D. Zhou and E. Greenbaum, Springer New York, New York, NY, 2010, pp. 217–252.
62. M. P. Prabhakaran, L. Ghasemi-Mobarakeh, G. Jin and S. Ramakrishna, *J. Biosci. Bioeng.*, 2011, **112**, 501.
63. A. Borriello, V. Guarino, L. Schiavo, M. A. Alvarez-Perez and L. Ambrosio, *J. Mater. Sci.: Mater. Med.*, 2011, **22**, 1053.
64. T. H. Qazi, R. Rai and A. R. Boccaccini, *Biomaterials*, 2014, **35**, 9068.
65. J. Yang and D. C. Martin, *Sens. Actuators, B*, 2004, **101**, 133.
66. X. T. Cui and D. D. Zhou, *IEEE Trans. Neural Syst. Rehabil. Eng.*, 2007, **15**, 502.
67. M. M. Perez-Madrigal, E. Armelin, L. J. del Valle, F. Estrany and C. Aleman, *Polym. Chem.*, 2012, **3**, 979.
68. E. Armelin, A. L. Gomes, M. M. Perez-Madrigal, J. Puiggali, L. Franco, L. J. d. Valle, A. Rodriguez-Galan, J. S. d. C. Campos, N. Ferrer-Anglada and C. Aleman, *J. Mater. Chem.*, 2012, **22**, 585.
69. L. Groenendaal, F. Jonas, D. Freitag, H. Pielartzik and J. R. Reynolds, *Adv. Mater.*, 2000, **12**, 481.
70. A. A. Argun, A. Cirpan and J. R. Reynolds, *Adv. Mater.*, 2003, **15**, 1338.
71. H. C. Ko, S. Kim, H. Lee and B. Moon, *Adv. Funct. Mater.*, 2005, **15**, 905.
72. X. Cui and D. C. Martin, *Sens. Actuators, B*, 2003, **89**, 92.
73. R. A. Green, N. H. Lovell and L. A. Poole-Warren, *Biomaterials*, 2009, **30**, 3637.
74. M. R.-B. Sarah, L. H. Jeffrey and C. M. David, *J. Neural Eng.*, 2007, **4**, L6.
75. A. Peramo, M. G. Urbanchek, S. A. Spanninga, L. K. Povlich, P. Cederna and D. C. Martin, *Tissue Eng., Part A*, 2008, **14**, 423.
76. M. Asplund, E. Thaning, J. Lundberg, A. C. Sandberg-Nordqvist, B. Kostyszyn, O. Inganäs and H. v. Holst, *Biomed. Mater.*, 2009, **4**, 045009.
77. C. Frias, J. Reis, F. Capela e Silva, J. Potes, J. Simões and A. T. Marques, *J. Biomech.*, 2010, **43**, 1061.
78. C. Ribeiro, V. Sencadas, D. M. Correia and S. Lanceros-Méndez, *Colloids Surf., B*, 2015, **136**, 46.
79. K. Heiji, *Jpn. J. Appl. Phys.*, 1969, **8**, 975.
80. F. S. Foster, K. A. Harasiewicz and M. D. Sherar, *IEEE Trans. Ultrason. Ferroelectr. Freq. Control*, 2000, **47**, 1363.
81. J. Serrado Nunes, A. Wu, J. Gomes, V. Sencadas, P. M. Vilarinho and S. Lanceros-Méndez, *Appl. Phys. A*, 2009, **95**, 875.
82. N. Weber, Y. S. Lee, S. Shanmugasundaram, M. Jaffe and T. L. Arinzeh, *Acta Biomater.*, 2010, **6**, 3550.
83. C. D. Klink, K. Junge, M. Binnebösel, H. P. Alizai, J. Otto, U. P. Neumann and U. Klinge, *J. Invest. Surg.*, 2011, **24**, 292.
84. L. Marques, L. A. Holgado, R. D. Simões, J. D. A. S. Pereira, J. F. Floriano, L. S. L. S. Mota, C. F. O. Graeff, C. J. L. Constantino, M. A. Rodriguez-Perez, M. Matsumoto and A. Kinoshita, *J. Biomed. Mater. Res., Part B*, 2013, **101**, 1284.

85. U. Klinge, B. Klosterhalfen, A. P. Öttinger, K. Junge and V. Schumpelick, *Biomaterials*, 2002, **23**, 3487.
86. J. Conze, K. Junge, C. Weiß, M. Anurov, A. Oettinger, U. Klinge and V. Schumpelick, *J. Biomed. Mater. Res., Part B*, 2008, **87B**, 321.
87. H. F. Guo, Z. S. Li, S. W. Dong, W. J. Chen, L. Deng, Y. F. Wang and D. J. Ying, *Colloids Surf., B*, 2012, **96**, 29.
88. P. L. Jansen, U. Klinge, M. Anurov, S. Titkova, P. R. Mertens and M. Jansen, *Eur. surg. Res.*, 2004, **36**, 104.
89. M. M. Beloti, P. T. de Oliveira, R. Gimenes, M. A. Zaghete, M. J. Bertolini and A. L. Rosa, *J. Biomed. Mater. Res., Part A*, 2006, **79A**, 282.
90. L. N. Teixeira, G. E. Crippa, A. C. Trabuco, R. Gimenes, M. A. Zaghete, D. B. Palioto, P. T. de Oliveira, A. L. Rosa and M. M. Beloti, *Acta Biomater.*, 2010, **6**, 979.
91. T. H. Young, H. H. Chang, D. J. Lin and L. P. Cheng, *J. Membr. Sci.*, 2010, **350**, 32.
92. H. Delaviz, A. Faghihi, A. A. Delshad, M. H. Bahadori, J. Mohamadi and A. Roozbehi, *Cell J.*, 2011, **13**, 137.
93. X. Liu, X. Wang, H. Zhao and Y. Du, *J. Phys.: Conf. Ser.*, 2014, **557**, 012057.
94. D. Zhai, B. Liu, Y. Shi, L. Pan, Y. Wang, W. Li, R. Zhang and G. Yu, *ACS Nano*, 2013, **7**, 3540.
95. W. Tang, L. Li and X. Zeng, *Talanta*, 2015, **131**, 417.
96. H.-C. Su, C.-M. Lin, S.-J. Yen, Y.-C. Chen, C.-H. Chen, S.-R. Yeh, W. Fang, H. Chen, D.-J. Yao, Y.-C. Chang and T.-R. Yew, *Biosens. Bioelectron.*, 2010, **26**, 220.
97. W. M. Tsang, A. L. Stone, D. Otten, Z. N. Aldworth, T. L. Daniel, J. G. Hildebrand, R. B. Levine and J. Voldman, *J. Neurosci. Methods*, 2012, **204**, 355.
98. S. R. Shin, S. M. Jung, M. Zalabany, K. Kim, P. Zorlutuna, S. b. Kim, M. Nikkhah, M. Khabiry, M. Azize, J. Kong, K.-t. Wan, T. Palacios, M. R. Dokmeci, H. Bae, X. Tang and A. Khademhosseini, *ACS Nano*, 2013, **7**, 2369.
99. M. Kharaziha, S. R. Shin, M. Nikkhah, S. N. Topkaya, N. Masoumi, N. Annabi, M. R. Dokmeci and A. Khademhosseini, *Biomaterials*, 2014, **35**, 7346.
100. X. Li, X. Liu, J. Huang, Y. Fan and F.-z. Cui, *Surf. Coat. Technol.*, 2011, **206**, 759.
101. E. Mooney, J. N. Mackle, D. J. P. Blond, E. O'Cearbhaill, G. Shaw, W. J. Blau, F. P. Barry, V. Barron and J. M. Murphy, *Biomaterials*, 2012, **33**, 6132.
102. F. Menaa, A. Abdelghani and B. Menaa, *J. Tissue Eng. Regener. Med.*, 2015, **9**, 1321.
103. Q. Lu, J. M. Moore, G. Huang, A. S. Mount, A. M. Rao, L. L. Larcom and P. C. Ke, *Nano Lett.*, 2004, **4**, 2473.
104. P. Cherukuri, S. M. Bachilo, S. H. Litovsky and R. B. Weisman, *J. Am. Chem. Soc.*, 2004, **126**, 15638.

105. B. S. Harrison and A. Atala, *Biomaterials*, 2007, **28**, 344.
106. J. Wen, Y. Xu, H. Li, A. Lu and S. Sun, *Chem. Commun.*, 2015, **51**, 11346.
107. M. Chakrabarti, R. Kiseleva, A. Vertegel and S. K. Ray, *J. Nanosci. Nanotechnol.*, 2015, **15**, 5501.
108. A. Bianco, J. Hoebeke, S. Godefroy, O. Chaloin, D. Pantarotto, J.-P. Briand, S. Muller, M. Prato and C. D. Partidos, *J. Am. Chem. Soc.*, 2005, **127**, 58.
109. X. Chen, U. C. Tam, J. L. Czlapinski, G. S. Lee, D. Rabuka, A. Zettl and C. R. Bertozzi, *J. Am. Chem. Soc.*, 2006, **128**, 6292.
110. L. P. Zanello, B. Zhao, H. Hu and R. C. Haddon, *Nano Lett.*, 2006, **6**, 562.
111. Y. Wenrong, T. Pall, J. J. Gooding, P. R. Simon and B. Filip, *Nanotechnology*, 2007, **18**, 412001.
112. L. Xiaoming, G. Hong, U. Motohiro, S. Yoshinori, A. Tsukasa, A. Shigeaki, F. Qingling, C. Fuzhai and W. Fumio, *Biomed. Mater.*, 2009, **4**, 015005.
113. H. Hu, Y. Ni, V. Montana, R. C. Haddon and V. Parpura, *Nano Lett.*, 2004, **4**, 507.
114. H. Hu, Y. Ni, S. K. Mandal, V. Montana, B. Zhao, R. C. Haddon and V. Parpura, *J. Phys. Chem. B*, 2005, **109**, 4285.
115. E. Hirata, M. Uo, H. Takita, T. Akasaka, F. Watari and A. Yokoyama, *J. Biomed. Mater. Res., Part B*, 2009, **90B**, 629.
116. J. Venkatesan, R. Pallela and S. K. Kim, *J. Biomed. Nanotechnol.*, 2014, **10**, 3105.
117. V. Khalili, J. Khalil-Allafi, W. Xia, A. B. Parsa, J. Frenzel, C. Somsen and G. Eggeler, *Appl. Surf. Sci.*, 2016, **366**, 158.
118. Y. Zhu, S. Murali, W. Cai, X. Li, J. W. Suk, J. R. Potts and R. S. Ruoff, *Adv. Mater.*, 2010, **22**, 3906.
119. B. Song, D. Li, W. Qi, M. Elstner, C. Fan and H. Fang, *ChemPhysChem*, 2010, **11**, 585.
120. T. Cohen-Karni, Q. Qing, Q. Li, Y. Fang and C. M. Lieber, *Nano Lett.*, 2010, **10**, 1098.
121. K. Yang, S. Zhang, G. Zhang, X. Sun, S.-T. Lee and Z. Liu, *Nano Lett.*, 2010, **10**, 3318.
122. M. Kalbacova, A. Broz, J. Kong and M. Kalbac, *Carbon*, 2010, **48**, 4323.
123. S. Y. Park, J. Park, S. H. Sim, M. G. Sung, K. S. Kim, B. H. Hong and S. Hong, *Adv. Mater.*, 2011, **23**, H263.
124. T. R. Nayak, H. Andersen, V. S. Makam, C. Khaw, S. Bae, X. Xu, P.-L. R. Ee, J.-H. Ahn, B. H. Hong, G. Pastorin and B. Özyilmaz, *ACS Nano*, 2011, **5**, 4670.
125. Y. Wang, W. C. Lee, K. K. Manga, P. K. Ang, J. Lu, Y. P. Liu, C. T. Lim and K. P. Loh, *Adv. Mater.*, 2012, **24**, 4285.
126. Z. Chen, W. Ren, L. Gao, B. Liu, S. Pei and H.-M. Cheng, *Nat. Mater.*, 2011, **10**, 424.
127. N. Li, Q. Zhang, S. Gao, Q. Song, R. Huang, L. Wang, L. Liu, J. Dai, M. Tang and G. Cheng, *Sci. Rep.*, 2013, **3**, 1604.
128. A. Guiseppi-Elie, *Biomaterials*, 2010, **31**, 2701.

129. J. P. Gong, I. Kawakami, V. G. Sergeyev and Y. Osada, *Macromolecules*, 1991, **24**, 5246.
130. S. Abraham, S. Brahim, K. Ishihara and A. Guiseppi-Elie, *Biomaterials*, 2005, **26**, 4767.
131. S. Brahim, D. Narinesingh and A. Guiseppi-Elie, *Biosens. Bioelectron.*, 2002, **17**, 53.
132. S. E. Moulton, M. D. Imisides, R. L. Shepherd and G. G. Wallace, *J. Mater. Chem.*, 2008, **18**, 3608.
133. L. M. Lira and S. I. Córdoba de Torresi, *Electrochem. Commun.*, 2005, **7**, 717.
134. E. A. Moschou, M. J. Madou, L. G. Bachas and S. Daunert, *Sens. Actuators, B*, 2006, **115**, 379.
135. D. A. Stout, B. Basu and T. J. Webster, *Acta Biomater.*, 2011, **7**, 3101.
136. M. R. Abidian, E. D. Daneshvar, B. M. Egeland, D. R. Kipke, P. S. Cederna and M. G. Urbanchek, *Adv. Healthcare Mater.*, 2012, **1**, 762.
137. S. R. Shin, S. M. Jung, M. Zalabany, K. Kim, P. Zorlutuna, S. b. Kim, M. Nikkhah, M. Khabiry, M. Azize, J. Kong, K.-t. Wan, T. Palacios, M. R. Dokmeci, H. Bae, X. Tang and A. Khademhosseini, *ACS Nano*, 2013, **7**, 2369.
138. S. R. Shin, C. Shin, A. Memic, S. Shadmehr, M. Miscuglio, H. Y. Jung, S. M. Jung, H. Bae, A. Khademhosseini, X. Tang and M. R. Dokmeci, *Adv. Funct. Mater.*, 2015, **25**, 4486.
139. J. H. Collier, J. P. Camp, T. W. Hudson and C. E. Schmidt, *J. Biomed. Mater. Res.*, 2000, **50**, 574.
140. Z. Zhang, R. Roy, F. J. Dugré, D. Tessier and L. H. Dao, *J. Biomed. Mater. Res.*, 2001, **57**, 63.
141. H. Castano, E. A. O'Rear, P. S. McFetridge and V. I. Sikavitsas, *Macromol. Biosci.*, 2004, **4**, 785.
142. X. Wang, X. Gu, C. Yuan, S. Chen, P. Zhang, T. Zhang, J. Yao, F. Chen and G. Chen, *J. Biomed. Mater. Res., Part A*, 2004, **68A**, 411.
143. A. Ramanaviciene, A. Kausaite, S. Tautkus and A. Ramanavicius, *J. Pharm. Pharmacol.*, 2007, **59**, 311.
144. N. Ferraz, M. Strømme, B. Fellström, S. Pradhan, L. Nyholm and A. Mihranyan, *J. Biomed. Mater. Res., Part A*, 2012, **100A**, 2128.
145. S. Kamalesh, P. Tan, J. Wang, T. Lee, E.-T. Kang and C.-H. Wang, *J. Biomed. Mater. Res.*, 2000, **52**, 467.
146. S.-C. Luo, E. Mohamed Ali, N. C. Tansil, H.-h. Yu, S. Gao, E. A. B. Kantchev and J. Y. Ying, *Langmuir*, 2008, **24**, 8071.
147. M. R. Abidian, K. A. Ludwig, T. C. Marzullo, D. C. Martin and D. R. Kipke, *Adv. Mater.*, 2009, **21**, 3764.
148. M. H. Bolin, K. Svennersten, X. Wang, I. S. Chronakis, A. Richter-Dahlfors, E. W. H. Jager and M. Berggren, *Sens. Actuators, B*, 2009, **142**, 451.
149. V. Karagkiozaki, P. G. Karagiannidis, M. Gioti, P. Kavatzikidou, D. Georgiou, E. Georgaraki and S. Logothetidis, *Biochim. Biophys. Acta, Gen. Subj.*, 2013, **1830**, 4294.
150. H. Zhou, X. Cheng, L. Rao, T. Li and Y. Y. Duan, *Acta Biomater.*, 2013, **9**, 6439.

151. G.-M. Qiu, L.-P. Zhu, B.-K. Zhu, Y.-Y. Xu and G.-L. Qiu, *J. Supercrit. Fluids*, 2008, **45**, 374.
152. H.-C. Chen, C.-H. Tsai and M.-C. Yang, *J. Polym. Res.*, 2010, **18**, 319.
153. Y. Zhu and W. Li, *Sci. China, Ser. B: Chem.*, 2008, **51**, 1021.
154. N. Li, X. Zhang, Q. Song, R. Su, Q. Zhang, T. Kong, L. Liu, G. Jin, M. Tang and G. Cheng, *Biomaterials*, 2011, **32**, 9374.
155. L. Huang, J. Hu, L. Lang, X. Wang, P. Zhang, X. Jing, X. Wang, X. Chen, P. I. Lelkes, A. G. MacDiarmid and Y. Wei, *Biomaterials*, 2007, **28**, 1741.
156. A. Subramanian, U. M. Krishnan and S. Sethuraman, *J. Biomed. Sci.*, 2009, **16**, 108.
157. Y. Mei, L. Youlong, G. Qingyuan, C. Jun and L. Yong, *Mater. Res. Express*, 2015, **2**, 042001.
158. A. N. Zelikin, D. M. Lynn, J. Farhadi, I. Martin, V. Shastri and R. Langer, *Angew. Chem., Int. Ed.*, 2002, **41**, 141.
159. B. Lakard, L. Ploux, K. Anselme, F. Lallemand, S. Lakard, M. Nardin and J. Y. Hihn, *Bioelectrochemistry*, 2009, **75**, 148.
160. L. Cen, K. G. Neoh and E. T. Kang, *Langmuir*, 2002, **18**, 8633.
161. X. Cui, J. Wiler, M. Dzaman, R. A. Altschuler and D. C. Martin, *Biomaterials*, 2003, **24**, 777.
162. J.-W. Lee, F. Serna, J. Nickels and C. E. Schmidt, *Biomacromolecules*, 2006, **7**, 1692.
163. W. R. Stauffer and X. T. Cui, *Biomaterials*, 2006, **27**, 2405.
164. J. Yang and D. C. Martin, *Sens. Actuators, A*, 2004, **113**, 204.
165. H. K. Song, B. Toste, K. Ahmann, D. Hoffman-Kim and G. T. R. Palmore, *Biomaterials*, 2006, **27**, 473.
166. M. R. Abidian and D. C. Martin, *Adv. Funct. Mater.*, 2009, **19**, 573.
167. R. A. Green, N. H. Lovell, G. G. Wallace and L. A. Poole-Warren, *Biomaterials*, 2008, **29**, 3393.
168. J. Y. Lee, J.-W. Lee and C. E. Schmidt, *J. R. Soc., Interface*, 2009, **6**, 801.
169. A. Akkouch, G. Shi, Z. Zhang and M. Rouabhia, *J. Biomed. Mater. Res., Part A*, 2010, **92A**, 221.
170. D. D. Ateh, P. Vadgama and H. A. Navsaria, *Tissue Eng.*, 2006, **12**, 645.
171. G. M. Xiong, S. Yuan, J. K. Wang, A. T. Do, N. S. Tan, K. S. Yeo and C. Choong, *Acta Biomater.*, 2015, **23**, 240.
172. A. Gelmi, M. J. Higgins and G. G. Wallace, *Biomaterials*, 2010, **31**, 1974.
173. K. J. Gilmore, M. Kita, Y. Han, A. Gelmi, M. J. Higgins, S. E. Moulton, G. M. Clark, R. Kapsa and G. G. Wallace, *Biomaterials*, 2009, **30**, 5292.
174. J. Huang, X. Hu, L. Lu, Z. Ye, Q. Zhang and Z. Luo, *J. Biomed. Mater. Res., Part A*, 2010, **93A**, 164.
175. L. Ghasemi-Mobarakeh, M. P. Prabhakaran, M. Morshed, M. H. Nasr-Esfahani and S. Ramakrishna, *Tissue Eng., Part A*, 2009, **15**, 3605.
176. Y. Liu, X. Liu, J. Chen, K. J. Gilmore and G. G. Wallace, *Chem. Commun.*, 2008, 3729.
177. A. Yang, Z. Huang, G. Yin and X. Pu, *Colloids Surf., B*, 2015, **134**, 469.
178. J. G. Hardy, M. K. Villancio-Wolter, R. C. Sukhavasi, D. J. Mouser, D. Aguilar, S. A. Geissler, D. L. Kaplan and C. E. Schmidt, *Macromol. Rapid Commun.*, 2015, **36**, 1884.

179. R. Borah, A. Kumar, M. K. Das and A. Ramteke, *RSC Adv.*, 2015, **5**, 48971.
180. T. Kmecko, G. Hughes, L. Cauller, J.-B. Lee and M. Romero-Ortega, *Mater. Res. Soc. Proc.*, 2006, **926**, 0926-CC04-06.
181. H. Xiao, M. Zhang, Y. Xiao and J. Che, *Colloids Surf., B*, 2015, **126**, 138.
182. M. R. Aufan, Y. Sumi, S. Kim and J. Y. Lee, *ACS Appl. Mater. Interfaces*, 2015, **7**, 23454.
183. S. Park, Y. J. Kang and S. Majd, *Adv. Mater.*, 2015, **27**, 7583.
184. J. Xie, M. R. MacEwan, S. M. Willerth, X. Li, D. W. Moran, S. E. Sakiyama-Elbert and Y. Xia, *Adv. Funct. Mater.*, 2009, **19**, 2312.
185. J. Y. Lee, C. A. Bashur, A. S. Goldstein and C. E. Schmidt, *Biomaterials*, 2009, **30**, 4325.
186. J. Y. Lee, C. A. Bashur, C. A. Milroy, L. Forciniti, A. S. Goldstein and C. E. Schmidt, *IEEE Trans. Nanobioscience*, 2012, **11**, 15.
187. L. Jin, Z.-Q. Feng, M.-L. Zhu, T. Wang, M. K. Leach and Q. Jiang, *J. Biomed. Nanotechnol.*, 2012, **8**, 779.
188. H. Xu, J. M. Holzwarth, Y. Yan, P. Xu, H. Zheng, Y. Yin, S. Li and P. X. Ma, *Biomaterials*, 2014, **35**, 225.
189. L. Yan, B. Zhao, X. Liu, X. Li, C. Zeng, H. Shi, X. Xu, T. Lin, L. Dai and Y. Liu, *ACS Appl. Mater. Interfaces*, 2016, **8**, 6834.
190. J. Zhang, K. Qiu, B. Sun, J. Fang, K. Zhang, H. Ei-Hamshary, S. S. Al-Deyab and X. Mo, *J. Mater. Chem. B*, 2014, **2**, 7945.
191. L. J. Juarez-Hernandez, N. Cornella, L. Pasquardini, S. Battistoni, L. Vidalino, L. Vanzetti, S. Caponi, M. D. Serra, S. Iannotta, C. Pederzolli, P. Macchi and C. Musio, *Biophys. Chem.*, 2016, **208**, 40.
192. N. Royo-Gascon, M. Wininger, J. I. Scheinbeim, B. L. Firestein and W. Craelius, *Ann. Biomed. Eng.*, 2013, **41**, 112.
193. Y.-S. Lee, G. Collins and T. Livingston Arinzeh, *Acta Biomater.*, 2011, **7**, 3877.
194. Y.-S. Lee and T. L. Arinzeh, *Tissue Eng., Part A*, 2012, **18**, 2063.
195. Y.-J. Huang, H.-C. Wu, N.-H. Tai and T.-W. Wang, *Small*, 2012, **8**, 2869.
196. S. Meng, M. Rouabhia and Z. Zhang, *Bioelectromagnetics*, 2013, **34**, 189.
197. A. Shahini, M. Yazdimamaghani, K. J. Walker, M. A. Eastman, H. Hatami-Marbini, B. J. Smith, J. L. Ricci, S. V. Madihally, D. Vashaee and L. Tayebi, *Int. J. Nanomed.*, 2014, **9**, 167.
198. C. Ribeiro, S. Moreira, V. Correia, V. Sencadas, J. G. Rocha, F. M. Gama, J. L. Gomez Ribelles and S. Lanceros-Mendez, *RSC Adv.*, 2012, **2**, 11504.
199. M. D. Sita, W. Siliang, J. Michael and A. Treena Livingston, *Biomed. Mater.*, 2013, **8**, 045007.
200. J. Pärssinen, H. Hammarén, R. Rahikainen, V. Sencadas, C. Ribeiro, S. Vanhatupa, S. Miettinen, S. Lanceros-Méndez and V. P. Hytönen, *J. Biomed. Mater. Res., Part A*, 2015, **103**, 919.
201. C. Ribeiro, J. Pärssinen, V. Sencadas, V. Correia, S. Miettinen, V. P. Hytönen and S. Lanceros-Méndez, *J. Biomed. Mater. Res., Part A*, 2015, **103**, 2172.
202. L. N. Teixeira, G. E. Crippa, R. Gimenes, M. A. Zaghete, P. T. Oliveira, A. L. Rosa and M. M. Beloti, *J. Mater. Sci.: Mater. Med.*, 2010, **22**, 151.

203. L. N. Teixeira, G. E. Crippa, A. C. Trabuco, R. Gimenes, M. A. Zaghete, D. B. Palioto, P. T. de Oliveira, A. L. Rosa and M. M. Beloti, *Acta Biomater.*, 2010, **6**, 979.
204. S. Shao, S. Zhou, L. Li, J. Li, C. Luo, J. Wang, X. Li and J. Weng, *Biomaterials*, 2011, **32**, 2821.
205. S. I. Jeong, I. D. Jun, M. J. Choi, Y. C. Nho, Y. M. Lee and H. Shin, *Macromol. Biosci.*, 2008, **8**, 627.
206. K. D. McKeon, A. Lewis and J. W. Freeman, *J. Appl. Polym. Sci.*, 2010, **115**, 1566.
207. S. H. Ku, S. H. Lee and C. B. Park, *Biomaterials*, 2012, **33**, 6098.
208. M.-C. Chen, Y.-C. Sun and Y.-H. Chen, *Acta Biomater.*, 2013, **9**, 5562.
209. P. M. Martins, S. Ribeiro, C. Ribeiro, V. Sencadas, A. C. Gomes, F. M. Gama and S. Lanceros-Mendez, *RSC Adv.*, 2013, **3**, 17938.
210. D. Kai, M. P. Prabhakaran, G. Jin and S. Ramakrishna, *J. Biomed. Mater. Res., Part A*, 2011, **99A**, 376.
211. M. Li, Y. Guo, Y. Wei, A. G. MacDiarmid and P. I. Lelkes, *Biomaterials*, 2006, **27**, 2705.
212. T. H. Qazi, R. Rai, D. Dippold, J. E. Roether, D. W. Schubert, E. Rosellini, N. Barbani and A. R. Boccaccini, *Acta Biomater.*, 2014, **10**, 2434.
213. A. M. Martins, G. Eng, S. G. Caridade, J. F. Mano, R. L. Reis and G. Vunjak-Novakovic, *Biomacromolecules*, 2014, **15**, 635.
214. C. Andrew, L. Bassett, R. J. Pawluk and A. A. Pilla, *Science*, 1974, **184**, 575.
215. M. A. Darendeliler, A. Darendeliler and P. M. Sinclair, *Int. J. Adult Orthodon. Orthognath. Surg.*, 1997, **12**, 43.
216. J. T. Ryaby, *Clin. Orthop. Relat. Res.*, 1998, **355**, S205.
217. P. Torricelli, M. Fini, G. Giavaresi, R. Botter, D. Beruto and R. Giardino, *J. Biomed. Mater. Res., Part A*, 2003, **64A**, 182.
218. C. F. Martino, D. Belchenko, V. Ferguson, S. Nielsen-Preiss and H. J. Qi, *Bioelectromagnetics*, 2008, **29**, 125.
219. S. Meng, Z. Zhang and M. Rouabhia, *J. Bone Miner. Metab.*, 2011, **29**, 535.
220. P. Aspenberg, *Int. Orthop.*, 2007, **31**, 783.
221. M. Pecina and S. Vukicevic, *Int. Orthop.*, 2007, **31**, 719.
222. D. L. Butler, N. Juncosa-Melvin, G. P. Boivin, M. T. Galloway, J. T. Shearn, C. Gooch and H. Awad, *J. Orthop. Res.*, 2008, **26**, 1.
223. K. R. Chien, I. J. Domian and K. K. Parker, *Science*, 2008, **322**, 1494.
224. G. Vunjak-Novakovic, N. Tandon, A. Godier, R. Maidhof, A. Marsano, T. P. Martens and M. Radisic, *Tissue Eng., Part B*, 2009, **16**, 169.

CHAPTER 6

Smart Biomaterials for Cell Encapsulation

HUI ZHU[a] AND ZHIQIANG CAO*[a]

[a]Wayne State University, Department of Chemical Engineering and Materials Science, Detroit, Michigan, 48202, USA
*E-mail: zcao@wayne.edu

6.1 Introduction

Cell encapsulation is a well-known technology applied in biomedicine. This technology could protect the living cells inside to be viable by providing a biocompatible microenvironment that allows good transport of oxygen and nutrients, as well as hazardous substances.[1] In order to avoid cells being attacked by the host immune system, reducing the amount of toxic metabolites reaching encapsulated cells and adjusting mechanical stress are the primary challenges in cell encapsulation.[2–4] Besides, another obstacle is how to design biomaterials and take advantage of monoclonal antibodies to deliver encapsulated cells to certain specific positions, which is called targeted delivery.[5–7] Cell encapsulation has been a basic research tool since 1954.[8] Over the past 60 years, recent advances have brought the technology of cell encapsulation from a simple laboratory tool to a promising bedside therapy.[9–23] Cell encapsulation has been used in therapeutic treatments for diabetes,[24] cancer,[25] hemophilia,[26] rental failure[27] and functional applicability in humans in several clinical trials.[28,29] However, lots of challenges remain for cell encapsulation. For the long-term successful application of cell encapsulation in the

Smart Materials No. 25
Smart Materials for Tissue Engineering: Applications
Edited by Qun Wang

Published by the Royal Society of Chemistry, www.rsc.org

Table 6.1 Key parameters could be optimized for cell encapsulation technology.[1] Reprinted from Life Sciences, 143, M. Hashemi and F. Kalalinia, Application of encapsulation technology in stem cell therapy, 139–146, Copyright (2015) with permission from Elsevier.

Field of challenges	Parameters
Materials science	-Purity -Mechanical properties -Toxicity and immunogenicity -Interactions with the encapsulated cells
Encapsulation technology	-Formation of uniform capsules with excellent repeatability and reproducibility -Stability of the cell capsules -Chemical and physical properties of polymer
Cell biology	-The quality of the cells -Nutrition of the encapsulated cells -Transplantation site of the cell capsules -Control of expansion, cultivation and differentiation of stem cells

clinic, scientific ingenuity should consider the sources of functional cells. Properties of materials, like biocompatibility and stability, are also critical to protect the encapsulated cells and maintain their long-term viability.[30] Therefore, many important parameters should be optimized (Table 6.1), which are summarized by Maryam.[1] These considerations significantly limit the number of materials suitable for this application. The new generation of smart biomaterials seems to further improve the feasibility for cell encapsulation to be applied.

Smart biomaterials are novel biomaterials that can respond to changes in the surrounding environment when one of their properties is changed by external conditions like pH, temperature, pressure and light.[31,32] Over the past few decades, a large amount of smart biomaterials has been created with improved responsiveness, biocompatibility, stealth properties, specificity and other critical properties, such as shape memory, promoting vascularization, directing cell phenotype, injectability, *etc.* Here, these new generations of smart biomaterials with different functions will be discussed and their application for cell encapsulation will be highlighted.

6.2 Recent Advances of Smart Biomaterials

6.2.1 Smart Biomaterials that Mimic the Native Microenvironment

Advances in various fields of biology have demonstrated that cells are highly sensitive to their environment. The native microenvironment consists of cells and the extracellular matrix (ECM). The mechanical, chemical and physical properties of the native microenvironment could affect the behavior of encapsulated cells directly or indirectly. Mimicking the native microenvironment

has been widely exploited as an effective approach in tissue engineering. A suitable microenvironment could control cell morphology, cellular attachment and even promote cell differentiation. The properties of the ECM, architectures of cells and signaling pathways in living cells are key factors to be considered when mimicking the native environment.[33–35]

Electrospun fibers have been identified for their use in numerous applications,[36] because of their large surface-to-volume ratio, controllable properties, comparatively low cost and relatively high production rate. Hydrogels are polymer networks that are extensively swollen in water and are highly similar to natural tissue.[37] Consequently, they have also received considerable attention over the last few decades. However, there are still several formidable problems when applying hydrogel materials, such as in mimicking the native microenvironment. Some researchers have found that a combination of electrospun fibers and hydrogels could overcome their respective intrinsic defects, and take advantage of their individual superiority; particularly, it has been found that the complex fiber/gel architecture is similar to a native microenvironment. In Xu's review,[38] they summarized approaches (Figure 6.1) that could be used to form various scaffolds with electrospun fibers and hydrogels, which could be applied in tissue engineering, drug delivery, and other biomedical fields. In the fiber/gel composite, the hydrogels are supporting materials for the formation of a 3D structure to encapsulate cells and the

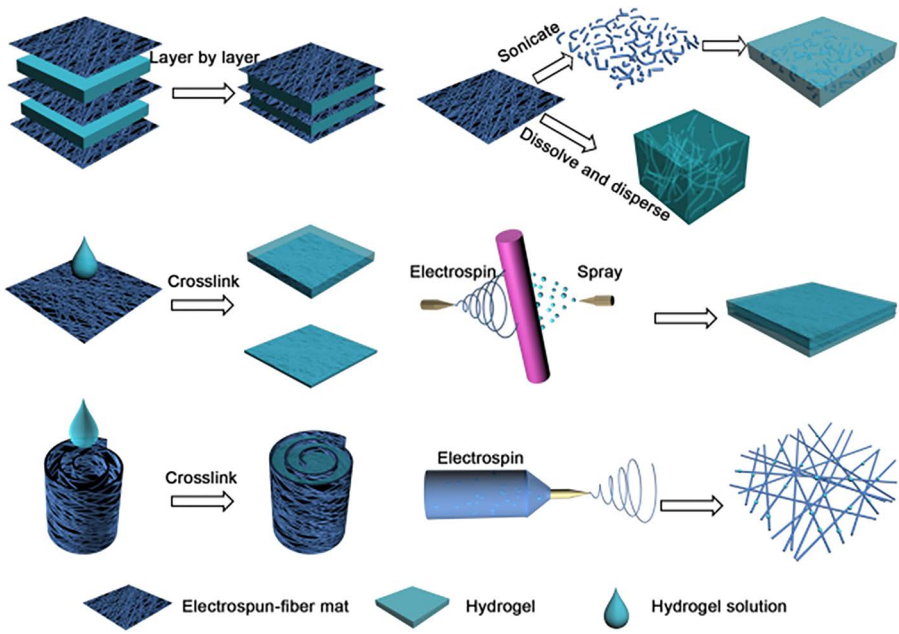

Figure 6.1 Numerous strategies to integrate electrospun fibers with hydrogels.[38] Reproduced with permission from S. Xu, L. Deng, J. Zhang, L. Yin and A. Dong, *J Biomed Mater Res B Appl Biomater*, 2015, **104**, 640. Copyright 2015: Wiley.

embedded aligned electrospun fibers could guide the growth of individual cells. Hsieh[39] seeded neural stem/progenitor cells (NSPCs) in the composite of a physical hydrogel blend of HA and methylcellulose (HAMC) and electrospun fiber segments of poly(ε-caprolactone-*co*-D,L-lactide) (P(CL:DLLA)) or collagen with different culture media. Their work demonstrated that a 3D microenvironment is very important to shape cell behavior, which is one of the critical factors for cell delivery applications.

Supramolecular biomaterials (Figure 6.2)[40] are assembled through reversible, non-covalent interactions, and offer unprecedented application possibilities as drug carriers, and tissue engineering scaffolds. Supramolecular biomaterials could also be applied to engineer cell microenvironments. Matthew highlighted the properties of supramolecular biomaterials compared with traditional biomaterials in terms of modularity, tunability, responsiveness and biomimicry.[40] The reversibility of supramolecular interactions has been applied to the technologies of preparing bioactive matrices from peptides or engineered proteins to control cell behavior[41–44] and support therapeutic cells.[45,46] In addition, materials designed with supramolecular principles could direct cell differentiation and guide cell phenotype. Gabriel reported self-assembled scaffolds consisting of supramolecular peptide nanofibers that direct the differentiation of neural progenitor cells into neurons.[47] A monodomain gel composed of massively aligned bundles of nanofibers was used as a platform to facilitate the differentiation and aligned growth of neural cells.[48]

Designing hydrogels with biomolecules present to promote specific cell–substrate interactions is another way to mimic a cell's microenvironment.

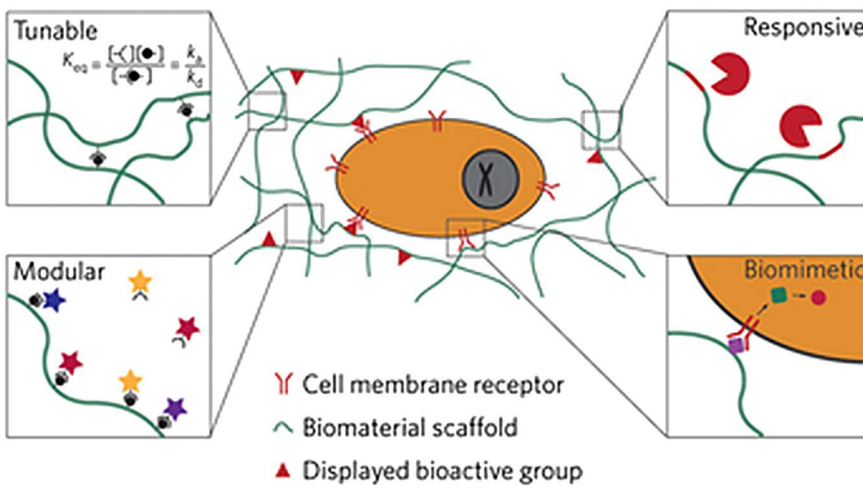

Figure 6.2 Special properties of supramolecular biomaterials.[40] Reproduced with permission from Macmillan Publishers Ltd: M. J. Webber, E. A. Appel, E. W. Meijer and R. Langer, *Nature Materials*, 2015, **15**, 13. Copyright 2015: Nature Publishing Group.

Chemical signals, mechanical cues, and physical cues play key roles in cell–ECM interactions. Firstly, growth factors are key components present within the ECM that dictate cell fate. The site-targeted combination of growth factors and hydrogels has been applied to promote cell development *in vitro.* Fibroblast growth factor 1 (FGF-1) and bone morphogenetic protein 4 (BMP-4) are two pro-adipogenic soluble factors present in ECM. Midori[49] encapsulated these two factors in alginate microgels, with the dual-stage delivery of FGF-1 and BMP-4 to induce adipogenesis. The development of mature adipocytes was promoted in this 3D, dual-stage delivery system. Secondly, cell fate could be influenced by the mechanical properties of an effective biomimetic hydrogel. Sur showed that dissociated hippocampal cells cultured on a softer peptide amphiphile hydrogel could significantly increase their differentiation and maturation.[50] Thirdly, biomaterials' size and shape are physical cues that affect cell microenvironments. Certain research has demonstrated that the behaviors of many cells can be modified by fibers of sub-micron dimension.[51]

6.2.2 Smart Biomaterials that Overcome Suffocation

There are many challenges in the technology of cell encapsulation, including protecting cells from immune attack by the host, and improving cell proliferation and maintaining cell viability.[1] These obstacles typically result in cell graft failure and have to be considered when rationally designing new biomaterials to improve graft survival. Before vascularization develops, if any, many cells in an encapsulation graft die in the first few days due to suffocation, which has been considered as a result of competition for oxygen from inflammatory cells.[52,53]

Hypoxia tolerance is related to the reduced generation of oxidative stress, which could result in significant destruction of cell death.[54] Oxidative stress is caused by an imbalance between the production of free radicals. It is detrimental to cell survival and is related to many pathological diseases. A composite hydrogel was engineered to be auto-catalytic, antioxidant and self-renewing by taking advantage of a cerium oxide nanoparticle (CONP).[55] Embedded CONPs within the encapsulating alginate hydrogel served as agents to release cellular oxidative stress, consequently improving cell survival (Figure 6.3).

Sufficient generation of oxygen is very important for cell viability and tissue function. Designing a hydrogel that generates oxygen is a promising way to control cell fate. Neslihan and his colleagues reported the preparation of an oxygen-generating hydrogel, a gelatin methacryloyl (GelMA), containing calcium peroxide (CPO) to provide oxygen for cardiac cells under ischemic conditions[56] (Figure 6.4). Calcium peroxide decomposes in water and generates oxygen. Solid peroxide was encapsulated within a hydrophilic material, polydimethylsiloxane (PDMS).[57] The resulting PDMS-CaO_2 disk was able to prolong the survival and function of encapsulated pancreatic islets that would otherwise be compromised by hypoxia. PDMS played the role of restricting the water from rapidly

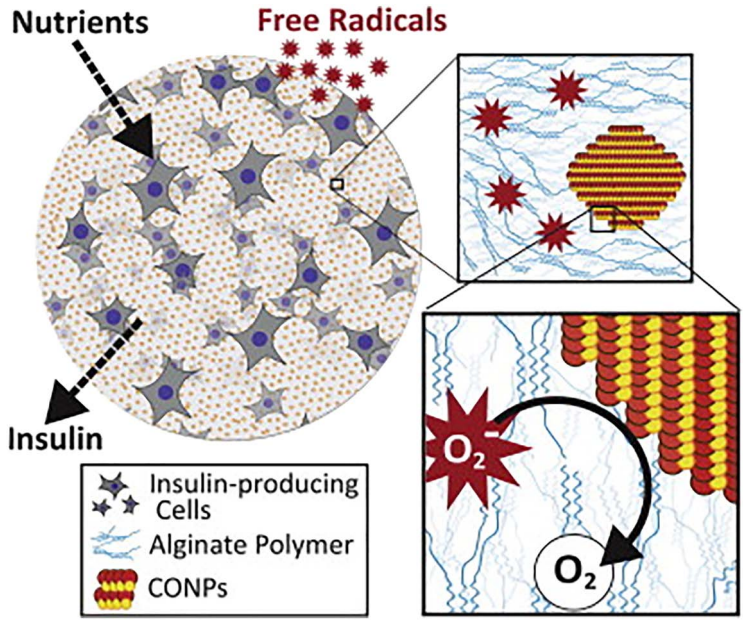

Figure 6.3 The way to release oxidative stress in a cerium oxide nanoparticle (CONP)-composite hydrogel.[55] Reproduced from *Acta Biomaterialia*, **16**, J. D. Weaver and C. L. Stabler, Antioxidant cerium oxide nanoparticle hydrogels for cellular encapsulation, 136–144, Copyright (2015) with permission from Elsevier.

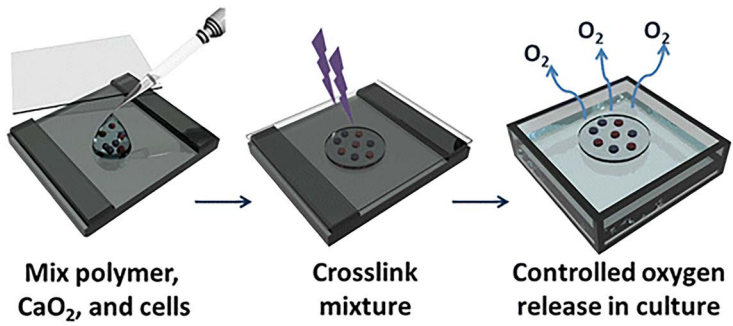

Figure 6.4 Illustration of CPO-GelMA hydrogels.[56] Reproduced with permission from N. Alemdar, J. Leijten, G. Camci-Unal, J. Hjortnaes, J. Ribas, A. Paul, P. Mostafalu, A.K. Gaharwar, Y. Qiu, S. Sonkusale, R. Liao and A. Khademhosseini, *ACS Biomater. Sci. Eng.*, 2016, doi:10.1021/acsbiomaterials.6b00109. Copyright 2016: American Chemical Society.

reacting with calcium peroxide. This allowed sustained oxygen generation from the PDMS-CaO_2 disk, which kept the β cell proliferating for more than three weeks.

Oxygen can also be generated from photoexcited C60 or C70.[58,59] Taking advantage of this feature, a water-soluble fullerene biomaterial was

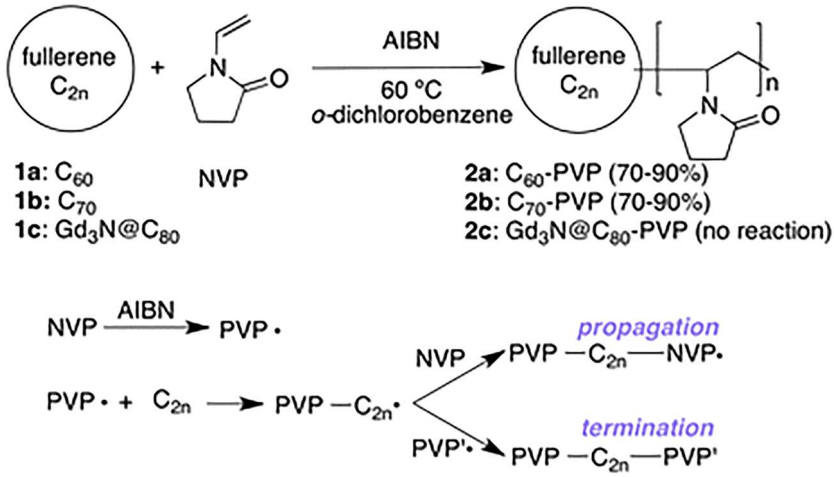

Figure 6.5 Preparation of (C_{2n})–PVP copolymers. Reproduced from ref. 59 with permission from The Royal Society of Chemistry.

developed, by integrating biocompatible poly(vinylpyrrolidone) (PVP) with C60 or C70 through covalent bonds[60] (Figure 6.5).

6.2.3 Smart Biomaterials that Promote Vascularization

Blood vessels and capillaries provide oxygen and nutrients to sustain cell viability and facilitate the removal of waste metabolic products. Therefore, promoting a well-vascularized microenvironment is critical for tissue engineering. For long-term cell encapsulation, besides overcoming suffocation, how to promote blood vessel formation in and/or surrounding the implanted biomaterials is extremely challenging. A good understanding of the biology background provides a fundamental basis for researchers to develop and optimize new biomaterials that could promote vascularization. In order to control neovasculature development, it's important to figure out which regulatory factors and cell types affect the formation of blood vessels.[61] Well-studied angiogenesis stimulatory factors include fibroblast growth factor (bFGF), certain matrix metalloproteinases (MMPs), vascular endothelial growth factor (VEGF) and platelet-derived growth factor (PDGF).[62] There are numerous cell types involved in vascular networks, such as vascular endothelial cells (VECs), smooth muscle cells (VSMCs) and mesenchymal stem cells (MSCs). Based on this knowledge of vascularization, vascularized biomaterials have been developed through various starategies.[61]

Encapsulating growth factors within a scaffold matrix and absorbing the factors to the matrix surface are popular approaches to delivering growth factors for neovascularization. Mejdi[63] engineered a fibrin gel by covalently linking major integrin-binding domain (FNIII 9-10) and the growth factor (GF)-binding domain (FNIII 12-14). The engineered gel could retain the

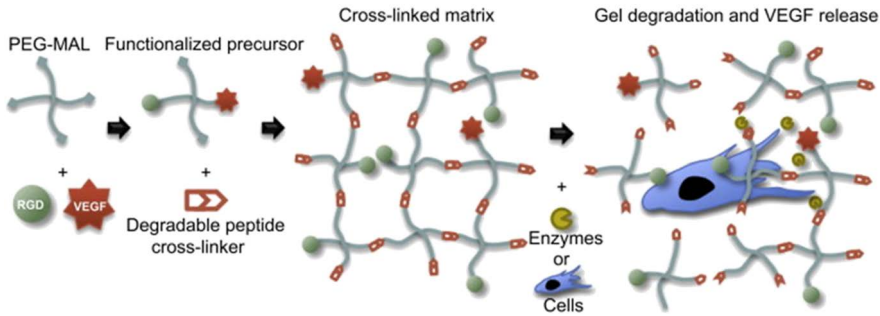

Figure 6.6 Illustration of functionalizing a PEG-MAL hydrogel with a bioactive molecular RGD peptide and VEGF growth factor.[64] Reproduced from *Biomaterials*, **34**(19), E. A. Phelps, D. M. Headen, W. R. Taylor, P. M. Thule and A. J. Garcia, Vasculogenic biosynthetic hydrogel for enhancement of pancreatic islet engraftment and function in type 1 diabetes, 4602–4611, Copyright (2013) with permission from Elsevier.

release of pro-angiogenic GFs, such as vascular endothelial GF (VEGFA165) and platelet-derived GF (PDGF-BB), and promote revascularization in a murine islet transplant model. Edward[64] pre-functionalized a PEG-maleimide hydrogel with VEGF-A165 (an angiogenic growth factor) and GRGDSPC (RGD) peptide for pancreatic islet encapsulation (Figure 6.6). This VEGF-releasing hydrogel showed improved islet engraftment and therapeutic function in treating type 1 diabetes.

Localized gene delivery is an alternative strategy to produce angiogenic growth factors within and/or surrounding the porous biomaterial implant. Lentivirus encoding for an angiogenic factor, VEGF, was used in macroporous PEG hydrogels to transfect the cells and promote vascularization[65] (Figure 6.7). Genetically modified cells enable the natural release of bioactive proteins at physiological doses.

To promote vascular formation, mature or progenitor endothelial cells, smooth muscle cells and mesenchymal stem cells (MSCs) can also be transplanted. They are expected to anastomose with invading host cells and form a functional vascular network within the scaffolds.[62]

Modifying the geometry and physical properties of biomaterials have also been shown to promote vascularization. It has been reported that a synthetic scaffold with pore size controlled at 30–40 μm in diameter can vascularize rapidly under *in vivo* conditions.[66,67] Lauran fabricated a poly(2-hydroxyethyl methacrylate-*co*-methacrylic acid) (pHEMA-*co*-MAA) hydrogel scaffold containing parallel channels through a micro templating method and observed that the micrometer-sized spherical pores promoted vascularization.[68] Besides, Hongyan reported the preparation of water-insoluble silk protein scaffolds by the use of acids.[69] It was believed that the soft mechanical property of the silk protein scaffold provides appropriate physical cues to support endothelial cell differentiation and neovascularization.[69]

6.2.4 Smart Biomaterials that Overcome a Foreign Body Reaction

As discussed above, protecting encapsulated cells from immune attack by the host system is one of the biggest barriers in cell encapsulation. Encapsulating cells in super-biocompatible materials and devices that provide a protective shell barrier is one method for preventing this immune destruction. However, the immune system recognizes materials or devices implanted in the body as foreign objects, and a foreign body reaction is triggered in most cases.

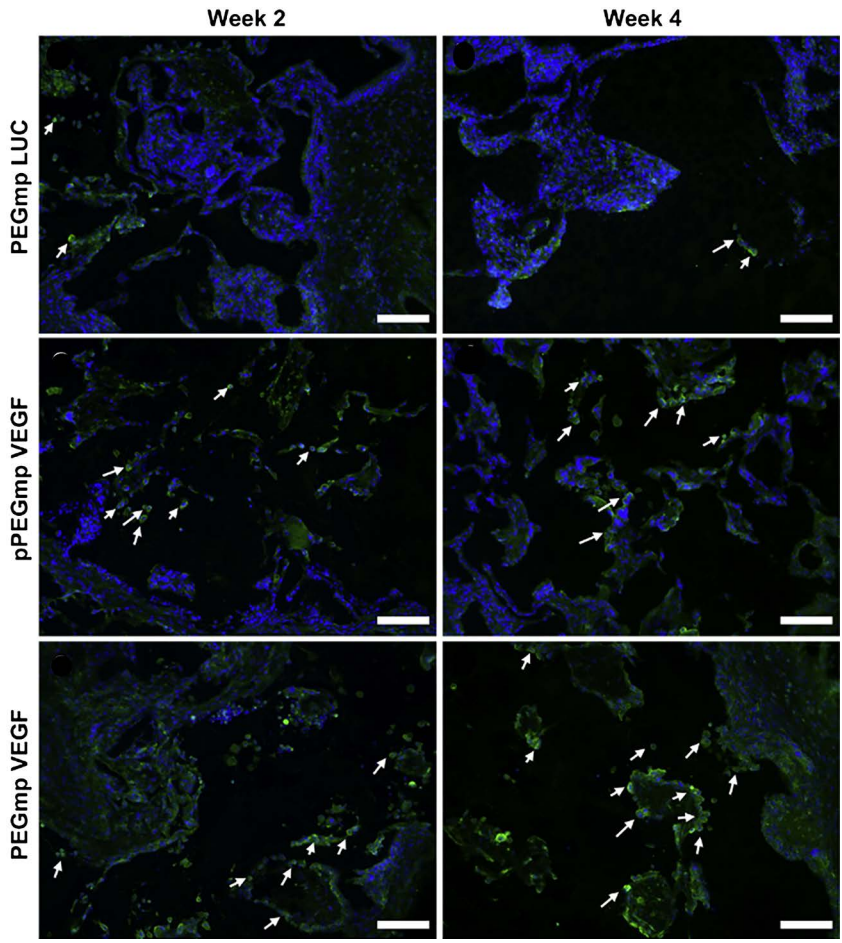

Figure 6.7 Vascularization of macroporous PEG hydrogels embedded with lentivirus, which could encode for VEGR factor after two and four weeks.[65] Reproduced from *Biomaterials*, **33**(30), J. A. Shepard, F. R. Virani, A. G. Goodman, T. D. Gossett, S. Shin and L. D. Shea, Hydrogel macroporosity and the prolongation of transgene expression and the enhancement of angiogenesis, 7412–7421, Copyright (2012) with permission from Elsevier.

A foreign body reaction involves the encapsulation of foreign objects within a dense collagen capsule (an avascular network), chronic inflammation, and damage to the surrounding tissue.[70–73] These immune-mediated reactions can lead to degradation, chronic pain, device rejection, and failure. Therefore, encapsulated cells would normally get destroyed after implantation unless the foreign body reaction to the encapsulating materials and devices can be regulated.

The initiation step for the foreign body reaction is believed to involve protein adsorption on the surfaces of implanted biomaterials.[71] It has been hypothesized that non-fouling biomaterials, being able to resist nonspecific protein absorption, can attenuate subsequent adverse inflammatory responses.[74,75] Shenfu summarized antifouling materials into two major categories: polyhydrophilic materials and polyzwitterionic materials (Table 6.2)[76]. PEG and PHEMA are two notable non-fouling materials in the

Table 6.2 Overview of hydrophilic and zwitterionic antifouling materials.[76] Reprinted from Polymer, 51(23), S. Chen, L. Li, C. Zhao and J. Zheng, Surface hydration: Principles and applications toward low-fouling/non-fouling biomaterials, 5283–5293, Copyright (2010) with permission from Elsevier.

Materials	Protein absorption	Cell adhesion
Hydrophilic materials		
PEG-based materials		
PS-*g*-PEGMA and PMMA-*g*-PEGMA	Yes	No
PEG-poly(phosphonate) terpolymer	Yes	No
PLL-*g*-PEG	Yes	Yes
PEGMA	Yes	No
$PPEG_xLys$	Yes	No
POEGMA	Yes	Yes
PEO-PU-PEO	Yes	No
PEO-PPO-PEO	Yes	No
PEO	Yes	No
PEG	Yes	Yes
Py-*g*-PEG	Yes	No
mPEG-DOPA	Yes	No
mPEG-MAPD	Yes	No
OEG-SAM	Yes	Yes
PMOXA	Yes	No
Dendron		
Glycerol dendron	Yes	No
HPG	Yes	No
Tetraglyme	Yes	Yes
Dextran	Yes	No
Polysaccharide	Yes	No
Poly (HEMA)	No	Yes
PVA	Yes	No
Polyamines functionalized with acetyl chloride	Yes	Yes
Mannitol-SAM	Yes	Yes
Peptide-based SAM	Yes	No

(*continued*)

Table 6.2 (*continued*)

Materials	Protein absorption	Cell adhesion
Polybetaine		
Poly(CBAA)	Yes	Yes
Poly(SBMA)	Yes	Yes
Poly(CBMA)	Yes	Yes
Poly(MPC)	Yes	Yes
PC-SAM	Yes	Yes
OPC-SAM	Yes	Yes
Polyampholyte		
SA/TMA-SAM	Yes	Yes
CA/TMA-SAM	Yes	Yes
PM/TMA-SAM	Yes	No
Peptide surfaces derived from natural amino acids	Yes	No
Poly(TM-SA)	Yes	No
Poly(METMA-MES)	Yes	No
PDDA/PSS	Yes	No

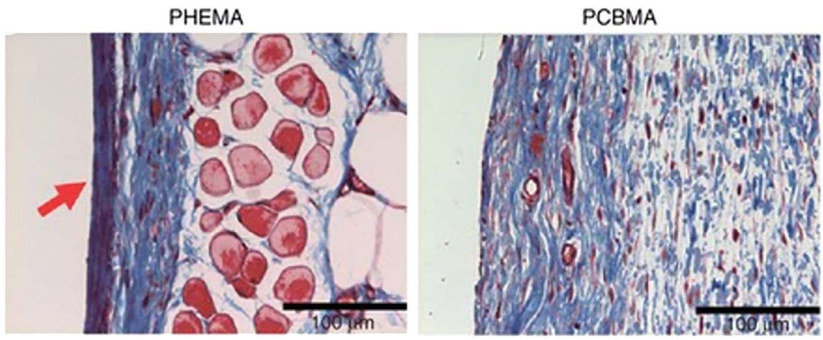

Figure 6.8 Masson's trichrome staining images to indicate the formation of a collagen capsule (red arrow) when encapsulated cells were implanted in mice subcutaneously after four weeks.[77] Reproduced with permission from Macmillan Publishers Ltd: L. Zhang, Z. Cao, T. Bai, L. Carr, J. R. Ella-Menye, C. Irvin, B. D. Ratner and S. Jiang, *Nature Biotechnology*, 2013, **31**, 553. Copyright 2013: Nature Publishing Group.

polyhydrophilic material category. Compared with these hydrophilic materials, zwitterionic polymers are more promising nonfouling biomaterials because of their biomimetic property, simplicity of synthesis, and availability of functional groups, and more importantly, the capability to inhibit the foreign body reaction. Lei reported a PCBMA-based zwitterionic hydrogel, which could resist the formation of a foreign body capsule for at least three months at the subcutaneous site as demonstrated in a mouse model.[77] Zwitterionic PCBMA hydrogel samples after the implantation showed much less capsule formation than PHEMA, a typical polyhydrophilic non-fouling material (Figure 6.8).

In addition to zwitterionic biomaterials, Arturo tried to chemically modify alginate, which is one of the most commonly used gel-forming materials using a combinatorial synthetic method.[78] A large library of the alginate variants has been created, and it has been identified that three triazole-containing analogs (Z2-Y12, Z1-Y15, Z1-Y19 in Figure 6.9) create unique hydrogel surfaces that substantially reduce foreign body reactions as tested in rodents and non-human primates.[78] This research group also prepared an alginate gel with a Z1-Y15 modification to encapsulate SC-β cells (a type of insulin-producing human embryonic stem cell) and demonstrated the implant's capability of mitigating the foreign body response and maintaining long-term glycemic control in mice.[79]

The geometry of materials and devices is an additional factor that modulates the foreign body response;[80,81] in particular, the size and shape affect the foreign body reaction and macrophage behavior. Omid showed that spherical alginate gel beads of 1.5 mm in diameter had improved biocompatibility compared with beads of a smaller size or gels of a different shape.[82] SLG20 alginate beads of 0.5 and 1.5 mm in diameter were used to encapsulate 500 IEs (islet equivalents) of rat islets and were later transplanted to the intraperitoneal space of streptozotocin (STZ)-induced C57BL/6 diabetic mice, a commonly used type 1 diabetes model (Figure 6.10). Transplanted islets encapsulated by 1.5 mm SLG20 alginate could lower the blood glucose to a healthy level for up to 180 days, which is five times longer than islets encapsulated by 0.5 mm SLG20 alginate. It was concluded that the capability for implanted materials to overcome foreign body reactions could be simply manipulated by their spherical dimensions.

6.2.5 Smart Biomaterials that Direct Cell Phenotype

Cell behaviors typically include adhesion, proliferation, and phenotypic expression.[83] These cell behaviors, such as phenotype, are typically directed by cues from their local microenvironment. When cells are encapsulated, various signaling molecules tethered to the biomaterial matrix become responsible for directing cell behaviors (Figure 6.11).[84] As a new trend towards smart biomaterials, researchers are trying to design new encapsulating materials to control cell behavior by closely mimicking the natural *in vivo* cellular microenvironment, such as by providing the necessary signaling molecules, and biophysical and bioactive cues.

Stem cells are non-specialized cells that could either proliferate to expand the stem cell population or differentiate into various other cell types during their development.[85] Stem cells play increasingly prominent roles in cell encapsulation, such as by differentiating into desired cell phenotypes wherein they are embedded. The differentiation of stem cells into specialized cell types is governed by a variety of factors, including micro-environmental cues from the surrounding ECM, soluble factors, matrix stiffness, substrate topography and direct cell–cell contact.[34] Designing smart biomaterials as cell carriers to deliver stem-cell-regulatory signals is a common strategy to direct cell phenotype.

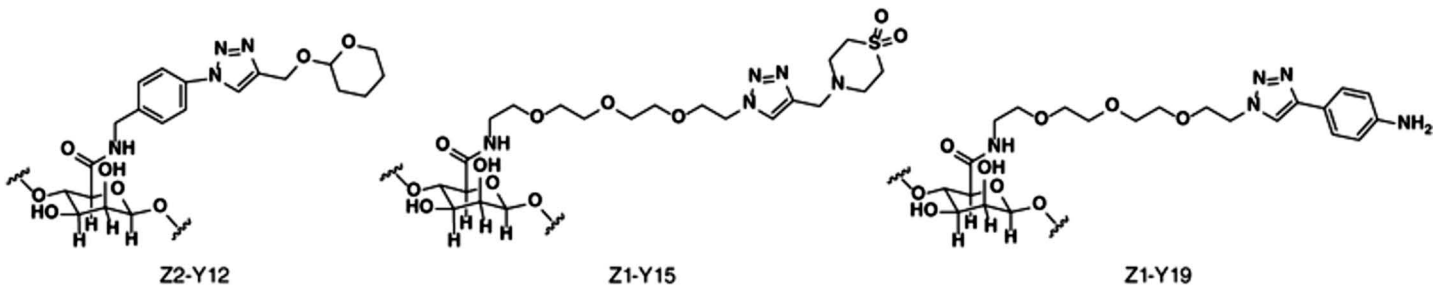

Figure 6.9 Chemical structures of the three materials.[78] Reproduced with permission from Macmillan Publishers Ltd: A. J. Vegas, O. Veiseh, J. C. Doloff, M. Ma, H. H. Tam, K. Bratlie, J. Li, A. R. Bader, E. Langan, K. Olejnik, P. Fenton, J. W. Kang, J. Hollister-Locke, M. A. Bochenek, A. Chiu, S. Siebert, K. Tang, S. Jhunjhunwala, S. Aresta-Dasilva, N. Dholakia, R. Thakrar, T. Vietti, M. Chen, J. Cohen, K. Siniakowicz, M. Qi, J. McGarrigle, S. Lyle, D. M. Harlan, D. L. Greiner, J. Oberholzer, G. C. Weir, R. Langer and D. G. Anderson, *Nature Biotechnology*, 2016, **34**, 345. Copyright 2016: Nature Publishing Group.

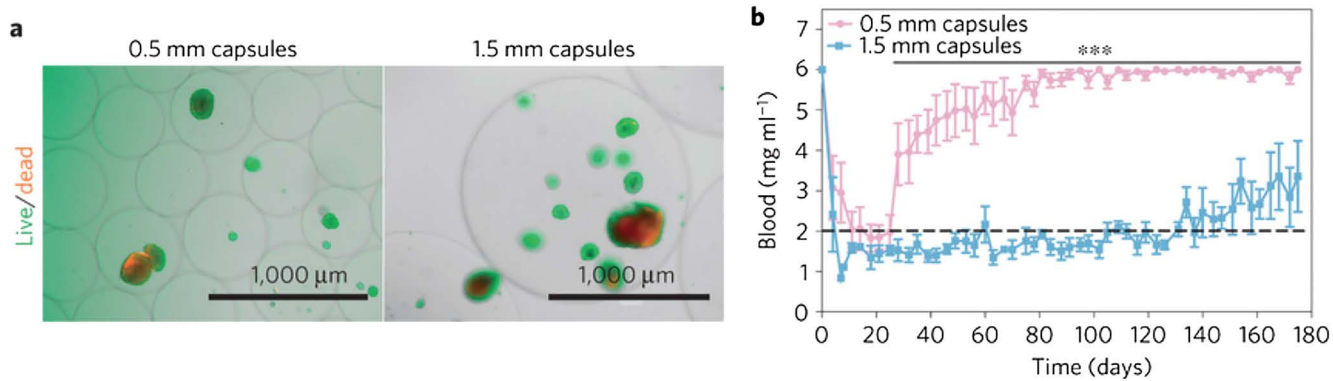

Figure 6.10 (a) Live/dead staining for islet cells encapsulated in 0.5 mm capsules and 1.5 mm capsules to verify their viability. (b) Blood–glucose concentration in implanted mice; the one with 1.5 mm capsules shows much longer normoglycemia than the one with 0.5 mm capsules.[82] Reproduced with permission from Macmillan Publishers Ltd: O. Veiseh, J. C. Doloff, M. Ma, A. J. Vegas, H. H. Tam, A. R. Bader, J. Li, E. Langan, J. Wyckoff, W. S. Loo, S. Jhunjhunwala, A. Chiu, S. Siebert, K. Tang, J. Hollister-Lock, S. Aresta-Dasilva, M. Bochenek, J. Mendoza-Elias, Y. Wang, M. Qi, D. M. Lavin, M. Chen, N. Dholakia, R. Thakrar, I. Lacik, G. C. Weir, J. Oberholzer, D. L. Greiner, R. Langer and D. G. Anderson, *Nature Materials*, 2015, **14**, 643. Copyright 2015: Nature Publishing Group.

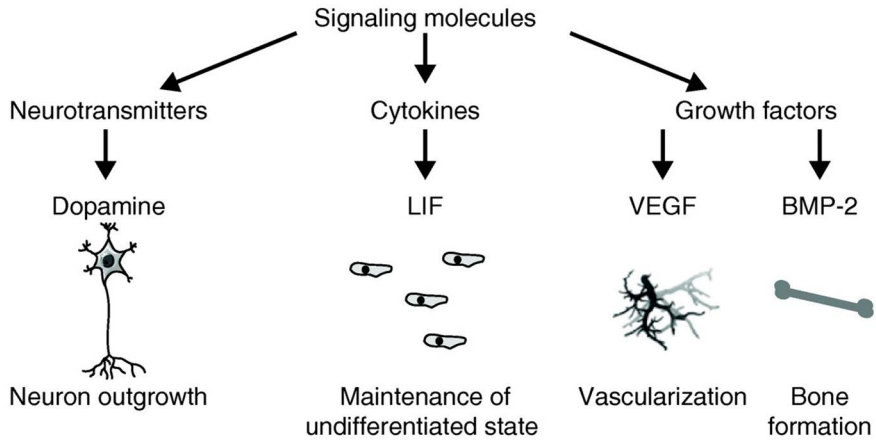

Figure 6.11 Most studied signaling molecules could affect the behaviors of cells in biomaterials applied for tissue engineering.[84] Reproduced with permission from A. J. Mieszawska and D. L. Kaplan, *Mieszawska and Kaplan BMC Biology*, 2010, **8**, 59. Copyright 2010: BioMed Central.

For example, alginate poly-L-lysine (PLL) was used to encapsulate a murine embryonic stem cell and this encapsulation system was able to control stem cell differentiation into hepatocytes.[86] In this system, alginate PLL microencapsulation was used as a vehicle to discretely control important culture parameters through variations in alginate composition, PLL concentration, and cell seeding density. Delivering signal molecules directly *via* biomaterials has many shortcomings, such as their rapid degradation and cleaving. Significant work has focused on the immobilization (or functionalization) of signal bio-molecules on cell encapsulation materials. Tzu-Yun reported a hydrogel assembled from functionalized peptides for neural stem cell encapsulation.[87] In their system, RADA16, one type of self-assembling peptide (SAP), was used to form a nanofibrous network structure as a cell encapsulating material. As a signal carrier, RADA16 was conjugated with a IKVAV sequence at its terminal residue. IKVAV is a motif from the α1 chain of laminin-1, which could promote neuronal differentiation.

In addition to delivering biomedical cues, introducing micro- and nanoscale features onto culture surfaces is another strategy to direct cell differentiation.[88] Studies revealed that cells could respond to topographical cues, such as elasticity, dimensionality and different combinations of biomaterials. Nathaniel found that manipulating the elasticity of materials could control stem cell behavior *in vitro*.[89] They encapsulated solid-phase porogens into a bulk hydrogel with cells encapsulated. The porogen was degraded *via* hydrolysis, forming void spaces inside the hydrogel. The chemical composition of the porogen determined its degradation rate, which directed the cell release, potential cell infiltration, and final tissue repair. Kelly examined the phenotypes of native valvular interstitial cells (VICs) when they were cultured on tissue culture polystyrene (TCPS), and 2D and 3D poly (ethylene glycol)

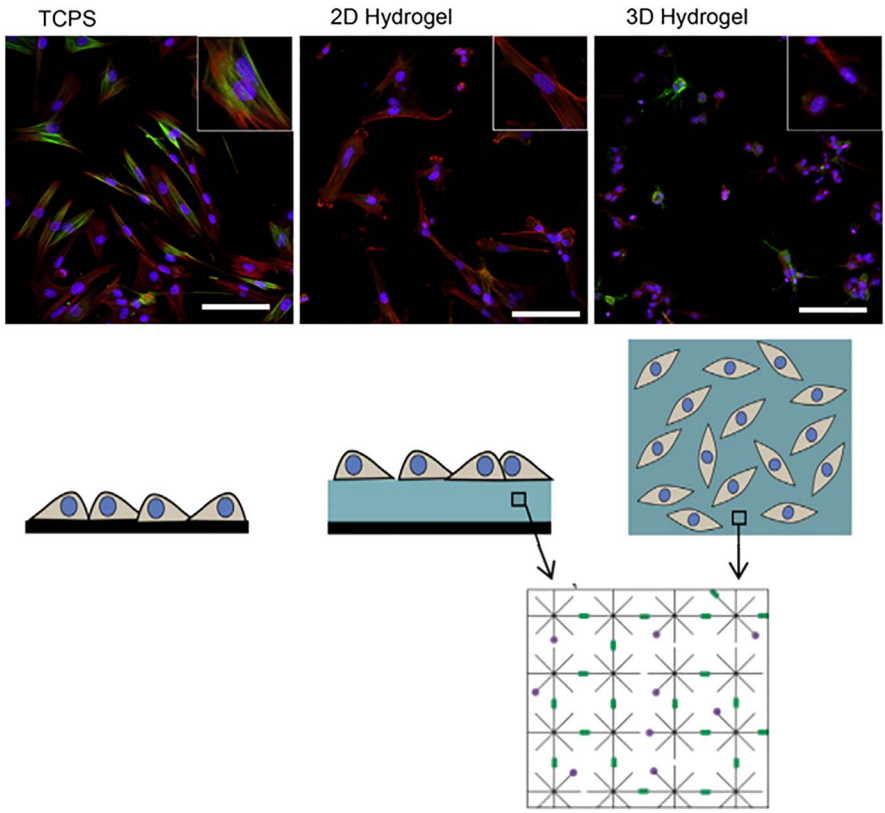

Figure 6.12 Native valvular interstitial cells (VICs) were cultured on different media (TCPS, hydrogels in a different dimensionality), staining cells with αSMA (α-smooth muscle actin) (green), f-actin (red) and nuclei (blue) to characterize the myofibroblast phenotype of the VICs.[91] Reproduced from *Biomaterials*, **74**, K. M. Mabry, S. Z. Payne and K. S. Anseth, Microarray analyses to quantify advantages of 2D and 3D hydrogel culture systems in maintaining the native valvular interstitial cell phenotype, 31–41, Copyright (2016) with permission from Elsevier.

(PEG) hydrogels (Figure 6.12).[90] Cells in 3D hydrogels were smaller and had more rounded morphology, but were less elongated than the ones in TCPS and 2D hydrogels. And most VICs on TCPS showed organized αSMA stress fibers immunostained in a green color. The results indicated that dimensionality affects cell phenotype significantly. Lonnissa showed how different combinations of biomaterials affected the differentiation of a marrow stem cell (MSC) population into different articular cartilage.[91] They combined various synthetic and natural biopolymers to create unique niches, such as PEG hydrogel with chondroitin sulfate (CS), PEG hydrogel with CS and matrix metalloproteinase-sensitive peptide (MMP-pep), and PEG hydrogel with hyaluronic acid (HA). They demonstrated that specific formulations of biomaterials can direct cell differentiation into the articular cartilage of various zones.

6.2.6 Injectable Smart Biomaterials

Encapsulating donor cells in numerous smart biomaterials is a conventional cell-based therapeutic approach for tissue engineering and regeneration. Delivering the living cells to the targeted location is critical for them to secrete therapeutic molecules or replace lost cells that can integrate and regenerate the damaged tissues.[92,93] There are many shortcomings with these conventional methods that potentially lead to scaffold failure,[94] including the risk of surgical implantation, high probability of infections, and difficult adaptation to the defect site. Therefore, more effective cell transplantation methods are required. Injectable biomaterial-based therapies are supposed to overcome these shortcomings, and injectable biomaterials can reach a defect located in very deep tissues, require minimum invasiveness, and enable improved defect margin adaptation (Figure 6.13)[94]. In recent years, injectable biomaterials have been widely applied to myocardial infarction (MI) and peripheral artery disease (PAD) to improve the cardiac function, reduce the infarct size and increase neovascularization.

Injectable hydrogels were the first injectable biomaterials used to transplant cells in the heart.[95,96] Among them, naturally derived materials were also tested on small animals.[97] When designing an injectable hydrogel, various parameters should be considered and must be kept in balance (Figure 6.14).[94] Dhanya reported a composite hydrogel that combined alginate/*O*-carboxymethyl chitosan (*O*-CMC) and alginate/poly(vinyl alcohol) (PVA) with fibrin nanoparticles to enhance the ability of cell adhesion and improve proliferation rates.[98] In this composite hydrogel, *O*-carboxymethyl chitosan (*O*-CMC) was well soluble in water and poly(vinyl alcohol) (PVA) was a more flexible polymer than alginate. Alginate became more flexible blended with *O*-CMC or PVA. Encapsulated adipose-derived stem cells

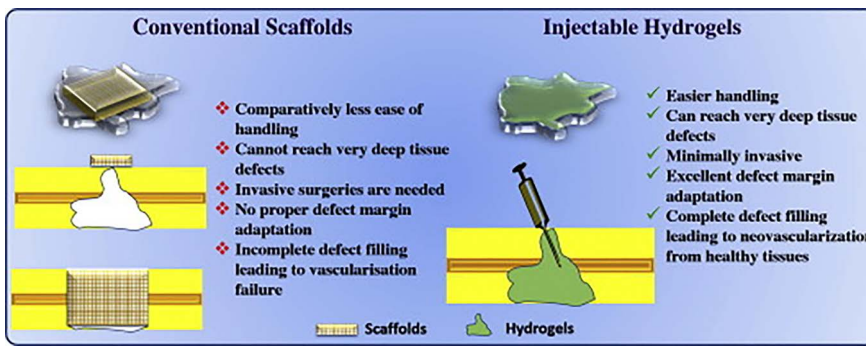

Figure 6.13 Advantages and disadvantages of injectable hydrogels and conventional scaffolds.[94] Reproduced from *European Polymer Journal*, **72**, A. Sivashanmugam, R. Arun Kumar, M. Vishnu Priya, S. V. Nair and R. Jayakumar, An overview of injectable polymeric hydrogels for tissue engineering, 543–565, Copyright (2015) with permission from Elsevier.

(ADSCs) could survive by cellular adhesion, proliferation and differentiation into adipocytes, showing the potential for adipose tissue engineering. In order to offer injectable hydrogels with higher bioactivity and improved mechanical properties, Ali combined a naturally-derived material (gelatin) with a synthetic thermo-responsive biomaterial (poly(*N*-isopropylacrylamide), PNIPAAm). This injectable biohybrid matrix was successfully applied in cardiac cell delivery and tissue engineering.[99] Kevin also developed an optimization method to improve the weak mechanical properties of injectable hydrogels, which limit their applications. Through physical and chemical cross-linking, Kevin incorporated cellulose nanocrystals (CNCs) into hydrazine cross-linked poly(oligoethylene glycol methacrylate) (POEGMA) hydrogels. The adsorbed amount of POEGMA can be adjusted by changing the side chain length of the POEGMA precursor polymers to create tighter-packed or heterogeneous hydrogel morphologies.[100] The properties of the POEGMA–CNC nanocomposite hydrogels show high potential for various biomedical applications, such as high-strength biodegradable tissue engineering scaffolds. Common injectable hydrogels also include fibrin gels, which have been demonstrated to be potential injectable scaffolds and cell carriers for tissue engineering.[101] Yuting reviewed the recent advancement in developing fibrin gels into injectable biomaterials for tissue engineering.[101]

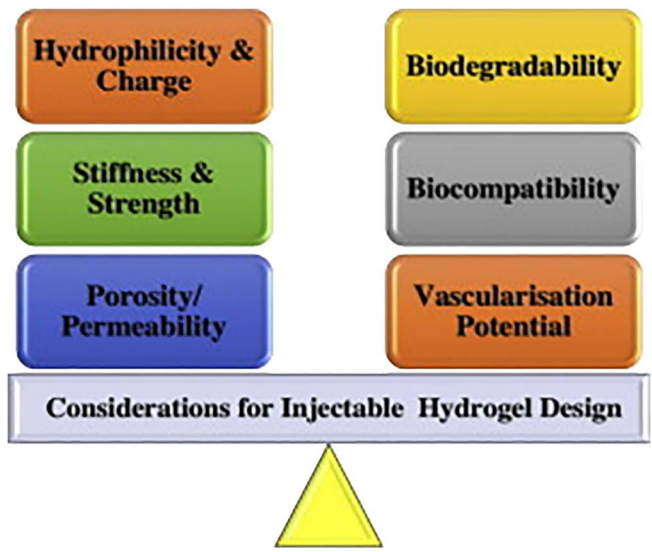

Figure 6.14 Parameters to consider while designing injectable hydrogels.[94] Reproduced from *European Polymer Journal*, **72**, A. Sivashanmugam, R. Arun Kumar, M. Vishnu Priya, S. V. Nair and R. Jayakumar, An overview of injectable polymeric hydrogels for tissue engineering, 543–565, Copyright (2015) with permission from Elsevier.

6.2.7 Smart Biomaterials that Remember Shapes

Shape memory polymers (SMPs) are stimuli-responsive polymers that respond to various stimuli with shape changes for potential medical applications. External stimuli include temperature, light, magnetic field, water, pH, ionic concentration, electrical currents, *etc.* SMPs could recover their permanent shapes or their programmed, temporary shapes after activation by different stimuli. There are three types of commonly seen SMPs: shape memory polymer blends, polymer composites, and hydrogels.[102] Each of them has various applications in biomedical fields, and most of them can be applied in tissue engineering due to their high water content and good biocompatibility.[103]

One ion-triggered shape memory hydrogel (termed as PVV) was reported to exhibit anti-inflammatory and wound healing efficacies.[104] This smart biomaterial was synthesized from 2-vinyl-4,6-diamino-1,3,5-triazine (VDT), 1-vinylimidazole (VI), and polyethylene glycol diacrylate, and was fixed with zinc ion. Cells cultured on the shape memory hydrogel had varied viability in response to Zn^{2+}, with decreased cell viability at high Zn^{2+} concentration (Figure 6.15). Wenjing synthesized a dipole–dipole reinforced copolymer hydrogel, named PVI–AN hydrogel, by photopolymerizing VI and an acrylonitrile (AN) comonomer with a polyethylene glycol-based crosslinker.[105] The mechanical property of the PVI–AN hydrogel changed with the concentration of Zn^{2+}, which firmly locked the temporary shape of the hydrogel.

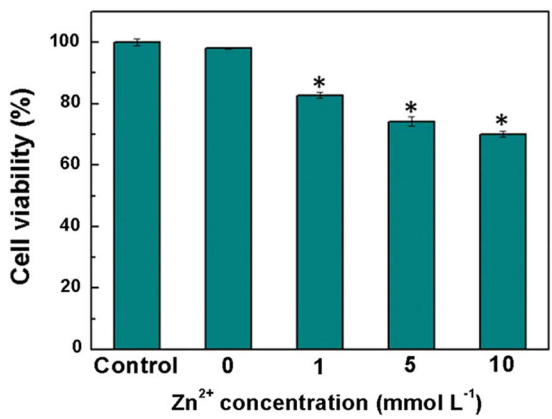

Figure 6.15 Culture L929 cells with PVV-2.5 hydrogel; the viability percentage of cells will decrease with an increase in zinc ion concentration.[104] Reproduced with permission from B. Xu, Y. Li, F. Gao, X. Zhai, M. Sun, W. Lu, Z. Cao and W. Liu, *ACS Appl Mater Interfaces*, 2015, 7, 16 865. Copyright (2015) American Chemical Society.

6.3 Conclusion and Perspective

Recent advances in the development of smart biomaterials presented here show the tremendous efforts made by numerous researchers in this field. These smart biomaterials bring a promising future for cell encapsulation. As outlined in this chapter, smart biomaterials are designed from various perspectives to address the obstacles in cell encapsulation, *e.g.*, by mimicking the native microenvironment, overcoming suffocation, promoting vascularization, overcoming the foreign body reaction, directing cell phenotype, and being injectable and shape memorable. Current smart biomaterials still have their limitations that must be overcome, and an ideal smart biomaterial is expected to have all quality attributes if needed. From the clinical side, currently, there are several cell encapsulation products under clinical trials in the United States, including an alginate-based human beta cell encapsulation product, and a stem-cell-derived insulin producing cell encapsulation product (VC-01™ Combination Product, Viacyte Inc), that are promising therapeutic solutions for type I diabetes. For a successful clinical application and/or commercialization of cell encapsulation technology, the simplicity of the product design and ease of consistent manufacturing are important attributes. These factors should be considered for future smart biomaterial design. In the coming years, research progress in molecular engineering and rational design will further the advancement of the field of smart biomaterials. They will be even smarter than those available to date.

Acknowledgements

This work was supported by the Juvenile Diabetes Research Foundation (1-SRA-2015-41 A-N), and the faculty start-up fund at Wayne State University, Chemical Engineering and Materials Science.

References

1. M. Hashemi and F. Kalalinia, *Life Sci.*, 2015, **143**, 139.
2. D. Freimark, P. Pino-Grace, S. Pohl, C. Weber, C. Wallrapp, P. Geigle, R. Portner and P. Czermak, *Transfus. Med. Hemother.*, 2010, **37**, 66.
3. L. Gasperini, J. F. Mano and R. L. Reis, *J. R. Soc., Interface*, 2014, **11**, 20140817.
4. R. Krishnan, M. Alexander, L. Robles, C. E. Foster and J. R. Lakey, *Rev. Diabet. Stud.*, 2014, **11**, 84.
5. F. Meng, G. H. Engbers and J. Feijen, *J. Controlled Release*, 2005, **101**, 187.
6. A. Moshaverinia, S. Ansari, C. Chen, X. Xu, K. Akiyama, M. L. Snead, H. H. Zadeh and S. Shi, *Biomaterials*, 2013, **34**, 6572–6579.
7. K. Shah, *Biomatter*, 2013, **3**(1), e24278.

8. G. H. Algire, J. M. Weaver and R. T. Prehn, *J. Natl. Cancer Inst.*, 1954, **15**, 493.
9. D. F. Emerich, S. R. Winn, L. Christenson, M. A. Palmatier, F. T. Gentile and P. R. Sanberg, *Neurosci. Biobehav. Rev.*, 1992, **16**, 437.
10. L. G. Cima and R. Langer, *Chem. Eng. Prog.*, 1993, 46.
11. J. P. Vacanti and R. Langer, *Science*, 1993, **260**, 920.
12. M. J. Lysaght, B. Frydel, F. Gentile, D. Emerich and S. Winn, *J. Cell. Biochem.*, 1994, **56**, 196.
13. R. Bellamkonda and P. Aebischer, *Biotechnol. Bioeng.*, 1994, **43**, 543.
14. P. A. Tresco, *J. Controlled Release*, 1994, **18**, 253.
15. C. Ezzell, *J. NIH Res.*, 1995, **7**, 47.
16. J. A. Hubbell, *Biotechnology*, 1995, **13**, 565.
17. P. M. Galletti, P. Aebischer and M. J. Lysaght, *ASAIO J.*, 1995, **41**, 49.
18. R. P. Lanza and W. L. Chick, *Sci. Am. Sci. Med.*, 1995, 16.
19. R. P. Lanza, J. L. Hayes and W. L. Chick, *Nat. Biotechnol.*, 1996, **14**, 1107.
20. S. Woerly, G. W. Plant and A. R. Harvey, *Biomaterials*, 1996, **17**, 301.
21. D. Maysinger and A. Morinville, *Trends Biotechnol.*, 1997, **15**, 418.
22. M. J. Lysaght and P. Aebischer, *Sci. Am.*, 1999, **280**, 76.
23. H. Uludag, P. De Vos and P. A. Tresco, *Adv. Drug Delivery Rev.*, 2000, **42**, 29.
24. Y. Sun, X. Ma, D. Zhou, I. Vacek and A. M. Sun, *J. Clin. Invest.*, 1996, **98**, 1417.
25. W. Xu, L. Liu and I. G. Charles, *FASEB J.*, 2002, **16**, 213.
26. G. Hortelano, A. Al-Hendy, F. A. Ofosu and P. L. Chang, *Blood*, 1996, **87**, 5095.
27. S. Prakash and T. M. S. Chang, *Nat. Med.*, 1996, **2**, 883.
28. P. Soon-Shiong, R. E. Heintz, N. Merideth, Q. X. Yao, Z. Yao, T. Zheng, M. Murphy, M. K. Moloney, M. Schmehl and M. Harris, *et al.*, *Lancet*, 1994, **343**, 950.
29. C. Hasse, G. Klock, A. Schlosser, U. Zimmermann and M. Rothmund, *Lancet*, 1997, **351**, 1296.
30. G. Orive, R. M. Hernandez, A. R. Gascon, R. Calafiore, T. M. S. Chang, P. D. VOS, G. Hortelano, D. Hunkeler, I. Lacik, A. M. J. Shapiro and J. L. Pedraz, *Nat. Med.*, 2003, **9**, 104.
31. S. V. Bhujbal, PhD Thesis from University of Groningen, 2015.
32. S. K. Bhullar, N. L. Lala and S. Ramkrishna, *Rev. Adv. Mater. Sci.*, 2015, **40**, 12.
33. A. Khademhosseini, R. Langer, J. Borenstein and J. P. Vacanti, *Proc. Natl. Acad. Sci. U. S. A.*, 2006, **103**, 2480.
34. A. Dolatshahi-Pirouz, M. Nikkhah, A. K. Gaharwar, B. Hashmi, E. Guermani, H. Aliabadi, G. Camci-Unal, T. Ferrante, M. Foss, D. E. Ingber and A. Khademhosseini, *Sci. Rep.*, 2014, **4**, 3896.
35. J. Kobolak, A. Dinnyes, A. Memic, A. Khademhosseini and A. Mobasheri, *Methods*, 2016, **99**, 62.
36. S. Ramakrishna, K. Fujihara, W. E. Teo, T. Yong, Z. Ma and R. Ramaseshan, *Mater. Today*, 2006, **9**, 40.
37. E. M. Ahmed, *J. Adv. Res.*, 2015, **6**, 105.

38. S. Xu, L. Deng, J. Zhang, L. Yin and A. Dong, *J. Biomed. Mater. Res., Part B*, 2015, **104**, 640.
39. A. Hsieh, T. Zahir, Y. Lapitsky, B. Amsden, W. Wan and M. S. Shoichet, *Soft Matter*, 2010, **6**, 2227.
40. M. J. Webber, E. A. Appel, E. W. Meijer and R. Langer, *Nat. Mater.*, 2015, **15**, 13.
41. P. Y. W. Dankers, M. C. Harmsen, L. A. Brouwer, M. J. A. V. Luyn and E. W. Meijer, *Nat. Mater.*, 2005, **4**, 568.
42. M. E. Davis, J. P. Motion, D. A. Narmoneva, T. Takahashi, D. Hakuno, R. D. Kamm, S. Zhang and R. T. Lee, *Circulation*, 2005, **111**, 442.
43. H. Storrie, M. O. Guler, S. N. Abu-Amara, T. Volberg, M. Rao and S. I. Stupp, *Biomaterials*, 2007, **28**, 4608.
44. T. S. Cheryl, F. P. Wong, J. S. Lee, W. Mulyasasmita, A. Parisi-Amon and S. C. Heilshorn, *Proc. Natl. Acad. Sci. U. S. A.*, 2009, **106**, 22067.
45. W. Mulyasasmita, L. Cai, R. E. Dewi, A. Jha, S. D. Ullmann, R. H. Luong, N. F. Huang and S. C. Heilshorn, *J. Controlled Release*, 2014, **191**, 71.
46. A. Parisi-Amon, W. Mulyasasmita, C. H. Chung and S. C. Heilshorn, *Adv. Healthcare Mater.*, 2013, **2**, 428.
47. G. A. Silva, C. Czeisler, K. L. Niece, E. Beniash, D. A. Harrington, J. A. Kessler and S. I. Stupp, *Science*, 2004, **303**, 1352.
48. E. J. Berns, S. Sur, L. Pan, J. E. Goldberger, S. Suresh, S. Zhang, J. A. Kessler and S. I. Stupp, *Biomaterials*, 2014, **35**, 185.
49. M. Greenwood-Goodwin, E. S. Teasley and S. C. Heilshorn, *Biomater. Sci.*, 2014, **2**, 1627.
50. S. Sur, C. J. Newcomb, M. J. Webber and S. I. Stupp, *Biomaterials*, 2013, **34**, 4749.
51. J. Bockelmann, K. Klinkhammer, A. V. Holst, N. Seiler, A. Faissner, G. A. Brook, D. Klee and J. Mey, *Tissue Eng., Part A*, 2011, **17**, 475.
52. G. C. Weir, *Diabetologia*, 2013, **56**, 1458.
53. S. Song and S. Roy, *Biotechnol. Bioeng.*, 2016, **113**, 1381.
54. J. Aragones, M. Schneider, K. V. Geyte, P. Fraisl, T. Dresselaers, M. Mazzone, R. Dirkx, S. Zacchigna, H. Lemieux, N. H. Jeoung, D. Lambrechts, T. Bishop, P. Lafuste, A. Diez-Juan, S. K. Harten, P. V. Noten, K. D. Bock, C. Willam, M. Tjwa, A. Grosfeld, R. Navet, L. Moons, T. Vandendriessche, C. Deroose, B. Wijeyekoon, J. Nuyts, B. Jordan, R. Silasi-Mansat, F. Lupu, M. Dewerchin, C. Pugh, P. Salmon, L. Mortelmans, B. Gallez, F. Gorus, J. Buyse, F. Sluse, R. A. Harris, E. Gnaiger, P. Hespel, P. Van Hecke, F. Schuit, P. V. Veldhoven, P. Ratcliffe, M. Baes, P. Maxwell and P. Carmeliet, *Nat. Genet.*, 2008, **40**, 170.
55. J. D. Weaver and C. L. Stabler, *Acta Biomater.*, 2015, **16**, 136.
56. N. Alemdar, J. Leijten, G. Camci-Unal, J. Hjortnaes, J. Ribas, A. Paul, P. Mostafalu, A. K. Gaharwar, Y. Qiu, S. Sonkusale, R. Liao and A. Khademhosseini, *ACS Biomater. Sci. Eng.*, 2016, DOI: 10.1021/acsbiomaterials.6b00109.
57. E. Pedraza, M. M. Coronel, C. A. Fraker, C. Ricordi and C. L. Stabler, *Proc. Natl. Acad. Sci. U. S. A.*, 2012, **109**, 4245.

58. J. W. Arbogast and C. S. Foote, *J. Am. Chem. Soc.*, 1991, **113**, 8886.
59. J. W. Arbogast, A. P. Darmanyan, C. S. Foote, Y. Rubin, F. N. Diederich, M. M. Alvarez, S. J. Anz and R. L. Whetten, *J. Phys. Chem.*, 1991, **95**, 11.
60. S. Oriana, S. Aroua, J. O. Sollner, X. J. Ma, Y. Iwamoto and Y. Yamakoshi, *Chem. Commun. (Camb.)*, 2013, **49**, 9302.
61. J. J. Moon and J. L. West, *Curr. Top. Med. Chem.*, 2008, **8**, 300.
62. E. Jabbarzadeh, J. Blanchette, T. Shazly, A. Khademhosseini, G. Camci-Unal and C. T. Laurencin, *Curr. Angiog.*, 2012, **1**, 180.
63. M. Najjar, V. Manzoli, M. Abreu, C. Villa, M. M. Martino, R. D. Molano, Y. Torrente, A. Pileggi, L. Inverardi, C. Ricordi, J. A. Hubbell and A. A. Tomei, *Biotechnol. Bioeng.*, 2015, **112**, 1916.
64. E. A. Phelps, D. M. Headen, W. R. Taylor, P. M. Thule and A. J. Garcia, *Biomaterials*, 2013, **34**, 4602.
65. J. A. Shepard, F. R. Virani, A. G. Goodman, T. D. Gossett, S. Shin and L. D. Shea, *Biomaterials*, 2012, **33**, 7412.
66. A. J. Marshall, C. A. Irvin, T. Barker, E. H. Sage, K. D. Hauch and B. D. Ratner, *Polym. Prepr.*, 2004, **45**, 100.
67. S. N. Isenhath, Y. Fukano, M. L. Usui, R. A. Underwood, C. A. Irvin, A. J. Marshall, K. D. Hauch, B. D. Ratner, P. Fleckman and J. E. Olerud, *J. Biomed. Mater. Res., Part A*, 2007, **83**, 915.
68. L. R. Madden, D. J. Mortisen, E. M. Sussman, S. K. Dupras, J. A. Fugate, J. L. Cuy, K. D. Hauch, M. A. Laflamme, C. E. Murry and B. D. Ratner, *Proc. Natl. Acad. Sci. U. S. A.*, 2010, **107**, 15211–15216.
69. H. Han, H. Ning, S. Liu, Q. Lu, Z. Fan, H. Lu, G. Lu and D. L. Kaplan, *Adv. Funct. Mater.*, 2016, **26**, 421.
70. B. D. Ratner, *J. Controlled Release*, 2002, **78**, 211.
71. J. M. Anderson, A. Rodriguez and D. T. Chang, *Semin. Immunol.*, 2008, **20**, 86.
72. D. F. Williams, *Biomaterials*, 2008, **29**, 2941.
73. R. Langer, *Adv. Mater.*, 2009, **21**, 3235.
74. E. Ostuni, R. G. Chapman, R. E. Holmlin, S. Takayama and G. M. Whitesides, *Langmuir*, 2001, **17**, 5605.
75. S. Jiang and Z. Cao, *Adv. Mater.*, 2010, **22**, 920.
76. S. Chen, L. Li, C. Zhao and J. Zheng, *Polymer*, 2010, **51**, 5283.
77. L. Zhang, Z. Cao, T. Bai, L. Carr, J. R. Ella-Menye, C. Irvin, B. D. Ratner and S. Jiang, *Nat. Biotechnol.*, 2013, **31**, 553.
78. A. J. Vegas, O. Veiseh, J. C. Doloff, M. Ma, H. H. Tam, K. Bratlie, J. Li, A. R. Bader, E. Langan, K. Olejnik, P. Fenton, J. W. Kang, J. Hollister-Locke, M. A. Bochenek, A. Chiu, S. Siebert, K. Tang, S. Jhunjhunwala, S. Aresta-Dasilva, N. Dholakia, R. Thakrar, T. Vietti, M. Chen, J. Cohen, K. Siniakowicz, M. Qi, J. McGarrigle, S. Lyle, D. M. Harlan, D. L. Greiner, J. Oberholzer, G. C. Weir, R. Langer and D. G. Anderson, *Nat. Biotechnol.*, 2016, **34**, 345.
79. A. J. Vegas, O. Veiseh, M. Gurtler, J. R. Millman, F. W. Pagliuca, A. R. Bader, J. C. Doloff, J. Li, M. Chen, K. Olejnik, H. H. Tam, S. Jhunjhunwala, E. Langan, S. Aresta-Dasilva, S. Gandham, J. J. McGarrigle, M. A.

Bochenek, J. Hollister-Lock, J. Oberholzer, D. L. Greiner, G. C. Weir, D. A. Melton, R. Langer and D. G. Anderson, *Nat. Med.*, 2016, **22**, 306.
80. T. Kusaka, M. Nakayama, K. Nakamura, M. Ishimiya, E. Furusawa and K. Ogasawara, *PloS One*, 2014, **9**, e92634.
81. J. Zandstra, C. Hiemstra, A. H. Petersen, G. J. Veldhuis, J. Zuidema, R. Steendam, M. M. V. Beuge, R. A. Bank, S. Rodriguez and E. R. Popa, *Eur. Cells Mater.*, 2014, **28**, 335.
82. O. Veiseh, J. C. Doloff, M. Ma, A. J. Vegas, H. H. Tam, A. R. Bader, J. Li, E. Langan, J. Wyckoff, W. S. Loo, S. Jhunjhunwala, A. Chiu, S. Siebert, K. Tang, J. Hollister-Lock, S. Aresta-Dasilva, M. Bochenek, J. Mendoza-Elias, Y. Wang, M. Qi, D. M. Lavin, M. Chen, N. Dholakia, R. Thakrar, I. Lacik, G. C. Weir, J. Oberholzer, D. L. Greiner, R. Langer and D. G. Anderson, *Nat. Mater.*, 2015, **14**, 643.
83. K. E. Healy, A. Rezania and R. A. Stite, *Ann. N. Y. Acad. Sci.*, 1999, **875**, 24.
84. A. J. Mieszawska and D. L. Kaplan, *BMC Biol.*, 2010, **8**, 59.
85. H. M. Blau, A. Sacco and P. M. Gilbert, in *Essentials of Stem Cell Biology*, ed. R. Lanza, *et al.*, 2nd edn, 2009, pp. 249–257.
86. T. Maguire, E. Novik, R. Schloss and M. Yarmush, *Biotechnol. Bioeng.*, 2006, **93**, 581.
87. T. Y. Cheng, M. H. Chen, W. H. Chang, M. Y. Huang and T. W. Wang, *Biomaterials*, 2013, **34**, 2005.
88. C. Chai and K. W. Leong, *Mol. Ther.*, 2007, **15**, 467.
89. N. Huebsch, E. Lippens, K. Lee, M. Mehta, S. T. Koshy, M. C. Darnell, R. M. Desai, C. M. Madl, M. Xu, X. Zhao, O. Chaudhuri, C. Verbeke, W. S. Kim, K. Alim, A. Mammoto, D. E. Ingber, G. N. Duda and D. J. Mooney, *Nat. Mater.*, 2015, **14**, 1269.
90. K. M. Mabry, S. Z. Payne and K. S. Anseth, *Biomaterials*, 2016, **74**, 31.
91. L. H. Nguyen, A. K. Kudva, N. L. Guckert, K. D. Linse and K. Roy, *Biomaterials*, 2011, **32**, 1327.
92. C. Wang, R. R. Varshney and D. A. Wang, *Adv. Drug Delivery Rev.*, 2010, **62**, 699.
93. M. M. Pakulska, B. G. Ballios and M. S. Shoichet, *Biomed. Mater.*, 2012, **7**, 024101.
94. A. Sivashanmugam, R. Arun Kumar, M. Vishnu Priya, S. V. Nair and R. Jayakumar, *Eur. Polym. J.*, 2015, **72**, 543.
95. T. Kofidis, J. L. de Bruin, G. Hoyt, D. R. Lebl, M. Tanaka, T. Yamane, C. P. Chang and R. C. Robbins, *J. Thorac. Cardiovasc. Surg.*, 2004, **128**, 571.
96. K. L. Christman, H. H. Fok, R. E. Sievers, Q. Fang and R. J. Lee, *Tissue Eng.*, 2004, **10**, 403.
97. J. L. Ungerleider and K. L. Christman, *Stem Cells Transl. Med.*, 2014, **3**, 1090.
98. D. Jaikumar, K. M. Sajesh, S. Soumya, T. R. Nimal, K. P. Chennazhi, S. V. Nair and R. Jayakumar, *Int. J. Biol. Macromol.*, 2015, **74**, 318.
99. A. Navaei, D. Truong, J. Heffernan, J. Cutts, D. Brafman, R. W. Sirianni, B. Vernon and M. Nikkhah, *Acta Biomater.*, 2016, **32**, 10.

100. K. J. De France, K. J. Chan, E. D. Cranston and T. Hoare, *Biomacromolecules*, 2016, **17**, 649.
101. Y. Li, H. Meng, Y. Liu and B. P. Lee, *Sci. World J.*, 2015, **2015**, 10.
102. B. Q. Chan, Z. W. Low, S. J. Heng, S. Y. Chan, C. Owh and X. J. Loh, *ACS Appl. Mater. Interfaces*, 2016, **8**, 10070.
103. N. A. Peppas, J. Z. Hilt, A. Khademhosseini and R. Langer, *Adv. Mater.*, 2006, **18**, 1345.
104. B. Xu, Y. Li, F. Gao, X. Zhai, M. Sun, W. Lu, Z. Cao and W. Liu, *ACS Appl. Mater. Interfaces*, 2015, **7**, 16865.
105. W. Nan, W. Wang, H. Gao and W. Liu, *Soft Matter*, 2013, **9**, 132.

CHAPTER 7

Multi-Functional Biomaterials for Bone Tissue Engineering

CHRISTIAN WIRAJA[a], MARK S. K. CHONG[a], YANWAN LIAO[a], SHARON W. T. CHEW[a] AND CHENJIE XU*[a,b]

[a]School of Chemical and Biomedical Engineering, Nanyang Technological University, 70 Nanyang Drive, Singapore 637457; [b]NTU-Northwestern Institute of Nanomedicine, Nanyang Technological University, 50 Nanyang Avenue, Singapore 639798
*E-mail: cjxu@ntu.edu.sg

7.1 Introduction

Bone tissue engineering combines principles from biology, medicine, material science, and engineering science to create functional replacements to facilitate bone regeneration,[1] or bone tissue analogues in experimental models of disease.[2] Driven by a shortage of bone tissue for transplantation along with an aging population, this field has been under intense development in the past decades and three major strategies have since been developed for engineering tissues, namely: (1) creating implantable pieces of the organism with the use of living cells seeded on a natural or synthetic extracellular substrate; (2) delivering tissue-inducing substances, and (3) injecting therapeutic cells placed on or within matrices.

Although these strategies sound technically different, the goal is the same: to fabricate new and functional bone tissues by incorporating living cells within a matrix or scaffold. Scaffolds can be natural, man-made, or

Smart Materials No. 25
Smart Materials for Tissue Engineering: Applications
Edited by Qun Wang

Published by the Royal Society of Chemistry, www.rsc.org

a composite of both. Living cells may be cultured *in vitro* to associate with the matrix prior to implantation or induced *in vivo* to migrate into the implant after implantation. Successful engineering strategies would necessitate the scaffold to guide organization, growth, and/or differentiation of cells to form a functional tissue.

Given the key role that scaffolds play, the development of bone tissue engineering strategies has been closely related with the advancement of material science.[3] For example, the first generation of scaffolds for bone tissue engineering was bioinert and adapted from materials used in other fields. These were selected on the basis of approximating mechanical properties to tissues of interest but were largely passive and lacked cues to promote tissue regeneration. Later, the focus shifted to resorbable biomaterials, based on the development of resorbable polymers such as polycaprolactone (PCL), poly(glycolic acid) (PGA), poly(lactic acid) (PLA), and poly(lactic-*co*-glycolic acid) (PLGA). These materials have significant advantages over their non-resorbable counterparts, with degradation byproducts that can be processed by the body through the citric acid cycle, a natural metabolic pathway.[4] Together with advances in additive manufacturing and drug delivery technologies, a new generation of scaffolds that could induce the migration of host cells into the scaffolds and the regeneration of natural tissues is ushered in.

The aim of this chapter is to highlight the impact of biomaterial advances on the bone tissue engineering field, starting from primarily providing structural support and cell–matrix interactions, to the delivery of biofunctional molecules to accelerate healing, and finally to act as a theranostic platform (Figure 7.1).

7.2 Multi-Functional Biomaterials for Bone Tissue Engineering

7.2.1 Passive Biomaterials for Mechanical Support

The cell and scaffold form the two basic components of engineered bone tissue. Conventionally, this involves a period of culture *in vitro*, in which the cells and scaffolds are assembled to form engineered constructs.[5]

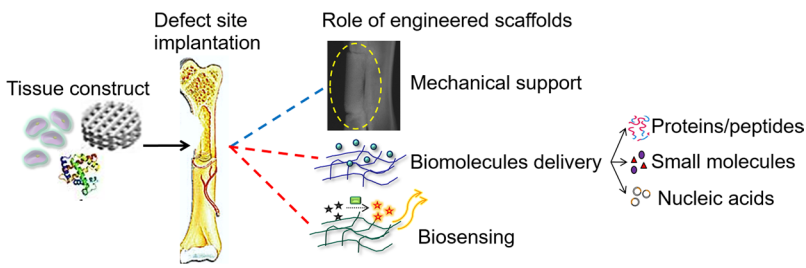

Figure 7.1 Summary of roles served by biomaterials in bone tissue engineering.

Post-implantation, the engineered bone grafts are assumed to integrate into the host skeleton, and further mature into woven bone. Scaffolds perform primarily to provide structural support for cells, both *in vitro* and *in vivo*, with the following key requirements:[6] (1) biocompatibility, in that the materials and degradation products of scaffolds should be non-toxic and non-teratogenic without eliciting excessive inflammatory response. (2) Sufficient mechanical properties to define and protect a physical space for cellular growth; these should ideally match the mechanical properties of the surrounding tissue. (3) High porosity (>90%), good interconnectivity, and average pore size between 200 μm and 400 μm to promote host cell infiltration and host integration. (4) Appropriate biodegradability with adjustable degradation rates. (5) Feasible sterilization methods that do not interfere with the function of the scaffold or change the chemical composition of scaffold biomaterials.

It is important to distinguish at this point the terms "osteoconductive" and "osteoinductive". Osteoconductivity refers to the ability of a porous scaffold to support the infiltration of host bone cells and blood vessels. As the scaffold undergoes degradation, this process ensures the formation of integrated bone tissue. In contrast, osteoinductive scaffolds actively drive osteogenesis and the formation of bone tissue. These include physical cues, including topography and the nano-/micro-structure of the scaffold's surface that influence cell proliferation and differentiation on scaffolds.[7] In the early years of tissue engineering, scaffolds were almost exclusively comprised of bio-inert materials. These "first generation" scaffolds provided ample mechanical support and room for osteoconduction, with no chemical or physical cues for osteoinduction of seeded cells.[8]

First generation scaffolds may be grouped into natural or synthetic materials. Proteins such as collagen,[9] gelatin,[10] fibrin[11] and silk fibroin,[12] polysaccharides like chitosan[13] and alginate[14] and inorganic materials like coralline apatite[15] are derived from natural sources; consequently, they approximate various components of the human bone extracellular matrix, and are observed to be cytocompatible. These materials exhibit various limitations, however, including immunological concerns attributed to the use of xenogeneic material and inadequate mechanical properties (due both to source variability and difficulties in modifying inherent properties). Additionally, scaffold-forming technologies to handle these materials are limited, necessitating highly-customized set-ups to address these concerns. Taking a pure chitosan scaffold as an example, its inadequate mechanical properties result in improper cell attachment and morphology, which in turn affects cell activities. The addition of 1 wt% nano-hydroxyapatite (HAp) to form a composite construct significantly improves scaffold stiffness and translates to 50% greater proliferation rate of pre-osteoblastic cells, one week after cell seeding.[16]

Compared with natural biomaterials, it is usually easier to shape or alter the chemical and mechanical properties of synthetic materials. In particular, polyesters, such as polycaprolactone (PCL), are commonly employed as

scaffold materials. Bioresorbable polymers have tailored degradation rates, and are designed to be absorbed by the host over time. Of course, synthetic materials have their own limitations, like acidolysis associated with scaffold breakdown, and the lack of biologically-recognizable surface motifs, which impedes cellular attachment.[17] Great efforts have been spent to address these challenges by incorporating tricalcium phosphate (TCP)[18] or employing surface-hydrolytic treatments to improve surface wettability, cell adhesion and thereby host tissue ingrowth.[19] HAp-coated or gelatin-coated PCL films and 3D honeycomb PCL scaffolds have also been designed for the development of vascularized tissue engineered bone.[20,21] The use of co-polymers is another way to control the degradation of scaffold materials. For example, poly(anhydride-*co*-imides) has a much more adjustable degradation rate than polyanhydride, a surface bioeroding polymer. As a homopolymer, aliphatic polyanhydride is rapidly degraded *in vivo* within a few weeks, while aromatic polyanhydride can take years to be fully degraded.[22,23] Degradation of poly(anhydride-*co*-imides) on the other hand, can be adjusted between weeks to a few months by simply tuning its monomer ratio.[24,25]

Aside from polymers, ceramics are renowned for their biocompatibility and the ease of forming highly porous structures. Besides HAp and TCP, non-degradable ceramics such as alumina and zirconia[26] are also applied in scaffold fabrication. Several studies have additionally demonstrated the tunable compressive strength of alumina,[27,28] with good cytocompatibility and lack of genotoxicity.[29] However, due to low fatigue strength, high rigidity and brittleness, the processing and application of pure ceramics remain limited.

Finally, metals that have traditionally been associated with orthopaedic reconstructions can perform similarly in bone tissue engineering as permanent scaffolds. Titanium (Ti) is widely applied in fracture fixation and repair of bone defects owing to its good biocompatibility and resistance to fatigue and corrosion.[30] Ti fiber web scaffolds coated with a thin HAp layer showed enhanced stress resistance and osteoconductivity in rabbit mandibular bone reconstruction.[31] Surface-grafted chitosan may further improve the safety and efficacy of Ti scaffolds by promoting cell attachment and reducing bacterial adhesion.[32] Composite coatings of chitosan, nano-HAp and nano-copper–zinc alloy have successfully combined the advantages of natural polymers, synthetic ceramics and metal alloys. This composite shows a low degradation rate for maintaining sufficient mechanical strength, increased protein adsorption to facilitate cell adhesion, and anti-bacterial activity.[33]

In recent years, other bioinert materials have emerged for bone tissue engineering applications, including nano-scale materials such as graphene[34,35] and carbon nanotubes, which can also provide mechanical reinforcement for scaffold materials. Multi-walled carbon nanotubes loaded on a poly(3-hydroxybutyrate-*co*-3-hydroxyvalerate) (PHBV) cylinder significantly increased the flexural and compressive strengths of a PHBV-based scaffold.[36] However, safety concerns over carbon nanotube toxicity and detachment from the implantation site remain significant; further research is required to better characterize its nano-toxicity.[37]

7.2.2 Active Scaffolds

Beyond providing structural support, scaffolds are also able to play more active roles in bone engineering. As described above, bone tissue engineering scaffolds are usually designed to be osteoconductive (*i.e.* to facilitate proliferation, differentiation and ECM deposition of osteoprogenitor cells), but may further be osteoinductive (*i.e.* be capable of stimulating bone formation).[38,39] To supplement the natural effects brought by the choice of the materials' structure and type, various active biomolecules can also be incorporated into these scaffolds. According to their roles in bone tissue engineering, this section classifies these scaffold constructs into two groups: scaffolds for (i) biomolecular delivery and (ii) biosensing. Subsequently, limitations of these active scaffolds will be discussed and potential solutions will be proposed.

7.2.2.1 Biomaterials for Biomolecular Delivery

One purpose of incorporating bioactive molecules into scaffold materials is to specifically stimulate/direct cellular responses at the target sites.[40,41] Scaffold-mediated delivery takes place in a more localized and defined manner, enhancing biomolecular internalization by target cells, whilst reducing potential complications from off-target uptake.[42,43] The scaffold further serves to protect the biological payload from biodegradation, permitting extended release profiles. Finally, they address problems associated with non-specific clearance when the biomolecules are delivered systemically.[44,45] Taken together, scaffold-mediated biomolecular delivery is safer, more efficacious and cost-effective than systemic administration.[46,47]

Functionalization of scaffolds with bioactive molecules is typically achieved through physical entrapment, physical adsorption or surface conjugation. Design considerations include chemical/biological properties of the bioactive molecules, desired release profile, and the chemical/physical/biological properties of the scaffold materials.[48] For instance, small molecules (*e.g.* dexamethasone) may be covalently-grafted on the surface of polymeric constructs *via* a cross-linker. Subsequently, as the linker is degraded, released dexamethasone retains its functionality to induce MSC osteogenic differentiation.[49] In this case, the release rate is strongly influenced by the strength of the covalent bond formed. In contrast, encapsulation of large and labile growth factors (GFs) would be favored to retain biological activity by eliminating/minimizing exposure towards extrinsic factors including pH, metal ions and proteases, which can cause structural changes/GF degradation.[50] In such configurations, GFs are only released and exposed to the biological environment in tandem with the breakdown of the polymer shell.[51]

7.2.2.1.1 Peptides and Proteins. Growth factors are the most commonly delivered molecules through scaffolds for bone tissue engineering. In particular, bone morphogenetic proteins (BMPs; mainly -2, -4 and -7) are often used to stimulate osteoblastic activity and induce MSC differentiation towards osteogenic lineage.[44,52] BMPs interact with cell surface receptors BMPR-I and -II

to trigger mobilization and phosphorylation of SMAD transducing molecules, which regulates the expression of downstream target genes.[46]

As highlighted recently by several review articles, BMPs slowly and continuously released from scaffolds show a better effect for inducing bone formation, compared to free BMPs.[53,54] These BMP–scaffold systems have enhanced recruitment of osteoprogenitor cells,[55] a significant increase in alkaline phosphatase activity,[56] as well as greater mineral deposition and higher compressive moduli.[57–59] Controlling the release profile of these biomolecules is a common research theme. Comparing a heparin-conjugated fibrin against a normal fibrin construct, Yang *et al.* reported that slower BMP-2 release (~80% after 13 days instead of three days) resulted in ~10-fold greater calcium concentration and more prominent osteocalcin and osteopontin expression, eight weeks after implantation in an ectopic rat model.[56] Meanwhile, Wei *et al.* demonstrated that a nanosphere-immobilized, but not adsorbed rhBMP-7 PLLA scaffold could induce significant ectopic bone formation six weeks after rat transplantation, as observed through von Kossa staining and radiographic density (Figure 7.2).[58]

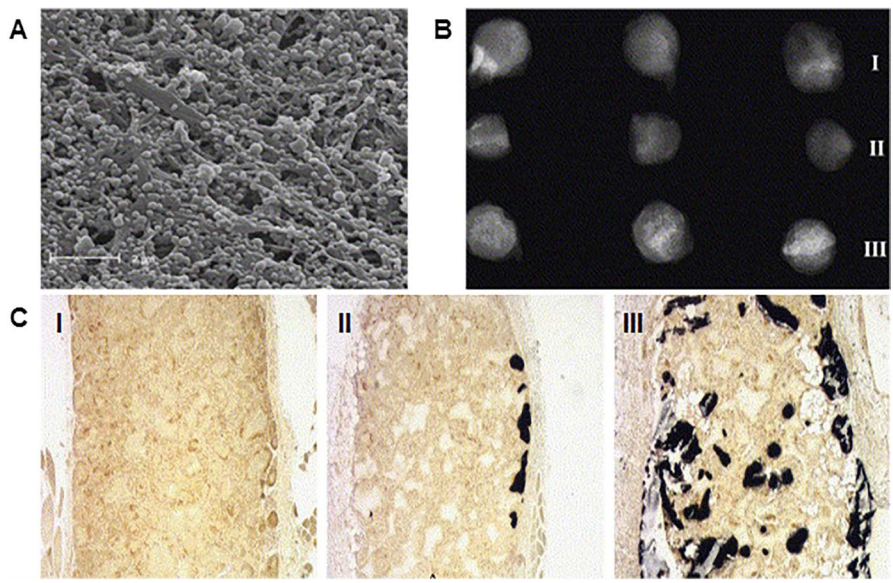

Figure 7.2 LGA nanospheres' immobilization on a PLLA scaffold enable sustained release of BMP-7 for ectopic bone formation. (A) Scanning electron micrograph of PLLA nanofibrous scaffolds after the nanospheres' incorporation. Nanosphere-immobilized scaffolds (III) showed significantly greater bone formation than BMP-7 adsorbed scaffolds (II) and blank scaffolds (I), as observed by radiographic imaging (B) and von Kossa staining (C). Reproduced from *Biomaterials*, **28**(12), Wei, G., Jin, Q., Giannobile, W. V., Ma, P. X. The enhancement of osteogenesis by nano-fibrous scaffolds incorporating rhBMP-7 nanospheres, 2087–2096, Copyright (2007) with permission from Elsevier.

After realizing the benefit of incorporating bioactive molecules, researchers began to utilize scaffolds for the delivery of two or more growth factors to achieve a synergistic effect.[47] One study co-delivered BMP-2 with Wnt1 inducible signaling protein-1 (WISP-1) using a β-TCP/gelatin scaffold. *In vitro*, introduction of both factors promoted more than two-fold osteopontin expression on MSCs after seven days, as compared to the singly-delivered molecules. *In vivo*, there was two-fold greater osteoid formation 10 days after subcutaneous implantation, relative to the BMP2-only group.[60] In another study, co-incorporation of BMP-2 and transforming growth factor beta-3 (TGFβ-3; which is involved in the up-regulation of endogenous BMP-2 expression[61]) in MSCs-containing alginate hydrogel was shown to stimulate significant bone formation from as early as six weeks after transplantation. Meanwhile, the introduction of individual growth factors resulted in negligible bone formation even after 22 weeks.[62] To achieve maximal therapeutic effect, the sequence of the GFs' release may also be manipulated through this co-administration. One such case is the co-delivery of BMP-2 and insulin-like growth factor 1 (IGF-1). While IGF-1 itself can stimulate osteoblast growth and proliferation,[63] sequential delivery of BMP-2/IGF-1 might potentiate these effects, as BMP-2 treatment upregulates the expression of IGF-1 receptors.[64] Indeed, Kim *et al.* showed that sequential release of BMP-2 from chitosan gel followed with IGF-1 from a gelatin microsphere provided ~50% greater alkaline phosphatase (ALP) activity of W-17-20 cells at day seven, when compared to scaffolds releasing only BMP-2 or simultaneously releasing BMP-2 and IGF-1 from chitosan gels.[65]

Aside from proteins with osteoinductive benefits, angiogenic ones including fibroblast growth factors (FGFs), vascular endothelial growth factors (VEGFs) and platelet-derived growth factors (PDGFs) have also been explored, particularly for applications in the treatment of large, critically-sized defects.[66–68] In one study involving polyelectrolyte multilayer films with BMP-2 and VEGF-165, the co-introduction of both factors resulted in a 33% increase in ectopic bone formation together with a higher trabecular thickness, taking the BMP-2 only treatment as a control.[69] In a similar study using a gelatin-microspheres-incorporated poly(propylene fumarate) (PPF) scaffold, co-delivery of BMP-2 and VEGF was shown to accelerate defect bridging and healing time in a critical-size cranial defect model, with two-fold bone formation over the BMP2-only group after four weeks of treatment, as evaluated through micro CT.[70]

Lastly, to mitigate problems associated with delivering large and full-scale proteins (*e.g.* high cost, rapid loss of bioactivity),[71] researchers have experimented as well with truncated versions containing only critical portions. While its effects may not be as extensive as its complete sequence counterpart, a dose-dependent stimulatory role on bone formation was attained when BMP-2 peptide was delivered using a HAp/collagen/PLA composite scaffold.[72] In another study, Luo *et al.* also reported a dose-dependent upregulation on MG63 osteogenic marker expression, 14 days following treatment with BMP-7-laden mesoporous silica nanoparticles.[73]

7.2.2.1.2 Small Molecules. Small molecules are promising alternatives to stimulate bone regeneration, with their ability to minimize the problems or limitations of GFs including limited synthesis scale, high cost and limited stability.[74,75] For instance, small molecular compounds can better withstand processing techniques utilized in material preparation (*e.g.* solvent exposure, thermal heating) as compared to GFs, hence retaining their bioactivity more efficiently after scaffold coupling.[76] Over the past decade, many osteoinductive small molecules have been identified with the advent of high-throughput screening.[77] One example is simvastatin, which helps fracture healing by up-regulating BMP-2 expression in osteoblasts.[78] Previously, it was shown that simvastatin increased bone formation when injected subcutaneously or orally administered to mice and rats.[79] However, statin drugs have limitations with solubility and adverse side effects at high dosage.[78] Therefore, sustained release from biomaterials is proposed to circumvent this issue. Tai *et al.* incorporated simvastatin within PLGA/HAp double emulsion microspheres, for subsequent avascular graft transplantation in a mouse fracture model. Compared to a graft-only control, they observed improved blood vessel and callus formation around the implant after two and four weeks, respectively. Cellular ingrowths that facilitated graft substitution were also observed.[80]

Purmorphamine is another example. It induces osteogenesis through the hedgehog signaling pathway.[81] When purmorphamine-containing HAp beads were injected into defect femurs, the proportion of the trabecular bone area was found to be significantly higher than the empty beads control (~70% to ~50% after seven days).[82] Last but not least, FTY720 is an analog of sphingosine-1-phosphate (S1P), which promotes recirculation of osteoclast precursors from a bone surface, an effect that ameliorates bone loss. When applied alongside dissolved PLGA as a coating for allograft samples, FTY720 promoted greater osteointegration of the implant interface with superior mechanical properties (*i.e.* elasticity and compressive strength) than both un-coated and PLGA-only control allografts six weeks post-implantation.[83]

7.2.2.1.3 Nucleic Acids. Another major area involves delivering nucleic acids, which encompass DNA plasmids and micro/small interfering RNAs (miRNAs/siRNAs). In general, the introduction of nucleic acids aims to alter cellular function and phenotype by causing either up- or down-regulation of gene expressions. Plasmid transfection is commonly used to trigger gene upregulation, while interfering RNA is applied to knock down target gene expression through mRNA cleavage.[84,85] Specifically in bone tissue engineering, various plasmids encoding for osteogenic differentiation genes have been studied, in addition to various interfering RNAs targeting osteo-inhibiting genes.[86,87]

For example, a BMP-2 DNA plasmid can be complexed with polyethyleneimine (PEI) and encapsulated within PLGA microspheres for gelatin sponge transplantation into a rat calvarial defect model. Eight weeks later, bone formation at the defect site was visible only in BMP-2-containing sponges, as observed through micro CT and histological staining.[88] BMP-2 plasmid

complexation with acetylated PEI prior to collagen/PGA-fiber scaffold incorporation has also been shown to promote osteogenesis on seeded MSCs. Following scaffold and cell implantation into the backs of rats, homogeneous bone formation was observed with ~10-fold ALP activity and osteocalcin content, as compared to a blank scaffold control.[89]

Apart from BMP-2, plasmids encoding other genes such as Runt-related transcription factor 2 (RUNX2) and PDGF were also successfully delivered through scaffold incorporation. Monteiro *et al.* loaded RUNX2 plasmids, a crucial gene to induce transition towards osteoblast phenotype, onto the surface of electrospun-PCL nanofibers through liposomal encapsulation and immobilization. Following internalization by seeded MSCs, the RUNX2-loaded liposomes induced continuous overexpression of the RUNX2 gene, which in turn triggered ~2.5-fold greater ALP activity at day 21 to unmodified nanofibers, without additional supplements.[90] For the purpose of enhancing scaffold vascularization, Shea *et al.* directly combined a PDGF plasmid with PLGA matrices for the formation of a plasmid-containing 3D sponge through a gas forming process. Here, PDGF was chosen for its angiogenesis-stimulating role in mediating endothelial cell proliferation and tube formation.[91] Following subcutaneous implantation in Lewis rats, plasmids released from the sponges transfected nearby cells at the adipose and muscle layers, which accelerated blood vessel formation (~three-fold vessel area to blank sponge at day 14); a useful trait for scaffold infiltration.[92]

Similar to protein delivery, multiple kinds of plasmids can be co-delivered through the same scaffold to achieve synergistic effects. By firstly condensing the plasmid with PEI for lyophilization, Huang *et al.* incorporated both BMP-4 and VEGF encoding plasmids into compressed PLGA pellets. When MSC-seeded PLGA constructs were subcutaneously implanted, significant bone deposition was observed with micro CT. Importantly, simultaneous loading of both plasmids resulted in three times stiffer bone as compared to when BMP-4 or the VEGF plasmid was independently incorporated, 15 weeks post implantation (Figure 7.3).[93]

Lastly, RNA moieties (such as miRNA and siRNA) have also been incorporated into biomaterials for bone tissue engineering. In one study, a positively-charged TransIT-TKO/BCL2L2 siRNA nanoparticle was proposed for retention within the cavities of NaOH-treated PCL films. This local BCL2L2 silencing enhanced early osteogenic differentiation, in terms of collagen type 1 deposition and organization.[94] Moreover, prolonged and sustained release of siNoggin (a gene which is reported to inactivate BMP-4 and prevent ossification[95]) in combination with miR-20a (which is predicted to upregulate BMP/Runx2 signaling by regulating PPARγ, Bambi and Crim1[96]) from a PEG hydrogel was shown to successfully direct MSCs' osteogenic differentiation and induce higher calcium content on day 28 (~two-fold), as compared to blank hydrogel.[87] With various osteogenic-inducing miRNAs identified recently (*e.g.* miRNA 26a, miRNA 148b, miR-196a),[97,98] further exploration to optimize their combination and release profile from scaffold materials is warranted.

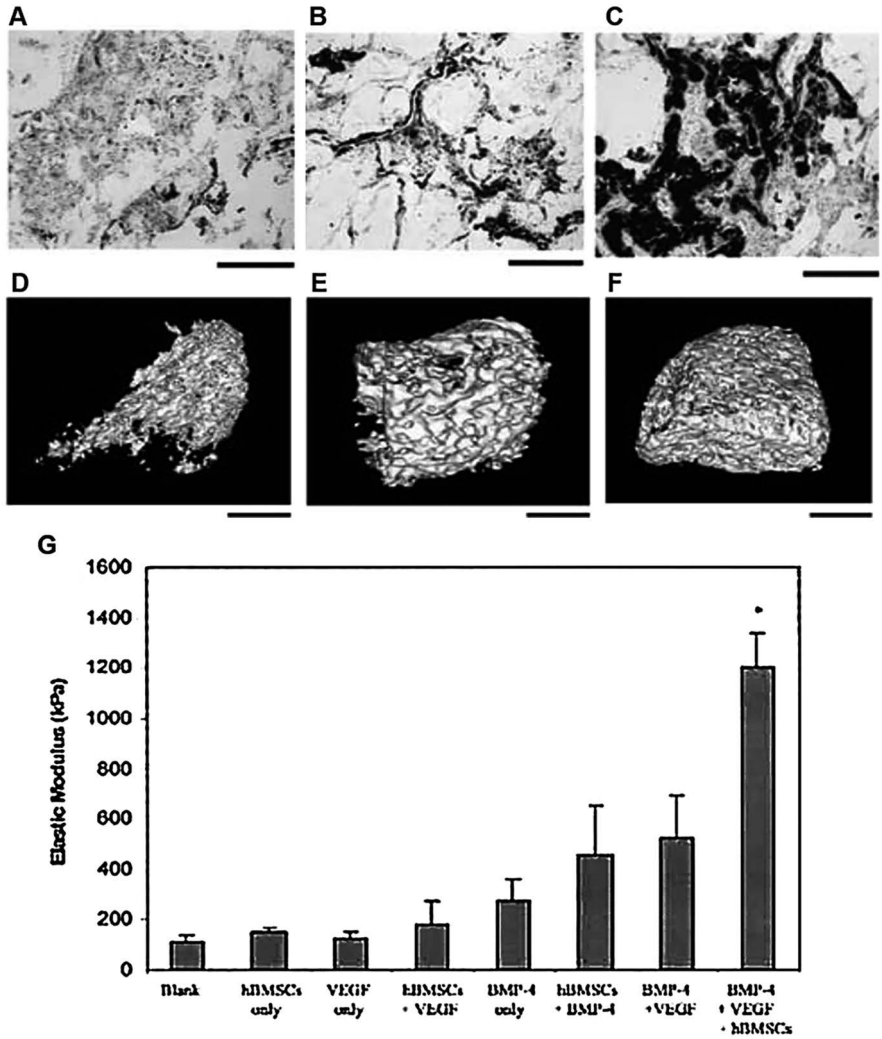

Figure 7.3 Co-delivery of VEGF and BMP-4 encoding plasmid enhances MSC-driven bone regeneration. Von Kossa staining revealed calcium deposition of MSC-seeded constructs incorporating VEGF plasmids (A), BMP-4 plasmids (B) and both plasmids (C). Micro-CT images of constructs delivering both plasmids at week three (D), eight (E) and 15 (F). (G) Elastic modulus of engineered bone recovered at week 15. Scale bar indicates 20 μm in (A)–(C), and 2 mm in (D)–(F). *Represents statistical significance against all other groups ($P < 0.05$). Reproduced with permission from Huang Y. C. *et al.*, *J. Bone Miner. Res.*, **20**, 848, 2005. Copyright 2005: John Wiley and Sons.

7.2.2.2 Biomaterials for Biosensing

In bone tissue engineering, non-invasive monitoring of bone regeneration can greatly facilitate the development of effective scaffolds, by enabling longitudinal assessment of the same sample post-implantation, without serial euthanization at each time point for sample collection.[99,100] These real-time and non-invasive assessments can also be used in clinics to guide clinical decisions on whether further interventions are required following bone graft implantations.[101] To achieve this goal, sensing functions have been coupled to the biomaterial constructs through incorporation of sensor moieties, either directly or facilitated through nanoparticle encapsulation.[102,103] Considering the functions, these platforms can be classified into two categories: (1) platforms that monitor local extracellular conditions (*e.g.* deposited calcium minerals), and (2) platforms that report intracellular molecules (*e.g.* mRNA, protein expression).

7.2.2.2.1 Biomaterial Constructs to Report Extracellular Conditions. Being a major component of bone, the extent of calcium mineral deposition is an important indicator of successful osteogenesis. In this aspect, various HAp-targeted fluorescence and magnetic resonance (MR)-probes have been developed.[104,105] Probes for fluorescence imaging include PamidronatePam78 (with IRDye78)[106] and PAM800 agent (with IRDye800CW).[107] In addition to optical detection of mineralization, these agents also serve to visualize bone remodeling and osteoclast activity.[108,109] For MR-based imaging, contrast agents (CA) act to accelerate the proton relaxation process, of either T1 (longitudinal) or T2 (transversal). Gadolinium(III) [Gd(III)] is widely applied for T1, while super-paramagnetic iron oxide nanoparticles are common for T2 imaging.[110,111] Hence, various HA-targeted ligands have been complexed with Gd(III) to achieve bone-targeted contrast enhancement, including DOTA and BPAMD.[104,112] Nevertheless, application of these probes is thus far limited with a short monitoring window, as contrast signals generated rapidly decay following their elimination.[113] Therefore, repeated injections are required for comprehensive analysis of tissue regeneration, even though this is inconvenient and costly.[114]

While it has not been applied for HAp-targeted agents, scaffold incorporation is a potential solution for protecting and tuning the amount of probes incorporated and released at any moment.[115] At the same time, the scaffold degradation process, which is necessary for complete osteointegration, can be monitored. For example, van der Zande *et al.* demonstrated that a Gd-labeled carbon nanotube (gado NT)-incorporated PLGA scaffold increased the T1 MR intensity of the scaffold's surrounding tissue over a three-week period, matching the scaffold degradation process observed through histology.[116]

Besides the extent of calcium mineral deposition, cell status at implanted sites is also important to understand the mechanism behind the successful bone engineering. Harrington *et al.* proposed a pH and O_2 self-reporting scaffold as a measure of cell viability, blood vessel formation and waste clearance.

Briefly, PLGA nanofibers were functionalized with ratiometric responsive nanosensors carrying either pH-sensitive (5-(and-6)-carboxy-fluorescein: FAM) and a pH reference dye (6-carboxytetramethylrhodamine: TAMRA), or O_2-sensitive (tris(4,7-diphenyl-1,10-phenanthroline)ruthenium(II) chloride: $Ru(dpp)_3^{2+}$) and an O_2 reference dye (Oregon Green Dextran) to monitor physiologically relevant conditions (pH 5.5–8; 0–21% O_2).[117] Meanwhile, Chan *et al.* demonstrated a MR-based pH detection platform to monitor cells undergoing apoptosis.[118] As shown in Figure 7.4, this platform integrates L-arginine liposome and protamine to provide abundant NH protons for exchange with water molecules within alginate microcapsules. In a low pH environment (*i.e.* as a result of apoptotic cells), less exchange would occur between water molecules and NH protons, which translates to a lower chemical exchange saturation transfer (CEST) contrast signal. In this way, observed

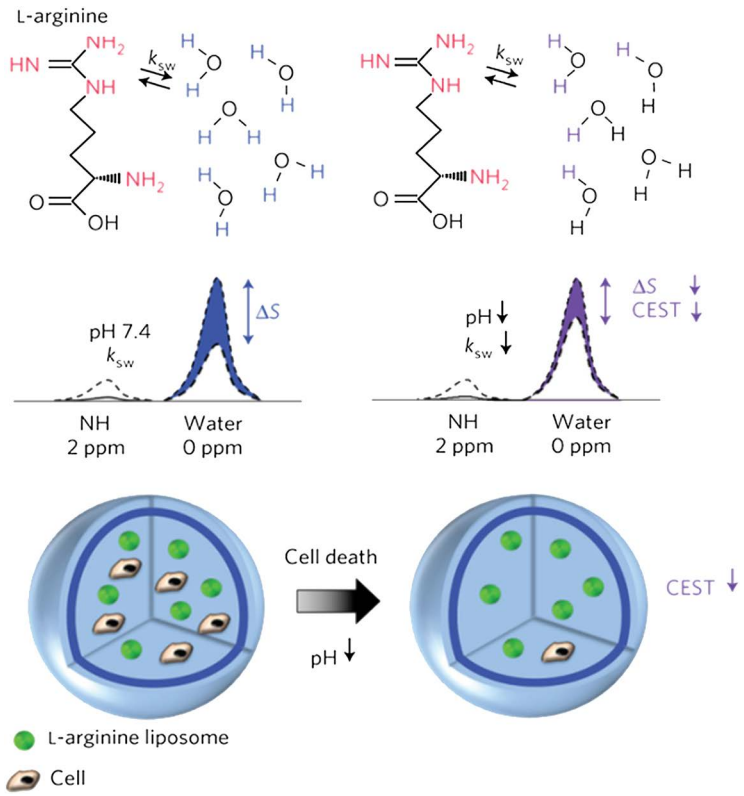

Figure 7.4 MR-based pH monitoring was developed and demonstrated on a hydrogel system, by measuring the CEST contrast, which relates the drop in water signal intensity (ΔS) with selective saturation of the NH-rich L-arginine (2 ppm). At a lower pH (*i.e.* due to cell death), the CEST contrast decreases alongside the drop in k_{sw}. Reproduced with permission from Macmillan Publishers Ltd: Chan K. W., *et al.*, *Nat. Mater.*, **12**, 268, 2013. Copyright 2013: Nature Publishing Group.

MR intensity can be correlated with hydrogel pH value. For bone tissue engineering, such a pH-reporting scaffold can greatly assist pre-clinical optimization of scaffold parameters and therapeutic procedures, by representing the status of seeded MSCs during or even prior to implantation. Crucially, it is reported that osteogenic differentiation is pH sensitive, and that careful pH control is necessary for optimal ALP activity, collagen synthesis and osteogenic marker expression in MSCs.[119,120]

Employing a similar concept based on proton exchange, Ganesh *et al.* displayed an interesting usage of doped HAp nanocrystals (nHAp) for dual purposes (osteoinducting and monitoring). Previously, they showed that Gd(III)-doped nHAp was a suitable agent for T1 weighted MR imaging.[121] Subsequently, doped nHAp was incorporated in electrospun PCL fibers to enable monitoring of cell adhesion and growth. Initially, proton exchange between water and agents was poor due to polymer hydrophobicity. As cells adhered and proliferated on days seven and 14, stronger proton exchange occurred from polymer interactions with the cell membrane, resulting in brighter T1 images. Later, the T1 signal declined following the deposition of calcium minerals. In this manner, correlation can be drawn between the T1 signal and the stages of osteogenesis.[102]

7.2.2.2.2 Biomaterial Constructs to Monitor Intracellular Expression. Besides the techniques mentioned above, validation of successful osteogenesis can also be achieved by evaluating osteogenic differentiation stages of recruited/implanted MSCs. Cell modification with gene reporter techniques is commonly used for non-invasive examination of cellular gene expression.[122,123] To this end, various reporter constructs for osteogenic markers have been developed, including green fluorescence protein (GFP)-tagged osteocalcin (OCN),[124] luciferase (luc)-tagged OCN,[125] yellow fluorescence protein (YFP)-tagged RUNX2[126], and luc-tagged Col1A1[127]. As mentioned in the previous section, these plasmids can be introduced through scaffold incorporation for adherent cell uptake. However, the transfection efficiency of this strategy is quite poor at the moment.[128]

More recently, nucleic acid-based molecular probes (*i.e.* aptamers and molecular beacons/MBs) have been receiving significant attention for cell tracking purposes, with their non-integrative, yet highly specific target recognition.[129] Their limitation comes from rapid degradation and elimination due to nuclease activity, which means that multiple introduction is required to obtain a sufficient monitoring window for differentiation tracking,[130] making them impracticable for use *in vivo*. To meet this need, our group recently demonstrated a simple yet effective solution involving probe encapsulation into biodegradable polymeric NPs. More specifically, PLGA nanoparticles that can be internalized and retained effectively by MSCs[111,131] are used to achieve sustained MB delivery, in order to drastically extend the monitoring period to two/three weeks.[132] Moreover, this nanosensor platform provides versatility in the simultaneous delivery of multiple probes, for a multiplexed cell functionality assessment.[131]

In the future, integrating such nanosensors into scaffold formulations may enable direct evaluation of bone repair. As scaffold materials begin to degrade, exposed nanosensors can then be internalized by adherent MSCs to report on their differentiation status.[133] Furthermore, although such a monitoring approach is currently applicable only in *in vitro* or small animal settings due to light penetration issues, further development of image acquisition tools (*e.g.* two photon intra-vital microscopy) and probes (*e.g.* to incorporate luminescence agents or agents with far-infrared spectra) may facilitate even deeper tissue imaging.[134,135]

7.2.2.3 Limitations with Current Active Scaffolds

While recent advances have made biomaterial scaffolds more functional with regards to promoting recovery and having sensing capability (highlighted in Table 7.1), most of these constructs rely on their passive biodegradation to release incorporated biomolecules. As such, there is not much control over the release profile of molecules.[136] Consequently, with different defect sizes and mechanical stresses expected for distinct application, constructs' parameters (*e.g.* thickness, porosity) require a comprehensive fine-tuning to obtain maximum functional benefit. This process can be highly laborious, time-consuming and costly.[137,138]

One solution is to employ a stimuli-responsive release mechanism, using external (*e.g.* ultrasound, laser), or better yet internal factors (*e.g.* pH, protein expression, secreted molecules) to trigger and control the release rate of bioactive molecules. A comprehensive list of triggers that have been utilized for responsive delivery can be found in recent review papers.[139,140] While not exclusively for bone tissue engineering purposes, pH-dependent carriers have been proposed multiple times. pH-Responsive hydrogels, which become ionized and swell under acidic conditions, have been widely studied for delivery towards gastrointestinal tract and anti-cancer treatments.[141,142] Noting that bone remodeling involves inflammatory and osteoclast activities which induce an acidic environment, a similar strategy may be extended for applications in bone regeneration.[143]

For bone tissue engineering applications, there have been a few externally-responsive carriers proposed. Kearney *et al.* employed an ultrasound trigger to induce the release of BMP-2-conjugated gold nanoparticles from crosslinked alginate hydrogels, which are otherwise entrapped due to steric hindrance.[144] Meanwhile, Qureshi *et al.* demonstrated the light-mediated delivery of miR-148b through photo-sensitive linkage with silver nanoparticles. Upon photo-activation, the complex stimulated ALP activity and osteogenic marker expression (*i.e.* RUNX2, OCN) on adipose-derived stem cells (Figure 7.5).[145]

In the future, the identification and study of more molecular triggers to activate functional scaffolds is expected. Thus, release mechanisms may instead be linked with multiple stimuli to achieve a finely-tuned delivery.[146] Ideally, this involves cell-responsive scaffolds with molecular release defined by an automated feed-back/forward system. In conjunction, biomaterial

Table 7.1 Examples of active scaffolds for bone tissue engineering.

Functionality	Material constructs	Incorporated molecules/ probes	Remarks	References
Protein/ peptide delivery	Gelatin microsphere/ chitosan gel	BMP-2 and IGF-1	Sequential release of BMP-2 and then IGF-1 promoted greater ALP activity	65
Protein/ peptide delivery	Gelatin microsphere/ PPF scaffold	BMP-2 and VEGF	Delivery of both factors enhanced bone bridging in critical-size cranial defect model	70
Small molecule delivery	PLGA/HA microspheres	Simvastatin	Low, sustained release of simvastatin promoted neo-vascularization, cell ingrowth in bone graft	80
Small molecule delivery	Porous CaP beads	Purmorphamine	Bead injection enhanced trabecular bone percentage in defect femurs	82
Nucleic acid delivery	PEG hydrogels	siNoggin and miRNA-20a	Induced osteogenic differentiation of MSCs and greater calcium content on day 28	87
Nucleic acid delivery	Liposome/ electrospun-PCL nanofibers	RUNX2-encoding plasmid	Continuous RUNX2 expression upregulated ALP activity of seeded MSCs	90
Biosensing	PLGA nanofibers	pH- and O_2-sensitive and insensitive fluorescence dyes	Ratiometric analysis to monitor 5–20% dissolved O_2, pH 5.5–8	117
Biosensing	Liposome and protamine-containing alginate hydrogels	NH-proton-rich L-arginine	MR CEST contrast-based pH nanosensor	118

constructs that carry both therapeutic and diagnostic benefits can be an interesting development to currently available scaffolds. Integrated theranostic platforms enable live verification of tissue formation, while at the same time accelerating its process. Therefore, such platforms can facilitate a more rapid and complete evaluation during their optimization stages.

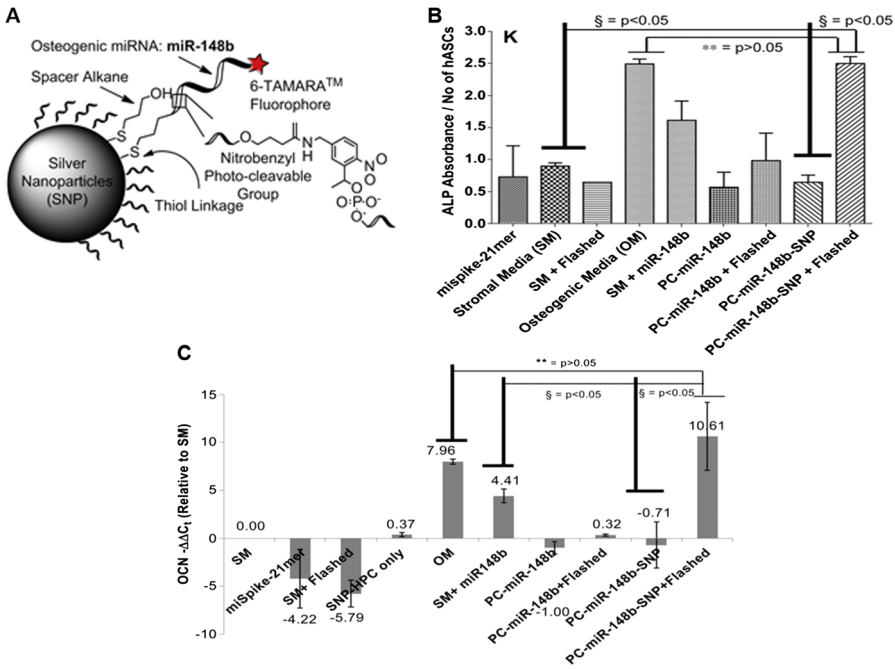

Figure 7.5 Photo-responsive miR-148b conjugates to facilitate controlled osteogenesis. (A) Schematic showing conjugation of miR-148b to silver NPs through a photo-sensitive linker group. Upon light activation, the NP conjugates release miR-148b, which translates into significantly greater ALP activity on day seven (B) and OCN expression on day 28 (C). Reproduced with permission from Qureshi A. T., *et al.*, *Biomaterials*, **34**, 7799, 2013. Copyright 2013: Elsevier. Reproduced from Biomaterials, 34(31), Quershi, A. T., Monroe, W. T., Dasa, V., Gimble, J. M., Hayes, D. J., miR-148b-Nanoparticle conjugates for light mediated osteogenesis of human adipose stromal/stem cells. 7799–7810. Copyright (2013) with permission from Elsevier.

Ventura *et al.* demonstrated incorporation of such theranostic agents inside ceramic phosphate cements. By coupling silica beads loaded with iron oxide agents with BMP-2 proteins, an improved osteogenesis was achieved alongside long-term MR contrast enhancement for longitudinal assessment of scaffold degradation and bone healing.[147] In the near future, it is conceivable that more theranostic agents will be developed and incorporated into scaffolds for bone tissue engineering applications.

7.2.3 Future Perspectives—Clinical Applications of Multi-Functional Biomaterials for Bone Tissue Engineering

As discussed above, advanced generation tissue engineering scaffolds may be loaded with myriad drugs and distinct release profiles,[148] as well as sensors that provide real-time feedback of local environments.[149] Such sophisticated designs yield new opportunities to improve clinical outcomes.

In musculoskeletal tissue engineering, successful bone regeneration is largely dependent on osteointegration and vascularization. A corollary to this, treatment of voluminous fractures with avascular engineered bone grafts has thus far been limited by an inadequate blood supply, resulting in ischaemia, necrosis and eventual graft failure.[150] In contrast, vascularized bone flaps used in autograft procedures are associated with improved functional and aesthetic outcomes in mandibular[151] and long bone reconstructions.[152] Various strategies to engineering bone grafts have been proposed, such as incorporation of heterogeneous cellular co-cultures,[153] or cytokine and growth factor delivery systems.[154] Jia *et al.* recently reported the simultaneous administration of BMP and VEGF, showing significantly improved osteogenesis and bone formation over groups where either cytokine was used alone, and suggesting synergistic effects of osteogenic and vasculogenic activation.[155] Similarly, administration of mesenchymal stem cells concurrently with PLGA-mediated delivery of BMP-2 and VEGF were shown to be useful in correcting mandibular defects, resulting in accelerated defect bridging.[156] These outcomes may likely be improved through the use of more sophisticated delivery systems that allow tailoring of release profiles, including increased payloads[157] and coordinated release systems for co-delivery of two or more factors,[158] in order to match the complex orchestration of chemokines and cytokines in the process of bone healing.[159] Using multiphasic PEG-based constructs, Barati *et al.* demonstrated the staggered release of VEGF and BMP to improve vasculogenesis and osteogenesis in an *in vitro* model.[160] *In vivo*, BMP-2 and VEGF loaded either in PLGA (for extended release) or gelatin (burst release), resulted in sequential release, and increased bone formation in an ectopic implant model.

In any surgical application, monitoring the surgical site is critical for successful clinical outcomes. In the practice of Ilizarov limb-lengthening, for example, non-invasive and quantitative observations on bone healing may be used to make informed clinical decisions on subsequent procedures.[101] Similarly, following implantation of the bone graft, continuous monitoring of the graft is highly desirable to guide interventions and improve outcomes. Besides direct observations of bone quality, various groups have looked at tracking metabolic processes, including pH[149] and oxygen[161] levels, in three-dimensional structures. Despite current technical limitations, it can be expected that future scaffolds, in which the delivery of multiple therapeutic agents and concurrent monitoring take place, can have important implications in tissue engineering. Emerging areas of development include multi-functional scaffolds for application in the treatment of bone cancer.[162]

7.3 Conclusions

In close to five decades of research and development, scaffold technologies have advanced significantly: from the “first-generation” scaffolds, which primarily served mechanical roles, to the current research theme focusing on bioactive scaffolds. These scaffolds address the major limitations of their predecessors, which were largely passive and bioinert, leading to sub-optimal

healing responses. By directly interfacing with seeded cells and/or surrounding host tissues, newer generation scaffolds are able to guide and direct healing responses, with significantly raised safety and efficacy profiles. Current research is focused on novel methods to customize release profiles and interrogate healing responses *in vivo*. Such advances will provide smart scaffolds with "theranostic" abilities in the future.

Acknowledgements

This work was supported by NTU-Northwestern Institute of Nanomedicine, Nanyang Technological University.

References

1. T. Dvir, B. P. Timko, D. S. Kohane and R. Langer, *Nat. Nanotechnol.*, 2010, **6**, 13–22.
2. M. Chong Seow Khoon, *Adv. Drug Delivery Rev.*, 2015, **94**, 141–150.
3. L. L. Hench and J. M. Polak, *Sci. Signaling*, 2002, **295**, 1014.
4. M. A. Woodruff and D. W. Hutmacher, *Prog. Polym. Sci.*, 2010, **35**, 1217–1256.
5. Z.-Y. Zhang, S. H. Teoh, E. Y. Teo, M. S. K. Chong, C. W. Shin, F. T. Tien, M. A. Choolani and J. K. Chan, *Biomaterials*, 2010, **31**, 8684–8695.
6. D. J. Barone, J. M. Raquez and P. Dubois, *Polym. Adv. Technol.*, 2011, **22**, 463–475.
7. J. Mitra, G. Tripathi, A. Sharma and B. Basu, *RSC Adv.*, 2013, **3**, 11073–11094.
8. K. J. L. Burg, S. Porter and J. F. Kellam, *Biomaterials*, 2000, **21**, 2347–2359.
9. A. M. Ferreira, P. Gentile, V. Chiono and G. Ciardelli, *Acta Biomater.*, 2012, **8**, 3191–3200.
10. Y. S. Chen, S. M. Kuo and C. H. Yao, *Biomed. Eng. Appl. Basis Commun.*, 2009, **21**, 233–238.
11. E. Soffer, J. P. Ouhayoun and F. Anagnostou, *Oral Surg. Oral Med. Oral Pathol. Oral Radiol. Endod.*, 2003, **95**, 521–528.
12. F. Mottaghitalab, H. Hosseinkhani, M. A. Shokrgozar, C. B. Mao, M. Y. Yang and M. Farokhi, *J. Controlled Release*, 2015, **215**, 112–128.
13. J. Venkatesan and S.-K. Kim, *Mar. Drugs*, 2010, **8**, 2252.
14. J. Venkatesan, I. Bhatnagar, P. Manivasagan, K.-H. Kang and S.-K. Kim, *Int. J. Biol. Macromol.*, 2015, **72**, 269–281.
15. B. Ben-Nissan, *Curr. Opin. Solid State Mater. Sci.*, 2003, **7**, 283–288.
16. W. Thein-Han and R. Misra, *Acta Biomater.*, 2009, **5**, 1182–1197.
17. P. Yilgor, R. A. Sousa, R. L. Reis, N. Hasirci and V. Hasirci, *Macromol. Symp.*, 2008, **269**, 92–99.
18. J. Lim, M. S. K. Chong, J. K. Y. Chan and S. H. Teoh, *Small*, 2014, **10**, 2495–2502.
19. A. Yeo, W. J. Wong, H. H. Khoo and S. H. Teoh, *J. Biomed. Mater. Res., Part A*, 2010, **92A**, 311–321.

20. Y. Liu, S. H. Teoh, M. S. Chong, E. S. Lee, C. N. Mattar, N. s. K. Randhawa, Z. Y. Zhang, R. J. Medina, R. D. Kamm and N. M. Fisk, *Stem Cells*, 2012, **30**, 1911–1924.
21. C. S. Choong, D. W. Hutmacher and J. T. Triffitt, *Tissue Eng.*, 2006, **12**, 2521–2531.
22. S. E. M. Ibim, K. E. Uhrich, M. Attawia, V. R. Shastri, S. F. El-Amin, R. Bronson, R. Langer and C. T. Laurencin, *J. Biomed. Mater. Res.*, 1998, **43**, 374–379.
23. M. A. Attawia, K. E. Uhrich, E. Botchwey, R. Langer and C. T. Laurencin, *J. Orthop. Res.*, 1996, **14**, 445–454.
24. K. Uhrich, S. Ibim, D. Larrier, R. Langer and C. Laurencin, *Biomaterials*, 1998, **19**, 2045–2050.
25. K. Uhrich, T. Thomas, C. Laurencin and R. Langer, *J. Appl. Polym. Sci.*, 1997, **63**, 1401–1411.
26. M. N. Aboushelib, E. Osman, I. Jansen, V. Everts and A. J. Feilzer, *J. Prosthodontics*, 2013, **22**, 190–195.
27. E. Soh, E. Kolos and A. J. Ruys, *Ceram. Int.*, 2015, **41**, 1031–1047.
28. B.-H. Yoon, W.-Y. Choi, H.-E. Kim, J.-H. Kim and Y.-H. Koh, *Scr. Mater.*, 2008, **58**, 537–540.
29. A. L. M. Maia Filho, F. P. d. M. d. Amaral, A. A. Martin and L. E. S. Soares, *Braz. Arch. Biol. Technol.*, 2014, **57**, 334–339.
30. A. B. Nover, S. L. Lee, M. S. Georgescu, D. R. Howard, R. A. Saunders, W. T. Yu, R. W. Klein, A. P. Napolitano, G. A. Ateshian and C. T. Hung, *Acta Biomater.*, 2015, **27**, 286–293.
31. M. Hirota, T. Shima, I. Sato, T. Ozawa, T. Iwai, A. Ametani, M. Sato, Y. Noishiki, T. Ogawa, T. Hayakawa and I. Tohnai, *Biomaterials*, 2016, **75**, 223–236.
32. B. L. Foss, N. Ghimire, R. Tang, Y. Sun and Y. Deng, *Colloids Surf., B*, 2015, **134**, 370–376.
33. A. Tripathi, S. Saravanan, S. Pattnaik, A. Moorthi, N. C. Partridge and N. Selvamurugan, *Int. J. Biol. Macromol.*, 2012, **50**, 294–299.
34. X. Y. Xie, K. W. Hu, D. D. Fang, L. H. Shang, S. D. Tran and M. Cerruti, *Nanoscale*, 2015, **7**, 7992–8002.
35. A. Oyefusi, O. Olanipekun, G. M. Neelgund, D. Peterson, J. M. Stone, E. Williams, L. Carson, G. Regisford and A. Oki, *Spectrochim. Acta, Part A*, 2014, **132**, 410–416.
36. J. L. Li, Z. Yang, W. T. Y. Loo, X. Xiao, D. J. Zhang, M. N. B. Cheung, W. W. N. Tsang, E. L. Y. Ng and M. Wang, *J. Bioact. Compat. Polym.*, 2014, **29**, 350–367.
37. P. Newman, A. Minett, R. Ellis-Behnke and H. Zreiqat, *Nanomed. Nanotechnol. Biol. Med.*, 2013, **9**, 1139–1158.
38. S. Bose, M. Roy and A. Bandyopadhyay, *Trends Biotechnol.*, 2012, **30**, 546–554.
39. A. J. Salgado, O. P. Coutinho and R. L. Reis, *Macromol. Biosci.*, 2004, **4**, 743–765.
40. Y. Liu, J. Lim and S.-H. Teoh, *Biotechnol. Adv.*, 2013, **31**, 688–705.

41. E. Quinlan, A. López-Noriega, E. Thompson, H. M. Kelly, S. A. Cryan and F. J. O'Brien, *J. Controlled Release*, 2015, **198**, 71–79.
42. V. P. Torchilin, *Eur. J. Pharm. Sci.*, 2000, **11**(suppl. 2), S81–S91.
43. M. Kessler, D. Goldsmith and H. Schellekens, *Nephrol., Dial., Transplant.*, 2006, **21**, v9–v12.
44. G. Wang, J. Qiu, L. Zheng, N. Ren, J. Li, H. Liu and J. Miao, *J. Biomater. Sci., Polym. Ed.*, 2014, **25**, 1813–1827.
45. Y. M. Kolambkar, J. D. Boerckel, K. M. Dupont, M. Bajin, N. Huebsch, D. J. Mooney, D. W. Hutmacher and R. E. Guldberg, *Bone*, 2011, **49**, 485–492.
46. A. C. F. Bassit, P. Moffatt, M.-H. Gaumond and R. Hamdy, *J. Nanomed. Nanotechnol.*, 2015, **6**, 1.
47. M. M. Martino, P. S. Briquez, K. Maruyama and J. A. Hubbell, *Adv. Drug Delivery Rev.*, 2015, **94**, 41–52.
48. F. R. Maia, S. J. Bidarra, P. L. Granja and C. C. Barrias, *Acta Biomater.*, 2013, **9**, 8773–8789.
49. C. R. Nuttelman, M. C. Tripodi and K. S. Anseth, *J. Biomed. Mater. Res., Part A*, 2006, **76**, 183–195.
50. X. Niu, Q. Feng, M. Wang, X. Guo and Q. Zheng, *J. Controlled Release*, 2009, **134**, 111–117.
51. K. Lee, E. A. Silva and D. J. Mooney, *J. R. Soc., Interface*, 2011, **8**, 153–170.
52. S.-H. Jun, E.-J. Lee, T.-S. Jang, H.-E. Kim, J.-H. Jang and Y.-H. Koh, *J. Mater. Sci.: Mater. Med.*, 2013, **24**, 773–782.
53. N. Monteiro, A. Martins, R. L. Reis and N. M. Neves, *Regener. Ther.*, 2015, **1**, 109–118.
54. T. N. Vo, F. K. Kasper and A. G. Mikos, *Adv. Drug Delivery Rev.*, 2012, **64**, 1292–1309.
55. Y. Kimura, N. Miyazaki, N. Hayashi, S. Otsuru, K. Tamai, Y. Kaneda and Y. Tabata, *Tissue Eng., Part A*, 2009, **16**, 1263–1270.
56. H. S. Yang, W.-G. La, S. H. Bhang, J.-Y. Jeon, J. H. Lee and B.-S. Kim, *Tissue Eng., Part A*, 2010, **16**, 1225–1233.
57. H. S. Yang, W.-G. La, S. H. Bhang, T.-J. Lee, M. Lee and B.-S. Kim, *Tissue Eng., Part A*, 2011, **17**, 2153–2164.
58. G. Wei, Q. Jin, W. V. Giannobile and P. X. Ma, *Biomaterials*, 2007, **28**, 2087–2096.
59. F. M. Phillips, A. S. Turner, H. Seim, J. MacLeay, C. A. Toth, A. R. Pierce and D. L. Wheeler, *Spine J.*, 2006, **6**, 500–506.
60. H. Kohara and Y. Tabata, *Biomaterials*, 2011, **32**, 5726–5732.
61. R. M. Klar, R. Duarte, T. Dix-Peek and U. Ripamonti, *Biomaterials*, 2014, **35**, 2773–2788.
62. C. A. Simmons, E. Alsberg, S. Hsiong, W. J. Kim and D. J. Mooney, *Bone*, 2004, **35**, 562–569.
63. A. Jaklenec, A. Hinckfuss, B. Bilgen, D. M. Ciombor, R. Aaron and E. Mathiowitz, *Biomaterials*, 2008, **29**, 1518–1525.
64. A. Raiche and D. Puleo, *Biomaterials*, 2004, **25**, 677–685.
65. S. Kim, Y. Kang, C. A. Krueger, M. Sen, J. B. Holcomb, D. Chen, J. C. Wenke and Y. Yang, *Acta Biomater.*, 2012, **8**, 1768–1777.

66. A. Sahni, L. A. Sporn and C. W. Francis, *J. Biol. Chem.*, 1999, **274**, 14936–14941.
67. A. H. Zisch, M. P. Lutolf, M. Ehrbar, G. P. Raeber, S. C. Rizzi, N. Davies, H. Schmökel, D. Bezuidenhout, V. Djonov and P. Zilla, *FASEB J.*, 2003, **17**, 2260–2262.
68. T. P. Richardson, M. C. Peters, A. B. Ennett and D. J. Mooney, *Nat. Biotechnol.*, 2001, **19**, 1029–1034.
69. N. J. Shah, M. L. Macdonald, Y. M. Beben, R. F. Padera, R. E. Samuel and P. T. Hammond, *Biomaterials*, 2011, **32**, 6183–6193.
70. Z. S. Patel, S. Young, Y. Tabata, J. A. Jansen, M. E. Wong and A. G. Mikos, *Bone*, 2008, **43**, 931–940.
71. J. Lock and H. Liu, *Int. J. Nanomed.*, 2011, **6**, 2769–2777.
72. B. Wu, Q. Zheng, X. Guo, Y. Wu, Y. Wang and F. Cui, *Biomed. Mater.*, 2008, **3**, 044111.
73. Z. Luo, Y. Deng, R. Zhang, M. Wang, Y. Bai, Q. Zhao, Y. Lyu, J. Wei and S. Wei, *Colloids Surf., B*, 2015, **131**, 73–82.
74. K. W. Lo, K. M. Ashe, H. M. Kan and C. T. Laurencin, *Regener. Med.*, 2012, **7**, 535–549.
75. C. E. Segar, M. E Ogle and E. A Botchwey, *Curr. Pharm. Des.*, 2013, **19**, 3403–3419.
76. K. A. Wieghaus, S. M. Capitosti, C. R. Anderson, R. J. Price, B. R. Blackman, M. L. Brown and E. A. Botchwey, *Tissue Eng.*, 2006, **12**, 1903–1913.
77. H. Hojo, K. Igawa, S. Ohba, F. Yano, K. Nakajima, Y. Komiyama, T. Ikeda, A. C. Lichtler, J.-T. Woo and T. Yonezawa, *Biochem. Biophys. Res. Commun.*, 2008, **376**, 375–379.
78. T. Ito, M. Takemasa, K. Makino and M. Otsuka, *J. Pharm. Pharmacol.*, 2013, **65**, 494–502.
79. G. Mundy, R. Garrett, S. Harris, J. Chan, D. Chen, G. Rossini, B. Boyce, M. Zhao and G. Gutierrez, *Science*, 1999, **286**, 1946–1949.
80. I.-c. Tai, Y.-C. Fu, C.-K. Wang, J.-K. Chang and M.-L. Ho, *Int. J. Nanomed.*, 2013, **8**, 3895.
81. X. Wu, J. Walker, J. Zhang, S. Ding and P. G. Schultz, *Chem. Biol.*, 2004, **11**, 1229–1238.
82. K. Gellynck, R. Shah, M. Parkar, A. Young, P. Buxton and P. Brett, *Bone*, 2013, **57**, 405–412.
83. C. E. P. Aronin, S. J. Shin, K. B. Naden, P. D. Rios, L. S. Sefcik, S. R. Zawodny, N. D. Bagayoko, Q. Cui, Y. Khan and E. A. Botchwey, *Biomaterials*, 2010, **31**, 6417–6424.
84. F. Wegman, A. Bijenhof, L. Schuijff, F. Oner, W. Dhert and J. Alblas, *Eur. Cells Mater.*, 2011, **21**, 230–242.
85. M. Sriram, R. Sainitya, V. Kalyanaraman, S. Dhivya and N. Selvamurugan, *Int. J. Biol. Macromol.*, 2015, **74**, 404–412.
86. L. C. Rose, C. Kucharski and H. Uludağ, *Biomaterials*, 2012, **33**, 3363–3374.
87. M. K. Nguyen, O. Jeon, M. D. Krebs, D. Schapira and E. Alsberg, *Biomaterials*, 2014, **35**, 6278–6286.

88. C. Qiao, K. Zhang, H. Jin, L. Miao, C. Shi, X. Liu, A. Yuan, J. Liu, D. Li and C. Zheng, *Int. J. Nanomed.*, 2013, **8**, 2985.
89. H. Hosseinkhani, M. Hosseinkhani, N. P. Gabrielson, D. W. Pack, A. Khademhosseini and H. Kobayashi, *J. Biomed. Mater. Res., Part A*, 2008, **85**, 47–60.
90. N. Monteiro, D. Ribeiro, A. Martins, S. Faria, N. A. Fonseca, J. N. Moreira, R. L. Reis and N. M. Neves, *ACS Nano*, 2014, **8**, 8082–8094.
91. S. Gehmert, S. Gehmert, M. Hidayat, M. Sultan, A. Berner, S. Klein, J. Zellner, M. Müller and L. Prantl, *Clin. Hemorheol. Microcirc.*, 2011, **48**, 5.
92. L. D. Shea, E. Smiley, J. Bonadio and D. J. Mooney, *Nat. Biotechnol.*, 1999, **17**, 551–554.
93. Y. C. Huang, D. Kaigler, K. G. Rice, P. H. Krebsbach and D. J. Mooney, *J. Bone Miner. Res.*, 2005, **20**, 848–857.
94. M. Ø. Andersen, J. V. Nygaard, J. S. Burns, M. K. Raarup, J. R. Nyengaard, C. Bünger, F. Besenbacher, K. A. Howard, M. Kassem and J. Kjems, *Mol. Ther.*, 2010, **18**, 2018–2027.
95. L. B. Zimmerman, J. M. De Jesús-Escobar and R. M. Harland, *Cell*, 1996, **86**, 599–606.
96. J.-f. Zhang, W.-m. Fu, M.-l. He, W.-d. Xie, Q. Lv, G. Wan, G. Li, H. Wang, G. Lu and X. Hu, *RNA Biol.*, 2011, **8**, 829–838.
97. Y. Li, L. Fan, S. Liu, W. Liu, H. Zhang, T. Zhou, D. Wu, P. Yang, L. Shen and J. Chen, *Biomaterials*, 2013, **34**, 5048–5058.
98. P. D. Mariner, E. Johannesen and K. S. Anseth, *J. Tissue Eng. Regener. Med.*, 2012, **6**, 314–324.
99. H. Hagenmüller, S. Hofmann, T. Kohler, H. P. Merkle, D. L. Kaplan, G. Vunjak-Novakovic, R. Müller and L. Meinel, *Ann. Biomed. Eng.*, 2007, **35**, 1657–1667.
100. J. de Boer, C. van Blitterswijk and C. Löwik, *Biomaterials*, 2006, **27**, 1851–1858.
101. O. M. Babatunde, A. T. Fragomen and S. R. Rozbruch, *HSS J.*, 2010, **6**, 71–78.
102. N. Ganesh, A. Ashokan, R. Rajeshkannan, K. Chennazhi, M. Koyakutty and S. V. Nair, *Tissue Eng., Part A*, 2014, **20**, 2783–2794.
103. H. Harrington, F. R. Rose, J. W. Aylott and A. M. Ghaemmaghami, *J. Visualized Exp.*, 2013, e50608.
104. V. Kubícek and I. Lukeš, *Future Med. Chem.*, 2010, **2**, 521–531.
105. J. S. Lee, J. D. Morrisett and C.-H. Tung, *Atherosclerosis*, 2012, **224**, 340–347.
106. A. Zaheer, R. E. Lenkinski, A. Mahmood, A. G. Jones, L. C. Cantley and J. V. Frangioni, *Nat. Biotechnol.*, 2001, **19**, 1148–1154.
107. E. A. Cowles, J. L. Kovar, E. T. Curtis, H. Xu and S. F. Othman, *BioRes. Open Access*, 2013, **2**, 186–191.
108. Y. Zilberman, I. Kallai, Y. Gafni, G. Pelled, S. Kossodo, W. Yared and D. Gazit, *J. Orthop. Res.*, 2008, **26**, 522–530.
109. K. M. Kozloff, L. Quinti, S. Patntirapong, P. V. Hauschka, C.-H. Tung, R. Weissleder and U. Mahmood, *Bone*, 2009, **44**, 190–198.

110. Y. Li, M. Beija, S. Laurent, L. v. Elst, R. N. Muller, H. T. Duong, A. B. Lowe, T. P. Davis and C. Boyer, *Macromolecules*, 2012, **45**, 4196–4204.
111. C. Xu, D. Miranda-Nieves, J. A. Ankrum, M. E. Matthiesen, J. A. Phillips, I. Roes, G. R. Wojtkiewicz, V. Juneja, J. R. Kultima and W. Zhao, *Nano Lett.*, 2012, **12**, 4131–4139.
112. V. Kubicek, J. Rudovský, J. Kotek, P. Hermann, L. Vander Elst, R. N. Muller, Z. I. Kolar, H. T. Wolterbeek, J. A. Peters and I. Lukeš, *J. Am. Chem. Soc.*, 2005, **127**, 16477–16485.
113. K. M. Harmatys, E. L. Cole and B. D. Smith, *Mol. Pharmaceutics*, 2013, **10**, 4263–4271.
114. J. E. Perosky, J. R. Peterson, O. N. Eboda, M. D. Morris, S. C. Wang, B. Levi and K. M. Kozloff, *J. Orthop. Res.*, 2014, **32**, 1416–1423.
115. A. M. Ghaemmaghami and J. W. Aylottb, *Cell. In Vitro Test.*, 2014, 89.
116. M. van der Zande, B. Sitharaman, X. F. Walboomers, L. Tran, J. S. Ananta, A. Veltien, L. J. Wilson, J. I. Álava, A. Heerschap and A. G. Mikos, *Tissue Eng., Part C*, 2010, **17**, 19–26.
117. H. Harrington, F. Rose, Y. Reinwald, L. Buttery, A. Ghaemmaghami and J. Aylott, *Anal. Methods*, 2013, **5**, 68–71.
118. K. W. Chan, G. Liu, X. Song, H. Kim, T. Yu, D. R. Arifin, A. A. Gilad, J. Hanes, P. Walczak and P. C. van Zijl, *Nat. Mater.*, 2013, **12**, 268–275.
119. D. H. Kohn, M. Sarmadi, J. I. Helman and P. H. Krebsbach, *J. Biomed. Mater. Res.*, 2002, **60**, 292–299.
120. L.-E. Monfoulet, P. Becquart, D. Marchat, K. Vandamme, M. Bourguignon, E. Pacard, V. Viateau, H. Petite and D. Logeart-Avramoglou, *Tissue Eng., Part A*, 2014, **20**, 1827–1840.
121. A. Ashokan, D. Menon, S. Nair and M. Koyakutty, *Biomaterials*, 2010, **31**, 2606–2616.
122. G. Zhang, X. Lan, T.-C. Yen, Q. Chen, Z. Pei, C. Qin and Y. Zhang, *Nucl. Med. Biol.*, 2012, **39**, 1243–1250.
123. J. R. Bagó, E. Aguilar, M. Alieva, C. Soler-Botija, O. F. Vila, S. Claros, J. A. Andrades, J. Becerra, N. Rubio and J. Blanco, *Tissue Eng., Part A*, 2012, **19**, 593–603.
124. A. K. Born, S. Lischer and K. Maniura-Weber, *J. Cell. Biochem.*, 2012, **113**, 313–321.
125. T. Narai, M. Katoh, T. Inoue, M. Taniguchi, K. Kazuki, Y. Kazuki, K. Sato, I. Kodani, K. Ryoke and M. Oshimura, *Yonago Acta Med.*, 2015, **58**, 23–29.
126. L. Zou, F. K. Kidwai, R. A. Kopher, J. Motl, C. A. Kellum, J. J. Westendorf and D. S. Kaufman, *Stem Cell Rep.*, 2015, **4**, 190–198.
127. D. J. Corn, Y. Kim, M. D. Krebs, T. Mounts, J. Molter, S. Gerson, E. Alsberg, J. E. Dennis and Z. Lee, *J. Orthop. Res.*, 2013, **31**, 871–879.
128. X. Cao, W. Deng, Y. Wei, W. Su, Y. Yang, Y. Wei, J. Yu and X. Xu, *Int. J. Nanomed.*, 2011, **6**, 3335.
129. C. Wiraja, D. Yeo, D. Lio, L. Labanieh, M. Lu, W. Zhao and C. Xu, *Mol. Cell. Ther.*, 2014, **2**, 33.
130. H. V. Desai, I. S. Voruganti, C. Jayasuriya, Q. Chen and E. M. Darling, *Tissue Eng., Part A*, 2014, **20**, 899–907.

131. D. Yeo, C. Wiraja, Y. J. Chuah, Y. Gao and C. Xu, *Sci. Rep.*, 2015, **5**, 14768.
132. C. Wiraja, D. C. Yeo, S. Y. Chew and C. Xu, *J. Mater. Chem. B*, 2015, **3**, 6148–6156.
133. C. K. K. Choi, J. Li, Y. J. Xu, L. W. C. Ho, Z. Meiling, K. K. W. To, C. H. J. Choi and L. Bian, *J. Am. Chem. Soc.*, 2015, **137**, 7337–7346.
134. H. Sano, J. Kikuta, M. Furuya, N. Kondo, N. Endo and M. Ishii, *Bone*, 2015, **74**, 134–139.
135. S. Qi, Y. Huang, Y. Li, P. Cai, S. I. Kim and H. J. Seo, *J. Mater. Chem. B*, 2014, **2**, 6387–6396.
136. X. Zhao, J. Kim, C. A. Cezar, N. Huebsch, K. Lee, K. Bouhadir and D. J. Mooney, *Proc. Natl. Acad. Sci.*, 2011, **108**, 67–72.
137. Y. Chen, S. Zhou and Q. Li, *Biomaterials*, 2011, **32**, 5003–5014.
138. E. Saito, E. E. Liao, W. W. Hu, P. H. Krebsbach and S. J. Hollister, *J. Tissue Eng. Regener. Med.*, 2013, **7**, 99–111.
139. Y. Qiu and K. Park, *Adv. Drug Delivery Rev.*, 2012, **64**, 49–60.
140. S. Mura, J. Nicolas and P. Couvreur, *Nat. Mater.*, 2013, **12**, 991–1003.
141. K.-Y. Lu, C.-W. Lin, C.-H. Hsu, Y.-C. Ho, E.-Y. Chuang, H.-W. Sung and F.-L. Mi, *ACS Appl. Mater. Interfaces*, 2014, **6**, 18275–18289.
142. C.-Y. Chen, T. H. Kim, W.-C. Wu, C.-M. Huang, H. Wei, C. W. Mount, Y. Tian, S.-H. Jang, S. H. Pun and A. K.-Y. Jen, *Biomaterials*, 2013, **34**, 4501–4509.
143. N. Zhang, T. Gao, Y. Wang, Z. Wang, P. Zhang and J. Liu, *Mater. Sci. Eng., C*, 2015, **46**, 158–165.
144. C. J. Kearney, H. Skaat, S. M. Kennedy, J. Hu, M. Darnell, T. M. Raimondo and D. J. Mooney, *Adv. Healthcare Mater.*, 2015, **4**, 1634–1639.
145. A. T. Qureshi, W. T. Monroe, V. Dasa, J. M. Gimble and D. J. Hayes, *Biomaterials*, 2013, **34**, 7799–7810.
146. A. P. Blum, J. K. Kammeyer, A. M. Rush, C. E. Callmann, M. E. Hahn and N. C. Gianneschi, *J. Am. Chem. Soc.*, 2015, **137**, 2140–2154.
147. M. Ventura, Y. Sun, S. Cremers, P. Borm, Z. T. Birgani, P. Habibovic, A. Heerschap, P. M. van der Kraan, J. A. Jansen and X. F. Walboomers, *Biomaterials*, 2014, **35**, 2227–2233.
148. V. Mouriño, J. P. Cattalini, J. A. Roether, P. Dubey, I. Roy and A. R. Boccaccini, *Expert Opin. Drug Delivery*, 2013, **10**, 1353–1365.
149. W. Di, R. S. Czarny, N. A. Fletcher, M. D. Krebs and H. A. Clark, *Pharm. Res.*, 2016, 1–12.
150. J. Lim, M. Chong, Y. Liu, A. Khademhosseini and S. Teoh, *Regenerative Engineering of Musculoskeletal Tissues and Interfaces*, 2015, p. 269.
151. H. Chim, C. J. Salgado, S. Mardini and H.-C. Chen, *Semin. Plast. Surg.*, 2010, **24**, 188–197.
152. Y. Sun, C. Zhang, D. Jin, J. Sheng, X. Cheng, X. Liu, S. Chen and B. Zeng, *Int. Orthop.*, 2010, **34**, 425–430.
153. Y. Liu, J. K. Chan and S. H. Teoh, *J. Tissue Eng. Regener. Med.*, 2015, **9**, 85–105.
154. G. D. Barabaschi, V. Manoharan, Q. Li and L. E. Bertassoni, *Engineering Mineralized and Load Bearing Tissues*, Springer, 2015, pp. 79–94.

155. J. Jia, W. Siheng, C. Fang, A. Chengchong and C. Shiyi, *RSC Adv.*, 2016, **6**, 41800–41808.
156. B. C. Tee, K. G. H. Desai, K. S. Kennedy, B. Sonnichsen, D.-G. Kim, H. W. Fields, S. R. Mallery, S. P. Schwendeman and Z. Sun, *Am. J. Transl. Res.*, 2016, **8**, 2693.
157. H.-y. Zhao, J. Wu, J.-j. Zhu, Z.-c. Xiao, C.-c. He, H.-x. Shi, X.-k. Li, S.-l. Yang and J. Xiao, *BioMed Res. Int.*, 2015, **2015**, 7.
158. M. Farokhi, F. Mottaghitalab, M. A. Shokrgozar, K.-L. Ou, C. Mao and H. Hosseinkhani, *J. Controlled Release*, 2016, **225**, 152–169.
159. S. Reed and B. Wu, *Ann. Biomed. Eng.*, 2014, **42**, 1528–1536.
160. D. Barati, S. R. P. Shariati, S. Moeinzadeh, J. M. Melero-Martin, A. Khademhosseini and E. Jabbari, *J. Controlled Release*, 2016, **223**, 126–136.
161. M. T. Raimondi, C. Giordano and R. Pietrabissa, *J. Appl. Biomater. Funct. Mater.*, 2015, **13**, e313–e319.
162. C. Marques, J. Ferreira, E. Andronescu, D. Ficai, M. Sonmez and A. Ficai, *Int. J. Nanomed.*, 2014, **9**, 2713–2725.

CHAPTER 8

Smart Biomaterials for Tissue Engineering of Cartilage

MINA D. FAHMY[a], BRINDA SHAH[a], MEHDI RAZAVI[b], HOSSEIN JAZAYERI[a], FARAHNAZ FAHIMIPOUR[a], JOSHUA WHITE[a], RADI MASRI[c] AND LOBAT TAYEBI*[a]

[a]Marquette University School of Dentistry, Milwaukee, WI 53201, USA; [b]Department of Radiology, School of Medicine, Stanford University, Palo Alto, California 94305, USA; [c]Department of Endodontics, Prosthodontics and Operative Dentistry, University of Maryland School of Dentistry, Baltimore, MD, USA
*E-mail: lobat.tayebi@marquette.edu

8.1 Introduction

The articular cartilage (AC) allows for painless, frictionless movement of synovial joints. Once the AC has been damaged, it has limited ability to regenerate or repair, and continued injury may progress to debilitating osteoarthritis (OA).[1] OA is considered to be the most common form of arthritis. It is associated with joint pain and dysfunction so much so that it is also considered a leading cause of disability among older adults.[2,3]

Due to their avascularity and low immunogenicity, AC allografts can be used to repair osteochondral lesions.[4] Donor AC allografts are typically preserved before transplantation by vitrification using cryoprotectant agents (CPAs).[5]

Smart Materials No. 25
Smart Materials for Tissue Engineering: Applications
Edited by Qun Wang

Published by the Royal Society of Chemistry, www.rsc.org

Despite their toxicity, strides have been made to determine dose–injury relationships of CPAs on AC so as to limit potential injury while maintaining a concentration adequate to vitrify the tissue.[6] Another method used to treat osteochondral lesions is tissue engineering; a technique that employs the use of biologically compatible materials to replace defected or worn tissue; in this instance, cartilage tissue.

In the early stages of tissue engineering of any organ, scaffolds or implants were built to provide minimal structural support while also regulating the diffusion of waste and nutrient products between newly forming tissue and host tissue.[7–15] Various biomaterials with different characteristics have been synthesized and used for tissue engineering and regeneration purposes.[16–24] Some biomaterials have been used successfully to replace the mechanical function of bodily tissues including vertebral discs and knees, however, they are still limited within the realm of tissue engineering due to their inadequate ability to regulate and modulate the repair and regeneration of host tissues.[25–30] However, clinical applications of tissue engineering have been limited due to limited availability of biomaterials that are available for human use but also due to inherent material properties that render them incompatible.[31–34] Due to these limitations, the use of innovative smart materials in tissue engineering have emerged.

Smart biomaterials are characterized by their capability to respond to even slight variations in their environment. These smart biomaterials have distinct properties and have been designed over the years to interact, in a specific fashion, with various biological systems producing specific biological responses. They are unique in that they undergo rapid structural macroscopic changes that can be reversible.[35] The need for specific and timely interactions between biomaterials and cellular bodies creates a need specifically for "smart" biomaterials that can both mimic the interactions between cells and their extracellular environment to properly facilitate cellular growth and development and also a need for practical application in a clinical setting.[36] Both synthetic and natural materials exist and can be used as smart biomaterials in the tissue regeneration process. The desired properties of these materials will be explored in detail in this chapter.

Within the realm of tissue regeneration, biomaterials are used to facilitate the cell differentiation and growth processes outside of the body in order to grow tissue that can be implanted into the body. During normal development, tissue differentiation and development is dependent on the interactions that occur between cells and their respective extracellular matrix (ECM). It takes a considerable amount of technology to recreate these interactions. Since simple polymers cannot adequately reproduce these complex interactions in order to regenerate tissue, the creation and development of smart biomaterials will be crucial to forming functional tissue.[37] Smart biomaterials are required and therefore have been designed to react appropriately when interacting with cells and the ECM in order to fit the needs of tissue regeneration, which is a complex process that requires a specific environment to facilitate growth and development.[36]

Smart biomaterials can be applied in many different ways. For example, they can be applied to the regeneration of cartilage by actively reproducing the interactions between precursor cells and differentiating stem cells within tissue. Such smart biomaterials are designed to target and enhance cell differentiation and cell metabolism in addition to the complex interactions that take place.[36] Therefore, cells are able to be grown on bio-scaffolds and can be strategically implanted into damaged areas of cartilage tissue to create healthy, functional cartilaginous tissue. To be useful in this application, "smart" biomaterials must be biodegradable, have the strength to physically support and protect cells through their development cycles, and boast a level of bioactivity to facilitate cell attachment and movement—all properties that would make them biocompatible in order to produce the optimum biological responses.[38]

It becomes necessary to modify the properties of biomaterials to regenerate different types of tissue. In the case of AC regeneration, the parameters of the matrix structures or biomaterial scaffolds that support chondrocyte growth and development should be modified. Both natural and synthetic materials can be used in this process. Different material factors need to be considered, such as the rate of degradation, biocompatibility, porosity, surface topography, and ease of handling in a clinical setting. Numerous new biomaterials have been generated in recent years that are also viable candidates for use in tissue engineering applications.

As introduced previously, the properties of the material chosen determine the metabolism and the longevity of the cells. During the growth of cartilage, the chondrocytes, or the precursor cells of cartilage, secrete the matrix of cartilage and eventually proliferate and differentiate into cartilage after they are embedded into that matrix. These biomaterial matrices are linked to the degradation rate of the ECM biomaterial and pore distribution, directly affecting their growth and proliferation rates, leading to the production of more or less cartilage, as cells can sense topography changes and differences in material surfaces.

Numerous challenges must be overcome in order for the future use of smart biomaterials in human trials. In the majority of studies involving biomaterials, it is mostly young adult subjects or fetal animal cells that are used.[39] The adult–elderly demographic would arguably benefit the most from tissue regeneration therapy. However, the feasibility of using elderly cells in regeneration is inconclusive. In addition, *in vitro* methods and animal testing are the current methods of choice for testing smart biomaterials; regulatory approval for human testing in clinical applications and eventually market introduction are still difficult milestones for biomaterials to reach.[40]

8.2 Required Biomaterial Properties for Cartilage Repair

In selecting smart biomaterials to repair cartilage, there are a number of desired properties that contribute to effective cartilage tissue regeneration. Cartilage tissue regeneration research is usually done by combining cells,

such as stem cells and chondrocytes, with bio-scaffolds.[41] The biomaterials used are either biological or synthetic in nature and are sometimes a combination of both. The physicochemical and biological properties of smart biomaterials need to be modified for specific tissue regeneration applications. In order to stimulate growth and development of cartilage tissue, it is necessary to adjust the specific property parameters of the smart matrix structures or the biomaterial scaffolds that support the growth and development of cell structures, as these parameters affect the status of the cells in these matrices.[42] Both natural materials, or materials synthesized from natural extracellular materials, and synthetic materials can be used in this process. Each of these materials has their advantages and disadvantages. Cells primarily interact with biomaterial scaffolding through ligands on the material's surface.[38] Scaffolds synthesized using natural materials naturally possess these ligands for cell adhesion while synthetic materials need incorporation of the appropriate ligands through specific means. Various factors need to be considered depending on the desired application, such as the rate of degradation, biocompatibility, porosity, surface topography, and ease of handling in a clinical setting.

Biodegradation is a chemical process that inevitably occurs in all biochemical compounds and the rate at which it occurs is determined by many variables. These variables include the presence of light, temperature, oxygen, bacteria, fungi, and even bioavailability. Through the chemical reactions and microorganisms, these substances transform into new materials.[43] Through careful manipulation of these variables and the use of degradation tests such as respirometer tests, the rate of degradation of the scaffold can be carefully controlled in order to manage waste production into the ECM. In addition, the biocompatibility of these materials is also an important property. Biocompatibility is the ability of a smart biomaterial to behave appropriately in certain environments with a specific host response.[44] Controlling the biocompatibility would prevent an increase in the toxicity of the ECM or prevent any change in pH levels, which would hinder chondrocyte attachment and proliferation needed in cartilage tissue repair.[36] Another property that is important to account for is porosity. Biomaterial scaffolds should have an interconnected pore structure with high porosity to ensure that cells can penetrate the scaffolding—in this way, proper nutrients can diffuse into the ECM of these cells and waste products from these cells can diffuse freely away without interfering with the surrounding tissues and organs.[44] A lack of vascularization, nutrient availability, and poor waste removal from the center of engineered scaffolding constructs are the main issues in core degradation in cartilage tissue engineering.[38]

Specific surface topography and area also affect the bulk properties of a biomaterial. Surface topography is determined by three main properties which are lay (the predominant direction in which the surface pattern is oriented), surface roughness, and waviness (irregularities in the surface pattern). What used to be flat and original surface textures can now become engineered surface topographies through several different machining methods and processes.[45] Specific surface area influences ligand density for cell

adhesion, thus the mean pore size of the scaffold must be large enough for cells to enter into the structure but small enough to allow for the binding of a specific amount of ligand on the material surface to adhere to the cells for tissue regeneration.[46] It is critical to control surface topography by manipulating its properties and by measuring it through both contact and non-contact methods.

There are a variety of materials that are currently used in cartilage tissue engineering. The benefits, drawbacks, and limitations of natural and synthetic biomaterials will be explored. The natural biomaterials discussed are collagen, hyaluronic acid, fibronectin, chitosan, and alginate. The synthetic biomaterials discussed are polyurethane, polytetrafluoroethylene, and poly butyric acid.

8.3 Natural Polymers

8.3.1 Collagen

Collagen, the fibrous protein that constitutes the fibrils of connective tissue, is used as a natural biomaterial extensively because of its abundance, ubiquity, and biocompatibility. It is used either alone or in conjunction with another substrate to enhance its structural properties. Collagen is a smart material because it can readjust and adapt its mechanical and molecular properties in response to any external resistance or force placed upon it. When this mechanical loading or force is placed on collagenous tissues, collagen can utilize its capability to convert mechanical forces into biochemical signals.[47] Collagen will alter and transform its molecular properties at the top and induce a host of downstream biochemical signals that will aid in biological processes such as wound healing and tissue regeneration. Though collagen synthesis is important in producing collagenous tissue in parts such as tendons, collagen degradation is also a key component in biological and pathological processes.[48] With the right amount of collagen degradation, remodeling and regeneration of tissue can occur; however, with an excess amount of collagen degradation, it could create extra porous sites and lead to pathologies such as arthritis. Type I and II fibril-forming (fibrillar) and Type IX fibril-associated collagen are used for the regeneration of cartilage tissue.[49,50] Degradation rates, porosity, and pore sizes can all be measured through various methods and then adjusted and adapted depending on specific design requirements. Collagen has both advantages and limitations when used as a scaffold, as listed in Table 8.1.[49]

8.3.2 Hyaluronic Acid

Hyaluronic acid (HA), also known as hyaluronan, is a polysaccharide and is a natural polymer found endogenously and evenly distributed between connective and epithelial tissue. HA acts as a smart biomaterial because it has been shown to be responsive to pH changes and has been able to alter and adapt its mechanical and chemical properties in order to function

Table 8.1 Collagen properties as a scaffold.

Advantages	Disadvantages
Biocompatibility	No inherent rigidity
Osteocompatibility	Potential for antigenicity through telopeptides
Adhesive	
Fibrous, cohesive, and nonfriable	
Suturable	
High porosity for neohistogenesis	
Fibers appear to become incorporated into the new tissue matrix	
The ability to be combined with other materials	
Medium can be perfused	
Fluid pressure can be transduced	

and behave appropriately to these changes in pH to reestablish a proper relationship between the macromolecules and their corresponding ECM environment.[51] Additionally, HA has high biocompatibility and is readily able to regulate angiogenesis—the process involving the formation of blood vessels—by stimulating endothelial precursor cells to proliferate and grow. Due to its pH-sensitive properties and adaptability, HA has been used in many drug delivery systems that are sensitive to changes in pH.[52] Due to its angiogenesis contribution, HA can be used as a tumor marker in various cancer types.[53] Additionally, HA serves as a coat around chondrocytes and is responsible for the resilience of cartilage in its aggregate form.[54] HA is often used in a hydrogel form in cartilage tissue scaffolding. Since HA and its associated elements in hydrogel form occur naturally in the body, scaffolding formation takes place in the presence of cells with minimal toxicity.[55]

8.3.3 Chitosan

Chitosan is a cationic amino polysaccharide formed by the alkaline deacetylation of chitin[56] and is both biocompatible and bioresorbable. Additionally, chitosan-based polymers are smart biomaterials due to their pH- and temperature-sensitive structures. Many smart biomaterials composed of chitosan are highly responsive to changes in pH and temperature and alter their structure accordingly.[57] Due to these smart properties, chitosan has been readily used in drug delivery systems, cell culture systems, graft modifications, *etc.* Chitosan is also often used in conjunction with HA to form natural hydrogels to serve as effective scaffolding for chondrocytes. The pore size, and thus the amount of chondrocytes that adhere to the scaffolding, changes depending on the concentrations of each component in the hydrogel in conjunction with other materials, like type II collagen.[56] Both chitosan and HA hydrogel scaffoldings have shown promise for cartilage regeneration applications and these biomaterial hydrogels have also been proven to be

injectable.[55,58] Superior differentiation of chondrogenic distribution of ECM, and better mechanical behavior make HA in hydrogel form a significant potential candidate in future cartilage tissue engineering applications.[59] Chitosan scaffolding can be seen in Figure 8.1 below from Griffon *et al.*[56]

8.3.4 Fibronectin

Fibronectin is a glycoprotein found in the ECM. Fibronectin is an essential determinant of many applications because it binds to integrin (a receptor protein), collagen, and fibrin and therefore plays a significant role in cellular

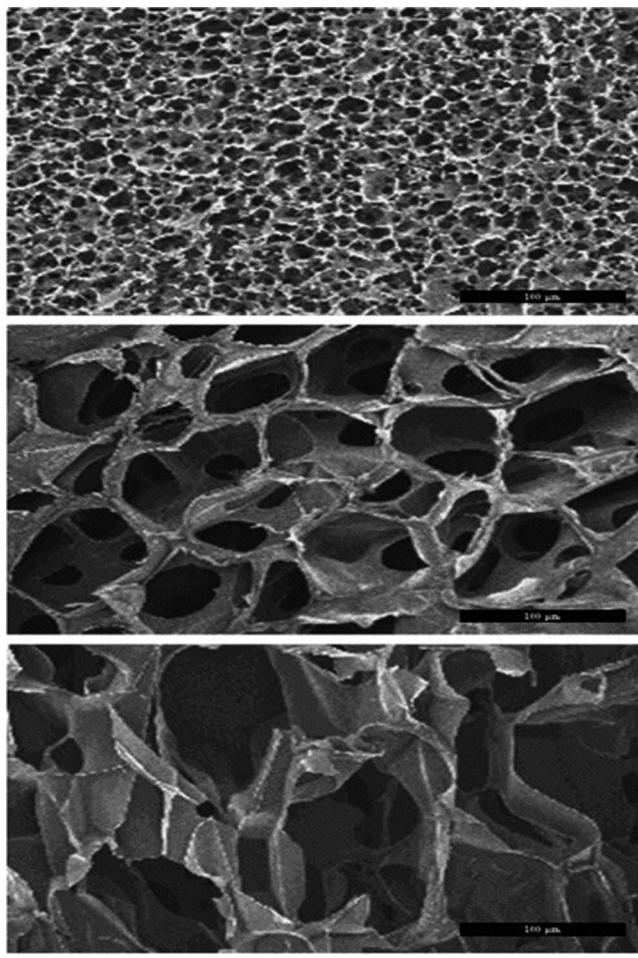

Figure 8.1 Scanning electron microscope examination of chitosan scaffolds with pore size measuring <10 micrometers (top), 10–50 micrometers (middle) and 70–120 micrometers (bottom) in diameter. Reprinted from *Acta Biomaterialia*, **2**, Griffon, D. J., Sedighi, M. R., Schaeffer, D. V., Eurell, J. A., Johnson, A. L. Chitosan scaffolds: Interconnective pore size and cartilage engineering, 313–320, Copyright (2006) with permission from Elsevier.

signaling, adhesion, transport, differentiation, growth, and regeneration.[60] Due to these properties, fibronectin can be used as a marker for the presence of cancer. Additionally, in its polymerized form, fibrin has a critical role in wound healing to avoid fibrosis (scar tissue). Sahni and colleagues found that fibrin bound to fibroblast growth factor 2 encouraged growth of endothelial cells as well as amplified the endothelial cells' proliferation.[61] Fibrin, and therefore, fibronectin, are presented as smart biomaterials because in addition to its binding properties, adhesive capabilities, signaling processes, and wound repairing, the adverse effects of fibrin gluing on chondrocytes haven't been seen in cell cultures.[62] Therefore, when important ECM molecules such as fibrin and collagen are used as cellular scaffolds, they are considered suitable and useful biological vehicles for wound healing. A disadvantage of fibrin is that its constructs can shrink, which can eventually impede cellular invasion and thus the healing response.[42]

8.3.5 Alginate

Alginate is a sugar-based natural polymer found extensively in the cell walls of brown algae. It has been used as a smart biomaterial because it has many favorable properties including its high biocompatibility, ease of gelation, low toxicity, and low cost.[63] Through several crosslinking processes, alginate also represents ECM both structurally and dynamically and therefore can be manipulated and altered to fit the needs of the specific application to create a specific host response.[64] Alginate hydrogels, therefore, can create a moist environment for wound healing while also minimizing bacterial infections at the site of interest. For drug delivery systems, alginate is used particularly because it can be administrated orally or injected into the body without the use of highly invasive mechanisms.[63] Alginate can be used in biomaterial scaffoldings for cartilage tissue regeneration as well due to its high biocompatibility and mild gelation. Alginate is used as a biomaterial in scaffoldings in the form of beads and as a component in the form of hydrogels or even sponges and pads. Alginate and chitosan are widely utilized *in vitro* while their role in *in vivo* cartilage regeneration is restricted and continues to be tested.[42]

8.4 Synthetic Polymers

8.4.1 Polyurethane, Polytetrafluoroethylene, Poly Butyric Acid

Synthetic polymers are emerging smart biomaterials used in several tissue engineering applications. They are selected because of their responsiveness to variables such as temperature, pH, chemicals, and even light. Very small changes in response to these variables cause significant changes in the mechanical and chemical properties of synthetic polymers.[65] Synthetic polymers are also selected for their biodegradability and mechanical properties in supporting chondrocyte cell structures in cartilage tissue regeneration.[7] The advantage of using synthetic polymers is their great flexibility in design

and elimination of disease transmission. Furthermore, synthetic polymers can be transformed into porous scaffolds. Though these synthetic polymers are often chosen for their biodegradability, they can be degraded in various ways—hydrolysis, cellular degradation, enzymatic pathways—and these degradation products that result from these reactions and processes can increase the pH of the scaffolding area and therefore can cause excess inflammation due to high molecular weight of the synthetic polymers.[42] However, due to their high molecular weight and formation of cartilaginous tissue, they also exhibit high resistance to loading which can be useful in many applications.

Polyurethane is a synthetic polymer composed of organic units. These units are considered smart biomaterials because they are thermo-responsive and therefore change significantly with changes in temperature of the external environment. They are also characterized by high-resiliency and high-flexibility making them useful in many applications.[66] They are prepared in scaffolds as bone graft substitutes because they can be made to have high interconnected pores and water permeability, a high pore/volume ratio, and high osteo-conductivity.[67] Additionally, polyurethane has shown promise in promoting the attachment of differentiated chondrocytes *in vitro* for extended periods of time, up to 42 days in some cases, although a significant release of matrix molecules into the culture medium was reported as well.[68]

Polytetrafluoroethylene, also known as Teflon, is also a thermoplastic polymer and therefore changes depending on the temperature of the external environment—it is useful in several applications because it is thermo-responsive. Additionally, it exhibits high strength and high flexibility.[69] Among the many applications it is used for, polytetrafluoroethylene has been proven to increase chondrocyte cell numbers when used as a plasma treated scaffolding.[70] However, there are still risks of increased toxicity levels or the potential development of complications.[71]

Poly butyric acid is also an organic compound that is thermoplastic and therefore it can be used in many bioengineering settings. What is very unique about this smart material is that it tends to resist biodegradation and is also highly biocompatible, making it useful for many medical applications.[43] Additionally, poly butyric acid possesses high tensile strength and therefore is useful in tissue regeneration and cartilage reconstruction as well.[72] Since it has few degradation products, it is generally associated with little inflammation and immune reactions.

8.5 Smart Matrices (Scaffolds)

8.5.1 Thermo-Responsive Matrices

The design of a scaffold with optimal fabrication parameters is crucial in the mechanical durability and regenerative capacity of the complex as a whole. Smart biomaterials are unique in their ability to undergo changes in morphology and properties as a result of external stimulants, such as pH and temperature.[73,74] Thermo-responsive polymers belong to the largest class of smart biomaterials, and the distinction between their characteristic lower

critical solution temperature (LCST) and upper critical solution temperature (UCST) manifests a difference in physical properties of the material.[75] The change in temperature induces a conformational change in the smart polymer structure by manipulating its interaction with water-soluble and water-insoluble environments.[76] A transition between different physical states, such as film, bulk, or solution, is made possible by external temperature variation, which can disrupt crosslinked molecular networks within the smart material.[77] Temperatures below the LCST stimulate the smart polymer to exhibit hydrophilic properties while temperatures above the LCST contrarily induce hydrophobicity following a phase separation.[78]

In an experiment involving poly(*N*-isopropylacrylamide; PNIPAAm), the LCST for the smart biomaterial was determined to be 33 °C, at which the substance can undergo a reversible globular structural alteration in water. At temperatures higher than 33 °C, the biomaterial yielded an insoluble gel, while below, it yielded the soluble form.[79] For cartilage tissue engineering, the solubility of the material is important in chondrogenic differentiation.[79] The aqueous gel formed by introducing an ambient temperature makes it clinically applicable to soft tissue engineering.[80] Examples of structural changes include micelle packing as well as reversible transitions between coil and helix conformations.[80] These thermos-responsive polymers are ideal for fabricating surfaces with variable adhesion capabilities.[81] Smart biomaterials, in this regard, show a fine equilibrium between hydrophilic and hydrophobic states, and the manipulation of temperature toward or away from its critical value will allow the structure to expand or collapse in response.[57]

The objective for using thermos-responsive polymers in cartilage tissue engineering is to create surfaces with adjustable cell attachment and detachment capabilities, which is ideal for cartilage tissue engineering strategies.[82] The switch that initiates or stops cell adhesion is PNIPAAm, and the temperature variation above or below the LCST determines the structural action of the thermo-responsive polymer as a whole.[83] Ibusuki *et al.* demonstrated in 2003 one of many ongoing experiments that apply the use of thermos-responsive, injectable hydrogels for cartilaginous defects of various shapes *in vitro*.[84] One example of a thermos-responsive hydrogel is lyophilized chitosan-pluronic hydrogel as an injectable cell delivery carrier as seen in Figure 8.2.[85] Muzzarelli *et al.* also went into detail describing carbohydrate polymers for cartilage tissue regeneration in a sol-to-gel manner exhibited by their intelligent polymer systems.[86] The key to sol–gel transitions of thermo-sensitive biomaterial systems is cooling or heating to body temperature following subcutaneous injection of the therapeutic agent, depending on the desired molecular mechanism, such as swelling or shrinking.[87] Inverse temperature dependence is indicative of swelling properties of the system in correlation to temperature change relative to the LCST. Furthermore, the composition of the hydrogel is either a combination of hydrophobic parts or the possession of both hydrophilic and hydrophobic groups. Lowering the temperature substantiates dissolution because the interactions between the hydrophilic segments and surrounding aqueous environment are strengthened, so its applicability in cartilage engineering is promising. Heightened hydrophobicity, however, has the reverse effect: shrinkage.

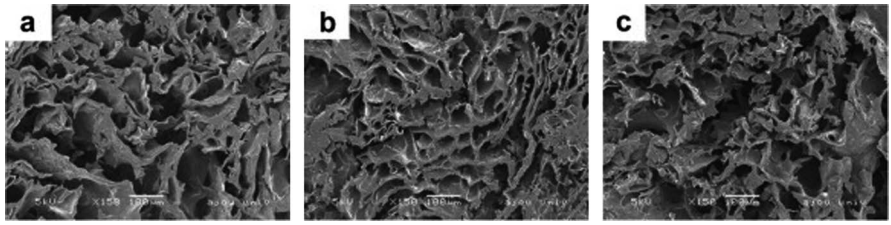

Figure 8.2 SEM images of lyophilized CP hydrogels at various concentrations (a) 16, (b) 18, and (c) 20 wt%. Reprinted from *Acta Biomaterialia*, **5**(6), Park, K. M., Lee, S. Y., Joung, Y. K., Na, J. S., Lee, M. C., Park, K. D. Thermosensitive chitosan-Pluronic hydrogel as an injectable cell delivery carrier for cartilage regeneration, 1956–1965, Copyright (2009) with permission from Elsevier.

This system's relevance in drug delivery is uncanny.[88,89] The incorporation of temperature-sensitive elements to the polymer or copolymer system can allow it to achieve smart capabilities.[88] It is also important to note that gelation can occur under heating or cooling conditions, depending on the physical properties of the material itself. Chemical crosslinking or association can be attributed with post-injection gelation.[90] Peptides have also been used as temperature-sensitive systems, often undergoing conformational changes from an alpha helix into a β-sheet, or *vice versa*, as a result of this environmental stimulus. Once again, the hydrophilicity of certain functional groups and hydrophobicity of other segments of the secondary peptide structure will be affected and shift to a conformational change in this process.[91]

8.5.2 pH-Responsive Systems

The pH of a polymer system for tissue engineering purposes also has an effect on structural change due to shifts in hydrophilicity and hydrophobicity. Poly((2-dimethyl amino)ethyl methacrylate) (P(DMAEMA)), for example, has an approximate pH of 8.5.[92] Protonation or deprotonation can change this relationship between the compound and an aqueous environment.[93] Similar to the nature and mechanism of thermos-responsive polymeric systems, a change in pH that can transform its relationship with hydrophilic and hydrophobic environments will result in swelling or shrinkage, depending on protonation or deprotonation.[94] The complexity of shrinkage/swelling behavior as a result of ionization and pH change is astounding. In a report from Gupta *et al.*, his team noted that hydrogel swelling occurred at a pH above the polymer's pK_a and shrinkage occurred below, as a result of varying ion concentrations in the solution.[94] Wu and colleagues discussed pH-responsive hydrogels and immersed the hydrogels into a buffer solution of either 7.4 pH or 5.0 pH, and found that the structure of *N*-[(2-hydroxyl-3-trimethylammonium) propyl] chitosan chloride/glycerophosphate (HTCC/GP) and chitosan hydrochloride/glycerophosphate (CS/GP) were both more compact before immersion as seen in the comparison of Figures 8.3 and 8.4.[95]

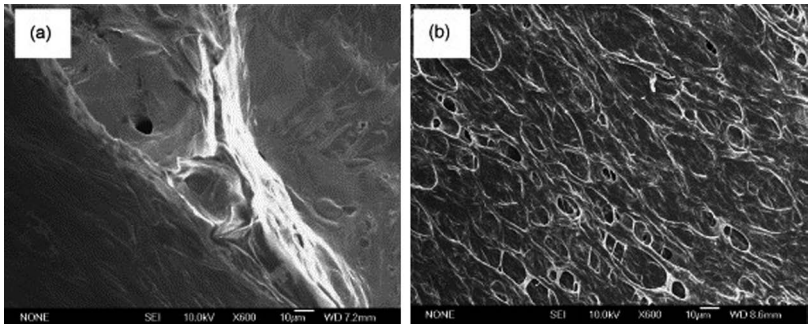

Figure 8.3 SEM micrographs of (a) HTCC/GP and (b) CS/GP hydrogels formed after heating at 37 °C for two hours. Reprinted from the *International Journal of Pharmaceutics*, **315**(1–2), Wu, J., Su, Z.-G., Ma, G.-H. A thermo- and pH-sensitive hydrogel composed of quaternized chitosan/glycerophosphate, 1–11, copyright (2006) with permission from Elsevier.

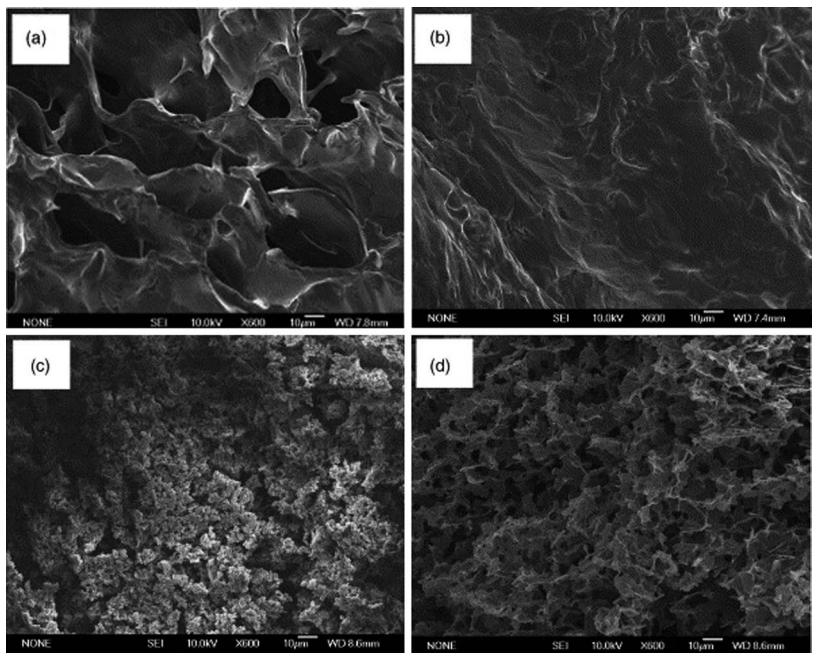

Figure 8.4 SEM micrographs of (a) HTCC/GP hydrogel at pH 5; (b) HTCC/GP hydrogel at pH 7.4; (c) CS/GP hydrogel at pH 5.0; and (d) CS/GP hydrogel at pH 7.4 formed after immersion in buffer (pH 5.0 or 7.4, at 37 °C) for one hour. Reprinted from the *International Journal of Pharmaceutics*, **315**(1–2), Wu, J., Su, Z.-G., Ma, G.-H. A thermo- and pH-sensitive hydrogel composed of quaternized chitosan/glycerophosphate, 1–11, Copyright (2006) with permission from Elsevier.

Because polymers are commonly used in cartilage engineering applications, it is relevant to point out that their miscibility in the solution also determines their extent of swelling. Acidic and basic functional groups can give off ions that increase osmotic pressure, thus affecting swelling/shrinkage behavior. Buffered solutions, in fact, can expedite the swelling mechanism.[96] Fibrin-based matrices can also be sensitive to changes in pH; for example, a somewhat basic pH of 10 can orient the matrix fibrils in a longitudinal fashion, proving to be suitable for vessel endothelial cells.[97]

The preparation of pH-responsive hydrogels entails the addition of a weak polyacid/polybase to the polymeric gel. They are very useful in orthopaedic drug delivery. Furthermore, these polyacids and polybases actually influence the conformational transition that the polymer undergoes as a result of pH change. The combination of electrostatic interactions between different functional groups, including other interactive forces, allows the therapeutic polymer system to swell. The difference in osmotic pressure in the inner and outer solutions is countered by gel swelling.[98] Sokker *et al.* described that pH change can also influence release rate in drug delivery applications. They explained that an alkaline medium was more contributive to the swelling nature of the hydrogel than a neutral medium.[99] Chen *et al.* formulated a way to calculate swelling degree (SD), typically sensitive to changes in pH. They used the original hydrogel weight in buffer solution and divided the value of the gel weight at a different swelling time by the original weight.[100]

The applications of pH-responsive systems are found in the gastrointestinal tract and systemic vasculature as well. Universally, the backbone is composed of a specific polymer. The variations in the chains attached to the backbone that participate in electrostatic interactions make each pH-responsive system unique. The groups ionize and build up a charge that makes them repulsive or attractive to other groups, rendering them capable of undergoing swelling/shrinkage behavior. A change in pH can also facilitate erosion of a pH-responsive polymer.[101,102] Insulin transport has also been effective with these polymeric networks. The diffusion of glucose into the gel leads to conversion of the monosaccharide to acid, decreasing the pH and causing the gel to swell. The opposite effect of shrinkage reverses the release rate of insulin.[102] Apart from charge and degree of ionization, crosslinking density is also a significant factor that affects pH-responsiveness. The environment, such as a buffer solution, similarly has a dramatic effect on swelling kinetics. Siegel *et al.* demonstrated that multivalent anions decrease swelling in buffer solutions compared to monovalent anions.[103] An increase in pK_a similarly substantiates swelling capacity.[104] A drug surrounded by a solution with a pH different to its own pK_a could end up charged or uncharged as a result of this environmental effect. Porosity of the polymer network contributes to pH sensitivity as well.[105] Because each organ and cell type has its own particular environment with an optimal pH, such as cancer tissue and the gastrointestinal tract of acidic nature,

manipulating the pH sensitivity of certain polymeric systems to meet the pH level of the targeted environment is a complex matter. The environment will cause protonation or deprotonation of the therapeutic system in order to render it capable of swelling/shrinkage.[73]

8.5.3 Self-Assembling Matrices

Self-assembling peptides have been explored for various tissues, such as cartilage.[41,106] These peptides not only control the delivery of bioactive agents,[107,108] but also provide a microenvironment to increase the chondrogenesis of bone marrow stromal cells.[106] The most common "natural" motifs used for peptide-based materials are the α-helix and the β-sheet.[109] Self-assembly is the reversible conversion of a group of molecules into one or more supramolecular structures by noncovalent interactions without external force.[110] The balance between force opposition, such as solvation and electrostatic repulsive forces, and favored forces in this regard, such as hydrogen bonding, cohesive interaction, hydrophobic forces and electrostatic interactions, determines the stable structure of self-assembled molecules.[111] The structures of the most self-assembling molecules are amphiphilic, which contain both hydrophilic and hydrophobic parts and is the basis of functional assemblies in nature. The cellular membrane, the extracellular matrix and the cytoskeleton are examples of assembled structures.[112] Natural or synthetic amphiphilic materials under aqueous conditions form ordered assemblies with noncovalent interactions and the external environment, including pH, temperature, and solution ionic strength, as well as the structure of the monomer, determine the final assembled structure.[112–116]

A variety of natural polymers, such as polysaccharides and proteins (hyaluronic acid (HA), chitosan and chondroitin sulfate are examples of these natural polymers), were used as amphiphilic polymers and some of the natural polymers are naturally amphiphilic or can be modified with amphiphiles.[117] A self-assembling hydrogel containing 40% chitosan and 60% chondroitin sulfate was investigated as a carrier for chondroitin sulfate—an agent that inhibits the synthesis of agents that are related to the death of chondrocytes and cartilage damage, such as proteolytic enzymes. This hydrogel reorganizes at a pH ranging from 6 to 12 and releases significant amounts of chondroitin sulfate at a pH higher than 6.5.[118]

Kisiday *et al.* encapsulated chondrocytes through a self-assembling peptide KLD-12 with sequence AcN-KLDLKLDLKLDL-CNH2 as 3D matrices. They demonstrated that the seeded chondrocytes in the peptide matrices maintained their morphology and produced large amounts of glycosaminoglycans as well as Type II and Type XI collagen.[119] Chondrocytes seeded within RAD16-I (RADARADARADARADA-PuraMatrix™) hydrogel and supplemented with TGF-β improve integration between two opposing pieces of articular cartilage.[120] Self-assembling peptides with the sequence AcN-(KLDL) 3-CNH2

were modified to encapsulate bone-marrow-derived stromal cells and to deliver TGF-β to induce chondrogenesis in cartilage tissue engineering.[121] Nanofibrillar self-assembling peptide hydrogels containing KLD12 and KDL-12-collagen mimetic peptide (CMP) made of a -(Pro-Hyp-Gly)$_n$- amino acid sequence stimulate the chondrogenesis of BMSc and increase glycosaminoglycan production.[122] Bell *et al.* have engineered a peptide gel (P11-9) with a similar feature of hyaluronic acid (HA) to enhance lubrication between articulating cartilage surfaces. P11-9 contained four serine (OCH_2OH) and three glutamic acid (OCH_2CH_2COOH) side chains per peptide. P11-9 self-assembles into gels under physiological conditions.[123] Amphiphilic synthetic polymers commonly consist of poly ethylene glycol (PEG), poly(*N*-(2-hydroxypropyl) methacrylamide), pluronics, peptide amphiphiles (PA) and different poly(esters) and poly(amino acids).[117] A thermogelling, biodegradable copolymer with the formulation of poly(DL-lactic acid-*co*-glycolic acid)-poly (ethylene glycol) (PEG-*g*-PLGA) was used as an injectable protein and cell delivery system in cartilage in a rabbit model. It has been stated that when a chondrocyte suspension was used in the thermogelling polymer, the cartilage defect was remarkably repaired. The PEG-*g*-PLGA system doesn't need any organic solvent or any surgical procedure.[124]

Peptide amphiphiles (PAs) have four regions, including bioactive domains, that aid in cellular response and growth factor delivery:[121,125] the polar domain which enhances solubility, the stabilization domain that is often formed by a β-sheet sequence[126] and alkyl chain tails which help micelle assembly.[127] PAs were fabricated by Shah *et al.*, with high density of binding epitopes to TGF-β to regulate the release rate. They reported that these materials stimulate chondrogenic differentiation and cartilage regeneration when injected into a chondral defect in a rabbit model after 12 weeks with or without exogenous TGF-β. These results showed the potential of biofunctional materials to enhance regeneration of cartilage.[128] Arg-Gly-Asp (RGD)-modified HA-*g*-pluronic copolymers are a self-assembling, injectable material that are used for chondrocyte encapsulation. It is reported that chondrocytes can produce GAG and type II collagen within the hydrogels.[129]

In Table 8.2, a summary of self-assembling matrices in cartilage regeneration is provided.

The potential complications associated with scaffolds can be avoided by using self-assembly. Possible scaffold problems may include phenotype alteration of cells, degradation product toxicity, inhibition of cell migration, and stress shielding.[130] Self-assembly was used to produce tissue engineering constructs over agarose without a scaffold. Histological, biochemical, and biomechanical properties revealed that the tissue engineering construct was hyaline-like in appearance.[130] The using of self-assembling structures with the appropriate balance of hydrophobic/hydrophilic components for any specific application as cell carriers or drug delivery systems in cartilage tissue engineering has many advantages, such as minimally invasive surgical procedures by using *in situ* formation of injectable hydrogels and scaffoldless cartilage tissue engineering.

Table 8.2 Self-assembling matrices in cartilage regeneration.[a]

Authors	Materials	Function
J. F. Piai *et al.*[118]	40% chitosan and 60% chondroitin sulfate	Chondroitin sulfate carrier
J. Kisiday *et al.*[119]	KLD-12 peptide	Chondrocyte encapsulation
P. W. Kopesky *et al.*[120]	RAD16-I supplemented with TGF-β	Improve integration between two opposing pieces of articular cartilage
G. A. Silva *et al.*[121]	AcN-(KLDL) 3-CNH2 peptide with TGF-β	Induce chondrogenesis
J. E. Kim *et al.*[122]	KDL-12-CMP	Stimulate the chondrogenesis of BMSc
C. J. Bell *et al.*[123]	P11-9 peptide	Enhance lubrication between articulating cartilage surfaces
B. Jeong *et al.*[124]	PEG-*g*-PLGA	Chondrocyte encapsulation
R. N. Shah *et al.*[128]	Pas	Enhance regeneration of cartilage
H. Lee *et al.*[129]	RGD modified HA-*g*-pluronic	Chondrocyte encapsulation

[a]Abbreviations: collagen mimetic peptide (CMP), poly(DL-lactic acid-*co*-glycolic acid) (PLGA), poly(ethylene glycol) (PEG), peptide amphiphiles (PAs), Arg-Gly-Asp (RGD).

8.5.4 Bioactive-Agent-Releasing Matrices

Growth factors commonly represent bioactive agents, which have an impact on stimulating or inhibiting cellular growth and differentiation.[131] In cartilage tissue engineering, numerous growth factors such as bone morphogenetic proteins (BMPs), insulin-like growth factor I (IGF-I), transform growth factor β (TGF-β), and fibroblast growth factor (FGF) have been utilized.[132] Many delivery systems are used as natural or synthetic polymers, and release rates of bioactive agents depend on the diffusion of the agents and degradation of the carrier.[133] However, release rates in smart matrices rely on the status of the environment, which can be externally regulated or self-regulated. External triggers, such as magnetics, are used for release in an externally regulated system, whereas in the self-controlled system, matrices respond to environmental changes, such as elevated temperatures and low pH, which are found in the body.[134]

Motoyama *et al.* investigated the impact of TGF-β-immobilized magnetic beads on chondrogenesis with an external magnetic force. TGF-β was bound to Ferri Sphere 100C® *via* an amide bond. They showed that at the local site, the magnetic forces could control the concentration of TGF-β.[135] Several studies have described the role of a member of the TGF-β family in cartilage tissue engineering. They are utilized to increase proliferation of chondrocytes[136,137] in order to enhance cartilage ECM formation[138] and to induce chondrogenesis.[139,140]

pNIPAAm is one of the most common thermo-sensitive polymers that have a sol–gel transition at 32 °C.[141] Because of the poor biocompatibility and

non-degradability of the pNIPAAm, it's generally used as a composite material.[142] The composite of pNIPAAm with other polymers not only enhances bioactivity but also modulates the transition point near body temperature.[142] Na *et al.* used pNIPAAm with hyaluronic acid as a thermo-reversible hydrogel for cartilage regeneration. They embedded TGFβ-3 and rabbit chondrocytes in the composite gel and injected it subcutaneously in mice. As a result of their study, the thermo-reversible hydrogel with TGFβ-3 increased the differentiation and the formation of cartilage-specific ECM.[143] For example, another smart material that employs agent release is poly(*N*-isopropylacrylamide-*co*-vinylimidazole) (P(NIPAAm-*co*-VI)). Rabbit chondrocytes and nanoparticles that contain TGFβ-1 were embedded in poly(*N*-isopropylacrylamide-*co*-vinylimidazole) (P(NIPAAm-*co*-VI)) for subcutaneous implantation into the backs of nude mice. The proliferation and differentiation of chondrocytes notably increased.[144]

A composite of oligo(poly(ethylene glycol) fumarate) (OPF) has also been used as a thermo-sensitive scaffold in cartilage tissue engineering. Park *et al.* described a composite of OPF with MSCs and the bioactive agent TGFβ-1 loaded into gelatin microparticles for cartilage tissue engineering. The loading capability is unique for these bioactive-agent-releasing thermo-sensitive matrices.[105] Any of the bioactive-agent-releasing matrices are also thermo-sensitive or pH sensitive. For example, Jung *et al.* described a thermo-sensitive composite hydrogel using pluronic F127 and hyaluronic acid for the delivery of TGF-β1 and human-adipose-derived stem cells. A sol–gel transition of the hydrogel was reported at body temperature. The release of TGF-β1 was moderate and the formation of a cartilaginous matrix was increased.[145]

The triblock copolymer of PLGA–PEG–PLGA is another thermo-sensitive polymer system that was used as a matrix material to deliver a model protein. Different phase diagrams and release profiles were achieved by changes in the copolymer concentration and the block length.[146] As an injectable polymer with a sol–gel transition at 37 °C, chitosan–β-glycerophosphate–hydroxyethyl cellulose (CH–GP–HEC) was loaded with chondrogenic factors or mesenchymal stem cells (MSCs) and injected into cartilage tissue defects. The results show that the CH–GP–HEC hydrogel provided an appropriate environment for MSC proliferation and chondrogenic differentiation. The CH–GP–HEC can be used with minimal pain and invasion.[147] Matsusaki *et al.* described a pH-sensitive controlled release of FGF from poly(γ-glutamic acid) (γ-PGA) and sulfonated γ-PGA. The release of FGF from the biodegradable gel retained its biological activity without denaturation.[148] FGF-2 has been utilized to increase cell proliferation of chondrocytes and to maintain the chondrogenic potential of chondrocytes in cartilage tissue engineering (Table 8.3).[149–152]

In Table 8.3, the summary of bioactive agent releasing matrices for cartilage regeneration is provided.

A temperature/pH-sensitive gel composed of chitosan and glycidyltrimethylammonium chloride was synthesized. Its composite was a solution at room temperature, and it was converted to a hydrogel at 37 °C. The profile of

Table 8.3 Bioactive-agent-releasing matrices for cartilage regeneration.[a]

Authors	Materials	Bioactive agents
M. Motoyama *et al.*[135]	Ferri Sphere 100C®	TGF-β
K. Na *et al.*[143]	PNIPAAm	TGFβ-3
K. H. Park *et al.*[144]	p(NIPAAm-*co*-VI)	TGFβ-1
H. Park *et al.*[131]	OPF	TGFβ-1
H. H. Jung *et al.*[145]	Pluronic F127 and hyaluronic acid	TGFβ-1
S. Chen *et al.*[146]	PLGA–PEG–PLGA	Model protein
H. Naderi-Meshkin *et al.*[147]	CH–GP–HEC	Chondrogenic factors
M. Matsusaki *et al.*[148]	γ-PGA	FGF

[a]Abbreviations: poly(*N*-isopropylacrylamide-*co*-vinylimidazole): p(NIPAAm-*co*-VI), oligo(poly(ethylene glycol)fumarate): (OPF), poly(DL-lactic acid-*co*-glycolic acid): PLGA, poly(ethylene glycol): PEG, chitosan-β-glycerophosphate-hydroxyethyl cellulose: CH–GP–HEC, poly(γ-glutamic acid): γ-PGA.

drug release was changed as a function of pH. This system is useful for the delivery of bioactive agents.[95] Smart matrices offer great advantages in bioactive agent delivery for cartilage. Externally or internally regulated systems can be used for controlled drug delivery in cartilage tissue engineering. For successful delivery of bioactive agents, it is necessary to synthesize polymers and crosslinking agents with better biocompatibility. The benefits of using smart matrices in delivery systems demonstrate better local concentration of bioactive agents and a lower need for surgical procedures.

8.6 Response to Dynamic Loading

As a hydrated tissue, articular cartilage has a load-bearing surface in synovial joints and shows specific mechanical behaviour. The cartilage's mechanical behaviour depends on the microstructure and composition of its components.[153] Hyaline cartilage is a dense white tissue that covers the articulating surfaces of bones to transfer the loads in diarthrodial joints up to 5–18 MPa in the human hip joint.[154,155] Due to the compressive equilibrium aggregate modulus (0.3–1.0 MPa), the tensile equilibrium modulus (15–40 MPa), and the permeability ($0.5–5 \times 10^{-15}$ $m^4/(N.S)$), articular cartilage can perform this function.[156] The dense ECM that creates the above-mentioned properties consists of collagen type II and glycosaminoglycan.[156] Chondrocytes exist in the dense matrix and through their biosynthetic processes keep and remodel the tissue's structure in response to the *in vivo* mechanochemical environment. Although its unique structure allows cartilage to function under a load, its dense composition and lack of vascularization restrict its regenerative abilities. In explant culture systems, physiologic dynamic loading results in an increase in the synthesis of proteoglycan and protein, whereas static loads cause a reduction.[157] While the mechanical environment is known to affect the activity of the chondrocytes within the matrix and its phenotypic expression, immobilization is obviously harmful to cartilage repair and

regeneration.[158,159] Thus, an agreement has been made that dynamic loading within suitable ranges of load or strain and frequency is more helpful to cartilage than sustained static loading, and also this loading may be a beneficial tool for the functional tissue engineering of AC.[154] Regarding cartilage, an appropriate porous scaffold should give initial mechanical integrity and supports cell adhesion.[153] Most of the developed scaffolds for cartilage applications have been successful in the case of the biochemical and morphological properties of hyaline cartilage; however, they are usually mechanically inferior to the tissue.[154]

In agarose as an uncharged hydrogel that supports the chondrocyte phenotype,[160] chondrocytes respond to deformational loading similar to that found in explants. According to the fact that deformational loading enhances biosynthesis of the extracellular matrix,[161] researchers produced a bioreactor for culturing the chondrocyte-seeded agarose constructs with dynamic deformational loading at a physiologic level and frequency over an extended culture period.[158] Applying 10% strain at 1 Hz, for three hours per day, for one month enhanced both the biochemical composition and aggregate modulus of agarose hydrogels with seeded chondrocytes.[154] When growth factors were applied with dynamic loading, a synergistic enhancement in mechanical behaviour was observed. Although the mechanical properties reported were less than that of the native tissue, these outcomes propose that the accurate mixture of mechanical and chemical organizers can improve the growth of tissue-engineered articular cartilage scaffolds.[154] Addition of hydroxyproline and sulfated glycosaminoglycan was also understood to be superior in dynamically-loaded disks compared with the unloaded (static) free-swelling controls at the third week.[158] Indeed, applied loading increased the growth of a tissue that has the appearance properties of the cartilage tissue. In addition, a 21-fold increase in the equilibrium aggregate modulus with respect to day controls was seen after four weeks in culture. In the absence of loading, chondrocyte–agarose constructs showed only a three–four-fold enhancement over the initial stiffness values after four weeks in culture.[162] For comparison, the development of tissue having a modulus comparable to the previously mentioned study for chondrocyte-seeded polyglycolide acid scaffolds cultured in a rotating wall bioreactor for three months has been reported[163] showing the effect of dynamic loading for tissue culture. Moreover, it can be concluded that the time for having the same modulus under dynamic loading for polyglycolide acid scaffolds (three months) is more than agarose constructs (one month).

Considering the time needed to achieve suitable mechanical behaviour under static conditions or a free swelling culture, many researchers resorted to designing bioreactors to accelerate cartilage generation *in vitro*. A complex system including accurate control of media, shear force, mixing, and hydrodynamic pressure, is required to culture the chondrocytes.[158] Malaviya *et al.*[164] used a parallel-plate flow chamber system to employ fluid-induced shear stress as a modulator of chondrocyte activity for cartilage tissue engineering. Perfusion systems, spinner flasks and rotating wall vessels have also

been used successfully.[165] Also, in perfusion culture, biodegradable scaffolds encapsulated by agarose enhanced the accumulation and retention of extracellular matrix proteins from chondrocytes.[166]

8.7 Matrix Metalloproteinase Response

The degradation rate of biodegradable scaffolds depends greatly on the hydrolysis rates of the materials. In bioresponsive hydrogels, the degradation rate can be moderated over time through the rate of enzyme secretion by the cells. As a modification, by changing the peptide sequence utilized as a crosslinker, a hydrogel is able to be degraded by any type of protease in the body.[167] Park *et al.*[167] developed a matrix metalloproteinase-sensitive polyethylene-glycol-based hydrogel as a cartilage scaffold. The properties of this hydrogel can be applied in liquid form directly to the affected site, where it polymerizes *in situ*.[167] The distinguishing feature of this research was using the matrix metalloproteinase-sensitive peptide as a gelation crosslinker.[168] This polymer scaffold can be remodelled using the cells' own mechanisms. Matrix metalloproteinase-sensitive peptides as crosslinkers lead to a material that is degraded by gelatinase and collagenase. The chondrocytes were cultured in both matrix metalloproteinase-sensitive and matrix metalloproteinase-insensitive hydrogels. Although most of the cells were viable after four weeks' culture time and formed cell clusters, gel matrices with sensitivity to matrix metalloproteinase-based matrix remodelling indicated superior clusters, further diffuse and less cell surface-constrained cell-derived matrix in the chondron.[167] The cells in the matrix metalloproteinase-insensitive gels express more collagenase. The cells have the capability to sense the greater matrix concentration and reduce their ECM gene expression. It is also possible that the cells have changed mechanisms by which matrix metalloproteinase expression is activated when a certain density of matrix or level of physical confinement is achieved.[167]

8.8 Shape-Memory Systems

Shape-memory polymers as a subclass of smart materials are developing from the academic labs into the clinical field, providing new functionality to often static implants. These kinds of polymers are able to recover large strains or apply stresses in response to a stimulus.[169] According to their name, they can recover their initial shape and rigidity after exposure to a particular stimulus including heat and light (Figure 8.5).[170] Shape-memory polymers can undergo a shape transformation after introduction of a particular external stimulus, which allows their application in minimally-invasive surgery with a small initial material transforming to a more voluminous structure in the body. Studies have shown that the differentiation capacity of MSCs is supported by the polymer and shape-memory effect and that activation does not influence cell adhesion.

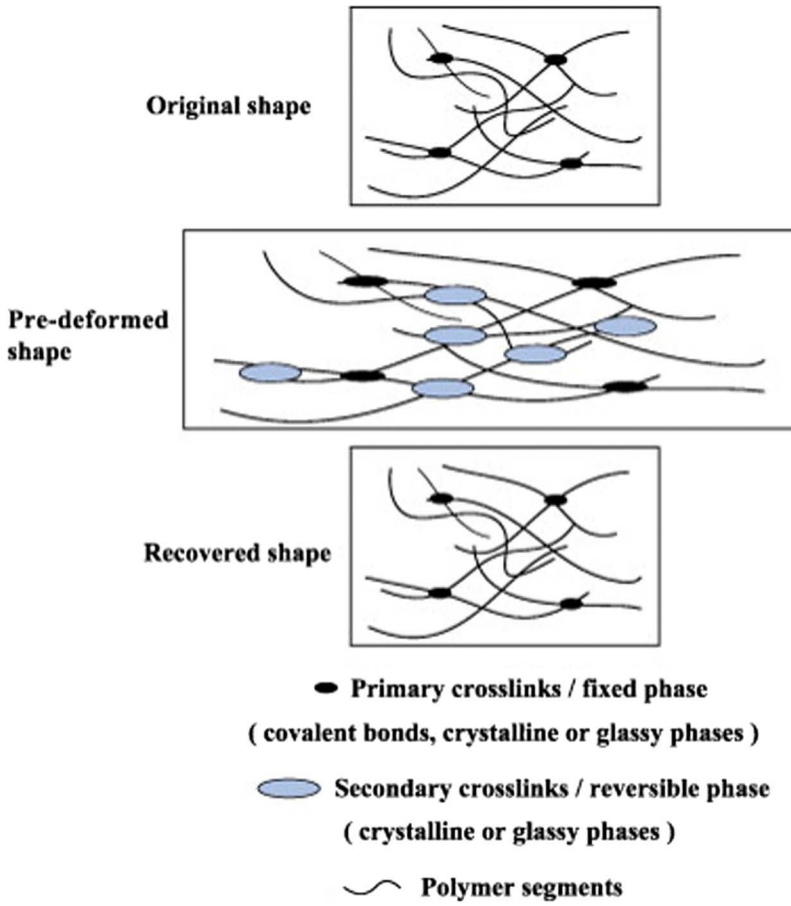

Figure 8.5 Schematic of polymer networks during shape recovery. Reprinted from *Progress in Materials Science*, **56**(7), Leng, J., Lan, X., Liu, Y., Du, S. Shape-memory polymers and their composites: Stimulus methods and applications, 1077–1135, Copyright (2011) with permission from Elsevier.

Degradable and nondegradable shape-memory polymers can be developed from various biopolymers, including cellulose, chitosan, poly(ε-caprolactone), polyetherurethanes, poly(ethylene terephthalate) and poly(ethylene oxide).[171] Shape-memory polymers can also be attained through a wide range of polymer chemistries, including poly(meth)acrylates, polyurethanes, poly(α-hydroxy) esters and their copolymers, and epoxies.[169] Although these polymers can be activated using a number of stimuli, the most usual ways for activation inside the body are force, temperature, and water. The recovery behaviour can be tuned for particular usages by tailoring the chemical structure of the shape-memory polymers.[172] For example, a shape-memory polymer for cardiovascular stents that deploy using thermal activation needs

an activation temperature around body temperature when implanted in the body. It's worth noting that the shape-memory polymers with activation temperatures above 37 °C may still be activated *in vivo*, however with a controlled laser light or resistive heating.[173]

While considering the shape memory process is important in the use of shape-memory polymer-based implants, their mechanical behaviour must also be considered for load-bearing applications, as this can dictate the *in vivo* performance. Particularly, the influence of temperature, moisture, immersion time, and degradation on the mechanical properties has important roles in the device performance. It has been shown that the modulus of several shape-memory polymers can be tailored to meet the physiological necessities,[172] however, the toughness is usually reduced when placed in the physiological solutions because of the water penetration into these networks.[174] In addition, shape-memory polymers lose a notable amount of toughness when they are above their activation temperature. These are issues that must be considered for these kinds of polymers to find their full potential as clinical biomaterials.[169]

AC has both low moduli and toughness. However, its physiological performances are partly mechanical, demanding it to be subjected to continuous loading cycles, in some cases, over large stress and strain ranges. The wide range of modulus and toughness values showed by physiological tissues demonstrates the necessity for diverse classes of biomaterials that can display the essential mechanical behaviours for a wide range of biomedical applications. Owing to the increasing interest in tissue engineering applications, shape-memory polymers are being developed with degradable chemistries, allowing them to be utilized as porous scaffolds to encourage the regeneration of tissue. Besides being able to undergo an initial shape change, these polymers are synthesized to degrade, while usually releasing some therapeutic agent; at the same rate, the tissue will regenerate itself such that the new tissue finally replaces the implant. Initial biodegradable shape-memory polymers were based on poly(lactide), poly(caprolactone) and poly(glycolide) whereas these networks are composed of semicrystalline polymers that have been methacrylated to allow for free-radical polymerization into the crosslinked networks.[169]

The mechanical properties, including tensile strength and failure strain, are tailored by enhancing the molecular weight of the semicrystalline degradable crosslinkers leading to a reduction in the biodegradability of the polymer. These shape-memory polymers present strain recovery ratios of more than 90% at initial time points.[175] Moreover, the activation temperature can be tailored by changing the molecular weight of the crosslinkers.[176] For example, block-copolymers based on poly(lactide) have been formed into networks that degraded by around five months and had appropriate mechanical behaviour at first degradation times. Through enhancing the poly (lactide) blocks, the strain recovery ratio was improved to 99%.[177] Poly(L-lactic acid) (PLLA) has quite low toughness but also presents advanced functionality by its capability to be degraded by the body. However, despite its low

toughness, biodegradability is possibly enough to justify its clinical applications. Researchers continue to toughen PLLA-based biomaterials.[178]

8.9 Future Prospects

Smart materials use a combination of bioactive molecules, response cells, and a support system to cause regeneration of cells. They provide a physical structure and architectural support for multiple molecules and a vast number of cells and allow for a large variety of shapes and sizes. Smart materials are capable of assisting cell proliferation, which helps in regeneration more than other materials. Thus, they are capable of decreasing the amount of time needed for tissue regeneration.[31] They are ideal for the synthesis of cartilage and other tissues that have a slow regenerative rate.

The use of smart materials is rapidly developing to meet the demand of tissue damage, cartilage damage, and bone loss. In the future, these materials may become the standard treatment in medicine. They will be used to treat osteoarthritis, rheumatoid arthritis, and many other autoimmune diseases. The lost or damaged cartilage that occurs from such diseases may be replaced with new synthetic cartilage that was produced using smart materials and tissue engineering. Smart materials may also be used to assist in the treatment of bone fractures. Using the architectural design of the pericardium to repair bone, the materials will help provide the foundation needed for the bones to properly suture. A 3D mold of smart materials is designed specifically for skeletal tissue as it allows for increased vascularization and adhesion, which are optimal factors for cellular growth.[179]

Traumatic and surgical wounds may be filled with smart materials as a form of treatment. The materials will assist in the healing and tissue regeneration processes of the body on a cellular level, leading to a quicker and more complete fibrous healing. Tissue regeneration primarily occurs in the extracellular matrix. Smart materials are capable of creating large gaps and spaces to assist in the health of the extracellular matrix and thus lead to effective tissue repair.[62] Also, the immune system has an important role in the repairing of tissues. It is likely that in future trials, we will see scaffolds that can manipulate the immune system into fighting diseases and heal tissue.[180] We have found that live tissue that is cultured from the skin can be used as a form of therapy for chronic wounds and conditions. Smart materials may be used to regenerate a wide variety of tissues including the tissue of the epidermis in addition to cartilage. It was discovered that smart materials can offer consistent wound closure upon the completion of surgical procedures.[181]

Cartilage engineering can be accomplished through the use of 3D-biomaterial printing technology. The degeneration of cartilage results in joint pain and arthritis, and can lead to the fusion of joints in advanced stages. Current surgical methods are not completely successful in restoring joints to their natural and healthy state. Through cartilage engineering, joints may be repaired to their natural state.[182] With this technology, researchers are able

to initiate cartilage tissue repair of hyaline, fibro, and elastic cartilages in the human body. They have developed scaffolds that are filled with chondrocytes and allow for the production of nasal cartilage. This discovery may be used as a means of therapy for patients who have experienced trauma or injury to their nasal tissue. The proper use of chondrocytes is a promising prospect for reconstructing nasal cartilage.[183]

Articular cartilage has been extensively studied and is primarily found in the human body. This cartilage has a very slow regeneration rate. It was found that through the use of type II collagen and chondroitin sulfate, cartilage that is similar to articular cartilage can be created. This newly generated cartilage will help to replace and maintain a healthy environment within the human body.[184] Articular cartilage was proven to undergo more of a timely regenerative process than elastic cartilage, however, the researchers were able to produce articular cartilage with the same consistency and cell to collagen ratio as healthy articular cartilage. This may be used to treat the joints of those who have osteoarthritis and other joint malfunctions or autoimmune diseases.

Traditional treatments that are currently used to treat osteoarthritis include autografts and allografts. These grafting materials are not as effective as the original cartilage tissue that is found in the joints. The grafted tissue material is not capable of withstanding heavy weight bearing loads as well as being flexible. Tissue engineering can replace this treatment by instilling growth and regeneration of the cartilage tissues in affected areas which will prevent further surgeries to replace worn out grafting materials.[185]

Elastic or auricular cartilage of the ear is a future prospect of cartilage engineering. Similar to hyaline cartilage, elastic cartilage has been proven to be highly regenerative when placed in particular scaffolds and bio-gels. The elastic cartilage produced was of a similar quality and dimension as the cartilage found in the human ear. The researchers discovered a high prevalence of elastin, collagen, and chondrocytes in the newly developed cartilage.[186] This discovery may lead to grafts and transplants of elastic cartilage to be placed on the outer ear as well as in the epiglottis. It may also be bioengineered to produce less elastin to give it more hyaline-cartilage-like properties.

In addition, temporomandibular joint disorders are highly common throughout the world. Many of the issues arise due to defects in the fibrocartilage portion that is present in the joint. Recent research has demonstrated that we have the ability to produce fibrocartilage similar in molecular composition to that found in the human body. With this ability, a physician may be able to replace damaged TMJ cartilage with a newly synthesized and fully functional one as a mode of treatment.[187] Fibrocartilage treatment may also be applicable to other areas of the body such as the intervertebral discs to help treat patients with spinal injuries. Intervertebral discs have been engineered by using mesenchymal stem cells. These cells allow for the differentiation of the tissue to take the appropriate shape and cellular composition of intervertebral cartilage.[188] This may become a modality of treatment for chronic and traumatic spinal injuries.

In addition, cartilage engineering may be used to cure patients who have generalized arthritis and/or tears in the meniscus. The meniscus is infamous for its lack of regeneration and thus cartilage engineering may be used as a new treatment for repair. Autologous meniscus cells are used to regenerate meniscus tissue; by using these cells with the assistance of smart material scaffolds, it may be possible to fully reproduce meniscus tissue and use it to replace damaged or inflamed tissue in the body. In some cases, it may be used to further stimulate the regeneration of meniscus tissue inside the body where tears have occurred.[189]

The future of patient treatment is to be found in the use of smart materials and cartilage engineering. Through the use of smart materials, all grafts, transplants, and tissue regeneration will become facilitated. We have only recently discovered smart materials, we have yet to touch the surface of the possibilities that they bring as a form of treatment among the practices of medicine and dentistry. Cartilage engineering is an exciting and innovative category of treatment. It can be used to treat many forms of trauma, arthritis, and growth related issues that occur among people. These are safer options for the patient as they do not involve the use of toxic and metallic substances that are not normally found in the human body. Using smart materials, the recovery time for treatment is presumed to be much quicker as the body will easily adapt to the material and less inflammation will occur. Through the use of cartilage engineering, full health and functionality may be restored.

8.10 Concluding Remarks

The regeneration and healing of cartilage tissue is a clinically challenging problem, due primarily to the poor vascularity of the cartilage. Fortunately, with technological advances in tissue engineering and bioprinting, innovative, naturally occurring and synthetic biomaterials can be used to regenerate and heal damaged cartilage. Of particular interest is the use of innovative, biocompatible smart biomaterials that are responsive to thermal, chemical, or mechanical stimuli. These smart biomaterials continue to be developed and are promising alternatives to existing technology. The biomaterials may prove effective for the treatment of several debilitating conditions including the treatment of patients with osteoarthritis, rheumatoid arthritis, and patients requiring cartilage replacement (*e.g.* nose, ear) due to neoplasms, burns or injuries.

References

1. X. Xu, Z. Cui and J. P. Urban, Measurement of the chondrocyte membrane permeability to Me2SO, glycerol and 1,2-propanediol, *Med. Eng. Phys.*, 2003, **25**(7), 573–579.
2. M. C. Corti and C. Rigon, Epidemiology of osteoarthritis: prevalence, risk factors and functional impact, *Aging: Clin. Exp. Res.*, 2003, **15**(5), 359–363.

3. K. L. Dominick and T. A. Baker, Racial and ethnic differences in osteoarthritis: prevalence, outcomes, and medical care, *Ethnic. Dis.*, 2003, **14**(4), 558–566.
4. A. Gross, *et al.*, Reconstruction of Skeletal Deficits at the Knee A Comprehensive Osteochondral Transplant Program, *Clin. Orthop. Relat. Res.*, 1983, **174**, 96–106.
5. N. M. Jomha, *et al.*, Vitrification of intact human articular cartilage, *Biomaterials*, 2012, **33**(26), 6061–6068.
6. M. Fahmy, *et al.*, Dose–injury relationships for cryoprotective agent injury to human chondrocytes, *Cryobiology*, 2014, **68**(1), 50–56.
7. M. Lutolf and J. Hubbell, Synthetic biomaterials as instructive extracellular microenvironments for morphogenesis in tissue engineering, *Nat. Biotech.*, 2005, **23**(1), 47–55.
8. M. Mozafari, *et al.*, *Electroconductive Nanocomposite Scaffolds: A New Strategy into Tissue Engineering and Regenerative Medicine*, INTECH Open Access Publisher, 2012.
9. M. Razavi, *et al.*, Biodegradation, bioactivity and in vivo biocompatibility analysis of plasma electrolytic oxidized (PEO) biodegradable Mg implants, *Phys. Sci. Int. J.*, 2014, **4**(5), 708.
10. M. Yazdimamaghani, *et al.*, Surface modification of biodegradable porous Mg bone scaffold using polycaprolactone/bioactive glass composite, *Mater. Sci. Eng. C*, 2015, **49**, 436–444.
11. M. Yazdimamaghani, *et al.*, Green synthesis of a new gelatin-based antimicrobial scaffold for tissue engineering, *Mater. Sci. Eng. C*, 2014, **39**, 235–244.
12. A. Tahmasbi Rad, *et al.*, Conducting scaffolds for liver tissue engineering, *J. Biomed. Mater. Res., Part A*, 2014, **102**(11), 4169–4181.
13. V. Shabafrooz, *et al.*, The effect of hyaluronic acid on biofunctionality of gelatin–collagen intestine tissue engineering scaffolds, *J. Biomed. Mater. Res., Part A*, 2014, **102**(9), 3130–3139.
14. M. Yazdimamaghani, *et al.*, Microstructural and mechanical study of PCL coated Mg scaffolds, *Surf. Eng.*, 2014, **30**(12), 920–926.
15. M. Yazdimamaghani, *et al.*, Significant degradability enhancement in multilayer coating of polycaprolactone-bioactive glass/gelatin-bioactive glass on magnesium scaffold for tissue engineering applications, *Appl. Surf. Sci.*, 2015, **338**, 137–145.
16. A. Ghafari-Nazari, *et al.*, Antibacterial activity of silver photodeposited nepheline thin film coatings, *Ceram. Int.*, 2012, **38**(7), 5445–5451.
17. M. Razavi, *et al.*, In vivo study of nanostructured diopside (CaMgSi2O6) coating on magnesium alloy as biodegradable orthopedic implants, *Appl. Surf. Sci.*, 2014, **313**, 60–66.
18. M. Razavi, *et al.*, Micro-arc oxidation and electrophoretic deposition of nano-grain merwinite (Ca3MgSi2O8) surface coating on magnesium alloy as biodegradable metallic implant, *Surf. Interface Anal.*, 2014, **46**(6), 387–392.

19. S. M. Rabiee, *et al.*, Effect of ion substitution on properties of bioactive glasses: A review, *Ceram. Int.*, 2015, **41**(6), 7241–7251.
20. M. Razavi, *et al.*, Biodegradable magnesium alloy coated by fluoridated hydroxyapatite using MAO/EPD technique, *Surf. Eng.*, 2014, **30**(8), 545–551.
21. M. Razavi, *et al.*, Improvement of biodegradability, bioactivity, mechanical integrity and cytocompatibility behavior of biodegradable mg based orthopedic implants using nanostructured bredigite (Ca7MgSi4O16) bioceramic coated via ASD/EPD technique, *Ann. Biomed. Eng.*, 2014, **42**(12), 2537–2550.
22. F. Heidari, *et al.*, In situ preparation of iron oxide nanoparticles in natural hydroxyapatite/chitosan matrix for bone tissue engineering application, *Ceram. Int.*, 2015, **41**(2), 3094–3100.
23. M. Razavi, *et al.*, Regenerative influence of nanostructured bredigite (Ca7MgSi4O16)/anodic spark coating on biodegradable AZ91 magnesium alloy implants for bone healing, *Mater. Lett.*, 2015, **155**, 97–101.
24. M. Razavi, *et al.*, Green Chemical and Biological Synthesis of Nanoparticles and Their Biomedical Applications, *Green Processes for Nanotechnology*, Springer, 2015, pp. 207–235.
25. G. Balasundaram and T. J. Webster, An Overview of Nano-Polymers for Orthopedic Applications, *Macromol. Biosci.*, 2007, **7**(5), 635–642.
26. E. Salahinejad, *et al.*, Multilayer zirconium titanate thin films prepared by a sol–gel deposition method, *Ceram. Int.*, 2013, **39**(2), 1271–1276.
27. P. Rouhani, *et al.*, Nanostructured zirconium titanate fibers prepared by particulate sol–gel and cellulose templating techniques, *J. Alloys Compd.*, 2013, **568**, 102–105.
28. E. Salahinejad, *et al.*, Zirconium titanate thin film prepared by an aqueous particulate sol–gel spin coating process using carboxymethyl cellulose as dispersant, *Mater. Lett.*, 2012, **88**, 5–8.
29. E. Salahinejad, *et al.*, Aqueous sol–gel synthesis of zirconium titanate (ZrTiO4) nanoparticles using chloride precursors, *Ceram. Int.*, 2012, **38**(8), 6145–6149.
30. M. Razavi, *et al.*, In vivo assessments of bioabsorbable AZ91 magnesium implants coated with nanostructured fluoridated hydroxyapatite by MAO/EPD technique for biomedical applications, *Mater. Sci. Eng. C*, 2015, **48**, 21–27.
31. M. E. Furth, A. Atala and M. E. Van Dyke, Smart biomaterials design for tissue engineering and regenerative medicine, *Biomaterials*, 2007, **28**(34), 5068–5073.
32. M. Razavi, *et al.*, In vitro study of nanostructured diopside coating on Mg alloy orthopedic implants, *Mater. Sci. Eng. C*, 2014, **41**, 168–177.
33. M. Razavi, *et al.*, Surface modification of magnesium alloy implants by nanostructured bredigite coating, *Mater. Lett.*, 2013, **113**, 174–178.
34. M. Yazdimamaghani, *et al.*, Development and degradation behavior of magnesium scaffolds coated with polycaprolactone for bone tissue engineering, *Mater. Lett.*, 2014, **132**, 106–110.

35. M. Ebara, *et al.*, Introductory Guide to Smart Biomaterials, *Smart Biomaterials*, Springer, 2014, pp. 1–7.
36. C. Sharma, *et al.*, Cartilage tissue engineering: current scenario and challenges, *Adv. Mater. Lett.*, 2011, **2**, 90–99.
37. N. R. Patel and P. P. Gohil, A review on biomaterials: scope, applications & human anatomy significance, *Int. J. Emerg. Techno. Advan. Eng.*, 2012, **2**(4), 91–101.
38. F. J. O'Brien, Biomaterials & scaffolds for tissue engineering, *Mater. Today*, 2011, **14**(3), 88–95.
39. L. Cen, *et al.*, Collagen tissue engineering: development of novel biomaterials and applications, *Pediatr. Res.*, 2008, **63**(5), 492–496.
40. W. Zhang, *Development and Characterization of Micro/Nano Scale Biomaterials for Biomedical Applications*, 2011.
41. I. L. Kim, R. L. Mauck and J. A. Burdick, Hydrogel design for cartilage tissue engineering: A case study with hyaluronic acid, *Biomaterials*, 2011, **32**(34), 8771–8782.
42. R. Stoop, Smart biomaterials for tissue engineering of cartilage, *Injury*, 2008, **39**(1), 77–87.
43. R. Balint, N. J. Cassidy and S. H. Cartmell, Conductive polymers: towards a smart biomaterial for tissue engineering, *Acta Biomater.*, 2014, **10**(6), 2341–2353.
44. J. M. Anderson and M. S. Shive, Biodegradation and biocompatibility of PLA and PLGA microspheres, *Adv. Drug Delivery Rev.*, 2012, **64**, 72–82.
45. H. Assender, V. Bliznyuk and K. Porfyrakis, How surface topography relates to materials' properties, *Science*, 2002, **297**(5583), 973–976.
46. M. M. Stevens and J. H. George, Exploring and engineering the cell surface interface, *Science*, 2005, **310**(5751), 1135–1138.
47. S.-W. Chang and M. J. Buehler, Molecular biomechanics of collagen molecules, *Mater. Today*, 2014, **17**(2), 70–76.
48. W. Chrzanowski and A. Khademhosseini, Biologically inspired 'smart'materials, *Adv. Drug Delivery Rev.*, 2013, **4**(65), 403–404.
49. J. Glowacki and S. Mizuno, Collagen scaffolds for tissue engineering, *Biopolymers*, 2008, **89**(5), 338–344.
50. R. Parenteau-Bareil, R. Gauvin and F. Berthod, Collagen-based biomaterials for tissue engineering applications, *Materials*, 2010, **3**(3), 1863–1887.
51. G. D. Prestwich, Hyaluronic acid-based clinical biomaterials derived for cell and molecule delivery in regenerative medicine, *J. Controlled Release*, 2011, **155**(2), 193–199.
52. T. E. Hardingham and H. Muir, The specific interaction of hyaluronic acid with cartilage proteoglycans, *Biochim. Biophys. Acta, Gen. Subj.*, 1972, **279**(2), 401–405.
53. D. C. West, *et al.*, Angiogenesis induced by degradation products of hyaluronic acid, *Science*, 1985, **228**(4705), 1324–1326.
54. P. J. Roughley and R. White, Age-related changes in the structure of the proteoglycan subunits from human articular cartilage, *J. Biol. Chem.*, 1980, **255**(1), 217–224.

55. C. D. Ren, *Injectable Hyaluronic Acid Scaffolds for Cartilage Tissue Engineering*, Massachusetts Institute of Technology, 2008.
56. D. J. Griffon, *et al.*, Chitosan scaffolds: interconnective pore size and cartilage engineering, *Acta Biomater.*, 2006, **2**(3), 313–320.
57. M. Aguilar, *et al.*, Smart polymers and their applications as biomaterials, *Topics in Tissue Engineering*, 2007, vol. 3, ch. 6.
58. H. Park, *et al.*, Injectable chitosan hyaluronic acid hydrogels for cartilage tissue engineering, *Acta Biomater.*, 2013, **9**(1), 4779–4786.
59. P. A. Levett, *et al.*, A biomimetic extracellular matrix for cartilage tissue engineering centered on photocurable gelatin, hyaluronic acid and chondroitin sulfate, *Acta Biomater.*, 2014, **10**(1), 214–223.
60. E. Engvall and E. Ruoslahti, Binding of soluble form of fibroblast surface protein, fibronectin, to collagen, *Int. J. Cancer*, 1977, **20**(1), 1–5.
61. A. J. Mieszawska and D. L. Kaplan, Smart biomaterials-regulating cell behavior through signaling molecules, *BMC Biol.*, 2010, **8**(1), 59.
62. F. Rosso, *et al.*, Smart materials as scaffolds for tissue engineering, *J. Cell. Physiol.*, 2005, **203**(3), 465–470.
63. K. Y. Lee and D. J. Mooney, Alginate: properties and biomedical applications, *Prog. Polym. Sci.*, 2012, **37**(1), 106–126.
64. A. D. Augst, H. J. Kong and D. J. Mooney, Alginate hydrogels as biomaterials, *Macromol. Biosci.*, 2006, **6**(8), 623–633.
65. R. A. Perez, *et al.*, Naturally and synthetic smart composite biomaterials for tissue regeneration, *Adv. Drug Delivery Rev.*, 2013, **65**(4), 471–496.
66. S.-H. Chen, *et al.*, Synthesis and characterization of thermal-responsive chitin-based polyurethane copolymer as a smart material, *Carbohydr. Polym.*, 2012, **88**(4), 1483–1487.
67. P. D. Costantino and C. D. Friedman, Synthetic bone graft substitutes, *Otolaryngol. Clin. North Am.*, 1994, **27**(5), 1037–1074.
68. S. Grad, *et al.*, The use of biodegradable polyurethane scaffolds for cartilage tissue engineering: potential and limitations, *Biomaterials*, 2003, **24**(28), 5163–5171.
69. J. Brun, *et al.*, Physical and biological characteristics of the main biomaterials used in pelvic surgery, *Bio-Med. Mater. Eng.*, 1991, **2**(4), 203–225.
70. R. Ghazanfar, *et al.*, Adhesion of human chondrocytes on medical-grade PTFE following surface-modification by plasma treatment in an oxygen atmosphere, http://www3.imperial.ac.uk/pls/portallive/docs/1/4535900.PDF.
71. P. J. Rubin and M. J. Yaremchuk, Complications and toxicities of implantable biomaterials used in facial reconstructive and aesthetic surgery: a comprehensive review of the literature, *Plast. Reconstr. Surg.*, 1997, **100**(5), 1336–1353.
72. W.-C. Hsieh, Y. Wada and C.-P. Chang, Fermentation, biodegradation and tensile strength of poly (3-hydroxybutyrate-co-4-hydroxybutyrate) synthesized by Delftia acidovorans, *J. Taiwan Inst. Chem. Eng.*, 2009, **40**(2), 143–147.
73. D. Schmaljohann, Thermo- and pH-responsive polymers in drug delivery, *Adv. Drug Delivery Rev.*, 2006, **58**(15), 1655–1670.

74. M. Yazdimamaghani, *et al.*, Synthesis and characterization of encapsulated nanosilica particles with an acrylic copolymer by in situ emulsion polymerization using thermoresponsive nonionic surfactant, *Materials*, 2013, **6**(9), 3727–3741.
75. F. D. Jochum and P. Theato, Temperature- and light-responsive smart polymer materials, *Chem. Soc. Rev.*, 2013, **42**(17), 7468–7483.
76. P. Bawa, *et al.*, Stimuli-responsive polymers and their applications in drug delivery, *Biomed. Mater.*, 2009, **4**(2), 022001.
77. J. Hu, *et al.*, A review of stimuli-responsive polymers for smart textile applications, *Smart Mater. Struct.*, 2012, **21**(5), 053001.
78. A. Kumar, *et al.*, Smart polymers: Physical forms and bioengineering applications, *Prog. Polym. Sci.*, 2007, **32**(10), 1205–1237.
79. H. Sa-Lima, *et al.*, Thermoresponsive poly(N-isopropylacrylamide)-g-methylcellulose hydrogel as a three-dimensional extracellular matrix for cartilage-engineered applications, *J. Biomed. Mater. Res., Part A*, 2011, **98**(4), 596–603.
80. L. Klouda and A. G. Mikos, Thermoresponsive hydrogels in biomedical applications, *Eur. J. Pharm. Biopharm.*, 2008, **68**(1), 34–45.
81. C. Custodio, *et al.*, Smart instructive polymer substrates for tissue engineering, *Smart Polymers and Their Applications*, Woodhead Publishing Limited, 2014, pp. 301–326.
82. R. M. da Silva, J. F. Mano and R. L. Reis, Smart thermoresponsive coatings and surfaces for tissue engineering: switching cell-material boundaries, *Trends Biotechnol.*, 2007, **25**(12), 577–583.
83. J. S. Scarpa, D. D. Mueller and I. M. Klotz, Slow Hydrogen-Deuterium Exchange in a Non-Alpha-Helical Polyamide, *J. Am. Chem. Soc.*, 1967, **89**(24), 6024–6030.
84. S. Ibusuki, *et al.*, Tissue-engineered cartilage using an injectable and in situ gelable thermoresponsive gelatin: fabrication and in vitro performance, *Tissue Eng.*, 2003, **9**(2), 371–384.
85. K. M. Park, *et al.*, Thermosensitive chitosan–Pluronic hydrogel as an injectable cell delivery carrier for cartilage regeneration, *Acta Biomater.*, 2009, **5**(6), 1956–1965.
86. R. A. Muzzarelli, *et al.*, Chitosan, hyaluronan and chondroitin sulfate in tissue engineering for cartilage regeneration: A review, *Carbohydr. Polym.*, 2012, **89**(3), 723–739.
87. I. Roy and M. N. Gupta, Smart polymeric materials: emerging biochemical applications, *Chem. Biol.*, 2003, **10**(12), 1161–1171.
88. S. K. Samal, *et al.*, Smart polymer hydrogels: properties, synthesis and applications, *Smart Polymers and Their Applications*, 2014, p. 237.
89. L. E. Bromberg and E. S. Ron, Temperature-responsive gels and thermogelling polymer matrices for protein and peptide delivery, *Adv. Drug Delivery Rev.*, 1998, **31**(3), 197–221.
90. L. Yu and J. Ding, Injectable hydrogels as unique biomedical materials, *Chem. Soc. Rev.*, 2008, **37**(8), 1473–1481.
91. R. Fairman and K. S. Åkerfeldt, Peptides as novel smart materials, *Curr. Opin. Struct. Biol.*, 2005, **15**(4), 453–463.

92. J. Amalvy, *et al.*, Synthesis and characterization of novel pH-responsive microgels based on tertiary amine methacrylates, *Langmuir*, 2004, **20**(21), 8992–8999.
93. F.-J. Xu, E.-T. Kang and K.-G. Neoh, pH-and temperature-responsive hydrogels from crosslinked triblock copolymers prepared via consecutive atom transfer radical polymerizations, *Biomaterials*, 2006, **27**(14), 2787–2797.
94. P. Gupta, K. Vermani and S. Garg, Hydrogels: from controlled release to pH-responsive drug delivery, *Drug Discovery Today*, 2002, **7**(10), 569–579.
95. J. Wu, Z.-G. Su and G.-H. Ma, A thermo-and pH-sensitive hydrogel composed of quaternized chitosan/glycerophosphate, *Int. J. Pharm.*, 2006, **315**(1), 1–11.
96. S. K. De, *et al.*, Equilibrium swelling and kinetics of pH-responsive hydrogels: Models, experiments, and simulations, *J. Microelectromech. Syst.*, 2002, **11**(5), 544–555.
97. F. Rosso, *et al.*, Smart materials as scaffolds for tissue engineering, *J. Cell. Physiol.*, 2005, **203**(3), 465–470.
98. M. F. Abou Taleb, Radiation synthesis of multifunctional polymeric hydrogels for oral delivery of insulin, *Int. J. Biol. Macromol.*, 2013, **62**, 341–347.
99. H. H. Sokker, *et al.*, Synthesis and characterization of hydrogels based on grafted chitosan for the controlled drug release, *Carbohydr. Polym.*, 2009, **75**(2), 222–229.
100. L. Chen, Z. Tian and Y. Du, Synthesis and pH sensitivity of carboxymethyl chitosan-based polyampholyte hydrogels for protein carrier matrices, *Biomaterials*, 2004, **25**(17), 3725–3732.
101. J. Heller, *et al.*, Controlled drug release from bioerodible hydrophobic ointments, *Biomaterials*, 1990, **11**(4), 235–237.
102. P. Gupta, K. Vermani and S. Garg, Hydrogels: from controlled release to pH-responsive drug delivery, *Drug Discovery Today*, 2002, **7**(10), 569–579.
103. R. A. Siegel and B. A. Firestone, pH-Dependent Equilibrium Swelling Properties of Hydrophobic Poly-Electrolyte Copolymer Gels, *Macromolecules*, 1988, **21**(11), 3254–3259.
104. R. A. Siegel, *et al.*, Buffer effects on swelling kinetics in polybasic gels, *Pharm. Res.*, 1992, **9**(1), 76–81.
105. R. Bettini, P. Colombo and N. A. Peppas, Solubility effects on drug transport through pH-sensitive, swelling-controlled release systems: Transport of theophylline and metoclopramide monohydrochloride, *J. Controlled Release*, 1995, **37**(1), 105–111.
106. T. Re'em, *et al.*, Chondrogenesis of hMSC in affinity-bound TGF-beta scaffolds, *Biomaterials*, 2012, **33**(3), 751–761.
107. A. B. Tekinay, *et al.*, Peptide nanofibers for controlled growth factor release, *Ther. Delivery*, 2013, **4**(6), 651–654.

108. Y. Zhang, *et al.*, In vitro observations of self-assembled ECM-mimetic bioceramic nanoreservoir delivering rFN/CDH to modulate osteogenesis, *Biomaterials*, 2012, **33**(30), 7468–7477.
109. R. J. Wade and J. A. Burdick, Advances in nanofibrous scaffolds for biomedical applications: From electrospinning to self-assembly, *Nano Today*, 2014, **9**(6), 722–742.
110. N. Stephanopoulos, J. H. Ortony and S. I. Stupp, Self-assembly for the synthesis of functional biomaterials, *Acta Mater.*, 2013, **61**(3), 912–930.
111. A. Sivashanmugam, *et al.*, An overview of injectable polymeric hydrogels for tissue engineering, *Eur. Polym. J.*, 2015, **72**, 543–565.
112. M. C. Branco and J. P. Schneider, Self-assembling materials for therapeutic delivery, *Acta Biomater.*, 2009, **5**(3), 817–831.
113. G. M. Whitesides and M. Boncheva, Beyond molecules: Self-assembly of mesoscopic and macroscopic components, *Proc. Natl. Acad. Sci. U. S. A.*, 2002, **99**(8), 4769–4774.
114. R. S. Tu and M. Tirrell, Bottom-up design of biomimetic assemblies, *Adv. Drug Delivery Rev.*, 2004, **56**(11), 1537–1563.
115. R. V. Rughani and J. P. Schneider, Molecular design of beta-hairpin peptides for material construction, *MRS Bull.*, 2008, **33**(5), 530–535.
116. K. Kita-Tokarczyk, *et al.*, Block copolymer vesicles - using concepts from polymer chemistry to mimic biomembranes, *Polymer*, 2005, **46**(11), 3540–3563.
117. J. S. Roman, *et al.*, Keynote: Self-assembling bioactive polymer systems for tissue engineering. Modulation of angiogenesis, *J. Tissue Eng. Regener. Med.*, 2012, **6**, 202.
118. J. F. Piai, A. F. Rubira and E. C. Muniz, Self-assembly of a swollen chitosan/chondroitin sulfate hydrogel by outward diffusion of the chondroitin sulfate chains, *Acta Biomater.*, 2009, **5**(7), 2601–2609.
119. J. Kisiday, *et al.*, Self-assembling peptide hydrogel fosters chondrocyte extracellular matrix production and cell division: Implications for cartilage tissue repair, *Proc. Natl. Acad. Sci. U. S. A.*, 2002, **99**(15), 9996–10001.
120. P. W. Kopesky, *et al.*, Controlled Delivery of Transforming Growth Factor beta 1 by Self-Assembling Peptide Hydrogels Induces Chondrogenesis of Bone Marrow Stromal Cells and Modulates Smad2/3 Signaling, *Tissue Eng., Part A*, 2011, **17**(1–2), 83–92.
121. G. A. Silva, *et al.*, Selective differentiation of neural progenitor cells by high-epitope density nanofibers, *Science*, 2004, **303**(5662), 1352–1355.
122. J. E. Kim, S. H. Kim and Y. Jung, In situ chondrogenic differentiation of bone marrow stromal cells in bioactive self-assembled peptide gels, *J. Biosci. Bioeng.*, 2015, **120**(1), 91–98.
123. C. J. Bell, *et al.*, Self-assembling peptides as injectable lubricants for osteoarthritis, *J. Biomed. Mater. Res., Part A*, 2006, **78A**(2), 236–246.
124. B. Jeong, *et al.*, Thermogelling biodegradable copolymer aqueous solutions for injectable protein delivery and tissue engineering, *Biomacromolecules*, 2002, **3**(4), 865–868.

125. M. J. Webber, *et al.*, Supramolecular nanostructures that mimic VEGF as a strategy for ischemic tissue repair, *Proc. Natl. Acad. Sci. U. S. A.*, 2012, **109**(23), 9220.
126. H. G. Cui, M. J. Webber and S. I. Stupp, Self-Assembly of Peptide Amphiphiles: From Molecules to Nanostructures to Biomaterials, *Biopolymers*, 2010, **94**(1), 1–18.
127. J. D. Hartgerink, E. Beniash and S. I. Stupp, Self-assembly and mineralization of peptide-amphiphile nanofibers, *Science*, 2001, **294**(5547), 1684–1688.
128. R. N. Shah, *et al.*, Supramolecular design of self-assembling nanofibers for cartilage regeneration, *Proc. Natl. Acad. Sci.*, 2010, **107**, 3293–3298.
129. H. Lee and T. G. Park, Photo-crosslinkable, biomimetic, and thermosensitive pluronic grafted hyaluronic acid copolymers for injectable delivery of chondrocytes, *J. Biomed. Mater. Res., Part A*, 2009, **88A**(3), 797–806.
130. J. C. Hu and K. A. Athanasiou, A self-assembling process in articular cartilage tissue engineering, *Tissue Eng.*, 2006, **12**(4), 969–979.
131. H. Park, *et al.*, Injectable biodegradable hydrogel composites for rabbit marrow mesenchymal stem cell and growth factor delivery for cartilage tissue engineering, *Biomaterials*, 2007, **28**(21), 3217–3227.
132. C. Chung and J. A. Burdick, Engineering cartilage tissue, *Adv. Drug Delivery Rev.*, 2008, **60**(2), 243–262.
133. R. Stoop, Smart biomaterials for tissue engineering of cartilage, *Injury*, 2008, **39**, S77–S87.
134. T. Traitel, R. Goldbart and J. Kost, Smart polymers for responsive drug-delivery systems, *J. Biomater. Sci., Polym. Ed.*, 2008, **19**(6), 755–767.
135. M. Motoyama, *et al.*, In vitro cartilage formation using TGF-beta-immobilized magnetic beads and mesenchymal stem cell-magnetic bead complexes under magnetic field conditions, *J. Biomed. Mater. Res., Part A*, 2010, **92**(1), 196–204.
136. R. N. Rosier, *et al.*, Transforming Growth-Factor Beta - an Autocrine Regulator of Chondrocytes, *Connect. Tissue Res.*, 1989, **20**(1–4), 295–301.
137. D. Vivien, *et al.*, Differential-Effects of Transforming Growth-Factor-Beta and Epidermal Growth-Factor on the Cell-Cycle of Cultured Rabbit Articular Chondrocytes, *J. Cell. Physiol.*, 1990, **143**(3), 534–545.
138. S. E. Kim, *et al.*, Porous chitosan scaffold containing microspheres loaded with transforming growth factor-beta 1: Implications for cartilage tissue engineering, *J. Controlled Release*, 2003, **91**(3), 365–374.
139. S. M. Seyedin, D. M. Rosen and P. R. Segarini, Modulation of Chondroblast Phenotype by Transforming Growth Factor-Beta, *Pathol. Immunopathol. Res.*, 1988, **7**(1–2), 38–42.
140. M. Iwasaki, *et al.*, Transforming Growth-Factor-Beta-1 Stimulates Chondrogenesis and Inhibits Osteogenesis in High-Density Culture of Periosteum-Derived Cells, *Endocrinology*, 1993, **132**(4), 1603–1608.
141. M. Prabaharan and J. F. Mano, Stimuli-responsive hydrogels based on polysaccharides incorporated with thermo-responsive polymers as novel biomaterials, *Macromol. Biosci.*, 2006, **6**(12), 991–1008.

142. R. A. Perez, *et al.*, Naturally and synthetic smart composite biomaterials for tissue regeneration, *Adv. Drug Delivery Rev.*, 2013, **65**(4), 471–496.
143. K. Na, *et al.*, Synergistic effect of TGF beta-3 on chondrogenic differentiation of rabbit chondrocytes in thermo-reversible hydrogel constructs blended with hyaluronic acid by in vivo test, *J. Biotechnol.*, 2007, **128**(2), 412–422.
144. K. H. Park, D. H. Lee and K. Na, Transplantation of poly(N-isopropylacrylamide-co-vinylimidazole) hydrogel constructs composed of rabbit chondrocytes and growth factor-loaded nanoparticles for neocartilage formation, *Biotechnol. Lett.*, 2009, **31**(3), 337–346.
145. H. H. Jung, K. Park and D. K. Han, Preparation of TGF-beta 1-conjugated biodegradable pluronic F127 hydrogel and its application with adipose-derived stem cells, *J. Controlled Release*, 2010, **147**(1), 84–91.
146. S. Chen, *et al.*, Triblock copolymers: synthesis, characterization, and delivery of a model protein, *Int. J. Pharm.*, 2005, **288**(2), 207–218.
147. H. Naderi-Meshkin, *et al.*, Chitosan-based injectable hydrogel as a promising in situ forming scaffold for cartilage tissue engineering, *Cell Biol. Int.*, 2014, **38**(1), 72–84.
148. M. Matsusaki and M. Akashi, Novel functional biodegradable polymer IV: pH-Sensitive controlled release of fibroblast growth factor-2 from a poly(gamma-glutamic acid)-sulfonate matrix for tissue engineering, *Biomacromolecules*, 2005, **6**(6), 3351–3356.
149. I. Martin, *et al.*, Enhanced cartilage tissue engineering by sequential exposure of chrondrocytes to FGF-2 during 2D expansion and BMP-2 during 3D cultivation, *J. Cell. Biochem.*, 2001, **83**(1), 121–128.
150. S. Miot, *et al.*, Cartilage tissue engineering by expanded goat articular chondrocytes, *J. Orthop. Res.*, 2006, **24**(5), 1078–1085.
151. H. Schmal, *et al.*, Stimulation of chondrocytes in vitro by gene transfer with plasmids coding for epidermal growth factor (hEGF) and basic fibroblast growth factor (bFGF), *Cytotherapy*, 2005, **7**(3), 292–300.
152. M. M. Stevens, *et al.*, FGF-2 enhances TGF-beta 1-induced periosteal chondrogenesis, *J. Orthop. Res.*, 2004, **22**(5), 1114–1119.
153. J. Jančář, *et al.*, Mechanical response of porous scaffolds for cartilage engineering, *Physiol. Res.*, 2007, **56**(suppl. 1), S17–S25.
154. R. L. Mauck, *et al.*, Synergistic action of growth factors and dynamic loading for articular cartilage tissue engineering, *Tissue Eng.*, 2003, **9**(4), 597–611.
155. N. Luepongsak, *et al.*, Hip stress during lifting with bent and straight knees, *Scand. J. Rehabil. Med.*, 1997, **29**(1), 57–64.
156. V. Mow, *et al.*, Biphasic and quasilinear viscoelastic theories for hydrated soft tissues, *Biomechanics of Diarthrodial Joints*, Springer, 1990, pp. 215–260.
157. A. J. Grodzinsky, *et al.*, Cartilage tissue remodeling in response to mechanical forces, *Annu. Rev. Biomed. Eng.*, 2000, **2**(1), 691–713.
158. R. L. Mauck, *et al.*, Functional tissue engineering of articular cartilage through dynamic loading of chondrocyte-seeded agarose gels, *J. Biomech. Eng.*, 2000, **122**(3), 252–260.

159. R. Grumbles, *et al.*, Cartilage metalloproteases in disuse atrophy, *J. Rheumatol. Suppl.*, 1995, **43**, 146–148.
160. P. D. Benya and J. D. Shaffer, Dedifferentiated chondrocytes reexpress the differentiated collagen phenotype when cultured in agarose gels, *Cell*, 1982, **30**(1), 215–224.
161. M. D. Buschmann, *et al.*, Mechanical compression modulates matrix biosynthesis in chondrocyte/agarose culture, *J. Cell Sci.*, 1995, **108**(4), 1497–1508.
162. M. D. Buschmann, *et al.*, Chondrocytes in agarose culture synthesize a mechanically functional extracellular matrix, *J. Orthop. Res.*, 1992, **10**(6), 745–758.
163. L. E. Freed, *et al.*, Tissue engineering of cartilage in space, *Proc. Natl. Acad. Sci.*, 1997, **94**(25), 13885–13890.
164. P. Malaviya and R. M. Nerem, Fluid-induced shear stress stimulates chondrocyte proliferation partially mediated via TGF-β 1, *Tissue Eng.*, 2002, **8**(4), 581–590.
165. N. S. Dunkelman, *et al.*, Cartilage production by rabbit articular chondrocytes on polyglycolic acid scaffolds in a closed bioreactor system, *Biotechnol. Bioeng.*, 1995, **46**(4), 299–305.
166. M. Sittinger, *et al.*, Engineering of cartilage tissue using bioresorbable polymer carriers in perfusion culture, *Biomaterials*, 1994, **15**(6), 451–456.
167. Y. Park, *et al.*, Bovine primary chondrocyte culture in synthetic matrix metalloproteinase-sensitive poly (ethylene glycol)-based hydrogels as a scaffold for cartilage repair, *Tissue Eng.*, 2004, **10**(3–4), 515–522.
168. M. Lutolf, *et al.*, Synthetic matrix metalloproteinase-sensitive hydrogels for the conduction of tissue regeneration: engineering cell-invasion characteristics, *Proc. Natl. Acad. Sci.*, 2003, **100**(9), 5413–5418.
169. D. L. Safranski, K. E. Smith and K. Gall, Mechanical requirements of shape-memory polymers in biomedical devices, *Polym. Rev.*, 2013, **53**(1), 76–91.
170. J. Leng, *et al.*, Shape-memory polymers and their composites: stimulus methods and applications, *Prog. Mater. Sci.*, 2011, **56**(7), 1077–1135.
171. S. Neuss, *et al.*, The use of a shape-memory poly (ε-caprolactone) dimethacrylate network as a tissue engineering scaffold, *Biomaterials*, 2009, **30**(9), 1697–1705.
172. C. M. Yakacki, *et al.*, Strong, Tailored, Biocompatible Shape-Memory Polymer Networks, *Adv. Funct. Mater.*, 2008, **18**(16), 2428–2435.
173. D. J. Maitland, *et al.*, Photothermal properties of shape memory polymer micro-actuators for treating stroke, *Lasers Surg. Med.*, 2002, **30**(1), 1–11.
174. K. E. Smith, *et al.*, The effect of the glass transition temperature on the toughness of photopolymerizable (meth) acrylate networks under physiological conditions, *Polymer*, 2009, **50**(21), 5112–5123.
175. A. Lendlein, A. M. Schmidt and R. Langer, AB-polymer networks based on oligo (ε-caprolactone) segments showing shape-memory properties, *Proc. Natl. Acad. Sci.*, 2001, **98**(3), 842–847.

176. A. Lendlein, *et al.*, Shape-memory polymer networks from oligo (ϵ-caprolactone) dimethacrylates, *J. Polym. Sci., Part A: Polym. Chem.*, 2005, **43**(7), 1369–1381.
177. N. Y. Choi, S. Kelch and A. Lendlein, Synthesis, Shape-Memory Functionality and Hydrolytical Degradation Studies on Polymer Networks from Poly (rac-lactide)-b-poly (propylene oxide)-b-poly (rac-lactide) dimethacrylates, *Adv. Eng. Mater.*, 2006, **8**(5), 439–445.
178. F. Jing and M. A. Hillmyer, A bifunctional monomer derived from lactide for toughening polylactide, *J. Am. Chem. Soc.*, 2008, **130**(42), 13826–13827.
179. M. Sittinger, D. W. Hutmacher and M. V. Risbud, Current strategies for cell delivery in cartilage and bone regeneration, *Curr. Opin. Biotechnol.*, 2004, **15**(5), 411–418.
180. G. Chan and D. J. Mooney, New materials for tissue engineering: towards greater control over the biological response, *Trends Biotechnol.*, 2008, **26**(7), 382–392.
181. M. L. Sabolinski, *et al.*, Cultured skin as a 'smart material' for healing wounds: experience in venous ulcers, *Biomaterials*, 1996, **17**(3), 311–320.
182. J. S. Temenoff and A. G. Mikos, Review: tissue engineering for regeneration of articular cartilage, *Biomaterials*, 2000, **21**(5), 431–440.
183. W. e. Kafienah, *et al.*, Three-dimensional tissue engineering of hyaline cartilage: comparison of adult nasal and articular chondrocytes, *Tissue Eng.*, 2002, **8**(5), 817–826.
184. J. Pieper, *et al.*, Crosslinked type II collagen matrices: preparation, characterization, and potential for cartilage engineering, *Biomaterials*, 2002, **23**(15), 3183–3192.
185. L. Zhang, J. Hu and K. A. Athanasiou, The role of tissue engineering in articular cartilage repair and regeneration, *Crit. Rev. Biomed. Eng.*, 2009, **37**(1–2), 1–57.
186. A. Rodriguez, *et al.*, Characteristics of cartilage engineered from human pediatric auricular cartilage, *Plast. Reconstr. Surg.*, 1999, **103**(4), 1111–1119.
187. K. N. Kalpakci, E. J. Kim and K. A. Athanasiou, Assessment of growth factor treatment on fibrochondrocyte and chondrocyte co-cultures for TMJ fibrocartilage engineering, *Acta Biomater.*, 2011, **7**(4), 1710–1718.
188. F. Mwale, P. Roughley and J. Antoniou, Distinction between the extracellular matrix of the nucleus pulposus and hyaline cartilage: a requisite for tissue engineering of intervertebral disc, *Eur. Cells Mater.*, 2004, **8**(58), 63–64.
189. P. Buma, *et al.*, Tissue engineering of the meniscus, *Biomaterials*, 2004, **25**(9), 1523–1532.

CHAPTER 9

Smart Biomaterials for Cardiovascular Tissue Engineering

SHINKA MIYAMOTO[a], TOSHIHIRO SHOJI[a], HIDEKI MIYACHI[a] AND TOSHIHARU SHINOKA*[a,b]

[a]The Tissue Engineering Program and Center for Cardiovascular and Pulmonary Research, Nationwide Children's Hospital, Columbus, OH, USA; [b]Department of Cardiothoracic Surgery, The Heart Center, Nationwide Children's Hospital, Columbus, OH, USA
*E-mail: Toshiharu.Shinoka@nationwidechildrens.org

9.1 Introduction—Clinical Motivation

Diverse clinical motivations drive research into engineered cardiovascular tissues, but perhaps the greatest impetus is the need for coronary artery bypass grafts to treat ischemic heart disease, the leading cause of death worldwide. This disease, often affecting multiple vessels, results from an excessive buildup of plaques within the arterial wall that gradually narrow the lumen of the vessel, impairing flow to downstream myocardium. In addition, rupture of unstable plaques can cause sudden occlusion of coronary vessels (*i.e.*, heart attack) in otherwise asymptomatic individuals. When angioplasty and stenting are not advised treatments, the only available option is coronary artery bypass. To date, the most successful graft conduits for coronary artery bypass procedures have been autografts, sourced from the patient's own

Smart Materials No. 25
Smart Materials for Tissue Engineering: Applications
Edited by Qun Wang

Published by the Royal Society of Chemistry, www.rsc.org

internal mammary artery or saphenous vein. However, autografts typically have a limited lifespan due to gradual stenosis and susceptibility to atherosclerosis. Thus, patients sometimes require recurrent interventions to revise previous bypass surgeries. Additionally, these autologous vessels are finite resources that become quickly depleted and are sometimes not suitable for bypass grafts due to issues such as size-mismatch. Therefore, patients commonly reach a point at which there are no more suitable autologous vessels that can be harvested and surgeons are forced to rely on synthetic alternatives. Current, clinically approved materials for peripheral artery bypass grafts include plastics such as expanded polytetrafluoroethylene (ePTFE, Gore-Tex®) and polyethylene terephthalate (PET, Dacron®). These materials address some limitations of autografts but are associated with a multitude of issues such as thromboembolization, calcification, increased infection risk, lack of growth potential, and the lifelong need for anticoagulation/antithrombotic therapy.

The need for cardiovascular tissue engineering extends beyond coronary artery bypass procedures as similar scaffolds could be used as bypass grafts to treat peripheral artery disease (PAD) and aortic aneurysm, vessels/patches during reconstructive surgery, and arteriovenous shunts for patients undergoing dialysis. Separate from vascular grafts and patches is the need for heart valve substitutes. Whether mechanical, or made with decellularized animal tissues, these valves have similar limitations and complications to synthetic vascular grafts. One must also consider children. Although certain prosthetics may be used successfully in the adult population, they might be inappropriate in fetal and pediatric populations that may outgrow or outlive a prosthetic. When this occurs, additional surgeries are necessary that increase the risk of complications and mortality. Tissue engineering holds the greatest promise of fulfilling these clinical needs and eliminating the complications associated with prosthetic devices. Furthermore, when used in a child, a tissue engineered vessel, patch, or valve will have the potential to integrate seamlessly and grow along with the child as native tissue would, reducing the potential for multiple surgeries.

9.2 Considerations for Vascular Neotissue Formation and TEVG Remodeling

A sound understanding of native tissue structure and function is crucial for rational tissue engineering design. The primary role of the cardiovascular system is to circulate blood throughout the body to support the metabolic needs of tissues and organs. This system is comprised of the heart, a muscular organ that rhythmically contracts to provide the driving force for blood flow, and a branching network of vessels that delivers a balanced flow of blood to the tissues before returning it to the heart. Within the heart, valves provide directionality so that blood circulates purposefully from the right heart through the lungs to the left heart before being sent throughout the body.

Each tissue is unique in its complexity and location in the cardiovascular system and has adapted a structure suitable to perform its function effectively in that specific environment. Due to the vital role of this system, failure of any component to perform its function, due to disease or injury, may threaten the life and well being of the affected individual.

Veins are perhaps the simplest of the cardiovascular structures that will be discussed in this chapter. Large-caliber veins experience low pressures and are thin structures with fewer layers of smooth muscle cells (SMCs) and extracellular matrix (ECM) relative to arteries. Arteries experience high cyclic pressures and therefore must have thicker walls than veins of comparable size. Heart valves are distinct not only in their form, but in that they also experience a more complex and hemodynamic environment. Valves experience wide swings in pressure and must alter their shape appropriately to both permit and restrict flow. They must be compliant enough to open easily and allow for blood to pass through freely, but strong enough when closed to prevent regurgitation. Thus, valves represent the most complex structures that will be discussed in this chapter (Figures 9.1 and 9.2).

These structures are similar in that they all require a confluent endothelial cell monolayer lining and are in direct contact with blood. Most importantly, these cells provide a surface that resists platelet adhesion and is

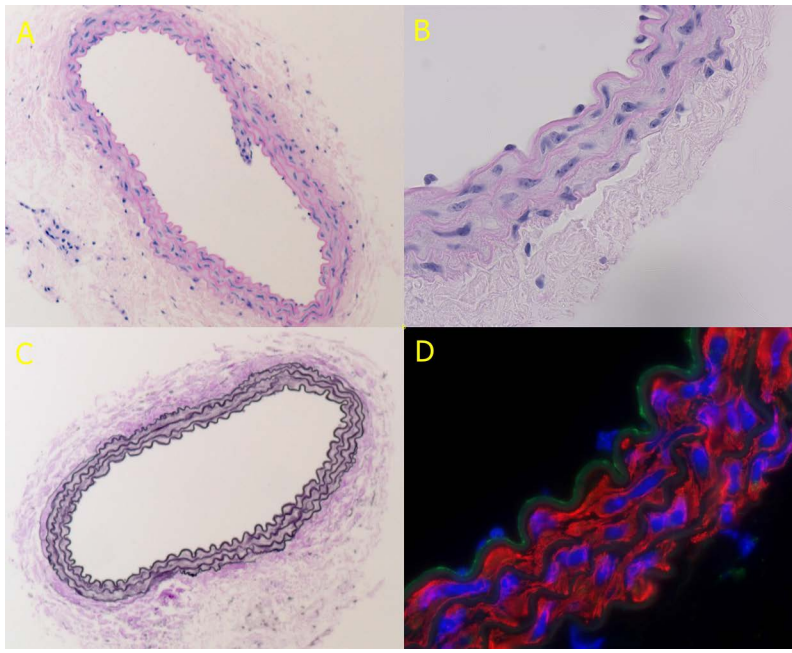

Figure 9.1 Microscopic image of mouse abdominal aorta. Hematoxylin and eosin (H&E) staining, 10× magnification (A), 63× magnification (B), Hart's staining, 10× magnification (C), immunofluorescence staining, green: CD31, red: alpha smooth muscle actin, 63× magnification (D).

anti-thrombogenic. In vessels, this endothelial cell lining is surrounded by a thin layer of basement membrane followed by outer layers containing smooth muscle cells and ECM. ECs also communicate with SMCs to alter vessel lumen diameter and regulate the flow of blood to tissues. In addition, ECs make the vessel selectively permeable to water, and they regulate the exchange of metabolites with the surrounding tissues.[1]

The ECM is what ultimately defines a vessel or valve's mechanical properties.[2] Collagen provides the ECM with the tensile strength to resist rupture, whereas elastin confers elasticity to tissues.[3] In arterial grafts, both properties are important, as they must be able to store the energy of contraction during systole so that blood can be released more steadily to downstream tissues. Proteoglycans give the ECM its resistance to compressibility.[4,5]

The common limitations associated with current prosthetic replacements suggest that no man-made substitute will fulfill all functions as effectively as native tissue that has been refined meticulously by nature over millennia. Tissue engineering, therefore, seeks to harness and encourage the body's natural abilities to heal and regenerate its tissues. The traditional model of tissue engineering required the isolation of cells, seeding, or incorporation of these cells into a scaffold,[6] and sometimes subsequent extended *in vitro* culture to allow for the construct/tissue to mature before implantation. However, cell isolation, seeding, and culture can be both costly and time consuming. Due to the high cost, risks of contamination during culture, and urgency often surrounding intervention for IHD or congenital heart defects, this approach is not a practical solution. With this in mind, several groups have investigated a

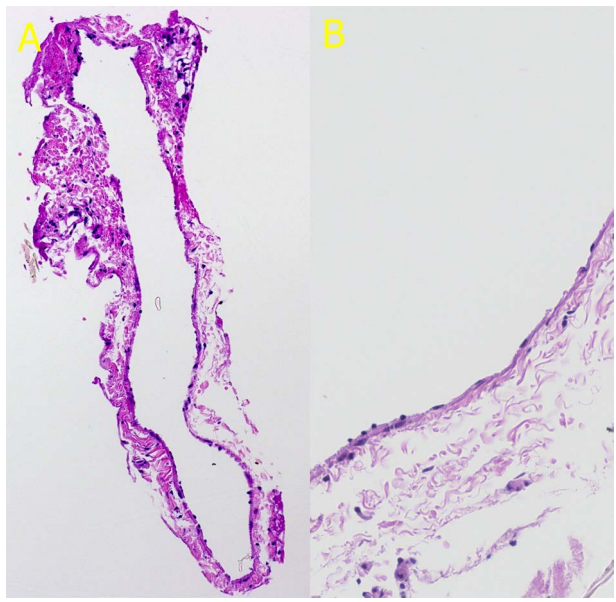

Figure 9.2 Microscopic image of mouse inferior vena cava. H&E staining, 10× magnification (A), 20× magnification (B).

different paradigm by which an unseeded scaffold is implanted and recruits host-derived cells to form neotissue closely resembling the native structure.

9.3 Smart Materials for Cardiovascular Tissue Engineering

A scaffold provides a temporary three-dimensional framework on which cells will adhere, proliferate, and produce extracellular matrix. They should be highly porous to encourage cellular infiltration, neotissue formation, and native tissue integration.[7] If a material is not porous enough or too porous, cells cannot infiltrate the scaffold or the mechanical properties will be insufficient, respectively. Before neotissue formation, biomechanical properties are determined solely by the scaffold. Eventually, graft biomechanical properties are reflective of the deposited ECM after the scaffold degrades or is remodeled. In between these times there is a transition period where the neotissue develops and increasingly bears the mechanical burden as the scaffold loses its mechanical integrity.[3]

A scaffold must meet high expectations in order to successfully perform as a vascular graft, patch, or valve. The ideal scaffold must be readily available ("off-the-shelf"), able to withstand handling during surgery and the mechanical loading experienced *in vivo* before neotissue maturation. In the acute period, the scaffold must be non-thrombogenic, non-immunogenic, and promote cellular adhesion and neotissue formation. Neotissue formation within a scaffold must be balanced, robust enough to quickly form neotissue, but not excessive so that the vessel or valve stenoses. The neotissue must also develop mechanical properties similar to the native tissue (*e.g.*, strength and compliance) and resist ectopic calcification.[8] If made of synthetic materials, a scaffold must be degradable so as to make room for neotissue formation, and not promote a persistent foreign body reaction, chronic inflammation, or ectopic calcification.[9,10] To date, no one material is the silver bullet or performs well for all applications. Therefore, research is ongoing into newer, smarter materials for TEVGs, patches and valves that are specialized for each application. These materials, designs, and modifications will be described herein. Of note, there is great overlap in the materials used for tissue engineered vessels, valves, patches, and myocardium. This review focuses heavily on examples of tissue-engineered vessels. We suggest the reader focuses on why a particular material was used and why specific modifications were made because this information is generalizable to other applications.

To prepare the reader for the chapter ahead, smart materials used in cardiovascular engineering will primarily be introduced within the specific context of vascular tissue engineering. This will be followed by a section on heart valve and myocardial tissue engineering with application of these materials. Included in the subsections, new materials will be introduced as appropriate. In addition, materials will be described in order beginning with those that are closest to natural materials and ending with those that are synthetic.

For many of the applications we describe, we state the success rate in a certain model or at a certain time point. We may need to put this information within a greater context. Some materials perform spectacularly early, but have dismal failure later. The time point/end point is critical to the "success" of the graft. We must make sure the reader does not fall into this trap and realizes that data may not go out long enough to fully evaluate a specific material. It is also important to determine whether failure is slow or catastrophic. Slow failure can be identified and interfered with. Catastrophic failure might be unpredictable and might have extreme consequences to the patient.

9.3.1 Decellularized Vascular Scaffolds

Though decellularized tissues can be derived from auto- and allografts, they are most often obtained from xenogenic sources. Decellularized tissues go through an involved process of physical agitation and chemical surfactant application to remove cellular components, DNA, and any other nucleotide remnants. The process will ideally leave an intact and structurally organized ECM after its completion. There are several commercially available ECM products tailored for cardiovascular use. Because many have been introduced to the marketplace only recently, the long-term prognosis and efficacy of these products remain unclear.

These scaffolds are desirable because they provide an environment for cells that closely mimics the *in vivo* environment in that it is compositionally diverse and includes a variety of biologically active binding sites. This complexity has implications for cell behaviors such as survival, proliferation, differentiation, and migration. Decellularized matrix is naturally highly porous to encourage cell infiltration. In addition, since the ECM is already present and organized, theoretically the tissue has a head start in maturing and would be expected to have mechanical properties approximating native tissue. Furthermore, this material was designed and perfected by nature to encourage cellular interaction, thus giving seeded or circulating cells an advantage with regards to remodeling.

ECM derived from the small intestinal submucosa (SIS) is widely utilized as a scaffold for tissue repair in the clinic. Autologous SIS were first investigated as small and large diameter vascular substitutes in a dog model during the late 1980s.[11,12] In 1999, a small diameter graft constructed from collagen derived from swine SIS and type I bovine was investigated. The construct was implanted in a rabbit arterial bypass model and demonstrated excellent hemostasis and 100% patency at 90 day follow-up.[13] However, a 2009 study found a graft failure rate of 70% in the carotid artery bovine model due to dilatation, stenosis, and aneurysm formation.[14] More recently, CorMatrix® has been utilized for a variety of cardiovascular surgical applications. It is a xenogenic porcine-SIS-derived ECM that has purportedly produced enough evidence to merit clinical trials. However, there is controversy regarding whether CorMatrix® elicits significant unwanted inflammatory responses.

In 2001, Kaushal *et al.* decellularized a xenogenic vessel and seeded the remaining construct with autologous cells before implantation.[15] The seeded scaffold was compared to an unseeded control. In this particular case, the seeded group remained patent whereas the unseeded control group occluded within 15 days. Therefore, in this investigation, decellularized vasculature by itself was not a viable vessel substitute.

Dahl and colleagues have produced promising results by culturing cadaveric SMCs onto a synthetic biodegradable scaffold for 10 weeks in a pulsatile bioreactor that mimics physiologic stress. The arteries grown *in vitro* were then decellularized and resulted in a readily available "off the shelf" construct. Even though the process is quite intricate and involved, a study reported 88% patency past six months as an arteriovenous TEVG in a baboon model.[16]

9.3.2 Natural Polymeric Biomaterials

Whereas decellularized scaffolds are complex structures containing a mixture of ECM proteins, purified matrix proteins are also used. There is greater control over the form, mechanical properties and biocompatibility/immunogenicity. Predictable biodegradation profiles, use, and limitations will be described below. Scaffolds fabricated from naturally occurring polymers are typically biocompatible and often induce desirable cellular responses without activating unwanted inflammatory or immunogenic responses. However, the biodegradation profiles and mechanical load bearing properties of these polymers are less than optimal.

9.3.2.1 Collagen Scaffolds

Type I collagen is one of the main proteins that form the vascular ECM and is primarily produced by medial SMCs and adventitial fibroblasts. Collagen fibers have high tensile strength and allow vessels to resist dilation and rupture in response to physiological pressures. Furthermore, collagen contains integrin binding sites for cells and encourages cellular attachment and proliferation.[17] Weinberg and Bell are credited with creating the first TEVG in 1986. Their hallmark construction incorporated SMCs, fibroblasts, and ECs into tubular collagen gels *in vitro*.[2] However, their graft lacked appropriate strength and was unsuitable for implantation *in vivo*.

The influence of crosslinking treatments on collagen scaffolds *in vitro* was investigated in 2003. The study found that tensile strength improved, but the constructs proved to be too stiff and lost elasticity.[18] Another group took a direct assembly approach and seeded the collagen construct with porcine SMCs and ECs. The *in vitro* study revealed cell proliferation and collagen remodeling over seven days but there were unacceptable burst pressures (18 mm Hg).[19] Collagen and elastin composites have been designed to overcome the burst pressure limitations of previous scaffolds.[20] These composite collagen grafts have shown adequate resilience, compliance, platelet adhesion

reduction, and patency two weeks after implantation in an aortic rodent model. However, these scaffolds must undergo longer-term studies in larger animals to better assess their possible clinical value.

9.3.2.2 *Gelatin*

Gelatin is a collagen derivative that has been used for wound healing, nerve, cartilage, bone, and skin tissue engineering constructs. This material is appealing for scaffold fabrication because it shares similar mechanical properties, biocompatibility, and biodegradation with collagen.

For vascular scaffolds, gelatin is typically used as a coating agent to enhance cellular adhesion. Additionally, gelatin invokes minimal immunogenic responses.[21] Similarly, a co-electrospun polyurethane/gelatin composite graft was found to enhance EC adhesion and proliferation.[22] A greater density of viable cells was also found on a scaffold composed of a blended electrospun solution of recombinant spider silk protein, PCL, and gelatin *versus* a 100% PCL scaffold *in vitro*.[23]

TEVGs incorporating gelatin have shown better biointegration, biocompatibility, and anti-thrombogenic characteristics when compared with non-gelatin scaffolds.[24] However, a major limitation of gelatin is that it degrades as a colloidal solution above 37 °C and will be a gel at room temperature or lower. Additionally, gelatin must be cross-linked to increase its stability, resulting in longer degradation times and increased water resistance.

9.3.2.3 *Elastin*

Elastin is a main organization element of vascular ECM and confers compliance to vessels, thereby ensuring smooth blood flow by storing elastic energy.[25] There are several different forms of elastin, such as tropoelastin, and soluble α, β, and κ elastin. Elastin is highly insoluble and a difficult material to handle when manufacturing scaffolds. Therefore, there are few scaffolds composed entirely of elastin. Instead, similar to gelatin, it is used primarily to supplement a scaffold composed primarily of another material. For example, scaffolds made of recombinant human tropoelastin, when presented as a monomer and cross-linked into a synthetic elastin/PCL scaffold, show low thrombogenicity. These constructs were implanted as carotid interposition grafts in a rabbit model and showed 100% patency past four weeks.[26] The incorporation of elastin and tropoelastin into biodegradable synthetic grafts appears promising, but longer-term and larger animal studies need to be conducted to better evaluate scaffold characteristics. Another tubular scaffold composed of purified elastin reinforced with fibrin-bonded layers of SIS was implanted as a carotid interposition graft in a porcine model. The elastin composites demonstrated longer average patency times (5.23 h) when compared to clinically acceptable ePTFE grafts (4.15 h).[27] New processing techniques are being introduced that enhance the ability to process elastin into scaffolds. *In vitro* scaffolds made of α-elastin and a diepoxy crosslinker

supported vascular SMC attachment and proliferation *in vitro*.[28] Therefore, scaffolds made primarily of elastin may be useful in cardiovascular tissue engineering applications.

9.3.2.4 *Fibrin*

Fibrin is a major structural protein that is needed for wound healing. What makes it appealing for scaffold design is that its primary constituents, fibrinogen and thrombin, can be directly isolated from a patient's blood. Other benefits of fibrin scaffolds include high-seeding efficiency, even cellular distribution, and controllable degradation rates with the use of protease inhibitors. Bovine SMCs and ECs were embedded in a fibrin gel construct which was cultured for two weeks before implantation as a jugular vein interposition graft in a lamb model. At 15 weeks postimplantation, the scaffold was infiltrated with SMCs that were oriented perpendicular to blood flow and both collagen and elastin fiber production was observed. Additionally, blood flow through the graft was 71% of the native control.[29] Without extensive *in vitro* culture, fibrin has shown poor mechanical properties that have limited its use as a scaffold in tissue engineering approaches. To address these limitations, some groups have reinforced fibrin *via* cross-linking or an underlying synthetic scaffold. A fibrin-based scaffold, supported with a PLA mesh and seeded with autologous arterial cells, was implanted as a carotid artery interposition graft and observed at one, three, and six months. At all time points, the grafts remained patent, though there was one incidence of stenosis at the three-month time point. Furthermore, the grafts displayed a complete lack of thrombosis and no evidence of aneurysm formation or calcification.[30] In 2016, Aper and colleagues reported a rapid manufacturing method that produced fibrin-based vascular grafts within one hour. Cross-linking between the fibrin fibrils yielded a significant increase in burst strength, and after explantation at six months, the structure looked similar to a native artery in sheep.[31]

9.3.2.5 *Chitosan Scaffolds and Blends*

Chitosan (CS) is obtained from the shells of shellfish and waste from the seafood industry. CS is widely used for biomedical applications because of its mechanical strength, porous structure, biocompatibility, biodegradability, antibacterial characteristics and ease of chemical modification.[32] CS has a well-documented and successful clinical history for bone, cartilage, and skin tissue engineering functions. By itself, CS scaffolds do not possess adequate mechanical strength, and therefore are often blended with other polymers to make up for their limitations. Electrospun hybrid CS/PCL grafts have presented satisfactory patency rates *in vivo*.[33,34] However, when implanted in an abdominal aortic rat model, CS/PCL grafts were bonded to heparin to prevent thrombus formation and stenosis.[33] Furthermore, when implanted as carotid artery conduits in a larger canine model, CS/PCL grafts had to be seeded with ECs to achieve acceptable patency and mechanical properties.

9.3.2.6 Silk Fibroin

In tissue engineering, the pertinent use of silk fibers has been limited to silk fibroin. Silk is comprised of two components: (1) a glue, such as the protein sericin, which acts as an adhesive for inclusive fibers and (2) fibroin filaments which provide mechanical strength. Silk fibroin is broken down *via* proteolytic degradation, and remnants are resorbed as biocompatible amino acids *in vivo*. Furthermore, silk fibroin constructs are attractive because they are easily fabricated into various materials such as films, fibers, sponges, or knitted scaffolds.

In 2008, human ECs and SMCs were successfully cultured onto an electrospun silk-based scaffold *in vitro*.[35] Mechanical tests demonstrated adequate burst strength to withstand arterial pressures. Later studies conducted in an abdominal aortic rat model revealed 100% graft patency at four weeks without acute thrombosis,[36] and 85% graft patency past 12 months.[37] Scaffolds composed of silk fibroin display host cell infiltration, ECM remodeling, and the development of an elastic lamina within seven days of implantation.[38] Silk fibroin is possibly a viable material to fabricate TEVGs, but it still needs to undergo longer-term and larger animal studies for evaluation.

9.3.3 Polymeric Scaffold

Early vascular substitutes were comprised of non-degradable polymers such as Dacron (polyethylene terephthalate, PET) or Gore-Tex (expanded polytetrafluoroethylene, ePTFE or Teflon). PET and PTFE have been used clinically since 1956 and 1976, respectively. These non-degradable polymeric scaffolds have since dominated the large diameter vascular market because they provide acceptable patency rates and are readily available and convenient ("off the shelf") when native vascular substitutes are not available. In large diameter vascular applications, these non-degradable substitutes have demonstrated comparable patency rates with autologous grafts but are greatly limited as small diameter vascular substitutes because of their poor patency and incapacity to form neotissue. Synthetic grafts for small diameter (<6 mm) arterial bypass procedures display patency rates of 40% and 25% at six months and three years, respectively. In the case of PTFE, randomized studies have found significant differences in below knee femoral popliteal bypass operations.[39] Additionally, the patency rate of secondary operations that are required to repair graft failures is overwhelmingly in favor of saphenous vein (70%) over PTFE (18%).[40]

9.3.3.1 Biostable Synthetic Polymers

9.3.3.1.1 PTFE. The GORE® PROPATEN® Vascular Graft was produced by W. L. Gore & Associates (Gore) in 2006. It was heparin-bonded PTFE vascular prostheses. Although the patency rate improved when compared to previous PTFE grafts, it was still not superior to the autologous saphenous vein.[41–44]

9.3.3.1.2 PU (PEUU). Polyurethanes have been researched extensively over the past two decades and are elastic materials with exceptional physical and mechanical properties. They are typically formed by polymerizing a monomer containing multiple hydroxyl groups with a monomer containing an isocyanate group. Polyurethanes are strong, flexible, durable, and can be manipulated by varying monomer ratios and compositions.[45,46] Furthermore, polyurethanes are composed of both hard and soft domains. The hard domains are dispersed in the amorphous and elastic soft domains, thus giving the materials their uniquely flexible and yet durable characteristics.

In the 1960s, Dupont developed a poly(ether-urethane urea) named Lycra®. It was a durable elastic material resistant to hydrolytic degradation. Biomer, a modified version of the material, was fabricated into vascular grafts and implanted beginning in 1967.[47–49] An electrospun Biomer vascular graft displayed a 65% patency rate past two years and all graft failures occurred within one year. A more recent investigation looked at a similar PEU named Pellethane. This particular vascular graft was implanted in a rat model as an abdominal aortic conduit and revealed a 95% patency past 26 weeks *in vivo*.[50] Though polyurethane vascular grafts were implanted with the purpose of being permanent prostheses, they were found to be vulnerable to hydrolytic degradation and macrophage-activated stress cracking.[51] With the discovery of a degradation mechanism, more attention was paid to the utilization of degradable polyurethane in TEVG applications.

An electrospun scaffold composed of degradable PEU was implanted in rats and reported 40% patency at eight weeks with failures attributed to thrombosis.[52,53] Later, a platelet adhesion polymer named MPC was blended with PEU to form the copolymer poly(2-methacryloyloxyethyl phosphorylcholine-*co*-methacryloyl-oxyethyl butylurethane) (PMBU), which reported 67% patency at eight weeks.[52] Another electrospun PEU graft covalently bonded MPC to the surface of the scaffold and reported a 92% patency rate, with failures due to acute thrombosis.[53] Thus as a class of materials, polyurethanes are viable vascular conduits, but require antithrombogenic treatment before graft implantation. Furthermore, before they are considered for clinical translation, polyurethanes need to undergo longer-term studies to evaluate graft performance after total polymer degradation.

9.3.3.2 Biodegradable Synthetic Polymers

9.3.3.2.1 Polyesters. Polyesters represent another class of synthetic polymers that differ most significantly from those previously mentioned in that they are readily biodegradable; ester bonds linking monomer subunits are susceptible to hydrolytic and proteolytic enzymatic degradation. One of the earliest biomedical uses of these materials was as absorbable sutures, composed of either PGA or PLA, due to their biodegradability and high tensile strength. These materials are synthesized from the condensation reaction between a variety of potential monomer subunits. This is a highly customizable system in which many material properties (*e.g.*, hydrophilicity,

degradation rate, tensile strength) can be altered by varying the composition of the subunits and methods of processing.

The choice to use a particular polyester or blend is often influenced by the degradation rate one desires for a particular application. This property depends upon the initial molecular weight of the polymer, crystallinity, and geometry/exposed surface area.[3] In the cardiovascular system, scaffolds are often designed with large pores to encourage cellular infiltration, quick degradation, and neotissue formation, as well as preventing residual polymer from contributing to inflammation and/or ectopic calcification.[8]

In 2001, Shin'oka *et al.* reported the first successful clinical implantation of a degradable TEVG composed of 50:50 PCL–PLLA copolymer reinforced with a PGA mesh seeded with autologous bone-marrow-derived mononuclear cells.[54] Long-term follow up of the original study revealed no evidence of aneurysm formation, graft rupture, graft infection, or ectopic calcification (Figure 9.3).[55,56]

It is important to note, however, that the procedures were performed in low pressure, venous systems. Therefore, the bulk of current research on degradable polymer scaffolds has been focused on novel constructs that can withstand the higher pressures of the arterial system and at the same time encourage healthy neotissue formation.

9.3.3.2.2 PGA. Poly(glycolic acid) (PGA) is among the most commonly used polymers in tissue engineering. It was one of the first biodegradable polymers utilized to fabricate a scaffold. PGA degrades into glycolic acid, which is metabolized by cells into water and carbon dioxide.

Figure 9.3 Macro image of a vein tissue engineering vascular graft.

In our murine model, a PGA IVC interposition graft takes up to six weeks for the scaffold to lose its mechanical integrity.

For use in arterial applications, scaffolds made of PGA alone have not had sufficient structural and chemical characteristics. Often, the grafts fail due to aneurysmal dilation because the neotissue cannot withstand physiological pressures as PGA begins to lose its mechanical integrity. PGA grafts have been improved by aortic smooth muscle cell seeding[57] or when used as a composite with gelatin.[21]

9.3.3.2.3 PLA. Poly(L-lactic acid) (PLA) is another widely used aliphatic polyester used for tissue engineering approaches. PLA is more hydrophobic than PGA due to the presence of an extra methyl group. The reduced affinity to water leads to longer degradation times. Thus, studies have reported that PLA takes months to years to lose the majority of its mechanical integrity *in vivo* or *in vitro*.

Hashi *et al.* were the first to investigate an electrospun, biodegradable TEVG constructed for the arterial circulation in rat aortas.[58] Specifically, the group compared an electrospun PLA graft seeded with bone-marrow-derived mesenchymal stem cells before implantation *versus* an unseeded control. The seeded scaffolds displayed a reduced thrombotic response compared to the unseeded group and there was no graft rupture or aneurysmal dilatation.

Subsequent experiments focused on improvements in graft construction and making chemical surface modifications. Hirudin is a thrombin inhibiting polypeptide.[58,59] An experimental hirudin-conjugated PLA scaffold was compared to a non-conjugated PLA scaffold. The experimental group displayed a 75% patency rate *versus* 50% in the non-conjugated control graft. Therefore, this investigation demonstrated the efficacy of making surface chemical modifications to improve material performance.

9.3.3.2.4 PCL. Poly(ε-caprolactone) (PCL) is an aliphatic polyester that has been thoroughly investigated. PCL is synthetic, hydrophobic, and slowly biodegradable with a low glass transition temp and low melting point. In fact, PCL has one of the slowest degradation profiles out of all biodegradable polymers. The semicrystalline polymer's low melting point makes the polymer pliable at lower temperatures, in addition to being easy to tune and fabricate. After slow ester linkage hydrolysis, PCL forms ε-hydroxycaproic acid as a degradation product, which is safely removed by giant cells.

A series of *in vivo* studies have evaluated electrospun PCL in rats with observations at 12, 24, and 78 weeks.[60–62] Even without the help of drugs, graft patency was 100% and did not provide evidence of thrombosis. PCL scaffolds were found to lose 20%, 51.5%, and 78.1% of their initial 80 kDa molecular weight at three, 12, and 18 months, respectively. However, cellular infiltration was reported to decrease after one year in addition to findings of chondroid metaplasia that led to gradual graft calcification.

PCL has been blended with collagen[63] and recombinant human tropoelastin.[26] Both scaffolds reported 100% patency in *in vivo* pilot experiments

as well as improved biocompatibility and reduced platelet attachment. Blending PCL with chitosan has been shown to improve its biocompatibility, degradation profile, and mechanical properties.[34,64] Other groups have incorporated or coated PCL scaffolds with peptides and reported increased endothelialization, cellular infiltration, and patency.[65–67]

Unfortunately, studies on PCL have been unable to ascertain graft viability after total scaffold degradation because its degradation period exceeds that of a typical rodent lifespan. Though it is a promising material, future studies must evaluate PCL over longer time periods before it can be clinically translated.

9.3.3.2.5 PHA. Polyhydroxyalkanoates are a class of natural polyesters.[68] PHA polymers, namely, polyhydroxybutyrate (PHB) and polyhydroxybutyrate-*co*-valerate (PHBV) have been evaluated for a variety of medical applications.[69] Hoerstrup *et al.* created small caliber vascular grafts made from polyglycolic-acid/poly-4-hydroxybutyrate, proving its feasibility for use in vascular tissue engineering.[70] Shum-Tim *et al.* subsequently implanted 7 mm diameter PHA–PGA tubular scaffolds in a lamb's abdominal aorta, but more recent investigations into the materials have been sparse.[71]

9.3.3.2.6 PGS. Unlike the other previously described polymers which are formed from the condensation reaction of single monomers, poly(glycerol sebacate) (PGS) is an elastomer formed from both glycerol and sebacic acid. PGS degrades within two months *in vivo* and displays excellent mechanical properties and biocompatibility. Khosravi *et al.* showed suitable bilayered, cell-free, PGS–PCL TEVGs in the arterial system over a 12 month implantation period.[72]

9.4 Myocardial Tissue Engineering

Current research focuses on creating apparatuses that support, repair, replace, or functionally enhance damaged myocardial tissue. Strategies for myocardial tissue engineering include the injection of cells alone (*e.g.*, intravenous, intracoronary or intramyocardial),[73] intramyocardial injection of biomaterials, or the surgical application of an epicardial patch (Figure 9.4).

The advantage of injectable approaches as compared to a patch is that they can deliver cells and biomaterials with minimally invasive procedures by a combination of catheter-mediated cell delivery approaches.[74,75] Just like vascular tissue engineered scaffolds, to generate neomyocardial tissue, cell ingrowth and maturation must replace and maintain structural integrity as the scaffold degrades and loses its mechanical properties. Considerations for thick myocardial tissue and the large metabolic demand required to provide oxygen and nutrients that diffusion cannot provide by itself also need to be taken into account.

The ideal biomaterial construction for heart regeneration must follow several general principles: the material should (1) be biocompatible and

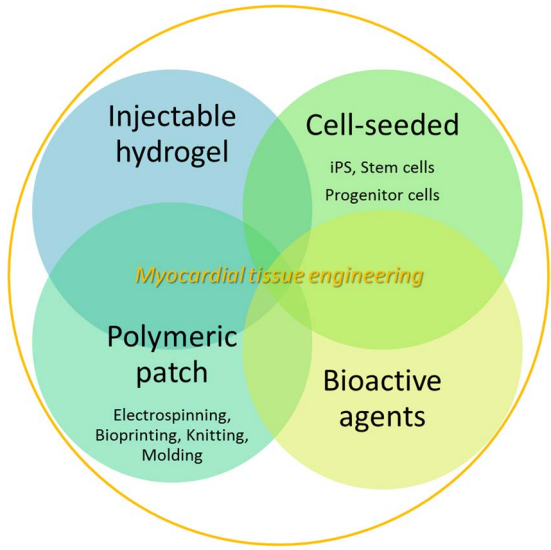

Figure 9.4 The schema of combined approaches for myocardial tissue engineering.

biodegradable, (2) support cell proliferation, differentiation, and integration into the host tissue while facilitating highly ordered and biomimetic neotissue, (3) possess the strength to withstand the large, cyclical mechanical stresses of the heart, and (4) be easy to manufacture and shape into patient-specific forms.

9.4.1 Injectable Biomaterials

Initial attempts at cardiovascular tissue engineering utilized direct intramyocardial cell injections. These early attempts were limited by poor cell retention and survival, irrespective of the cell type or the administration route. The injection of hydrogels, such as collagen,[76] with cells in suspension attempts to address the problems of limited cell retention and survival by providing a temporary ECM support structure for cellular adherence. This method has successfully increased cell retention and survival after injection.[74]

Following the initial pioneering studies, hydrogel injection for cardiovascular tissue engineering has since been investigated with a variety of materials with or without cells. These materials include synthetic polyethylene glycol (PEG),[77–80] PEGylated fibrin + HGF,[81] MPEG–PCL–MPEG,[82,83] collagen,[84] fibrin,[85–88] matrigel,[89,90] acrylamid,[91,92] fibrin–alginate composite,[93] chitosan chloride–glutathione (CSCl–GSH),[94] methylcellulose,[95] naturally occurring polysaccharides[96] such as xylan,[97] dextran,[98] pullulan,[98] chitosan,[99–101] hyaluronan,[102–104] and alginates.[105–111] However, despite promising results achieved using several biomaterials, only Algisyl-LVR (LoneStar Heart, Inc., CA) and IK-5001[112], both alginate-based hydrogels, have reached clinical trials.[112–114] Algisyl-LVR™ was shown to improve peak VO_2, a convalescence

estimation indicator of heart failure, at six months in NYHA Functional Class II trials. As alginate hydrogel approaches in cardiovascular tissue engineering are still in their infancy, future studies must observe and assess the pros and cons of such therapies over longer-term clinical trials.

9.4.2 Patch-Forming Scaffolds

Epicardial patches are a more invasive approach to myocardial tissue engineering, but are better than injectable approaches in providing mechanical support in efforts to reduce dilation of damaged or disease heart tissue. Like hydrogels, epicardial patches can be cell seeded or embedded with bioactive molecules. A multitude of biomaterials has been studied in efforts to create the ideal epicardial patch such as chitosan–hyaluronan–silk fibroin,[115] PLGA,[116] collagen,[117–119] polyester urethane,[120,121] PGS,[122–124] PCL,[123,125] poly(3-hydroxybutyrate) (PHB),[126] poly-L-lactic acid (PLLA), and poly-chitosan-*g*-lactic acid (PCLA).[127] Decellularized ECMs generated from small intestine submucosa[128] or xenogeneic porcine pericardium[129] have also been used. Although numerous biomaterials have improved cardiac cell growth *in vitro* and possess good biocompatibility *in vivo*, an ideal material has not yet emerged and engineering functional cardiac tissue remains a challenging and elusive endeavor.

9.5 Heart Valve Tissue Engineering

When malfunctioning heart valves cannot be repaired surgically, the next alternative is replacement with a mechanical or bioprosthetic valve.[130,131] Mechanical heart valves, made of metals and plastics, have excellent durability, but are prone to causing inflammation, infection, and thromboembolic complications that necessitate long-term anticoagulation therapy. Non-decellularized porcine or bovine bioprosthetic heart valves are not as thrombogenic, but are prone to calcification and progressive deterioration 10 to 15 years after surgery, particularly when implanted in younger individuals (Figure 9.5).[132]

The tissue engineered heart valve (TEHV) is a promising alternative approach in an effort to eliminate these limitations. Conceptually, a TEHV will be comparable to a native valve and exhibit adequate mechanical strength, cellular adhesion and proliferation to grow, repair, and remodel into a long-lasting valve. Additionally it will be less inflammatory and immunogenic when compared to current prosthetics. The traditional approach to construct a tissue engineered heart valve is to seed autologous cells onto a three-dimensional scaffold, and subsequently culture the construct *in vitro* until sufficient neotissue has formed before implantation. More recently, researchers have been pursuing an approach that exploits implanting cell-free materials that guide the neotissue formation process *in vivo*.[133] In the latter case, scaffold matrices must function as valves immediately, withstand

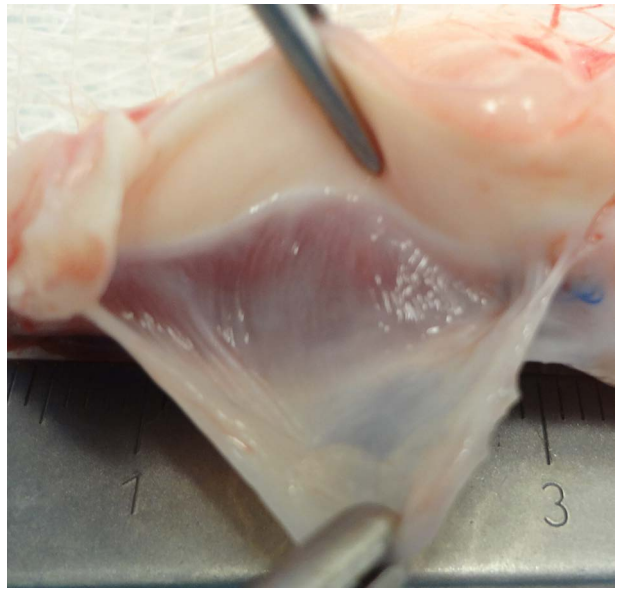

Figure 9.5 Macro image of a sheep pulmonary valve.

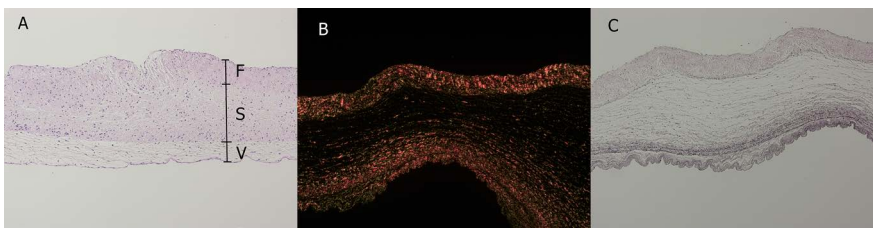

Figure 9.6 Microscopic image of a sheep pulmonary valve leaflet. Circumferential collagen alignment in the fibrosa layer. Radial elastin alignment in the ventricularis layer. (A) H&E staining, (B) Picrosirius red staining, (C) Hart's staining, magnification 10×, F: fibrosa, S: spongiosa, V: ventricularis.

in vivo forces, and provide a short-term biomechanical structure to support cells until they have remodeled into adequately strong neotissue. Primarily, two approaches to heart valve substitute scaffold designs have been studied: (1) decellularized biological scaffolds, from allo- or xenogeneic sources[134,135] and (2) synthetic-based scaffolds (Figure 9.6).

9.5.1 Biological-Based Scaffold

The main sources of biological material used to make decellularized heart valves are provided by homografts or xenografts.[136] Several decellularization strategies have been investigated to leave behind an intact ECM with the

structural characteristics that allow for host cell attachment, migration, and proliferation.[137] The inherent structure and biological activity of these scaffolds make them an attractive choice for tissue repair and reconstruction.[138] Though limited by availability, homografts are more desirable than xenogenic scaffolds due to the risk of zoonotic infection and greater immunogenicity of non-human tissues. Cross-linking is one method that reduces immunogenicity and minimizes disease transmission from decellularized xenogenic scaffolds.[139,140]

In large animal studies, decellularized scaffolds have exhibited structural stability, in addition to robust cellular regrowth, and migration without observed thromboembolisms.[141–144] In humans, encouraging results have been reported with decellularized allogenic valves and allografts with respect to immunological responses, durability and overall clinical performance.[145–147] Though many experimental studies in preclinical animal models have demonstrated that decellularized allografts are fully repopulated *in vivo* after implantation,[148–150] repopulation in humans was only focal. There were a few cells with a fibroblast appearance coming both from the luminal side and from the periadventitial inflammatory reaction, but they were sparse and did not penetrate into the deep layers of the media. These findings are very similar to those reported by Miller and colleagues,[151] who studied one SynerGraft decellularized aortic valve allograft explanted two years after the operation.

However, despite these results and the many decellularization approaches that have been developed, clinical outcomes when using decellularized xenogenic heart valves have been far less encouraging as evidenced by the SynerGraft trial, which was a catastrophic failure.[152] Thus, the main limitations in using decellularized scaffolds remain the lack of availability of homografts and the risk of transferring zoonoses and immunogenicity when using xenogenic valves. At present, the adoption of decellularized tissue for use as replacement heart valves remains limited.

9.5.2 Degradable Synthetic Scaffolds

Synthetic scaffolds are attractive alternatives to decellularized tissues since they do not contain antigenic epitopes, and thus are generally less immunogenic and thrombogenic.[153] Additionally, these scaffolds can be designed to have reproducible mechanical properties, high durability, and controlled degradation. Furthermore, as cell-free medical products, they would undergo less stringent regulatory processes during medical device classification and more easily achieve approval for clinical use. There is high interest among regenerative medical researchers to design scaffolds in such a way that they can be used in combination with minimally invasive implantation procedures to reduce trauma and surgical complications.

The first TEHV concept appeared in the mid-nineties[154–156] with the hope of reconstructing right posterior pulmonary heart valve leaflets. These scaffolds were seeded with myofibroblasts and ECs. Due to the thickness and stiffness of the scaffolds, they behaved like stenotic trileaflet valves and were not functional. In the two decades since, several synthetic materials and

blends have been investigated *in vivo*, such as PHA and poly-4-hydroxybutyrate (P4HB),[157,158] poly-hydroxyoctanoate (PHO),[159] PGA[160–162] and PLLA.[163] However, synthetic heart valve substitutes have not yet been clinically translated.

9.6 The Clinical Potentials and Applications of Smart Materials in Cardiovascular Disease

Patients with cardiovascular disease or congenital heart defects sometimes require vascular graft implantations. Autologous grafts remain the gold standard in treatment, but are in short supply and often run into size mismatch issues. Non-biodegradable, synthetic scaffolds address both of these concerns. In fact, synthetic, large-diameter vessel replacements, such as Dacron and Teflon, have already proven their clinical utility. However, as small-diameter conduits, these non-biodegradable synthetic graft substitutes display much lower patency rates and difficulties with neotissue growth and remodeling, and are more prone to infection when compared to autologous grafts. TEVGs hold great promise to resolve the clinical failures of non-biodegradable, synthetic grafts in small-diameter applications.

Designing a functional TEVG greatly depends upon factors such as cell seeding, biomechanical properties, and suitable material selection. Additionally, arterial TEVGs should be minimally invasive and able to withstand the high-pressure arterial circulation until it is completely reconstituted by host-derived cells. Currently, grafts constructed from cultured cell sheets or cadaveric cells appear to be quite promising. Although cell culturing and seeding scaffold technologies have progressed rapidly, they have several limitations such as being technically complicated to construct, long production times, and high costs. In cases where the cardiovascular disease must be immediately addressed, it may not be possible to wait the several weeks or months required for cells to be collected, cultured, and conditioned into a transplantable graft. Vascular grafts fabricated solely out of synthetic biomaterials have so far been limited by low hemocompatibility or biomechanical properties. Therefore, current approaches have looked at synthetic biomaterials by themselves or blended with natural ECM proteins.

In order to be widely accepted in the clinic, future TEVGs should be cost-effective and readily available "off-the-shelf". To address current scaffold limitations, it is believed that mimicking the biological and mechanical properties of native vessels will be critical in designing future TEVGs. Despite the breadth of research on the subject matter, consensus on what makes materials suitable for clinical applications has not yet been established. Current TEVGs still need to be evaluated over longer-term studies with appropriate clinical application lengths in large animal models. These investigations should focus on vascular neotissue characterization after complete scaffold degradation in addition to finding means of inhibiting thrombosis and calcification.

Although engineering cell-free valves that are functional and long lasting will have its own unique challenges, these issues will be very similar to those

with TEVGs and vascular patches. Therefore, progress made on an individual cardiovascular apparatus is likely to be highly translatable to other similar tissues and technologies. On the contrary, myocardial tissue engineering is expected to have distinct challenges reflective of this complex, metabolically demanding tissue and the high mechanical forces it experiences. In an effort to better mimic native cardiac tissue, research focused on treating diseased or injured myocardium has been dedicated to designing materials to attract and sustain cells by incorporating bioactive molecules to encourage vascularization. Two prominent methods being pursued involve injection of hydrogels (with or without cells) or implantation of an epicardial scaffold. To date, only injectable cell-free biomaterials have reached clinical application.

References

1. J. P. Stegemann, S. N. Kaszuba and S. L. Rowe, *Tissue Eng.*, 2007, **13**, 2601–2613.
2. C. B. Weinberg and E. Bell, *Science*, 1986, **231**, 397–400.
3. S. Tara, H. Kurobe, M. W. Maxfield, K. A. Rocco, T. Yi, Y. Naito, C. K. Breuer and T. Shinoka, *J. Vasc. Surg.*, 2015, **62**, 734–743.
4. A. Ratcliffe, *Matrix Biol.*, 2000, **19**, 353–357.
5. L. Buttafoco, N. G. Kolkman, P. Engbers-Buijtenhuijs, A. A. Poot, P. J. Dijkstra, I. Vermes and J. Feijen, *Biomaterials*, 2006, **27**, 724–734.
6. R. Langer and J. P. Vacanti, *Science*, 1993, **260**, 920–926.
7. K. C. Rustad, M. Sorkin, B. Levi, M. T. Longaker and G. C. Gurtner, *Organogenesis*, 2010, **6**, 151–157.
8. S. Tara, H. Kurobe, K. A. Rocco, M. W. Maxfield, C. A. Best, T. Yi, Y. Naito, C. K. Breuer and T. Shinoka, *Atherosclerosis*, 2014, **237**, 684–691.
9. W. Wu, R. A. Allen and Y. Wang, *Nat. Med.*, 2012, **18**, 1148–1153.
10. R. A. Allen, W. Wu, M. Yao, D. Dutta, X. Duan, T. N. Bachman, H. C. Champion, D. B. Stolz, A. M. Robertson, K. Kim, J. S. Isenberg and Y. Wang, *Biomaterials*, 2014, **35**, 165–173.
11. S. F. Badylak, G. C. Lantz, A. Coffey and L. A. Geddes, *J. Surg. Res.*, 1989, **47**, 74–80.
12. G. C. Lantz, S. F. Badylak, A. C. Coffey, L. A. Geddes and W. E. Blevins, *J. Invest. Surg.*, 1990, **3**, 217–227.
13. T. Huynh, G. Abraham, J. Murray, K. Brockbank, P. O. Hagen and S. Sullivan, *Nat. Biotechnol.*, 1999, **17**, 1083–1086.
14. D. Pavcnik, J. Obermiller, B. T. Uchida, W. Van Alstine, J. M. Edwards, G. J. Landry, J. A. Kaufman, F. S. Keller and J. Rosch, *Cardiovasc. Intervent. Radiol.*, 2009, **32**, 106–113.
15. S. Kaushal, G. E. Amiel, K. J. Guleserian, O. M. Shapira, T. Perry, F. W. Sutherland, E. Rabkin, A. M. Moran, F. J. Schoen, A. Atala, S. Soker, J. Bischoff and J. E. Mayer Jr, *Nat. Med.*, 2001, **7**, 1035–1040.
16. S. L. Dahl, A. P. Kypson, J. H. Lawson, J. L. Blum, J. T. Strader, Y. Li, R. J. Manson, W. E. Tente, L. DiBernardo, M. T. Hensley, R. Carter,

T. P. Williams, H. L. Prichard, M. S. Dey, K. G. Begelman and L. E. Niklason, *Sci. Transl. Med.*, 2011, **3**, 68ra69.
17. J. Hirai and T. Matsuda, *Cell Transplant.*, 1996, **5**, 93–105.
18. V. Charulatha and A. Rajaram, *Biomaterials*, 2003, **24**, 759–767.
19. F. Boccafoschi, N. Rajan, J. Habermehl and D. Mantovani, *Macromol. Biosci.*, 2007, **7**, 719–726.
20. V. A. Kumar, J. M. Caves, C. A. Haller, E. Dai, L. Liu, S. Grainger and E. L. Chaikof, *Acta Biomater.*, 2013, **9**, 8067–8074.
21. H. Hajiali, S. Shahgasempour, M. R. Naimi-Jamal and H. Peirovi, *Int. J. Nanomed.*, 2011, **6**, 2133–2141.
22. N. Detta, C. Errico, D. Dinucci, D. Puppi, D. A. Clarke, G. C. Reilly and F. Chiellini, *J. Mater. Sci.: Mater. Med.*, 2010, **21**, 1761–1769.
23. P. Xiang, M. Li, C. Y. Zhang, D. L. Chen and Z. H. Zhou, *Int. J. Biol. Macromol.*, 2011, **49**, 281–288.
24. L. Bordenave, J. Caix, B. Basse-Cathalinat, C. Baquey, D. Midy, J. C. Baste and H. Constans, *Biomaterials*, 1989, **10**, 235–242.
25. M. Rabaud, F. Lefebvre and D. Ducassou, *Biomaterials*, 1991, **12**, 313–319.
26. S. G. Wise, M. J. Byrom, A. Waterhouse, P. G. Bannon, A. S. Weiss and M. K. Ng, *Acta Biomater.*, 2011, **7**, 295–303.
27. M. T. Hinds, R. C. Rowe, Z. Ren, J. Teach, P. C. Wu, S. J. Kirkpatrick, K. D. Breneman, K. W. Gregory and D. W. Courtman, *J. Biomed. Mater. Res., Part A*, 2006, **77**, 458–469.
28. J. B. Leach, J. B. Wolinsky, P. J. Stone and J. Y. Wong, *Acta Biomater.*, 2005, **1**, 155–164.
29. D. D. Swartz, J. A. Russell and S. T. Andreadis, *Am. J. Physiol.: Heart Circ. Physiol.*, 2005, **288**, H1451–H1460.
30. S. Koch, T. C. Flanagan, J. S. Sachweh, F. Tanios, H. Schnoering, T. Deichmann, V. Ella, M. Kellomaki, N. Gronloh, T. Gries, R. Tolba, T. Schmitz-Rode and S. Jockenhoevel, *Biomaterials*, 2010, **31**, 4731–4739.
31. T. Aper, M. Wilhelmi, C. Gebhardt, K. Hoeffler, N. Benecke, A. Hilfiker and A. Haverich, *Acta Biomater.*, 2016, **29**, 21–32.
32. I. Y. Kim, S. J. Seo, H. S. Moon, M. K. Yoo, I. Y. Park, B. C. Kim and C. S. Cho, *Biotechnol. Adv.*, 2008, **26**, 1–21.
33. Y. Yao, J. Wang, Y. Cui, R. Xu, Z. Wang, J. Zhang, K. Wang, Y. Li, Q. Zhao and D. Kong, *Acta Biomater.*, 2014, **10**, 2739–2749.
34. M. Zhou, W. Qiao, Z. Liu, T. Shang, T. Qiao, C. Mao and C. Liu, *Tissue Eng., Part A*, 2014, **20**, 79–91.
35. L. Soffer, X. Wang, X. Zhang, J. Kluge, L. Dorfmann, D. L. Kaplan and G. Leisk, *J. Biomater. Sci., Polym. Ed.*, 2008, **19**, 653–664.
36. M. Lovett, G. Eng, J. A. Kluge, C. Cannizzaro, G. Vunjak-Novakovic and D. L. Kaplan, *Organogenesis*, 2010, **6**, 217–224.
37. Y. Nakazawa, M. Sato, R. Takahashi, D. Aytemiz, C. Takabayashi, T. Tamura, S. Enomoto, M. Sata and T. Asakura, *J. Biomater. Sci., Polym. Ed.*, 2011, **22**, 195–206.

38. I. Cattaneo, M. Figliuzzi, N. Azzollini, V. Catto, S. Fare, M. C. Tanzi, A. Alessandrino, G. Freddi and A. Remuzzi, *Int. J. Artif. Organs*, 2013, **36**, 166–174.
39. F. J. Veith, S. K. Gupta, E. Ascer, S. White-Flores, R. H. Samson, L. A. Scher, J. B. Towne, V. M. Bernhard, P. Bonier and W. R. Flinn, *et al.*, *J. Vasc. Surg.*, 1986, **3**, 104–114.
40. W. J. Quinones-Baldrich, R. W. Busuttil, J. D. Baker, C. L. Vescera, S. S. Ahn, H. I. Machleder and W. S. Moore, *J. Vasc. Surg.*, 1988, **8**, 219–228.
41. P. Peeters, J. Verbist, K. Deloose and M. Bosiers, *J. Cardiovasc. Surg.*, 2006, **47**, 407–413.
42. K. Daenens, S. Schepers, I. Fourneau, S. Houthoofd and A. Nevelsteen, *J. Vasc. Surg.*, 2009, **49**, 1210–1216.
43. R. Pulli, W. Dorigo, P. Castelli, V. Dorrucci, F. Ferilli, G. De Blasis, V. Monaca, E. Vecchiati, C. Pratesi and G. Propaten Italian Registry, *J. Vasc. Surg.*, 2010, **51**, 1167–1177.e1161.
44. J. S. Lindholt, B. Gottschalksen, N. Johannesen, D. Dueholm, H. Ravn, E. D. Christensen, B. Viddal, T. Florenes, G. Pedersen, M. Rasmussen, M. Carstensen, N. Grondal and H. Fasting, *Eur. J. Vasc. Endovasc. Surg.*, 2011, **41**, 668–673.
45. A. Tiwari, H. Salacinski, A. M. Seifalian and G. Hamilton, *Cardiovasc. Surg.*, 2002, **10**, 191–197.
46. E. M. Christenson, M. Dadsetan, M. Wiggins, J. M. Anderson and A. Hiltner, *J. Biomed. Mater. Res., Part A*, 2004, **69**, 407–416.
47. J. W. Boretos and W. S. Pierce, *Science*, 1967, **158**, 1481–1482.
48. D. Annis, A. Bornat, R. O. Edwards, A. Higham, B. Loveday and J. Wilson, *Trans.–Am. Soc. Artif. Intern. Organs*, 1978, **24**, 209–214.
49. A. C. Fisher, L. De Cossart, T. V. How and D. Annis, *Life Support Syst.*, 1985, **3**(suppl. 1), 462–465.
50. H. Bergmeister, C. Grasl, I. Walter, R. Plasenzotti, M. Stoiber, C. Schreiber, U. Losert, G. Weigel and H. Schima, *Artif. Organs*, 2012, **36**, 54–61.
51. K. A. Rocco, M. W. Maxfield, C. A. Best, E. W. Dean and C. K. Breuer, *Tissue Eng., Part B*, 2014, **20**, 628–640.
52. Y. Hong, S. H. Ye, A. Nieponice, L. Soletti, D. A. Vorp and W. R. Wagner, *Biomaterials*, 2009, **30**, 2457–2467.
53. L. Soletti, A. Nieponice, Y. Hong, S. H. Ye, J. J. Stankus, W. R. Wagner and D. A. Vorp, *J. Biomed. Mater. Res., Part A*, 2011, **96**, 436–448.
54. T. Shin'oka, Y. Imai and Y. Ikada, *N. Engl. J. Med.*, 2001, **344**, 532–533.
55. T. Shin'oka, G. Matsumura, N. Hibino, Y. Naito, M. Watanabe, T. Konuma, T. Sakamoto, M. Nagatsu and H. Kurosawa, *J. Thorac. Cardiovasc. Surg.*, 2005, **129**, 1330–1338.
56. N. Hibino, E. McGillicuddy, G. Matsumura, Y. Ichihara, Y. Naito, C. Breuer and T. Shinoka, *J. Thorac. Cardiovasc. Surg.*, 2010, **139**, 431–436, 436.e431–432.
57. L. E. Niklason, J. Gao, W. M. Abbott, K. K. Hirschi, S. Houser, R. Marini and R. Langer, *Science*, 1999, **284**, 489–493.

58. C. K. Hashi, Y. Zhu, G. Y. Yang, W. L. Young, B. S. Hsiao, K. Wang, B. Chu and S. Li, *Proc. Natl. Acad. Sci. U. S. A.*, 2007, **104**, 11915–11920.
59. C. K. Hashi, N. Derugin, R. R. Janairo, R. Lee, D. Schultz, J. Lotz and S. Li, *Arterioscler., Thromb., Vasc. Biol.*, 2010, **30**, 1621–1627.
60. E. Pektok, B. Nottelet, J. C. Tille, R. Gurny, A. Kalangos, M. Moeller and B. H. Walpoth, *Circulation*, 2008, **118**, 2563–2570.
61. S. de Valence, J. C. Tille, D. Mugnai, W. Mrowczynski, R. Gurny, M. Moller and B. H. Walpoth, *Biomaterials*, 2012, **33**, 38–47.
62. B. Nottelet, E. Pektok, D. Mandracchia, J. C. Tille, B. Walpoth, R. Gurny and M. Moller, *J. Biomed. Mater. Res., Part A*, 2009, **89**, 865–875.
63. B. W. Tillman, S. K. Yazdani, S. J. Lee, R. L. Geary, A. Atala and J. J. Yoo, *Biomaterials*, 2009, **30**, 583–588.
64. J. Zhao, H. Qiu, D. L. Chen, W. X. Zhang, D. C. Zhang and M. Li, *Int. J. Biol. Macromol.*, 2013, **56**, 106–113.
65. R. Kato, C. Kaga, M. Kunimatsu, T. Kobayashi and H. Honda, *J. Biosci. Bioeng.*, 2006, **101**, 485–495.
66. F. Kuwabara, Y. Narita, A. Yamawaki-Ogata, K. Kanie, R. Kato, M. Satake, H. Kaneko, H. Oshima, A. Usui and Y. Ueda, *Ann. Thorac. Surg.*, 2012, **93**, 156–163, discussion 163.
67. W. Zheng, Z. Wang, L. Song, Q. Zhao, J. Zhang, D. Li, S. Wang, J. Han, X. L. Zheng, Z. Yang and D. Kong, *Biomaterials*, 2012, **33**, 2880–2891.
68. S. F. Williams, D. P. Martin, D. M. Horowitz and O. P. Peoples, *Int. J. Biol. Macromol.*, 1999, **25**, 111–121.
69. O. Duvernoy, T. Malm, J. Ramstrom and S. Bowald, *Thorac. Cardiovasc. Surg.*, 1995, **43**, 271–274.
70. S. P. Hoerstrup, G. Zund, R. Sodian, A. M. Schnell, J. Grunenfelder and M. I. Turina, *Eur. J. Cardiothorac. Surg.*, 2001, **20**, 164–169.
71. D. Shum-Tim, U. Stock, J. Hrkach, T. Shinoka, J. Lien, M. A. Moses, A. Stamp, G. Taylor, A. M. Moran, W. Landis, R. Langer, J. P. Vacanti and J. E. Mayer Jr, *Ann. Thorac. Surg.*, 1999, **68**, 2298–2304, discussion 2305.
72. R. Khosravi, C. A. Best, R. A. Allen, C. E. Stowell, E. Onwuka, J. J. Zhuang, Y. U. Lee, T. Yi, M. R. Bersi, T. Shinoka, J. D. Humphrey, Y. Wang and C. K. Breuer, *Ann. Biomed. Eng.*, 2016, **44**(8), 2402–2416.
73. K. L. Christman and R. J. Lee, *J. Am. Coll. Cardiol.*, 2006, **48**, 907–913.
74. J. M. Singelyn, J. A. DeQuach, S. B. Seif-Naraghi, R. B. Littlefield, P. J. Schup-Magoffin and K. L. Christman, *Biomaterials*, 2009, **30**, 5409–5416.
75. J. M. Singelyn, P. Sundaramurthy, T. D. Johnson, P. J. Schup-Magoffin, D. P. Hu, D. M. Faulk, J. Wang, K. M. Mayle, K. Bartels, M. Salvatore, A. M. Kinsey, A. N. Demaria, N. Dib and K. L. Christman, *J. Am. Coll. Cardiol.*, 2012, **59**, 751–763.
76. T. Eschenhagen, C. Fink, U. Remmers, H. Scholz, J. Wattchow, J. Weil, W. Zimmermann, H. H. Dohmen, H. Schafer, N. Bishopric, T. Wakatsuki and E. L. Elson, *FASEB J.*, 1997, **11**, 683–694.
77. S. Dobner, D. Bezuidenhout, P. Govender, P. Zilla and N. Davies, *J. Card. Failure*, 2009, **15**, 629–636.

78. X. J. Jiang, T. Wang, X. Y. Li, D. Q. Wu, Z. B. Zheng, J. F. Zhang, J. L. Chen, B. Peng, H. Jiang, C. Huang and X. Z. Zhang, *J. Biomed. Mater. Res., Part A*, 2009, **90**, 472–477.
79. T. Wang, X. J. Jiang, T. Lin, S. Ren, X. Y. Li, X. Z. Zhang and Q. Z. Tang, *Biomaterials*, 2009, **30**, 4161–4167.
80. M. Habib, K. Shapira-Schweitzer, O. Caspi, A. Gepstein, G. Arbel, D. Aronson, D. Seliktar and L. Gepstein, *Biomaterials*, 2011, **32**, 7514–7523.
81. G. Zhang, Q. Hu, E. A. Braunlin, L. J. Suggs and J. Zhang, *Tissue Eng., Part A*, 2008, **14**, 1025–1036.
82. T. Wang, X. J. Jiang, Q. Z. Tang, X. Y. Li, T. Lin, D. Q. Wu, X. Z. Zhang and E. Okello, *Acta Biomater.*, 2009, **5**, 2939–2944.
83. J. Chen, R. Guo, Q. Zhou and T. Wang, *Kaohsiung J. Med. Sci.*, 2014, **30**, 173–180.
84. W. Dai, L. E. Wold, J. S. Dow and R. A. Kloner, *J. Am. Coll. Cardiol.*, 2005, **46**, 714–719.
85. K. L. Christman, A. J. Vardanian, Q. Fang, R. E. Sievers, H. H. Fok and R. J. Lee, *J. Am. Coll. Cardiol.*, 2004, **44**, 654–660.
86. K. L. Christman, H. H. Fok, R. E. Sievers, Q. Fang and R. J. Lee, *Tissue Eng.*, 2004, **10**, 403–409.
87. X. Zhang, H. Wang, X. Ma, A. Adila, B. Wang, F. Liu, B. Chen, C. Wang and Y. Ma, *Exp. Biol. Med.*, 2010, **235**, 1505–1515.
88. T. P. Martens, A. F. Godier, J. J. Parks, L. Q. Wan, M. S. Koeckert, G. M. Eng, B. I. Hudson, W. Sherman and G. Vunjak-Novakovic, *Cell Transplant.*, 2009, **18**, 297–304.
89. T. Kofidis, A. Lenz, J. Boublik, P. Akhyari, B. Wachsmann, K. M. Stahl, A. Haverich and R. G. Leyh, *Eur. J. Cardiothorac. Surg.*, 2003, **24**, 906–911.
90. T. Kofidis, J. L. de Bruin, G. Hoyt, D. R. Lebl, M. Tanaka, T. Yamane, C. P. Chang and R. C. Robbins, *J. Thorac. Cardiovasc. Surg.*, 2004, **128**, 571–578.
91. K. L. Fujimoto, Z. Ma, D. M. Nelson, R. Hashizume, J. Guan, K. Tobita and W. R. Wagner, *Biomaterials*, 2009, **30**, 4357–4368.
92. T. Wang, D. Q. Wu, X. J. Jiang, X. Z. Zhang, X. Y. Li, J. F. Zhang, Z. B. Zheng, R. Zhuo, H. Jiang and C. Huang, *Eur. J. Heart Failure*, 2009, **11**, 14–19.
93. R. Mukherjee, J. A. Zavadzkas, S. M. Saunders, J. E. McLean, L. B. Jeffords, C. Beck, R. E. Stroud, A. M. Leone, C. N. Koval, W. T. Rivers, S. Basu, A. Sheehy, G. Michal and F. G. Spinale, *Ann. Thorac. Surg.*, 2008, **86**, 1268–1276.
94. J. Li, Y. Shu, T. Hao, Y. Wang, Y. Qian, C. Duan, H. Sun, Q. Lin and C. Wang, *Biomaterials*, 2013, **34**, 9071–9081.
95. C. C. Huang, Z. X. Liao, D. Y. Chen, C. W. Hsiao, Y. Chang and H. W. Sung, *Adv. Healthcare Mater.*, 2014, **3**, 1133–1148.
96. A. K. Silva, M. Juenet, A. Meddahi-Pelle and D. Letourneur, *Carbohydr. Polym.*, 2015, **116**, 267–277.
97. J. Venugopal, R. Rajeswari, M. Shayanti, R. Sridhar, S. Sundarrajan, R. Balamurugan and S. Ramakrishna, *Mater. Sci. Eng. C Mater. Biol. Appl.*, 2013, **33**, 1325–1331.

98. M. Lavergne, M. Derkaoui, C. Delmau, D. Letourneur, G. Uzan and C. Le Visage, *Macromol. Biosci.*, 2012, **12**, 901–910.
99. H. Wang, J. Shi, Y. Wang, Y. Yin, L. Wang, J. Liu, Z. Liu, C. Duan, P. Zhu and C. Wang, *Biomaterials*, 2014, **35**, 3986–3998.
100. W. N. Lu, S. H. Lu, H. B. Wang, D. X. Li, C. M. Duan, Z. Q. Liu, T. Hao, W. J. He, B. Xu, Q. Fu, Y. C. Song, X. H. Xie and C. Y. Wang, *Tissue Eng., Part A*, 2009, **15**, 1437–1447.
101. Z. Liu, H. Wang, Y. Wang, Q. Lin, A. Yao, F. Cao, D. Li, J. Zhou, C. Duan, Z. Du, Y. Wang and C. Wang, *Biomaterials*, 2012, **33**, 3093–3106.
102. S. J. Yoon, Y. H. Fang, C. H. Lim, B. S. Kim, H. S. Son, Y. Park and K. Sun, *J. Biomed. Mater. Res., Part B*, 2009, **91**, 163–171.
103. J. L. Ifkovits, E. Tous, M. Minakawa, M. Morita, J. D. Robb, K. J. Koomalsingh, J. H. Gorman 3rd, R. C. Gorman and J. A. Burdick, *Proc. Natl. Acad. Sci. U. S. A.*, 2010, **107**, 11507–11512.
104. C. H. Chen, M. Y. Chang, S. S. Wang and P. C. Hsieh, *Am. J. Physiol.: Heart Circ. Physiol.*, 2014, **306**, H1078–H1086.
105. X. Hao, E. A. Silva, A. Mansson-Broberg, K. H. Grinnemo, A. J. Siddiqui, G. Dellgren, E. Wardell, L. A. Brodin, D. J. Mooney and C. Sylven, *Cardiovasc. Res.*, 2007, **75**, 178–185.
106. J. Yu, Y. Gu, K. T. Du, S. Mihardja, R. E. Sievers and R. J. Lee, *Biomaterials*, 2009, **30**, 751–756.
107. O. Tsur-Gang, E. Ruvinov, N. Landa, R. Holbova, M. S. Feinberg, J. Leor and S. Cohen, *Biomaterials*, 2009, **30**, 189–195.
108. N. Landa, L. Miller, M. S. Feinberg, R. Holbova, M. Shachar, I. Freeman, S. Cohen and J. Leor, *Circulation*, 2008, **117**, 1388–1396.
109. J. Leor, S. Tuvia, V. Guetta, F. Manczur, D. Castel, U. Willenz, O. Petnehazy, N. Landa, M. S. Feinberg, E. Konen, O. Goitein, O. Tsur-Gang, M. Shaul, L. Klapper and S. Cohen, *J. Am. Coll. Cardiol.*, 2009, **54**, 1014–1023.
110. J. Yu, K. T. Du, Q. Fang, Y. Gu, S. S. Mihardja, R. E. Sievers, J. C. Wu and R. J. Lee, *Biomaterials*, 2010, **31**, 7012–7020.
111. N. C. Panda, S. T. Zuckerman, O. O. Mesubi, D. S. Rosenbaum, M. S. Penn, J. K. Donahue, E. Alsberg and K. R. Laurita, *J. Interv. Card. Electrophysiol.*, 2014, **41**, 117–127.
112. N. Frey, A. Linke, T. Suselbeck, J. Muller-Ehmsen, P. Vermeersch, D. Schoors, M. Rosenberg, F. Bea, S. Tuvia and J. Leor, *Circ.: Cardiovasc. Interventions*, 2014, **7**, 806–812.
113. L. C. Lee, S. T. Wall, D. Klepach, L. Ge, Z. Zhang, R. J. Lee, A. Hinson, J. H. Gorman 3rd, R. C. Gorman and J. M. Guccione, *Int. J. Cardiol.*, 2013, **168**, 2022–2028.
114. S. D. Anker, A. J. Coats, G. Cristian, D. Dragomir, E. Pusineri, M. Piredda, L. Bettari, R. Dowling, M. Volterrani, B. A. Kirwan, G. Filippatos, J. L. Mas, N. Danchin, S. D. Solomon, R. J. Lee, F. Ahmann, A. Hinson, H. N. Sabbah and D. L. Mann, *Eur. Heart J.*, 2015, **36**, 2297–2309.
115. N. H. Chi, M. C. Yang, T. W. Chung, N. K. Chou and S. S. Wang, *Carbohydr. Polym.*, 2013, **92**, 591–597.
116. J. Yu, A. R. Lee, W. H. Lin, C. W. Lin, Y. K. Wu and W. B. Tsai, *Tissue Eng., Part A*, 2014, **20**, 1896–1907.

117. J. Gao, J. Liu, Y. Gao, C. Wang, Y. Zhao, B. Chen, Z. Xiao, Q. Miao and J. Dai, *Tissue Eng., Part A*, 2011, **17**, 2739–2747.
118. P. Maureira, P. Y. Marie, F. Yu, S. Poussier, Y. Liu, F. Groubatch, A. Falanga and N. Tran, *J. Biomed. Sci.*, 2012, **19**, 93.
119. V. Serpooshan, M. Zhao, S. A. Metzler, K. Wei, P. B. Shah, A. Wang, M. Mahmoudi, A. V. Malkovskiy, J. Rajadas, M. J. Butte, D. Bernstein and P. Ruiz-Lozano, *Biomaterials*, 2013, **34**, 9048–9055.
120. R. Hashizume, K. L. Fujimoto, Y. Hong, J. Guan, C. Toma, K. Tobita and W. R. Wagner, *J. Thorac. Cardiovasc. Surg.*, 2013, **146**, 391–399.e391.
121. R. Hashizume, Y. Hong, K. Takanari, K. L. Fujimoto, K. Tobita and W. R. Wagner, *Biomaterials*, 2013, **34**, 7353–7363.
122. Q. Z. Chen, H. Ishii, G. A. Thouas, A. R. Lyon, J. S. Wright, J. J. Blaker, W. Chrzanowski, A. R. Boccaccini, N. N. Ali, J. C. Knowles and S. E. Harding, *Biomaterials*, 2010, **31**, 3885–3893.
123. R. Ravichandran, J. R. Venugopal, S. Sundarrajan, S. Mukherjee, R. Sridhar and S. Ramakrishna, *Int. J. Cardiol.*, 2013, **167**, 1461–1468.
124. R. Rai, M. Tallawi, C. Frati, A. Falco, A. Gervasi, F. Quaini, J. A. Roether, T. Hochburger, D. W. Schubert, L. Seik, N. Barbani, L. Lazzeri, E. Rosellini and A. R. Boccaccini, *Adv. Healthcare Mater.*, 2015, **4**, 2012–2025.
125. A. G. Guex, A. Frobert, J. Valentin, G. Fortunato, D. Hegemann, S. Cook, T. P. Carrel, H. T. Tevaearai and M. N. Giraud, *Acta Biomater.*, 2014, **10**, 2996–3006.
126. D. Castellano, M. Blanes, B. Marco, I. Cerrada, A. Ruiz-Sauri, B. Pelacho, M. Arana, J. A. Montero, V. Cambra, F. Prosper and P. Sepulveda, *Stem Cells Dev.*, 2014, **23**, 1479–1490.
127. A. Lesman, M. Habib, O. Caspi, A. Gepstein, G. Arbel, S. Levenberg and L. Gepstein, *Tissue Eng., Part A*, 2010, **16**, 115–125.
128. Z. Vukadinovic-Nikolic, B. Andree, S. E. Dorfman, M. Pflaum, T. Horvath, M. Lux, L. Venturini, A. Bar, G. Kensah, A. R. Lara, I. Tudorache, S. Cebotari, D. Hilfiker-Kleiner, A. Haverich and A. Hilfiker, *Tissue Eng., Part A*, 2014, **20**, 799–809.
129. A. F. Godier-Furnemont, T. P. Martens, M. S. Koeckert, L. Wan, J. Parks, K. Arai, G. Zhang, B. Hudson, S. Homma and G. Vunjak-Novakovic, *Proc. Natl. Acad. Sci. U. S. A.*, 2011, **108**, 7974–7979.
130. K. E. Hammermeister, G. K. Sethi, W. G. Henderson, C. Oprian, T. Kim and S. Rahimtoola, *N. Engl. J. Med.*, 1993, **328**, 1289–1296.
131. W. Vongpatanasin, L. D. Hillis and R. A. Lange, *N. Engl. J. Med.*, 1996, **335**, 407–416.
132. P. Pibarot and J. G. Dumesnil, *Circulation*, 2009, **119**, 1034–1048.
133. S. Brody and A. Pandit, *J. Biomed. Mater. Res., Part B*, 2007, **83**, 16–43.
134. P. M. Dohmen and W. Konertz, *Ann. Thorac. Cardiovasc. Surg.*, 2009, **15**, 362–367.
135. S. Neuenschwander and S. P. Hoerstrup, *Transplant Immunol.*, 2004, **12**, 359–365.
136. K. Schenke-Layland, F. Opitz, M. Gross, C. Doring, K. J. Halbhuber, F. Schirrmeister, T. Wahlers and U. A. Stock, *Cardiovasc. Res.*, 2003, **60**, 497–509.

137. F. Moroni and T. Mirabella, *Am. J. Stem Cells*, 2014, **3**, 1–20.
138. S. F. Badylak, *Semin. Cell Dev. Biol.*, 2002, **13**, 377–383.
139. M. E. Tedder, J. Liao, B. Weed, C. Stabler, H. Zhang, A. Simionescu and D. T. Simionescu, *Tissue Eng., Part A*, 2009, **15**, 1257–1268.
140. X. Lu, W. Zhai, Y. Zhou, Y. Zhou, H. Zhang and J. Chang, *J. Mater. Sci.: Mater. Med.*, 2010, **21**, 473–480.
141. H. Baraki, I. Tudorache, M. Braun, K. Hoffler, A. Gorler, A. Lichtenberg, C. Bara, A. Calistru, G. Brandes, M. Hewicker-Trautwein, A. Hilfiker, A. Haverich and S. Cebotari, *Biomaterials*, 2009, **30**, 6240–6246.
142. P. M. Dohmen, F. Costa, S. V. Lopes, S. Yoshi, F. P. Souza, R. Vilani, M. B. Costa and W. Konertz, *Heart Surg. Forum*, 2005, **8**, E100–E104, discussion E104.
143. S. S. Kim, S. H. Lim, Y. S. Hong, S. W. Cho, J. H. Ryu, B. C. Chang, C. Y. Choi and B. S. Kim, *Artif. Organs*, 2006, **30**, 554–557.
144. M. F. O'Brien, S. Goldstein, S. Walsh, K. S. Black, R. Elkins and D. Clarke, *Semin. Thorac. Cardiovasc. Surg.*, 1999, **11**, 194–200.
145. J. F. Bechtel, U. Stierle and H. H. Sievers, *J. Heart Valve Dis.*, 2008, **17**, 98–104, discussion 104.
146. J. W. Brown, M. Ruzmetov, O. Eltayeb, M. D. Rodefeld and M. W. Turrentine, *Ann. Thorac. Surg.*, 2011, **91**, 416–422, discussion 422–413.
147. F. D. da Costa, A. C. Costa, R. Prestes, A. C. Domanski, E. M. Balbi, A. D. Ferreira and S. V. Lopes, *Ann. Thorac. Surg.*, 2010, **90**, 1854–1860.
148. P. M. Dohmen, F. da Costa, S. Yoshi, S. V. Lopes, F. P. da Souza, R. Vilani, A. F. Wouk, M. da Costa and W. Konertz, *J. Heart Valve Dis.*, 2006, **15**, 823–829.
149. F. D. Affonso da Costa, P. M. Dohmen, S. V. Lopes, G. Lacerda, F. Pohl, R. Vilani, M. B. Affonso Da Costa, E. D. Vieira, S. Yoschi, W. Konertz and I. Affonso da Costa, *Artif. Organs*, 2004, **28**, 366–370.
150. K. J. Zehr, M. Yagubyan, H. M. Connolly, S. M. Nelson and H. V. Schaff, *J. Thorac. Cardiovasc. Surg.*, 2005, **130**, 1010–1015.
151. D. V. Miller, W. D. Edwards and K. J. Zehr, *J. Thorac. Cardiovasc. Surg.*, 2006, **132**, 175–176.
152. P. Simon, M. T. Kasimir, G. Seebacher, G. Weigel, R. Ullrich, U. Salzer-Muhar, E. Rieder and E. Wolner, *Eur. J. Cardiothorac. Surg.*, 2003, **23**, 1002–1006, discussion 1006.
153. S. Ravi and E. L. Chaikof, *Regener. Med.*, 2010, **5**, 107–120.
154. T. Shinoka, C. K. Breuer, R. E. Tanel, G. Zund, T. Miura, P. X. Ma, R. Langer, J. P. Vacanti and J. E. Mayer Jr, *Ann. Thorac. Surg.*, 1995, **60**, S513–S516.
155. T. Shinoka, *Artif. Organs*, 2002, **26**, 402–406.
156. T. Shinoka, P. X. Ma, D. Shum-Tim, C. K. Breuer, R. A. Cusick, G. Zund, R. Langer, J. P. Vacanti and J. E. Mayer Jr, *Circulation*, 1996, **94**, II164–II168.
157. R. Sodian, S. P. Hoerstrup, J. S. Sperling, S. Daebritz, D. P. Martin, A. M. Moran, B. S. Kim, F. J. Schoen, J. P. Vacanti and J. E. Mayer Jr, *Circulation*, 2000, **102**, III22–III29.

158. R. Sodian, J. S. Sperling, D. P. Martin, A. Egozy, U. Stock, J. E. Mayer Jr and J. P. Vacanti, *Tissue Eng.*, 2000, **6**, 183–188.
159. U. A. Stock, M. Nagashima, P. N. Khalil, G. D. Nollert, T. Herden, J. S. Sperling, A. Moran, J. Lien, D. P. Martin, F. J. Schoen, J. P. Vacanti and J. E. Mayer Jr, *J. Thorac. Cardiovasc. Surg.*, 2000, **119**, 732–740.
160. S. P. Hoerstrup, R. Sodian, S. Daebritz, J. Wang, E. A. Bacha, D. P. Martin, A. M. Moran, K. J. Guleserian, J. S. Sperling, S. Kaushal, J. P. Vacanti, F. J. Schoen and J. E. Mayer Jr, *Circulation*, 2000, **102**, III44–III49.
161. B. Weber, J. Scherman, M. Y. Emmert, J. Gruenenfelder, R. Verbeek, M. Bracher, M. Black, J. Kortsmit, T. Franz, R. Schoenauer, L. Baumgartner, C. Brokopp, I. Agarkova, P. Wolint, G. Zund, V. Falk, P. Zilla and S. P. Hoerstrup, *Eur. Heart J.*, 2011, **32**, 2830–2840.
162. M. Y. Emmert, B. Weber, P. Wolint, L. Behr, S. Sammut, T. Frauenfelder, L. Frese, J. Scherman, C. E. Brokopp, C. Templin, J. Grunenfelder, G. Zund, V. Falk and S. P. Hoerstrup, *JACC Cardiovasc. Interv.*, 2012, **5**, 874–883.
163. F. W. Sutherland, T. E. Perry, Y. Yu, M. C. Sherwood, E. Rabkin, Y. Masuda, G. A. Garcia, D. L. McLellan, G. C. Engelmayr Jr, M. S. Sacks, F. J. Schoen and J. E. Mayer Jr, *Circulation*, 2005, **111**, 2783–2791.

CHAPTER 10

Advances of Smart Materials for Wound Healing

JUNJIE DENG[a], PETER Y. LI[a] AND HAO CHENG*[a]

[a]Department of Materials Science and Engineering, Drexel University, Philadelphia, PA 19104, USA
*E-mail: hcheng@drexel.edu

10.1 Introduction

Acute and chronic wounds severely affect the quality-of-life of millions of patients each year.[1] The market for chronic wound care alone is worth more than US$20 billion annually.[2] In the past several decades, the number of people suffering from chronic wounds has dramatically increased, due to reasons such as diabetic foot ulcers and vascular ulcers. According to data from the World Health Organization, the prevalence of diabetes worldwide in 2014 was approximately 9% of all adults. There were 29.1 million diabetic patients in the United States, and approximately 15% of these patients developed a diabetic foot ulcer, representing an estimated four million patients. The huge cost of treating wounds strongly drives the development of advanced therapies for effective wound healing. Due to the complexity of the healing process, it is optimal to target wound sites and precisely regulate signaling mediators based on the status of wounds. Recently, smart materials that alter their structure and/or physicochemical properties in response to stimuli have attracted increased attention in wound healing applications because these materials are able to integrate self-adjusted treatments into

Smart Materials No. 25
Smart Materials for Tissue Engineering: Applications
Edited by Qun Wang

Published by the Royal Society of Chemistry, www.rsc.org

the complicated process of tissue regeneration. This chapter provides a general overview of the wound healing process and the current applications of smart materials in wound healing.

10.2 Overview of Wound Healing Stages

10.2.1 Wounds

A wound often refers to the disruption of the normal anatomic structure and function of the skin,[3] but also includes internal injuries such as myocardial infarction and portal hypertension-caused bleeding in patients with liver cirrhosis.[4,5] Pathological conditions due to diseases and external factors such as chemical, physical and thermal damages all can cause wounds.[6] Based on the wound healing process, wounds have been classified as either acute or chronic. Acute wounds mainly occur as a result of surgery or mechanical damages from abrasions, incisions, lacerations, *etc.*, and usually heal in 8–12 weeks. Another category of acute wounds involves burns and chemical injuries, which are mainly because of exposure to irradiation, heat, electrical shock or corrosive chemicals.[7] Chronic wounds normally result from specific diseases, take longer than 12 weeks to heal, and often relapse due to a failure to restore the anatomical and functional integrity of diseased tissues.[7] The variety of wound types underlines the complexity of the wound healing process. Thus, an expanding number of research programs now focus on elaborating the wound healing process and identifying compounds/entities that promote wound repair and regeneration.

10.2.2 Phases of Wound Healing

Wound healing involves orchestrated interactions among different types of cells, chemicals and biologics.[4,8] The process has been categorized into three main phases: inflammation, proliferation, and remodeling, as illustrated in Figure 10.1, though there are overlaps between these phases. Unbalanced interactions cause dysfunctional healing such as fibrotic healing due to excessive deposition of collagen, and further damage of healthy tissues surrounding wounds from excessive inflammatory signals.

10.2.2.1 Inflammation

Hemostasis is the initiating step in wound healing to stop bleeding. It is achieved by the formation of a platelet plug and a fibrin network, generating a clot in the wound site.[4] Immediately after blood vessel injury, vascular smooth muscle cells release intracellular signals to contract. The vascular spasm leads to vasoconstriction followed by platelet adhesion on collagen in the subendothelium of the vasculature. The binding activates platelets to initiate the coagulation cascade that converts fibrinogen to fibrin and forms fibrin fiber networks. Activated platelets release thromboxane A2 (TXA2)

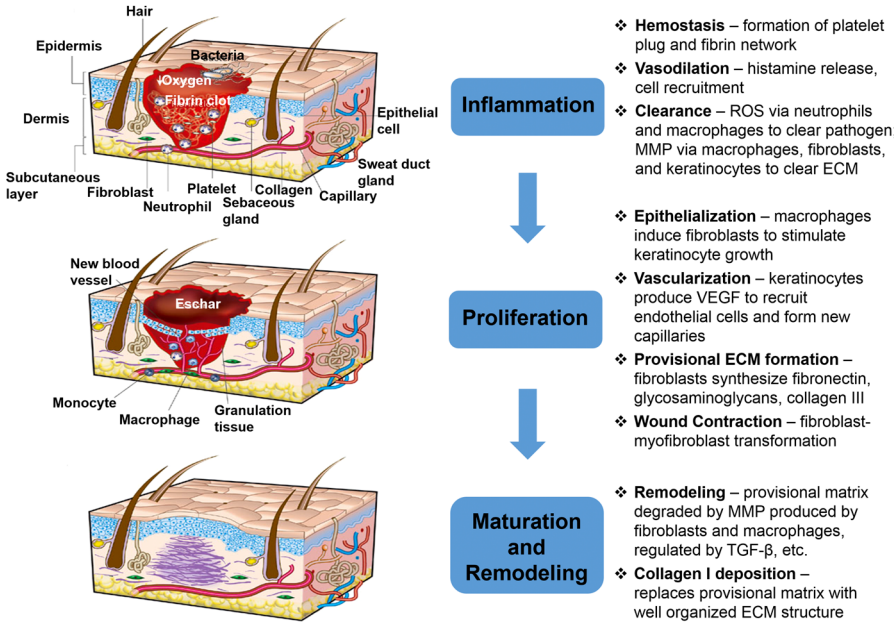

Figure 10.1 The classic wound healing stages. The process has been categorized into three phases: inflammation, proliferation, and remodeling, though there are overlaps between these phases. (Reproduced with permission from ref. 4. Copyright© 2008, Nature Publishing Group.)

to increase vasoconstriction, induce platelet aggregation and recruit more platelets to the clot for reducing blood loss.[9] Following hemostasis, mast cells and activated platelets release histamine for vasodilation that increases blood cell traffic to the injured area. In addition, the platelets secrete growth factors and inflammatory cytokines to enhance leukocyte adhesion to inflamed blood vessel walls and extravasation to enter wound sites.[10] Clots serve as matrices to house recruited neutrophils, monocytes, fibroblasts, and endothelial cells and generate a local environment with high concentrations of secreted cytokines and growth factors.[11] In the inflammatory phase, neutrophils are first recruited to clots by platelet-released chemokines such as transforming growth factor beta (TGF-β), tumor necrosis factor (TNF-α), and interleukin (IL)-1. TNF-α and IL-1 also stimulate endothelial cells to express selectins that mediate neutrophil adhesion and rolling, two important steps of cell homing to wound areas.[12] Neutrophils release proteolytic enzymes and reactive oxygen free radicals to digest bacteria and dead tissue/cells. Neutrophils quickly undergo apoptosis and are replaced by monocyte-derived macrophages two to four days post-injury.[8,13] Macrophages remove bacteria, cell debris, and apoptotic neutrophils in wound areas through phagocytosis. The cells also generate a large amount of nitric oxide (NO), which is converted into peroxynitrite and hydroxyl radicals after NO reacts with superoxide radicals and hydrogen peroxide respectively.[14,15] These chemicals kill pathogens and prevent viral DNA replication.[16] In addition, under

the stimulation of TNF-α, macrophages along with fibroblasts, keratinocytes and monocytes produce matrix metalloproteinases (MMPs) to clear damaged extracellular matrix, assisting cell migration for wound repair. However, excessive amounts of MMPs or other inflammatory signals such as reactive oxygen species (ROS) can damage surrounding tissues and even cause systemic problems such as shock, respiratory failure, and renal failure.[17]

10.2.2.2 Proliferation

The proliferative phase usually occurs about two days after injury and involves epithelialization, angiogenesis, provisional matrix formation, and wound contraction. In skin wound healing, macrophages secrete inflammatory cytokines, IL-1 and TNF-α, to stimulate fibroblast cells, which produce keratinocyte growth factor 2 (KGF-2), and IL-6.[18,19] These cytokines and growth factors stimulate keratinocyte growth in the wound area and recruit more keratinocytes from surrounding tissues. The specialized epithelial cells then reconstruct epithelium to prevent pathogen invasion and fluid loss. Keratinocytes also have an important role in angiogenesis by releasing vascular endothelial growth factor (VEGF), which recruits endothelial cells and stimulates the cell proliferation and formation of new capillaries. Activated platelets and macrophages release platelet-derived growth factor (PDGF) and epidermal growth factor (EGF) to recruit neighboring fibroblasts to the wound site. Fibroblasts also produce PDGF by autocrine and paracrine stimulation. Activated fibroblasts proliferate and synthesize glycosaminoglycans, fibronectin, and collagen III to create a provisional matrix,[20,21] which together with macrophages, fibroblasts and newly generated capillaries, forms granulation tissue, replacing the fibrin matrix. Granulation tissue typically grows from the wound base.[22] In the early proliferation phase, TGF-β1, 2, and 3 play important roles to recruit fibroblasts and keratinocytes. TGF-β1 also induces the fibroblast–myofibroblast transformation for wound contraction.[1,22]

10.2.2.3 Maturation and Remodeling

The maturation and remodeling phase is characterized by the deposition of collagen with a well-organized structure. It begins about two weeks after injury and can last for more than a year. In the remodeling phase, macrophages, fibroblasts and endothelial cells gradually exit the wound area or undergo apoptosis, reducing cell numbers in the wound matrix dramatically.[4] Provisional matrix is gradually degraded and replaced by organized collagen matrix with increased percentage of collagen I, which improves the mechanical properties of the new matrix. Problems in new matrix deposition can compromise the strength of wounds. MMPs are the major proteinases in remodeling, and their production by fibroblasts and macrophages is regulated by the concentrations of TGF-β and other growth factors and cytokines.[8] Although collagen matrix becomes thicker and stronger in the remodeling process, the wound will never regain the strength of uninjured skin due to the non-ideal structure of new collagen.[23]

10.3 Current Methods and Material Applications in Wound Healing

10.3.1 Wound Dressings

Wound dressings are widely used in current wound care by providing a favorable local environment for natural healing. Wound dressings maintain moisture over wound areas, prevent infection, permit gas exchange, absorb exudates, and protect the wound base.[7,24] In recent years, many advanced dressings have been developed for delivering therapeutics to the wound site and/or possessing intrinsic functionalities to assist wound healing. Most of these materials are made of natural polysaccharides such as chitosan, hyaluronic acid (HA), alginates, and cellulose, or synthetic polymers such as polyvinyl alcohol (PVA),[25] polyethylene oxide (PEO),[26] and polyvinylpyrrolidone.[27] Alginate-based wound dressings are broadly used in wound healing. In addition, HA is an appealing wound dressing material because it is highly biocompatible as a natural component of extracellular matrix, and its biodegradation products can improve fibroblast proliferation and migration in a wound site.[28] Ong *et al.* reported that a chitosan dressing that contains a procoagulant (polyphosphate) and antimicrobial agent (silver) effectively improved the hemostatic and antimicrobial activity within wounds.[29]

10.3.2 Delivery Systems for Controlled Release of Growth Factors and Other Biomolecules

Growth factors regulate cell proliferation, cytokine production, cell–cell and cell–matrix interactions during wound repair. However, in chronic wounds, the level of growth factors has been shown to be low due to diminished synthesis and/or excessive protease-mediated degradation.[30] For instance, PDGF levels were found to be low within non-healing human ulcers, while improved healing of chronic wounds has been achieved by the delivery of recombinant PDGF into wound sites.[31] Drug delivery systems have focused on improving the stability of growth factors and allowing sustained release at wound sites, using materials such as polymeric micro and nanospheres,[32] lipid nanoparticles,[33,34] nanofibers,[35,36] and hydrogels.[37,38] Chu *et al.* utilized poly(lactic-*co*-glycolic acid) (PLGA) nanoparticles encapsulating recombinant human EGF to promote fibroblast proliferation. This was demonstrated by the increased expression of proliferating cell nuclear antigen in cells in diabetic rats.[39] Lai *et al.* developed a biomimetic nanofibrous matrix using collagen and hyaluronic acid for the multi-stage delivery of bFGF, EGF, VEGF and PDGF. The cytokines were encapsulated in nanofibers directly or in gelatin nanoparticles that were incorporated into nanofibers for sequential release by the slow degradation of the nanofibers/nanoparticles.[40]

In addition, polymeric delivery systems have been widely used as carriers for anti-oxidant and anti-inflammatory drugs to accelerate wound healing by curbing excessive inflammation in the inflammatory phase. Li and coworkers reported that the rate of re-epithelialization was greatly elevated using a

methoxypoly(ethylene glycol)-*graft*-chitosan film containing curcumin, an anti-inflammatory and antioxidant drug naturally produced by some plants.[41] Furthermore, DNA encoding growth factors or cytokines have been used to treat wounds through viral or non-viral gene delivery.[42] For example, cationic liposomal complexes have been employed to deliver genes for the co-expression of insulin-like growth factor-I (IGF-I) and KGF to improve dermal and epidermal regeneration of wounds *via* increased neovascularization.[43]

10.3.3 Stem Cell Therapy in Wound Repair

Another potential new approach for wound healing is stem cell therapy. Stem cells can self-renew and differentiate into various cell types, offering an alternative approach to reconstitute complex structures of wounds. Stem cells from various tissues, such as bone marrow, peripheral blood, adipose tissue, skin, and hair follicles, have been applied to modulate the healing of acute and chronic wounds.[42,44,45] Bone marrow-derived mesenchymal stem cells (MSCs) have been widely studied for tissue regeneration because of their multilineage potential and immune system evading characteristics, enabling the use of allogeneic MSCs in regeneration.[46] Falanga and coworkers showed that autologous MSCs could be safely and effectively delivered to wounds to accelerate their healing rate using a fibrin polymer spray.[47] Despite the successful demonstration of stem cell therapy in wound healing, the strategy still suffers from many limitations, such as maintaining cell viability long enough in the hostile wound microenvironment to create a therapeutic response.

In summary, wound healing is a well-orchestrated and choreographed process that involves the mediation of many components in the healing process. A variety of approaches and materials have been developed for regulating these mediators to promote the healing of both acute and chronic wounds. However, many challenges remain in the selection of optimal target sites, delivery of mediators with precise spatiotemporal controls, and development of programmed delivery systems. To overcome these limitations, multiple smart materials have recently been developed. In this review, we mainly focus on the classification and discussion of smart materials for wound healing according to the stimuli-responsive mechanisms. In addition, we offer some perspectives for the next generation of smart materials in wound healing.

10.4 Stimuli-Responsive Materials for Wound Healing

10.4.1 Reactive Oxygen Species (ROS)-Responsive Materials for Inflammation Treatment

Reactive oxygen species (ROS) such as hydrogen peroxide (H_2O_2), superoxide (O_2^-), and peroxynitrite ($ONOO^-$), are mediators of a variety of biological and pathological events. Elevated ROS result in oxidative stresses that can impair organs and tissues in acute and chronic inflammatory processes.

Table 10.1 ROS-responsive materials and their oxidation products.

ROS-responsive materials	Chemical structure and reaction	Ref.
Polypropylene sulfide (PPS)	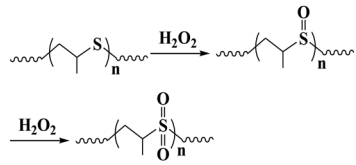	53–59
Poly(thiolketal)	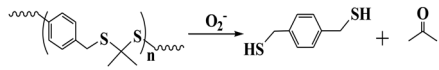	61–64
Polyoxalate	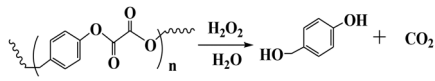	65,66,69,70,73 and 74
Boronic ester based polymer	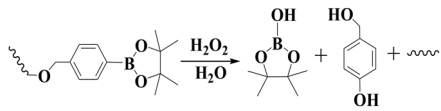	78
ROS-responsive materials *via* Fenton's reaction	$C_2H_5OH + H_2O_2 \xrightarrow{Fe^{2+}} CH_3COOH + H_2O$ $CH_3COOH \rightarrow CH_3COO^- + H^+$ $HCO_3^- + H^+ \rightarrow H_2CO_3 \rightarrow H_2O + CO_{2[g]}$	81

For example, unregulated ROS in chronic pro-inflammatory environments can lead to endothelial dysfunction and a predisposition to peripheral arterial disease.[48,49] Patients with chronic wounds usually remain in a constant pathological inflammatory state and are susceptible to oxidative stresses due to the excessive production of ROS. To harness the ability of ROS to degrade materials, ROS signals have been used to precisely trigger various interventions for wound inflammation treatment. In the past few decades, several classes of ROS-responsive materials have been designed and synthesized for targeted delivery of therapeutic and imaging agents (Table 10.1).[50,51] Current applications of ROS-responsive biomaterials for wound inflammation treatment are discussed in this section.

10.4.1.1 ROS-Responsive Materials via *Solubility Switch*

Poly(propylene sulfide) (PPS) is a hydrophobic polymer with a low glass-transition temperature (~230 K).[52] The sulfide groups in the backbone are sensitive to ROS through a solubility-switch mechanism whereby the sulfide group under oxidative conditions transforms to the more hydrophilic sulfoxide or sulfone group. Hubbell *et al.* first utilized ABA triblock copolymer

poly(ethylene glycol)-poly(propylene sulfide)-poly(ethylene glycol) (PEG-PPS-PEG) to fabricate ROS-responsive polymeric vesicles. These polymeric vesicles remained stable in aqueous solution and underwent a morphology transition from vesicles to worm-like and spherical micelles, and finally to water soluble substances after exposing to 10% H_2O_2.[53] PPS has also been found to be responsive to superoxides[54] and peroxynitrites.[55] The oxidation-responsive properties of PPS-based nanoparticles were explored by Hubbell *et al.* for delivering antigens to dendritic cells because the oxidative environment of dendritic cell endosomes can potentially improve cross-presentation of PPS nanoparticle-carried anitigens.[56,57] In addition to on-demand release of therapeutics, PPS alone showed inherent therapeutic properties for reducing the oxidative stress of wounds because of its ROS scavenging characteristics. Recently, Duvall *et al.* reported a physically cross-linked PPS-based hydrogel for ROS-triggered degradation and on-demand release of a fluorescent dye as a model drug.[58] The PPS hydrogel was shown to protect cells from H_2O_2-induced death *via* PPS scavenging. Utilizing this property, the same group developed ROS-responsive PPS microspheres for the on-demand delivery of curcumin for treating a mouse ischemic limb.[59] Micro-sized PPS particles encapsulating curcumin (curcumin–PPS microspheres) were fabricated *via* oil-in-water emulsion. Below 0.5 mM H_2O_2, both blank PPS and curcumin–PPS microspheres increased cell survival due to the H_2O_2 scavenging effects of PPS. Above 0.5 mM H_2O_2, curcumin–PPS (27.1 mM curcumin, 20.4 mg mL^{-1} PPS) microspheres showed significantly enhanced cell viability over blank PPS microspheres. In the mouse model of diabetic hind limb ischemia, the ROS level was significantly reduced at day seven in the extracted gastrocnemius muscles of mice that were treated with curcumin–PPS microspheres compared to those treated with PPS microspheres alone. Furthermore, curcumin–PPS microspheres also improved the recovery of blood oxygenation, perfusion, and vessel remodeling properties in the ischemic limb due to the synergistic effect of curcumin and PPS as ROS scavengers.

10.4.1.2 ROS-Responsive Materials via *Degradation*

10.4.1.2.1 Thioketal-Based Materials. Polymers containing thioketal linkages are cleaved into hydrophilic fragments such as ketones and organic thiols (or disulfides) in the presence of ROS, leading to degradation of polymers and the release of cargo.[60] Wilson *et al.* created a polymeric nanoparticle that contains ROS-reactive poly-(1,4-phenyleneacetone dimethylene thioketal) (PPADT), for oral delivery of siRNA to inhibit the expression of inflammatory proteins in the intestinal tissue (Figure 10.2). The PPADT nanoparticles remained stable in the gastrointestinal tract after oral administration, until they reached the inflammatory site where PPADT was degraded into acetone and 4-(mercaptomethyl)phenyl methanethiol in an oxidative environment. In a murine model of ulcerative colitis, the release of siRNA from PPADT nanoparticles

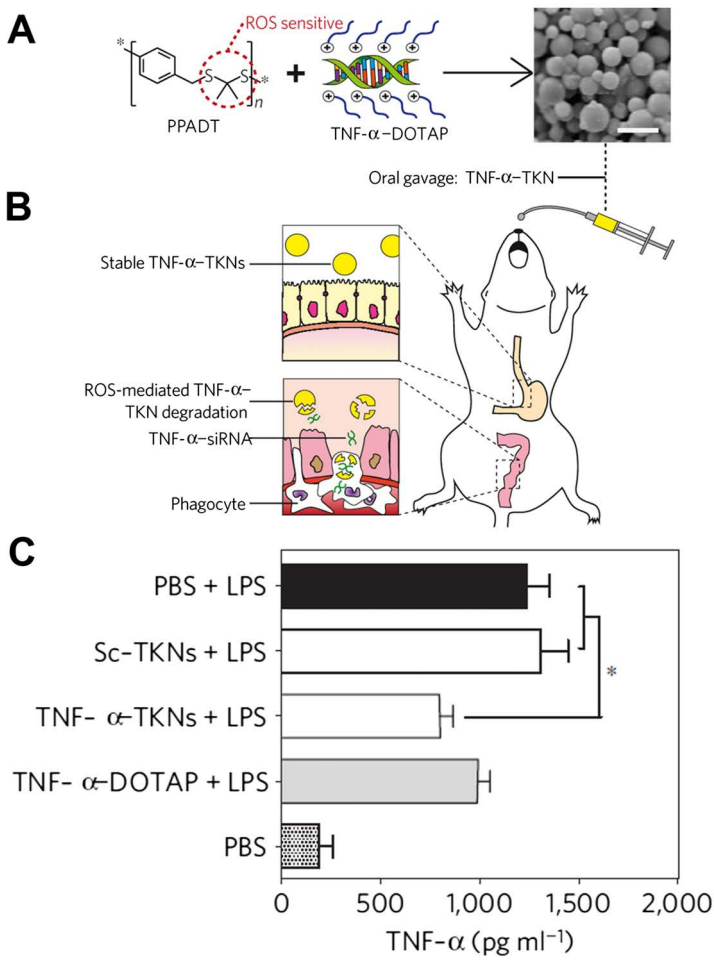

Figure 10.2 Schematic illustration of the fabrication and application of ROS-sensitive thioketal nanoparticles (TKNs). (A) TKNs encapsulating siRNA that specifically knock down TNF-α expression (TNF-α-TKNs) were prepared by adding TNF-α-siRNA and cationic lipid DOTAP complexes into PPADT solution. The SEM image shows TNF-α-TKNs (scale bar: 1.5 μm). (B) After being orally administered, TKN protected TNF-α-siRNA in the gastrointestinal tract and released the siRNA under elevated ROS concentrations at sites of intestinal inflammation. (C) TNF-α-TKNs treatment significantly reduced TNF-α production by lipopolysaccharide-activated macrophages. Values indicate mean ± s.e.m. (n = 3). (Reproduced with permission from ref. 61. Copyright© 2010, Nature Publishing Group.)

upon ROS triggering significantly reduced the expression of proinflammatory cytokine TNF-α in the colon and suppressed tissue inflammation.[61]

In order to accelerate neovascularization in wound areas, ROS-responsive nanoparticles based on poly-(1,4-phenyleneacetone dimethylene thioketal) were fabricated to encapsulate stromal cell-derived factor-1α (SDF-1α). The responsive release of SDF-1α in mice with full-thickness skin defects promoted the migration of MSCs toward the wound and its periphery, enhancing wound vascularization and healing.[62] Pu *et al.* reported ROS/pH dual-responsive chitosan-derived nanoparticles encapsulating PPADT for the delivery of curcumin to inflamed tissues.[63] Additionally, since the encapsulated curcumin and conjugated Cy3 formed an energy donor and acceptor pair, the nanoparticles could be used to monitor the intracellular release of drug *via* Förster resonance energy transfer (FRET). The oxidative stress and pH-triggered curcumin release from the nanoparticles were able to efficiently reduce ROS from lipopolysaccharide-stimulated macrophages thanks to the combined effects of extracellular free radical scavenging and intracellular inhibition of the oxidant production.

In a recent study, Martin and coworkers developed ROS-degradable porous scaffolds of poly(thioketal)-derived polyurethanes. Since the rate of cell-mediated degradation better matches the rate of tissue ingrowth in ROS-responsive scaffolds, they showed a performance superior to non-responsive poly(ester urethane) scaffolds in subcutaneous rat wounds as indicated by improved cellular infiltration, granulation tissue formation, and mechanical stability of subcutaneous implants.[64]

10.4.1.2.2 Polyoxalate-Based Materials. Aryl oxalate ester-containing polymers have been studied to reduce the oxidative stress in injuries because of their potent H_2O_2 scavenging activity.[65,66] In one example, H_2O_2-responsive polyoxalate was synthesized by polycondensation of 1,4-cyclohexamethanol with oxalyl chloride and 4-hydroxybenzyl alcohol (HBA), a phenolic compound for treating injuries with oxidative stress, such as ischemic brain injury and coronary heart disease.[51,67,68] The polyoxalate exerted excellent antioxidant activity by scavenging H_2O_2 *via* the peroxalate ester linkages and releasing HBA. *In vitro* and *in vivo* studies revealed that this polymeric antioxidant significantly reduced oxidative stress, inhibited NO by reducing the production of inducible nitric oxide synthases, and attenuated allergic inflammation.[69] Furthermore, multifunctional polyoxalate-based micelles were fabricated for therapeutic and diagnostic applications. This micelle was able to detect H_2O_2 at concentrations of 100 nM and illuminate H_2O_2 in inflamed mouse ankles.[70] In addition to HBA, vanillyl alcohol is also potent for anti-inflammation and antioxidation by scavenging ROS and suppressing pro-inflammatory cytokines, such as IL-1β, TNF-α, interferon-γ, and IL-6.[67,71,72] Lee and coworkers incorporated vanillyl alcohol into polyoxalate to synthesize inflammation-responsive nanoparticles,[65,73] which targeted ischemia/reperfusion (I/R) sites, and exhibited significant anti-oxidant and anti-apoptotic effects *in vivo* by inhibiting the activation of polyADP ribose polymerase-1 and caspase-3 in a mouse model of hind-limb I/R.[74]

10.4.1.2.3 Boronic Ester-Based Polymers. Boronic ester-containing polymers have been shown to generate phenol and boronic acid under H_2O_2-induced degradation. In past decades, several boronic ester derivatives have been studied as ROS-responsive materials for targeted delivery.[75–77] Lee and coworkers reported a H_2O_2-activatable antioxidant prodrug that contains a self-immolative boronic ester protecting group to release HBA by reacting with H_2O_2.[78] The prodrug showed antioxidant, anti-inflammatory and anti-apoptotic activities in hepatic I/R and cardiac I/R mouse models because of the combined effects of H_2O_2 consumption and HBA generation.

10.4.1.3 ROS-Responsive Materials via *Mediation of Fenton's Reaction*

Previous research of ROS-responsive drug delivery systems has focused on the synthesis of various ROS-sensitive polymers. However, these studies have limited clinical applications due to the reduced sensitivity of polymers under biologically relevant concentrations of ROS.[76] In 1894, Fenton discovered that many metals, such as iron, can catalyze H_2O_2 to generate highly reactive hydroxyl radicals ($OH^{\bullet}$).[79] H_2O_2 is a precursor of most ROS, while iron is an essential element in biological processes.[80] Some studies have utilized Fenton's reaction to trigger drug release in inflammatory environments. Recently, Chung and coworkers fabricated ROS-responsive PLGA microspheres for local inhibition of inflammation. The PLGA microsphere encapsulating dexamethasone sodium phosphate (DEX-P), ethanol, iron(II) salt ($FeCl_2$), and sodium bicarbonate (SBC) was prepared by a water-in-oil-in-water double emulsion using a microfluidic device. Within the inflammatory environment, H_2O_2 can diffuse into the PLGA microsphere to oxidize the encapsulated ethanol under catalysis of Fe^{2+}, forming acetic acid, which then reacts with SBC to generate CO_2 gas, disrupting the PLGA microsphere and releasing DEX-P. In an *in vivo* study, the inflammation-responsive PLGA microsphere showed sufficient sensitivity to a low concentration of H_2O_2 (50 μM) (Figure 10.3).[81] Similarly, Muhammad *et al.* reported an inflammation-responsive drug delivery system *via* mediation of Fenton's reaction. The nanochannels of mesoporous silica nanoparticles were capped by ultra-small thiol-stabilized ZnS quantum dots. Reactive hydroxyl radicals were generated at the site of inflammation by the catalysis of H_2O_2 in the presence of iron, which oxidized the thiol group of capped ZnS nanoparticles to open the drug-loaded nanochannels.[82]

In summary, ROS-responsive materials exhibit intrinsic advantages for alleviating excessive inflammation and are a novel and promising therapeutic platform to assist healing of acute and chronic wounds. However, some challenges have yet to be addressed, such as designing ultra-sensitive ROS-responsive materials that can distinguish the difference in ROS concentrations between pathological and normal cellular activities.

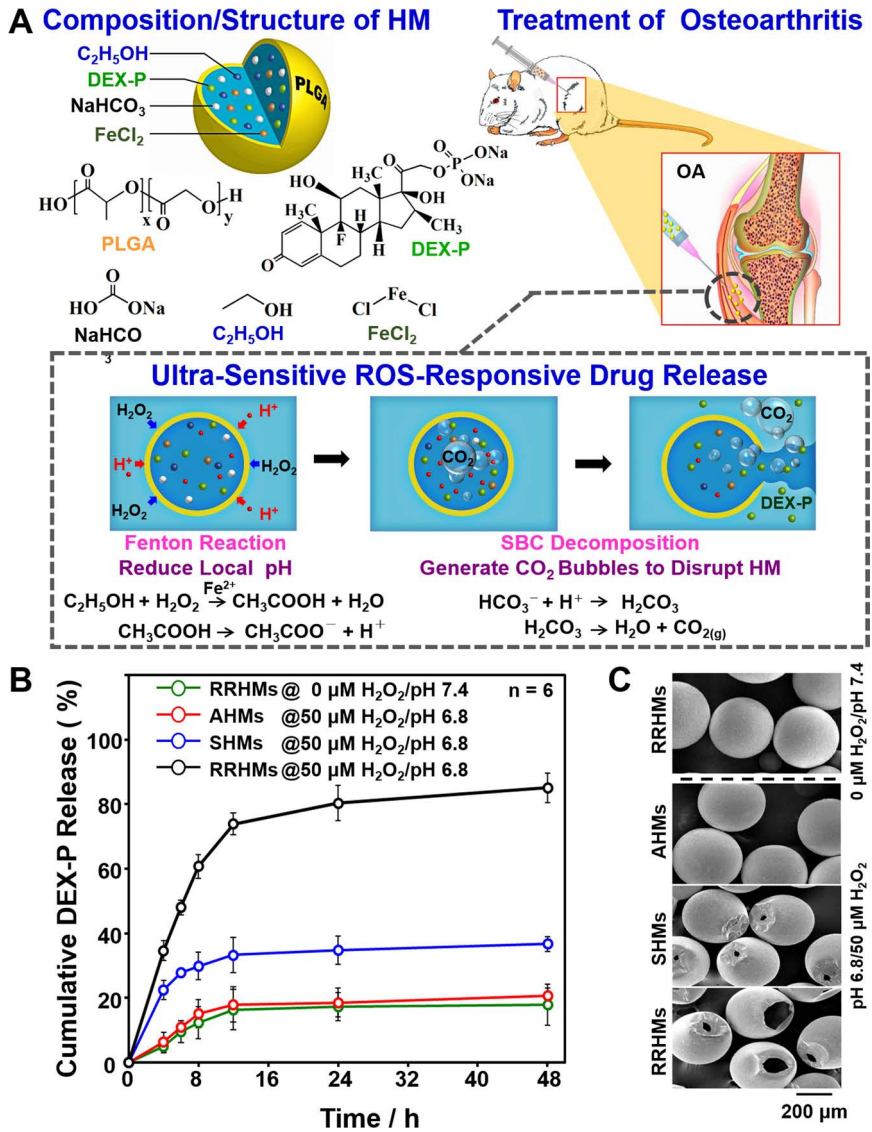

Figure 10.3 An ROS-responsive gas-generating hollow microsphere (HM). (A) Schematic illustration of fabricating an ROS-responsive gas-generating hollow microsphere and anti-inflammatory drug release in response to H_2O_2. (B) Release profile of dexamethasone sodium phosphate (DEX-P) from different HMs: ROS-responsive HMs (RRHMs), HMs encapsulating ethanol and $FeCl_2$ (AHMs), and HMs encapsulating sodium bicarbonate (SHMs). (C) SEM images of HMs with and without H_2O_2 treatment. (Reproduced with permission from ref. 81. Copyright© 2015, American Chemical Society.)

10.4.2 Temperature-Responsive Materials for Wound Healing

10.4.2.1 Temperature-Responsive Materials as Wound Dressings

Wound dressings can improve healing by providing an optimum environment for growth and regeneration. An ideal dressing should not adhere to the regenerated and surrounding tissues since removal of the adherent dressing from the wound bed is painful and may induce secondary injury.[24] Thermo-responsive materials have great potential for the fabrication of wound dressings with adhesion control because of their unique hydration–dehydration transition in response to temperature change. An extensively studied temperature-responsive polymer is poly(*N*-isopropylacrylamide) (PNIPAAm), which has a lower critical solution temperature (LCST) of around 32 °C in water.[83] Below the LCST, intermolecular hydrogen bonds between PNIPAAm and water stabilize the polymer. The polymer exhibits an extended chain conformation in aqueous solution. Above the LCST, PNIPAAm is dehydrated with a coil or globule chain conformation due to the formation of intramolecular hydrogen bonds and hydrophobic interactions between chain segments. As a result of this unique thermo-responsive property, PNIPAAm has been successfully used in cell culture where the cells can detach from the polymer without enzyme treatment,[84] implying that thermo-responsive PNIPAAm can be easily and painlessly detached as a wound dressing. In recent years, various PNIPAAm-based membranes, fibers, and hydrogels have been designed and synthesized as wound dressings.[85–91] For example, Lin and co-workers reported a drug-loaded wound dressing composed of a self-adhesive film with PNIPAAm microgel beads. The strength to peel the film at 25 °C is significantly lower than that at 37 °C.[24] PNIPAAm microgel beads contained in the film swelled at 25 °C, decreasing the adhesive property and causing the lower peel strength. Moreover, Yang *et al.* prepared transparent and thermo-sensitive membranes as wound dressings by bicontinuous microemulsion polymerization of *N*-isopropylacrylamide, methyl methacrylate, and 2-hydroxyethyl methacrylate.[92,93] The membranes exhibited a temperature-dependent cell detachment with increased water uptake at low temperatures.

Another important property of wound dressings is having the flexibility to mold to the shape of the wound during application and improve cell grafting. Additionally, the transparency of the membrane is useful to visualize the healing process and prevent premature removal of the dressing. Reddy *et al.* reported a wound dressing using flexible semi-interpenetrating polymer networks (semi-IPNs) consisting of polyurethane urea and PNIPAAm.[94] The semi-IPNs exhibited thermo-sensitivity in swelling and cell adhesion. When the environmental temperature was reduced to 15 °C, the cells detached from all the semi-IPN surfaces. In addition, poly(2-hydroxypropyl methacrylate) (PHPMA) is another polymer with thermo-responsive behavior in aqueous conditions.[95] Madsen *et al.* synthesized a thermo-responsive ABA triblock copolymer hydrogel for biocompatible wound dressings in which the A block is PHPMA and the B block is poly(2-(methacryloyloxy)ethyl

phosphorylcholine).[96] Gong *et al.* reported a drug delivery system with the ability to form a gel *in situ* for cutaneous wound healing.[97] Polymer micelles containing curcumin were encapsulated into a thermo-sensitive poly(ethylene glycol)-poly(ε-caprolactone)-poly(ethylene glycol) (PEG-PCL-PEG) hydrogel. The polymer formed a hydrogel *in situ* at body temperature and could easily fill irregularly shaped wounds. The hydrogel released curcumin in a sustained manner, promoting the tissue reconstruction processes.

10.4.2.2 Thermo-Responsive Materials for Inflammation Reduction

Using a similar strategy for local inflammation treatment, thermo-responsive polymer solutions can be injected locally at room temperature for complete wound coverage, and rapidly form a gel *in situ* at body temperature.[98] For example, Yang *et al.* synthesized a thermo-responsive poly(polyethylene glycol citrate-*co*-*N*-isopropylacrylamide) (PPCN) gel with a LCST of 26 °C. The gel has intrinsic antioxidant properties through scavenging free radicals, chelating metal ions, and inhibiting lipid peroxidation likely because of the citrate in the PPCN backbone.[99] Further, PPCN gels were able to deliver the chemokine SDF-1α in a controlled manner and support the viability and proliferation of vascular cells.

Nagasaki and coworkers developed an injectable system of thermo-responsive flower-like micelles *via* complexation of anionic poly(acrylic acid) with cationic poly[4-(2,2,6,6-tetramethylpiperidine-*N*-oxyl)aminomethylstyrene]-*b*-poly(ethyleneglycol)-*b*-poly[4-(2,2,6,6-tetramethylpiperidine-*N*-oxyl) aminomethylstyrene] (PMNT-PEG-PMNT) triblock copolymer.[100] The side chains of the PMNT segment are nitroxide radical compounds, which can scavenge ROS to prevent ROS-dependent reactions. The micelle solution undergoes sol–gel transition at body temperature. Different to the fast clearance of nitroxide radical compounds in injection sites, the gel can remain more than three days after subcutaneous injection. The injected hydrogel suppressed hyperalgesia *via* inhibiting neutrophil infiltration and cytokine production. Recently, the same group extended this system to function as an anti-adhesion agent for inflammation treatment.[101] Compared to a commercial anti-adhesion agent (Seprafilm®, Genzyme, Cambridge, MA), the injected hydrogel inhibited tissue adhesions and significantly suppressed inflammation *in vivo*.

10.4.2.3 Thermo-Responsive Materials with Antimicrobial Properties

There is an increased interest in designing wound dressings that possess antimicrobial properties. In the past few decades, a large number of silver-containing dressings had been used for wound management.[102–104] However, the leak of silver from the dressings could delay wound healing, especially in

large wounds such as burns, thus limiting their clinical application.[105] One property of infected wounds and skin is an elevated temperature compared with healthy surrounding tissue, for instance, the average temperature of infected leg ulcers is 2.46 °C higher than healthy skin.[106] Thus, a dressing that releases its antimicrobial payload in response to a change in temperature in an infected wound has attracted the attention of researchers. Jenkins *et al.* reported a thermo-responsive antimicrobial fabric made of poly(*N*-isopropylacrylamide)-*co*-allylamine (PNIPAM-*co*-ALA) nanogels that encapsulated silver nitrate and were grafted onto non-woven polypropylene.[107] The fabric showed greater anti-bacterial properties at 37 °C than at 28 °C due to the fast release of silver nitrate after the collapse of nanogels at 37 °C. Sui and co-workers also reported thermo- and redox-dual responsive antimicrobial poly(*N*-isopropylacrylamide)-poly(ferrocenylsilane) hydrogels, in which silver nanoparticles formed *in situ via* reduction of silver nitrate with the poly(ferrocenylsilane) chain.[108]

10.4.3 pH-Responsive Materials for Wound Healing

Scaffolds provide a structural support for cell adhesion, infiltration, and vascularization for wound healing. Since infection and inflammation can cause an acidic local microenvironment, pH-responsive scaffolds have the ability to swell and lead to increased oxygen penetration and cell infiltration for enhancing tissue regeneration. Recently, Auguste and coworkers prepared a series of pH-responsive scaffolds with different poly(dimethylaminoethyl methacrylate) (PDMAEMA) content.[109] The scaffolds that were able to expand in response to a decrease in pH improved macrophage infiltration and promoted wound healing. After being implanted subcutaneously in rats, the scaffolds showed increased granulation tissue and upregulated growth factor expression. Cui *et al.* also reported an acid-responsive PLLA fibrous scaffold encapsulating ibuprofen for inhibiting inflammation and promoting muscle wound healing.[110,111] Sodium bicarbonate as an acid-triggered gas generator was also encapsulated in the scaffold to achieve responsive release of ibuprofen. The *in vivo* study showed this acid-responsive PLLA fibrous scaffold reduced inflammatory factors (IL-6 and TNF-α), while increasing the expression of repair factors (VEGF and TGF-β1).

Micro/nanoparticle systems with pH-responsive properties have also been developed for inflammation treatment. Sung *et al.* reported an injectable calcium phosphate (CP) cement that contained pH-responsive PLGA hollow microspheres (HMs).[112] Under acidic conditions, CO_2 bubbles were quickly generated through the reaction of encapsulated sodium bicarbonate with acid. The bubbles disrupted the PLGA shells and triggered vancomycin release from the HMs. The cement exhibited highly effective local antibacterial activity in a rabbit model study. Nagasaki *et al.* developed a pH-responsive nitroxide radical-containing nanoparticle (RNP^{pH}) for protection against acute kidney injury.[113] RNP^{pH} is made of copolymers with 2,2,6,6-tetramethylpiperidine-*N*-oxyl (TEMPO) moieties, which is a strong ROS scavenger,

while nitroxide radicals can catalyze ROS scavenging. RNP^{pH} disassembled at low pH due to the amino group protonation in the hydrophobic core. The exposure of TEMPO and nitroxide radicals efficiently scavenged ROS and led to renal protective effects in a renal ischemia-reperfusion AKI mouse model.

10.4.4 Enzyme-Responsive Materials in Wound Healing

Materials that mimic extracellular matrix (ECM) such as hydrogels and films have emerged as valuable tools to examine the dynamic interactions between cells and ECM in tissue generation because these materials allow for two- and three-dimensional cell culture in defined environments with spatial and temporal property controls. Moreover, it is ideal to match the degradation rate of ECM-mimicking materials to tissue regeneration and achieve on-demand delivery of growth factors and cytokines in response to intrinsic wound repair signals. Scaffold materials that degrade too quickly will attenuate the support to tissue ingrowth, while those that degrade too slowly will prevent proper tissue development.[114] Recently, inspired by the fact that many degradation processes in living organisms are mediated by enzymes, enzyme-responsive biomimetic materials with degradation rates and on-demand delivery of bioactive agents consistent to the local microenvironment have been developed.[115–118]

10.4.4.1 Matrix Metalloproteinase-Responsive Materials in Wound Healing

Matrix metalloproteinases (MMPs) are a family of proteases that degrade ECM proteins and also cleave many other proteins such as cell surface receptors.[119] As discussed in Section 10.3, MMPs play a critical role in wound healing. These unique features make MMPs special enzymes for designing responsive materials in the wound healing process. Hubbell and coworkers first synthesized MMP-responsive PEG-based hydrogel scaffolds that permit cell migration.[120–122] The MMP degradable hydrogel was prepared *via* a Michael-type addition reaction between vinyl sulfone groups at the end of four-arm PEGs and the thiol groups in the MMP cleavable substrate peptides flanked by two cysteine residues. RGD peptides were also incorporated in the gel formation step to support cell attachment. Primary human fibroblasts were able to invade the hydrogel by secreting MMPs to degrade hydrogel cross-linkers. Their *in vivo* study demonstrated that tissue regeneration mainly depended on the MMP sensitivity of the networks. In addition, the group also studied cell migration using MMP-degradable PEG hydrogel (M-PEG) and plasmin-degradable PEG hydrogel (P-PEG) mimicking ECM.[123] The morphology of human fibroblasts and their migration patterns were found to be significantly different in M-PEG and P-PEG. Cell migration in M-PEG was highly dependent on MMP modulation. M-PEG containing an MMP inhibitor suppressed cell migration, while M-PEG containing an MMP

stimulator enhanced cell migration. Steinhagen *et al.* chemically conjugated SDF-1α on polymeric films *via* a MMP-9 cleavable peptide as the linker.[124] Since the upregulation of MMP-9 is important for ECM breakdown and cell invasion during inflammation, the MMP-9 cleavage linker allowed for on-demand release of SDF-1α, which recruited stem cells for potential wound regeneration. Separately, Nguyen and co-workers synthesized peptide–polymer amphiphiles, in which the peptides are the substrates of MMP-2 and MMP-9. Spherical nanoparticles formed *via* the polymer self-assembly could accumulate in the infarct after systemic administration due to the leaky vasculature after myocardial infarction (MI). The degradation of peptides close to nanoparticle surfaces by MMPs in MI converted the discrete nanoparticles into network-like scaffolds, enhancing nanoparticle retention times for up to 28 d post-injection and prevented the progression of negative left ventricular remodeling (Figure 10.4).[125]

Excessive MMP activity is a hallmark of many inflammation-related diseases and contributes to adverse tissue remodeling.[126] However, inhibition of MMP activities may delay or prevent wound healing if not controlled properly. Burdick *et al.* have developed an injectable hydrogel containing MMP-degradable crosslinks and encapsulated a recombinant tissue inhibitor of MMPs (rTIMP-3).[127] This system released rTIMP-3 under excessive MMP concentrations following a MI. rTIMP-3 was bound to negatively charged polysaccharide in hydrogels through electrostatic interactions to reduce passive diffusion/release. The degradation of the hydrogel under elevated MMPs after MI expedited the release of rTIMP-3, reducing MMP activity to attenuate adverse ventricular remodeling. The active release of rTIMP-3 was turned off when MMP concentration decreased (Figure 10.5). This design is the first to establish a negative-feedback mechanism between wound and biomaterials.

10.4.4.2 Other Enzyme-Responsive Materials in Wound Healing

In addition to MMPs, the inflammatory phase is also accompanied by up-regulation of elastase and hydrolytic proteases, such as human neutrophil elastase (HNE).[128,129] Anseth and coworkers reported a PEG hydrogel platform with HNE substrate peptides as cross-linkers, making the gel degradable in inflammatory areas.[130,131] Additionally, the same authors showed that RGD peptide can be incorporated into the hydrogel to study adhesion of valvular interstitial cells, which display a myofibroblastic phenotype upon heart valve injury.[132,133] Zhao and co-workers fabricated a β-galactosidase-responsive hydrogel by the self-assembly of short peptides and caged NO molecules. The gel sustained released NO by the addition of β-galactosidase to remove the sugar capping group on the caged NO molecule.[134] The *in vivo* study showed that this β-galactosidase-responsive hydrogel could accelerate wound healing by promoting angiogenesis in the wound bed. Zhang and Karp *et al.* reported negatively charged hydrogel microfibers that bound to a positively charged inflamed colon surface in a mouse model of ulcerative colitis.[135] The hydrogel

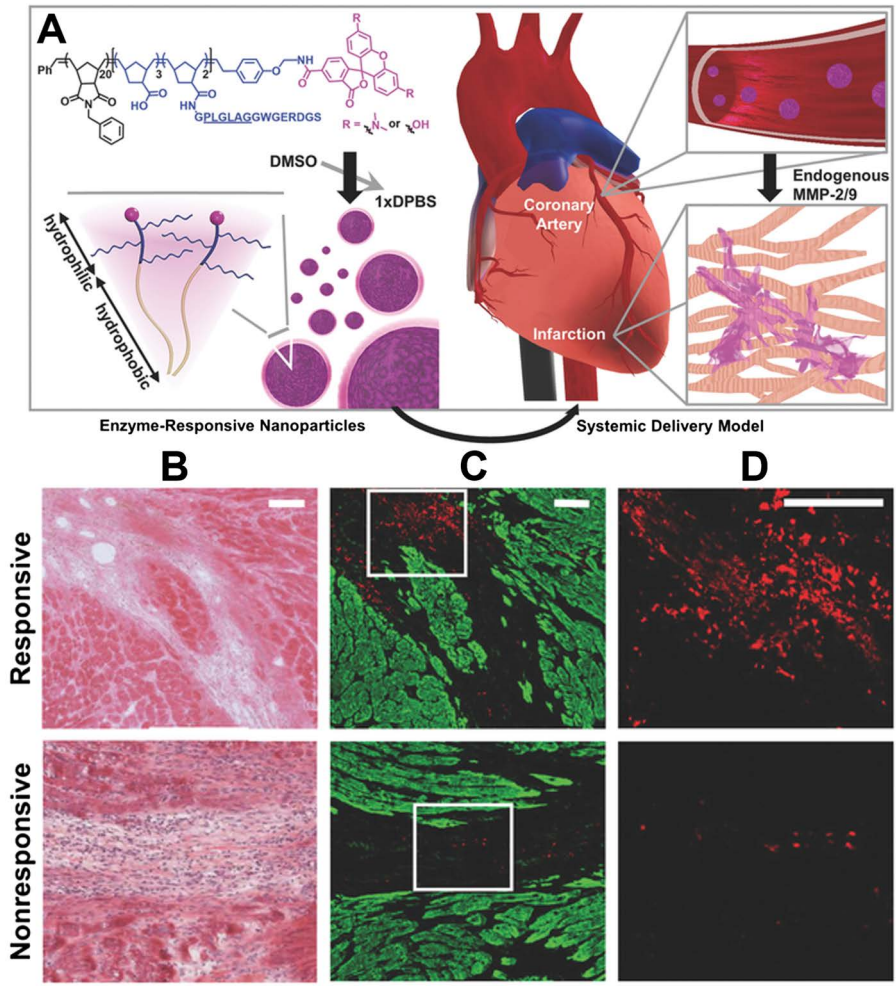

Figure 10.4 Accumulation and prolonged retention of enzyme-responsive nanoparticles in heart tissue after myocardial infarction. (A) Schematic illustration of MMP-responsive nanoparticles that converted from the discrete nanoparticles into network-like scaffolds in myocardial infarction. The nanoparticles were formed by the self-assembly of a peptide–polymer amphiphile containing an MMP-2 and MMP-9 specific recognition sequence. The generation of a network-like scaffold resulted in prolonged particle retention. (B) H&E images of the infarct area, and (C) fluorescence images showing particles (red) retained in the myocardium, which was illustrated by anti-α-actin in staining (green). (D) High magnification images of the selected regions in (C). Scale bar: 100 μm. (Reproduced with permission from ref. 125. Copyright© 2015, John Wiley & Sons, Inc.)

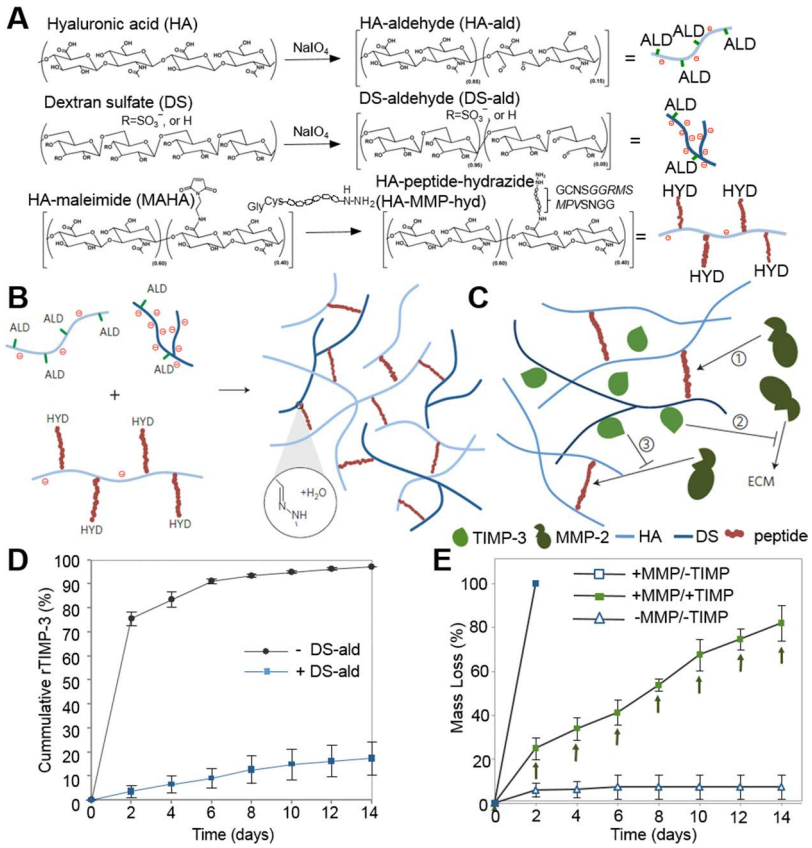

Figure 10.5 Schematic illustration of MMP-responsive hydrogel synthesis and rTIMP-3 release from hydrogels. (A) Synthesis of aldehyde (ALD)-modified hyaluronic acid (HA) and ALD-modified dextran sulfate (DS) and peptide-modified HA. The peptide is a substrate of MMP and contains a hydrazide (HYD) group for reacting with the ALD group. (B) Hydrogel formation. The rationale to incorporate DS is to utilize its interaction with rTIMP-3 to reduce rTIMP-3 passive release. (C) Schematic illustration of rTIMP-3 release under MMP by degrading peptide linker of the hydrogel (1). Increased rTIMP-3 release (2) inhibits local MMP activity and reduces further hydrogel degradation (3). (D) Passive release profile of rTIMP-3 from hydrogel with and without DS. (E) Degradation of hydrogels with (filled symbols) and without (open symbols) encapsulated rTIMP-3 under conditions with (squares) or without (triangles) MMP. Arrows indicate the date to add fresh MMP. (Reproduced with permission from ref. 127. Copyright© 2014, Nature Publishing Group.)

microfibers were generated from the self-assembly of ascorbyl palmitate and were loaded with dexamethasone (DEX), an anti-inflammatory corticosteroid. At the inflammatory site, macrophages and other immune cells secrete hydrolytic enzymes, which degrade the hydrogel and trigger the local release of DEX from the hydrogel microfibers. Griffin and coworkers developed an

injectable, microporous scaffold formed by microgel particles that crosslink *in situ* in wound sites under activated Factor XIII (FXIIIa). FXIIIa is an enzyme that is involved in blood co-agulation to form fibrin networks. The scaffold was shown to facilitate cell infiltration and accelerate cutaneous-tissue regeneration and tissue-structure formation.[136]

The programmable presentation of growth factors, cytokines, and enzymes is highly important for the hierarchical remodeling of a wound. Thus, the delivery of multiple signaling molecules in a desired sequence using responsive materials has attracted the attention of researchers. Wang *et al.* successfully demonstrated that multiple proteins can be sequentially released in predetermined stages from hydrogels that were functionalized with nucleic acid aptamers. Aptamers bind to specific proteins, and protein release is triggered when nucleic acids with complementary sequences change the aptamer conformation, reducing their interaction with the proteins. Sequential release of proteins was achieved by using a few pairs of aptamer-triggers (nucleic acids with a complementary sequence) and sequentially applying different triggers (Figure 10.6).[137] Segura and Lu *et al.* developed enzyme-responsive delivery of proteins through *in situ* encapsulation of protein and polymerization of monomers using cleavable peptide linkers.[138] Proteolytic kinetics of peptide substrates depends on their chirality structures (*i.e.* approximately 10-fold slower for the D enantiomer than the L enantiomer). Thus, by changing the chirality ratios of the peptide crosslinkers, the investigators were able to control sequential release of multiple encapsulated proteins under proteolytic enzymes in wound sites (Figure 10.7). The sequential release of VEGF and PDGF from nanocapsules enhanced the growth of granulation tissue and pericyte-covered blood vessels in a diabetic skin wound model.

10.4.4.3 Bacterial Enzyme-Responsive Materials for Infection Control

The invasion and proliferation of pathogenic bacteria in wound sites represent a ubiquitous problem in the wound healing process. Therefore, smart materials that can detect pathogenic bacteria in advance or are capable of triggering the release of antibacterial agents by the presence of bacteria are promising strategies to improve wound healing. Recently, Schönherr *et al.* reported a chitosan-based platform for *in situ* detection of the enzyme β-glucuronidase (β-GUS), which is secreted by the bacterium *Escherichia coli*.[139] In the presence of β-GUS, the covalent coupled dyes on the surface were rapidly cleaved and produced a signal which was detectable by the naked eye under appropriate illumination. In another example, Landfester *et al.* synthesized hyaluronic acid-based nanocapsules that encapsulate polyhexanide, an antimicrobial agent.[140] The nanocapsules were selectively degraded by gram-positive staphylococcus bacteria-secreted hyaluronidase in wounds. The hyaluronidase-triggered release of polyhexanide demonstrated a higher antibacterial efficiency than the control capsules made of hydroxyethyl starch.

In summary, proteases are essential in tissue regeneration. Therefore, it is expected that research efforts will continue to be directed towards

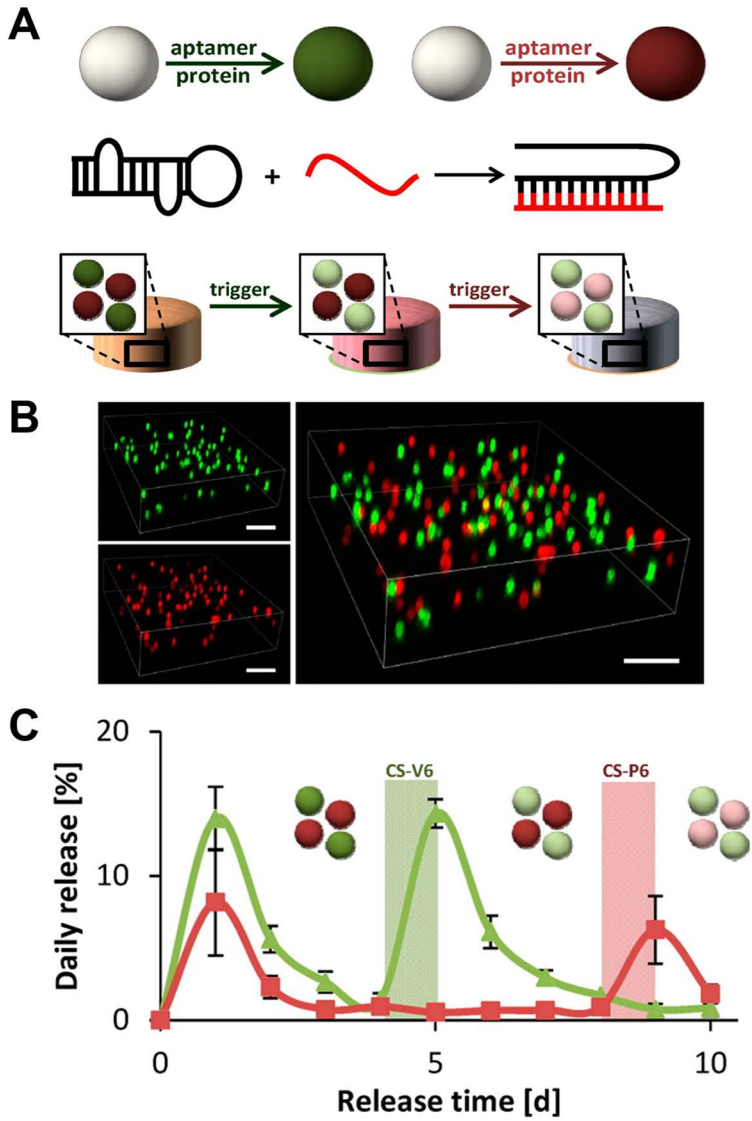

Figure 10.6 Programmable release of multiple protein from aptamer-functionalized hydrogels. (A) Schematic illustration of aptamer-functionalized hydrogel fabrication and programmable release of multiple protein. The release is triggered by nucleic acids with complementary sequence. (B) Confocal microscopy images of the two aptamer-functionalized particles in the hydrogel. Scale bars: 10 μm. (C) VEGF (green) and PDGF-BB (red) release from hydrogels *via* sequence-specific trigger. The amounts of proteins were illustrated by the color intensity of the balls. The light colors indicate fewer proteins. (Reproduced with permission from ref. 137. Copyright© 2012, American Chemical Society.)

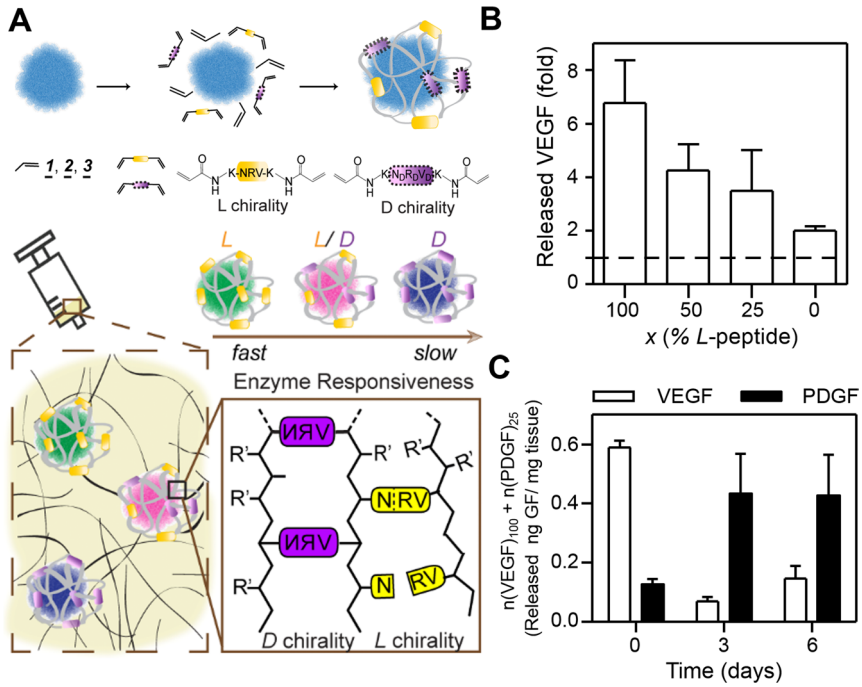

Figure 10.7 Enzyme-responsive delivery of multiple proteins with spatiotemporal control. (A) Schematic illustration of the fabrication of enzyme-responsive protein nanocapsules and their chirality-controlled enzymatic degradation. Nanocapsules are synthesized by *in situ* polymerization of monomers and crosslinkers around individual proteins. The plasmin-sensitive peptides served as labile crosslinkers that included a mixture of peptide enantiomers with designed molar ratios of L and D. Nanocapsules with multi-protein delivery are achieved by controlling the enzyme degradation rate of individual nanocapsules *via* adjusting the molar ratio of L to D in peptide crosslinkers. A higher L content resulted in a faster protein release rate. (B) Plasmin-triggered release profile of VEGF from nanocapsules with different L to D ratios. (C) Temporally controlled release of VEGF and PDGF from nanocapsules in diabetic mouse skin wounds. (Reproduced with permission from ref. 138. Copyright© 2015, John Wiley & Sons, Inc.)

enzyme-responsive materials for wound healing. Enzyme-triggered self-assembly of materials mimicking the cell matrix *in situ* and on-demand degradation of biomimetic materials may represent promising approaches for targeted and precise therapies for certain wounds.

10.4.5 Activated Platelet-Responsive Materials in Wound Healing

Although much progress has been made in developing stimuli-responsive materials for topical and easily accessible wounds, improving the treatment of internal bleeding has been more challenging. Approaches to promote

hemostasis after severe internal bleeding have used modified cells, liposomes, or polymeric particles to target the glycoprotein IIb/IIIa receptor on activated platelets to expedite the generation of a robust clot.[141] Critical design features for this objective include being small enough to circulate through lung capillaries, being easily producible and cost effective, having a sufficiently long circulation time, and not causing unwanted clots or side effects. To address these issues, Lavik and colleagues have developed intravenously injected polymeric nanoparticles to facilitate clotting at sites of internal injury.[141] The system is selectively activated at the site of injury by conjugating RGD peptide *via* a PEG linker to poly(lactic-*co*-glycolic) acid-poly-L-lysine (PLGA-PLL) nanoparticles, which binds to activated platelets at a site of injury. This creates a nanostructure that decreases the time of coagulation by promoting the aggregation of more platelets. Away from the site of injury, the nanoparticles do not cause clots and are rapidly cleared by the body within 24 hours. Their group showed that i.v. administration of these particles to mice five minutes after a blast injury with multiorgan hemorrhaging resulted in a significant improvement in survival.[142]

10.5 Recent Advances in Wound Healing and Future Directions

As our understanding of the biological processes involved in wound healing increases, materials can be engineered more effectively to promote high-quality wound healing. A deeper knowledge of the specific cell types and signaling molecules involved in healing different types of wounds, along with their temporal distribution, has enabled more efficacious wound treatments. Whereas many smart material systems in the past have been designed to release therapeutics in response to a single stimulus, precision treatments that respond to the dynamic nature of the wound healing environment are needed. Such treatments are beginning to emerge, as demonstrated by Wang and colleagues, who designed a novel aptamer-based hydrogel system that was able to release different growth factors in response to different stimuli in the form of complementary aptamer sequences.[137] However, more research is needed to develop multi-responsive systems that precisely respond to physiological signals of *in vivo* wound healing processes. Other novel treatments in development, such as gene therapy, stem cell-based therapies, and targeted immunotherapies, have also shown promise in improving wound healing.[143–146]

10.5.1 Gene Therapy in Biomaterials

As previously stated, many growth factors play key roles in the process of tissue regeneration and are insufficient at the sites of injuries. However, topical delivery of growth factors has had limited success, due to the presence of proteolytic enzymes and low diffusion rates into the wound.[146]

Thus, genetically engineered cells producing desired growth factors can greatly increase the effectiveness of therapy. Traditional approaches of delivering genetic material involve viral vectors, liposomes, or various direct seeding methods.[147] However, while these methods have demonstrated accelerated re-epithelialization and improved wound healing in many animal models, few have been translated for use in human trials. Furthermore, the majority of existing studies focus on delivering a single gene, which does not reflect the dynamic and complex needs of wound healing. Studies have begun to explore the delivery of a combination of growth factor genes, which have shown higher efficacy than delivery of individual genes.[148] The ability to control sequential delivery of different genes in response to signals in the wound microenvironment would further increase the applicability of the strategy. Such a goal is well-suited for stimuli-responsive biomaterials *via* incorporation of genes in modified liposomes, polymeric particles, or scaffolds.

More recently, gene therapy has advanced to include the use of microRNA (miRNA) for wound healing applications.[149] MiRNA are short, non-coding sequences of RNA that have functions in post-transcriptional gene regulation by pairing with complementary sequences in messenger RNA (mRNA) to control cell proliferation, differentiation, apoptosis, and protein production. The small size of miRNA sequences of 20–24 nucleotides has made them attractive targets for controlled delivery using a variety of biomaterials strategies. One emerging modality for wound healing applications is the use of three-dimensional polymeric scaffolds to locally present miRNA to cell populations seeded or recruited to the scaffold. For instance, sustained release of the miRNA miR-29b in a hydrogel scaffold was shown to help restore the natural composition of collagen type I and III, and increase granulation tissue in Lewis rats with full thickness excisional dermal wounds.[150] The use of stimuli-responsive scaffolds has also been explored, such as the release of nucleic acids from hyaluronic acid-based scaffolds that degrade in the presence of hyaluronidase.[151,152] These studies demonstrate the therapeutic potential of using multi-responsive scaffolds to deliver multiple types of miRNA in a sequential fashion at different stages of wound healing.

10.5.2 Stem Cell Delivery

Another developing strategy for wound repair aims to harness the regenerative capabilities of stem cells to improve the healing capacity of serious acute and chronic wounds. Stem cell-based technologies have shown great potential in accelerating wound closure, increasing re-epithelialization, and improving angiogenesis in both animals and humans.[47,153,154] However, as previously mentioned, one limiting factor when delivering stem cells to wound sites is the hostile oxidative and inflammatory local environment, which leads to death or undesired differentiation of stem cells and decreases their effectiveness.[155] Delivering cells *via* injection further decreases cell engraftment, possibly due to shear forces during the injection process.[156] Scaffold-based technologies can therefore play an important role in protecting cells during

delivery and maintaining their regenerative abilities. Composed of materials such as collagen, hyaluronic acid, or other natural or synthetic polymers, these scaffolds can deliver pre-seeded cells to the wound site while maintaining a more controlled extracellular environment, which has been shown to better preserve the stemness of injected cells.[157] Furthermore, it has been shown that a pullulan–collagen scaffold can intrinsically quench free radicals present in the wound site, thereby increasing cell survival.[158] The tunability of polymeric scaffolds enables an increasing control of the timing, rate, and quality of stem cell delivery. Moreover, the ability of the scaffold environment to maintain cytokines, anti-inflammatory substances, and small molecules may help direct or maintain the regenerative ability of the cells. Nowadays, researchers are beginning to explore the effects of combining gene and stem cell therapy, a potentially powerful tool for engineering regenerative environments.[159]

10.5.3 Advances in Immunotherapy

Recently, advances in immunology have begun to uncover the roles of recruited immune cells in sites of injuries. This has led to an increased understanding of how to engineer biomaterials to improve the process of wound healing. For instance, monocytes have been shown to exhibit distinct phenotypes with inflammatory or anti-inflammatory roles for clearing debris or promoting angiogenesis and tissue regeneration, respectively.[143,160] Botchwey and colleagues used PLGA thin films to deliver FTY720, which is a sphingosine 1-phosphate receptor 3 (S1PR) agonist, to inflamed and ischemic tissues, resulting in the local enrichment of anti-inflammatory monocytes and improved angiogenesis. They demonstrated the recruitment of regenerative immune cells and the degree of vascular remodeling were highly dependent on the gradient of S1PR agonists, a property that can be controlled using smart biomaterials systems.[161] As another example, Elisseeff and colleagues demonstrated the importance of T helper 2 (Th2) cells in regenerative scaffolds. This was a surprising finding due to the classical role of Th2 cells as part of the adaptive immune system, rather than the innate immune system typically implicated in healing responses.[162] In the study, it was shown that IL-4 produced by Th2 cells is necessary to direct macrophage polarization towards a regenerative response. These types of discoveries in wound immunology will inform the design of smart materials systems, such as by designing an environment that fosters Th2 cell recruitment and differentiation. Wound healing will undoubtedly benefit from such advances in immunological understanding in the future.

10.6 Conclusion

A variety of stimuli-responsive materials have been developed in the past two decades to selectively release their payloads and/or support cell growth *in situ* for improving wound healing. Although great progresses have been made in

this field, many challenges remain and require continued research and innovative solutions. For instance, wound healing is a complicated process involving orchestrated expression of cytokines, growth factors, and proteolytic enzymes. Hence, it is necessary to develop stimuli-responsive materials that can sequentially deliver multiple signaling molecules in a pre-defined manner or in a step-by-step manner in response to different triggers. Furthermore, the most studied stimuli for controlled release in wounds include pH gradient, temperature, ROS, and a few enzymes. The abundant proteins, cells and other biomolecules present in the wound site are just beginning to be integrated into the design of biomaterials. Finally, only a few stimuli-responsive materials have been translated to clinical applications. In order to address these limitations, it is important to develop stimuli-responsive materials that rigorously meet clinical standards and are reproducible on a large scale in a cost efficient manner.[163] In summary, the reviewed studies shed light on the great potential of stimuli-responsive materials for wound healing. Further development of new materials will pave the way to develop more accurate delivery systems for the next generation of wound care.

References

1. T. N. Demidova-Rice, M. R. Hamblin and I. M. Herman, *Adv. Skin Wound Care*, 2012, **25**, 304.
2. C. K. Sen, G. M. Gordillo, S. Roy, R. Kirsner, L. Lambert, T. K. Hunt, F. Gottrup, G. C. Gurtner and M. T. Longaker, *Wound Repair Regen.*, 2009, **17**, 763.
3. G. S. Lazarus, D. M. Cooper, D. R. Knighton, D. J. Margolis, R. E. Pecoraro, G. Rodeheaver and M. C. Robson, *Arch. Dermatol.*, 1994, **130**, 489.
4. G. C. Gurtner, S. Werner, Y. Barrandon and M. T. Longaker, *Nature*, 2008, **453**, 314.
5. C. Merkel, M. Bolognesi, D. Sacerdoti, G. Bombonato, B. Bellini, R. Bighin and A. Gatta, *Hepatology*, 2000, **32**, 930.
6. J. S. Boateng, K. H. Matthews, H. N. Stevens and G. M. Eccleston, *J. Pharm. Sci.*, 2008, **97**, 2892.
7. N. Mayet, Y. E. Choonara, P. Kumar, L. K. Tomar, C. Tyagi, L. C. Du Toit and V. Pillay, *J. Pharm. Sci.*, 2014, **103**, 2211.
8. G. Broughton, J. E. Janis and C. E. Attinger, *Plast. Reconstr. Surg.*, 2006, **117**, 12S.
9. H. O. Ogedegbe, *Lab. Med.*, 2002, **33**, 948.
10. T. N. Mayadas, R. C. Johnson, H. Rayburn, R. O. Hynes and D. D. Wagner, *Cell*, 1993, **74**, 541.
11. M. B. Witte and A. Barbul, *Surg. Clin. North Am.*, 1997, **77**, 509.
12. C. W. Wyble, K. L. Hynes, J. Kuchibhotla, B. C. Marcus, D. Hallahan and B. L. Gewertz, *J. Surg. Res.*, 1997, **73**, 107.
13. D. R. Yager and B. C. Nwomeh, *Wound Repair Regen.*, 1999, **7**, 433.
14. C. Szabo, H. Ischiropoulos and R. Radi, *Nat. Rev. Drug Discovery*, 2007, **6**, 662.

15. A. J. Nappi and E. Vass, *Biochim. Biophys. Acta, Gen. Subj.*, 1998, **1380**, 55.
16. R. Goldman, *Adv. Skin Wound Care*, 2004, **17**, 24.
17. L. H. Evers, D. Bhavsar and P. Mailander, *Exp. Dermatol.*, 2010, **19**, 777.
18. Y. P. Xia, Y. N. Zhao, J. Marcus, P. A. Jimenez, S. M. Ruben, P. A. Moore, F. Khan and T. A. Mustoe, *J. Pathol.*, 1999, **188**, 431.
19. P. A. Jimenez and M. A. Rampy, *J. Surg. Res.*, 1999, **81**, 238.
20. G. F. Pierce, T. A. Mustoe, B. W. Altrock, T. F. Deuel and A. Thomason, *J. Cell. Biochem.*, 1991, **45**, 319.
21. S. E. Lynch, J. C. Nixon, R. B. Colvin and H. N. Antoniades, *Proc. Natl. Acad. Sci. U. S. A.*, 1987, **84**, 7696.
22. A. J. Singer and R. A. F. Clark, *N. Engl. J. Med.*, 1999, **341**, 738.
23. S. M. Levenson, E. F. Geever, L. V. Crowley, J. F. Oates 3rd, C. W. Berard and H. Rosen, *Ann. Surg.*, 1965, **161**, 293.
24. S. Y. Lin, K. S. Chen and L. Run-Chu, *Biomaterials*, 2001, **22**, 2999.
25. R. A. Perez, J. E. Won, J. C. Knowles and H. W. Kim, *Adv. Drug Delivery Rev.*, 2013, **65**, 471.
26. K. Y. Lee and D. J. Mooney, *Chem. Rev.*, 2001, **101**, 1869.
27. L. Y. Qiu and Y. H. Bae, *Pharm. Res.*, 2006, **23**, 1.
28. M. Moczar and L. Robert, *Exp. Gerontol.*, 1993, **28**, 59.
29. S. Y. Ong, J. Wu, S. M. Moochhala, M. H. Tan and J. Lu, *Biomaterials*, 2008, **29**, 4323.
30. S. Barrientos, O. Stojadinovic, M. S. Golinko, H. Brem and M. Tomic-Canic, *Wound Repair Regen.*, 2008, **16**, 585.
31. G. F. Pierce, J. E. Tarpley, J. Tseng, J. Bready, D. Chang, W. C. Kenney, R. Rudolph, M. C. Robson, J. Vande Berg and P. Reid, *et al.*, *J. Clin. Invest.*, 1995, **96**, 1336.
32. M. L. Ye, S. Kim and K. Park, *J. Controlled Release*, 2010, **146**, 241.
33. A. J. Almeida and E. Souto, *Adv. Drug Delivery Rev.*, 2007, **59**, 478.
34. G. Gainza, D. C. Bonafonte, B. Moreno, J. J. Aguirre, F. B. Gutierrez, S. Villullas, J. L. Pedraz, M. Igartua and R. M. Hernandez, *J. Controlled Release*, 2015, **197**, 41.
35. J. S. Choi, K. W. Leong and H. S. Yoo, *Biomaterials*, 2008, **29**, 587.
36. Y. Yang, T. Xia, W. Zhi, L. Wei, J. Weng, C. Zhang and X. H. Li, *Biomaterials*, 2011, **32**, 4243.
37. A. C. Brown and T. H. Barker, *Acta Biomater.*, 2014, **10**, 1502.
38. Y. Xie, Z. Upton, S. Richards, S. C. Rizzi and D. I. Leavesley, *J. Controlled Release*, 2011, **153**, 225.
39. Y. J. Chu, D. M. Yu, P. H. Wang, J. Xu, D. Q. Li and M. Ding, *Wound Repair Regen.*, 2010, **18**, 499.
40. H. J. Lai, C. H. Kuan, H. C. Wu, J. C. Tsai, T. M. Chen, D. J. Hsieh and T. W. Wang, *Acta Biomater.*, 2014, **10**, 4156.
41. X. Y. Li, K. H. Nan, L. L. Li, Z. L. Zhang and H. Chen, *Carbohydr. Polym.*, 2012, **88**, 84.
42. L. K. Branski, G. G. Gauglitz, D. N. Herndon and M. G. Jeschke, *Burns*, 2009, **35**, 171.
43. M. G. Jeschke and D. N. Herndon, *Gene Ther.*, 2007, **14**, 1235.

44. K. Yoshimura, H. Suga and H. Eto, *Regener. Med.*, 2009, **4**, 265.
45. D. S. Kwon, X. Gao, Y. B. Liu, D. S. Dulchavsky, A. L. Danyluk, M. Bansal, M. Chopp, K. McIntosh, A. S. Arbab, S. A. Dulchavsky and S. C. Gautam, *Int. Wound J.*, 2008, **5**, 453.
46. J. A. Ankrum, J. F. Ong and J. M. Karp, *Nat. Biotechnol.*, 2014, **32**, 252.
47. V. Falanga, S. Iwamoto, M. Chartier, T. Yufit, J. Butmarc, N. Kouttab, D. Shrayer and P. Carson, *Tissue Eng.*, 2007, **13**, 1299.
48. D. Giugliano, A. Ceriello and G. Paolisso, *Diabetes Care*, 1996, **19**, 257.
49. G. Kojda and D. Harrison, *Cardiovasc. Res.*, 1999, **43**, 562.
50. S. H. Lee, M. K. Gupta, J. B. Bang, H. Bae and H. J. Sung, *Adv. Healthcare Mater.*, 2013, **2**, 908.
51. C.-C. Song, F.-S. Du and Z.-C. Li, *J. Mater. Chem. B*, 2014, **2**, 3413.
52. E. Nicol, T. Nicolai and D. Durand, *Macromolecules*, 1999, **32**, 7530.
53. A. Napoli, M. Valentini, N. Tirelli, M. Muller and J. A. Hubbell, *Nat. Mater.*, 2004, **3**, 183.
54. P. Hu and N. Tirelli, *Bioconjugate Chem.*, 2012, **23**, 438.
55. M. K. Gupta, T. A. Meyer, C. E. Nelson and C. L. Duvall, *J. Controlled Release*, 2012, **162**, 591.
56. E. A. Scott, A. Stano, M. Gillard, A. C. Maio-Liu, M. A. Swartz and J. A. Hubbell, *Biomaterials*, 2012, **33**, 6211.
57. S. T. Reddy, A. Rehor, H. G. Schmoekel, J. A. Hubbell and M. A. Swartz, *J. Controlled Release*, 2006, **112**, 26.
58. M. K. Gupta, J. R. Martin, T. A. Werfel, T. Shen, J. M. Page and C. L. Duvall, *J. Am. Chem. Soc.*, 2014, **136**, 14896.
59. K. M. Poole, C. E. Nelson, R. V. Joshi, J. R. Martin, M. K. Gupta, S. C. Haws, T. E. Kavanaugh, M. C. Skala and C. L. Duvall, *Biomaterials*, 2015, **41**, 166.
60. S. C. Yang, M. Bhide, I. N. Crispe, R. H. Pierce and N. Murthy, *Bioconjugate Chem.*, 2008, **19**, 1164.
61. D. S. Wilson, G. Dalmasso, L. X. Wang, S. V. Sitaraman, D. Merlin and N. Murthy, *Nat. Mater.*, 2010, **9**, 923.
62. T. Tang, H. Jiang, Y. Yu, F. He, S. Z. Ji, Y. Y. Liu, Z. S. Wang, S. C. Xiao, C. Tang, G. Y. Wang and Z. F. Xia, *Int. J. Nanomed.*, 2015, **10**, 6571.
63. H. L. Pu, W. L. Chiang, B. Maiti, Z. X. Liao, Y. C. Ho, M. S. Shim, E. Y. Chuang, Y. N. Xia and H. W. Sung, *ACS Nano*, 2014, **8**, 1213.
64. J. R. Martin, M. K. Gupta, J. M. Page, F. Yu, J. M. Davidson, S. A. Guelcher and C. L. Duvall, *Biomaterials*, 2014, **35**, 3766.
65. S. Park, J. Yoon, S. Bae, M. Park, C. Kang, Q. Ke, D. Lee and P. M. Kang, *Biomaterials*, 2014, **35**, 5944.
66. H. Park, S. Kim, S. Kim, Y. Song, K. Seung, D. Hong, G. Khang and D. Lee, *Biomacromolecules*, 2010, **11**, 2103.
67. H. J. Kim, I. K. Hwang and M. H. Won, *Brain Res.*, 2007, **1181**, 130.
68. E. J. Lim, H. J. Kang, H. J. Jung and E. H. Park, *J. Pharm. Pharmacol.*, 2007, **59**, 1235.
69. S. Kim, H. Park, Y. Song, D. Hong, O. Kim, E. Jo, G. Khang and D. Lee, *Biomaterials*, 2011, **32**, 3021.

70. S. Cho, O. Hwang, I. Lee, G. Lee, D. Yoo, G. Khang, P. M. Kang and D. Lee, *Adv. Funct. Mater.*, 2012, **22**, 4038.
71. M. Makni, Y. Chtourou, H. Fetoui, M. Garoui el, T. Boudawara and N. Zeghal, *Eur. J. Pharmacol.*, 2011, **668**, 133.
72. Y. Murakami, A. Hirata, S. Ito, M. Shoji, S. Tanaka, T. Yasui, M. Machino and S. Fujisawa, *Anticancer Res.*, 2007, **27**, 801.
73. J. Kwon, J. Kim, S. Park, G. Khang, P. M. Kang and D. Lee, *Biomacromolecules*, 2013, **14**, 1618.
74. D. Lee, S. Bae, D. Hong, H. Lim, J. H. Yoon, O. Hwang, S. Park, Q. Ke, G. Khang and P. M. Kang, *Sci. Rep.*, 2013, **3**, 2233.
75. D. L. Zhang, Y. L. Wei, K. Chen, X. J. Zhang, X. Q. Xu, Q. Shi, S. L. Han, X. Chen, H. Gong, X. H. Li and J. X. Zhang, *Adv. Healthcare Mater.*, 2015, **4**, 69.
76. C. de Gracia Lux, S. Joshi-Barr, T. Nguyen, E. Mahmoud, E. Schopf, N. Fomina and A. Almutairi, *J. Am. Chem. Soc.*, 2012, **134**, 15758.
77. K. E. Broaders, S. Grandhe and J. M. Frechet, *J. Am. Chem. Soc.*, 2011, **133**, 756.
78. D. Lee, S. Park, S. Bae, D. Jeong, M. Park, C. Kang, W. Yoo, M. A. Samad, Q. Ke, G. Khang and P. M. Kang, *Sci. Rep.*, 2015, **5**, 16592.
79. H. J. H. Fenton, *J. Chem. Soc., Trans.*, 1894, **65**, 899.
80. C. Walling and S. Kato, *J. Am. Chem. Soc.*, 1971, **93**, 4275.
81. M. F. Chung, W. T. Chia, W. L. Wan, Y. J. Lin and H. W. Sung, *J. Am. Chem. Soc.*, 2015, **137**, 12462.
82. F. Muhammad, W. X. Qi, A. F. Wang, J. K. Gu, J. S. Du and G. S. Zhu, *J. Mater. Chem. B*, 2015, **3**, 1597.
83. M. Heskins and J. E. Guillet, *J. Macromol. Sci., Chem.*, 1968, **2**, 1441.
84. T. Takezawa, Y. Mori and K. Yoshizato, *Bio/Technology*, 1990, **8**, 854.
85. Z. Abdali, H. Yeganeh, A. Solouk, R. Gharibi and M. Sorayya, *RSC Adv.*, 2015, **5**, 66024.
86. J.-P. Chen, C.-Y. Kuo and W.-L. Lee, *Appl. Surf. Sci.*, 2012, **262**, 95.
87. J. M. Yang and H. T. Lin, *J. Membr. Sci.*, 2004, **243**, 1.
88. K.-S. Chen, Y.-A. Ku, C.-H. Lee, H.-R. Lin, F.-H. Lin and T.-M. Chen, *Mater. Sci. Eng., C*, 2005, **25**, 472.
89. J. I. Ngadaonye, L. M. Geever, J. Killion and C. L. Higginbotham, *J. Polym. Res.*, 2013, **20**, 1.
90. J. M. Yang, S. J. Yang, H. T. Lin, T.-H. Wu and H.-J. Chen, *Mater. Sci. Eng., C*, 2008, **28**, 150.
91. M. D. Pawar, G. V. Rathna, S. Agrawal and B. S. Kuchekar, *Mater. Sci. Eng., C*, 2015, **48**, 126.
92. L. S. Wang, P. Y. Chow, T. T. Phan, I. J. Lim and Y. Y. Yang, *Adv. Funct. Mater.*, 2006, **16**, 1171.
93. L. S. Wang, P. Y. Chow, D. C. W. Tan, W. D. Zhang and Y. Y. Yang, *Adv. Mater.*, 2004, **16**, 1790.
94. T. T. Reddy, A. Kano, A. Maruyama, M. Hadano and A. Takahara, *Biomacromolecules*, 2008, **9**, 1313.
95. J. Madsen, S. P. Armes and A. L. Lewis, *Macromolecules*, 2006, **39**, 7455.

96. J. Madsen, S. P. Armes, K. Bertal, H. Lomas, S. Macneil and A. L. Lewis, *Biomacromolecules*, 2008, **9**, 2265.
97. C. Gong, Q. Wu, Y. Wang, D. Zhang, F. Luo, X. Zhao, Y. Wei and Z. Qian, *Biomaterials*, 2013, **34**, 6377.
98. Y. Yin, S. Jiao, C. Lang and J. Liu, *Soft Matter*, 2014, **10**, 3374.
99. J. Yang, R. van Lith, K. Baler, R. A. Hoshi and G. A. Ameer, *Biomacromolecules*, 2014, **15**, 3942.
100. M. L. Pua, T. Yoshitomi, P. Chonpathompikunlert, A. Hirayama and Y. Nagasaki, *J. Controlled Release*, 2013, **172**, 914.
101. H. Nakagawa, Y. Matsumoto, Y. Matsumoto, Y. Miwa and Y. Nagasaki, *Biomaterials*, 2015, **69**, 165.
102. S. Y. Lu, W. J. Gao and H. Y. Gu, *Burns*, 2008, **34**, 623.
103. A. M. Abdelgawad, S. M. Hudson and O. J. Rojas, *Carbohydr. Polym.*, 2014, **100**, 166.
104. T. Maneerung, S. Tokura and R. Rujiravanit, *Carbohydr. Polym.*, 2008, **72**, 43.
105. V. K. M. Poon and A. Burd, *Burns*, 2004, **30**, 140.
106. M. Fierheller and R. G. Sibbald, *Adv. Skin Wound Care*, 2010, **23**, 369.
107. C. James, A. L. Johnson and A. T. A. Jenkins, *Chem. Commun.*, 2011, **47**, 12777.
108. X. F. Sui, X. L. Feng, A. Di Luca, C. A. van Blitterswijk, L. Moroni, M. A. Hempenius and G. J. Vancso, *Polym. Chem.*, 2013, **4**, 337.
109. J. O. You, M. Rafat, D. Almeda, N. Maldonado, P. Guo, C. S. Nabzdyk, M. Chun, F. W. LoGerfo, J. W. Hutchinson, L. K. Pradhan-Nabzdyk and D. T. Auguste, *Biomaterials*, 2015, **57**, 22.
110. Z. Yuan, J. Zhao, Y. Chen, Z. Yang, W. Cui and Q. Zheng, *Mediators Inflammation*, 2014, **2014**, 858045.
111. Z. M. Yuan, J. W. Zhao, W. K. Zhu, Z. L. Yang, B. Li, H. L. Yang, Q. Zheng and W. G. Cui, *Biomater. Sci.*, 2014, **2**, 502.
112. M. F. Chung, W. T. Chia, H. Y. Liu, C. W. Hsiao, H. C. Hsiao, C. M. Yang and H. W. Sung, *Adv. Healthcare Mater.*, 2014, **3**, 1854.
113. T. Yoshitomi, A. Hirayama and Y. Nagasaki, *Biomaterials*, 2011, **32**, 8021.
114. J. Alijotas-Reig, M. T. Fernandez-Figueras and L. Puig, *Clin. Rev. Allergy Immunol.*, 2013, **45**, 97.
115. M. Zelzer and R. V. Ulijn, *Chem. Soc. Rev.*, 2010, **39**, 3351.
116. R. J. Williams, R. J. Mart and R. V. Ulijn, *Biopolymers*, 2010, **94**, 107.
117. J. E. Ghadiali and M. M. Stevens, *Adv. Mater.*, 2008, **20**, 4359.
118. D. Roy, J. N. Cambre and B. S. Sumerlin, *Prog. Polym. Sci.*, 2010, **35**, 278.
119. P. Van Lint and C. Libert, *J. Leukocyte Biol.*, 2007, **82**, 1375.
120. J. L. West and J. A. Hubbell, *Macromolecules*, 1999, **32**, 241.
121. M. P. Lutolf and J. A. Hubbell, *Nat. Biotechnol.*, 2005, **23**, 47.
122. M. P. Lutolf, J. L. Lauer-Fields, H. G. Schmoekel, A. T. Metters, F. E. Weber, G. B. Fields and J. A. Hubbell, *Proc. Natl. Acad. Sci. U. S. A.*, 2003, **100**, 5413.
123. G. P. Raeber, M. P. Lutolf and J. A. Hubbell, *Biophys. J.*, 2005, **89**, 1374.

124. M. Steinhagen, P. G. Hoffmeister, K. Nordsieck, R. Hotzel, L. Baumann, M. C. Hacker, M. Schulz-Siegmund and A. G. Beck-Sickinger, *ACS Appl. Mater. Interfaces*, 2014, **6**, 5891.
125. M. M. Nguyen, A. S. Carlini, M. P. Chien, S. Sonnenberg, C. L. Luo, R. L. Braden, K. G. Osborn, Y. W. Li, N. C. Gianneschi and K. L. Christman, *Adv. Mater.*, 2015, **27**, 5547.
126. B. Fingleton, *Curr. Pharm. Des.*, 2007, **13**, 333.
127. B. P. Purcell, D. Lobb, M. B. Charati, S. M. Dorsey, R. J. Wade, K. N. Zellars, H. Doviak, S. Pettaway, C. B. Logdon, J. A. Shuman, P. D. Freels, J. H. Gorman, R. C. Gorman, F. G. Spinale and J. A. Burdick, *Nat. Mater.*, 2014, **13**, 653.
128. L. Sorokin, *Nat. Rev. Immunol.*, 2010, **10**, 712.
129. E. Wiener and D. Levanon, *Science*, 1968, **159**, 217.
130. A. A. Aimetti, A. J. Machen and K. S. Anseth, *Biomaterials*, 2009, **30**, 6048.
131. A. A. Aimetti, M. W. Tibbitt and K. S. Anseth, *Biomacromolecules*, 2009, **10**, 1484.
132. J. A. Benton, B. D. Fairbanks and K. S. Anseth, *Biomaterials*, 2009, **30**, 6593.
133. S. T. Gould, N. J. Darling and K. S. Anseth, *Acta Biomater.*, 2012, **8**, 3201.
134. J. Gao, W. T. Zheng, J. M. Zhang, D. Guan, Z. M. Yang, D. L. Kong and Q. Zhao, *Chem. Commun.*, 2013, **49**, 9173.
135. S. F. Zhang, J. Ermann, M. D. Succi, A. Zhou, M. J. Hamilton, B. N. Cao, J. R. Korzenik, J. N. Glickman, P. K. Vemula, L. H. Glimcher, G. Traverso, R. Langer and J. M. Karp, *Sci. Transl. Med.*, 2015, **7**, 300ra128.
136. D. R. Griffin, W. M. Weaver, P. O. Scumpia, D. Di Carlo and T. Segura, *Nat Mater*, 2015, **14**, 737.
137. M. R. Battig, B. Soontornworajit and Y. Wang, *J. Am. Chem. Soc.*, 2012, **134**, 12410.
138. S. Zhu, L. Nih, S. T. Carmichael, Y. Lu and T. Segura, *Adv. Mater.*, 2015, **27**, 3620.
139. M. M. S. Ebrahimi, Y. Voss and H. Schonherr, *ACS Appl. Mater. Interfaces*, 2015, **7**, 20190.
140. G. Baier, A. Cavallaro, K. Vasilev, V. Mailander, A. Musyanovych and K. Landfester, *Biomacromolecules*, 2013, **14**, 1103.
141. M. Lashof-Sullivan, A. Shoffstall and E. Lavik, *Nanoscale*, 2013, **5**, 10719.
142. M. M. Lashof-Sullivan, E. Shoffstall, K. T. Atkins, N. Keane, C. Bir, P. Vande-Vord and E. B. Lavik, *Proc. Natl. Acad. Sci. U. S. A.*, 2014, **111**, 10293.
143. A. O. Awojoodu, M. E. Ogle, L. S. Sefcik, D. T. Bowers, K. Martin, K. L. Brayman, K. R. Lynch, S. M. Peirce-Cottler and E. Botchwey, *Proc. Natl. Acad. Sci. U. S. A.*, 2013, **110**, 13785.
144. A. Das, D. A. Barker, T. Wang, C. M. Lau, Y. Lin and E. A. Botchwey, *PLoS One*, 2014, **9**, e101276.
145. O. Jeon and E. Alsberg, *Adv. Funct. Mater.*, 2013, **23**, 4765.
146. L. K. Branski, C. T. Pereira, D. N. Herndon and M. G. Jeschke, *Gene Ther.*, 2007, **14**, 1.

147. M. G. Jeschke, R. E. Barrow, H. K. Hawkins, Z. Tao, J. R. Perez-Polo and D. N. Herndon, *Lab. Invest.*, 2000, **80**, 151.
148. M. G. Jeschke and D. Klein, *Gene Ther.*, 2004, **11**, 847.
149. B. Peng, Y. Chen and K. W. Leong, *Adv. Drug Delivery Rev.*, 2015, **88**, 108.
150. M. Monaghan, S. Browne, K. Schenke-Layland and A. Pandit, *Mol. Ther.*, 2014, **22**, 786.
151. M. Dimitrova, C. Affolter, F. Meyer, I. Nguyen, D. G. Richard, C. Schuster, R. Bartenschlager, J. C. Voegel, J. Ogier and T. F. Baumert, *Proc. Natl. Acad. Sci. U. S. A.*, 2008, **105**, 16320.
152. T. Segura, P. H. Chung and L. D. Shea, *Biomaterials*, 2005, **26**, 1575.
153. Y. Wu, L. Chen, P. G. Scott and E. E. Tredget, *Stem Cells*, 2007, **25**, 2648.
154. E. V. Badiavas and V. Falanga, *Arch. Dermatol.*, 2003, **139**, 510.
155. D. Duscher, J. Barrera, V. W. Wong, Z. N. Maan, A. J. Whittam, M. Januszyk and G. C. Gurtner, *Gerontology*, 2016, **62**, 216.
156. R. K. Garg, R. C. Rennert, D. Duscher, M. Sorkin, R. Kosaraju, L. J. Auerbach, J. Lennon, M. T. Chung, K. Paik, J. Nimpf, J. Rajadas, M. T. Longaker and G. C. Gurtner, *Stem Cells Transl. Med.*, 2014, **3**, 1079.
157. K. C. Rustad, V. W. Wong, M. Sorkin, J. P. Glotzbach, M. R. Major, J. Rajadas, M. T. Longaker and G. C. Gurtner, *Biomaterials*, 2012, **33**, 80.
158. V. W. Wong, K. C. Rustad, J. P. Glotzbach, M. Sorkin, M. Inayathullah, M. R. Major, M. T. Longaker, J. Rajadas and G. C. Gurtner, *Macromol. Biosci.*, 2011, **11**, 1458.
159. G. G. Gauglitz and M. G. Jeschke, *Mol. Pharm.*, 2011, **8**, 1471.
160. F. Geissmann, S. Jung and D. R. Littman, *Immunity*, 2003, **19**, 71.
161. M. E. Ogle, L. S. Sefcik, A. O. Awojoodu, N. F. Chiappa, K. Lynch, S. Peirce-Cottler and E. A. Botchwey, *Acta Biomater.*, 2014, **10**, 4704.
162. K. Sadtler, K. Estrellas, B. W. Allen, M. T. Wolf, H. N. Fan, A. J. Tam, C. H. Patel, B. S. Luber, H. Wang, K. R. Wagner, J. D. Powell, F. Housseau, D. M. Pardoll and J. H. Elisseeff, *Science*, 2016, **352**, 366.
163. B. M. Holzapfel, J. C. Reichert, J. T. Schantz, U. Gbureck, L. Rackwitz, U. Noth, F. Jakob, M. Rudert, J. Groll and D. W. Hutmacher, *Adv. Drug Delivery Rev.*, 2013, **65**, 581.

CHAPTER 11

Applications of Magnetic-Responsive Materials for Cardiovascular Tissue Engineering

LINDSAY STEELE[a,e], GAL MARGOLIS[b], SMADAR COHEN*[b,c,d] AND BORIS POLYAK*[e,f]

[a]Molecular Cell Biology and Genetics (MCBG) Program, Drexel University College of Medicine, Philadelphia, PA 19102, USA; [b]The Avram and Stella Goldstein-Goren Department of Biotechnology Engineering, Ben-Gurion University of the Negev, Beer-Sheva 84105, Israel; [c]Ilse Katz Institute for Nanoscale Science and Technology, Ben-Gurion University of the Negev, Beer-Sheva 84105, Israel; [d]Regenerative Medicine and Stem Cell (RMSC) Research Center, Ben-Gurion University of the Negev, Beer-Sheva 84105, Israel; [e]Department of Surgery, Drexel University College of Medicine, Philadelphia, PA 19102, USA; [f]Department of Pharmacology and Physiology, Drexel University, Philadelphia, PA 19102, USA
*E-mail: scohen@bgu.ac.il, bpolyak@drexelmed.edu

11.1 Introduction

Heart attacks are a leading cause of mortality worldwide. In the late fetal development and soon after birth, cardiomyocytes transition from the proliferative, mono-nucleate to the mature bi-nucleate non-proliferative

Smart Materials No. 25
Smart Materials for Tissue Engineering: Applications
Edited by Qun Wang

Published by the Royal Society of Chemistry, www.rsc.org

phenotype. Lack of proliferative ability in adult cardiomyocytes hampers natural regeneration of cardiac tissue after myocardial infarction (MI), resulting in progressive cardiac tissue damage, left ventricular remodeling, and subsequent heart failure (HF). To date, the only clinical solution for terminal HF patients is heart transplantation, which is severely limited due to the shortage of donors.

Cell therapy lies at the core of many meritorious efforts to restore heart function after MI, either by injecting cell suspensions[1] or implanting cardiac patches fabricated by tissue engineering methodologies.[2,3] Several studies illustrate that implantation of a cardiac patch onto the myocardial scar in a rat model of MI prevented left ventricular remodeling and expansion.[2,3] The cardiac patch consisted of neonatal cardiomyocytes seeded within alginate scaffolds,[2,4] fabricated as a sponge with 90% porosity and pore sizes of ≥50 μm[5,6] enabling vascularization after patch implantation.[7] Three-dimensional cultures of cardiac cells[8] were studied both (i) under perfusion conditions to enhance mass transport and (ii) with the implementation of mechanical,[8] electrical, and chemical (MI serum) stimulation.[9] Encouraging results have been achieved with thin-walled tissues, *e.g.*, engineered skin,[10] trachea[11] and urinary bladder.[12] However, engineering dense tissues and solid organs (*e.g.*, the heart) that depend on vascular supply remains a challenge.

Pre-vascularization of engineered constructs *in vitro* is one option to enable efficient integration with host tissue.[13,14] During the *in vitro* construct growth, vasculature structures enable sufficient supply of oxygen and nutrients to ensure maximal cell survival, and promote cellular differentiation and functional tissue organization.[15,16] Upon implantation, the established graft vascular network can efficiently anastomose with the vasculature of a recipient tissue, augmenting tissue transplant perfusion and accelerating recipient tissue neovascularization *via* tissue transplant-driven paracrine signaling.[13,14]

One of the fundamental goals in the development of artificial tissues for regenerative needs is a creation of appropriate stimulatory conditions leading to an inductive microenvironment for efficient tissue growth *in vitro* and *in vivo*. It is well known that both molecular signals (*e.g.* growth factors, cytokines and chemokines) and physical cues (*e.g.* stretching, bending and compression) are necessary components of a functional tissue promoting microenvironment. Physical cues are particularly relevant to the engineering of biological tissues that experience physical loads and stresses under normal physiological conditions. In such tissues, mechanical cues stimulate mechano-sensitive receptors, triggering biochemical pathways initiating synthesis of proteins involved in the formation of functionally organized tissue. Magnetically responsive nanoparticles (MNPs) attached to the surface of cell membranes or incorporated within the walls of three-dimensional (3D) scaffolds and coupled with either uniform magnetic fields or field gradients can apply physical forces to cells directly linked with nanoparticles or present in the 3D scaffold near the source of generated force. Additionally, uniform magnetic fields and field gradients can be used to magnetically guide

and target cell-based therapies to improve cell homing and engraftment in the targeted tissue.

In this chapter, we will overview strategies based on magnetic-responsive scaffolds or nanoparticles for application of mechanical cues and present a novel methodology for obtaining a pre-vascularized functional cardiac muscle patch suitable to replace damaged myocardial tissue. We will demonstrate the feasibility of 'magneto-mechanical' actuation achieved by a uniform magnetic field translated to a mechanical conditioning of endothelial and cardiac cells cultivated within 3D magnetically-responsive alginate scaffolds In addition, we will present the implementation of this strategy to design tissue scaffolds with special topography/morphology, such as the formation of anisotropic scaffolds.

11.2 Application of Mechanical Cues *via* Magnetic Force

Physical cues are critically involved in several cellular processes, including differentiation, migration, and proliferation. Cells translate physical cues into biochemical signaling through mechanotransduction to ensure proper tissue development and function. Consequently, appropriate mechanical priming of cells is necessary for successful tissue engineering. One way to mechanically stimulate cells is to use magnetic force in combination with magnetically-responsive cells or materials. In comparison with other mechanical systems, such as piston/compression systems or fluid shear force, magnetically-based systems are advantageous because they can be applied remotely, *in vivo*, and in a spatially or temporally diverse manner. Other mechanical systems require direct contact with cells or materials, increasing the risk of contamination. Furthermore, magnetic-based systems are more versatile. Magnetic nanoparticles (MNPs) have been used to improve contrast in magnetic resonance imaging,[17,18] target cells within the body,[19–24] improve transfection efficiency,[25–27] and trigger biochemical signaling within cells.[28–30] Magnetic nanoparticles can be easily attached to or loaded within cells or materials, providing a means to directly or indirectly stimulate cells. These characteristics make magnetically-based systems an attractive option for engineering complex tissues, such as cardiac tissue, that consist of various cell types, require efficient vascularization, and rely on mechanical cues for proper function. This section will review various methods for utilizing magnetic stimulation to apply mechanical force on cells.

11.2.1 Magneto-Mechanical Cues Applied *via* Magnetic Particles

In 2006, Dobson *et al.* described the theoretical design of a magnetic-force bioreactor that remotely applied stress to cells.[31] Magnetic force bioreactors require two components: a magnetic field and magnetically-responsive cells.

The bioreactor described utilized either a linear array of neodymium rare-earth magnets (NdFeB) or electromagnetic coils to generate a magnetic field. Magnetic nanoparticles tagged to the cell membrane or loaded within the cytosol make cells magnetically responsive. Often, the magnetic nanoparticles are composed of magnetite and display superparamagnetic behavior. Therefore, when applied, the magnetic field magnetizes the magnetic nanoparticles, causing them to align with the applied field, resulting in tensile or compressive forces on the cells. The combined features of the bioreactor and magnetically-responsive cells allow researchers to easily vary the mechanical load transferred to cells by altering the magnetic strength, frequency, and field gradient.[31] The outcome of stimulated magnetically-responsive cells largely depends on the method used to functionalize cells with MNPs. MNPs tagged to the cell surface can be used to spatially organize or target cells, or they can be used to elicit a desired biochemical response.[27,31–33] Cellular internalization of MNPs is typically required for therapeutic cell targeting or gene delivery.[34–38]

In follow up studies, Dobson and colleagues confirmed the ability of magnetic-force bioreactors to promote force-based biochemical signaling within cells by activating membrane components.[32,33] In 2014, they successfully differentiated human bone marrow stem cells (hBMSCs) towards a smooth muscle cell lineage by activating platelet-derived growth factor receptors located on the cell surface (Figure 11.1(A)).[31,32] Platelet-derived growth factor receptor, PDGFα, is mechanosensitive and has an important role in the differentiation of mesenchymal stem cells (MSCs). Magnetically-responsive nanoparticles, functionalized with antibodies against PDGFα, activated PDGFRα signaling in the presence of magnetic stimulation independent of soluble growth factors. PDGFRα activation, demonstrated by a significant increase in total tyrosine phosphorylation, occurred as early as thirty minutes of stimulation. Magnetic stimulation and activation of PDGFRα resulted in the differentiation of hBMSCs towards smooth muscle cells, shown by the upregulation smooth muscle actin-α (SMA-α) expression. Whether PDGF receptor activation was achieved by a strain-induced conformational change in the receptor or magnetically-induced receptor clustering remains unknown. Collectively, these results demonstrate the ability of magnetic bioreactors to activate membrane receptors and influence stem cell differentiation in the absence of soluble factors.[32]

In 2008, Hughes *et al.* demonstrated the ability to apply highly localized forces to specific ion channels.[33] They activated the TREK-1 ion channel by targeting the extended loop region of the channel that is hypothesized to be responsible for mechano-gating of the ion channel. To apply localized magnetic force to the extended loop of the channel, researchers expressed a mutant TREK-1 channel in cos-7 cells, which do not normally exhibit outward rectifying potassium current. The mutant TREK-1 channel contained a six histidine repeat inserted into the extended loop between two transmembrane spanning regions of the channel. They then grafted antibodies against the histidine repeat or nickel-nitrilotriacetic acid onto magnetic nanoparticles to target the magnetic nanoparticles to the histidine repeat

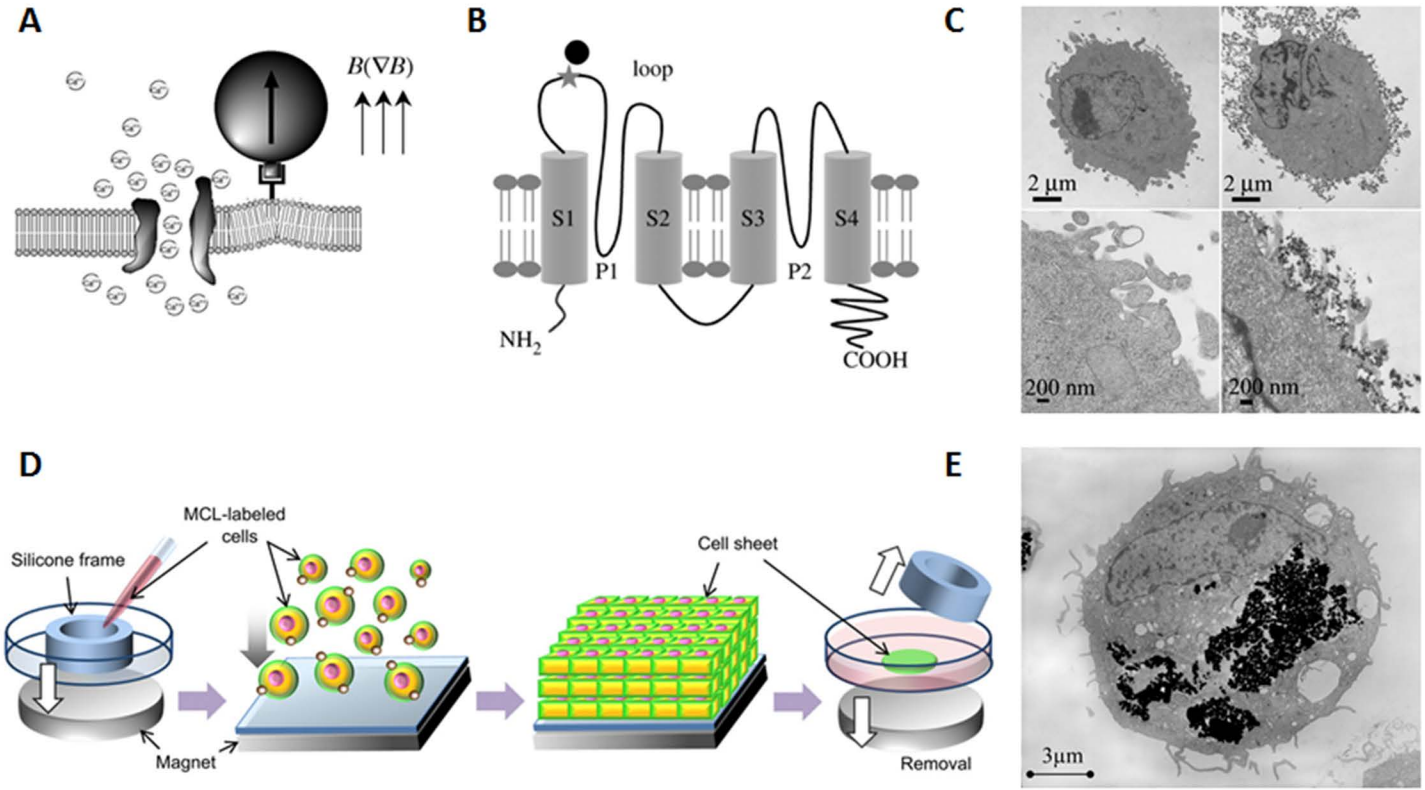

Figure 11.1 Methods for making cells magnetically responsive. (A) Depiction of magnetic nanoparticles attached to membrane receptors. Activation of an adjacent mechanosensitive ion channel occurs when magnetic nanoparticles experience a translational force directed along the magnetic field vector. Copyright © 2006 IEEE. Reprinted with permission from *IEEE Transactions on NanoBioscience*. Dobson J., Cartmell S. H., Keramane A., El Haj A. J. Principles and design of a novel magnetic force

mechanical conditioning bioreactor for tissue engineering, stem cell conditioning, and dynamic *in vitro* screening. **5**(3):173–177.[31] (B) Depiction of a mutant TREK-1 channel designed for application of highly localized forces. Six-histidine repeat (star) inserted into the extended loop between two transmembrane spanning regions of the channel. Location of targeted magnetic nanoparticles engrafted with antibodies against the histidine repeat represented by black circle. Adapted with permission from *Current Opinion in Cell Biology*. **13**(4) Patel A. J., Lazdunski M., Honoré E., Lipid and mechano-gated 2P domain K(+) channels. pgs. 422–428, Copyright © 2001, with permission from Elsevier.[158] Reprinted with permission from *The Journal of Royal Society Interface*. Hughes,S., McBain,S., Dobson,J., El Haj, A., Selective activation of mechanosensitive ion channels using magnetic particles. **5**(25):855–863 Copyright © 2007 The Royal Society. http://rsif.royalsocietypublishing.org/content/5/25/855.long DOI: 10.1098/rsif.2007.1274.[33] All rights reserved. Available under a Creative Commons Attribution license. (C) Transmission electron microscopy images of SPIONS stabilized with a polyelectrolyte, (poly)allyl amine hydrochloride, electrostatically interacting with the negatively charged HeLa cell membrane (right top and bottom) or HeLa cells without SPIONs (left top and bottom). Adapted with permission from *Langmuir*, Dzamukova M. R., Zamaleeva A. I., Ishmuchametova D. G., Osin Y. N., Kiyasov A. P., Nurgaliev D. K., Ilinskaya O. N., Fakhrullin R. F., A direct technique for magnetic functionalization of living human cells. **27**(23):14 386–14 393. DOI: 10.1021/la203839v. Copyright © 2011. American Chemical Society.[39] (D) Fabrication of cell sheets. MCL-labeled cells seeded inside a silicone-rubber tube frame placed in the dish. The cells accumulate on the bottom of the dish by a magnet placed beneath the dish, and then are cultured to form a multilayered cell sheet. Reprinted from *Biomaterials*. **31**(6), Akiyama H., Ito A., Kawabe Y., Kamihira M. Genetically engineered angiogenic cell sheets using magnetic force-based gene delivery and tissue fabrication techniques, pgs. 1251–1259. Copyright © 2010, with permission from Elsevier.[42] (E) Herceptin functionalized polypyrrole-Fe_3O_4 nanospheres (NS-HER) internalized within cell cytoplasm. Transmission electron micrograph. Reprinted from *Biomaterials*. **29**(14), Wuang S. C., Neoh K. G., Kang E. T., Pack D. W., Leckband D. E. HER-2-mediated endocytosis of magnetic nanospheres and the implications in cell targeting and particle magnetization, pgs. 2270–2279. Copyright © 2010, with permission from Elsevier.[47]

(Figure 11.1(B)).[33] Magnetic stimulation of cells expressing magnetically-responsive TREK-1 channels resulted in an increase in the number of traces exhibiting changes in outward potassium current recorded from cells.[33] These results indicate increased TREK-1 channel activity in response to magnetic treatment. Since TREK-1 is a tandem pore potassium channel that regulates the resting cell membrane potential in excitable tissues, including vascular tissue and the heart, these results are relevant to cardiac tissue engineering.

Typically, magnetic nanoparticles are targeted to specific membrane components. However, in some cases, it is useful to magnetically functionalize the entire cell membrane. Dzamukoa *et al.*, 2011, demonstrated a method for dispersing superparamagnetic iron oxide nanoparticles (SPION) onto the cell membrane in a simple procedure utilizing electrostatic attraction.[39] Stabilizing the iron oxide nanoparticles with (poly) allyl amine hydrochloride, a cationic polyelectrolyte confers a positive charge onto the magnetic nanoparticles. Consequently, the nanoparticles quickly and strongly interact with the negatively charged cell membrane (Figure 11.1(C)).[39] The iron oxide magnetic nanoparticles were deposited between the microvilli network and did not penetrate the cytoplasm.[39] The authors showed that the nanoparticle coating did not affect cell viability or proliferation.

Employing the same principles of electrostatic attraction, Ito *et al.*, 2005, established a methodology called 'magnetic force-based tissue engineering' (Mag-TE).[40] Their method uses magnetite-cationic liposomes (MCLs), which consist of magnetite nanoparticles, with a diameter of 10 nm, entrapped in a cationic liposome.[40] The positively charged MCL electrostatically interacts with the negatively charged cell membrane. This interaction enhances the uptake of the MCLs by the cells conferring magnetic responsiveness onto the cells. Cells become magnetically responsive after one step incubation with MCLs. This group has been able to use this method to improve cell seeding of polymer scaffolds,[41] enhance retroviral-transduction efficiency in myoblasts,[42] engineer complex tubular structures,[40] and engineer polymer-free cell sheet constructs capable of inducing angiogenesis in ischemic tissues (Figure 11.1(D)).[42–45]

Finally, endocytosis of magnetic nanoparticles into the cytoplasm offers a simple and effective method to load cells with MNPs. Endocytosed MNPs are distributed between daughter cells during mitosis and can be maintained within cells at measurable levels for multiple generations.[46] Internalization of particles by cells is not a result of passive membrane deformation. Several studies show that particle uptake, including MNPs, is an active process requiring cytoskeletal rearrangement. Treatment of cells with inhibitors of actin polymerization, like cytochalasin D, or decreasing reaction temperatures to 4 °C will significantly reduce particle internalization (Figure 11.1(E)).[37,46,47] As demonstrated by Rejman *et al.*, 2004, the mechanism of particle internalization depends on particle size.[48] For this study, fluorescent-latex beads ranging in diameters from 50 nm to 1000 nm were incubated with mouse melanoma cells. They showed that particles with diameters of 200 nm or less are endocytosed by a clathrin-mediated pathway and became distributed

throughout the cell. Particles with a diameter of 500 nm were internalized by a caveolae-mediated pathway and remained localized to the cell periphery. Cells were unable to internalize particles with a diameter of 1000 nm.[48]

In another study, endocytosis was enhanced by mechanical stimulation. Localized stretching forces applied to β1-integrin receptors on endothelial cells *via* the displacement of fibronectin-coated glass beads by a piezo-driven glass pipette results in accelerated internalization of integrin receptors.[49] As elucidated by Kiyoshima *et al.*, 2011, uniaxial forces applied to the integrin receptor transiently activate calcium-permeable stretch activated channels resulting in a significant rise in intracellular calcium in the vicinity of the receptor.[49] Concomitantly, tension in actin stress fibers beneath the receptor significantly decreases. The coordinated increase in calcium and decrease in tension mediates a de-phosphorylation of focal-contact proteins and subsequent endocytosis of integrin clusters.[49] In agreement with these results, endocytosis of MNPs by endothelial cells is enhanced by magnetic force.[37] In MacDonald *et al.*, 2012, poly(lactic acid) (PLA)-based MNPs with varied concentrations of magnetite were incubated with endothelial cells under a static magnetic field of 500 G and surface force density of 66 T^2 m^{-1}.[37] The diameters of MNPs were approximately 300 nm. Magnetic force significantly increased the efficiency of MNP internalization by approximately three-fold compared to cell loading without magnetic force. By increasing the magnetite concentration of MNPs and applying a magnetic field, the authors achieved a 91% loading efficiency. Interestingly, magnetic force enhanced the mechanism of MNP uptake, not just MNP–cell contact. Endothelial cells experiencing magnetic force were able to internalize a higher proportion of MNPs than cells not exposed to a magnetic field. Furthermore, removal of the magnetic field after one hour of MNP incubation arrested MNP uptake. These results indicate a limit to the amount of magnetite endothelial cells that can internalize statically, which can be surpassed with magnetic force.[37]

Not only is the uptake of nanoparticles dependent on particle characteristics, but it is also highly dependent on cell type.[37,46,47] While cells like endothelial cells efficiently take up MNPs,[35,37,49] other cell types are deemed 'hard-to-label'. One cell type that is difficult to label is neural stem cells. Adams *et al.*, 2015, demonstrated that increasing the magnetite content of PLA-based MNPs significantly increased the proportion of cells that internalized MNPs and enhanced magnetic capture of neural stem cells.[36] At the highest concentration of magnetite, the authors achieved a 95.8 ± 1.0% efficiency of MNP loading, resulting in an internal iron content 5.7 pg Fe/cell. Surprisingly, short-term varying of the magnetic force did not significantly increase MNP loading in neural stem cells. These results highlight the specificity of MNP loading efficiency to cell type.

11.2.1.1 Safety of Nanoparticles in Cells

Iron oxide nanoparticles exhibit several characteristics that make them attractive for use in tissue engineering, regenerative medicine, and diagnostics.

They display superparamagnetic behavior, becoming magnetized only when a magnetic field is applied, they have a large surface area that is amenable for chemical modifications, and it is easy to control their physical shape and size. Due to their growing potential for use in the medical field, it is important to thoroughly assess the biocompatibility and cytotoxicity of iron oxide nanoparticles. Three separate studies evaluated the bio-distribution and biocompatibility of intravenously injected MNPs in rats and did not report any observable changes in animal survival, organ function, body weight, or food consumption.[51–53] Two of the papers assessed particles ranging from 50 to 200 nm in diameter at dose concentrations ranging from 0 to 30 mg Fe/kg both with and without applied magnetic fields.[51,52] Additionally, Weissleder *et al.*, 1989, performed pharmacokinetic analysis of intravenously injected (1 mg Fe/kg) radioactive superparamagnetic-iron oxide particles (^{59}Fe-AMI-25) on both rats and beagle dogs.[53] The magnetic nanoparticles were predominantly distributed to the liver and spleen within hours post injection. There was very low or no distribution to the heart, lung, brain, and kidneys. An initial increase in iron serum levels was observed after injection, but levels decreased and remained within normal levels by 2–3 weeks post injection.[51–53] Weissleder *et al.* reported a time dependent incorporation of iron into the hemoglobin of erythrocytes, indicating the biodegradability and bioavailability of these particles *in vivo*.[53] There were no reported long term changes in oxidative stress, liver function, or toxicity after the administration of iron oxide nanoparticles both with and without applied magnetic fields.[51,52] Toxicity studies did not show any acute or subacute toxic effects of injected MNPs even at doses as high as 128 mg Fe/kg. A negative impact on the endothelium of mice was reported in a different study when ultrafine magnetic particles (<100 nm) were intravenously injected at doses of 20 mg kg^{-1} of magnetic nanoparticles. No endothelium damage occurred when the MNPs were injected at doses of 5 mg kg^{-1}. In general, this paper also reported no significant changes to animal health and no obvious impacts on heat, liver, or spleen function.[54]

Intravenously injected magnetic nanoparticles will come into direct contact with endothelial cells lining blood vessels before reaching target tissues. Therefore, the effects of these nanoparticles on endothelial cell viability, morphology, and function must be taken into consideration when designing new magnetically-based therapies and materials. A 2007 study by Gojova *et al.* revealed that direct exposure of endothelial cells to magnetic nanoparticles induced an inflammatory response that was dependent on the composition and concentration of the nanoparticles.[55] Magnetic nanoparticles that were approximately 50 nm in diameter and made of yttrium oxide or zinc oxide increased expression of inflammatory markers, intracellular adhesion molecule 1, interleukin-8, and monocyte chemotactic protein-1, in endothelial cells at concentrations of 10 μg mL^{-1}. These concentrations corresponded to approximately 80–100 pg of zinc or yttrium per cell. Conversely, iron oxide nanoparticles did not result in increased expression of inflammatory markers at concentrations ranging from 0.001 to 50 μg mL^{-1} (approximately

3.5–100 pg Fe/cell) or exposure times from one to eight hours.[55,56] Indicating magnetic nanoparticles composed of iron oxide may be more favorable for biomedical applications. In a study by Buyukhatipoglu and Clyne, 2010, iron oxide nanoparticles with diameters between 20–40 nm were readily taken up by endothelial cells into the cytoplasm but did not enter the nucleus. The cytoplasmic nanoparticles significantly increased production of reactive oxygen species (ROS) in a dose- and time-dependent manner. Doses of 0.1 mg mL^{-1} or higher of nanoparticles, corresponding to 11–54 pg/cell or higher, resulted in significantly increased ROS production compared to unloaded cells.[56] The reported adverse effects have the potential to negatively impact endothelial cell function and viability. In a separate study, researchers showed that treating endothelial cells with MNPs with diameters of 15–20 nm at doses that were 400 μg mL^{-1} or greater resulted in decreased cell viability and proliferation.[54] Endothelial cell dysfunction was also observed at high MNP doses as demonstrated by a decreased ability of cells to take up acetylated low-density lipoprotein, increased activity of endothelial nitric oxide synthase (eNOS) and increased production of nitric oxide (NO) indicating potentially harmful effects on endothelium function and vasodilation of blood vessels.[54] These results are partially in disagreement with results reported in a 2016 study by Zhang *et al.*, investigating the effects of bare iron oxide nanoparticles with diameters ranging from 10–15 nm on endothelial cells.[57] In this report, exposure of endothelial cells to doses of MNPs that are 400 μg mL^{-1} and above decreases the ability of cells to take up acetylated low density lipoprotein, but eNOS activity was impaired with significantly decreased NO production. The impaired endothelial cell function is attributed to enhanced autophagic activity but decreased autophagic flux in these cells as shown by increases in the formation of acidic compartments, lysosomes and autophagolysosomes, along with significant increases in p62 protein, which is normally degraded along the autophagic pathways.[57] Dysfunction in autophagic flux may be partly responsible for the observed disruption in endothelial cell function and for increased expression of pro-inflammatory factors such as interleukin 1β, tumor necrotic factor α, and c-reactive protein that were observed 24 hours after exposure to nanoparticles.[57]

While these studies highlight dysfunction in endothelial cells caused by magnetic nanoparticles, they indicate the occurrence of adverse effects at high concentrations of ultrafine magnetic nanoparticles and a reduced number of effects at lower concentrations. These studies focused on magnetic particles with diameters less than 100 nm. A report by Orynbayeva *et al.*, 2015, systematically assessed the potential adverse effects of MNPs on primary endothelial cells.[34] Poly(lactic acid)-based-magnetite loaded MNPs with diameters of approximately 280 nm were incubated with primary endothelial cells in the presence of a static magnetic field of 500 G for 24 hours. This procedure corresponded to an intracellular magnetite concentration of 25.3 ± 0.75 pg magnetite/cell. Primary endothelial cells laden with MNPs remained viable and capable of proliferating. Cellular structure remained intact with continuous actin and microtubule networks despite small, localized

displacement of actin by MNPs. Overall cellular health and function were not adversely affected by MNP loading, but some changes in cellular metabolism did occur to account for the stressful conditions of internalization. MNPs occupied the perinuclear space and partially destroyed local endoplasmic reticulum (ER) cisterns resulting in a decrease in calcium released from the ER upon stimulation with thapsigargin, 388 ± 52.4 nmol *versus* 271 ± 20.7 nmol of calcium in unloaded and loaded cells respectively. However, overall calcium homeostasis was maintained and cells retained functional cell signaling. Additionally, the mechanical stress of internalization did cause some mitochondria to be degraded, resulting in a decrease in the total number of mitochondria in loaded cells compared to unloaded cells. Despite a decrease in the number of mitochondria, rates of oxygen consumption were similar between the two groups, implying that MNP internalization did degrade some mitochondria but the remaining mitochondria were able to acquire a higher membrane potential to support cellular demands and compensate for missing mitochondria.[34] Zohra *et al.*, 2015, evaluated changes in cellular function and gene expression when endothelial cells were loaded with the same PLA-based MNPs resulting in the same loading of 25.3 ± 0.75 pg magnetite/cell.[35] Endothelial cells loaded with poly(lactic acid) (PLA)-based magnetic nanoparticles, approximately 280 nm in diameter, did not display altered function compared to unloaded cells as shown by comparable results in adhesion, tube formation, and NO production assays. This paper reports significant changes in endothelial cell genes involved in inflammation, angiogenesis, and coagulation in response to MNP loading. Interestingly, significant changes in endothelial cell genes between MNP loaded and unloaded cells were no longer observed when cells were circulating in a closed loop system and magnetically captured on a stainless steel mesh.[35] Collectively, these studies indicate that magnetic nanoparticles do have an impact on endothelial cell function that varies significantly depending on MNP composition, size, surface modifications, dosage, and exposure time. Most adverse effects were reported at high concentrations of ultrafine MNPs. While MNPs do not appear to have immediate consequences on overall organism health using an animal model, long term effects on vascular function may be possible. Therefore, it is important to take into consideration the effects of MNPs on endothelial cells when designing new MNPs for use in magnetic materials and technologies.

11.2.2 Magneto-Mechanical Cues Applied Through Magnetic Scaffolds

An alternative method to directly tagging and stimulating cells with magnetic nanoparticles is to indirectly stimulate cells by impregnation of magnetic nanoparticles into a polymeric scaffold. Use of a magnetically-responsive polymer scaffold offers the advantage of simplifying cell culture procedures, as cells do not need to be magnetically functionalized or altered in any manner. All engineered alterations are applied to the premade-polymer scaffold

before cell cultivation. Additionally, use of magnetically-responsive scaffolds facilitates the application of magnetically-induced mechanical strain *in vivo* without disrupting the targeting or location of implanted cells. The feasibility of using magnetically actuated scaffolds as a mechanism for physical stimulation was demonstrated by Sapir-Lekhovitser *et al.*, 2016 (Figure 11.2).[58]

Atomic force microscopy showed that time-varying, uniform magnetic fields with strengths ranging from 15 to 100 Oe and a frequency of 1 Hz were capable of inducing reversible shape deformations in magnetite-embedded alginate scaffolds crosslinked to various degrees (Figure 11.3(A) and (B)).[58]

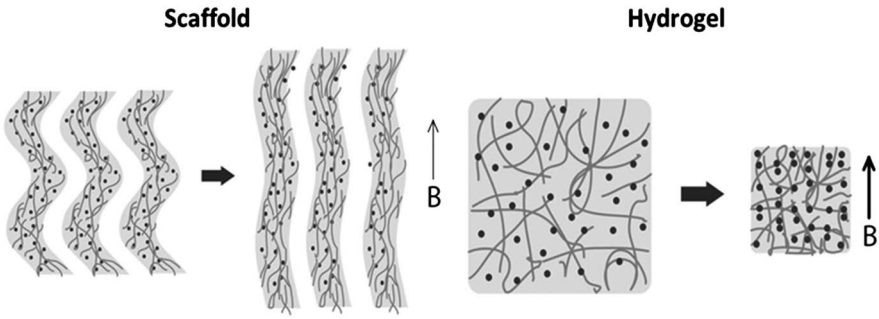

Figure 11.2 Hypothesized deformations of a magnetically-responsive alginate scaffold within a magnetic field. Reprinted from *Nanoscale*. Sapir-Lekhovitser Y., Rotenberg M. Y., Jopp J., Friedman G., Polyak B., Cohen S., Magnetically actuated tissue engineered scaffold: insights into mechanism of physical stimulation, **8**(6):3386–3399. Copyright © 2016, with permission from the Royal Society of Chemistry.[58]

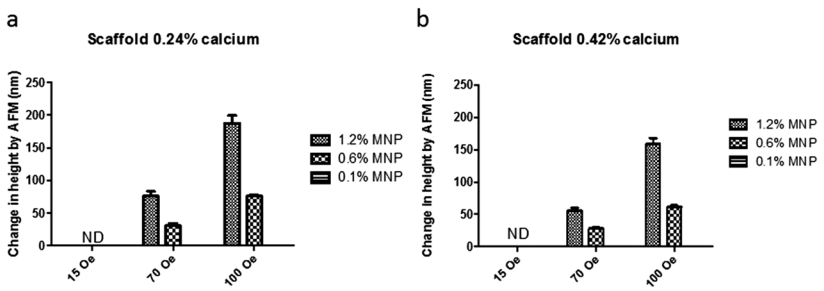

Figure 11.3 Atomic force microscopy (AFM)-based measurements of changes in scaffold height of hydrated scaffolds with crosslinked with 0.24% calcium (a) or 0.42% calcium (b) during treatment with a field of 15 Oe, 70 Oe, or 100 Oe at a frequency of 1 Hz. Scaffolds were fabricated with 1.2%, 0.6%, or 0.1% MNP. Adapted from *Nanoscale*. Sapir-Lekhovitser Y., Rotenberg M. Y., Jopp J., Friedman G., Polyak B., Cohen S., Magnetically actuated tissue engineered scaffold: insights into mechanism of physical stimulation, **8**(6):3386–3399. Copyright © 2016, with permission from The Royal Society of Chemistry.[58]

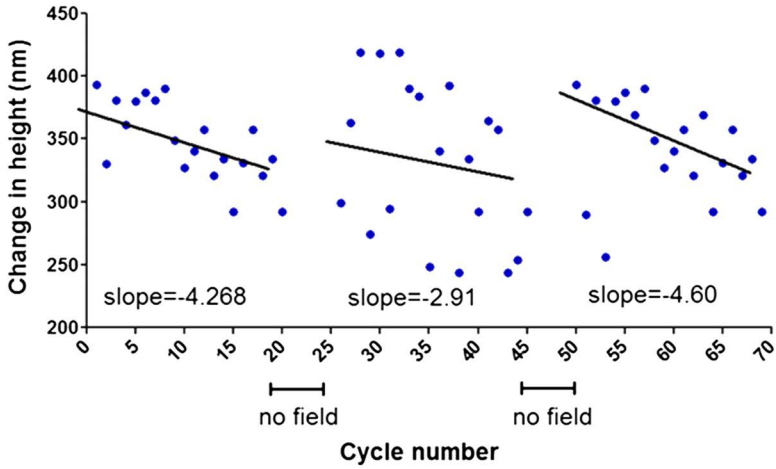

Figure 11.4 AFM measurements over three stimulation intervals made over 20 cycles followed by non-stimulation intervals of five cycles. Changes in scaffold height quantified. Adapted from *Nanoscale*. Sapir-Lekhovitser Y., Rotenberg M. Y., Jopp J., Friedman G., Polyak B., Cohen S., Magnetically actuated tissue engineered scaffold: insights into mechanism of physical stimulation, **8**(6):3386–3399. Copyright © 2016, with permission from The Royal Society of Chemistry.[58]

While the shape deformations, as measured by a change in scaffold height, gradually decreased over the course of 20 cycles at a 1 Hz frequency, it was possible to completely recover the original shape after deformation within a one-minute time-frame post magnetic stimulation (Figure 11.4).[58]

This result implies that a frequency less than 1 Hz may be necessary for optimal scaffold relaxation between applied magnetic currents to prevent attenuation of shape deformation. Translation of the shape deformation into force imparted by the scaffold bending/stretching onto theoretically seeded cells was calculated to be approximately 1 pN. Low mechanical forces activate various intracellular biochemical signaling pathways.[58] Forces as low as 0.2 pN activate the TREK-1 ion channels located in the study discussed earlier. Therefore, it is reasonable to assume that the translation of 1 pN onto cells embedded within a magnetically-responsive scaffold would alter intracellular biochemical signaling and influence cellular behavior.[33]

11.2.3 Cellular Response to Mechanical Stress

The above methods represent different ways to apply mechanical strain on cells using magnetic particles attached to specific membrane components, materials, or loaded intracellularly in combination with magnetic fields. As discussed above, cells respond to mechanical stress by transducing mechanical strain into biochemical signaling pathways. Magnetic strategies can precisely control activation of mechanically sensitive signaling pathways.

In multiple studies, Ingber and colleagues have demonstrated the ability to activate diverse intracellular signaling responses by treating cells with ligand bound magnetic nanobeads and subsequently applying magnetic twisting forces.[28–30,59] Meyer *et al.*, 2000, showed that coating magnetic nanobeads with the integrin-adhesion peptide, RGD, resulted in a 50% increase in intracellular cyclic AMP (cAMP) signaling in endothelial cells.[30] When combined with a magnetically-induced twisting force of 15.6 dyn cm^{-2}, intracellular levels of the cAMP second messenger tripled. The authors demonstrated a concomitant increase in nuclear translocation of protein kinase A and phosphorylated CREB indicating altered cAMP levels results in downstream signaling in both endothelial cells and fibroblasts. Interestingly, alterations in intracellular signaling were both mechanically and chemically dependent. cAMP signaling increased proportionally with increases in stress applied to RGD beads (2.6 to 15.6 dyn cm^{-2}) whereas magnetic nanobeads coated with non-activating antibodies specific for integrin-β1 did not alter cAMP signaling in response to magnetic twisting.[30] In a follow up study, researchers used this technique to elucidate that mechanically induced cAMP signaling is mediated by the heterotrimeric Gαs protein. They demonstrated that binding of RGD-coated magnetic nanobeads to integrin receptors in combination with magnetic twisting significantly increased the recruitment of Gαs protein to focal adhesions formed beneath magnetic beads, intracellularly. Furthermore, Gαs protein was not only recruited, but it was also biochemically activated as shown by an increase in GTP-bound Gαs. Activated Gαs, in turn, increased cAMP signaling and nuclear localization of its downstream effectors, PKA and phosphorylated CREB. These results were attenuated with Gαs protein either pharmacologically inhibited or knocked down by RNAi techniques.[28]

Another study by this group (Mannix *et al.*, 2008) utilized the precise control conferred by magnetic actuation to establish a method using magnetic stimulation as a switch that can rapidly trigger a specific intracellular signaling response.[29] In this study, mast cells and their high-affinity immunoglobulin E (IgE) receptors (FcεRI) were used as a model system for inducing robust intracellular signaling in response to magnetically-induced strain. By priming mast cells with IgE directed against dinitrophenyl antigen (DNP), the authors were able to fabricate superparamagnetic nanobeads capable of binding the mast cell FcεRI receptors by covalently conjugating a single monovalent DNP-lysine (DNP-lys) ligand to the bead. DNP-lys nanobeads could bind the FcεRI receptors, but could not activate signaling because FcεRI receptors are normally activated by multivalent ligands that induce receptor clustering. Exposure of mast cells to a magnetic field, applied by an electromagnetic needle at a current of 1 A for multiple one-minute stimulation periods, resulted in FcεRI receptor clustering and significantly increased intracellular signaling as demonstrated by an increase in intracellular calcium. The force applied to the cells (10^{-17} N) was too low to induce mechanosensitive signaling through integrin receptors, which requires pN to nN forces, indicating signaling was a result of receptor oligomerization. The observed increase in intracellular calcium was comparable to the calcium increase seen when

FcεRI receptors are activated by multivalent ligands. Due to the nature of superparamagnetic particles, the fabricated nanobeads for this study only became magnetized when the magnetic field was applied, allowing magnetic stimulation to function as a switch for physically inducing receptor clustering.[29] Since receptor clustering is a common activation mechanism for cell surface receptors, this method represents a non-invasive way to rapidly and reversibly control a diverse number of signal transduction pathways.

The discussed studies validate the importance of both physical and chemical cues when activating cell surface receptors, like integrin. However, the duration, strength, and cyclic nature of a physical stimulus also have a role in eliciting a desired cellular response. Just as cells respond to different biochemical cues by activating different arrays of intracellular signaling pathways, cells respond to different types of physical cues in biochemically and mechanistically distinct ways. Cells receive a wide range of physical cues *in vivo*. These cues include the stiffness of the extracellular matrix, cyclical mechanical load, and fluid shear force. Not only do these signals differ in different locations within the body, but they also differ significantly throughout development. Similarly, the strain exerted by a cell on the surrounding extracellular matrix is spatially and temporally diverse. Therefore, lack of dynamic mechanical strain can be a hindrance in achieving functional engineered tissue constructs.

Matthews *et al.*, 2006, used magnetically-induced mechanical strain to show how cells adapt to different types of mechanical stress.[59] Magnetic microbeads bound to cell surface receptors on bovine capillary endothelial cells combined with magnetic pulling cytometry analysis, showed three unique cellular responses to applied physical strain. Three second pulses of forces ranging from 0 to 350 pN elicited an immediate viscoelastic response of focal adhesions formed between the magnetic bead, integrin receptor, and cytoskeleton. This response was dependent upon baseline tension present in the cytoskeleton and receptor tyrosine kinase signaling. Continuous-pulsatile forces, defined as the cyclical application of three second forces (130 pN) followed by four seconds of recovery, known to be enough time for full bead recoil, resulted in an early adaptive strengthening response in cells. Bead displacement showed a small but significant attenuation that plateaued by the third cycle. This response was also dependent on cytoskeletal tension, myosin dependent contractility, and tyrosine kinase activity. Interestingly, when cells were exposed to a prolonged strain (250 pN), greater than 15 sec, there was an adaptive and sustained strengthening response initiated within the cell that significantly decreased bead displacement in response to pulsatile forces applied after the prolonged force. This adaptive increase in cell strength was not dependent on myosin contractility or tyrosine kinase activity, indicating that an alternate biochemical pathway was facilitating cell strengthening in response to static forces compared to pulsatile forces. Furthermore, sustained forces longer than 20 sec resulted in a repositioning reaction in the cell that increased the cellular strength enough to pull the magnetic bead in the opposite direction of the applied magnetic force.[59]

These results demonstrate that cells respond to mechanical strain using different biochemical pathways to produce different physical responses. Consequently, design of an appropriate mechanical strain regimen must be taken into consideration when engineering different tissues to more closely mimic the endogenous physiological environment for a specific cell type. The flexibility of magnetically-based systems to apply a wide range of spatially and temporally diverse physical cues makes them a promising method for engineering complex tissue.

11.3 Vascularization Challenge and Current Studies

Efficient vascularization remains a challenge for engineering thick tissues, like cardiac tissue. Cell survival and function require a sufficient supply of oxygen and nutrients as well as a means to remove waste. Since diffusion of oxygen and nutrients is limited to only a few hundred microns, a robust vascularization network is necessary to support viability of inner tissue layers. Magnetically-based systems offer a promising method to vascularize a tissue construct by stimulating the secretion of angiogenic factors or by inducing cellular reorganization into vascular structures.

11.3.1 Vessel Structure Formation

One method for engineering complex vascular structures is to utilize tubular shaped magnets to culture magnetically-responsive cells into a tubular structure. Using the Mag-TE approach mentioned earlier, Ito *et al.*, 2005, engineered a tubular structure made of heterotypic cell layers.[40] Using a cylindrical permanent magnet, endothelial cells, smooth muscle cells, and fibroblasts were cultured in a sequential manner to create a multilayer 3-D construct. The multilayer-tubular construct was stabilized by collagen type I solution injected into the tube and allowed to gel. Upon removal of the magnet, histological examination and imaging of the construct showed a tubular structure made up of more than 30 cell layers that had an internal lumen diameter of 5 mm.[40]

11.3.2 Induction of Vessel Structure Organization

In follow up studies, using the same Mag-TE method, researchers were able to demonstrate the fabrication of multilayer cell sheet structures made of myoblasts transduced with VEGF,[42] mesenchymal stem cells,[45] induced pluripotent stem cells (iPS),[44] and adipose-derived regenerative cells (ADRCs)[43] without the use of a polymer scaffold that were capable of inducing angiogenesis in ischemia damaged tissues upon implantation. The cell sheets consisted of approximately 15 cellular layers and were 300 μm thick.[42–45] The researchers did not observe significant cell death or inhibition of cell proliferation within the constructs. The application of a vertically applied magnetic

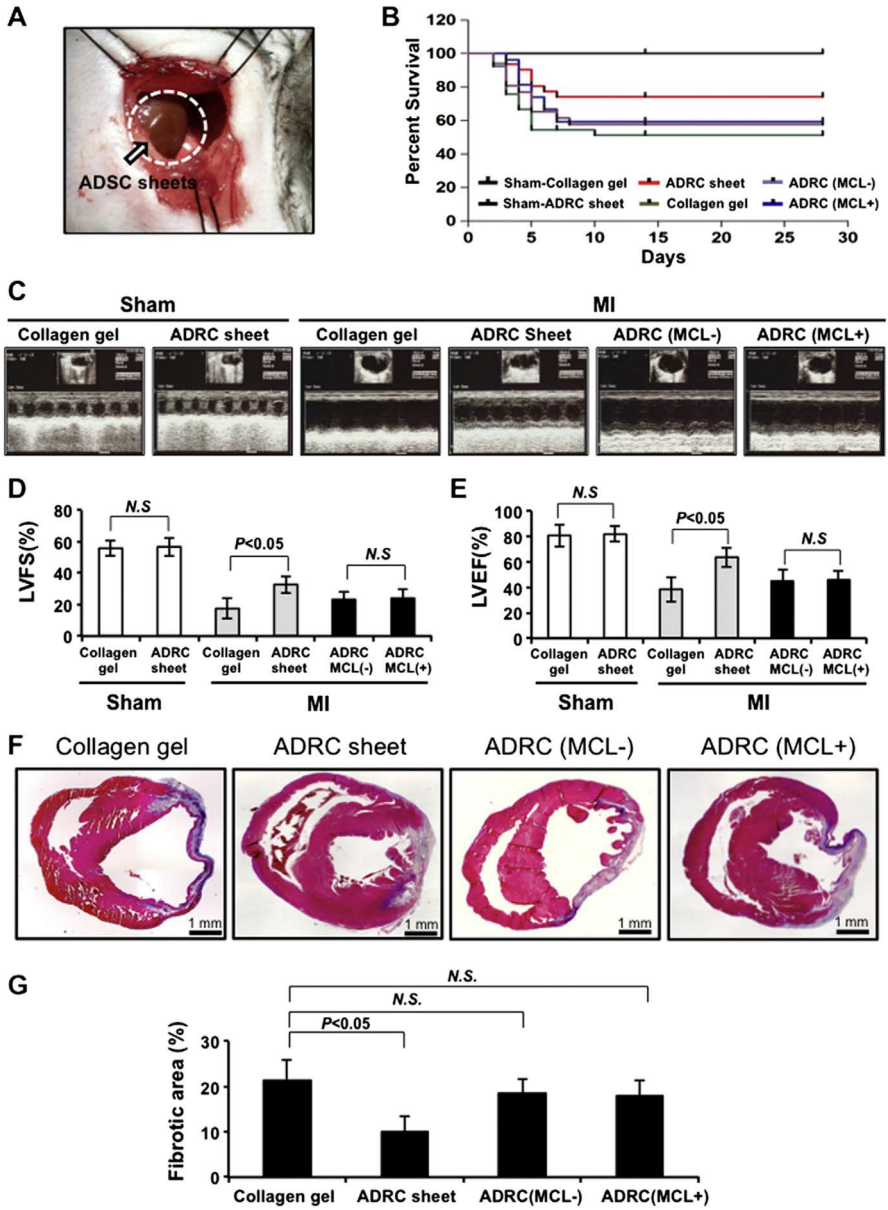

Figure 11.5 (A) Image of ARDC sheets attached to the heart surface in mice. (B) Kaplan–Meier survival curves over the course of four weeks after sheet implantation. Six experimental groups: (1) cell-free collagen gel sheet implanted after a sham-operation (sham-collagen gel). (2) Cell-loaded ADRC sheet implanted after sham-operation (sham-ARDC sheet). (3) Cell-free collagen gel sheet implanted after MI (collagen gel). (4) Cell-loaded ADRC sheet implanted after MI (ARDC sheet). (5)

force enhanced cell–cell contact, facilitating cell adhesion both vertically and laterally. Cell sheets consisting of mesenchymal stem cells or induced pluripotent stem cells (iPSCs), showed improved capillary density and blood perfusion in an ischemic hind limb model. Implantation of cell sheets over hind limb tissue post induction of unilateral hind limb ischemia resulted in increased blood perfusion by post-operative day seven as demonstrated by laser dopler blood flow analysis. Histological analysis also demonstrated a significant increase in capillary density by day 21 post implantation.[44,45] Furthermore, ADRC cell sheets implanted post myocardial infarction in mice resulted in improved survival and cardiac function compared to cell injection and cell-free collagen implantation (Figure 11.5(A) and (B)).[43] Echocardiography analysis at 28 days post myocardial infarction showed a significant increase in left ventricular function (Figure 11.5(C)–(E)).[43] Histological analysis using Masson's trichrome staining and immunofluorescence showed a decrease in cardiac fibrosis (Figure 11.5(F) and (G)) and increase in capillary density (Figure 11.6), respectively.[43] The improved angiogenesis was not due to differentiation of progenitors into endothelial cells, but rather due to the increased expression of angiogenic factors.[43] These results highlight the use of magnetically engineered cell sheets for treatment of ischemic tissue and have significant implications for cardiac tissue engineering.

This group also demonstrated that their Mag-TE methodology can be used to enhance gene therapy in addition to and in combination with cell therapy. MCL-retroviral complexes with retroviral vectors containing the vascular endothelial growth factor (VEGF) gene resulted in a 6.7-fold increase in transduction efficiency of mouse myoblasts compared to standard retroviral transduction. Transduction efficiency increased with increasing magnetic field strength. The transduced myoblasts were then cultured into cell sheets using a permanent magnet placed beneath the cell culture plate. The transduced myoblast cell sheet significantly increased the amount of bioactive VEGF secreted from the cell sheet as demonstrated by the significantly enhanced ability of the myoblast conditioned media to induce proliferation in HUVEC cells compared to non-transduced myoblast sheets and increased

Cell-loaded ADRCs, unlabeled with MCLs, needle injected after MI (ARDC(MCL−)). (6) Cell-loaded ADRCs, labeled with MCLs, needle injected after MI (ARDC(MCL+)) (n = 25 for each group). (C) M-mode echocardiograms for the six experimental groups. (D) and (E) Quantitative analysis of left ventricular fractional shortening (LVFS) and left ventricular ejection fraction (LVEF). (F) Masson trichrome staining. Scale bar: 1 mm. (G) Quantitative analysis of cardiac fibrosis area using Masson trichrome staining (n = 5 for each group). Reprinted from *International Journal of Cardiology*. **175**(3), Ishii M., Shibata R., Shimizu Y., Yamamoto T., Kondo K., Inoue Y., Ouchi N., Tanigawa T., Kanemura N., Ito A., Honda H., Murohara T. Multilayered adipose-derived regenerative cell sheets created by a novel magnetite tissue engineering method for myocardial infarction. pgs. 545–553. Copyright © 2014, with permission from Elsevier.[43]

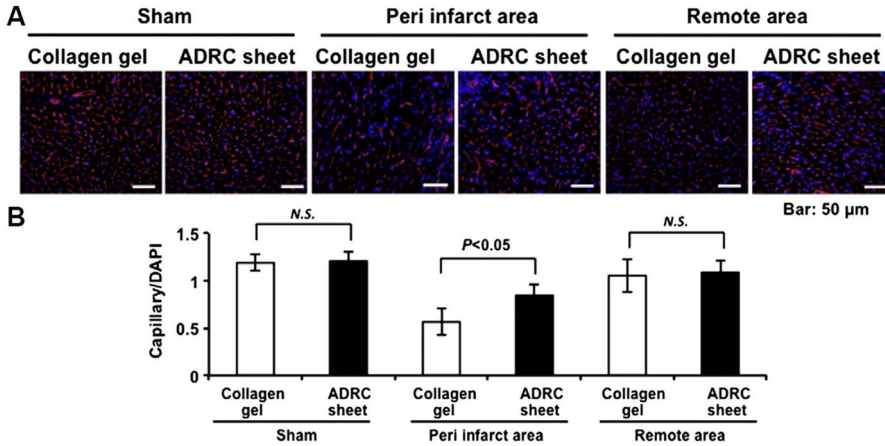

Figure 11.6 Capillary density 14 days after surgery. (A) Microscopic photographs of the peri-infarct areas and remote areas in either the collagen gel or ARDC sheet experimental groups. Anti-CD31 antibodies were used to stain capillaries. (B) Quantitative analysis of capillary density. Reprinted from *International Journal of Cardiology*. **175**(3), Ishii M., Shibata R., Shimizu Y., Yamamoto T., Kondo K., Inoue Y., Ouchi N., Tanigawa T., Kanemura N., Ito A., Honda H., Murohara T. Multilayered adipose-derived regenerative cell sheets created by a novel magnetite tissue engineering method for myocardial infarction. pgs. 545–553. Copyright © 2014, with permission from Elsevier.[43]

tube length of HUVECs in a tubular formation assay. Subcutaneous implantation of sheets resulted in significantly increased size of constructs *in vivo* and angiogenesis of host vessels into the construct as shown by histological data showing an increased micro vessel area.[42] In a separate study, magnetic nanoparticle beads conjugated to an adenovirus encoding the VEGF gene were directly delivered to ischemic heart tissue *via* intravenous injection and magnetic guidance. Use of magnetic force significantly enhances the expression of VEGF in ischemic heart tissue post myocardial infarction compared to non-treated control groups. Hemodynamic measurement of cardiac performance demonstrated a significant increase in functional cardiac parameters and histological analysis showed improved left ventricular wall thickness and decreased fibrotic scarring in infarcted hearts receiving treatment compared to untreated controls and delivery of adenovirus without magnetic targeting.[38] These results demonstrate the increased effectiveness of magneto-transduction compared to standard gene transduction therapies and show the potential for this technique to be used both *in vitro* and *in vivo*.

Beyond the fabrication of a construct that can induce vascularization *via* secretion of angiogenic factors, recent evidence has shown the ability of magnetic nanoparticles to modulate angiogenesis directly or be utilized in magnetically-responsive scaffolds to promote the morphological

rearrangement of endothelial cells into vessel structures. Inoculation of five-day-old fertile chick eggs with nanoparticles of spinel ferrites (MFe_2O_4) incorporating the transition metals copper, manganese, and nickel induces angiogenesis in the chick chorioallantoic membrane (CAM). Evaluation of the CAM 14 days post inoculation showed a significant increase in blood vessel sprouting and branching compared to the untreated control.[60]

Sapir *et al.*, 2012, demonstrated the morphological re-arrangement of endothelial cells into vessel structures in response to magnetic stimulation of a magnetite-embedded alginate scaffold.[61] Endothelial cells were seeded onto macroporous alginate scaffolds modified with RGD and HBP peptides and impregnated with superparamagnetic magnetite nanoparticles to promote cell adhesion and cell stimulation, respectively. The researchers showed that application of an alternating magnetic field with a strength of 10–15 Oe and a frequency of 40 Hz for seven days resulted in a 1.5-fold increase in the number of endothelial cell vessel structures formed within the scaffold compared to non-magnetic scaffolds (Figure 11.7(A) and (B)).[61] The increase in the vessel structure formation occurred alongside an increase in cell metabolic activity during magnetic stimulation that returned to baseline when the magnetic stimulus was removed. The increase in metabolic activity was not associated with an increase in cell proliferation as shown by the lack of a significant upregulation of the proliferation marker, PCNA, during stimulation. This result implies that the magnetic stimulation increased metabolic activity in endothelial cells seeded within the scaffolds that gave rise to morphological rearrangement of cells into vessel structures instead of cellular proliferation.[61]

11.4 Generation of Functional Cardiac Tissue

Damaged cardiac tissue is unable to regenerate post myocardial infarction. This is due to the severely limited ability of adult cardiomyocytes to proliferate.[62–66] Over time, injured ischemic tissue is replaced by non-functional fibrotic scarring. Fibrotic scarring can lead to left ventricle wall thinning and adverse tissue remodeling, resulting in eventual heart failure.[67,68] Despite improvements in pharmacological treatments post myocardial infarction that aim to repress fibrotic scarring, there is still no clinical treatment available that can effectively regenerate damaged tissue outside of a heart transplant, which is limited due to a lack of donors. Cell therapy has been the focus of developing new regenerative treatments, however injection of cells alone leads to mass cellular attrition, incomplete engraftment into host tissue, and only modest improvements in tissue function.[1,69–73] Therefore, methods to improve cell delivery and engraftment are necessary. Magnetic attraction and manipulation of magnetically-responsive cells has shown to be a promising method for *in vitro* construction of cardiac tissue, induction of cardiomyogenesis in

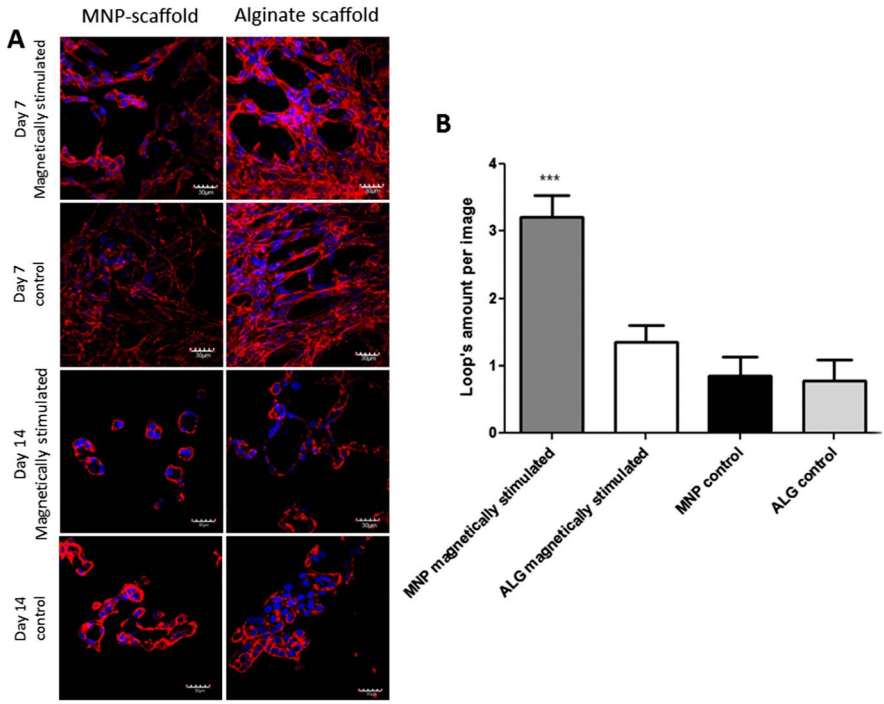

Figure 11.7 Endothelial cell organization in response to magnetic stimulation. (A) Endothelial cells stained for F-actin (red) and nuclei (blue) seven or 14 days after cell seeding onto MNP-alginate scaffolds (scale bar: 30 μm). (B) Quantitation of average loop number per image field observed 14 days post cell seeding. 25 randomly selective fields per group. Asterisks denote significant difference (by two-way ANOVA), $*p < 0.05$, $**p < 0.01$ and $***p < 0.005$ (Bonferronis post-hoc test was used for comparison between the groups). Adapted from *Biomaterials*. **33**(16), Sapir Y., Cohen S., Friedman G., Polyak B. The promotion of *in vitro* vessel-like organization of endothelial cells in magnetically responsive alginate scaffolds. pgs. 4100–4109. Copyright © 2012, with permission from Elsevier.[61]

stem cells, and gene delivery that can enhance cardiac tissue function post damage due to ischemia.

Utilizing the Mag-TE method, Akiyama *et al.*, 2010, were able to construct rings of cardiac tissue that possess contractile and force generating properties.[42] MCL-labeled primary cardiomyocytes were cultivated in a ring-shaped culture plate with a permanent magnet exerting a vertical magnetic force directly beneath the plate. The magnetic force attracted the cardiomyocytes downward to form a compact, densely populated cardiomyocyte construct. This densely populated structure closely mimics the native myocardium, which consists of highly organized, densely populated cardiomyocytes functioning in a coordinated manner. Achievement

of a construct highly populated with cardiomyocytes has not been realized by other tissue engineering methods and may be critical for proper tissue function upon implantation. Collagen type I solution was used to stabilize the cardiomyocytes and support the construct structure and function. The researchers demonstrated that the cardiac rings constructed had a thickness of approximately 247 μm and did not display significant necrosis within the interior cardiomyocyte layers. Using force transducer analysis, the cardiac rings demonstrated the ability to generate force up on the μN scale when a strain was applied that was 14% of the original length or higher. The generation of force decreased when a fixed strain of 20% was applied, a phenomenon that was observed in native cardiac tissue. The researchers also showed the ability of cardiac rings to generate contractile forces in response to electrical pulses as well as longitudinal alignment of cardiomyocytes on the surface of their construct.[42] These are properties indicative of mature cardiac tissue, implying the feasibility of using magnetic force to create a cardiac tissue construct from primary cardiomyocytes *in vitro*.

Alternatively, generating a cardiac tissue construct using a magnetically-responsive polymer scaffold instead of magnetically-responsive cells is another feasible method. Sapir *et al.*, 2014, utilized magnetically-responsive alginate scaffolds embedded with primary neonatal rat cardiomyocytes and cardiac fibroblasts in combination with alternating magnetic currents to indirectly exert mechanical strain on cardiac cells.[74] Using a physiologically relevant frequency of 5 Hz, and a field strength of 10–15 Oe, stimulation of constructs for as little as five minutes increased pro-survival Akt signaling within cells almost two-fold compared to non-stimulated controls. Pro-apoptotic p38 signaling was not different between control and stimulated groups, indicating that stimulation triggers a pro-survival biochemical response within cardiac cells. Furthermore, seven days of stimulation, followed by seven days of cultivation without magnetic treatment significantly increased metabolic activity within cells. The change in metabolic activity appeared immediately after magnetic stimulation and was not only sustained, but further enhanced one week post stimulation in treated cells. Immunohistochemical analysis of the contractile protein α-sarcomeric actinin post magnetic stimulation revealed an increase in cardiac fiber morphology with striation that is characteristic of mature cardiomyocytes in both magnetically treated and untreated samples. However, this striation morphology was only sustained throughout the entire two weeks of cultivation in the magnetically stimulated group (Figure 11.8).[74] Additionally, expression of the contractile protein, Troponin-T, showed a significant increase in cardiac cells that were magnetically stimulated compared to controls (Figure 11.9).[74] These results indicate the ability of cardiomyocytes to adhere and mature in 3D cultures both with and without magnetically-induced strain. However, sustained cardiac maturation and organization was observed during application of magnetically-induced strain.

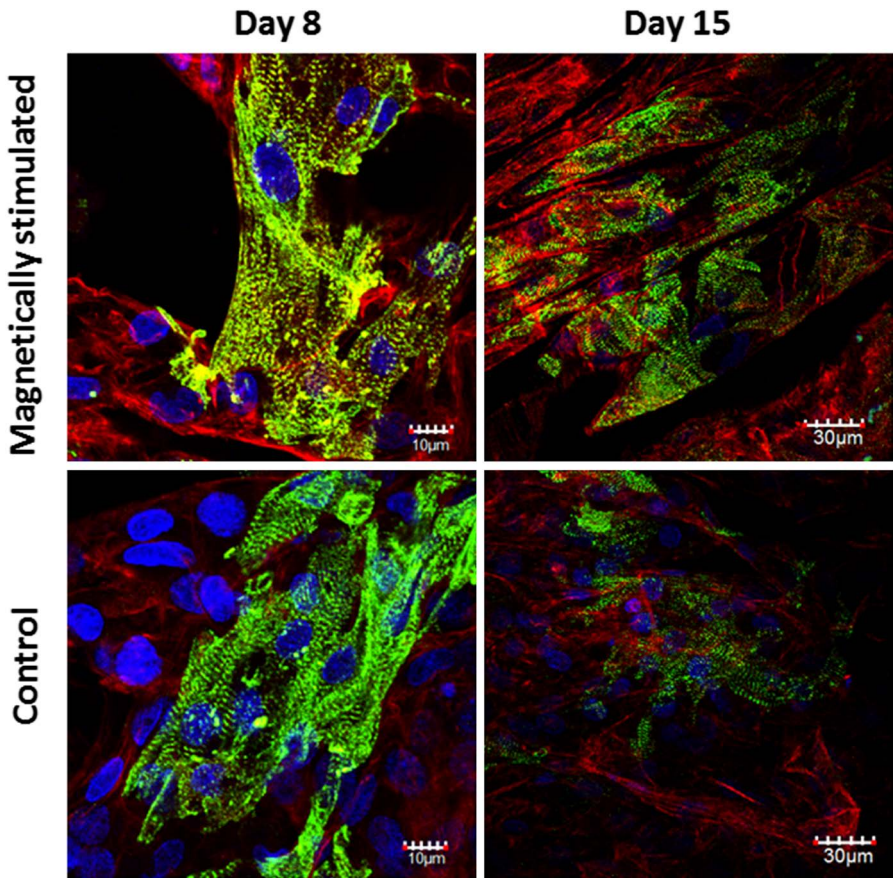

Figure 11.8 Cardiac cell organization in response to magnetic stimulation. MNP–alginate scaffolds seeded with cardiomyocytes. Cells were stained for alpha-actinin (green), F-actin (red) and nuclei (blue) on day eight or 15 post cell seeding. Reprinted from: Sapir Y., Polyak B., Cohen S., Cardiac tissue engineering in magnetically actuated scaffolds. *Nanotechnology*, **25**(1):014009, Published 11 December 2013. DOI: 10.1088/0957-4484/25/1/014009. Copyright © 2014, reproduced with permission from IOP Publishing Ltd. All rights reserved.[74]

11.4.1 Effects of Magneto-Mechanical Stimuli on Maturation of Cardiomyocytes

While application of magnetic force has been shown to enhance primary cardiac cell maturation and organization *in vitro*, the clinical translation of techniques relying on the use of differentiated adult cardiac cells may be limited due to the difficulty of harvesting a sufficiently large population of cardiomyocytes from a donor or patient for *in vitro* tissue engineering.

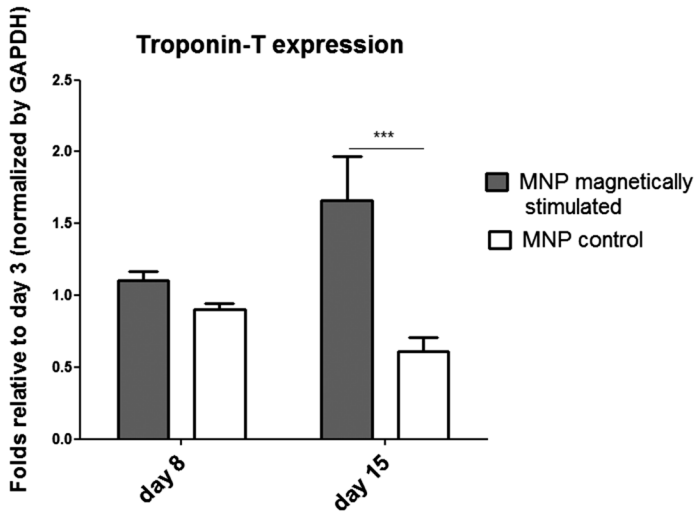

Figure 11.9 Expression of cardiac cell marker Troponin-T in response to magnetic stimulation. Western blot analysis of Troponin-T expression on day eight or 15 post cell seeding, relative to day three (before magnetic stimulation). Asterisks denote significant difference (by two-way ANOVA), $p < 0.05$; $p < 0.01$ and $p < 0.005$ (Bonferroni's post-hoc test was used for comparison between the groups), ns represents non-significant difference. Reprinted from: Sapir Y., Polyak B., Cohen S., Cardiac tissue engineering in magnetically actuated scaffolds. *Nanotechnology*, **25**(1):014009, Published 11 December 2013. DOI: 10.1088/0957-4484/25/1/014009. Copyright © 2014, reproduced with permission from IOP Publishing Ltd. All rights reserved.[74]

Therefore, an alternative cell source for cardiomyocytes may be necessary. The proliferative capabilities and pluripotency of stem cells make them promising cellular sources that can be harvested, expanded, and differentiated in culture to generate a source of cardiomyocytes. The use of soluble factors alone to differentiate stem cells into cardiomyocytes results in a low yield, ~20% for embryonic stem cells.[75] Mechanical strain is known to help guide differentiation of pluripotent cells during tissue development. Therefore, the combination of magnetically-induced mechanical strain and soluble factors to enhance differentiation of stem cells into functional cardiomyocytes represents a promising strategy. Geuss *et al.*, 2014, incorporated magnetically-induced mechanical strain with morphogen supplementation to significantly enhance differentiation of embryonic stem cell embryoid bodies into cardiomyocytes.[76] Embryonic stem cells tagged with RGD-functionalized paramagnetic beads were cultured into embryoid bodies and treated with a magnetic field of 0.2 T. Application of the magnetic field of 0.2 T alone was able to activate integrin signaling as shown by an increase in expression of the second messenger, protein kinase A (PKA). When combined with bone morphogenetic protein-4 (BMP4)

supplementation, a morphogen that induces cardiomyogenesis, magnetic stimulation resulted in a significantly increased number of cells expressing sarcomeric α-actinin, a cardiomyocyte marker, as shown by FACs analysis. BMP4 supplementation alone did produce an increasing trend in the number of cardiomyocytes compared to a control, however the combination with magnetically-induced strain further enhanced cardiomyogenesis in embryoid bodies that were aged day three or later.[76]

11.5 Magnetic Cell Targeting

Cell therapy based on the fully differentiated progeny of autologous induced pluripotent stem cells (iPSCs) or undifferentiated stem cells holds great promise to promote tissue regeneration and repair.[77–83] Cell therapy has shown potential in regenerating cardiac tissue in models of myocardial infarction, inducing formation of new blood vessels and restoring endothelial cell linings in stented arteries.[84–87] Advancement of new tools enabling us to obtain iPSCs and development of cell-based therapeutic approaches have resulted in a paradigm shift from transplantable donor organs to artificially generated tissues and organs. The development of artificial organs holds promise for more than 120 000 patients that need a lifesaving organ transplant (United Networks for organ sharing).[88]

Poor cell homing, retention and engraftment are the major obstacles faced by cell therapy, irrespective of the cell type, route of administration or animal model. These obstacles prevent cell therapies from achieving a significant functional benefit when applied *in vivo*.[89,90] Retention and long-term engraftment of cells delivered to the heart is extremely suboptimal. Heart contraction and coronary blood flow account for the substantial elimination of delivered cells shortly after cell administration.[89] This, in part, may be a reason for the non-significant and highly variable therapeutic benefits observed in clinical trials involving stem cell-based therapies for the treatment of acute myocardial infarction (MI). Therefore, there is still a critical need for novel approaches that can improve the homing and retention of therapeutic cells delivered to treat infarcted heart muscle and atherosclerotic blood vessels.

Magnetically-mediated targeting is an intriguing physical approach that utilizes magnetic forces to localize and retain magnetic carriers associated with drugs, genes or cells.[50,91] This technology was initially suggested for targeting chemotherapeutic agents to tumors[92–96] with the intention of reducing the overall administered drug dose and minimizing the toxic systemic side effects of the chemotherapy. Today, however, this technology is becoming more and more popular for cell delivery applications. This section focuses on the recent progress of magnetic cell delivery for cardiac and vascular regeneration, highlighting its potential to improve cell homing, retention, and engraftment, leading to better therapeutic outcomes.

11.5.1 Magnetic Cell Therapy for Heart Regeneration

A magnetic targeting strategy to improve localization of the transplanted cells in the heart was first assessed by Cheng and colleagues.[97] This group showed that magnetically-assisted homing of intramyocardially injected cells augmented short-term cell retention (at 24 hours) and long-term engraftment (at three weeks) in the recipient hearts by nearly three-fold compared to non-targeted cells. Magnetically-enhanced cell engraftment used in this study translated to a greater functional outcome demonstrating superior reduction of left ventricular remodeling in the animals of a magnetic targeting group. Chaudeurge and co-workers utilized a magnetic cell targeting approach to study the retention of endothelial progenitor cells (EPCs) after direct intraventricular injection.[98] Although per RT-PCR quantification, no statistically significant differences in cell retention between groups were observed, quantitative immunostaining showed a ten-fold greater engraftment of EPCs in magnetically-targeted animals in comparison to non-targeted controls. In another study, magnetic targeting was used to investigate cell homing and retention after intracoronary administration of magnetically-responsive cardiosphere-derived cells.[99] These authors demonstrated that improved cell engraftment was preserved for at least three weeks, leading to a higher ejection fraction and decreased left ventricular remodeling in the animals of the magnetic targeting group. Ge and co-workers demonstrated that magnetic targeting enhanced cell retention in a rat model of myocardial infarction using a retrograde coronary venous administration.[100] In this study, magnetically-labeled mesenchymal stem cells, MSCs, were transjugularly injected into the left cardiac vein under magnetic conditions. Cardiac tissue retention of transplanted MSCs was shown to increase nearly three-fold with magnetic targeting. Per histologic evaluation, a larger fraction of transplanted cells was found to distribute in the anterior wall of the left ventricle. The augmented cell engraftment three weeks after cell administration resulted in attenuated remodeling of the left ventricle and improved cardiac function. In a recent study, syngeneic human cardiosphere-derived stem cells (hCDCs) laden with FDA-approved ferumoxytol nanoparticles were infused into the coronary arteries of rats.[21] Magnetic targeting significantly enhanced cell retention without exacerbating cardiac inflammation and resulted in reduced left ventricular remodeling, a higher ejection fraction and greater extent of angiogenesis in the animals of the magnetic targeting group.

The above studies demonstrated that magnetic targeting was instrumental in enhancing cell retention and engraftment resulting in improved functional outcomes of the targeted cell therapy, indicating high translational potential of this modality for clinical applications. In most cases, however, cell transplantation for tissue repair relies on exogenously administered cells, which usually necessitates access to appropriate cell sources and is associated with prolonged cell isolation and propagation procedures. To address these limitations, an appealing alternative has recently been suggested: using bispecific antibodies (BiAb) that enable coupling of an endogenous

therapeutic cell population to specific antigens of a diseased tissue. Bispecific antibodies that target hematopoietic marker CD45 and myosin light chain (MLC)-1, a marker for ischemic injury, were used to target hematopoietic stem cells (HSC) to the injured myocardium achieving definitive therapeutic improvements.[101–103]

A recent innovative study suggested functionalization of magnetic particles with bispecific antibodies to target and link endogenous circulating therapeutically relevant cells with exposed antigens of injured cells in diseased tissue to realize a so-called magnetic bifunctional cell engager, (MagBICE). Such innovative 'nanomatchmakers' intravenously administered in rats with induced MI direct endogenous circulating bone marrow-derived stem cells or CD34-positive stem cells and concentrate them by magnetic forces in the injured heart, thus reducing the formation of scar tissue and improving cardiac pump function.[104] This approach doesn't require cell transplantation, which may significantly shorten and simplify the treatment protocol, making it very attractive for translation into clinical settings.

11.5.2 Magnetic Cell Therapy for Blood Vessel Regeneration

Repair of injured vasculature is another area where cell-based therapy has the potential to make significant improvements. Obstructive coronary artery disease, a result of progressive atherosclerosis, is managed today by percutaneous coronary interventions with implantation of endovascular stents.[105–108] Although these procedures have become the current treatment of choice for vascular disease patients, they inevitably cause severe trauma to the arterial wall with concurrent endothelial denudation[109] and inflammatory response,[110] often leading to a recurrent blockage of the stented artery or in-stent restenosis.[111,112] The primary mechanism responsible for restenosis is attributed to uncontrollable proliferation and migration of vascular smooth muscle cells (VSMCs) into the intima, eventually leading to re-narrowing of the vessel lumen.[109,113,114] Currently used in clinical practice, drug eluting stents (DES) effectively prevent proliferation of VSMCs by releasing potent antiproliferative drugs.[105,115] However, these non-selective drugs also inhibit the growth and function of endothelial cells, significantly delaying re-endothelialization and subsequent vascular healing.[116–120] A healthy and intact endothelial cell lining forms a physical barrier that modulates vascular hemostasis and fibrinolysis and controls the proliferative and functional state of the VSMCs.[120,121] Thus, rapid and efficient restoration of the competent endothelial layer after vascular injury represents a promising strategy to minimize severe complications associated with the use of DES, with the potential to improve long-term prognosis for vascular disease patients.

Magnetic targeting of endothelial cells to the injured vessels is a captivating approach that has been investigated over the last decade in animal models with and without stenting. The feasibility of magnetically-guided cell delivery to the stented vessels has been demonstrated using transiently magnetized[24] and permanently magnetized[122] vascular stents. A circular

Halbach array, which augments the magnetic field at its center, was used to demonstrate six-fold enhancement in cell retention following balloon angioplasty in a rabbit model, which, however, did not translate to a statistically significant anti-restenotic effect.[123] More recent studies showed that magnetically-guided endothelial cells to transiently magnetized stents in a rat carotid stent angioplasty model augmented capture, retention and proliferation of delivered cells at the site of stent implantation.[124] Circumferential magnetic localization of endothelial cells overexpressing endothelial nitric oxide synthase (eNOS) in the non-stented vessels in a murine balloon angioplasty model showed improved vascular function after mechanical injury.[125] Although these studies provide supporting indications that magnetically-mediated cell delivery to the injured vasculature has the potential to restore structural and functional endothelial lining mitigating the deleterious sequelae of mechanical revascularizations, more studies will need to be conducted to demonstrate this promising potential on the long-term scale.

11.6 Effects of Electro-Magnetic Fields on Cells

The technology of magnetic targeting or magneto-mechanical stimulation is inevitably associated with exposure of biological systems to static or time-varying (alternating) magnetic fields and field gradients, which may cause both negative and positive effects. Static fields and field gradients usually used for targeting applications are very short (up to 30 min) and their effects are expected to be quite transient with negligible consequences to affect the biological balance of a live organism. Extremely low frequency electromagnetic fields (1–100 Hz) used for magneto-mechanical stimulation during prolonged periods of time (up to a week)[61,74] could be potentially of a greater concern by causing arrhythmias, especially for *in vivo* stimulation. Although this effect was not studied under controlled conditions (*e.g.* frequency, field strength), the literature indicates that no associated risk of severe arrhythmia-related heart disease was associated with prolonged exposure of humans to low frequency electromagnetic fields (16–50 Hz).[126,127]

Most studies describing the effects of magnetic fields investigated the influence of electromagnetic fields on the healing of bone, tendons, and skin.[128–131] A small number of studies have been devoted to assessing the effects of magnetic fields on cardiac cells and cardiomyogenesis of stem cells.[132–135] However, considering the limited regenerative ability of cardiomyocytes, viable sources for these cells are greatly required.[136] In this context, electromagnetic fields represent one of the attractive strategies to controllably modulate differentiation of stem cells in cardiomyogenic direction without the use of pharmacological or genetic manipulation.

Application of sinusoidal magnetic fields (50 Hz, 8 G) to embryonic stem cells (ES) have shown to increase the yield of ES cell-derived cardiomyocytes without the aid of genetic or pharmacological agents.[135] In another study, the extremely low frequency electromagnetic fields tuned at calcium (Ca^{2+}) ion cyclotron energy resonance (7 Hz, 0.025 G) have been effective in driving

cardiac specific differentiation of adult cardiac stem cells.[132] Moreover, it has recently been reported that a static magnetic field of 10 G also promoted cardiomyogenesis of FLK-1^{+} cardiac progenitor cells derived from mouse ES cells indicating that magnetic field-mediated generation of reactive oxygen species (ROS) and cytosolic Ca^{2+} may potentially serve as secondary messengers in signaling pathways leading to cardiomyocyte differentiation.[137]

11.7 Magnetic Methods for Preparation of Specially Designed Tissue Scaffolds

11.7.1 Anisotropic Morphology/Topography

The ventricular myocardium is an anisotropic tissue, with tensile mechanical and electrical properties dictated by cardiac muscle fiber orientation.[138] To promote the anisotropy microstructure in tissue scaffolds, several approaches have been employed. Engelmayr *et al.* used a micro laser-ablation technique to create honeycomb-like poly(glycerol sebacate) structures that had both mechanical and morphological anisotropy.[139] Neonatal rat cardiomyocytes seeded on such structures created cardiac tissues with greater contractility and alignment than when seeded in isotropic scaffolds. Bian *et al.* used soft lithography to create molds with 600 μm and 1.2 mm posts on them. They later used the molds to create anisotropic fibrinogen-Matrigel hydrogels with elliptical pores, created by the posts in the mold.[140] Their findings showed that the anisotropic scaffold structure promoted local and global alignment of the cardiomyocytes and the ECM, which led to anisotropy of the action potential and faster conductivity on the longitudal axis. These works and others have showed the importance of appropriate anisotropic topography to cardiac tissue engineering.

Magnetic fields (below 1 MHz), coupled with magnetizable nanoparticles (MNPs) embedded in a fiber or matrix, can be a relatively simple and effective way, applied from a distance, to achieve a tissue scaffold with an anisotropic, aligned structure. Shefi and Antman-Passig have successfully created a directionally-oriented collagen-based scaffold using MNPs and a magnetic field (Figure 11.10).[141] They mixed MNPs into collagen hydrogels and applied a permanent external field, causing the MNPs to align along the magnetic field lines. The aligned MNPs formed strings that led to the alignment of the collagen fibers, eventually leading to a scaffold that is oriented in the direction of the magnetic field.

De Santis *et al.* used advanced biofabrication techniques such as fiber deposition and stereolithography to create MNP-containing scaffolds with various shapes, compositions and structures.[142] They prepared MNP-embedded poly(ε-caprolactone) and poly(ethylene glycol) scaffolds with a coaxial or bilayered structure. The scaffolds showed varying mechanical behavior based not only on the materials and their compositions but also on the scaffold structures such as monolithic, co-axial or bi-layered. Another interesting combination of advanced biofabrication technique and MNPs was presented

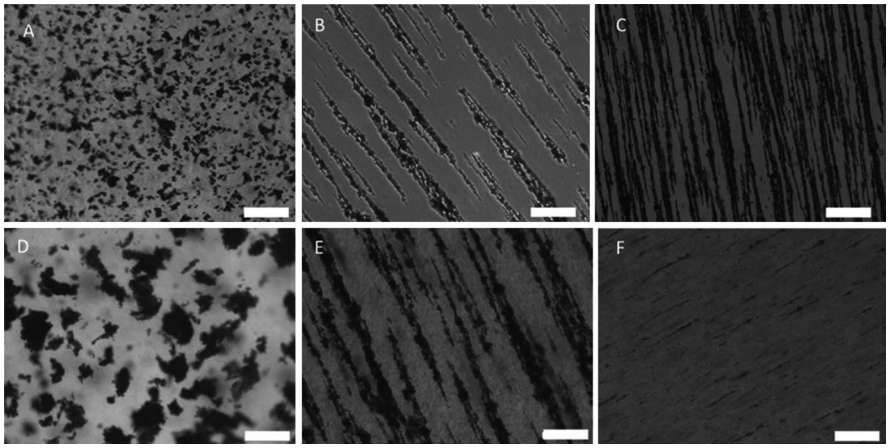

Figure 11.10 Formation of aligned magnetic particle strings within 1.4 mg mL^{-1} (top panels) and 3 mg mL^{-1} (bottom panels) collagen gels. (A, D) Magnetic particles (1μm and 100 nm respectively) were mixed into collagen gels, and solidified with no magnetic field present. (B, E) 100 nm MNP formed strings within the gel under a magnetic field of 255 G. (C, F) Strings were also formed using 1 μm magnetic particles, solidified under a 255 G magnetic field. Adapted with permission from *Nano Letters*, Merav Antman-Passig and Orit Shefi. Remote Magnetic Orientation of 3D Collagen Hydrogels for Directed Neuronal Regeneration, **16**(4), 2567–2573 DOI: 10.1021/acs.nanolett.6b00131. Copyright © 2016. American Chemical Society.[141]

by Sun *et al.* They used electrospinning to eject MNP-containing alginate hydrogel onto a designed support model.[143] A vertical magnetic force, created by a ring magnet, made the electrospun fibers attach to the model and acquire their shape, thus allowing the creation of a scaffold with a direction-dependent macroscopic structure.

11.7.2 Remote Controlled Release Scaffold

The natural microenvironment of cells provides them with various chemical stimuli. To mimic biochemical stimuli in tissue engineering, numerous growth factors (GFs) are delivered to the cells, most commonly by preloading scaffolds with GFs before cell seeding and cultivation. GFs are crucial signaling molecules that promote cell survival, development and host integration by driving processes such as angiogenesis and anastomosis.[144] Physical encapsulation of GFs in hydrogels or scaffolds allows their controlled release. Non-magnetic methods for the controlled release of GFs include their encapsulation in micro[145] or nano[146,147] particles that are incorporated in the scaffold. These particles can be made from gelatin,[148] PLGA,[149] PHBV poly(3-hydroxybutyrate-*co*-3-hydroxyvalerate)[146] and many others. Another interesting approach involves coating the scaffold with a gelatin hydrogel

preloaded with a GF.[150] Controlled release of GFs from hydrogels can be achieved by electrostatic affinity binding of multiple heparin-binding proteins (*via* alginate-sulfate).[151,152] These studies resulted in a consecutive release of factors, at rates dictated by the equilibrium binding constants of the specific factor. While controlled release of GFs is achievable with non-magnetic approaches, the release profiles from these systems are determined during the fabrication process, prior to implantation. Magnetic approaches hold the ability to adjust the release profile as needed *in vivo*.

Magnetically-induced GF delivery generally uses one of three mechanisms. The first is increasing the flow of GF-containing medium by large deformations of macroporous ferrogels.[153] The second approach utilizes thermoresponsive polymers.[7,154–156] Exposure of these MNP-containing polymers to an alternating, high-frequency magnetic field, causes a local temperature increase due to magnetic hysteresis loss and Brownian relaxation. The elevated temperature causes a phase transition of the polymer and GF release. The third approach is based on mechanical force application to a magnetically-responsive scaffold by a time-varying or continuous field.[157] Although none of the studies mentioned is relevant to CTE, it is clear that magnetically-induced controlled release of GF has great potential for CTE—having the advantage of on-demand, remotely controlled, GF release both *in vitro* and *in vivo*.

11.8 Concluding Remarks

This chapter presented the potential of magnetic-responsive materials and their recent implementation in the fast-growing field of CTE. Magnetic materials are of a substantial interest for regenerative medicine because the properties of these materials can be controlled and tuned remotely enabling non-invasive application of physical effects. The remote application of physical cues is highly desired for applications *in vivo* for promoting a more efficient vascular integration of the cellular graft with the vasculature of a recipient. In particular, hydrogel-based magnetic nanocomposites are beneficial for achieving remote mechanical conditioning of cultivated cells with tunable spatial directionality and amplitude. In these structures, a magnetic field is non-invasively coupled with magnetically-responsive particles to trigger a biochemical processes within cultivated cells fostering their organization into functionally mature tissue. Among the cases discussed, the materials and approaches that utilize static or time-varying uniform magnetic fields seem to be the most promising for clinical translation, because generation of uniform magnetic fields across large animals or even humans is a relatively scalable task in contrast to approaches where gradient fields are utilized for the same goal. Although methodologies involving magnetic-responsive biomaterials demonstrate great potential for developing functional and vascularized tissues, efficient delivery of cell-based therapies and capabilities to control directional cell growth, the future clinical success of this methodology will depend on addressing the current challenges of the field.

First, the acute toxicity and potential long-term adverse effects of magnetic biomaterials should be well understood. Although most materials used in CTE are biodegradable or derived from a biological origin, the biocompatibility and safety of the materials need to be thoroughly assessed to eliminate the potential risks associated with their future clinical use. Second, there is a need for materials that enable a high degree of spatial control of cell behavior. Current materials are mainly prepared using bulk methods, which do not allow precise and custom control of the nanomaterial patterns. Modern 3D biological printing may provide great opportunities to print out magnetic biomaterials with custom-designed patterns that will allow a higher degree of spatial control of the cellular environment. Third, future tissue engineers have to learn to work with complex multicellular constructs, representing models that are closer to real biological tissue. Stimulation conditions and temporal control in the multicellular structures will need to be carefully considered and optimized. Finally, understanding the immune system response to the implanted magnetic materials is necessary to design the materials that will elicit minimal inflammation responses that can affect implant survival and integration in the host environment.

Acknowledgements

This work was supported by the NIH award R01HL107771, W. W. Smith Charitable Trust award H1504, Drexel University College of Medicine Clinical & Translational Research Institute (CTRI), Drexel University IVIS grant, 2016 Commonwealth Universal Research Enhancement (CURE) grant to BP and by a grant from the United States-Israel Binational Science Foundation (BSF), Jerusalem, Israel, to BP and SC. The content is solely the responsibility of the authors and does not necessarily represent the official views of the National Heart, Lung and Blood Institute or the National Institutes of Health.

Prof. Cohen holds the Claire and Harold Oshry Professor Chair in Biotechnology.

References

1. D. Orlic, J. Kajstura, S. Chimenti, I. Jakoniuk, S. M. Anderson, B. Li, J. Pickel, R. McKay, B. Nadal-Ginard, D. M. Bodine, A. Leri and P. Anversa, *Nature*, 2001, **410**, 701–705.
2. J. Leor, S. Aboulafia-Etzion, A. Dar, L. Shapiro, I. M. Barbash, A. Battler, Y. Granot and S. Cohen, *Circulation*, 2000, **102**, III56–III61.
3. W. H. Zimmermann, I. Melnychenko, G. Wasmeier, M. Didie, H. Naito, U. Nixdorff, A. Hess, L. Budinsky, K. Brune, B. Michaelis, S. Dhein, A. Schwoerer, H. Ehmke and T. Eschenhagen, *Nat. Med.*, 2006, **12**, 452–458.
4. A. Dar, M. Shachar, J. Leor and S. Cohen, *Biotechnol. Bioeng.*, 2002, **80**, 305–312.
5. S. Zmora, R. Glicklis and S. Cohen, *Biomaterials*, 2002, **23**, 4087–4094.
6. L. Shapiro and S. Cohen, *Biomaterials*, 1997, **18**, 583–590.

7. T. Hoare, B. P. Timko, J. Santamaria, G. F. Goya, S. Irusta, S. Lau, C. F. Stefanescu, D. B. Lin, R. Langer and D. S. Kohane, *Nano Lett.*, 2011, **11**, 1395–1400.
8. T. Dvir, O. Levy, M. Shachar, Y. Granot and S. Cohen, *Tissue Eng.*, 2007, **13**, 2185–2193.
9. R. Schwarzkopf, M. Shachar, T. Dvir, Y. Dayan, R. Holbova, J. Leor and S. Cohen, *Tissue Eng.*, 2006, **12**, 3467–3475.
10. H. Bannasch, M. Fohn, T. Unterberg, A. D. Bach, B. Weyand and G. B. Stark, *Clin. Plast. Surg.*, 2003, **30**, 573–579.
11. P. Macchiarini, P. Jungebluth, T. Go, M. A. Asnaghi, L. E. Rees, T. A. Cogan, A. Dodson, J. Martorell, S. Bellini, P. P. Parnigotto, S. C. Dickinson, A. P. Hollander, S. Mantero, M. T. Conconi and M. A. Birchall, *Lancet*, 2008, **372**, 2023–2030.
12. A. Atala, S. B. Bauer, S. Soker, J. J. Yoo and A. B. Retik, *Lancet*, 2006, **367**, 1241–1246.
13. S. Levenberg, J. Rouwkema, M. Macdonald, E. S. Garfein, D. S. Kohane, D. C. Darland, R. Marini, C. A. van Blitterswijk, R. C. Mulligan, P. A. D'Amore and R. Langer, *Nat. Biotechnol.*, 2005, **23**, 879–884.
14. K. R. Stevens, K. L. Kreutziger, S. K. Dupras, F. S. Korte, M. Regnier, V. Muskheli, M. B. Nourse, K. Bendixen, H. Reinecke and C. E. Murry, *Proc. Natl. Acad. Sci. U. S. A.*, 2009, **106**, 16568–16573.
15. T. Kaully, K. Kaufman-Francis, A. Lesman and S. Levenberg, *Tissue Eng., Part B*, 2009, **15**, 159–169.
16. M. W. Laschke, Y. Harder, M. Amon, I. Martin, J. Farhadi, A. Ring, N. Torio-Padron, R. Schramm, M. Rucker, D. Junker, J. M. Haufel, C. Carvalho, M. Heberer, G. Germann, B. Vollmar and M. D. Menger, *Tissue Eng.*, 2006, **12**, 2093–2104.
17. J. Halavaara, P. Tervahartiala, H. Isoniemi and K. Hockerstedt, *Acta Radiol.*, 2002, **43**, 180–185.
18. B. Bonnemain, *J. Drug Targeting*, 1998, **6**, 167–174.
19. R. P. Zhang, L. J. Wang, S. He, J. Xie and J. D. Li, *Stem Cells Int.*, 2016, **2016**, 2018474.
20. E. E. Mahmoud, G. Kamei, Y. Harada, R. Shimizu, N. Kamei, N. Adachi, N. A. Misk and M. Ochi, *Cell Transplant.*, 2016, **25**, 1073–1083.
21. A. C. Vandergriff, T. M. Hensley, E. T. Henry, D. Shen, S. Anthony, J. Zhang and K. Cheng, *Biomaterials*, 2014, **35**, 8528–8539.
22. A. Luciani, C. Wilhelm, P. Bruneval, P. Cunin, G. Autret, A. Rahmouni, O. Clement and F. Gazeau, *Eur. Radiol.*, 2009, **19**, 1087–1096.
23. P. G. Kyrtatos, P. Lehtolainen, M. Junemann-Ramirez, A. Garcia-Prieto, A. N. Price, J. F. Martin, D. G. Gadian, Q. A. Pankhurst and M. F. Lythgoe, *JACC Cardiovasc. Interv.*, 2009, **2**, 794–802.
24. B. Polyak, I. Fishbein, M. Chorny, I. Alferiev, D. Williams, B. Yellen, G. Friedman and R. J. Levy, *Proc. Natl. Acad. Sci. U. S. A.*, 2008, **105**, 698–703.
25. M. Subramanian, J. Lim and J. Dobson, *PLoS One*, 2013, **8**, e69812.
26. S. C. McBain, H. H. Yiu and J. Dobson, *Int. J. Nanomed.*, 2008, **3**, 169–180.

27. J. Dobson, *Gene Ther.*, 2006, **13**, 283–287.
28. F. J. Alenghat, J. D. Tytell, C. K. Thodeti, A. Derrien and D. E. Ingber, *J. Cell. Biochem.*, 2009, **106**, 529–538.
29. R. J. Mannix, S. Kumar, F. Cassiola, M. Montoya-Zavala, E. Feinstein, M. Prentiss and D. E. Ingber, *Nat. Nanotechnol.*, 2008, **3**, 36–40.
30. C. J. Meyer, F. J. Alenghat, P. Rim, J. H. Fong, B. Fabry and D. E. Ingber, *Nat. Cell Biol.*, 2000, **2**, 666–668.
31. J. Dobson, S. H. Cartmell, A. Keramane and A. J. El Haj, *IEEE Trans. Nanobioscience*, 2006, **5**, 173–177.
32. B. Hu, J. Dobson and A. J. El Haj, *Nanomedicine*, 2014, **10**, 45–55.
33. S. Hughes, S. McBain, J. Dobson and A. J. El Haj, *J. R. Soc., Interface*, 2008, **5**, 855–863.
34. Z. Orynbayeva, R. Sensenig and B. Polyak, *Nanomedicine (Lond.)*, 2015, **10**, 1555–1568.
35. F. T. Zohra, M. Medved, N. Lazareva and B. Polyak, *Nanomedicine (Lond.)*, 2015, **10**, 1391–1406.
36. C. F. Adams, A. Rai, G. Sneddon, H. H. Yiu, B. Polyak and D. M. Chari, *Nanomedicine*, 2015, **11**, 19–29.
37. C. MacDonald, K. Barbee and B. Polyak, *Pharm. Res.*, 2012, **29**, 1270–1281.
38. Y. Zhang, W. Li, L. Ou, W. Wang, E. Delyagina, C. Lux, H. Sorg, K. Riehemann, G. Steinhoff and N. Ma, *PLoS One*, 2012, **7**, e39490.
39. M. R. Dzamukova, A. I. Zamaleeva, D. G. Ishmuchametova, Y. N. Osin, A. P. Kiyasov, D. K. Nurgaliev, O. N. Ilinskaya and R. F. Fakhrullin, *Langmuir*, 2011, **27**, 14386–14393.
40. A. Ito, K. Ino, M. Hayashida, T. Kobayashi, H. Matsunuma, H. Kagami, M. Ueda and H. Honda, *Tissue Eng.*, 2005, **11**, 1553–1561.
41. K. Shimizu, A. Ito and H. Honda, *J. Biomed. Mater. Res., Part B*, 2006, **77**, 265–272.
42. H. Akiyama, A. Ito, Y. Kawabe and M. Kamihira, *Biomaterials*, 2010, **31**, 1251–1259.
43. M. Ishii, R. Shibata, Y. Shimizu, T. Yamamoto, K. Kondo, Y. Inoue, N. Ouchi, T. Tanigawa, N. Kanemura, A. Ito, H. Honda and T. Murohara, *Int. J. Cardiol.*, 2014, **175**, 545–553.
44. T. Kito, R. Shibata, M. Ishii, H. Suzuki, T. Himeno, Y. Kataoka, Y. Yamamura, T. Yamamoto, N. Nishio, S. Ito, Y. Numaguchi, T. Tanigawa, J. K. Yamashita, N. Ouchi, H. Honda, K. Isobe and T. Murohara, *Sci. Rep.*, 2013, **3**, 1418.
45. M. Ishii, R. Shibata, Y. Numaguchi, T. Kito, H. Suzuki, K. Shimizu, A. Ito, H. Honda and T. Murohara, *Arterioscler., Thromb., Vasc. Biol.*, 2011, **31**, 2210–2215.
46. Y. J. Ma and H. C. Gu, *J. Mater. Sci.: Mater. Med.Journal of Materials Science. Materials in Medicine*, 2007, **18**, 2145–2149.
47. S. C. Wuang, K. G. Neoh, E. T. Kang, D. W. Pack and D. E. Leckband, *Biomaterials*, 2008, **29**, 2270–2279.
48. J. Rejman, V. Oberle, I. S. Zuhorn and D. Hoekstra, *Biochem. J.*, 2004, **377**, 159–169.

49. D. Kiyoshima, K. Kawakami, K. Hayakawa, H. Tatsumi and M. Sokabe, *J. Cell Sci.*, 2011, **124**, 3859–3870.
50. R. Sensenig, Y. Sapir, C. MacDonald, S. Cohen and B. Polyak, *Nanomedicine (Lond.)*, 2012, **7**, 1425–1442.
51. T. K. Jain, M. K. Reddy, M. A. Morales, D. L. Leslie-Pelecky and V. Labhasetwar, *Mol. Pharm.*, 2008, **5**, 316–327.
52. J. Tate, J. Ogden, R. Strawbridge, Z. Pierce and P. Hoopes, *Proc. SPIE-Int. Soc. Opt. Eng.*, 2009, **7181**, 71810L.
53. R. Weissleder, D. D. Stark, B. L. Engelstad, B. R. Bacon, C. C. Compton, D. L. White, P. Jacobs and J. Lewis, *AJR, Am. J. Roentgenol.*, 1989, **152**, 167–173.
54. L. Su, L. Han, F. Ge, S. L. Zhang, Y. Zhang, B. X. Zhao, J. Zhao and J. Y. Miao, *J. Hazard. Mater.*, 2012, **235–236**, 316–325.
55. A. Gojova, B. Guo, R. S. Kota, J. C. Rutledge, I. M. Kennedy and A. I. Barakat, *Environ. Health Perspect.*, 2007, **115**, 403–409.
56. K. Buyukhatipoglu and A. M. Clyne, *J. Biomed. Mater. Res., Part A*, 2011, **96**, 186–195.
57. L. Zhang, X. Wang, Y. Miao, Z. Chen, P. Qiang, L. Cui, H. Jing and Y. Guo, *J. Hazard. Mater.*, 2016, **304**, 186–195.
58. Y. Sapir-Lekhovitser, M. Y. Rotenberg, J. Jopp, G. Friedman, B. Polyak and S. Cohen, *Nanoscale*, 2016, **8**, 3386–3399.
59. B. D. Matthews, D. R. Overby, R. Mannix and D. E. Ingber, *J. Cell Sci.*, 2006, **119**, 508–518.
60. M. Nooris, D. Aparna and S. Radha, *Eur. Biophys. J.*, 2016, **45**, 139–148.
61. Y. Sapir, S. Cohen, G. Friedman and B. Polyak, *Biomaterials*, 2012, **33**, 4100–4109.
62. M. Xin, E. N. Olson and R. Bassel-Duby, *Nat. Rev. Mol. Cell Biol.*, 2013, **14**, 529–541.
63. J. H. van Berlo and J. D. Molkentin, *Nat. Med.*, 2014, **20**, 1386–1393.
64. F. Li, X. Wang, J. M. Capasso and A. M. Gerdes, *J. Mol. Cell. Cardiol.*, 1996, **28**, 1737–1746.
65. M. H. Soonpaa and L. J. Field, *Am. J. Physiol.*, 1997, **272**, H220–H226.
66. O. Bergmann, R. D. Bhardwaj, S. Bernard, S. Zdunek, F. Barnabe-Heider, S. Walsh, J. Zupicich, K. Alkass, B. A. Buchholz, H. Druid, S. Jovinge and J. Frisen, *Science*, 2009, **324**, 98–102.
67. P. C. Westman, M. J. Lipinski, D. Luger, R. Waksman, R. O. Bonow, E. Wu and S. E. Epstein, *J. Am. Coll. Cardiol.*, 2016, **67**, 2050–2060.
68. R. S. Whelan, V. Kaplinskiy and R. N. Kitsis, *Annu. Rev. Physiol.*, 2010, **72**, 19–44.
69. S. K. Sanganalmath and R. Bolli, *Circ. Res.*, 2013, **113**, 810–834.
70. S. Zhang, Z. Jia, J. Ge, L. Gong, Y. Ma, T. Li, J. Guo, P. Chen, Q. Hu, P. Zhang, Y. Liu, Z. Li, K. Ma, L. Li and C. Zhou, *Cell Transplant.*, 2005, **14**, 787–798.
71. M. Hofmann, K. C. Wollert, G. P. Meyer, A. Menke, L. Arseniev, B. Hertenstein, A. Ganser, W. H. Knapp and H. Drexler, *Circulation*, 2005, **111**, 2198–2202.

72. J. M. Collins and B. Russell, *J. Cardiovasc. Nurs.*, 2009, **24**, 93–97.
73. T. I. van der Spoel, K. R. Vrijsen, S. Koudstaal, J. P. Sluijter, J. F. Nijsen, H. W. de Jong, I. E. Hoefer, M. J. Cramer, P. A. Doevendans, E. van Belle and S. A. Chamuleau, *J. Cell. Mol. Med.*, 2012, **16**, 2768–2776.
74. Y. Sapir, B. Polyak and S. Cohen, *Nanotechnology*, 2014, **25**, 014009.
75. M. Y. Lee, E. Cagavi Bozkulak, S. Schliffke, P. J. Amos, Y. Ren, X. Ge, B. E. Ehrlich and Y. Qyang, *Biochem. Biophys. Res. Commun.Biochem. Biophys. Res. Commun.*, 2011, **416**, 51–57.
76. L. R. Geuss, D. C. Wu, D. Ramamoorthy, C. D. Alford and L. J. Suggs, *PLoS One*, 2014, **9**, e113982.
77. A. P. Beltrami, L. Barlucchi, D. Torella, M. Baker, F. Limana, S. Chimenti, H. Kasahara, M. Rota, E. Musso, K. Urbanek, A. Leri, J. Kajstura, B. Nadal-Ginard and P. Anversa, *Cell*, 2003, **114**, 763–776.
78. A. S. Boyd, N. P. Rodrigues, K. O. Lui, X. Fu and Y. Xu, *Stem Cells*, 2012, **30**, 797–803.
79. M. Dezawa, H. Ishikawa, Y. Itokazu, T. Yoshihara, M. Hoshino, S. Takeda, C. Ide and Y. Nabeshima, *Science*, 2005, **309**, 314–317.
80. M. A. Laflamme and C. E. Murry, *Nature*, 2011, **473**, 326–335.
81. C. E. Murry and G. Keller, *Cell*, 2008, **132**, 661–680.
82. V. F. Segers and R. T. Lee, *Nature*, 2008, **451**, 937–942.
83. V. Tabar, M. Tomishima, G. Panagiotakos, S. Wakayama, J. Menon, B. Chan, E. Mizutani, G. Al-Shamy, H. Ohta, T. Wakayama and L. Studer, *Nat. Med.*, 2008, **14**, 379–381.
84. R. Gulati, A. Lerman and R. D. Simari, *Clin. Sci. (Lond.)*, 2005, **109**, 27–37.
85. S. A. Parikh and E. R. Edelman, *Adv. Drug Delivery Rev.*, 2000, **42**, 139–161.
86. X. Wu, G. Wang, C. Tang, D. Zhang, Z. Li, D. Du and Z. Zhang, *J. Biomed. Mater. Res., Part A*, 2011, **98**, 442–449.
87. X. Wu, T. Yin, J. Tian, C. Tang, J. Huang, Y. Zhao, X. Zhang, X. Deng, Y. Fan, D. Yu and G. Wang, *Regener. Biomater.*, 2015, **2**, 87–96.
88. https://www.unos.org.
89. A. Al Kindi, Y. Ge, D. Shum-Tim and R. C. Chiu, *Front. Biosci.*, 2008, **13**, 2421–2434.
90. I. L. Weissman, *Science*, 2000, **287**, 1442–1446.
91. B. Polyak and G. Friedman, *Expert Opin. Drug Delivery*, 2009, **6**, 53–70.
92. R. Tietze, J. Zaloga, H. Unterweger, S. Lyer, R. P. Friedrich, C. Janko, M. Pottler, S. Durr and C. Alexiou, *Biochem. Biophys. Res. Commun.*, 2015, **468**, 463–470.
93. R. Tietze, S. Lyer, S. Durr and C. Alexiou, *Nanomedicine (Lond.)*, 2012, **7**, 447–457.
94. C. Alexiou, R. J. Schmid, R. Jurgons, M. Kremer, G. Wanner, C. Bergemann, E. Huenges, T. Nawroth, W. Arnold and F. G. Parak, *Eur. Biophys. J.*, 2006, **35**, 446–450.
95. A. S. Lubbe, C. Alexiou and C. Bergemann, *J. Surg. Res.*, 2001, **95**, 200–206.
96. C. Alexiou, W. Arnold, R. J. Klein, F. G. Parak, P. Hulin, C. Bergemann, W. Erhardt, S. Wagenpfeil and A. S. Lubbe, *Cancer Res.*, 2000, **60**, 6641–6648.

97. K. Cheng, T. S. Li, K. Malliaras, D. R. Davis, Y. Zhang and E. Marban, *Circ. Res.*, 2010, **106**, 1570–1581.
98. A. Chaudeurge, C. Wilhelm, A. Chen-Tournoux, P. Farahmand, V. Bellamy, G. Autret, C. Menager, A. Hagege, J. Larghero, F. Gazeau, O. Clement and P. Menasche, *Cell Transplant.*, 2012, **21**, 679–691.
99. K. Cheng, K. Malliaras, T. S. Li, B. Sun, C. Houde, G. Galang, J. Smith, N. Matsushita and E. Marban, *Cell Transplant.*, 2012, **21**, 1121–1135.
100. Z. Huang, Y. Shen, A. Sun, G. Huang, H. Zhu, B. Huang, J. Xu, Y. Song, N. Pei, J. Ma, X. Yang, Y. Zou, J. Qian and J. Ge, *Stem Cell Res. Ther.*, 2013, **4**, 149.
101. L. G. Lum, P. A. Davol and R. J. Lee, *Exp. Hematol.*, 2006, **34**, 1–6.
102. L. G. Lum, H. Fok, R. Sievers, M. Abedi, P. J. Quesenberry and R. J. Lee, *Blood Cells, Mol., Dis.*, 2004, **32**, 82–87.
103. T. C. Zhao, A. Tseng, N. Yano, Y. Tseng, P. A. Davol, R. J. Lee, L. G. Lum and J. F. Padbury, *J. Appl. Physiol. (1985)*, 2008, **104**, 1793–1800.
104. K. Cheng, D. Shen, M. T. Hensley, R. Middleton, B. Sun, W. Liu, G. De Couto and E. Marban, *Nat. Commun.*, 2014, **5**, 4880.
105. G. De Luca, M. T. Dirksen, C. Spaulding, H. Kelbaek, M. Schalij, L. Thuesen, B. van der Hoeven, M. A. Vink, C. Kaiser, C. Musto, T. Chechi, G. Spaziani, L. S. Diaz de la Llera, V. Pasceri, E. Di Lorenzo, R. Violini, G. Cortese, H. Suryapranata and G. W. Stone, *Arch. Intern. Med.*, 2012, **172**, 611–621.
106. E. G. Nabel and E. Braunwald, *N. Engl. J. Med.*, 2012, **366**, 54–63.
107. P. W. Serruys, M. J. Kutryk and A. T. Ong, *N. Engl. J. Med.*, 2006, **354**, 483–495.
108. G. G. Stefanini and D. R. Holmes Jr, *N. Engl. J. Med.*, 2013, **368**, 254–265.
109. C. Chaabane, F. Otsuka, R. Virmani and M. L. Bochaton-Piallat, *Cardiovasc. Res.*, 2013, **99**, 353–363.
110. R. Kornowski, M. K. Hong, F. O. Tio, O. Bramwell, H. Wu and M. B. Leon, *J. Am. Coll. Cardiol.*, 1998, **31**, 224–230.
111. F. Alfonso, R. A. Byrne, F. Rivero and A. Kastrati, *J. Am. Coll. Cardiol.*, 2014, **63**, 2659–2673.
112. M. S. Kim and L. S. Dean, *Cardiovasc. Ther.*, 2011, **29**, 190–198.
113. S. O. Marx, H. Totary-Jain and A. R. Marks, *Circ. Cardiovasc. Interv.*, 2011, **4**, 104–111.
114. G. K. Owens, M. S. Kumar and B. R. Wamhoff, *Physiol. Rev.*, 2004, **84**, 767–801.
115. A. R. Marks, *N. Engl. J. Med.*, 2003, **349**, 1307–1309.
116. S. Cassese and A. Kastrati, *JAMA*, 2012, **308**, 814–815.
117. G. Guagliumi, V. Sirbu, G. Musumeci, R. Gerber, G. Biondi-Zoccai, H. Ikejima, E. Ladich, N. Lortkipanidze, A. Matiashvili, O. Valsecchi, R. Virmani and G. W. Stone, *JACC Cardiovasc. Interv.*, 2012, **5**, 12–20.
118. M. Joner, G. Nakazawa, A. V. Finn, S. C. Quee, L. Coleman, E. Acampado, P. S. Wilson, K. Skorija, Q. Cheng, X. Xu, H. K. Gold, F. D. Kolodgie and R. Virmani, *J. Am. Coll. Cardiol.*, 2008, **52**, 333–342.

119. H. T. Liu, F. Li, W. Y. Wang, X. J. Li, Y. M. Liu, R. A. Wang, W. Y. Guo and H. C. Wang, *Tex. Heart Inst. J.*, 2010, **37**, 194–201.
120. F. Otsuka, A. V. Finn, S. K. Yazdani, M. Nakano, F. D. Kolodgie and R. Virmani, *Nat. Rev. Cardiol.*, 2012, **9**, 439–453.
121. A. T. Fuchs, A. Kuehnl, J. Pelisek, P. H. Rolland, C. Mekkaoui, H. Netz and S. Nikol, *Endothelium*, 2008, **15**, 85–92.
122. S. V. Pislaru, A. Harbuzariu, R. Gulati, T. Witt, N. P. Sandhu, R. D. Simari and G. S. Sandhu, *J. Am. Coll. Cardiol.*, 2006, **48**, 1839–1845.
123. J. Riegler, A. Liew, S. O. Hynes, D. Ortega, T. O'Brien, R. M. Day, T. Richards, F. Sharif, Q. A. Pankhurst and M. F. Lythgoe, *Biomaterials*, 2013, **34**, 1987–1994.
124. R. F. Adamo, I. Fishbein, K. Zhang, J. Wen, R. J. Levy, I. S. Alferiev and M. Chorny, *J. Controlled Release*, 2016, **222**, 169–175.
125. S. Vosen, S. Rieck, A. Heidsieck, O. Mykhaylyk, K. Zimmermann, W. Bloch, D. Eberbeck, C. Plank, B. Gleich, A. Pfeifer, B. K. Fleischmann and D. Wenzel, *ACS Nano*, 2016, **10**, 369–376.
126. C. Johansen, *Scand. J. Work, Environ. Health*, 2004, **30**(suppl. 1), 1–30.
127. M. Roosli, M. Egger, D. Pfluger and C. Minder, *Environ. Health*, 2008, **7**, 35.
128. S. L. Henry, M. J. Concannon and G. J. Yee, *Eplasty*, 2008, **8**, e40.
129. P. Kovacic and R. Somanathan, *J. Recept. Signal Transduction Res.*, 2010, **30**, 214–226.
130. G. Scott and J. B. King, *J. Bone Jt. Surg., Am. Vol.*, 1994, **76**, 820–826.
131. W. J. Sharrard, *J. Bone Jt. Surg., Br. Vol.*, 1990, **72**, 347–355.
132. R. Gaetani, M. Ledda, L. Barile, I. Chimenti, F. De Carlo, E. Forte, V. Ionta, L. Giuliani, E. D'Emilia, G. Frati, F. Miraldi, D. Pozzi, E. Messina, S. Grimaldi, A. Giacomello and A. Lisi, *Cardiovasc. Res.*, 2009, **82**, 411–420.
133. A. Lisi, M. Ledda, F. De Carlo, A. Foletti, L. Giuliani, E. D'Emilia and S. Grimaldi, *Electromagn. Biol. Med.*, 2008, **27**, 230–240.
134. A. Lisi, M. Ledda, F. de Carlo, D. Pozzi, E. Messina, R. Gaetani, I. Chimenti, L. Barile, A. Giacomello, E. D'Emilia, L. Giuliani, A. Foletti, A. Patti, A. Vulcano and S. Grimaldi, *Electromagn. Biol. Med.*, 2008, **27**, 127–133.
135. C. Ventura, M. Maioli, Y. Asara, D. Santoni, P. Mesirca, D. Remondini and F. Bersani, *FASEB J.*, 2005, **19**, 155–157.
136. J. H. Dinsmore and N. Dib, *J. Cardiovasc. Transl. Res.*, 2008, **1**, 41–54.
137. M. M. Bekhite, H. R. Figulla, H. Sauer and M. Wartenberg, *Int. J. Cardiol.*, 2013, **167**, 798–808.
138. J. W. Holmes, T. K. Borg and J. W. Covell, *Annu. Rev. Biomed. Eng.*, 2005, **7**, 223–253.
139. G. C. Engelmayr Jr, M. Cheng, C. J. Bettinger, J. T. Borenstein, R. Langer and L. E. Freed, *Nat. Mater.*, 2008, **7**, 1003–1010.
140. W. Bian, C. P. Jackman and N. Bursac, *Biofabrication*, 2014, **6**, 024109.
141. M. Antman-Passig and O. Shefi, *Nano Lett.*, 2016, **16**, 2567–2573.

142. R. De Santis, U. D'Amora, T. Russo, A. Ronca, A. Gloria and L. Ambrosio, *J. Mater. Sci.: Mater. Med.*, 2015, **26**, 250.
143. T. Sun, Q. Huang, Q. Shi, H. P. Wang, X. M. Liu, M. Seki, M. Nakajima and T. Fukuda, *Microfluid. Nanofluid.*, 2015, **19**, 1169–1180.
144. J. Rouwkema, N. C. Rivron and C. A. van Blitterswijk, *Trends Biotechnol.*, 2008, **26**, 434–441.
145. A. Perets, Y. Baruch, F. Weisbuch, G. Shoshany, G. Neufeld and S. Cohen, *J. Biomed. Mater. Res., Part A*, 2003, **65A**, 489–497.
146. P. Yilgor, N. Hasirci and V. Hasirci, *J. Biomed. Mater. Res., Part A*, 2010, **93A**, 528–536.
147. P. Yilgor, K. Tuzlakoglu, R. L. Reis, N. Hasirci and V. Hasirci, *Biomaterials*, 2009, **30**, 3551–3559.
148. Z. S. Patel, H. Ueda, M. Yamamoto, Y. Tabata and A. G. Mikos, *Pharm. Res.*, 2008, **25**, 2370–2378.
149. J. Panyam and V. Labhasetwar, *Adv. Drug Delivery Rev.*, 2003, **55**, 329–347.
150. D. H. R. Kempen, L. C. Lu, A. Heijink, T. E. Hefferan, L. B. Creemers, A. Maran, M. J. Yaszemski and W. J. A. Dhert, *Biomaterials*, 2009, **30**, 2816–2825.
151. I. Freeman and S. Cohen, *Biomaterials*, 2009, **30**, 2122–2131.
152. I. Freeman, A. Kedem and S. Cohen, *Biomaterials*, 2008, **29**, 3260–3268.
153. X. H. Zhao, J. Kim, C. A. Cezar, N. Huebsch, K. Lee, K. Bouhadir and D. J. Mooney, *Proc. Natl. Acad. Sci. U. S. A.*, 2011, **108**, 67–72.
154. S. Brule, M. Levy, C. Wilhelm, D. Letourneur, F. Gazeau, C. Menager and C. Le Visage, *Adv. Mater.*, 2011, **23**, 787–790.
155. A. M. Derfus, G. von Maltzahn, T. J. Harris, T. Duza, K. S. Vecchio, E. Ruoslahti and S. N. Bhatia, *Adv. Mater.*, 2007, **19**, 3932–3936.
156. T. Y. Liu, S. H. Hu, D. M. Liu, S. Y. Chen and I. W. Chen, *Nano Today*, 2009, **4**, 52–65.
157. S. H. Hu, T. Y. Liu, C. H. Tsai and S. Y. Chen, *J. Magn. Magn. Mater.*, 2007, **310**, 2871–2873.
158. A. J. Patel, M. Lazdunski and E. Honore, *Curr. Opin. Cell Biol.*, 2001, **13**, 422–428.

CHAPTER 12

Intestinal Tissue Engineering with Intestinal Stem Cells

ZAHRA DAVOUDI[a] AND QUN WANG*[a]

[a]Department of Chemical and Biological Engineering, Iowa State University, Ames, IA 50011, USA
*E-mail: qunwang@iastate.edu

12.1 Introduction

Tissue engineering (TE) refers to an interdisciplinary field of science that employs biological and engineering sciences with the aim of replacing or repairing a malfunctioning, missing, or injured organ.[1] This approach has been proposed as an alternative to autologous or allogeneic grafts when these cannot be used, *e.g.*, because of a lack of donor tissues and potential transmission of disease such as infection, or triggered immune response, respectively.[2,3] Cells and scaffolds play the most significant roles in designing a tissue-engineered organ. TE uses different cells and different scaffold materials to regenerate vital tissues.[4] Employment of different cells is associated with different advantages. Two basic types of cells are being considered: parenchymal or tissue-specific cells, and progenitor cells or stem cells.[5] On the other hand, scaffolds provide an appropriate structure for cell growth and act as extracellular matrix (ECM) for the incorporated cells until the formation of innate ECM by these cells.[6–8] Moreover, scaffolds have a role in maintaining and delivering biological components requisite for tissue growth, such as growth factors or cytokines.[9] Therefore, selection of the appropriate

Smart Materials No. 25
Smart Materials for Tissue Engineering: Applications
Edited by Qun Wang

Published by the Royal Society of Chemistry, www.rsc.org

scaffold material is essential. In addition, great effort is dedicated to designing 3D-structured scaffolds instead of the typical 2D scaffolds because of their superior capability of mimicking the ECM structure.[2,10]

The engineered tissue should display the highest possible similarity to the original organ and, more importantly, proliferate and grow into the regenerated tissue. In order to improve the function of a tissue-engineered organ, different capabilities, such as gradual degradation and angiogenesis, are added to the designed scaffold.[11] Different organs are currently under investigation for TE, including the skin, bladder, the liver, the heart, bones, the pancreas, cornea, *etc.*[4]

The gastrointestinal (GI) tract is a complex organ composed of different parts with diverse functions, including ingestion, digestion, nutrient absorption, and excretion of waste. The small intestine and colon are two major sections of the intestinal tract, and form the lower part of the GI tract.[12] Because of its finger-shaped villi structures, the small intestinal epithelium has a large surface area (Figure 12.1). This enlarged surface enables it to absorb great quantities of substances such as nutrients, electrolytes and water.[13,14] A layer of differentiated epithelium covers the villus, extending over blood and lymph vessels that absorb the nutrients. The cavities between villi are called crypts of Lieberkühn and lie beneath the mucus layer.[14] The small intestinal epithelium has the highest self-renewal rate among all the tissues because of stem cells that are located at the bottom of the crypts. The villus–crypt structure of the small intestine acts in an orderly manner to impart different functions onto the differentiated cells. Stem cells residing at

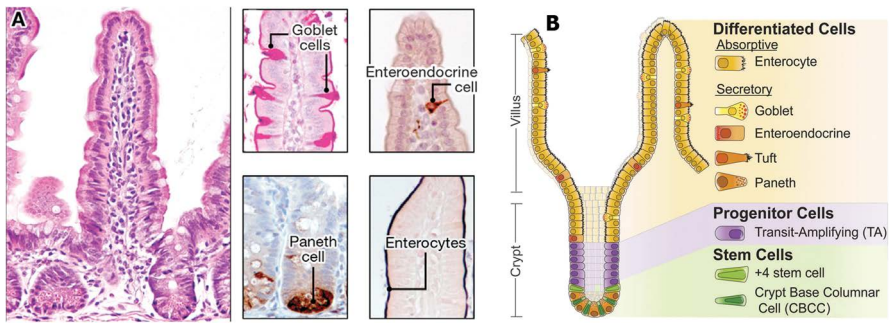

Figure 12.1 (A) Hematoxylin and eosin staining of the human intestinal epithelium. The location of stained differentiated cells (goblet cells, enteroendocrine cells, Paneth cells and enterocytes) are highlighted.[14] (Reproduced with permission from H. Clevers, *Cell*, 2013, **154**, 274–284. Copyright 2013: Elsevier). (B) Schematic of finger-like structured human intestinal tissue containing stem cells and Paneth cells residing at the bottom of the crypt and differentiated cells (enterocytes, goblet cells and enteroendocrine cells) located at the epithelium of the villus. Stem cells, by proliferating and migrating upward, differentiate into intestinal differentiated cells. Reproduced from ref. 106 with permission from The Royal Society of Chemistry.

the bottom of the crypts constantly proliferate, differentiate, and migrate to the top of the villus, then die and are shed.[15]

Various types of differentiated cells exist in the intestine, each having a distinct functionality. Absorptive enterocytes, monolayer polarized epithelial cells, are in charge of the brush border structure of the gut epithelium. It takes ~3–4 days for the absorptive cells to migrate from the crypt to the villus before they can reside at the mucus intestinal layer.[16] Enterocytes are responsible for digestion of nutrients as well as controlled antigen uptake. They act as a diffusion barrier, with the help of a mucus layer secreted by goblet cells, the second category of differentiated intestinal epithelial cells.[12,17] The volume density of goblet cells in the villi increases in the small intestine, from the duodenum to the distal ileum, although it is constant in crypts across the entire intestine length. As a result, mucin (mucus glycoprotein) secretion differs in different parts of the intestine.[18] Enteroendocrine cells are differentiated cells that are located in deeper parts of the mucosa. They are sparse and, therefore, localized far from one other.[19] Their most important function is the secretion or export of hormones.[12,17] Paneth cells comprise the last important type of differentiated cells. They are different from the other three groups in that upon differentiation they migrate downward from the villus to the crypt, where they can remain for almost 23 days before removal by phagocytosis.[17] Many important roles are attributed to Paneth cells, with secretion of antimicrobial peptides helping the body's defense system as the most significant one. Maintaining the intestinal microbiota homeostasis and nourishing stem cells of the small intestine are their other important functions.[20] The structure of the intestinal epithelium is shown in Figure 12.1. Beneath the mucosa layer of the small intestine are two muscle layers, inner and external, both containing smooth muscle cells (SMCs), albeit in different orientations. Their main function is the support of intestinal peristaltic function.[21]

Because of the broad functionality of the intestinal tissue, its defects may compromise the operation of the entire body. The intestine may be affected by grave diseases. Inflammatory bowel disease (IBD), colorectal cancer (CRC), and short bowel syndrome (SBS) are the three major intestinal diseases. IBDs belong to a group of diseases that result in the inflammation of any part of the GI tract, including the small intestine.[22] Genetic and environmental factors, such as infection, smoking, stress, *etc.*, are now considered as important IBD-predisposing factors.[23,24] Diarrhea, fever, abdominal pain, vomiting, and weight loss are diagnosed as clinical signs of IBD.[24] No definite permanent cure for IBD exists. Prescribed anti-inflammatory and immunosuppressive agents, removal of inflamed intestinal tissue section and drug delivery systems are not fully effective as treatment methods, respectively because of the dependency of curative capability on the intensity of the disease, imposed inconvenience to the patient and the obstacle of direct transport to the inflamed region.[24–26] CRC is another serious and, unfortunately, common disease of the GI tract.[27] Environmental and genetic factors both lead to CRC development. CRC can be inherited, familial, or sporadic.[28] Chemotherapeutic agents remain as the only traditional treatment,

but molecular targeting agents are also being developed to substitute these agents to eliminate their side effects.[29] SBS results from insufficient intestine length, as a consequence of surgical resections (*e.g.*, tumor), neonatal condition, trauma, or IBD.[11,30] The intestine is the major organ of nutrient absorption and, therefore, losing intestine during SBS results in an insufficient absorption area, leading to malnutrition and, subsequently, weight loss. Diarrhea, electrolyte imbalance, and vitamin deficiency are other SBS symptoms.[31] Transplantation is considered as a common method to improve the life expectancy in SBS patients, which is challenging because of a lack of donors, low compatibility between the donor and the acceptor, the requirement for immune suppression, high cost, and complexity.[11] The Binachi method (longitudinally dividing the bowel into two tubes) and parenteral nutrition are also counted as treatment methods. However, the efficacy of these approaches is disputed.[11,32–34]

Different methods of curing the intestinal diseases are available, with their own shortcomings. To avoid surgical interventions and the risk of side effects of conventional drug administration, a great need exists for tissue replacement and this requirement should be met with the help of new methods of TE.[21,34] Employing a tissue-engineered intestine would circumvent the disadvantages of other therapies and be a conclusive method to cure intestinal diseases. However, in order to prepare an effective intestine by TE, certain obstacles should first be overcome, including identification of the appropriate source of cells and materials.[35] An appropriate cell source should be considered before a useful tissue-engineered intestine can be created. Furthermore, the complicated anatomy of the small intestine renders intestinal TE complex.[21] A thorough understanding of the different elements of intestinal TE is of great importance and will be required before scientists will be able to design an appropriate tissue-engineered small intestine (TESI). In this chapter, different TESI components are described and intestinal stem cells (ISCs) are introduced as a unique cell source for TESI. Moreover, as ISCs should be employed in an appropriate environment in order to regenerate into the intestinal tissue, elements contributed to an efficient environment or niche of ISCs should be studied. The second major focus of this chapter is assigned to the two substantial environments that should be prepared for the ISCs in order for them to have their complete functionality. Two of the most significant environments, specifically chemical and mechanical environments, are further discussed and the connectivity between ISCs and environmental elements in TESI is highlighted.

12.2 Tissue-Engineered Intestine Components

12.2.1 Cells

Different types of cells can be used to seed the intestinal TE scaffolds (shown in Figure 12.2). In general, we can categorize these cells into two distinct classes: differentiated cells and stem cells. The most used differentiated cells possess characteristics most similar to the intestinal epithelial cells.

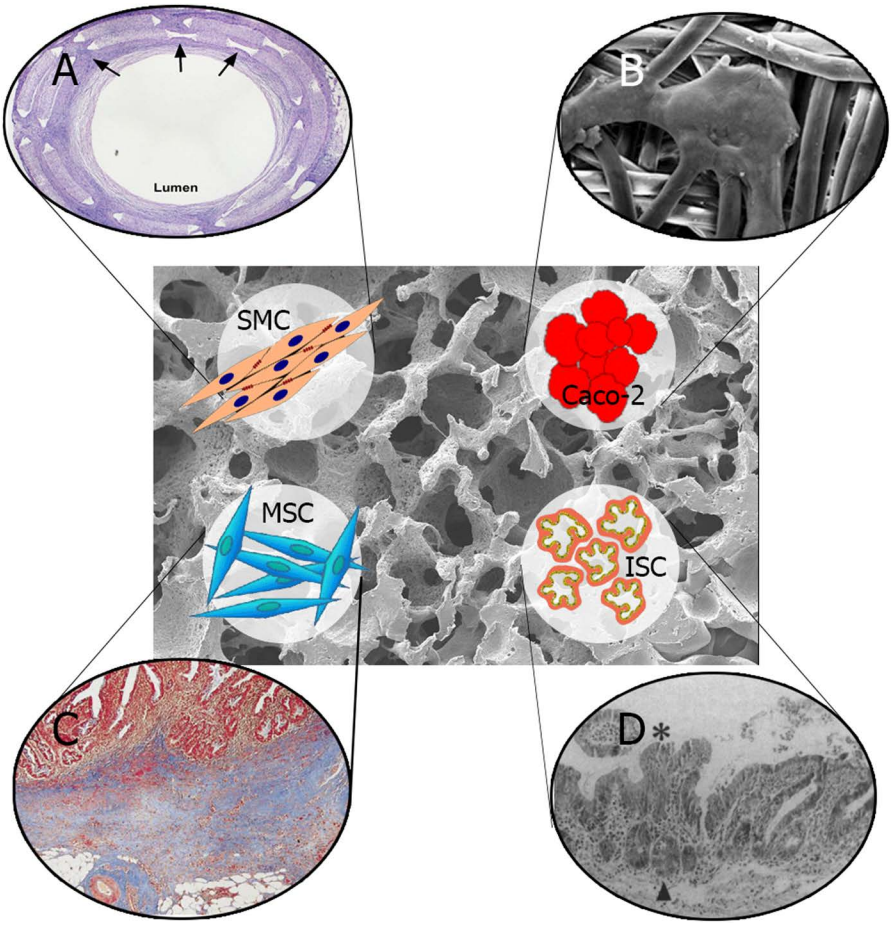

Figure 12.2 Different cells that can be used in TESI. (A) Isolated smooth muscle cells seeded on the PCL scaffold. Laser cut pores, which are shown with arrows, are responsible for vascular and cellular penetration into the scaffold.[38] (Reproduced with permission from C. M. Walthers, *et al.*, *PLoS One*, 2014, **9**, 1–20. Copyright (2014) Walthers *et al.*) (B) Attachment of Caco-2 cells on HYAFF 3D (hyaluronic acid scaffold).[37] Reproduced from *Journal of Materials Science*: Materials in Medicine, Hyaluronic acid based materials for intestine tissue engineering: A morphological and biochemical study of cell–material interaction, **17**(12), 2006, 1365–1372, Esposito, A., Mezzogiorno, A., Sannino, A., De Rosa, A., Menditti, D., Esposito, V., Ambrosio, L., with permission of Springer. (C) Microscopic picture of regenerated intestine, 16 weeks after implantation of collagen sponge scaffold seeded with MSCs in beagle dogs.[34] Reprinted from *Journal of Surgical Research*, **102**(2), Hori, Y., Nakamura, T., Kimura, D., Kaino, K., Kurokawa, Y., Satomi, S., Shimizu, Y. Experimental Study on Tissue Engineering of the Small Intestine by Mesenchymal Stem Cell Seeding, 156–160. Copyright (2001), with permission from Elsevier. (D) ISC. Epithelium formation in polyglycolic acid scaffold seed with organoids six weeks after implantation in a mouse model.[70] Reproduced from the *Journal of Pediatric Surgery*, **33**(7), Choi, R. S., Riegler, M., Pothoulakis, C., Kim, B. S., Mooney, D., Vacanti, M., Vacanti, J. P., Studies of brush border enzymes, basement membrane components, and electrophysiology of tissue-engineered neointestine, 991–997. Copyright (1998) with permission from Elsevier.

The Caco-2 cell line, which is derived from GI tumors, is being employed as the intestinal epithelial cell model in many *in vitro* experiments examining cell attachment, differentiation, and proliferation on different scaffolds.[36]

Esposito and his research group used Caco-2 cells as a tool to investigate the biocompatibility of hyaluronic acid (HA) ester groups as epithelial cell scaffolds. This resulted in greater differentiation of Caco-2 cells on 2D scaffolds in comparison with 3D scaffolds, considering the similar surface chemistry.[37] Caco-2 cell attachment and penetration of a composite scaffold have been reported to be enhanced by increasing the amount of HA (Figure 12.2(B)).[37] SMCs have also been used as a differentiated cell type for TESI[38] (Figure 12.2(A)) because, despite the fact that SMCs are present in different organs, their functionality differs depending on the tissue.[39] Therefore, Nakase attempted to extract SMCs from the stomach wall to use as an autologous seed for a collagen sponge scaffold to dampen the immune reaction to tissue-engineered intestine.[39] The development of a muscle layer in addition to a well-developed epithelial layer is a positive effect of SMC use.[39]

Other promising cell sources are undifferentiated or stem cells.[40] The two main characteristics of stem cells are their prolonged proliferation as well as their capacity to differentiate into one, multiple, or several cell types.[41] Adult tissue-specific or organ-specific stem cells are multi-potent cells that can differentiate into multiple cell types. Mesenchymal stem cells (MSCs) are specific types of adult stem cells that are normally present in connective tissues.[40] The ability of MSCs to differentiate into multiple types of cells and their easy culture render them a remarkable cell resource for TE.[42] For these reasons, researchers have been investigating the formation of muscle layers by seeding autologous MSCs onto collagen sponge scaffolds (Figure 12.2(C)). However, the outcome of the long-term use of such tissue-engineered organs in Beagles was not satisfactory. In the study, a lack of muscle layer recovery was attributed to the inadequate cell seeding or lack of pre-induction.[34] Thus, the demand for a promising cell source still exists. Researchers have suggested another type of cells, called ISCs, which in addition to retaining their ability to differentiate into various types of cells, are more specific to the intestinal tissue (Figure 12.2(D)).

12.2.2 Intestinal Stem Cells

As has been illustrated, tissue-specific stem cells reside in most tissues and are recognized by their ability to self-renew and differentiate into particular cells in that organ.[43] The high turnover rate of the intestinal epithelium (~3–4 days) in comparison with other mucous layers encourages researchers to consider the existence of a source of stem cells with an ability to differentiate into all types of intestinal epithelial cells.[44,45] Cheng and Leblond first proposed the existence of stem cells at the base of the crypts and introduced the term crypt-based columnar (CBC) stem cells.[15] CBC cells are at the origin of the differentiating process. As is shown in Figure 12.1(B), CBC cells residing among Paneth cells start to proliferate into daughter cells

(TA cells), which progressively transfer into differentiated cells. As the cells move upward through the crypt, their modality changes from progenitor to differentiated cells until the crypt–villus junction where two major categories of epithelial lineage cells, absorptive and secretory lineages, exists. Enterocytes are included in the absorptive lineage, and goblet and enteroendocrine cells belong to the secretory lineage. Paneth cells are also members of the secretory lineage, however, they are located at the bottom of the crypt.[43] Hans Clevers was the one who in 2007 recognized a G protein-coupled receptor with leucine rich-extracellular domain (LGR5) as a marker of CBC cycling, and $LGR5^+$ CBC cells as small intestinal stem cells.[46] Moreover, it has been speculated that in addition to $LGR5^+$ CBC and TA amplifying cells, a specific type of stem cell is located at the +4 position (shown in Figure 12.1(B)) above the Paneth cells, which is entirely different from $LGR5^+$ CBC cells.[46] These +4 cells are also known as DNA label-retaining cells with several markers attributed to them including Bmi-1, Hopx, mTert, and Lrig1.[15,47–50] Actually, little information is available concerning their culture and microenvironment, and more focus is being placed on $LGR5^+$ CBC cells.[15]

It has been reported that ~15 $LGR5^+$ CBC cells are present in every murine crypt, and that within a timescale of 24 h, each $LGR5^+$ CBC cell differentiates into 16–32 epithelial cells, *via* TA cells.[15] The homeostasis and fate of $LGR5^+$ CBC cells are directly related to their niche or microenvironment.[43] Some major pathways that regulate the stemness or differentiation of cells will now be briefly delineated (shown in Figure 12.3). One of the most significant pathways is Wnt signaling that plays an important role in maintaining the undifferentiated state of stem cells.[51] Wnt signaling is amplified by R-spondin family proteins (Wnt agonists) that themselves are activated by a LGR5 stem cell marker.[43] Wnt ligand binding leads to accumulation of β-catenin inside the nucleus as a result of an intracellular signaling cascade. T-cell factor (Tcf)/β-catenin transcription is a significant element of stemness maintenance. Moreover, the Wnt signal is also responsible for the terminal differentiation of Paneth cells.[51]

A second major pathway is the Notch pathway. Notch signaling plays two important roles in the intestine. First, it affords negative regulation that inhibits differentiation of stem cells and, as a result, maintains their stemness. Second, it promotes unidirectional cell differentiation, controlling the absorptive to secretory lineage ratio. This regulation occurs because of cell-to-cell signaling. Delta-like or Notch ligands of Paneth cells (DLL1 and DLL4) receive a Notch signal from the adjacent CBC cells and bind to the Notch receptor on the cell surface. Upon this binding, proteolytic cleavages result in shedding of the extracellular domain of the receptor and the release of Notch intracellular domain (NICD), NICD translocation to the nucleus and subsequent gene expression, with cell differentiation or proliferation as the final outcome. This process may inhibit differentiation of CBC cells.[43] Loss of contact between DLL1 ligand-containing Paneth cells and daughter cells results in daughter cell differentiation.[15] It can be noted that lateral inhibition is

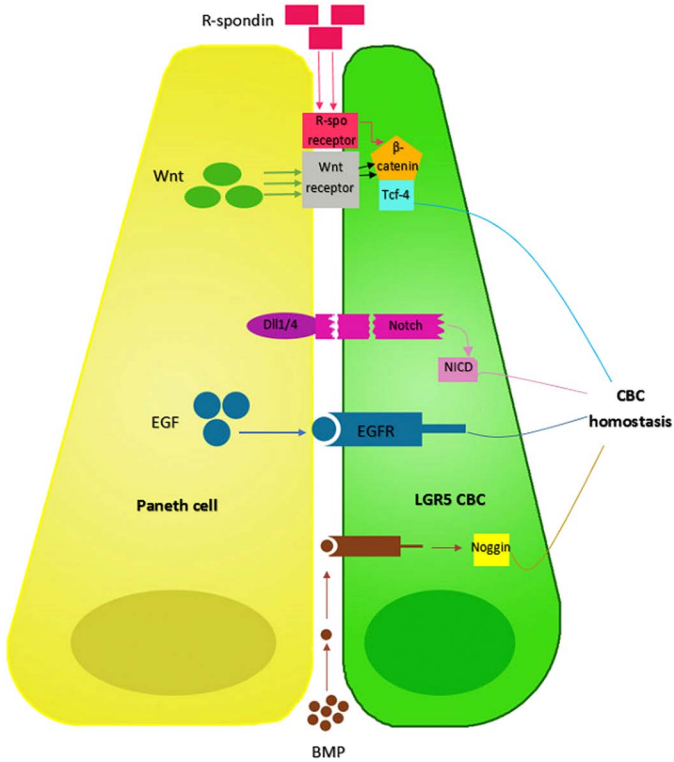

Figure 12.3 Major pathways necessary for the homeostasis of LGR5 CBCs. Wnt, Notch and EGF signaling, which are originated from Paneth cells, by affecting their receptors, maintain the stemness of LGR5 CBC. BMP located at the surrounding environment and the effect of BMPR is blocked by Noggin inside CBC that results in the maintaining of the CBC undifferentiated state. R-spondin amplifies the effect of Wnt signaling.

responsible for this type of differentiation. As a result of lateral inhibition, Notch activation leads to Notch ligand production. Thus, lower Notch activity accompanies higher Notch ligand concentrations, and higher ligand concentrations lead to increased Notch signaling in proximal cells and, subsequently, reduce the amount of neighboring cell ligands. Decreasing the neighboring cell ligands leads to an increase in the original cell ligands to a greater extent than upon initial activation and thus, the differentiation fates of two neighboring cells are different. Notch-high progenitor cells differentiate into enterocytes and, therefore, their neighboring cells will become secretory cells.[43]

Bone morphogenetic protein (BMP) signaling comprises another regulatory pathway in the differentiation of stem cells to epithelial layers. By binding to type-II receptor, BMP recruits a type-I receptor that transfers the signal to the nucleus and has a role in differentiation. However, Noggin (Nog),

an extracellular protein, antagonizes the BMP signal and inhibits its activity, leading to the formation of crypt-like structures among villi.[44]

Epidermal growth factor (EGF) is activated upon binding to its receptors on the cell surface, normally EGFR (epidermal growth factor receptors), enhancing cell proliferation.[52] Thus, EGF binds EGFRs of ISCs and TA cells and causes them to divide into the same stem cells.[15]

Considering the fact that stemness of LGR5$^+$ CBC cells strongly depends on the niche, naturally, there should be an element in the intestine that controls the microenvironment and accordingly manages the signaling pathways. Researchers have demonstrated that the presence of Paneth cells adjacent to LGR5$^+$ CBC cells is of great importance for maintaining their proper condition to stay undifferentiated. Paneth cells secrete EGF and Wnt3 in addition to their bactericidal secretions. Production of Notch ligands Dll1 and Dll4 comprises another role of Paneth cells. To conclude, Paneth cells are considered a niche-controlling element and the interaction between Paneth and LGR5$^+$ CBC cells is critical for cell fate. Moreover, in order to gain the full characteristics of a stem cell niche, BMP and R-spondin are provided by non-Paneth cell sources.[15]

Understanding stem cells' homeostasis, the effect of different elements on their differentiation, and, generally, the stem cells' biology, as well as their potential therapeutic applications, requires long-term *ex vivo* culturing. However, it is generally agreed that conventional long-term culture of adult tissues is not feasible.[51] Although a lot of effort has been dedicated toward identifying culture conditions appropriate for ISC culture, only short-term maintenance of cells, ~2–4, weeks could be achieved.[53–55] Finally, in 2009, Sato succeeded in developing a culture system for maintaining viable cells for over 1.5 years.[56] Sato simply assumed that inclusion of all the elements important for stemness maintenance of stem cells in the culture system, *i.e.*, Wnt signaling, R-spondin-1 (Wnt agonist), EGF, and Nog (BMP inhibitor) would aid cellular survival and prepare similar conditions to the natural biology of the human intestine for stem cell maintenance. Moreover, cell detachment from the extracellular matrix (ECM) may result in a lack of proliferation. Therefore, an appropriate matrix, as similar to the crypts as possible, was designed for the cells to reside in. Because of the high laminin (α1 and α2) content of the crypt base, laminin-rich Matrigel was proposed as a matrix.[56] Under the stated conditions, a single LGR5$^+$ stem cell can be used to generate intestinal epithelium that would mimic normal intestinal epithelium. The resulting organoid structure consists of several crypts, presented as buds around a hollow cyst, and a villus-like epithelium located between the crypts. The crypts contain LGR5$^+$ stem cells in addition to adjacent Paneth cells and TA proliferating cells that are located at the crypt necks. Over the course of five days, stem cells at the bottom of the crypts differentiate, move towards the cyst, and finally shed into the hollow cyst.[51] The organoid structure is shown in Figure 12.4. Upon culturing a stem cell, a symmetric cyst containing stem cells forms. After 2–3 days, by the effect of Paneth cells, Wnt signaling is initiated and the presence of R-spondin makes the signaling focal.[15]

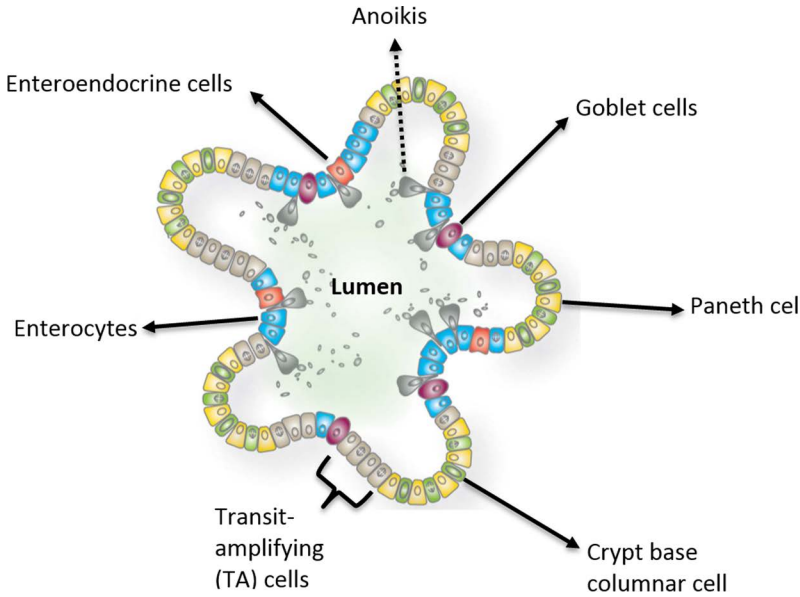

Figure 12.4 Organoid structure containing all types of differentiated cells in addition to CBCs. The CBCs are located at the buds of the organoid. At the end of the differentiated cell life span, cells shed off into the lumen of the organoid (a process called anoikis).[51] (Reproduced with permission from M. Leushacke, *et al.*, *Gut*, 2014, **63**, 1345–1354. Copyright 2014: BMJ Publishing Group Ltd and the British Society of Gastroenterology).

It is interesting that just as in a normal crypt–villus structure, the *EphB/EphrinB* interaction underlies bud formation in organoid structures. *Eph* receptors are a family of tyrosine kinase receptors that specifically bind *Ephrin* ligands. Repulsion is a consequence of *Eph–Ephrin* interactions in cell–cell interactions. Paneth cells express *EphB3*, a Wnt target gene. When TA cells differentiate, they travel upstream of the Wnt gradient from the crypt to the villus and, therefore, express EphrinB1.[57]

Regarding focal Wnt signaling and the subsequent Eph/EphrinB repulsion, the crypt part of the organoid region containing stem and Paneth cells is repelled from the cyst and creates buds (Figure 12.5).[15]

There were some important attainments in Sato's experiment.[56] First, although LGR5$^+$ are not dependent on the submucosal layer beneath the epithelial layer, some important growth factors were required for cell survival. Furthermore, it is possible to prevent cell apoptosis (anoikis) by using Rho-associated protein kinase (ROCK).[56] Despite the conclusion of Garabedian in 1997 that Paneth cells are not needed in a stem cell niche, Sato did not focus on the effect of Paneth cells on LGR5$^+$ culture in 2009.[56,58] Nevertheless, in 2010 Sato proved that a direct physical contact between Paneth cells and stem cells initiates Notch signaling.[59] Moreover, Paneth cells are

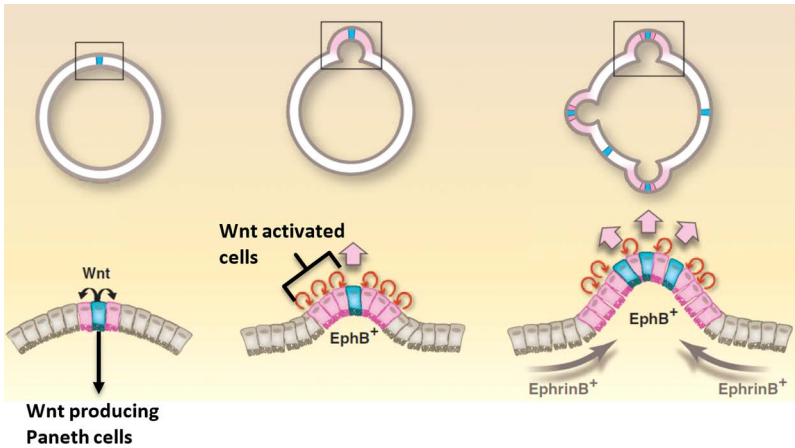

Figure 12.5 Bud formation in the organoid structure. Focal Wnt signaling by Paneth cell (blue parts) results in EphB expression and bud formation because of the repulsion between EphB and the EphrinB ligand.[15] (Reproduced with permission from T. Sato, *et al.*, *Science*, 2013, **340**, 1190–1194. Copyright 2013: American Association for the Advancement of Science).

responsible for EGF and Wnt3 support. It is true that Wnt may originate in cells other than Paneth cells, however, it has been confirmed that R-spondin amplifies local Wnt signaling of Paneth cells. Localized Wnt signaling of Paneth cells also affects the asymmetrical crypt–villus construction in organoids. It has been demonstrated that touching Paneth cells are vital for stem cell maintenance.[59] In comparison with 15 $LGR5^+$ stem cells, there are ~10 Paneth cells in each crypt. Therefore, because of the fewer numbers of Paneth cells, stem cells should compete for their niche, and, according to the "neutral competition model", the number of stem cells remaining in the crypt is related to the size of the Paneth cells' surface.[14] It has been observed that the lack of Notch signal leads to the formation of Paneth cells capable of Wnt signaling and to the production of more Paneth cells and stem cells. Therefore, this would be a positive feedback loop for increasing the number of stem and Paneth cells.[14] However, this signaling pathway should be balanced to prevent the ever-expanding cryptal growth. An investigation by Koo (2012), showed that RNF43 and ZNRF3, Wnt signaling inhibitors, limit the crypt size by affecting Frizzled receptors (G protein-coupled receptors in the Wnt signaling pathway).[60] Other reports also demonstrated the effect of Lrgi1 (leucine-rich repeats and immunoglobulin-like domains protein 1), a +4 stem cell marker, on stem cell proliferation and crypt homeostasis. Lrgi1 was inversely related to the amount of protein and the activity of receptors like the Erb B family, and prevented ISC over-expansion by interacting with them.[61] A long-term organoid culture, with some alterations, was also successfully conducted with a human GI epithelium.[62,63]

In conclusion, culturing ISCs for long-term use in the form organoids has been extremely successful. Therefore, there is great hope in the application of ISCs for different medical purposes, including microbial and toxicological investigations of different GI tract diseases and employing organoids as disease models.[63] There is also a great potential for using organoid structures in the pharmaceutical field, for instance for drug screening and drug targeting to treat specific diseases of the GI tract.[64] Moreover, a mild GI tract biopsy and culturing of the extracted tissues would render organoids an effective tool to be used in regenerative medicine.[65]

12.3 Environmental Factors

Due to the fact that each type of cell needs a specific environment to fulfil its requirement, the niche of each cell should be evaluated individually. The ISC environment as the focus of this chapter is delineated. The combination of ISCs that form epithelial layers of the small intestine with an appropriate environment for maintaining stem cell niche and organ structure results in TESI. TESI can grow into the intestinal tissue to treat or improve intestinal function. The important point in designing a TESI is the selection of appropriate factors required for stem cell growth. These important factors can be divided into two major groups: mechanical factors, or the environment, and chemical environment.

12.3.1 Mechanical Environment

Mechanical environment refers to all the factors that are mechanistically required for stem cell growth and they are generally known as scaffolds.

TESI was first introduced in 1988 by the Vacanti group that designed different scaffolds (polyglactin, polyorthoesters, and polyanhydride) to be loaded with parenchymal intestinal cells as a substitute of transplantations with surgical implications, or as a cell suspension injected into the tissue.[66] The rate of cellular scaffold attachment and survival was acceptable and differentiated epithelium cells were arising on the scaffolds.[66]

After organoid development, the Vacanti group used this source of cells as seeds in polyglycolic acid (PGA) fiber scaffolds in intestinal TE in Lewis rats.[53,67] PGA is a polyester, and polyesters are a group of synthetic biodegradable polymers.[68] PGA undergoes bulk degradation that leads to a decrease in its molecular weight even in the first days post implantation.[69] The biocompatibility of its degradation product, glycolic acid, renders it appropriate for use in medical fields.[68] In Vacanti's report, PGA was shown as a promising organoid-supporting scaffold. Beyond survival, organoids supported by PGA were proliferating and differentiating into columnar epithelium, goblet cells, Paneth cells, and crypt–villus structures typical for the intestinal tissue, that were all surrounded by vascularized tissue, fibroblast extracellular matrix (ECM) SMCs, and polymer degradation products.

Moreover, it was noted that increasing the implant length resulted in larger cysts with more natural crypt–villus structures.[67]

To illustrate the morphological and functional aspects of tissue-engineered neointestine, non-woven tubular PGA sprayed with PLLA (poly-L-lactic acid) and coated with type I collagen was prepared, seeded with organoids, and implanted in Lewis rats.[70] PLLA is an isomeric form of poly-lactic acid and a member of the polyester group of compounds. PLLA is more hydrophobic than PGA and, therefore, it shows less degradation.[68] It was concluded that the presence of PLLA on the surface of a degradable tubular scaffold results in a lower scaffold degradation rate.[70] Collagen is a biomolecule that can be extracted from different sources, *e.g.*, bovine skin and tendons, porcine skin, and murine tails. This highly compatible polymer is mainly produced by fibroblasts and forms the organic part of the ECM.[71,72] The presence of collagen on the surface of PGA/PLLA scaffolds resulted in better engraftment and larger cysts. The resulting neointestine mimicked the intestine in the formation of polarized epithelium layer with differentiated cells, basement membrane, and brush border enzymes. It has been also shown that epithelial maturation occurred over 2–6 weeks, including increased crypt and villus formation, numerous differentiated cells, and more mature columnar epithelium. A subepithelial layer containing a fibrous layer similar to lamina propria and SMC layers of different thicknesses in different regions were also obtained. It was also discovered that transepithelial resistance of the neointestine was similar to the intestine, which indicated that epithelial permeability of the neointestine was the same as in the intestine. However, a lesser maturation of the neointestine compared with the intestine resulted in decreased ion movement across the epithelial layer.[70] Other reports presented the formation of complete neomucosa and immune system in tissue-engineered neointestines.[73,74] These investigations confirmed the existence of B cells, T cells, and natural killer (NK) cells in the neointestine, following a period of time of ~20 weeks after anastomosis. Without luminal stimuli or within a shorter timeframe (~10 weeks), the numbers of some immune cells were lower with respect to a 20 weeks' timescale.[73] It has also been shown that TESI can greatly improve the functionality and regeneration of the intestine after small bowel resection. TESI-exerted positive effects included decreased recovery time, improved absorptive function, and creation of muscular, vascular, and neural components, and a thicker muscularis mucosae layer. An attractive insight gained from this experiment was that small bowel resection positively affected cell differentiation.[75] A perfusion bioreactor has been designed for the same system to render the stem cell environment more similar to natural *in vivo* conditions in order to make long-term *ex vivo* culture feasible. Constant oxygen exposure of cells increased cellular survival, proliferation, and differentiation. The possibility of investigating the effect of different factors on TESI and dynamic seeding thus constituted the advantages of bioreactor use. However, these experiments were performed for just two days and applicable results have not been obtained.[76] Sala *et al.* (2011) succeeded in establishing a multicellular approach of cell extraction and

seeded the cells onto a collagen-covered PGA/PLLA scaffold.[11] The method involved extracting full-thickness sections of mouse intestine and saving the mesenchymal components (muscle and nerve), instead of extracting low quantities of single cells for long-time culturing with subsequent cell transformation. Fully-differentiated epithelium, in addition to other vital components of TESI, including the muscularis layer, nerves, and blood supply, was thus obtained. Immediately after implantation, vast amounts of differentiated cells from the full-thickness intestine were dying and the neointestine was only generated from the stem cells presented. This may have also been caused by a lack of oxygen supply and nutrition in the bulk scaffold. Wound healing had just started upon implant insertion, by forming undifferentiated flat epithelium at the scaffold ends. It was concluded that "mesenchymal-epithelial cross-talk" results in tissue repair and regeneration.[11]

To decrease the immune response of the body to TESI, it is vital for the donor and the host to be the same. Since the ultimate aim of TESI is its employment as a substitute of the human intestine, extracting organoids from human intestine is a step in the right direction. One of the major problems necessitating the use of TESI in humans is SBS, which usually occurs in newborns. Levin used postnatal human intestine as a source for organoid derivation.[77] Postnatal organoids were seeded onto a collagen-coated PGA/PLLA scaffold and inserted into the omentum of adult non-obese diabetic/severe combined immunodeficiency (NOD/SCID) gamma chain-deficient mice. Clusters of cells were extracted from fresh postnatal small intestine to add intestinal subepithelial myofibroblasts (ISEMF) and differentiated epithelial cells to the intestinal cells, with the goal of a fully-functional neointestine. An increased absorptive area associated with the presence of enterocytes and flat epithelium, assumed to have the ability to develop into crypt–villus structures, was the result of this arrangement. In addition, all secretory cell lineages, including goblet cells, enteroendocrine cells, and Paneth cells, were detected. This TESI also comprised mesenchymal and nerve components in addition to adjacent ISEMF and epithelial layers. Neurovascular components were also confirmed in that experiment. The existence of all types of differentiated cells is an indication of similarity between a normal intestine and TESI. The presence of all intestinal factors is an indicator of the full-thickness TESI achievement using postnatal organoids.[77] It was expected that if TESI containing human postnatal organoids placed in a murine omentum has the same functional profile as mouse TESI in a mouse, autologous human TESI (hTESI) will be practically achievable. It has been reported that mouse TESI (mTESI) and hTESI result in the formation of a fully differentiated epithelium, containing fully functional secretory cells. A well-polarized epithelium determined the ion flux potential of both types of TESI. Actin localization resulting in tight epithelial junctions was observed in both TESIs. A high expression of cell division control protein 42 homolog (Cdc42) in secretory cells was related to tissue development and normal homeostasis, confirming the notion of the identical function of TESI and normal intestine. It was also shown that mTESI and hTESI expressed enough ion and water transporters and channels to act

as a normal intestine. Sodium-glucose linked transporter (SGLT-1) TESI localization was similar to a control, confirming adequate nutrient absorption. Strong intestinal alkaline phosphatase (IAP) activity in mTESI and hTESI indicated the integration of the gut barrier properties and an increase in food digestion. It can be concluded that satisfactory functional properties were achieved by both kinds of TESI and both had similar characteristics, which gives hope for using TESIs to treat deficiencies such as SBS in humans. However, engineering an extensive injury treatment remains difficult.[78]

Matrigel is a soluble extract of basement membrane that converts to a gel at 37 °C.[79] The principal components of Matrigel are laminin, collagen IV, and enactin. Matrigel is widely used in cell culture and it is believed that cell responses change after the cells are inserted into Matrigel. This is believed to be associated with the presence of growth factors, such as basic fibroblast growth factor (bFGF), EGF, insulin-like growth factor1 (IGF-1), transforming growth factor β (TGF-β), platelet-derived growth factor (PDGF), and nerve growth factor (NGF) inside a standard Matrigel.[80] An Engelbreth–Holm–Swarm (EHS) tumor (murine tumor with high ECM content) is the source of Matrigel.[79] Because of its unique properties, Matrigel can maintain cell progeny and pluripotency. Thus, it is widely used as the ECM in stem cell culture.[80] Matrigel is also common in intestinal organoid unit culture. However, because of its origin, it may provoke a foreign body response and thus might not be useful in regenerative applications.[81]

Collagen has been introduced as a 3D substitute for Matrigel in an *ex vivo* culture of ISCs.[10] Although the combination of collagen and laminin showed lower ISC proliferation than Matrigel, multilineage differentiation and long-time proliferation of ISCs are indicative of collagen's ability as a 3D matrix for ISC culture.[10] *In vitro* culture and *in vivo* implantation of collagen-coated PGA organoid scaffolds were also evaluated to determine the effect of collagen presence instead of Matrigel.[81] *In vitro* culture revealed different organoid morphology on Matrigel and collagen structures. As anticipated, crypts displayed bud-surrounded lumen on the Matrigel substrate. However, a smooth structure without buds arose on the collagen matrix. Moreover, a differentiated epithelium monolayer emerged in culture when the collagen matrix was used. This was not observed with Matrigel. Cells could survive on both matrices and fully differentiated cells, including enterocytes, goblet cells, enteroendocrine cells, and Paneth cells, in addition to stem cells, were observed as enteroid structures on Matrigel and monolayers on collagen. However, LGR5 expression was noticeably higher on Matrigel than on the collagen matrix because of its similarity to the intestine's crypt-like structure. A co-culture of organoids and ISEMFs, combined with either collagen or Matrigel, was applied to scaffolds and implanted in wild-type mice. Cells within both matrices, having been provided with the appropriate niche, proceeded through the growth process and the presence of myofibroblasts aided scaffold engraftment. Interestingly, collagen-containing scaffolds regained bud structure *in vivo*, which may be associated with the cellular microenvironment.[81] The different scaffolds used in ISC TE are summarized in Table 12.1.

Table 12.1 Scaffolds used in intestinal stem cell tissue engineering.

Scaffold	Organoid source	Model	Effect of the scaffold	Reference
PGA[a]	Lewis rats	Lewis rats	Organoid survival, proliferation, and differentiation to columnar epithelium; Paneth cells' and goblet cells' formation	67
Collagen-coated (PGA/PLLA[b])	Lewis rats	Lewis rats	Decreased degradation rate, better engraftment and larger cysts; formation of columnar epithelial layer, differentiated cells, basement membrane, and enzyme brush border; similar transepithelial resistance to the intestine but lower transepithelial ion movement	70
	Lewis rats	Lewis rats	Formation of immune system	73
	Lewis rats	Lewis rats	Formation of neomucosa	74
	Lewis rats	Lewis rats	Formation of differentiated epithelium; formation of muscular, vascular, and neural components; formation of thicker muscularis mucosae layer; decreased recovery time after massive resection; increased differentiation	75
	Mice	(NOD/SCID)[c] gamma chain-deficient mice	Mesenchyme-epithelial cross-talk; formation of fully differentiated epithelium, muscularis, nerves, and blood vessels; death of large numbers of original cells; formation of flat epithelium at the ends of scaffold	11
	Postnatal human small intestine	(NOD/SCID) gamma chain-deficient mice	Presence of all types of differentiated epithelial cells (enterocytes, goblet cells, enteroendocrine cells, and Paneth cells); appearance of mesenchymal and nerve components, muscularis, and neurovascular components	77
	Mice	C57BL/6[d] mice	Fully differentiated cells, fully functional secretory cells, ion fluxes; tight junctions of the epithelium; developed TESI; adequate channels for ion-water transport; adequate nutrient absorption and integrated gut barrier properties	78
	Postnatal human small intestine	(NOD/SCID) gamma chain-deficient mice	Fully differentiated cells, fully functional secretory cells, ion fluxes; tight junctions of the epithelium; developed TESI; adequate channels for ion-water transport, adequate nutrient absorption and limiting passage of epithelium	78
Collagen-coated PGA/Matrigel	Transgenic C57BL/6 mice	Wild-type mice	Recapitulates stem cell niche; regained crypt-like structure and growth of organoids; better engraftment because of ISEMF cells	81
Collagen-coated PGA/collagen	Transgenic C57BL/6 mice	Wild-type mice	Recapitulates stem cell niche; regained crypt-like structure and growth of organoids; better engraftment because of ISEMF cells	81

[a]Polyglycolic acid.
[b]Poly-L-lactic acid.
[c]Non-obese diabetic/severe combined immunodeficiency.
[d]C57 black 6.

12.3.2 Chemical Environment

The chemical environment encompasses all factors that are chemically required for ISC function maintenance, as a TE cell source. Growth factors play the most important role here. Several reports on the effect of different growth factors on the proliferation and growth of the epithelium layer have been published, concerning specific disease treatment or renewal of the intestinal organ.[82–84]

Circulating growth hormone (GH) binds cellular GH receptors, which leads to IGF-1 production. Both GH and IGF-1 are responsible for somatic growth.[85] Inconsistencies in clinical results regarding the administration of recombinant GH (rhGH) are considered to be associated with the methods used, patient diet, and diet supplements.[86,87] IGFs can improve the growth of the small bowel, where their receptors are expressed.[88] Factors, such as bFGFs and IGFs, are responsible for the proliferative characteristics of the crypts in the gut.[89] Glucan-like peptide-2 (GLP-2), a PGDP (peptide derived from post-translational processing of proglucagons), has the ability to regulate epithelial cell proliferation.[90] GLP-2s are peptides that are secreted from enteroendocrine cells that, because of their location, can affect the entire length of the intestinal epithelium.[91] It has been reported that, unlike IGFs, the increase of cell proliferation by GLP-2 is "tissue-specific only in the intestine".[90,92] Decreased cell apoptosis, and increased crypt cell population and villus height in rodents have been attributed to GLP-2 administration.[92] Clinical administration of GLP-2 is controversial because of its short half-life, and use of teduglutide, a GLP-2 analog resistant to enzymatic degradation, is more common. However, the variability of results of teduglutide administration should be resolved by a comprehensive study.[87] Administration of EGF as another growth factor can also enhance the proliferation rate and absorptive properties of the intestine by binding to enterocyte receptors.[93,94] EGF has been successfully used in the treatment of different GI tract diseases.[87] EGF's stimulatory role has also been considered in epithelial growth. PDGFs are also regarded as stimulatory growth factors.[95] Similarly, TGF-α exerts a stimulatory effect on proliferation of stem cells in crypts, while TGF-β is mostly known for its inhibitory function.[89] By decreasing the duration of the stem cell mitotic cycle, subsequently increasing the number of dividing cells, EGF and TGF-α increase the cell proliferation rate in the crypt region. However, TGF-β prevents cell proliferation in 50–75% of the crypt region.[89] It is worth noting that different tissue reactions would be expected because of different cell responses to TGF-β. Time-related inhibition or stimulatory TGF-β effects can be seen on different timescales. Hepatocyte growth factor (HGF), a protein synthesized in digestive tissues, is responsible for epithelium repair, and mucosal regeneration and recovery.[96] Interestingly, none of these factors can perform their roles in their entirety individually and only their combination leads to an appropriate tissue response.[89]

The brief summary above described the most important growth factors in the GI tract, however, not all of these elements are useful in TE.[97] Some practical examples of their employment in TE will now be delineated.

GLP-2 has been subcutaneously administered as a growth factor to enhance the functionality of TESI formed by a PGA scaffold with a PLLA surface layer seeded with organoid units in adult rats.[98] Different aspects of the effect of GLP-2 on TESI were then investigated. First, endogenous regulatory effects of GLP-2, including increased villus length and crypt depth, increased crypt cell proliferation, and decreased apoptosis, were successfully observed. Moreover, GLP-2 increased nutrient absorption of neointestine epithelium by increasing SGLT-1 expression and its distribution along the entire villus length. Furthermore, GLP-2 affected the expression of sucrase but not GLUT2, suggesting different regulation mechanisms. These experiments confirmed the subepithelial layer localization of GLP-2R.[98]

In 2011, Wulkersdorfer and his colleagues used locally-delivered growth factors (GLP-2, HGF, and transferrin) on PGA felt disks to increase growth factor bioavailability in target tissue and decrease growth factor requirement. The simplicity and lack of protein degradation in this method were apparent when compared with the microsphere delivery method.[99] Seeded growth factor-containing scaffolds were used and tested in Lewis rats. The effect of Matrigel was also investigated, by suspending the PGA scaffolds in a Matrigel solution. Although, since Matrigel was used, the distinct effects of growth factors in all samples that contained them were not obvious, comparisons of TESIs with and without growth factors helped in understanding some of their effects. Matrigel results in a "complex neomucosal structure and increased surface area" (shown in Figure 12.6(C)).[99] However, increased cyst numbers were attributed to GLP-2. GLP-2 did not affect the diameter of the neomucosal area but GLP-2 effects described in Ramsanahie's report were also observed.[98] It was concluded that the localized GLP-2 effects were identical to the effects generated by systematic administration. No significant HGF effects were observed, which was related to its low dose in TESI (shown in Figure 12.6(A)). However, transferrin samples displayed a more complex structure in addition to a higher neomucosal surface area (shown in Figure 12.6(D)).[99]

Fgf10 is a fibroblast growth factor that has been used in the intestinal TE of extensive injuries or deficiencies on account of its attractive GI tract properties, such as control of epithelium proliferation, differentiation, survival, and expression inside the GI tract. It is assumed that *Fgf10* overexpression may improve TESI formation. Therefore, organoids were extracted from transgenic mice with inducible *Fgf10* overexpression. Organoids were seeded on PLLA-coated PGA scaffolds and implanted in mice. As expected, *Fgf10* overexpression resulted in greater villus length and deeper crypts, which consequently improved the absorptive area (shown in Figure 12.6(B)). Proliferation of the epithelium in *Fgf10*-overexpressing TESI was higher than in the control sample. However, the amount of epithelial proliferation is not enough to consider it as an appropriate TESI. Cells should sufficiently differentiate and distribute along the epithelium before TESI can be considered suitable for mimicking the small intestine. *Fgf10*-overexpressing TESI contained completely differentiated cells of all kinds, reminiscent of a normal intestine.[100]

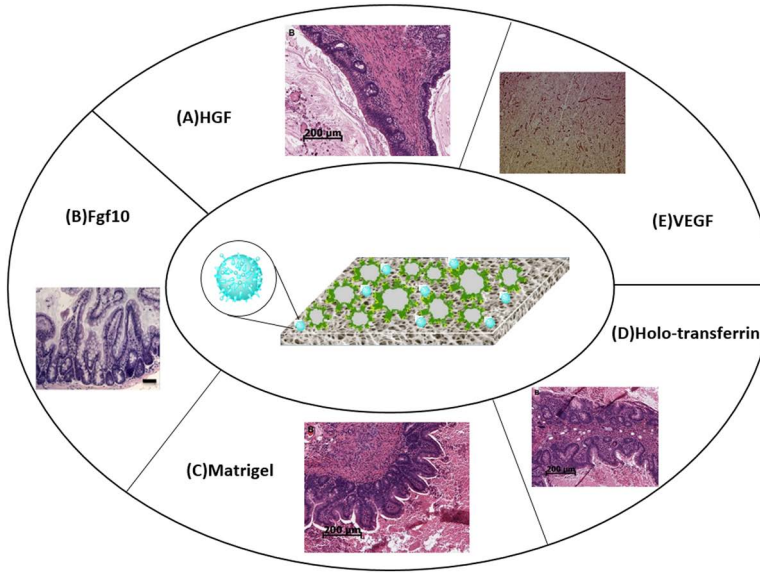

Figure 12.6 Different chemical elements used for TESI improvement. (A) Using HGF on PGA scaffolds seeded with organoids showed no significant differences in neomucosal structure after four weeks' implantation in Lewis rats.[99] Reproduced from the *Journal of Surgical Research*, **169**(2), Wulkersdorfer, B., Kao, K. K., Agopian, V. G., Dunn, J. C., Wu, B. M., Stelzner, M. Growth Factors Adsorbed on Polyglycolic Acid Mesh Augment Growth of Bioengineered Intestinal Neomucosa, 169–178, Copyright (2011) with permission from Elsevier. (B) Crypt–villus structure formed by a TESI-containing organoid-unit-seeded-collagen-coated PGA/PLLA scaffold and *Fgf10* overexpression.[100] (Reproduced with permission from Y. Torashima, *et al.*, *J Tissue Eng Regen Med*, 2016, **10**, 132–139. Copyright 2013: John Wiley & Sons, Ltd.) (C) Complex mucosal structure formed by implanting PGA scaffolds seeded with organoids and treated with Matrigel after four weeks' implantation in Lewis rats.[99] Reproduced from the *Journal of Surgical Research*, **169**(2), Wulkersdorfer, B., Kao, K. K., Agopian, V. G., Dunn, J. C., Wu, B. M., Stelzner, M. Growth Factors Adsorbed on Polyglycolic Acid Mesh Augment Growth of Bioengineered Intestinal Neomucosa, 169–178. Copyright (2011) with permission from Elsevier. (D) Complex cyst morphology obtained from using holo-transferrin in PGA scaffolds seeded with organoids implanted in Lewis rats for four weeks.[99] Reproduced from the *Journal of Surgical Research*, **169**(2), Wulkersdorfer, B., Kao, K. K., Agopian, V. G., Dunn, J. C., Wu, B. M., Stelzner, M. Growth Factors Adsorbed on Polyglycolic Acid Mesh Augment Growth of Bioengineered Intestinal Neomucosa, 169–178, Copyright (2011) with permission from Elsevier. (E) High level of neointestinal capillary marked by CD31 (endothelial cell marker) in the neointestine, formed by an organoid-seeded PGA/PLLA scaffold containing PLLA microspheres loaded with VEGF, after four weeks' implantation in Lewis rats.[102] Reproduced from *Biomaterials*, **29**(19), Rocha, F. G., Sundback, C. A., Krebs, N. J., Leach, J. K., Mooney, D. J., Ashley, S. W., Vacanti, J. P., Whang, E. E. The effect of sustained delivery of vascular endothelial growth factor on angiogenesis in tissue-engineered intestine, 2884–2890, Copyright (2008) with permission from Elsevier.

In order to provide TESI with nutrients and oxygen, Rocha *et al.* used PLGA ((poly(lactic-*co*-glycolic acid)), a biodegradable and biocompatible polymer[101]) microspheres containing VEGF (vascular endothelial growth factor) as an angiogenesis factor.[102] PLGA/VEGF microspheres were loaded onto PLLA-coated PGA scaffolds that were afterwards seeded with organoids and implanted in adult Lewis rats. VEGF-containing TESIs showed increased construct size and weight, which has been related to TESI VEGF delivery. A higher capillary network density in comparison with control samples was observed (shown in Figure 12.6(E)). Epithelial cell proliferation increased in response to higher amounts of nutrients and oxygen supply, as a result of increased vascularity. Apoptosis rates were similar to the control sample and it thus can be concluded that degradation of PLGA does not exert any harmful effects on the TESI function. A TE system mimicking the natural intestine was thus obtained.[102]

Considering the probability of microsphere degradation and also the inability to control the villus–crypt height, researchers have devised another method of VEGF application.[103] Instead of microspheres, VEGF overexpression was used in the Rocha system described above.[102,103] A triple transgenic *CMV*^{Cre}*-rtTA*$^{flox/flox}$ *-tet(o)-VEGF* mouse was selected as the donor of organoids and the host of TESI because of its ability to induce VEGF overexpression upon doxycycline treatment. A sustained VEGF expression was thus attained, unaffected by polymer degradation. Complete neovascularization was achieved and nutrient transport to the bulk scaffold resulted in mucosal layer growth. Increased crypt cell proliferation may also be attributed to sufficient nutrition. Complete differentiation of intestinal epithelial cells without inhibition took place in the TESI. A fully-developed mucous layer, in addition to different types of differentiated intestinal cells, was assumed to be associated with the presence of Flt-1 and Flk-1 (VEGF receptors) and their signaling in the epithelium layer. High villi and deep crypts were observed in the VEGF overexpression system at a higher density compared with the control system.[103]

It is crucial that, as mentioned before, elements required for stem cell niche maintenance should be included in the TESI. In addition to growth factors, other factors facilitate acceptable TESI generation. Matrigel is an important factor facilitating the formation of a more complex TESI structure resembling the naturally occurring crypt–villus structures. An increased mucosal surface area and cyst formation were obtained after using Matrigel on PLGA scaffolds. Improved differentiation of cells on Matrigel is regarded as an effect of cell–cell interactions on or in the Matrigel matrix, and, in consequence, differentiated cells similar to those naturally occurring in the organs are formed.[79] The complexity of the tissue-engineered structure of the intestine is thus explained. Longer, narrower, and densely spaced villi were observed when using Matrigel on PLGA scaffolds, as compared with PLGA suspended in Hanks' buffered saline solution (HBSS). However, cyst numbers decreased when Matrigel was used.[99]

Some growth factors are also required for preparing important signaling pathways to maintain the stem cell nature of cells in culture and for long-time maintenance, which seems necessary for the long-term usage of these cells. In small intestinal murine cultures, ENR (murine EGF, murine Nog, and human R-spondin-1) are essential for differentiation of stem cells to all types of intestinal cells.[56,63,65] Addition of Wnt3 to the culture medium results in the generation of cells that are mostly undifferentiated. Even though the specified chemical conditions favored mouse crypt formation, such was not the case for human intestinal culture and seven days was the maximum lifespan of human stem cells under these conditions. To improve the efficiency of the culture, gastrin (neoendocrine hormone secreted by G-cells in the stomach[104]) and nicotinamide (a form of vitamin B3 or niacin[105]) were added to the system. Gastrin does not play a major role in culture systems and does not intervene with differentiation but it was preferred to use gastrin in all human culture systems. In contrast, nicotinamide increased the lifespan of cells to one month. After one month, the organoids converted from bud-like structures to cystic structures and their proliferation decreased significantly. By adding a combination of A83-01 (Alk4/5/7 inhibitor) and SB202190 (p38 inhibitor), the viable culture period was increased to six months. Differentiated cells did not arise under these conditions. Wnt3, SB202190, and nicotinamide were considered as differentiation-inhibiting factors. Differentiation was achieved by eliminating these factors.[63] A single biopsy of a patient and culturing organoid units of the intestinal tract under the specified chemical conditions can lead to generation of a "transplantable epithelium" for treating intestinal organ malfunction.[63] All steps of human ISC culture are shown in Figure 12.7. A summary of all chemical factors required for TE is presented in Table 12.2.

12.4 Conclusions and Future Perspectives

Intestinal TE, as an alternative approach circumventing the limitations of other techniques like drug therapy, chemotherapy and surgical methods, will help patients to regain their health more easily. However, because of the complex intestine structure and functionality, detailed investigations of various components of TESI have to be undertaken. TESI components can be divided into two distinct categories: cells and the cellular growth environment. Although different types of cells have been used in TESI design, a cell source that meets all the requirements of intestinal structure and also affords all functionalities is the best choice. Stem cells comprise a promising cell source as they can convert into differentiated cells with the ability to perform an intended role in an organ. ISCs, residing at the bottom of intestinal crypts, appear to be the best option because they can proliferate into identical stem cells and can also differentiate into all cell lineages of the intestinal epithelium. The obstacle in their application is that ISCs do not survive under conventional cell culture conditions. Therefore, an environment has to be created that would simulate the niche that they occupy, similar

Table 12.2 Chemical factors used in intestinal stem cell tissue engineering.

Chemical element	Organoid source	Model	Effect of the growth factor	Reference
GLP-2[a]	Lewis rats	Lewis rats	Increased villus height and crypt depth; increased crypt cell proliferation; decreased apoptosis; increased nutrient absorption; expression of sucrase and absence of GLUT2 expression; location of GLP-2R in the subepithelial layer	98
	Lewis rats	Lewis rats	Elevated cyst numbers, increased villus height, increased crypt depth	99
HGF[b]	Lewis rats	Lewis rats	No distinguishable effect	99
Fgf10[c]	*Fgf10*^{LacZ}, littermate control mice[d] or *R26*^{rtTA}*; tet(O)Fgf10* mutant mice[e]	(NOD/SCID) gamma-chain-deficient mice	Increased villus height, increased crypt depth, increased cell proliferation; fully differentiated intestinal cells in normal population were obtained	100
VEGF[f]	Lewis rats	Lewis rats	Increased size and weight of TESI; increased vascularity and epithelial proliferation, no change in apoptosis	102
	Triple transgenic *CMV* ^{Cre} *rtTA*-$^{flox/flox}$ *-tet(O)-VEGF* mice[g]	Irradiated (350 cGy) (NOD/SCID) gamma-chain-deficient mice	Increased villus height and crypt depth, increased crypt cell proliferation, increased mucous thickness, complete cell differentiation	103
Matrigel	Lewis rats	Lewis rats	Greater surface area and cyst diameter, more complex neomucosal structure (longer, narrower, and packed villi)	99
EGF[h]	*Lgr5–EGFP–ires–CreERT2* mice,[i] *APC*$^{flox/flox}$ mice, *Axin2-lacZ* mice, C57B/6 wild-type mice	—	Intestinal proliferation	56,63,65
	Human	—		

Noggin	*Lgr5–EGFP–ires–CreERT2* mice, *APC*$^{flox/flox}$ mice, *Axin2-lacZ* mice, C57B/6 wild-type mice	—	Expansion of crypts	56,63,65
	Human	—		
R-spondin	*Lgr5–EGFP–ires–CreERT2* mice, *APC*$^{flox/flox}$ mice, *Axin2-lacZ* mice, C57B/6 wild-type mice	—	Crypt hyperplasia; Wnt activation	56,63,65
	Human	—		
Gastrin	Human	—	Improved culture efficiency	63
Nicotinamide	Human	—	Improved culture efficiency, prolongation of culturing period, differentiation inhibition	63
Wnt3	Human	—	Differentiation inhibition	63
A83-01[j]	Human	—	Synergic effect with SB202190 in prolonging the culture period	63
SB202190[k]	Human	—	Synergic effect with A83-01 in prolonging the culture period; differentiation inhibition	63

[a]Glucan-like peptide-2.
[b]Hepatocyte growth factor.
[c]Fibroblast growth factor.
[d]Fibroblast growth factor 10; transgene insertion 24, Margaret E. Buckingham.
[e]*R26*^{rtTA}: gene trap ROSA 26, Philippe Soriano; targeted mutation 1, Anton Wutz.
[f]Vascular endothelial growth factor.
[g]*CMV Cre*: transgene insertion 1, University of Cologne.
[h]Epidermal growth factor.
[i]Leucine-rich repeat containing G protein coupled receptor 5; targeted mutation 1, Hans Clevers (reproduced from *Cell*, 154(2), Clevers, H., The Intestinal Crypt, A Prototype Stem Cell Compartment, 274–284. Copyright (2013) with permission from Elsevier).
[j]3-(6-Methyl-2-pyridinyl)-*N*-phenyl-4-(4-quinolinyl)-1*H*-pyrazole-1-carbothioamide.
[k]4-[4-(4-Fluorophenyl)-5-(4-pyridinyl)-1*H*-imidazol-2-yl]phenol.

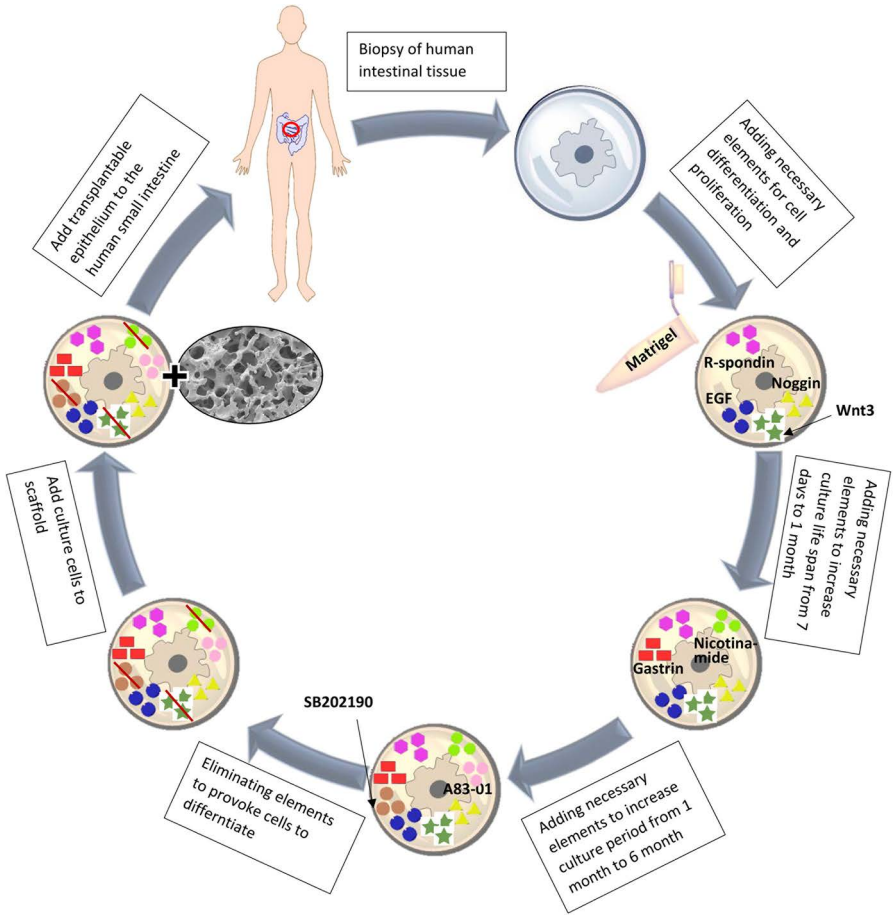

Figure 12.7 Different steps in a long-term culture of human ISCs and the future of making a transplantable epithelium to regenerate intestinal tissue.[63]

to biological microenvironments. Stem cells convert into crypt–villus-like structures termed organoids. Organoids, or mini guts, contain differentiated epithelium-forming cells as well as ISCs that can renew the entire organ. The key point here is that organoids should be provided with a proper surrounding environment to enable them to grow into a whole organ. Chemical and mechanical aspects of the environment should be fulfilled. The chemical environment encompasses all the chemical components, such as proteins, growth factors, *etc.*, that are necessary to aid organoid proliferation and differentiation into intestinal cells capable of carrying out all the necessary intestinal epithelial functions, including nutrition, absorption, lubrication, and barrier function. The mechanical environment encompasses supporting materials required for the organoids to act as an ECM for the cells. This chapter presented a comprehensive overview of every concept of ISC TE,

including organoids as the cell source; such chemical elements as GLP-2, FGF, and VEGF; and scaffolds, *e.g.*, PGA and collagen-coated PGA/PLLA.

Despite the great effort in ISC TE, there are still some sections of this topic that have not been evaluated or need further investigations. One of the first attempts of future work should be directed towards the culture condition of human ISCs. Since a working human intestine is the ultimate goal of TESI, further studies should focus on more effective culture conditions to maintain long-term human organoids in a more controlled manner and make the ISCs able to proliferate constantly and differentiate into epithelial cells. More operative factors should be investigated and added to the culture system that have positive effects on maintaining the normal niche of ISCs. The other area of future research should be assigned to involve polymer technologies in the manufacturing and chemical processes of scaffold preparation in order to provide scaffolds with the highest similarity to the human intestine. Subsequently, mimicking the intestinal structure and complete organ functionality can be expected from TESI. A similarity between the scaffold and intestine should be achieved in diverse aspects including shape and size (possessing the most similar shape to the finger-like structure of the small intestine), materials used, and surface and bulk properties. These strategies will facilitate the engineering of a regenerating intestine to replace the native intestine during disease.

Acknowledgements

Dr Wang thanks for the support from Crohn's & Colitis Foundation of America (CCFA) Career Award (No. 348137), Iowa State University (ISU) President's Initiative on Interdisciplinary Research (PIIR) program, and McGee-Wagner Interdisciplinary Research Award.

References

1. F. G. Rocha and E. E. Whang, *J. Surg. Res.*, 2004, **120**, 320–325.
2. H. Naderi, M. M. Matin and A. reza Bahrami, *J. Biomater. Appl.*, 2011, **26**, 383–417.
3. J. A. Fishman, M. A. Greenwald and P. A. Grossi, *Clin. Infect. Dis.*, 2012, **55**, 720–727.
4. E. Zakhem, S. Raghavan, R. R. Gilmont and K. N. Bitar, *Biomaterials*, 2012, **33**, 4810–4817.
5. C. A. Heath, *Trends Biotechnol.*, 2000, **18**, 17–19.
6. L. Lamboni, M. Gauthier, G. Yang and Q. Wang, *Biotechnol. Adv.*, 2015, **33**, 1855–1867.
7. F. Ding, H. Deng, Y. Du, X. Shi and Q. Wang, *Nanoscale*, 2014, **6**, 9477–9493.
8. F. Song, X. Li, Q. Wang, L. Liao and C. Zhang, *J. Biomed. Nanotechnol.*, 2015, **11**, 40–52.
9. M. Jafari, Z. Paknejad, M. Rezai Rad, S. R. Motamedian, M. J. Eghbal, N. Nadjmi and A. Khojasteh, *J. Biomed. Mater. Res., Part B*, 2015, **00B**, 1–29.

10. H. Peng, N. Poovaiah, M. Forrester, E. Cochran and Q. Wang, *ACS Biomater. Sci. Eng.*, 2015, **1**, 37–42.
11. F. G. Sala, J. A. Matthews, A. L. Speer, Y. Torashima, E. R. Barthel and T. C. Grikscheit, *Tissue Eng., Part A*, 2011, **17**, 1841–1850.
12. N. Barker, A. Van Oudenaarden and H. Clevers, *Cell Stem Cell*, 2012, **11**, 452–460.
13. P. Artursson, A.-L. Ungell and J.-E. Lofroth, *Pharm. Res.*, 1993, **10**, 1123–1129.
14. H. Clevers, *Cell*, 2013, **154**, 274–284.
15. T. Sato and H. Clevers, *Science*, 2013, **340**, 1190–1194.
16. A. W. Overeem, C. Posovszky, E. H. M. M. Rings, B. N. G. Giepmans and S. C. D. Van Ijzendoorn, *Dis. Models & Mech.*, 2016, **9**, 1–12.
17. V. Snoeck, B. Goddeeris and E. Cox, *Microbes Infect.*, 2005, **7**, 997–1004.
18. R. D. Specian and M. G. Oliver, *Am. J. Physiol.*, 1991, **260**, 83–93.
19. A. R. Gunawardene, B. M. Corfe and C. A. Staton, *Int. J. Exp. Pathol.*, 2011, **92**, 219–231.
20. C. L. Bevins and N. H. Salzman, *Nat. Rev. Microbiol.*, 2011, **9**, 356–368.
21. E. Zakhem, S. Raghavan, R. R. Gilmont and K. N. Bitar, *Biomaterials*, 2012, **33**, 4810–4817.
22. R. B. Michalčíková, K. Dryahina and P. Španěl, *Int. J. Mass Spectrom.*, 2016, **396**, 35–41.
23. H. Ali, B. Weigmann, E. Collnot, S. A. Khan, M. Windbergs and C. Lehr, *Pharm. Res.*, 2015, **33**, 1085–1092.
24. C. Lautenschläger, C. Schmidt, D. Fischer and A. Stallmach, *Adv. Drug Delivery Rev.*, 2014, **71**, 58–76.
25. C. Kriegel and M. Amiji, *J. Controlled Release*, 2011, **150**, 77–86.
26. U. Klotz and M. Schwab, *Adv. Drug Delivery Rev.*, 2005, **57**, 267–279.
27. E. Cetinkaya, A. B. Dogrul and M. B. Tirnaksiz, *World J. Gastrointest. Oncol.*, 2016, **8**, 113–120.
28. E. E. Yörüker, S. Holdenrieder and U. Gezer, *Clin. Chim. Acta*, 2016, **455**, 26–32.
29. H. Kocoglu, F. M. Velibeyoglu, M. Karaca and D. Tural, *World J. Gastrointest. Oncol.*, 2016, **8**, 1–7.
30. M. K. Chen and E. A. Beierle, *Biomaterials*, 2004, **25**, 1675–1681.
31. M. K. Chen and S. F. Badylak, *J. Surg. Res.*, 2001, **99**, 352–358.
32. M. Nakao, T. Ueno, A. Oga, Y. Kuramitsu, H. Nakatsu and M. Oka, *J. Pediatr. Surg.*, 2015, **50**, 573–580.
33. M. Lee, P. C. Y. Chang and J. C. Y. Dunn, *J. Surg. Res.*, 2008, **147**, 168–171.
34. Y. Hori, T. Nakamura, D. Kimura, K. Kaino, Y. Kurokawa, S. Satomi and Y. Shimizu, *J. Surg. Res.*, 2002, **102**, 156–160.
35. Y. Liu, T. Rager, J. Johnson, J. Enmark and G. E. Besner, *Tissue Eng., Part C*, 2015, **21**, 816–824.
36. Y. Sambuy, I. De Angelis, G. Ranaldi, M. L. Scarino, A. Stammati and F. Zucco, *Cell Biol. Toxicol.*, 2005, **21**, 1–26.
37. A. Esposito, A. Mezzogiorno, A. De Rosa, D. Menditti, V. Esposito and L. Ambrosio, *J. Mater. Sci.: Mater. Med.*, 2006, **17**, 1365–1372.

38. C. M. Walthers, M. Lee, B. M. Wu and J. C. Y. Dunn, *PLoS One*, 2014, **9**, 1–20.
39. Y. Nakase, A. Hagiwara, T. Nakamura, S. Kin, S. Nakashima, T. Yoshikawa, K.-I. Fukuda, Y. Kuriu, K. Miyagawa, C. Sakakura, E. Otsuji, Y. Shimizu, Y. Ikada and H. Yamagishi, *Tissue Eng.*, 2006, **12**, 403–412.
40. M. Raff, *Annu. Rev. Cell Dev. Biol.*, 2003, **19**, 1–22.
41. H. Rippon and A. Bishop, *Cell Proliferation*, 2004, **37**, 23–34.
42. L. Muller, R. Jones and A. Hunt, *Stem Cells*, 2007, **25**, 2739–2749.
43. R. Sancho, C. A. Cremona and A. Behrens, *EMBO Rep.*, 2015, **16**, 571–581.
44. S. J. Leedham, M. Brittan, S. A. C. Mcdonald and N. A. Wright, *J. Cell. Mol. Med.*, 2005, **9**, 11–24.
45. S. Asfaha, *Curr. Opin. Pharmacol.*, 2015, **25**, 62–66.
46. N. Barker, J. H. Van Es, J. Kuipers, P. Kujala, M. Van Den Born, M. Cozijnsen, A. Haegebarth, J. Korving, H. Begthel, P. J. Peters and H. Clevers, *Nature*, 2007, **449**, 1003–1008.
47. E. Sangiorgi and M. R. Capecchi, *Nat. Genet.*, 2008, **40**, 915–920.
48. N. Takeda, R. Jain, M. R. Leboeuf, Q. Wang, M. Lu and J. A. Epstein, *Science*, 2011, **334**, 1420–1424.
49. R. K. Montgomery, D. L. Carlone, C. A. Richmond, L. Farilla, L. K. Fogli, S. Algra and D. T. Breault, *Proc. Natl. Acad. Sci.*, 2010, **108**, 179–184.
50. A. E. Powell, Y. Wang, Y. Li, E. J. Poulin, A. L. Means, M. K. Washington, J. N. Higginbotham, A. Juchheim, N. Prasad, S. E. Levy, Y. Guo, Y. Shyr, B. J. Aronow, K. M. Haigis, J. L. Franklin and R. J. Coffey, *Cell*, 2012, **149**, 146–158.
51. M. Leushacke and N. Barker, *Gut*, 2014, **63**, 1345–1354.
52. A. U. Dignass and A. Sturm, *Eur. J. Gastroenterol. Hepatol.*, 2001, **13**, 763–770.
53. G. S. Evans, N. Flint, A. S. Somers, B. Eyden and C. S. Potten, *J. Cell Sci.*, 1992, **101**, 219–231.
54. R. H. Whitehead, K. Demmler, S. P. Rockman and N. K. Watson, *Gastroenterology*, 1999, **117**, 858–865.
55. H. Fukamachi, *J. Cell Sci.*, 2016, **103**, 511–519.
56. T. Sato, R. G. Vries, H. J. Snippert, M. Van De Wetering, N. Barker, D. E. Stange, J. H. Van Es, A. Abo, P. Kujala, P. J. Peters and H. Clevers, *Nature*, 2009, **459**, 262–266.
57. E. Batlle, J. T. Henderson, H. Beghtel, M. M. W. Van Den Born, E. Sancho, G. Huls, J. Meeldijk, J. Robertson, M. Van De Wetering, T. Pawson and H. Clevers, *Cell*, 2002, **111**, 251–263.
58. E. M. Garabedian, L. J. J. Roberts, M. S. Mcnevin and J. I. Gordon, *J. Biol. Chem.*, 1997, **272**, 23729–23740.
59. T. Sato, J. H. Van Es, H. J. Snippert, D. E. Stange, R. G. Vries, M. Van Den Born, N. Barker, N. F. Shroyer, M. Van De Wetering and H. Clevers, *Nature*, 2010, **469**, 415–418.
60. B. Koo, M. Spit, I. Jordens, T. Y. Low, D. E. Stange, M. Van De Wetering, J. H. Van Es, S. Mohammed, A. J. R. Heck, M. M. Maurice and H. Clevers, *Nature*, 2012, **488**, 665–669.

61. V. W. Y. Wong, D. E. Stange, M. E. Page, S. Buczacki, A. Wabik, S. Itami, M. Van De Wetering, R. Poulsom, N. A. Wright, M. W. B. Trotter, F. M. Watt, D. J. Winton, H. Clevers and K. B. Jensen, *Nat. Cell Biol.*, 2012, **14**, 401–408.
62. P. Jung, T. Sato, A. Merlos-suárez, F. M. Barriga, M. Iglesias, D. Rossell, H. Auer, M. Gallardo, M. A. Blasco, E. Sancho, H. Clevers and E. Batlle, *Nat. Med.*, 2011, 1225–1227.
63. T. Sato, D. E. Stange, M. Ferrante, R. G. J. Vries, J. H. VAN Es, S. Van den brink, W. J. Van houdt, A. Pronk, J. Van gorp, P. D. Siersema and V. Clevers, *Gastroenterology*, 2011, **141**, 1762–1772.
64. N. Barker, *Nat. Rev. Mol. Cell Biol.*, 2013, **15**, 19–33.
65. S. Yui, T. Nakamura, T. Sato, Y. Nemoto, T. Mizutani, X. Zheng, S. Ichinose, T. Nagaishi, R. Okamoto, K. Tsuchiya, H. Clevers and M. Watanabe, *Nat. Med.*, 2012, 1–7.
66. J. P. Vacanti, M. A. Morse, W. M. Saltzman, A. J. Domb, A. Perez-atayde and R. Langer, *J. Pediatr. Surg.*, 1988, **23**, 3–9.
67. R. S. Choi and J. P. Vacanti, *Transplant. Proc.*, 1997, **29**, 848–851.
68. P. A. Gunatillake and R. Adhikari, *Eur. Cells Mater.*, 2003, **5**, 1–16.
69. D. W. Hutmacher, *Biomaterials*, 2000, **21**, 2529–2543.
70. R. S. Choi, M. Riegler, C. Pothoulakis, B. S. Kim, D. Mooney and M. Vacanti, *J. Pediafr. Surg.*, 1998, **33**, 991–997.
71. R. Parenteau-bareil, R. Gauvin and F. Berthod, *Materials*, 2010, **3**, 1863–1887.
72. H. Peng, X. Liu, R. Wang, F. Jia, L. Dong and Q. Wang, *J. Mater. Chem. B*, 2014, **2**, 6435–6461.
73. A. Perez, T. C. Grikscheit, R. S. Blumberg, S. W. Ashley, J. P. Vacanti and E. E. Whang, *Transplantation*, 2002, **74**, 619–623.
74. A. Tavakkolizadeh, U. V. Berger, A. E. Stephen, B. S. Kim, D. Mooney, M. A. Hediger, S. W. Ashley, J. O. P. Vacanti and E. E. Whang, *Transplantation*, 2003, **75**, 181–185.
75. T. C. Grikscheit, A. Sliddique, E. R. Ochoa, A. Srinivasan, E. Alsberg, R. A. Hodin and J. P. Vacanti, *Ann. Surg.*, 2004, **240**, 748–754.
76. S. S. Kim, R. Penkala and P. Abrahimi, *J. Surg. Res.*, 2007, **142**, 327–331.
77. D. E. Levin, E. R. Barthel, A. L. Speer, F. G. Sala, X. Hou, Y. Torashima and T. C. Grikscheit, *J. Pediatr. Surg.*, 2013, **48**, 129–137.
78. C. N. Grant, S. G. Mojica, F. G. Sala, J. R. Hill, D. E. Levin, A. L. Speer, E. R. Barthel, H. Shimada, N. C. Zachos, T. C. Grikscheit and G. Cn, *Am. J. Physiol.: Gastrointest. Liver Physiol.*, 2015, **308**, 664–677.
79. H. K. Kleinman and G. R. Martin, *Semin. Cancer Biol.*, 2005, **15**, 378–386.
80. C. S. Hughes, L. M. Postovit and G. A. Lajoie, *Proteomics*, 2010, **10**, 1886–1890.
81. Z. Jabaji, C. M. Sears, G. J. Brinkley, N. Y. Lei, V. S. Joshi, J. Wang, M. Lewis, M. Stelzner, G. M. Martin and J. C. Y. Dunn, *Tissue Eng., Part C*, 2013, **19**, 961–969.
82. S. James, *JPEN, J. Parenter. Enteral Nutr.*, 1999, **23**, 309–313.
83. X. Zhou, Y. Li, N. Li and J. Li, *J. Surg. Res.*, 2001, **99**, 47–52.

84. Y. Gu, Z. H. Wu, J. X. Xie, D. Y. Jin and H. C. Zhuo, *Clin. Nutr.*, 2001, **20**, 159–166.
85. A. L. Thesis, S. Fruchtman and P. K. Lund, *Inflammatory Bowel Dis.*, 2004, **10**, 871–880.
86. A. Tavakkolizadeh and E. E. Whang, *JPEN, J. Parenter. Enteral Nutr.*, 2002, **26**, 251–257.
87. P. M. Pereira and J. E. Bines, *J. Gastroenterol. Hepatol.*, 2006, **21**, 932–940.
88. K. Ohneda, M. H. Ulshen, C. R. Fuller, A. J. D. Ercole and P. K. A. Y. Lund, *Gastroenterology*, 1997, **112**, 444–454.
89. C. S. Potten, G. Owen, D. Hewitt, C. A. Chadwick, H. Hendry, B. I. Lord and L. B. Woolford, *Gut*, 1995, **36**, 864–873.
90. C. Tsai, M. Hill, S. L. Asa, P. L. Brubaker and D. Druckeri, *Am. J. Physiol.*, 1997, **273**, 77–84.
91. B. Yusta, L. Huang, D. Munroe, G. Wolff, R. Fantaske, S. Sharma, L. Demchyshyn, S. L. Asa and D. J. Drucker, *Gastroenterology*, 2000, **119**, 744–755.
92. D. J. Drucker, P. Ehrlich, S. L. Asat and P. L. Brubaker, *Proc. Natl. Acad. Sci. U. S. A.*, 1996, **93**, 7911–7916.
93. M. A. Helmrath, C. R. Erwin, D. Ph and B. W. Warner, *J. Surg. Res.*, 1997, **80**, 76–80.
94. M. A. Helmrath, C. E. Shin, J. W. Fox, C. R. Erwin and W. Warner, *Surgery*, 1998, **124**, 848–854.
95. C. Booth, G. S. Evans and C. S. Potten, *In Vitro Cell. Dev. Biol.*, 1995, **31**, 234–243.
96. C. J. Xian, R. Couper, G. S. Howarth, L. C. Read and N. C. Kallincos, *Br. J. Cancer*, 2000, **82**, 945–952.
97. G. Gross Belchior, M. Cleide Sogayar and T. Cannon Grischeit, *Semin. Pediatr. Surg.*, 2014, **23**, 141–149.
98. A. Ramsanahie, M. S. Duxbury, T. C. Grikscheit, A. Perez, D. B. Rhoads, J. Gardner-thorpe, J. Ogilvie, S. W. Ashley, J. P. Vacanti, E. E. Whang, M. S. Duxbury, C. Tracy, A. Perez, D. B. Rhoads, J. Ogilvie, S. W. Ashley, J. P. Vacanti and E. E. Whang, *Am. J. Physiol.: Gastrointest. Liver Physiol.*, 2003, **285**, 1345–1352.
99. B. Wulkersdorfer, K. K. Kao, V. G. Agopian, J. C. Dunn, B. M. Wu and M. Stelzner, *J. Surg. Res.*, 2011, **169**, 169–178.
100. Y. Torashima, D. E. Levin, E. R. Barthel, A. L. Speer, F. G. Sala, X. Hou and T. C. Grikscheit, *J. Tissue Eng. Regener. Med.*, 2016, **10**, 132–139.
101. Q. Wang, L. Wang, M. S. Detamore and C. Berkland, *Adv. Mater.*, 2008, **20**, 236–239.
102. F. G. Rocha, C. A. Sundback, N. J. Krebs, J. K. Leach, D. J. Mooney, S. W. Ashley, J. P. Vacanti and E. E. Whang, *Biomaterials*, 2008, **29**, 2884–2890.
103. J. Mattew, F. Sala, A. Speer and E. Al, *Regener. Med.*, 2011, **6**, 559–567.
104. Z. Liu, Y. Luo, Y. Cheng, D. Zou, A. Zeng, C. Yang and J. Xu, *Exp. Biol. Med.*, 2016, **241**, 873–881.
105. J. M. Denu, *Trends Biochem. Sci.*, 2005, **30**, 479–483.
106. A. J. Carulli, L. C. Samuelson and S. Schnell, *Integr. Biol.*, 2014, **6**, 243–257.

CHAPTER 13

Smart Materials and Systems as Artificial Pancreas for Diabetes Treatment

YUQI ZHANG*[a,b], MENGZHE WANG[a], JICHENG YU[a,b] AND ZHEN GU*[a,b,c]

[a]Pharmacoengineering Division, Joint Department of Biomedical Engineering, University of North Carolina at Chapel Hill and North Carolina State University, Raleigh, NC 27695, USA; [b]Center of Nanomedicine and Molecular Pharmaceutics Division, Eshelman School of Pharmacy University of North Carolina at Chapel Hill, Chapel Hill, NC 27599, USA; [c]Department of Medicine, University of North Carolina School of Medicine, Chapel Hill, NC 27599, USA
*E-mail: yuqi@email.unc.edu, zgu@email.unc.edu

13.1 Introduction

Diabetes mellitus (DM) is a metabolic disorder disease caused by a defect in insulin secretion (type 1 diabetes),[1–3] insulin action (type 2 diabetes)[4–6] or both. According to the International Diabetes Federation, diabetes affected over 415 million people in 2015, which is almost 9.1% of the population worldwide and the figure is expected to rise to 645 million people by 2040.[7]

Currently, insulin pumps clinically help to regulate the blood glucose levels (BGLs) of type 1 and advanced type 2 diabetic patients, functionalizing as an alternative pancreas.[8,9] When incorporated with a real-time glucose monitor,

Smart Materials No. 25
Smart Materials for Tissue Engineering: Applications
Edited by Qun Wang

Published by the Royal Society of Chemistry, www.rsc.org

the pump can realize closed-loop insulin delivery with an appropriate algorithm, which can deliver precise doses of rapid-acting insulin to closely match patients' needs.[10] Nevertheless, current glucose sensors, which are limited in reliability and accuracy, do not meet the requirements for commercial acceptability.[11] Moreover, a high risk of infusion set failure due to patients' education on infusion site care and pump operation ensures that this electronic device still strives towards a closed-loop performance.[12,13] Over the last decades, chemically synthesized smart systems as an artificial pancreas have been explored for achieving closed-loop insulin delivery.[14–16] Generally, glucose-responsive materials are integrated into these systems to provide BGL-dependent delivery of insulin.[14,17] Then the systems can sense an increase in BGL and respond accordingly with the release of a certain amount of insulin for closed-loop therapy, which can mimic the nature dynamics of glycemic control. Besides a synthetic-material based therapy, the transplant of a pancreatic β-cell offers another approach to treat diabetes. By transplanting exogenous normal β-cells to diabetes patients, insulin can then be secreted by implanted β-cells to retain the normal BGLs in the body.[18] Thus these external β-cells may serve as an artificial pancreas. In this chapter, synthetic materials for closed-loop insulin delivery and pancreatic β-cell-based therapy will be surveyed.

13.2 Smart Synthetic Systems as an Artificial Pancreas

Artificial pancreas-like synthetic closed-loop insulin delivery systems that can simulate normal pancreatic function, and continuously and intelligently release insulin in response to changing blood glucose levels (BGLs) have gained increasing attention in recent years. These systems may utilize polymeric hydrogels, nanoparticle formulations and swelling or degradable membrane-sealed reservoirs to release the insulin with the help of certain glucose-sensing factors.[19,20] Currently, most of the smart synthetic systems are based on glucose-responsive biomaterials with glucose-sensing moieties, including glucose oxidase (GOx), phenylboronic acids (PBA), or glucose binding proteins (GBP). Chemically modified insulin also serves as an alternative approach for controlled insulin delivery. The main mechanisms of diverse systems and the most recent studies will be discussed in this section.

13.2.1 GOx-Mediated Systems

GOx-based insulin delivery is one of the classic glucose-responsive systems. The first development of a glucose-responsive material was a GOx-associated pH-sensitive hydrogel.[21,22] GOx is a glucose specific enzyme that will oxidize glucose to gluconic acid:[23]

$$\text{Glucose} + O_2 + H_2O \xrightarrow{\text{GOx}} \text{gluconic acid} + H_2O_2$$

During this process, a low pH value, hypoxic environment and H_2O_2 will be generated, which can all serve as the trigger of insulin release. Since the over-production of H_2O_2 can lead to local cytotoxicity and also inhibit the activity of GOx, catalase (CAT), an enzyme that can scavenge H_2O_2 to water and O_2, is usually introduced into the systems. The following section will introduce GOx-integrated glucose-responsive systems based on different stimuli.

13.2.1.1 pH-Responsive Materials

GOx-mediated pH-sensitive matrices are widely applied in insulin delivery, which usually release insulin *via* volume change or hydrolysis in response to a pH decrease.[24,25] Specifically, protonation-induced swelling or shrinking of systems can propel insulin release; or acidity-caused degradation can disintegrate the carrier and subsequently release a drug. Wu and coworkers designed a glucose-responsive plug to control insulin release from a reservoir, which was made of surface-modified silicone.[26] The plug consisted of crosslinked bovine serum albumin, enzymes (GOx and CAT), MnO_2 nanoparticles, and the embedded pH-responsive hydrogel nanoparticles (NPs). GOx was used to induce a pH stimulus. Meanwhile, CAT was able to quench undesired H_2O_2 and enhance the GOx half-life. MnO_2 NPs can not only stabilize the enzymes by fully converting H_2O_2 to O_2, but also reinforce the mechanical strength of the plug. Under a high BGL, the decrease in pH generated through the oxidation of glucose caused the hydrogel NPs to shrink, resulting in an interconnected porous structure to allow insulin permeation across the membrane. They demonstrated the reversibility of this glucose-mediated insulin release *in vitro*. Furthermore, through intraperitoneal implantation of the insulin device, the BGLs of diabetic rats can be regulated well *in vivo*.

Gu *et al.* have reported several acidity-responsive drug carriers for closed-loop insulin delivery.[27–29] They fabricated a chitosan-based sponge-like matrix for insulin reservation, which showed a five-fold volume increase in response to glucose (Figure 13.1). Chitosan is a natural polysaccharide that can be degraded by lysozymes and glycosidases, which are ubiquitous in the body.[30] Tripolyphosphate (TPP) crosslinked chitosan entrapped insulin and enzyme nanocapsules inside and formed sponge-like microgels. When a high glucose level was sensed, the encapsulated glucose-specific enzyme (GOx) catalyzed glucose into gluconic acid, leading to the protonation of amine groups on the polymer chains. Thus the microgels continuously swelled as a result of the increasing charge in the matrix, which in turn triggered the release of insulin. Additionally, this system was reversible under normoglycemic conditions, which means the microgels could shrink and cease insulin release until the next high glucose challenge.

They also explored dextran as an acidity-sensitive material for glucose responsiveness.[28] In this system, dextran was modified with an acetal group for acid sensitivity, which can be hydrolyzed into water-soluble dextran, ethanol and acetone in the presence of gluconic acid. A double emulsion method

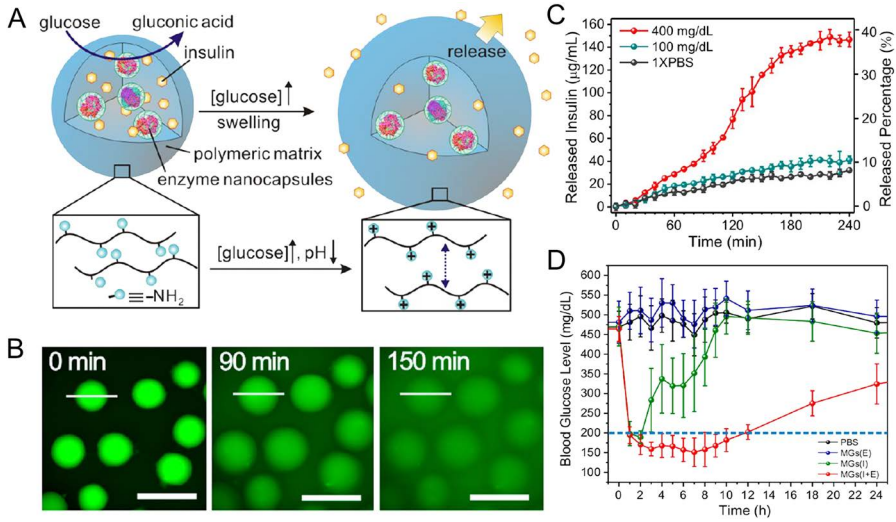

Figure 13.1 Chitosan-based microgels for glucose-responsive insulin delivery. (A) Schematic of insulin and enzyme nanocapsule-encapsulated microgel showing swelling response to glucose. (B) Fluorescence images of FITC-stained insulin released from microgels incubated in 400 mg dL^{-1} glucose PBS solution at 37 °C. (C) *In vitro* release profiles of insulin from the microgels incubated with different glucose concentrations (0, 100 and 400 mg dL^{-1}). (D) The change of BGLs in diabetic mice after subcutaneous injection of PBS solution, microgels loaded with insulin and enzymes (MGs(E + I)), microgels loaded with insulin only (MGs(I)), microgels loaded with enzymes only (MGs(E)). Reproduced with permission from ref. 27. Copyright 2013 American Chemical Society.

was utilized to fabricate acetal-modified dextran (*m*-dextran) NPs encapsulating insulin and GOx as well as CAT (Figure 13.2). Under hyperglycemic conditions, the catalytically-generated gluconic acid degraded *m*-dextran, and subsequently contributed to the collapse of the NPs and the release of insulin. To further enhance the stability of the NPs and make them injectable, the 3D-structured nano-network was formed *via* mixing oppositely charged *m*-dextran NPs coated with chitosan and alginate respectively. The resulting nano-network had a cohesive and porous structure with microchannels. These microchannels allowed the diffusion of glucose and insulin throughout the network, thus providing a center for a high-efficiency catalytic reaction. The results demonstrated fast glucose responsiveness and insulin release at a hyperglycemic level, while the network was quite stable under normoglycemic conditions. One single injection of the nano-network could help type 1 diabetic mice maintain normal BGLs for up to 10 days.

Recently, Gu's group established a glucose-responsive polymersome by packing insulin, GOx and CAT inside.[29] The polymersome was self-assembled by the amphiphilic polymer PEG-poly(Ser-Ketal), which was pH sensitive as

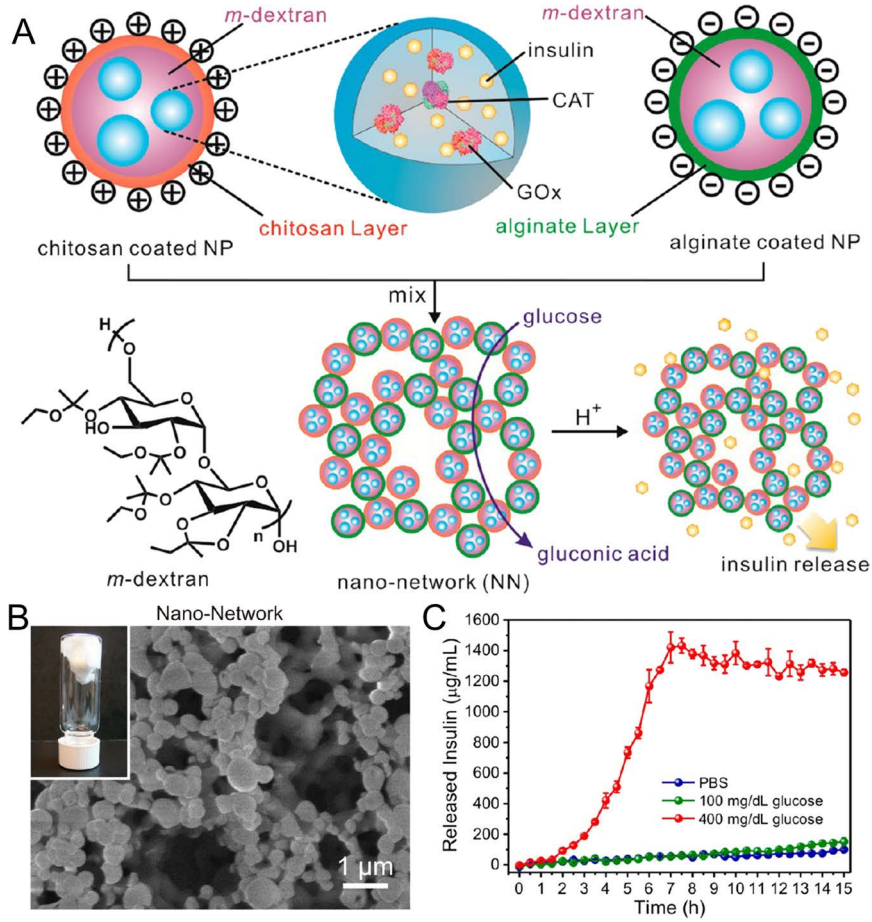

Figure 13.2 Injectable glucose-responsive nano-network for insulin delivery. (A) Schematic of the formation and the glucose-sensitive mechanism of the nano-network. (B) A SEM image of the nano-network. Inset: a photograph of the gel-like nano-network. (C) *In vitro* insulin release profile of the nano-network in PBS solution with different glucose concentrations at 37 °C. Reproduced with permission from ref. 28. Copyright 2013 American Chemical Society.

it was supposed to be hydrolyzed into water-soluble PEG-polyserine and acetone/ethanol under an acidic environment (Figure 13.3). When glucose crossed the bilayer membrane of the nanocapsule, GOx converted it into gluconic acid and acidified the aqueous core of the polymersome nanocapsule, leading to hydrolysis of the polymeric bilayer shell and subsequent dissociation of the nanocapsule, resulting in a glucose-responsive insulin release. A thermoresponsive and biodegradable polymer, Pluronic-127 (PF127), was mixed with the polymersome to form a suspension. Once subcutaneously injected, the suspension quickly formed a stable hydrogel, in which

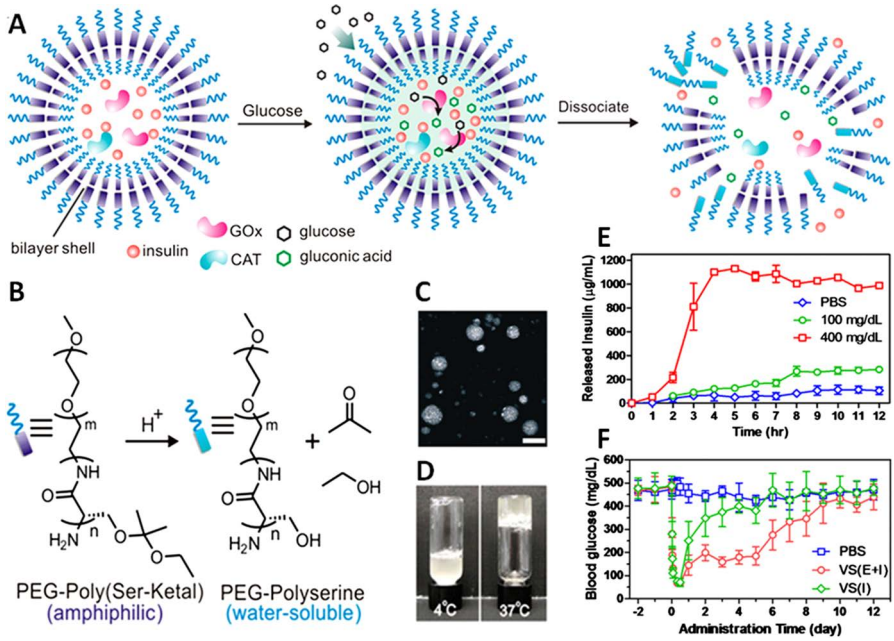

Figure 13.3 GOx-encapsulated polymersome for closed-loop insulin delivery. (A) GOx converts glucose into gluconic acid and acidifies the aqueous core of the polymersome nanovesicle, leading to hydrolysis of the polymeric bilayer shell and subsequent dissociation of vesicles. (B) The chemical structure of the pH-sensitive diblock copolymer PEG-poly(Ser-Ketal), which can be hydrolyzed into water-soluble PEG-polyserine and acetone/ethanol in an acidic environment. (C) TEM image of polymersome. Scale bar: 500 nm. (D) The polymersome was mixed with PF127 to form a thermoresponsive suspension. (E) *In vitro* accumulated insulin release from the vesicles incubated in the solutions with different glucose concentrations. (F) The BGLs of STZ-induced diabetic mice after treatment with PBS solution, polymersome encapsulating both enzyme and insulin (VS(E + I)) and polymersome encapsulating insulin only (VS(I)). Adapted with permission from ref. 29. Copyright 2014 American Chemical Society.

nanocapsules were evenly dispersed, and was able to stabilize the BGLs in the normoglycemic state (<200 mg dL^{-1}) for up to five days.

13.2.1.2 H_2O_2-Responsive Materials

Several polymers, such as poly(acrylic acid) (PAA), poly(vinylpyrrolidone) (PVP), poly(methacrylic acid) (PMA),and poly(ethylene oxide) (PEO) can be degraded by H_2O_2.[31] Uchiyama and Kiritoshi *et al.* used poly-2-methacryloyloxyethyl phosphorylcholine (PMPC) to form a matrix that could readily be degraded in H_2O_2 aqueous solution.[32] The degradation contributed to the main chain scission (elimination of the acyl group and the methyl group) of PMPC by

hydroxy and/or hydroperoxy radicals (HO$^{\bullet}$ and HOO$^{\bullet}$) that were produced by H_2O_2. The release rate of the drug model was dependent on the H_2O_2 concentration. They also applied this material to an implantable artificial pancreas device, in which PMPC functioned as a glucose-responsive insulin diffusion membrane.[33] In these systems, PMPC not only plays a role in responsiveness, but also offers enhanced biocompatibility by consuming H_2O_2.[34]

13.2.1.3 Hypoxia-Responsive Materials

Although GOx-based pH-sensitive materials allow closed-loop insulin delivery dependent on BGLs, the slow responsiveness has limited their application.[35] Besides enzymatically-induced pH change, Gu's group took advantage of the local hypoxic environment generated by GOx to trigger insulin release in response to hyperglycemia.[36] A hypoxia-sensitive moiety, 2-nitroimidazole, was introduced to hyaluronic acid (HA) for hypoxia-responsive transduction. HA is a hydrophilic polysaccharide, which is chosen due to its high biodegradability and biocompatibility; while the conjugated side chain, 2-nitroimidazole, is a hydrophobic component. Thus, this hypoxia-sensitive HA (HS-HA) could readily encapsulate insulin and GOx to form glucose-responsive nanoscale vesicles (GRVs) (Figure 13.4(A)). Once subjected to elevated BGLs, the oxygen could be quickly consumed during the glucose oxidation reaction catalyzed by GOx, which leads to local hypoxia. Under this condition, the hydrophobic nitroimidazole groups were bio-reduced into the hydrophilic aminoimidazole groups, further causing the disassembly of GRVs and subsequent release of the cargo. To achieve a convenient administration, the GRVs were deposited into a microneedle-array patch for continuous and painless insulin delivery. The GRVs in microneedles would maintain their stability under normoglycemic conditions, while they would quickly disassemble to release encapsulated insulin once exposed to high glucose levels in the blood and lymph vascular networks. This "smart insulin patch" using hypoxic signals as a novel trigger exhibited good responsiveness (Figure 13.4(D)) for glucose control, and presented a reversible control of insulin release between the normoglycemic and hyperglycemic states (Figure 13.4(E)). *In vivo* results implied that with one single patch, the BGLs of type 1 diabetes mice could stay around 200 mg dL^{-1} for 4 h (Figure 13.4(F)) without causing any risk of hypoglycemia (Figure 13.4(G)) even with one more administration of a MN patch. This smart insulin patch provides a promising platform to realize a fast glucose-responsive, pain-free, and safe insulin delivery.

13.2.2 Phenylboronic Acid (PBA)-Modified Systems

PBA was found to have a reversible binding reaction with sugar in 1959 by Lorand and Edwards.[37] PBA has two forms—neutral and anionic—dissociating in equilibrium (pK_a = 9) in the aqueous environment.[38] Only the charged formulation can bind to diols reversibly by the formation of a five- or six-membered ring structure (Figure 13.5). Based on this mechanism,

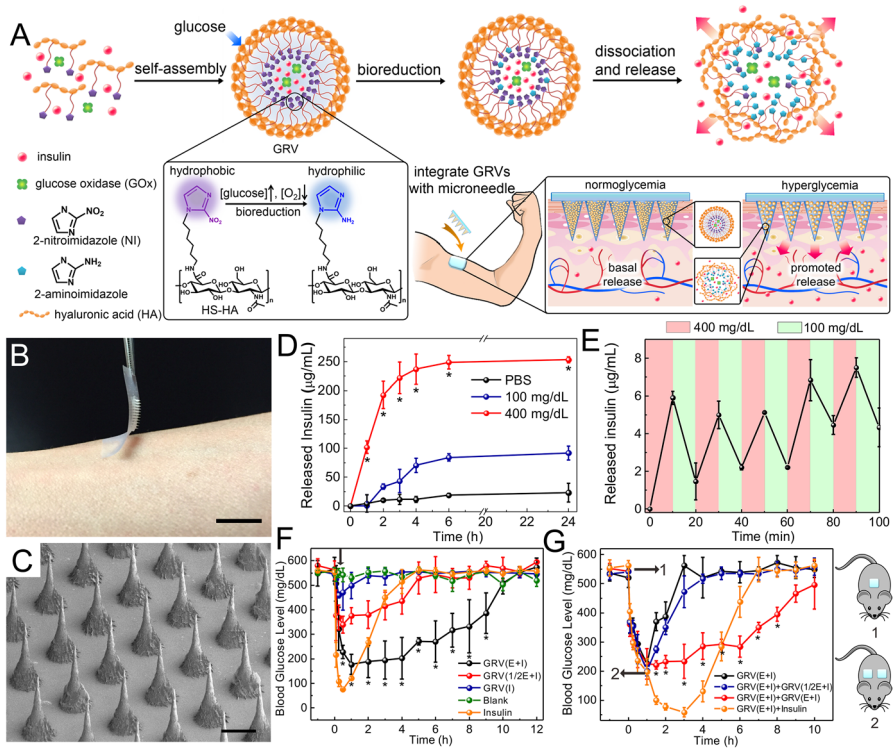

Figure 13.4 Hypoxia-sensitive vesicle-loading microneedle array patches for glucose-responsive insulin delivery. (A) Schematic of the formation and glucose-responsive mechanism of GRV and schematic of the GRV-loading MN-array patch for *in vivo* insulin delivery. (B) A photograph of the insulin MN patch (scale bar: 1 cm.) (C) A SEM image of the MN-array patch (scale bar: 200 μm.) (D) *In vitro* insulin release from the GRVs in PBS solution with different glucose concentrations at 37 °C. (E) Pulsatile release profile of GRVs by changing the glucose concentration between 100 and 400 mg dL^{-1}. (F) BGL changes in STZ-induced diabetic mice post-administration of blank MNs, MNs loaded with only insulin, MNs loaded with GRV(E + I), MNs loaded with GRV(1/2E + I), and MNs loaded with GRV(I). (G) BGL changes in mice with an additional MN-array patch 1 h after treatment of GRV(E + I)-loaded MNs. Adapted with permission from ref. 36. Copyright 2015 National Academy of Sciences.

PBA and its derivatives were extensively utilized in the detection, analysis, and purification of polyol compounds in organisms. In 1994, Kataoka *et al.* first reported a PBA-based glucose-sensitive delivery of insulin.[39] Since then, diverse PBA-modified materials have been explored for insulin delivery.[40–42] To enhance the sensibility of PBA in a physiological environment (pH ≈ 7.4), many derivatives with a lower pK_a, such as DDOPBA[43] and AmECFPBA,[44] were explored.

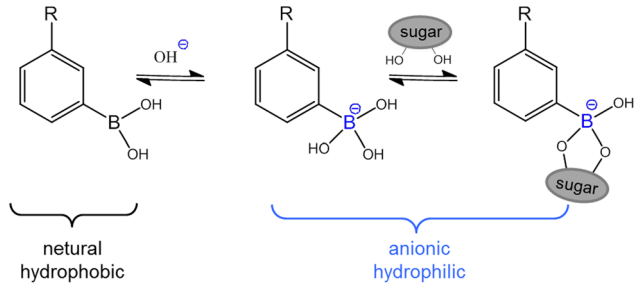

Figure 13.5 Equilibrium between different forms of phenylboronic acid (PBA) in an aqueous system.

13.2.2.1 Responsive Materials Based on Charge Change

Many systems incorporate PBA in hydrogels to initiate swelling by charge-change-induced electrostatic repulsion. Matsumoto *et al.* conjugated AmECFPBA to a thermo-sensitive PNIPMAAm polymer and achieved a glucose-responsive hydrogel (Figure 13.6).[44] They applied the localized dehydration of the surface to inhibit the diffusion of insulin. This dehydration can be efficiently controlled by the glucose levels between normo- and hyperglycemia. Specifically, the equilibrium of AmECFPBA between the anionically charged and uncharged structures shifted based on the glucose concentrations, which would lead to the volume change of the gel as was driven by counterions' osmotic pressure. Then the resulting abrupt and rapid change in the hydration further led to surface dehydration as a "skin layer", which could instantly control the insulin release rate corresponding to glucose concentrations from 100 mg dL^{-1} to 200 mg dL^{-1} (Figure 13.6(C)).

De Smedt *et al.* used a layer-by-layer (LbL) technique to prepare glucose-sensitive hollow multilayer capsules from a phenylboronic-acid-containing polyelectrolyte.[45] The polyanion PSS (polystyrene sulfonate) and polycation PAD (poly-AAPBA-*co*-DMAEA) were electrostatically adhered to form a PSS/PAD polyelectrolyte multilayer, which was stable without glucose. However, when exposed to a certain concentration of glucose, the AAPBA component in the PAD reversed from the uncharged form to a negatively charged form and attracted the positively charged DMAEA, then led to the decomplexation of the system as well as insulin release (Figure 13.7). Zhang's group further explored more sensitive systems based on the same mechanism.[46] In this case, they fabricated the LbL films from poly[acrylamide-*co*-(acrylamido)phenylboronic acid] [P(AAm-AAPBA)] and poly(vinylalcohol) (PVA) based on the formation of a covalent phenylboronate ester. The obtained PVA/P(AAm-AAPBA) films could gradually dissolve in the glucose solution due to the reversible phenylboronate ester bonding. The enhanced glucose-responsiveness of this system at physiological

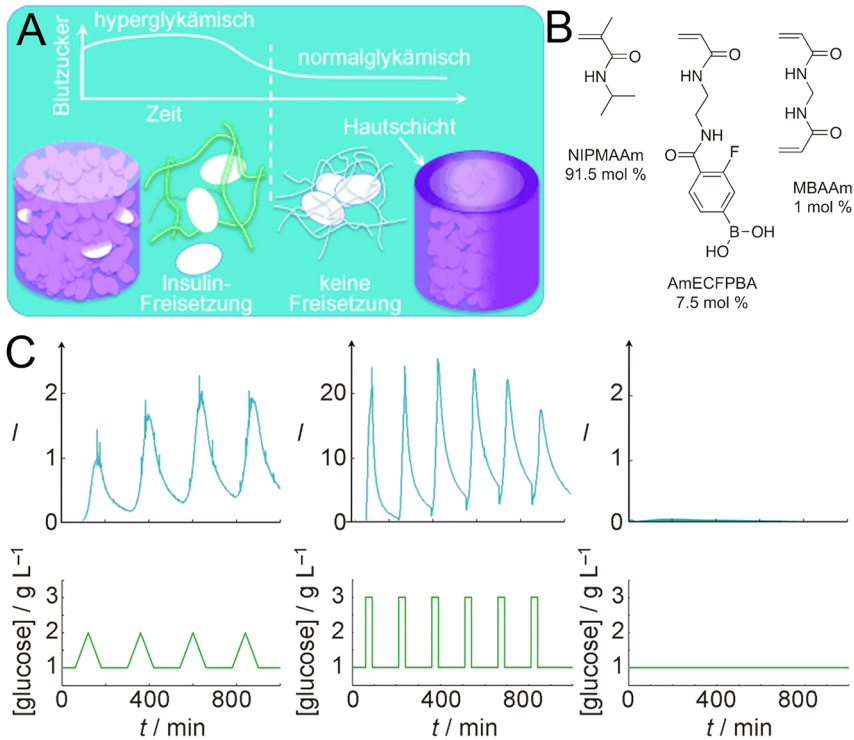

Figure 13.6 A hydrogel containing phenylboronate for glucose-responsive control of insulin diffusion. (A) Schematic of glucose-responsive mechanism. (B) Structures of the monomers and their optimized molar amounts for preparation of a glucose-responsive gel. (C) (Top) Fluorescence intensity of FITC-tagged insulin released from the glucose-responsive gel under physiological conditions over time. (Bottom) The fluctuation of glucose concentration in a corresponding experiment. Adapted with permission from ref. 44. Copyright 2012 Wiley-VCH.

conditions may be attributed to the adjacent amide group, which further stabilized the phenylboronate ester.

The hydrophilic reversion of PBA was also applied as a trigger of system dissociation.[47,48] Kim and coworkers synthesized an amphiphilic copolymer composed of a boroxole-containing styrenic monomer and poly(ethylene glycol) (PEG) *via* a reversible addition–fragmentation chain transfer method.[49] The amphiphilic copolymer poly(ethylene glycol)-*b*-poly(styreneboroxole) (PEG_{45}-*b*-PBOx) could form a monosaccharide-responsive polymersome with a PEG hydrophilic shell and a PBO hydrophobic core by self-assembling. When exposed to a monosaccharide solution, the PBO block could bind to glucose and form the charged phenylboronate, which converted this hydrophobic PBO block into a hydrophilic one. Then, the encapsulated insulin was released as a result of the disassembled system.

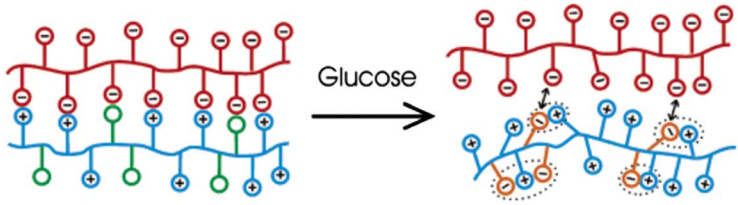

Figure 13.7 Glucose-sensitive mechanism of the polyelectrolyte bilayer. The blue and red circles represent the amino groups and the sulfonates, respectively. The uncharged phenylboronic acid groups are indicated by green circles, which can bind to glucose to become anionic (orange circles). Reproduced with permission from ref. 45. Copyright 2006 American Chemical Society.

13.2.2.2 Responsive Materials Based on Binding Competition

Another mechanism is to use the competition between free glucose and modified insulin attributed to the reversible affinity of PBA to glucose. Gluconated insulin (G-lns) was first prepared by Okano and coworkers for insulin delivery.[50] They discovered free glucose could replace the G-Ins that was bound in the PBA-containing hydrogel, and realize responsive insulin release to glucose concentration. To further optimize the sensitivity of their system under physiological pH, they introduced an amine group to decrease the pK_a.[51] Mesoporous silica nanoparticles (MSN) can also act as insulin carriers (Figure 13.8).[52] Insulin as well as cyclic adenosine monophosphate (cAMP) were loaded into MSN, while G-Ins was utilized to cap the pores by interacting with the PBA-decorated exterior surface. Encapsulated insulin could not be released unless glucose replaced the gated G-Ins. The simultaneously released cAMP could also facilitate the BGL regulation *via* stimulating insulin secretion through the activation of Ca^{2+} channels on pancreas β cells.

On the other hand, based on a PBA competition mechanism, a glycopolymer that can bind to PBA can also be designed for glucose-responsive drug delivery.[45,53] One example is from Li's group; they synthesized a block glycopolymer containing phenylboronic acid (AAPBA) and carbohydrates (GAMA) named as *p*(AAPBA-*b*-GAMA) (Figure 13.9(A)).[54] The amphiphilic glycopolymers could self-assemble into nanocarriers through crosslinking inter- and intramolecular complexation between the phenylboronic acid and the diol groups of the carbohydrates. While the diol group of the free glucose binds to AAPBA and simultaneously breaks the crosslinking between GAMA and AAPBA, the NPs would undergo partial disassembly. The different swelling ratios at different glucose concentrations indicated the good glucose-responsive capability of the NPs (Figure 13.9(B)). The corresponding insulin release rate was further verified to be a function of the glucose level (Figure 13.9(C)).

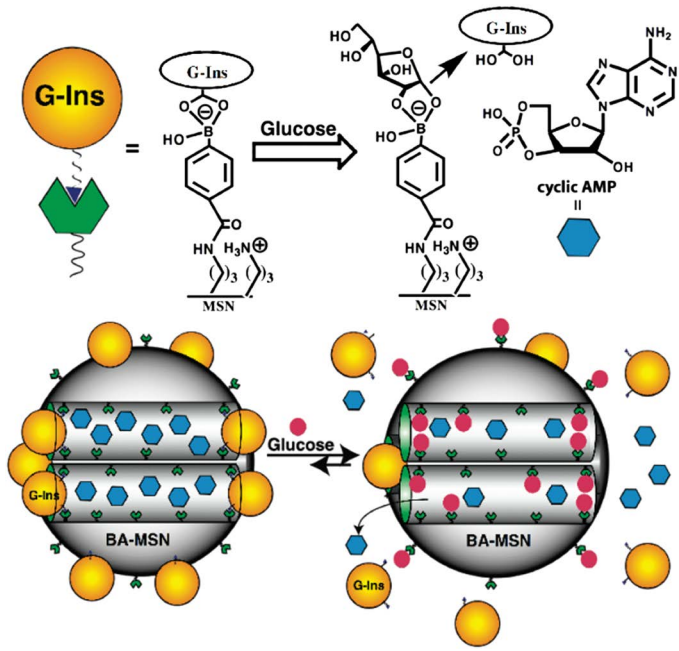

Figure 13.8 Glucose-triggered G-Ins and cAMP release from PBA-functionalized MSN. Reproduced with permission from ref. 52. Copyright 2009 American Chemical Society.

13.2.3 Glucose Binding Protein (GBP)-Modified Systems

Glucose binding proteins are a group of natural carbohydrate-binding proteins, which can bind to glycosylated receptors or lipids to transmit cell signals. Among them, concanavalin A (Con A) is commonly utilized for insulin delivery.[55,56] Con A has four binding sites under neutral pH, which all show good affinity to D-glucose as well as D-glucosyl substances.[57] Thus Brownlee and Cerami creatively developed a glucose-regulated insulin delivery matrix *via* taking advantage of the affinity between Con A and glucose.[58] Due to α-D-glucose residues at the terminal of the glycosylated insulin derivative, G-Ins could complementarily bind to Con A. The release rate of bound G-Ins was determined by the glucose concentration and the binding constant to the Con A. The most generally used G-Ins are SAPG-Ins and SAPM-Ins (*p*-succinylamidophenyl-α-D-mannopyranoside-insulin and *p*-succinylamidophenyl-α-D-glucopyranoside-insulin).[59] Moreover, the binding capability between natural polysaccharide polymers and Con A could be used to design a glucose-responsive polymeric matrix for insulin delivery.[59–63] Miyata *et al.* discovered the glucose-induced gel–sol transition of PGEMA/Con A (poly (2-glucosyloxyethyl methacrylate)-concanavalin A) complexation.[64] The different concentrations could control the swelling ratio of the hydrogel, which promoted its potential application for glucose sensing and glucose-responsive insulin

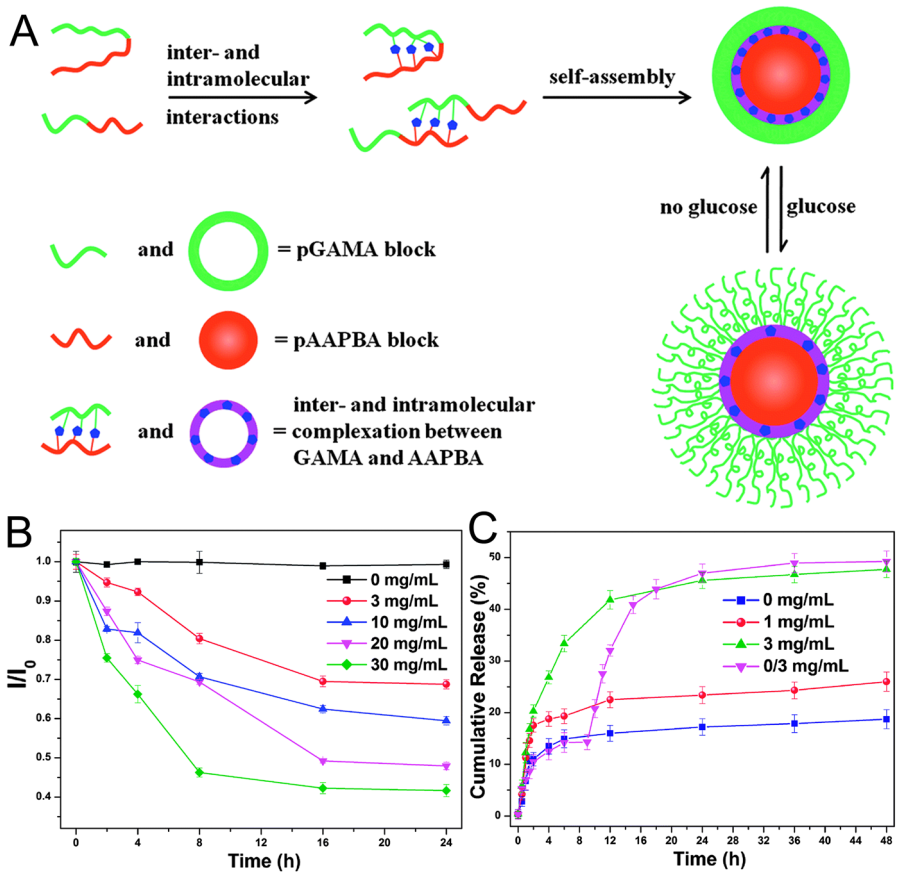

Figure 13.9 Glycopolymeric nanocarriers based on phenylboronate–diol interactions for glucose-responsive insulin delivery. (A) Schematic of the formation and glucose-sensitive mechanism of *p*(AAPBA-*b*-GAMA) NPs. (B) The light scattering intensity of *p*(AAPAB4-*b*-GAMA1) NPs in PBS solution with different glucose concentrations. (C) *In vitro* release profile of insulin in PBS solution with various glucose concentrations (0, 100 and 300 mg dL^{-1}) and medium only for the first 12 h and then 300 mg dL^{-1}. Reproduced with permission from ref. 54. Copyright 2014 Royal Society of Chemistry.

delivery (Figure 13.10). Nie *et al.* further established a glucose and pH dual-responsive microhydrogel, respectively, based on the complex of Con A and glycopolymer (PGEMA), and a pH-responsive polymer (PDMAEMA).[62] The protonation/deprotonation of tertiary amine groups on PDMAEMA resulted in pH-dependent swelling of the hydrogel and release of encapsulated insulin; on the other hand, external glucose reopening the saccharide-binding sites also led to the disassociation of hydrogel. MSNs were also engineered as insulin carriers by Wu *et al.*[65] Con A was used to cap the pores of the MSNs *via* its binding to mannose decorated on the surface. Through this strategy,

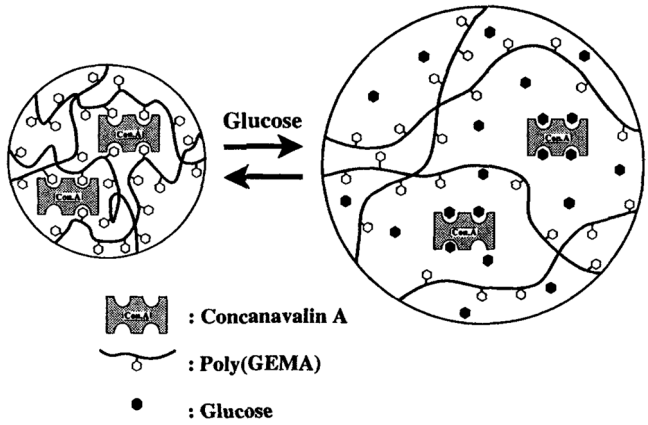

Figure 13.10 Schematic of glucose-triggered swelling of a poly(GEMA)–Con A hydrogel. Reproduced with permission from ref. 64. Copyright 1996 Wiley-VCH.

loaded cargo would only be released if the Con A gates were opened by introducing a competitive binding with free glucose.

13.2.4 Insulin Modification

Besides chemical synthesis of glucose-responsive materials, modification of insulin with glucose-sensing groups would also serve as an alternative strategy for controlled insulin delivery.[66,67] Hoeg-Jensen *et al.* investigated PBA-modified insulin in glucose-responsive therapy.[68–70] As insulin is a protein, its bioactivity is dependent on multiple properties including its molecular weight and structure.[71] Monomeric insulin has a faster diffusion rate than hexameric insulin, but it also has a shorter half-life time ($t_{1/2}$ 1 hour *vs.* $t_{1/2}$ 2–4 h). Insulin bound to high molecular weight proteins has a more than 10 h acting period. Based on this mechanism, they modified insulin with diol groups and PBA in order to force them to be self-assembled into hexamers.[68] Therefore, injected hexameric insulin would circulate in the blood for a relatively longer time without performing a bioactivity. In the presence of high BGLs, the reversible self-assembled insulin disassociated within five minutes to release bioactive monomeric insulin and regulated the BGLs (Figure 13.11).

Recently, Langer and Anderson's group demonstrated that aliphatic PBA-conjugated insulin had a glucose-responsive and long-lasting ability.[72] The PBA moieties were modified to the aliphatic domain of insulin through direct amidation of PBA followed by a Suzuki coupling reaction (Figure 13.12(A)). The modified aliphatic domain could bind to serum albumin or other hydrophobic serum components, which led to a prolonged circulation half-life. The resulting insulin derivatives provided good glycemia control in diabetic mice following several glucose challenges during 13 hours (Figure 13.12(B)). These insulin

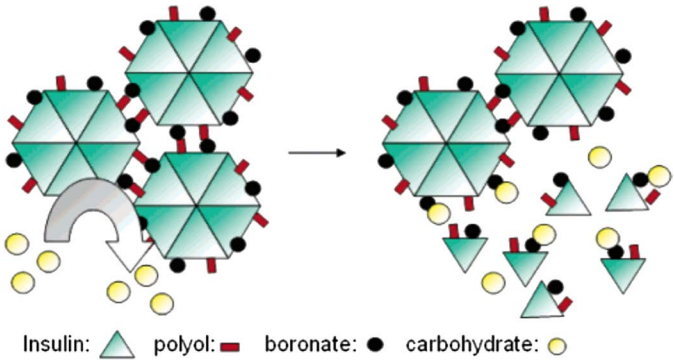

Figure 13.11 Illustration of insulin self-assembly controlled by a carbohydrate. Reproduced with permission from ref. 68. Copyright 2005 American Chemical Society.

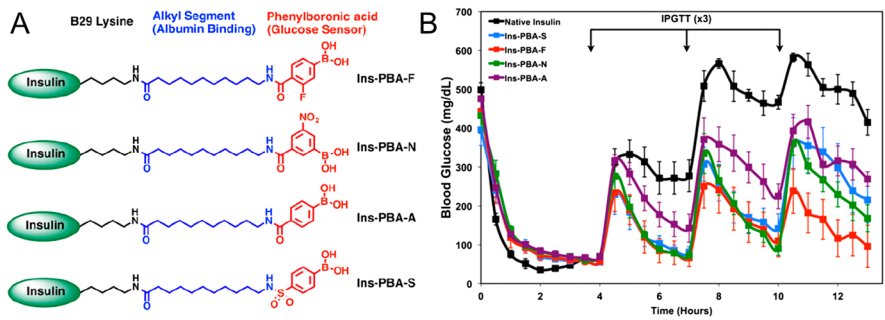

Figure 13.12 Chemically modified insulin for glycemia regulation. (A) Chemical structures of the four PBA-modified insulin derivatives. (B) BLGs of STZ-induced diabetic mice after injection of insulin derivatives or native insulin followed by a series of i. p. glucose tolerance tests performed at 4, 7, and 10 h. Reproduced with permission from ref. 72. Copyright 2015 National Academy of Sciences.

derivatives exhibited even faster and superior BGL control than native insulin. Furthermore, their good glucose responsiveness was revealed to be similar to the function of the pancreas by continuous glucose monitoring.

13.3 Pancreatic Cell-Based Systems as an Artificial Pancreas

Transplants of pancreas or β-cells to type 1 diabetes patients have been widely explored as an approach to help retain insulin secretion.[18] Recently, the advance of *in vitro* differentiation from human pluripotent stem cells (hPSCs) into functional pancreatic β-cells has provided a good source of human-insulin-producing cells, further promoting the development of a cell-based diabetes

therapy.[73] However, allogenic implants typically suffer a foreign body immune response, which requires the long-term need of immunosuppressive drugs and may pose a challenge for normal function, even the survival of implanted cells.[74] One alternative strategy is cell encapsulation, which can prevent therapeutic cells being rejected by the immune system *via* using semi-permeable containers. Materials used in cell carriers need to be biocompatible and enable immuno-isolation, and allow the diffusion of glucose and insulin. Alginate is the most commonly used material to form microbeads *via* electrostatic droplet generation for islet encapsulation.[75,76] The chemical structures of alginate derivatives and the sizes or shapes of alginate microspheres were all studied for their effects on immunological responses.[77,78] Recent work by Anderson's group realized a long-term glycemic control of up to 174 days without immunosuppression by using triazole–thiomorpholine (TMTD)-alginate-encapsulated human-stem-cell-derived β-cells (SC-β cells).[79] The TMTD alginate beads of 1.5-mm diameter showed the longest normoglycemia maintenance in STZ-induced diabetic mice after SC-β cell transplantation compared to other groups of 500-μm and 1.5-mm alginate spheres (Figure 13.13). It was demonstrated that the increased sphere size of the alginate sphere could efficiently mitigate the immunological responses.

Besides transplantation of cells, Gu's group reported a new microneedle-based cell therapy through transcutaneous administration.[80] They integrated exogenous pancreatic β-cells with microneedles to achieve glucose-responsive insulin secretion without implantation. Under a hyperglycemic state, the encapsulated β-cells were expected to secrete insulin. In order to transport the internal glucose signal to the external β-cells, synthetic "glucose-signal amplifiers" (GSAs) were developed and loaded in a MN matrix to effectively trigger the cellular response (Figure 13.14(A)). This GSA contained self-assembled polymeric vesicles encapsulating GOx, α-amylase (AM) and glucoamylase (GA). GOx would oxidize glucose and consume oxygen, while AM and GA can hydrolyze the α-amylose into glucose. In the presence of a high BGL, the GSA based on hypoxia-sensitive HA quickly dissociated due to the rapid oxygen consumption by GOx. The released enzymes subsequently generated a local condensed glucose site, resulting in effective diffusion of glucose to the β-cell capsules and further facilitating the insulin secretion. Thereafter, the secreted insulin diffused into the vascular networks through MN channels to regulate the BGLs. Their design involved both live and synthetic glucose-responsive systems to amplify the glucose signal to the β-cell capsules for insulin secretion and realize transdermal insulin delivery in a painless and convenient manner. One single MN patch was demonstrated to maintain BGLs at a reduced level for over 10 h in type-1 diabetic mice (Figure 13.14(E) and 13.14(F)).

13.4 Emerging Translation to Clinical Practice

Chemically controlled closed-loop insulin delivery systems provide highly promising platforms for self-regulation of glucose levels. However, they are still in their infancy regarding clinical production and implementation.

The specificity of PBA and Con A mediated systems remains a concern. Besides glucose, they can also react with other sugars, which leads the precise report of physiological BGLs in body to be a challenge. For PBA-based materials, derivatives with a low pK_a at physiological pH (7.4) are needed to adjust the *in vivo* glucose responsiveness of PBA. Moreover, the most existing materials reported cannot survive repeatable glucose challenges, as they usually lose their responsive ability or drug release control as a result of system destruction. How to achieve a reversible and stable delivery of insulin is an issue that needs to be resolved.

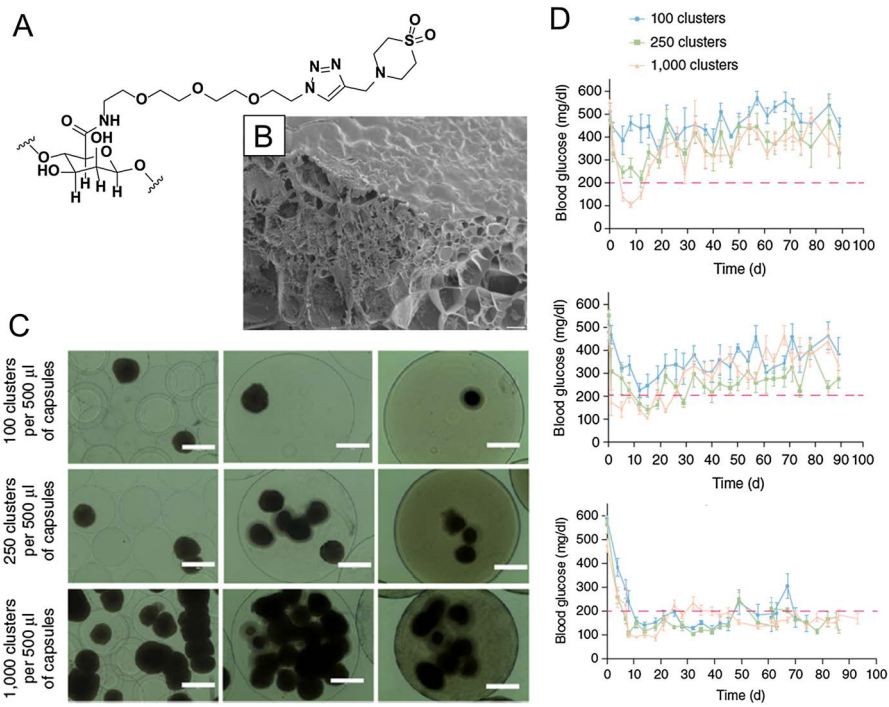

Figure 13.13 TMTD alginate encapsulating SC-β cells for glucose regulation in immune-competent diabetic mice. (A) Chemical structure of TMTD alginate. (B) Cryo-SEM image of TMTD alginate spheres (scale bar: 3 μm). (C) Representative bright-field images of SC-β cells encapsulated in 500-μm alginate microcapsules (left), 1.5-mm alginate spheres (middle) and 1.5-mm TMTD alginate spheres (right) with various doses (scale bars: 400 μm). (D) BLGs in diabetic mice after transplantation of SC-β cells encapsulated in 500-μm alginate microcapsules (top), 1.5-mm alginate spheres (middle) and 1.5-mm TMTD alginate spheres (bottom) at various doses of cell clusters. The blood glucose cut-off for normoglycemia is indicated by the red dashed line. Reprinted by permission from Macmillan Publishers Ltd: Nature Medicine, ref. 79. Copyright Nature Publishing Group.

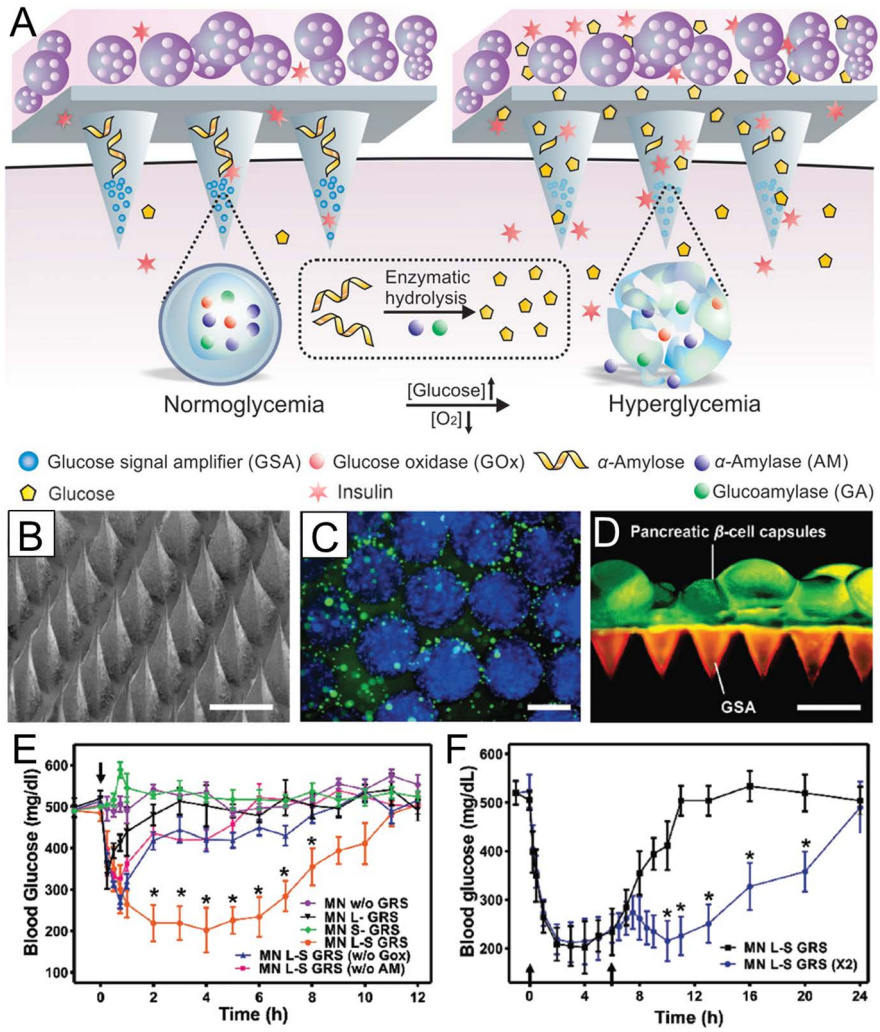

Figure 13.14 (A) Schematic of a microneedle-array patch loaded with glucose signal amplifiers (GSA) integrated with pancreatic β-cells for glucose regulation. (B) A SEM image of the MN patch. (C) Immunofluorescence image of the pancreatic β-cell capsules (green: insulin, and blue: nucleus). (D) Fluorescence image of the MN patch loaded with GSA (red) and pancreatic β-cell capsules (green). (E) *In vivo* studies of the MN patches in STZ-induced diabetic mice. Mice were transcutaneously administrated with different MN samples: blank MNs (w/o GRS), MNs loaded with only L-GRS (L-GRS), MNs loaded with only S-GRS (S-GRS), MNs loaded with both L-GRS and S-GRS (L-S GRS), MNs loaded with both L-GRS and S-GRS without GOx (L-S GRS (w/o GOx)), and MNs loaded with both L-GRS and S-GRS without α-amylose (L-S GRS (w/o AM)). (F) BGLs in diabetic mice after additional treatment of MN (L-S GRS) six h post administration. Scale bars: 500 μm. Reproduced with permission from ref. 80. Copyright 2016 Wiley-VCH.

Table 13.1 Recent Clinical Trials Evaluating Cell Transplantation for the Treatment of Type 1 Diabetes (retrieved from www.clinicaltrials.gov).

Intervention	Technique	Cell type	Phase	Clinical trial identifier	Year
Novocell	PEG coating	Allogenic islets	I/II	NCT00260234	2005
Baylor Research Institute	Two-layer pancreatic ductal preservation method	Allogenic islets	I	NCT00214786	2005
Baylor Research Institute	Ductal injection method	Allogenic islets	I	NCT00214786	2007
National Institute of Allergy and Infectious Diseases	Immunosuppressive drug (antithymocyte globulin, sirolimus, and tacrolimus)	Allogenic islets	III	NCT00434811	2007
University of Chicago	Intraportal infusion through the portal vein in the liver	Allogenic islets	II	NCT01241864	2010
Living cell Technologies (Diabecell®)	Alginate microencapsulation	Porcine islets	II	NCT01736228	2012
ViaCyte (VC-01™)	Encaptra®	Allogenic pancreatic endoderm cells from embryonic stem cells	I/II	NCT02239354	2014
Medical University of South Carolina	—	Autologous mesenchymal stromal cells	I	NCT02384018	2014
DiaVacs	Immunoregulatory (intradermal injection)	Autologous dendritic cells	II	NCT02354911	2015

Clinical studies on cell transplantations for type 1 diabetes treatments started in the 1890s,[81] and significant progress has been achieved during the past several decades,[82] especially in cell encapsulation.[83,84] Many trials have been carried out with different cell sources, biomaterials and techniques to evaluate the safety and efficacy of cell transplantations (Table 13.1). The key of cell therapy is to maintain the bioactivity of implants: how to minimize immunosuppression and provide sufficient oxygen supply within the islets. Immunosuppressive drugs have been introduced to facilitate the cell survival;[85–87] materials with good biocompatibility and diffusion properties have been explored;[88] some anti-oxidant enzymes that reduce free radical levels have also been applied to help resist the hypoxic environment around the islets.[89] Moreover, desired revascularization around transplanted islets is also crucial as a rapid response to blood glucose levels demands close proximity to blood vessels.[90]

13.5 Conclusions

Diabetes treatments with smart materials and systems have attracted more and more attention in the last decade. For closed-loop insulin delivery, a number of different systems have been explored. However, more efforts are needed for potential clinical applications. First of all, the most challenging task is how to achieve fast responsiveness *in vivo*. To date, many studies have presented ideal glucose-responsive behaviors in test tubes without *in vivo* investigations. The real-time monitoring of *in vivo* pharmacokinetics of formulations in a complex physiological environment is essential to validate the performance to further tailor the material and formulation design. Second, several safety concerns associated with insulin dosage should be addressed. For example, the burst release of insulin should be avoided for depot-based formulations. Additionally, co-delivery of glucagon might be incorporated to serve as a safeguard to prevent the risk of hypoglycemia, a result of the release of unexpected insulin in a large amount. Third, biocompatibility of glucose-responsive formulations or modified insulin should be carefully assessed. Acute inflammation and long-term immunogenicity should be alleviated. In terms of cell-based therapy, how to maintain their long-term bioactivity is still the key challenge. High-throughput screening biomaterials for evaluating the performance of cell capsules both *in vitro* and *in vivo* provide an effective strategy to identify excellent candidates. In addition, the development of novel methodologies to help by-pass immunology issues, such as the way of externally positioning β-cells, would be another direction.

References

1. M. A. Atkinson and G. S. Eisenbarth, *Lancet*, 2001, **358**, 221–229.
2. J. A. Bluestone, K. Herold and G. Eisenbarth, *Nature*, 2010, **464**, 1293–1300.
3. T. L. Van Belle, K. T. Coppieters and M. G. Von Herrath, *Physiol. Rev.*, 2011, **91**, 79–118.

4. M. Stumvoll, B. J. Goldstein and T. W. van Haeften, *Lancet*, 2005, **365**, 1333–1346.
5. A. E. Butler, J. Janson, S. Bonner-Weir, R. Ritzel, R. A. Rizza and P. C. Butler, *Diabetes*, 2003, **52**, 102–110.
6. R. A. DeFronzo, R. Eldor and M. Abdul-Ghani, *Diabetes Care*, 2013, **36**, S127–S138.
7. International Diabetes Federation, *IDF Diabetes*, Brussels, Belgium, 9782930229812, 7 edn, 2015.
8. C. Mameli, A. E. Scaramuzza, J. Ho, R. Cardona-Hernandez, L. Suarez-Ortega and G. V. Zuccotti, *Acta Diabetol.*, 2014, **51**, 205–210.
9. J. C. Pickup, *Nat. Rev. Endocrinol.*, 2014, **10**, 647–649.
10. F. Alsaleh, F. Smith, S. Keady and K. Taylor, *J. Clin. Pharm. Ther.*, 2010, **35**, 127–138.
11. R. Hovorka, *Diabetic Med.*, 2006, **23**, 1–12.
12. L. Heinemann and L. Krinelke, *J. Diabetes Sci. Technol.*, 2012, **6**, 954–964.
13. V. N. Shah, A. Shoskes, B. Tawfik and S. K. Garg, *Diabetes Technol. Ther.*, 2014, **16**, 477–490.
14. Q. Wu, L. Wang, H. Yu, J. Wang and Z. Chen, *Chem. Rev.*, 2011, **111**, 7855–7875.
15. R. Mo, T. Jiang, J. Di, W. Tai and Z. Gu, *Chem. Soc. Rev.*, 2014, **43**, 3595–3629.
16. O. Veiseh, B. C. Tang, K. A. Whitehead, D. G. Anderson and R. Langer, *Nat. Rev. Drug Discovery*, 2015, **14**, 45–57.
17. W. Wu and S. Zhou, *Macromol. Biosci.*, 2013, **13**, 1464–1477.
18. R. P. Robertson, *N. Engl. J. Med.*, 2004, **350**, 694–705.
19. K. M. Bratlie, R. L. York, M. A. Invernale, R. Langer and D. G. Anderson, *Adv. Healthcare Mater.*, 2012, **1**, 267–284.
20. M. J. Webber and D. G. Anderson, *J. Drug Targeting*, 2015, **23**, 651–655.
21. F. Fischel-Ghodsian, L. Brown, E. Mathiowitz, D. Brandenburg and R. Langer, *Proc. Natl. Acad. Sci.*, 1988, **85**, 2403–2406.
22. V. Ravaine, C. Ancla and B. Catargi, *J. Controlled Release*, 2008, **132**, 2–11.
23. S. B. Bankar, M. V. Bule, R. S. Singhal and L. Ananthanarayan, *Biotechnol. Adv.*, 2009, **27**, 489–501.
24. C. M. Hassan, F. J. Doyle and N. A. Peppas, *Macromolecules*, 1997, **30**, 6166–6173.
25. A. Lowman, M. Morishita, M. Kajita, T. Nagai and N. Peppas, *J. Pharm. Sci.*, 1999, **88**, 933–937.
26. C. R. Gordijo, K. Koulajian, A. J. Shuhendler, L. D. Bonifacio, H. Y. Huang, S. Chiang, G. A. Ozin, A. Giacca and X. Y. Wu, *Adv. Funct. Mater.*, 2011, **21**, 73–82.
27. Z. Gu, T. T. Dang, M. Ma, B. C. Tang, H. Cheng, S. Jiang, Y. Dong, Y. Zhang and D. G. Anderson, *ACS Nano*, 2013, **7**, 6758–6766.
28. Z. Gu, A. A. Aimetti, Q. Wang, T. T. Dang, Y. Zhang, O. Veiseh, H. Cheng, R. S. Langer and D. G. Anderson, *ACS Nano*, 2013, **7**, 4194–4201.
29. W. Tai, R. Mo, J. Di, V. Subramanian, X. Gu, J. B. Buse and Z. Gu, *Biomacromolecules*, 2014, **15**, 3495–3502.

30. M. R. Kumar, R. A. Muzzarelli, C. Muzzarelli, H. Sashiwa and A. Domb, *Chem. Rev.*, 2004, **104**, 6017–6084.
31. C. Mai, A. Majcherczyk, W. Schormann and A. Hüttermann, *Polym. Degrad. Stab.*, 2002, **75**, 107–112.
32. T. Uchiyama, Y. Kiritoshi, J. Watanabe and K. Ishihara, *Biomaterials*, 2003, **24**, 5183–5190.
33. T. Uchiyama, J. Watanabe and K. Ishihara, *J. Membr. Sci.*, 2002, **210**, 423–431.
34. T. Uchiyama, J. Watanabe and K. Ishihara, *J. Biomater. Sci., Polym. Ed.*, 2004, **15**, 1237–1262.
35. O. Veiseh and R. Langer, *Nature*, 2015, **524**, 39–40.
36. J. Yu, Y. Zhang, Y. Ye, R. DiSanto, W. Sun, D. Ranson, F. S. Ligler, J. B. Buse and Z. Gu, *Proc. Natl. Acad. Sci.*, 2015, **112**, 8260–8265.
37. J. P. Lorand and J. O. Edwards, *J. Org. Chem.*, 1959, **24**, 769–774.
38. S. Angyal, D. Greeves and V. Pickles, *Carbohydr. Res.*, 1974, **35**, 165–173.
39. K. Kataoka, H. Miyazaki, T. Okano and Y. Sakurai, *Macromolecules*, 1994, **27**, 1061–1062.
40. K. Kataoka, H. Miyazaki, M. Bunya, T. Okano and Y. Sakurai, *J. Am. Chem. Soc.*, 1998, **120**, 12694–12695.
41. R. Ma and L. Shi, *Polym. Chem.*, 2014, **5**, 1503–1518.
42. R. S. Langer, D. G. Anderson, Z. Gu and A. A. Aimetti, Pat., WO 2013123491 A1, 2013.
43. A. Matsumoto, S. Ikeda, A. Harada and K. Kataoka, *Biomacromolecules*, 2003, **4**, 1410–1416.
44. A. Matsumoto, T. Ishii, J. Nishida, H. Matsumoto, K. Kataoka and Y. Miyahara, *Angew. Chem., Int. Ed.*, 2012, **51**, 2124–2128.
45. B. G. De Geest, A. M. Jonas, J. Demeester and S. C. De Smedt, *Langmuir*, 2006, **22**, 5070–5074.
46. Z. Ding, Y. Guan, Y. Zhang and X. Zhu, *Soft Matter*, 2009, **5**, 2302–2309.
47. B. Wang, R. Ma, G. Liu, Y. Li, X. Liu, Y. An and L. Shi, *Langmuir*, 2009, **25**, 12522–12528.
48. Y. Yao, L. Zhao, J. Yang and J. Yang, *Biomacromolecules*, 2012, **13**, 1837–1844.
49. H. Kim, Y. J. Kang, S. Kang and K. T. Kim, *J. Am. Chem. Soc.*, 2012, **134**, 4030–4033.
50. D. Shiino, Y. Murata, K. Kataoka, Y. Koyama, M. Yokoyama, T. Okano and Y. Sakurai, *Biomaterials*, 1994, **15**, 121–128.
51. D. Shiino, Y. Murata, A. Kubo, Y. J. Kim, K. Kataoka, Y. Koyama, A. Kikuchi, M. Yokoyama, Y. Sakurai and T. Okano, *J. Controlled Release*, 1995, **37**, 269–276.
52. Y. Zhao, B. G. Trewyn, I. I. Slowing and V. S.-Y. Lin, *J. Am. Chem. Soc.*, 2009, **131**, 8398–8400.
53. X. Jin, X. Zhang, Z. Wu, D. Teng, X. Zhang, Y. Wang, Z. Wang and C. Li, *Biomacromolecules*, 2009, **10**, 1337–1345.
54. Q. Guo, Z. Wu, X. Zhang, L. Sun and C. Li, *Soft Matter*, 2014, **10**, 911–920.

55. M. Brudner, M. Karpel, C. Lear, L. Chen, L. M. Yantosca, C. Scully, A. Sarraju, A. Sokolovska, M. R. Zariffard, D. P. Eisen, B. A. Mungall, D. N. Kotton, A. Omari, I. C. Huang, M. Farzan, K. Takahashi, L. Stuart, G. L. Stahl, A. B. Ezekowitz, G. T. Spear, G. G. Olinger, E. V. Schmidt and I. C. Michelow, *PLoS One*, 2013, **8**, e60838.
56. T. B. Geijtenbeek and S. I. Gringhuis, *Nat. Rev. Immunol.*, 2009, **9**, 465–479.
57. N. Sharon and H. Lis, *Science*, 1972, **177**, 949–959.
58. M. Brownlee and A. Cerami, *Science*, 1979, **206**, 1190–1191.
59. S. Y. Jeong, S. W. Kimn, M. J. Eenink and J. Feijen, *J. Controlled Release*, 1984, **1**, 57–66.
60. M. J. Taylor, S. Tanna, P. M. Taylor and G. Adams, *J. Drug Targeting*, 1995, **3**, 209–216.
61. K. Nakamae, T. Miyata, A. Jikihara and A. S. Hoffman, *J. Biomater. Sci., Polym. Ed.*, 1994, **6**, 79–90.
62. R. Yin, Z. Tong, D. Yang and J. Nie, *Int. J. Biol. Macromol.*, 2011, **49**, 1137–1142.
63. R. Yin, Z. Tong, D. Yang and J. Nie, *J. Controlled Release*, 2011, **152**(suppl. 1), e163–e165.
64. T. Miyata, A. Jikihara, K. Nakamae and A. S. Hoffman, *Macromol. Chem. Phys.*, 1996, **197**, 1135–1146.
65. S. Wu, X. Huang and X. Du, *Angew. Chem., Int. Ed. Engl.*, 2013, **52**, 5580–5584.
66. M. J. Webber, D. G. Anderson and R. Langer, *Expert Rev. Endocrinol. Metab.*, 2015, **10**, 483–489.
67. A. N. Zaykov, J. P. Mayer and R. D. DiMarchi, *Nat. Rev. Drug Discovery*, 2016, **15**, 425–439.
68. T. Hoeg-Jensen, S. Havelund, P. K. Nielsen and J. Markussen, *J. Am. Chem. Soc.*, 2005, **127**, 6158–6159.
69. T. Hoeg-Jensen, S. Ridderberg, S. Havelund, L. Schäffer, P. Balschmidt, I. Jonassen, P. Vedsø, P. H. Olesen and J. Markussen, *J. Pept. Sci.*, 2005, **11**, 339–346.
70. T. Hoeg-Jensen, S. Havelund, J. Markussen, S. Ostergaard, S. Ridderberg, P. Balschmidt, L. Schaffer and I. Jonassen, Pat., WO 2001092334 A1, 2008.
71. V. Sluzky, J. A. Tamada, A. M. Klibanov and R. Langer, *Proc. Natl. Acad. Sci.*, 1991, **88**, 9377–9381.
72. D. H.-C. Chou, M. J. Webber, B. C. Tang, A. B. Lin, L. S. Thapa, D. Deng, J. V. Truong, A. B. Cortinas, R. Langer and D. G. Anderson, *Proc. Natl. Acad. Sci.*, 2015, **112**, 2401–2406.
73. F. W. Pagliuca, J. R. Millman, M. Gürtler, M. Segel, A. Van Dervort, J. H. Ryu, Q. P. Peterson, D. Greiner and D. A. Melton, *Cell*, 2014, **159**, 428–439.
74. A. J. Shapiro, C. Ricordi, B. J. Hering, H. Auchincloss, R. Lindblad, R. P. Robertson, A. Secchi, M. D. Brendel, T. Berney and D. C. Brennan, *N. Engl. J. Med.*, 2006, **355**, 1318–1330.
75. D. Jacobs-Tulleneers-Thevissen, M. Chintinne, Z. Ling, P. Gillard, L. Schoonjans, G. Delvaux, B. L. Strand, F. Gorus, B. Keymeulen and D. Pipeleers, *Diabetologia*, 2013, **56**, 1605–1614.

76. D. W. Scharp and P. Marchetti, *Adv. Drug Delivery Rev.*, 2014, **67**, 35–73.
77. O. Veiseh, J. C. Doloff, M. Ma, A. J. Vegas, H. H. Tam, A. R. Bader, J. Li, E. Langan, J. Wyckoff and W. S. Loo, *Nat. Mater.*, 2015, **14**, 643–651.
78. A. J. Vegas, O. Veiseh, J. C. Doloff, M. Ma, H. H. Tam, K. Bratlie, J. Li, A. R. Bader, E. Langan and K. Olejnik, *Nat. Biotechnol.*, 2016, **34**, 345–352.
79. A. J. Vegas, O. Veiseh, M. Gürtler, J. R. Millman, F. W. Pagliuca, A. R. Bader, J. C. Doloff, J. Li, M. Chen and K. Olejnik, *Nat. Med.*, 2016, **22**, 306–311.
80. Y. Ye, J. Yu, C. Wang, N. Y. Nguyen, G. M. Walker, J. B. Buse and Z. Gu, *Adv. Mater.*, 2016, **28**, 3115–3121.
81. P. W. Williams, *BMJ*, 1894, **19**, 1303–1304.
82. A. Shapiro, S. A. Nanji and J. R. Lakey, *Immunol. Rev.*, 2003, **196**, 219–236.
83. P. Soon-Shiong, R. Heintz, N. Merideth, Q. Yao, Z. Yao, T. Zheng, M. Murphy, M. Moloney, M. Schmehl and M. Harris, *Lancet*, 1994, **343**, 950–951.
84. G. Orive, R. M. Hernández, A. R. Gascón, R. Calafiore, T. M. Chang, P. De Vos, G. Hortelano, D. Hunkeler, I. Lacík and A. J. Shapiro, *Nat. Med.*, 2003, **9**, 104–107.
85. A. J. Shapiro, J. R. Lakey, E. A. Ryan, G. S. Korbutt, E. Toth, G. L. Warnock, N. M. Kneteman and R. V. Rajotte, *N. Engl. J. Med.*, 2000, **343**, 230–238.
86. E. A. Ryan, B. W. Paty, P. A. Senior, D. Bigam, E. Alfadhli, N. M. Kneteman, J. R. Lakey and A. J. Shapiro, *Diabetes*, 2005, **54**, 2060–2069.
87. C. Ricordi and T. B. Strom, *Nat. Rev. Immunol.*, 2004, **4**, 259–268.
88. Y. Teramura and H. Iwata, *Adv. Drug Delivery Rev.*, 2010, **62**, 827–840.
89. J. D. Acharya and S. S. Ghaskadbi, *Islets*, 2010, **2**, 225–235.
90. J. C. Stendahl, D. B. Kaufman and S. I. Stupp, *Cell Transplant.*, 2009, **18**, 1–12.

CHAPTER 14

Smart Materials for Nerve Regeneration and Neural Tissue Engineering

METIN UZ[a] AND SURYA K. MALLAPRAGADA*[a,b]

[a]Department of Chemical and Biological Engineering, Iowa State University, Ames, IA 50011, USA; [b]Neuroscience Program, Iowa State University, Ames, IA 50011, USA
*E-mail: suryakm@iastate.edu

14.1 Introduction

Physical damage to the central nervous system (CNS) and the presence of chronic neurodegenerative diseases, such as Parkinson's and Alzheimer's, causing loss of neuronal cells, axons, and associated glial support, are the main reasons for the disruption of brain architecture.[1,2] The self-repairing capacity of the CNS and replacement potential of lost neurons are limited due to injury or disease-associated inflammatory responses causing microglial infiltration, astrocyte proliferation and glial scarring, as well as reduced neuronal proliferation.[3] A combination of these effects suppresses the reparative and proliferative processes in the CNS. Therefore, the presence of cues and signals for cell migration, axonal guidance and synapse formation as well as the neuronal phenotypes, are needed in order to facilitate the participation of intrinsically derived neurons or implanted stem-cell-based therapies in adult CNS repair.[3] In addition, the transport of applied drugs

Smart Materials No. 25
Smart Materials for Tissue Engineering: Applications
Edited by Qun Wang

Published by the Royal Society of Chemistry, www.rsc.org

or neurotrophic factors across the blood–brain barrier (BBB) to target brain sites for long-term activity is also another fundamental challenge.[4] On the other hand, compared to the adult CNS possessing a growth inhibitory environment, the presence of Schwann cells, facilitating axonal regrowth upon damage, provides a greater repairing capacity for peripheral nervous system (PNS) neurons.[5,6] The myelin and axon debris formed after traumatic injury to peripheral nerves are removed by macrophages and monocytes migrating into the nerve stumps. At the same time, Schwann cells proliferate to secrete neurotrophic factors and extracellular matrix (ECM) molecules. These synergistic actions facilitate axon regeneration to achieve functional recovery. Despite the self-healing capacity, peripheral nerve repair with poor functional recovery is achieved, particularly for large peripheral nerve gaps.[6] In order to address these issues in the CNS and PNS, various approaches, including delivery of drugs, neurotrophic factors and stem cell therapies, allowing reprogramming and transdifferentiation, based on different biomaterials and 3D scaffold fabrication techniques, have been applied in neural tissue engineering and nerve regeneration.[2,7–11]

Biomaterials fabricated from natural and synthetic sources, possessing many features (including biocompatibility, biodegradability, biological activity, mechanical properties, surface chemistry, and growth factor binding capabilities) have been used for the fabrication of 3D scaffolds providing an available ECM microenvironment that enables cell (native or transplanted) growth and differentiation along with an efficient drug/neurotrophic factor delivery platform.[12–33] Among these materials, stimuli-responsive smart biomaterials, that are capable of showing large conformation- or property-based responses to small physical or chemical changes, have been addressed as promising candidates providing 3D scaffolds and drug/neurotrophic factor delivery platforms for neural tissue engineering and nerve regeneration.

This review chapter overviews recent advances in the use of stimuli-responsive smart-biomaterial-based strategies to overcome the key hurdles of neural tissue engineering and nerve regeneration. The chapter specifically focuses on temperature-, pH-, enzyme- and photo-triggered self-assembling mono- or multi-responsive biomaterial-based 3D scaffolds and delivery platforms for drug/neurotrophic factors and stem cell therapies used in neural tissue engineering and nerve regeneration. A separate section emphasizing electrically conductive materials and graphene is also included. In the last part, surface functionalized delivery systems for traversing the BBB and gene delivery systems and strategies are mentioned briefly. The chapter ends with a discussion about the clinical potential and applications of smart materials in neural tissue engineering followed by concluding remarks and future perspectives.

14.2 Stimuli-Responsive Biomaterials for Neural Tissue Engineering and Nerve Regeneration

Different types of stimuli-responsive smart biomaterials have been used for neural tissue engineering and nerve regeneration purposes as promising candidates providing 3D scaffolds and drug/neurotrophic factor delivery

platforms. They respond sensitively to physical or chemical changes, such as temperature, pH, enzymatic reactions, light and electrical stimuli by showing relatively large conformation or property changes. The types of materials, their stimuli responses and descriptions are discussed below and outlined in Table 14.1.

14.2.1 Temperature-Responsive Biomaterials

Temperature-responsive materials have been mostly used to develop injectable *in situ* forming hydrogel scaffolds, allowing precise and controlled localization at the desired site in the liquid phase, for neural tissue engineering. A commonly used thermoresponsive polymer, poly(*N*-isopropylacrylamide) (poly(NIPAAM)), is capable of changing conformation from a coil to a globule at temperatures higher than the lower critical solution temperature (LCST: 32 °C). At these temperatures, the water molecules attached to the isopropyl side groups are released, leading to poly(NIPAAM) phase separation and enhancement in hydrophobic interactions.[89–92] However, the large shrinkage of poly(NIPAAM) upon a temperature change reduces the cell encapsulation and protein delivery efficacy of this polymer. In order to prevent the shrinking problem and enhance cell entrapment and compatibility, poly(NIPAAM) chains have been further modified by hydrophilic blocks including acrylic acid or polyethylene glycol (PEG).[93,94] For instance, PNIPAAm modified with PEG was used as a biocompatible, injectable scaffold for the treatment of spinal cord injuries.[34] The temperature-responsive injectable PNIPAAm–PEG-based scaffold allowed bone marrow stromal cell attachment and a sustained release of neurotrophic factors along with providing mechanical support matching the native neuronal tissue.[34] Besides the large shrinkage, the lack of biodegradation of poly(NIPAAM) is also another problem for tissue engineering applications. In order to address this issue, poly(NIPAAM) has been introduced to the backbone of biodegradable polymers such as chitosan, gelatin, hyaluronic acid and dextran.[35,36,95,96]

Biodegradable and biocompatible gelatin with thermoreversible properties and facile modification at the amino acid level is considered as another potential biopolymer. Below 25 °C, triple helix formation occurs, causing the solidification of aqueous gelatin and creation of a rigid 3D network, while above 30 °C, the reverse is exhibited through a conformation change from a helix to a flexible coil.[35,36] Since this thermal behavior of gelatin is opposite to what is usually required in biomedical applications, a combination of gelatin with other polymers is also needed to show thermal gelation close to body temperature. For this purpose, poly(*N*-isopropylacrylamide)-grafted gelatin (PNIPAM–gelatin) was also examined as a temperature-responsive biodegradable *in situ* formed injectable 3D scaffold.[36]

Amphiphilic block copolymers, containing both hydrophobic and hydrophilic blocks, along with temperature-responsive properties (such as PEO–PPO–PEO (PluronicF127), PLGA–PEG–PLGA, PEG–PLLA–PEG, PCL–PEG–PCL and PEG–PCL–PEG) are other potential scaffold materials for neural tissue

Table 14.1 Types of biomaterials, their stimuli responses and descriptions.

Material	Stimuli response	Application/description	Outcome	References
PNIPAAm–PEG	Thermo-responsive	Injectable scaffold for bone marrow stromal cells' attachment and a sustained release of neurotrophic factors	Provided mechanical support matching the native neuronal tissue and enhanced cell encapsulation	34
PNIPAM–gelatin	Thermo-responsive	*In situ* formed injectable 3D scaffold for cells	Provided enhanced biodegradability to PNIPAM	35 and 36
PEG-(poly-L-alanine)	Thermo-responsive	3D hybrid scaffolds comprising neuronal differentiated MSCs and growth factor releasing microspheres	Exhibited mechanical properties similar to brain tissue, capable of baring the microspheres and MSCs throughout 3D culture	37
Methylcellulose-tethered laminin-1	Thermo-responsive	Bioactive scaffold as a delivery vehicle for CNS and neural cell transplantation laminin-1 to methylcellulose through Schiff base reaction	Enhanced low protein adsorption and cell adhesion of methylcellulose for neural tissue engineering applications	38
Chitosan/glycerophosphate salt hydrogel with PDLA	Thermo-responsive	3D chitosan/glycerophosphate salt hydrogels, containing immobilized poly-D-lysine onto chitosan *via* azidoaniline photocoupling	Certain peptide polylysine concentrations improved neuronal adhesion and neurite outgrowth in 3D gel geometry	39
Xyloglucan hydrogels	Thermo-responsive	Xyloglucan hydrogel scaffolds functionalized through the immobilization and grafting of poly-D-lysine	Promoted neuron adhesion and neurite outgrowth for the spinal cord. Native spinal cord mimicking mechanical properties, allowing migration of neural stem cells, direction of neurite growth and infiltration of axons, astrocytes and neurites with higher concentrations	5,40–42
PDEAEM–PluronicF127–PDEAEM	pH and temperature responsive	Hydrogels composed of temperature-responsive Pluronic F127 and pH-responsive cationic PDEAEM	Potential as 3D scaffolds for cellular growth and depot for drug/neurotrophic factor delivery for neural tissue engineering applications	43–59

(*continued*)

Table 14.1 (*continued*)

Material	Stimuli response	Application/description	Outcome	References
IKVAV, LDLK12, RADA16 peptides	Self-assembly	Nanofibrillar gels and scaffolds developed through spontaneous self-assembly of ionic self-complementary peptides	Mimicking ECM. Enhanced neural cell attachment, proliferation, migration and differentiation. Induced neurite outgrowth and synapse formation	60–71
Photocrosslinkable methacrylamide chitosan	Photoresponsive	Photocrosslinkable methacrylamide chitosan-based porous 3D scaffold	Provide differentiation of neural stem/progenitor cells into neurons, astrocytes and oligodendrocytes	72
Amino ethyl methacrylate – Chitosan	Photoresponsive	Amino-ethyl methacrylate derivatized, degradable, photocrosslinkable chitosan 3D scaffolds	The scaffolds showed toxic effect against MSCs while enhancing the NSC differentiation into neurons and astrocytes	73
HRP catalyzed gelatin-hydroxyphenylpropionic acid hydrogels	Enzyme responsive	Provided the stiffness-dependent differentiation of human mesenchymal stem cells (hMCSs) on HRP catalyzed gelatin-hydroxyphenylpropionic acid hydrogels	The hydrogel stiffness stimulated neurogenesis and myogenesis of hMSCs along with high migration and proliferation rate. hMSCs encapsulated in soft hydrogels provided enhanced proliferation rate and neuronal protein marker expression compared to the hydrogels with higher stiffness	74 and 75
HRP catalyzed gelatin-hydroxyphenyl-propionic acid hydrogels	Enzyme responsive	Provided the stiffness-dependent differentiation of adult neural stem cells (aNSCs) on HRP catalyzed gelatin-hydroxyphenylpropionic acid hydrogels	Observed self-renewal and differentiation of aNSCs into central nervous system cell types. Stiffer hydrogels enhanced neuronal lineage differentiation of aNSCs, improved cell adhesion, oxidative stress resistance and cell proliferation and migration	76
Conductive polymers	Electrical stimuli responsive	NGF-doped PPy films,[77] PPy–PLGA,[78] PPy–PDLLA[79] and PLLA–PANI[80] scaffolds	Promoted survival, neurite outgrowth and density of viable neurons resulting in neural network formation	77–80

Collagen coated PPy scaffold	Electrical stimuli responsive	Inkjet-printed collagen-coated conductive PPy scaffold with guidance tracks	Enhanced guided neurite outgrowth	81
Gelatin-*graft*-polyaniline	Electrical stimuli responsive	*In situ* forming biodegradable electroactive gelatin-*graft*-polyaniline hydrogels by crosslinking with genipin at body temperature	Enhanced MSC adhesion and proliferation upon electrical stimuli	82
PPy/PMAS	Electrical stimuli responsive	PPy/PMAS composite films	Enhanced the NGF triggered neural differentiation of cells	83
Fibrillar collagen-coated PPy	Electrical stimuli responsive	Fibrillar collagen-coated PPy scaffolds	Enhanced neural differentiation of rat pheochromocytoma nerve cells when electrical stimulus was applied	84
Graphene foam	Electrical stimuli responsive	3D porous graphene foam with electrically conductive properties	Supported neural stem cell (NSC) growth with active proliferation state and enhanced NSC differentiation towards astrocytes and neurons through efficient electrical stimulation	85
Graphene	Electrical stimuli responsive	Graphene-coated substrate	Extremely low frequency electromagnetic fields enhanced neuronal differentiation of bone marrow-derived hMSCs	86
Graphene oxide	Electrical stimuli responsive	3D conductive nanofibers achieved through the controlled assembly of graphene oxide sheets into the electrospun polymer nanofiber surface	Enhanced electrical stimulation, accelerated cellular growth and primary motor neurons	87
Graphene oxide and gold nanoparticles	Electrical stimuli responsive	Gold nanoparticles containing 3D graphene oxide to monitor and detect the differentiation potential of neural stem cells (NSCs) using surface-enhanced Raman spectroscopy (SERS)	Promoted SERS signals of graphene oxide and gold nanoparticles for undifferentiated NSCs. Promising *in situ* monitoring tool for stem cell differentiation	88

engineering and cell delivery.[97–99] In these stimuli-responsive copolymer designs, the amphiphilic polymer chains self-assemble into micellar structures at low temperatures, whereas more hydrophobic segments leading to increased hydrophobicity and micellar aggregation form hydrogels at LCST.[100,101] For example, 3D hybrid scaffolds based on a temperature-responsive poly(ethylene glycol)–poly(L-alanine) (PEG–L-PA) polymer comprising neuronal differentiated tonsil-derived mesenchymal stem cells (TMSCs) and microspheres releasing growth factors were developed previously (Figure 14.1(A)).[37] The *in situ* formed gel mimicked the mechanical properties of brain tissue and showed robust characteristics enabling the presence of microspheres in the structure during 3D TMSCs culturing (Figure 14.1(B) and (C)).[37]

These synthetic block copolymers can also be used in combination with natural polymers to enhance their biocompatibility, biodegradability and mechanical properties. In a study, thermoresponsive and biodegradable scaffolds composed of thermoresponsive poly(*N*-isopropylacrylamide) (PNIPAAm), hydrolytically degradable and hydrophobic poly(L-lactic acid) (PLLA) and enzymatically degradable and hydrophilic natural dextran blocks were designed for nerve growth factor controlled release.[102]

Many natural temperature-responsive materials, such as cellulose derivatives, chitosan, gelatin, dextran *etc.*, have been used alone or in combination with synthetic polymers for the fabrication of thermoresponsive scaffolds.[103] Among those, a cellulose derivative, methylcellulose (MC), shows thermoresponsive gelation between 60 and 80 °C and liquification upon cooling.[104,105] Although the LCST range of MC is not suitable to show a thermoresponsive effect by direct body injection, particularly for neural tissue engineering applications, adjusting the LCST range is possible through grafting MC with other thermoresponsive materials (*i.e.* synthetic *N*-isopropylacrylamide) by changing their relative ratios as mentioned in previous work.[106] However, the application of methylcellulose for neural tissue engineering is limited by the low protein adsorption and cell adhesion properties. This issue was addressed through a bioactive scaffold, which was developed as a delivery vehicle for neural cell transplantation strategies in injured CNS tissue. In this strategy, laminin-1 was tethered to thermoresponsive MC through a Schiff base reaction occurring between the primary amine groups of laminin and the carbonyl groups of the oxidized MC chain.[38]

Another natural material, chitosan, obtained by deacetylation of chitin, mostly forms thermosensitive hydrogels with polyol salts.[107] A chitosan/glycerophosphate salt hydrogel was first developed for potential neural tissue engineering applications.[108] Following that, 3D chitosan/glycerophosphate salt hydrogels with thermoresponsive properties, containing immobilized poly-D-lysine, were fabricated *via* azidoaniline photocoupling, enhancing neurite outgrowth for neural tissue engineering.[39] It was noted that certain peptide polylysine concentrations improved neuronal adhesion and neurite outgrowth in 3D gel architectures mimicking the extracellular matrix. One problem with chitosan is the solubility and gelation issue at physiological pH, which can also be adjusted by grafting some hydrophilic moieties such as PEG.[103,109]

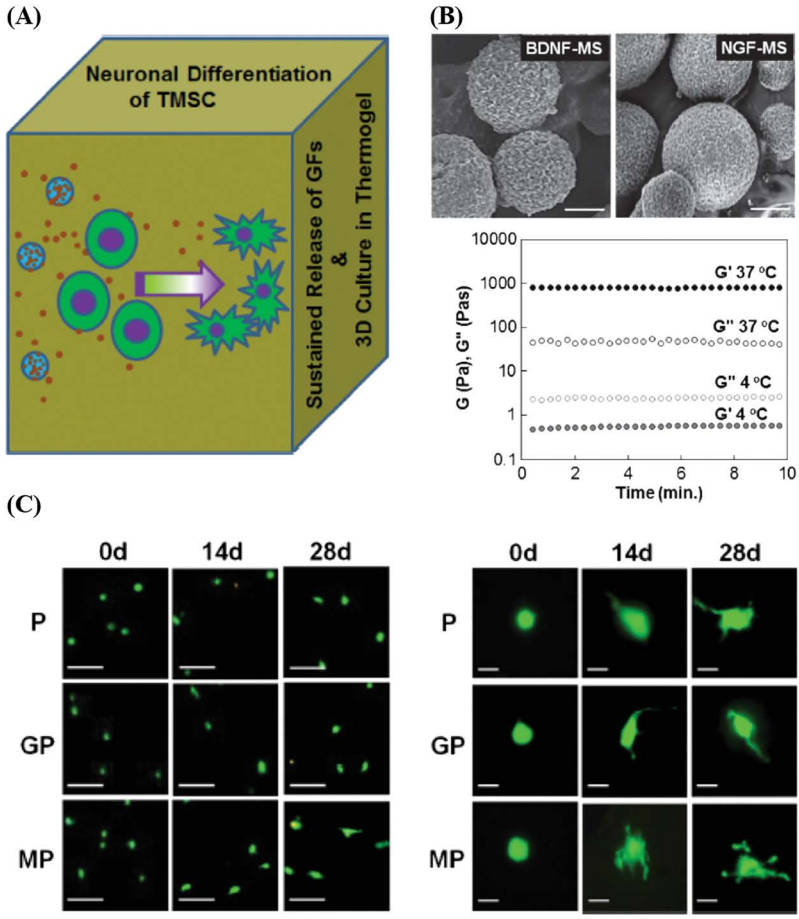

Figure 14.1 (A) 3D PEG–L-PA thermogel cell culture matrix incorporated with alginate microspheres containing neuronal growth factor. TMSCs' neuronal differentiation was manipulated by the controlled release of neuronal growth factors, BDNF and NGF. (B) SEM images of BDNF-loaded (BDNF–MS) and NGF-loaded (NGF–MS) alginate microspheres and storage (G′) and loss (G″) modulus of PEG–L-PA aqueous polymer solutions. (C) Cell images of TMSC after 3D culturing 0, 14, and 28 d in the absence of growth factor (P), presence of growth factor (GP), and 3D cell culture (MP) systems.[37] (Reproduced with permission from Patel *et al.*, *Adv. Healthcare Mater.*, **4**, 1565–1574, 2015. Copyright 2015: John Wiley and Sons.)

Xyloglucan, a biocompatible polysaccharide, shows thermoresponsive characteristics upon removal of more than 35% of galactose residues.[110] Although xyloglucan gels were previously demonstrated as potential drug carriers for different applications,[107] their application in neural tissue engineering was rare due to the limited rheological and morphological characteristics. Previous work examined the gelation properties and morphology of xyloglucan

hydrogels at physiological conditions,[111] which led to further development in thermoresponsive xyloglucan hydrogel scaffold functionalization through the immobilization and grafting of poly-D-lysine to promote neuron adhesion and neurite outgrowth for the spinal cord. It was shown that mechanical properties mimicking the native spinal cord and allowing neural stem cell migration, directed neurite growth and infiltration of axons, astrocytes and neurites with higher concentrations, were possible with these gels.[5,40–42]

14.2.2 pH-Responsive Biomaterials

The copolymerization of poly(NIPAAM) or block copolymer hydrogels with pH-sensitive acrylates, such as 2-(dimethylamino) ethyl methacrylate (DMAEMA) or 2-(diethylaminoethyl) methyl methacrylate (DEAEMA), enables both temperature- and pH-responsiveness. These dual-responsive polymers provided extended protein release in previous work.[112,113] Similarly, in our group, pH- and temperature-responsive, amphiphilic and cationic pentablock copolymers, composed of temperature-responsive Pluronic F127 (poly(ethyleneoxide)-*block*-poly(propyleneoxide)-*block*-poly(ethyleneoxide) (PEO-*b*-PPO-*b*-PEO)) mid-block and pH-responsive cationic PDEAEM (poly(2-diethylaminoethyl methacrylate)) end-blocks, were synthesized *via* atom transfer radical polymerization (ATRP). These polymers were used for both pDNA and siRNA delivery, as well as a vaccine carrier, due to their several advantages in eliminating the intra/extra cellular barriers over their counterparts (Figure 14.2). The central triblock, Pluronic F127, facilitates cellular entry *via* thermoresponsive micellization while the pH-responsive cationic end blocks, PDEAEM, enable complexation with negatively charged nucleic acids and endosomal escape.[43–47,50,51,54–59] The hydrophobic poly(propyleneoxide) (PPO) block in the middle of Pluronic F127 with a LCST of ~8 °C is responsible for the thermoreversible micellization. In addition, the hydrophobic nature of PPO chains enhances the particle–cell interactions, facilitates the particle incorporation into cell membranes and promotes cellular entry of delivery systems without altering cell membrane integrity.[48,49,53] The cationic end blocks, poly(diethylaminoethyl methacrylate) (PDEAEM) with a pK_a of ~7.3, provide electrostatic complexation with negatively charged pDNA or siRNA. Moreover, the pH buffering capacity of these segments through the presence of protonatable tertiary amine groups, facilitates the endosomal escape of the delivery system *via* the proton sponge mechanism at the low pH of the endosome.[45,48,57] Despite the advantages, pH-responsive hydrogels are not generally considered preferred cell carriers due to the *in vivo* biocompatibility and stability concerns. However, adjusting the balance between the cationic and non-ionic blocks makes it possible to manipulate the cytotoxicity of these copolymers.[47] In addition, the temperature- and pH-responsive gelation of these polymers was also reported as addressing the potential for 3D scaffolds, providing available space for cellular growth as well as acting like a depot for drug/neurotrophic factor delivery for neural tissue engineering applications.

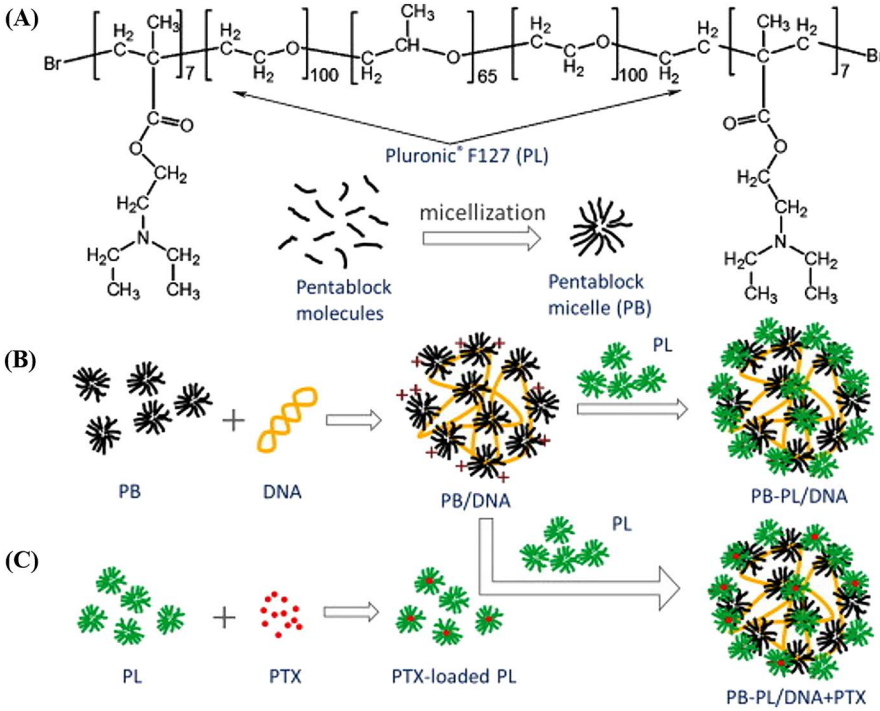

Figure 14.2 (A) Temperature- and pH-responsive self-assembly and micelle formation of pentablock copolymer molecules. (B) Polyplex formation with DNA through electrostatic attraction and shielding of excess positive charges *via* Pluronic self-assembly. (C) Self-assembly of polyplexes with Paclitaxel (PTX) encapsulated Pluronic to create a carrier loaded by both DNA and PTX for dual delivery.[56] Reproduced from *International Journal of Pharmaceuticals*, **427**(1), Zhang, B., Jia, F., Fleming, M. Q., Mallapragada, S. K., Injectable self-assembled block copolymers for sustained gene and drug co-delivery: An *in vitro* study, 88–96, Copyright (2012) with permission from Elsevier.

14.2.3 Self-Assembling Biomaterials

Responsive short peptides with self-assembly properties have shown promise in the development of 3D scaffolds for tissue engineering.[114,115] These peptides form higher order self-assembled structures through weak and non-covalent interactions. The adjustment of the amino acid sequence controls the formation of various secondary structures (such as β-sheets, β-hairpins and α-helices) and their bonding interactions (such as hydrogen bonding, ionic, electrostatic, hydrophobic and van der Waals), which in turn affect the spontaneous formation of nanofibers, 3D hydrogels and scaffolds.[116,117] These peptides have the advantage of possessing a shear thinning property and they form scaffolds under physiological conditions giving the ability of post-stress *in situ* self-assembly and mechanical recovery.

Various self-assembling peptides have successfully been used for neural cell culture. For example, nanofibrillar gels and scaffolds have been developed through spontaneous self-assembly of ionic self-complementary peptides while self-assembling peptide amphiphiles with biological signaling properties, such as IKVAV (isoleucine–lysine–valine–alanine–valine), have been used for 3D cell culture.[64,67,70,71] IKVAV, a laminin epitope, has been shown to enhance the differentiation of neural progenitor cells into neurons.[69] Similarly, the binding of LDLK12 self-assembling peptide to murine neural stem cell (NSC) derived neural precursor cells (NPCs) enhanced the viability and differentiation.[62] On the other hand, the spontaneous self-assembly of RADA16-like peptides (RADA16-I and RADA16-II) into antiparallel β-sheets under physiological conditions resulted in the formation of nano and microfibers. These fiber structures mimic the ECM structure, induce neurite outgrowth and synapse formation in PC12 cells[65,66] and facilitate neural stem cell proliferation and differentiation.[61,68] Moreover, RADA16-I has also been reported to induce osteoblast proliferation, differentiation, and migration. RADA16-I, possessing 99% water content, can resolve into natural amino acids and further be custom designed for the incorporation of functional segments (such as BMHP1 and 2). Because of these features, this peptide has been addressed as a promising self-assembling peptide for neural tissue engineering applications (Figure 14.3).[60,63] Considering their properties, self-assembling peptides are promising candidates for neural tissue engineering as responsive polymers.

14.2.4 Photo-Responsive Biomaterials

Photopolymerization enables the *in situ* formation of hydrogel scaffolds at physiological pH and temperature. Hydrogel scaffolds are mainly formed upon visible light/UV exposure through a reaction between free radicals, produced by decomposition of the photoinitiator, and polymerizable acrylate or methacrylate groups. Photo stimuli can be used for the encapsulation of viable cells without damaging the cell structure and by allowing favorable gelation conditions.[118] Photocrosslinkable polymers, such as poly(ethylene glycol)-diacrylate (PEGDA), poly(ethylene glycol)-dimethacrylate (PEGDMA), poly(propylene fumarate) (PPF) and oligo(poly(ethylene glyco) fumarate) (OPF) have been investigated for tissue engineering applications.[119–123] For instance, as an alternative to traditional photocuring methods, a 3D hydrogel scaffold based on photocurable poly(ethylene glycol) resin using novel custom built laser-based microstereolithography has recently been developed for the manufacture of a nerve growth conduit aimed at large peripheral nerve gaps. This method was proposed as a new platform for rapid microfabrication and the development of advanced designs.[118]

As an alternative to synthetic materials, natural photocrosslinkable hydrogel materials such as dextran, alginate, chitosan and hyaluronic acid have also been investigated recently along with methacrylation or copolymerization.[124–127] Photocrosslinkable methacrylamide chitosan was used to develop

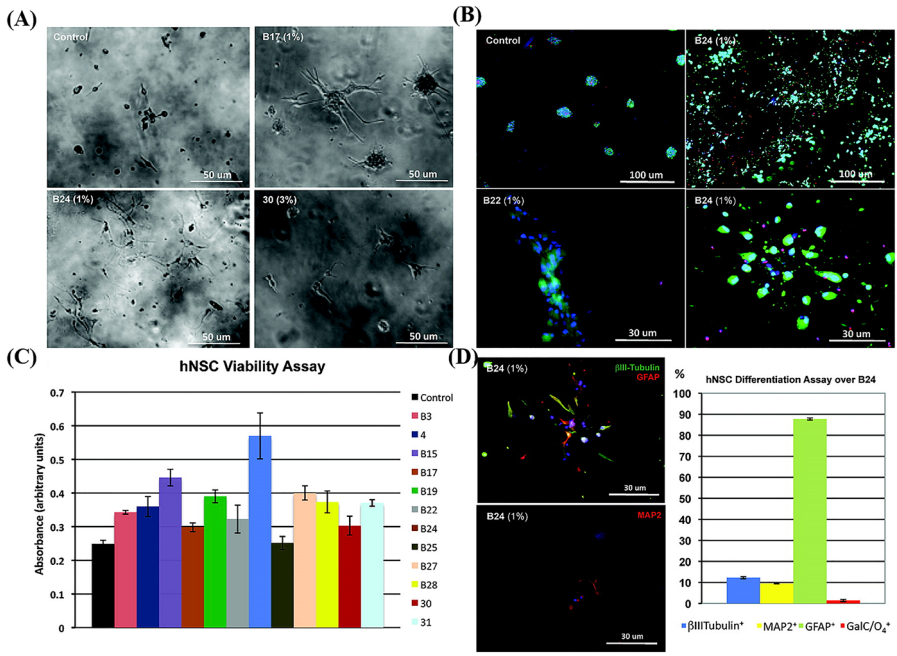

Figure 14.3 Human neural stem cells cultured on BMHP1-SAPs self-assembled scaffolds. (A) Branched and adhered cells. (B) Live/dead cell assays. (C) Cell titer assay of cells cultured for seven days over BMHP1-SAP scaffolds. (D) NSCs cultured for 14 DIV over B24 scaffolds.[63] (Reproduced with permission from Gelain *et al.*, *ACS Nano*, **5**, 1845–1859, 2011. Copyright 2011: American Chemical Society.)

a porous 3D scaffold for differentiation of neural stem/progenitor cells into neurons, astrocytes and oligodendrocytes.[72] In other work, amino-ethyl methacrylate derivatized, degradable, photocrosslinkable chitosan was developed to create 3D scaffolds for MSCs and neural stem cells. The scaffolds showed a toxic effect against MSCs while enhancing NSC differentiation into neurons and astrocytes.[73] Although the overall scaffolding performance of photo-responsive materials for stem-cell-based therapies is promising, they are not perfectly applicable for clinical purposes.

14.2.5 Enzyme-Responsive Biomaterials

Some materials show endogenous or exogenous enzyme initiated responses by forming *in situ* cross linking and gelation to create scaffolds. This approach is advantageous compared to the other scaffolding techniques by avoiding side reactions and potential toxicity issues due to the enzyme specificity. Although different enzymes have been used to provide *in situ* crosslinking or gelation, transglutaminases and horseradish peroxidases are the most

utilized enzymes to form scaffolds in tissue engineering applications.[128] A family of thiol enzymes, transglutaminases, catalyzes the reaction between the free amine groups of lysine and the g-carboxamide group of glutamine in a relatively fast time range (5–20 min) resulting in the formation of a stable covalent bond that is highly resistant to proteolysis. Although the applications of transglutaminases, particularly for promoting blood clotting, preventing bleeding and enhancing wound healing, are not common in neural regeneration, they have been used in combination with peptides or PEG for various biomedical applications.[129]

On the other hand, horseradish peroxidase (HRP), catalyzing the conjugation of phenol and aniline derivatives in the presence of hydrogen peroxide, is the most commonly used peroxidase in hydrogel scaffold formation along with natural and synthetic polymers for neural tissue engineering providing advantages such as adjustable stiffness, reaction rates, mild cross-linking conditions and good biocompatibility.[128] In particular, this approach provides wide control over the scaffold stiffness that affects cell proliferation, spreading migration and differentiation.

The stiffness-dependent differentiation of human mesenchymal stem cells (hMCSs) on HRP-catalyzed gelatin-hydroxyphenylpropionic acid hydrogels was shown previously.[74] The stiffness of the hydrogels was controlled within the range of 629–12 780 Pa by manipulating the hydrogen peroxide concentration. The neurogenesis and myogenesis of hMSCs along with high migration and proliferation rate were manipulated by hydrogel stiffness (Figure 14.4).[74] The same group also studied the differentiation behavior of hMSCs cultured in 3D hydrogels and reported an enhanced proliferation rate and neuronal protein marker expression in soft hydrogels containing hMSCs.[75] Similarly, adult neural stem cells (aNSCs) were cultured on the same 3D hydrogel system and showed growth and differentiation of aNSCs into central nervous system cell types. Interestingly, they reported enhanced differentiation of aNSCs into neuronal lineages in stiffer hydrogels as well as increased cell adhesion, proliferation, migration and oxidative stress resistance.[76]

14.2.6 Conductive, Electrical-Stimuli-Responsive Biomaterials

Electrical signals provide communication in the nervous system at physiological levels and cause charge gradients across cell membranes and nerves. Electrical fields or stimulations alter the ion channel distribution, modulate voltage-influenced channels and influence nerves at the molecular level by affecting proliferation, migration and axonal regeneration of cells.[130] Since damaged peripheral or spinal nerves require axonal regeneration and function for recovery, electrical stimulation has been used to enhance axonal growth and neuronal, astrocyte, and Schwann cell migration.[130–132] In order to facilitate these requirements, electrical-stimuli-responsive biomaterials, such as conductive polymers, electrets, piezoelectric and photovoltaic materials, are considered a new class of smart materials that can stimulate cells,

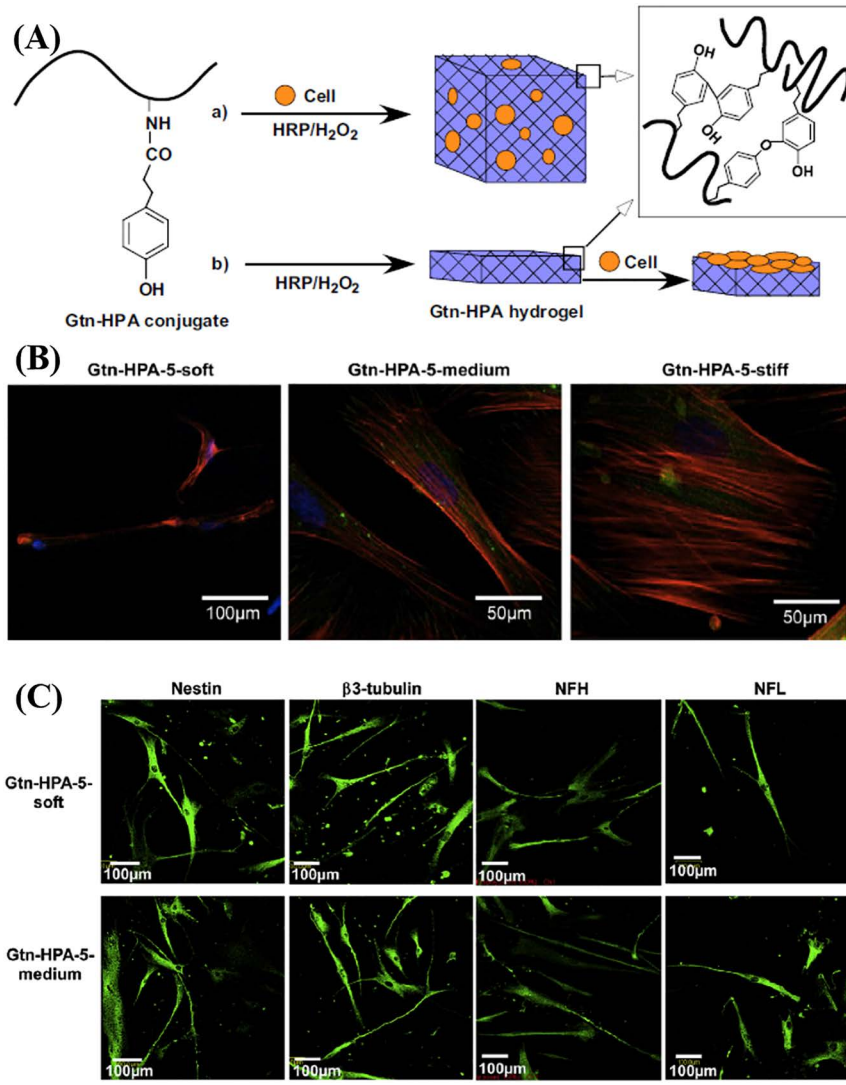

Figure 14.4 (A) Formation of GtneHPA hydrogels by enzyme-catalyzed oxidation for 3D and 2D cell growth and differentiation. (B) Confocal fluorescence microscopy of hMSCs cultured on GtneHPA hydrogels. (C) Immunofluorescence images of neurogenic protein markers.[74] Reproduced from *Biomaterials*, **31**(33), Wang, L.-S., Boulaire, J., Chan, P. P. Y., Chung, J. E., Kurisawa, M. The role of stiffness in gelatin–hydroxyphenylpropionic acid hydrogels formed by enzyme-mediated crosslinking on the differentiation of human mesenchymal stem cell, 8608–8616, Copyright (2010) with permission from Elsevier.

regulate specific cellular activities and influence nerve regeneration processes upon electrical exposure.[133] Amongst the others, since the self-powered electrets and piezoelectric materials do not need an external power source to transmit an electrical stimulus, the electrical stimulus control of these materials is limited.[134,135] On the other hand, conductive polymers, such as polypyrrole, polyaniline and poly(3,4-ethylenedioxythiophene), possessing good electrical properties with high conductivity/weight ratios, provide wide external control over the electrical stimulus. Moreover, the chemical, electrical, physical and structural properties of conductive materials along with their biocompatibility and biodegradability can be tailored through the incorporation of biological moieties such as antibodies, enzymes and others, and further controlled by external or internal stimulation depending on the type of application.[134–136] Considering the advantages of conductive materials, particularly conductive polymers, and the noted positive effects of electrical stimulation on nerve regeneration, these materials lend themselves as excellent scaffolds for neural tissue engineering purposes.

The application of electrical stimuli resulted in significant neurite extension in nerve cells. For example, PC-12 cells have been reported to show enhanced neurite outgrowth on NGF-doped PPy films[77] and PPy–PLGA,[78] PPy–PDLLA[79] and PLLA–PANI[80] scaffolds upon electrical stimuli exposure. In a recent study, an inkjet-printed collagen-coated conductive PPy scaffold was developed with guidance tracks and showed enhanced guided neurite outgrowth along with the direction of the tracks upon electrical stimuli in PC-12 cells.[81] Similar effects were also reported for the electrically stimulated neural cells on nanofibrous PANI–PG scaffolds.[137] In a different study, the potential of small diameter (<400 μm) fibers consisting of electrically conductive polyaniline and polypropylene (PA–PP) blends was addressed for neural regeneration. These conductive fibers embedded in an agarose matrix along with primary dorsal root ganglion neurons promoted survival, adhesion, neurite outgrowth and density of viable neurons resulting in neural network formation directly along the fibers.[138] The enhanced neurite growth, increased neuron density and formation of neural networks upon electrical stimuli could be a result of the improved fibronectin adsorption onto the conductive polymer scaffolds along with the formed proteins and ion channels within the cell membrane.

The applied electrical stimuli can also enhance the adhesion, proliferation, spreading and migration of the neural cells. *In situ* forming biodegradable electroactive hydrogel gelatin-*graft*-polyaniline was developed by crosslinking with genipin at body temperature. This *in situ* formed degradable electroactive biomimetic hydrogel scaffold provided efficient electrical stimuli enhancing MSC adhesion and proliferation.[82]

Besides the neurite outgrowth, cellular adhesion and proliferation, applied electrical stimuli also promote neural differentiation. For instance, the 250 Hz biphasic current applied through PPy/PMAS composite films was observed to enhance the neural differentiation in the presence of NGF.[83] Similarly, rat pheochromocytoma nerve cells, grown on fibrillar collagen-coated

PPy scaffolds, enhanced neural differentiation when an electrical stimulus was applied.[84] Schwann cells, producing a myelin sheath around neuronal axons for the peripheral nervous system, also demonstrated good viability and increased NGF and BDNF secretion capacity upon application of an electrical stimulus of 100 mV mm^{-1} on chitosan–PPy composite scaffolds.[139] The enhanced adhesion, proliferation and differentiation of neural cells cultured on hybrid hydrogel scaffolds obtained by chemical and electropolymerization of poly(3,4-ethylenedioxythiophene) (PEDOT) and polyurethane (PU), giving rise to strong bonding of a conductive composite with an elastic double-network was also reported.[140] The possible mechanisms of electrical stimulation on cell differentiation were hypothesized to be based on altering membrane potential through hyperpolarization and depolarization,[141] modification of ion channels including density and distribution of receptors, calcium channel activation,[142] and up-regulation of the ERK pathway.[143–145] In addition, the activation of various signaling pathways such as MAPK, PI3K and ROCK,[146,147] and the increase in intracellular ROS generation[148] were pointed out as other reasons of electro-trans differentiation.[146,149] However, all of these studies used chemical- or growth-factor-based stimuli along with the electrical stimuli for the differentiation. Therefore, the exact mechanism of electrical stimuli in stem cell differentiation is still unresolved.

Graphene, composed of a single-atom-thick sheet of carbon atoms arranged in a hexagonal lattice, has been extensively used in a plethora of biotechnological/biomedical applications and translational research including bioassays,[150] biosensors,[151,152] photothermal anticancer therapy,[153] electrical stimulation of cells[154] and drug delivery.[155] Recently, the potential of this non-cytotoxic and biocompatible and conductive material has been exploited as a scaffold for cell growth, differentiation, and fate conversion in tissue engineering and regenerative medicine.[156–159] The unique physical, chemical and mechanical properties[160,161] as well as the non-toxic, biocompatible, conductive and stable nature of graphene have revealed its potential as a functional scaffold material mediating cell growth, proliferation, differentiation, and alteration of cell fate in tissue engineering.[86,154,162–168] Graphene-based conductive substrates support electrically stimulated neuronal differentiation of stem cells and provide a promising platform for neural regeneration. It was previously reported that a 3D porous graphene foam with electrically conductive properties supported neural stem cell (NSC) growth with an active proliferation state and enhanced NSC differentiation towards astrocytes and neurons through efficient electrical stimulation implicating the potential use of graphene for neural tissue engineering.[85] In another study, extremely low frequency electromagnetic fields (50 Hz, 1 mT) were reported to enhance neuronal differentiation of bone-marrow-derived human mesenchymal stem cells grown on a graphene-coated substrate (Figure 14.5). It was noted that the enhancement in neurogenesis resulted from the alteration of gene expression profile, up-regulation of cell adhesion through intracellular calcium influx and the activation of the focal adhesion kinase signaling pathway, which is stimulated by extracellular matrix production.[86]

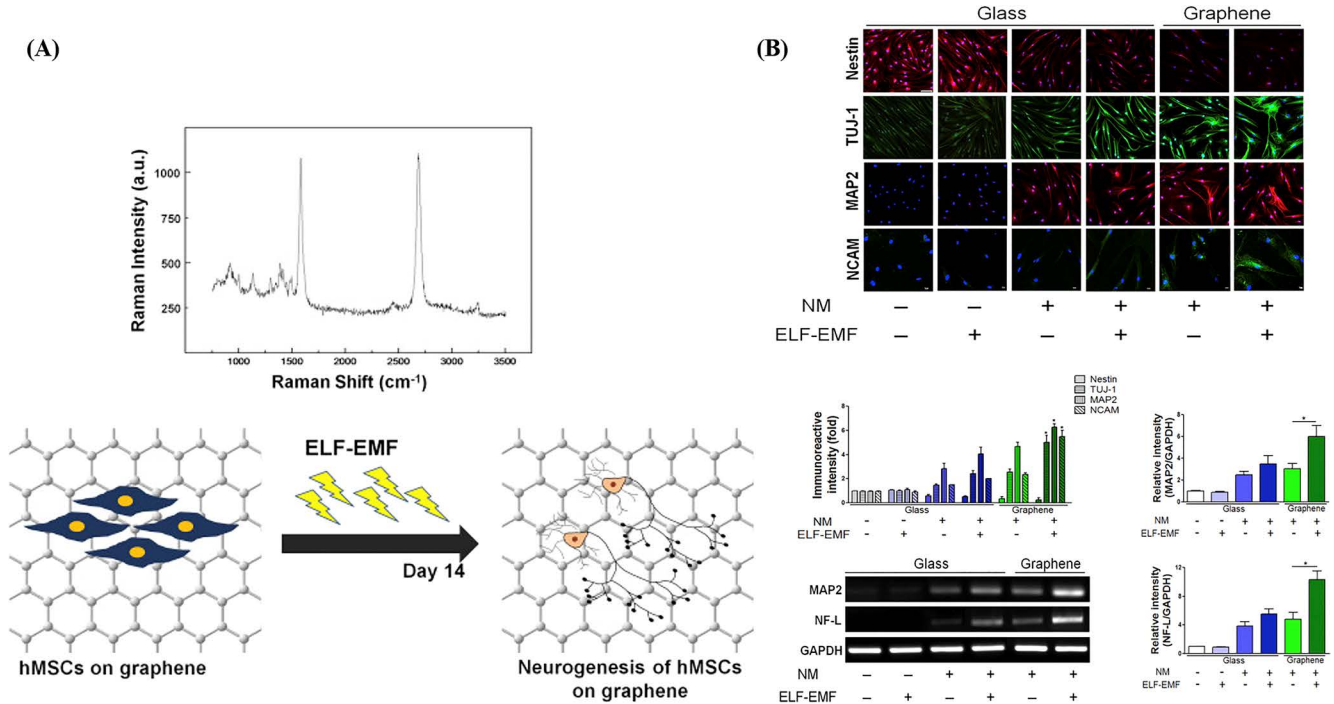

Figure 14.5 (A) Electromagnetic field (EMF)-triggered neuronal differentiation of hMSCs on the graphene-coated substrate. (B) Confocal images indicating the immunostaining of nestin, TUJ-1, MAP2, and NCAM neuronal markers and quantification of fluorescent intensities in hMSCs.[86] Reproduced from *Current Applied Physics*, **15**, Lee, Y.-J., Jang, W., Im, H., Sung, J.-S. Extremely low frequency electromagnetic fields enhance neuronal differentiation of human mesenchymal stem cells on grapheme-based substrates, S95–S102, Copyright (2015) with permission from Elsevier.

A novel strategy has been introduced to fabricate 3D conductive nanofibers through the controlled assembly of graphene oxide sheets into an electrospun polymer nanofiber surface providing flexibility, high electrical conductivity, and uniform 3D nanofiber morphology. This novel strategy and nanofibers enhanced electrical stimulation, accelerated cellular growth and primary motor neuron development.[87] Although the electrically conductive nature of graphene promotes many cellular properties, the exact differentiation mechanism mediated by the graphene substrate is not fully understood. In addition to being used as a 3D conductive scaffold for neural differentiation, graphene can also be used as a monitoring device. Gold nanoparticles encapsulated with 3D graphene oxide were used as a non-destructive detection tool to monitor and detect neural stem cells' (NSCs) differentiation by surface-enhanced Raman spectroscopy (SERS). This new material was capable of promoting the double enhancement effect of graphene oxide and gold nanoparticles on SERS signals for undifferentiated NSCs and showed promise as a non-destructive *in situ* monitoring tool for the identification of the differentiation potential of various kinds of stem cells.[88]

14.3 Functional Delivery Systems for the BBB

The efficient treatment of neurodegenerative diseases affecting the central nervous system lies in the development of smart delivery systems that can cross the blood–brain barrier (BBB) and reach target tissues with their payloads. The recent advances in smart and stimuli-responsive natural or synthetic functional materials offer various opportunities for the development and design of smart vehicles able to cross the BBB.[4]

There are two common strategies for nanoparticles to cross the BBB: (1) receptor-mediated, which is achieved by ligand binding, targeting the surface expressed receptor on the brain capillary endothelial cells or (2) adsorptive mediated, in which the particle is adsorbed to the brain capillary endothelial cell membrane. These methods have been applied to polymer-, liposome-, solid-lipid-nanoparticle- and inorganic-nanoparticle-based delivery systems to improve the delivery of therapeutics across the BBB. In the receptor-mediated transcytosis, surface nanoparticles were modified by endogenous ligands, peptides and antibodies against the receptors including low density lipoprotein receptor, transferrins, leptins, epidermal growth factor, diphtheria toxin, and insulin to improve transport through the BBB. Surface modifications of particles to create smart systems through a receptor-mediated approach for BBB penetration were summarized in our previous work.[2] Despite the advantages, receptor-mediated endothelial transcytosis is limited by the quantity of receptors on the cell surface and the lack of specificity. On the other hand, cell-penetrating peptides, responding to intracellular or extracellular stimuli, enhance the delivery of nanoparticles by adsorption-mediated transcytosis. Examples include the human immunodeficiency virus type 1 transactivator of transcription protein, poly-arginines, and Syn-B vectors. The herpes simplex virus type 1 peptide (gH625) has also been shown

to increase the transport of polystyrene particles across the BBB. Peptides have been used in combination with polymers. Recently, a dual-functional drug delivery carrier was developed based on a PEG–PLA polymer surface modified by a 12-amino acid peptide, TGNYKALHPHNG (TGN) and a D-enantiomeric peptide, QSHYRHISPAQV (QSH), to target and potentially treat Alzheimer's disease. This dual-functional drug delivery system can diminish cytotoxicity to normal tissues and help to improve early diagnosis or treatment of Alzheimer's disease.[169,170]

14.4 Clinical Potential and Applications of Smart Materials in Neural Tissue Engineering

Smart biomaterials have been considered as potent tools to overcome various clinical challenges in drug delivery, imaging, diagnostics and therapeutics.[171] However, their potential for neural tissue engineering and nerve regeneration is still limited and needs further development.

A number of clinical trials employing bioengineering strategies have been conducted for the treatment of spinal cord injuries. In one of the studies, autologous transplantation of neural stem cells with a biocompatible matrix, RMx Biomatrix, for traumatic spinal cord injuries is currently in the recruitment phase (NCT0232666) (Federal Research Clinical Center of Federal Medical & Biological Agency 2015). In another study, a company, InVivo Therapeutics, is testing PLGA poly-L-lysine-based scaffolds seeded with neural stem cells for the treatment of complete thoracic traumatic acute spinal cord injuries (NCT02138110). Another functional collagen scaffold is also being tested for transplantation in acute spinal cord injury patients by The Chinese Academy of Sciences (NCT02510365). A similar clinical trial based on collagen-scaffold-containing mesenchymal stem cells for transplantation in spinal cord injuries has also been supported by the same institute (NCT02352077). There are also other biomaterial-based clinical trials for the treatment of peripheral nerve damage. Bovine-type-I-collagen-based conduits of varying caliber have been tested in clinical trials by NeuraGen to recover peripheral nerve gaps larger than 5 mm.[172,173] RWTH Aachen University sponsored a clinical trial to test the porcine-collagen-based nerve guide, Neuromaix, to create a conduit for axonal growth and to bridge large peripheral nerve discontinuity (NCT01884376). Neuromaix is composed of two parts: Epimaix enables the structural characteristics and avoids ingrowth of scar tissue while Perimaix provides structure-mimicking endoneurial tubes providing guidance for the regenerating axons. The University of Alberta is conducting a clinical trial to evaluate the possible benefit of electrical stimulation of the injured nerve following surgery (NCT02403661), which can further be improved by using electrically conductive biomaterials for peripheral nerve regeneration.

As summarized above, there is a huge potential and effort for the clinical applications of biomaterials to facilitate nerve regeneration. However, the clinical translation of smart biomaterials still needs further evaluation and development.

14.5 Conclusions and Future Outlook

As summarized above, stimuli-responsive smart biomaterials serve as enabling technologies to overcome significant challenges associated with drug- and cell-based therapies addressing disorders in neural tissue engineering and nerve regeneration. As described here, smart-biomaterial-based systems with appropriate chemistries and functionalization can be extremely promising for safe, effective, targeted, site-specific, and sustained delivery of bioactive agents and stem-cell-based therapies to treat disorders of the nervous system. A combination of bioactive agent delivery and stem-cell-based therapies along with the use of smart biomaterials can significantly impact neuroregeneration. They also offer new ways for therapeutics and imaging agents to traverse the BBB. Future studies will continue to investigate strategies using stimuli-responsive smart biomaterials to engineer 3D biomimetic scaffolds with various functionalities that can be used to regulate stem cell fate. These smart biomaterials can significantly impact not only the therapies of nervous system disorders but also potentially facilitate diagnosis for the detection of neural disorders paving the way for translation to clinic.

Acknowledgements

The authors would like to acknowledge the US Army Medical Research and Materiel Command under contract W81XWH-11–1–0700 and the Stem Cell Biology Fund for funding this work. We are also grateful to the Stanley Endowed Chair for providing additional funds in support of this work.

References

1. X. Gu, *Front. Med.*, 2015, **9**, 401–411.
2. S. K. Mallapragada, T. M. Brenza, J. M. McMillan, B. Narasimhan, D. S. Sakaguchi, A. D. Sharma, S. Zbarska and H. E. Gendelman, *Nanomedicine*, 2015, **11**, 715–729.
3. I. E. Donaghue, R. Tam, M. V. Sefton and M. S. Shoichet, *J. Controlled Release*, 2014, **190**, 219–227.
4. H. Peluffo, U. Unzueta, M. L. Negro-Demontel, Z. Xu, E. Vaquez, N. Ferrer-Miralles and A. Villaverde, *Biotechnol. Adv.*, 2015, **33**, 277–287.
5. D. R. Nisbet, K. E. Crompton, M. K. Horne, D. I. Finkelstein and J. S. Forsythe, *J. Biomed. Mater. Res., Part B*, 2008, **87B**, 251–263.
6. X. Gu, F. Ding and D. F. Williams, *Biomaterials*, 2014, **35**, 6143–6156.
7. S. M. Willerth and S. E. Sakiyama-Elbert, *Adv. Drug Delivery Rev.*, 2007, **59**, 325–338.
8. G. A. A. Saracino, D. Cigognini, D. Silva, A. Caprini and F. Gelain, *Chem. Soc. Rev.*, 2013, **42**, 225–262.
9. M. S. Kim and H. B. Lee, *Tissue Eng., Part A*, 2014, **20**, 1781–1783.
10. M. Goldsmith, L. Abramovitz and D. Peer, *ACS Nano*, 2014, **8**, 1958–1965.

11. A. Rajaram, X.-B. Chen and D. J. Schreyer, *Tissue Eng., Part B*, 2012, **18**, 454–467.
12. S. Abraham, N. Eroshenko and R. R. Rao, *Regener. Med.*, 2009, **4**, 561–578.
13. C. Chai and K. W. Leong, *Mol. Ther.*, 2007, **15**, 467–480.
14. J. M. Corey, D. Y. Lin, K. B. Mycek, Q. Chen, S. Samuel, E. L. Feldman and D. C. Martin, *J. Biomed. Mater. Res., Part A*, 2007, **83**, 636–645.
15. C. Cunha, S. Panseri and S. Antonini, *Nanomedicine*, 2011, **7**, 50–59.
16. J. M. Dang and K. W. Leong, *Adv. Drug Delivery Rev.*, 2006, **58**, 487–499.
17. P. de Vos, H. A. Lazarjani, D. Poncelet and M. M. Faas, *Adv. Drug Delivery Rev.*, 2014, **67–68**, 15–34.
18. B. Dhandayuthapani, Y. Yoshida, T. Maekawa and D. S. Kumar, *Int. J. Polym. Sci.*, 2011, **2011**, 1–19.
19. I. Elliott Donaghue, R. Tam, M. V. Sefton and M. S. Shoichet, *J. Controlled Release*, 2014, **190**, 219–227.
20. L. Gasperini, J. F. Mano and R. L. Reis, *J. R. Soc., Interface*, 2014, **11**, 20140817.
21. L. Ghasemi-Mobarakeh, M. P. Prabhakaran, M. Morshed, M.-H. Nasr-Esfahani and S. Ramakrishna, *Biomaterials*, 2008, **29**, 4532–4539.
22. S. GhoshMitra, D. R. Diercks, N. C. Mills, D. L. Hynds and S. Ghosh, *Adv. Drug Delivery Rev.*, 2012, **64**, 110–125.
23. R. D. Keeley, K. D. Nguyen, M. J. Stephanides, J. Padilla and J. M. Rosen, *J. Reconstr. Microsurg.*, 1991, **7**, 93–100.
24. H. F. Ko, C. Sfeir and P. N. Kumta, *Philos. Trans. R. Soc., A*, 2010, **368**, 1981–1997.
25. S. G. Kumbar, C. T. Laurencin and M. Deng, *Nat. Synth. Biomed. Polym.*, 2014, 1–402.
26. W. B. Liechty, D. R. Kryscio, B. V. Slaughter and N. A. Peppas, *Annu. Rev. Chem. Biomol. Eng.*, 2010, **1**, 149–173.
27. S. Panseri, C. Cunha, J. Lowery, U. Del Carro, F. Taraballi, S. Amadio, A. Vescovi and F. Gelain, *BMC Biotechnol.*, 2008, **8**, 39.
28. S. Patel, K. Kurpinski, R. Quigley, H. Gao, B. S. Hsiao, M. M. Poo and S. Li, *Nano Lett.*, 2007, **7**, 2122–2128.
29. E. Schnell, K. Klinkhammer, S. Balzer, G. Brook, D. Klee, P. Dalton and J. Mey, *Biomaterials*, 2007, **28**, 3012–3025.
30. S. A. Sell, P. S. Wolfe, K. Garg, J. M. McCool, I. A. Rodriguez and G. L. Bowlin, *Polymers*, 2010, **2**, 522–553.
31. F. Yang, R. Murugan, S. Wang and S. Ramakrishna, *Biomaterials*, 2005, **26**, 2603–2610.
32. D. M. Yoon and J. P. Fisher, *Biomed. Mater.*, 2009, 415–442.
33. J. Zhu and R. E. Marchant, *Expert Rev. Med. Devices*, 2011, **8**, 607–626.
34. N. Comolli, B. Neuhuber, I. Fischer and A. Lowman, *Acta Biomater.*, 2009, **5**, 1046–1055.
35. R. Liu, M. Fraylich and B. R. Saunders, *Colloid Polym. Sci.*, 2009, **287**, 627–643.
36. S. Ohya, Y. Nakayama and T. Matsuda, *J. Artif. Organs*, 2004, **7**, 181–186.
37. M. Patel, H. J. Moon, B. K. Jung and B. Jeong, *Adv. Healthcare Mater.*, 2015, **4**, 1565–1574.

38. S. E. Stabenfeldt, A. J. Garcia and M. C. LaPlaca, *J. Biomed. Mater. Res., Part A*, 2006, **77A**, 718–725.
39. K. E. Crompton, J. D. Goud, R. V. Bellamkonda, T. R. Gengenbach, D. I. Finkelstein, M. K. Horne and J. S. Forsythe, *Biomaterials*, 2007, **28**, 441–449.
40. D. R. Nisbet, D. Moses, T. R. Gengenbach, J. S. Forsythe, D. I. Finkelstein and M. K. Horne, *J. Biomed. Mater. Res., Part A*, 2009, **89A**, 24–35.
41. D. R. Nisbet, D. Moses, T. R. Gengenbach, J. S. Forsythe, D. I. Finkelstein and M. K. Horne, *J. Biomed. Mater. Res., Part A*, 2009, **89**, 24–35.
42. D. R. Nisbet, A. E. Rodda, M. K. Horne, J. S. Forsythe and D. I. Finkelstein, *Tissue Eng., Part A*, 2010, **16**, 2833–2842.
43. J. R. Adams and S. K. Mallapragada, *Macromol. Chem. Phys.*, 2013, **214**, 1321–1325.
44. A. Agarwal and S. K. Mallapragada, *Curr. Top. Med. Chem.*, 2008, **8**, 311–330.
45. A. Agarwal, R. Unfer and S. K. Mallapragada, *J. Controlled Release*, 2005, **103**, 245–258.
46. A. Agarwal, R. Unfer and S. K. Mallapragada, *J. Biomed. Mater. Res., Part A*, 2007, **81A**, 24–39.
47. A. Agarwal, R. C. Unfer and S. K. Mallapragada, *Biomaterials*, 2008, **29**, 607–617.
48. A. Agarwal, R. Vilensky, A. Stockdale, Y. Talmon, R. C. Unfer and S. K. Mallapragada, *J. Controlled Release*, 2007, **121**, 28–37.
49. E. V. Batrakova, S. Li, S. V. Vinogradov, V. Y. Alakhov, D. W. Miller and A. V. Kabanov, *J. Pharmacol. Exp. Ther.*, 2001, **299**, 483–493.
50. M. D. Determan, J. P. Cox and S. K. Mallapragada, *J. Biomed. Mater. Res., Part A*, 2007, **81A**, 326–333.
51. M. D. Determan, J. P. Cox, S. Seifert, P. Thiyagarajan and S. K. Mallapragada, *Polymer*, 2005, **46**, 6933–6946.
52. A. V. Kabanov, E. V. Batrakova and V. Y. Alakhov, *J. Controlled Release*, 2002, **82**, 189–212.
53. N. S. Melik-Nubarov, O. O. Pomaz, T. Dorodnych, G. A. Badun, A. L. Ksenofontov, O. B. Schemchukova and S. A. Arzhakov, *FEBS Lett.*, 1999, **446**, 194–198.
54. M. Uz, S. K. Mallapragada and S. A. Altinkaya, *RSC Adv.*, 2015, **5**, 43515–43527.
55. B. Zhang, Y. Zhang, S. K. Mallapragada and A. R. Clapp, *ACS Nano*, 2011, **5**, 129–138.
56. B. Q. Zhang, F. Jia, M. Q. Fleming and S. K. Mallapragada, *Int. J. Pharm.*, 2012, **427**, 88–96.
57. B. Q. Zhang, M. Kanapathipillai, P. Bisso and S. Mallapragada, *Pharm. Res.*, 2009, **26**, 700–713.
58. B. Q. Zhang and S. Mallapragada, *Acta Biomater.*, 2011, **7**, 1570–1579.
59. B. Q. Zhang and S. Mallapragada, *Acta Biomater.*, 2011, **7**, 1580–1587.
60. C. Cunha, S. Panseri, O. Villa, D. Silva and F. Gelain, *Int. J. Nanomed.*, 2011, **6**, 943–955.
61. F. Gelain, D. Bottai, A. Vescovi and S. Zhang, *PLoS One*, 2006, **1**, e119.

62. F. Gelain, D. Cigognini, A. Caprini, D. Silva, B. Colleoni, M. Donega, S. Antonini, B. E. Cohen and A. Vescovi, *Nanoscale*, 2012, **4**, 2946–2957.
63. F. Gelain, D. Silva, A. Caprini, F. Taraballi, A. Natalello, O. Villa, K. T. Nam, R. N. Zuckermann, S. M. Doglia and A. Vescovi, *ACS Nano*, 2011, **5**, 1845–1859.
64. A. Gritti, E. A. Parati, L. Cova, P. Frolichsthal, R. Galli, E. Wanke, L. Faravelli, D. J. Morassutti, F. Roisen, D. D. Nickel and A. L. Vescovi, *J. Neurosci.*, 1996, **16**, 1091–1100.
65. T. C. Holmes, S. de Lacalle, X. Su, G. Liu, A. Rich and S. Zhang, *Proc. Natl. Acad. Sci. U. S. A.*, 2000, **97**, 6728–6733.
66. Q. Li and Y. Chau, *J. Biomed. Mater. Res., Part A*, 2010, **94**, 688–699.
67. B. A. Reynolds and S. Weiss, *Science*, 1992, **255**, 1707–1710.
68. C. E. Semino, J. Kasahara, Y. Hayashi and S. Zhang, *Tissue Eng.*, 2004, **10**, 643–655.
69. G. A. Silva, C. Czeisler, K. L. Niece, E. Beniash, D. A. Harrington, J. A. Kessler and S. I. Stupp, *Science*, 2004, **303**, 1352–1355.
70. F. Taraballi, M. Campione, A. Sassella, A. Vescovi, A. Paleari, W. Hwang and F. Gelain, *Soft Matter*, 2009, **5**, 660–668.
71. A. L. Vescovi, E. A. Parati, A. Gritti, P. Poulin, M. Ferrario, E. Wanke, P. Frolichsthal-Schoeller, L. Cova, M. Arcellana-Panlilio, A. Colombo and R. Galli, *Exp. Neurol.*, 1999, **156**, 71–83.
72. H. Li, A. Wijekoon and N. D. Leipzig, *PLoS One*, 2012, **7**(11), e48824.
73. C. M. Valmikinathan, V. J. Mukhatyar, A. Jain, L. Karumbaiah, M. Dasari and R. V. Bellamkonda, *Soft Matter*, 2012, **8**, 1964–1976.
74. L.-S. Wang, J. Boulaire, P. P. Y. Chan, J. E. Chung and M. Kurisawa, *Biomaterials*, 2010, **31**, 8608–8616.
75. L.-S. Wang, J. E. Chung, P. Pui-Yik Chan and M. Kurisawa, *Biomaterials*, 2010, **31**, 1148–1157.
76. T. C. Lim, W. S. Toh, L.-S. Wang, M. Kurisawa and M. Spector, *Biomaterials*, 2012, **33**, 3446–3455.
77. N. Gomez and C. E. Schmidt, *J. Biomed. Mater. Res., Part A*, 2007, **81A**, 135–149.
78. J. Y. Lee, C. A. Bashur, A. S. Goldstein and C. E. Schmidt, *Biomaterials*, 2009, **30**, 4325–4335.
79. H. Xu, J. M. Holzwarth, Y. Yan, P. Xu, H. Zheng, Y. Yin, S. Li and P. X. Ma, *Biomaterials*, 2014, **35**, 225–235.
80. M. P. Prabhakaran, L. Ghasemi-Mobarakeh, G. Jin and S. Ramakrishna, *J. Biosci. Bioeng.*, 2011, **112**, 501–507.
81. B. Weng, X. Liu, R. Shepherd and G. G. Wallace, *Synth. Met.*, 2012, **162**, 1375–1380.
82. L. Li, J. Ge, B. Guo and P. X. Ma, *Polym. Chem.*, 2014, **5**, 2880–2890.
83. X. Liu, K. J. Gilmore, S. E. Moulton and G. G. Wallace, *J. Neural. Eng.*, 2009, **6**, 065002.
84. X. Liu, Z. Yue, M. J. Higgins and G. G. Wallace, *Biomaterials*, 2011, **32**, 7309–7317.
85. N. Li, Q. Zhang, S. Gao, Q. Song, R. Huang, L. Wang, L. Liu, J. Dai, M. Tang and G. Cheng, *Sci. Rep.*, 2013, **3**, 1604.

86. Y.-J. Lee, W. Jang, H. Im and J.-S. Sung, *Curr. Appl. Phys.*, 2015, **15**, S95–S102.
87. Z.-Q. Feng, T. Wang, B. Zhao, J. Li and L. Jin, *Adv. Mater.*, 2015, **27**, 6462–6468.
88. T.-H. Kim, K.-B. Lee and J.-W. Choi, *Biomaterials*, 2013, **34**, 8660–8670.
89. C. Alexander, *Expert Opin. Drug Delivery*, 2006, **3**, 573–581.
90. Z. Mao, L. Ma, J. Yan, M. Yan, C. Gao and J. Shen, *Biomaterials*, 2007, **28**, 4488–4500.
91. E. Salcher and E. Wagner, in *Nucleic Acid Transfection*, ed. W. Bielke and C. Erbacher, Springer Berlin Heidelberg, 2010, vol. 296, pp. 227–249.
92. M. Talelli and W. E. Hennink, *Nanomedicine (Lond.)*, 2011, **6**, 1245–1255.
93. J. Guan, Y. Hong, Z. Ma and W. R. Wagner, *Biomacromolecules*, 2008, **9**, 1283–1292.
94. S. Qin, Y. Geng, D. E. Discher and S. Yang, *Adv. Mater.*, 2006, **18**, 2905–2909.
95. S. B. Lee, D. I. Ha, S. K. Cho, S. J. Kim and Y. M. Lee, *J. Appl. Polym. Sci.*, 2004, **92**, 2612–2620.
96. H. Tan, C. M. Ramirez, N. Miljkovic, H. Li, J. P. Rubin and K. G. Marra, *Biomaterials*, 2009, **30**, 6844–6853.
97. C. Gong, S. Shi, P. Dong, B. Kan, M. Gou, X. Wang, X. Li, F. Luo, X. Zhao, Y. Wei and Z. Qian, *Int. J. Pharm.*, 2009, **365**, 89–99.
98. C. Hiemstra, Z. Zhong, L. Li, P. J. Dijkstra and J. Feijen, *Biomacromolecules*, 2006, **7**, 2790–2795.
99. W. S. Shim, J.-H. Kim, H. Park, K. Kim, I. Chan Kwon and D. S. Lee, *Biomaterials*, 2006, **27**, 5178–5185.
100. M. D. Determan, L. Guo, C. T. Lo, P. Thiyagarajan and S. K. Mallapragada, *Phys. Rev. E*, 2008, **78**, 9.
101. S. Peleshanko, K. D. Anderson, M. Goodman, M. D. Determan, S. K. Mallapragada and V. V. Tsukruk, *Langmuir*, 2007, **23**, 25–30.
102. X. Huang, L. Wu, X. Li and T. L. Lowe, *Macromol. Symp.*, 2012, **317–318**, 301–309.
103. L. Klouda and A. G. Mikos, *Eur. J. Pharm. Biopharm.*, 2008, **68**, 34–45.
104. L. Li, H. Shan, C. Y. Yue, Y. C. Lam, K. C. Tam and X. Hu, *Langmuir*, 2002, **18**, 7291–7298.
105. M. Takahashi, M. Shimazaki and J. Yamamoto, *J. Polym. Sci., Part B: Polym. Phys.*, 2001, **39**, 91–100.
106. W. Liu, B. Zhang, W. W. Lu, X. Li, D. Zhu, K. De Yao, Q. Wang, C. Zhao and C. Wang, *Biomaterials*, 2004, **25**, 3005–3012.
107. E. Ruel-Gariépy and J.-C. Leroux, *Eur. J. Pharm. Biopharm.*, 2004, **58**, 409–426.
108. A. Chenite, C. Chaput, D. Wang, C. Combes, M. D. Buschmann, C. D. Hoemann, J. C. Leroux, B. L. Atkinson, F. Binette and A. Selmani, *Biomaterials*, 2000, **21**, 2155–2161.
109. N. Bhattarai, F. A. Matsen and M. Zhang, *Macromol. Biosci.*, 2005, **5**, 107–111.
110. M. Shirakawa, K. Yamatoya and K. Nishinari, *Food Hydrocolloids*, 1998, **12**, 25–28.

111. D. R. Nisbet, K. E. Crompton, S. D. Hamilton, S. Shirakawa, R. J. Prankerd, D. I. Finkelstein, M. K. Horne and J. S. Forsythe, *Biophys. Chem.*, 2006, **121**, 14–20.
112. J. C. Garbern, A. S. Hoffman and P. S. Stayton, *Biomacromolecules*, 2010, **11**, 1833–1839.
113. K. Nagase, J. Kobayashi, A. Kikuchi, Y. Akiyama, H. Kanazawa and T. Okano, *Biomacromolecules*, 2008, **9**, 1340–1347.
114. S. Zhang, *Adv. Cancer Res.*, 2008, **99**, 335–362.
115. S. Zhang, F. Gelain and X. Zhao, *Semin. Cancer Biol.*, 2005, **15**, 413–420.
116. G. S. Nowakowski, M. S. Dooner, H. M. Valinski, A. M. Mihaliak, P. J. Quesenberry and P. S. Becker, *Stem Cells*, 2004, **22**, 1030–1038.
117. E. Ruoslahti and M. D. Pierschbacher, *Science*, 1987, **238**, 491–497.
118. C. J. Pateman, A. J. Harding, A. Glen, C. S. Taylor, C. R. Christmas, P. P. Robinson, S. Rimmer, F. M. Boissonade, F. Claeyssens and J. W. Haycock, *Biomaterials*, 2015, **49**, 77–89.
119. J. Caddick, P. J. Kingham, N. J. Gardiner, M. Wiberg and G. Terenghi, *Glia*, 2006, **54**, 840–849.
120. P. G. di Summa, D. F. Kalbermatten, E. Pralong, W. Raffoul, P. J. Kingham and G. Terenghi, *Neuroscience*, 2011, **181**, 278–291.
121. P. G. di Summa, P. J. Kingham, W. Raffoul, M. Wiberg, G. Terenghi and D. F. Kalbermatten, *J. Plast. Reconstr. Aesthet. Surg.*, 2010, **63**, 1544–1552.
122. A. Mosahebi, P. Fuller, M. Wiberg and G. Terenghi, *Exp. Neurol.*, 2002, **173**, 213–223.
123. A. Mosahebi, B. Woodward, M. Wiberg, R. Martin and G. Terenghi, *Glia*, 2001, **34**, 8–17.
124. K. Arcaute, B. Mann and R. Wicker, *Acta Biomater.*, 2010, **6**, 1047–1054.
125. P. Erba, C. Mantovani, D. F. Kalbermatten, G. Pierer, G. Terenghi and P. J. Kingham, *J. Plast. Reconstr. Aesthet. Surg.*, 2010, **63**, e811–e817.
126. P. J. Kingham, D. F. Kalbermatten, D. Mahay, S. J. Armstrong, M. Wiberg and G. Terenghi, *Exp. Neurol.*, 2007, **207**, 267–274.
127. Q. G. Xu, R. Midha, J. A. Martinez, G. F. Guo and D. W. Zochodne, *Neuroscience*, 2008, **152**, 877–887.
128. J. W. Bae, J. H. Choi, Y. Lee and K. D. Park, *J. Tissue Eng. Regener. Med.*, 2015, **9**, 1225–1232.
129. M. Ehrbar, S. C. Rizzi, R. G. Schoenmakers, B. S. Miguel, J. A. Hubbell, F. E. Weber and M. P. Lutolf, *Biomacromolecules*, 2007, **8**, 3000–3007.
130. A. N. Koppes, A. L. Nordberg, G. M. Paolillo, N. M. Goodsell, H. A. Darwish, L. Zhang and D. M. Thompson, *Tissue Eng., Part A*, 2014, **20**, 494–506.
131. E. Beaumont, E. Guevara, S. Dubeau, F. Lesage, M. Nagai and M. Popovic, *J. Spinal Cord Med.*, 2014, **37**, 93–100.
132. Y.-J. Chang, C.-M. Hsu, C.-H. Lin, M. S.-C. Lu and L. Chen, *Biochim. Biophys. Acta, Gen. Subj.*, 2013, **1830**, 4130–4136.
133. L. Ghasemi-Mobarakeh, M. P. Prabhakaran, M. Morshed, M. H. Nasr-Esfahani, H. Baharvand, S. Kiani, S. S. Al-Deyab and S. Ramakrishna, *J. Tissue Eng. Regener. Med.*, 2011, **5**, e17–e35.

134. A. Kotwal and C. E. Schmidt, *Biomaterials*, 2001, **22**, 1055–1064.
135. T. J. Rivers, T. W. Hudson and C. E. Schmidt, *Adv. Funct. Mater.*, 2002, **12**, 33–37.
136. A. Guiseppi-Elie, *Biomaterials*, 2010, **31**, 2701–2716.
137. L. Ghasemi-Mobarakeh, M. P. Prabhakaran, M. Morshed, M. H. Nasr-Esfahani and S. Ramakrishna, *Tissue Eng., Part A*, 2009, **15**, 3605–3619.
138. D. K. Cullen, A. R. Patel, J. F. Doorish, D. H. Smith and B. J. Pfister, *J. Neural Eng.*, 2008, **5**, 374–384.
139. J. Huang, X. Hu, L. Lu, Z. Ye, Q. Zhang and Z. Luo, *J. Biomed. Mater. Res., Part A*, 2010, **93**, 164–174.
140. M. Sasaki, B. C. Karikkineth, K. Nagamine, H. Kaji, K. Torimitsu and M. Nishizawa, *Adv. Healthcare Mater.*, 2014, **3**, 1919–1927.
141. S. H. Ku, M. Lee and C. B. Park, *Adv. Healthcare Mater.*, 2013, **2**, 244–260.
142. H.-J. Kim, J. Jung, J.-H. Park, J.-H. Kim, K.-N. Ko and C.-W. Kim, *Exp. Biol. Med.*, 2013, **238**, 923–931.
143. J. Henley and M.-m. Poo, *Trends Cell Biol.*, 2004, **14**, 320–330.
144. L. Sheng, I. Leshchyns'ka and V. Sytnyk, *Cell Commun. Signaling*, 2013, **11**, 1–13.
145. M. Takeichi and T. S. Okada, *Exp. Cell Res.*, 1972, **74**, 51–60.
146. J.-E. Park, Y.-K. Seo, H.-H. Yoon, C.-W. Kim, J.-K. Park and S. Jeon, *Neurochem. Int.*, 2013, **62**, 418–424.
147. K. E. Hammerick, M. T. Longaker and F. B. Prinz, *Biochem. Biophys. Res. Commun.*, 2010, **397**, 12–17.
148. H. Sauer, G. Rahimi, J. Hescheler and M. Wartenberg, *J. Cell. Biochem.*, 1999, **75**, 710–723.
149. G. Thrivikraman, G. Madras and B. Basu, *Biomaterials*, 2014, **35**, 6219–6235.
150. Y. Cai, H. Li, B. Du, M. Yang, Y. Li, D. Wu, Y. Zhao, Y. Dai and Q. Wei, *Biomaterials*, 2011, **32**, 2117–2123.
151. L. Feng, Y. Chen, J. Ren and X. Qu, *Biomaterials*, 2011, **32**, 2930–2937.
152. D. Yin, B. Liu, L. Zhang and M. Wu, *J. Biomed. Nanotechnol.*, 2012, **8**, 458–464.
153. Z. M. Markovic, L. M. Harhaji-Trajkovic, B. M. Todorovic-Markovic, D. P. Kepic, K. M. Arsikin, S. P. Jovanovic, A. C. Pantovic, M. D. Dramicanin and V. S. Trajkovic, *Biomaterials*, 2011, **32**, 1121–1129.
154. C. Heo, J. Yoo, S. Lee, A. Jo, S. Jung, H. Yoo, Y. H. Lee and M. Suh, *Biomaterials*, 2011, **32**, 19–27.
155. O. C. Farokhzad and R. Langer, *ACS Nano*, 2009, **3**, 16–20.
156. S. Hu, Y. Zeng, S. Yang, H. Qin, H. Cai and J. Wang, *J. Nanosci. Nanotechnol.*, 2015, **15**, 6327–6341.
157. T. Dvir, B. P. Timko, D. S. Kohane and R. Langer, *Nat. Nanotechnol.*, 2011, **6**, 13–22.
158. L. Zhang and T. J. Webster, *Nano Today*, 2009, **4**, 66–80.
159. W. C. Lee, C. H. Y. X. Lim, H. Shi, L. A. L. Tang, Y. Wang, C. T. Lim and K. P. Loh, *ACS Nano*, 2011, **5**, 7334–7341.

160. K. S. Novoselov, A. K. Geim, S. V. Morozov, D. Jiang, Y. Zhang, S. V. Dubonos, I. V. Grigorieva and A. A. Firsov, *Science*, 2004, **306**, 666–669.
161. C. N. Rao, A. K. Sood, K. S. Subrahmanyam and A. Govindaraj, *Angew. Chem., Int. Ed. Engl.*, 2009, **48**, 7752–7777.
162. C. Chung, Y.-K. Kim, D. Shin, S.-R. Ryoo, B. H. Hong and D.-H. Min, *Acc. Chem. Res.*, 2013, **46**, 2211–2224.
163. E. Mooney, P. Dockery, U. Greiser, M. Murphy and V. Barron, *Nano Lett.*, 2008, **8**, 2137–2143.
164. A. Aryaei, A. H. Jayatissa and A. C. Jayasuriya, *J. Biomed. Mater. Res., Part A*, 2014, **102**, 3282–3290.
165. D. H. Kim, Y. S. Yun, H. Bak, S. Y. Cho and H.-J. Jin, *Curr. Appl. Phys.*, 2011, **11**, S376–S380.
166. Y. U. Jung, S.-i. Oh, S.-H. Choa, H.-K. Kim and S. J. Kang, *Curr. Appl. Phys.*, 2013, **13**, 1331–1334.
167. T. R. Nayak, H. Andersen, V. S. Makam, C. Khaw, S. Bae, X. Xu, P.-L. R. Ee, J.-H. Ahn, B. H. Hong, G. Pastorin and B. Özyilmaz, *ACS Nano*, 2011, **5**, 4670–4678.
168. G. Y. Chen, D. W. P. Pang, S. M. Hwang, H. Y. Tuan and Y. C. Hu, *Biomaterials*, 2012, **33**, 418–427.
169. B. L. Banik, P. Fattahi and J. L. Brown, *Wiley Interdiscip. Rev.: Nanomed. Nanobiotechnol.*, 2016, **8**, 271–299.
170. C. Zhang, X. Wan, X. Zheng, X. Shao, Q. Liu, Q. Zhang and Y. Qian, *Biomaterials*, 2014, **35**, 456–465.
171. C. Alvarez-Lorenzo and A. Concheiro, *Chem. Commun.*, 2014, **50**, 7743–7765.
172. K. J. Wangensteen and L. K. Kalliainen, *Hand (N. Y.)*, 2010, **5**, 273–277.
173. D. Schmauss, T. Finck, E. Liodaki, F. Stang, K. Megerle, H. G. Machens and J. A. Lohmeyer, *J. Reconstr. Microsurg.*, 2014, **30**, 561–568.

CHAPTER 15

Smart Cell Culture for Tissue Engineering

YEHUDAH PARDO[a] AND MINGLIN MA*[b]

[a]Meinig School of Biomedical Engineering, Cornell University, Ithaca, New York 14853, USA; [b]Department of Biological and Environmental Engineering, Cornell University, Ithaca, New York 14853, USA
*E-mail: mm826@cornell.edu

15.1 Introduction

The traditional model for tissue engineering begins with *in vitro* cell culture. Cells, isolated from patients or differentiated from stem cells, are seeded on a biomaterial substrate or culture dish and grown in the laboratory until ready for implantation (Figure 15.1). *In vitro* culture of human cells necessarily involves removing the cells from their natural environment. Consequently, cell behavior and properties *in vitro* may not be reflective of their characteristics *in vivo*. Furthermore, cells can "remember" conditions to which they were previously exposed, affecting cellular behavior even after the original stimulus is removed.[1] This suggests that inappropriate conditions *in vitro* could potentially affect the *in vivo* response after implantation.

How can tissue engineers avoid subjecting cells to stimuli that will negatively impact their performance *in vivo*? The answer begins with the substrate on which cells are grown. Cell culture is traditionally carried out on a flat (2D) plastic dish. However, an increasingly large body of work has demonstrated that the geometric (2D *vs.* 3D)[2–8] and mechanical

Smart Materials No. 25
Smart Materials for Tissue Engineering: Applications
Edited by Qun Wang

Published by the Royal Society of Chemistry, www.rsc.org

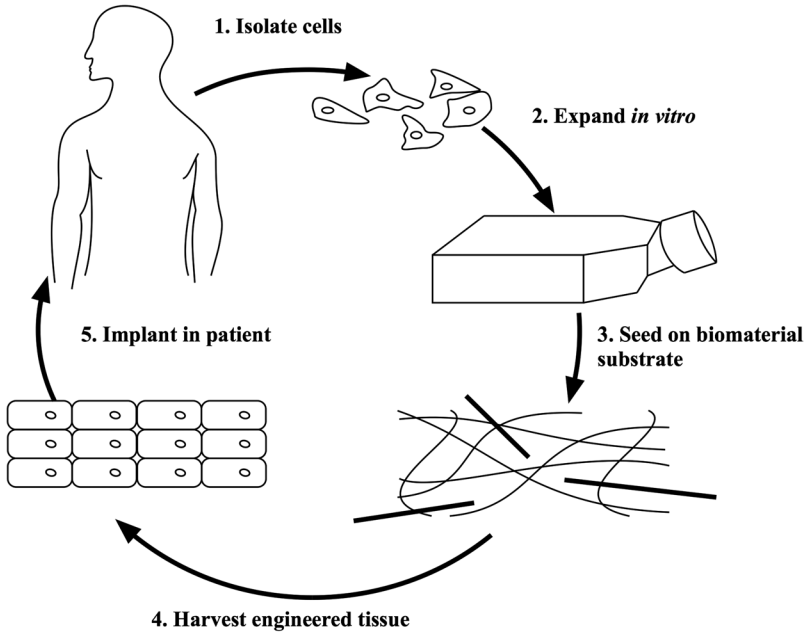

Figure 15.1 Schematic of the traditional model of tissue engineering.

(stiffness)[9–12] differences between plastic culture flasks and the extracellular matrix (ECM) in which cells naturally reside, fundamentally alter cellular characteristics. The ECM is a heterogeneous mix of biomolecules ranging from fibrillar structural proteins and glycoproteins to growth factors and small-molecule signals. Its complex structure reflects the vast array of functions it performs. Perfectly mimicking the complexity of the ECM is thus an extremely challenging task.

Despite the difficulty in replicating *in vivo* conditions, *in vitro* culture does have the distinct advantage of allowing greater access to and greater control over the growing cells. *In vitro*, the cell culture substrate is completely defined by the researchers, reducing the number of factors that could negatively impact the functionality or viability of cells during the tissue growth stage of tissue engineering. The introduction of smart materials as cell culture substrates allows an additional level of control over the cell culture to be realized. Rather than a single substrate defining a single environment for cell culture, smart substrates are dynamic, changing in response to an external stimulus. Most commonly, smart materials have been applied to dynamically modulate cell adhesion. The ability to alter the adhesive characteristics of a substrate has a wide range of applications from simply enabling facile cell collection while maintaining maximum cell viability to the development of complex-shaped tissues. Due to its pervasiveness in the literature, as well as its relevance to clinically translational tissue engineering, modulation of cell adhesion is the main focus of this chapter.

Clinically translational tissue engineering is supported by basic research. In discovery-oriented experiments, it is often useful to be able to subject cells repeatedly to a stimulus and observe the response in a time-dependent fashion. These stimuli may include the delivery of chemical factors, the application of compressive, tensile, or shear stresses to living cells, or even the relative positions of cells in co-cultures. Whereas non-responsive substrates represent a single set of static culture conditions, the properties of smart culture substrates can be altered within a single culture. In addition, smart materials may provide the actuation necessary to apply forces at the single cellular or subcellular scale. The final sections of this chapter will touch on some of these basic science applications of smart cell culture.

15.2 Materials for Modulating Cell Adhesion and Detachment

Providing cellular adhesion sites can be considered the most critical role of tissue culture substrates. Adhesion of cells to a substrate provides the structure that determines the final shape of the tissue being grown. Furthermore, the majority of cell types relevant to tissue engineering actually require some sort of adhesion for survival, undergoing anoikis (programmed cell death caused by lack of adhesion) in the absence of both cell–cell and cell–matrix attachment.

The biology behind cell adhesion is extremely complicated and will not be discussed in detail here. However, for the purpose of understanding the material in this chapter, a few points are worth mentioning. Cell adhesion to a substrate can occur through both specific, *i.e.* receptor–ligand, and non-specific interactions. The specific interactions are mediated by various cell surface proteins, most notably a family of proteins known as integrins. Integrins are heterodimers consisting of an α and β subunit of which there are several types. Altogether, a total of 24 different integrins have been identified in humans.[13] Multiple integrins cluster to form focal adhesions that tightly bond cells to the underlying substrate. Different integrins recognize and adhere to specific amino acid sequences. The arginine-glycine-aspartic acid (RGD) motif is especially widely used in *in vitro* culture substrates as it is recognized by a variety of integrin types. In the human body, the RGD sequence as well as the other motifs to which integrins bind, occur in ECM proteins such as fibronectin or collagen. This highlights an important point in understanding cell adhesion: cells adhere to proteins. When developing cell culture substrates, even so-called "adhesive" surfaces do not typically bind to cells directly. Rather, they promote the adsorption of ECM proteins to which the cells can then adhere.

In cell culture, the adhesiveness of cells is both a boon and a challenge. Cells adhered to a culture dish are relatively easy to wash, observe, and manipulate. However, transferring cells from one substrate to another, *e.g.* during passaging, necessitates that the cells be detached. In cell culture this is most

commonly achieved through the addition of a combination of the proteolytic enzyme trypsin and ethylenediaminetetraacetic acid (EDTA). This mix effectively digests focal adhesions as well as adsorbed proteins, causing the cells to lift off the surface. However, cell–cell connections that may be important for communication or tissue integrity are also digested. Furthermore, this process can actually damage the cells themselves, reducing cell viability.[14,15]

Smart materials provide one possible solution to this dilemma. Materials have been developed that have switchable adhesion properties, *i.e.* in one state cells adhere and grow, yet once the material is exposed to a specific stimulus, the state switches and cells are released. Thermo-responsive materials are particularly common for this purpose. At physiological temperature (37 °C), they are designed to adhere to cells, yet when cooled to room temperature or below, they release the cells.[16,17] Since only the cell–substrate interactions are affected, cell–cell adhesions and the natural ECM remain intact during detachment, allowing a complete tissue to be released from the smart substrate.

15.2.1 Poly(*N*-Isopropyl Acrylamide), a Material Worth Noting

Thermo-responsive biomaterials are based on polymers that decrease in solubility above a specific temperature, known as the lower critical solution temperature (LCST). Below the LCST, the polymer is hydrophilic, and extended. However, when the temperature of the solution increases beyond the LCST, the polymer collapses, becomes more hydrophobic, and precipitates from solution. In the hydrophilic, extended state, these polymers act as a barrier that prevents protein adsorption and cell adhesion, but when collapsed, the barrier is removed. Thus, thermo-responsive materials are not particularly adhesive to cells; rather, they simply do not resist cell attachment above the LCST.

Although several types of thermo-responsive biomaterials exist and have been applied in the literature, poly(*N*-isopropyl acrylamide), or PNIPAAm, is by far the most common. In fact, commercially available thermo-responsive cell culture substrates are based on this polymer. We therefore felt that PNIPAAm merited a more in-depth discussion than the myriad of other smart materials in existence. The LCST of PNIPAAm is approximately 32 °C. Therefore, at 37 °C the polymer is collapsed and supports cell adhesion. However, at room temperature (~25 °C), PNIPAAm becomes more hydrophilic and the cells are released.

Halperin and Kroger[18,19] posited that two main mechanisms are responsible for cell detachment from PNIPAAm surfaces (Figure 15.2). The first is a force, termed F_{cell}, which results from the compression of PNIPAAm brushes by an approaching cell membrane. The cell membrane is impermeable to the polymer, yet the cell is large enough that it cannot simply attach to the underlying substrate between polymer chains. Therefore, the cell confines the polymer brushes, resulting in the observed force. In their collapsed state, the thermo-responsive polymers are closer to the surface already and do not resist the approach of a cell as strongly (Figure 15.2(A)). However, when the

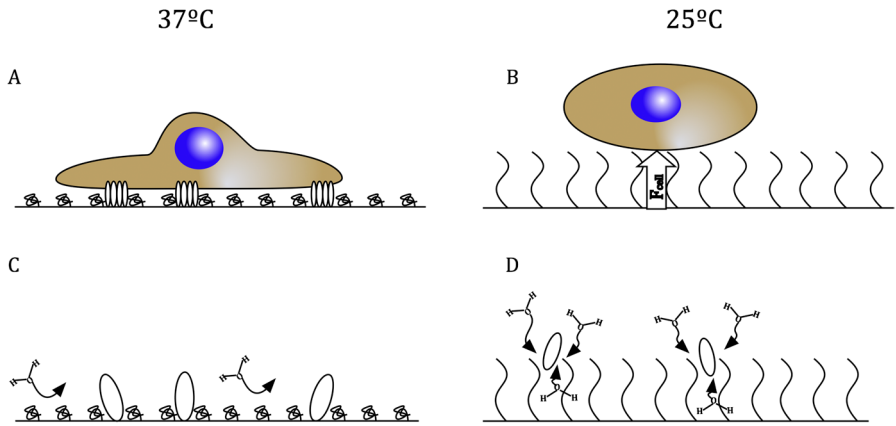

Figure 15.2 The mechanism of cell (A), (B) and protein (C), (D) detachment from a PNIPAAm-coated surface.

polymer becomes extended below its LCST, F_{cell} increases, putting any focal adhesions that have formed between the cell and the substrate under tension (Figure 15.2(B)). This tension increases the probability that the integrin–substrate interaction will break down, facilitating cell detachment.

Proteins are smaller than cells and have the potential to insert themselves between polymer chains. Thus, protein adhesion does not necessarily result in polymer brush confinement. Rather, the adhesion of a protein to the already crowded surface upsets the osmotic balance, resulting in an influx of water that drives the protein away from the substrate (Figure 15.2(D)). Above the LCST, the thermo-responsive polymer is not only collapsed and takes up less space, but also is more hydrophobic, reducing water influx (Figure 15.2(C)).

Despite the logic of these explanations, the presence of a detaching force (either F_{cell} or osmotic pressure) is not sufficient to cause the complete release of cells and their associated matrix from a culture substrate. Yamato *et al.* discovered that cells actively participate in the detachment process.[20] It was previously observed that cell detachment from thermo-responsive surfaces occurred more slowly than detachment *via* trypsin/EDTA. Furthermore, antibodies that block cell surface receptors involved in cell attachment had little to no effect at 4 °C, yet caused cell rounding (an indicator of loss of cell adhesion) when incubated at 37 °C.[21] These results suggested that metabolic processes (active only at 37 °C) were involved in cell detachment. Yamato *et al.* further discovered that sodium azide and genistein, inhibitors of ATP synthesis and tyrosine kinases, respectively, completely eliminated the ability of cells to detach from a PNIPAAm-grafted surface at low temperature. They therefore concluded that ATP-dependent tyrosine kinase signal transduction was a critical part of cell detachment. In addition, both actin stabilizers and depolymerizers reduced the ability of cells to detach from the same thermo-responsive surface, indicating that cytoskeleton rearrangements were involved.

15.2.2 Alternatives to PNIPAAm

Although PNIPAAm scaffolds are rarely implanted directly *in vivo*, the release of tissue engineered constructs from PNIPAAm surfaces raises the possibility that any PNIPAAm polymers or fragments remaining attached to a cell-sheet might cause a toxic reaction following implantation.[22] The NIPAAm monomer has been shown to be cytotoxic *in vitro*,[23] and there is limited evidence that the biocompatibility of PNIPAAm, the polymerized form, may deteriorate with repeated use.[24] These questions about the biocompatibility of PNIPAAm have led to a search for alternative thermo-responsive materials. It would be impossible to describe every thermo-responsive material that has been created and could potentially be applied to cell culture, but we will briefly review a few here. Each new material solves some issues associated with previous biomaterials while introducing new issues. Depending on the specific tissue engineering challenge, some may be more applicable than others.

15.2.2.1 Poly(Ethylene Glycol)-Based Materials

Unsurprisingly, the search for PNIPAAm alternatives began with compounds that had already been approved by the Federal Drug Administration (FDA) for other applications. In particular, poly(ethylene glycol) (PEG) was an attractive candidate. PEG has long been applied to *in vivo* applications, most notably as a biocompatible coating through "PEGylation"[25] of pharmaceuticals or drug delivery vehicles. In the majority of biomedical applications of PEG, it is intended to prevent rather than promote cell adhesion. The anti-adhesive properties of PEG derive from its highly hydrophilic nature. However, PEG does display an LCST above which it becomes more hydrophobic and allows cells to adhere.

Unfortunately, the LCST of PEG itself is around 85 °C.[26] Consequently, it is not very useful for tissue engineering applications. A solution to this problem was devised by copolymerizing high-LCST PEG derivatives with polymers having much lower LCST values. The methacrylated PEG derivative, oligo(ethylene glycol) methacrylate (OEGMA), was co-polymerized with 2-(2'-methoxyethoxy)ethyl methacrylate (MEO_2MA), which has an LCST around 26 °C.[27] OEGMA was used rather than an ethylene glycol monomer to enable the application of atom transfer radical polymerization, which provides a higher degree of control over the molecular weight distribution of the final polymer than conventional anionic ring-opening polymerization. Lutz and Hoth[27] altered the fraction of OEGMA to effectively tune the LCST of poly(MEO_2MA-*co*-OEGMA) (PMO) from 28 to 90 °C.

Lutz and colleagues later investigated the effectiveness of PMO as a switchable culture surface. Their studies revealed that cells have a reduced adhesiveness for PMO compared with PNIPAAm surfaces. While cells grown on PNIPAAm achieved 80% attachment after only an hour, it took 48 hours to achieve a similar degree of attachment on PMO surfaces. One hypothesis for this reduced attachment to PMO was the relatively small temperature gap

between the LCST of the PMO surface (34 °C) and the culture temperature (37 °C). Therefore, at 37 °C, the PMO may not have been fully collapsed, inhibiting cell attachment. Interestingly, after multiple cycles of cell attachment and detachment, this effect was reduced, allowing cells to adhere at rates comparable to those displayed on PNIPAAm and tissue culture plastic.[24]

Due to the extraordinary ability of PEG to resist protein adhesion, the principal challenge associated with developing switchable PEG-like materials for tissue culture is reducing the non-adhesive capacity sufficiently to achieve cell attachment. In the case of PMO, this was achieved by cycling the PMO surfaces in the presence of serum proteins. An alternative approach was taken to develop a glycerol-based switchable material.[28] Poly(methyl glycerol) is structurally very similar to PEG and displays the same non-adhesive properties. In order to allow cells to adhere to the polymer above its LCST, it was co-polymerized with either ethyl glycidyl ether or ethoxy ethyl glycidyl ether.[28] These monomers are more hydrophobic than glycidyl methyl ether, the monomer of poly(methyl glycerol), and thus reduce the ability of this polymer to resist cell and protein adhesion. Furthermore, the inclusion of hydrophobic moieties reduces the LCST from approximately 60 °C to between 30 and 40 °C,[28] making the final product useful for cell culture applications.

15.2.2.2 Cellulose-Based Materials

PEG, like many other hydrocarbons, is typically derived from fossil fuel precursors. This raises concerns about the potential sustainability and cost-effectiveness of the large-scale industrial production of PEG-based culture substrates. Cellulose is one of the most abundant polymers found in nature and is a renewable resource. Furthermore, it is highly cytocompatible. Consequently, cellulose-based materials are particularly attractive for large-scale cell culture. Unmodified cellulose is insoluble in water. Therefore, in order to make it useful for aqueous applications such as cell culture, it requires chemical functionalization. Methylcellulose is an aqueously soluble cellulose derivative. It has both hydrophobic and hydrophilic zones. In solution, the hydrophilic zones remain hydrated, while the hydrophobic zones condense in micelle structures.[29] An interesting property of methylcellulose is that it forms a gel upon heating. While the precise mechanism is not fully understood, it is believed that heating reduces the amount of hydration of the hydrophilic zones, causing the polymer to precipitate from solution in the form of a gel. Furthermore, this process is reversible, allowing the polymer to go back into solution upon cooling.[29,30] Hydration of methylcellulose can be manipulated through the addition of salt. Increasing the salt concentration in solution draws water away from the hydrated hydrophilic zones of the methylcellulose polymer and toward the salt ions. This makes gelation comparatively easier and is manifested by a decrease in gelation temperature.[29,30]

This ability to reversibly become more hydrophobic or hydrophilic combined with the ability to tune the gelation temperature *via* salt addition makes methylcellulose a potential candidate as a switchable culture substrate. Cells

were successfully grown on a methylcellulose gel and released upon cooling to 20 °C within as little as 10 minutes.[30] The extreme rapidity of this release process (as compared to the 30–60 min often needed for PNIPAAm) may be due to the extremely low adhesive properties of methylcellulose. In fact, in order to allow cells to attach at all, a thin layer of collagen gel over the methylcellulose surface was needed. Upon cooling, the collagen gel and the attached cells lifted off. In repeated cycles of switching between adhesive and non-adhesive states, the collagen was continuously replaced, while the methylcellulose was reusable.

In addition to methylcellulose, hydroxypropyl cellulose has also been applied as a thermo-responsive culture substrate. Like methylcellulose, it is a water-soluble derivative of cellulose. Unlike methylcellulose, it does not form a gel in its natural configuration. In order to create a hydrogel material, hydroxypropyl cellulose was modified with photo-cross-linkable methacrylate groups.[31] Upon exposure of a hydroxypropyl cellulose methacrylate solution to UV light, it rapidly crosslinks and forms a hydrogel. The LCST of this polymer was found to be between 37 and 38 °C. This makes it just useable as a thermo-responsive culture surface. CoS-7 cells were successfully grown on hydroxypropyl cellulose hydrogels and released upon incubation at 4 °C.[31]

15.2.2.3 Chitosan-Based Materials

Chitosan is another abundant, cytocompatible polymer that has been widely used in cell culture applications. It is a polysaccharide found in arthropod exoskeletons as well as the cell walls of certain fungi.[32] The modification of chitosan with hydroxyl butyl groups confers thermo-responsive properties on this polymer. Originally, hydroxybutyl chitosan was applied as an encapsulation material for stem cells and intervertebral disc cells as a treatment for vertebral disc degeneration.[33] Above 26 °C, hydroxybutyl chitosan forms a hydrogel. Thus, cells bound for implantation can be mixed with a solution of the polymer kept at cool temperatures, injected, and allowed to gel *in vivo*. Similar to methylcellulose, the same properties that allow temperature dependent gelation of chitosan also affect the ability of cells to adhere to a chitosan-coated surface. An in-depth study of smooth muscle cell culture on hydroxybutyl chitosan substrates demonstrated an 80% reduction in adhesion area within one hour of incubating the culture substrate at 18 °C.[34]

In another approach to endow chitosan with thermo-responsive properties, it was grafted with PMO chains *via* click chemistry.[35] The hydrophobicity of chitosan, combined with the hydrophilicity of PMO, allowed the polymer to form micelles in solutions that could swell and shrink reversibly with temperature changes. Depending on the ratio of chitosan to PMO, the LCST of the grafted polymer was tuned from 29 to 43 °C. Although in this particular study, they did not apply their polymer to cell culture directly, its LCST is within a physiologically relevant range and the component parts have previously been established as biocompatible. Consequently, chitosan-*graft*-PMO has the potential to be applied successfully as a thermo-responsive tissue engineering substrate.

15.2.3 Beyond Thermo-Responsive Materials

15.2.3.1 pH-Responsiveness

The successes of PNIPAAm-based surfaces have perhaps biased the field of cell attachment and detachment control toward thermo-responsive materials. Certainly, these are the most commonly studied materials for manipulating cell adhesion. However, research on switchable surfaces for controlling adhesion of cells has not been limited to thermo-responsive materials alone. In fact, some of the materials that were discussed in the context of thermo-responsive substrates above are, in fact, better suited to other stimulus methods. Chitosan is a good example. In its natural state, chitosan is not thermo-responsive at all. However, amino groups that can be protonated and deprotonated at near physiological pH heavily populate the backbone of chitosan. These functional groups confer on chitosan natural pH-responsiveness. In general, pH is not a stimulus considered for cell culture due to the relatively high sensitivity of mammalian cells to even small pH changes. However, the isoelectric point of chitosan happens to be approximately 7.4, the pH generally considered to be physiologically normal.[36–38] Below this pH, a higher proportion of the amino groups are protonated, giving chitosan a positive charge. Both cell membranes and the majority of ECM proteins have a net negative charge at physiological pH. Consequently, even minute changes of the net charge of the chitosan backbone can have dramatic effects on the ability of cells and proteins to adhere to a chitosan surface (see Figure 15.3).

Chen *et al.*[36] took advantage of this unique feature of chitosan to create a pH-responsive, switchable cell culture surface. At pH 7.2, both HeLa cells and fibronectin adhered strongly to the surface. However, when the medium pH was increased to 7.65, the proteins and cells detached with greater than 80% efficiency. Furthermore, viability studies showed that greater than 95% viability was maintained in the detached cells. Perhaps the most intriguing result of this study was that the pH changes required for efficient cell detachment could be achieved simply by altering the partial pressure of CO_2 in the incubator. The majority of cell culture incubators supplement the ambient CO_2 with external tanks. It is therefore exceedingly simple to adjust the percentage of CO_2 in a standard cell culture incubator in order to reduce or increase the pH of the media.

15.2.3.2 Electro-Responsiveness

Electro-responsive surfaces may be broadly classified into two main categories: reversible and non-reversible. Here we consider a surface reversibly electro-responsive if after the application of a voltage the surface can be returned to its original state without the need to add additional materials. Conversely, a surface is non-reversible if after the electrical stimulus is applied a physical change has taken place such that new chemical reactions must occur in

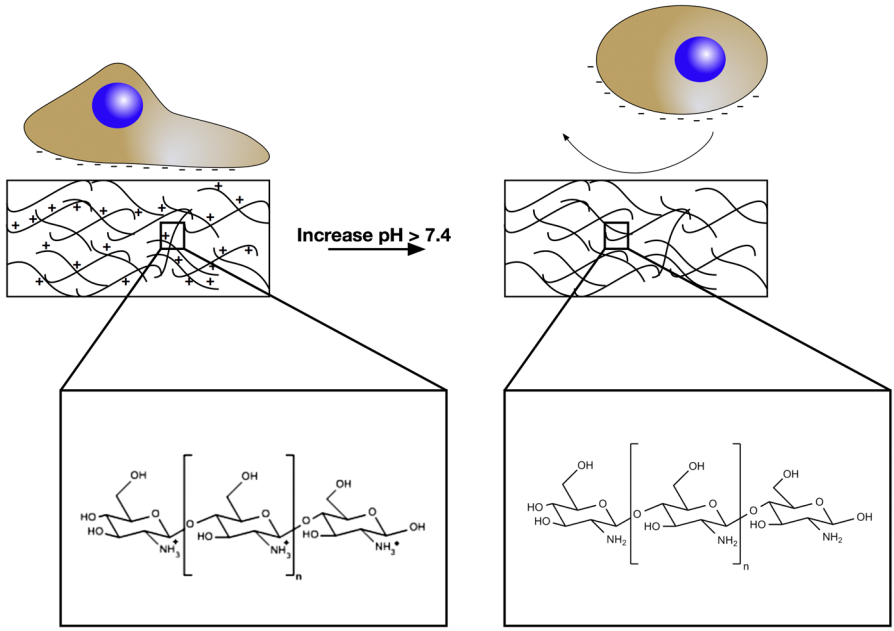

Figure 15.3 Cell adhesion and detachment from a pH-responsive chitosan surface. At low pH, the amines on the chitosan backbone become protonated resulting in a net positive charge, which promotes cell adhesion.

order to return the surface to its original state. The Langer lab first developed reversible electro-responsive surfaces in 2003.[39] The concept is simple, yet was challenging to create in practice. A polymer brush of (16-mercapto) hexadecanoic acid (MHA) was grown on a gold surface. MHA consists of a long hydrophobic chain capped by a hydrophilic, anionically charged carboxylate group. In the absence of a stimulus, only the hydrophilic carboxylate is exposed, rendering the entire surface hydrophilic. However, with the application of an electrical potential, the negatively charged carboxylate is attracted to the positively charged gold surface, bending the polymer chains and exposing the hydrophobic regions (Figure 15.4(A)). When the voltage is removed, the polymer returns to its original conformation. In this way, the application of an electrical potential switches the surface from hydrophilic to hydrophobic in a reversible manner.

The challenge associated with creating such a surface is the crowding of the polymer chains. Self-assembled monolayers (SAMs), such as the layer of MHA on gold, are typically tightly packed. Therefore, the polymer does not have the freedom to bend despite the electrical driving force. In order to overcome this challenge, Lahaan *et al.*[39] created first an SAM of MHA modified with a bulky head group. Although the head groups became tightly packed, the hydrophobic chains were relatively sparsely distributed. Following hydrolytic cleavage of the head group, the much smaller carboxylate was left with sufficient spacing between polymer chains to allow for bending.

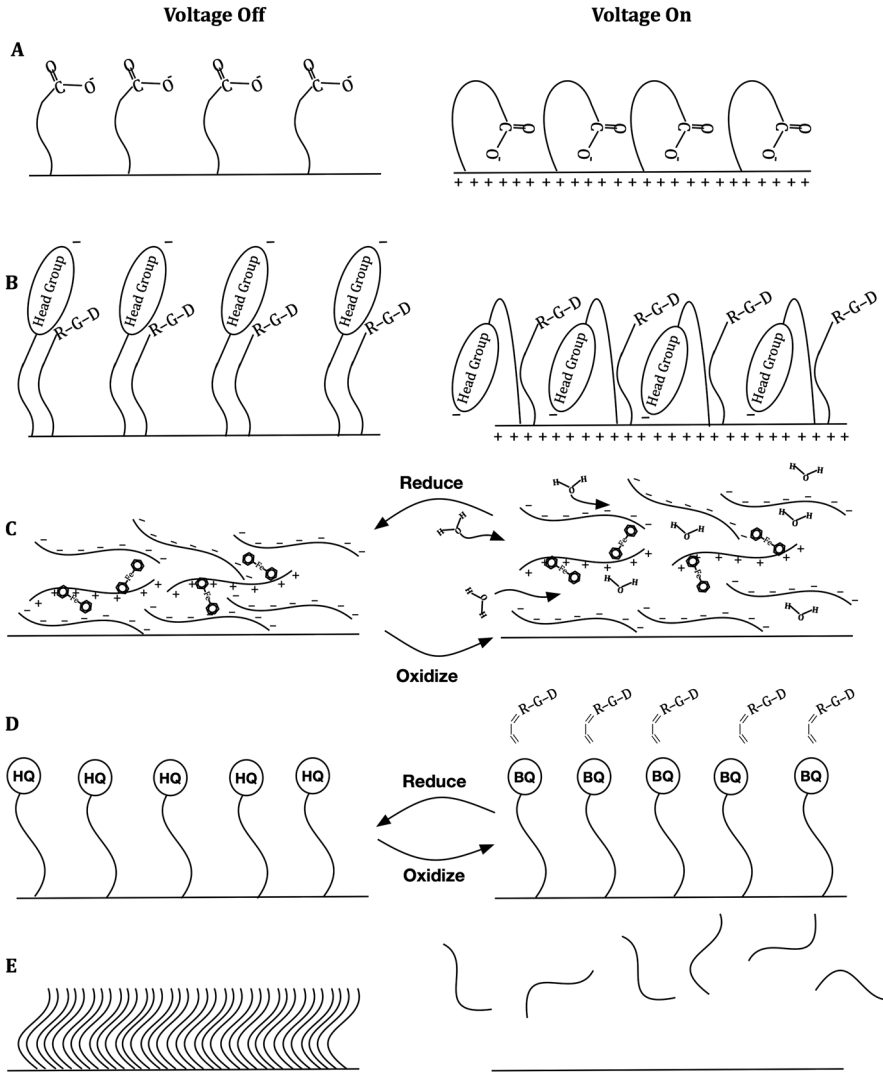

Figure 15.4 Reversible (A)–(C) and non-reversible (D), (E) electro-responsive surfaces. (A) The original mechanism proposed for electro-responsive surfaces. (B) Cells can adhere to an RGD peptide only when unobstructed by the charged head group. (C) The oxidation of ferrocene by an applied voltage results in water influx and swelling that disrupts cell adhesion. (D) Oxidation of hydroquinone to benzoquinone makes a surface reactive to diene-modified RGD peptides. (E) Densely packed, hydrophobic alkane-thiols resist cell adhesion, but desorb from a gold surface under electrical stimulation.

Building on this original work, electro-responsive technology has been extended to reversibly switch cell adhesion. In one approach, a SAM composed of hexa(ethylene glycol) was modified with RGD adhesion peptides and bulky, charged head groups.[40] The bulky head groups concealed neighboring RGD peptides, preventing cell adhesion. However, with the application of an electrical charge, the head group would bend toward the surface, exposing the RGD and allowing cells to adhere (Figure 15.4(B)). Furthermore, regions of the surface were engineered to respond differently to the same electrical potential by altering the type of charged head group in that region (either negatively charged sulfonate or positively charged ammonium).

Yet another approach toward the development of a reversible electro-responsive surface focused on controlling bulk swelling of a multilayered surface to render it non-adhesive to cells.[41] DNA (negatively charged polymer) and poly(ethylene imine) (PEI, positively charged polymer) were alternately deposited in a layer-by-layer assembly approach. The PEI was modified with ferrocene. Ferrocene changes from a reductive to oxidative state when exposed to an electrical voltage. This change altered the ionic balance in the assembly, causing the influx of counter ions to neutralize the charge differences and creating an osmotic gradient. The ensuing water influx caused the assembly to swell, detaching adhered cells (Figure 15.4(C)).

Reversible electro-responsive surfaces are relatively permanent constructions. As such, they are continuously reusable. This can be highly advantageous for applications in which cell layers are grown and released in a repeated fashion. However, for many research applications, an adjustable surface with the capability of altering the exposed ligand is desirable. Taking advantage of redox chemistry, Mrksich and co-workers developed just such a surface. They created a SAM of oligo(ethylene glycol) on a gold film to which cells would not attach and terminated the ethylene glycol chains with hydroquinone. Upon application of a voltage, the hydroquinone is oxidized to a benzoquinone that reacts *via* the Diels–Alder reaction with a diene. An RGD peptide was modified with a diene tag, allowing it to be covalently bonded to the benzoquinone-terminated oligo(ethylene glycol)[42] (Figure 15.4(D)). What is particularly interesting about this methodology is the redox reaction is reversible and the ligand can be released with the application of the opposite voltage.[43] Since cells are bound exclusively to the RGD ligand, once it is released, the cells are released as well. Thus, dynamic control over cell adhesion is achieved. Furthermore, once one ligand is released, it can be washed away and replaced with a second, different ligand, changing the functionality of the surface.[43]

In the presence of serum proteins such as fibronectin, cells have a remarkable ability to adhere to surfaces without the need for specific modification of the surfaces with adhesive ligands. As such, the removal of a barrier to protein adhesion is sufficient to induce cell attachment. Alkane-thiols may provide this type of removable barrier. The Whitesides lab has performed extensive work patterning alkane thiols onto gold substrates *via* micro contact printing.[44,45] The spontaneous reaction between thiol-functional

groups and gold allows rapid, permanent transfer of alkane-thiol "ink" from an elastomeric stamp to a gold substrate. The highly hydrophobic alkane-thiols resist cell and protein adhesion, thus allowing certain regions of a gold-coated surface to be protected from cell attachment. An electric stimulus can cause the alkane-thiol SAMs to desorb from the gold, removing the barrier and allowing cell adhesion to occur[46,47] (Figure 15.4(E)). Clearly such an approach is not particularly useful as a method for cell-sheet engineering, as the cells cannot be uniformly released from the surface. However, it may be applicable as a tool to study certain cellular behaviors such as cell migration. Cells can be confined to a pattern defined by regions not coated by alkane-thiols and then spontaneously allowed to begin migration from those patterns by releasing the surrounding alkane-thiol SAM.[46]

Compared to other types of smart materials (*e.g.* thermo-responsive or pH-responsive), electro-responsive materials are relatively difficult to construct. In order to transmit the electrical stimulus, such surfaces must be formed on a conductive electrode, typically gold. Furthermore, the chemistry involved in creating surfaces such as the hydroquinone-terminated oligo (ethylene glycol) requires a certain level of expertise with organic chemistry that is beyond many cell biology or tissue engineering laboratories. What then is the advantage of electro-responsive materials? One could argue that the application of an electrical impulse is less likely to have a damaging effect on cells than would changes in temperature or medium pH. While there is some truth to this, the evidence in the literature supports the conclusion that the temperature changes or pH changes required to achieve cell detachment have minimal to no harmful effects on cell viability. However, unlike any other smart material type, the development of electro-responsive surfaces provides the opportunity for collaboration between the fields of cell biology and tissue engineering and modern electronics. The techniques perfected for creating integrated circuitry are potentially applicable to electro-responsive cell culture as well, allowing a degree of control over cell culture that is difficult to otherwise achieve.

Perhaps the simplest example of such fine-tuned control is the ability to manipulate the adhesion of single cells. In a culture of thousands or millions of cells, this goal may seem unrealistic. However, by borrowing from computer technology, such a feat may be possible.[48] Cells can be seeded on an array of individually addressed elements that can be electrically stimulated one at a time. Considering these addressable elements as pixels, the same technology that is employed to develop computers can be applied to create electrically responsive cell substrates. Persson *et al.*[48] recently created a "passive" array of 64 pixels capable of individually responding to an electrical stimulus to release cells attached to that pixel exclusively. A single patterned gold wire addresses each row and column of the array. The pixel itself consists of a layer of poly(4-(2,3-dihydrothieno[3,4-*b*]-[1,4]-dioxin-2-yl-methoxy)-1-butanesulfonic acid) (PEDOT-S : H). When oxidized by a positive voltage above a certain threshold, this polymer desorbs from the surface to which it is attached. Because a certain minimum threshold is

necessary to achieve desorption, only the pixel corresponding to both the row and column to which voltages are applied is activated. Although other pixels along the row or column may experience an increase in electrical potential, it does not exceed the threshold necessary to cause detachment. The system was demonstrated with a co-culture of primary keratinocytes and fibroblasts as a method to segregate these two cell types. While far from fully developed, this technology is suggestive of the potential of collaboration with computer engineering to transform the field of cell-culture and tissue engineering.

15.3 Modulation of the Culture Environment

Cells are constantly exposed to a plethora of signals ranging from soluble paracrine signals to cell–cell contact to cell–ECM interactions. The signals themselves are transduced into cellular behaviors through lengthy, highly integrated signal cascades. In order to understand these signaling networks to the degree necessary to design effective tissues, researchers require the ability to controllably and predictably introduce and remove the signals a few at a time. Such precise control over cell signaling is not easily achievable in conventional cell culture. The relatively large volumes of conventional culture flasks make the high throughput experiments needed to investigate extensive signaling networks impractical and expensive. On the other hand, manual handling of small volume cell cultures such as multi-well plates is extremely time consuming and typically results in high losses and low reproducibility. With the introduction of electronic control systems and robotics, high-throughput, low volume, reproducible cultures are possible. However, pipetting robots are expensive, and cannot be directly used to study the effect of mechanical signals. Smart materials provide inexpensive automation that can be adapted to small volumes easily. In addition, since the mechanical properties of smart materials can dynamically be adjusted, smart cell culture can potentially be used to investigate mechanical signals as well.

15.3.1 Microfluidic-Based Cell Culture

Microfluidic devices are flexible and powerful platforms for high-throughput cell culture. By definition, they use low volumes (microliter scales) thus consuming few resources. This has inspired the use of microfluidics to create drug discovery platforms that allow many drug candidates to be rapidly screened for effectiveness *in vitro*.[49–51] In addition, the small size of microfluidic channels results in low Reynold's number, laminar flows, allowing highly predictable flow patterns to be created. Finally, microfluidic technology has been combined with tissue culture to generate tissues or even organs on a chip,[52–54] allowing multiple physiological systems and their interactions to be studied simultaneously. Organ systems that have been simulated on microchips include the liver, kidneys, lungs, vasculature, and the gastrointestinal tract.[54]

There are two principle advantages to gaining precise control over fluid flow. First, precise control allows for controlled transport of solutes between cells or tissues. This is particularly useful for studying cell–cell paracrine signaling or cellular response to soluble ligands in general. For example, clever microfluidic designs have been applied to create concentration gradients supporting studies of chemotaxis (cellular migration in response to soluble chemical stimuli).[51,52] The second major benefit of precise fluid control is the ability to apply defined shear stress to cells in culture. Many cell types not only sense and respond to mechanical stress, but also depend on the presence of stress for many of their functions. *In vivo*, endothelial cells, blood cells such as neutrophils, macrophages and erythrocytes, and bone cells, among others, are all regularly exposed to significant mechanical stress. In microfluidic cell culture systems, the fluid flow applies shear stress to the cells cultured inside. Thus, microfluidic systems are a convenient platform for studying the effect of shear stress on a variety of cell types.[51,52] In order to control flow in microfluidic devices, smart materials have been applied to create microvalves.[55–58] Valves in microfluidics extend far beyond smart materials.[59,60] However, without responsive materials, automation, *i.e.* self-regulation, of microfluidic valves requires computer-based controllers. Such systems typically require external power sources, can be expensive, and may require significant electronics expertise to construct. Responsive materials, on the other hand, can be implemented as valves without reliance on expensive electronics technology.

Some of the first smart valves consisted of small pH-responsive hydrogels polymerized *in situ* in microfluidic channels.[56] Hydrogels displaying pH-responsiveness typically gain a net positive charge in acidic (cationic hydrogels) or net negative charge in basic conditions (anionic hydrogels).[61] The presence of a net charge is balanced by an influx of counter ions, upsetting the osmotic balance and causing the hydrogel to swell.[62] In the original work of Beebe *et al.*,[56] the hydrogel micro-valve swelled under basic conditions closing off the channel. When returned to an acidic environment, the hydrogel shrank to its original size and shape allowing free fluid flow. In order to create such valves, a mixture of monomers (acrylic acid, 2-hydroxyethyl methacrylate, and ethylene glycol dimethacrylate) and a photoinitiator were injected into the channel. A specific region was then exposed to UV light through a photomask to initiate polymerization. Importantly, the authors noted that the UV exposure required to form such a hydrogel is achievable with a standard fluorescence microscope.[56] Therefore, their method is accessible to a variety of biological laboratories, even those lacking the specific expertise or equipment necessary for advanced microfabrication.

One potential pitfall with using pH-responsive valves is that actuation of the valve depends on changing the pH of the fluid in the microfluidic channel. While the precise pH at which the valve transitions from a closed to an open pH can be tuned, even small pH changes can have a devastating effect on live cells. As such, such valves may have limited applicability to cell culture. Thermally-responsive materials represent an alternative to pH-responsive

valves that can be actuated with minimal risk of cell damage. As thermally-responsive materials such as PNIPAAm collapse and contract above their LCST value, they can also be applied to block fluid flow. Thermo-responsive valves were first demonstrated on a macro scale (cm length scales) in 1997.[63] PNIPAAm chains were grafted to a porous polymer monolith and blocked the flow through the pores upon immersion of the entire system in a warm water bath. The same group later applied their method to micro-channels, by polymerizing a PNIPAAm monolith *in situ*.[58] In this system, the valves were actuated *via* an external array of thermoelectric elements opening or closing the valves in 3.5 and 5.0 seconds, respectively. This thermoelectric array provided more precise spatial control over the heating of the thermo-responsive valves than did their original method of immersing the entire device in a heated water bath.

While resistive heating circuits are relatively simple to construct, they do require some degree of expertise with circuits. Furthermore, if such circuits were created by hand, it would be nearly impossible to achieve spatial resolutions on the order of microns or even tens of microns. Instead, more advanced electronic fabrication methods would be needed. A more recent paper investigated light as an actuation method for thermo-responsive valves.[57] A halogen light source was focused on the valve in a plastic channel causing local heating and rapidly opening the valve (~4 sec). When the light was turned off, the heat quickly dissipated and the valve reopened (~6.2 sec). Light can be easily focused with standard optics supplies enabling high spatial resolutions to be achieved. Polymers that directly respond to light rather than heat generated by the light, *i.e.* photoresponsive polymers, have also been applied as micro-valves. However, once opened, the valves returned to their original state at a much slower rate (~1 hour) effectively restricting them to a single use during a given experiment.[64]

15.3.2 Mechanical Actuation

Although microfluidics can be used to apply defined amounts of shear stress to cell culture, cells also experience compressive and tensile stresses *in vivo*. The same ability of smart materials to expand and contract that makes them effective as valves can make them effective actuators of compressive and tensile stresses as well. Pelah *et al.* implemented a PNIPAAm actuator to compress and stretch red blood cells.[65,66] In order to apply a compressive stress, cells were confined between two layers of PNIPAAm beads. As the temperature was decreased below 32 °C, the beads expanded, compressing the red blood cells (see Figure 15.5(A)). In order to stretch cells, they were confined between a single layer of PNIPAAm and a coverslip. As the temperature was increased to 37 °C, the PNIPAAm became more hydrophobic allowing the red blood cells to adhere. At the same time, the PNIPAAm gel contracted, stretching the adhered cells (see Figure 15.5(B)).

Mechanical actuation has even been achieved at the molecular level through the streptavidin–biotin interaction. Streptavidin is a protein that

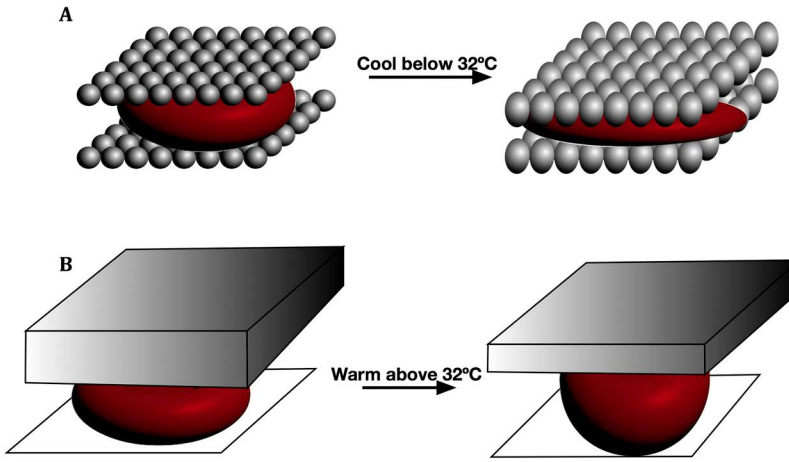

Figure 15.5 Mechanical actuation achieved through thermo-responsive materials. (A) PNIPAAm beads expand on cooling, compressing a red blood cell. (B) A red blood cell confined between a glass coverslip and a layer of PNIPAAm is stretched when the PNIPAAm contracts with increasing temperature.

binds biotin with a remarkably high affinity (K_d on the order of femtomolar).[67] However, this interaction can be interrupted in a reversible manner by conjugating PNIPAAm to the biotin-binding site of streptavidin. When below its LCST, the extended PNIPAAm polymer had little effect on the ability of streptavidin to bind biotin. When the temperature was raised above its LCST, the PNIPAAm collapsed, blocking access to the binding site.[68] In cells, such a methodology might be used to reversibly interrupt protein–ligand interactions providing molecular level insight into cellular processes. Toward this end, biotin was conjugated to PNIPAAm and packaged in erythrocyte ghosts.[69] Erythrocyte ghosts are intact red blood cell membranes lacking the internal components of red blood cells. They can fuse with other plasma membranes and thus act as effective delivery vehicles. As an illustration, the PNIPAAm-conjugated biotin was delivered to other erythrocyte ghosts containing streptavidin. Upon binding to the PNIPAAm-conjugated biotin, the streptavidin could be reversibly aggregated by increasing the temperature above PNIPAAm's LCST. While such a system is clearly useful only as a demonstration, the same experimental methods could be employed to aggregate more biologically important proteins, thus rapidly restricting their accessibility.

Besides PNIPAAm, there is a vast collection of materials that display mechanical actuation in response to non-mechanical stimuli including thermo-responsive, pH-responsive, light-sensitive, electro-responsive and even magneto-responsive polymers.[70] In addition, novel hydrogel actuators have been created from composite materials. In one study, elastin-like synthetic peptides (ELPs) were combined with graphene oxide to create a

light-responsive mechanical actuator.[71] The ELPs are thermally responsive, and like PNIPAAm, collapse and become insoluble upon heating. Graphene oxide generates heat when exposed to near-infrared radiation. The ELPs were bound to a graphene oxide sheet and then exposed to near-infrared radiation. This caused local heating of the graphene oxide and subsequent collapse of the ELPs at the site. As a result, the entire material bent.

15.3.3 Repositioning of Cells

The spatial organization and position of cells affects not only the architecture of a tissue, but its function as well. As discussed more fully in earlier sections of this chapter, cells arranged in three-dimensions behave differently than cells grown on 2D substrates. In addition, many types of cell signaling are dependent on cell–cell contacts rather than soluble signaling molecules. Finally, the specific organization of multiple cell types in co-culture or *in vivo* often defines tissue function. Consider for example, the organization of vascular tissue: an inner sheath of endothelial cells wrapped by vascular smooth muscle cells and pericytes. The role of each cell type is defined by its position in the tissue and is specialized accordingly.

Smart materials allow researchers to gain control over the spatial positioning of cells in tissue culture. This enables the elucidation of the effects and mechanisms behind cell–cell contacts as well as the creation of complex tissue architectures. Magnetically-responsive materials are the principle workhorses of such studies. Magnetic nanoparticles, typically made of magnetite (Fe_3O_4), can be incorporated into cell culture substrates, bound to cell surfaces or delivered to the cytoplasm of cells. Under a magnetic field, these systems can be repositioned quickly and efficiently.

Magnetite particles, like other nanoparticles, are naturally endocytosed by cells and incorporated into the cytoplasm upon introduction to cell culture media.[72] Packaging of the magnetic nanoparticles in drug-delivery vehicles may increase the uptake efficiency. Cationic liposomes were designed for just such a purpose.[73] The positive charge on the surface of the liposomes allows them to bind to anionic cell membranes. The liposomes then fuse with the plasma membrane, dumping their load of magnetite nanoparticles into the cytoplasm.

Dynamic aggregation of magnetically labeled cells has led to insights into cell–cell adhesive properties. Building on previous work by their group with magnetically labeled MSCs,[74] Frasca *et al.* tested the cohesive properties of nine different cell types.[75] The cells were labeled with maghemite nanoparticles and aggregated to form spheroids with a magnet. Once the magnetic field was removed, the shape of the cell aggregate evolved, providing insight into the ability of the cells to adhere to one another. Adherent cell types such as fibroblasts retained a stable spheroid structure, while aggregates of non-adherent cell types such as monocytes disintegrated under gravitational force. Unlike conventional methods of forming spheroids *via* non-adhesive culture surfaces (discussed below), magnetically driven cell aggregation can be

applied to virtually any cell type. Thus, the methods developed by Frasca and colleagues can be applied to study cell–cell adhesive capacity in cells derived from a wide variety of tissues.

Separate studies have taken advantage of magnetically manipulable cells to study cancer invasion.[76,77] BALB/3T3/*v-src* cells, a type of malignant fibroblasts, were aggregated and embedded in type I collagen gel.[76] The BALB/3T3/*v-src* cells were labeled with cationic liposomes and positioned over an array of magnetized iron pins. This generated a large number of cell aggregates enabling high throughput study of their invasion into the surrounding collagen. As a further demonstration of the utility of their system, the authors exposed the cells to matrix metallo-protease (MMP) inhibitors, restricting the invasive capacity of the malignant cells. In the future, a similar setup might be used to screen drug candidates designed to limit cancer cell metastasis.

Magnetic manipulation is not limited to the formation of spheroids. Cells can be patterned into stripes[78] and magnetic fields have even been focused to manipulate individual microparticles.[79] This fine-tuned method of patterning cells can be harnessed to study the effect of the spatial arrangement of cells. For example, skeletal myoblasts have been proposed as a potential treatment for cardiac failure.[80] However, there is concern that the lack of conductive properties of these cells may interrupt the propagation of electrical signals through the heart thereby generating arrhythmias.[81] In order to test this hypothesis, skeletal myoblasts were magnetically labeled with cationic liposomes and co-cultured with cardiomyocytes.[78] The conductivity and calcium transport through the culture were monitored to assess the enervation of this *in vitro* heart model. It was discovered that randomly dispersed skeletal myoblasts significantly impaired cardiac conductivity, while localizing the myoblasts to a striped region *via* magnetic manipulation mitigated this effect.

Cells themselves do not need to be labeled to enable magnetic repositioning. Cell culture substrates have been designed that incorporate magnetic nanoparticles. Magnetite nanoparticles take on a negative charge in neutral pH allowing them, along with gold nanoparticles, to crosslink positively charged filamentous viral phages together to form a hydrogel.[77,82] The phages were engineered to display a peptide sequence specific to the αv integrin allowing cells to adhere to the hydrogel. Neural stem cells cultured within this hydrogel were magnetically levitated at the air–media interface, creating a static suspension culture.[77]

Magnetite nanoparticles were also embedded in molded PEG-hydrogels.[83] The hydrogels were dispersed on a surface and impregnated with cells to generate small cell culture "bricks" that could be recombined to form complex geometries. A magnetic field was employed to aggregate the PEG gels over curved, dome-shaped or tubular molds forming a signal tissue structure. Before the magnetic field was removed, the entire construct was crosslinked within a fresh layer of PEG to preserve its shape.[83]

In a recent study, magnetically responsive vortex ring particles were reported that are broadly applicable for cell encapsulation.[84] The unique

torus shape of these particles maximizes the diffusion of nutrients and oxygen necessary to keep encapsulated cells alive. Iron oxide nanoparticles embedded in the vortex rings provide a mechanism by which the rings can be manipulated and efficiently organized. This capability suggests that cells growing on and in the vortex ring particles could be rapidly reorganized into a variety of complex geometries.

15.4 Applications of Smart Cell Culture and Clinical Perspectives

15.4.1 Cell-Sheet Engineering

Thermo-responsive technology has inspired a fundamentally new tissue engineering paradigm known as cell-sheet engineering.[14] The concept is to harvest 2D sheets of cells with cell–cell junctions and ECM intact from the tissue culture substrate (see Figure 15.6). It should be noted that cell-sheet engineering is not strictly limited to thermo-responsive culture substrates. For example, Itabashi *et al.* produced myocardial cell-sheets simply by growing cells on a fibrin layer that was gradually digested by proteases secreted by the cells themselves.[85] In addition, cell-sheets have been derived from electro-responsive, pH-responsive, photo-responsive and even magnetic-responsive substrates.[86]

The applications of cell-sheets are diverse. They may be implanted directly when a monolayer format is relevant, as in the case of epithelial cells.[87] Alternatively, they may be layered together to form more complex three-dimensional tissues.[14] Furthermore, cell-sheets containing different cell types may be easily combined, creating co-cultures that more accurately model physiology.[88] In recent years, cell-sheet engineering has been applied to develop therapies for an impressive array of different tissue types and diseases. These have included myocardial infarction, mandibular defects, tracheal grafts, islet therapies (for treatment of diabetes), and even as *in vitro* tumor models.[89–93] In addition to the flexibility of cell-sheet engineering, the ability to completely separate cells from the biomaterial substrate reduces the chance that the implantation of the tissue-engineered construct will result in a toxic reaction.

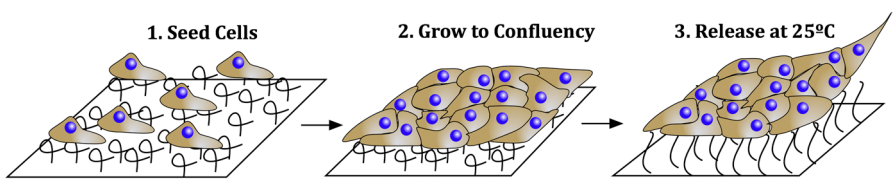

Figure 15.6 Cell-sheet engineering. This is a unique paradigm for tissue engineering in which cells are grown on a layer of thermo-responsive PNIPAAm and then released as a 2D sheet upon cooling of the substrate below its LCST (32 °C).

One of the disadvantages of completely isolating cell layers from the biomaterial substrate prior to implantation is the lack of mechanical support. Without the presence of a biomaterial, the cellular junctions must withstand the stresses associated with manipulation of the cell-sheet on their own. In order to overcome this difficulty, layers of gelatin, chitosan and alginate were deposited on a cell-sheet, forming a supportive backing that enabled easier physical manipulation.[94] While the addition of such "nano-clothing" has the desired effect of enabling easier manipulation of the cell-sheet, the potential for a negative host response to the gelatin, alginate and chitosan is a concern.

Nevertheless, the combination of cell-sheet engineering with appropriate biomaterial scaffolds can be a formidable tool in the tissue engineer's arsenal. Cell-sheets can rapidly assume the shape of a scaffold, while cells seeded as a suspension may take weeks to reach the same level of scaffold coverage. Vascular grafts are a good example of when this property of cell-sheet engineering is advantageous. Blood vessels consist of a lining of endothelial cells supported by a basement membrane and vascular smooth muscle cells. Humans do not naturally endothelialize (generate an endothelial lining) vascular grafts,[95] frequently leading to a thrombotic response and graft failure. In order to improve graft outcome, extensive research has focused on the addition of cells to vascular grafts prior to implantation, especially the addition of endothelial cells.[96–98] Cell-sheet engineering has been applied to accomplish the same goal with smooth muscle cells. Scaffolds were electrospun from poly(caprolactone) and collagen I and wrapped with a smooth muscle cell–cell-sheet.[99] This resulted in more rapid and complete coverage of the graft with a cell layer compared to seeding with a cell suspension.

The ubiquitous interactions between multiple cell types *in vivo*, such as endothelial and smooth muscle cells in blood vessels, highlights the importance of the co-culture of two or more cell types in tissue engineering. Furthermore, in many tissues, different cell types occupy separate regions of the tissue in well-defined architectures. Applying conventional micro-patterning techniques, cells can be organized during the initial *in vitro* culture, thus creating a patterned cell-sheet. For example, in one study, a thermo-responsive substrate was patterned with stripes of fibronectin (an ECM protein) to which human epidermal fibroblasts were adhered.[100] The spaces between the stripes were then filled with bovine aortic endothelial cells. Once the cells reached confluency, the entire cell-sheet consisting of both cell types was separated from the culture substrate.[100]

Cell-sheet engineering in particular holds the advantage of allowing multiple cell types to be combined simply by layering together different cell-sheets. Therefore, even if two cell types cannot easily be cultured together *in vitro* (*e.g.* due to different media requirements), they can still be combined *via* cell-sheet technology. In addition, layering of cell-sheets enables the combination of multiple tissue types to form an organ. While a fully functional engineered organ has not yet been realized, remarkable steps toward this goal have been made. One such step has been the successful vascularization of implantable tissues. The diffusion of nutrients, especially oxygen, is one

of the major factors limiting the engineering of large (millimeter scale and greater) tissues and organs.[101] This limitation can be circumvented if native vasculature can be encouraged to connect and penetrate the tissue-engineered organ. Following up on their original work with cell-sheet engineering, the Okano lab has tackled this problem in the context of cardiac tissue engineering.[102] They created thick cardiac tissue by layering together multiple sheets of cardiomyocytes. In order to ensure that the sheets would become well vascularized upon implantation, they interspersed the cardiomyocytes with endothelial cells. *In vivo*, the endothelial cells migrated through the cell-sheets and combined to form a vascular network that connected with blood vessels at the implantation site.[103] By repeating this procedure with several sets of a few cell-sheets at a time, a vascularized cardiac tissue with a total of twelve layers was created.[103] A similar process was achieved *in vitro* with a specially designed bioreactor consisting of microchannels embedded in collagen gel through which media could flow.[104]

Desiring to create vascular networks with more controlled structures, the Okano lab began investigating methods to pattern the endothelial cells incorporated into these tissue structures. They discovered that orientation of one cell-sheet could affect the orientation of cells in another sheet.[105,106] Endothelial cells previously aligned in a stripe pattern lost their orientation when put in contact with a randomly oriented cell-sheet. However, by sandwiching a randomly oriented endothelial cell-sheet between two aligned fibroblast cell-sheets, the endothelial cells spontaneously formed an aligned pattern.[105] Furthermore, the aligned fibroblasts were shown to produce higher levels of vascular endothelial growth factor (VEGF), a stimulator of angiogenesis (new blood vessel growth).[107] This suggests that such aligned sheets may be vascularized more easily than their randomly oriented counterparts.

15.4.2 3D Culture

Cell-sheet engineering inherently depends on 2D cell culture, *i.e.* cells cultured on a flat substrate. However, cells *in vivo* exist in three-dimensional matrices. For more than a decade, evidence has been steadily mounting showing that cells behave fundamentally differently on 2D *vs.* more realistic 3D culture substrates.[2–8] Notably, gene expression regulation is altered by the dimensionality of the culture substrate, suggesting that even once released from a 2D surface, its effect would linger.[108] As such, it is desirable to translate the flexibility and utility of cell-sheet engineering to 3D platforms.

In order to accomplish this, a variety of 3D fiber matrices (polypropylene, polyethylene terephthalate, and nylon) were grafted with PNIPAAm *via* solution free-radical polymerization.[108] In this particular study, two hepatocyte cell lines were grown on the 3D scaffold (HC04 and HepG2). Hepatocyte cells are known to have reduced expression of cytochrome P450 (CYP) isozymes, a family of proteins important for drug metabolism, when cultured on 2D surfaces.[109,110] Rossouw *et al.* showed significantly higher expression of several forms of CYP on the thermo-responsive 3D substrates compared with

a 2D control. Furthermore, as with other thermo-responsive substrates, the viability of harvested cells was higher than that obtained by trypsin-mediated release. Cells released from a 3D culture substrate do not form a single sheet as they do when released from 2D substrates. Two geometries were observed depending on the cell type. HC04 formed multi-layered strips of cells, while released HepG2 cells formed spheroids. While the activities of these hepatocyte constructs released from the thermo-responsive matrix were not tested *in vivo*, it is reasonable to expect that their 3D nature would enable them to maintain the phenotype developed *in vitro* leading up to and through implantation.

Although not every cell type will form spheroids, many cells do form spheroids spontaneously when cultured on a non-adherent surface. Spheroids are perhaps the simplest form of 3D culture and are one of the oldest methods to culture cells in 3D. Furthermore, spheroids obviate the need for a realistic 3D culture substrate, since they are composed exclusively of the cells themselves and any matrix excreted by those cells. The greatest challenge with spheroids is controlling the size. Since they are formed spontaneously, it is difficult to ensure that a specific number of cells aggregate in each spheroid. Thermo-responsive surfaces have provided one solution to this issue. Since the adhesiveness of thermo-responsive surfaces can be precisely controlled, cells can be grown to a particular density, detached and then aggregated into a single multicellular spheroid.

This phenomenon was originally observed with fibroblasts.[111] When cultured on collagen conjugated with PNIPAAm, the fibroblasts proliferated until reaching confluency. The fibroblasts were released as a cell-sheet and then transferred to a second hydrophobic surface (coated with PNIPAAm without collagen). Rather than attaching to the plate, the fibroblasts coalesced to form a multicellular spheroid. The size of the spheroid is thus dependent on the size of the cell-sheet.

Later work performed by the same group took advantage of this fact to create multiple size-controlled spheroids.[112] Collagen is a naturally UV-cross-linkable polymer.[113] Exploiting this property, PNIPAAm-conjugated collagen was patterned into defined pads *via* photolithography. Cell-sheets grown on these pads were restricted to the size of the collagen pattern and therefore produced spheroids with defined diameter and cell number. The idea of using collagen conjugated with PNIPAAm to produce spheroids has been extended to a variety of cell types. In a 1995 study, Yamazaki *et al.* systematically tested 23 different cell types on this type of substrate, 15 of which were found to form spheroids.[114] In addition, heterospheroids containing both fibroblasts and hepatocytes in a single spheroid have been created.[115]

Besides simply providing a more natural environment for cells, 3D *in vitro* culture allows for more geometrically complex tissue engineering constructs to be generated. A tubular endothelial cell construct was created with the aid of a thermo-responsive 3D substrate.[116,117] Endothelial cells form a single monolayer *in vivo*, and therefore it is not necessary to develop *in vitro* tissues consisting of multiple layers of endothelial cells. However, endothelial cells

in vivo are wrapped in a tubular configuration on the luminal surface of blood vessels. This raises the possibility that cells grown in other configurations *in vitro* might be phenotypically different from cells *in vivo*. While this tubular configuration can and has been achieved by wrapping cell-sheets around a cylindrical scaffold (see Section 15.2.3.1),[99] culturing cells initially in a 2D environment can result in lasting changes to gene expression. Matsuda circumvented this issue by directly seeding and culturing endothelial cells on the luminal side of a capillary tube, thus mimicking the *in vivo* geometry.[117] The capillary tube was coated with a layer of PNIPAAm-grafted gelatin. The gelatin created a favorable environment for cell attachment and growth while the PNIPAAm chains allowed for thermally induced release of the confluent endothelial cell construct. This approach successfully produced an intact tubular graft consisting exclusively of endothelial cells. One may speculate that such approaches could be made more complex in the future in order to incorporate the other cell types (smooth muscle cells and pericytes, *etc.*) necessary to create a complete, functioning blood vessel.

15.4.3 Cell Segregation

Tissues are composed of a heterogeneous cell population. Although tissue engineering methods often attempt to recapitulate this heterogeneity through co-cultures, controlled *in vitro* culture requires that cell types must be fully purified and segregated from neighboring cells.[118] Conventional methods for cell separation, such as flow activated cell sorting (FACS), often rely on specific cell labeling making them expensive and technically challenging. A simpler method was devised to separate cell types based on differing surface tension and proliferative capacity employing microwells.[119] In a similar vein, differential adhesive capabilities provide a convenient route for segregating cell types with thermo-responsive materials. Even among cells that do adhere to PNIPAAm, there is significant variability in the strength of adhesion. Furthermore, these differences in adhesive capacity can be enhanced through the reduction of the total surface area available for cell attachment. Three different cell lines (HeLa cells, HUVECs and 3T3 fibroblasts) were segregated on a striped pattern of PNIPAAm.[118] The stripes were only 3 μm in diameter, far smaller than the cellular footprint. The area between the stripes was filled with polyacrylamide, a polymer that resists cell adhesion. As such, cells extended over both adhesive PNIPAAm and non-adhesive polyacrylamide, causing cells with lower adhesive capacities to more easily detach from the PNIPAAm surface. HeLa cells did not attach to the PNIPAAm at all. HUVECs (human umbilical vein endothelial cells) attached for the first 12 hours and then detached. Only fibroblasts were able to remain attached to the surface over an extended period. In order to recover these cells, the surface was cooled to 20 °C, hydrating the PNIPAAm stripes and causing the cells to lift off the pattern.

In a separate study, immune cells (monocytes, macrophages and foreign body giant cells) were segregated based on their differential adhesive properties.[120]

Over time, in culture, monocytes differentiate into macrophages, which then fuse to form foreign body giant cells. All three cell types might therefore be found in a single culture necessitating some form of separation. When cultured on PNIPAAm, monocytes, macrophages and foreign body giant cells adhere. However, monocytes more rapidly detach from the culture surface upon cooling than do macrophages, and macrophages more rapidly detach than foreign body giant cells. Therefore, by cooling the thermo-responsive surface for increasing times, the cell types may be segregated.

15.4.4 Clinical Perspectives

Ultimately, any tissue engineering technology is only useful as long as it benefits patients in the clinic, either directly or by advancing scientific knowledge of health and disease. Smart cell culture has the potential to achieve both. Smart tissue culture substrates have produced viable engineered tissues in complex geometries and containing multiple cell types with direct clinical applications. Furthermore, the control afforded by smart materials over the culture environment promises to provide unique insights into cell biology.

As with any tissue engineering substrates, the toxicity and immunogenicity of smart materials are potential barriers to clinical translation. As noted in section 15.4.1, cell-sheet engineering reduces the chance of a toxic reaction to culture substrates by allowing the substrates to be completely separated from the engineered tissue. This characteristic, combined with its simplicity, makes cell-sheet engineering one of the most readily clinically translatable smart cell culture technologies. In fact, cell-sheet engineering has already been applied with reasonable success in human trials.[121] Autologous epithelial cells derived from the oral mucosa were cultured on a thermo-responsive surface to form cell-sheets that were subsequently implanted to replace opacified corneal tissue. In their study, Nishida *et al.* noted that the implants integrated seamlessly with the surrounding tissue and remained transparent throughout a 14 month follow-up period. Thus, the intervention restored sight to all patients participating in the study. While still a far cry from the ultimate goal of tissue engineering of regenerating complex 3D organs and tissues, this case demonstrates the immediate and impactful clinical applications of smart cell culture.

15.5 Conclusion

In vitro culture is an important stage of the tissue engineering process during which researchers have maximum control over the cell culture conditions. Smart materials provide an additional level of autonomous control over a variety of aspects of cell culture including cell adhesion, cell signaling, and mechanical actuation, among others. This control has resulted in significant advancements in the development of more complex tissue engineered constructs such as 3D, vascularized myocardial tissue and endothelialized vascular grafts. Furthermore, these constructs can be rapidly separated from the

smart substrates, reducing the likelihood of a negative host reaction to the biomaterial. Smart cell culture has also contributed to an improved understanding of cellular biology through its incorporation into *in vitro* culture models. The field of tissue engineering is reaching ever closer to the *de novo* creation of functional organs. Smart materials promise to play a vital role in this technological development, providing an active role for *in vitro* culture substrates in replicating the complexities of human physiology.

References

1. J. L. Balestrini, S. Chaudhry, V. Sarrazy, A. Koehler and B. Hinz, *Integr. Biol.*, 2012, **4**, 410–421.
2. E. Cukierman, R. Pankov, D. R. Stevens and K. M. Yamada, *Science*, 2001, **294**, 1708–1712.
3. K. A. Beningo, M. Dembo and Y. L. Wang, *Proc. Natl. Acad. Sci. U. S. A.*, 2004, **101**, 18024–18029.
4. E. Cukierman, R. Pankov and K. M. Yamada, *Curr. Opin. Cell Biol.*, 2002, **14**, 633–639.
5. P. Friedl and E. B. Brocker, *Cell. Mol. Life Sci.*, 2000, **57**, 41–64.
6. M. Bokhari, R. J. Carnachan, N. R. Cameron and S. A. Przyborski, *J. Anat.*, 2007, **211**, 567–576.
7. F. Grinnell, *Trends Cell Biol.*, 2003, **13**, 264–269.
8. K. L. Schmeichel and M. J. Bissell, *J. Cell Sci.*, 2003, **116**, 2377–2388.
9. R. J. Pelham Jr and Y. Wang, *Proc. Natl. Acad. Sci. U. S. A.*, 1997, **94**, 13661–13665.
10. T. Yeung, P. C. Georges, L. A. Flanagan, B. Marg, M. Ortiz, M. Funaki, N. Zahir, W. Y. Ming, V. Weaver and P. A. Janmey, *Cell Motil. Cytoskeleton*, 2005, **60**, 24–34.
11. Y. S. Pek, A. C. A. Wan and J. Y. Ying, *Biomaterials*, 2010, **31**, 385–391.
12. J. D. Mih, A. Marinkovic, F. Liu, A. S. Sharif and D. J. Tschumperlin, *J. Cell Sci.*, 2012, **125**, 5974–5983.
13. Y. Takada, X. Ye and S. Simon, *Genome Biol.*, 2007, **8**, 215.
14. T. Shimizu, M. Yamato, A. Kikuchi and T. Okano, *Biomaterials*, 2003, **24**, 2309–2316.
15. L. Yang, F. Cheng, T. Liu, J. R. Lu, K. Song, L. Jiang, S. Wu and W. Guo, *Biomed. Mater.*, 2012, **7**, 035003.
16. T. Okano, N. Yamada, H. Sakai and Y. Sakurai, *J. Biomed. Mater. Res.*, 1993, **27**, 1243–1251.
17. N. Yamada, T. Okano, H. Sakai, F. Karikusa, Y. Sawasaki and Y. Sakurai, *Makromol. Chem.*, 1990, **11**, 571–576.
18. A. Halperin and M. Kroger, *Langmuir*, 2012, **28**, 16623–16637.
19. A. Halperin and M. Kroger, *Biomaterials*, 2012, **33**, 4975–4987.
20. M. Yamato, M. Okuhara, F. Karikusa, A. Kikuchi, Y. Sakurai and T. Okano, *J. Biomed. Mater. Res.*, 1999, **44**, 44–52.
21. N. Oppenheimer-Marks and F. Grinnell, *J. Cell Biol.*, 1982, **95**, 876–884.
22. M. A. Cooperstein, B. M. Bluestein and H. E. Canavan, *Biointerphases*, 2015, **10**, 019001.

23. M. A. Cooperstein and H. E. Canavan, *Biointerphases*, 2013, **8**, 19.
24. L. S. Sefcik, A. Kaminski, K. Ling, A. Laschewsky, J. F. Lutz and E. Wischerhoff, *Cell. Mol. Bioeng.*, 2013, **6**, 287–298.
25. A. Abuchowski, T. van Es, N. C. Palczuk and F. F. Davis, *J. Biol. Chem.*, 1977, **252**, 3578–3581.
26. M. A. Ward and T. K. Georgiou, *Polymers*, 2011, **3**, 1215–1242.
27. J. F. Lutz and A. Hoth, *Macromolecules*, 2006, **39**, 893–896.
28. M. Weinhart, T. Becherer and R. Haag, *Chem. Commun.*, 2011, **47**, 1553–1555.
29. P. P. Kundu and M. Kundu, *Polymer*, 2001, **42**, 2015–2020.
30. C. H. Chen, C. C. Tsai, W. Chen, F. L. Mi, H. F. Liang, S. C. Chen and H. W. Sung, *Biomacromolecules*, 2006, **7**, 736–743.
31. S. P. Hoo, F. Sarvi, W. H. Li, P. P. Y. Chan and Z. L. Yue, *ACS Appl. Mater. Interfaces*, 2013, **5**, 5592–5600.
32. M. N. V. R. Kumar, *React. Funct. Polym.*, 2000, **46**, 1–27.
33. J. M. Dang, D. D. Sun, Y. Shin-Ya, A. N. Sieber, J. P. Kostuik and K. W. Leong, *Biomaterials*, 2006, **27**, 406–418.
34. B. Chen, J. Dang, T. L. Tan, N. Fang, W. N. Chen, K. W. Leong and V. Chan, *Biomaterials*, 2007, **28**, 1503–1514.
35. X. F. Li, W. Z. Yuan, S. Y. Gu and J. Ren, *Mater. Lett.*, 2010, **64**, 2663–2666.
36. Y. H. Chen, Y. C. Chung, I. J. Wang and T. H. Young, *Biomaterials*, 2012, **33**, 1336–1342.
37. T. Lopez-Leon, E. L. Carvalho, B. Seijo, J. L. Ortega-Vinuesa and D. Bastos-Gonzalez, *J. Colloid Interface Sci.*, 2005, **283**, 344–351.
38. H. Y. Yeh and J. C. Lin, *J. Biomater. Sci., Polym. Ed.*, 2008, **19**, 291–310.
39. J. Lahann, S. Mitragotri, T. N. Tran, H. Kaido, J. Sundaram, I. S. Choi, S. Hoffer, G. A. Somorjai and R. Langer, *Science*, 2003, **299**, 371–374.
40. C. C. Ng, A. Magenau, S. H. Ngalim, S. Ciampi, M. Chockalingham, J. B. Harper, K. Gaus and J. J. Gooding, *Angew. Chem.*, 2012, **51**, 7706–7710.
41. Y. X. Sun, K. F. Ren, J. L. Wang, G. X. Chang and J. Ji, *ACS Appl. Mater. Interfaces*, 2013, **5**, 4597–4602.
42. M. N. Yousaf, B. T. Houseman and M. Mrksich, *Angew. Chem.*, 2001, **40**, 1093–1096.
43. W. S. Yeo, M. N. Yousaf and M. Mrksich, *J. Am. Chem. Soc.*, 2003, **125**, 14994–14995.
44. R. J. Jackman, J. L. Wilbur and G. M. Whitesides, *Science*, 1995, **269**, 664–666.
45. M. Mrksich, C. S. Chen, Y. Xia, L. E. Dike, D. E. Ingber and G. M. Whitesides, *Proc. Natl. Acad. Sci. U. S. A.*, 1996, **93**, 10775–10778.
46. X. Jiang, R. Ferrigno, M. Mrksich and G. M. Whitesides, *J. Am. Chem. Soc.*, 2003, **125**, 2366–2367.
47. M. M. Walczak, D. D. Popenoe, R. S. Deinhammer, B. D. Lamp, C. K. Chung and M. D. Porter, *Langmuir*, 1991, **7**, 2687–2693.
48. K. M. Persson, S. Lönnqvist, K. Tybrandt, R. Gabrielsson, D. Nilsson, G. Kratz and M. Berggren, *Adv. Funct. Mater.*, 2015, **25**, 7056–7063.
49. P. S. Dittrich and A. Manz, *Nat. Rev. Drug Discovery*, 2006, **5**, 210–218.

50. P. J. Hung, P. J. Lee, P. Sabounchi, R. Lin and L. P. Lee, *Biotechnol. Bioeng.*, 2005, **89**, 1–8.
51. I. Meyvantsson and D. J. Beebe, *Annu. Rev. Anal. Chem.*, 2008, **1**, 423–449.
52. J. El-Ali, P. K. Sorger and K. F. Jensen, *Nature*, 2006, **442**, 403–411.
53. D. Huh, G. A. Hamilton and D. E. Ingber, *Trends Cell Biol.*, 2011, **21**, 745–754.
54. N. K. Inamdar and J. T. Borenstein, *Curr. Opin. Biotechnol.*, 2011, **22**, 681–689.
55. B. D. Kieviet, P. M. Schon and G. J. Vancso, *Lab Chip*, 2014, **14**, 4159–4170.
56. D. J. Beebe, J. S. Moore, J. M. Bauer, Q. Yu, R. H. Liu, C. Devadoss and B. H. Jo, *Nature*, 2000, **404**, 588–590.
57. G. F. Chen, F. Svec and D. R. Knapp, *Lab Chip*, 2008, **8**, 1198–1204.
58. C. Yu, S. Mutlu, P. Selvaganapathy, C. H. Mastrangelo, F. Svec and J. M. J. Frechett, *Anal. Chem.*, 2003, **75**, 1958–1961.
59. A. K. Au, H. Lai, B. R. Utela and A. Folch, *Micromachines*, 2011, **2**, 179–220.
60. M. Hitzbleck, L. Avrain, V. Smekens, R. D. Lovchik, P. Mertens and E. Delamarche, *Lab Chip*, 2012, **12**, 1972–1978.
61. P. Gupta, K. Vermani and S. Garg, *Drug Discovery Today*, 2002, **7**, 569–579.
62. M. A. Cole, N. H. Voelcker, H. Thissen and H. J. Griesser, *Biomaterials*, 2009, **30**, 1827–1850.
63. E. C. Peters, F. Svec and J. M. J. Frechet, *Adv. Mater.*, 1997, **9**, 630–633.
64. S. Sugiura, K. Sumaru, K. Ohi, K. Hiroki, T. Takagi and T. Kanamori, *Sens. Actuators, A*, 2007, **140**, 176–184.
65. A. Pelah, R. Seemann and T. M. Jovin, *J. Am. Chem. Soc.*, 2007, **129**, 468–469.
66. A. Pelah and T. M. Jovin, *ChemPhysChem*, 2007, **8**, 1757–1760.
67. P. C. Weber, D. H. Ohlendorf, J. J. Wendoloski and F. R. Salemme, *Science*, 1989, **243**, 85–88.
68. P. S. Stayton, T. Shimoboji, C. Long, A. Chilkoti, G. H. Chen, J. M. Harris and A. S. Hoffman, *Nature*, 1995, **378**, 472–474.
69. A. Pelah, A. Bharde and T. M. Jovin, *Soft Matter*, 2009, **5**, 1006–1010.
70. S.-k. Ahn, R. M. Kasi, S.-C. Kim, N. Sharma and Y. Zhou, *Soft Matter*, 2008, **4**, 1151.
71. E. Wang, M. S. Desai and S. W. Lee, *Nano Lett.*, 2013, **13**, 2826–2830.
72. S. Gil, C. R. Correia and J. F. Mano, *Adv. Healthcare Mater.*, 2015, **4**, 883–891.
73. M. Shinkai, M. Yanase, H. Honda, T. Wakabayashi, J. Yoshida and T. Kobayashi, *Jpn. J. Cancer Res.*, 1996, **87**, 1179–1183.
74. D. Fayol, G. Frasca, C. Le Visage, F. Gazeau, N. Luciani and C. Wilhelm, *Adv. Mater.*, 2013, **25**, 2611–2616.
75. G. Frasca, V. Du, J. C. Bacri, F. Gazeau, C. Gay and C. Wilhelm, *Soft Matter*, 2014, **10**, 5045–5054.
76. M. Okochi, S. Takano, Y. Isaji, T. Senga, M. Hamaguchi and H. Honda, *Lab Chip*, 2009, **9**, 3378–3384.
77. G. R. Souza, J. R. Molina, R. M. Raphael, M. G. Ozawa, D. J. Stark, C. S. Levin, L. F. Bronk, J. S. Ananta, J. Mandelin, M. M. Georgescu,

J. A. Bankson, J. G. Gelovani, T. C. Killian, W. Arap and R. Pasqualini, *Nat. Nanotechnol.*, 2010, **5**, 291–296.
78. H. Takanari, K. Miwa, X. Fu, J. Nakai, A. Ito, K. Ino, H. Honda, W. Tonomura, S. Konishi, T. Opthof, M. A. van der Heyden, I. Kodama and J. K. Lee, *J. Cell. Physiol.*, 2016, **231**, 2249–2256.
79. Y. Yamanishi, S. Sakuma, K. Onda and F. Arai, *Biomed. Microdevices*, 2010, **12**, 745–752.
80. C. E. Murry, R. W. Wiseman, S. M. Schwartz and S. D. Hauschka, *J. Clin. Invest.*, 1996, **98**, 2512–2523.
81. P. Menasche, A. A. Hagege, J. T. Vilquin, M. Desnos, E. Abergel, B. Pouzet, A. Bel, S. Sarateanu, M. Scorsin, K. Schwartz, P. Bruneval, M. Benbunan, J. P. Marolleau and D. Duboc, *J. Am. Coll. Cardiol.*, 2003, **41**, 1078–1083.
82. G. R. Souza, D. R. Christianson, F. I. Staquicini, M. G. Ozawa, E. Y. Snyder, R. L. Sidman, J. H. Miller, W. Arap and R. Pasqualini, *Proc. Natl. Acad. Sci. U. S. A.*, 2006, **103**, 1215–1220.
83. F. Xu, C. A. Wu, V. Rengarajan, T. D. Finley, H. O. Keles, Y. Sung, B. Li, U. A. Gurkan and U. Demirci, *Adv. Mater.*, 2011, **23**, 4254–4260.
84. D. An, A. Warning, K. G. Yancey, C.-T. Chang, V. R. Kern, A. K. Datta, P. H. Steen, D. Luo and M. Ma, *Nat. Commun.*, 2016, **7**, 12401.
85. Y. Itabashi, S. Miyoshi, H. Kawaguchi, S. Yuasa, K. Tanimoto, A. Furuta, T. Shimizu, T. Okano, K. Fukuda and S. Ogawa, *Artif. Organs*, 2005, **29**, 95–103.
86. N. G. Patel and G. Zhang, *Organogenesis*, 2013, **9**, 93–100.
87. M. Yamato, M. Utsumi, A. Kushida, C. Konno, A. Kikushi and T. Okano, *Tissue Eng.*, 2001, **7**, 473–480.
88. M. Harimoto, M. Yamato, M. Hirose, C. Takahashi, Y. Isoi, A. Kikuchi and T. Okano, *J. Biomed. Mater. Res.*, 2002, **62**, 464–470.
89. C. H. Du, C. Yao, N. Y. Li, S. Y. Wang, Y. Y. Feng and X. C. Yang, *Exp. Ther. Med.*, 2015, **10**, 2216–2220.
90. M. Hirabaru, T. Kuroki, T. Adachi, A. Kitasato, S. Ono, T. Tanaka, H. Matsushima, Y. Sakai, A. Soyama, M. Hidaka, K. Yamanouchi, M. Takatsuki, T. Okano and S. Eguchi, *Tissue Eng., Part C*, 2015, **21**, 1205–1215.
91. Y. Otsuki, Y. Nakamura, S. Harada, Y. Yamamoto, K. Ogino, K. Morikawa, H. Ninomiya, S. Miyagawa, Y. Sawa, I. Hisatome and M. Nishimura, *Biomed. Res.*, 2015, **36**, 11–19.
92. J. H. Park, J. Y. Park, I. C. Nam, S. H. Hwang, C. S. Kim, J. W. Jung, J. Jang, H. Lee, Y. Choi, S. H. Park, S. W. Kim and D. W. Cho, *Acta Biomater.*, 2015, **25**, 56–64.
93. R. Suzuki, A. Aruga, H. Kobayashi, M. Yamato and M. Yamamoto, *Anticancer Res.*, 2014, **34**, 4747–4754.
94. J. Chen, X. Z. Qiu, L. Y. Wang, W. Zhong, J. M. Kong and M. M. Q. Xing, *Adv. Funct. Mater.*, 2014, **24**, 2216–2223.
95. P. Dixit, D. Hern-Anderson, J. Ranieri and C. E. Schmidt, *J. Biomed. Mater. Res.*, 2001, **56**, 545–555.
96. R. M. Nerem and D. Seliktar, *Annu. Rev. Biomed. Eng.*, 2001, **3**, 225–243.
97. M. S. Baguneid, A. M. Seifalian, H. J. Salacinski, D. Murray, G. Hamilton and M. G. Walker, *Br. J. Surg.*, 2006, **93**, 282–290.

98. S. J. Lee, J. Liu, S. H. Oh, S. Soker, A. Atala and J. J. Yoo, *Biomaterials*, 2008, **29**, 2891–2898.
99. H. Ahn, Y. M. Ju, H. Takahashi, D. F. Williams, J. J. Yoo, S. J. Lee, T. Okano and A. Atala, *Acta Biomater.*, 2015, **16**, 14–22.
100. N. Tanaka, H. Ota, K. Fukumori, J. Miyake, M. Yamato and T. Okano, *Biomaterials*, 2014, **35**, 9802–9810.
101. C. K. Colton, *Cell Transplant.*, 1995, **4**, 415–436.
102. K. Sakaguchi, T. Shimizu and T. Okano, *J. Controlled Release*, 2015, **205**, 83–88.
103. T. Shimizu, H. Sekine, J. Yang, Y. Isoi, M. Yamato, A. Kikuchi, E. Kobayashi and T. Okano, *FASEB J.*, 2006, **20**, 708–710.
104. K. Sakaguchi, T. Shimizu, S. Horaguchi, H. Sekine, M. Yamato, M. Umezu and T. Okano, *Sci. Rep.*, 2013, **3**, 1316.
105. M. Muraoka, T. Shimizu, K. Itoga, H. Takahashi and T. Okano, *Biomaterials*, 2013, **34**, 696–703.
106. H. Takahashi, T. Shimizu, M. Nakayama, M. Yamato and T. Okano, *Biomaterials*, 2013, **34**, 7372–7380.
107. H. Takahashi, M. Nakayama, T. Shimizu, M. Yamato and T. Okano, *Biomaterials*, 2011, **32**, 8830–8838.
108. C. L. Rossouw, A. Chetty, F. S. Moolman, L. M. Birkholtz, H. Hoppe and D. T. Mancama, *Biotechnol. Bioeng.*, 2012, **109**, 2147–2158.
109. G. D. Prestwich, *Acc. Chem. Res.*, 2008, **41**, 139–148.
110. D. Mooney, L. Hansen, J. Vacanti, R. Langer, S. Farmer and D. Ingber, *J. Cell. Physiol.*, 1992, **151**, 497–505.
111. T. Takezawa, Y. Mori and K. Yoshizato, *Bio/Technology*, 1990, **8**, 854–856.
112. M. Yamazaki, M. Tsuchida, K. Y. Kobayashi, T. Takezawa and Y. Mori, *Biotechnol. Bioeng.*, 1994, **44**, 38–44.
113. T. Miyata, T. Sohde, A. L. Rubin and K. H. Stenzel, *Biochim. Biophys. Acta*, 1971, **229**, 672–680.
114. M. Yamazaki, M. Tsuchida, K. Kobayashi, T. Takezawa and Y. Mori, *Biotechnol. Bioeng.*, 1995, **48**, 17–24.
115. T. Takezawa, M. Y. , Y. Mori, T. Yonaha and K. Yoshizato, *J. Cell Sci.*, 1992, **101**, 495–501.
116. M. A. Cooperstein and H. E. Canavan, *Langmuir*, 2010, **26**, 7695–7707.
117. T. Matsuda, *J. Biomater. Sci., Polym. Ed.*, 2004, **15**, 947–955.
118. Y. Kumashiro, J. Ishihara, T. Umemoto, K. Itoga, J. Kobayashi, T. Shimizu, M. Yamato and T. Okano, *Small*, 2015, **11**, 681–687.
119. W. Song, C. K. Tung, Y. C. Lu, Y. Pardo, M. Wu, M. Das, D. I. Kao, S. Chen and M. Ma, *Soft Matter*, 2016, 5739–5746.
120. T. O. Collier, J. M. Anderson, A. Kikuchi and T. Okano, *J. Biomed. Mater. Res.*, 2002, **59**, 136–143.
121. K. Nishida, M. Yamato, Y. Hayashida, K. Watanabe, K. Yamamoto, E. Adachi, S. Nagai, A. Kikuchi, N. Maeda, H. Watanabe, T. Okano and Y. Tano, *N. Engl. J. Med.*, 2004, **351**, 1187–1196.

CHAPTER 16

Flexible Micro- and Nanoelectronics for Tissue Engineering

H. ACARÓN LEDESMA[a], K. KOEHLER[b] AND B. TIAN*[b,c,d]

[a]Biophysical Sciences Program, University of Chicago, Chicago, IL 60637, USA; [b]Department of Chemistry, University of Chicago, Chicago, IL 60637, USA; [c]The James Franck Institute, University of Chicago, Chicago, IL 60637, USA; [d]The Institute for Biophysical Dynamics, University of Chicago, IL 60637, USA
*E-mail: btian@uchicago.edu

16.1 Introduction

Tissue engineering aims to assemble functional constructs that restore, maintain, or improve damaged tissues or whole organs. To achieve this goal, the field has focused on designing materials capable of providing functionality to biological systems,[1–4] assessing biological activity,[5,6] and mimicking the properties of biological systems.[7,8] Traditionally, constructs developed for tissue engineering are composed of scaffolds, cells, and biologically active molecules that attempt to recreate the chemical and mechanical composition of many biological environments. However, with many advances in electroceuticals[9] and discoveries of the underlying mechanisms of excitable membranes,[10–14] there has been a momentous push to incorporate electronics into tissue engineering. In this chapter, we will focus on the work done

Smart Materials No. 25
Smart Materials for Tissue Engineering: Applications
Edited by Qun Wang

Published by the Royal Society of Chemistry, www.rsc.org

over the past decade in designing and implementing micro- and nanoscale electronics in biological systems.

Cell membranes are embedded with many different types of ion pumps and ion channels that are selective for transporting Na^+, K^+, Cl^-, and Ca^{2+} ions, among others, across a cell's semipermeable membrane.[15] The transport of these ions is governed by the electrochemical gradients established across the cell membrane, creating an asymmetric ion distribution between the intra- and extracellular fluids. The unequal distribution of charged molecules in addition to the selective permeability of cell membranes give rise to membrane potentials, which can be probed using electrodes or field effect transistors. Virtually all biological cells exhibit this bioelectric behavior and have either stable or variable membrane potentials. In particular, some eukaryotic cells, such as neurons, cardiomyocytes, smooth and skeletal muscle cells, and some secretory cells, are electrically excitable since cellular events can lead to the opening and closing of ion channels. In excitable cells, the membrane potential can be depolarized or hyperpolarized relative to resting potential (between −40 and −80 mV for most cells) depending on which ion channels are activated. Neurons in the brain and cardiomyocytes in the heart use these electrophysiological signals to communicate and trigger processes such as propagation of information and the heartbeat.

Excitable cells can assemble into tissues and organs such as the brain, heart, and muscles, which partially use bioelectric signals to maintain proper function. For example, the human brain is composed of approximately 100 billion neurons and each makes approximately 7000 connections to other neurons. This leads to complex electrical patterns across the central nervous system and proper brain function being dependent on the reliable signaling between neurons. Damaged or diseased states can disrupt this electrical signaling in specific areas of the brain. The activity of cardiomyocytes in the heart is coordinated by similar electrical signals. Traditionally, these systems have been interrogated with bulky electrodes, such as patch-clamp electrophysiology[16] and multi-electrode arrays,[17] which are not suitable for long-term probing. Traditional probes tend to be highly invasive both because of their large-scale dimensions and mechanical mismatch with targeted tissue.[18,19] As a solution to bulky and invasive probes, flexible micro- and nanoscale materials could be developed with the capacity to read out the activity of these tissues and provide electrical signals where such function has been lost. This alternative would significantly advance the maintenance and treatment of many disorders that pertain to natural or engineered neural and cardiac tissues.

In general, there are two main approaches to fabricating micro- and nanoscale objects commonly referred to as top-down and bottom-up paradigms.[20] In the top-down approach, combinations of lithography, etching, and deposition are used to create small patterns in bulk materials. In the bottom-up approach, the intrinsic chemical properties of atomic, molecular, and nanoscale building blocks are employed to assemble structures and patterns. These approaches are used exclusively or together to create complex

electronic structures and devices. With these techniques, micro- and nanoelectronic devices fabricated at the same length scales of many sub-cellular structures can be developed to interface biological systems. Specifically, the similar size scale of micro-/nanostructures and biological building blocks facilitates the seamless integration of electronics with cells and tissues and enables promising opportunities for the development of engineered tissues and biomedical prosthetics. Recent studies have demonstrated that devices with small-scale dimensions exhibit increased biocompatibility and create less invasive interfaces with cells and tissues. These studies include experiments showing the internalization of nanoscale inorganic devices by individual cells, *in vitro* cell culture on substrates containing nanopillar arrays, and single-cell nanowire endoscopy.[21–23] From a material and device perspective, micro- and nanoscale devices can have improved spatial resolution, enhanced carrier transport properties, and reduced power consumption. Existing evidence suggests that flexible micro- and nanoscale electronics represent new avenues for tissue engineering.

16.2 Material Building Blocks and Their Interfaces with Cells and Tissues

Before going into detail about state-of-the-art bioelectronic devices, a basic understanding of the nanostructured material building blocks used in the design and development of these devices is required. A variety of novel nanomaterials exhibiting strengthened carrier transport have emerged over the past several decades, including zero-dimensional nanoparticles, one-dimensional nanotubes[24–26] and nanowires,[26–28] and two-dimensional nanosheets.[29,30] Nanoparticles have unique properties due to quantum confinement[31,32] and large surface areas; but their use in electronics has been limited by challenges in establishing robust and reproducible electrical contacts. On the other hand, one-dimensional nanostructures, such as nanowires and nanotubes, represent the smallest material systems that can efficiently transport electrical carriers. The small-scale dimensions of these materials dramatically decreases the mechanical rigidity of devices while acting as electrodes, field effect transistors, and diodes.[33,34] The unprecedented augmented physical properties in these materials are advantageous for tissue engineering applications, because they can lead to the fabrication of flexible electronic devices that are desired for biointerfaces.

The key component in a micro- or nanoscale bioelectronic device is the active device element used to interface with a biological component with the purpose of recording or stimulating a biological event. The high surface-to-volume ratio of nanomaterials offers high sensitivity to surface processes.[35] In addition, the size scale of nanostructures can be comparable to biological building blocks, such as proteins and nucleic acids, offering new ways to perturb living systems from subcellular to tissue levels,[36] which can be particularly useful in a tissue engineering process. Indeed, recent work

has shown that the structure, size, morphology, and topography of nanoscale materials determine their chemical and physical properties needed for biological interfaces.[37] Therefore, the development of bioelectronic devices involves rational design in order to exploit the unique properties of different nanomaterials with the goal of providing unique capabilities of interfacing with and studying diverse biological behaviors. The following sections in this chapter will focus on the synthesis, structure, and properties of silicon- and carbon-based nanomaterials, nanostructured polymers, and nanoscale metal electrodes.

16.2.1 Inorganic Semiconductors

One-dimensional semiconductor nanomaterials, including nanowires, nanotubes, and nanorods, have been of particular interest over the past several decades because of their novel electrical, optical and mechanical properties, and demonstrated applications in biology and medicine. For example, semiconductor nanowires have been exploited in a wide range of device configurations, such as light-emitting diodes,[38] lasers,[39,40] biological and chemical sensors,[41,42] and solar cells.[43] Silicon nanowires (SiNWs) are particularly powerful, and they are generally synthesized *via* the vapor–liquid–solid growth mechanism, where a metallic nanoparticle catalyzes the formation of a metal-semiconductor alloy in the presence of a vapor-phase silicon source above the eutectic temperature.[44] During the synthesis, vapor-phase silicon is continuously fed into the growth system, allowing the liquid alloy to become supersaturated and in this state the semiconductor solid can nucleate and precipitate. This process over time leads to the vertical growth of SiNWs on a substrate. Overall, the ability to control and modulate the doping,[45,46] composition,[47,48] crystal structure,[49] and morphology[21,41,50] of semiconductor nanowires during the synthesis process has allowed researchers to explore various applications of nanowires.

The morphology and surface topography of SiNWs are of great importance since these features dictate how the material will interact with target cells and tissues. The rational design and fabrication of complex nanowires offers great potential for creating integrated systems capable of exploring novel bioelectronic interfaces. For example, Tian *et al.* demonstrated how transient modifications of growth parameters can lead to *in situ* morphological changes in one-dimensional materials during their synthesis.[41] Specifically, kinks were introduced along the length of nanowires by creating abrupt pressure variations.[41] This method also confers control over the stereochemistry of adjacent kinks, which can be beneficial for the synthesis of complex 2D and 3D structures.[41] As shown in Figure 16.1(a) and (b), this method was used to introduce two *cis*-linked kinked units in SiNWs to yield 60° angle probes.[41] In addition, dopants were introduced during the synthesis of these nanowires in order to fabricate a nanoscale FET capable of performing intracellular recordings from excitable cells.[41] Results from this study emphasize how nanowire-based bioprobe arrays could be particularly advantageous for

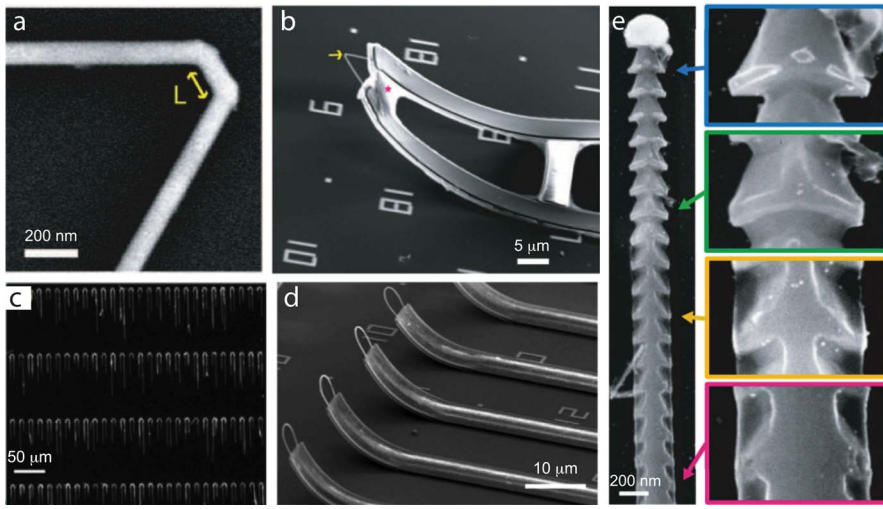

Figure 16.1 Silicon nanomaterials as building blocks for biomedical devices. (a) Double kinked SiNW two-terminal FET probe for electrophysiological recordings. (b) SEM image of a free-stranding three-dimensional device with kinked probe sandwiched between SU-8 polymer and metal contacts. (c) Shape-controlled assembly of U-shaped silicon nanowire arrays. (d) SEM image of large-scale three-dimensional curved nanowire probe with bend up geometry. (e) Skeleton-like Si spicules synthesized by pressure modulation and selective etching of silicon. Reproduced with permission from B. Tian *et al.*, *Science*, 2010, **329**(5993), 830 (a), (b), reprinted with permission from Y. Zhao *et al.*, *Nano Lett.*, 2016, **16**, 2644, copyright (2016) American Chemical Society (c), (d), from Z. Luo *et al.*, *Science*, 2015, **348**(6242), 1451, reprinted with permission from AAAS (e).

probing cellular networks of an excitable engineered tissue, or recording from acute brain slices and possibly *in vivo*. Kinked SiNWs have also been used as a probe for intracellular and intercellular force dynamics.[21] In experiments by Zimmerman *et al.*, human umbilical vein endothelial cells (HUVECs) and human aortic smooth muscle cells (HASMCs) internalized singly-kinked SiNWs *via* the cells' natural endocytic pathway.[21] The kink in the internalized nanostructure served as an anchoring point that limited the rotation and translation of the SiNWs and enabled accurate monitoring of the deflection over time during live cell imaging. Intracellular forces experienced by single cells during ordinary cellular processes, such as cell migration, division, and contraction, were calculated by applying the Euler–Bernoulli beam theory on the measurements of kinked-SiNW bending.[21]

As mentioned above, kinked nanowires can be utilized as building blocks for integrated bioelectronics; however, *in situ* perturbations are not the only way of fabricating 1D structures with innovative morphology. The morphology of traditional, straight SiNWs can also be modified post-synthesis. Recent work in Charles Lieber's research group at Harvard University described

a novel technique for the large-scale assembly of U-shaped nanowires with well-defined curvature.[50] In this study, the authors employed a modified version of the nanocombing technique previously described by Yao *et al.* for aligned assembly of nanowires.[50,51] Essentially, the nanocombing technique is comprised of sliding the nanowire growth substrate over a target substrate containing lithographically patterned trenches that serve as anchoring regions for nanowires. Zhao *et al.* used photolithography to pattern U-shaped trenches with a 1.5 μm radius and 260 nm depth on a Si wafer. Their experiments showed that the trench depth was ~4 times the nanowire diameter or greater and a trench with >2 μm yielded a >90% success rate for the assembly of U-shaped nanowires.[50] (Figure 16.1(c)) Experimental data and modeling suggest that the U-shape trenches serve to initially anchor and mechanically trap the nanowires, and then the shear force produced during the transfer bends the nanowires around the shaped trench and aligns their arms in the transfer direction.[50] The assembly of nanowires with defined curvature could lead to novel applications not feasible with straight wires. For this reason, the authors explored the potential of these curved nanowires for the fabrication of large-scale three-dimensional (3D) nanowire bioprobe arrays. As demonstrated in Figure 16.1(d), U-shaped silicon nanowires were organized in a 3D bent geometry similar to the studies testing kinked SiNWs.[41] Analysis of device conductance and signal-to-noise ratios revealed yields comparable to, or better than, the performance of kinked nanowire devices,[50] suggesting that U-shaped nanowires could provide improved signal recording. Zhao *et al.* were able to attain innovative structural configurations for integrated nanodevices by combining the strengths of wafer-scale top-down fabrication with the tunable properties of one-dimensional building blocks.

So far, we have reviewed several techniques for the modification of SiNW morphology. Another key parameter to be considered for nano-bioelectronics is the surface topography of one-dimensional building blocks as it determines the interactions that occur at the material–biology interface. Mesoscale and nanoscale patterning on one-dimensional materials has been limited due to the resolution of top-down approaches and the need for precise and controlled assembly of molecular building blocks in the bottom-up approach.[52] While lithography at these length scales remains a difficult task, some research groups have developed techniques capable of fabricating meso- and nanostructured 1D semiconductors. For example, Luo *et al.* took advantage of the pressure-dependent Au diffusion in Si to create etchant-resistant patterns in SiNWs during synthesis. As you can see in Figure 16.1(e), post-synthesis wet chemical etching removed Si in the regions that were not protected by Au, creating silicon spicules with complex surface topography.[53] Here, gold had two functions in the fabrication of these structures: (1) as a catalyst to nucleate and elongate silicon nanowires from the vapor phase and (2) as a mask to protect Si from etchants. Varying the pressure of the growth process altered the rate of gold diffusion along the surface of the wire. The authors were thus able to make a series of mesoscale ridges and notches in one-dimensional silicon materials strictly by chemical methods. The anisotropic mesoscale topography of Si spicules, when compared to more isotropic Si structures, suggests that these structures could experience enhanced surface

interactions with surrounding environments such as hydrogels or biological tissues. These enhanced surface interactions were measured by atomic force microscopy (AFM) experiments. Single mesostructured Si spicules mounted onto cantilever tips *via* focused ion-beam (FIB) lithography were inserted and retracted from collagen type I hydrogels while monitoring the force and work

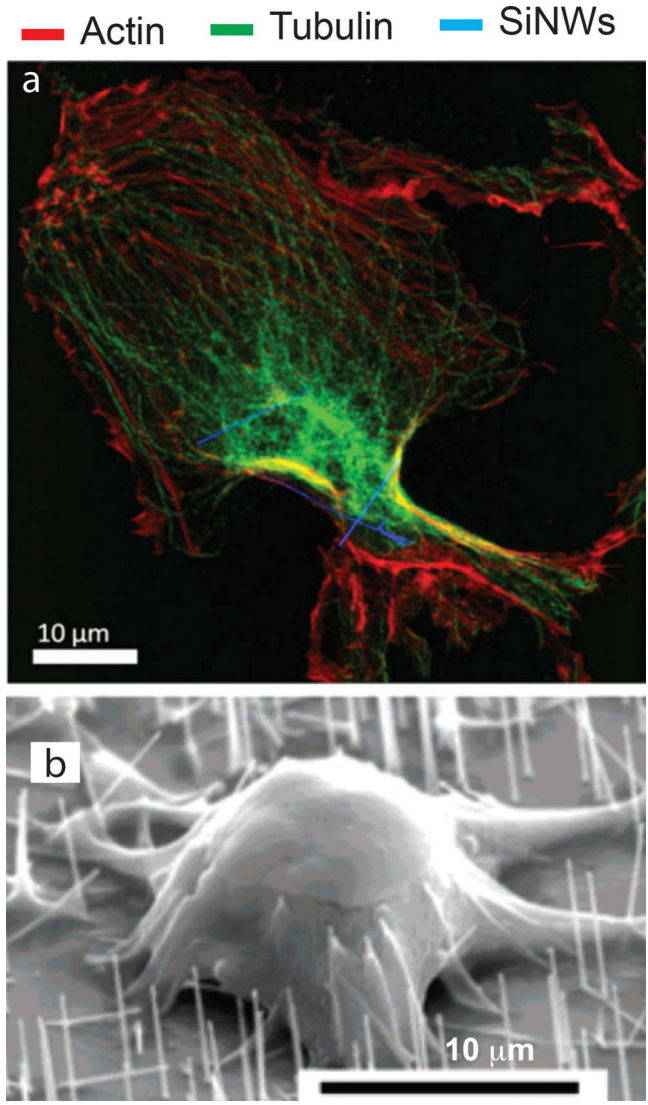

Figure 16.2 Interface between SiNWs and biological systems. (a) Interaction between internalized kinked SiNWs and cytoskeletal elements in HUVECs. (b) Mouse embryonic stem cells cultured on a Si substrate with vertically aligned SiNW array. Reproduced with permission from J. F. Zimmerman *et al.*, *Nano Lett.*, 2015, **15**(8), 5492, copyright (2015) American Chemical Society (a) and reprinted with permission from W. Kim *et al. J. Am. Chem. Soc.*, 2007, **129**(23), 7228, copyright (2007) American Chemical Society (b).

of the spicule–matrix interactions. These AFM experiments indicated that the Si spicule probe exhibits a higher detachment force (~4.16 nN) compared to un-etched nanowires (~0.455 nN), modulated nanowires (~1.03 nN), and nanoporous nanowires (~0.827 nN).[53] These results highlight the potential for creating tight junctions in tissue engineering or bioelectronics by adopting mesostructured Si spicules to interface with soft materials.

A final hurdle for nano-bioelectronics is biocompatibility. The biocompatibility of SiNWs has been evaluated by internalization experiments performed by Zimmerman *et al.* and has been confirmed by other studies evaluating cell activity and viability. Zimmerman *et al.* used confocal microscopy and histochemical analysis to reveal extensive interactions of the internalized SiNWs with the cytoskeletal elements of cells (Figure 16.2(a)).[21] Confluence and metabolic activity experiments demonstrated that these interactions did not cause a significant effect on cell viability. Studies from Peidong Yang's research group at the University of California, Berkeley, have also demonstrated that cell–nanowire interactions do not create conflicts with routine cell behavior. For example, in experiments where embryonic stem cells were cultured on penetrating vertical silicon nanowire arrays (Figure 16.2(b)), they reported cell survival up to seven days.[22] In addition, no cell toxicity was observed when nanowires penetrating cells were used as endoscopes.[23] The design capabilities, enhanced electronic performance, and the high biocompatibility of SiNWs make them an excellent candidate for building blocks for tissue engineering devices.

16.2.2 Carbon-Based Materials

Carbon nanostructures, including single-walled carbon nanotubes (SWCNT), multi-walled carbon nanotubes (MWCNT), graphene sheets, and graphene ribbons, are allotropes of carbon that represent an organic alternative to the semiconductor building blocks we discussed above. These nanoscale materials are typically synthesized to have dimensions ranging from several hundred nanometers to several microns[54] and they exhibit large aspect ratios (above 10^6).[55] The length scale of these materials is similar to that of subcellular structures,[56] making carbon nanomaterial solutions noninvasive. The large aspect ratio of these materials is able to provide a large surface area[57] for functionalization and interaction with biological targets. Carbon nanostructures are uniquely poised to advance the field of tissue engineering because their electrical, mechanical, and surface properties depend heavily on the structural configurations of these building blocks. With an extensive range of potential geometric orientations and physical properties, carbon nanostructures have great potential for use in a wide array of applications. In particular, the highly tunable electrical properties can result in promising novel solutions for interfacing electrically excitable cells, such as neurons or cardiomyocytes. In addition, the flexible and resilient nature of CNTs makes them a good candidate to conform to soft tissue interfaces.

Due to the heavy dependence of physical properties on structure, methods for synthesizing carbon nanoscale building blocks with controlled morphology have become crucial.[58] There are many established synthetic methods including arc discharge,[59] laser ablation,[60] electrolysis, flame synthesis,[61] and the most commonly used method chemical vapor deposition (CVD). CVD becomes a preferred technique then because it affords more control over quality and type of CNTs produced and bulk production is less of a challenge.[60] CVD for CNT growth is determined by the metallic nanoparticle catalyst that serves as a decomposition site for carbon feedstock gas and the template for CNT elongation. One of the most elusive challenges has remained the difficulty in synthesizing specific geometries with a high yield. Purification and isolation steps are employed to circumvent difficulties in synthesizing monodisperse products. Solution phase separation,[54] tube sorting *via* chromatography, density gradient centrifugation, electrophoresis, and purification by refluxing CNTs in an oxidizing acid like nitric acid[63] have all been used for this purpose.

Single-walled carbon nanotubes (SWNT) are generally thought of as graphene sheets rolled into hollow tubes. This encompasses a wide range of structural orientations defined by the chiral index (n,m). Within these parameters there are three types of geometries: zigzag (n,0), armchair (n,n), and rest are considered chiral nanotubes. The chiral index denotes the orientation and magnitude of the chiral vector, and determines the electronic properties of the SWNT. The morphology, size, and diameter of the nanotube will determine the electrical properties that can range from a metallic state to a semiconducting state. For this reason, electronic applications require monodisperse samples that are isomerically pure and electronically similar. Multi-walled carbon nanotubes consist of coaxial nanotubes with a spacing of around 0.34 nm.[61] CNTs are not biodegradable[64] meaning that cell–material interfaces created with these materials are stable and well suited for long-term applications such as neural prostheses.

Although there are effective solution-based separation and isolation techniques, synthetic routes for the fabrication of tailored carbon nanostructures will provide the most effective method for accessing the unique electronic properties these materials can provide. Often the focus is on tailoring the shape and composition of the metallic nanoparticles used in CVD as a method of patterning the resulting geometry,[54] but other methods include end-cap engineering or cloning.[62] Several groups have made exciting advances towards this goal by demonstrating the high yield synthesis of single-chirality single-walled carbon nanotubes and graphene nanoribbons with zigzag edge topology. These advancements indicate that improvements in synthetic techniques will continue to advance the potential for the bottom-up synthetic direction of NT geometry for specific purposes.

Sanchez-Valencia *et al.* successfully synthesized single chirality (6,6) armchair carbon nanotubes *via* a two-step bottom up synthetic strategy.[62] The first step involves patterning a precursor compound that undergoes intramolecular cyclodehydrogenation to produce ultra-short seeds of (6,6) SWNTs.

In the second step, these seeds underwent selective epitaxial growth into monodisperse SWNTs. Both careful precursor design and use of a planar catalyst gave this method a significant advantage over other synthetic patterning approaches. The rational design of the precursor compound resulted in singly capped ultra-short SWNT seeds that dictated the unidirectional growth and precise geometry of subsequent SWCNT growth. Furthermore, integration of planar Pt(111) as the catalyst, *in lieu* of traditional metal nanoparticles, suppressed spontaneous production of seed structures, which would elongate into CNTs of varied geometries and reduce the overall purity of the fabrication technique. In a different approach to directing CNT geometry, Yang *et al.* tailored the size and composition of the metallic nanoparticle (W_6Co_7) catalyst key to the CVD growth of carbon nanotubes (Figure 16.3).[65] With this approach they were able to grow single chirality (12,6) SWCNTs at an abundance of 92%. Previous attempts to tailor catalysts had resulted

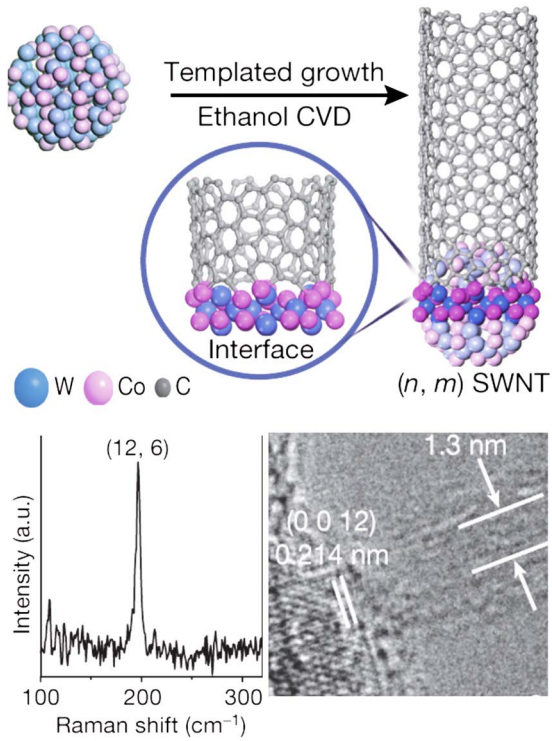

Figure 16.3 Carbon-based nanomaterial building blocks. Chirality-specific growth of single-walled carbon nanotubes on solid alloy catalysts. Diagram (upper) of the W–Co solid nanocrystal catalyst that templates SWCNT with specific (n,m). Raman spectrum (lower left) of SWCNT templated from W–Co nanocrystal catalyst. HRTEM of SWCNT perpendicular to W–Co nanocrystal (lower right). Reproduced with permission from Macmillan Publishers Ltd: F. Yang *et al.*, *Nature*, 2014, **510**, 522, copyright (2014).

in the highest yields around 55% of a single chirality, so the authors looked to alloy nanoparticles that could provide very specific structural features for directing CNT growth. To achieve this drastic increase in purity, a tungsten alloy with a high melting point was used as the CVD growth catalyst. W_6Co_7 nanoparticles likely retain their crystalline structure and ordered facets during CVD growth at 1030 °C as they remain crystalline in a vacuum up to 1100 °C. This indicates that the solid nanoparticles are able to provide optimized structural association with carbon atoms arranged around the nanotube circumference; a key parameter in directing strict (12,6) CNT structure growth. AFM height profile measurements supported this uniform growth confirming the diameter of about 1.28 nm for SWCNTs. Although carbon nanostructures have the potential to produce a large diversity of interesting electrical properties, the sensitivity of these properties to structural conditions necessitates the development of precise and tunable fabrication methods. Advancements such as these towards synthetic control over highly pure carbon nanostructures will be essential to the future developments of carbon nanostructures and their integration into tissue engineering applications.

The tailorable electrical conductivity, flexible and resilient mechanical properties, and large surface area have allowed carbon nanostructures to be a popular research topic for bio-integration. Early studies that interfaced CNTs with cellular platforms saw long term viability and alterations in cell morphology including increased neurite length and branching when neurons were cultured on functionalized MWNT supports.[64,66] In a related study by Malarkey *et al.*[67] SWNT films with a specific conductivity range and surface coatings promoted the greatest increase in cell body area. These results indicated that CNTs, with tailored conductivity and functionality, could have success in serving as a platform for neural prostheses in cases where long-term directed growth would be required. In the case of implants for neural regeneration with damaged brain or spinal cord tissue, CNTs seemed to have the proper requirements to serve as scaffolds that would promote growth and reestablishment of neuron connections. Following these studies, Gabay *et al.*[68] patterned substrates with CNT islands such that neurons and glial cells preferentially migrated to CNT-coated locations. Patterned geometries directed network formation between the islands. Gabay *et al.* then utilized this lithographically patterned island network and neuronal interface to develop a micro electrode array.[68] Lithographically defined titanium nitride conductors were deposited on a silicon dioxide substrate and then dense islands of CNTs were grown *via* CVD on top of the defined electrode array. This fabrication process resulted in a 3D microelectrode array that promoted neuronal attachment without further functionalization. Spontaneously induced extracellular signals were recorded from the neuron culture, which demonstrated typical signal shapes and a high signal-to-noise ratio due to strong cell–electrode coupling. Expanding on this concept David-Pur *et al.* integrated a CNT microelectrode array into a soft polymeric support with the goal of demonstrating efficacy as a neuro-prosthetic device.[69] This soft implantable microelectrode array was designed to record and locally

stimulate nervous system activity. To fabricate this device, they lithographically patterned the circuit and grew the MWNT islands *via* CVD (Figure 16.4). Then the polymeric support PDMS or polyimide was cast over the patterned circuit and cured, making intimate contact with the MWNTs. The device was tested by recording electrical activity from an embryonic chick retina. As with previous studies, the CNT islands anchored the neuronal cells, making intimate contact for recording and stimulation. They were able to record spontaneous extracellular activity, but also demonstrated stimulation of cellular activity with currents of 4 μA and a pulse width of 1 ms (Figure 16.4). These prior results have demonstrated the potential of utilizing CNTs' electrical and physical properties for interfacing with excitable cells such as neurons, but further fundamental studies of the cell–nanostructure interface will be critical. Research to this end will be greatly supported by developments in synthetic approaches and greater degrees of control over nanostructure architecture and purity.

As our understanding of the carbon nanostructure cellular interface advances, the biocompatibility of these structures will become increasingly

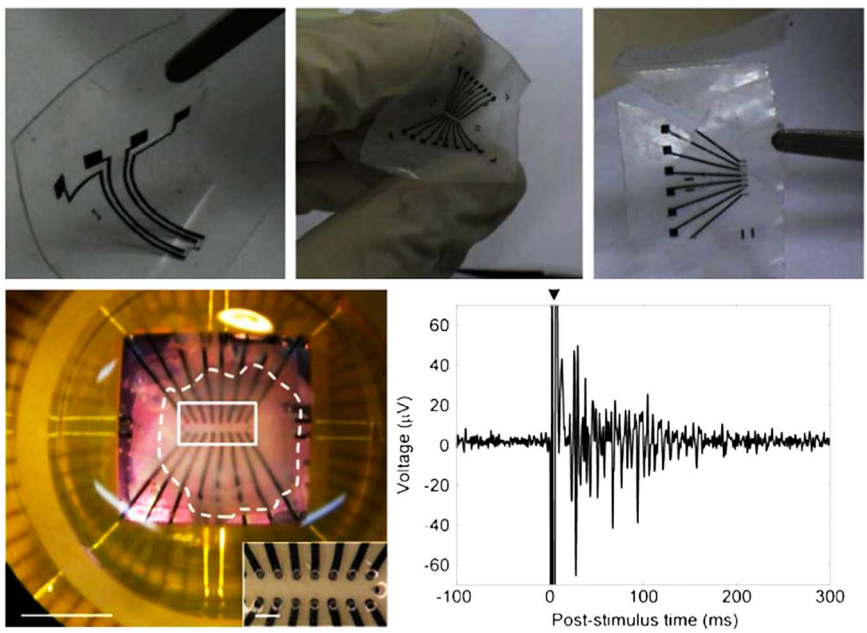

Figure 16.4 Carbon nanotube bio-Interface. All-carbon-nanotube flexible multi-electrode array for neuronal recording and stimulation. Demonstration of flexible PDMS polymeric support bearing fabricated CNT micro electrode array (upper panel). Embryonic chick retina (white dotted line) is mounted onto the flexible microelectrode array (lower left). Recording of stimulated activity of chick retina (lower right). Electrical response matched a typical pre-synaptic cell activation. Reproduced from M. David-Pur *et al.*, *Biomed. Microdevices.*, 2014, **16**(1), 43.

important. Currently, research on this topic is inconsistent and there is a large degree of contradictory evidence.[55] But, for these materials to be truly advantageous in tissue engineering developments, they must be decidedly biocompatible so a comprehensive understanding of the carbon nanostructure–biology interface must be established. Initial toxicology studies indicated the potentially harmful effects of these nanomaterials. Pulmonary studies by Lam *et al.*[70] indicated a higher toxicity for CNTs compared to carbon black from inhalation exposure, with a study of the lungs of mice after seven and 90 days showing interstitial inflammation and in some cases necrosis. Cui *et al.*[71] investigated the toxicity of SWNTs in HEK293 kidney cells and observed inhibition of cell proliferation, limited cell adhesion, and signs of apoptosis evident above 25 μg mL^{-1} SWNT. Despite these observations, numerous other studies demonstrated long-term cell survival and general biocompatibility with CNTs.[64,66] Dumortier *et al.*[72] investigated the immune response of functionalized CNTs. They observed no effect on primary immune cell viability *in vitro* with functionalized CNTs. Some studies even observe greater cell viability with CNT platforms. Gheith *et al.*[73] demonstrated long-term viability of 94–98% of neurons cultured on SWNT thin polymer films. Notably, they observed that for cells grown on films without the SWNT, cell viability dropped to 65%, indicating that the SWNT contributed to the biocompatibility of the polymer films. Although there is no clear answer regarding the biocompatibility of carbon nanomaterials, new research developments such as functionalized CNTs supporting neuron growth and development[64,66] are promising steps towards biocompatible carbon nanomaterials for tissue engineering.

16.2.3 Nanostructured Polymers

In their native environments, cells rely on various mechanical and biochemical cues provided by the extracellular matrix (ECM) to maintain proper function. Nanostructured polymer scaffolds developed for tissue engineering have evolved to mimic natural cellular microenvironments and provide proper cues to encourage cell viability, growth, adhesion, or proliferation.[74] Implantable devices fabricated from soft elastomeric materials can minimize inflammatory responses[75] and improve intimate association with the curvilinear surfaces of complex biological systems. Both natural and synthetic polymers can be modified *via* chemical methods to obtain scaffolds with structural configurations and chemical functionality that closely resemble the natural ECM of many tissues. Numerous reports have demonstrated that these scaffolds can generate morphological anisotropy,[76] provide a compressive modulus and mechanical properties similar to native ECM,[75] and replicate high aspect ratio structures seen with collagen or other ECM fibers. In addition to favorable mechanical properties, polymer scaffolds can also be designed to exhibit electronic properties important for interfacing with excitable cell types, such as neurons or cardiomyocytes.[6,77,78]

Recent work in this field has provided a wide array of biocompatible or biodegradable options of elastomeric polymers that can be synthesized, functionalized, or hybridized to produce nanostructured geometries and physical properties tailored for varied cell types and applications. Polymer systems include (1) natural polymers: collagen,[79] gelatin,[80] chitosan,[84] silk[76] or alginate,[6,81] (2) synthetic biodegradable polymers: poly(L-lactic acid),[77,82] poly(glycerol sebacate),[80] or polycaprolactone,[83] and (3) hybrid systems of synthetic polymers, natural polymers, and inorganic nanostructures. Alterations in structure and material properties are achieved by modifying synthetic methods: solvent casting, phase separation[82] electrospinning,[77] molecular self-assembly,[85] and lyophilization *via* freeze-drying.[76,80]

Hybridizing soft elastomeric polymers with inorganic nanomaterials such as CNTs,[78–80] SiNW,[86] gold nanowires,[6] and silver nanoparticles[81] presents a platform for improving electronic functionality, mechanical properties, or the nanostructure geometry of non-conducting polymer scaffolds. Soft polymers are advantageous for tissue integration due to their flexible nature, but often these scaffolds face challenges due to poor mechanical and electrical properties. For example, alginate gels provide many desirable mechanical and biological cues required for cell growth and viability; however, their insulating nature is a challenge for excitable tissues.[6] A common solution is integrating inorganic nanostructures to improve material conductance, while maintaining desired flexible and elastomeric properties. As demonstrated by Dvir *et al.*, gold NWs[6] integrated into alginate scaffolds improved electrical conductivity and allowed the propagation of bioelectric signals along a 3D cardiac patch. Immunostaining for troponin I and connexin-43, two indicators for cardiomyocyte viability, revealed higher expression of both factors and a more aligned and physiologically relevant phenotype.

In addition, nanostructure polymeric components serve as key intermediates between cellular components and the electrical sensing/stimulating components used for bioelectronic devices. Tian *et al.* developed a 3D synthetic nanoelectronic network[5] based on a flexible nanowire scaffold hybridized with macroporous polymers for intimate cellular support (Figure 16.5(a)). In this work, the authors used a variety of techniques, including gel casting, lyophilization, and electrospinning, to functionalize this scaffold with several common biomaterials to demonstrate its potential in various types of engineered tissues. Each polymer was fully entangled in the mesh framework and demonstrated the potential to recruit cellular components to the surfaces of sensing elements. Results from this study highlight how interactions between inorganic nanostructures and polymer components can lead to the generation of synthetic 3D tissues with the potential for real-time local monitoring functionality.

In another approach to sensing and stimulating tissue activity, Feiner *et al.* utilized an electroactive polymer to integrate regulatory drug-delivery

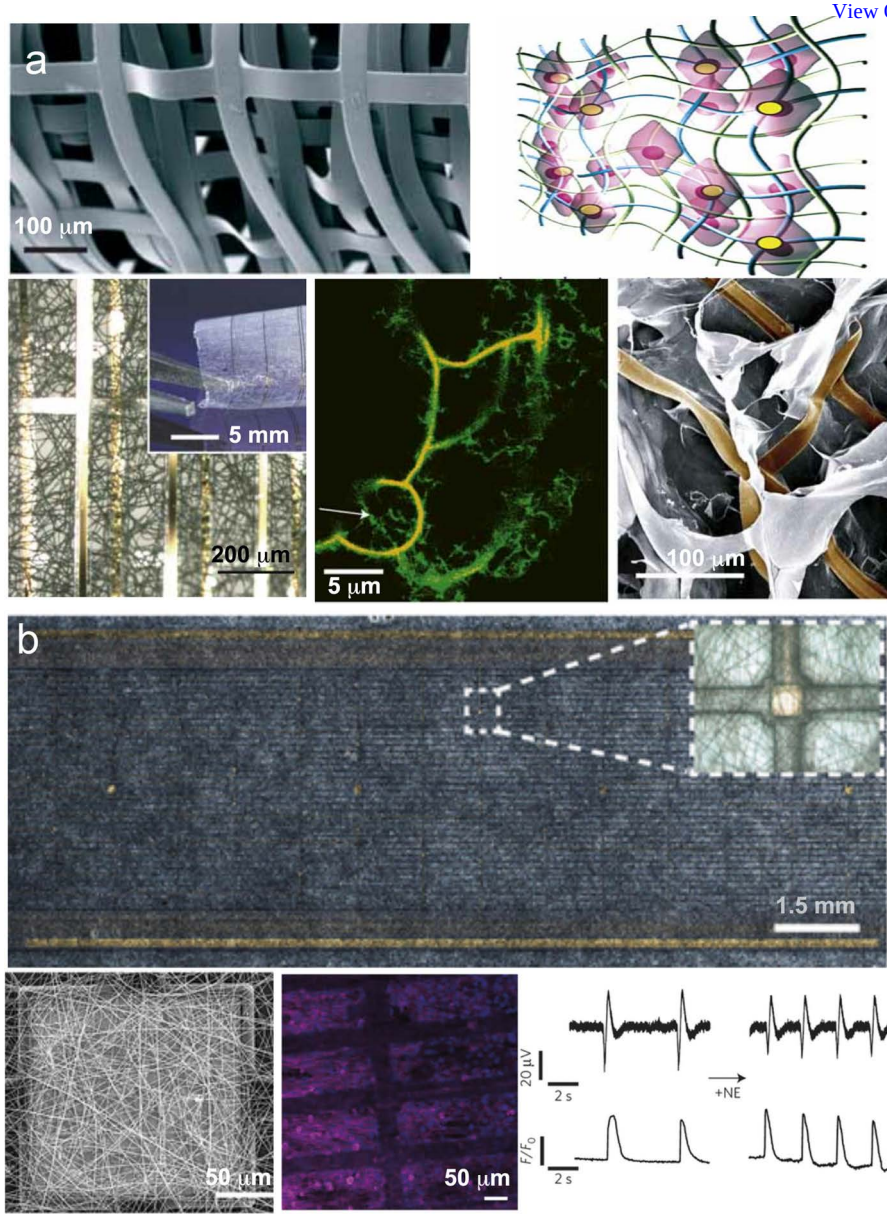

Figure 16.5 Synthesis of nanostructured polymers and bio-interface. (a) Macroporous nanowire nanoelectronic scaffolds for synthetic tissues, showing an SEM image of a nanoES mesh, a diagram of a nanoES mesh seeded with cells, a bright-field micrograph of a nanoES/PLGA fibers hybrid construct, a confocal fluorescence image of a hybrid nanoES/collagen matrix, and an SEM image of a nanoEM/alginate scaffold. (b) Engineered hybrid cardiac patches with multifunctional electronics for online monitoring and regulation of tissue function, showing an optical image of hybrid polycaprolactone-gelatin nanocomposite fibers/electronic mesh, an SEM image of a sensing and stimulating electrode surrounded by electrospun polymer fibers, a confocal image of cardiac cells grown on a hybrid construct, and typical recording traces. Reproduced with permission from Macmillan Publishers Ltd: B. Tian *et al.*, *Nat. Mater.*, 2012, **11**(11), 986–994, copyright (2012) (a) and reprinted with permission from Macmillan Publishers Ltd: R. Feiner *et al.*, *Nature Mater.*, 2016. DOI: 10.1038/nmat4590, copyright (2016) (b).

functionality into a cardiac patch device (Figure 16.5(b)).[87] Two types of electroactive polymers were tested for storage and release of biological factors in the form of negatively charged small molecules or positively charged proteins: polypyrrole and chondroitin-4-sulfate crosslinked with ethylene diglycidyl ether, respectively. The charged compounds loaded into the pores of the swollen hydrogel fibers due to electrostatics. To demonstrate the proof of concept of this functionality, the authors loaded the hydrogel with the negatively charged drug dexamethasone, an anti-inflammatory drug. When stimulated, the polypyrrole gel released the trapped drug, indicating the potential to, *in vivo*, monitor and curb inflammation caused by device implantation. To test the positively charged protein release, the authors stored stromal cell-derived factor-1 (SDF-1), a chemokine protein involved in the recruitment of bone-marrow-derived stem cell migration.[87] When the chondroitin-4-sulfate hydrogel was stimulated *in vitro*, cell migration greatly increased. Devices such as this pave the way towards engineered tissue implants that can monitor and respond to cellular activity, release SDF-1 or dexamethasone, to recruit stem cells and direct vascularization or limit inflammatory responses to implantation. With a widely explored range of polymeric supports, fabrication methods, and hybridization capabilities, biocompatible polymers can truly be tailored to both mimic natural ECM nanostructure cellular environments and confer improved functionality and physical properties to advance tissue engineering scaffolds.

16.3 Flexible Micro- and Nanoelectronics for Monitoring Biological Activity

The development of intracellular recording technology was a groundbreaking invention that revealed the biophysical mechanisms by which individual neurons transmit electrical information, communicate, and compute sub-threshold synaptic information.[10,15] Electrophysiological recording of brain tissue has become common practice for diagnosing and treating neurological disorders such as epilepsy, Parkinson's disease, and depression. The current technology available for recording brain activity relies on sharp micrometer-sized electrodes or electrode arrays on planar rigid substrates that are mechanically invasive and not suitable for implantation. The mechanical mismatch between these electrodes and the target tissue leads to excessive inflammation and scarring. These clinical needs motivate efforts to develop flexible electrode technologies for neurophysiologic monitoring that incorporate inorganic and organic nanomaterials. As previously discussed, the rational design of next generation devices requires a fundamental understanding of the properties of these materials and how they depend on dimensionality and size. The following sections will discuss state-of-the-art developments in the fabrication of flexible, implantable, and bioresorbable recording electrodes using semiconductor, metallic, carbon, and polymer nanomaterial building blocks.

16.3.1 Nanoscale Electronics Based on Field-Effect Transistor Technology

The field-effect transistor (FET) has become one of the most important devices for high-density integrated circuits. Transistors, by definition, are three-terminal devices where the channel resistance between two of the contacts is controlled by a third contact, called the gate. In FETs, the channel is controlled capacitively by an electric field facilitating carriers to flow from source to drain. The first FETs were designed during the first half of the 20th century and since then, various semiconductor FETs have been made with Ge, Si, and GaAs using many different oxides and insulators, such as SiO_2, Si_3N_4, and Al_2O_3. Currently, the Si–SiO_2 system is the most widely used system because of the extensive fabrication techniques for silicon. As previously described in Section 16.2.1, numerous studies have demonstrated that one-dimensional semiconductors building blocks are capable of transporting electronic carriers with high efficiency. Semiconductor nanowires synthesized with controlled doping levels exhibit gate voltage-dependent conductance behavior,[46] allowing them to function as FETs.[33] The insulating oxide layer that forms on the surface of SiNWs plays a role in enabling large conductance modulations observed in nanowire FETs.[39] SiNW FETs have been configured by placing the nanowires on the surface of an insulating substrate, making source and drain contacts at the nanowire ends, and then configuring either a bottom or top gate electrode.[28,33,46]

One advantage of semiconductor nanowires is that they are fabricated in bulk, representing a readily available material for assembling devices. Controlled assembly and integration of these building blocks into high-density array devices have led to the design of novel and innovative technologies.[88] Silicon nanoscale FET arrays have been fabricated for many applications in biology, including the detection of ionic species,[42] nucleic acids,[89] proteins,[42,90] cancer biomarkers,[91] and electrophysiological events.[41,92,93] Patolsky *et al.* described one of the most impressive uses of nanoscale FETs.[92] In their study, they report the electrical detection of single virus particles using SiNWs whose surfaces were modified to contain antibody receptors against influenza A.[92] The underlying principle for this detection scheme relies on conductance changes upon binding/unbinding events. For instance, when a virus particle binds to the conjugated antibody receptor on a nanowire surface, the conductance of that device should change from the baseline value, and when the virus unbinds, the conductance returns to the baseline. In addition, this detection scheme allows for the monitoring of the binding and unbinding of single virus particles in real time; making this device capable of providing insight on the binding/unbinding kinetics of virus particles on receptors.[92] This is just one example of how silicon nanoelectronics can revolutionize the medical diagnostics industry.

Devices based on SiNW FETs have also been used to monitor the activity of excitable cells and tissues.[41,92,93] One limitation of traditional microelectrodes is that the tip size (usually between ~0.2 to 5 μm) needs to be small enough to minimize cell damage during membrane rupture, but large enough to minimize impedance and maintain a favorable signal-to-noise ratio. An advantage of FET technology is that device performance does not

depend on impedance; therefore, it can be designed to have dimensions as small as tens of nanometers. Tian *et al.* demonstrated that kinks can be introduced along the length of SiNWs to fabricate sharp nanoscale probes.[41] In their experiments, two *cis*-linked kinks were introduced into heavy-doped SiNWs *via* pressure perturbations during synthesis to create 60° tip angles. A FET detector region was also incorporated into these wires by introducing a ~200 nm lightly-doped region following the kinks in heavily n-type doped nanowires.[41] After synthesis, the kinked SiNWs were modified to include a phospholipid bilayer along their surface and they were assembled into a 3D bent configuration (Figure 16.6(a)). The phospholipid coating allows for the

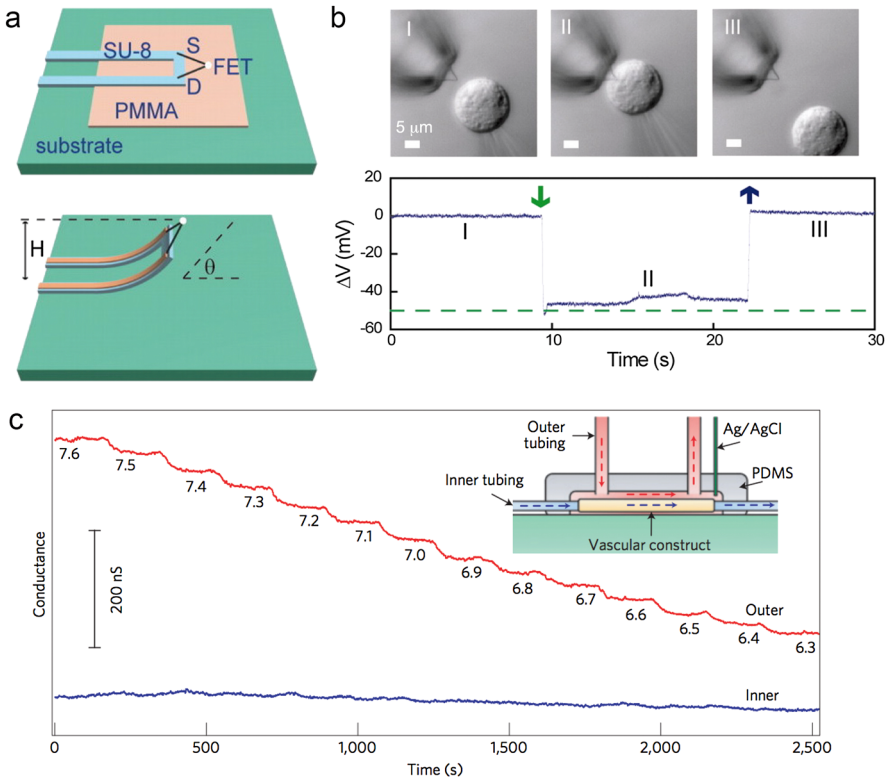

Figure 16.6 SiNW-based devices for monitoring electrophysiological activity. (a) Schematic of the fabrication of a three-dimensional kinked nanowire FET device using SU-8 and PMMA as sacrificial layers. (b) Differential interference contrast microscopy images (upper panels) and electrical recording (lower panel) of a HL-1 cell and nanowire probe as the cell approaches (I), contacts and internalizes (II), and is retracted from (III) the nanoprobe. (c) Electrical recording of pH over time in a vascular nanoelectronic hybrid construct. Reproduced with permission from B. Tian *et al.*, *Science*, 2010, **329**(5993), 830 (a) and reproduced with permission from Macmillan Publishers Ltd: B. Tian *et al.*, *Nat. Mater.*, 2012, **11**(11), 986–994, copyright (2012) (b).

fusion of these probes with the membrane of voltage-clamped HL-1 cells. The SiNW FETs achieved accurate and stable recordings of the clamped potential while the probe tip was within the cell and returned to baseline once the cell was retracted (Figure 16.6(b)). In comparison, FETs without the phospholipid modifications exhibited baseline fluctuations, highlighting the importance of the surface chemistry in the interactions between nanoscale electronics and biological systems.

Other nanoscale devices capable of monitoring bioelectric signals have been fabricated based on similar FET technologies.[5,93–95] For example, Duan *et al.* reported the intracellular recording of action potentials using SiO_2 nanotubes that branch off from p-type SiNW FETs.[93] In this device, the SiO_2 nanotube connects the cytosol of the targeted cell to the FET detector region of the SiNW. Results from these studies emphasize the potential of nanoscale probes as routine tools in electrophysiology. Nevertheless, devices capable of multiplexed recordings would be ideal to monitor activity across larger brain areas. In a landmark study, Tian *et al.* were able to merge nanoelectronic scaffolds (nanoES) with biomaterial matrices and cells to design the first electrically bioactive synthetic tissue.[5] The authors constructed hybrid, synthetic tissues by incorporating biomimetic and biological elements into a nanoelectronic scaffold in a stepwise fashion. First, SiNW FETs were synthesized by the VLS mechanism and lithographically patterned to form a freestanding, flexible macroporous network. Second, natural or synthetic extracellular matrix (ECM) elements, such as type I collagen, matrigel, alginate, and poly(lactic-*co*-glycolic acid) (PLGA), were combined with the nanoES network (Figure 16.5(a)), creating a three-dimensional environment suitable for cell culture. Lastly, neurons, cardiomyocytes, or smooth muscle cells were cultured in the nanoES hybrid environment. Viability assays showed no significant differences between cells cultured in the nanoES system *versus* those cultured in an ECM gel, emphasizing the biocompatibility of this platform.

The nanoES has great bioelectronic sensing capability since it is an assembly of highly efficient electrical transporting building blocks. In fact, the semiconductor network exhibited an average conductance of ~3 μS and a sensitivity of ~7 μS V^{-1}. In addition to its electrical properties, this device is highly flexible and it can be rolled up into a tubular configuration, enabling the use of this platform for vascular tissue engineering applications. Once seeded with neurons, cardiomyocytes, or smooth muscle cells, multiplexed recordings demonstrated that the nanoES hybrid platform can be used to measure physiological activity, study the effect of drugs on tissue activity, and detect time-dependent pH changes during fluid flow[5] (Figure 16.6(c)). This study and the work done by Liu *et al.*[96] demonstrate how nanoES can be a powerful device for the spatial-mapping and time-dependent monitoring of activity in engineered tissues. These devices also demonstrate the novel idea of implementing synthetic engineered tissues as a device that can extract information from a biological system.[5,96]

16.3.2 Implantable Devices for *In vivo* Recordings

Thus far, we have discussed how nanomaterials can be incorporated into flexible high performance integrated devices capable of interfacing biological tissues and monitoring their activity. However, in order for these devices to be practical in a clinical setting, they need to be mechanically robust for delivery and implantation to specific anatomical regions and they must be durable for their intended lifetime. This can be somewhat challenging when working with nanoscale building blocks that are flexible, foldable, and stretchable. Therefore, device administration and delivery are design parameters that need to be considered during development. In a study by Kozai *et al.*, the authors developed novel composite materials to create an ultra-small organic electrode interface that is mechanically compliant and capable of long-lasting device performance.[97] They fabricated microthread electrodes (MTEs) by mounting 7-μm-diameter carbon fibers onto a microelectrode printed circuit board following subsequent deposition of layers of poly(*p*-xylylene), poly((*p*-xylylene-4-methyl-2-bromoisobutyrate)-*co*-(*p*-xylylene)), and poly(ethylene glycol) methacrylate (PEGMA) as an antifouling polymer.[97] Finally, a poly(3,4-ethylenedioxythiophene)/poly(styrenesulfonate) (PEDOT:PSS) recording site was added to the tip of the probe *via* electrochemical deposition. The calculated stiffness of MTEs is approximately ~4540 N m^{-1}, which is an order of magnitude lower than that for silicon microelectrodes of similar dimensions, ~151 000 N m^{-1}.[97] These flexible MTEs were implanted 1.6-mm-deep into a rat motor cortex and were able to record spikes from individual neurons *in vivo*. After implantation, an initial inflammation period lasting up to one week was reported where the signal-to-noise ratio decreased. However, after this inflammation period, the authors observed an increase in signal-to-noise ratio until it stabilized. Electrophysiological recordings performed five weeks after the initial implantation did not show any evidence of signal degradation, suggesting that MTEs represent a novel platform for long-term monitoring of brain activity.

Flexible and stretchable nanoelectronics are mechanically compliant and can create better interfaces with biological tissues. However, these devices are fabricated using biologically foreign materials and device rejection can occur. The medical electronics industry aims to design devices that seamlessly integrate into biological systems. For these reasons, some studies have taken measures to include bio-integration aiding elements in their device fabrication process.[98] For example, Kim *et al.* fabricated a cell-sheet-coated mesh-patterned Au–graphene hybrid electrode to achieve high quality integration for simultaneous monitoring and therapy of muscle tissue. The Au doping on the graphene mesh electrode helps reduce impedance and increase the conductivity of the material. An advantage of this platform is that the device is composed of transparent materials, allowing for optical imaging or stimulation of the tissue below. This flexible hybrid device was implanted onto the hind limb skeletal muscle region of mice and tested for effective electromyography (EMG) sensing.[98] In their experiments, they were

able to couple nanoelectronic EMG sensing with optogenetics by expressing channelrhodopsin (ChR2), a light-activated ion channel, in the muscle cells of the hind limb. ChR2 enables the use of blue light to control the opening and closing of these channels and therefore the activation and inactivation of these cells. The cell-sheet graphene hybrid was implanted into a ChR2-expressing region of the hind limb and using a 470-nm blue LED, they simultaneously performed optical stimulation and *in vivo* recordings. The successful stimulation was confirmed visually since twitching of the legs was also observed. These elegant experiments demonstrate that cell-sheet graphene hybrid electrodes are a highly flexible, stretchable, and bio-integratable platform for *in vivo* electrophysiological recording capable of keeping tissues optically accessible.

As one can imagine, implantable devices capable of monitoring brain activity have potential for many applications in medicine, such as the tracking of seizures in epileptic patients. Researchers from Charles Lieber's group were able to fabricate a device and a delivery method that minimizes the implantation footprint.[99] Liu *et al.* demonstrated that flexible mesh electronics can be delivered into biological materials by syringe injection.[99] The mesh flexible electronics platform used by Liu *et al.* was fabricated using similar methods as those designed by Tian *et al.* (discussed above).[5] As shown in Figure 16.7(a)–(e), glass needles with outer diameters on the scale of hundreds of micrometers were used to inject the mesh electronic device into the lateral ventricle and hippocampus of live mice.[99] This delivery method reduces the invasiveness of the surgery since the dimensions of the cranial window that are needed are much smaller than those of other electronic platforms. Imaging of brain slices using confocal microscopy revealed that (1) the mesh expands from the initial 200-μm needle diameter to integrate within the local extracellular matrix (Figure 16.7(f)), (2) cells around the mesh stained with neuronal marker NeuN form tight junctions with the device, and (3) brain regions with and without the mesh device show very similar levels of glial fibrillary acidic protein (an indicator of inflammation in the central nervous system). The authors report the accurate multiplexed recordings of local field potentials in the hippocampus of anaesthetized mice (Figure 16.7(g) and (h)). Although the injectable electronics was demonstrated *in vivo*, the approach can be readily extended to existing engineered tissues for biological activity monitoring and control.

16.3.3 Bioresorbable Electronics

The treatment and care of many neurological disorders involve the constant monitoring of brain activity or monitoring after specific procedures. In many cases, recording electrodes are implanted and used to monitor brain activity, but a second surgery is required to remove the device once it is no longer necessary. This increases the cost, risk, and footprint of the treatment. The use of bioresorbable electrodes for these implants would eliminate the risk and cost of removing electrodes at the end of treatment periods. This idea can

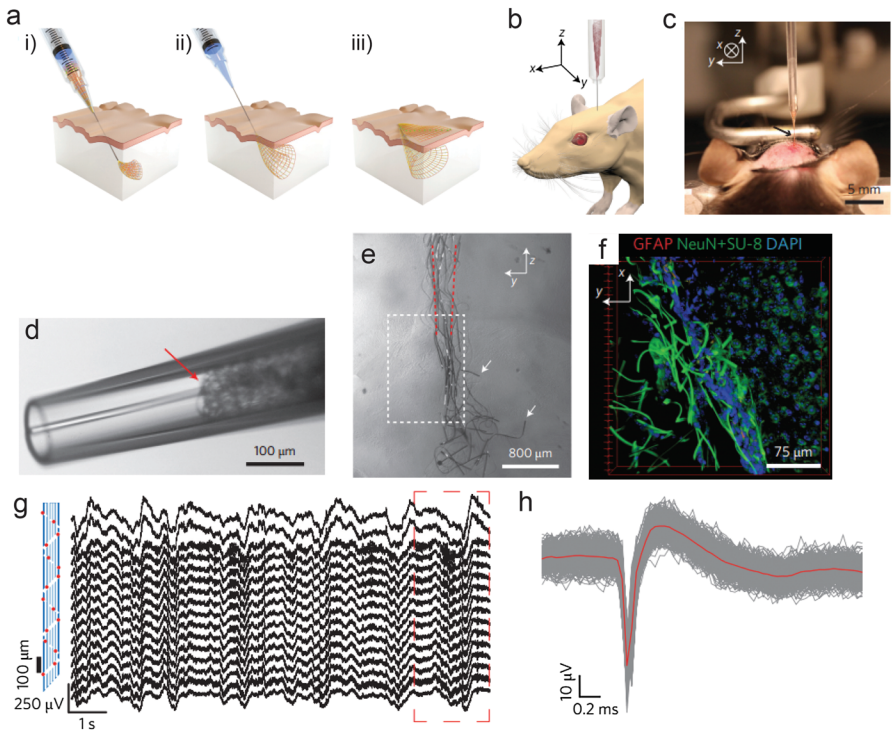

Figure 16.7 Implantable devices for monitoring neuronal activity. (a) Schematics of the delivery of a syringe-injectable expanding network into a mouse brain. (b) Three-dimensional schematic of the stereotaxic injection of a mesh nanoelectronic through a syringe into a mouse brain. (c) Photograph of an *in vivo* experiment. (d) Image of mesh electronic network inside a glass needle before injection. (e) Bright-field image of a coronal slice of the HIP five weeks after injection. (f) Confocal microscopy images showing tight association between neurons and mesh electronics. (g) *In vivo* 16 channel recording from nanoelectronic mesh network. (h) Single unit recording from one channel. Reproduced with permission from Macmillan Publishers Ltd: J. Liu *et al.*, *Nat. Nanotechnol.*, 2015, **10**(7), 629, copyright (2015).

equally be applied to engineered tissues. A research team led by John Rogers has developed unprecedented technology through designing the first bioresorbable electrodes for transient electrophysiological recordings of neural tissue. Bioresorbable pressure and temperature sensors have been recently reported;[100] but, *in vivo* multiplexed recordings of neural activity on a transient interface were not possible until Yu *et al.*, from John Rogers' group, fabricated an implantable platform based on highly-doped silicon nanomembrane technology. Their device consists of a photolithographically patterned, n-type 300-nm-thick silicon nanomembrane encapsulated between a 100-nm layer of SiO_2 and a 30-µm sheet of PLGA, which is also a bioresorbable polymer[101](Figure 16.8(a)). The dissolution of Si under physiological

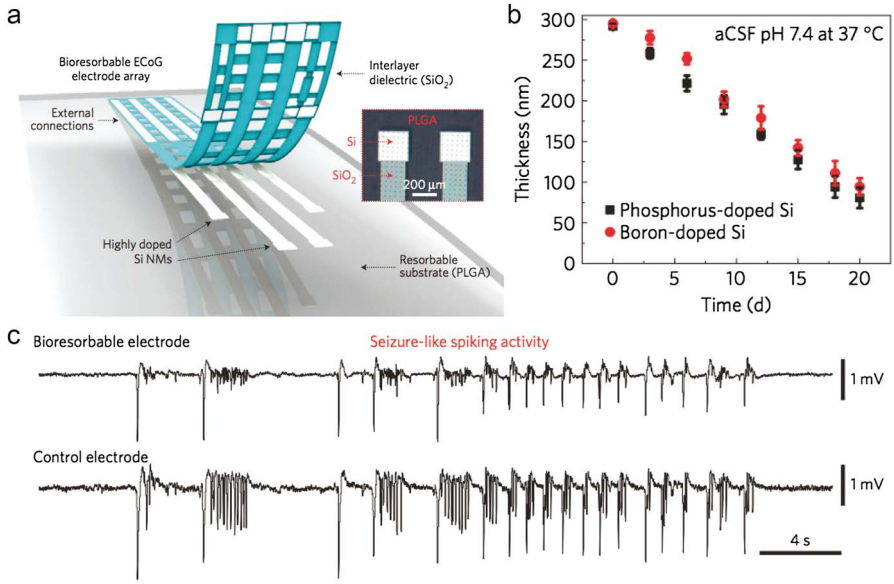

Figure 16.8 Monitoring of electrophysiological activity using bioresorbable materials. (a) Schematic of a Si nanomembrane device on a bioresorbable PLGA substrate with a silicon dioxide insulating layer. (b) Plot showing the thickness degradation of the Si nanomembrane in PBS. (c) Epileptiform activity recorded using the bioresorbable device and a control electrode. Reproduced with permission from Macmillan Publishers Ltd: K. J. Yu *et al.*, *Nat. Mater.*, 2016, DOI: 10.1038/nmat4624, copyright (2016).

conditions occurs by hydrolysis into silicic acid, $Si(OH)_4$, and the kinetics of this process depend on factors such as ionic content, pH, temperature, and doping level of silicon. Yu *et al.* observed[101] that the fabricated 300-nm-thick Si nanomembranes dissolved at a rate of 11 nm/day in artificial cerebrospinal fluid at physiological temperature and the total dissolution of the device, including the SiO_2 and PLGA layers, takes place over a ~5–6 week period (Figure 16.8(b)). This represents a long enough time window for the monitoring of activity during the recovery of different treatments and procedures.

Yu *et al.* implanted the Si nanomembrane electrode array on the cortical surface of the left hemisphere of an anaesthetized rat in a stereotaxic apparatus to test the efficiency of this platform in performing electrophysiological recordings *in vivo*.[101] In their experiments, the authors applied bicuculline methoxide to induce seizures in the brain and recorded epileptiform spiking activity using bioresorbable electrodes and a control electrode.[101](Figure 16.8(c)) In addition to epileptiform activity, evoked cortical activity was reported by using the bioresorbable multiplexed array on the surface of the barrel cortex of these rats. Evoked potentials were observed when the whiskers were mechanically stimulated. These results demonstrate that bioresorbable recording platforms can intracortically record stimulus-evoked

physiological and pathological activity with high signal-to-noise ratio. The principles discussed in this section provide a very promising argument about the capabilities of bioresorbable implantable electrode technology for various clinical problems, including post-operation monitoring of brain activity and electrical monitoring of organ function. Likewise, this technique can be applicable to various types of engineered tissues as well.

16.4 Flexible Electronics for the Stimulation of Excitable Tissues

As discussed above, electronic nanostructures can be used to monitor the electrophysiological activity of a wide range of tissues; but they also have the potential to provide electrical stimulation to the tissues into which they are incorporated. Stimulation can provide electronic functionality to synthetic tissues and aid in the treatment of many diseases. Recent studies have described the extensive communication between the brain and the immune system, suggesting that immune cells have the capacity of understanding the bioelectric signals used by the nervous system.[9] This opens up a wide array of opportunities for using electronic devices as therapeutics for boosting or suppressing immune responses. In fact, leading pharmaceutical companies, such as GlaxoSmithKline, predict that "electroceuticals", or nanoelectronic biomedical devices, could take the place of many prescription drugs on the market today. Currently, electronic stimulation has become a common treatment for many medical conditions. For example, cochlear implants restore hearing in deaf patients, deep brain stimulation alleviates symptoms of Parkinson's disease, pacemakers regulate the rhythm of heartbeats, and spinal cord neuromodulation attenuates chronic neuropathic pain. However, the current stimulation technologies cannot be applied to all scenarios because of the dimensional and mechanical gaps between the electronics and targeted tissues. This section will cover the emerging flexible and nanoscale technologies for achieving localized electrical stimulation of biological systems.

Inorganic nanostructures can be incorporated into ECM scaffolds for enhanced bioelectric control over the electrophysiological activity of the embedded cells. In the following example, Dvir *et al.* created an alginate and gold nanowire (Alg–NW) nanocomposite scaffold[6] by mixing nanowires with sodium alginate with the purpose of fabricating functional cardiac patches. Alginate has been used extensively in cardiac regeneration applications because of its defined porous structure and biocompatibility. But, the insulating nature of the scaffold prevents the propagation of electric signals and ultimately limits the potential of pristine alginate scaffolds for regeneration of damaged cardiac tissue. In this study, the authors demonstrated that the inclusion of metal conductive nanowires was sufficient to add electronic functionality to alginate scaffolds and induce synchronous cell contraction.[6]

Results from conductive AFM showed that Alg–NW scaffolds exhibit conductive properties, while the scaffolds with no nanowires do not (Figure 16.9(d)). Cardiomyocytes were cultured in the Alg–NW scaffold and were incubated with a calcium-sensitive dye to test for the capability of electrophysiological stimulation. As shown in Figure 16.9(e) and (f), imaging of calcium transients demonstrated that bioelectric signals efficiently propagated through the cardiomyocytes in the Alg–NW scaffold.[6] Signal propagation and synchronous cardiomyocyte contraction highlight the potential for this device to restore function in infarcted hearts.

Devices capable of the simultaneous delivery of electrical and chemical therapy would be ideal for cases in which drugs are necessary to reduce side effects and achieve seamless biointegration. Minev *et al.* constructed an implantable spinal cord device,[19] which they termed e-dura, by patterning microfluidic channels and platinum/silicone electrodes with stretchable gold interconnects onto a transparent silicone substrate (Figure 16.9(a)). The microfluidic channels enable the localized delivery of drugs into the targeted tissue, while the electrodes and gold interconnects allow for electrical excitation. The e-dura was implanted into the spinal subdural space of adult rats that received a thoracic contusion to induce a spinal cord injury. Serotonergic replacement therapy (5HT1A/7 and 5HT2 agonists) was administered through the microfluidic channels along with continuous electrical stimulation.[19] After a six-week rehabilitation period, the rats were placed on a treadmill to test their ability to walk. As shown in Figure 16.9(b), e-dura implanted rats missed significantly fewer steps on the treadmill test compared to sham-operated and stiff implant rats.[19] This suggests that flexible and stretchable implants capable of concurrent delivery of electrical and chemical therapy are more effective in promoting spinal cord healing than their stiff counterparts. In addition, another advantage of the e-dura is that the silicone substrate is transparent, leaving the tissue below the implant optically accessible for other applications such as optogenetics and imaging.

The work by Minev *et al.* demonstrated that the combination of electrical and chemical methods of treatment can lead to improved therapy and that implantable devices for concurrent stimulations can be fabricated.[19] Similarly, targeting multiple cellular pathways in engineered tissues, such as biochemical and bioelectric ones, increases the demand of devices capable of fine control over both drug and electrical delivery. In their recent work, Feiner *et al.* introduced a novel device that can be controlled remotely to deliver electrical stimulation, release charged biomolecules, and sense engineered tissue activity.[87] The foundation of this device was based on similar nanoES technology to that first presented by Tian *et al.*[5] Specifically, Feiner *et al.* designed a nanoelectronic mesh network that included micrometer-scaled gold electrodes and deposited electroactive polymers for drug loading. Incorporation of electroactive polymers onto these electrodes enables fine control over the release of biological factors that may promote tissue growth and tissue integration. This electronic network was integrated into a

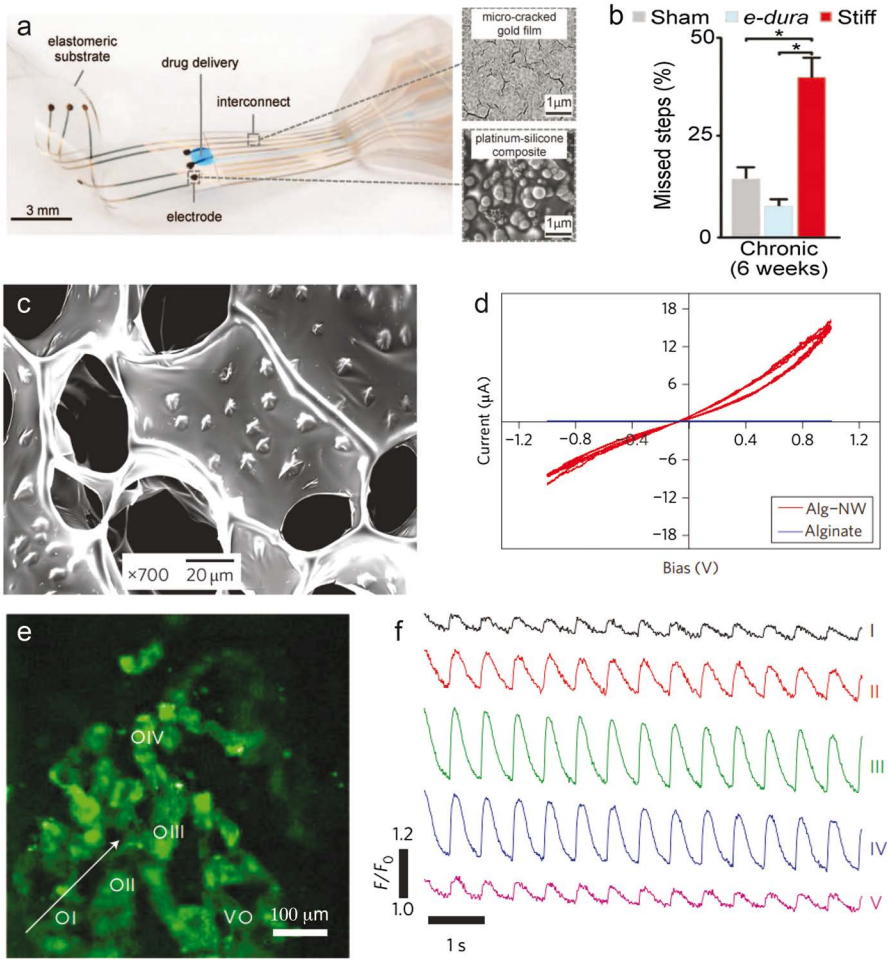

Figure 16.9 Flexible electronics for the stimulation of neural tissue. (a) Optical image of electronic dura mater spinal cord implant, along with SEM images of the gold film and platinum–silicone composite. (b) Bar plot showing the average percentage of missed steps in sham operated, e-dura implanted, and stiff implant groups. (c) SEM image of alginate scaffold showing AuNWs at 1 mg ml^{-1} for star-shaped aggregates. (d) Plot showing increased electrical conductivity in AuNW-modified alginate scaffolds. (e) Fluorescence image of cardiac cells in an alginate–AuNW scaffold incubated with a calcium dye. Circles represent recording sites I–V. The white arrow shows the direction of the propagation of the initial stimulation. (f) Calcium transients recorded at all points. Reproduced with permission from I. R. Minev *et al.*, *Science*, 2015, **347**(6218), 159, reprinted with permission from AAAS (a), (b) and reprinted with permission from Macmillan Publishers Ltd: T. Dvir *et al.*, *Nat. Nanotechnol.*, 2011, **6**(11), 720, copyright (2011) (c)–(f).

polycaprolactone–gelatin nanofiber matrix to create a biocompatible microenvironment for cardiac cells. Confocal microscopy revealed that cardiac cells cultured in this hybrid device made intimate interactions with nanofibers and showed elongated conformation indicative of cell maturation.[87] Electrical stimulation through the gold electrodes synchronized the contraction of mature cardiac cells, demonstrating the potential of this device as an implantable patch for cardiac pacing. This device represents a novel platform capable of unprecedented control over engineered tissues by providing on-demand, remote interference through electrical stimulation and delivery of biochemical factors.

16.5 Clinical Applications of Smart Materials in Tissue Engineering

While there have been many advances in optical tools for brain science, from imaging techniques such as CLARITY[102] and optical sensors[103,104] to stimulation techniques like optogenetics,[105] the synaptic physiology of deep brain circuits and their role in disease remain poorly understood in part because of the limited tools available for recording. For decades, invasive *in vivo* recordings were the only possible way to gain access to the human brain and many clinical neurology studies relied on bulky and rigid electrodes to attempt to understand how neural activity is affected in diseased states, such as Parkinson's, stroke, tumors, and other neurodegenerative diseases.[106] Even with these electrodes, it has become apparent that aberrant neural conditions can originate from the activity of a small number of neurons. For example, Smith *et al.* recently demonstrated that the sustenance and termination of seizures depend on the intense activity of small, spatially restricted populations of neurons.[107] As already discussed in this chapter, devices fabricated from flexible nanomaterials exhibit higher spatiotemporal resolution and are suitable for long-term experiments since they are mechanically compliant. Recordings from next generation devices can extract physiological information from the brain with cellular resolution. We believe that such devices will bridge the gap in clinical neurology with the information necessary to understand how neurons interact to form functionally coherent cell assemblies and if diseases are correlated to the disruption of circuit activity.[108]

In addition to the use of nanoelectronics as research tools, these can also play a more direct role in the clinic as therapeutics and health monitors. For example, bioresorbable electronics can reduce the surgical footprint associated with epilepsy,[101] multi-site nanoscale electrodes can provide long-term monitoring of tissue with reduced inflammation and scarring,[99] and these devices can be equipped for localized drug delivery,[19] which is particularly advantageous for drugs incapable of crossing the blood–brain barrier. Implantable nanoelectronic devices have the potential of restoring the neural activity of postsynaptic targets when inputs are lost. For example,

Mandel *et al.* were able to restore light-evoked responses in the primary visual cortex (V1) of blind rats by implanting a microscale photodiode array in the inner nuclear layer of the retina of these animals. This device converts photons of light into a current capable of stimulating retinal bipolar cells, the cells responsible for relaying information from the photoreceptors onto the output neurons of the retina.[109] This is just one example of how nanoscale devices can restore normal neural activity. Lastly, the use of nanoelectronic devices in medicine does not have to be restricted to patients with symptoms of brain damage. We expect that next generation devices will also help in the prevention of disease. As electronic circuits become smaller and devices are fabricated to be flexible, bendable and stretchable, we can imagine technologies that are easily integrated with the body. Several research groups are working on fabricating ultra-thin devices that can adhere on to the surface of the skin and monitor vital signs, such as blood pressure,[110] temperature,[110,111] hydration,[111] and arterial stiffening.[112] These platforms, termed "wearable electronics", aim to bring healthcare into homes and aid in the early detection of disease onset and progression.

16.6 Conclusions and Outlook

In this chapter, we have discussed the role flexible micro- and nanoelectronics will play in the design and implementation of next generation engineered tissues. The work presented here emphasizes the advantages of nanostructured building blocks in interfacing, monitoring, and manipulating the activity of soft tissues. In particular, we have addressed how scientists and researchers have overcome many challenges and limitations that current technologies face, such as fabricating mechanically compliant materials, designing easily implantable devices, reducing autoimmune responses, and exerting fine control over tissue interference. The enhanced physical and chemical properties observed at the nanoscale led the way for novel material platforms in electronics and has also sparked an interest in the study of the physical laws governing these phenomena. In addition, the similar lengthscale of nanomaterials and biological structures has enabled the interrogation of cells and tissue with increased spatial resolution. As described in this chapter, we have observed a rise in the number of nanoscale platforms available for monitoring the activity and manipulating the bioelectric signals in engineered tissue systems. Nevertheless, there are still many possibilities for new discoveries and the fabrication of novel systems that can revolutionize modern regenerative medicine. We can imagine the design of a tissue engineering platform that incorporates sensing and stimulating elements into a logic-gated feedback loop. This platform would be able to provide electrical stimulation when atypical bioelectric signals are detected. In addition, we envision a push for stimulation devices that can be triggered by wireless stimuli, such as light or radio frequencies.

References

1. N. Bock, A. Riminucci, C. Dionigi, A. Russo, A. Tampieri, E. Landi and V. Dediu, *Acta Biomater.*, 2010, **6**(3), 786.
2. A. Ratcliffe, *Biomaterials*, 2011, **32**(18), 4215.
3. B. Li, K. V. Brown, J. C. Wenke and S. A. Guelcher, *J. Controlled Release*, 2010, **145**(3), 221.
4. J. S. Laursen, P. Harris, P. Fristrup and C. A. Olsen, *Nat. Commun.*, 2015, **6**, 7013.
5. B. Tian, J. Liu, T. Dvir, L. Jin, J. H. Tsui, Q. Qing, Z. Suo, R. Langer, D. S. Kohane and C. M. Lieber, *Nat. Mater.*, 2012, **11**(11), 986–994.
6. T. Dvir, B. P. Timko, M. D. Brigham, S. R. Naik, S. S. Karajanagi, O. Levy and D. S. Kohane, *Nat. Nanotechnol.*, 2011, **6**(11), 720.
7. P. M. Baptista, M. M. Siddiqui, G. Lozier, S. R. Rodriguez, A. Atala and S. Soker, *Hepatology*, 2011, **53**(2), 604.
8. R. P. Lanza, H. Y. Chung, J. J. Yoo, P. J. Wettstein, C. Blackwell, N. Borson and M. D. West, *Nat. Biotechnol.*, 2002, **20**(7), 689.
9. K. Famm, B. Litt, K. J. Tracey, E. S. Boyden and M. Slaoui, *Nature*, 2013, **496**(7444), 159.
10. B. Sakmann and E. Neher, *Annu. Rev. Physiol.*, 1984, **46**(1), 455.
11. R. D. Keynes, *Nature*, 1972, **239**, 29.
12. A. N. Lopatin, E. N. Makhina and C. G. Nichols, *Nature*, 1994, **372**(6504), 366.
13. R. A. Kumpf and D. A. Dougherty, *Science*, 1993, **261**(5129), 1708.
14. D. A. Doyle, J. M. Cabral, R. A. Pfuetzner, A. Kuo, J. M. Gulbis, S. L. Cohen and R. MacKinnon, *Science*, 1998, **280**(5360), 69.
15. E. Neher, B. Sakmann and J. H. Steinbach, *Pflügers Arch.*, 1978, **375**(2), 219.
16. O. P. Hamill, A. Marty, E. Neher, B. Sakmann and F. J. Sigworth, *Pflügers Arch.*, 1981, **391**(2), 85.
17. M. E. Spira and A. Hai, *Nat. Nanotechnol.*, 2013, **8**(2), 83.
18. R. Biran, D. C. Martin and P. A. Tresco, *Exp. Neurol.*, 2005, **195**(1), 115.
19. I. R. Minev, P. Musienko, A. Hirsch, Q. Barraud, N. Wenger, E. M. Moraud, J. Gandar, M. Capogrosso, T. Milekovic, L. Asboth, R. F. Torres, N. Vachicouras, Q. Liu, N. Pavlova, S. Duis, A. Larmagnac, J. Voros, S. Micera, Z. Suo, G. Courtine and S. P. Lacour, *Science*, 2015, **347**(6218), 159.
20. *Nanofabrication: Techniques and Principles*, ed. M. Stepanova and S. Dew, Springer Science & Business M, 2011.
21. J. F. Zimmerman, G. F. Murray, Y. Wang, J. M. Jumper, J. R. Austin and B. Tian, *Nano Lett.*, 2015, **15**(8), 5492.
22. W. Kim, J. K. Ng, M. E. Kunitake, B. R. Conklin and P. Yang, *J. Am. Chem. Soc.*, 2007, **129**(23), 7228.
23. R. Yan, J. H. Park, Y. Choi, C. J. Heo, S. M. Yang, L. P. Lee and P. Yang, *Nat. Nanotechnol.*, 2012, **7**(3), 191.
24. Z. Yao, C. L. Kane and C. Dekker, *Phys. Rev. Lett.*, 2000, **84**(13), 2941.

25. H. Dai, E. W. Wong and C. M. Lieber, *Science*, 1996, **272**(5261), 523.
26. J. Hu, M. Ouyang, P. Yang and C. M. Lieber, *Nature*, 1999, **399**(6731), 48.
27. A. I. Hochbaum, R. Chen, R. D. Delgado, W. Liang, E. C. Garnett, M. Najarian and P. Yang, *Nature*, 2008, **451**(7175), 163.
28. Y. Cui, Z. Zhong, D. Wang, W. U. Wang and C. M. Lieber, *Nano Lett.*, 2003, **3**(2), 149.
29. A. C. Neto, F. Guinea, N. M. R. Peres, K. S. Novoselov and A. K. Geim, *Mod. Phys.*, 2009, **81**(1), 109.
30. H. Chen, M. B. Müller, K. J. Gilmore, G. G. Wallace and D. Li, *Adv. Mater.*, 2008, **20**(18), 3557.
31. Y. Sun and Y. Xia, *Science*, 2002, **298**(5601), 2176.
32. V. I. Klimov, A. A. Mikhailovsky, D. W. McBranch, C. A. Leatherdale and M. G. Bawendi, *Science*, 2000, **287**(5455), 1011.
33. X. Duan, Y. Huang, Y. Cui, J. Wang and C. M. Lieber, *Nature*, 2001, **409**(6816), 66.
34. E. S. Snow, F. K. Perkins, E. J. Houser, S. C. Badescu and T. L. Reinecke, *Science*, 2005, **307**(5717), 1942.
35. E. Roduner, *Chem. Soc. Rev.*, 2006, **35**(7), 583.
36. G. Zheng and M. Xu, in *Semiconducting Silicon Nanowires for Biomedical Applications*, ed. J. L. Coffer, Elsevier, Ch. 2, 2014.
37. P. C. Ray, *Chem. Rev.*, 2010, **110**(9), 5332.
38. F. Qian, S. Gradecak, Y. Li, C. Y. Wen and C. M. Lieber, *Nano Lett.*, 2005, **5**(11), 2287.
39. X. Duan, Y. Huang, R. Agarwal and C. M. Lieber, *Nature*, 2003, **421**(6920), 241.
40. M. H. Huang, S. Mao, H. Feick, H. Yan, Y. Wu, H. Kind and P. Yang, *Science*, 2001, **292**(5523), 1897.
41. B. Tian, T. Cohen-Karni, Q. Qing, X. Duan, P. Xie and C. M. Lieber, *Science*, 2010, **329**(5993), 830.
42. Y. Cui, Q. Wei, H. Park and C. M. Lieber, *Science*, 2001, **293**(5533), 1289.
43. M. Law, L. E. Greene, J. C. Johnson, R. Saykally and P. Yang, *Nat. Mater.*, 2005, **4**(6), 455.
44. A. M. Morales and C. M. Lieber, *Science*, 1998, **279**(5348), 208.
45. J. Huang, S. Y. Chiam, H. H. Tan, S. Wang and W. K. Chim, *Chem. Mater.*, 2010, **22**(13), 4111.
46. Y. Cui, X. Duan, J. Hu and C. M. Lieber, *J. Phys. Chem. B*, 2000, **104**(22), 5213.
47. M. S. Gudiksen, L. J. Lauhon, J. Wang, D. C. Smith and C. M. Lieber, *Nature*, 2002, **415**(6872), 617.
48. L. J. Lauhon, M. S. Gudiksen, D. Wang and C. M. Lieber, *Nature*, 2002, **420**(6911), 57.
49. R. E. Algra, M. A. Verheijen, M. T. Borgström, L. F. Feiner, G. Immink, W. J. van Enckevort and E. P. Bakkers, *Nature*, 2008, **456**(7220), 369.

50. Y. Zhao, J. Yao, L. Xu, M. N. Mankin, Y. Zhu, H. Wu, L. Mai, Q. Zhang and C. M. Lieber, *Nano Lett.*, 2016, **16**, 2644.
51. J. Yao, H. Yan and C. M. Lieber, *Nat. Nanotechnol.*, 2013, **8**(5), 329.
52. A. Biswas, I. S. Bayer, A. S. Biris, T. Wang, E. Dervishi and F. Faupel, *Adv. Colloid Interface Sci.*, 2012, **170**(1), 2.
53. Z. Luo, Y. Jiang, B. D. Myers, D. Isheim, J. Wu, J. F. Zimmerman, Z. Wang, Q. Li, Y. Wang, X. Chen, V. P. Dravid, D. N. Seidman and B. Tian, *Science*, 2015, **348**(6242), 1451.
54. W. Yang, P. Thordarson, J. J. Gooding, S. P. Ringer and F. Braet, *Nanotechnology*, 2007, **18**(41), 412001.
55. C. P. Firme III and P. R. Bandaru, *Nanomedicine*, 2010, **6**(2), 245.
56. L. Zhang and T. J. Webster, *Nano Today*, 2009, **4**(1), 66.
57. E. W. Keefer, B. R. Botterman, M. I. Romero, A. F. Rossi and G. W. Gross, *Nat. Nanotechnol.*, 2008, **3**, 434.
58. E. B. Malarkey, K. A. Fisher, E. Bekyarova, W. Liu, R. C. Haddon and V. Parpura, *Nano Lett.*, 2009, **9**(1), 264.
59. S. Iijima, *Nature*, 1991, **354**, 56.
60. E. T. Thostensona, Z. Renb and T. Chou, *Compos. Sci. Technol.*, 2001, **61**(13), 1899.
61. G. Mittal, V. Dhand, K. Y. Rhee, S. Park and W. R. Lee, *J. Ind. Eng. Chem.*, 2015, **21**(25), 11.
62. J. R. Sanchez-Valencia, T. Dienel, O. Gröning, I. Shorubalko, A. Mueller, M. Jansen, K. Amsharov, P. Ruffieux and R. Fasel, *Nature*, 2014, **512**, 61.
63. B. Harrison and A. Atala, *Biomaterials*, 2007, **28**(2), 344.
64. H. Hu, Y. Ni, V. Montana, R. C. Haddon and V. Parpura, *Nano Lett.*, 2004, **4**(3), 507.
65. F. Yang, X. Wang, D. Zhang, J. Yang, D. Luo, Z. Xu, J. Wei, J.-Q. Wang, Z. Xu, F. Peng, X. Li, R. Li, Y. Li, M. Li, X. Bai, F. Ding and Y. Li, *Nature*, 2014, **510**, 522.
66. M. P. Mattson, R. C. Haddon and A. M. Rao, *J. Mol. Neurosci.*, 2000, **14**(3), 175.
67. E. B. Malarkey, K. A. Fisher, E. Bekyarova, W. Liu, R. C. Haddon and V. Parpura, *Nano Lett.*, 2009, **9**, 264.
68. T. Gabay, M. Ben-David, I. Kalifa, R. Sorkin, Z. R. Abrams, E. Ben-Jacob and Y. Hanein, *Nanotechnology*, 2007, **18**(3), 035201.
69. M. David-Pur, L. Bareket-Keren, G. Beit-Yaakov, D. Raz-Prag and Y. Hanein, *Biomed. Microdevices*, 2014, **16**(1), 43.
70. C. Lam, J. T. James, R. McCluskey and R. L. Hunter, *Toxicol. Sci.*, 2004, **77**(1), 126.
71. D. Cui, F. Tian, C. S. Ozkan, M. Wang and H. Gao, *Toxicol. Lett.*, 2005, **155**(1), 73.
72. H. Dumortier, S. Lacotte, G. Pastorin, R. Marega, W. Wu, D. Bonifazi, J. P. Briand, M. Prato, S. Muller and A. Bianco, *Nano Lett.*, 2006, **6**(7), 1522.

73. M. K. Gheith, V. A. Sinani, J. P. Wicksted, R. L. Matts and N. A. Kotov, *Adv. Mater.*, 2005, **17**(22), 2663.
74. C. Zhao, A. Tan, G. Pastorin and H. K. Ho, *Biotechnol. Adv.*, 2013, **31**(5), 654.
75. W. Shen, L. Karumbaiah, X. Liu, T. Saxena, S. Chen, R. Patkar, R. V. Bellamkonda and M. G. Allen, *Microsyst. Nanoeng.*, 2015, **1**, 15010.
76. W. L. Stoppel, D. Hu, I. J. Domian, D. L. Kaplan and L. D. Black, *Biomed. Mater.*, 2015, **10**(3), 034105.
77. M. P. Prabhakaran, L. Ghasemi-Mobarakeh, G. Jin and S. Ramakrishna, *J. Biosci. Bioeng.*, 2011, **112**(5), 501.
78. S. Pok, F. Vitale, S. L. Eichmann, O. M. Benavides, M. Pasquali and J. G. Jacot, *ACS Nano*, 2014, **8**(10), 9822.
79. R. A. MacDonald, B. F. Laurenzi, G. Viswanathan, P. M. Ajayan and J. P. Stegemann, *J. Biomed. Mater. Res., Part A*, 2005, **74**(3), 489.
80. M. Kharaziha, M. Nikkhah, S. R. Shin, N. Annabi, N. Masoumi, A. K. Gaharwar, G. Camci-Unal and A. Khademhosseini, *Biomaterials*, 2013, **34**(27), 6355.
81. M. S. Mannoor, Z. Jiang, T. James, Y. L. Kong, K. A. Malatesta, W. O. Soboyejo, N. Verma, D. H. Gracias and M. C. McAlpine, *Nano Lett.*, 2013, **13**(6), 2634.
82. Q. Liu, S. Tian, C. Zhao, X. Chen, I. Lei, Z. Wang and P. X. Ma, *Acta Biomater.*, 2015, **26**(105), 14.
83. N. Baheiraei, H. Yeganeh, J. Ai, R. Gharibi, S. Ebrahimi-Barough, M. Azami, S. Vahdat and H. Baharvand, *J. Biomed. Mater. Res., Part A*, 2015, **103**(10), 3179.
84. S. Pok, J. D. Myers, S. Madihally and J. G. Jacot, *Acta Biomater.*, 2013, **9**(3), 5630.
85. L. E. O'Leary, J. A. Fallas, E. L. Bakota, M. K. Kang and J. D. Hartgerink, *Nat. Chem.*, 2011, **3**, 821.
86. Y. Tan, D. Richards, R. Xu, S. Stewart-Clark, S. K. Mani, T. K. Borg, D. R. Menick, B. Tian and Y. Mei, *Nano Lett.*, 2015, **15**(5), 2765.
87. R. Feiner, L. Engel, S. Fleischer, M. Malki, I. Gal, A. Shapira, Y. Shacham-Diamand and T. Dvir, *Nat. Mater.*, 2016, **15**, 679–685.
88. D. Whang, S. Jin, Y. Wu and C. M. Lieber, *Nano Lett.*, 2003, **3**(9), 1255.
89. J. I. Hahm and C. M. Lieber, *Nano Lett.*, 2004, **4**(1), 51.
90. W. U. Wang, C. Chen, K. H. Lin, Y. Fang and C. M. Lieber, *Proc. Natl. Acad. Sci. U. S. A.*, 2005, **102**(9), 3208.
91. G. Zheng, F. Patolsky, Y. Cui, W. U. Wang and C. M. Lieber, *Nat. Biotechnol.*, 2005, **23**(10), 1294.
92. F. Patolsky, G. Zheng, O. Hayden, M. Lakadamyali, X. Zhuang and C. M. Lieber, *Proc. Natl. Acad. Sci. U. S. A.*, 2004, **101**, 14017.
93. X. Duan, R. Gao, P. Xie, T. Cohen-Karni, Q. Qing, H. S. Choe and C. M. Lieber, *Nat. Nanotechnol.*, 2012, **7**(3), 174.
94. J. T. Robinson, M. Jorgolli, A. K. Shalek, M. H. Yoon, R. S. Gertner and H. Park, *Nat. Nanotechnol.*, 2012, **7**(3), 180.

95. C. Xie, Z. Lin, L. Hanson, Y. Cui and B. Cui, *Nat. Nanotechnol.*, 2012, **7**(3), 185.
96. J. Liu, C. Xie, X. Dai, L. Jin, W. Zhou and C. M. Lieber, *Proc. Natl. Acad. Sci. U. S. A.*, 2013, **110**(17), 6694.
97. T. D. Kozai, N. B. Langhals, P. R. Patel, X. Deng, H. Zhang, K. L. Smith, J. Lahann, N. A. Kotov and D. R. Kipke, *Nat. Mater.*, 2012, **11**(12), 1065.
98. S. J. Kim, K. W. Cho, H. R. Cho, L. Wang, S. Y. Park, S. E. Lee, T. Hyeon, N. Lu, S. H. Choi and D. H. Kim, *Adv. Funct. Mater.*, 2016, **26**, 3207–3217.
99. J. Liu, T. M. Fu, Z. Cheng, G. Hong, T. Zhou, L. Jin, M. Duvvuri, Z. Jiang, P. Kruskal, C. Xie, Z. Suo, Y. Fang and C. M. Lieber, *Nat. Nanotechnol.*, 2015, **10**(7), 629.
100. S. K. Kang, R. K. Murphy, S. W. Hwang, S. M. Lee, D. V. Harburg, N. A. Krueger, J. Shin, P. Gamble, H. Cheng, S. Yu, Z. Liu, J. G. McCall, M. Stephen, H. Ying, J. Kim, G. Park, R. C. Webb, C. H. Lee, S. Chung, D. S. Wie, A. D. Gujar, B. Vemulapalli, A. H. Kim, K. M. Lee, J. Cheng, Y. Huang, S. H. Lee, P. V. Braun, W. Z. Ray and J. A. Rogers, *Nature*, 2016, **530**, 71.
101. K. J. Yu, D. Kuzum, S. W. Hwang, B. H. Kim, H. Juul, N. H. Kim, S. M. Won, K. Chiang, M. Trumpis, A. G. Richardson, H. Cheng, H. Fang, M. Thompson, H. Bink, D. Talos, K. J. Seo, H. N. Lee, S. K. Kang, J. H. Kim, J. Y. Lee, Y. Huang, F. E. Jensen, M. A. Dichter, T. H. Lucas, J. Viventi, B. Litt and J. A. Rogers, *Nat. Mater.*, 2016, **15**, 782–791.
102. K. Chung, J. Wallace, S. Y. Kim, S. Kalyanasundaram, A. S. Andalman, T. J. Davidson, J. J. Mirzabekov, K. A. Zalocusky, J. Mattis, A. K. Denisin, S. Pak, H. Bernstein, C. Ramakrishnan, L. Grosenick, V. Gradinaru and K. Deisseroth, *Nature*, 2013, **497**(7449), 332–337.
103. F. St-Pierre, J. D. Marshall, Y. Yang, Y. Gong, M. J. Schnitzer and M. Z. Lin, *Nat. Neurosci.*, 2014, **17**(6), 884–889.
104. T. W. Chen, T. J. Wardill, Y. Sun, S. R. Pulver, S. L. Renninger, A. Baohan, E. R. Schreiter, R. A. Kerr, M. B. Orger, V. Jayaraman, L. L. Looger, K. Svoboda and D. S. Kim, *Nature*, 2013, **499**(7458), 295–300.
105. E. S. Boyden, F. Zhang, E. Bamberg, G. Nagel and K. Deisseroth, *Nat. Neurosci.*, 2005, **8**(9), 1263–1268.
106. S. S. Cash and L. R. Hochberg, *Neuron*, 2015, **86**(1), 79–91.
107. E. H. Smith, J. Y. Liou, T. S. Davis, E. M. Merricks, S. S. Kellis, S. A. Weiss, B. Greger, P. A. House, G. M. McKhann, R. R. Goodman, R. G. Emerson, L. M. Bateman, A. J. Trevelyan and C. A. Schevon, *Nat. Commun.*, 2016, **7**, 11098.
108. A. K. Engel, C. K. Moll, I. Fried and G. A. Ojemann, *Nat. Rev. Neurol.*, 2005, **6**(1), 35–47.
109. Y. Mandel, G. Goetz, D. Lavinsky, P. Huie, K. Mathieson, L. Wang, T. Kamins, L. Galambos, R. Manivanh, J. Harris and D. Palanker, *Nat. Commun.*, 2013, **4**, 1980.

110. D. H. Kim, N. Lu, R. Ma, Y. S. Kim, R. H. Kim, S. Wang, J. Wu, S. M. Won, H. Tao, A. Islam, K. J. Yu, T. Kim, R. Chowdhury, M. Ying, L. Xu, M. Li, H. Chung, H. Keum, M. McCormick, P. Liu, Y. Zhang, F. G. Omenetto, Y. Huang, T. Coleman and J. A. Rogers, *Science*, 2011, **333**(6044), 838–843.
111. M. Kaltenbrunner, T. Sekitani, J. Reeder, T. Yokota, K. Kuribara, T. Tokuhara, M. Drack, R. Schwodiauer, I. Graz, S. Bauer and T. Someya, An ultra-lightweight design for imperceptible plastic electronics, *Nature*, 2013, **499**(7459), 458–463.
112. G. Schwartz, B. C. K. Tee, J. Mei, A. L. Appleton, D. H. Kim, H. Wang and Z. Bao, *Nat. Commun.*, 2013, **4**, 1859.

CHAPTER 17

Smart Materials to Regulate the Fate of Stem Cells

JIABIN ZHANG[a], HU ZHANG*[a] AND XIA XU[b]

[a]School of Chemical Engineering, The University of Adelaide, Adelaide, SA 5005, Australia; [b]Institute of Process Engineering, Chinese Academy of Sciences, Beijing, 100190, China
*E-mail: hu.zhang@adelaide.edu.au

17.1 Introduction

Many serious diseases, such as Parkinson's disease (PD), acute myocardial infarction (MI), and acute low back pain (LBP), are caused by either tissue/organ degeneration or accident damage and they interrupt the normal daily activities of patients.[1–3] Stem cell therapy, as a potential treatment for these diseases, is currently being intensively explored by many researchers.[4] Stem cells, such as embryonic stem cells (ESCs) or adult stem cells, together with biocompatible support materials are injected into the defect or damaged site, allowing stem cells to proliferate and then differentiate into target cells *in situ*. In the last decades, more and more researchers have focused on the applicability of the implanted materials for stem cell cultivation.[5] Scaffolds or hydrogels generated from various materials are modified to mimic the properties of the extracellular matrix (ECM),[6] which is an essential component of the surrounding environment of cells to provide mechanical supports for stem cells and facilitate signal communications between cells or cells–ECM. However, most of the reported materials provide passive supports for the stem cells,[7] while only a few have functions of active regulation in the proper differentiation of stem cells.[8]

Smart Materials No. 25
Smart Materials for Tissue Engineering: Applications
Edited by Qun Wang

Published by the Royal Society of Chemistry, www.rsc.org

Smart materials, just like traditional normal biomaterials, can provide ECM-like topography for stem cells. More importantly, smart materials can be physically or chemically modified by actively responding to external stimuli, such as temperature, electricity, pH, shear stress, light and ions.[9,10] Smart materials with finely tuned properties can be utilised to accurately and directly regulate differentiation of the encapsulated stem cells (Figure 17.1) because stem cell differentiation, to a great extent, depends on the mechanical/chemical properties of the surrounding microenvironment.[11,12]

Smart materials are divided into groups according to external stimuli, such as thermosensitive (temperature), thixotropic (shear stress), conductive/electroactive (electricity), photo-responsive (light), pH-responsive (pH) and others. They are widely reported to be used as injectable materials in the liquid form of hydrogels containing stem cells, which can turn into the gel form and encapsulate stem cells inside the hydrogels in response to temperature, light, shear stress, or pH after injection.[13,14] These hydrogels further recruit internal chemical growth factors or signal factors, or receive physical simulations *in situ*[9] so that the encapsulated stem cells are differentiated into cell types in the damaged site for effective repair and regeneration.[1] Stem cell differentiation

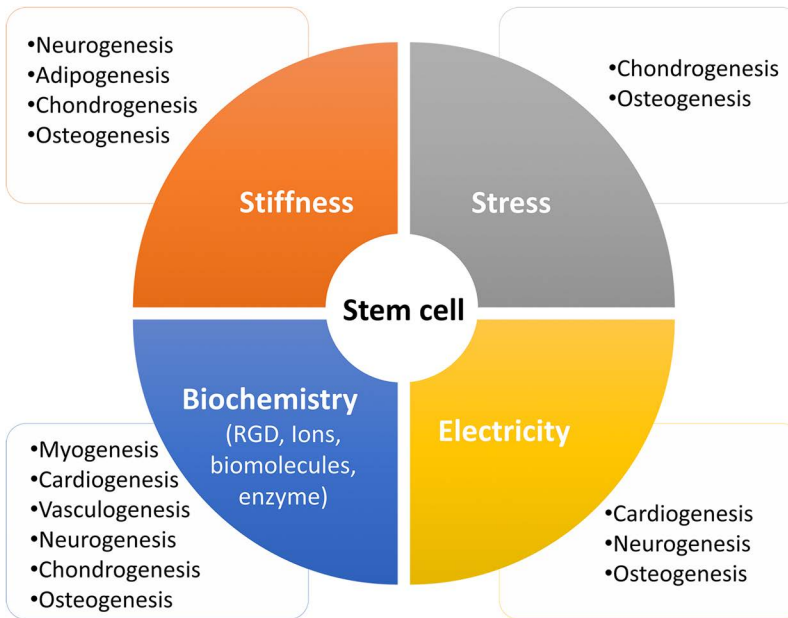

Figure 17.1 Differentiation of stem cells in response to external stimuli. Chemical stimuli, such as RGDs, ionic strength, growth factors and enzymes, facilitate directing the differentiation of stem cells into a wide range of cell types,[14] while neurogenesis, cardiogenesis and osteogenesis are enhanced through electrical stimulus[20] and mechanical stimulus of the supported materials.[15] Moreover, shear stress is often utilised to induce bone and cartilage formation.[10]

can also be regulated by either the property changes or inherent stiffness and topography of the smart materials.[15] Conductive/electroactive materials that have bulk property changes in response to electrical stimuli have been widely applied in osteogenesis and neural differentiation for bone and neural regeneration, respectively.[16,17] Light-responsive and pH-responsive hydrogels allow control of the concentration and distribution of incorporated biomolecules in the gel, which play a role in guiding the differentiation of stem cells.[14] Each type of smart material can even respond to more than one single stimulus[18] and a combination of two or more smart materials is used to achieve spatial and temporal control over stem cell differentiation.[19]

There have been excellent reviews on smart materials. A few reviews address the application of smart materials in drug/gene delivery for cancer treatment[14,21,22] and some of them focus on the modelling of physical cues and elucidation of the mechanisms that influence cell behaviours,[12,23] such as cell attachment, spreading and proliferation. However, very few of them cover the details in the differentiation of stem cells.[10,11] Among a very few of them, piezoelectric materials are comprehensively reviewed in regulating stem cell fate.[20] Therefore, the present review focuses mainly on the application of smart materials, including scaffolds and hydrogels, in guiding stem cell differentiation in response to external stimuli, such as temperature, electricity, pH, shear stress, light and ions.

17.2 Thermosensitive Materials

Thermosensitive materials, usually in the form of hydrogels for applications in tissue engineering and regenerative medicines, not only have a hydrophilic property but also allow a sol–gel transition by a simple increase or decrease of the surrounding temperature (Figure 17.2). The gelation can be initiated

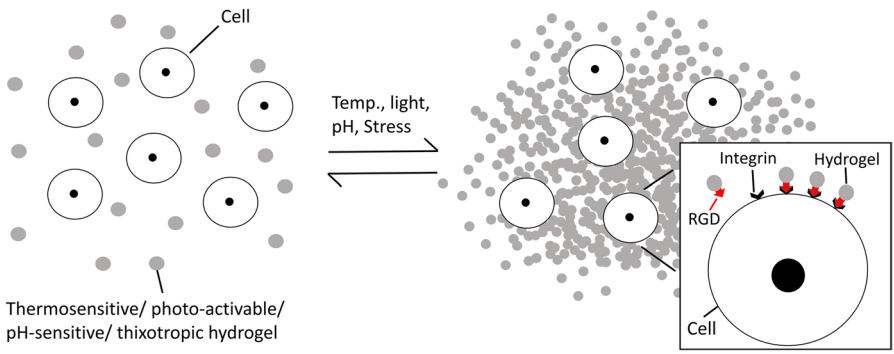

Figure 17.2 Schematic of encapsulation of stem cells in thermosensitive, photoactive, pH-sensitive or thixotropic hydrogels due to external stimuli. The incorporated biomolecules or the conjugated RGDs interact with the integrin of the encapsulated stem cells and direct differentiation of stem cells into defined cells.[14] Adapted from ref. 25 with permission from the Royal Society of Chemistry.

above the lower critical solution temperature (LCST) or below the upper critical solution temperature (UCST). LCST thermosensitive hydrogels, such as polyethylene glycol (PEG)-based copolymers, polyethylene oxide-polypropylene oxide-polyethylene triblock copolymers (PEO–PPO–PEO)[24] and poly(*N*-isopropylacrylamide) (PNIPAAm),[25,26] are more popularly utilised since the LCST is close to body temperature (Table 17.1). In addition, the inherent properties of LCST thermosensitive hydrogels, including stiffness, biocompatibility and gelation temperature, can be adjusted by copolymerizing with other biocompatible components. Conjugation of RGD peptides/proteins with the hydrogels facilitates cell binding to the receptors of cells for better adhesion or guided differentiation.[27]

17.2.1 Facilitating Cell Differentiation by *in vivo* Gelation

Because of the adjustability of the gelation temperature for thermosensitive materials, LCST thermosensitive hydrogels are often employed as injectable carriers for stem cells, which can not only supply *in situ* gel formation to localize stem cells in the damaged/degenerative site, but also provide assistive functions for guiding stem cell differentiation. After implantation, the hydrogels turn into a three-dimensional (3D) gel-like network structure to retain the encapsulated stem cells, avoiding stem cell migration into other sites or circulation in the blood vessels. Physiological stimuli produced by the host are received by cells through the thermosensitive hydrogels, and these localized stimuli can guide differentiation of stem cells into specific lineage cells in the injection site. For instance, Gao *et al.* directly injected rat adipose-derived mesenchymal stem cells (ASCs), which were encapsulated in a chitosan-based thermosensitive hydrogel (chitosan chloride and β-glycerophosphate (β-GP)), into the ischemia-induced acute kidney injury site.[28] Four weeks after the transplantation, pre-labelled rat ASCs were found to hold a positive epithelial cell marker (Anti-pan-CK antibody) and vascular endothelial cell marker (anti-CD31 antibody), which indicated that the encapsulated stem cells were induced for differentiation into renal epithelial cells and vascular endothelial cells. Through analysing the concentration level of creatinine and blood urea nitrogen (BUN), it was shown that the concentration of both components continuously decreased from a significant value to a relatively normal level during the implantation period, which meant that the function of the injured kidneys was repaired and improved by the thermosensitive hydrogel–ASCs hybrid. Another *in vivo* study of the impact of thermosensitive hydrogels upon the differentiation of stem cells was reported by Li *et al.*, who injected Dil-labelled brown ASCs and a single-wall carbon nanotube-modified poly(*N*-isopropylacrylamide) (PNIPAAm) mixture into myocardial infarction (MI) lesion sites.[29] The improvement in the left ventricular shortening fraction (LVSF) and the left ventricular ejection fraction (LVEF) was observed by echocardiography in four weeks. In addition, the MI area and the thickness of the ventricular wall at the MI lesion site was significantly

decreased and prominently increased, respectively. The immunofluorescent images of the cardiac section also indicated that the implanted ASCs differentiated towards cardiac lineage cells with expression of cardiac proteins, such as cTnT and α-SA.

17.2.2 Determining Cell Differentiation by Gel Modification

Thermosensitive hydrogels can also induce differentiation of stem cells through changes of their hydrogel properties.[5] It was reported that over 76% of bone-marrow-derived MSCs cultured in the stiffer thermosensitive hydrogel (NIPAAm/AAc/NAS/HEMA-PTMC) at a Young's modulus of 45 kPa and 65 kPa for fourteen days were detected to proceed with cardiac differentiation by expressing specific genes and proteins (cTnI and MEF2C).[30] Moreover, incorporation of biomolecules inside the thermosensitive hydrogel and conjugation of proteins/peptides with the thermosensitive polymers are both effective methods to regulate the fate of stem cells (Figure 17.2). L-Alanine was copolymerized with ethylene glycol to form a thermosensitive polymer poly(ethylene glycol)-*block*-poly(L-alanine) (PEG-L-PA) by Yeon *et al.*[31] The ASCs encapsulated in the thermosensitive hydrogel expressed a high level of collagen II *in vitro* and generated sulfated glycosaminoglycan *in vivo*, which indicated chondrogenic differentiation of ASCs within the hydrogels. Chun *et al.* also conjugated the GRGDS peptide, a cell-binding ligand, into poly(organophosphazene) and investigated expression of genes and proteins for rabbit MSCs encapsulated in the poly(organophosphazene)–RGD hydrogel.[32] Four weeks after transplantation of the MSCs–hydrogel hybrid in mice, it was observed that osteocalcin (OCN) and collagen I were significantly expressed in addition to calcium deposition. This illustrated that the thermosensitive hydrogel poly(organophosphazene)–RGD can be utilised to direct osteogenesis of stem cells. Apart from peptide/protein conjugation, bioactive molecules can also be incorporated into the hydrogel and regulate differentiation of the encapsulated stem cells. By co-encapsulating TGF-β3 and human-bone-marrow-derived MSCs (hBMSCs) into the thermosensitive hydrogel, the hBMSCs were directed to osteogenesis with the evidence of collagen II and glycosaminoglycan (GAG) expression.[33] In addition, it was reported that the encapsulated bFGF inside the thermosensitive hydrogel, NIPAAm/AAc/NAS/HEMA-PTMC, improved survival of MSCs and their differentiation towards cardiomyocyte-like cells, which could be potentially applied in the treatment of myocardial infarction.[34] Researchers also attempted to incorporate other small components inside the thermosensitive hydrogels to achieve fate regulation of stem cells. For instance, nanohydroxyapatite (nHAp) was shown not only to enhance the properties of the thermosensitive hydrogel, such as swelling and protein adsorption, but also to promote expression of osteogenic genes and proteins, such as Runx2, ALP, COL-I and OCN, as well as calcium deposition for the encapsulated mouse MSCs inside the chitosan-based hydrogel.[35]

Table 17.1 Thermosensitive materials and their regulation for the fate of stem cells.

Material	Crosslink method	Biodegradability	Phase change temperature range	Responded property change	Dimension (2D/3D)	Encapsulated cell type	Differentiation type	Differentiation evidence	Application	References
PNIPAAm/SWCNTs (single-wall carbon nanotubes)	—	No	32 °C	Phase change: sol under 32 °C and gel above 32 °C	3D	ASCs	Cardiac differentiation	*In vivo* test; protein: cTnT, α-SA	Injectable gel formation for myocardial repair	29 and 71
Poly (NIPAAm/AAc/NAS/HEMA-PTMC) molar 85 : 6 : 5 : 4 (adjust stiffness by bFGF)	Ionic crosslinking (DPBS, pH 7.4)	Degradable (thermal transition temperature of degraded hydrogel elevated to 49.4 °C)	23.8 ± 0.6 °C	Phase change at 23.8 ± 0.6 °C; rapid gelation at 37 °C <7 s	3D	BMSCs	76% Cardiomyocyte-like cells	mRNA: MEF2C, CACNA1c; protein: cTnI	Injectable *in situ* gel formation for infarcted hearts	30 and 72
Poly(NIPAM-*co*-HEMA-*co*-DBA)-*b*-PCL-poly-(NIPAM-*co*-HEMA-*co*-DBA) (adjust stiffness by collagen I)	Ionic crosslinking (DPBS, pH 7.4)	Degradable (LCST of degraded hydrogel is 47.5 °C)	17.7–22.4 °C	Rapid gelation at 37 °C <5 s	3D	Cardiosphere-derived cells (CDCs)	Mature cardiomyocyte lineage	Cardiac markers: cTnT, MYH6; pre-mature cardiac marker: GATA4; protein: cTnI	Injectable *in situ* gel formation for infarcted hearts	73
Aminated hyaluronic acid-*g*-poly(*N*-isopropylacrylamide) (AHA-*g*-PNIPAAm)	—	Partially	30 °C	Phase change: sol under 30 °C and gel above 30 °C	3D	hASCs	—	*In vivo* test	Adipose tissue engineering	74

PNIPAAm-AA-HEMA-macromers (oligoLA/oligoHB/oligoTMC)	—	Degradable (LCST of degrade production poly(NIPAAm-*co*-AAc-*co*-HEMA) is 44 °C)	14.6–23.7 °C	Phase change: sol at 4 °C and gel at 37 °C within 7 s	3D	mBMSCs	Myogenic differentiation	Myosin heavy chain (MHC), myogenin, MyoD1, MEF2 in 14 days 20 kPa elastic expansion moduli	Skeletal muscle regeneration	75
PNIPAAm-*co*-AAc with TGF- β3	—	No	—	—	3D	hBMSCs	Chondrogenesis	*In vivo* test; collagen II; glycosaminoglycan (GAG) for ECM	Chondrogenic engineering	33
PNIPAAm–PAA	—	No	—	Phase change: sol under 37 °C and gel above 37 °C	3D	mASCs	Adipocyte	*In vivo* test	Depressed defects	76
PNIPAAm-MAA-mPEGMA-MDO-TA (PN-TA)	—	Degradable	39–31 °C	Phase change: sol at25 °C and gel at 37 °C	3D	Rat cardiac myoblast H9c2	—	*In vivo* test inflammatory responses, enhance the intracellular calcium level and induce a large intracellular calcium transient	Myocardial infarction therapy	77

(*continued*)

Table 17.1 (*continued*)

Material	Crosslink method	Biodegradability	Phase change temperature range	Responded property change	Dimension (2D/3D)	Encapsulated cell type	Differentiation type	Differentiation evidence	Application	References
Chitosan-*g*-PNIPAAm	Ionic cross-linking (PBS, pH 7.4)	No	25–37 °C	Phase change: sol under 37 °C and gel above 37 °C	3D	Mouse embryonic mesenchymal progenitor cells C3H/10T1/2	—	—	Regenerative medicine	78
Chitosan/nanohydroxyapatite/collagen	Ionic cross-linking (β-glycerophosphate , β-GP)	No	31 °C	Phase change: sol under 31 °C and gel above 31 °C	3D	Rat BMSCs	—	*In vivo* test	Cell delivery	79
2.5 wt% Chitosan and 1 wt% gelatin + Sr	Ionic cross-linking (β-GP)	Degradable	36 °C	Phase change: sol under 36 °C and gel above 36 °C	3D	Human exfoliated deciduous teeth (SHEDs) MSCs	Osteoblast	ALP; mRNA: Collagen I, Runx2, OP, ON; protein: BMP-2; calcium deposit	Bone formation	71
Zinc-doped chitosan/nanohydroxyapatite/beta-glycerophosphate (Zn-CS/nHAp/ β-GP)	Ionic cross-linking (β-GP)	Degradable	37 °C	Phase change: sol at 4 °C and gel at 37 °C	3D	mMSCs	Osteoblasts	*In vivo*; mRNA: Runx2, ALP, COL-I, OCN; protein: Runx2; calcium deposition	Bone regeneration	35

Chitosan chloride	Ionic cross-linking (β-GP)	Degradable	37 °C	Phase change: sol under 37 °C and gel above 37 °C	3D	mASCs	Renal tubular epithelial-like and vascular endothelial-like cells	*In vivo* test Pan-CK for epithelial cells and CD31 for vascular endothelial cells	Acute kidney injury	28
Poly(ethylene glycol)-*b*-poly(L-alanine) (PEG-L-PA)	—	Degradable	The sol-to-gel transition temperatures decreased from 47 to 20 °C, from 34 to 14 °C, and from 18 to 6 °C as the concentrations were increased from 8.0 to 17.0 wt%, from 2.0 to 6.0 wt%, and from 1.0 to 2.0 wt% for P50–06, P50–11, and P50–25, respectively		3D	ASCs	Chondrogenesis	Collagen II *in vitro*; sulfated glycosaminoglycan *in vivo*	Injectable tissue engineering	31
Tetronic–tyramine with FN or RGD	—	No	37 °C	Phase change: sol at 4 °C and gel at 37 °C	2D	hMSCs	—	*In vivo* test	Cell patch	80
Poly(organophosphazene)-RGD	—	Degradable	37 °C	Phase change: sol under 37 °C and gel above 37 °C	3D	Rabbit MSCs	Osteoblast	*In vivo* test; mRNA: OCN; calcium deposition; protein: collagen I	Bone tissue engineering	32

Table 17.2 Electroactive materials and their regulation for the fate of stem cells.

Material	Stimuli	Dimension (2D/3D)	Culture medium	Encapsulated cell type	Differentiation type	Differentiation evidence	Application	Reference
Laminin-coated PPy-DBS	±0.25 mA cm^{-2} biphasic waveform of 100 μs pulses with 20 μs interphase open circuit potential and a 3.78 ms short circuit (250 Hz) 8 h day^{-1} for 3 days	2D	Differentiation media	hNSCs	Neurons and glial cells	β-III tubulin (TUJ1) for neurons and glial fibrillary acidic protein (GFAP) for glial cells	*In vitro* modelling, translational drug discovery and regeneration medicine	43
PPy	Direct current field (DCF), 0.035, 0.35, 3.5 V cm^{-1} for 2, 4, 12 h	2D	Differentiation medium	Rat bone marrow stromal cells (rBMSCs)	Osteoblasts	Up-regulated mRNA: core binding factor 1 (Cbfa1), osteocalcin (OCN); earlier expressed alkaline phosphatase activity (ALP); improved calcium deposition and mineralization	Coating on the medical devices with a transparent appearance	44
(Fibronectin/pyrrole/2-hydroxy-5-sulfonic aniline)-coated PVDF	3 d without stimulation, 6 d with stimulation at 100 mV mm^{-1} for 4 h day^{-1}, no stimulation thereafter	3D	Differentiation medium	hBMSCs	Osteoblasts	Improved ALP express, calcium and collagen deposition, mineralization	Formation of calcified extracellular matrix associated with bone	17

(Collagen I alone or with sulfated hyaluronan)-coated PANI (PANI/Col I/sHya)	Pulsed electric field (PEF) 7 ms rectangular pulses 3.6 mV cm^{-1} 10 Hz	2D	Differentiation medium	Primary hMSCs	Osteoblasts	Up-regulated ALP and OCN, calcium deposition	Regulate stem cell behaviour with controlled physicochemical cues and optimal stimulation modalities	40
(Laminin/poly-L-ornithine)-coated PEDOT:PSS	Pulsed stimulation potential 100 Hz 24 h during the first 4 days' culture with EGF, FGF-2 and B27 on crosslinked PEDOT:PSS and 12 h during differentiation time (following 8 days)	2D	Differentiation medium	Human neural progenitor cell line (ReNcell VM)	Neuronal and glial lineages	Tuj1 for neurons	Neuronal engineering	41
HCl doped PANI	10 days of 100 mV cm^{-1} electrical field stimuli in cycle of 10 min day^{-1}	2D	Standard cell culture medium	hMSCs	Neural-like cells	Decreased expression in nestin and higher expression of β-III tubulin	Integrating substrate conductivity and external electric stimuli to manipulate the cell functionality *in vitro*	42

17.3 Electroactive/Conductive Materials

Electroactive materials are conductive and they change their bulk properties in response to different frequencies of applied electricity. Electrochemistry and inverse piezoelectricity are the two main contributing factors for bulk change when applying alternating electricity. Electrochemistry utilises the ionic exchange between the electroactive materials and the electrolytes to achieve swelling and contraction,[36] while inverse piezoelectricity induces deformation due to the inherent inverse piezoelectric property of the electroactive materials in an applied electrical field.[20] Hence, electroactive materials can be divided into two categories: (a) electrochemical materials, such as polypyrrole (PPy) and PPy-coated films/scaffolds, polyaniline (PANI) and PANI-coated films/scaffolds, poly(3,4-ethylenedioxythiophene) (PEDOT) and PEDOT-coated films/scaffolds, and (b) piezoelectric materials, such as polyvinylidene fluoride (PVDF), PVDF-*co*-polymers, and collagen (Table 17.2). Moreover, piezoelectric materials can also generate electricity due to mechanical deformation, which is called piezoelectricity.

17.3.1 Electrochemical Materials

Firstly, the effect of electroactive materials on differentiation of stem cells can be merely based on the inherent conductivity and stiffness. It was reported that polylactide with chondroitin sulfate-doped PPy (PLA–PPy) slightly improved expression of alkaline phosphatase (ALP), an osteogenic marker, while this enhancement was considered as a typical impact of 3D scaffolds on the hASCs supplied with the standard cell culture medium.[37] The effect of electrical stimulation on the early osteogenic differentiation of hASCs was not observed, however, electrical stimulation-induced differentiation into fibroblastic and vasculogenic cells was detected in another study by Tandon *et al.* in the standard cell culture medium.[38] Furthermore, when supplying hASCs with the osteogenic medium in a two-dimensional (2D) system, mineralization and expression of osteogenic genes and proteins were observed.[39] Compared to direct chemical stimulation, electrical stimulation showed less influence on the early osteogenesis of hASCs, because electrical stimulation helps in improving osteogenic induction of the osteogenic medium on hASCs but not osteogenic initiation. In addition, the source of stem cells may also play a role in the tendency of cell differentiation, which could explain why hASCs showed fibroblastic and vasculogenic behaviour rather than osteogenesis in response to electrical stimulation in the standard cell culture medium.

Secondly, when appropriately combining electrical and chemical stimulation, differentiation of stem cells can be well controlled (Figure 17.3(A)). Electrical stimulation in the osteogenic or neurobasal medium induced osteogenesis[17,40] or neural differentiation,[41] respectively. Even without the neurobasal medium, hMSCs were found to differentiate into neuron-like cells on a HCl-doped PANI film charged with a cycled electrical field.[42] Stewart

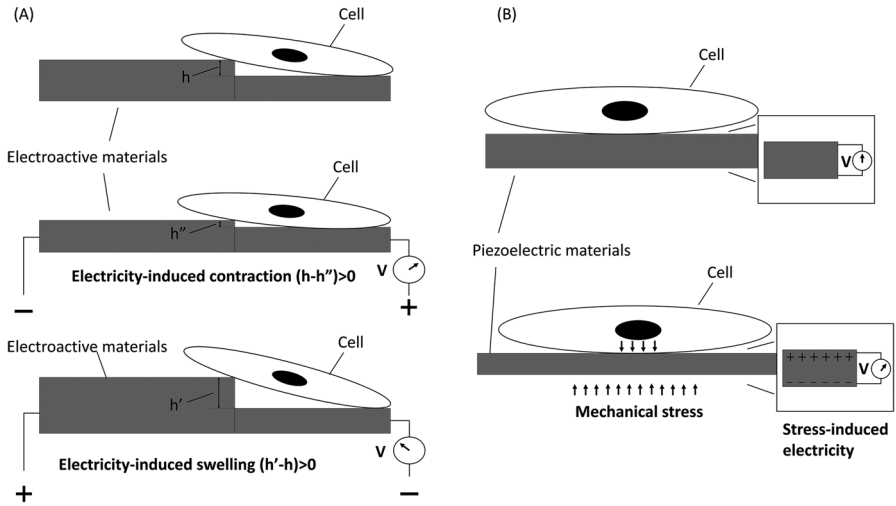

Figure 17.3 Schematic of electroactive materials regulating the fate of stem cells. Swelling and contraction of the electroactive scaffolds due to external electricity are shown in (A). When an altered electrical field is applied to the electroactive scaffolds, the scaffolds contract and swell due to the ion exchange between the scaffold and the electrolyte[36] or the inverse piezoelectricity.[20] Hence, the attached stem cells are stimulated by mechanical stress to induce specific cell differentiation. The electricity produced by piezoelectric materials is shown in (B). When the scaffolds are stressed or attached stem cells contract, the piezoelectric materials produce electricity on the surface, which is in turn utilised as an electrical stimulus to differentiate the stem cells, such as neurogenesis or osteogenesis.[45] Adapted with permission from *Journal of Biomedical Materials Research A*, **136**, Ribeiro, C., Sencadas, V., Correia, D. M., Lanceros-Mendez, S. Piezoelectric polymers as biomaterials for tissue engineering applications, 46–55, copyright (2015) with permission from Elsevier.

et al. reported that human neural stem cells (hNSCs) were predominantly differentiated into neurons, while fewer glial cells were detected, seven days after they were cultured on a dodecylbenzenesulfonate-doped polypyrrole (PPy-DBS) film in the neurobasal medium and exposed to an alternating electrical field.[43] In addition, accelerated osteogenesis was also reported when rat bone marrow stromal cells (rBMSCs) were cultured on the PPy film in the osteogenic medium in a direct current field.[44]

17.3.2 Piezoelectric Materials

Piezoelectric materials can be utilised to direct differentiation of stem cells by piezoelectricity or inverse piezoelectricity (Figure 17.3(B)). Piezoelectricity was applied to direct hASCs towards osteogenic differentiation.[45] The hASCs dynamically cultured on the β-poly(vinylidene fluoride) (β-PVDF) film coating with fibronectin in a standard cell culture medium expressed much

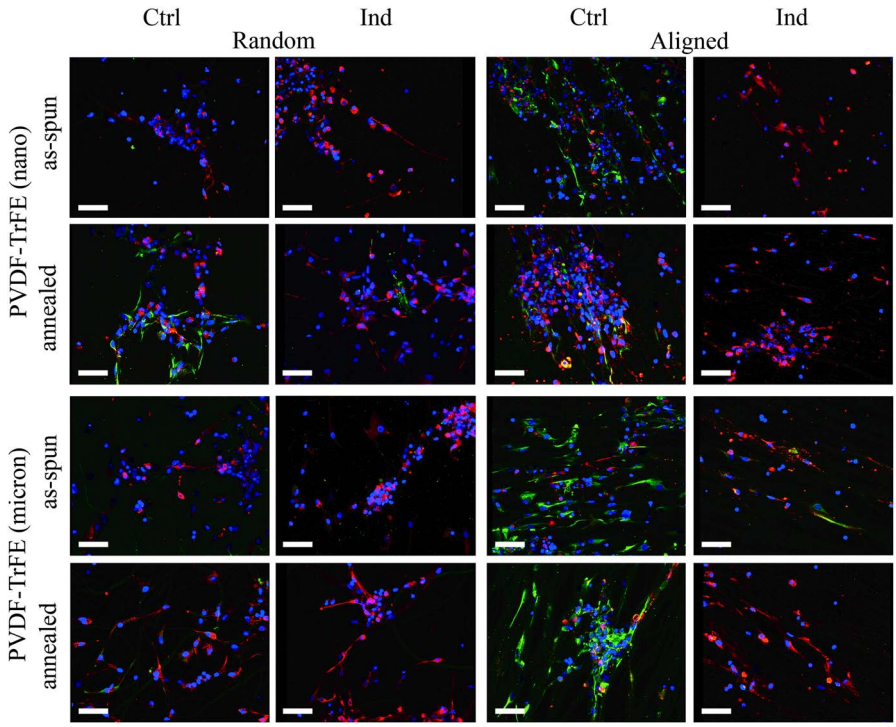

Figure 17.4 Immunofluorescent staining of hNPCs cultured on piezoelectric micro- and nano-sized PVDF-TrFE as-spun (without annealing), annealed (enhanced piezoelectricity), random and aligned scaffolds in control and induced medium at day nine.[16] Green: nestin; red: β-III tubulin; blue: GFAP and DAPI. (Scale bar = 50 μm). Reproduced with permission from Lee Y. S., *et al.*, *Tissue Eng Part A*, **18**, 2063, 2012. Copyright 2012: Mary Ann Liebert, Inc.

higher ALP than those statically cultured. Furthermore, Lee *et al.* successfully directed human neural progenitors (hNPCs) into mature neural cells on a piezoelectric scaffold, which was generated by electrospinning poly(vinylidene fluoride trifluoroethylene) (PVDF-TrFE, 65/35), even without a cell differentiation medium. PVDF-TrFE produced electricity, due to a cell-induced minute bulk change, and enhanced expression of the neuronal cell marker (β-III tubulin) (Figure 17.4).[16] In addition, a longer neurite was observed on the enhanced piezoelectric, micro-, and aligned PVDF-TrFE scaffolds.

17.4 Photo-Responsive Materials

Photo-responsive materials respond to certain wavelengths of light and change their properties, for instance, photo-polymerization induced by photo-initiators and gelation of acrylated monomers or biopolymers, such as

acrylamide, acrylic acid, hydroxyethyl acrylate, NIPAAm, and PEG-monoacrylate.[13] In addition, photo-responsive materials may be activated to release electrons to induce electricity,[19] or activate reactive oxygen species (ROS) inside the cells.[46] Moreover, photo-responsive polymers can perform photolysis[47,48] or reversible isomerization[10] in response to a certain wavelength of light.

According to the reversibility of the responsive behaviour, photo-responsive materials can be divided into two categories: (a) photo-activatable/photo-cleavable materials, such as TiO_2, 5-aminolevulinic acid (5-ALA), polymers containing *o*-nitrobenzyl (*o*NB) moieties, 2-(2-nitrophenyl) propyl 2-(2-(2-(2-azidoethoxy)ethoxy)ethoxy)ethoxycarbamate (N3-TEG-ONH-NPPOC), 3-(4,5-dimethoxy-2-nitrophenyl)-2-butyl (DMNPB), and (b) reversible isomers, such as azobenzene groups or spiropyran groups containing polymers (Table 17.3).

17.4.1 Photo-Activatable Materials

When exposed to a certain wavelength of light, photo-initiated polymerization and gelation of a hydrogel (Figure 17.2) can provide mechanical support for the encapsulated stem cells to form a 3D *in-vivo*-ECM-mimicking environment, where the inherent stiffness of the hydrogel and the incorporated biomolecules can play a synergistic role in the differentiation of stem cells. Shell *et al.* successfully initiated the gelation of bis(acrylamide) and PEG-diacrylate with a vitamin B12 derivative, alkyl-cob(III)alamins Cy5-labeled ethyl-Cbl at a wavelength of 660 nm.[13] Due to the biocompatibility and biodegradability of PEG and the vitamin B12 derivative, stem cells were mixed with the photo-responsive materials and the PEG-diacrylate monomers, and the hybrids were implanted into the damaged cartilage. *In situ* gel formation was initiated under irradiation at 660 nm, which falls within the "optical window of tissue" (600–900 nm), a range of light wavelengths that allow maximal tissue penetration.[13] After gelation, stem cells were retained inside the hydrogel and further differentiated into chondrocytes for regeneration of the damaged cartilage by responding to the internal stimuli generated by the host.

Apart from polymerization and gelation for *in situ* regulation of stem cells, photo-responsive materials can also generate ROS under irradiation.[46] A high level of ROS is toxic to cells, but ROS at a certain dosage range can regulate intracellular signalling, and therefore, change the final cell lineage of stem cells.[49] Kushibiki *et al.* exposed the photo-responsive material, 5-aminolevulinic acid (5-ALA), to weak illumination to generate a low level of ROS inside primary rat MSCs.[46] The generated ROS promoted osteogenesis of MSCs by regulating the activator protein-1 (AP-1)-mediated signalling pathway. In addition, the excited photo-responsive materials generate electricity on the conductive substrate by accumulating released electrons (Figure 17.5(A)) and the minute electricity stimulated hNSCs to differentiate into mature neurons rather than glial cells.[19]

Table 17.3 Photo-responsive materials and their regulation for the fate of stem cells.

Material	Stimuli	Responded property change	Dimension (2D/3D)	Status (hydrogel/scaffold)	Culture medium	Encapsulated cell type	Differentiation type	Differentiation evidence	Application	Reference
Reduced graphene oxide (rGO)/TiO_2 heterojunction	Repeated pulse duration of 4 s and frequency of 1 Hz (4 flashes s^{-1} with xenon lamp) with intervals of 60 s for a total time of 30 min at each 12 h	Excited electrons transported from TiO_2 to cells on rGO through Ti–C and Ti–O–C bond	2D	Film	Extracellular medium: 140 mM NaCl, 5.0 mM KCl, 2.0 mM $CaCl_2$, 1.5 mM $MgCl_2$, 15.0 mM ascorbic acid (under the optimum conditions of this work), 10 mM 4-(2-hydroxyethyl)-1-piperazineethanesulfonic acid (HEPES), 10 mM glucose at pH 6.4	Human neural stem cells	Neurons (23-fold increase in the neuronal to glial cell ratio)	Neuron-specific β-III tubulin (TUJ1), glial fibrillary acidic protein (GFAP)	As nanostructure scaffold in neural regeneration and repair	19
5-ALA	Irradiation at 635 nm 30 mW cm^{-2} for 0, 24, 67, 102 sec (0, 1, 2, 3 J cm^{-2})	Intracellular reactive oxygen species (ROS) formation (CellROX reagent became fluorescent red)	2D	Film	Differentiation medium (complete medium + 10 nM dexamethasone + 10 mM β-glycerophosphate + 50 ug mL^{-1} ascorbic acid)	Rat BMSCs	Osteogenic differentiation	Calcium deposition with Alizarin red staining; ALP (early osteogenic marker) and osteocalcin (late osteogenic marker) expression	Bone engineering	46

Vitamin B12 derivative alkyl-cob(III) alamins (unlabeled and Cy5-labeled ethyl-Cbl)	Certain wavelength illumination 520 nm for unlabeled and Cy5-labeled ethyl-Cbl, and 660 nm for Cy5-labeled ethyl-Cbl	Photohomolysis of unlabeled or Cy5-labeled ethyl-Cbl at 520 nm or 660 nm, respectively, induces polymerization or gelation of acrylated monomers or biopolymers (by the ethyl radical)	3D	Hydrogel	—	—	—	—	Light-induced injectable hydrogel for tissue regeneration (phototherapeutics)	13
Heparin photogel contains thiolated heparin molecules and PEG molecules with bifunctional acryl terminated photolabile *o*-nitrobenzyl moieties	365 nm 600 W UV light exposure for 10 s	Heparin photogel degraded	2D	Hydrogel (FGF2 inside)	Differentiation medium contains IMDM + 1% FBS + 2% penicillin/streptomycin + 0.001 M nonessential amino acids + 0.5 U mL^{-1} insulin + 14 ng mL^{-1} glucagon + 100 × 10^{-9} M dexamethasone for 4 d and 1% FBS replaced with 1% B27 after 4 d	mESCs	Endoderm (encapsulated FGF2 induce differentiation)	Sox17 and FOXA2	Stem cell culture and study	81

(*continued*)

Table 17.3 (*continued*)

Material	Stimuli	Responded property change	Dimension (2D/3D)	Status (hydrogel/ scaffold)	Culture medium	Encapsulated cell type	Differentiation type	Differentiation evidence	Application	Reference
SPAAC-based gel (PEG, 10 wt%), NPPOC-(photo-caged) for vitronectin-*o*NB to anchor (cells attach)	Collimated UV light (wavelength 365 nm, 5–20 mW cm^{-2}, 0–600 s) with a patterned chrome photomask or pulsed laser light for 3D photomediated protein ligation or photorelease	UV exposure to photolyze NPPOC and then immobilize VTN-CHO onto the gel and same light exposure to induce photoremoval of VTN-CHO	3D	Hydrogel	stemXVivo human osteogenic inductive medium + 1% penicillin/ streptomycin	hBMSCs	Osteogenic differentiation (differentiation media induced together with cell attaching and spreading because of vitronectins)	OCN and ALP	Tissue engineering	50
Cyclic RGD peptide (cyclo-[RGDfK])-&cyclo[RGD-(DMNPB)] fK]-tethered SAMs of alkanethiols	Irradiation at 355 nm 3.5 mW cm^{-2} for 3 min	Decaged RGD and phototriggered cell attachment	2D	Monolayer	DMEM + 1% penicillin-streptomycin + 1% insulin-transferrin-selenium-X (ITS)	Murine C2C12 myoblast	Myogenic differentiation	Sarcomeric myosin positive	Biomedical devices	47
PEG5000 containing *o*-NB caged PFSST-KTC peptide (SAM)	UV exposure for 5 min	Detachment of PEG shell and enhancement of cell attachment	2D	Monolayer	DMEM + 10% FBS + 1% penicillin-streptomycin	Rat BMSCs	Osteogenesis	Calcium deposition and OPN expression	Regeneration medicine	48

Dynamic photo-responsive zwitterionic hydrogel consists of static zwitterionic monomer carboxybetaine acrylamide (CBAA), cyclic-RGD (cRGD)-functionalized CBAA and photo-switchable monomer spiropyran methacrylate (SPMA), cross-linked with zwitterionic carboxybetaine dimethacrylate (CBDMA)	Illumination at near-infrared light (NIR, 800 nm, 50 mW); NG-1 (50 mW NIR + 10 mW visible green light); NG-2 (50 mW NIR + 30 mW visible green light); visible green light (560 nm, 50 mW) for continuous 14 days	NIR transfers closed-ring hydrophobic form isomer (spiropyran, SP) to zwitterionic hydrophilic form isomer (merocyanine, MC) by two-photon excitation (TPE); visible green light transfers MC to SP by SPE	2D and 3D	Hydrogel	Bipotential (osteogenic and adipogenic) differentiation media	hMSCs	Osteogenesis and adipogenic differentiation	Adipogenic surface antigens (PPARG and FABP4) and neutral lipids; osteogenic surface antigens (Runx2 and OPN) and ALP	Regenerative medicine	82

17.4.2 Photo-Cleavable Materials

Some photo-responsive materials provide specific binding sites for stem cells by conjugating the materials with RGD peptides/proteins or a cage to prevent such specific binding (Figure 17.5(C) and (D)). When irradiated at a certain wavelength, the covalent bonds between the photo-responsive materials and the RGD peptides/proteins are broken by photolysis. The released RGD peptides/proteins either are detached from the main structure of the polymer backbone or become available for cell binding after opening the caged components. Both approaches can be employed to control the duration and intensity of binding by adjusting the concentration of RGD binding ligands in the hydrogels. Based on this concept, Weis *et al.* caged cyclo[RGDfk]-tethered self-assembled monolayers (SAMs) with DMNPB and successfully achieved a controllable concentration of the RGD for cell binding on the SAMs by sequential irradiation.[47] The seeded myoblasts on the substrate were guided towards myogenic differentiation and achieved the maximal myogenesis when RGD was exposed to cells under illumination for six hours. Polymers are also modified to control caging and uncaging of RGD peptides under illumination. For instance, PEG with a photo-sensitive

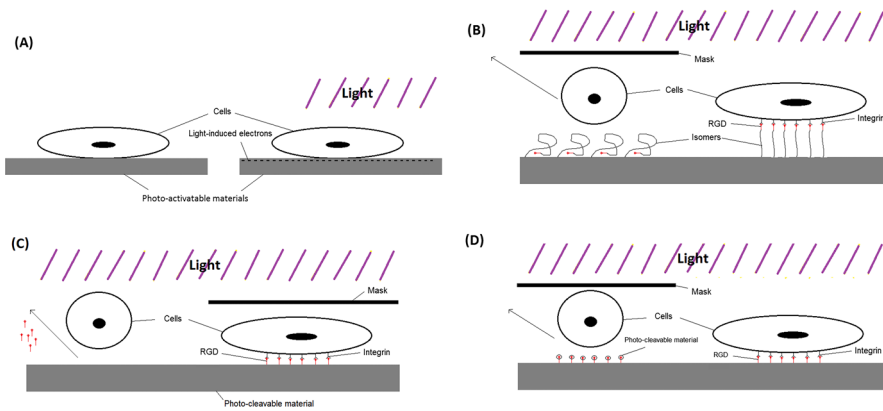

Figure 17.5 Schematic of photo-responsive materials regulating the fate of stem cells. (A) When a certain wavelength of light is applied to the photo-activatable materials, the excited electrons are released and play a role in stem cell differentiation.[19] (B) When illuminated by a certain wavelength of light, the RGDs conjugated to the isomers are reversibly exposed to the stem cells by light-induced isomerization and the differentiation of stem cells is regulated by the concentration of RGDs.[10] (C) The RGDs are pre-conjugated to the photo-cleavable materials and released upon illumination from the surface of scaffolds/hydrogels, which leads to stem cell detachment from the surface. (D) The RGDs mounted on the scaffolds/hydrogels are caged by the photo-cleavable materials, but released and exposed to the stem cells after illumination. In both ways, the concentration and the exposure time of RGDs in the scaffolds/hydrogels can be manually controlled for defined regulation of stem cell differentiation.[10]

o-nitrobenzyl group was utilised to control the concentration of the peptides exposed to rat BMSCs. It was shown that the uncaged PFSSTKTC (Pro–Phe–Ser–Ser–Thr–Lys–Thr–Cys) peptide improved cell attachment[5] and directed rat BMSCs towards osteogenic differentiation in the standard cell culture medium.[48] Moreover, DeForest *et al.* reported the use of photocleavable materials to achieve defined distribution of proteins within a hydrogel.[50] Briefly, the first protein, bovine serum albumin (BSA_{488}) modified with 2,5-dioxopyrrolidin-1-yl 4-(4-(1-((4-(4-formylbenzamido)butanoyl)oxy) ethyl)-2-methoxy-5-nitrophenoxy)butanoate (NHS-*o*NB-CHO), was combined with PEG hydrogel.[50] On the other hand, the alkoxyamine groups of the PEG hydrogel were caged by NPPOC and these groups were activated upon illumination to anchor the second protein. Hence, when irradiation was applied to the PEG hydrogel, BSA_{488}-*o*BN-CHO was first photo-cleaved from the hydrogel by photolysis of *o*BN; at the same time, the cage by NPPOC was open to release the alkoxyamine groups to form the second protein complex BSA_{594}-*o*BN-CHO. Based on the concept, it was able to achieve controlled anchor or removal of vitronectins from the PEG hydrogel. By controlling concentration and spatial distribution of vitronectins exposed to hBMSCs, the stem cells were significantly promoted to express the early osteogenic marker ALP at day 4. After removal of vitronectins from the PEG hydrogel, expression of ALP in hBMSCs dropped back to the initial level at day 10.

17.4.3 Reversible Isomers

Photo-induced isomerization of spiropyran- or azobenzene-polymers can help to regulate differentiation by balancing specific and non-specific cell adhesion (Figure 17.5(B)). *Cis*-transition of azobenzene-polymers is triggered upon illumination of UV/visible light, which results in a complete change in the electronic structure, shape and polarity of the polymer. Through the transition, specific binding between the conjugated RGD sequences and stem cell integrin receptors can be manipulated and therefore the stem cell fate can be regulated. PEG is often incorporated inside the hydrogels to minimize non-specific binding.[8] On the contrary, spiropyran-polymers perform reversible transition between the hydrophilic zwitterionic form (merocyanine, MC) and the hydrophobic closed-ring form (spiropyran, SP), which has been used to demonstrate the effect of non-specific binding on stem cell differentiation. When near-infrared (NIR) light was applied to the photo-responsive hydrogel, the spiropyran moieties were transformed to the merocyanine moieties, and this transformation was inversed when a visible green light illuminated on the hydrogel. Exposure to green light resulted in an increase in the spiropyran form, thus an increase in non-specific cell–substrate interactions.[10] It was demonstrated that hMSCs hardly performed differentiation under the pure NIR light (in the zwitterionic form), while osteogenesis was preferred under the green light and adipogenesis was predominant after illumination under the NG-1 light (50 mW NIR and 10 mW green) (Figure 17.6). It was also noticed that differentiation of hMSCs was suspended after switching from the green light back to NIR.[51]

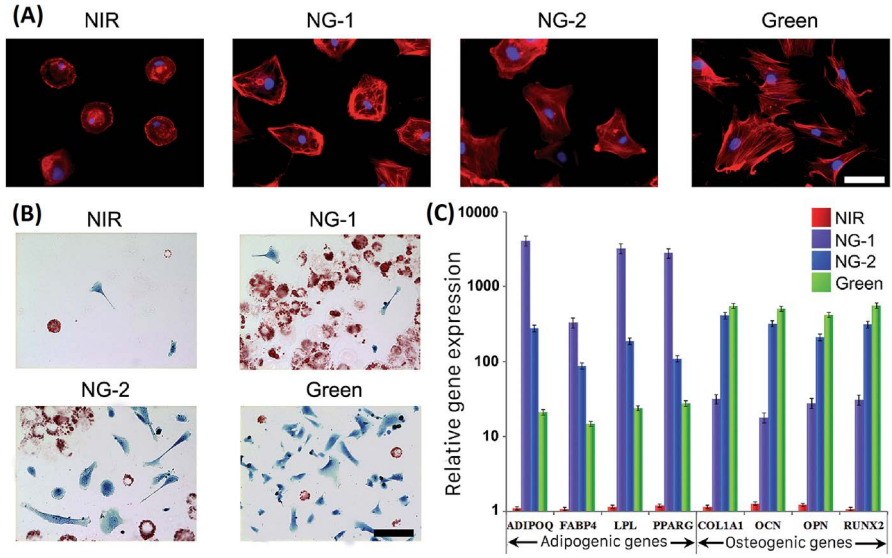

Figure 17.6 (A) Immunofluorescent staining of hMSCs cultured on the photo-responsive hydrogel in the osteogenic and adipogenic differentiation media under different illumination (NIR (800 nm): 50 mW; NG-1: 50 mW NIR + 10 mW green; NG-2: 50 mW NIR + 30 mW green; green (560 nm): 50 mW at day 14). Red: TRITC-phalloidin; blue: DAPI. (Scale bar = 15 μm). (B) Histological staining of adipogenic and osteogenic hMSCs by Oil Red O and Fast Blue salt, respectively, in the osteogenic and adipogenic differentiation media under different illumination at day 14. Red: neutral lipids; blue: alkaline phosphatase. (Scale bar = 100 μm). (C) Adipogenesis and osteogenesis level under various illumination ($p < 0.05$).[51] Adapted from ref. 51 with permission from the Royal Society of Chemistry.

17.5 Thixotropic Materials

Thixotropic materials change their properties in response to an applied shear stress. The viscoelasticity of thixotropic materials allows them to reversibly change their status between gel and sol at different shear stress levels. When being stressed or pipetted, the viscous property is over the elastic one, namely the loss modulus G″ is higher than the storage modulus G′, and the thixotropic hydrogel becomes sol.[14] Under stressed conditions, molecular interactions inside the thixotropic material, such as hydrogen bonding and hydrophobic and/or electrostatic interactions, become weak, which results in mechanical deformation of the hydrogel to form the sol status. After the stress is removed, the internal interactions are reconstructed and the mechanical gel structure is reformed. The recovery process from the sol back to the gel status is dependent on time as well as the interactions in the hydrogels,[14] and the process can be selectively manipulated by temperature,[14,52] pH,[53] or ionic components.[18]

Thixotropic materials used in regeneration medicines are divided into two categories: (a) polymeric hydrogels formed by covalent crosslinking, such as a blend of silk fibroin (SF) and hydroxypropylcellulose (HPC), a blend of hyaluronic acid (HA) and methylcellulose, polyethylene glycol–silica (PEG–silica), nanofibrillar cellulose (NFC), and (b) supra-molecular hydrogels formed by non-covalent self-assembly, such as naphthalene-oligopeptide, the Max family (MAX1 and MAX8), tryptophan (W)-rich oligopeptides (CC 43 and Nedd 4.3), amyloids, and SF protein (Table 17.4).

17.5.1 Stiffness-Induced Cell Differentiation

Stem cells are homogeneously dispersed into thixotropic hydrogels in the form of a sol. The cell–sol hybrid is directly injected into the lesion site, and under stressed conditions, the hybrid is in the form of a sol so the solution can exactly fit into the *in vivo* damaged tissue (Figure 17.2). In the lesion site after removal of the applied stress, the hybrid turns back into a gel to retain stem cells in the damaged tissue. The injected hydrogel also plays a role in directing the fate of the incorporated stem cells by the stiffness of the hydrogel and *in vivo* electrical, mechanical, and chemical stimulation under physiological conditions. Pek *et al.* cultured hBMSCs in a 3D PEG-silica-based thixotropic hydrogel and demonstrated that various stiffnesses of the injectable hydrogel, which were measured by the minimal liquefaction stress (τ_y) required to transform gel to sol, promoted differentiation of the encapsulated stem cells towards different lineages: neural differentiation, myogenesis and osteogenesis at τ_y of 7 Pa, 25 Pa and 75 Pa, respectively.[54] In addition, when cell-binding RGD peptides were conjugated to the PEG-silica hydrogel, osteogenesis at a τ_y of 75 Pa was markedly enhanced with 13% higher expression of Runx2 and OCN, because the specific binding between the immobilized RGD ligands and the cellular membrane integrin at a stiffer hydrogel was tighter, and the tighter binding induced osteogenic differentiation.[54] Jacob *et al.* adjusted the inherent stiffness of an amyloid hydrogel by changing the concentrations of amyloid and ions, at which the encapsulated hBMSCs were detected to differentiate into the neural lineage.[55] The peptide Nap-GFFYGG-KOGEOGKOGSO in the supra-molecular-peptide/protein-formed thixotropic hydrogels was reported to work as a stimulus and selectively improved differentiation of mouse ESCs into vascular progenitor cells with a significantly high expression of the *Flk 1* gene.[56]

17.5.2 Stress Stiffening/Relaxation-Induced Cell Differentiation

Most hydrogels generated from filamentous biopolymers, such as collagen, F-actin and fibrin, become stiffer when the applied stress is above their critical stress (σ_C) level, which is called stress stiffening. It was recently reported that stress stiffening also plays an important role in regulation of stem cell fate

Table 17.4 Thixotropic materials and their regulation for the fate of stem cells.

Material	Dimension (2D/3D)	Culture medium	Encapsulated cell type	Differentiation type	Differentiation efficiency	Differentiation evidence	Application	Reference
RGD-conjugated PEG-silica gel (with varied liquefaction stress and RGD concentration)	3D	Culture media	hBMSCs	Neural differentiation for 7 Pa; myogenic differentiation for 25 Pa; osteogenesis for 75 Pa	RGD promoted proliferation and differentiation of hMSCs for stiffer gels with liquefaction stress >75 Pa	Neural (*ENO 2*), myogenic (*MYOG*). Osteogenic (*Runx2*, *OCN*) transcription factors	Tissue engineering	54
Amyloid hydrogel (Fmoc-conjugate peptides (Aβ42)), varying stiffness by changing peptide and salt concentration	2D	Knockout DMEM + 10% FBS + 2 mM glutamax + 0.25% penicillin and streptomycin	hBMSCs	Neuronal lineage for softest gel P5 6 mg mL^{-1}	—	Maximal spreading and elongation, β-III tubulin ENO2, GRIA3	Tissue engineering	55
Nap-GFFYGGKO-GEOGKOGSO	2D	Differentiation media	mESCs	Vascular progenitors	—	Mesoderm marker (*Flk 1*)	Vascular formation in regeneration medicine	56

RGD-PICs; modify the critical stress by changing the polymer length	3D	1 : 1 v/v osteogenic and adipogenic media	hMSCs	Adipocyte lowest critical stress ~9.4 Pa; predominant osteogenesis over adipogenesis with increasing critical stress	—	Rsterix stain and *Runx2* RT-PCR for osteogenesis; neural lipid and *PPAR-γ* for adipogenesis	Tissue engineering	57
Alginate (crosslinked with calcium and covalently coupled with RGD); modify stress relaxation time by changing the molecular weight polymers and the crosslinking densities of calcium	3D	DMEM + 10% FBS + 1% PS + 50 mg mL^{-1} L-ascorbic acid + 10 mM β-glycerophosphate + 0.1 μM dexamethasone	mBMSCs	Adipocyte at ~9 kPa and osteoblast at ~17 kPa	Adipogenesis differentiation decrease in rapidly relaxing gels ~1 minute; osteogenic differentiation significantly enhanced with faster stress relaxation	Neural lipid for adipogenesis and ALP for osteogenesis	Bone regeneration	58

besides the inherent stiffness of the hydrogel.[57] By simply changing the polymer length of RGD-conjugated helical oligo(ethylene) glycol polyisocyanopeptides (RGD-PICs), the σ_C was accordingly adjusted without any influence on the stiffness and the density of RGD peptides. When hMSCs were encapsulated in the hydrogel, hMSCs were attached to the RGD ligand through specific interactions between RGD and cellular integrin (Figure 17.2), during which cells applied traction stress on the surrounding gel and the traction triggered stress stiffening of the hydrogel. The stress stiffening in turn affected differentiation of the stem cells.[57] It was shown that adipogenic differentiation was predominantly performed at a lower σ_C (~9.4 Pa), while osteogenesis was preferred at a higher σ_C (14.6–19.3 Pa).[57] Furthermore, it was reported that the stress relaxation time of the RGD-alginate hydrogel also influenced the differentiation of mouse mBMSCs.[58] Decreased adipogenesis at a stiffness of ~9 kPa and significantly enhanced osteogenesis at a stiffness of ~17 kPa in the faster relaxing gel (~1 minute) were observed, because the relaxation time of the hydrogel influenced the interaction between RGD and the cell integrin, and accordingly played a role in cell adhesion and differentiation.[58]

17.6 pH-Sensitive Materials

pH-Sensitive materials usually have certain pendant groups or bonds, which can be ionized or broken when the external pH is higher or lower than their acid dissociation constants (pK_a).[14] Ionization increases the osmotic pressure inside the hydrogel, which leads to water absorption and hydrogel swelling. In addition, electrostatic repulsion generated by the ionized anionic or cationic pendant components further enhances the ionization impact. Opposite to swelling, the hydrogel may also contract by simply inhibiting ionization of pendant groups and electrostatic repulsion.[14] pH-Sensitive materials include zwitterionic amino acid/peptide amphiphiles (H_2N-peptide/oligopeptide-COOH)[59] or polymers that consist of an amino group ($-NH_2$), or carboxyl group (–COOH),[60] or catechol ($C_6H_4(OH)_2$),[61] or a hydrogen bond (–NH–CO–),[62,63] or an ionic bond ($-NH_4^+\cdots OSO_3^-$–),[64] or an imine bond (–N=CH–).[65]

Most pH-sensitive materials are reported as carriers for drug/gene delivery, because the bonds in the drug-immobilized pH-sensitive materials are ionized in the abnormal pH condition of the tumour, and then the drug is released to achieve target treatment.[14,66,67] Based on this concept, bone morphogenetic protein 2 (BMP-2) was immobilized to pH-sensitive chitosan-functionalized mesoporous silica nanoparticles through hydrogen bond formation and the protein was selectively released to rat BMSCs, to control differentiation towards osteogenesis with the evidence of enhanced expression of ALP, Runx2, OPN and Col I.[62]

Furthermore, chondrogenic differentiation, adipogenesis, and osteogenesis of hASCs were all demonstrated when the stem cells were encapsulated inside a pH-sensitive chitosan-poly (acrylic acid) (chi-PAA) hydrogel, which might be due to the contraction and swelling properties of the chi-PAA

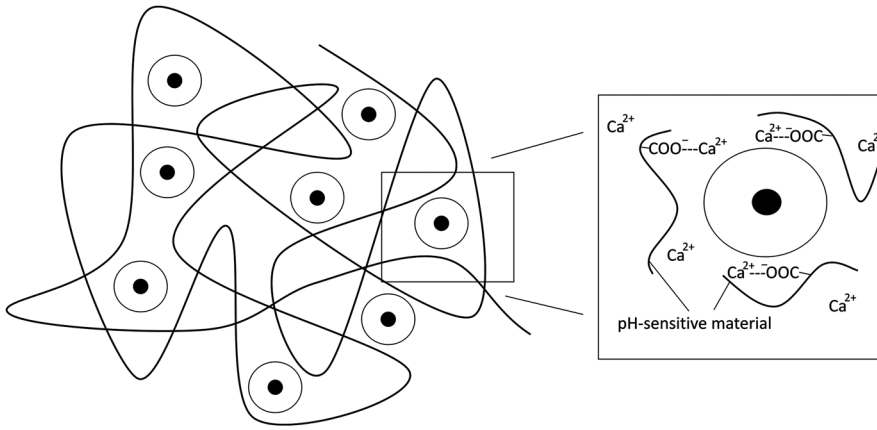

Figure 17.7 Schematic of pH-sensitive materials regulating the fate of stem cells. The carboxyl groups of PNIPAAm–AA were ionized as the anions when the pH was higher than their pK_a, which could attract cations, such as Ca^{2+}. As a result, the encapsulated stem cells were surrounded by the rich Ca^{2+} hydrogel and enhanced osteogenesis.[25,60]

hydrogel.[63] In addition, ionization and bond dissociation always improve the hydrophilicity of the hydrogels. Hence, pH-sensitive materials are easily transformed between sol and gel by simply varying the pH value (Figure 17.2), and they can be potentially applied as injectable hydrogels to provide an *in vivo* ECM-mimicking environment for encapsulated stem cells at physiological pH. Growth factors and RGD peptides/proteins are also incorporated or conjugated into the pH-sensitive hydrogels for regulation of stem cell fate (Figure 17.2). Dai *et al.* achieved selective improvement in expression of ALP and calcium deposition by encapsulating mBMSCs in a thermosensitive and pH-sensitive hydrogel (PNIPAAm–AA).[60] The ionized carboxyl groups of PNIPAAm–AA may play an important role in the capture of calcium, which is an osteogenic stimulus and further promotes osteogenesis of stem cells (Figure 17.7).[60]

17.7 Smart Materials in Clinical Applications

Currently, most cell culturing systems made of smart materials for stem cell therapy are still at the *in vitro* or *in vivo* animal research stage.[24] They were mainly designed to maximally mimic the properties of the extracellular matrix (ECM) so as to facilitate functioning of implanted stem cells similar to host cells *via in vivo* physiological stimulation. Thus, the stem cells can be induced to transform to the required cell types. One of the few successful applications of smart materials in the clinical trails of stem cell therapy was reported by Menasché *et al.* in 2015.[68,69] A hybrid of enzyme-sensitive fibrinogen and hESCs-derived cardiac progenitor cells was induced to form a thin layer of a 3D fibrin gel by thrombin, which was then implanted onto the

infarcted area of a patient suffering from MI. Three months after the implantation, an improved left ventricular ejection fraction (LVEF) from 26% to 36% and contractility in the infarcted area were found. In addition, no adverse complications were shown. Even though it was hard to say that the improvement of cardiac function was due to the differentiation of the implanted hESCs-derived cardiac progenitor cells since vascular bypass surgery in a no-infarcted area was performed at the same time, the smart material utilised in this trial showed a good example for their future clinical applications. In addition, a monolayer of autologous oral mucosal epithelium was generated from the temperature-sensitive material PNIPAAm and implanted into a patient suffering total bilateral corneal limbal epithelial stem cell deficiency, which showed another possible clinical application of smart materials.[70] However, before full regulation of stem cells in clinical applications, the complicated mechanism of cell differentiation should be completely and clearly understood. Then the fate of stem cells can be controlled well either *in vivo* or *in vitro* by physical or chemical modification of the smart materials.[24]

17.8 Conclusions and Perspectives

Compared to traditional materials, smart materials are better alternatives for advancing stem cell therapy because they allow remote control of regulating the fate of the encapsulated stem cells both *in vitro* and *in vivo*. Most smart materials are easily modified for injectable stem cell carriers for implantation, and they not only facilitate delivery of stem cells into the lesion site but also provide an *in situ* ECM-mimicking environment for the stem cells.

Smart materials are also employed to direct the differentiation of stem cells through a variety of physical/chemical cues, including inherent stiffness, controlled release of encapsulated biomolecules, hydrophobic or electrostatic interactions, generated electricity or reactive oxygen species, and others, when they change their properties in response to external stimuli, such as temperature, pH, stress, or light.

However, how these physical/chemical cues created by the smart materials in response to external stimuli switch the gene expression of stem cells to another remains to be clarified. More importantly, precise control of interactions between these physical/chemical cues and stem cells are mandatory for spatially and temporarily regulating stem cell differentiation, which requires the development of novel "smarter" biomaterials. These biomaterials are able to make the cues available for stem cells by external stimuli when requested by cellular differentiation.

Acknowledgements

HZ would like to acknowledge financial support from the ARC Discovery Project (DP160104632) and The Medical Advancement Without Animal (MAWA) Trust. JBZ thanks the IPE-UoA Scholarship (BES).

References

1. X. Li, E. Katsanevakis, X. Liu, N. Zhang and X. Wen, *Prog. Polym. Sci.*, 2012, **37**, 1105–1129.
2. J. Hou, L. Wang, J. Jiang, C. Zhou, T. Guo, S. Zheng and T. Wang, *Stem Cell Rev.*, 2013, **9**, 326–338.
3. T. Goldschlager, D. Oehme, P. Ghosh, A. Zannettino, J. V. Rosenfeld and G. Jenkin, *Curr. Stem Cell Res. Ther.*, 2013, **8**, 381–393.
4. S. Kriks, J.-W. Shim, J. Piao, Y. M. Ganat, D. R. Wakeman, Z. Xie, L. Carrillo-Reid, G. Auyeung, C. Antonacci, A. Buch, L. Yang, M. F. Beal, D. J. Surmeier, J. H. Kordower, V. Tabar and L. Studer, *Nature*, 2011, **480**, 547–551.
5. W. L. Murphy, T. C. McDevitt and A. J. Engler, *Nat. Mater.*, 2014, **13**, 547–557.
6. T. P. Kraehenbuehl, R. Langer and L. S. Ferreira, *Nat. Methods*, 2011, **8**, 731–736.
7. M. G.-F. Sandra Hofmann, in *Regenerative Medicine and Tissue Engineering: Cells and Biomaterials*, ed. D. Eberli, InTech, 2011, ch. 18, DOI: 10.5772/22061.
8. R. Ravichandran, S. Sundarrajan, J. R. Venugopal, S. Mukherjee and S. Ramakrishna, *Macromol. Biosci.*, 2012, **12**, 286–311.
9. A. Chan, R. P. Orme, R. A. Fricker and P. Roach, *Adv. Drug Delivery Rev.*, 2013, **65**, 497–514.
10. A. Higuchi, Q.-D. Ling, S. S. Kumar, Y. Chang, T.-C. Kao, M. A. Munusamy, A. A. Alarfaj, S.-T. Hsu and A. Umezawa, *Prog. Polym. Sci.*, 2014, **39**, 1585–1613.
11. A. Higuchi, Q.-D. Ling, Y. Chang, S.-T. Hsu and A. Umezawa, *Chem. Rev.*, 2013, **113**, 3297–3328.
12. H. Zhang, S. Dai, J. Bi and K.-K. Liu, *Interface Focus*, 2011, **1**, 792–803.
13. T. A. Shell and D. S. Lawrence, *Acc. Chem. Res.*, 2015, **48**, 2866–2874.
14. M. C. Koetting, J. T. Peters, S. D. Steichen and N. A. Peppas, *Mater. Sci. Eng., R*, 2015, **93**, 1–49.
15. A. Higuchi, Q.-D. Ling, S. S. Kumar, Y. Chang, A. A. Alarfaj, M. A. Munusamy, K. Murugan, S.-T. Hsu and A. Umezawa, *J. Mater. Chem. B*, 2015, **3**, 8032–8058.
16. Y. S. Lee and T. L. Arinzeh, *Tissue Eng., Part A*, 2012, **18**, 2063–2072.
17. J. G. Hardy, S. A. Geissler, D. Aguilar Jr, M. K. Villancio-Wolter, D. J. Mouser, R. C. Sukhavasi, R. C. Cornelison, L. W. Tien, R. C. Preda, R. S. Hayden, J. K. Chow, L. Nguy, D. L. Kaplan and C. E. Schmidt, *Macromol. Biosci.*, 2015, **15**, 1490–1496.
18. J. Mierczynska, J. Cybulska, B. Solowiej and A. Zdunek, *Carbohydr. Polym.*, 2015, **133**, 547–555.
19. O. Akhavan and E. Ghaderi, *Nanoscale*, 2013, **5**, 10316–10326.
20. C. Ribeiro, V. Sencadas, D. M. Correia and S. Lanceros-Méndez, *Colloids Surf., B*, 2015, **136**, 46–55.
21. B. Shi, H. Zhang, S. Z. Qiao, J. Bi and S. Dai, *Adv. Healthcare Mater.*, 2014, **3**, 1839–1848.

22. Z. Shen, B. Shi, H. Zhang, J. Bi and S. Dai, *Soft Matter*, 2012, **8**, 1385–1394.
23. Z. Shen, A. Mellati, J. Bi, H. Zhang and S. Dai, *RSC Adv.*, 2014, **4**, 29146–29156.
24. D. Y. Kim, D. Y. Kwon, J. S. Kwon, J. H. Kim, B. H. Min and M. S. Kim, *Polym. Rev.*, 2015, **55**, 407–452.
25. Z. Shen, J. Bi, B. Shi, D. Nguyen, C. J. Xian, H. Zhang and S. Dai, *Soft Matter*, 2012, **8**, 7250–7257.
26. A. Mellati, M. Valizadeh Kiamahalleh, S. Dai, J. Bi, B. Jin and H. Zhang, *Mater. Sci. Eng., C*, 2016, **59**, 509–513.
27. S. A. Fisher, R. Y. Tam and M. S. Shoichet, *Tissue Eng., Part A*, 2014, **20**, 895–898.
28. J. Gao, R. Liu, J. Wu, Z. Liu, J. Li, J. Zhou, T. Hao, Y. Wang, Z. Du, C. Duan and C. Wang, *Biomaterials*, 2012, **33**, 3673–3681.
29. X. Li, J. Zhou, Z. Liu, J. Chen, S. Lü, H. Sun, J. Li, Q. Lin, B. Yang, C. Duan, M. Xing and C. Wang, *Biomaterials*, 2014, **35**, 5679–5688.
30. Z. Li, X. Guo, A. F. Palmer, H. Das and J. Guan, *Acta Biomater.*, 2012, **8**, 3586–3595.
31. B. Yeon, M. H. Park, H. J. Moon, S.-J. Kim, Y. W. Cheon and B. Jeong, *Biomacromolecules*, 2013, **14**, 3256–3266.
32. C. Chun, H. J. Lim, K. Y. Hong, K. H. Park and S. C. Song, *Biomaterials*, 2009, **30**, 6295–6308.
33. J. S. Park, D. G. Woo, H. N. Yang, H. J. Lim, K. M. Park, K. Na and K. H. Park, *J. Biomed. Mater. Res., Part A*, 2010, **92**, 988–996.
34. Z. Li, X. Guo and J. Guan, *Biomacromolecules*, 2012, **13**, 1956–1964.
35. S. Dhivya, S. Saravanan, T. P. Sastry and N. Selvamurugan, *J. Nanobiotechnol.*, 2015, **13**, 40.
36. A. Gelmi, J. Zhang, A. Cieslar-Pobuda, M. K. Ljunngren, M. J. Los, M. Rafat and E. W. H. Jager, *Proc. SPIE, Electroactive Polymer Actuators and Devices (EAPAD)*, 2015, **9430**, 94301T.
37. J. Pelto, M. Bjorninen, A. Palli, E. Talvitie, J. Hyttinen, B. Mannerstrom, R. Suuronen Seppanen, M. Kellomaki, S. Miettinen and S. Haimi, *Tissue Eng., Part A*, 2013, **19**, 882–892.
38. N. Tandon, B. Goh, A. Marsano, P.-H. G. Chao, C. Montouri-Sorrentino, J. Gimble and G. Vunjak-Novakovic, *Conf. Proc. IEEE Eng. Med. Biol. Soc.*, 2009, **1**, 6517–6521.
39. S. D. McCullen, J. P. McQuilling, R. M. Grossfeld, J. L. Lubischer, L. I. Clarke and E. G. Loboa, *Tissue Eng., Part C*, 2010, **16**, 1377–1386.
40. G. Thrivikraman, P. S. Lee, R. Hess, V. Haenchen, B. Basu and D. Scharnweber, *ACS Appl. Mater. Interfaces*, 2015, **7**, 23015–23028.
41. F. Pires, Q. Ferreira, C. A. V. Rodrigues, J. Morgado and F. C. Ferreira, *Biochim. Biophys. Acta, Gen. Subj.*, 2015, **1850**, 1158–1168.
42. G. Thrivikraman, G. Madras and B. Basu, *Biomaterials*, 2014, **35**, 6219–6235.
43. E. Stewart, N. R. Kobayashi, M. J. Higgins, A. F. Quigley, S. Jamali, S. E. Moulton, R. M. Kapsa, G. G. Wallace and J. M. Crook, *Tissue Eng., Part C*, 2015, **21**, 385–393.

44. W. W. Hu, Y. T. Hsu, Y. C. Cheng, C. Li, R. C. Ruaan, C. C. Chien, C. A. Chung and C. W. Tsao, *Mater. Sci. Eng., C*, 2014, **37**, 28–36.
45. C. Ribeiro, J. Parssinen, V. Sencadas, V. Correia, S. Miettinen, V. P. Hytonen and S. Lanceros-Mendez, *J. Biomed. Mater. Res., Part A*, 2015, **103**, 2172–2175.
46. T. Kushibiki, Y. Tu, A. O. Abu-Yousif and T. Hasan, *Sci. Rep.*, 2015, **5**, 13114.
47. S. Weis, T. T. Lee, A. del Campo and A. J. Garcia, *Acta Biomater.*, 2013, **9**, 8059–8066.
48. K. Han, W. N. Yin, J. X. Fan, F. Y. Cao and X. Z. Zhang, *ACS Appl. Mater. Interfaces*, 2015, **7**, 23679–23684.
49. K. M. Holmstrom and T. Finkel, *Nat. Rev. Mol. Cell Biol.*, 2014, **15**, 411–421.
50. C. A. DeForest and D. A. Tirrell, *Nat. Mater.*, 2015, **14**, 523–531.
51. T. Bai, A. Sinclair, F. Sun, P. Jain, H.-C. Hung, P. Zhang, J.-R. Ella-Menye, W. Liu and S. Jiang, *Chem. Sci.*, 2016, **7**, 333–338.
52. X. Jia, Y. Chen, C. Shi, Y. Ye, M. Abid, S. Jabbar, P. Wang, X. Zeng and T. Wu, *Food Hydrocolloids*, 2014, **39**, 27–33.
53. S. M. Reddy, G. Shanmugam, N. Duraipandy, M. S. Kiran and A. B. Mandal, *Soft Matter*, 2015, **11**, 8126–8140.
54. Y. S. Pek, A. C. Wan and J. Y. Ying, *Biomaterials*, 2010, **31**, 385–391.
55. R. S. Jacob, D. Ghosh, P. K. Singh, S. K. Basu, N. N. Jha, S. Das, P. K. Sukul, S. Patil, S. Sathaye, A. Kumar, A. Chowdhury, S. Malik, S. Sen and S. K. Maji, *Biomaterials*, 2015, **54**, 97–105.
56. H. Liu, Y. Hu, H. Wang, J. Wang, D. Kong, L. Wang, L. Chen and Z. Yang, *Soft Matter*, 2011, **7**, 5430–5436.
57. R. K. Das, V. Gocheva, R. Hammink, O. F. Zouani and A. E. Rowan, *Nat. Mater.*, 2016, **15**, 318–325.
58. O. Chaudhuri, L. Gu, D. Klumpers, M. Darnell, S. A. Bencherif, J. C. Weaver, N. Huebsch, H.-p. Lee, E. Lippens, G. N. Duda and D. J. Mooney, *Nat. Mater.*, 2016, **15**, 326–334.
59. B. F. Lin, K. A. Megley, N. Viswanathan, D. V. Krogstad, L. B. Drews, M. J. Kade, Y. Qian and M. V. Tirrell, *J. Mater. Chem.*, 2012, **22**, 19447–19454.
60. Z. Dai, Y. Shu, C. Wan and C. Wu, *J. Biomater. Appl.*, 2015, **29**, 1272–1283.
61. S. Hong, K. Yang, B. Kang, C. Lee, I. T. Song, E. Byun, K. I. Park, S.-W. Cho and H. Lee, *Adv. Funct. Mater.*, 2013, **23**, 1856.
62. Q. Gan, J. Zhu, Y. Yuan, H. Liu, J. Qian, Y. Li and C. Liu, *J. Mater. Chem. B*, 2015, **3**, 2056–2066.
63. T. Debnath, S. Ghosh, U. S. Potlapuvu, L. Kona, S. R. Kamaraju, S. Sarkar, S. Gaddam and L. K. Chelluri, *PLoS One*, 2015, **10**, e0120803.
64. J. V. Araujo, N. Davidenko, M. Danner, R. E. Cameron and S. M. Best, *J. Biomed. Mater. Res., Part A*, 2014, **102**, 4415–4426.
65. K. Raghupathi, L. Li, J. Ventura, M. Jennings and S. Thayumanavan, *Polym. Chem.*, 2014, **5**, 1737–1742.
66. B. Shi, H. Zhang, J. Bi and S. Dai, *Colloids Surf., B*, 2014, **119**, 55–65.
67. B. Shi, H. Zhang, S. Dai, X. Du, J. Bi and S. Z. Qiao, *Small*, 2014, **10**, 871–877.
68. P. Menasché, V. Vanneaux, A. Hagege, A. Bel, B. Cholley, I. Cacciapuoti, A. Parouchev, N. Benhamouda, G. Tachdjian, L. Tosca, J. H. Trouvin, J. R.

Fabreguettes, V. Bellamy, R. Guillemain, C. Suberbielle Boissel, E. Tartour, M. Desnos and J. Larghero, *Eur. Heart J.*, 2015, **36**, 2011–2017.
69. P. Menasche, V. Vanneaux, J. R. Fabreguettes, A. Bel, L. Tosca, S. Garcia, V. Bellamy, Y. Farouz, J. Pouly, O. Damour, M. C. Perier, M. Desnos, A. Hagege, O. Agbulut, P. Bruneval, G. Tachdjian, J. H. Trouvin and J. Larghero, *Eur. Heart J.*, 2015, **36**, 743–750.
70. C. Burillon, L. Huot, V. Justin, S. Nataf, F. Chapuis, E. Decullier and O. Damour, *Invest. Ophthalmol. Visual Sci.*, 2012, **53**, 1325–1331.
71. W.-T. Su, W.-L. Chou and C.-M. Chou, *Mater. Sci. Eng. C*, 2015, **52**, 46–53.
72. Z. Li, X. Guo and J. Guan, *Biomacromolecules*, 2012, **13**, 1956–1964.
73. Z. Li, X. Guo, S. Matsushita and J. Guan, *Biomaterials*, 2011, **32**, 3220–3232.
74. H. Tan, C. M. Ramirez, N. Miljkovic, H. Li, J. P. Rubin and K. G. Marra, *Biomaterials*, 2009, **30**, 6844–6853.
75. Y. Rui, L. Xu, R. Chen, T. Zhang, S. Lin, Y. Hou, Y. Liu, F. Meng, Z. Liu, M. Ni, K. Sze Tsang, F. Yang, C. Wang, H. Chang Chan, X. Jiang and G. Li, *Sci. Rep.*, 2015, **5**, 11056.
76. X. Xiao, L. Yu, Z. Dong, R. Mbelek, K. Xu, C. Lei, W. Zhong, F. Lu and M. Xing, *J. Mater. Chem. B*, 2015, **3**, 5635–5644.
77. H. Cui, Y. Liu, Y. Cheng, Z. Zhang, P. Zhang, X. Chen and Y. Wei, *Biomacromolecules*, 2014, **15**, 1115–1123.
78. A. Mellati, S. Dai, J. Bi, B. Jin and H. Zhang, *RSC Adv.*, 2014, **4**, 63951–63961.
79. Z. Huang, B. Yu, Q. Feng, S. Li, Y. Chen and L. Luo, *Carbohydr. Polym.*, 2011, **85**, 261–267.
80. I. Jun, Y. B. Lee, Y. S. Choi, A. J. Engler, H. Park and H. Shin, *Biomaterials*, 2015, **54**, 44–54.
81. J. You, A. Haque, D.-S. Shin, K. J. Son, C. Siltanen and A. Revzin, *Adv. Funct. Mater.*, 2015, **25**, 4650–4656.
82. C. M. Kirschner and K. S. Anseth, *Small*, 2013, **9**, 578–584.

CHAPTER 18

Smart Drug Delivery Systems for Tissue Engineering

MUHANAD ALI[a], FANG YANG[a] AND JOHN JANSEN*[a]

[a]Department of Biomaterials/Dentistry, Radboud University Medical Center, Nijmegen, PO Box 9010, 6500 HB, Nijmegen, The Netherlands
*E-mail: John.Jansen@radboudumc.nl

18.1 Introduction

In tissue engineering (TE), there is a growing demand for target-selective drug delivery systems (DDSs) with high clinical efficacy and long-term therapeutic properties. In conventional drug delivery methods, plasma drug concentration tends to peak rapidly and then declines. Despite some positive pre-clinical results, many of these "first-generation" DDSs display less optimistic results in the clinic due to their inability to control drug release, insufficient access to target tissues and difficulty averting pre-mature degradation.[1] The limitations of "first-generation" DDSs prompted research into smarter forms of DDSs that induce "rate-controlled release" in response to certain physical, chemical or biochemical processes, such as pH gradient or enzymatic activity.[2] Additionally, these systems were also able to induce "feed-back control" by altering the drug release characteristics in response to physiological or pathological conditions.

The concept of smart drug delivery was first introduced in the 1970s when liposomes where designed to induce local release in response to hyperthermia.[3] The last decade has witnessed a great deal of research using

Smart Materials No. 25
Smart Materials for Tissue Engineering: Applications
Edited by Qun Wang

Published by the Royal Society of Chemistry, www.rsc.org

stimuli-responsive nanoparticles (NPs) and macromolecular carriers as efficient drug carriers for improving the efficacy of chemotherapeutics *in vivo*, particularly in cancer therapy.[4] Since then, there has been great progress in thermo-, light-, pH-, magnetic field- and other responsive DDSs. Smart DDSs fall within the area of polymer therapeutics, which is a sub-category of nanomedicine. In 2009, the global market of smart biomaterials was estimated at $47 billion; by 2025, this figure will increase to $113 billion, according to a EU report on nanotechnology.[5]

Smart DDSs are systems that exert a noticeable microscopic shift in their properties in response to small environmental triggers (Figure 18.1).[6,7] They aim to maintain drug levels at a therapeutically desirable range by increasing bioavailability to target sites, while minimizing adverse effects.[3] They mimic the smartness of natural systems in the body by displaying environmentally driven responses. Just as immune cells are programmed to migrate to specific regions in response to specific chemical signals, smart DDSs respond by releasing drugs in response to environmental triggers. They enable targeted delivery using variations that exist between healthy and diseased tissues,

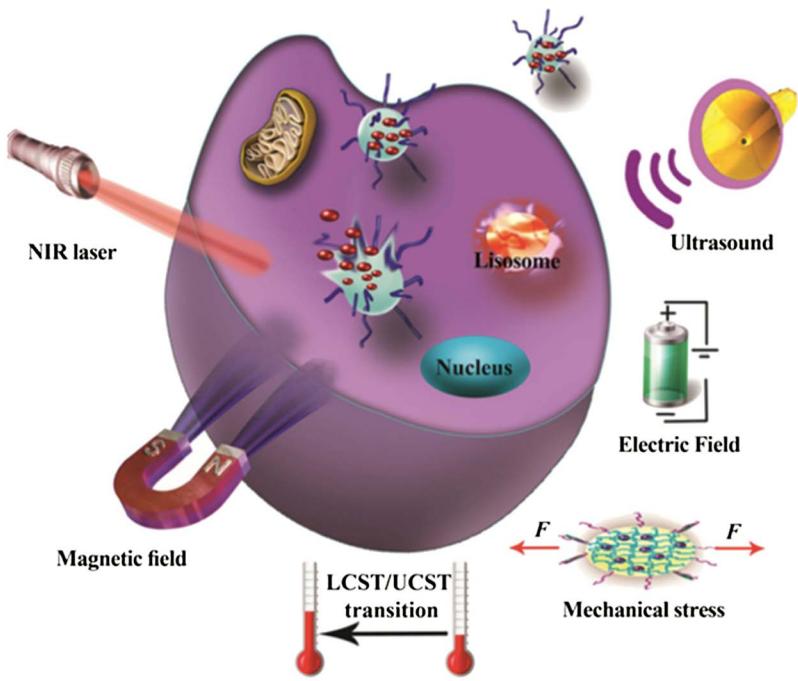

Figure 18.1 Schematic diagram of external stimuli (*e.g.* electric and magnetic field, light and ultrasound) that act as triggers for smart drug delivery systems (DDSs). NIR = near infrared, LCST = low critical solution temperature, UCST = upper critical solution temperature. (Reproduced with permission from Karimi M., *et al.*, 1–3, 2015. Copyright 2015: Morgan & Pool Publishers.)

for example pH and temperature.[8] This offers the possibility of using environmentally responsive DDSs as therapy in response to external (light, magnetism, electric field, *etc.*) or internal (pH, temperature) environmental stimuli.

Stimuli-responsive (or smart) DDSs are mostly made from biocompatible materials, such as peptides, polymers, and lipids, which react in a dynamic manner in response to specific signals in their microenvironment.[9] Stimuli-responsive materials are designed to enhance the localization and efficacy of drugs compared to the free form of drugs. The unique stimuli-responsive physiochemical behaviour exhibited by these materials is exploited in the development of drug carriers (*e.g.* hydrogels, polymersomes, NPs, *etc.*), which respond to variations in physiological and/or pathological conditions.[9] In addition to achieving targeted delivery, they also aim to decrease toxicity, degradation or immunogenicity of active drugs.[10] Often, these materials mimic human molecules with naturally derived stimuli-responsive physiochemical properties (*e.g.* tropoelastin).

This chapter aims to give an overview of stimuli-responsive or "smart" DDSs. A range of smart delivery vehicles will be discussed first to emphasize the diverse drug carriers used in novel DDSs. Subsequently, a review of the diverse self-regulated and externally controlled "smart" DDSs will be provided (in addition to their biomedical applications). Due to the vastness of this subject, only selected examples will be discussed. Examples that are not covered can be easily accessed using a number of available reviews on this field.[11–13]

18.2 Smart Drug Delivery Vehicles

Common problems of conventional drugs relate to poor bioavailability, solubility and dissolution velocity. It is estimated that around 40% of newly developed drugs are poorly soluble. Thus, efforts have focused on developing strategies to improve the solubility of poorly soluble drugs. This led to formulation techniques designed to overcome the solubility and bioavailability problems, such as pro-drug formulations, emulsions, liposomes, micelle systems and soft gelatine capsules. Entrapment techniques are incorporated in the formulation using passive and active strategies. Selecting the best encapsulation design is important in order to obtain the desired release profile (fast or slow release) (Figure 18.2). Finding the right vehicle is vital for ensuring that the medication arrives intact at its destination, just as it is easier to transport a solution in a beaker rather than on a Petri dish.

Nanoparticles (NPs) are taken up by cells more efficiently than larger macromolecules and enable effective transport of drug molecules due to their ability to enter the cytoplasmic space across the cellular membranes.[14] A decrease in size (*e.g.* NPs, dendrimers, *etc.*) below 100 nanometres has shown advantageous properties in novel DDSs used in drug targeting, diagnostics and TE. NPs are divided into two categories: organic and inorganic NPs (Figure 18.2). Organic NPs are further sub-divided into three categories: polymeric matrix NPs, lipidic matrix NPs (*e.g.* nano-emulsions, liposomes and lipid NPs), and drug nanocrystals (NCs).

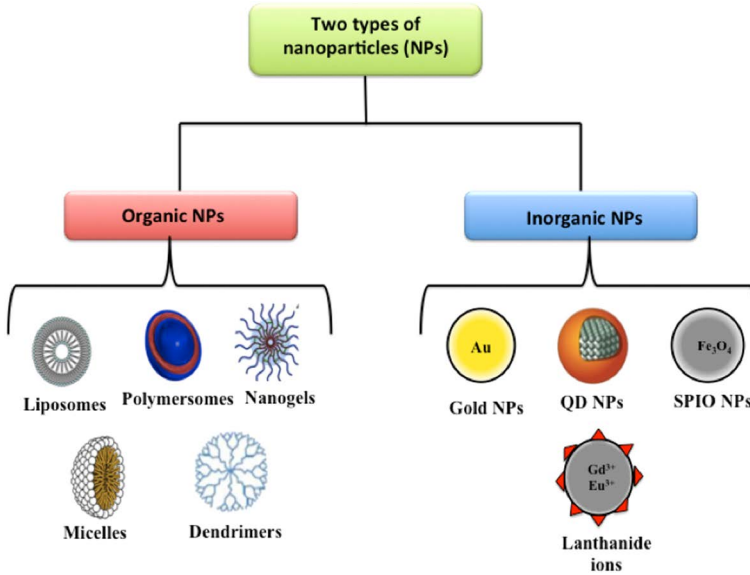

Figure 18.2 Summary of different types of organic and inorganic nanoparticle (NP) materials. There are two basic types of NPs used to synthesize multifunctional NPs: organic (liposomes, polymersomes, nanogels, micelles, dendrimers) and inorganic (gold NPs, quantum dots (QDs) NPs, superparamagnetic iron (SPIO) and lanthanide ions).

Apart from NPs, increasingly, more DDSs are utilising complex polymeric materials, such as hydrogels and scaffolds, which have favourable properties. Hydrogels in particular have been used for many clinical applications due to their cross-linked network that transitions from a collapsed (shrunken) to an expanded (swollen) state. Additionally, surface modifications may be applied to a polymer chain to make it responsive to small changes in environmental parameters. For example, adding pH-sensitive polymers can make the polymer network responsive to pH. Additionally, dual-stimuli responsive hydrogels can respond to two environmental parameters, such as pH and temperature, simultaneously. This reversible behaviour exhibited by hydrogels is attractive for use in DDSs because it can be used to provide a pulsed form of drug delivery.[15]

18.2.1 Polymersomes

Polymersomes are a class of polymeric vesicles that range from 50 nm to 5 μm depending on the preparation process used. They are composed of an aqueous hydrophobic hollow core surrounded by a bilayer membrane composed of a hydrophobic middle part and surrounded by hydrophilic coronas.[16] The function of the hydrophilic bilayer membrane is to protect the core from the external medium. Therapeutic biomolecules can be encapsulated in the

aqueous core of polymersomes prepared with different properties, including stimuli-responsiveness, membrane thickness (3–4 μm) and permeability.[16]

Polymersomes have received substantial attention over the last decades due to their unique properties such as large surface-to-volume ratio, small size and a tuneable surface chemistry. They provide many advantages, including stability of volatile therapeutic agents, cost efficiency and the ease to formulate them into large quantities using many proven methods. Improved bioavailability, increased half-life for clearance and target specificity are some of the key advantages of using polymersomes. These advantages lead to higher intracellular uptake and sustained release of drug payload.[17] This may result in a reduction in the quantity of drug needed to induce a therapeutic effect and enables the delivery of potentially toxic therapeutic drugs safely to target regions. Polymersomes also provide protection to non-targeted regions of the body from exposure and severe side effects.[18] The coating provides a protective barrier to active therapeutic agents, which prevents rapid diffusion and/or erosion, which increase drug circulation time. Polymersomes are becoming increasingly prevalent as drug delivery carriers for a wide range of applications because they are particularly good at passing organ barriers, such as the blood–brain barrier (BBB), and cell membranes.[19]

Polymersomes are functionalised into smart drug delivery vehicles *via* passive and active targeting strategies. Passive targeting relies on the enhanced permeation and retention (EPR) effect to selectively accumulate in targeted tissues—a pathophysiologic characteristic of tumour blood vessels.[20] Alternatively, active targeting strategies increase the binding affinity to target tissues using targeting moieties such as antibodies, peptides and other small molecules. Active biomolecules are easily loaded into the polymersome system due to the versatility of their structure *e.g.* large surface area and multiple sub-compartments. Polymersomes are a unique platform that can form multimodal targeted delivery systems leading to effective treatment and fewer side effects.[21]

18.2.2 Liposomes

Liposomes are vesicular microstructures composed of an aqueous core and surrounded by a hydrophobic phospholipid bilayer. They are synthesised by extrusion of phospholipids through filters of specific sizes, which typically range from 15–200 nm. Liposomes are characterised based on size, surface charge, and number of bilayers present. Liposomes are generally regarded as safe, which minimizes the potential for severe side effects. Liposomes can function as drug delivery vehicles because they are able to encapsulate both hydrophilic and hydrophobic drugs in the core without any chemical modifications.[19] To promote the release of their contents, liposomes fuse with other bilayers after systemic administration. Additionally, functionalities are inserted into liposomes *via* surface modifications to enhance drug potency, stability and to enable preferential delivery *in vivo.* Therefore, they are a suitable platform for delivery of biotech drugs, such as insulin, antibacterial, antivirals and plasmid DNA.

In the 1960s, scientists started experimenting with the use of liposomes as possible drug or protein carriers for treatment of disease.[22] Since then, there have been great advances in the field due to increasing knowledge and funding. The US FDA has approved several liposome-based therapeutic products for clinical and preclinical development.[23] However, many of these "first generation" nanomedicines were not designed with selectivity towards biological targets. The liposomal formulation of Doxil®, for example, is a first generation nanomedicine approved by the FDA in 1995, which significantly improved circulating half-life and maximized drug accumulation in tumour tissue.[23] However, it failed to provide controlled release, stability, and localisation in metastatic breast cancer, ovarian cancer and multiple myeloma.[23] Since then, an increasing number of liposomal formulations of active biomolecules have been in the process of clinical development, *e.g.* liposomes which incorporate surface modifications, including cisplatin, cytarabine and daunorubicin.[23]

Issues regarding non-targeted delivery are solved by means of utilising smart delivery liposomes that selectively target tumour cells. Increasing the liposome circulation time is vital for application in targeted liposomal drug delivery. The intermolecular forces dictate the type of interaction between the liposome and proteins. Thus, the incorporation of molecules that achieve target specificity in addition to circulation longevity should improve drug efficacy. Conjugating surface modification using targeting peptides (*e.g.* polyethylene glycol (PEG)) into the liposome design (*i.e.* PEGylation) increases the circulation lifetime.[24] PEG prevents rapid clearance by forming a steric and hydrated barrier that shields defective regions in the lipid bilayer and inhibits protein adosprtion.[25] It has been attempted to improve the pharmacokinetics and delivery of cargo across the BBB by first coating liposomes with PEG to ensure prolonged circulation time in the plasma, then functionalizing the liposomes with ligands that target specific cell types in the brain. Results showed a four-fold increase in the efficacy of targeted liposomes compared to non-targeted liposomes.[26]

18.2.3 Hydrogels

Hydrogels are three-dimensional polymeric networks with the capacity to transition from a solution to a viscous gel (sol–gel) when exposed to external stimuli. Hydrogels are composed by simple reactions combining monomers together into a polymer chain. Hydrogels swell by water occupying free space between macromolecules and collapse, due to breakdown of polymeric networks, in response to an external stimulus. Hydrogels exhibit the unique ability to swell and retain a large portion of water within their structure but they do not become dissolved in the same medium. Hydrophilic functional groups attached to the polymeric backbone give hydrogels the ability to absorb water, while cross-links between their network chains give them resistance to dissolution. Volume phase transition results from changes in the polymer's physical properties, such as size, shape, hydrophobicity and degradation rate, which depend on the nature of the intermolecular forces.[27]

Hydrogels are used for a range of biomedical applications due to their flexibility and similarity to natural tissues because of their large water content.

Increasingly, synthetic hydrogels are replacing natural hydrogels due to improved shelf life and their modification opportunities. Moreover, functional groups are easier to implement in synthetic polymers due to their well-defined structure, which can be modified and functionalised to obtain a desired degradability. It is also a relatively simple procedure to synthesize them using "classical" chemical reactions such as polymerization and cross-linking techniques. This tailored approach to polymer design is an advantage because properties such as biodegradation, mechanical strength and biological response to stimuli can be fine-tuned in the robust polymer framework.[28]

Hydrogels can be functionalised by cross-linking stimuli-responsive polymers to equip hydrogels with multifunctional capabilities, such as biological response to stimuli. This allows for a range of possibilities. For example, temperature-sensitive hydrogels are currently being exploited for multiple purposes, which involves administering therapeutic agents to local targets. Tailoring the gel's properties by altering the cross-linking density of the polymer chains or changing molecular weight may optimize the rate of drug release and allow for an effective form of drug delivery.[29,30]

18.2.4 Dendrimers

Dendrimers have emerged as an attractive drug delivery vehicle due to their ability to control their molecular structure and incorporate surface functionalization. Surface functionalization enables conjugation of drug targeting moieties, which enhances their versatility. They are distinguished from other vehicles by the presence of multiple functional groups at the periphery and internal cavities. Dendrimers are composed from monomers using either step-growth or convergent polymerization. They are typically composed of one or more of the following polymers: poly(L-glutamic acid) (PG), polyethyleneimine (PEI), poly(ethylene glycol) (PEG), or chitin. Drug molecules are incorporated into dendrimers using encapsulation or complexion techniques. Dendrimers have been used as drug or gene delivery vehicles, for example, as carriers of antibiotics and anticancer drugs.[31] They have a strong potential for use as drug carrier systems because they have a well-defined structure, which can be easily fine-tuned by manipulating the dendritic architecture. Due to the small size of dendrimers (~10 nm), it is reasonably easy for them to cross cell membranes and avoid premature clearance from the body. Thus, they have the potential to exert a clinical effect and target specific tissues in the body.

18.2.5 Other Delivery Vehicles

Silicon-, carbon- and metal-based vehicles have received a lot of attention in the last few years for use in drug delivery systems. This is mainly because their size and architecture can be accurately controlled. Moreover, they allow

for surface modification such as platinum coating. Their hollow nature and small size can range from tens to hundreds of nanometers, which further adds to their usability as drug delivery vehicles. These unique vehicles have been used as drug- and DNA-based carriers for drug delivery applications because their hollow nanoshells are able to incorporate drug molecules. Metal-based vehicles are usually composed of one of the following metals: gold, silver, platinum or palladium metals. They are incorporated (linked or imbedded) within polymeric drug carriers (*e.g.* hydrogels) to induce thermal release when excited by light or a magnetic field.

18.3 Self-Regulated Smart Drug Delivery Systems and Their Applications

Smart drug delivery systems (DDSs) are categorised into either open or closed-loop systems.[12] Open-loop systems are externally regulated by electrical, ultrasonic, thermal or magnetic stimuli. Closed-loop systems are self-regulated and use rate-controlled mechanisms, such as pH-sensitive polymers or pH-dependent drug solubility. Self-regulated systems are controlled by internal signals (*e.g.* glucose blood levels, pH and temperature), which regulate the release rate in response to feedback control.

18.3.1 pH-Responsive

There are remarkable variations in pH in the human body (blood pH 7.35–7.45; stomach pH 1.0–3.0; duodenum pH 4.8–8.2; colon pH 7.0–7.5; endosomal pH 5.0–6.0; lyosomal pH 4.5–5.0; extratumoral pH 6.5–7.2).[8] This variation in body pH is exploited for controlled drug delivery by using pH-responsive DDSs. pH-Responsive polymers are polyelectrolytes, meaning they either accept or release protons in response to environmental pH, depending on the pedant acidic or basic groups present.

pH-Responsive polymers are polyelectrolytes that contain a large number of ionisable groups in their chemical structure, as side groups or end groups. They typically consist of cationic and/or anionic functional polymers, such as poly(*N*,*N*′-diethyl-aminoethyl methacrylate) (PDEAEM) and poly(acrylic acid) (PAA), respectively, which possess phase transition behaviour in response to external environmental pH conditions.[8] Phase transition behaviour can be explained as a charge along the polymer backbone, which undergoes electrostatic repulsion exerted by adjacent ionised groups, leading to an increase in hydrodynamic volume in the polymer.[15] pH-Responsive systems are modulated by choosing the most suitable polyacids or polybases to match the desired pH range.

Polymers such as PAA (*e.g.* Carbopol®), polyacrylamide (PAAm) and poly(methacrylic acid) (PMAA) are known as polyacids (or polyanions) because they contain a large number of ionisable acid groups such as carboxylic and sulfonic acids in their molecular structure. At low pH values,

carboxylic groups accept protons and at high pH values, they release them. When exposed to high pH values, a PAA-based hydrogel swells due to electrostatic repulsions created from the negatively charged groups (Figure 18.3(A) and (B)).

pH-Sensitive polymers with alkaline functional groups are referred to as polybases (or polycations) because they contain amino groups in their

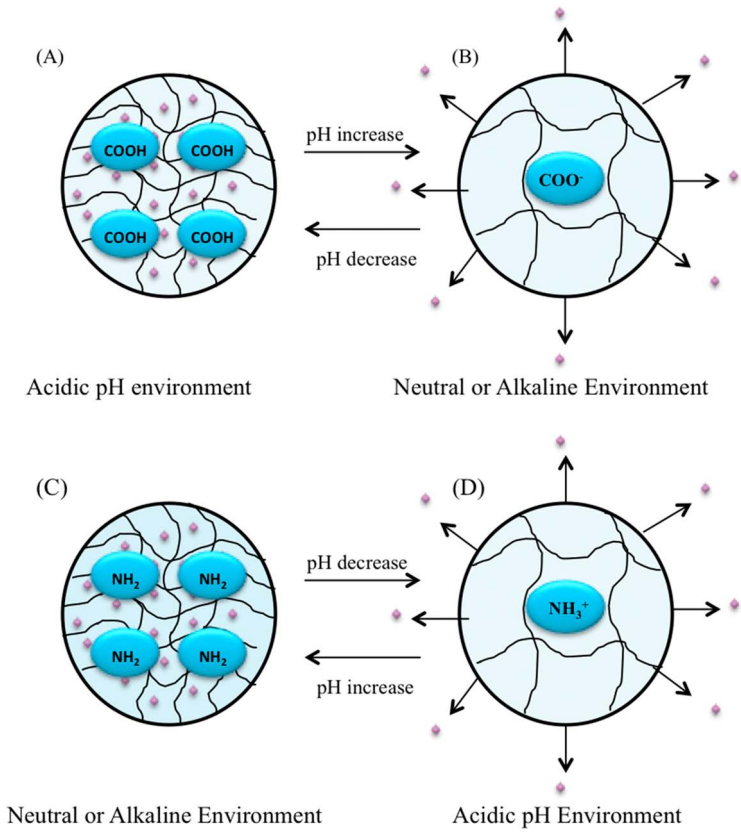

Figure 18.3 (A) Schematic diagram of a specific drug carried by an anionic polymer *e.g.* poly(acrylic acid) (AA). At low pH values, the pendent carboxylic acid groups are not ionised and the polymer retains the drug in its interior. (B) However, at high pH values, the carboxylic acid groups become ionised and the groups undergo electrostatic repulsions and enable drug release. (C) Schematic representation of a cationic polymer *e.g.* poly(vinyl amine) (NH_2) with a specific drug. The amino groups remain un-ionised at high pH and retain their drug molecule in their interior. (D) At an acidic pH environment, however, the amino groups become protonated, which results in swelling of the polymeric net due to electrostatic repulsion between the positive groups. (Reproduced with permission from 'Stimuli-sensitive particles for drug delivery' from *Biologically-Responsive Hybrid Biomaterials*, Grainger S. J. and El-Sayed M. E. H., 171–190, 2012. Copyright 2012: World Scientfic.)

structure, such as poly(*N*,*N*-dimethylaminoethylmethacrylate) (PDMAEMA) and poly(2-diethylaminoethylmethacrylate) (PDEAEMA). In alkaline (or basic) pH environments, polybases become deprotonated, while at acidic pH values they become positively ionized (or protonated) by gaining protons from their acidic environment. At acidic pH values, polybases will undergo phase transition by swelling due to the electrostatic repulsions created between the positively charged groups by protonation of the amino groups.[32] This will usually result in a shift in balance between hydrophilicity and hydrophobicity of the matrix surface of the polymer resulting from the decrease in pH value (Figure 18.3(C) and (D)).[33]

When pH-responsive polymer chains are cross-linked into hydrogels, micelles, or hollow NPs, they can be used for drug and gene delivery. For example, pH-sensitive vehicles have been used to trigger release of encapsulated materials from the inner hollow compartment.[15] The unique feature of pH-responsive materials to undergo phase transition in response to pH makes them an attractive vehicle for drug delivery. This shift in solubility is exploited in the delivery of therapeutic agents locally to regions where pH values are abnormal, for example the tumour microenvironment, where values can drop as low as pH 6.5. Moreover, the nature of pH-responsive polymers can be manipulated by the addition of alkaline or acidic functional groups, depending on the region that is being targeted.

pH-Sensitive polymers have potential for application in cancer immunotherapy. One promising application for pH-responsive polymers is to function as carriers of DNA molecules because it is difficult to transfect "naked" DNA into cells. There is a considerable potential for using nucleic acid molecules as therapy against cancer, inflammation and neurodegenerative disease. The success of these molecules depends on their ability to reach intracellular cell compartments. However, nucleic acids are usually degraded by nuclease enzymes after systemic administration. Thus, the body eliminates them before cells take them up. Additionally, DNA molecules are too electronegative and large to incorporate successfully inside cells. In such cases, pH-responsive polymers can function as an effective strategy for incorporation of DNA into cells.

pH-Responsive nanocarriers (~200 nm) are used as gene carriers due to favourable bio-related functions. For example, pH-responsive liposomes are able to condense membrane impermeable substances (*e.g.* proteins, DNA, RNA) into spherical-shaped polymers and transfer them across cellular membranes to enhance protein and DNA intracellular transfection.[34,35] This is due to their ability to retain drug and DNA molecules at physiologic pH yet they are capable of inducing release of their contents into the cytosol as they undergo destabilization and merging with endosomes under mildly acidic microenvironments. It is due to the fusogenic property of these pH-sensitive liposomes that they have access into the cytosol *via* membrane-destabilising mechanisms that originate from the liposomal lipid's intrinsic character.[13] Upon internalisation, the cationic pH-responsive polymers will undergo a phase transition in response to low intracellular pH values by altering their hydrophobicity. This leads to disruption of the endosome membrane,

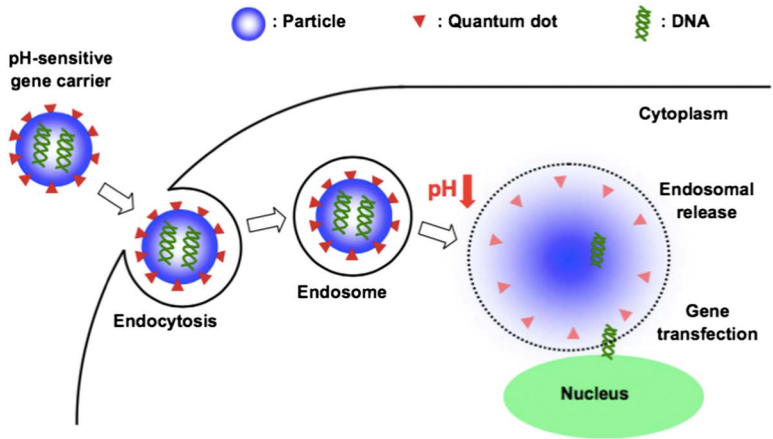

Figure 18.4 Schematic diagram of gene delivery through pH-responsive gene carrier. pH-Responsive NPs (*e.g.* DMAEMA/HEMA) release DNA upon experiencing the low pH value of the endosome. (Reproduced with permission from You J.-O., *et al.*, *J. Biol. Eng.*, **4**, 15, 2010. Copyright 2010: Biomed Central.)

resulting in the delivery of the encapsulated content into the nucleus (Figure 18.4). This mechanism of intracellular delivery is regarded as highly important and the use of pH-sensitive liposomes has been exploited to improve the delivery of biomolecules (DNA, proteins) to intracellular targets. pH-Responsive polymers can be used to give liposomes added functionality *via* surface modifications. This gives the added benefit of producing stable yet highly membrane-permeable liposomes with strong membrane fusion properties efficient for cytoplasmic delivery.

18.3.2 Temperature-Responsive

Thermosensitive polymers are soluble in aqueous solutions at low temperatures and undergo phase separation in response to higher temperatures (Figure 18.5). The temperature at which the thermoresponsive polymer will enter phase separation is called the lower critical temperature (LCT) or lower critical solution temperature (LCST). At lower temperatures, the polymer dissolves in water due to favourable hydrogen bonding between water molecules and the polymer chains (*i.e.* hydration). However, at higher temperatures the polymer chains will undergo phase separation because the supermolecular interaction strength decreases and water molecules will start to diffuse back into the aqueous solution, leaving behind partially dehydrated polymer chains.[36] This phenomenon is completely reversible because the polymer chains can once again become miscible in aqueous solution by reversing the temperature. The upper critical temperature (UCT) is the temperature at which thermoresponsive polymers reverse their configuration.

Thermoresponsive polymers are currently being exploited to improve the physicochemical stability of therapeutic agents by controlling the rate of drug

release and maintaining the biological activity of drugs. A common practice in using thermoresponsive polymers is to alter the LCT to body temperature by chemical modifications of the polymer structure. Increasing the polymer molecular weight will usually decrease the LCT due to enhanced polymer–polymer interactions.[37] Moreover, introducing hydrophilic (co)monomers to the polymer chain or hydrophilic end-groups will increase the LCT. Attempts have been made to reduce the initial burst drug release of thermosensitive polymer gels by optimising the chain length ratio between hydrophobic and hydrophilic segments, which has shown significant improvements in the release profile.[8] Moreover, incorporating poly(ethylene glycol) (PEG) into a polymeric chain has shown significant improvements in the initial burst and displayed sustained release for over one month.[8]

There is a wide variety of thermoresponsive polymers available that have been covered extensively in a number of reviews.[8,38,39] The most widely investigated thermoresponsive polymer is poly(*N*-isopropylacrylamide) (PNIPAM) (Figure 18.6(A)) owing to its LCT of 32 °C, robust phase behaviour

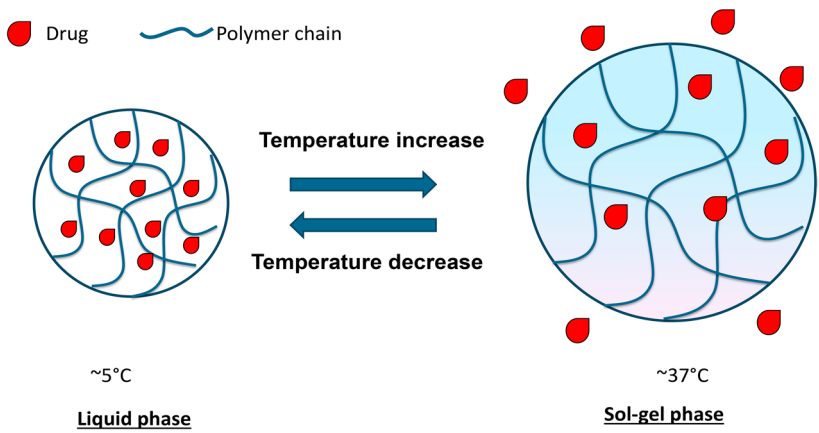

Figure 18.5 Schematic representation of collapsed and swollen states of polymeric chains of thermoresponsive hydrogels in response to external temperature.

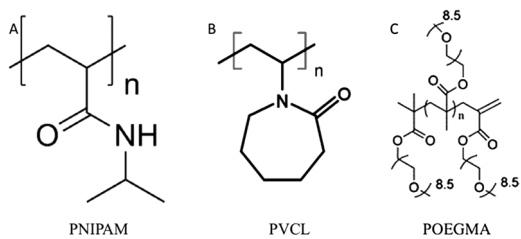

Figure 18.6 Chemical structures of thermoresponsive polymers (A) poly(*N*-isopropylacrylamide) (PNIPAM), (B) poly(*N*-vinyl caprolactam) (PVCL) and (C) poly(oligo ethylene glycol)methacrylate (POEGMA).

and biocompatibility, which make this polymer an ideal candidate for biomedical applications. Since the discovery of PNIPAM, a new thermosensitive polymer was described with a similar LCT (31 °C) and biocompatibility roughly similar to PNIPAM, called poly(*N*-vinyl caprolactam) (PVCL) (Figure 18.6(B)). Despite the relative similarity of PNIPAM and PVCL, PNIPAM remains the gold standard of thermoresponsive polymers possible due to its wide availability.

PNIPAM and PVCL present opportunities as drug carriers for *in situ* drug delivery and other biomedical applications. Interestingly, functional endgroups or conjugation with biological species can be inserted into the polymer chain to enable preferential binding to biological targets. However, their use remains limited due their very high glass transition temperature (T_g = ~140–150 °C). T_g is the temperature at which polymer transition from a hard glassy-like material to a soft gel-like rubbery material occurs.[37] Below the T_g, PNIPAM and PVCL become very hard and brittle, like glass—a process known as hysteresis. Poly(oligoethylene glycol) methacrylate (POEGMA) (Figure 18.6(C)) is an alternative polymer with thermoresponsive behavior similar to PNIPAM. POEGMA is composed of a poly(meth)acrylate backbone with oligoethylene glycol side chains which can be modified by varying the number of ethylene glycol repeats and side-chain functionality.[37,40] More importantly, POEGMA does not have a high T_g like PNIPAM and does not show hysteresis in response to repeated exposure to high- and low-temperature cycles.[36]

18.3.3 Glucose-Responsive

Diabetes is a major health problem and it is estimated that it will affect 4.4% of the world's population by the year 2030, equal to 366 million sufferers world-wide.[41] In 2012, 1.5 million deaths were caused by diabetes, according to the World Health Organization (WHO).[42] Diabetic patients are normally given frequent intravascular injections of insulin, which leads to low patient compliance. Thus, there is an urgent need to resolve this inconvenience for patients suffering from diabetes and to develop alternative effective forms of insulin administration.

Glucose-responsive insulin delivery systems are a relatively new concept that has garnered considerable attention recently. They can be divided into three main categories: glucose oxidase, lectin, and phenylboronic acid (PBA)-modified systems.[43] The aim is to mimic insulin secretion in the same controlled manner as natural endogenous insulin secretion by responding to external stimuli. In addition to controlled insulin delivery, glucose-responsive systems are used in diagnostics to monitor glucose concentrations.[6]

Glucose-oxidase-based glucose systems consist of the glucose oxidase conjugated to the side chains of a pH-responsive polymer backbone. Glucose oxidase catalyses the oxidation of glucose in the blood to gluconic acid and hydrogen peroxide (H_2O_2). The continuous conversion of glucose to gluconic acid leads to a decrease in the pH of the solution, eventually triggering swelling or deswelling of the pH-responsive groups, depending on the type of group used (alkaline or acid). As a result, the polymer will release

encapsulated insulin molecules from the polymer network in response to the by-products from the enzymatic oxidation of glucose.[6] Polycationic polymers, such as PAA, are incorporated into insulin delivery polymers because PAA carboxylate moieties become protonated by the acidic environment as a result of glucose oxidation, which finally facilitates insulin release.[44] Unfortunately, this system has several disadvantages when applied to clinical practice, such as low stability and high toxicity. Other forms of glucose-systems utilise the unique carbohydrate/glucose affinitive properties of lectins. Concanavalin (Con A), for example, is a lectin with four different binding sites with a strong affinity for glucose, which has been complexed with a saccharide-modified polymer chain.[42] Insulin will become released when free glucose molecules become attached to Con A, leading to displacement of the complex and eventually the release of insulin within the surrounding tissue.

Phenylboronic acid (PBA) plays a central role in glucose-responsive systems because they become converted to hydrophilic moieties in response to elevated glucose levels.[42] Additionally, PBA-based systems are less toxic compared to glucose-oxidase- and lecti- based glucose-responsive systems. Insulin carriers, such as nanogels, are functionalized with PBA and used to encapsulate and release insulin at therapeutic doses *in vitro* (Figure 18.7). Upon increasing glucose concentrations, boron atoms bind to the hydroxyl groups of glucose molecules forming a glucose–PBA complex. It induces a conformational change resulting in swelling and subsequent release of insulin due to negative ionisation of PBA.[38]

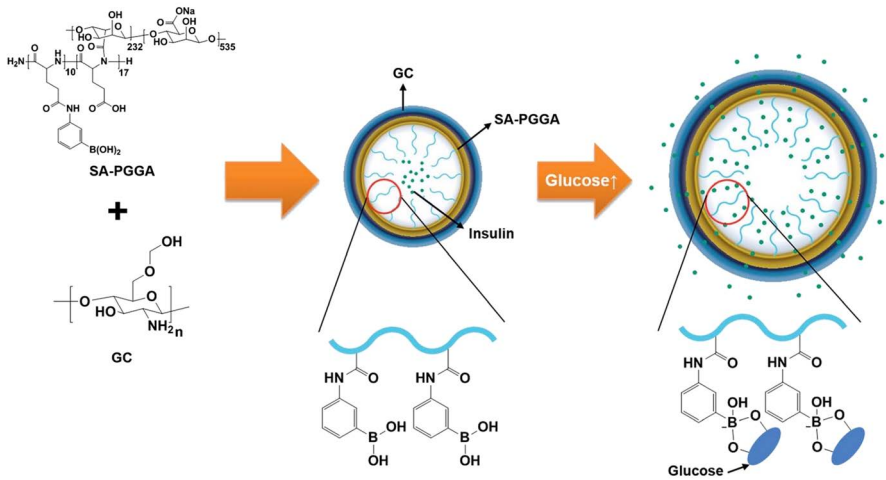

Figure 18.7 Self-regulated glucose delivery systems composed of a phenylboronic acid (PBA)-based nanogel. Glucose molecules bind to boron atoms and induce negative ionization of PBA leading to swelling and release of insulin. (Reproduced from ref. 42 with permission from The Royal Society of Chemistry.)

Nanogels are exploited in self-regulating glucose-responsive systems because they exhibit excellent biocompatibility and glucose-responsive features. For example, poly(L-glutmate-*co*-*N*-3-L-glutamylphenylboronic acid) (PGGA) graft polymer double-layered nanogel was used to release insulin controllably *in vitro*.[42] Incorporating nanogels into glucose-responsive systems is beneficial because they provide a unique network structure as carriers of insulin molecules. The cross-linking density of glucose-responsive nanogels usually decreases as the concentration of glucose increases, which facilitates the release of insulin molecules from the eroded gel.[6] The unique ability of nanogels to bounce back into their original structure after glucose molecules are absorbed away from the blood by insulin makes them an ideal delivery vehicle for targeted insulin delivery.

PBA-modified glucose-responsive nanogels can incorporate NPs for added therapeutic benefit. A recent study showed sustained release of insulin encapsulated in poly(lactic-*co*-glycolic acid) PLGA NPs from pluronic® (F-127) nanogels over a few days in a rat following subcutaneous injection.[45] Additionally, silver (Ag)-NP-based nanogels can function as biological probes for monitoring blood glucose levels by capping them with phenylboronic acid (PBA) derivatives to bind preferentially to glucose (Figure 18.8).[43] Results from the study showed that the incorporation of silver NPs provided stronger fluorescence signals due to higher excitation coefficients, which displayed significant improvement in the fluorescence intensity.[46]

18.3.4 Multiple-Responsive Drug Delivery Systems

DDSs can respond to multiple stimuli, simultaneously. In addition, they may combine delivery of a drug with other functionalities such as real-time imaging. Diseased tissues are known for having different environmental

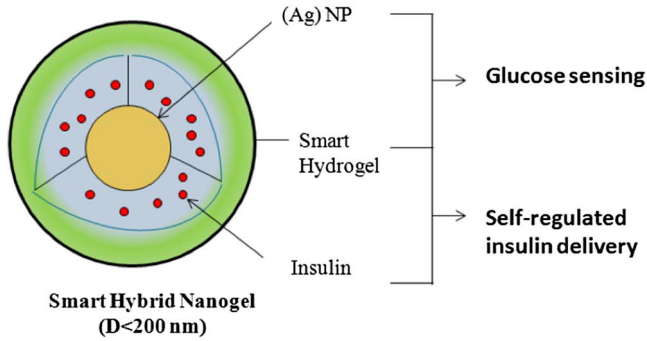

Figure 18.8 Glucose-responsive insulin delivery system composed of silver (Ag) NPs coated with glucose-responsive boronate derivative poly(4-vinylphenylboronic acid-*co*-2-dimethylamino)ethylacrylate, [p(VPBA-DMAEA)], nanogel network chains. Upon exposure to glucose (~30 mM), the gel shell will adapt to the surroundings by releasing preloaded insulin (D = diameter). (Reproduced from ref. 64 with permission from The Royal Society of Chemistry.)

conditions, including temperature and pH. For this reason, polymeric macromolecules have been developed to respond to these two stimuli simultaneously by combining PNIPAM temperature-responsive polymers with pH-responsive polymers, like acrylic acid (AA) and its alkyl ester, methacrylic acid (MAA).[36] Moreover, adjusting the molar ratio of PNIPAM to MAA can significantly increase the permeability of the pH/temperature-responsive NPs.[47]

18.4 Externally Regulated Smart Drug Delivery Systems and Their Applications

Externally regulated smart drug systems release drug molecules in response to external stimuli. In this section, light, electric-field, and magnetic-field-responsive DDSs will be reviewed. External environmental triggers are used to localise drug carriers in the region being exposed to the stimulus. Above a certain threshold, environmental triggers permit stimuli-responsive vehicles to undergo abrupt changes in their microstructure, such as protonation, swelling or degradation.[6,39,48] Subsequently, the smart material returns to its initial state after the triggering factor is removed.[49]

18.4.1 Magnetic-Field-Responsive

Magnetic NPs (MNPs) have been traditionally used for their intrinsic magnetic properties to enable local delivery of imaging agents *e.g.* contrast agents for magnetic resonance imaging (MRI).[50] MNPs provide favourable properties which can be used to tailor drug release characteristics and improve treatment efficacy. Additionally, immunogenicity and side effects can be minimised. More importantly, imaging agents and drugs have been combined to enable *in vivo* drug delivery and diagnostic imaging by real-time treatment tracking.[51] Some examples of MNPs include metallic, bimetallic and superparamagnetic iron oxide NPs (SPIONs).

The blood–brain barrier (BBB) protects the brain from potentially harmful foreign substances and prevents therapeutic agents greater than 400 Da from entering into the brain parenchyma. Rather than significantly decreasing the molecular weight of therapeutic agents, the use of low-energy focused ultrasound (FUS) was found to disrupt the BBB locally by increasing its permeability, which allowed the passage of large therapeutic agents into the brain.[52] Results from this experiment led to the development of magnetic-field sensitive DDSs, which rely on FUS providing a window of opportunity to achieve local delivery of chemotherapeutic agents in the brain. MNPs can then be used as drug carriers to enhance the deposition of therapeutic agents at target sites where a combination of magnetic targeting (MT) and FUS is used to enhance deposition of MNPs at the target site. Essentially, FUS provides the window of opportunity to deliver therapeutic MNPs passively *via* the EPR effect in solid tumours, whilst magnetic forces actively increase the local deposition of MNPs of target tissues (Figure 18.9).

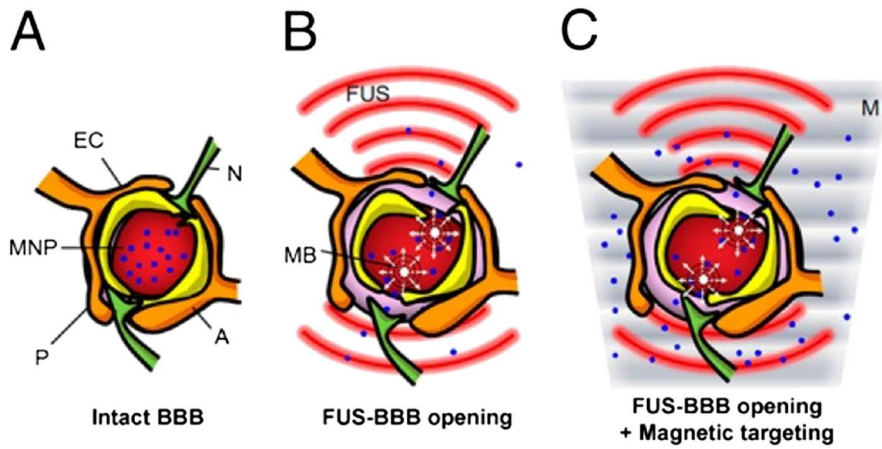

Figure 18.9 A cross-section of a central nervous system (CNS) capillary with intact BBB. (A) An intact CNS capillary block delivery of therapeutic agent into the brain parenchyma. (B) Presence of focused (low-energy) ultrasound (FUS) increases the permeability of the BBB, which enhances deposition at the target site. (C) The combination of magnetic targeting (MT) and FUS actively targets magnetic NPs to the brain. (A, astrocytes; EC, endothelial cell; N, neuron; P, pericyte). (Reproduced with permission from H. L. Liu., *et al.*, *Proc. Natl. Acad. Sci.*, **107**, 15 205–15 210, 2010. Copyright 2010: PNAS.)

One application of using magnetic-field-sensitive DDSs is for delivery of therapeutic biomolecules into brain tumours. For instance, gemcitabine is a widely used drug to target solid tumours in a variety of tissues. However, it has several drawbacks, including short biological half-life and tumour resistance. In an attempt to improve its anticancer activity, squalenoyl gemcitabine, a pro-drug of gemcitabine was coated to the shell of MNPs composed of magnetite nuclei, which were designed to induce drug release *in vivo* to solid tumour tissue in response to an externally applied magnetic field. Optical microscopic images obtained showed alignment of MNPs in response to the magnetic field.[53] Moreover, they resisted rapid deamination and overcame drug resistance *in vitro*. They also presented superior anticancer activity compared to the free-form of gemcitabine, *e.g.* in the treatment of leukaemia, which resulted in several long-term survivors.[54] Other similar studies dealing with the application of the FUS/MT treatment showed enhanced local deposition of doxorubicin-MNPs in breast carcinomas.[55]

18.4.2 Light-Responsive

Exposure to light induces phase transition in light-sensitive polymers. Light-sensitive polymers, like many other smart polymers in this section, have several advantages for incorporation in novel DDSs including water solubility, biocompatibility and biodegradability. They have the capacity to

trigger and control drug release in response to external irradiation from a light source. They are classified as either visible-light-sensitive or UV-sensitive, depending on the wavelength of the light source that triggers the phase transition. However, visible light sources are preferred because they are readily available, safe and easy to use.

The polymer structure of UV-sensitive hydrogels consists of a "leuco" derivative molecule (Figure 18.10), such as bis(4-dimethylamino)phenylmethyl leucocyanide. In response to UV irradiation, the leuco derivative molecule becomes ionised, which produces triphenylmethyl cations by dissociating into ion pairs. This leads to swelling of the hydrogel, because the increase in osmotic pressure within the gel results in the formation of isocyanide ions. Once the light source is removed, the hydrogel polymer returns to its original collapsed form.[56] The temperature increase is proportional to the light intensity registered by the chromophores.

Visible light hydrogels (*e.g.* poly(*N*-isopropylacrylamide)) contain light-sensitive chromophores, such as trisodium salt or copper chlorophyllin, designed to absorb light within the wavelength of 488 nm. This light then dissipates locally as heat by radiationless transitions.[56] The temperature-sensitive polymers, as incorporated into the polymer structure, respond to the increase in heat by altering its swelling behaviour.

Light-sensitive polymers are particularly attractive for biomedical application because the intensity and wavelength of the light source can be easily manipulated. Light-sensitive micelles and vesicles induce site-specific release of encapsulated agents *in vivo* using an external stimulus in the drug delivery field. Upon light exposure, the micelles and vesicles will release their contents to diseased tissues, such as tumours, using selective irradiation of the target site.[57] Site-specific delivery of drugs can improve the therapeutic index and enable a greater dose of drug release at the target site, which reduces systemic exposure and debilitates side effects associated with non-targeted delivery.

Light-responsive catanionic vesicles have also been used as carriers to improve non-viral gene delivery, where light illumination is used to induce vesicle formation and disruption.[58] Ruptured vesicles trigger the release of the DNA molecules into the external environmental milieu. Catanionic light-responsive surfactants are used to trigger vesicle disruption and spontaneous

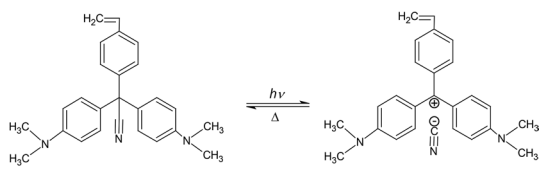

Figure 18.10 Structure of leuco-derivative molecule, bis(4-dimethylamino)-phenylmethyl-leucocyanide. Reprinted from *Advanced Drug Delivery Reviews*, **53**(3), Qiu Y. and Park K., Environment-sensitive hydrogels for drug delivery, 321–339, Copyright (2001) with permission from Elsevier.

reformation because they allow a combination of electrostatic attractions between the surfactant head groups and hydrophobic interactions between the surfactant tails (Figure 18.11).[57] The light-sensitive liposomes remain relatively stable in "*trans*" conformation with little release taking place. However, upon UV light exposure (350 nm), isomerisation from the "*trans*" to the "*cis*" conformation takes place and results in release of DNA molecules.[57] The photo-isomerisation process is reversible as exposure to 436 nm visible light (or thermal relaxation) leads to reassembly from "*cis*" to "*trans*". Thus, upon UV illumination, the vesicles will rupture (*cis* form) and release DNA, which leads to higher DNA transfection efficiencies.[58]

18.4.3 Electric-Field-Responsive

Electroactive polymers (EAPs) are divided into two categories based on the activation mechanism: electronic EAPs, which are driven by the electric field forces, and ionic EAPs, which are driven by the movement of ions.[59] The physical structure of electronic EAPs undergoes physical changes in response to an externally applied electric field. Chitosan, alginate and hyaluronic acid are naturally occurring polymers commonly employed in EAPs. Some major synthetic electro-sensitive polymers have also been used, including allyl amine, vinyl alcohol and methacrylic acid. Natural and synthetic polymers have also been combined simultaneously to construct novel electro-sensitive DDSs. EAPs are mostly polyelectrolytes that undergo anisotropic deformation in

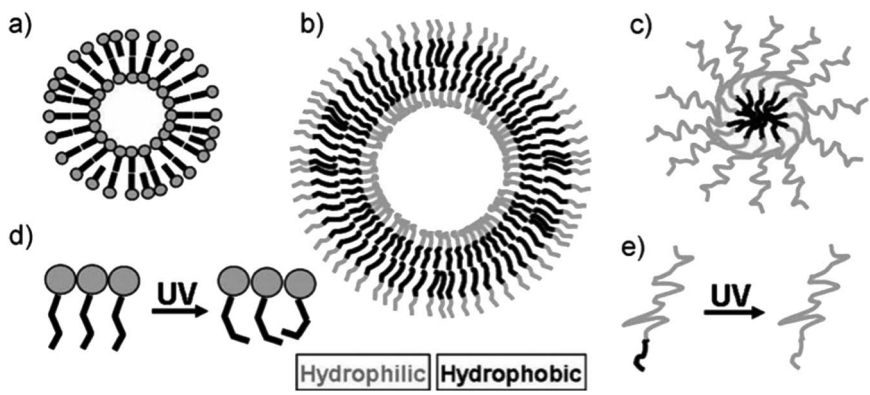

Figure 18.11 Schematic diagram depicting the self-assembly of macromolecular structures. (a) Self-assembly of lipid molecules into vesicle structures composed of a hydrophobic head and hydrophilic tail. (b) Larger vesicles composed of diblock copolymers of hydrophilic and hydrophobic blocks. (c) Light-responsive vesicles. (d) Isomerisation of azo-containing lipids with UV-light. (e) UV-light-induced changes to the hydrophilic/hydrophobic balance of macromolecules leading to micelle breakdown. Black = hydrophobic, grey = hydrophilic. (Reproduced with permission from Katz J.S. and Burdick J.A., *Macromol. Biosci.*, **10**, 339–348, 2010. Copyright 2010: John Wiley and Sons.)

response to stress caused by an electric field leading to swelling or de-swelling, depending on the direction in which the charged ions move—towards either the cathode or anode.[6]

EAPs offer advantageous properties for applications in biotechnology and smart drug delivery, similar to the other stimuli-responsive materials described previously. By inducing drug release in response to an external stimulus, EAPs can provide treatment of chronic conditions requiring medication on a daily basis. For example, conducting polymeric materials and implantable electronic devices have been used previously to facilitate drug release in response to external electrical stimuli in the delivery of neurotransmitters (such as γ-aminobutyric acid (GABA), glutamate, aspartate). A variety of nervous system disorders and neuropsychiatric disorders can be treated by modulating neurotransmitters (*e.g.* anxiety and depression).

EAPs are widely used in smart DDSs and in other TE applications, for example, in sensory applications such as hepatic sensing, blood pressure and pulse monitoring or even chemical sensing.[59–61] Conducting polymeric materials and electronic delivery devices have been used to trigger release of molecules using electric stimuli. This is due to the electro-kinetic phenomenon, which provides several favorable properties, such as high mechanical stability, flexibility and customizable capabilities.

A group from Kyoto University in Japan developed an organic electronic device composed of electronically insulating yet ionically conducting biocompatible conducting polymers.[62] These devices were found to be capable of mimicking nerve synapses by precisely delivery neurotransmitters *in vivo* and *in vitro*. When a voltage is applied, it leads to the establishment of an electrochemical circuit, which leads to modulation of mammalian sensory functions by precisely delivering neurotransmitters using an organic electric device. This form of smart drug delivery has several advantages including regulation of cell signalling, on–off functionality and it is minimally disruptive. Overall, it offers a good prospect for the treatment of central nervous system disorders because it is able to deliver pulsed, rather than a continuous, delivery of neurotransmitters. Continuous delivery is problematic to the CNS because it desensitises the receptors leading to down-regulation or malfunctioning signalling pathways.[62]

The disadvantage of using electronic delivery devices is that they require implantation, which can be invasive. However, polymerization techniques for drug encapsulation provide an alternative delivery vehicle to produce a stimuli-triggered localised release of cargos in response to a small external electric field. Conducting polypyrrole nanoparticles are used as drug reservoirs using polymerization techniques to encapsulate drug compounds designed for electric-field-triggered release. Smart DDSs often incorporate a combination of other stimuli-responsive materials. For example, conducting nanoparticles are suspended in temperature-responsive hydrogels to develop a hybrid delivery system able to induce local release of drugs *in vivo*. This mixture composed of conducting nanoparticles and thermosensitive hydrogels can then be applied locally to induce electric-field-triggered release of drug compounds

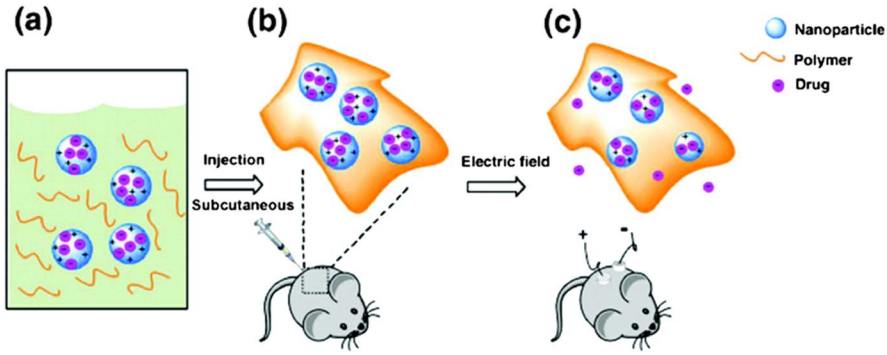

Figure 18.12 Application of an electric-field-sensitive system for the delivery of drugs. (a) Polymer solution containing nanoparticles is (b) subcutaneously applied into a mouse, which is followed by (c) application of an electric current (DC) to facilitate release of encapsulated nanoparticles into the surrounding tissue. (Reproduced with permission from Ge J., *et al.*, *ACS Nano*, **6**, 227–233, 2012. Copyright (2012) American Chemical Society.)

(Figure 18.12). Conducting materials, such as poly(3,4-ethylenedioxythiophene) (PED-OT)-coated poly(L-lactide) (PLLA) or PLGA nanofibers have incorporated drugs to controlled release of dexamethasone (Dex), a corticosteroid.[63]

18.5 Conclusion and Future Perspective

Smart environmentally-sensitive polymers will play a crucial role as advanced delivery vehicles for the future treatment of a wide range of diseases. Over the last decade, there has been tremendous interest in using targeted drug delivery systems as carriers for tissue- and cell-specific drug delivery. This has coincided with the development of sophisticated carriers that can trigger release of their contents in a controlled fashion. The next generation of stimuli-sensitive carriers will become more advanced by continuing to exploit the physiological differences that exist between a diseased (cancer, inflammation) and non-diseased (pH variations in the GI tract) human body state. This will be achieved by combining polymeric structures with natural biological motifs to enable them to reach their target tissue.

Despite the great potential of stimuli-sensitive polymers, many have unfortunately failed to make it to clinical trials. This is because there are issues regarding the cytotoxicity of peptides, proteins or nucleic acid molecules associated with the delivery of bimolecular drugs. Slow responding polymers are another reason why polymers have not made it past pre-clinical drug development, where faster-acting polymer systems are desired. Biodegradability is another disadvantage because many molecules used in smart DDSs, such as acrylic acid or acrylamide polymers, are, unfortunately, not hydrolytically degradable and in most cases are associated with neurotoxicity, which limit their usability as targeted polymeric drug systems.

Another issue with high molecular weight smart polymers is that despite their effective targeting properties, they cannot be eliminated by the body leading to their accumulation, deeming them non-biodegradable. This is one major reason why many smart polymers have not been tested in clinical trials. Despite the successful targeting strategies employed by stimuli-responsive polymers, they are unable to completely remove cancerous cells due to rapid metastasis of these cells, which makes them very difficult to kill. It also presents a huge barrier to the clinical use of smart polymers.

The molecular microstructure of the smart polymers needs to have an appropriate balance of hydrophobicity and hydrophilicity for the phase transition to take place.[49] Stimuli-responsive polymers are becoming increasingly attractive for biotechnology and nanomedicine because they provide versatility and add functionalities, which allow them to interact more locally and effectively without compromising healthy tissues around the body. The versatility of smart polymers makes their use widespread for many applications, from active targeting drug delivery systems to smart diagnostic agents, which is an equally important field. Smart DDSs will continue to exploit stimuli-responsive polymers that incorporate delivery vehicles to achieve a desired therapeutic effect.

References

1. C. Alvarez-Lorenzo and A. Concheiro, *Chem. Commun.*, 2014, **50**, 7743–7765.
2. Y. Chien and S. Lin, *Clin. Pharmacokinet.*, 2002, **41**, 1267–1299.
3. M. B. Yatvin, J. N. Weinstein, W. H. Dennis and R. Blumenthal, *Science*, 1978, **202**, 1290–1293.
4. T. A. Elbayoumi and V. P. Torchilin, *Mol. Pharm.*, 2009, **6**, 246–254.
5. B. M. Holzapfel, J. C. Reichert, J. T. Schantz, U. Gbureck, L. Rackwitz, U. Noth, F. Jakob, M. Rudert, J. Groll and D. W. Hutmacher, *Adv. Drug Delivery Rev.*, 2013, **65**, 581–603.
6. H. Priya James, R. John, A. Alex and K. R. Anoop, *Acta Pharm. Sin. B*, 2014, **4**, 120–127.
7. T. Lammers, *Int. J. Pharm.*, 2013, **454**, 527–529.
8. K. Huh, H. Kang, Y. Lee and Y. Bae, *Macromol. Res.*, 2012, **20**, 224–233.
9. S. Mura, J. Nicolas and P. Couvreur, *Nat. Mater.*, 2013, **12**, 991–1003.
10. D. Schmaljohann, *Adv. Drug Delivery Rev.*, 2006, **58**, 1655–1670.
11. H.-K. A. Tsai, E. A. Moschou, S. Daunert, M. Madou and L. Kulinsky, *Adv. Mater.*, 2009, **21**, 656–660.
12. J. Kost and R. Langer, *Adv. Drug Delivery Rev.*, 2012, **64**, 327–341.
13. B. Priya, P. Viness, E. C. Yahya and C. d. T. Lisa, *Biomed. Mater.*, 2009, **4**, 022001.
14. M. I. Yatoo, A. Saxena, M. H. Malik, M. K. Sharma and U. Dimri, *J. Anim. Sci. Adv.*, 2014, **4**, 705–709.
15. C. E. M. R. Aguilar, A. Gallardo, B. Vazquez and J. S. Roman, in *Topics in Tissue Engineering*, ed. N. Ashammakhi, R. L. Reis and E. Chiellini, 2007, vol. 3, Chapter 3, pp. 1–27, (http://www.oulu.fi/spareparts/ebook_topics_in_t_e_vol3/abstracts/aguilar_01.pdf).

16. J. S. Lee and J. Feijen, *J. Controlled Release*, 2012, **161**, 473–483.
17. X. Xu, W. Ho, X. Zhang, N. Bertrand and O. Farokhzad, *Trends Mol. Med.*, 2015, **21**, 223–232.
18. S. R. Mudshinge, A. B. Deore, S. Patil and C. M. Bhalgat, *Saudi Pharm. J.*, 2011, **19**, 129–141.
19. F. Lai, A. M. Fadda and C. Sinico, *Expert Opin. Drug Delivery.*, 2013, **10**, 1003–1022.
20. M. K. Yu, J. Park and S. Jon, *Theranostics*, 2012, **2**, 3–44.
21. H. De Oliveira, J. Thevenot and S. Lecommandoux, *Wiley Interdiscip. Rev.: Nanomed. Nanobiotechnol.*, 2012, **4**, 525–546.
22. G. Bozzuto and A. Molinari, *Int. J. Nanomed.*, 2015, **10**, 975–999.
23. V. Sanna, N. Pala and M. Sechi, *Int. J. Nanomed.*, 2014, **9**, 467–483.
24. W. Alshaer, H. Hillaireau, J. Vergnaud, S. Ismail and E. Fattal, *Bioconjugate Chem.*, 2015, **26**, 1307–1313.
25. B. J. Lestini, S. M. Sagnella, Z. Xu, M. S. Shive, N. J. Richter, J. Jayaseharan, A. J. Case, K. Kottke-Marchant, J. M. Anderson and R. E. Marchant, *J. Controlled Release*, 2002, **78**, 235–247.
26. J. Rip, L. Chen, R. Hartman, A. van den Heuvel, A. Reijerkerk, J. van Kregten, B. van der Boom, C. Appeldoorn, M. de Boer, D. Maussang, E. C. M. de Lange and P. J. Gaillard, *J. Drug Targeting*, 2014, **22**, 460–467.
27. F. Ilmain, T. Tanaka and E. Kokufuta, *Nature*, 1991, **349**, 400–401.
28. E. M. Ahmed, *J. Adv. Res.*, 2015, **6**, 105–121.
29. K. E. Uhrich, S. M. Cannizzaro and R. S. Langer, *Chem. Rev.*, 1999, **11**, 3181–3198.
30. M. Hamidi, A. Azadi and P. Rafiei, *Adv. Drug Delivery Rev.*, 2008, **60**, 1638–1649.
31. P. Kesharwani, K. Jain and N. K. Jain, *Prog. Polym. Sci.*, 2014, **39**, 268–307.
32. E. S. Gil and S. M. Hudson, *Prog. Polym. Sci.*, 2004, **29**, 1173–1222.
33. P. Bawa, V. Pillay, Y. E. Choonara and L. C. du Toit, *Biomed. Mater.*, 2009, **4**, 022001.
34. B. Jeong and A. Gutowska, *Trends Biotechnol.*, 2002, **20**, 305–311.
35. E. Yuba, Y. Kono, A. Harada, S. Yokoyama, M. Arai, K. Kubo and K. Kono, *Biomaterials*, 2013, **34**, 5711–5721.
36. J.-O. You, D. Almeda, G. J. C. Ye and D. T. Auguste, *J. Biol. Eng.*, 2010, **4**, 15.
37. M. A. Ward and T. K. Georgiou, *Polymers*, 2011, **3**, 1215–1242.
38. A. Gandhi, A. Paul, S. O. Sen and K. K. Sen, *Asian J. Pharm. Sci.*, 2015, **10**, 99–107.
39. D. Schmaljohann, *Adv. Drug Delivery Rev.*, 2006, **58**, 1655–1670.
40. S. Han, M. Hagiwara and T. Ishizone, *Macromolecules*, 2003, **36**, 8312–8319.
41. C. D. Mathers and D. Loncar, *PloS Med.*, 2006, **3**, e442.
42. D. Lee, K. Choe, Y. Jeong, J. Yoo, S. M. Lee, J.-H. Park, P. Kim and Y.-C. Kim, *RSC Adv.*, 2015, **5**, 14482–14491.
43. W. Wu, N. Mitra, E. C. Y. Yan and S. Zhou, *ACS Nano*, 2010, **4**, 4831–4839.
44. L. R. Fogueri and S. Singh, *Recent Pat. Drug Delivery Formulation*, 2009, **3**, 40–48.

45. J. M. Barichello, M. Morishita, K. Takayama and T. Nagai, *Int. J. Pharm.*, 1999, **184**, 189–198.
46. K. Aslan, J. Zhang, J. Lakowicz and C. Geddes, *J. Fluoresc.*, 2004, **14**, 391–400.
47. K. Zhang and X. Y. Wu, *Biomaterials*, 2004, **25**, 5281–5291.
48. B. Jeong and A. Gutowska, *Trends Biotechnol.*, 2002, **20**, 305–311.
49. I. Y. Galaev and B. Mattiasson, *Trends Biotechnol.*, 1999, **17**, 335–340.
50. O. Veiseh, J. W. Gunn and M. Zhang, *Adv. Drug Delivery Rev.*, 2010, **62**, 284–304.
51. O. Veiseh, J. W. Gunn and M. Zhang, *Adv. Drug Delivery Rev.*, 2010, **62**, 284–304.
52. K. Hynynen, N. McDannold, N. Vykhodtseva, S. Raymond, R. Weissleder, F. A. Jolesz and N. Sheikov, *J. Neurosurg.*, 2006, **105**, 445–454.
53. J. L. Arias, L. H. Reddy and P. Couvreur, *Langmuir*, 2008, **24**, 7512–7519.
54. L. H. Reddy, C. Dubernet, S. L. Mouelhi, P. E. Marque, D. Desmaele and P. Couvreur, *J. Controlled Release*, 2007, **124**, 20–27.
55. H. L. Liu, M. Y. Hua, H. W. Yang, C. Y. Huang, P. C. Chu, J. S. Wu, I. C. Tseng, J. J. Wang, T. C. Yen, P. Y. Chen and K. C. Wei, *Proc. Natl. Acad. Sci. U. S. A.*, 2010, **107**, 15205–15210.
56. Y. Qiu and K. Park, *Adv. Drug Delivery Rev.*, 2001, **53**, 321–339.
57. J. S. Katz and J. A. Burdick, *Macromol. Biosci.*, 2010, **10**, 339–348.
58. Y. C. Liu, A. L. Le Ny, J. Schmidt, Y. Talmon, B. F. Chmelka and C. T. Lee Jr, *Langmuir*, 2009, **25**, 5713–5724.
59. T. Wang, M. Farajollahi, Y. S. Choi, I. T. Lin, J. E. Marshall, N. M. Thompson, S. Kar-Narayan, J. D. W. Madden and S. K. Smoukov, *Interface Focus*, 2016, **6**, 1–19.
60. E. Biddiss and T. Chau, *J. Biomed. Eng.*, 2006, **28**, 568–578.
61. A. Keshavarzi, M. Shahinpoor, K. J. Kim and J. W. Lantz, *Smart Mater. Struct.*, 1999, **3669**, 369–376.
62. D. T. Simon, S. Kurup, K. C. Larsson, R. Hori, K. Tybrandt, M. Goiny, E. W. Jager, M. Berggren, B. Canlon and A. Richter-Dahlfors, *Nat. Mater.*, 2009, **8**, 742–746.
63. J. Ge, E. Neofytou, T. J. Cahill, R. E. Beygui and R. N. Zare, *ACS Nano*, 2012, **6**, 227–233.
64. G. Pasparakis and M. Vamvakaki, *Polym. Chem.*, 2011, **2**, 1234–1248.

CHAPTER 19

Smart Materials for Central Nervous System Cell Delivery and Tissue Engineering

TIMOTHY M. O'SHEA[a], ALEXANDER L. WOLLENBERG[b], ALEXANDER M. BERNSTEIN[a], DARREN B. SARTE[b], TIMOTHY J. DEMING[b] AND MICHAEL V. SOFRONIEW*[a]

[a]Department of Neurobiology, David Geffen School of Medicine, University of California, Los Angeles, California 90095-1763, USA; [b]Departments of Bioengineering, Chemistry and Biochemistry, University of California Los Angeles, Los Angeles, California 90095-1600, USA
*E-mail: sofroniew@mednet.ucla.edu

19.1 Introduction

Severe sudden focal CNS damage that occurs following stroke, traumatic spinal cord injury (SCI) or brain injury (TBI) in humans causes irreversible destruction of neural circuitry, often resulting in permanent dysfunction or paralysis. In these conditions, large lesions of non-neural repair tissue persist that contain diverse cellular and extracellular elements such as fluid-filled cysts, abundant inflammatory cells and a surrounding border of astrocyte scar.[1–4] The large areas of persistent non-neural tissue are key impediments to endogenous axonal regrowth across CNS lesions. Bridging neuronal connections to re-establish functionally meaningful neural activity across such large and complex lesions is a major goal of, and a major challenge for,

Smart Materials No. 25
Smart Materials for Tissue Engineering: Applications
Edited by Qun Wang

Published by the Royal Society of Chemistry, www.rsc.org

therapeutic approaches to focal CNS injury. By contrast, chronic neurodegenerative CNS diseases such as glaucoma, retinopathies, Parkinson's, multiple sclerosis and amyotrophic lateral sclerosis (ALS) display pathophysiology characterized by the progressive loss of functionally distinct neuronal cell populations in anatomically defined sites within the CNS.[5–7] For such diseases, therapeutic options that recapitulate the vital cellular functions of lost cells remain largely elusive.

CNS tissue engineering, involving the transplantation of neural cells or neural-cell-derived tissue aided by supporting biomaterial matrices and/or bioactive morphogens, represents a potential therapeutic approach for re-establishing neuronal circuitry and/or function, either by providing trophic support and substrates for growth of host axons, and/or by providing a source of new neurons that may restore lost functionality.[8,9] Despite the promise of cell therapies for a variety of CNS diseases, this treatment paradigm faces considerable unresolved challenges including: (i) widespread death of grafted cells upon transplantation; (ii) uncontrolled migration and cell fate decision making in the surviving cell population; (iii) localized and extended tumor and ectopic colony formation; (iv) inadequate cellular integration with apposed endogenous tissue, and (v) immune rejection of the graft.[9–14] Unsatisfactory control over one or many of these properties has impaired the extent of functional benefits provided by grafted cells. Realizing the potential of cell transplantation in CNS disease is likely to benefit from innovative biomaterial engineering strategies that: (1) enhance the survival of cells injected into sub-acute or chronic tissue lesions; (2) control/guide progenitor differentiation and cell functionality *in vivo*; and (3) optimize interactions between host and grafted cells. In this review we focus on how biomaterials are being used to address CNS cell transplantation challenges and discuss how emerging innovation in the biomaterials field can be applied to develop "smarter" materials for this application.

19.2 A Brief History of CNS Cell Transplantation

The concept of transplanting viable CNS cells or tissue as a means of treating CNS injury or disease has its origins in the late 19th century when the first known report of a cortical tissue transplant in dogs and cats was published.[15] (For an excellent early historical overview of CNS transplantation the reader is directed to Dunnett *et al.*, 2009.[16]) Although there was a smattering of individual reports throughout the subsequent decades that built on this early work, the widespread study of cell transplantation in the CNS did not gain significant traction or systematic investigation until the 1970s. In this decade a number of pioneering studies set the scene for the modern day field of CNS cell transplantation. Such studies included: (1) Olson's work on grafting catecholamine expressing cells from the adrenal medullar into the eye demonstrating survival and partial reinnervation of functioning cells;[17] (2) the first transplantation of developing CNS tissue into another developing brain by Das and Altman;[18] (3) the first use of "dispersed cell culture in the brain"

by Bjorklund and colleagues who transplanted embryonic-brainstem-derived neural cells that expressed several catecholamines such as dopamine and observed partial reinnervation of the denervated hippocampus;[19] and (4) the first reports of partial functional restoration of a chronic CNS disease state using dopamine-expressing neurons implanted adjacent to a damaged caudate nucleus.[20] The concept of cell graft "bridging" across traumatic CNS lesions emerged shortly thereafter when Aguayo and others extended the work of Cajal and Tello from the early 1900s[21,22] by using peripheral nerve grafts to explore: (i) the reconnection of the completely transected mid-thoracic spinal cord,[23,24] (ii) extraspinal linkage of the medulla oblongata and the upper thoracic spinal cord with a peripheral graft to bypass a spinal cord lesion,[25] and (iii) the re-establishment of functional synapse connectivity between the retina and brain so as to restore light responses.[26] These studies introduced the idea of using a growth supporting environment containing exogenous cellular and extracellular constituents to encourage regrowth of damaged neural fibers. However, unsatisfactory integration of peripheral nerve grafts limited outcomes in these studies and as a result, immature CNS tissue grafts were subsequently explored. In addition to providing bridging support for host axon regrowth, these CNS fetal tissue grafts demonstrated the potential to be a source of new viable CNS neurons to replace those lost by injury and recapitulate local neuronal circuitry as well as deliver specific local trophic support.[27–30] The cell transplantation field has subsequently focused on transplanting more purified populations of neural cells in order to augment specific effects that were seen within these pioneering grafted tissue studies.[31]

19.3 Objectives and Challenges for Modern CNS Cell Transplantation

There are many diverse cell candidates that have been investigated to date as possible treatments for a multitude of CNS disease and injury states. Cell candidates that have been explored across a number of independent studies in the CNS include: olfactory ensheathing glial cells,[32] Schwann cells,[33] bone marrow stromal cells,[34–36] human umbilical cord blood (HUCB) stem cells[37] and a variety of neural stem progenitor cells[38,39] (NSPCs) derived from primary, embryonic or genetically induced sources. NSPCs are currently regarded as preferred candidates for cell grafting because their fate is sufficiently restricted that tumor formation is improbable, but they still possess the adequate immaturity to survive injection into CNS lesions. Furthermore, NSPCs, unlike the other cell types explored, have the capacity to recapitulate neural tissue as well as support host cell survival and axon growth through production of contact-mediated and diffusible bioactive cues. A number of different neural progenitor cell candidates have been applied to CNS lesions including embryonic stem (ES)-cell-derived progenitors,[40,41] fetal and adult neural stem cells[9,42,43] and induced pluripotent stem (iPS) cells.[44]

Various transplanted progenitors show a capacity to differentiate into glial or neuronal phenotypes. Some grafted cells favorably impact on host neuronal survival, axon regeneration, re-myelination and lesion re-vascularization, which in several cases has been correlated with some behaviorally observable motor and sensory recovery.

A number of different strategies for CNS cell transplantation have been employed to date with the approach largely depending on the specific CNS disease or injury type under investigation (Figure 19.1). For chronic neurodegenerative diseases, NSPCs have been used to derive specific neuronal subtypes that demonstrate cellular functions that can be used to replace the equivalent host cells that have been lost or damaged due to the disease pathology. For example, ES-derived NSPCs with midbrain characteristics were differentiated into dopamine expressing neurons, which have demonstrated a capacity to promote functional recovery in a Parkinson's disease model.[45,46] Similarly, in a model of retinal degeneration, transplantation

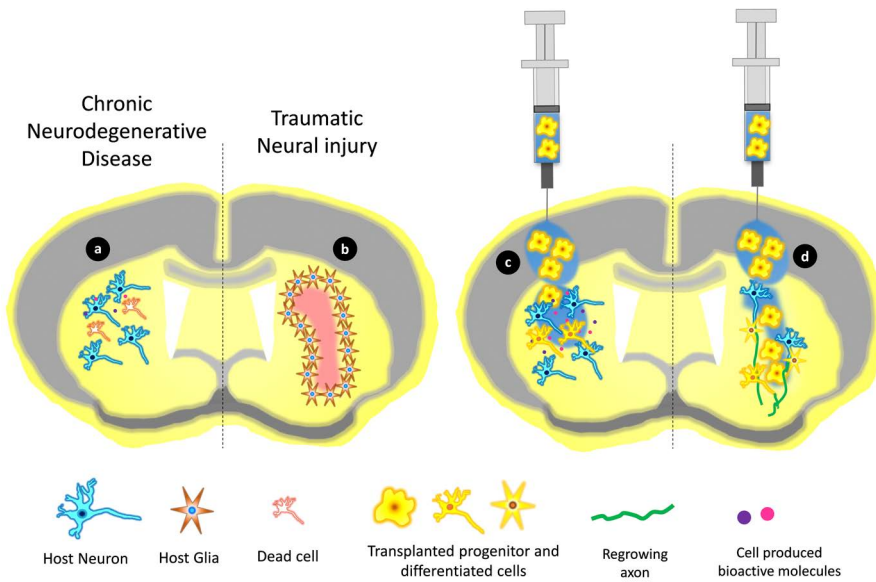

Figure 19.1 There are at least two categories of CNS injury/disease that may be amenable to CNS cell transplantation therapies: (a) chronic neurodegenerative diseases, which are characterized by the progressive loss of functional neural cell populations, and (b) focal traumatic injuries, which result in large lesions of non-neural repair tissue and a surrounding border of astrocyte scar. The two main strategies for CNS cell transplantation are to: (c) provide a cell source to replace the equivalent host cells that have been lost or damaged in chronic neurodegenerative diseases, and (d) provide a cell source that offers trophic support and substrates for growth of host axons as well as a population of new neurons that may restore lost functionality following traumatic injury.

of post-mitotic rod photoreceptor precursors integrated well into the host and improved visual function.[47] While results using the cell replacement approach have been promising to date, it is important to note that success with such strategies has been mostly limited to cases where sufficiently restricted progenitors that are destined for the desired cell fates are used for transplantation. By contrast, the more immature and multipotent NSPCs often fail to satisfactorily differentiate into the desired cell candidates when transplanted into the host disease site. The ability to generate and preserve the viability of sufficient numbers of these more restricted progenitors represents a considerable manufacturing challenge. Smart biomaterials may assist in overcoming these challenges by allowing for directed differentiation of the more immature NSPCs into the specific cell type *in vivo*.

An alternative strategy for cell transplantation, apart from direct cell replacement, is to use grafted cells to induce or impart some effect on the host either by: (i) acting as local reservoirs for the production and delivery of bioactive molecules, (ii) supporting cell growth through cell–cell contacts or (iii) by acting as major players in newly formed relay circuits that may re-establish viable neural connections. Early studies, as described above, demonstrate the capacity for cell grafts of various types to be used to deliver dopamine and neurotrophic support. This concept was subsequently expanded upon by employing genetically modified cells to overproduce and deliver neurotrophic factors at local sites of injury or disease in order to: (i) provide neuroprotection from stressors, (ii) to keep host neurons from degenerating,[48] or (iii) to attract regrowing axons.[49–52] The concept of being able to direct the transplanted cell secretome either through genetic manipulations or through specific physiochemical biomaterial properties is a concept that is starting to gain traction within the CNS cell transplantation field.[53,54] Finally, endogenous propriospinal neurons can form new relay connections that mediate hindlimb locomotor recovery in the absence of long descending supraspinal connections.[55,56] Recently, it has been shown that fetal-spinal-cord-derived NSPC can give rise to neurons when grafted into SCI lesions,[9,57] raising the possibility that if their differentiation and integration can be regulated, NSPC-derived neurons may be able to form functional relay circuits.

Despite extensive investigations of many different cell types and strategies for CNS cell transplantation, there remain several unresolved challenges that continue to limit efficacy and represent barriers for potential clinical translation (Figure 19.2). The first main challenge involves keeping the cell grafts viable both during injection procedures (as a result of shear stresses imparted on the cells during injection through narrow diameter needles and glass pipettes) as well as upon exposure to the harsh CNS injury/disease environment (Figure 19.2(a) and (b)). It has been shown that injured CNS tissue significantly decreases transplanted cell survival[58,59] and as few as 10–15% of transplanted cells remain viable after a few days post injection into the CNS.[13] Given that CNS lesions represent inhospitable environments with poor tissue integrity, a second challenge affecting CNS cell transplantation

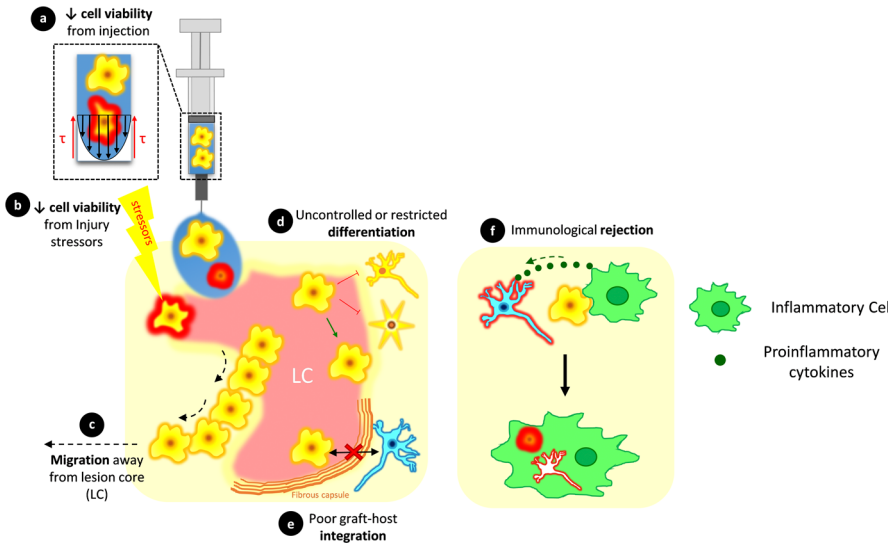

Figure 19.2 There are several unresolved challenges impacting CNS cell transplantation outcomes. These challenges include: (a), (b) widespread transplant cell death due to injection shear stresses and injury environment stressors; (c) migration of transplanted cells away from the inhospitable lesion core (LC); (d) inadequate control over the differentiation of transplanted progenitor cells; (e) unsatisfactory integration of grafted cells with host tissue due to inflammation and/or fibrosis that is induced upon cell transplantation; and (f) immunological rejection of cell transplants, which can lead to the death of the graft and neighboring host cells by elements of the innate immune system.

is the uncontrolled migration of transplanted cells away from inhospitable damaged CNS[10,59] (Figure 19.2(c)). Associated with this is the formation of ectopic colonies elsewhere in the CNS as a result of uncontrolled migration along open tissue planes such as within the central canal in the spinal cord, along the ventricles within the brain, or through the periependymal and periventricular tissue niches that provide hospitable environments for adult neural progenitor cells throughout life. Developing strategies that ensure cells stay localized to the lesion transplant site is imperative for CNS cell transplantation success. As mentioned above, controlling the differentiation *in vivo* of NSPCs represents another currently unaddressed challenge (Figure 19.2(d)). More mature/restricted neurons and glia do not survive transplantation, yet neural progenitors with greater viability after implantation can turn into a variety of cell types without appropriate direction and can pose a tumorigenic risk if too immature.[60–63] Poor integration of grafted cells with host tissue can also significantly influence grafting outcomes and can lead to physical rifts within the graft and at the host tissue interface (such as that seen in SCI transection studies), which disrupts the integrity of the transplant[64,65] (Figure 19.2(e)). Unsatisfactory integration has been a major issue for retinal engraftment of stem cells.[66] Finally, transplanted cell immunological rejection is a major challenge facing the field with the effect

of mismatched stem cell histocompatibility antigens on graft immunogenicity as well as clonal variations in induced autologous stem cells often being underappreciated[67] (Figure 19.2(f)). Evidently, there are still considerable barriers that need to be overcome in order to realize the full potential of CNS cell transplantation. Irrespective of the specific source or protocol used to derive cells, realizing the potential of cell transplantation in CNS disease and injury is likely to benefit from innovative bioengineering strategies that: (1) enhance the survival of cells injected into sub-acute or chronic tissue lesions; (2) control/guide progenitor differentiation *in vivo*; and (3) optimize interactions between host and grafted cells.

19.4 The Development of Biomaterials for CNS Cell Transplantation

The application of biomaterials as carriers for the transplantation of cells into the diseased and injured CNS has an extensive history with a variety of different formulations being explored (Figure 19.3). The concept of using

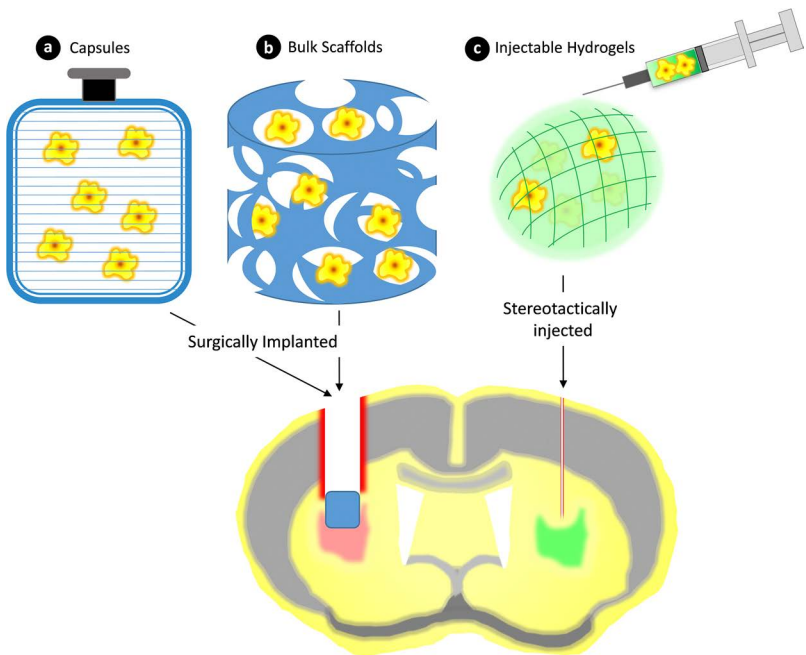

Figure 19.3 A number of different biomaterial-based approaches have been used to improve cell transplant outcomes in CNS applications: (a) semipermeable synthetic membrane capsules can be used to protect cells from immune rejection following transplantation; (b) bulk 3D scaffolds provide seeded cells with a solid support to adhere and grow while the porous structure facilitates nutrient and waste exchange; and (c) injectable hydrogels can be used to suspend cells for grafting and can be applied to host tissue using minimally invasive procedures.

biomaterials for molecular delivery in the CNS dates back to the late 19th and early 20th centuries and the pioneering experiments of Cajal, Tello and others.[21,22] These authors had observed that injured CNS axons that were unable to grow across CNS lesions, were, however, able to regrow into grafts of peripheral nerves. Subsequent experiments to investigate potential mechanisms showed that axons did not regrow into peripheral nerves that had been killed (with chloroform), suggesting that axon growth might be induced and attracted by chemical factors produced by live cells in the peripheral nerves. To test this possibility, the authors prepared high concentration extracts from peripheral nerves and soaked these into elder pith (pith from the elder tree), a well-known and widely available porous material. The elder pith was then implanted in injured CNS, and pith previously soaked in peripheral nerve extract attracted CNS axons, whereas pith soaked in control liquid did not (see pages 79–80, 188–127 and 742–750 of ref. 22). These experiments represent imaginative and powerful early experimental applications of biomaterials for molecular delivery in the CNS. The resulting observations enabled Cajal to extend his theory of "chemotactism" or chemical attraction of nerve growth by "neurotropic substances" (a term that he first coined) from occurring only in the developmental stage to also occurring after injury of axons (see pages 388–392 and 742–750 of ref. 22). More recent studies have confirmed these early experiments and have shown that live peripheral nerve grafts contain Schwann cells that produce a variety of different neurotrophic substances that attract the ingrowth of CNS axons.[68–70]

More recently, in an effort to address the major CNS cell transplantation challenges, cell biologists have searched for excipients or carrier systems that can be used to enhance cell integration, localization and viability *in vivo*. As a first approach, researchers applied immunosuppressive drugs such as Cyclosporin A systemically as an adjunct therapy to improve survival of cross-species-grafted cells in the CNS.[71] However, despite improved outcomes, the still unsatisfactory cell survival achieved prompted the search for alternative strategies. In a series of papers by Aebischer and colleagues, the first use of a modern biomaterial vehicle was described and involved using semipermeable synthetic membrane capsules to protect xenogeneic cells upon transplantation as part of a dopamine replacement therapy in models of Parkinson's disease[72–75] (Figure 19.3(a)). Specifically, non-resorbable polyvinyl chloride acrylic copolymer XM-50 tubes were used as an isolating capsule to implant embryonic mouse mesencephalon[72] or an immortalized cell line derived from an adrenal medulla pheochromocytoma (PC12)[73–75] into the rat parietal cortex. In these pioneering studies, the researchers attempted to provide a xenograft source of dopamine-expressing cells that could be leveraged to provide localized delivery of this important neurotransmitter, which is depleted in Parkinson's disease as a result of the death of dopaminergic neurons in the substantia nigra. They rationalized that encapsulation of cells within a material possessing a semipermeable membrane (50 kDa cut-off) would allow for free transport of nutrients from the local environment to xenogeneic cells as well as diffusion of neurotransmitters to local host targets

but would ultimately exclude elements of the local immune attack system (*e.g.* complement complex, leukocytes *etc.*). In all these studies, preserved transplanted cells were identified within the tubes upon retrieval at chronic implantation time points. Interestingly, the same authors noted that the extent of fibrosis (or extent of local collagen deposition) seen at the capsule–brain tissue interface was significantly reduced compared to that seen when the same system was implanted into other places in the body such as in the subcutaneous space, peritoneal cavity or near visceral organs.[76] Subsequent studies in non-human primates identified that the polymer capsules promoted survival of cells for up to five months and this corresponded with behaviorally detectable improvements in a model of Parkinson's disease.[77] Application of similar cell encapsulation technology has progressed to clinical trials for other CNS relevant diseases such as ALS, macular degeneration and chronic retinal degeneration with engineered immortalized cells being used in these instances as a means of delivering the neurotrophin, CNTF.[78,79] The cell isolation and encapsulation strategy provides for a potentially effective means of prolonging the availability of secreted soluble biologically active factors to the local CNS environment. However, the inability to control: (i) cell viability and proliferation within the capsule; and (ii) the distribution and concentration of secreted factors will likely limit the widespread adoption of this technique in CNS applications.

The use of non-resorbable synthetic membranes such as those described above to isolate cell therapies prevents any transplanted cell integration or synaptic reconnection with the host. In many of the CNS diseases amenable to possible cell transplantation therapy, satisfactory host integration is fundamental to ensuring long-term viability of the graft as well as for promoting the repopulation of viable new neural tissue at the local diseased or injured site. An alternative strategy that emerged shortly after the cell encapsulation approach involved the use of porous scaffolds/membranes or hydrogel vehicles that could act to guide the regrowth of endogenous tissue as well as support transplanted cell integration with the host. Silver and colleagues in a series of papers explored the use of nitrocellulose membranes, alone or in combination with grafted immature astrocytes, to guide the axon growth of the corpus callosum upon implantation within acallosal mice.[80–83] In the first of these studies, they showed that postnatal formation of the disrupted corpus callosum was amenable to manipulation or guidance *via* the implantation of the nitrocellulose bridge (at t = P4), which subsequently became coated with host-derived immature glial cells on the surface, creating a favorable substrate/scaffold for aligned fiber growth.[80] Following these exciting observations, the same group explored the potential of grafting similar exogenously sourced immature astrocytes onto the nitrocellulose scaffold, demonstrating a capacity to promote similar axon growth in older, adult acallosal mice[81,82] but that this capacity was lost when mature astrocytes were grafted.[83] Similar axon regrowth guidance results using the immature astrocyte-grafted nitrocellulose implants were observed for dorsal root fibers in the spinal cord.[84] Others subsequently explored similar strategies using

laminin- or polylysine-coated nitrocellulose membranes to graft dissociated cells derived from the forebrains or spinal cords of P1 rat pups into the spinal cords of neonate rats and the capacity to guide the growing CST along the substrate was characterized.[85] These grafted cells were predominately GFAP positive cells, characteristic of immature astrocytes similar to those used in the Silver studies. It was observed that the cell- and laminin-coated implants supported the adhesion and growth of CST axons while the polylysine-coated and uncoated control did not. Similar results were subsequently seen for the regrowth of sensory axons into the dorsal root entry zone when fetal spinal cord cells were grafted on nitrocellulose aided by bound NGF.[86] These early studies are important reading for anyone developing smart biomaterials for CNS cell transplantation applications.

While exciting results were obtained using these relatively inert nitrocellulose membranes, the desire to establish three-dimensional grafts, the need to facilitate direct host–graft adhesion/contact as well as the ability to perform transplantation *via* a minimally invasively injection led to the investigation of hydrogel-based systems for use in CNS cell grafting. The foundation work for the hydrogel CNS cell transplantation field was performed by Woerly and colleagues.[87–91] In this work, a thermally induced physically crosslinked collagen gel was used to introduce fetal grafts into induced cortex injuries. At chronic time points post implantation, a modest number of grafted cells was observed to have survived using this hydrogel system. An interesting observation in these studies was that only after two months of implantation, and once the collagen network had been consumed and replaced by a glial cell containing matrix, did any observable host axon regrowth occur.[88,91] Just like in the nitrocellulose membrane experiments, it would seem that axon contact with supporting astrocytes is necessary for facilitating regrowth.[88] Furthermore, the authors suggest that some extent of glial reorganization at the hydrogel scar interface results in a more permeable matrix, allowing penetration of the regrowing axons into the newly produced glial matrix. In a follow-up study, the same group used a hydrogel composed of co-precipitated chondroitin-6-sulfate (C-6-S) and collagen to form a heterogeneous strengthened network. The C-6-S incorporation increased the residence time of the hydrogel matrix *in vivo* within the CNS lesion and again it was the glial-containing secondary matrix formed upon resorption of the implanted material that facilitated the axonal regrowth.[90] There was no observed inhibition of axon growth associated with the C-6-S-containing hydrogel. These findings are not only consistent with, but anticipate, transgenic loss-of-function studies showing that newly proliferated scar-forming astrocytes aid, rather than inhibit, the regeneration of damaged axons.[92]

Since the first uses of materials for grafting cells in the CNS, a greater diversity of materials has been explored using a variety of naturally and synthetically derived polymers that provide unique properties. These systems can be broadly classified into two main groups: (1) bulk three-dimensional porous scaffolds whereby cells are seeded onto and/or within the structure and then implanted (Figure 19.3(b)); or (ii) as hydrogels whereby cells are suspended

within the hydrated network of the material and then injected (Figure 19.3(c)). Porous scaffolds made of a poly(lactic-*co*-glycolic acid) (PLGA) or block copolymer of PLGA-polylysine formed through solvent casting/particulate leaching processes have been used to graft various cell candidates in spinal cord injury models in rats[93–95] and primates.[96] The use of these resorbable materials results in the formation of remodeled tissue within the implant site that forms as host cells migrate into the scaffold structure and the material degrades by hydrolysis through a combination of surface and bulk erosion processes. This newly synthesized tissue, which appears to be formed by predominantly glial and fibroblast-like cells as part of a general foreign body response to the implant appears to be a permissible environment for the regrowth of CNS axons. Similar porous materials made of the synthetic low hydration polymer poly(2-hydroxyethyl methacrylate) (pHEMA) that were coated with collagen, have been used to graft Schwann cells into the optic nerve.[97] In this study by Plant and Harvey, GFAP-positive astrocytes were the dominant infiltrating cell, with these cells appearing to support the regrowth of axon fibers. The authors observed that the seeded Schwann cells acted to recruit larger numbers of GFAP-positive astrocytes into the pores of the implant resulting in increased axon regeneration compared to the cell-free implants.[97] In a follow-up study employing an RGD-peptide-coated porous bulk implant made of a similar polymer to that of pHEMA, poly *N*-(2-hydroxypropyl)-methacrylamide (HPMA), Woerly and Harvey seeded onto the material genetically engineered fibroblasts that produce high concentrations of neurotrophic factors BDNF and CNTF.[98] This resulted in a construct that when implanted into the optic nerve demonstrated enhanced fiber growth in a neurotrophin-production-dependent manner. Another bulk scaffold with aligned pores made of the natural polymer alginate was used to graft adult primary neural progenitor cells into a dorsal hemisection spinal cord injury.[99] In this study, the scaffold supported the non-directed differentiation of the grafted cells that included subpopulations with immature astrocyte-like morphology that seemed to support axon growth. A common and important observation in all these studies, and which was consistently noted in the original nitrocellulose membrane work discussed above, is that regrowing axon fibers seem to prefer growing upon cellular-based bridges usually provided by astrocytes or fibroblasts rather than along the material itself regardless of whether the material contains specific bioactive molecules (*e.g.* laminin, fibronectin or RGD/IKVAV peptides) on its contact surface. However, it is apparent that these different bioactive molecules likely influence the type and phenotype of the cell that is able to interact with the surface of the material, which may greatly influence the performance of these cellular bridges. Regardless, these observations suggest that focusing on modulating the grafted or host cell type that predominately adheres/interacts with the surface of these biomaterial scaffolds will likely be the key regulator of axon growth outcomes. While the results from the growing body of bulk scaffold literature studies provides important information, a significant limitation of the bulk scaffold structures is the need to implant the material

into a "free space" or cavity within the CNS. In many of the preclinical rodent studies that are used to study these materials in models of CNS injury such as in the spinal cord for example, a hemisection lesion is used, which has the benefit of creating both the injury and the scaffold implantation cavity in the same procedure in a very anatomically controlled way. Since most clinical CNS lesions are non-penetrating irregularly shaped injuries, the physical implantation of these bulk structures requires additional injury to the CNS tissue to be made *via* a myelotomy or similar procedure in order to be able to implant the scaffold.[100] The desire for minimally invasive implantation of biomaterial–cell constructs has led to an increased interest in injectable biomaterials as an alternative to bulk scaffolds.

Since the collagen hydrogel work of Woerly in the early 1990s as described above, a number of other naturally-derived and synthetic-based polymers have also been explored for CNS cell grafting. The dominant materials by far in these studies have been fibrin-based constructs, which are fibrous matrices established through the thrombin-induced polymerization of fibrinogen. Using this system, Tuszynski and colleagues have produced several reports exploring the grafting of various neural progenitor cell candidates (derived from ES, iPS and E14 spinal cord origin) in models of transection SCI.[9,101,102] In these studies, the fibrin matrix is loaded with a cocktail of several growth factors that ensures local survival of the grafted cells within transection injuries. These progenitors differentiate into a mixed population of neural cells that support host axon growth of the corticospinal tract and other axon fibers again through an apparent cell contact mediated mechanism.[102] Identification of ectopic colonies of grafted cells within the brain and brainstem using this biomaterial system in follow-up studies suggests that the material and cocktail of growth factors may not be sufficient for ensuring localization of the graft at the injury site in all cases.[10,64] Sakiyama-Elbert and colleagues have used similar fibrin-based biomaterials to graft ES-cell-derived neural progenitors.[103–106] Aided by co-suspended heparin binding peptides and growth factors (NT-3 and PDGF), the NSPCs have showed increased cell survival and neuronal differentiation *in vivo* in a dorsal hemisection spinal cord injury model.[105,106] Using injectable hydrogels composed of the predominant ECM biomacromolecule, hyaluronan, Shoichet's group have produced shear thinning hyaluronan-methylcellulose blended (HAMC) hydrogels[107] and demonstrated enhanced survival and integration of retinal stem cell (RSC)-derived rods upon transplantation into the eye[108,109] leading to improved visual function in a model of retinal injury. This biomaterial system has also been employed for NSPC grafting into stroke injuries, resulting in enhanced graft cell survival[108] as well as in SCI where the same group used conjugated PDGF to induce a modest increase in oligodendrocyte differentiation.[110] Hyaluronan interacts specifically with CD44 receptors present on NSPCs, which may influence intracellular survival pathways.[108] The CD44 receptor is also highly expressed on endothelial cells allowing hyaluronan to stimulate proliferation of these cells by the host and consequently enhance local angiogenesis at the graft site, which has been attributed to

an improved overall performance of hyaluronan biomaterials in cell transplant studies.[111] Others have utilized covalently crosslinked hydrogels that contain hyaluronan as carriers for NSPCs derived from ES origin in order to graft these cells into brain lesions in a stroke model.[112] The use of this particular biomaterial carrier, which also included collagen and heparin components within the network, promoted increased cell survival as well as a reduction in macrophages and microglia infiltrating into the graft. However, in a follow-up study by the same group using iPS-derived NSPCs suspended in a similar hyaluronan-containing material (with additional RGD and MMP degradable peptide fragments), the presence of hyaluronan did not confer a survival advantage to grafted cells at the examined one week time point but did enhance differentiation towards a neuronal phenotype.[113] Other injectable hydrogel materials derived from alternative natural materials such as salmon fibrin[114] or decellularized CNS extracellular matrix[115,116] may provide other uniquely favorable bioactive properties than those offered by the currently studied selection of materials and may warrant further exploration as *in vivo* cell carriers in the future.

Despite their promise, some major limitations associated with naturally-derived materials include an inability to meaningfully tune the physiochemical properties of the matrix as well as inherent immunogenic risks associated with pyrogens and other potential contaminants that cannot be readily removed from these biologically sourced materials. Although there is considerable *in vitro* literature describing the use of synthetic polymers such as PEG, PVA, PEG-PLGA, and poloxamers for neural tissue engineering applications there are seldom *in vivo* reports employing such materials in the CNS.

To enhance the performance of NSPC grafted into the CNS, a small contingent including ourselves are developing synthetic biomaterial vehicles that can provide favorable and versatile microenvironments *in vivo* and also possess the capacity to deliver vital molecular cues in a controlled spatial and temporal manner. For our studies the synthetic biomaterial vehicles used are based on diblock copolypeptide hydrogels (DCH), which we have shown to be versatile carriers that are compatible with the CNS *in vivo*.[117] DCH are fabricated using synthetic copolymer amphiphiles derived from the controlled living polymerization of cyclized *N*-carboxyanhydride amino acid derivatives, and can be synthesized with highly tunable mechanical, chemical and biological properties.[118] DCH can be modified to demonstrate thermoreversible gelation and/or shear thinning behavior allowing for facile and minimally invasive delivery of cargo molecules such as polypeptide neurotrophic factors and small molecule hydrophobic drugs to the CNS.[117,119,120] Recent studies from our lab also indicate that transplantation of mouse-fetal-brain-derived primary neural stem cells (pNSC) after SCI in DCH vehicles without cargo molecules improves pNSC viability, localization and integration compared to pNSC in culture media alone.[121,122] The DCH platform offers unprecedented versatility and control over the delivery of cells and molecules compared to many of the other hydrogel materials currently studied in CNS applications.[123] Others have applied related synthetic small

peptide-based amphiphiles also capable of self-assembling into hydrogels to deliver cells in a model of stroke.[124] By attaching the IKVAV peptide sequence derived from the cell binding motif of laminin the authors showed enhanced neuronal differentiation *in vivo* whereas in the absence of this bioactive peptide sequence, the hydrogels demonstrated increased astrocyte differentiation. Developing new synthetic biomaterials that provide tunable chemical, mechanical, biological and stimuli-responsive properties that allow for the systematic evaluation of important cell transplantation parameters should be the focus of future work in the neural biomaterials space.

19.5 Emerging Smart Biomaterials for CNS-Based Cell Delivery Applications

In the final section of this chapter we provide emerging concepts from smart biomaterials research using synthetic biomaterials that may be of potential benefit for improving CNS cell transplantation outcomes. There are a number of promising smart material approaches and concepts developed in recent times that may be applied to address the challenges posed by CNS cell therapy transplantation (Figure 19.4). Within this section we detail concepts that may have not yet been studied in CNS applications but that are prime for future exploration in this space.

19.5.1 Protecting Cells during CNS Cell Transplantation

Arguably the greatest challenge for CNS cell transplantation is the ability to ensure adequate cell viability both during CNS transplantation and during initial exposure to a hostile CNS lesion. Smart biomaterials are being developed to address both of these stressors of cell survival. Smart biomaterials that demonstrate the capacity to self-heal upon shearing or possess thermoresponsive mechanical properties may be used to aid injection and improve survival of cells injected through narrow gauge needles or glass pipettes (Figure 19.4(a)). Our group has demonstrated that non-ionic DCH formulations, which contain γ-[2-(2-methoxyethoxy)ethyl]-L-glutamate (E^{P2}) functional groups within the hydrophobic segments, provide for thermoresponsive materials which undergo a sol to gel transition near physiological temperatures as a result of a LCST of the E^{P2}-containing segments that desolvate from water leading to aggregation of the α-helical hydrophobic domains. This thermoresponsive DCH provides a liquid at room temperature with tunable viscosity that allows for facile surgical injection of the cell material construct into the CNS but is still sufficiently viscous to prevent cell sedimentation and clumping within the pipette.[121,122] This system demonstrated improved cell viability upon gelation and recovery immediately following injection through the pipette as well as after three weeks' post transplantation *in vivo*. Using other polypeptide-based materials that also leverage non-covalent chemical interactions to facilitate gelation,

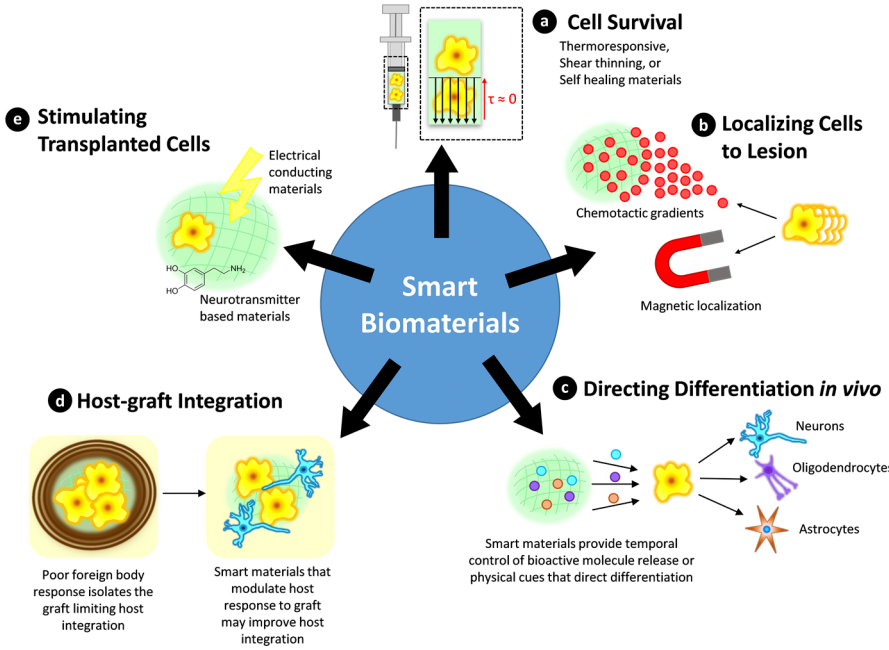

Figure 19.4 There are a number of promising smart material approaches that can be used to improve CNS cell transplant outcomes: (a) thermoresponsive, shear thinning and/or self-healing injectable materials can be used to mitigate cell death during injection by minimizing the shear stress at the pipette–hydrogel boundary; (b) using materials to establish chemotactic gradients or the application of magnetic nanoparticles and fields to encourage the transplanted cells to localize to the CNS lesion; (c) smart materials that provide specific differentiation-directing cues, such as bioactive morphogens or physical stimuli, can be used to ensure the establishment of a heterogeneous tissue graft from transplanted neural progenitor cells; (d) smart materials that minimize the foreign body response can improve graft–host integration outcomes; (e) electrical conducting materials and neurotransmitter-based materials may be used to stimulate grafted cells in order to form specific network connections with the host.

the Heilshorn lab has developed smart biomaterial systems for improved cell survival during injection. Their mixing-induced two-component hydrogels (MITCH), which make use of engineered proteins that contain conserved tryptophan and proline-rich peptide domains on individual chains that associate together upon mixing, demonstrated shear thinning and self-healing properties as well as being supportive of cell encapsulation.[125] To improve the *in vivo* longevity and strength of these hydrogels the same group next developed multifunctional star-shaped proline peptide-polyethylene glycol (PEG)-poly(*N*-isopropylacrylamide) (PNIPAM) copolymers, which when combined with the linear tryptophan-rich-domain-containing polymers resulted in materials with a reinforced network at physiological temperatures owing

to the thermally-induced phase transition and aggregation of the PNIPAM segment.[126] Using human adipose-derived stem cells as a model cell system this strengthened hydrogel provided for enhanced survival following injection through a 28 gauge needle as well as improved local retention of cells for up to 14 days within a subcutaneous site compared to that achieved with the media carrier alone. Interestingly, this group has also demonstrated that for these and other hydrogel materials, a storage modulus of less than 50 Pa provides the most protective physical environment for suspended cells during the injection procedure.[127] It is theorized that these low strength easily injectable hydrogels may protect cells by a phenomenon known as shear banding in which the hydrogel creates a central wide plug flow region that consequently reduces cell membrane shearing and disruption during injection.[127,128] However, it is likely that high dynamic viscosity of the carriers at high strain also contributes to enhanced cell viability by mitigating cell sedimentation and clumping. Further development of facile synthetic materials that can provide for highly tunable dynamic viscosity and flow properties in order to rigorously study and optimize cell viability outcomes during injection will be important future work. An alternative approach to furthering cell viability gains during injection, in addition to the development of new material carriers, may be to modify the surface properties of the injection tools themselves with smart functionalities. For example, by leveraging standardized silanization chemistry[129] or oxidized polydopamine derivatives,[130] it would be possible to functionalize the surface of the glass pipettes with a variety of different non-fouling or protective functional moieties that may act to favorably modify the boundary layer flow profile of the viscous hydrogel carrier to enhance the plug flow profile achieved during injection. However, to date, this has been an under-researched area and it is unclear how significant such modifications will be on improving cell viability outcomes.

Once the cell–biomaterial construct is transplanted into the site of CNS injury it is barraged by a multitude of stressors including (but not limited to): damage-associated molecular pattern molecules (DAMPs), highly reactive lipid peroxidation products and constituents of the innate immune system which create a hostile injury CNS microenvironment.[131] Smart biomaterial systems could be used to mitigate the effects of these injury induced stressors by either: (i) delivering stressor antagonizing drugs locally, (ii) scavenging reactive injury stressors through some sacrificial functional groups on the biomaterial itself, or (iii) by providing a physical protection barrier between the stressors and the cells. Langer and colleagues used a biomaterial local drug delivery system in combination with a porous scaffold to protect neural stem cells grafts from peroxynitrite-induced death upon transplantation into SCI.[132] Others are developing smart biomaterials and polymers which possess chemical functionality that can mitigate cell death upon exposure to various stressors as can occur during cryopreservation.[133,134] Similar biomaterial approaches could be applied to transiently protect transplanted cells during the initial *in vivo* incubation periods.

19.5.2 Localizing Transplanted Cells to CNS Injuries and Preventing Migration

Localization of transplanted cells to CNS lesions can be challenging given that these injury regions are often not very supportive microenvironments because they are devoid of adequate vascularization and supportive glial cells. As such, migration of grafted cells away from injured tissue is frequently observed. To ensure localization of transplanted cells a number of different smart biomaterial approaches may be used (Figure 19.4(b)). Recently, magnetic cell localization techniques have been explored by a number of groups as an approach to localize or "home" neural stem cell therapies to sites of CNS injury in models of stroke and spinal cord injury.[135–137] By first labeling cells with magnetite-containing poly(lactic acid) (PLA)-coated nanoparticles, superparamagnetic iron oxide nanoparticles or ferumoxide and then subsequently applying magnetic fields locally, these groups were able to improve the numbers of cells that homed to sites of CNS injury when injected intravenously or transplanted within the intrathecal space. Similar approaches could be applied periodically to locally injected cells in order to prevent excessive cell migration away from lesions. Smart biomaterial systems have also been used to establish chemotactic gradients of bioactive molecules that act to recruit endogenous neural stem cells to sites of injury.[138,139] With the identification of appropriate bioactive molecules, such approaches could also be easily adapted to maintain grafted cells locally within the lesion site over a chronic time course.

19.5.3 Regulating Grafted Cell Differentiation *In vivo*

In order to facilitate the re-establishment of functional neural tissue at sites of CNS injury or disease, repopulation of the CNS lesions with an appropriately proportioned distribution of neuronal and glial cells will be necessary. As has been demonstrated within endogenous tissue, graft-derived neurons will not survive on their own without appropriate glial support. The most viable approach to achieve a heterogeneous cell graft is to transplant multipotent progenitors and guide differentiation *in vivo* in an appropriately controlled manner. Using smart biomaterials to present multiple diverse differentiation directing cues to grafted cells in a specific spatiotemporal manner will be critical to realizing the recapitulation of functionally viable neural tissue (Figure 19.4(c)). These cues can include: (i) the delivery of hydrophilic growth factors and small molecules that modulate transcription factors or other intracellular processes, (ii) the selection of the compliance/mechanical properties of the biomaterial substrate that the cells are seeded upon/within, or (iii) by presenting specific extracellular moieties or cell adhesion molecules to grafted cells that interact with specific transmembrane receptors. While there is considerable literature on the use of biomaterials to direct differentiation of neural progenitors *in vitro* using all three of these approaches, there are few reports of corresponding studies *in vivo*. However, some studies

have emerged that warrant a mention here. Using biotin-streptavidin immobilization of specific growth factors known to regulate NSPC differentiation to chitosan conduits, Leipzig and colleagues studied directed differentiation outcomes upon implantation of the cell loaded conduits into the subcutaneous space of rats over a four-week period.[140] Using immobilized interferon-γ (IFN-γ), platelet derived growth factor-AA (PDGF-AA), or bone morphogenic protein-2 (BMP-2) as a bioactive cue to induce neuronal, oligodendrocyte and astrocyte differentiation respectively, some qualitative enhancement of desired cell populations was observed. However, a systematic evaluation to determine the relative proportional increase of one cell type over another was not performed in this study and it is uncertain whether comparable results would be obtained upon transplantation within a CNS injury environment. Directed differentiation of NSPC can be controlled through careful selection of the mechanical properties of the biomaterial used to suspend/seed the cells for transplantation.[141,142] In many *in vitro* studies, softer materials have been consistently shown to result in predominant neuronal phenotypes while slightly stiffer materials confer an astrocyte fate. The effects of biomaterial mechanical properties on *in vivo* directed differentiation are primed for further study and open up many unique possibilities for new smart biomaterials that may be capable of undergoing temporally or external stimuli guided mechanical property changes *in vivo* in order to influence differentiation outcomes at various points in time post transplantation.[143] Such a dynamic approach would seem analogous to how the endogenous neural stem cell niche alters the structural and mechanical properties of the extracellular environment in order to guide differentiation changes.[144] The chemical functionality of the biomaterial matrix can also be used as a way of directing differentiation outcomes of neural progenitors with a variety of different synthetic chemistries having recently demonstrated some interesting differentiation outcomes *in vitro*.[145–147] However, much like the effect of biomaterial mechanical properties, no systematic evaluation of directed differentiation outcomes *in vivo* has been reported as yet and will certainly be required as part of future exploration to validate the legitimacy of such an approach for guiding CNS transplantation outcomes.

19.5.4 Promoting Optimal Cell Graft–Host Integration through Modulation of the Biomaterial Host Interface

While it is generally recognized that favorable integration of the grafted cells with the host is imperative for achieving favorable CNS cell transplant outcomes, there is limited literature that directly addresses this property. As mentioned above, hyaluronan-based materials have generally shown good cell–host integration perhaps due to the fact that hyaluronan is a major constituent of the host ECM and also because it directly stimulates local angiogenesis, which likely aids favorable local ECM remodeling. A major determinant of cell graft–host tissue integration is the extent/severity of the

foreign body response that is induced upon introduction of the transplant into the CNS injury site. An unfavorable foreign body response involving the walling off of the implant through an activated microglia/macrophage and astrocyte response limits the extent of graft integration (Figure 19.4(d)). Recently, Langer and Anderson have developed a library of modified alginate-based polymers and demonstrated how certain chemical modifications could be used to modulate the foreign body response of the material when encapsulating progenitor-derived islet cells within the material and implanting it within subcutaneous tissue sites.[148,149] Similar approaches using these or other non-fouling materials containing similar triazole or sulfoxide functional groups or even zwitterionic moieties[150] may be useful for various CNS cell transplantation applications. Another approach to improving integrating could be to include specific biological cues delivered from smart biomaterials to stimulate transplanted or host cells to synthesize and reorganize the local extracellular matrix within the lesion non-neural tissue to improve graft integration. Some applicable examples could include: (i) stimulating host astrocytes around the CNS lesion to synthesize important extracellular matrix molecules such as laminin, which appear necessary for supporting and guiding regrowing neural tissue[92] or (ii) stimulating the re-synthesis of the dominant extracellular matrix constituent, high molecular weight hyaluronan,[151] by up-regulating hyaluronan synthase (Has1, Has2) activity in grafted or local host cells analogous to processes used by the neural stem cell niche and in neural tissue development.[152]

19.5.5 Stimulating Transplanted Neural Cells with Smart Biomaterials

Electrical and/or neurotransmitter stimulation of host neurons such as the propriospinal neurons in the spinal cord can facilitate favorable circuitry rewiring after injury and has been correlated with recovery of function in various models of CNS injury.[153,154] Smart biomaterials that employ similar functional stimulation of transplanted cells may be useful in guiding the formation of new circuits between host and grafted cells (Figure 19.4(e)). Electrically conductive polymers such as polypyrrole, polyaniline and carbon nanotubes (CNT) have already been incorporated extensively as biomaterials in peripheral and central nerve regeneration applications.[155–158] Furthermore electrically conducting biomaterials have demonstrated the potential to guide differentiation outcomes.[159,160] However, while the use of electrically conducting materials for cell transplantation applications appears to have exciting prospects, mitigating the potential cytotoxicity associated with these materials as well as tuning and dynamically controlling the amount of electrical stimulation still remain to be adequately addressed and as such there are no *in vivo* studies involving cell transplantation with electrically conductive materials reported to date. An alternative smart biomaterial platform approach that may find utility in guiding circuit reorganization would

be neurotransmitter functionalized materials.[161,162] Biomaterials that contain pendant dopamine and acetylcholine have demonstrated promising *in vitro* primary neuron sprouting results, however, again the use of these materials *in vivo* remains to be explored. Overall, these stimulation-based materials represent a class of materials with exciting potential that are ready to undergo *in vivo* evaluation as part of a CNS transplantation strategy.

19.5.6 Clinical Potential and Applications of Smart Materials for Central Nervous System Tissue Engineering

The past decade has seen the commencement of a number of institutional review board (IRB) and regulatory agency approved clinical trials of neural cell therapies applied to a variety of CNS disease and injury conditions such as ALS,[163] SCI,[164] stroke,[165] macular degeneration[166] and others. However, concurrently there have also been a multitude of reports describing the effects of an unregulated stem cell tourism industry where for-profit companies across the world exploit vulnerable patients with unsafe and unproven cell therapies resulting in alarming adverse events.[61,167] While the progression of cell grafting approaches to clinical evaluation should be viewed as encouraging progress, it is clear that there are still many cell manufacturing, quality assurance and *in vivo* performance issues such as the ones raised in this review that make such treatment paradigms in their current form far from optimal.[168] If preclinical results are any indication, smart biomaterials may be a powerful means of improving the clinical performance of CNS cell therapies. However, other than a number of different cell encapsulation biomaterial systems,[169] to date there has been limited investigation of the use of smart biomaterials for improved delivery of cell therapies in human CNS disease. In order to ensure clinical conversion of smart biomaterials, important design considerations such as manufacturability, scalability, material sterilization and packaging, surgical preparation and use as well as cost must be examined with priority during the preclinical research and development process. Following newly defined ASTM and ISO guidance documents for tissue engineering medical products[170] will assist in these efforts, although the development of specific standards for CNS disease and injury applications is still desperately needed in order to aid translation efforts.

19.6 Conclusions and Future Directions

This chapter provided an overview of the research to date that has applied biomaterial carriers to aid CNS cell transplantation. Here we document how the use and development of biomaterials, from initial primitive substrates to formulations with advanced smart properties, have evolved in tandem with the study of various cell candidates as therapeutic strategies for a variety of different CNS injuries and diseases. Moving forward, the CNS tissue engineering field should focus on advancing the many smart biomaterial

concepts raised in this chapter that have demonstrated promising *in vitro* results through to systematic *in vivo* study in models of CNS disease. As new biological techniques and tools such as *in vivo* imaging, cell-type-specific RNA isolation from whole tissue and gene editing begin to see more widespread adoption, the rigorous *in vivo* evaluation and biomolecular profiling of cell transplantation outcomes will become possible. Using these emerging tools in conjunction with smart biomaterials to aid cell transplant survival, differentiation outcomes and graft–host integration will be critically important in furthering our understanding of the potential and limitations of CNS cell transplantation. As the field strives to develop even smarter biomaterials for CNS cell transplantation applications in the future, a key focus should be on creating dynamic systems that can demonstrate the capacity to evolve or modulate properties so as to best meet the needs and demands of the cells suspended or seeded within them which will undoubtedly be different during the injection phase as well as at acute or chronic implant time points. Furthermore, developing smart biomaterials that can control the presentation of survival or differentiation directing cues to suspended cells in response to some external stimuli from the host would seem to be worthy of future study. To achieve such dynamic biomaterial systems, researchers should consider learning from, and replicating, how the neural stem cell niche and other biochemical allosteric regulation mechanisms are used by biology to respond to altered environmental states. Such materials are already in the works[171] and further progress in these and other smart and dynamic biomaterial systems will be essential for realizing the therapeutic potential of cell transplantation for CNS injury and disease.

Acknowledgements

This work was supported by the US National Institutes of Health (NS057624 and NS084030 to MVS), the National Science Foundation (NSF#1308081 to TJD) and the Dr Miriam and Sheldon G. Adelson Medical Foundation (MVS,TJD), and Wings for Life (MVS).

References

1. J. R. Faulkner, J. E. Herrmann, M. J. Woo, K. E. Tansey, N. B. Doan and M. V. Sofroniew, *J. Neurosci.*, 2004, **24**, 2143–2155.
2. J. C. Fleming, M. D. Norenberg, D. A. Ramsay, G. A. Dekaban, A. E. Marcillo, A. D. Saenz, M. Pasquale-Styles, W. D. Dietrich and L. C. Weaver, *Brain*, 2006, **129**, 3249–3269.
3. M. D. Norenberg, J. Smith and A. Marcillo, *J. Neurotrauma*, 2004, **21**, 429–440.
4. I. B. Wanner, M. A. Anderson, B. Song, J. Levine, A. Fernandez, Z. Gray-Thompson, Y. Ao and M. V. Sofroniew, *J. Neurosci.*, 2013, **33**, 12870–12886.

5. B. D. Trapp and K.-A. Nave, *Annu. Rev. Neurosci.*, 2008, **31**, 247–269.
6. N. Gupta and Y. H. Yücel, *Curr. Opin. Ophthalmol.*, 2007, **18**, 110–114.
7. T. Wyss-Coray and L. Mucke, *Neuron*, 2002, **35**, 419–432.
8. J. F. Bonner, T. M. Connors, W. F. Silverman, D. P. Kowalski, M. A. Lemay and I. Fischer, *J. Neurosci.*, 2011, **31**, 4675–4686.
9. P. Lu, Y. Wang, L. Graham, K. McHale, M. Gao, D. Wu, J. Brock, A. Blesch, E. S. Rosenzweig, L. A. Havton, B. Zheng, J. M. Conner, M. Marsala and M. H. Tuszynski, *Cell*, 2012, **150**, 1264–1273.
10. O. Steward, K. G. Sharp, K. M. Yee, M. N. Hatch and J. F. Bonner, *J. Neurosci.*, 2014, **34**, 14013–14021.
11. M. H. Tuszynski, Y. Wang, L. Graham, M. Gao, D. Wu, J. Brock, A. Blesch, E. S. Rosenzweig, L. A. Havton, B. Zheng, J. M. Conner, M. Marsala and P. Lu, *Cell*, 2014, **156**, 388–389.
12. K. M. Piltti, S. N. Avakian, G. M. Funes, A. Hu, N. Uchida, A. J. Anderson and B. J. Cummings, *Stem Cell Res.*, 2015, **15**, 341–353.
13. S. Nishimura, A. Yasuda, H. Iwai, M. Takano, Y. Kobayashi, S. Nori, O. Tsuji, K. Fujiyoshi, H. Ebise, Y. Toyama, H. Okano and M. Nakamura, *Mol. Brain*, 2013, **6**, 1–15.
14. A. M. Parr, I. Kulbatski, T. Zahir, X. Wang, C. Yue, A. Keating and C. H. Tator, *Neuroscience*, 2008, **155**, 760–770.
15. W. G. Thompson, *N. Y. Med. J.*, 1890, **51**, 701.
16. S. B. Dunnett, in *Handbook of Clinical Neurology*, ed. F. B. Michael, J. Aminoff and F. S. Dick, Elsevier, 2009, vol. 95, pp. 885–912.
17. L. Olson, *Histochemie*, 1970, **22**, 1–7.
18. G. D. Das and J. Altman, *Brain Res.*, 1972, **38**, 233–249.
19. A. Bjorklund, U. L. F. Stenevi and N.-A. Svendgaard, *Nature*, 1976, **262**, 787–790.
20. M. Perlow, W. Freed, B. Hoffer, A. Seiger, L. Olson and R. Wyatt, *Science*, 1979, **204**, 643–647.
21. S. Ramon y Cajal, *Degeneration and Regeneration of the Nervous System*, Oxford University Press, London, 1928.
22. J. DePhillipe and E. G. Jones, *Cajal's Degeneration and Regeneration of the Nervous System*, Oxford University Press, Oxford, New York, 1991.
23. P. M. Richardson, U. M. McGuinness and A. J. Aguayo, *Nature*, 1980, **284**, 264–265.
24. C. C. Kao, L. W. Chang and J. M. B. Bloodworth, *Exp. Neurol.*, 1977, **54**, 591–615.
25. S. David and A. Aguayo, *Science*, 1981, **214**, 931–933.
26. M. Vidal-Sanz, G. M. Bray, M. P. Villegas-Perez, S. Thanos and A. J. Aguayo, *J. Neurosci.*, 1987, **7**, 2894–2909.
27. P. J. Reier, B. S. Bregman and J. R. Wujek, *J. Comp. Neurol.*, 1986, **247**, 275–296.
28. J. D. Houlé and P. J. Reier, *J. Comp. Neurol.*, 1988, **269**, 535–547.
29. A. Bjorklund and U. Stenevi, *Annu. Rev. Neurosci.*, 1984, **7**, 279–308.
30. M. V. Sofroniew, O. Isacson and A. Björklund, *Brain Res.*, 1986, **378**, 409–415.

31. W. Tetzlaff, E. B. Okon, S. Karimi-Abdolrezaee, C. E. Hill, J. S. Sparling, J. R. Plemel, W. T. Plunet, E. C. Tsai, D. Baptiste, L. J. Smithson, M. D. Kawaja, M. G. Fehlings and B. K. Kwon, *J. Neurotrauma*, 2011, **28**, 1611–1682.
32. A. Ramón-Cueto, M. I. Cordero, F. F. Santos-Benito and J. Avila, *Neuron*, 2000, **25**, 425–435.
33. X. M. Xu, A. Chen, V. Guenard, N. Kleitman and M. B. Bunge, *J. Neurocytol.*, 1997, **26**, 1–16.
34. C. P. Hofstetter, E. J. Schwarz, D. Hess, J. Widenfalk, A. El Manira, D. J. Prockop and L. Olson, *Proc. Natl. Acad. Sci.*, 2002, **99**, 2199–2204.
35. D. Karussis, C. Karageorgiou and A. Vaknin-Dembinsky, *et al.*, *Arch. Neurol.*, 2010, **67**, 1187–1194.
36. P. Lu, L. L. Jones and M. H. Tuszynski, *Exp. Neurol.*, 2007, **203**, 8–21.
37. S. Saporta, J.-J. Kim, A. E. Willing, E. S. Fu, C. D. Davis and P. R. Sanberg, *J. Hematother. Stem Cell Res.*, 2003, **12**, 271–278.
38. C. N. Svendsen, M. A. Caldwell, J. Shen, M. G. ter Borg, A. E. Rosser, P. Tyers, S. Karmiol and S. B. Dunnett, *Exp. Neurol.*, 1997, **148**, 135–146.
39. N. Uchida, D. W. Buck, D. He, M. J. Reitsma, M. Masek, T. V. Phan, A. S. Tsukamoto, F. H. Gage and I. L. Weissman, *Proc. Natl. Acad. Sci.*, 2000, **97**, 14720–14725.
40. A. J. Mothe and C. H. Tator, *J. Clin. Invest.*, 2012, **122**, 3824–3834.
41. S. Vadivelu, T. J. Stewart, Y. Qu, K. Horn, S. Liu, Q. Li, J. Silver and J. W. McDonald, *Stem Cells Transl. Med.*, 2015, **4**, 401–411.
42. Q.-l. Cao, Y. P. Zhang, R. M. Howard, W. M. Walters, P. Tsoulfas and S. R. Whittemore, *Exp. Neurol.*, 2001, **167**, 48–58.
43. S. Wu, Y. Suzuki, M. Kitada, M. Kitaura, K. Kataoka, J. Takahashi, C. Ide and Y. Nishimura, *Neurosci. Lett.*, 2001, **312**, 173–176.
44. S. Nori, Y. Okada, A. Yasuda, O. Tsuji, Y. Takahashi, Y. Kobayashi, K. Fujiyoshi, M. Koike, Y. Uchiyama, E. Ikeda, Y. Toyama, S. Yamanaka, M. Nakamura and H. Okano, *Proc. Natl. Acad. Sci.*, 2011, **108**, 16825–16830.
45. J.-H. Kim, J. M. Auerbach, J. A. Rodriguez-Gomez, I. Velasco, D. Gavin, N. Lumelsky, S.-H. Lee, J. Nguyen, R. Sanchez-Pernaute, K. Bankiewicz and R. McKay, *Nature*, 2002, **418**, 50–56.
46. L. H. Thompson and A. Björklund, *Neurobiol. Dis.*, 2015, **79**, 28–40.
47. R. E. MacLaren, R. A. Pearson, A. MacNeil, R. H. Douglas, T. E. Salt, M. Akimoto, A. Swaroop, J. C. Sowden and R. R. Ali, *Nature*, 2006, **444**, 203–207.
48. J. Wang, J. Xia, F. Zhang, Y. Shi, Y. Wu, H. Pu, A. K. F. Liou, R. K. Leak, X. Yu, L. Chen and J. Chen, *Sci. Rep.*, 2015, **5**, 9621.
49. M. Rosenberg, T. Friedmann, R. Robertson, M. Tuszynski, J. Wolff, X. Breakefield and F. Gage, *Science*, 1988, **242**, 1575–1578.
50. R. Grill, K. Murai, A. Blesch, F. H. Gage and M. H. Tuszynski, *J. Neurosci.*, 1997, **17**, 5560–5572.
51. M. H. Tuszynski, D. A. Peterson, J. Ray, A. Baird, Y. Nakahara and F. H. Gages, *Exp. Neurol.*, 1994, **126**, 1–14.
52. P. Lu, L. L. Jones, E. Y. Snyder and M. H. Tuszynski, *Exp. Neurol.*, 2003, **181**, 115–129.

53. D. Drago, C. Cossetti, N. Iraci, E. Gaude, G. Musco, A. Bachi and S. Pluchino, *Biochimie*, 2013, **95**, 2271–2285.
54. M. P. Lutolf, P. M. Gilbert and H. M. Blau, *Nature*, 2009, **462**, 433–441.
55. G. Courtine, B. Song, R. R. Roy, H. Zhong, J. E. Herrmann, Y. Ao, J. Qi, V. R. Edgerton and M. V. Sofroniew, *Nat. Med.*, 2008, **14**, 69–74.
56. F. M. Bareyre, M. Kerschensteiner, O. Raineteau, T. C. Mettenleiter, O. Weinmann and M. E. Schwab, *Nat. Neurosci.*, 2004, **7**, 269–277.
57. M. Abematsu, K. Tsujimura, M. Yamano, M. Saito, K. Kohno, J. Kohyama, M. Namihira, S. Komiya and K. Nakashima, *J. Clin. Invest.*, 2010, **120**, 3255–3266.
58. C. J. Sontag, N. Uchida, B. J. Cummings and A. J. Anderson, *Stem Cell Rep.*, 2014, **2**, 620–632.
59. S. Kelly, T. M. Bliss, A. K. Shah, G. H. Sun, M. Ma, W. C. Foo, J. Masel, M. A. Yenari, I. L. Weissman, N. Uchida, T. Palmer and G. K. Steinberg, *Proc. Natl. Acad. Sci. U. S. A.*, 2004, **101**, 11839–11844.
60. N. Amariglio, A. Hirshberg, B. W. Scheithauer, Y. Cohen, R. Loewenthal, L. Trakhtenbrot, N. Paz, M. Koren-Michowitz, D. Waldman, L. Leider-Trejo, A. Toren, S. Constantini and G. Rechavi, *PLoS Med.*, 2009, **6**, e1000029.
61. B. J. Dlouhy, O. Awe, R. C. Rao, P. A. Kirby and P. W. Hitchon, *J. Neurosurg. Spine*, 2014, **21**, 618–622.
62. A. I. Teixeira, J. K. Duckworth and O. Hermanson, *Cell Res.*, 2007, **17**, 56–61.
63. O. Tsuji, K. Miura, Y. Okada, K. Fujiyoshi, M. Mukaino, N. Nagoshi, K. Kitamura, G. Kumagai, M. Nishino, S. Tomisato, H. Higashi, T. Nagai, H. Katoh, K. Kohda, Y. Matsuzaki, M. Yuzaki, E. Ikeda, Y. Toyama, M. Nakamura, S. Yamanaka and H. Okano, *Proc. Natl. Acad. Sci.*, 2010, **107**, 12704–12709.
64. K. G. Sharp, K. M. Yee and O. Steward, *Exp. Neurol.*, 2014, **257**, 186–204.
65. M. H. Tuszynski, Y. Wang, L. Graham, K. McHale, M. Gao, D. Wu, J. Brock, A. Blesch, E. S. Rosenzweig, L. A. Havton, B. Zheng, J. M. Conner, M. Marsala and P. Lu, *Exp. Neurol.*, 2014, **261**, 494–500.
66. T. V. Johnson, N. D. Bull and K. R. Martin, *Invest. Ophthalmol. Visual Sci.*, 2010, **51**, 960–970.
67. K. J. Wood, F. Issa and J. Hester, *Trends Immunol.*, 2016, **37**, 5–16.
68. G. V. Smith and J. A. Stevenson, *Exp. Brain Res.*, 1988, **69**, 299–306.
69. T. Hagg, A. K. Gulati, M. A. Behzadian, H. L. Vahlsing, S. Varon and M. Manthorpe, *Exp. Neurol.*, 1991, **112**, 79–88.
70. S. P. Frostick, Q. Yin and G. J. Kemp, *Microsurgery*, 1998, **18**, 397–405.
71. P. Brundin, O. G. Nilsson, F. H. Gage and A. Bjorklund, *Exp. Brain Res.*, 1985, **60**, 204–208.
72. P. Aebischer, S. R. Winn and P. M. Galletti, *Brain Res.*, 1988, **448**, 364–368.
73. C. B. Jaeger, L. A. Greene, P. A. Tresco, S. R. Winn and P. Aebischer, *Prog. Brain Res.*, 1990, **82**, 41–46.
74. P. Aebischer, P. A. Tresco, S. R. Winn, L. A. Greene and C. B. Jaeger, *Exp. Neurol.*, 1991, **111**, 269–275.

75. P. A. Tresco, S. R. Winn, S. Tan, C. B. Jaeger, L. A. Greene and P. Aebischer, *Cell Transplant.*, 1992, **1**, 255–264.
76. S. R. Winn, P. Aebischer and P. M. Galletti, *J. Biomed. Mater. Res.*, 1989, **23**, 31–44.
77. P. Aebischer, M. Goddard, A. P. Signore and R. L. Timpson, *Exp. Neurol.*, 1994, **126**, 151–158.
78. P. Aebischer, M. Schluep, N. Deglon, J.-M. Joseph, L. Hirt, B. Heyd, M. Goddard, J. P. Hammang, A. D. Zurn, A. C. Kato, F. Regli and E. E. Baetge, *Nat. Med.*, 1996, **2**, 696–699.
79. K. Zhang, J. J. Hopkins, J. S. Heier, D. G. Birch, L. S. Halperin, T. A. Albini, D. M. Brown, G. J. Jaffe, W. Tao and G. A. Williams, *Proc. Natl. Acad. Sci.*, 2011, **108**, 6241–6245.
80. J. Silver and M. Ogawa, *Science*, 1983, **220**, 1067–1069.
81. G. M. Smith, R. H. Miller and J. Silver, *J. Comp. Neurol.*, 1986, **251**, 23–43.
82. G. M. Smith, R. H. Miller and J. Silver, *Ann. N. Y. Acad. Sci.*, 1987, **495**, 185–205.
83. G. M. Smith and J. Silver, *Prog. Brain Res.*, 1988, **78**, 353–361.
84. M. Kliot, G. M. Smith, J. D. Siegal and J. Silver, *Exp. Neurol.*, 1990, **109**, 57–69.
85. D. J. Schreyer and E. G. Jones, *Dev. Brain Res.*, 1987, **35**, 291–299.
86. J. D. Houle and J. E. Johnson, *Neurosci. Lett.*, 1989, **103**, 17–23.
87. S. Woerly, *Biomaterials*, 1993, **14**, 1056–1058.
88. S. Woerly and R. Marchand, *Restor. Neurol. Neurosci.*, 1990, **1**, 369–385.
89. S. Woerly and D. J. Morassutti, *Neurosurg. Rev.*, 1993, **16**, 93–104.
90. S. Woerly and R. Marchand, *Restor. Neurol. Neurosci.*, 1991, **3**, 95–99.
91. R. Marchand and S. Woerly, *Neuroscience*, 1990, **36**, 45–60.
92. M. A. Anderson, J. E. Burda, Y. Ren, Y. Ao, T. M. O'Shea, R. Kawaguchi, G. Coppola, B. S. Khakh, T. J. Deming and M. V. Sofroniew, *Nature*, 2016, **532**, 195–200.
93. Y. D. Teng, E. B. Lavik, X. Qu, K. I. Park, J. Ourednik, D. Zurakowski, R. Langer and E. Y. Snyder, *Proc. Natl. Acad. Sci.*, 2002, **99**, 3024–3029.
94. H. E. Olson, G. E. Rooney, L. Gross, J. J. Nesbitt, K. E. Galvin, A. Knight, B. Chen, M. J. Yaszemski and A. J. Windebank, *Tissue Eng., Part A*, 2009, **15**, 1797–1805.
95. M. J. Moore, J. A. Friedman, E. B. Lewellyn, S. M. Mantila, A. J. Krych, S. Ameenuddin, A. M. Knight, L. Lu, B. L. Currier, R. J. Spinner, R. W. Marsh, A. J. Windebank and M. J. Yaszemski, *Biomaterials*, 2006, **27**, 419–429.
96. C. D. Pritchard, J. R. Slotkin, D. Yu, H. Dai, M. S. Lawrence, R. T. Bronson, F. M. Reynolds, Y. D. Teng, E. J. Woodard and R. S. Langer, *J. Neurosci. Methods*, 2010, **188**, 258–269.
97. G. W. Plant, A. R. Harvey and T. V. Chirila, *Brain Res.*, 1995, **671**, 119–130.
98. N. K. Loh, S. Woerly, S. M. Bunt, S. D. Wilton and A. R. Harvey, *Exp. Neurol.*, 2001, **170**, 72–84.
99. P. Prang, R. Müller, A. Eljaouhari, K. Heckmann, W. Kunz, T. Weber, C. Faber, M. Vroemen, U. Bogdahn and N. Weidner, *Biomaterials*, 2006, **27**, 3560–3569.

100. N. Theodore, R. Hlubek, J. Danielson, K. Neff, L. Vaickus, T. R. Ulich and A. E. Ropper, *Neurosurgery*, 2016, **79**, E305–E312.
101. P. Lu, G. Woodruff, Y. Wang, L. Graham, M. Hunt, D. Wu, E. Boehle, R. Ahmad, G. Poplawski, J. Brock, L. S. B. Goldstein and M. H. Tuszynski, *Neuron*, 2014, **83**, 789–796.
102. K. Kadoya, P. Lu, K. Nguyen, C. Lee-Kubli, H. Kumamaru, L. Yao, J. Knackert, G. Poplawski, J. N. Dulin, H. Strobl, Y. Takashima, J. Biane, J. Conner, S.-C. Zhang and M. H. Tuszynski, *Nat. Med.*, 2016, **22**, 479–487.
103. S. M. Willerth, K. J. Arendas, D. I. Gottlieb and S. E. Sakiyama-Elbert, *Biomaterials*, 2006, **27**, 5990–6003.
104. T. S. Wilems, J. Pardieck, N. Iyer and S. E. Sakiyama-Elbert, *Acta Biomater.*, 2015, **28**, 23–32.
105. D. A. McCreedy, T. S. Wilems, H. Xu, J. C. Butts, C. R. Brown, A. W. Smith and S. E. Sakiyama-Elbert, *Biomater. Sci.*, 2014, **2**, 1672–1682.
106. P. J. Johnson, A. Tatara, A. Shiu and S. E. Sakiyama-Elbert, *Cell Transplant.*, 2010, **19**, 89–101.
107. D. Gupta, C. H. Tator and M. S. Shoichet, *Biomaterials*, 2006, **27**, 2370–2379.
108. B. G. Ballios, M. J. Cooke, L. Donaldson, B. L. Coles, C. M. Morshead, D. van der Kooy and M. S. Shoichet, *Stem Cell Rep.*, 2015, **4**, 1031–1045.
109. B. G. Ballios, M. J. Cooke, D. van der Kooy and M. S. Shoichet, *Biomaterials*, 2010, **31**, 2555–2564.
110. A. J. Mothe, R. Y. Tam, T. Zahir, C. H. Tator and M. S. Shoichet, *Biomaterials*, 2013, **34**, 3775–3783.
111. P. Moshayedi and S. T. Carmichael, *Biomatter*, 2013, **3**, e23863.
112. J. Zhong, A. Chan, L. Morad, H. I. Kornblum, G. Fan and S. T. Carmichael, *Neurorehabil. Neural Repair*, 2010, **24**, 636–644.
113. J. Lam, W. E. Lowry, S. T. Carmichael and T. Segura, *Adv. Funct. Mater.*, 2014, **24**, 7053–7062.
114. Y.-E. Ju, P. A. Janmey, M. E. McCormick, E. S. Sawyer and L. A. Flanagan, *Biomaterials*, 2007, **28**, 2097–2108.
115. C. J. Medberry, P. M. Crapo, B. F. Siu, C. A. Carruthers, M. T. Wolf, S. P. Nagarkar, V. Agrawal, K. E. Jones, J. Kelly, S. A. Johnson, S. S. Velankar, S. C. Watkins, M. Modo and S. F. Badylak, *Biomaterials*, 2013, **34**, 1033–1040.
116. P. M. Crapo, C. J. Medberry, J. E. Reing, S. Tottey, Y. van der Merwe, K. E. Jones and S. F. Badylak, *Biomaterials*, 2012, **33**, 3539–3547.
117. C.-Y. Yang, B. Song, Y. Ao, A. P. Nowak, R. B. Abelowitz, R. A. Korsak, L. A. Havton, T. J. Deming and M. V. Sofroniew, *Biomaterials*, 2009, **30**, 2881–2898.
118. A. P. Nowak, V. Breedveld, L. Pakstis, B. Ozbas, D. J. Pine, D. Pochan and T. J. Deming, *Nature*, 2002, **417**, 424–428.
119. B. Song, J. Song, S. Zhang, M. A. Anderson, Y. Ao, C.-Y. Yang, T. J. Deming and M. V. Sofroniew, *Biomaterials*, 2012, **33**, 9105–9116.
120. S. Zhang, M. A. Anderson, Y. Ao, B. S. Khakh, J. Fan, T. J. Deming and M. V. Sofroniew, *Biomaterials*, 2014, **35**, 1989–2000.

121. S. Zhang, J. E. Burda, M. A. Anderson, Z. Zhao, Y. Ao, Y. Cheng, Y. Sun, T. J. Deming and M. V. Sofroniew, *ACS Biomater. Sci. Eng.*, 2015, **1**, 705–717.
122. S. Zhang, D. J. Alvarez, M. V. Sofroniew and T. J. Deming, *Biomacromolecules*, 2015, **16**, 1331–1340.
123. I. Elliott Donaghue, R. Tam, M. V. Sefton and M. S. Shoichet, *J. Controlled Release*, 2014, **190**, 219–227.
124. T.-Y. Cheng, M.-H. Chen, W.-H. Chang, M.-Y. Huang and T.-W. Wang, *Biomaterials*, 2013, **34**, 2005–2016.
125. C. T. S. Wong Po Foo, J. S. Lee, W. Mulyasasmita, A. Parisi-Amon and S. C. Heilshorn, *Proc. Natl. Acad. Sci.*, 2009, **106**, 22067–22072.
126. L. Cai, R. E. Dewi and S. C. Heilshorn, *Adv. Funct. Mater.*, 2015, **25**, 1344–1351.
127. B. A. Aguado, W. Mulyasasmita, J. Su, K. J. Lampe and S. C. Heilshorn, *Tissue Eng., Part A*, 2011, **18**, 806–815.
128. C. Yan, M. E. Mackay, K. Czymmek, R. P. Nagarkar, J. P. Schneider and D. J. Pochan, *Langmuir*, 2012, **28**, 6076–6087.
129. S. P. Massia and J. A. Hubbell, *Anal. Biochem.*, 1990, **187**, 292–301.
130. H. Lee, J. Rho and P. B. Messersmith, *Adv. Mater.*, 2009, **21**, 431–434.
131. J. E. Burda and M. V. Sofroniew, *Neuron*, 2014, **81**, 229–248.
132. D. Yu, W. L. Neeley, C. D. Pritchard, J. R. Slotkin, E. J. Woodard, R. Langer and Y. D. Teng, *Stem Cells*, 2009, **27**, 1212–1222.
133. D. M. C. Sharp, A. Picken, T. J. Morris, C. J. Hewitt, K. Coopman and N. K. H. Slater, *Cryobiology*, 2013, **67**, 305–311.
134. R. C. Deller, M. Vatish, D. A. Mitchell and M. I. Gibson, *Nat. Commun.*, 2014, **5**, 324.
135. C. F. Adams, A. Rai, G. Sneddon, H. H. P. Yiu, B. Polyak and D. M. Chari, *Nanomedicine*, 2015, **11**, 19–29.
136. M. Song, Y. J. Kim, Y. H. Kim, J. Roh, S. U. Kim and B. W. Yoon, *Hum. Gene Ther.*, 2010, **21**, 603–610.
137. V. Vanecek, V. Zablotskii, S. Forostyak, J. Ruzicka, V. Herynek, M. Babic, P. Jendelova, S. Kubinova, A. Dejneka and E. Sykova, *Int. J. Nanomed.*, 2012, **7**, 3719–3730.
138. T. C. Lim, S. Rokkappanavar, W. S. Toh, L. S. Wang, M. Kurisawa and M. Spector, *FASEB J.*, 2013, **27**, 1023–1033.
139. I. K. Ko, S. J. Lee, A. Atala and J. J. Yoo, *Exp. Mol. Med.*, 2013, **45**, e57.
140. H. Li, A. M. Koenig, P. Sloan and N. D. Leipzig, *Biomaterials*, 2014, **35**, 9049–9057.
141. K. Saha, A. J. Keung, E. F. Irwin, Y. Li, L. Little, D. V. Schaffer and K. E. Healy, *Biophys. J.*, 2008, **95**, 4426–4438.
142. P. C. Georges, W. J. Miller, D. F. Meaney, E. S. Sawyer and P. A. Janmey, *Biophys. J.*, 2006, **90**, 3012–3018.
143. J. A. Burdick and W. L. Murphy, *Nat. Commun.*, 2012, **3**, 1269.
144. F. Gattazzo, A. Urciuolo and P. Bonaldo, *Biochim. Biophys. Acta, Gen. Subj.*, 2014, **1840**, 2506–2519.
145. D. S. W. Benoit, M. P. Schwartz, A. R. Durney and K. S. Anseth, *Nat. Mater.*, 2008, **7**, 816–823.

146. Y. Tsai, J. Cutts, A. Kimura, D. Varun and D. A. Brafman, *Stem Cell Res.*, 2015, **15**, 75–87.
147. X. Liu, Y. Wang, J. He, X.-M. Wang, F.-Z. Cui and Q.-Y. Xu, *Front. Mater. Sci.*, 2011, **5**, 358–366.
148. A. J. Vegas, O. Veiseh, J. C. Doloff, M. Ma, H. H. Tam, K. Bratlie, J. Li, A. R. Bader, E. Langan, K. Olejnik, P. Fenton, J. W. Kang, J. Hollister-Locke, M. A. Bochenek, A. Chiu, S. Siebert, K. Tang, S. Jhunjhunwala, S. Aresta-Dasilva, N. Dholakia, R. Thakrar, T. Vietti, M. Chen, J. Cohen, K. Siniakowicz, M. Qi, J. McGarrigle, S. Lyle, D. M. Harlan, D. L. Greiner, J. Oberholzer, G. C. Weir, R. Langer and D. G. Anderson, *Nat. Biotechnol.*, 2016, **34**, 345–352.
149. A. J. Vegas, O. Veiseh, M. Gurtler, J. R. Millman, F. W. Pagliuca, A. R. Bader, J. C. Doloff, J. Li, M. Chen, K. Olejnik, H. H. Tam, S. Jhunjhunwala, E. Langan, S. Aresta-Dasilva, S. Gandham, J. J. McGarrigle, M. A. Bochenek, J. Hollister-Lock, J. Oberholzer, D. L. Greiner, G. C. Weir, D. A. Melton, R. Langer and D. G. Anderson, *Nat. Med.*, 2016, **22**, 306–311.
150. S. Jiang and Z. Cao, *Adv. Mater.*, 2010, **22**, 920–932.
151. A. D. Gaudet and P. G. Popovich, *Exp. Neurol.*, 2014, **258**, 24–34.
152. M. Preston and L. S. Sherman, *Front. Biosci. (Schol. Ed.)*, 2011, **3**, 1165–1179.
153. R. van den Brand, J. Heutschi, Q. Barraud, J. DiGiovanna, K. Bartholdi, M. Huerlimann, L. Friedli, I. Vollenweider, E. M. Moraud, S. Duis, N. Dominici, S. Micera, P. Musienko and G. Courtine, *Science*, 2012, **336**, 1182–1185.
154. K. C. Cowley, B. J. MacNeil, J. W. Chopek, S. Sutherland and B. J. Schmidt, *Exp. Neurol.*, 2015, **264**, 174–187.
155. Z. Zhang, M. Rouabhia, Z. Wang, C. Roberge, G. Shi, P. Roche, J. Li and L. H. Dao, *Artif. Organs*, 2007, **31**, 13–22.
156. C. E. Schmidt, V. R. Shastri, J. P. Vacanti and R. Langer, *Proc. Natl. Acad. Sci.*, 1997, **94**, 8948–8953.
157. V. Guarino, M. A. Alvarez-Perez, A. Borriello, T. Napolitano and L. Ambrosio, *Adv. Healthcare Mater.*, 2013, **2**, 218–227.
158. A. Fabbro, M. Prato and L. Ballerini, *Adv. Drug Delivery Rev.*, 2013, **65**, 2034–2044.
159. F. Pires, Q. Ferreira, C. A. V. Rodrigues, J. Morgado and F. C. Ferreira, *Biochim. Biophys. Acta, Gen. Subj.*, 2015, **1850**, 1158–1168.
160. E. Jan and N. A. Kotov, *Nano Lett.*, 2007, **7**, 1123–1128.
161. C. Gumera, B. Rauck and Y. Wang, *J. Mater. Chem.*, 2011, **21**, 7033–7051.
162. J. Gao, Y. M. Kim, H. Coe, B. Zern, B. Sheppard and Y. Wang, *Proc. Natl. Acad. Sci.*, 2006, **103**, 16681–16686.
163. G. M. Thomsen, G. Gowing, S. Svendsen and C. N. Svendsen, *Exp. Neurol.*, 2014, **262**(Pt B), 127–137.
164. A. J. Mothe and C. H. Tator, *J. Clin. Invest.*, 2012, **122**, 3824–3834.
165. D. Kalladka, J. Sinden, K. Pollock, C. Haig, J. McLean, W. Smith, A. McConnachie, C. Santosh, P. M. Bath, L. Dunn and K. W. Muir, *Lancet*, 2016, **388**, 787–796.

166. S. D. Schwartz, C. D. Regillo, B. L. Lam, D. Eliott, P. J. Rosenfeld, N. Z. Gregori, J.-P. Hubschman, J. L. Davis, G. Heilwell, M. Spirn, J. Maguire, R. Gay, J. Bateman, R. M. Ostrick, D. Morris, M. Vincent, E. Anglade, L. V. Del Priore and R. Lanza, *Lancet*, 2015, **385**, 509–516.
167. A. L. Berkowitz, M. B. Miller, S. A. Mir, D. Cagney, V. Chavakula, I. Guleria, A. Aizer, K. L. Ligon and J. H. Chi, *N. Engl. J. Med.*, 2016, **375**, 196–198.
168. A. French, C. Bravery, J. Smith, A. Chandra, P. Archibald, J. D. Gold, N. Artzi, H.-W. Kim, R. W. Barker, A. Meissner, J. C. Wu, J. C. Knowles, D. Williams, G. García-Cardeña, D. Sipp, S. Oh, J. F. Loring, M. S. Rao, B. Reeve, I. Wall, A. J. Carr, K. Bure, G. Stacey, J. M. Karp, E. Y. Snyder and D. A. Brindley, *Stem Cells Transl. Med.*, 2015, **4**, 217–223.
169. D. F. Emerich, G. Orive, C. Thanos, J. Tornoe and L. U. Wahlberg, *Adv. Drug Delivery Rev.*, 2014, **67–68**, 131–141.
170. ASTM, *ASTM Int.*, 2013, vol. ASTM F2150–13.
171. K. Dooley, Y. H. Kim, H. D. Lu, R. Tu and S. Banta, *Biomacromolecules*, 2012, **13**, 1758–1764.

CHAPTER 20

Smart Multifunctional Tissue Engineering Scaffolds

QILONG ZHAO[a] AND MIN WANG*[a]

[a]Department of Mechanical Engineering, The University of Hong Kong, Pokfulam Road, Hong Kong, China
*E-mail: memwang@hku.hk

20.1 Introduction

Human body tissues and organs encounter many medical problems, such as disease, lesions, trauma and aging, which require appropriate therapy for repair or regeneration. At present, severe dysfunctions or massive loss of human body tissues or organs are normally treated by prosthesis implantation or organ transplantation. However, implanted prostheses cannot perfectly substitute the original human body tissues or organs and will degrade gradually after implantation and hence a second surgery is often required. As for the use of donated organs, immune rejection and risk of infection are inherent problems. Besides, there is a large gap in the numbers between patients on the organ transplantation waiting list and available donated organs. To address the drawbacks of these medical treatments, tissue engineering, also termed "regenerative medicine", has emerged in recent decades, offering an alternative or advanced therapy for treating diseases or defects in human body tissues and organs.[1–3] Tissue engineering, which requires multidisciplinary efforts in biology, chemistry, physics, engineering and medicine, has attracted worldwide attention. The structure and functions of human

Smart Materials No. 25
Smart Materials for Tissue Engineering: Applications
Edited by Qun Wang

Published by the Royal Society of Chemistry, www.rsc.org

body tissues can be restored, maintained, or remodelled by applying suitable tissue engineering strategies. Unlike conventional approaches which use non-viable materials for tissue substitutes, tissue engineering aims to utilize bioactive materials/scaffolds for better promoting the native tissue regeneration process or to build artificial, live tissue-like constructs for implantation.

With our increasing knowledge in the life sciences and the rapid development in manufacture technology, tissue engineering has achieved some degree of success for the regeneration of human body tissues with relatively simple structures, such as skin,[4,5] cartilage,[6,7] and bone.[8,9] However, due to the high complexity of the structures and functions of some body tissues and solid organs and the complex tissue regeneration process in human bodies, many problems in tissue engineering still require major research efforts.[10–13] In particular, the regeneration and remodelling of whole organs with complex structures and complicated physiological functions pose great challenges.[14–16] Biomaterials or bioactive constructs built for the regeneration or remodelling of these complex human body tissues should be carefully designed and fabricated, and sometimes need to be "smart" and "multifunctional" to meet specific clinical requirements.

This chapter focuses on the advances in tissue engineering scaffolds for promoting tissue regeneration, including new biomaterials as well as technologies for scaffold manufacture, with an emphasis on the recent progress in smart multifunctional tissue engineering scaffolds. Various smart multifunctional tissue engineering scaffolds can be fabricated using different novel techniques, which exhibit superior properties for tissue regeneration.

20.2 Materials and Fabrication Techniques for Tissue Engineering Scaffolds

20.2.1 Tissue Engineering Strategies

There are three key components in human body tissues that determine the native tissue regeneration process, which are the cell, bio-signals and extracellular matrix (ECM). With different emphases, different tissue engineering strategies, including cell-based tissue engineering, factor-based tissue engineering and scaffold-based tissue engineering, have been investigated and developed.

In cell-based tissue engineering, cells or cell clusters are normally introduced into the defect sites of diseased or damaged tissues for assisting tissue regeneration.[17] Sources of cells for implantation include autologous cells from the patients themselves, allogeneic cells from human donors, and xenogeneic cells from other species. Since the utilization of xenogeneic cells for tissue repair have the risk of transmitting animal pathogens to humans,[10] allogeneic cells or autologous adult cells are commonly selected. However, cells or cell clusters alone are not adequate for the repair of large defects of human body tissues due to their low structural stability. Scaffolds are usually used to provide mechanically stable platforms for cell incorporation and to

subsequently make cell-laden constructs for implantation. For example, neonatal dermal fibroblasts obtained from humans (either the patients themselves or other people) can be cultured on a porous biodegradable scaffold and then incubated in a customized bioreactor. After cell expansion, the cell-laden constructs formed, which resemble the dermal layer of skin, can be employed for skin transplantation.[18]

To engineer complex tissue-like multicellular constructs *via* a cell-based strategy, a novel method, namely cell assembly, has been developed.[19] Different types of living cells were assembled to a multicellular system through the bonding of DNA strands pre-grafted on the cell membrane. Also, a cell sheeting technique has been investigated for building laminated multicellular structures at the tissue level.[20] In the cell sheeting approach, cells are accumulated and expanded on a film coated by ECM proteins to form a cell monolayer. After repeating this cell accumulation procedure, multilayered cell sheets can be made through this bottom-up approach. The number of layers, cell type, and cell location can be controlled. And the ingrowth of vascular structures can be achieved with the accumulation of endothelial cells in interlayers, which shows great promise in making living substitutes for laminated tissues such as skin.

Stem cells are attracting increasing attention now in regenerative medicine for their high capabilities of self-renewal and specialized progeny.[21] Stem cells play a vital role in the tissue regeneration process. When injury, disease or damage occurs in human tissues, stem cells will release suitable bio-signals to activate surrounding cells, proliferate and differentiate towards specific cell lineages for assisting tissue regeneration. In cell-based tissue engineering, appropriate stem cells can be implanted into the defects of target tissues to work as either the factory of bio-signals or the cell source for directing the regeneration or neo-formation of human body tissues. Categorized by their different sources, stem cells include embryonic stem cells, adult stem cells, and induced pluripotent stem cells (iPSCs). Embryonic stem cells derived from blastocysts are pluripotent and can differentiate to any cell lineages. But the use of embryonic stem cells has problems such as limited cell sources, immune tolerance and controversial ethical issues. Adult stem cells have the capability to differentiate towards specialized cell lineages, which have been widely employed for the regeneration of different body tissues. But the relatively low self-renewal of adult stem cells *in vitro* leads to the difficulty to yield adult stem cells with clinically useful cell numbers. In comparison, iPSCs hold greater promise since they have similar properties to embryonic stem cells but a wider cell source, which can be derived from adult cells, such as somatic skin fibroblasts.[22] Moreover, the self-renewal potential of iPSCs in cell culture is unlimited, which makes the *in vitro* massive expansion of iPSCs for tissue regeneration feasible.

In the tissue regeneration process, bio-signals such as growth factors, chemokines, and cytokines, are important factors in directing cell functions, which have been predominantly used in factor-based tissue engineering to modulate cell behaviours *in vitro*. In particular, growth factors are widely

used due to their direct and obvious effects on promoting tissue regeneration.[23] Growth factors are mostly proteins which can affect various cell behaviours, including cell proliferation, migration, differentiation, *etc.* Normally, growth factors can be produced by healthy cells for repairing diseased or damaged tissues and organs by the human body itself. However, when tissues have low capability of self-regeneration or the regeneration process does not occur naturally, appropriate growth factors need to be provided exogenously for properly activating cell functions and simultaneously promoting tissue regeneration. Different types of growth factors have different biological effects on affecting cell functions, which are summarized in Table 20.1. Appropriate administration of specific growth factors into the human

Table 20.1 Biological activity of major growth factors for tissue regeneration.

Growth factors	Abbreviation	Primary activity
Bone morphogenetic protein-2	BMP-2	Osteoinductive agent that stimulates chondrogenic differentiation of MSCs and induces endochondral bone formation
Bone morphogenetic protein-7	BMP-7	Osteoinductive agent and stimulating cartilage maturation
Epidermal growth factor	EGF	Promoting proliferation of mesenchymal, glial and epithelial cells
Basic fibroblast growth factor	bFGF	Promoting proliferation of many cell types, inhibiting some stem cells and inducing mesoderm to form in early embryos
Insulin-like growth factor-I	IGF-I	Promoting proliferation of many cell types
Insulin-like growth factor-II	IGF-II	Promoting proliferation of many cell types primarily of fetal origin
Nerve growth factor	NGF	Promoting neurite outgrowth and neural cell survival
Platelet-derived growth factor-BB	PDGF-BB	Promoting proliferation of connective tissue, glial and smooth muscle cells
Transforming growth factor-beta	TGF-β	Anti-inflammatory, promoting wound healing and inhibiting macrophage and lymphocyte proliferation
Vascular endothelial growth factor	VEGF	Regulating blood vessel formation, stimulates skeletal muscle regeneration, regulating endothelial cell proliferation, angiogenesis, and vascular permeability

body can facilitate the native regeneration process of diseased or damaged tissues and organs, whereas the improper utilization of growth factors may incur carcinogenic risks.

Owing to the crucial role of the ECM in the native tissue regeneration process, numerous efforts have been made to form artificial ECM with similar structure and functions for promoting tissue regeneration, which leads to "scaffold-based tissue engineering". Tissue engineering scaffolds can be developed as the structural platform for cell incorporation and as the reservoir for the delivery of bio-signals. For achieving good regenerative effects, the structure and properties of tissue engineering scaffolds should be well designed and controlled. The materials for scaffolds and fabrication techniques for scaffold manufacture should be carefully considered.

20.2.2 Materials for Tissue Engineering Scaffolds

For achieving good cell incorporation and suitable host responses upon implantation in the human body, materials for making tissue engineering scaffolds should be firstly biocompatible. And to avoid a second surgery, the degradability of tissue engineering scaffolds is required. A series of biocompatible and biodegradable synthetic polymers, such as poly(lactic acid) (PLA), poly(glycolic acid) (PGA), poly(ε-caprolactone) (PCL), poly(hydroxybutyrate-*co*-hydroxyvalerate) (PHBV), and co-polymers poly(lactic-*co*-glycolic acid) (PLGA) and poly(lactic acid-*co*-caprolactone) (PLACL), have been widely used for making tissue engineering scaffolds to meet these two requirements.[24] Most of these synthetic polymers have been approved by the U.S. Food and Drug Administration (FDA) for biomedical applications. These polymers are either crystalline or amorphous, which exhibit different properties under mechanical loading and in degradation. The biological performance of tissue engineering scaffolds is influenced by the synthetic polymers used. For example, PCL and PLGA scaffolds formed by the same fabrication technique were examined for bone tissue engineering.[25] The PCL scaffolds with relatively slow degradation rate showed a tendency to regenerate more dense bone tissues as compared to the PLGA scaffolds. Besides, due to the high elastic modulus of PLGA over PCL, urinary tract stromal cells cultured on the PLGA scaffolds were found to exhibit a contractile phenotype and a relatively low proliferation rate, while the PCL scaffolds formed under the same conditions showed better potential for the tissue engineering of the bladder and other soft tissues.[26] Some biocompatible and water-soluble synthetic polymers, such as poly(vinyl alcohol) (PVA), poly(ethylene glycol) (PEG) and poly(ethylene oxide) (PEO), are also widely used to make blends with biodegradable polymers for the manufacture of tissue engineering scaffolds, where the properties and structure of scaffolds are modified.

Enzymatically degradable natural polymers such as proteins, polysaccharides, lipids and polynucleotides, are also suitable materials for tissue engineering scaffolds. These natural polymers usually have superior biocompatibility. However, tissue engineering scaffolds made of natural polymers

are limited by their poor physical and mechanical properties, which may be improved through appropriate post-treatments such as crosslinking. Another common problem for scaffolds made of allogeneic or xenogeneic sourced natural polymers is the immune rejection by patients, which demands an additional procedure for minimizing the immunogenicity of materials.[27] De-cellularized ECMs are the best nature-simulating scaffolds with totally preserved structural cues and residual growth factors, which are effective for the regeneration or neo-formation of tissues with an identical or similar structure.[28] However, using de-cellularized ECMs as tissue engineering scaffolds also has limitations.[29] The sources for obtaining adequate de-cellularized ECM are limited. Moreover, due to the dense structure of de-cellularized ECM, it is hard to achieve homogeneous cell distribution in the scaffolds. And the incomplete removal of antigenic components for de-cellularized ECM could cause severe problems for patients.

In recent decades, bioactive materials such as bioceramics have emerged as "new materials" for tissue engineering scaffolds with specific bioactivity. Commonly used bioceramics include hydroxyapatite (HA) and bioactive calcium phosphates (Ca-P) such as tricalcium phosphate (TCP) and biphasic calcium phosphate (BCP, which contains HA and TCP in different proportions), which exhibit osteoconductive capabilities in promoting osteoblast growth and the mineralization process.[30] Among them, TCP and BCP are biodegradable, which holds great promise for bone tissue engineering. The biocompatibility of tissue engineering scaffolds made by bioceramics can be improved through surface modification using natural polymers such as collagen.[31] For making tissue engineering scaffolds with optimized properties, synthetic polymers, natural polymers and bioceramics should be carefully selected. Appropriate composite or hybridization approaches are also promising.[32–35]

20.2.3 Technologies for Scaffold Manufacture

20.2.3.1 Conventional Techniques

Technologies used for scaffold manufacture play a major role in affecting the properties of resultant tissue engineering scaffolds. For achieving good cell incorporation, the structure of scaffolds should be three-dimensional (3D) and highly porous, which can allow the migration and growth of cells. Various common techniques for making porous tissue engineering scaffolds, such as particulate leaching/solvent casting, gas foaming and phase separation, have been developed and are discussed here.

In the particulate leaching/solvent casting process, suitable porogens of appropriate average size (usually water-soluble inorganic compounds such as NaCl and/or sugars) are firstly added to a polymer solution of proper viscosity to form a solid polymer–porogen mixture in a mold. Highly porous scaffolds are then fabricated by the subsequent leaching of porogens through an immersion treatment using a suitable liquid. This technique takes advantage

of the insolubility of porogens in the organic solvent of a polymer solution. And the porogens can be selectively removed through immersion treatment, which leaves the water-insoluble polymer component with a highly porous structure. Porous and biodegradable polymer scaffolds fabricated by solvent casting/particulate leaching using grinded NaCl particles as porogens were investigated for tissue engineering scaffold fabrication, which showed high cost-effectiveness.[36] However, it is difficult to use the solvent casting/particulate leaching technique for making porous scaffolds with homogeneous and interconnected pores. And the pore size in the scaffolds, which was highly dependent on the size of porogens, could not be easily adjusted. Besides, the properties of scaffolds, particularly their mechanical properties, would be degraded during the salt leaching process. The cytotoxicity of residual porogens and the difficulty of incorporating bio-signals (*e.g.* growth factors) both limit the application of the solvent casting/particulate leaching technique for tissue engineering scaffold fabrication.

The gas foaming technique is another frequently used method for porous tissue engineering scaffold fabrication. A typical gas foaming process involves an inflation process to dissolve gas molecules (*e.g.* nitrogen, helium and carbon dioxide) with high pressure into a polymer solution or molten polymer and a subsequent deflation process to let the gas pressure return to ambient pressure, which leads to the release of gas molecules from the polymer matrix. In the inflation–deflation process, gas molecules tend to form clusters for minimizing their free energy, and pores are consequently formed with the escape and diffusion of gas molecules to the surroundings. The inflation process causes a significant expansion of the polymer volume, which results in final polymer scaffolds with a highly porous structure (*e.g.* 95%).[37] The gas foaming process is influenced by different processing parameters, including the type of gas used and the molecular weight of the raw polymer. Compared to nitrogen and helium, carbon dioxide has been found to be a better foaming agent as the scaffolds formed possessed a more porous structure, which was supposed to result from the higher intermolecular interactions between carbon dioxide and the carbonyl groups of commonly used polymers (*e.g.* PLGA).[38] Polymers with a relatively low molecular weight (low intrinsic viscosity) used in the gas foaming process result in scaffolds with high porosity, which is caused by the more homogeneous distribution of gas molecules in the inflation process.[39] However, pores in the scaffolds formed by gas foaming are usually closed pores, not interconnected with one another. With the assistance of solvent casting/particulate leaching, the porosity and pore structure of scaffolds produced by gas foaming can be significantly improved.[40] In this hybrid process, polymers and porogens are pre-mixed in a suitable ratio and homogeneously mixed prior to the inflation process. Additional immersion treatment is performed after the deflation process for removing the embedded porogens. Scaffolds made by this hybrid method are sponge-like and highly porous, and the pores formed in the scaffolds are open and interconnected.

The formation of interconnected pores is important for porous scaffolds in tissue engineering, since the interconnected pores can provide space for cell metabolism and cell contacts. Developing simple and effective methods for fabricating scaffolds with open porous structures is thus crucial in regenerative medicine. Through thermally induced phase separation (TIPS), interconnected porous structures can be simply built, which makes TIPS popular for the fabrication of tissue engineering scaffolds.[41] In a typical TIPS process, the temperature of a polymer solution is reduced to a specific value to induce the separation of the original polymer solution into two phases: one is the polymer-rich phase with a high polymer concentration, and the other is the polymer-lean phase with a low polymer concentration. The solvent is subsequently removed through extraction, evaporation, or sublimation, which results in the formation of open pores in the polymer-lean phase and the solidification of polymer in the polymer-rich phase to form the scaffold skeleton. The properties of the polymer solution (particularly the solvent in the polymer solution) and the operating temperature strongly influence TIPS processes, causing either the solid–liquid phase separation process or liquid–liquid phase separation process to proceed. Biodegradable scaffolds with interconnected pores ranging from several micrometres to hundreds of micrometres can be made by TIPS,[42] which have been extensively investigated for tissue regeneration.

20.2.3.2 Additive Manufacture

While different conventional techniques have been investigated and developed for making porous tissue engineering scaffolds, the generation of scaffolds with customized shapes and well-controlled macro- to micro-architectures is generally difficult. With the emergence of different additive manufacturing techniques, which were initially developed in engineering fields for fabricating complex engineering parts, additive manufacturing has attracted the attention of researchers in the biomedical field. In recent decades, additive manufacture technologies have become popular for manufacturing tissue engineering scaffolds with complex, designed architectures.[43] Several specific types of additive manufacturing techniques have been investigated for making 3D porous tissue engineering scaffolds, which include melt extrusion/fused deposition modelling,[44] stereolithography,[45] inkjet printing,[46] and selective laser sintering (SLS).[47]

SLS is a popular additive manufacturing technique for making tissue engineering scaffolds due to its high efficiency and accuracy in building 3D porous structures.[48] The fabrication of tissue engineering scaffolds *via* SLS involves two steps: object modelling and object construction. For object modelling, a data file describing the 3D structural information of the target object is created, which can be obtained from a 3D computer model of the object created by either software or 3D images captured by modern medical imaging techniques, such as computed tomography (CT) or magnetic resonance imaging (MRI).[49] The data file created is then processed to be

sliced into many-layered two-dimensional (2D) files, which will be used for directing the operation of the hardware of a SLS machine. Subsequently, a 3D object is constructed through a computer controlled layer-by-layer (LBL) manufacturing process in the SLS machine. The raw materials to be used for making porous tissue engineering scaffolds *via* SLS can be either polymers or the composites of polymers and bioceramics, which must be in the form of granules with suitable sizes. The SLS machine consists of a part bed, a powder dispensing roller on one side of the part bed and a laser beam on the top. In a typical SLS object construction process, the part bed is preheated by the laser to a temperature just below the glass transition temperature of the polymer for reducing the energy required in the subsequent laser-caused fusion process of granules. A layer of powders is then spread over the part bed by the powder dispensing roller and subsequently fused by the laser scanning in a programed way to form a specific solidified 2D pattern in a layer. Afterwards, the part bed moves downward to a specific distance as programed and the powder dispensing roller travels over the part bed to deposit another layer of fresh powders on the solidified pattern, where another layer of a 2D pattern is built. Through repeating these procedures, scaffolds with designed architectures can be made LBL. Post-processing is then conducted to remove loose, un-sintered powders in the scaffolds. Through SLS, high-quality nanocomposite scaffolds with anatomy specific exterior architectures and totally interconnected porous interior architectures can be made for bone tissue engineering.[50]

20.2.3.3 Technologies for Fibrous Scaffolds

The structure of the ECM in human body tissues and organs is nanofibrous; tissue engineering scaffolds with ECM-like nanofibrous structures are therefore very attractive. Through some conventional scaffold manufacture techniques with specific modifications, scaffolds with fibrous structures can be made. For example, a novel solvent casting/particulate leaching technique with the assistance of a complex extrusion process has been studied for making scaffolds with fibrous structures.[51] Besides, polymer microspheres with nanofibrous topography could be fabricated by a novel concurrent surfactant-free emulsification and liquid–liquid phase separation method.[52] However, the fabrication of fibrous scaffolds using these techniques requires the use of special materials and hence have many limitations in the tissue engineering field. There is a clear requirement for an effective and versatile technique suitable for making fibrous tissue engineering scaffolds.

The self-assembly of suitable macromolecules through complex non-covalent interactions, such as van der Waals forces, electrostatic forces, hydrogen bonding and/or π stacking, is an effective bottom-up approach for making fibrous structures.[53] These self-assembly processes mimic the native formation process of ECM proteins and the self-assembled nanofibrous structures have been investigated for different tissue engineering applications.[54] However, nanofibrous structures formed by macromolecular self-assembly are

usually short in length and weak in mechanical properties, which result in difficulties in offering adequate structural cues to cells. Besides, the complex mechanisms involved make it difficult to control the nanofibrous structures formed by self-assembly.

In contrast, electrospinning, a mature engineering technique, can produce submicron- and nano-fibers in a simple manner using various materials (polymers, ceramics, and their composites) with desired efficiency,[55] which have been widely studied for making fibrous tissue engineering scaffolds.[56–58] The setup for conducting electrospinning is simple and low-cost; it consists of a syringe filled with precursor solution (usually polymer solution), a syringe pump for controlling the solution feeding rate, a high-voltage power supply, and a grounded collector. In a typical electrospinning process (Figure 20.1), droplets of the precursor solution flowing out of the syringe spinneret are stretched by the electrostatic force generated in the electric field between the metallic syringe spinneret connecting to the power supply and the grounded collector. The jetting of precursor solution then occurs when the electrostatic force overcomes the surface tension of droplets out of the spinneret. The solvent in the solution evaporates during the journey of the jet towards the collector, and fibers with diameters ranging from dozens of nanometres to tens of micrometres are finally collected. The morphology and structure (*e.g.*, fiber diameter, fiber uniformity, surface pore structure) of fibrous scaffolds formed by electrospinning are governed by different solution properties (*e.g.*, viscosity, conductivity, polymer molecular weight, and polymer

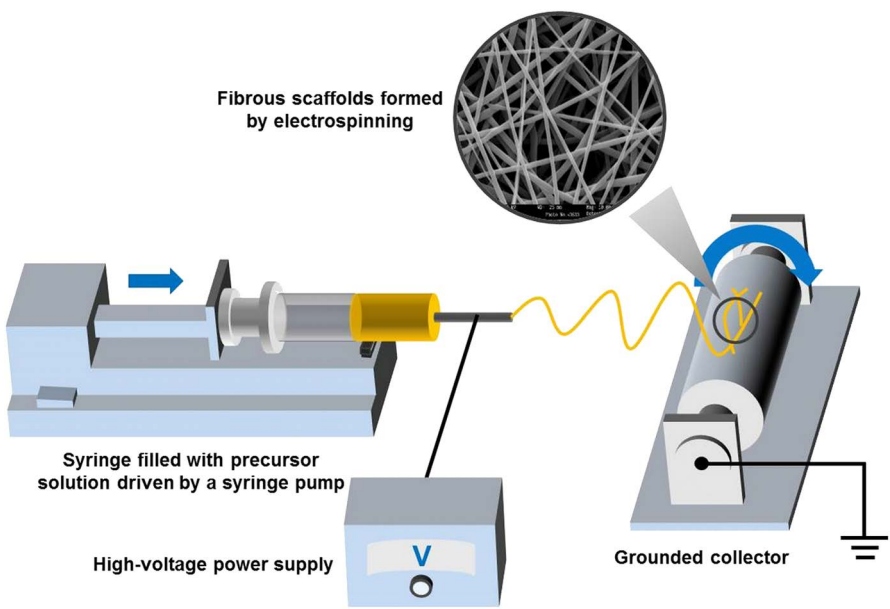

Figure 20.1 A schematic diagram illustrating the conventional electrospinning process.

solution concentration) and processing parameters (*e.g.*, feeding rate, field strength, nozzle configuration). Through specific electrospinning processes, scaffolds with either randomly oriented fibers or aligned fibers (parallel or radially oriented) can be fabricated.[59,60] Electrospun scaffolds with different fibrous architectures can cause different cell responses (*e.g.*, contraction or elongation) and result in different cell behaviours (*e.g.*, attachment, migration, proliferation, and differentiation). Through some modifications of electrospinning, such as blend electrospinning, emulsion electrospinning or coaxial electrospinning, bioactive agents can be incorporated in electrospun fibers, resulting in bioactive fibrous scaffolds with superior biological performance in promoting tissue regeneration.[61]

20.3 Design and Manufacture of Multifunctional Tissue Engineering Scaffolds

20.3.1 Complexity in Native Tissue Regeneration Process

In the human body, many tissues and organs have a regenerative capability for repairing and regenerating themselves even when there is no, or only a simple, therapeutic intervention involved. For instance, bone fractures and skin wounds below a critical size can self-heal. A healthy liver, with its complex structure and functions, can also regrow to its original size after being partially excised.[62] However, the regenerative capabilities of different tissues or for different individuals are different. For old-age people and patients with disorders or diseases in tissues, usually, the self-regenerative capability is not sufficient for repairing or regenerating lost tissues perfectly. Therapy for enhancing tissue regeneration is thus required. Tissue engineering aims to develop appropriate approaches for stimulating the innate regenerative potential of human tissues and organs that have insufficient regenerative capability. To achieve this goal, the native tissue regeneration process should be understood well.

For different types of human tissue, their regeneration processes have similarities and differences. For all the tissue regeneration processes, the involvement of cells, bio-signals, and the ECM and their interactions are important. But different cell lineages participate in the regeneration process of different human tissues. The spatiotemporal administration manners of multiple bio-signals are different in different tissue regeneration processes. Even for some human tissues with relatively simple structures, such as bones and blood vessels, their regeneration processes still involve complex biological processes with complicated interactions among cells, bio-signals and the matrix.

For instance, once a bone fracture occurs, inflammatory cells and fibroblasts will migrate towards the fracture site to form granulation tissue as the platform for the subsequent cell migration and vascular ingrowth in the early stage of healing. The collagen matrix is then mineralized by the osteoid secreted by osteoblasts to form a soft callus for repairing the lost bone in

the first 4–6 weeks. Eventually, bone remodelling is completed and the bone regrows to its original shape and strength in the subsequent months as parts of osteoblasts differentiate towards osteocytes in the new bone and osteoclasts works to remove the foci of damaged bone.[63] During the whole bone healing process, different types of growth factors are present in a sequential manner for regulating different cell functions.[64] For example, BMP-2 and VEGF are mainly expressed in the early stage for supporting the recruitment of osteoblasts and for vascular ingrowth, respectively. BMP-7 is a critical growth factor directing bone maturation in the late stage of the bone healing process. The sequential secretion of different growth factors is determined by specific cell–cell and cell–matrix interactions in the designated stage of bone healing. And any abnormal condition during the bone healing process may result in severe conditions such as osteoporosis and Paget's disease.[65] Likewise, the formation of new blood vessels is not a simple process and involves the participation of different cell lineages and growth factors.[66] In the early stage of new blood vessel formation, endothelial cells are recruited and self-organized into tube-like structures which are activated by the administration of VEGF. PDGF-BB is then expressed to stimulate the migration and proliferation of smooth muscle cells. Smooth muscle cells are coated on the outer layer of the endothelial tube to form matured new blood vessels.

20.3.2 Requirements for Multiple Functions of Scaffolds in Tissue Regeneration

Current tissue engineering strategies (*i.e.*, cell-based tissue engineering, factor-based tissue engineering and scaffold-based tissue engineering) for promoting tissue regeneration have their respective advantages. In all these strategies, tissue engineering scaffolds play a crucial role as structurally stable platforms in supporting cell attachment, cell growth and incorporation of bio-signals. In the human body, ECM is the natural "scaffold", directing the native tissue regeneration process. It is a highly difficult task to make "ideal" artificial scaffolds *ex vivo* that can recreate all the features of natural ECM due to its complexity in components and properties. Fortunately, suitable tissue engineering scaffolds with simplified ECM-mimicking characteristics can be appropriately designed and fabricated to meet specific requirements for properties and functions to affect cell behaviours, which can stimulate the innate regenerative potential of human body tissues and promote tissue regeneration.[67]

For achieving good therapeutic effects in promoting tissue regeneration, multiple properties and functions are required for tissue engineering scaffolds (Figure 20.2). First, scaffolds should be 3D and highly porous to offer space for cell incorporation and the ingrowth of cells from host tissues after implantation. The 3D and porous structure of scaffolds should have sufficient strength and rigidity to maintain their structural stability under mechanical loading. Second, materials used in making tissue engineering scaffolds should be biocompatible and scaffolds should have suitable

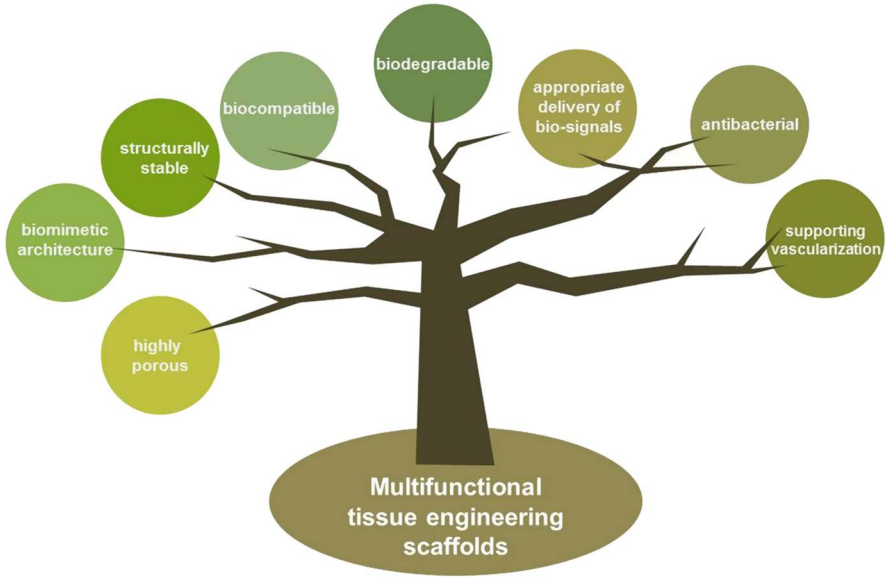

Figure 20.2 An illustration for the multiple requirements for advanced tissue engineering scaffolds.

surface chemistry in supporting cell attachment. Besides, scaffolds should degrade at a suitable rate to match the remodelling process of neo-tissue formation. The degradation process and the by-products generated during *in vivo* degradation of scaffolds should have no, or minimum, adverse effects on tissue regeneration and the host human body. For the new generation of biomaterials and tissue engineering scaffolds, both a suitable biodegradation property and good bioactivity are required.[11] For instance, bioactive scaffolds for bone tissue engineering should have osteoconductive capability in enhancing the growth of osteoblasts and the mineralization process and also osteoinductive potential in inducing the osteogenic differentiation of progenitor cells and stem cells.[68] Tissue engineering scaffolds should be both biodegradable and bioactive, which exhibit suitable properties in directing cell functions for better *in situ* tissue regeneration and can be gradually degraded within the entire tissue remodelling process. The most direct way to affect cell behaviours is to incorporate suitable bio-signals such as growth factors and genes into tissue engineering scaffolds.[69] Scaffolds functionalized with growth factors have been popular in tissue engineering.[70] According to the complexity of the native tissue regeneration process and the specific sequence of different growth factors administrated in certain tissue regeneration processes, multiple growth factors should be incorporated and the incorporated growth factors should be released in an appropriate spatiotemporal manner for different therapeutic purposes.[71] Although many growth-factor-incorporated scaffolds can provide good biological performance in directing cell functions and have achieved some degree of success

in promoting the regeneration of some human body tissues with relatively simple structures such as bones and blood vessels, the reconstruction and regeneration of whole functional tissues and organs such as the gastrointestinal tract, heart, lungs and kidneys, are still big challenges. These tissues and organs have complex multicellular structures, where different layers of tissues and organs consist of different types of cells with specific cell morphologies and cell arrangements.[13] Scaffolds for promoting the regeneration of these complex tissues and organs should possess biomimetic multilayer structures, in which different layers of scaffolds can have suitable properties for promoting the regeneration of specific tissue layers. Furthermore, in the tissue regeneration process, particularly for the regeneration of solid tissues with large thicknesses, the ingrowth of vascular structures, including blood vessels, lymphatic vessel and nerves, into the scaffolds after implantation is necessary for metabolism and specific functions. A "living" scaffold is required to achieve good vascularization.[72] Moreover, some additional functions, such as antibacterial or anticancer effects, are required for scaffolds used in specific clinical applications. Overall, "ideal" tissue engineering scaffolds should be multifunctional and exhibit appropriate characteristics in structure, physical properties, chemistry, biology, as well as good cell incorporation and bio-signal delivery.

20.3.3 Composite or Hybridization Approaches in Developing Multifunctional Tissue Engineering Scaffolds

As stated previously, tissue engineering scaffolds should be multifunctional to meet multiple requirements when used for promoting the regeneration of tissues and organs. It is very difficult or impossible to use one single biomaterial for scaffold fabrication and function to meet the multifunctional requirements for scaffolds. Composite or hybridization approaches are therefore being investigated and employed in developing multifunctional tissue engineering scaffolds. Due to the nano-composite nature of native bone, biodegradable and bioactive porous composite scaffolds have been extensively investigated for bone tissue engineering.[73] Bioactive bioceramics such as HA, TCP and BCP show good osteoconductive properties in enhancing osteogenesis. However, porous scaffolds made by neat bioceramics are fragile and lack sufficient elasticity,[74] which require improvement by using suitable biodegradable polymers. The addition of bioceramics in a polymer matrix also reinforces the mechanical strength and compressive modulus of neat polymer scaffolds. Popular techniques for producing porous composite scaffolds are developed on the basis of conventional techniques for making porous polymer scaffolds such as particulate leaching and phase separation/freeze-drying. In the particulate leaching process, a compound solution is used, which contains polymer solution, dispersed bioceramic particles and dispersed porogens.[32] Using different fabrication methods, various biodegradable and bioactive composite scaffolds such as HA/PCL,[75] HA/PHBV,[33] HA/PHBV/PLA,[34] HA/PLA/collagen,[76] TCP/PGA,[77] TCP/chitosan/gelatin,[78]

BCP/chitosan[79] and BCP/PCL[80] have been fabricated and studied for bone tissue engineering. Both the structure (*e.g.*, pore size, pore shape, pore interconnectivity, *etc.*) and components (*e.g.*, polymer, size of bioceramic particles, bioceramic content, dispersion of bioceramics in polymer matrix, *etc.*) of porous composite scaffolds influence their mechanical and degradation properties and also affect their biological performance for bone tissue engineering.[73] Due to limitations of various existing fabrication techniques, the formation of porous composite scaffolds with designed interconnected pores, biomimetic micro- to nano-architecture, customized shape, suitable mechanical properties, and good bioactivity is still challenging.

Apart from using the composite approach to enrich and improve the properties of tissue engineering scaffolds, hybridization strategies such as scaffold surface functionalization are alternatives to make scaffolds with specific functions. By tailoring the surface chemistry of tissue engineering scaffolds through techniques such as plasma treatment, interactions between scaffolds and proteins are affected as the wettability and surface charge of scaffolds are changed, which subsequently influences cell attachment on scaffolds.[81] The method more commonly used for the surface functionalization of tissue engineering scaffolds is to graft functional molecules onto the scaffold surface. Since cell behaviours, including cell polarization, spreading, migration, proliferation and differentiation, highly depend on the interactive signalling between cell integrin and the ECM,[82] ECM-adhesive proteins such as laminin and fibronectin or the short peptide sequences in the ECM-adhesive proteins affecting the cell binding such as YISGR (displayed in laminin) and tri-peptide arginine–glycine–aspartic acid (RGD, displayed in fibronectin) have been immobilized on the surface of tissue engineering scaffolds for improving the cell–scaffold anchorage, which is particularly important in directing cellular fate in a stem cell culture.[83] Growth factors play important roles in guiding cell functions in the tissue regeneration process. Surface functionalization using growth factors towards tissue engineering scaffolds has become popular for making bioactive scaffolds, where growth factors are commonly immobilized onto scaffold surfaces through covalent bonding.[84] The co-immobilization of growth factors, such as VEGF, and drug molecules, such as the anti-inflammatory and anti-thrombogenic drug acetylsalicylic acid, onto conventional biodegradable polymer scaffolds could achieve synergistic effects in activating cell functions, such as enhancing endothelial growth in promoting new blood vessel formation.[85] However, the bioactivity of covalently bonded molecules, especially proteins, may be influenced by the lesser mobility of the molecular structure or the change of active molecular conformation after immobilization. Chemicals used for molecular grafting, which remain in the functionalized surface of tissue engineering scaffolds, may also reduce scaffold biocompatibility. To address these drawbacks, the non-covalent incorporation of bioactive components within tissue engineering scaffolds has been studied by many researchers for achieving multifunction for scaffolds. A wide range of bioactive substances, ranging from bioactive polymers, proteins, peptides, and genes to

small molecular drugs, can be incorporated to make multifunctional tissue engineering scaffolds. The addition of natural polymers such as gelatin, collagen and hyaluronic acid into synthetic biodegradable polymer scaffolds through surface coating or blending can significantly enhance the bioactivity of scaffolds. For instance, the attachment of chondrocytes on porous PLGA scaffolds for bone tissue engineering made by using a gas forming/salt leaching method and with the surface modification of hyaluronic acid was much enhanced when compared to the unmodified scaffolds, and the proliferation and differentiation of chondrocytes were also stimulated.[86] As for the incorporation of bioactive proteins or genes in tissue engineering scaffolds, the preservation of bio-functionality for the molecules to be delivered is critical. Scaffolds functionalized with heparin or polydopamine on the surface can form specific binding sites for some growth factors such as VEGF, bFGF and BMP-2, which subsequently achieves the incorporation of these growth factors in scaffolds.[87–89] Another approach for effective incorporation of growth factors or genes in scaffolds is to make tissue engineering scaffolds with core–shell structures through advanced fabrication techniques such as emulsion electrospinning/electrospray and coaxial electrospinning/electrospray, where bioactive substances are protected in the core, which provides a biocompatible microenvironment.[90] Small molecular drugs with different therapeutic effects such as anti-inflammation, anti-infection and anti-cancer functions have also been widely investigated for incorporation in tissue engineering scaffolds for realizing different functionalities.[91,92] To better mimic the native tissue regeneration process, scaffolds with the incorporation of multiple bioactive factors are emerging in tissue engineering. For instance, TCP/PLGA composite scaffolds with dual-released dexamethasone and proteins were developed for bone tissue engineering.[93] Bi-layered biodegradable fibrous scaffolds with one layer incorporated with VEGF and one layer incorporated with PDGF-BB were found to simultaneously stimulate the activities of endothelial cell and smooth muscle cells, which could therefore facilitate vascularization.[94] Inappropriate administration of growth factors can cause problems in bio-safety and cost-effectiveness.[95] For tissue engineering scaffolds capable of multiple bioactive factor delivery, how to design and control the release profiles of different factors in a specific spatiotemporal manner is really challenging.

20.4 Fabrication, Properties and Biological Evaluation of Multifunctional Tissue Engineering Scaffolds—Case Studies

Multifunctional tissue engineering scaffolds hold great promise for effective tissue regeneration through comprehensive interventions. The design and fabrication of suitable multifunctional tissue engineering scaffolds for specific clinical applications are of high importance. Over the years, our research group, as well as many other researchers, has investigated different types of

multifunctional tissue engineering scaffolds formed by using different fabrication techniques. The multifunctional scaffolds can be either specifically designed bioactive composite scaffolds or functional cell-laden scaffolds, which have their respective advantages for promoting the regeneration of different types of human body tissues or organs. This section presents some of our research on multifunctional tissue engineering scaffolds.

20.4.1 Selective Laser Sintered Multifunctional Scaffolds for Bone Tissue Regeneration

Tissue engineering scaffolds for promoting bone tissue regeneration need to possess well-designed macro- to micro-architectures. Compared to conventional techniques for scaffold manufacture, additive manufacture techniques have distinctive advantages in controlling the shape, structure, and pore size of scaffolds formed. As one member of the additive manufacture family, selective laser sintering (SLS) is effective for processing a wide range of biomaterials, ranging from biopolymers and bioceramics to composites. Hence SLS has been investigated by our research group and a few other groups for making multifunctional tissue engineering scaffolds for bone tissue engineering.

The fabrication of tissue engineering scaffolds through SLS involves the preparation of raw biomaterials in the particulate form, the design and building of target 3D computer-aided design (CAD) models, and the construction of scaffolds using an SLS machine. During the formation of scaffolds in an SLS machine, one layer of the raw biomaterial powders is spread on the part bed of the SLS machine and heated up to a pre-set temperature by a laser beam scanning in a programmed route, which leads to the fusion of powders and subsequent formation of a solid structure with a designed pattern. After one layer of scaffold structure is formed, new biomaterial powders are spread over the formed part and then sintered in the same way to form another solid layer of the scaffold. Through repeating these processes, tissue engineering scaffolds with a designed structure and controlled pore size, according to the CAD model previously built, can be fabricated. Biodegradable polymers such as PCL and poly(L-lactic acid) (PLLA) have been studied for making porous tissue engineering scaffolds *via* SLS.[96] The scaffolds formed exhibit both anatomy specific exterior architecture and totally interconnected porous interior architecture, which are intended for customized tissue engineering applications.

For bone tissue engineering, composite scaffolds containing osteoconductive bioceramics are preferred. Using SLS techniques, different composite scaffolds have been investigated for bone tissue engineering, in which different biomaterials were used, including HA/poly(etheretherketone) (PEEK),[97] HA/PCL,[98] and carbonate HA/PLLA.[99] Although these composite scaffolds made by SLS exhibit favourable properties in facilitating osteogenesis, drawbacks still exist. According to the biomaterials used, these scaffolds cannot be totally degraded (synthetic HA is perceived as a stable bioceramic); and the

dispersion of bioceramic particles in the polymer matrix is inhomogeneous since blends of polymer powders and bioceramic powders are co-sintered in the SLS process for making these composite scaffolds. These drawbacks limit the scope of clinical applications of the scaffolds for bone regeneration.

To make good biodegradable composite scaffolds using the SLS technique, raw biomaterials in a new form should be prepared instead of using dry-blended powders. Through a solid-in-oil-in-water (s/o/w) emulsion solvent evaporation process, PLLA/carbonate HA nanocomposite microspheres with uniformly dispersed bioceramic nanoparticles were produced,[100] which would be suitable as raw biomaterials for the optimized SLS process for making composite scaffolds. However, carbonate HA in the composite scaffolds cannot be completely degraded. Using bioactive Ca-P nanoparticles (which are similar to TCP in composition) synthesized in-house and a natural biodegradable polymer (PHBV), through a similar fabrication process, biodegradable Ca-P/PHBV microspheres were made, which were suitable as raw materials for constructing totally biodegradable composite scaffolds *via* SLS.[35]

Detailed studies were conducted for fabricating suitable PHBV and Ca-P/PHBV nanocomposite microspheres for the SLS process. First, PHBV microspheres were prepared using a water in oil (o/w) emulsion solvent evaporation, where PHBV polymer solution (dissolved in chloroform, "oil phase") was added in a PVA aqueous solution and then stirred at room temperature until the solvent was evaporated, followed by filtering, washing and freeze-drying. The PHBV microspheres formed had a uniform spherical shape with an average diameter of around 50 μm. As for the preparation of Ca-P/PHBV nanocomposite microspheres, Ca-P nanoparticles with diameters ranging from 10–30 nm were firstly synthesized. The PHBV microspheres filled with Ca-P nanoparticles were then formed using a previously established s/o/w emulsion solvent evaporation method,[35] where the as-synthesized Ca-P nanoparticles were dispersed in the PHBV polymer solution. The average diameter of the Ca-P/PHBV nanocomposite microspheres formed was slightly smaller than that of neat PHBV microspheres, about 48 μm. For the composite microspheres, the distribution of Ca-P nanoparticles in the PHBV polymer matrix of microspheres was uniform, which would be suitable for the SLS process.

For making Ca-P/PHBV nanocomposite scaffolds with a preciously controlled structure (*i.e.*, desired dimensional accuracy, structural stability and mechanical properties) using the SLS technique, various processing parameters during the SLS process should be carefully studied and optimized. The influence of five SLS parameters, namely laser power, laser scan speed, laser scan spacing, part bed temperature and powder layer delay interval, on the properties of the Ca-P/PHBV nanocomposite scaffolds formed was systematically investigated and the optimized SLS processing parameters for the scaffold manufacture were demonstrated.[47] A previous study also indicated that the mechanical properties of scaffolds formed by SLS were affected by the laser scanning direction. Sintered scaffolds exhibited the weakest strength in the axis parallel to the laser scan direction,[101] which should be considered too in the fabrication of tissue engineering scaffolds *via* SLS.

Using the optimized parameters, Ca-P/PHBV nanocomposite scaffolds with a customized structure, orthogonal interconnected pore (square-shaped or round-shaped) and controlled pore size were successfully fabricated by SLS.[47,102] The scaffolds with square-shaped pores had a strut size of 0.5 mm and a pore size of 1.0 mm. As for the scaffolds with round-shaped pores, the diameters of the strut and pore were 1.0 mm and 0.8 mm, respectively. The microstructure of the scaffolds formed mainly preserved a spherical shape while only the surfaces of the microspheres were fused to connect with each other to form solid structures in both sintered PHBV scaffolds (Figure 20.3(a)) and Ca-P/PHBV nanocomposite scaffolds (Figure 20.3(b)). Owing to the microspherical shapes of raw materials for SLS, good porosity was achieved for the scaffolds. Compared to the neat PHBV scaffolds, the scaffolds with embedded Ca-P nanoparticles exhibited an enhanced compressive strength and modulus. Besides, for the sintered Ca-P/PHBV nanocomposite scaffolds with different pore sizes, the scaffolds with a relatively small pore size had the higher compressive strength and modulus. There would be a balance between the suitable pore size for cell ingrowth and mechanical properties for stable structural loading in the fabrication of porous composite scaffolds using the SLS technique.

Porous and biodegradable composite scaffolds alone can only provide appropriate structural cues and osteoconductive properties in promoting bone tissue regeneration. The incorporation and controlled delivery of suitable bioactive molecules as bio-signals for better directing cell functions, particularly for guiding the osteogenic differentiation of stem cells, are of high importance for the new generation of bone tissue engineering scaffolds. For tissue engineering scaffolds made by SLS, it is difficult or impossible to directly incorporate biomolecules during SLS since the high temperature generated in the SLS process can cause the denaturation of bioactive molecules. To investigate the protection of the bioactivity of biomolecules to be incorporated, a solid-in-water-in-oil-in-water (s/w/o/w) double-emulsion

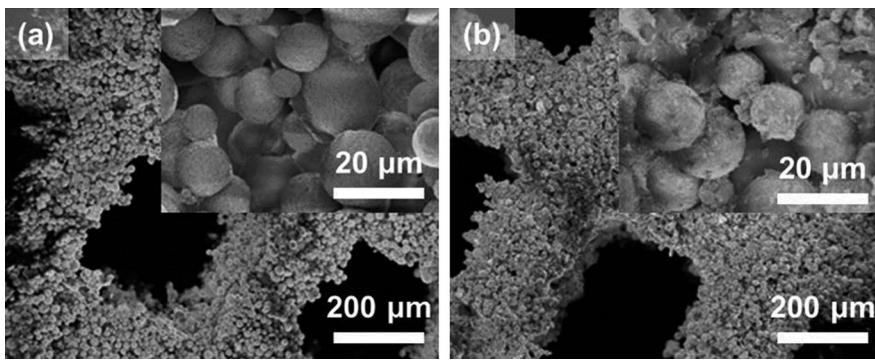

Figure 20.3 Structure of scaffolds formed by SLS: (a) PHBV scaffold; (b) Ca-P/PHBV nanocomposite scaffold. (Insets: SEM micrographs showing the sintered struts of respective scaffolds.)

solvent evaporation method was developed and a model biomolecule, bovine serum albumin (BSA), was encapsulated in the nanocomposite microspheres. Using BSA-encapsulated nanocomposite microspheres, Ca-P/PHBV nanocomposite scaffolds with incorporated BSA could be formed by SLS and the encapsulation and release behaviours of BSA in the scaffolds were studied.[103] Since only surfaces of nanocomposite microspheres were fused during SLS, the BSA of about 13% could be successfully loaded in the scaffolds and subsequently gradually released over time. However, the low encapsulation efficiency of BSA in scaffolds caused by denaturation and loss of BSA molecules during the fabrication process limits the potential of these direct biomolecule-incorporated scaffolds for tissue engineering. Post-SLA treatment, such as surface modification of scaffolds, is an alternative for the scaffolds made by SLS to contain and deliver biomolecules. For instance, Ca-P/PHBV nanocomposite scaffolds made by SLS were modified by a gelatin coating through a physical entrapment method, which improved the surface wettability of the scaffolds and enhanced the attachment and proliferation of osteoblasts on the modified scaffolds.[104] Furthermore, through a 1-ethyl-3-(3-dimethylaminopropyl)-carbodiimide hydrochloride (EDC)/*N*-hydroxysuccinimide (NHS)-catalysed reaction, heparin could be successfully grafted onto the surface of gelatin-coated Ca-P/PHBV nanocomposite scaffolds. Through the specific binding between heparin and growth factor, an osteoinductive factor such as BMP-2, could be incorporated with a Ca-P/PHBV nanocomposite with high efficiency.[102] The Ca-P/PHBV nanocomposite formed by SLS and modified by gelatin coating, heparin grafting and BMP-2 incorporation could achieve customized macro- to micro-architectures, good mechanical properties, osteoconductive potential and the sustained delivery of growth factor. These scaffolds exhibited an enhanced bone regeneration capability, meeting the multiple requirements for bone tissue engineering.[105,106]

20.4.2 Electrospun Multicomponent Scaffolds for Bone Tissue Regeneration

Electrospinning is a simple and effective method for producing fibrous scaffolds, which resemble the nanofibrous structure of native ECM and hence have caught attention in the tissue engineering field. Submicron- or nanofibers of various biopolymers can be made by electrospinning.[107] With specific adaptions, modified electrospinning techniques have been developed to make multifunctional fibrous scaffolds for tissue engineering. For example, electrospun multicomponent scaffolds with the incorporation of bioactive agents, including bioceramics and growth factors, can be formed by advanced electrospinning techniques, which display enhanced osteoconductive and osteoinductive potential for bone tissue engineering.[59,108,109]

Conventional electrospinning can process a polymer solution to form monocomponent scaffolds consisting of dried polymer nanofibers. For bone tissue engineering scaffolds, nanocomposite fibers with suitable combinations of bioceramics nanoparticles and biodegradable polymers are

desirable. To make these nanocomposite fibers, electrospinning techniques need to be investigated and tuned. One conventional technique, blend electrospinning, can be used for making electrospun multicomponent fibers. In blend electrospinning, the mixture solution containing different components is electrospun to form composite fibers. Blend electrospinning has been widely investigated to make polymer scaffolds loaded with small molecular drugs for drug delivery and tissue engineering,[58,110] where drug molecules are embedded in the polymer matrix of as-electrospun fibers. The release of loaded drugs from electrospun fibers made by biodegradable polymers *via* blend electrospinning usually follows almost a zero-order kinetic.[111] Blend electrospinning is also used for making tissue engineering scaffolds consisting of polymer blend fibers. For instance, fibrous scaffolds with fibers composed of one synthetic biodegradable polymer such as PLGA and PCL and one natural polymer such as gelatin and elastin were fabricated by blend electrospinning,[112,113] which combined the advantages of different polymers and were structurally stable in an aqueous environment without crosslinking. These composite fibrous scaffolds had adequate mechanical stability and exhibited improved biocompatibility in promoting cell attachment and cell growth. The fibrous scaffolds made by polyaniline/gelatin blends were biocompatible and had enhanced conductivity to better promote the growth of rat cardiac myoblast cells.[114] Blend electrospinning has also been investigated for making composite fibrous scaffolds using bioceramic nanoparticles and biodegradable polymers. Using PLGA solution with the addition of Ca-P nanoparticles, fibrous nanocomposite scaffolds were fabricated by blend electrospinning.[109] Compared to the neat PLGA scaffolds formed under the same formulation, the morphology and fiber diameter for the Ca-P/PLGA nanocomposite scaffolds had no obvious change, both exhibiting uniform nanofibrous structure (Figure 20.4(a)). A homogeneous distribution of Ca-P nanoparticles in the electrospun nanocomposite fibers was observed

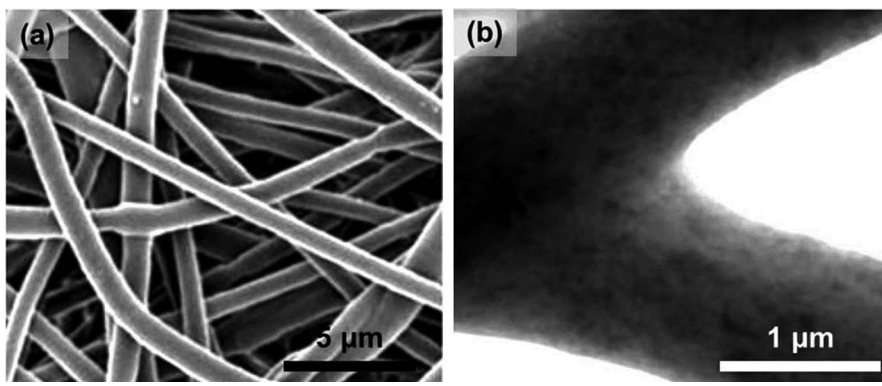

Figure 20.4 Fibrous Ca-P/PLGA nanocomposite scaffolds made by blend electrospinning: (a) fibrous morphology of a scaffold; (b) dispersion of Ca-P nanoparticles in fibers.

under TEM (Figure 20.4(b)). The incorporation of Ca-P nanoparticles also enhanced the hydrophilicity of resultant scaffolds,[115] which would be beneficial for cell attachment.

The incorporation of osteoinductive growth factor is a challenge for electrospun tissue engineering scaffolds. Blend electrospinning of a protein-containing polymer solution was investigated for making lysozyme-incorporated PCL/PEO scaffolds.[116] However, blend electrospinning has inherent limitations for the incorporation of growth factors. Specifically, since the use of, and direct contact with, organic solvent can cause the denaturation of growth factors, only blending solution made by water-soluble polymers using water as a "solvent" can be suitable for blend electrospinning to make effective growth-factor-incorporated scaffolds. But the scaffolds made of water-soluble polymers are difficult to handle for tissue engineering applications and usually require additional post-electrospinning treatments such as crosslinking to stabilize the scaffolds. As stated previously, a desired approach for growth factor delivery is to make a core–shell structured delivery vehicle with a biocompatible microenvironment (the "core") for protecting the bioactivity of the growth factor. Coaxial electrospinning and emulsion electrospinning can make polymer fibers with desired core–shell structures. Through coaxial electrospinning using a coaxial needle where the inner capillary was fed by a protein-containing aqueous solution and the outer capillary was fed by a polymer solution of a suitable biodegradable polymer, biomolecules such as BSA and lysozyme were successfully encapsulated in core–shell structured fibers.[117] The bioactivity of incorporated biomolecules was well preserved and the subsequent controlled release of biomolecules was achieved. Growth-factor-incorporated fibrous scaffolds, such as NGF-incorporated PLACL scaffolds, were also fabricated by coaxial electrospinning, which could effectively enhance the bioactivity of the scaffolds and promote peripheral nerve regeneration in rats.[118] However, the process of coaxial electrospinning is often difficult to control since two separated immiscible solutions are involved. The changes in the properties of two solutions, feeding rates for these two solutions, nozzle diameters, field strength, and even environmental factors will affect the structure of the fibers formed, and hence the encapsulation and release of growth factors. The repeatability of coaxial electrospinning as a technique to make growth-factor-incorporated scaffolds may therefore be influenced. In contrast, emulsion electrospinning to make core–shell structured nanofibers and the evolution of the core–shell structure during emulsion electrospinning have been studied in detail.[119,120] In the emulsion electrospinning process, a stable water-in-oil emulsion is subjected to electrospinning where a biomolecule-containing aqueous solution (the "water phase") is dispersed in a polymer solution (the "oil phase") with the addition of a suitable surfactant that does not compromise the biocompatibility either. The formation of a core–shell structure is strongly related to the utilization of surfactant and the fraction of water phase in the emulsion system, which can be relatively easily controlled. Using optimized processing parameters, poly(D,L-lactic acid) (PDLLA) scaffolds with core–shell structured nanofibers (Figure 20.5), where BMP-2 was encapsulated in the aqueous core, could be

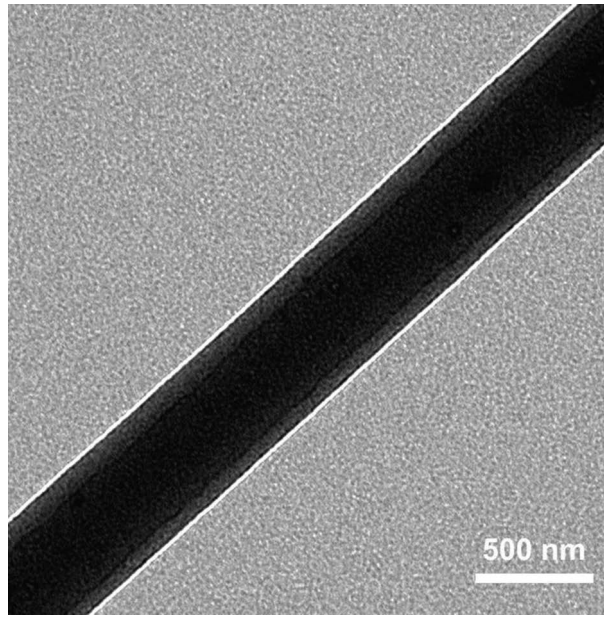

Figure 20.5 Core–shell structure of a PDLLA nanofiber made by emulsion electrospinning.

formed by emulsion electrospinning.[109] The bioactivity of incorporated BMP-2 was well protected and the release behaviours could be changed by varying the ratio between the water phase and oil phase. The sustained release of BMP-2 for more than one month was achieved along with the degradation of polymer fibers, which displayed promising osteoinductive potential for bone tissue engineering. Although the release of growth factors from fibrous scaffolds made by emulsion electrospinning have drawbacks, such as initial rapid release due to the charge repulsion effect, improvements such as control over the surface charge of emulsion electrospun scaffolds have been investigated, which were shown to be effective in modulating the release behaviours of growth factors.[121] After incorporating an appropriate negatively charged polyelectrolyte, namely cellulose acetate, in emulsion electrospun PLGA scaffolds through different approaches, a designed steady and sustained release of positively charged growth factors such as bFGF could be achieved from the modified fibrous scaffolds (Figure 20.6).

To combine the osteoconductive potential of fibrous nanocomposite scaffolds made by blend electrospinning and the osteoinductive potential of BMP-2 incorporated scaffolds made by emulsion electrospinning, a novel multi-source multi-power (MSMP) electrospinning approach was established for making multicomponent fibrous scaffolds.[108] A similar multi-jet electrospinning technique had been investigated for the mass production of electrospun fibrous scaffolds while one single polymer solution source was used. The interactions among the applied electrostatic field

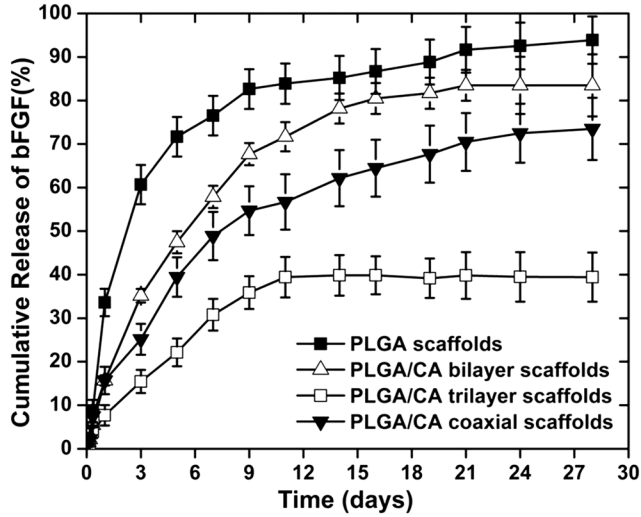

Figure 20.6 Release profiles of bFGF from emulsion electrospun PLGA scaffolds with or without CA incorporation.

and multiple charged jets were investigated.[122] In the MSMP electrospinning process, multiple electrospinning nozzles are fed by different polymer solution sources and connected to different power supplies. To minimize the influence of electric interactions on fiber collection, the blend electrospinning source for making nanocomposite fibers and the emulsion electrospinning source for making growth-factor-incorporated fibers were placed on the two sides of a grounded collecting drum, which could move reciprocally along its long axis and simultaneously rotate to ensure that the collected fibers were evenly distributed on the collector surface (Figure 20.7). Through MSMP electrospinning, multicomponent fibrous scaffolds with intermeshed Ca-P nanoparticle-embedded PLGA nanofibers and BMP-2-incorporated PDLLA nanofibers were successfully fabricated, which exhibited synergistic effects on promoting the mineralization process and osteogenic differentiation of mesenchymal stem cells (Figure 20.8), hence significantly improving bone tissue regeneration.[108] MSMP electrospinning could be extended for making fibrous scaffolds with controlled delivery of multiple growth factors required in the tissue regeneration process of tissues such as bone[123] and peripheral nerves.[124] For instance, through a previously described MSMP electrospinning process[108] with the addition of another emulsion electrospinning source using a VEGF-containing PLGA emulsion, tricomponent fibrous scaffolds with the dual delivery of BMP-2 and VEGF were formed.[123] Sequential release of VEGF and BMP-2 from the new tricomponent fibrous scaffolds was achieved according to the different degradation rates for the PLGA and PDLLA fibrous vehicles, which holds promise for the regeneration and neo-formation of vascularized living bone.

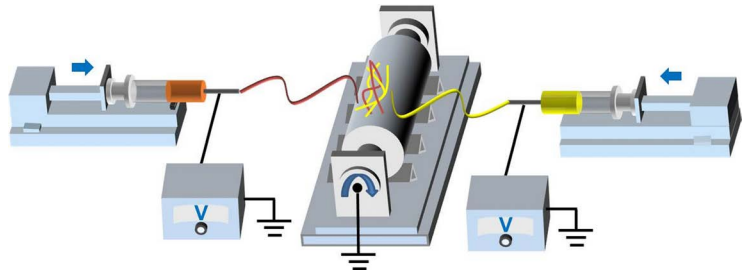

Figure 20.7 A schematic diagram showing the MSMP electrospinning setup.

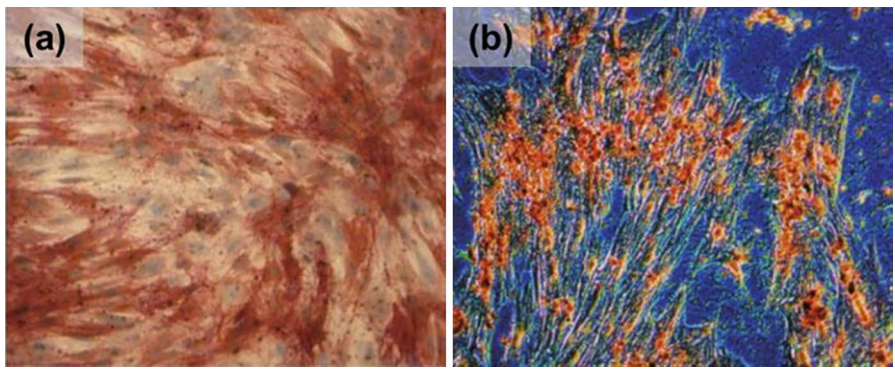

Figure 20.8 MSCs cultured on multicomponent fibrous scaffolds: (a) MSCs with alkaline phosphatase staining showing osteogenic differentiation; (b) MSCs with immunochemical staining showing MSC mineralization.

20.4.3 Nanofibrous Cell-Laden Scaffolds for the Regeneration of Complex Body Tissues

"Ideal" tissue regeneration requires the integration of scaffolds, cells and bio-signals. Cell incorporation is particularly important for tissue engineering scaffolds. Remarkable achievements have been made by using electrospun nanofibrous scaffolds for promoting the regeneration of various human body tissues with relatively simple structures. But electrospun scaffolds have limitations in poor cell infiltration due to very dense nanofibrous structures and small interconnected pores, which lead to a difficulty in forming 3D cell-laden structures for promoting the regeneration of complex body tissues and organs. The construction of multifunctional scaffolds with optimized incorporation of bio-signals and cells, in which the cell–scaffold organization is 3D and biomimetic, is a major challenge for electrospun tissue engineering scaffolds.[125]

Different efforts have been made for fabricating 3D cell-laden scaffolds *via* electrospinning. A direct way is to enlarge the sizes of interconnected pores in electrospun nanofibrous scaffolds, which aims to enhance cell infiltration and consequently make 3D cell-laden scaffolds. Combining

electrospinning with some other techniques, such as particulate leaching and gas foaming,[126,127] nanofibrous scaffolds with enlarged pores were fabricated. However, the engineered micropores in the scaffolds generated using these methods were usually neither interconnected nor homogeneous, and sometimes were unstable. Increasing the diameters of electrospun fibers is another method for making fibrous scaffolds with enlarged and structurally stable pores, which was shown to achieve improved cell infiltration,[128] while microfibrous scaffolds would influence cell attachment and 3D cell–scaffold organization.[129] It is of high importance to develop effective strategies that can effectively enlarge the pore sizes of electrospun scaffolds without disturbing their nanofibrous structures. Our investigations demonstrated a method of using concurrent electrospinning on a MSMP electrospinning setup to make bicomponent scaffolds with intermeshed nanofibers, where one component was a water-soluble polymer, namely gelatin, and one component was a biodegradable water-insoluble polymer, namely PLGA. After post-electrospinning immersion treatments to selectively remove the sacrificial gelatin fibers, as-formed nanofibrous PLGA scaffolds with some large interconnected micropores over 20 μm were fabricated, which would be adequate for cell migration and deep cell infiltration.[130] However, after the removal of sacrificial nanofibers from the bicomponent scaffolds, the mechanical properties, particularly ultimate tensile strength, of the scaffolds formed were reduced. An alternative approach of concurrently performing the positive voltage electrospinning and negative voltage electrospinning was then investigated.[131] Due to the charge neutralization effect, the nanofibrous PLGA scaffolds formed exhibited relatively loose-packed structures and slightly enlarged interconnected pores as compared to electrospun scaffolds made by conventional positive voltage electrospinning. The influence of this fabrication method on the mechanical properties of scaffolds was noticeable but small. However, this fabrication method also had a problem in that the effect to enlarge the pore sizes of scaffolds was limited.

Existing techniques for making electrospun nanofibrous scaffolds with enlarged pore sizes have respective drawbacks. Furthermore, even with effective cell infiltration, cells in electrospun scaffolds *via* conventional manual cell seeding will be inhomogeneous; and for the application of regenerating complex body tissues with different layers of cells, the particular type of cell cannot be distributed in the specific location of the scaffolds. To build nanofibrous cell-laden scaffolds with biomimetic 3D cell-scaffold organization and precisely controlled cell distribution, different novel cell incorporation methods for electrospun scaffolds have been studied.[132,133] For instance, different layers of cells were manually seeded onto electrospun scaffolds during electrospinning intervals.[132] Through a concurrent electrospinning–electrospray process, a cell suspension was sprayed *via* electrospray with simultaneous deposition of polymer nanofibers *via* electrospinning, which resulted in 3D cell-laden scaffolds.[132,133] The scaffolds formed using this method showed superior cell penetration while cell viability was affected due to inadequate protection during the direct electrospraying of an aqueous cell suspension.

Through electrospinning or electrospraying with specific modifications, cell-encapsulated structures can be produced for better cell protection. Compared to the electrospinning process, which leads to fibers that are too thin to effectively encapsulate mammalian cells and involves a high interfacial shear force causing cell death,[134] cell electrospraying, also termed "bio-electrospraying" by some researchers, has attracted much attention for cell microencapsulation and cell delivery.[135] Using suitable bio-polymers, semi-rigid, cell-bearing structures could be formed by electrospraying, where cell viability was well preserved. To ease handling in tissue engineering, the cell electrospray technique for making solidified live cell-encapsulated microspheres and subsequent controlled cell delivery were investigated by our group. Similar to the delivery of bioactive proteins, the delivery of live mammalian cells also needs to have a biocompatible microenvironment to protect the bioactivity. Coaxial electrospraying is an effective method for making core–shell structured microspheres with a polymer shell and a core filled with an aqueous component, which have been widely investigated for the delivery of drugs and proteins.[136] The structures (microsphere diameter, polymer shell thickness, aqueous core volume, *etc.*) and degradation properties of coaxial electrosprayed microspheres are adjustable by using different process parameters. Using optimized conditions and carefully selected biopolymer blends (gelatin and sodium alginate), a coaxial electrospray process with the inner capillary fed by a cell suspension was studied to make solidified polymer microspheres for live cell microencapsulation.[137] Although microspheres with an average diameter of about 5 μm could be formed (Figure 20.9(a)), the number of cells successfully encapsulated in the microspheres was low and the viability of encapsulated cells was not high (Figure 20.9(b)). To increase cell encapsulation efficiency and improve cell viability, a new coaxial electrospray method for making cell-encapsulated hydrogel

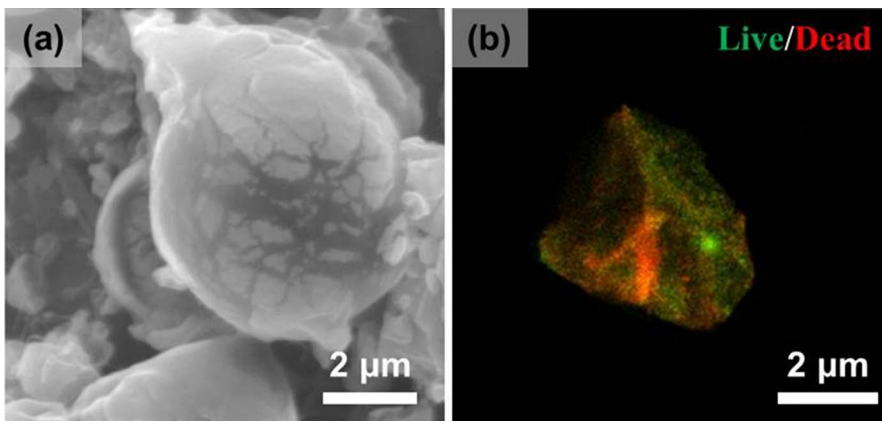

Figure 20.9 Polymer microspheres formed by coaxial electrospray for cell encapsulation: (a) morphology of microspheres; (b) cells in a microsphere revealed by live/dead cell staining.

microspheres was developed.[138] The jetting of cell-containing alginate microdroplets, instead of the direct formation of solidified cell-encapsulated polymer microspheres, was done during the coaxial electrospray process, and the microdroplets were then solidified in a collecting bath filled with an aqueous $CaCl_2$ solution for alginate crosslinking. Through this novel coaxial electrospray process, cell-encapsulated alginate-based hydrogel microspheres with an average diameter of around 100 μm could be successfully formed under suitable solution properties and processing parameters (Figure 20.10(a)). The results of a live/dead cell viability assay indicated that a very high cell survival rate (over 95%) was achieved by using this cell encapsulation technique (Figure 20.10(b)). Moreover, since the microspheres were formed by the crosslinking of alginate with calcium ions, through dripping a sodium citrate aqueous solution for disrupting alginate-based hydrogel structures, cell-encapsulated microspheres could be broken down and live cells would be released.

As effective live cell encapsulation and controlled cell delivery could be achieved through the novel coaxial cell electrospray approach, a combined process in which coaxial cell electrospray and emulsion electrospinning were concurrently performed to simultaneously fabricate cell-encapsulated alginate-based hydrogel microspheres and growth-factor-incorporated PLGA nanofibers was then developed for making complex nanofibrous growth-factor-incorporated and cell-laden scaffolds.[139] In the complex scaffolds, microspheres with encapsulated cells were randomly deposited on the polymer nanofibers with core–shell structures (Figure 20.11). After the dripping of sodium citrate solution, the encapsulated cells could be triggered to be released from the microspheres to be directly laid in the nanofibrous scaffolds. Using this method, nanofibrous PLGA scaffolds with incorporated

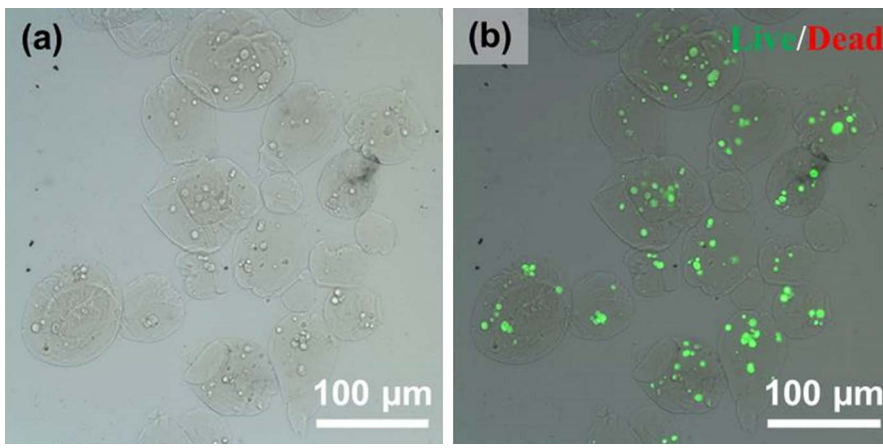

Figure 20.10 Cell encapsulation by alginate-based hydrogel microspheres formed *via* coaxial electrospray: (a) morphology and structure of microspheres; (b): cell-encapsulated microsphere with live/dead cell staining.

VEGF and endothelial cells (ECs) could be fabricated. The subsequent sustained release of VEGF (Figure 20.12(a)) and good spreading of ECs in the nanofibrous matrix of scaffolds (Figure 20.12(b)) highly resembled natural conditions during vascular formation and development. Compared to the growth of ECs on normal PLGA scaffolds using a conventional post-electrospinning manual cell seeding method, ECs grown in the complex scaffolds showed enhanced cell proliferation owing to the sustained delivery of VEGF and exhibited better cytoskeleton development due to the 3D and biomimetic cell–scaffold organization, which both offered positive stimuli for vascular tissue engineering. Furthermore, through sequentially performing the concurrent coaxial cell electrospray and emulsion electrospinning using different cells, biodegradable polymers and growth factors, multilayered nanofibrous scaffolds with different scaffold layers in accordance with the

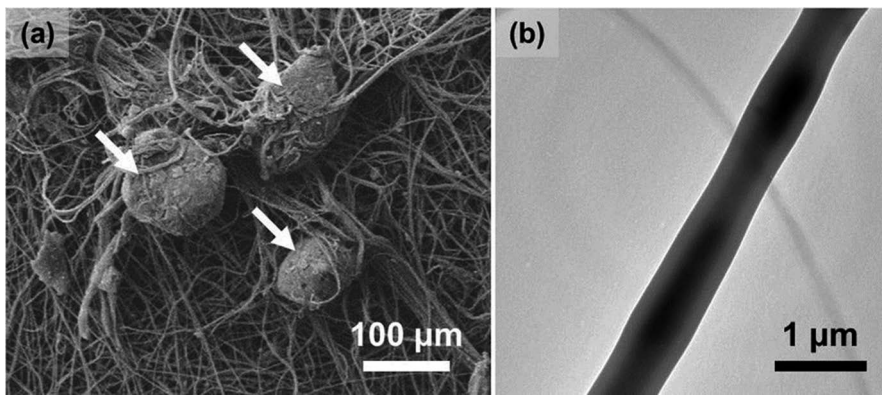

Figure 20.11 Complex fibrous scaffolds made by a concurrent fabrication process: (a) a scaffold with embedded cell-encapsulated microspheres; (b) growth factor-containing core–shell structured nanofibers in the complex scaffolds.

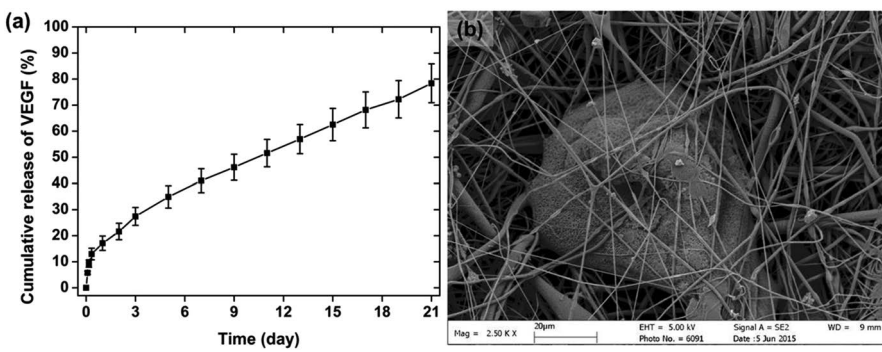

Figure 20.12 Complex scaffolds with incorporated cells and growth factor: (a) release behaviour of VEGF from the scaffolds; (b) spreading of ECs in the complex scaffolds after two-day cell culture.

different tissue layers of complex body tissues could be made. For example, multilayered scaffolds with one non-woven PLGA nanofibrous layer with incorporated VEGF and ECs and one aligned nanofibrous PDLLA layer with incorporated PDGF and smooth muscle cells (SMCs) were formed by using this concurrent fabrication method.[140] VEGF and PDGF were released in a controlled manner and in turn, due to the different degradation rates of PLGA fibers and PDLLA fibers (Figure 20.13), which respectively promoted the proliferation of ECs and SMCs and mimicked the native tissue regeneration process for angiogenesis and smooth muscle layer remodelling. Overall, the nanofibrous cell-laden scaffolds formed by concurrent coaxial cell electrospray and emulsion electrospinning can provide multiple functions including a biodegradable scaffold matrix, ECM-like nanofibrous structural cues, spatiotemporally controlled delivery of multiple growth factors, and a 3D biomimetic cell–scaffold organization, which hold great promise for the regeneration of complex human body tissues.

20.4.4 Theranostic-Embedded Scaffolds for Cancer Patients

For some specific medical applications, tissue engineering scaffolds with only a regenerative capability are not adequate. For instance, postoperative cancer patients usually have an urgent need for tissue regeneration as surgery is still the most commonly used method for cancer treatment and the resection of parts of cancerous tissues can cause abnormal functions of human body tissues or severe complications.[141,142] Furthermore, cancer patients after surgical resection also confront a high risk of cancer recurrence, which has been

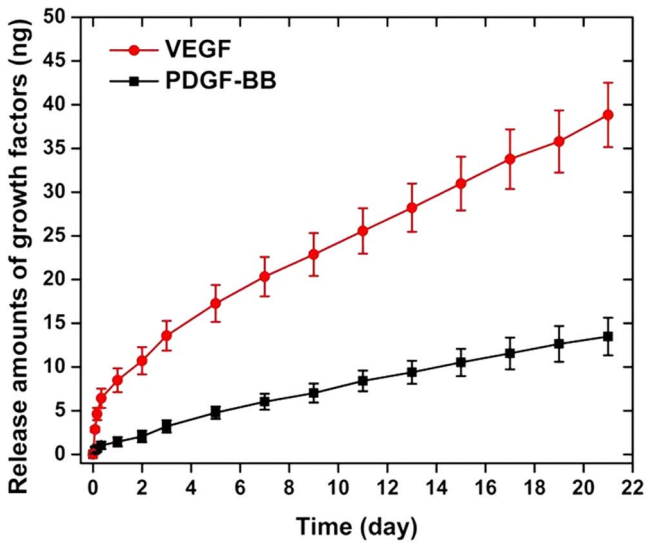

Figure 20.13 Release profiles for the dual delivery of VEGF and PDGF from multifunctional nanofibrous cell-laden scaffolds.

the main cause of death for cancer patients. Additional functions, such as the ability to monitor and inhibit cancer recurrence, are necessary for the tissue engineering scaffolds used for postoperative cancer patients.

Conventional techniques for fulfilling the anti-cancer property for tissue engineering scaffolds is to incorporate anti-cancer drugs in scaffolds through different approaches.[143] Electrospinning is a promising technique for making fibrous scaffolds enabling controlled delivery of anti-cancer drugs and simultaneously to promote tissue regeneration.[58] Through blend electrospinning, fibrous PLGA scaffolds with a loaded hydrophobic anti-cancer drug, paclitaxel, were formed.[144] A high drug loading efficiency (90%) and the sustained release of paclitaxel over 60 days were achieved, showing potential in chemotherapy. However, untargeted chemotherapy can bring problems such as toxicity to the surrounding healthy tissues. As effective agents for cancer detection and simultaneously cancer therapy, various functionalized nanoparticles, termed "theranostics", have emerged in recent years for cancer diagnosis and treatment.[145] Typical examples are gold nanoparticle (AuNP)-based theranostics, which can achieve cancer targeting through the functionalization of tumor-specific ligands, non-invasive cancer detection on the basis of their unique properties of surface-enhanced Raman scattering (SERS) activity or surface plasmon resonance (SPR) absorption, and cancer treatment arising from laser-irradiation-induced photo-thermal effects or the capability of anti-cancer drug delivery. Our group has developed a simple one-pot synthesis method to make folic-acid-chitosan-capped AuNPs as potential theranostics for cancer.[146] Through coaxial electrospraying, AuNP-based theranostics could be effectively encapsulated in core–shell structured PLGA microspheres (Figure 20.14(a)). The electrospray process was then combined with a concurrent PDLLA electrospinning process and,

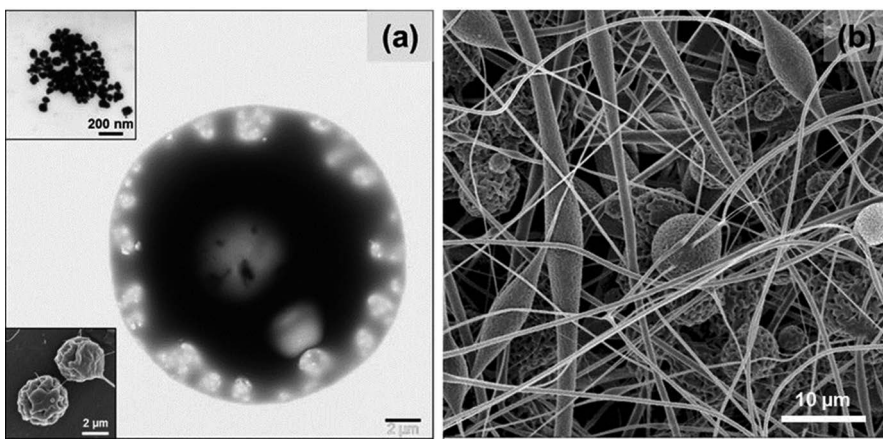

Figure 20.14 Multifunctional scaffolds for cancer patients: (a) PLGA microspheres with encapsulated AuNP-based theranostics; (b) theranostic-embedded scaffolds formed by concurrent coaxial electrospray and electrospinning.

consequently, novel nanofibrous composite scaffolds with embedded theranostics were subsequently formed.[147] In these new scaffolds, theranostic-encapsulated PLGA microspheres were randomly laid in the PDLLA nanofibrous matrix (Figure 20.14(b)). The encapsulated theranostics would be released along with the degradation of the PLGA microsphere shells while their SERS activity was well maintained for cancer detection. The released theranostics would be desirable agents for detecting cancer recurrence and also for the targeted clearance of residual cancer cells for cancer patients after tumor resection. At the same time, the PDLLA nanofibrous matrix with a relatively slow degradation rate would provide desired ECM-like microenvironments for promoting the healing and *in situ* regeneration of resected tissue. These theranostic-embedded scaffolds investigated in our studies have great potential to offer combined therapies for postoperative cancer patients.

20.5 Concluding Remarks

Smart multifunctional scaffolds are needed for meeting the multiple requirements for promoting the regeneration of human body tissues. The structure, property and microenvironment of the target tissue to be regenerated must be carefully considered when designing the multifunctional scaffolds, which should possess essential, desired functional abilities. There are a variety of fabrication techniques for constructing tissue engineering scaffolds. While conventional scaffolds can be produced by many of these techniques, the fabrication of smart multifunctional scaffolds is often difficult and can use only one or just a few techniques due to the limitations or shortcomings of other techniques as well as the additional requirements when scaffold multifunctionality is to be achieved. For the manufacture of smart multifunctional tissue engineering scaffolds, biomaterials should be carefully chosen, which should meet the requirements for the target tissue and be suitable for the specific scaffold fabrication technique to be used, and very often novel scaffold fabrication techniques need to be developed.

Worldwide, researchers in different countries are investigating different multifunctional scaffolds according to their philosophy and strategy for tissue regeneration. In this chapter, using our research work, four examples have been given for the design, fabrication and properties of multifunctional scaffolds for tissue engineering, with their potential applications for regenerating different body tissues and for cancer patients. Using SLS and with the assistance of nanocomposite and surface functionalization, biodegradable nanocomposite scaffolds with customized architecture, controlled pore size and porosity, incorporated osteoconductive component and sustained delivery of osteoinductive growth factor could be made, which showed excellent performance in promoting bone tissue regeneration. New multifunctional scaffolds for bone tissue engineering could be made *via* MSMP electrospinning, where multiple components, including biodegradable polymer nanofibers, well-dispersed osteoconductive Ca-P nanoparticles, and controlled released growth factors (BMP-2 and VEGF), could be integrated in one fibrous

scaffold. Furthermore, nanofibrous growth-factor-incorporated and cell-laden scaffolds better resembling the native 3D cell–ECM organization and the spatiotemporal administration of multiple growth factors could be made through concurrent coaxial cell electrospraying and emulsion electrospinning, which could be used for achieving better regeneration of complex body tissues. For postoperative cancer patients, aiming to achieve the synergetic effects of promoting tissue regeneration after surgical removal of cancer and simultaneously preventing cancer recurrence, nanofibrous tissue engineering scaffolds with controlled release of anti-cancer theranostics could be produced by concurrent electrospinning and coaxial electrospraying. These multifunctional scaffolds would provide comprehensive care for people suffering from cancer.

Current multifunctional scaffolds have shown great potential for tissue regeneration. With more and a better understanding of the development and regeneration of human body tissues and organs as well as significant advances in new biomaterials and engineering techniques, novel multifunctional scaffolds will be designed and investigated, accelerating the pace of developments in the tissue engineering field.

Acknowledgements

Min Wang thanks his research staff and students in Nanyang Technological University, Singapore, The Hong Kong Polytechnic University and The University of Hong Kong, Hong Kong, for conducting the research work on tissue engineering scaffolds with him. He thanks his collaborators in these universities and also other universities for their useful discussions and support. Assistance provided by technical staff in various laboratories of the universities is much appreciated. Research funding from Singapore's Ministry of Education, Research Grants Council of Hong Kong, National Natural Science Foundation of China and the universities is gratefully acknowledged. He thanks his research staff and students, past and present, for providing the figures used in this chapter. The credit goes to: B. Duan for Figure 20.3; C. Wang for Figures 20.4 and 20.8; and Y. Zhou for Figure 20.13. Qilong Zhao's post-doctoral position is supported by a grant (HKU7177/13E) from the Research Grants Council of Hong Kong.

References

1. R. M. Nerem, *Ann. Biomed. Eng.*, 1991, **19**, 529.
2. R. Langer and J. P. Vacanti, *Science*, 1993, **260**, 920.
3. D. J. Mooney and A. G. Mikos, *Sci. Am.*, 1999, **280**, 60.
4. S. G. Priya, H. Jungvid and A. Kumar, *Tissue Eng., Part B*, 2008, **14**, 105.
5. F. Groeber, M. Holeiter, M. Hampel, S. Hinderer and K. Schenke-Layland, *Adv. Drug Delivery Rev.*, 2011, **63**, 352.
6. J. S. Temenoff and A. G. Mikos, *Biomaterials*, 2000, **21**, 431.

7. E. B. Hunziker, *Osteoarthritis Cartilage*, 2002, **10**, 432.
8. D. W. Hutmacher, *Biomaterials*, 2000, **21**, 2529.
9. J. D. Kretlow and A. G. Mikos, *Tissue Eng.*, 2007, **13**, 927.
10. L. G. Griffith and G. Naughton, *Science*, 2002, **295**, 1009.
11. L. L. Hench and J. M. Polak, *Science*, 2002, **295**, 1014.
12. E. S. Place, N. D. Evans and M. M. Stevens, *Nat. Mater.*, 2009, **8**, 457.
13. I. Martin, P. J. Simmons and D. F. Williams, *Sci. Transl. Med.*, 2014, **6**, 232fs16.
14. R. C. Rennert, M. Sorkin, V. W. Wong and G. C. Gurtner, *Curr. Stem Cell Res. Ther.*, 2014, **9**, 2.
15. S. V. Murphy and A. Atala, *BioEssays*, 2013, **35**, 163.
16. K. C. Rustad, M. Sorkin, B. Levi, M. T. Longaker and G. C. Gurtner, *Organogenesis*, 2010, **6**, 151.
17. G. F. Muschler, C. Nakamoto and L. G. Griffith, *J. Bone Jt. Surg., Am. Vol.*, 2004, **86-A**, 1541.
18. S. F. Badylak, D. Taylor and K. Uygun, *Annu. Rev. Biomed. Eng.*, 2011, **13**, 27.
19. Z. J. Gartner and C. R. Bertozzi, *Proc. Natl. Acad. Sci. U. S. A.*, 2009, **106**, 4606.
20. A. Nishiguchi, H. Yoshida, M. Matsusaki and M. Akashi, *Adv. Mater.*, 2011, **23**, 3506.
21. G. Q. Daley and D. T. Scadden, *Cell*, 2008, **132**, 544.
22. K. Takahashi and S. Yamanaka, *Cell*, 2006, **126**, 663.
23. R. Vasita and D. S. Katti, *Expert Rev. Med. Devices*, 2006, **3**, 29.
24. L. S. Nair and C. T. Laurencin, *Prog. Polym. Sci.*, 2007, **32**, 762.
25. S. H. Park, D. S. Park, J. W. Shin, Y. G. Kang, H. K. Kim, T. R. Yoon and J. W. Shin, *J. Mater. Sci.: Mater. Med.*, 2012, **23**, 2671.
26. S. C. Baker, G. Rohman, J. Southgate and N. R. Cameron, *Biomaterials*, 2009, **30**, 1321.
27. A. Sano, M. Maeda, S. Nagahara, T. Ochiya, K. Honma, H. Itoh, T. Miyata and K. Fujioka, *Adv. Drug Delivery Rev.*, 2003, **55**, 1651.
28. S. Sabetkish, A. M. Kajbafzadeh, N. Sabetkish, R. Khorramirouz, A. Akbarzadeh, S. L. Seyedian, P. Pasalar, S. Orangian, R. S. Beigi, Z. Aryan, H. Akbari and S. M. Tavangar, *J. Biomed. Mater. Res., Part A*, 2015, **103**, 1498.
29. M. H. Zheng, J. Chen, Y. Kirilak, C. Willers, J. Xu and D. Wood, *J. Biomed. Mater. Res., Part B*, 2005, **73B**, 61.
30. R. Z. LeGeros, *Clin. Orthop. Relat. Res.*, 2002, 81.
31. J. C. Brodie, E. Goldie, G. Connel, J. Merry and M. H. Grant, *J. Biomed. Mater. Res., Part A*, 2005, **73**, 409.
32. M. Wang, *Biomaterials*, 2003, **24**, 2133.
33. N. Sultana and M. Wang, *J. Mater. Sci.: Mater. Med.*, 2008, **19**, 2555.
34. N. Sultana and M. Wang, *Biofabrication*, 2012, **4**, 015003.
35. B. Duan, M. Wang, W. Y. Zhou and W. L. Cheung, *Appl. Surf. Sci.*, 2008, **255**, 529.
36. A. G. Mikos, G. Sarakinos, S. M. Leite, J. P. Vacanti and R. Langer, *Biomaterials*, 1993, **14**, 323.

37. D. J. Mooney, D. F. Baldwin, N. P. Suh, L. P. Vacanti and R. Langer, *Biomaterials*, 1996, **17**, 1417.
38. S. G. Kazarian, M. F. Vincent, F. V. Bright, C. L. Liotta and C. A. Eckert, *J. Am. Chem. Soc.*, 1996, **118**, 1729.
39. M. H. Sheridan, L. D. Shea, M. C. Peters and D. J. Mooney, *J. Controlled Release*, 2000, **64**, 91.
40. W. L. Murphy, R. G. Dennis, J. L. Kileny and D. J. Mooney, *Tissue Eng.*, 2002, **8**, 43.
41. X. H. Liu and P. X. Ma, *Ann. Biomed. Eng.*, 2004, **32**, 477.
42. Y. S. Nam and T. G. Park, *J. Biomed. Mater. Res.*, 1999, **47**, 8.
43. W. Y. Yeong, C. K. Chua, K. F. Leong and M. Chandrasekaran, *Trends Biotechnol.*, 2004, **22**, 643.
44. I. Zein, D. W. Hutmacher, K. C. Tan and S. H. Teoh, *Biomaterials*, 2002, **23**, 1169.
45. R. Gauvin, Y.-C. Chen, J. W. Lee, P. Soman, P. Zorlutuna, J. W. Nichol, H. Bae, S. Chen and A. Khademhosseini, *Biomaterials*, 2012, **33**, 3824.
46. T. Boland, T. Xu, B. Damon and X. Cui, *Biotechnol. J.*, 2006, **1**, 910.
47. B. Duan, W. L. Cheung and M. Wang, *Biofabrication*, 2011, **3**, 015001.
48. S. Kumar, *JOM*, 2003, **55**, 43.
49. S. F. Yang, K. F. Leong, Z. H. Du and C. K. Chua, *Tissue Eng.*, 2002, **8**, 1.
50. B. Duan, M. Wang, W. Y. Zhou, W. L. Cheung, Z. Y. Li and W. W. Lu, *Acta Biomater.*, 2010, **6**, 4495.
51. G. R. Evans, K. Brandt, S. Katz, P. Chauvin, L. Otto, M. Bogle, B. Wang, R. K. Meszlenyi, L. Lu, A. G. Mikos and C. W. Patrick Jr, *Biomaterials*, 2002, **23**, 841.
52. X. Liu, X. Jin and P. X. Ma, *Nat. Mater.*, 2011, **10**, 398.
53. T. Aida, E. W. Meijer and S. I. Stupp, *Science*, 2012, **335**, 813.
54. R. J. Wade and J. A. Burdick, *Nano Today*, 2014, **9**, 722.
55. D. Li and Y. N. Xia, *Adv. Mater.*, 2004, **16**, 1151.
56. Q. P. Pham, U. Sharma and A. G. Mikos, *Tissue Eng.*, 2006, **12**, 1197.
57. W. Liu, S. Thomopoulos and Y. Xia, *Adv. Healthcare Mater.*, 2012, **1**, 10.
58. T. J. Sill and H. A. von Recum, *Biomaterials*, 2008, **29**, 1989.
59. H. W. Tong and M. Wang, *J. Nanosci. Nanotechnol.*, 2007, **7**, 3834.
60. J. W. Xie, M. R. MacEwan, W. Z. Ray, W. Y. Liu, D. Y. Siewe and Y. N. Xia, *ACS Nano*, 2010, **4**, 5027.
61. A. Szentivanyi, T. Chakradeo, H. Zernetsch and B. Glasmacher, *Adv. Drug Delivery Rev.*, 2011, **63**, 209.
62. G. K. Michalopoulos and M. C. DeFrances, *Science*, 1997, **276**, 60.
63. I. H. Kalfas, *Neurosurg. Focus*, 2001, **10**, E1.
64. T. N. Vo, F. K. Kasper and A. G. Mikos, *Adv. Drug Delivery Rev.*, 2012, **64**, 1292.
65. J. Kular, J. Tickner, S. M. Chim and J. K. Xu, *Clin. Biochem.*, 2012, **45**, 863.
66. G. D. Yancopoulos, S. Davis, N. W. Gale, J. S. Rudge, S. J. Wiegand and J. Holash, *Nature*, 2000, **407**, 242.
67. E. S. Place, N. D. Evans and M. M. Stevens, *Nat. Mater.*, 2009, **8**, 457.

68. S. Bose, M. Roy and A. Bandyopadhyay, *Trends Biotechnol.*, 2012, **30**, 546.
69. R. R. Chen and D. J. Mooney, *Pharm. Res.*, 2003, **20**, 1103.
70. J. E. Babensee, L. V. McIntire and A. G. Mikos, *Pharm. Res.*, 2000, **17**, 497.
71. F. M. Chen, M. Zhang and Z. F. Wu, *Biomaterials*, 2010, **31**, 6279.
72. E. C. Novosel, C. Kleinhans and P. J. Kluger, *Adv. Drug Delivery Rev.*, 2011, **63**, 300.
73. K. Rezwan, Q. Z. Chen, J. J. Blaker and A. R. Boccaccini, *Biomaterials*, 2006, **27**, 3413.
74. C. X. Wang and M. Wang, *Proc 10th Int Conf Biomed Eng*, 2000, p. 547.
75. S. J. Heo, S. E. Kim, J. Wei, Y. T. Hyun, H. S. Yun, D. H. Kim, J. W. Shin and J. W. Shin, *J. Biomed. Mater. Res., Part A*, 2009, **89A**, 108.
76. Y. Chen, A. F. T. Mak, M. Wang, J. S. Li and M. S. Wong, *Surf. Coat. Technol.*, 2006, **201**, 575.
77. H. Cao and N. Kuboyama, *Bone*, 2010, **46**, 386.
78. Y. Yin, F. Ye, J. Cui, F. Zhang, X. Li and K. Yao, *J. Biomed. Mater. Res., Part A*, 2003, **67**, 844.
79. A. Sendemir-Urkmez and R. D. Jamison, *J. Biomed. Mater. Res., Part A*, 2007, **81**, 624.
80. S. I. Roohani-Esfahani, S. Nouri-Khorasani, Z. Lu, R. Appleyard and H. Zreiqat, *Biomaterials*, 2010, **31**, 5498.
81. E. S. Place, J. H. George, C. K. Williams and M. M. Stevens, *Chem. Soc. Rev.*, 2009, **38**, 1139.
82. R. O. Hynes, *Nat. Rev. Mol. Cell Biol.*, 2014, **15**, 761.
83. A. Leal-Egana, A. Diaz-Cuenca and A. R. Boccaccini, *Adv. Mater.*, 2013, **25**, 4049.
84. J. K. Tessmar and A. M. Gopferich, *Adv. Drug Delivery Rev.*, 2007, **59**, 274.
85. K. Wulf, M. Teske, M. Lobler, F. Luderer, K. P. Schmitz and K. Sternberg, *J. Biomed. Mater. Res., Part B*, 2011, **98B**, 89.
86. H. S. Yoo, E. A. Lee, J. J. Yoon and T. G. Park, *Biomaterials*, 2005, **26**, 1925.
87. R. F. Luo, L. L. Tang, J. Wang, Y. C. Zhao, Q. F. Tu, Y. J. Weng, R. Shen and N. Huang, *Colloids Surf., B*, 2013, **106**, 66.
88. O. Jeon, S. J. Song, S. W. Kang, A. J. Putnam and B. S. Kim, *Biomaterials*, 2007, **28**, 2763.
89. J. J. Yoon, H. J. Chung, H. J. Lee and T. G. Park, *J. Biomed. Mater. Res., Part A*, 2006, **79A**, 934.
90. R. A. Perez and H. W. Kim, *Acta Biomater.*, 2015, **21**, 2.
91. H. S. Yoo, T. G. Kim and T. G. Park, *Adv. Drug Delivery Rev.*, 2009, **61**, 1033.
92. J. J. Xue, M. He, H. Liu, Y. Z. Niu, A. Crawford, P. D. Coates, D. F. Chen, R. Shi and L. Q. Zhang, *Biomaterials*, 2014, **35**, 9395.
93. Y. Yang, G. Tang, H. Zhang, Y. Zhao, X. Yuan, M. Wang and X. Yuan, *J. Biomed. Mater. Res., Part B*, 2011, **96**, 139.
94. H. Zhang, X. Jia, F. Han, J. Zhao, Y. Zhao, Y. Fan and X. Yuan, *Biomaterials*, 2013, **34**, 2202.

95. J. J. Rice, M. M. Martino, L. De Laporte, F. Tortelli, P. S. Briquez and J. A. Hubbell, *Adv. Healthcare Mater.*, 2013, **2**, 57.
96. S. H. Lee, W. Y. Zhou, M. Wang, W. L. Cheung and W. Y. Ip, *J. Biomimetics, Biomater., Tissue Eng.*, 2008, **1**, 81.
97. K. H. Tan, C. K. Chua, K. F. Leong, C. M. Cheah, P. Cheang, M. S. Abu Bakar and S. W. Cha, *Biomaterials*, 2003, **24**, 3115.
98. F. E. Wiria, K. F. Leong, C. K. Chua and Y. Liu, *Acta Biomater.*, 2007, **3**, 1.
99. W. Y. Zhou, S. H. Lee, M. Wang, W. L. Cheung and W. Y. Ip, *J. Mater. Sci.: Mater. Med.*, 2008, **19**, 2535.
100. W. Y. Zhou, M. Wang, W. L. Cheung, B. C. Guo and D. M. Jia, *J. Mater. Sci.: Mater. Med.*, 2008, **19**, 103.
101. S. Eosoly, D. Brabazon, S. Lohfeld and L. Looney, *Acta Biomater.*, 2010, **6**, 2511.
102. B. Duan and M. Wang, *J. R. Soc., Interface*, 2010, **7**, S615.
103. B. Duan and M. Wang, *Polym. Degrad. Stab.*, 2010, **95**, 1655.
104. B. Duan, M. Wang, Z. Y. Li, W. C. Chan and W. W. Lu, *Front. Mater. Sci.*, 2011, **5**, 57.
105. B. Duan and M. Wang, *MRS Bull.*, 2011, **36**, 998.
106. B. Duan, M. Wang and W. W. Lu, *Nano LIFE*, 2012, **2**, 1250005.
107. A. Greiner and J. H. Wendorff, *Angew. Chem., Int. Ed.*, 2007, **46**, 5670.
108. C. Wang and M. Wang, *Front. Mater. Sci.*, 2014, **8**, 3.
109. C. Wang and M. Wang, *J. Mater. Sci.: Mater. Med.*, 2012, **23**, 2381.
110. C. Wang, M. Wang and X. Y. Yuan, *Proc 9th World Biomater Congr*, 2012.
111. Z. Jing, X. Y. Xu, X. S. Chen, Q. Z. Liang, X. C. Bian, L. X. Yang and X. B. Jing, *J. Controlled Release*, 2003, **92**, 227.
112. H. M. Powell and S. T. Boyce, *Tissue Eng., Part A*, 2009, **15**, 2177.
113. M. Y. Li, M. J. Mondrinos, X. S. Chen and P. I. Lelkes, *Tissue Eng.*, 2006, **12**, 989.
114. M. Y. Li, Y. Guo, Y. Wei, A. G. MacDiarmid and P. I. Lelkes, *Biomaterials*, 2006, **27**, 2705.
115. C. H. Kim, M. S. Khil, H. Y. Kim, H. U. Lee and K. Y. Jahng, *J. Biomed. Mater. Res., Part B*, 2006, **78**, 283.
116. T. G. Kim, D. S. Lee and T. G. Park, *Int. J. Pharm.*, 2007, **338**, 276.
117. H. L. Jiang, Y. Q. Hu, Y. Li, P. C. Zhao, K. J. Zhu and W. L. Chen, *J. Controlled Release*, 2005, **108**, 237.
118. J. J. Liu, C. Y. Wang, J. G. Wang, H. J. Ruan and C. Y. Fan, *J. Biomed. Mater. Res., Part A*, 2011, **96A**, 13.
119. X. L. Xu, X. L. Zhuang, X. S. Chen, X. R. Wang, L. X. Yang and X. B. Jing, *Macromol. Rapid Commun.*, 2006, **27**, 1637.
120. C. Wang, L. Q. Wang and M. Wang, *Mater. Lett.*, 2014, **124**, 192.
121. Q. L. Zhao and M. Wang, *Mater. Lett.*, 2016, **162**, 48.
122. S. A. Theron, A. L. Yarin, E. Zussman and E. Kroll, *Polymer*, 2005, **46**, 2889.
123. C. Wang and M. Wang, *Proc MRS Fall Meet*, 2013.
124. C. Y. Liu and M. Wang, *Proc SFB 2015 Annu Meet*, 2015.

125. S. Khorshidi, A. Solouk, H. Mirzadeh, S. Mazinani, J. M. Lagaron, S. Sharifi and S. Ramakrishna, *J. Tissue Eng. Regener. Med.*, 2015, **10**, 175.
126. J. Nam, Y. Huang, S. Agarwal and J. Lannutti, *Tissue Eng.*, 2007, **13**, 2249.
127. G. Kim and W. Kim, *J. Biomed. Mater. Res., Part B*, 2007, **81B**, 104.
128. A. Thorvaldsson, H. Stenhamre, P. Gatenholm and P. Walkenstrom, *Biomacromolecules*, 2008, **9**, 1044.
129. M. M. Stevens and J. H. George, *Science*, 2005, **310**, 1135.
130. Q. L. Zhao and M. Wang, *Proc 38th Int Conf Expo Adv Ceram Compos*, 2014.
131. Q. L. Zhao, O. I. So and M. Wang, *Proc 38th Int Conf Expo Adv Ceram Compos*, 2015.
132. X. C. Yang, J. D. Shah and H. J. Wang, *Tissue Eng., Part A*, 2009, **15**, 945.
133. A. K. Ekaputra, G. D. Prestwich, S. M. Cool and D. W. Hutmacher, *Biomacromolecules*, 2008, **9**, 2097.
134. M. F. Canbolat, C. Tang, S. H. Bernacki, B. Pourdeyhimi and S. Khan, *Macromol. Biosci.*, 2011, **11**, 1346.
135. S. N. Jayasinghe, J. Auguste and C. J. Scotton, *Adv. Mater.*, 2015, **27**, 7794.
136. N. Bock, M. A. Woodruff, D. W. Hutmacher and T. R. Dargaville, *Polymers*, 2011, **3**, 131.
137. Q. L. Zhao and M. Wang, *Proc 4th Asian Biomater Congrs*, 2013.
138. Q. L. Zhao and M. Wang, *Proc MRS Fall Meet*, 2014.
139. Q. L. Zhao and M. Wang, *Proc 39th Int Conf Expo Adv Ceram Compos*, 2015.
140. Y. Zhou, Q. L. Zhao and M. Wang, *Proc 5th Asian Biomater Congr*, 2015.
141. K. S. Chian, M. F. Leong and K. Kono, *Lancet Oncol.*, 2015, **16**, e84.
142. J. C. Haag, P. Jungebluth and P. Macchiarini, *Curr. Opin. Otolaryngol. Head Neck Surg.*, 2013, **21**, 171.
143. L. S. Nair and C. T. Laurencin, *Adv. Biochem. Eng./Biotechnol.*, 2006, **102**, 47.
144. J. W. Xie and C. H. Wang, *Pharm. Res.*, 2006, **23**, 1817.
145. J. Xie, S. Lee and X. Y. Chen, *Adv. Drug Delivery Rev.*, 2010, **62**, 1064.
146. S. Y. Li and M. Wang, *IET Nanobiotechnol.*, 2012, **6**, 136.
147. L. Guo, Q. L. Zhao and M. Wang, *Proc MRS Fall Meet*, 2015.

CHAPTER 21

Applications of Smart Microfluidic Systems in Tissue Engineering

YIN CHEN[a], LU HUANG[a,b], KANGNING REN[c], XUETAO SHI[d] AND HONGKAI WU*[a,b]

[a]Division of Biomedical Engineering, The Hong Kong University of Science and Technology, Kowloon, Hong Kong, China; [b]Department of Chemistry, The Hong Kong University of Science and Technology, Kowloon, Hong Kong, China; [c]Department of Chemistry, Hong Kong Baptist University, Kowloon, Hong Kong, China; [d]Department of Biomedical Engineering, School of Materials Science and Engineering, South China University of Technology, Guangzhou 510641, China
*E-mail: chhkwu@ust.hk

21.1 Introduction

Microfluidics is a multidisciplinary subject, which employs fluids in microchannels to solve miscellaneous problems from physics, chemistry and biology.[1–8] In the field of biology, microfluidic systems have proved to be particularly useful due to their micro-sized feature that perfectly matches the dimension of cells.[1,7,8] As a result of that, microfluidic systems are extensively used in the areas of biomedical science and engineering, such as single cell analysis, disease diagnosis, biosynthesis and tissue engineering.[7–22]

Smart Materials No. 25
Smart Materials for Tissue Engineering: Applications
Edited by Qun Wang

Published by the Royal Society of Chemistry, www.rsc.org

Among these applications, tissue engineering has attracted a lot of attention because of the enormous growth in the population with degenerative diseases, including heart diseases, diabetes, osteoporosis, atherosclerosis, and macular degeneration.[23] For those patients suffering from severe symptoms, transplantation is their last resort.[24,25] However, this is seriously restricted by the small number of donors available in stark contrast to the huge amount of patients in need.[24,25] In the past few decades, the huge progresses in tissue engineering has ignited new hope for those patients thanks to the great advances made in stem cell technology, materials science and manipulation techniques.[26–39] The achievement in stem cell technology has provided human beings with unlimited amounts of specialized cells with desired biological functions while the development of new materials has rendered us with resources to construct various scaffolds with competent performance for artificial tissues.[19,26,29–31,34,37] Moreover, the emergence of 3D bioprinting and new microfluidic systems has given mankind the ability to build complex tissues or even integrated organs using a bottom-up strategy from the cellular level.[40–46]

As a powerful tool, microfluidic systems play an important role in tissue engineering.[44–46] Specifically, smart microfluidic systems have emerged as a new platform for fundamental studies and practical applications in this area in recent years.[47–57] This sort of system is capable of sensitively responding to changes or stimuli generated in the surrounding environment, thus possessing unique functions that are not owned by conventional microfluidic devices.[58] As a relatively new field, it has great potential in biomedical science and engineering. In this chapter, we will briefly introduce some of the smart microfluidic systems based on the stimuli they respond to. Their applications in tissue engineering will also be covered.

21.2 Thermo-Responsive Microfluidic System

Temperature is one of the most important factors that is frequently utilized to tune the properties of materials.[59–62] Poly(*N*-isopropylacrylamide) (PNIPAAm) is probably the most well-known polymer, which has a lower critical solution temperature (LCST) around 32 °C.[63–69] It is hydrophilic below the LCST and transforms into a hydrophobic polymer above it.[63–69] Because of this unique character, it is widely applied as a thermo-responsive coating on common substrates such as a glass slide, polystyrene culture dish and silicon water.[63–69] A surface grafted with a layer of PNIPAAm is cell-adhesive when the temperature is above 32 °C in a normal incubator so that it can promote cell adhesion and the formation of a compact monolayer of cells.[65–69] When the temperature is lowered below 32 °C, it becomes hydrophilic and anti-cell-adhesive.[65–69] Therefore, cells are detached and can be harvested as an integrated sheet with careful manipulation.[65–69] Compared to detachment by trypsin treatment, cells are much less impaired and their junctions as well as extracellular matrix (ECM) are well preserved, making the cell sheet ideal for the fabrication of artificial tissues based on layer-by-layer stacking.[65,67,68]

It is not surprising that PNIPAAm has also found applications in microfluidic systems for tissue engineering. Kitamori *et al.* reported a good study.[51] They designed and made a separable microchip-based cell culture and recovery device (Figure 21.1(a)). The microchip was assembled with two identical glass substrates, each containing half parts of the microfluidic channels. Cells were seeded in the microchannels grafted with a layer of PNIPAAm. The culture medium was kept within the microchannels by Laplace pressure induced by octadecyltrimethoxysilane (ODS)-modified microchip surfaces that are hydrophobic.[70,71] When the cells had grown to confluence, the temperature was lowered to release the cells from the surface as a result of the wettability transition of PNIPAAm. In the end, the top and bottom substrates of the microchip were split to recover the cells from the microchannels. With the increase of photoinitiator concentration (0 to 10 wt%), the grafting density of PNIPAAm on the substrate increased correspondingly (Figure 21.1(b)), leading to over 70% detached cells when the temperature was reduced (Figure 21.1(c)). This study demonstrated that a living cell monolayer could be

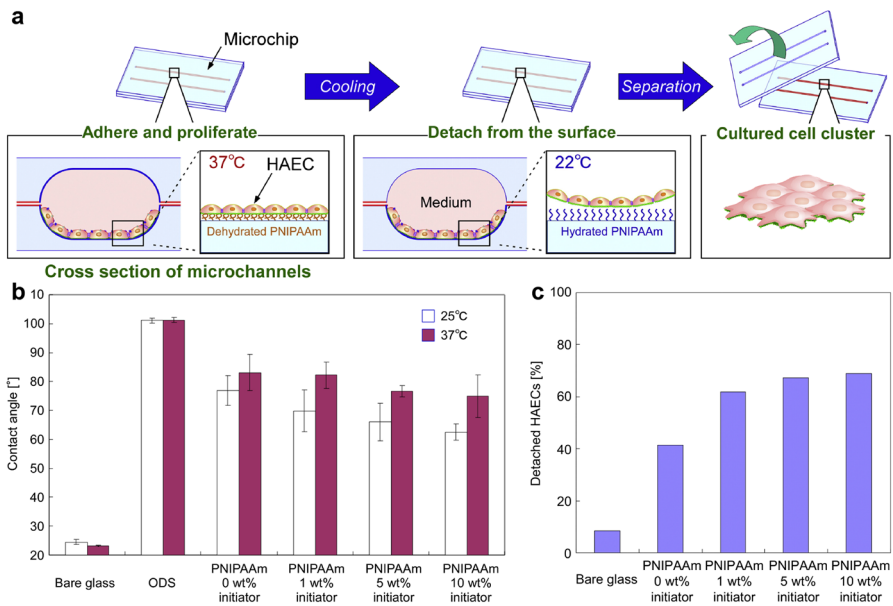

Figure 21.1 Cultivation and recovery of human aortic endothelial cells (HAECs) in thermo-responsive microchannels of a separable microchip.[51] (a) Schematic illustration for the device. (b) Water contact angles on bare, octadecyltrimethoxysilane (ODS)-modified, and PNIPAAm-grafted (0 to 10 wt% initiator solutions) glass substrates at 25 °C and 37 °C. (c) Detachment rate of HAECs grown on bare and PNIPAAm-grafted (0 to 10 wt% initiator solutions) glass substrates at 25 °C. Reprinted from *Biomaterials*, **32**(10), Cultivation and recovery of vascular endothelial cells in microchannels of separable micro-chemical chip. T. Yamashita, Y. Tanaka, N. Idota, K. Sato, K. Mawatari and T. Kitamori, 2459–2465, Copyright (2011) with permission from Elsevier.

recovered in a thermo-responsive microfluidic system for the first time, thus it may be a useful technique for vascular tissue engineering.

Human eyes can readily tune their focus by adjusting their lens' shape with the aid of ciliary muscles despite their compactness.[72,73] The development of optical systems that mimic the functions of human eyes has wide applications in photonics, displays and biomedical engineering.[74–76] However, traditional artificial ones rely on the displacement of lenses to achieve focusing, which requires complicated mechanical accessories. In the past few decades, the enormous progress in miniaturization technology has brought about new optical systems that are no longer dependent on them.[47,77–80] Among these works, an intriguing biomimetic "eye" based on a microfluidic system was presented by Jiang *et al.* (Figure 21.2(a)).[47]

In their work, they created a meniscus-shaped interface between water and oil, which acted as an optical lens. Its focal length can be adjusted by tuning the curvature of the meniscus. The core of the design is a ring made of a stimulus-responsive hydrogel (PNIPAAm for thermo-responsiveness) in a microchannel that is sandwiched between a glass plate and an aperture slip with an opening centered over the ring. The microchannels were filled with water, and oil was added on top of the aperture slip, which was further covered with a cover slip. A meniscus-shaped interface between water and oil was generated due to interfacial tensions. In their device, a polymer protecting layer was made around the hydrogel ring so as to prevent water leakage and physically restrict the latter's movement at its inner periphery (Figure 21.2(c)). When PNIPAAm is prepared as the hydrogel ring, its volume can be tuned by temperature (*i.e.* expands when lowering it and shrinks when raising it) so that the curvature of the meniscus can be adjusted. By tuning the temperature, the focal length can be adjusted from divergent (−11.7 mm to −∞ at 23 to 33 °C) to convergent (+∞ to 22.8 mm at 33 to 47 °C) (Figure 21.2(d)).

21.3 pH-Sensitive Microfluidic System

pH, another crucial stimulus, is often applied in smart systems.[60,81,82] Despite that, there are almost no reports about the applications of pH-sensitive microfluidic systems in tissue engineering, probably on account of the lability of mammalian cells to even a small change of environmental pH from the physiological condition. In fact, the system designed by Jiang *et al.* can also be made pH-sensitive by replacing the PNIPAAm-based hydrogel with a pH-sensitive polymer such as a poly(acrylic acid) (PAA)-based one (Figure 21.3(a)).[47,83] The PAA-based hydrogel contracts and expands at acidic and basic pHs, respectively (Figure 21.3(b) and (c)). Therefore, the microlens' focal length can be controlled by environmental pH (Figure 21.3(d)). As a proof of concept, they demonstrated the smart focusing of two objects by simply changing the pH of the aqueous solution in the microchannels (Figure 21.3(e)). When the pH was 2.0, both objects were out of focus. When the pH was increased to 4.0, the needle tip was focused. At pH 6.0, the focus point

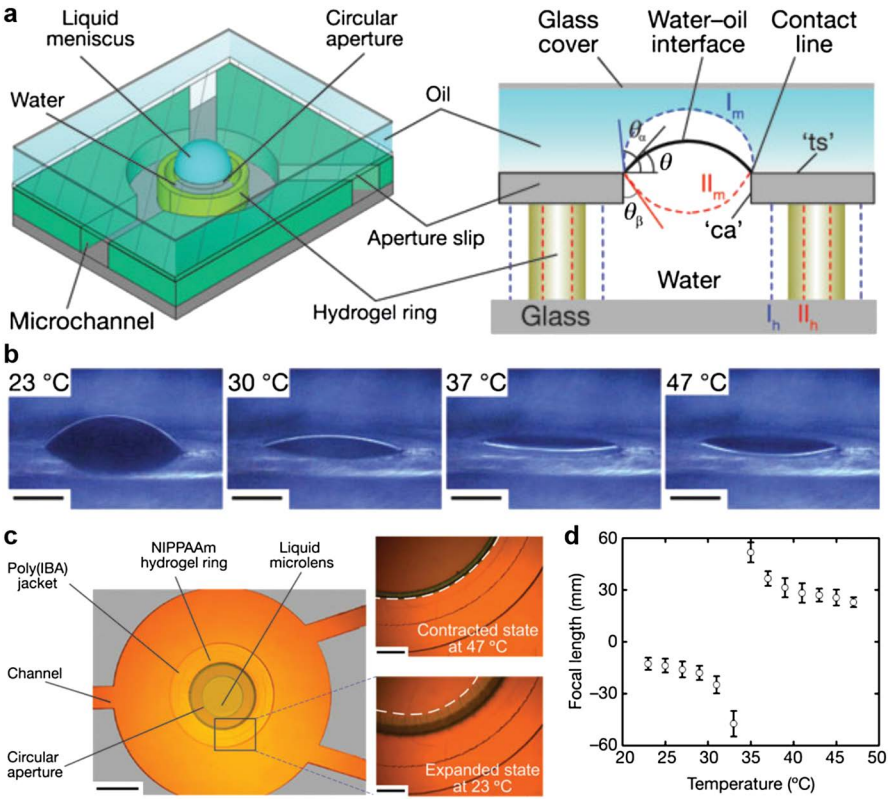

Figure 21.2 Biomimetic "eye" based on a thermo-responsive microfluidic system.[47] (a) Operational mechanism of the biomimetic "eye". The blue dashed lines indicate the expanded state of the hydrogel ring ('I_h'), corresponding to the divergent microlens ('I_m'). The red dashed lines show the contracted state of the hydrogel ring ('II_h'), corresponding to the convergent microlens ('II_m'). (b) Pictures showing the adjustment in the shape of the liquid microlens with the increase of local environmental temperature. Scale bars: 1 mm. (c) Optical images of the device. The dashed lines delineate the boundaries of the inner periphery of the hydrogel ring at two distinct temperatures. Scale bars: 2 mm in the left image, 500 μm in the right ones. (d) The temperature dependence of the focal length of the microlens. (Adapted by permission from Macmillan Publishers Ltd: ref. 47, copyright 2006.)

moved to somewhere between the two objects while at pH 10.0, the ball was finally focused.

21.4 Electro-Active Microfluidic System

Electrical stimulation is also an essential trigger for smart systems.[60,84,85] Rubloff *et al.*[52] developed an electro-active microfluidic system for three-dimensional (3D) cell assembly (Figure 21.4(a)). In their work, they used angled

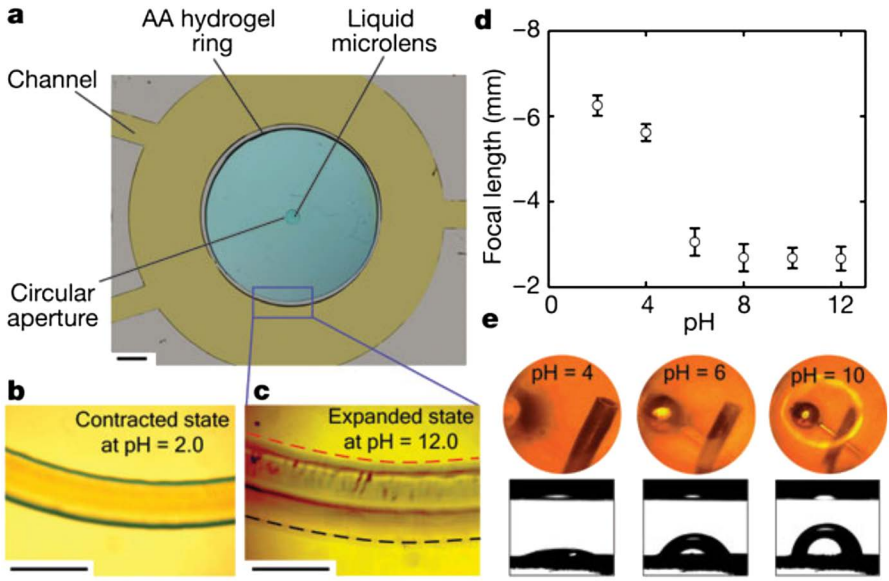

Figure 21.3 Biomimetic "eye" based on a smart pH-sensitive microfluidic system.[47] (a) A bright-field image of the device. PNIPAAm-based hydrogel was replaced by a poly(acrylic acid) (PAA)-based one for pH-sensitivity. Scale bar: 1 mm. (b), (c) The contracted (b) and expanded (c) states of the hydrogel ring at pH 2.0 and pH 12.0, respectively. The red and black dashed lines indicate the boundaries of the inner and outer peripheries of the hydrogel ring, respectively. Scale bars: 500 μm. (d) The dependence of the focal length of the microlens on pH. (e) "Smart" focusing of two objects (a pillar connected to a ball and a needle tip, with a distance of 1.38 cm). (Adapted by permission from Macmillan Publishers Ltd: ref. 47, copyright 2006.)

thermal evaporation of chromium and gold with the aid of a bent shadow mask to fabricate several parallel electrodes and leads on a glass plate. They placed two identical glass plates with the electrodes and leads side by side with a spacing of 1 mm, and sandwiched them between two pieces of poly(dimethylsiloxane) (PDMS) slab to construct a microfluidic system. A deposition solution composed of sodium alginate, $CaCO_3$ particles and cells filled the microchannel. By applying an electric potential, H^+ ions were generated at the anode by the electrolysis of water, which dissolved the $CaCO_3$ particles and released Ca^{2+} ions. The crosslinking of sodium alginate was then triggered by the presence of free Ca^{2+} ions.[86] 3D cell assembly was subsequently achieved by the sol–gel transition (Figure 21.4(b)). Since $CaCO_3$ particles can prevent the accumulation of H^+, pH deviation from neutral was so minimal that the cells encapsulated in the hydrogel maintained a high viability (Figure 21.4(c)). Besides multiple parallel electrodes, an electrode array (Figure 21.4(d)) was made as well with photolithography so that the spatially programmable assembly of cells was realized. The assembled 3D tissue enables

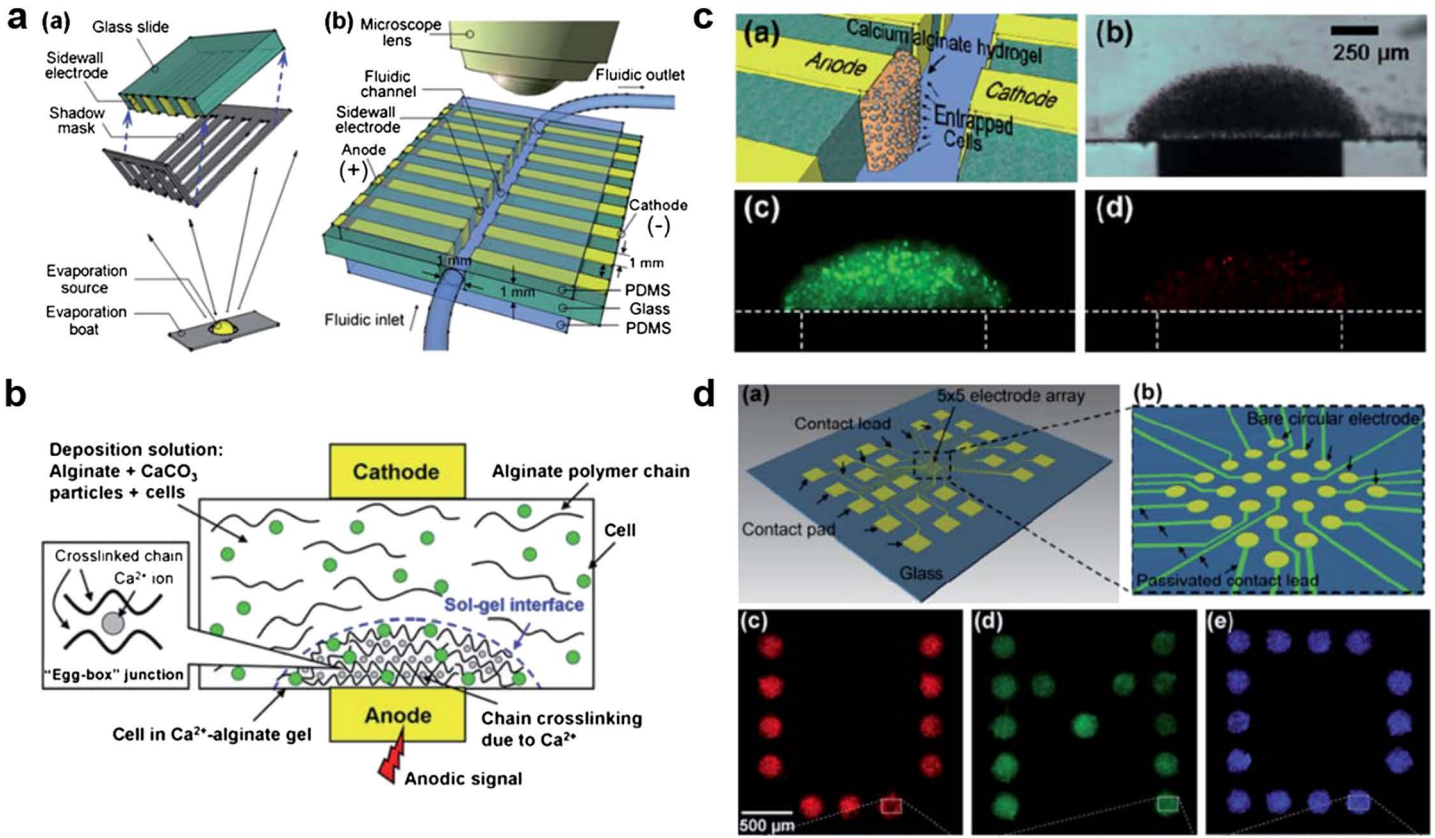

Figure 21.4 An electro-active microfluidic system for 3D cell assembly.[52] (a) Design of the electro-active microfluidic system. Angled thermal evaporation was used to build the parallel sidewall electrodes. (b) Schematic for the mechanism of 3D cell assembly through electrodeposition of calcium alginate hydrogel. (c) Assembly of mammalian cells (mouse B cells) on the sidewall of an electrode in a microfluidic device. Live (green)/dead (red) staining demonstrated a high viability of the assembled cells. (d) Spatially programmed assembly of *E. coli* cells expressing red fluorescent protein (RFP), green fluorescent protein (GFP), and blue fluorescent protein (BFP) on a 5 × 5 electrode array. (All the images were adapted from ref. 52 with permission from The Royal Society of Chemistry.)

the *in vitro* study of interactions between cells and their behaviors to stimuli at a more biologically relevant state.

Dielectrophoresis (DEP) is a physical phenomenon in which an external force is exerted on a particle when it is subjected to a non-uniform electric field.[87,88] In microfluidic systems, it is normally exploited as a tool for manipulating microparticles including mammalian cells.[89–91] Liu *et al.*[54] successfully reconstructed a liver tissue on a chip by making use of DEP. In their work, a lobule-mimetic stellate electrode array was constructed on a glass substrate, which consisted of two sets of electrodes, one for trapping hepatic cells and the other for endothelial cells (Figure 21.5(a)). A microfluidic system was then built by bonding the glass substrate to a transparent indium–tin–oxide

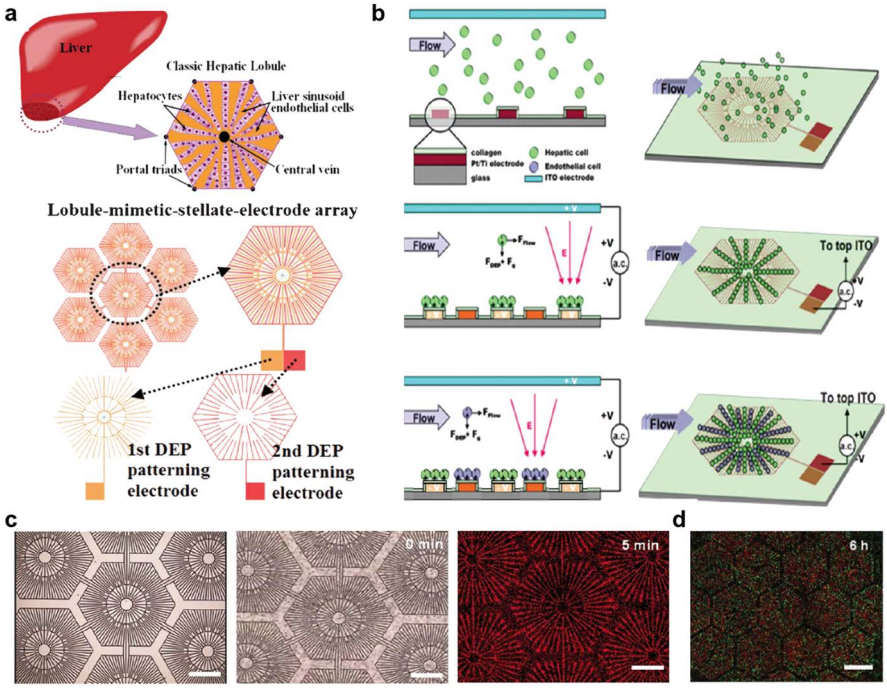

Figure 21.5 Liver-cell patterning on a microfluidic chip by dielectrophoresis (DEP).[54] (a) The fundamental structures of a hepatic lobule in liver and a stellate electrode array that mimics lobule. (b) The configuration and operational principle of heterogeneous lobule-mimetic cell patterning based on DEP. (c) DEP-based cell patterning on a chip in parallel. Bright-field pictures exhibit the lobule-mimetic electrode array before (left) and after (middle) cell infusion. After an alternating potential of 5 V at 1 MHz was applied, the originally randomly distributed HepG2 were patterned and snared onto the electrode array, as revealed by the fluorescence image (right). Scale bars: 500 μm. (d) The biomimetic liver tissue with heterogeneous distribution of HepG2 and HUVEC cells. (All the images were adapted from ref. 54 with permission from The Royal Society of Chemistry.)

(ITO) glass slide with inlet and outlet openings (Figure 21.5(b)). By applying alternating potentials, *Homo sapiens* carcinoma (HePG2) cells and human umbilical vein endothelial (HUVEC) cells were patterned and trapped sequentially onto the electrode array that mimics the lobule (Figure 21.5(d)), generating a centimeter-scale engineered liver tissue that recapitulated the structure of native hepatic lobules. This technique was claimed to be highly biocompatible for cell assembly as about 95% of cells were still alive after cell patterning based on DEP. More interestingly, the liver function (as reflected by CYP450-1A1 enzyme activity) of the biomimetic tissue (HePG2+HUVEC) exhibited an 80% enhancement over the non-patterned pure HepG2 after two days' culture.

21.5 Light-Responsive Microfluidic System

Light is an extremely valuable energy source for triggering chemical reactions.[92–95] By virtue of its ease of manipulation, it is also a powerful tool in the manufacture of microchips, specifically for micropatterning using photolithography.[96–100] Some microfluidic systems even exploit light to create engineered microtissues. For instance, Kwon *et al.*[49] established a microfluidic system for fabricating heterogeneous 3D microstructures based on optofluidic maskless lithography. As shown in Figure 21.6(a), their system is basically composed of a PDMS microfluidic channel with tunable height and an optical module that can generate desired digital patterns. The height of the channel is controlled under pneumatic pressure *via* the deformation of the PDMS membrane of the top chamber. Through programmed height regulation of the channel, prepolymer solution injection (Figure 21.6(b)) and digital pattern projection, heterogeneous 3D micron-scale objects can be formed. By substituting hydrogel precursor solutions encapsulating different cell types (Figure 21.6(c)) for prepolymer solutions, microtissues with complex 3D structures can be engineered (Figure 21.6(d)). Since the ultraviolet (UV) light exposure time for patterning was relatively short (0.2 s), high viabilities (>90%) of cells were maintained in the micro-tissues (Figure 21.6(e)). The proposed technique is simple and allows rapid synthesis of complex 3D heterogeneous microtissues so that it is a robust platform for studying cell-to-cell interactions and for microfluidic bioassays.

Although the technique invented by Kwon *et al.*[49] can generate complex heterogeneous 3D structures, it is not capable of engineering microtissues on a large scale even in one dimension such as with muscle fibers. Our group has established a light-responsive microfluidic system that can produce cell-responsive grooved microfibers *via* spinning (Figure 21.7(a)).[56] To introduce a grooved feature on the microfibers, a special micronozzle with a complementary structure was fabricated *via* repeated replica molding (Figure 21.7(b)), which was then connected to a syringe through a needle. Methacrylamide-modified gelatin (GelMA) solution was prepared as the scaffold material for cell encapsulation or seeding. The hydrogel precursor solution was injected through the micronozzle and immersed in cold ethanol.

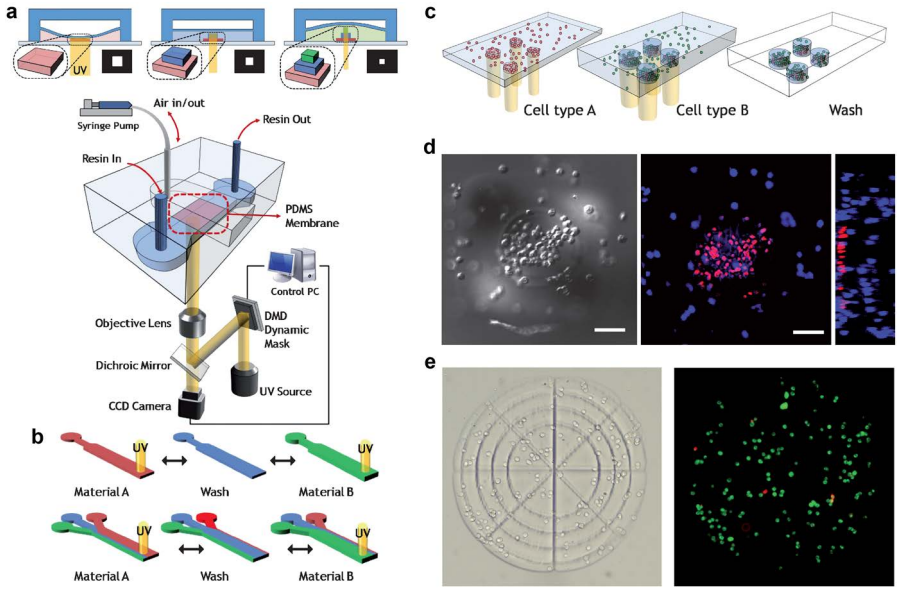

Figure 21.6 Fabrication of heterogeneous 3D microstructures using the deformation of soft membrane and maskless optofluidic lithography.[49] (a) Schematic illustration of the microfluidic system. (b) Control of microfluids for exchanging prepolymer solutions for generating hybrid microstructures. Prepolymer solutions can be loaded through the same inlet sequentially (top) or multilaminar flow (bottom). (c) Diagram depicting the fabrication of heterogeneous 3D hydrogel microstructures encapsulating living cells. (d) Confocal laser scanning microscope (CLSM) images of a heterogeneous hydrogel block containing sequentially patterned *Homo sapiens* cervix adenocarcinoma (HeLa) cells (left: differential interference contrast image; right: fluorescence image). (e) Cell viability assay in a cell-containing hydrogel block (left: bright-field image; right: fluorescence image). (All the images were adapted from ref. 49 with permission from The Royal Society of Chemistry.)

The as-prepared fibers were crosslinked by UV exposure. To generate GelMA microfibers continuously, the solution of GelMA was kept warm (60 °C) in the syringe before being injected into the micronozzle.

As shown by scanning electron microscopy (SEM) images (Figure 21.7(c)), GelMA microfibers with well-defined grooves could be acquired with our device. Owing to the outstanding biocompatibility of gelatin, high viabilities (>80%) of cells were achieved for both those cultured on it (Figure 21.7(d)) and encapsulated in it (data not shown). Moreover, a nice alignment of cells was achieved with the assistance of the grooved structure on GelMA fibers, in contrast to the random orientation of cells on smooth ones (Figure 21.7(d) and (e)). Encouragingly, our GelMA fibers can even support the co-culture of different cell types as demonstrated by the simultaneous seeding of HUVECs in the microfibers and C2C12 cells on them (Figure 21.7(f)). It is believed

that this co-culture model can facilitate the construction of complicated tissues such as blood vessels, which are constituted of smooth muscle cells and endothelial cells. Because of the merits of our system, it would be helpful in engineering artificial tissues with well-aligned structures such as muscle and blood vessels.

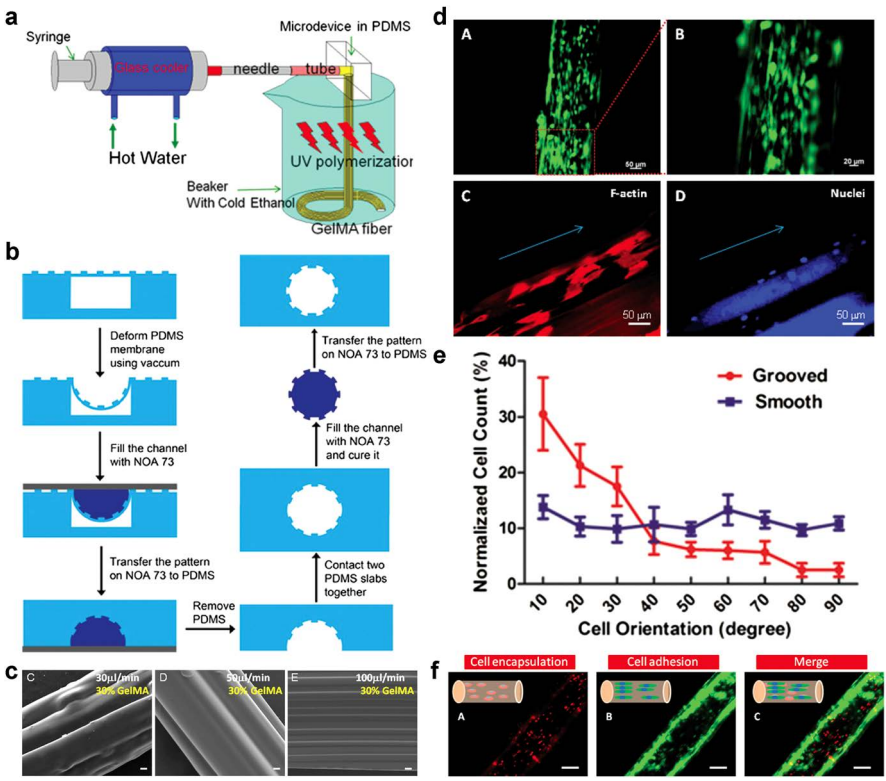

Figure 21.7 Grooved cell-responsive microfibers prepared by microfluidic spinning.[56] (a) Schematic for the principle of the spinning of grooved methacrylamide-modified gelatin (GelMA) microfibers. The fibers are crosslinked by UV exposure. (b) Workflow for the fabrication process of a PDMS micronozzle. (c) Scanning electron microscopy (SEM) images showing the grooved GelMA microfibers spun at varying flow rates. Scale bars: 20 μm. (d) Fluorescence images revealing the alignment of Mus musculus muscle (C2C12) cells caused by the induction of the grooved microstructures on the surface of GelMA fibers. The top panels present live (green)/dead (red) cell assay results while the bottom ones exhibit the orientation of filamentous actin (red) and cell nuclei (blue), respectively. (e) Quantification of cell alignment on grooved GelMA microfibers and smooth ones. (f) Fluorescence images displaying co-culture of two different cell types. HUVECs (red) were encapsulated in the grooved GelMA microfibers and C2C12 cells (green) were seeded on them. (Scale bars: 200 μm) (From ref. 56. Copyright © 1999–2016 by John Wiley & Sons, Inc. Reprinted by permission of John Wiley & Sons, Inc.)

21.6 Magneto-Responsive Microfluidic System

It is generally known that many organs and tissues such as the heart, stomach, bone and blood vessels possess multi-layered structures with varying orientations in each layer.[101–105] So it is imperative to fabricate multi-layered scaffolds with tunable alignment in each layer for the purpose of engineering tissues that resemble their native counterparts. Jiang *et al.*[48] have designed a magneto-responsive microfluidic system to spin aligned nanofibers (Figure 21.8(a)). The key part of their apparatus is a set of two parallel-positioned permanent magnets, which generates a magnetic field that can induce the alignment of electrospun fibers doped with magnetic particles. Poly(vinyl alcohol) (PVA) nanofibers with excellent alignment were successfully obtained (Figure 21.8(b)). By rotating the substrate after each cycle of fiber collection (Figure 21.8(c)), multi-layered fibrous grids with varying orientations could be formed (Figure 21.8(d)). Compared to other methods, their approach has at least the following advantages: (a) the whole system is simple, only including two additional magnets in contrast to conventional designs; (b) the magnetic field can be readily handled; (c) multi-layered fibrous grids with any orientations can be formed; (d) a much larger area of aligned fibers can be harvested compared to other methods.

To facilitate more precise control, Sun *et al.*[57] invented a smart system using microfluidic printing for 3D magnetic assembly of alginate microfibers (Figure 21.9). In their system, a permanent magnet disc was placed under a culture dish filled with deionized water. Fe_3O_4 magnetic nanoparticles (MNs)-doped sodium alginate solution was laden with cells and injected into a microfluidic

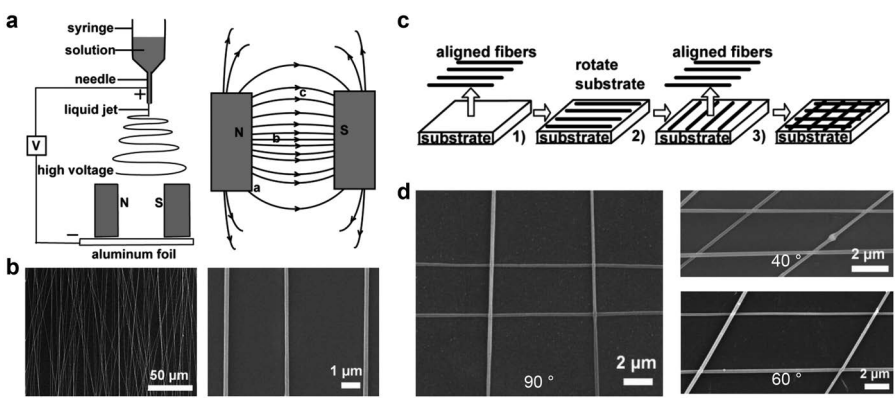

Figure 21.8 Magnetic electrospinning of aligned nanofibers.[48] (a) Schematic illustration for the preparation of aligned fibers using magnetic electrospinning (MES). The two parallel-positioned permanent magnets generated a magnetic field that induced the alignment of fibers. (b) SEM images of the aligned poly(vinyl alcohol) (PVA) nanofibers. (c) Strategy for the formation of multi-layered fibrous grids with varying orientations. (d) SEM images of two-layer fibrous grids with different angles of rotation. (From ref. 48. Copyright © 1999–2016 by John Wiley & Sons, Inc. Reprinted by permission of John Wiley & Sons, Inc.)

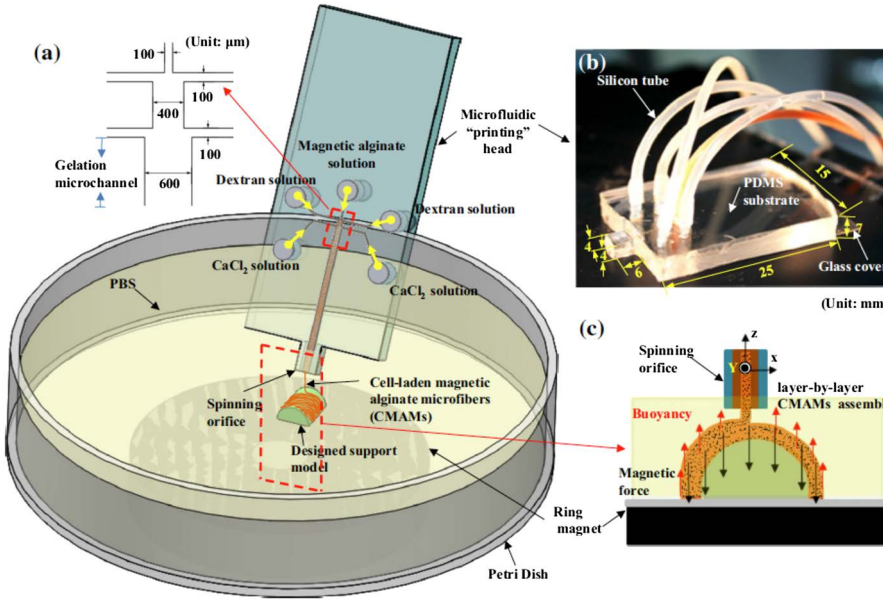

Figure 21.9 Printed 3D assembly of magnetic alginate microfibers using a microfluidic method.[57] (a) Diagram of the system for 3D magnetic assembly. (b) Image of a microfluidic print head for the system. (c) Mechanism of the 3D magnetic assembly. (ref. 57, with permission of Springer.)

chip. The solution was partially crosslinked in the microchannel by Ca^{2+} from other inlets and ejected from the device. The magnetic force imposed on the magnetic alginate microfibers (MAMs) could counteract the buoyancy of the water so that they would deposit onto a supporting substrate fixed in a Petri dish. Guided by the magnetic field, the movement of MAMs in the *z* direction made it possible to fabricate 3D assemblies with well-defined alignment of microfibers simply by moving the microfluidic device on the *xy* plane. Owing to the excellent biocompatibility of alginate, the cells maintained a high viability in the fibers. By using this "bottom-up" approach, 3D assemblies of MAMs with complex geometries can be produced since various shapes of the supporting substrate can be manufactured with modern technologies.

21.7 Enzymatically Degradable Microfluidic System

In the past few years, enzymatically degradable microfluidic systems have come out for the purpose of mimicking biological phenomena at tissue level in microfluidic chips.[50,53,55] Among these studies, the one reported by Chung *et al.*[53] is likely to be the most representative. Their device (Figure 21.10(a) and (b)) is made up of four major parts, *i.e.* a cell culture channel, two hydrogel channels, a stimuli channel, and a control channel. All the channels were firstly loaded with poly(L-lysine) (PLL) solution for surface coating to

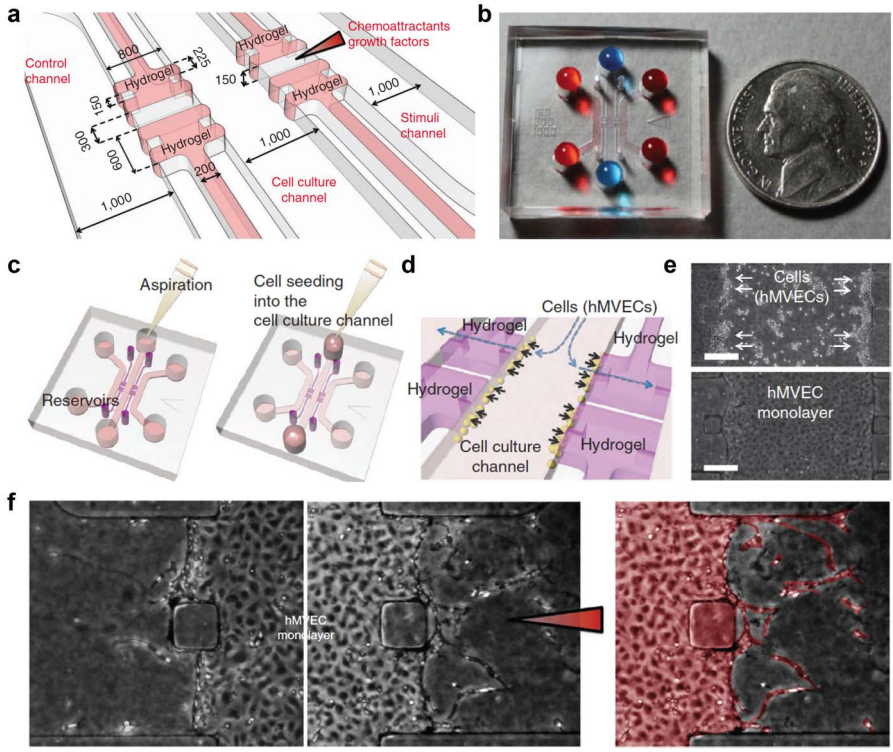

Figure 21.10 Simultaneous culture of multiple types of cells on the surfaces of a channel and within an enzymatically degradable collagen hydrogel in a microfluidic system.[53] (a) Schematic of the microfluidic system for cell culture. The units of all the figures are μm. (b) Photograph of the microfluidic chip. (c) Seeding of cells into one reservoir connected to the central channel. (d) Hydrostatic pressure gradient pushing the suspended cells onto the collagen hydrogel. (e) Optical images showing suspended human microvascular endothelial cells (hMVECs) right after cell seeding (top) and tight cell monolayer at day one (bottom). Scale bars: 250 μm. (f) Optical images exhibiting angiogenesis of the hMVEC monolayer into the collagen hydrogel induced by the diffusion of vascular endothelial growth factor (VEGF) from the right channel. (Adapted by permission from Macmillan Publishers Ltd: ref. 53, copyright 2012.)

enhance cell adhesion. Collagen hydrogel was then formed in the hydrogel channels to mimic the ECM. Subsequently, cells were injected into the cell culture channel (Figure 21.10(c)) and the hydrostatic pressure pushed the suspended cells onto the collagen hydrogel (Figure 21.10(d)). After the attachment of cells, media with and without stimulating reagents were added into the stimuli channel and control channel, respectively. Due to the presence of the PLL coating, cells attached onto the surface of the microchannel and formed a tight monolayer (Figure 21.10(e)). As collagen is enzymatically degradable, cells could digest the hydrogel and grow into it, being attracted

by growth factors or chemoattractants, as demonstrated by the angiogenesis of human microvascular endothelial cells (hMVECs) into the collagen hydrogel induced by the diffusion of vascular endothelial growth factor (VEGF) from the right channel (Figure 21.10(f)).

In addition to biochemical reagents, a second cell type could be raised in the stimuli channel to investigate interactions between different types of cells. Cells may even be embedded in the hydrogel for 3D culture. Well-defined biochemical and biophysical stimuli could be established by using this platform to study various biological phenomena. Thereby, it can help researchers to better understand fundamental issues in developmental biology, disease and tissue engineering.

21.8 Conclusion and Outlook

In this chapter, we have briefly reviewed several representative smart microfluidic systems according to the type of responsiveness, and their applications in tissue engineering. Although microfluidics is a discipline with a history of about 30 years, smart microfluidic systems have emerged only in the past decade. As a matter of fact, the number of reports about the applications of smart microfluidic systems in tissue engineering is still relatively small. With the continuous growth in the population with degenerative diseases in contrast to the scarcity of donor organs and tissues, one can foresee that more and more resources will be invested into tissue engineering. As a powerful technique to manipulate cells at the microscale, it comes naturally that microfluidics will continue to serve purposes related to biomedical science and engineering. Smart microfluidic systems based on other response mechanisms or capable of solving new problems are expected to come out. It is definite that they will prove their great value in tissue engineering and even demonstrate their clinical potential. Hopefully, with the advances in this, and other new techniques such as 3D bioprinting, practically implantable artificial tissues or even organs would be constructed in the near future.

Acknowledgements

We gratefully appreciate financial support from the Theme-based Research Scheme Fund (T13–706/11–2), Collaborative Research Fund (CUHK4/CRF/12G), and General Research Fund (GRF604712, GRF16306115) provided by the Research Grant Council (RGC) of Hong Kong. Y. Chen and L. Huang contributed equally to this chapter.

References

1. G. M. Whitesides, *Nature*, 2006, **442**, 368.
2. U. F. Keyser, B. N. Koeleman, S. van Dorp, D. Krapf, R. M. M. Smeets, S. G. Lemay, N. H. Dekker and C. Dekker, *Nat. Phys.*, 2006, **2**, 473.
3. T. Beatus, T. Tlusty and R. Bar-Ziv, *Nat. Phys.*, 2006, **2**, 743.

4. D. H. Kelley and N. T. Ouellette, *Nat. Phys.*, 2011, **7**, 477.
5. H. Song, J. D. Tice and R. F. Ismagilov, *Angew. Chem., Int. Ed.*, 2003, **42**, 768.
6. A. J. deMello, *Nature*, 2006, **442**, 394.
7. K. Ren, Y. Chen and H. Wu, *Curr. Opin. Biotechnol.*, 2014, **25**, 78.
8. B. Xiong, K. Ren, Y. Shu, Y. Chen, B. Shen and H. Wu, *Adv. Mater.*, 2014, **26**, 5525.
9. F. K. Balagaddé, L. You, C. L. Hansen, F. H. Arnold and S. R. Quake, *Science*, 2005, **309**, 137.
10. B. Huang, H. Wu, D. Bhaya, A. Grossman, S. Granier, B. K. Kobilka and R. N. Zare, *Science*, 2007, **315**, 81.
11. A. K. White, M. VanInsberghe, O. I. Petriv, M. Hamidi, D. Sikorski, M. A. Marra, J. Piret, S. Aparicio and C. L. Hansen, *Proc. Natl. Acad. Sci. U. S. A.*, 2011, **108**, 13999.
12. L. Huang, Y. Chen, Y. Chen and H. Wu, *Anal. Chem.*, 2015, **87**, 12169.
13. S. Nagrath, L. V. Sequist, S. Maheswaran, D. W. Bell, D. Irimia, L. Ulkus, M. R. Smith, E. L. Kwak, S. Digumarthy, A. Muzikansky, P. Ryan, U. J. Balis, R. G. Tompkins, D. A. Haber and M. Toner, *Nature*, 2007, **450**, 1235.
14. R. Fan, O. Vermesh, A. Srivastava, B. K. H. Yen, L. Qin, H. Ahmad, G. A. Kwong, C.-C. Liu, J. Gould, L. Hood and J. R. Heath, *Nat. Biotechnol.*, 2008, **26**, 1373.
15. S. L. Stott, C.-H. Hsu, D. I. Tsukrov, M. Yu, D. T. Miyamoto, B. A. Waltman, S. M. Rothenberg, A. M. Shah, M. E. Smas, G. K. Korir, F. P. Floyd, A. J. Gilman, J. B. Lord, D. Winokur, S. Springer, D. Irimia, S. Nagrath, L. V. Sequist, R. J. Lee, K. J. Isselbacher, S. Maheswaran, D. A. Haber and M. Toner, *Proc. Natl. Acad. Sci. U. S. A.*, 2010, **107**, 18392.
16. J. Tian, H. Gong, N. Sheng, X. Zhou, E. Gulari, X. Gao and G. Church, *Nature*, 2004, **432**, 1050.
17. Q. Mei, C. K. Fredrickson, A. Simon, R. Khnouf and Z. H. Fan, *Biotechnol. Prog.*, 2007, **23**, 1305.
18. J. G. Martin, M. Gupta, Y. Xu, S. Akella, J. Liu, J. S. Dordick and R. J. Linhardt, *J. Am. Chem. Soc.*, 2009, **131**, 11041.
19. N. W. Choi, M. Cabodi, B. Held, J. P. Gleghorn, L. J. Bonassar and A. D. Stroock, *Nat. Mater.*, 2007, **6**, 908.
20. D. Huh, B. D. Matthews, A. Mammoto, M. Montoya-Zavala, H. Y. Hsin and D. E. Ingber, *Science*, 2010, **328**, 1662.
21. X. Mu, W. Zheng, L. Xiao, W. Zhang and X. Jiang, *Lab Chip*, 2013, **13**, 1612.
22. J. Su, Y. Zheng and H. Wu, *Lab Chip*, 2009, **9**, 996.
23. J. A. Salomon, H. Wang, M. K. Freeman, T. Vos, A. D. Flaxman, A. D. Lopez and C. J. L. Murray, *Lancet*, 2012, **380**, 2144.
24. R. I. Lechler, M. Sykes, A. W. Thomson and L. A. Turka, *Nat. Med.*, 2005, **11**, 605.
25. G. Orlando, K. J. Wood, R. J. Stratta, J. J. Yoo, A. Atala and S. Soker, *Transplantation*, 2011, **91**, 1310.
26. P. Bianco and P. G. Robey, *Nature*, 2001, **414**, 118.

27. U. A. Stock and J. P. Vacanti, *Annu. Rev. Med.*, 2001, **52**, 443.
28. L. G. Griffith and G. Naughton, *Science*, 2002, **295**, 1009.
29. H. Shin, S. Jo and A. G. Mikos, *Biomaterials*, 2003, **24**, 4353.
30. S. J. Hollister, *Nat. Mater.*, 2005, **4**, 518.
31. G. Chan and D. J. Mooney, *Trends Biotechnol.*, 2008, **26**, 382.
32. L. Moroni, J. R. de Wijn and C. A. van Blitterswijk, *J. Biomater. Sci., Polym. Ed.*, 2008, **19**, 543.
33. D. Meng, M. Erol and A. R. Boccaccini, *Adv. Eng. Mater.*, 2010, **12**, B467.
34. F. J. O'Brien, *Mater. Today*, 2011, **14**, 88.
35. S. F. Badylak, D. J. Weiss, A. Caplan and P. Macchiarini, *Lancet*, 2012, **379**, 943.
36. D. G. Seifu, A. Purnama, K. Mequanint and D. Mantovani, *Nat. Rev. Cardiol.*, 2013, **10**, 410.
37. S. Wu, X. Liu, K. W. K. Yeung, C. Liu and X. Yang, *Mater. Sci. Eng., R*, 2014, **80**, 1.
38. Y. Chen, J. Wang, B. Shen, C. W. Y. Chan, C. Wang, Y. Zhao, H. N. Chan, Q. Tian, Y. Chen, C. Yao, I.-M. Hsing, R. A. Li and H. Wu, *Macromol. Biosci.*, 2015, **15**, 426.
39. Y. Chen, X. Dai, L. Huang, Y. Sun, H. N. Chan, B. Shen, X. Zeng, Z. Wu, I.-M. Hsing, Z. Guo and H. Wu, *Adv. Funct. Mater.*, 2015, **25**, 6189.
40. V. Mironov, V. Kasyanov, C. Drake and R. R. Markwald, *Regener. Med.*, 2008, **3**, 93.
41. V. Mironov, R. P. Visconti, V. Kasyanov, G. Forgacs, C. J. Drake and R. R. Markwald, *Biomaterials*, 2009, **30**, 2164.
42. G. Villar, A. D. Graham and H. Bayley, *Science*, 2013, **340**, 48.
43. S. V. Murphy and A. Atala, *Nat. Biotechnol.*, 2014, **32**, 773.
44. H. Onoe, T. Okitsu, A. Itou, M. Kato-Negishi, R. Gojo, D. Kiriya, K. Sato, S. Miura, S. Iwanaga, K. Kuribayashi-Shigetomi, Y. T. Matsunaga, Y. Shimoyama and S. Takeuchi, *Nat. Mater.*, 2013, **12**, 584.
45. S. N. Bhatia and D. E. Ingber, *Nat. Biotechnol.*, 2014, **32**, 760.
46. A. Hasan, A. Paul, N. E. Vrana, X. Zhao, A. Memic, Y.-S. Hwang, M. R. Dokmeci and A. Khademhosseini, *Biomaterials*, 2014, **35**, 7308.
47. L. Dong, A. K. Agarwal, D. J. Beebe and H. Jiang, *Nature*, 2006, **442**, 551.
48. D. Yang, B. Lu, Y. Zhao and X. Jiang, *Adv. Mater.*, 2007, **19**, 3702.
49. S. A. Lee, S. E. Chung, W. Park, S. H. Lee and S. Kwon, *Lab Chip*, 2009, **9**, 1670.
50. G. M. Price, K. H. K. Wong, J. G. Truslow, A. D. Leung, C. Acharya and J. Tien, *Biomaterials*, 2010, **31**, 6182.
51. T. Yamashita, Y. Tanaka, N. Idota, K. Sato, K. Mawatari and T. Kitamori, *Biomaterials*, 2011, **32**, 2459.
52. Y. Cheng, X. Luo, C.-Y. Tsao, H.-C. Wu, J. Betz, G. F. Payne, W. E. Bentley and G. W. Rubloff, *Lab Chip*, 2011, **11**, 2316.
53. Y. Shin, S. Han, J. S. Jeon, K. Yamamoto, I. K. Zervantonakis, R. Sudo, R. D. Kamm and S. Chung, *Nat. Protoc.*, 2012, **7**, 1247.
54. C.-T. Ho, R.-Z. Lin, R.-J. Chen, C.-K. Chin, S.-E. Gong, H.-Y. Chang, H.-L. Peng, L. Hsu, T.-R. Yew, S.-F. Chang and C.-H. Liu, *Lab Chip*, 2013, **13**, 3578.

55. P. A. Galie, D.-H. T. Nguyen, C. K. Choi, D. M. Cohen, P. A. Janmey and C. S. Chen, *Proc. Natl. Acad. Sci. U. S. A.*, 2014, **111**, 7968.
56. X. Shi, S. Ostrovidov, Y. Zhao, X. Liang, M. Kasuya, K. Kurihara, K. Nakajima, H. Bae, H. Wu and A. Khademhosseini, *Adv. Funct. Mater.*, 2015, **25**, 2250.
57. T. Sun, Q. Huang, Q. Shi, H. Wang, X. Liu, M. Seki, M. Nakajima and T. Fukuda, *Microfluid. Nanofluid.*, 2015, **19**, 1169.
58. L. Ionov, N. Houbenov, A. Sidorenko, M. Stamm and S. Minko, *Adv. Funct. Mater.*, 2006, **16**, 1153.
59. M. A. Ward and T. K. Georgiou, *Polymers*, 2011, **3**, 1215.
60. M. A. C. Stuart, W. T. S. Huck, J. Genzer, M. Müller, C. Ober, M. Stamm, G. B. Sukhorukov, I. Szleifer, V. V. Tsukruk, M. Urban, F. Winnik, S. Zauscher, I. Luzinov and S. Minko, *Nat. Mater.*, 2010, **9**, 101.
61. N. Shimada and A. Maruyama, in *Tailored Polymer Architectures for Pharmaceutical and Biomedical Applications*, ed. C. Scholz and J. Kressler, American Chemical Society, Washington, DC, 2013, vol. 14, pp. 235–241.
62. D. Roy, W. L. A. Brooks and B. S. Sumerlin, *Chem. Soc. Rev.*, 2013, **42**, 7214.
63. T. Okano, N. Yamada, H. Sakai and Y. Sakurai, *J. Biomed. Mater. Res.*, 1993, **27**, 1243.
64. Y. G. Takei, T. Aoki, K. Sanui, N. Ogata, Y. Sakurai and T. Okano, *Macromolecules*, 1994, **27**, 6163.
65. T. Shimizu, M. Yamato, A. Kikuchi and T. Okano, *Biomaterials*, 2003, **24**, 2309.
66. Y. Akiyama, A. Kikuchi, M. Yamato and T. Okano, *Langmuir*, 2004, **20**, 5506.
67. Y. Tsuda, T. Shimizu, M. Yarnato, A. Kikuchi, T. Sasagawa, S. Sekiya, J. Kobayashi, G. Chen and T. Okano, *Biomaterials*, 2007, **28**, 4939.
68. C. Williams, A. W. Xie, M. Yamato, T. Okano and J. Y. Wong, *Biomaterials*, 2011, **32**, 5625.
69. Z. Tang, Y. Akiyama and T. Okano, *J. Polym. Sci., Part B: Polym. Phys.*, 2014, **52**, 917.
70. A. Hozumi, K. Ushiyama, H. Sugimura and O. Takai, *Langmuir*, 1999, **15**, 7600.
71. A. Hibara, S. Iwayama, S. Matsuoka, M. Ueno, Y. Kikutani, M. Tokeshi and T. Kitamori, *Anal. Chem.*, 2005, **77**, 943.
72. F. M. Toates, *Physiol. Rev.*, 1972, **52**, 828.
73. N. López-Gil, I. Iglesias and P. Artal, *Vision Res.*, 1998, **38**, 2897.
74. L. P. Lee and R. Szema, *Science*, 2005, **310**, 1148.
75. T. Hirai, T. Ogiwara, K. Fujii, T. Ueki, K. Kinoshita and M. Takasaki, *Adv. Mater.*, 2009, **21**, 2886.
76. S. Schuhladen, F. Preller, R. Rix, S. Petsch, R. Zentel and H. Zappe, *Adv. Mater.*, 2014, **26**, 7247.
77. D.-Y. Zhang, V. Lien, Y. Berdichevsky, J. Choi and Y.-H. Lo, *Appl. Phys. Lett.*, 2003, **82**, 3171.
78. R. Yang, W. Wang and S. A. Soper, *Appl. Phys. Lett.*, 2005, **86**, 161110.

79. S. Yang, G. Chen, M. Megens, C. K. Ullal, Y.-J. Han, R. Rapaport, E. L. Thomas and J. Aizenberg, *Adv. Mater.*, 2005, **17**, 435.
80. C. A. López, C.-C. Lee and A. H. Hirsa, *Appl. Phys. Lett.*, 2005, **87**, 134102.
81. S. Dai, P. Ravi and K. C. Tam, *Soft Matter*, 2008, **4**, 435.
82. D. Schmaljohann, *Adv. Drug Delivery Rev.*, 2006, **58**, 1655.
83. E. S. Gil and S. M. Hudson, *Prog. Polym. Sci.*, 2004, **29**, 1173.
84. J. Lahann, S. Mitragotri, T.-N. Tran, H. Kaido, J. Sundaram, I. S. Choi, S. Hoffer, G. A. Somorjai and R. Langer, *Science*, 2003, **299**, 371.
85. W.-S. Yeo, M. N. Yousaf and M. Mrksich, *J. Am. Chem. Soc.*, 2003, **125**, 14994.
86. J. A. Rowley, G. Madlambayan and D. J. Mooney, *Biomaterials*, 1999, **20**, 45.
87. R. Pethig and G. H. Markx, *Trends Biotechnol.*, 1997, **15**, 426.
88. P. R. C. Gascoyne and J. Vykoukal, *Electrophoresis*, 2002, **23**, 1973.
89. M. Dürr, J. Kentsch, T. Müller, T. Schnelle and M. Stelzle, *Electrophoresis*, 2003, **24**, 722.
90. J. Voldman, *Annu. Rev. Biomed. Eng.*, 2006, **8**, 425.
91. K. Khoshmanesh, S. Nahavandi, S. Baratchi, A. Mitchell and K. Kalantar-zadeh, *Biosens. Bioelectron.*, 2011, **26**, 1800.
92. N. S. Allen and J. F. Mckellar, *Chem. Soc. Rev.*, 1975, **4**, 533.
93. M. Kaur and A. K. Srivastava, *J. Macromol. Sci., Polym. Rev.*, 2002, **42**, 481.
94. J. D. Clapper, L. Sievens-Figueroa and C. A. Guymon, *Chem. Mater.*, 2008, **20**, 768.
95. Y. Fuchs, O. Soppera and K. Haupt, *Anal. Chim. Acta*, 2012, **717**, 7.
96. B. J. Lin, *J. Vac. Sci. Technol.*, 1975, **12**, 1317.
97. T. Ito and S. Okazaki, *Nature*, 2000, **406**, 1027.
98. J. C. McDonald, D. C. Duffy, J. R. Anderson, D. T. Chiu, H. Wu, O. J. A. Schueller and G. M. Whitesides, *Electrophoresis*, 2000, **21**, 27.
99. D.-S. Lee, H. Yang, K.-H. Chung and H.-B. Pyo, *Anal. Chem.*, 2005, **77**, 5414.
100. W. Wei, J. Liu, H. Li, Q. Mu and X. Liu, *Prog. Chem.*, 2014, **26**, 1867.
101. D. D. Streeter, H. M. Spotnitz, D. P. Patel, J. Ross and E. H. Sonnenblick, *Circ. Res.*, 1969, **24**, 339.
102. W. N. Lee, B. Larrat, M. Pernot and M. Tanter, *Phys. Med. Biol.*, 2012, **57**, 5075.
103. H. Minami, H. Isomoto, N. Yamaguchi, K. Matsushima, Y. Akazawa, K. Ohnita, F. Takeshima, H. Inoue and K. Nakao, *Dig. Endosc.*, 2014, **26**, 43.
104. S. Weiner, W. Traub and H. D. Wagner, *J. Struct. Biol.*, 1999, **126**, 241.
105. C. Hahn and M. A. Schwartz, *Nat. Rev. Mol. Cell Biol.*, 2009, **10**, 53.

CHAPTER 22

Smart 3D Printing Materials for Tissue Engineering

SHAN-HUI HSU*[a], KUN-CHE HUNG[a] AND CHENG-WEI CHEN[a]

[a]National Taiwan University, Institute of Polymer Science and Engineering, Sec. 4, Roosevelt Rd, Taipei City, Taiwan
*E-mail: shhsu@ntu.edu.tw

22.1 Introduction

The developments and breakthroughs of metals and ceramics have been in place for many years, while for polymers, it was not until 100 years ago that there had been shown some major progress. Compared with metals and ceramics, the chemical structures of polymers are not only more complex but also can be devised at will. As a result, the variations in their properties can be even more complicated. For applications in tissue engineering, human bones are of a great hardness that can be replaced by metals and ceramics. However, the mechanical properties of these two types of materials are difficult to adjust. Moreover, the biomimeticity of metals and ceramics is unfavorable for use in human bodies. For these reasons, choosing polymers that are more similar to organisms in terms of biological properties for the development of smart materials allows us to fine tune the mechanical properties to meet the standards for use in human bodies as well as making up microenvironments with the real tissues through various mechanisms. Besides, metals and ceramics are mostly bio-inert and therefore are hardly degradable or absorbable in human bodies. In contrast, certain kinds

Smart Materials No. 25
Smart Materials for Tissue Engineering: Applications
Edited by Qun Wang

Published by the Royal Society of Chemistry, www.rsc.org

of polymers such as polyester-based ones can be decomposed gradually by hydrolytic enzymes and subsequently released from human bodies without the need of removal by surgery.

Most structures in organisms can adjust or respond to changes in the surrounding environment. For example, when they encounter changes in light, temperature, pH value, magnetic field or biomolecules, the natural materials in organisms will adapt automatically. Therefore, developing polymers with auto-adjusting abilities is a reasonable strategy from the viewpoint of biomimicry, for which these materials are also called smart polymers. By both physical and chemical mechanisms, polymers can exhibit various kinds of reversible properties and consequently have many applications. Different aspects of smartness may play distinctive roles for use in the biomedical field. Therefore, we will list the developments of a variety of smart polymers in the biomedical field in recent years including smart polymer hydrogels, shape-memory polymers, conductive and piezoelectric smart polymers, detailing the applications in the three-dimensional (3D) printing of these polymers.

22.2 Smart Materials

Smart materials are specifically designed materials that could serve a wide range of purposes, in which they are able to respond to stimuli in their surroundings, *i.e.* pressure, temperature, pH, electric field, and magnetic field, *etc.* These responses include shape memory and self-healing, and the materials could be metals or polymers.[1]

22.2.1 Smart Polymers

Smart polymers cover a wide variety of materials including shape-memory polymers, self-healing polymers, and environment-sensitive hydrogels. As mentioned above, they could adjust in response to changes in the environment.[2] Among these materials, smart degradable polymers have been widely used in the biomedical field, which include polylactide (PLA), polycaprolactone (PCL), polyglycolide (PGA), and poly(lactic-*co*-glycolic acid) (PLGA), which can be prepared through different physical or chemical processes.

22.3 The Introduction of Hydrogels

Hydrogels are networks of hydrophilic polymers that are formed by crosslinking, in which a large quantity of water is trapped inside the network structure, leading to gels whose fluidity is between that of solids and liquids.[3] The crosslinking process can be classified into two types depending on how the crosslinks form, namely chemical crosslinking and physical crosslinking. Chemical crosslinking relies on the crosslinking agents to form covalent networks between polymers, whereas physical crosslinking generally refers

to the networks created through secondary interactions such as electrostatic force, hydrogen bonding, or hydrophobic interactions (Figure 22.1).[4] The hydrogels are of excellent biocompatibility because of the high water content, and therefore are commonly used for biomedical applications including tissue engineering, as drug carriers, or 3D printing inks.[5] The hydrogels can be categorized into two groups based on the materials from which they are prepared: natural polymers and synthesized polymers. Natural polymers include collagen, gelatin, hyaluronic acid, chitosan, alginate, and agar. These polymers are suitable for the preparation of hydrogels. Moreover, the raw materials to synthesize these polymers are obtained from natural sources; thus, they have good biocompatibility and are easily acquired due to their abundance in nature. These polymers are much cheaper, yet their stability could be a concern. Synthesized polymers include various plastic, synthetic fibers, and synthetic rubber, such as those made from polyethylene glycol (PEG), PLA, poly(2-hydroxypropyl methacrylamide) (pHPMAm), poly(vinyl alcohol) (PVA), poly(2-hydroxyethyl methacrylate) (pHEMA), poly(methyl methacrylate) (PMMA), and polytetrafluoroethylene (PTFE). In the same way as mentioned previously, we can prepare hydrogels from synthetic polymers through crosslinking.[6,7]

In order to serve as biomaterials, the properties of hydrogels should meet certain standards: (1) superior biocompatibility, (2) good oxygen permeability, (3) soft and tissue-like physical properties, (4) microporous structures for additional transport channels, and (5) low protein adsorption and cell adhesion. In short, apart from adopting materials that have good biocompatibility, different hydrogels are prepared based on the conditions in which

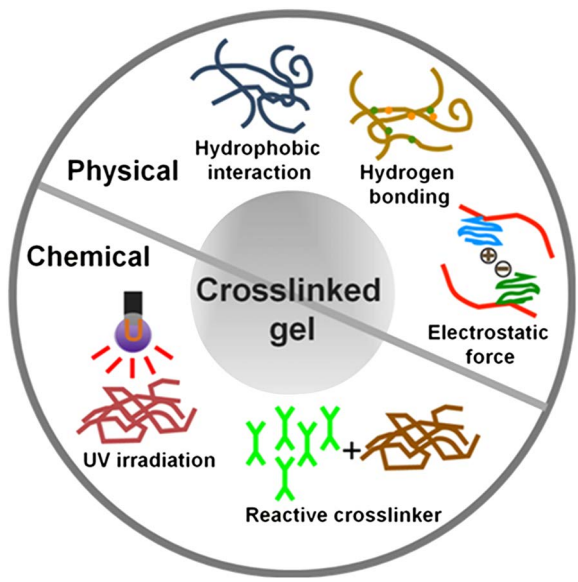

Figure 22.1 Typical crosslinking mechanisms of hydrogels.

they are being used and the purposes they are going to serve. In this way, the hydrogels work the most effectively and pose the least danger to organisms. Biomedical hydrogels are mostly used as drug carriers, cell or DNA carriers, and scaffolds in tissue engineering.[8]

22.3.1 Environment-Responsive Hydrogels

"Environment-responsive hydrogels" refers to the hydrogels that can adjust to slight changes in the environment, in which the crosslinking networks may become either more compact or collapse altogether, consequently affecting the swelling, mechanical properties, and water permeability of the hydrogels. Some common changes include temperature, pH, enzymatic catalysis, visible and ultraviolet light, electric field, magnetic field, and pressure. The subtle changes of these variables may have a huge influence on the properties of hydrogels.[9,10]

22.3.1.1 Thermo-Responsive Hydrogels

In recent years, much research on hydrogels has been done because of the wide range of applications. In particular, biomedical applications such as drug carriers, injectable hydrogel systems, scaffolds in tissue engineering, and even biosensors have all been considered. The mechanisms by which the hydrogels work are pretty simple.[11] For example, a thermo-responsive hydrogel with excellent biocompatibility could be prepared, which is designed to be in liquid form at room temperature. Meanwhile, upon a temperature rise to body temperature, that is 37 °C, crosslinking occurs and the liquid transforms into a gel. This enables us to mix the thermo-responsive hydrogels with drugs, and then inject the solution into the human body through a syringe. Upon injection into the human body, with a temperature change to 37 °C, the gel forms in a short period of time with the drugs embedded inside. The subsequent drug release can be adjusted depending on the circumstances. In this way, a non-intrusive therapy is accomplished that reduces the cost of labor as well as avoids the pain caused by other treatments. Thus, treatments involving thermo-responsive hydrogels have great potential in biomedical areas.[12]

22.3.1.2 pH-Responsive Hydrogels

pH-Responsive hydrogels involve polymers with ionic groups carrying electric charges such as COO_3^-, NH_3^+, or SO_3^+ on the polymer chain, which can either be proton-donors or proton-acceptors in order to adapt to changes in pH in the surrounding environment. When the pH value in the environment reaches a certain pK_a or pK_b, the electrostatic interaction on the polymer chain would be altered, leading to strong repulsive forces that change the total volume instantly. Based on the ionic groups, the hydrogels can be

classified into two categories: anionic and cationic hydrogels. When the pH value is larger than that of the pK_a, the ionic groups in anionic hydrogels would release protons into their surroundings, and therefore increase the swelling of the hydrogels. On the other hand, when the pH value is smaller than that of pK_b, cationic hydrogels can accept protons in the environment and also increase the swelling, leading to larger volumes. Therefore, these hydrogels can be fine-tuned to respond to pH changes in order to achieve the expected goals.[13]

22.3.1.3 Light-Responsive Hydrogels

Light-responsive hydrogels can form crosslinking structures in a short time and in a highly accurate way; thus are advantageous over the other types of environment-responsive hydrogels.[14] However, in the light-induced crosslinking process, crosslinking agents are required. Moreover, ultraviolet (UV) light must be applied to prompt the chain reactions and the subsequent chemical crosslinking to occur. Both crosslinking agents and UV light are somewhat hazardous to organisms, and therefore must be used with caution.[14,15]

22.3.2 Environment-Responsive Hydrogels in 3D Printing

Previously we have mentioned that in a number of works and literature, stimuli-responsive polymers that could transform into gels were used as substrates for 3D cell culture. In recent years, there has been a surge in the research on 3D printing, and much has been invested in the development of smart hydrogels. Among them, bio-inks involving cells have drawn much attention. The additive layer manufacturing technique not only overcomes problems in the freeze-drying process of the traditional preparation of 3D scaffolds, it also allows mixing of the hydrogel in liquid form with cells beforehand, and then the biomimetic tissues are printed out layer by layer into a 3D structure. In the following paragraphs, we introduce the strategies and applications of smart polymers serving as bio-inks in recent years, roughly categorizing them into degradable and non-degradable ones.

22.3.2.1 Degradable Hydrogels

Gelatin is a natural degradable polymer with arginyl-glycyl-aspartic acid (RGD) peptides. In addition, it can undergo reversible sol–gel transition, in which, at 30 °C or higher, gelatins are liquid-like, while below 20 °C, they are in the solid state. Aortic valves consist of two types of structures, namely vessel walls and valves. Butcher *et al.* fabricated the scaffolds of aortic valves by 3D bioprinting of gelatin/alginate hydrogels incorporated with aortic root sinus smooth muscle cells (SMCs) and aortic valve leaflet interstitial cells (VICs) through a uniaxial double nozzle. By adjusting the volumes of vessel walls and valves, cell viability could be raised to over 80%. Furthermore, alginate improved the

ductility of the hydrogels.[16] On the other hand, owing to the lysine functional groups on the peptides of gelatins, light-induced crosslinking bio-inks could be prepared by modifying the amide part on the lysine functional group into methacrylamide, which was named gelatin methacrylate (GelMA).[17] GelMA incorporated gelatins that have excellent biocompatibility as well as introduced methacrylamide that underwent crosslinking under UV light after printing was completed. Moreover, the hydrogels would degrade in human bodies within two months. Dubruel *et al.* fabricated scaffolds by 3D printing at low temperatures, exposed them to UV light to solidify the material, and investigated the varying activity of HepG2 cells when printer nozzles of different geometric shapes were used.[18] Ali *et al.* employed GelMA and agarose for the printing of scaffolds for blood vessels. First, they combined agarose and cells to print out a cylindrical-shaped structure, namely, the blood vessel template. GelMA embedded with SMCs was then added to wrap up the blood vessel template and GelMA was cured. Lastly, agarose was washed away by water, forming blood vessel channels inside GelMA,[19,20] functioning as the scaffolds for blood vessels. Kolesky *et al.* used Pluronic F127 (poly(ethylene oxide)-poly(propylene oxide)-poly(ethylene oxide) (PEO-PPO-PEO)) thermo-sensitive hydrogels as a fugitive ink in order to form open channels in the GelMA substrate. They made use of the lower critical solution temperature of Pluronic F127. In detail, Pluronic F127 was 3D-printed within GelMA at a temperature above the lower critical solution temperature (LCST) of Pluronic F127, followed by photopolymerization of GelMA. The temperature was then dropped below the LCST of Pluronic F127, at which Pluronic F127 changed to a liquid form that could be removed easily.[21]

Alginate is a responsive hydrogel based on polysaccharides, and its water absorption could reach 200 to 300 times as much as the original total volume. Huang *et al.* took advantage of this peculiar property to prepare a hydrogel solution containing both alginate and calcium ions to print out zigzag cellular tubes, which mimicked the scaffolds of blood vessels that have angles.[22] On the other hand, Yu *et al.* developed a process that could overcome the difficulties in the hydrogel printing operation concerning the exceedingly high viscosity, in which they applied the methods of coaxial bioprinting and dual solutions. Specifically, the solution of alginate with unreactive ions was placed in the outer tubes, while the inner tube was filled with a solution containing calcium ions that could cause crosslinking of alginate to occur. By simultaneously printing the two solutions and solidifying them, bioprinting involving cells was achieved in the absence of shear stress, which is harmful to cells.[23]

Hsu *et al.* employed biodegradable waterborne polyurethane (PU) to develop thermo-sensitive hydrogels for 3D printing, finding out that by combining PCL diol with poly(L-lactic acid) (PLLA) diol, poly (D,L-lactic acid) (PDLLA) diol or PLLA-PEG diol to serve as soft segments of PU, the prepared PU nanoparticle dispersions underwent sol–gel transition to form a hydrogel at some specific temperatures (Figure 22.2).[24–26] The mechanism was based on the changes in secondary forces of PU polymer chains upon the rise in temperature, leading to the swelling of particles, reduced interparticle distance, and subsequent aggregation. This kind of PU hydrogel had good

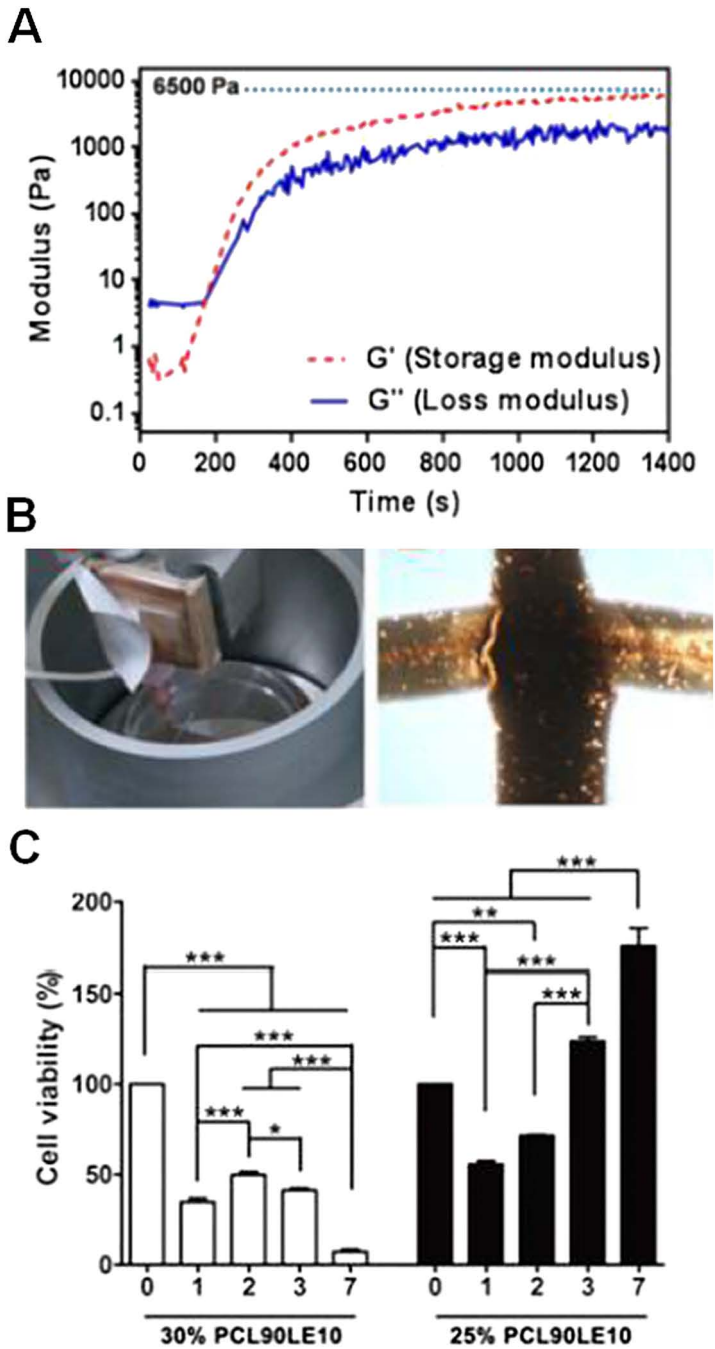

Figure 22.2 The rheological properties, processing properties, and cytocompatibility of thermoresponsive PU hydrogels. (A) Sol–gel transition of thermoresponsive PU inks at 37 °C. (B) Images of 3D printed stacking fibers of PU hydrogels. (C) The cell viability of mesenchymal stem cells embedded in 3D printed PU hydrogels. Adapted from ref. 26. Copyright 2015 American Chemical Society.

cytocompatibility as well as the possibility to adjust the gelation time and mechanical strength of the fabricated 3D-printed scaffolds by altering the designed chemical structure. Recent research also demonstrated the capacity of the 3D-printed neural stem cells with PU hydrogels in central nerve regeneration.[27]

22.3.2.2 Non-degradable Hydrogels

Although PEG diacrylate (PEGDA) is non-degradable, compared with other natural polymers, they have superior mechanical properties. In addition, the methacrylate groups at the end of the polymer chains are able to photocrosslink under UV light. Zhang *et al.* adopted digital light processing (DLP) to form lithographic patterns on PEGDA substrates to fabricate porous scaffolds. They further modified PEGDA by grafting RGD onto the structure, significantly improving the mechanical properties, bioadhesivity, and biocompatibility.[28] Lewis *et al.* printed non-degradable pHEMA and then exposed the scaffolds to UV light to induce the photopolymerization and photocrosslinking. The pHEMA microperiodic scaffolds with fibers were in the scales ranging from sub-micrometer to tens of micrometers. Moreover, the pores on the fibers were of sizes comparable to those of cells and could guide the cell growth.[29] It was also observed that the pHEMA microperiodic scaffolds could promote the growth and alignment of neuronal cells.[30]

22.3.3 Self-Healing Hydrogels

The development of self-healing hydrogels originated from phenomena seen in organisms. Once the microstructure is damaged, some chemical reactions occur through certain mechanisms, in which biological materials repair themselves and restore the original functions. This is the fundamental concept of self-healing materials. By combining 3D network hydrogels and a self-healing function, biomimetic smart hydrogels with properties resembling real tissues could be prepared. Self-healing hydrogels could be classified into two categories: autonomic and non-autonomic self-healing. The latter requires some stimulus such as light, heat, magnetic field, acids or bases to trigger the healing process. In contrast, autonomic self-healing does not need any stimulus; the damage itself sets off the repair.[31] Physical self-healing of hydrogels is obtained through the formation of non-covalent bonds, such as hydrogen bonding, van der Waals forces, ionic forces, and electrostatic forces, whereas chemical self-healing involves covalent crosslinking.

In the literature regarding physical self-healing, research teams made use of the self-assembly of liposomes into microscopic spherical vesicles in an aqueous environment. Physical crosslinks formed between self-assembled liposome vesicles and the cholesterol-end-capped PEG (Chol-PEG-Chol), and liposome gels with a quick self-healing behavior were prepared. Three possible ways of binding Chol-PEG-Chol to the liposomes existed. The first

was named 'bridge', referring to the case when both ends of Chol-PEG-Chol were embedded into the bilayers of two separate vesicles. 'Loop' indicated that the two cholesterol ends on the modified PEG were inserted into the same vesicle. The last one was called 'dangling' and simply meant only one end of Chol-PEG-Chol successfully bound to the liposome with the other end still in contact with water. Rheological analyses were used to investigate the self-healing ability of the liposome gels. Upon high deformation, cholesterol groups were squeezed out of the bilayers, causing the gel to collapse and transform back into a liquid form. Nevertheless, when the deformation strain was reduced, a sol–gel transition occurred again and the gels recovered the original mechanical strength in a very short time. Even if a 1000% deformation strain was applied, which destroyed the networks completely, the self-healing ability of the gels remained unaffected.[32]

Chen *et al.* obtained a self-healing elastomer with hydrogen bonding. A polystyrene (PS) backbone was chosen as the hard segment and polyacrylate amides (PA-A) grafted onto the backbone served as the soft phase. The nitrogen atoms on PA-A allowed hydrogen bonds to form between PA-A soft segments, leading to the self-assembly and the subsequent self-healing behavior. The PS hard segment contributed to the stiffness and elasticity of the material, while the self-healing ability was attributed to the soft segments due to the formation of hydrogen bonds. The designed polymer structure consisted of the hard backbone of PS and the soft 'brush' of PA-A. When placed in a polar solvent, the synthesized polymers would self-assemble into a hydrophobic core–shell nanostructure, with the interior consisting of PS and the exterior covered with PA-A brushes. The polymers further assembled to a nanostructure in which PS and PA-A part aggregated into two phases separately. The hydrogen bonding between the PA-A segments on the shell enabled the polymers to repair themselves after mechanical damage.[33]

Another commonly known chemical self-healing process involves the dynamic crosslinking of imine. The two hydroxyl ends of PEG were modified by reacting with benzaldehydes to act as crosslinking agents. The modified PEG reacted with chitosan solutions at low concentrations, in which the amine groups on chitosan underwent Schiff base (a class of imine) reactions to form hydrogels with metastable secondary amine groups. Upon mechanical damage, metastable amines formed; thus, the material is capable of self-healing. A research group has employed the self-healing gels in repairing the central nervous system of zebrafish embryos (Figure 22.3).[34] According to the study, the expression of neural stem cells (NSCs) was influenced by the hardness of hydrogels.[12,35,36]

22.3.4 Self-Healing Hydrogels in 3D Printing

The development of additive manufacturing and self-healing hydrogels has been very active in recent years. However, when combining the two, one would encounter some contradicting aspects. In particular, the structure of the manufactured scaffolds would be damaged by the self-healing of hydrogels.

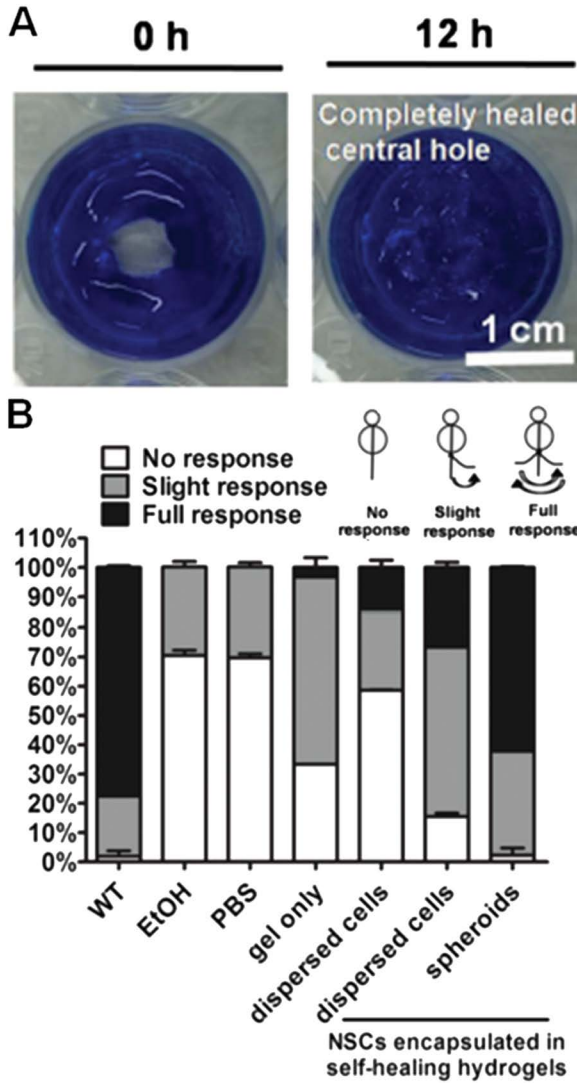

Figure 22.3 Self-healing properties of chitosan-based hydrogels and functional assay for central nervous system rescue in zebrafish embryos by injection of neural stem cell-laden self-healing hydrogels. (A) Gross appearance of self-healing hydrogels. (B) The spontaneous contraction of the zebrafish embryos. WT represents wild-type blank control. EtOH represents the untreated damaged group. Adapted from ref. 34. Copyright 2015: Wiley-VCH Verlag GmbH & Co. KGaA.

Therefore, one research group chose monomers that could undergo reversible Diels–Alder (D–A) reactions for use in inkjet printing on carbon fibers. In detail, the cracks on the carbon-fiber composite could be repaired and the mechanical strength was restored through the reversible D–A mechanism.[37] In the biomedical field, Burdick *et al.* adopted direct 3D printing of

shear-thinning hydrogels into self-healing hydrogels. Non-covalent, reversible bonds between the two hydrogels were disrupted under shear stress and re-formed after the mechanical stimulus was removed. These hydrogels are based on modified hyaluronic acids (HAs). The materials could be used in the printing of stem cells and fibroblasts and in the fabrication of specific structures such as tunnels within the substrate *via* various techniques.[38]

Combining 3D printing techniques and smart hydrogels enables us to produce cell-laden 3D-printed scaffolds. Moreover, by choosing different chemical structures, densities of polymer networks, and mechanical strengths of the hydrogels, the proliferation and differentiation of cells can be adjusted. In fact, the density of networks and mechanical strength are influenced by the designed chemical structure and the degree of response of hydrogels to the surrounding environment when being printed. In addition, the scaffolds fabricated *via* 3D printing of self-healing hydrogels may self-heal when being damaged. The pH-sensitive self-healing hydrogels could be degraded by acidic products during the cell culture, providing sufficient space for the cells to proliferate.[12] Therefore, combining smart hydrogels and 3D printing techniques to fabricate cell-laden 3D-printed scaffolds is very promising for applications in tissue engineering.

22.4 Shape-Memory Materials

Shape-memory materials refer to the stimulus-responsive materials that change to a temporary shape in response to external stress, but return to their original shape when an appropriate stimulus is applied, such as heat, light, magnetic field, electric field, pH value, and solvents.[15,39–43]

Shape-memory alloys were the earliest shape-memory materials to be developed. The first one-way shape-memory alloys were the gold–cadmium alloys observed by Chang and Read in 1951. The shape-memory effect took place in the form of martensitic transformation in which no diffusion of atoms occurred. The shape-memory effect of alloys was mainly controlled by changes in temperature.[41]

Next to shape-memory alloys are shape-memory polymers. These polymers have some characteristics including the facts that the volume could either expand or contract, and the stimuli inducing the shape-memory effect could be changes in temperature as well as light, pH value or solvents (Figure 22.4).[44] For example, the elasticity of polymer chains might be a function of temperature. One possible switch for the shape-memory effect is the transition temperatures in a certain range. When placed at a temperature lower than the transition temperature, which could be the melting temperature (T_m) or glass transition temperature (T_g) of the polymer, the elasticity of the polymers was limited.[40] In contrast, when the temperature rose above the transition temperatures, the polymer chains became softer and the shape of the material started to change. The temperature was then made to drop to obtain a fixed temporary shape. Lastly, the temperature was raised to over the transition temperatures once again to verify the shape-memory ability of the material.

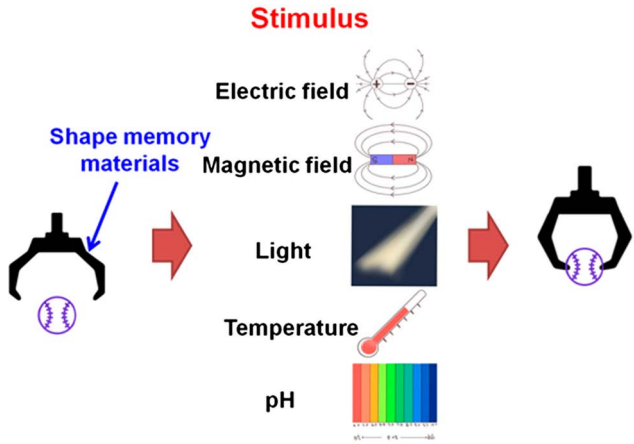

Figure 22.4 Illustration of the shape-memory effect.

22.4.1 Shape-Memory Materials for Biological Applications

Shape-memory polymers are very promising for applications as biomedical materials, which include medical devices in minimally invasive techniques,[45] drug delivery systems,[46] and implants in tissue engineering.[47,48]

PLLA is one polymer with a shape-memory ability. The shape-memory effect is attributed to the small crystallites and the amorphous phase in the structure of the material.[49,50] In addition, PLLA could be used as a shape-memory dressing because of its spinnability.[51] PCL polymers can also be employed as shape-memory materials by chemically crosslinking PCL using pentaerythritol tetrakis(3-mercaptopropionate) as the crosslinking agent. The crystallites in the structure of PCL served as the stationary phase, whereas the crosslinked amorphous PCL chains were the reversible phase. PCL scaffolds with shape-memory ability were prepared in this way.[52] PVA is a water-soluble polymer that is commonly used as a biomedical hydrogel. It can be used to prepare shape-memory polymer hydrogels as well. First, chemical networks formed in PVA solutions by using glutaraldehyde as a crosslinking agent. Then PVA polymers were deformed and the shape of the material was fixed by crystallites forming in freeze–thaw cycles. These materials recovered to the original shape upon heating, which caused the crystallites to melt.[53,54]

PU is a commonly used biomedical elastomer that has a shape-memory property.[55,56] PU elastomers have many applications in the biomedical field. The PU polymer chains consist of soft and hard segments that undergo microphase separation. The extent of the microphase separation may affect the physio–chemical properties and biocompatibility of the material. As Hsu *et al.* mentioned in their study, by choosing poly(3-hydroxybutyrate) (PHB) diol, which is biodegradable and has fairly good biocompatibility, as part of the soft segment along with PCL diol at a ratio of 2 : 8 to synthesize PU elastomers, materials with excellent mechanical properties, processability,

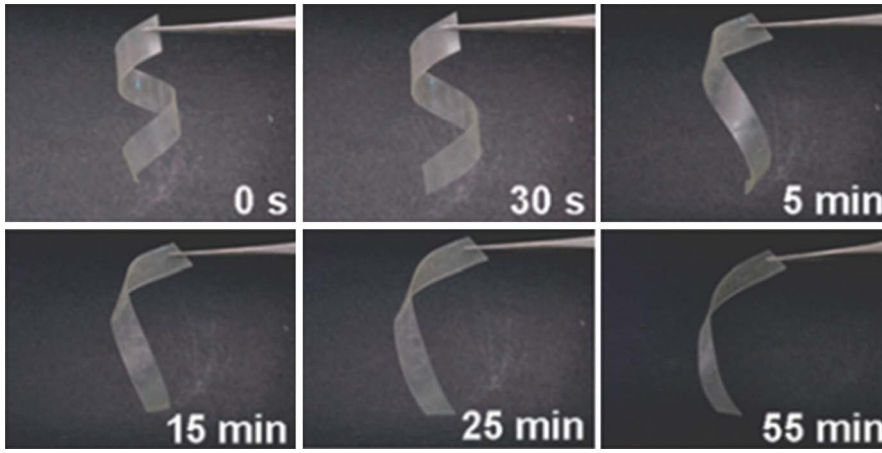

Figure 22.5 Images of the recovery process of shape-memory PU films at 37 °C. Adapted from ref. 57. Copyright 2015: the Royal Society of Chemistry.

biocompatibility, and biodegradability could be obtained. In addition, these PU elastomers have some shape-memory behavior (up to ~80% shape recovery) (Figure 22.5).[57] Therefore, the materials belong to a new category of potential biomaterials for cardiovascular applications.

22.4.2 Applications of Thermo-Responsive Shape-Memory Materials

Thermo-responsive shape-memory polymers are deformed and processed above transition temperatures, whereas below transition temperatures, the redefined shape can be temporarily fixed. The crystallization temperatures, T_m, or the T_g of thermo-responsive shape-memory polymers can be used as switches at which the shape-memory effect occurs.[49,51,52,58–61]

Moreover, in materials with significant microphase separation, the shape-memory effect is more obvious, such as that of PUs, which possess hard and soft segments that could serve as stationary and reversible phases, respectively. Thermo-responsive shape-memory materials have the potential for applications in minimally invasive surgeries. Those used in minimally invasive surgeries generally have a particular property, namely, their transition temperatures are close to the human body temperature. Therefore, the materials could be compressed to the minimum volume and remain stable at low temperatures. After being implanted into the human body, the materials would respond to the rising temperature, which causes the shape-memory effect to occur, and subsequently return to their original shape. For example, like those described in the study of Wang *et al.*, through minimally invasive techniques, the scaffolds made of a shape-memory polymer consisting of alginate were put into the tibialis anterior muscles of mice, and the repair of injured skeletal muscles was observed.[62] Guillaume *et al.*

implanted shape-memory porous alginate scaffolds in the smallest volume into the human body and then rehydrated them, restoring the scaffolds to their initial geometry. These scaffolds could be used in the repair of annulus fibrous enclosing the intervertebral discs.[63] Rychter *et al.* fabricated porous shape-memory scaffolds for the ingrowth of osteoblasts, and then implanted the cultured cells into the bone defects.[45]

22.4.3 Applications of Photo-Responsive Shape-Memory Materials

Apart from the thermo-responsive shape-memory materials, photo-responsive shape-memory materials are of another commonly seen category. The shape-memory effect of these materials is controlled by wavelengths of light, which cause different chemical bonds to form, leading to the contraction, bending or volume changes of the polymers. As described in the study of Lendlein *et al.*, polymers containing cinnamic groups can be deformed and fixed into a certain shape upon exposure to UV light at different wavelengths. In detail, the material was stretched, irradiated with UV light at a wavelength over 260 nm to fix the elongated shape. Then UV light with a wavelength under 260 nm was applied to make the material recover its original shape. The shape-memory behavior was due to the C–C double bonds on the cinnamic groups, which were able to undergo photoreversible [2+2] cycloaddition reactions when exposed to certain wavelengths. Upon exposure to UV light of a wavelength over 260 nm, the elongated shape was fixed by the photo-induced crosslinks. On the contrary, when exposed to UV light of a wavelength under 260 nm, the crosslinks were cleaved; and thus, the material returned to its original shape. The photo-responsive shape-memory effect of liquid-crystal polymers containing azobenzene was also reported, in which azobenzene entities changed from a *trans*-conformation to *cis*-conformation upon exposure to light of wavelengths ranging from 300 to 400 nm. Meanwhile, when exposed to visible light, azobenzene changed from a *cis*-conformation to *trans*-conformation.[64,65]

For photo-responsive shape-memory materials, the strain-recovery rates are comparable with those of thermo-responsive materials, whereas the strain-fixity rates are much lower due to the different fixation mechanisms. Nevertheless, the unique characteristics of photo-responsive shape-memory polymers enable the remote activation of shape recovery at ambient temperatures. Furthermore, the constraints on temperatures at which the thermo-responsive polymers are employed for applications involving external heating can be eliminated.[66]

22.4.4 Applications of Other Shape-Memory Materials Such as pH-Sensitive Polymers

Besides the aforementioned thermo-responsive and photo-responsive shape-memory polymers in Sections 22.2 and 22.3, there are other widely used stimuli that could induce the shape-memory effect, such as electric field, magnetic field, and pH.

Some less commonly seen shape-memory materials are stimulated by ultrasonication. Li *et al.* prepared a PVA hydrogel containing a small amount of melamine. The shape recovery was triggered by the ultrasound-induced thermal effect.[67] pH-Responsive polymers contain atoms that could be protonated at low pH and deprotonated at high pH. The commonly adopted approach is introducing pyridine rings into the chemical structure. For example, Chen *et al.* introduced pyridine rings by incorporating *N*,*N*-bis(2-hydroxylethyl)isonicotinamine (BIN) into the backbones of PU. The synthesized PU could maintain the redefined shape at a pH value of 10 and recover to the original shape at a pH value of 1.3. The shape-memory behavior was employed in a controlled drug release system. Under acidic conditions, pyridine rings swelled and released the drug, whereas under basic conditions, the formation of hydrogen bonds led to de-swelling of the material and therefore the drug release was suppressed.[68] Li *et al.* blended PU with functionalized cellulose nanocrystals (CNCs). The cellulose part was modified with carboxyl groups *via* 2,2,6,6-tetramethyl-1-piperidinyloxy (TEMPO)-mediated surface modification. The CNCs formed hydrogen bonds at low pH values, while they were ionized and negatively charged at high pH values, resulting in electrostatic repulsions. Therefore, the prepared PU could be deformed and processed at a pH value of 10, and then the shape was fixed at a pH value of 1. When the pH value changed to 10 again, the shape recovery occurred.[69]

22.4.5 Applications of Shape-Memory Polymers in 3D Printing

The products fabricated by 3D printing shape-memory polymers not only have the advantages of 3D-printed scaffolds such as high accuracy, but the materials are also capable of self-sensing and self-actuating. Therefore, the process is also called four-dimensional (4D) printing.[70] In determining whether a certain kind of material is suitable for 3D printing of shape-memory scaffolds, not only should the shape-memory behavior be taken into account, but the processability of the material also needs to be considered. Zhang *et al.* used 3D-printed shape-memory PLLA, forming a two-dimensional (2D) hexagonal pattern consisting of several circular rings, which could change shape under varying temperatures.[71] Yang *et al.* fabricated three-jaw grippers by 3D printing the shape-memory PLLA material. The material was deformed as the temperature changed, enabling the device to pick up items.[72] Yu *et al.* used epoxy as 3D-printable ink for the fabrication of 3D-printed interlocking components with shape-memory ability. These components underwent shape changes that transformed the unlocking structure into the locking structure upon changes in temperature.[73] Ge *et al.* used 3D-printed shape-memory acrylate-based polymers in box-like shapes, which would self-fold or self-unfold depending on the temperature, leading to the opening and closing of the boxes.[74] Balasubramanian *et al.* printed acrylate polymers into microfluidic networks in an attempt to mimic the expansion and contraction of human blood vessels.[75,76]

So far, there has been very little research on the applications of shape-memory polymers combined with 3D printing techniques in the biomedical field. Nonetheless, the combination has both the advantages of 3D printing and shape-memory polymers, *i.e.* the ability to fabricate highly accurate complex structures that can deform in response to different environments. Therefore, more biomimetic and multi-functioning biomedical products may be fabricated by the technique and they have a lot of potential applications in the biomedical field in the future.

22.5 Conductive Polymers Combined with 3D Printing Techniques for Applications in Tissue Engineering

Because conventional polymer backbones consist of C–C single bonds, the electrons cannot move freely, and this leads to non-conductivity. Currently, there are two types of approach to make polymers conductive. The first type involves blending polymers with conductive inorganic materials, such as metal particles, carbon black, or carbon nanotubes, to fabricate the conductive composites.[77–79] The second approach is to incorporate π–π conjugated double bonds onto the polymer backbone, on which π electrons could move freely *via* resonance structure, leading to the conductivity of the polymers. Some commonly seen conductive polymers include polyacetylene, polypyrrole, polythiophene, and polyanilines,[79,80] whose chemical structures are shown in Figure 22.6. Conductive polymers combine the conductivity of inorganic materials and the softness of organic materials and therefore are currently used in the fields of storage energy, electromagnetic interference shielding, and biomedical materials.[80]

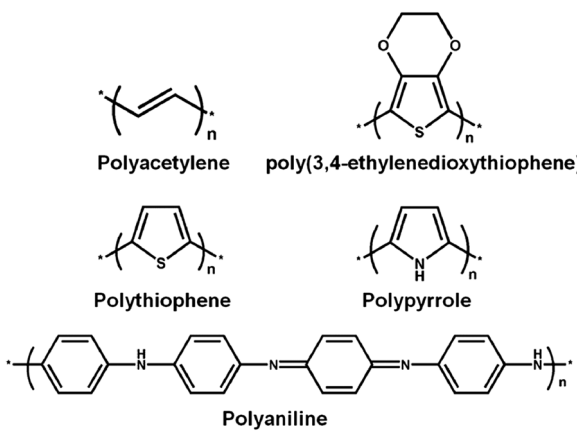

Figure 22.6 Chemical structures of some common conductive polymers.

22.5.1 Applications of Conductive Polymers in Tissue Engineering

In the field of biomedicine, conductive polymers were mainly used in biosensors. Studies conducted between the years of 1990 and 2000 established that the cell activity of nerves, bones, cardiac muscles, and skeletal muscles was affected by electrical stimulation, which altered the cell adhesion, cell migration, and protein adsorption.[81–84] These polymers also have excellent biocompatibility. Apart from the nerves, bones, and muscles, damage to the skin and cartilage was reported to have better repair by electrical stimulation.[85,86] Therefore, in recent years, conductive polymers have been used in neural probes as well as in tissue engineering.[87]

Polypyrrole is a frequently used conductive polymer in tissue engineering. Despite the fact that it is non-biodegradable, polypyrrole showed excellent biocompatibility after six months of *in vivo* experiments.[82] Moreover, the extracts of pyrrole were also non-cytotoxic. The immune response of polypyrrole after two weeks was lower than that of PLGA, implying the favorable bio-inert property.[82,88] Schmidt *et al.* cultured PC-12 neuron-like cells on the polypyrrole substrate and found that in comparison with those grown on the surface of PLA and PLGA, PC-12 cells had higher adhesion. In addition, when electrical stimulation was applied, the median neurite length was about twice as long as that of the cells cultivated without the stimulus (18.14 μm compared with 9.5 μm).[82] Shi *et al.* prepared polypyrrole nanoparticles in diameters ranging from 50 to 200 nm, which organized into a conductive network within a PDLLA matrix, and found that the growth of fibroblasts cultured on the polypyrrole/PDLLA membrane was promoted by electrical stimulation.[89] Moreno *et al.* conducted osteoblast cultures on the polypyrrole films and also found that the cell proliferation was enhanced by electrical stimulation.[90] However, the melting point of polypyrrole is almost 300 °C. In addition, the solubility of polypyrrole is low in most solvents. Therefore, the material is difficult to process and manufacture into scaffolds for tissue engineering. To overcome these disadvantages, surface modifications were usually applied, or alternatively, the polymerization of pyrrole took place on templates and the templates were then removed to obtain the scaffolds. Gomez *et al.* used e-beam lithography and electropolymerization to fabricate polypyrrole microchannels, onto which embryonic rat hippocampal cells were cultured. The results showed that the cells proliferated significantly faster on the conductive polymers and the axon orientations were more aligned.[91] Sudwilai *et al.* modified electrospun PLA fibrous scaffolds with polypyrrole and cultured neural progenitor cells on the scaffolds. Under electrical stimulation, the neural progenitor cells were differentiated into neurons and exhibited long neurite outgrowths.[92] Kai *et al.* blended polypyrrole with PCL/gelatin solution to fabricate electrospun fibers, and then cultured cardiac cells on the eletrospun fibrous scaffolds. It was observed that the growth rate of cardiac cells was higher on the electrospun fibrous scaffolds containing polypyrrole.[93]

Chen *et al.* adopted electropolymerization to polymerize polypyrrole onto templates. After the templates were removed, polypyrrole tubes serving as a guidance channel for nerve regeneration were obtained. After these tubes were implanted into rats for 20 weeks, the action potential of the repaired sciatic nerves was very close to those of the normal nerves.[94]

Polyaniline has several advantages, such as low cost, good environmental stability,[95] and no signs of allergic reactions in contact with human skin.[96] Inflammation associated with the implantation of various forms of polyaniline was insignificant after 50 weeks, indicating excellent biocompatibility.[97] Wang *et al.* blended PCL, silk fibroin, and polyaniline all together to prepare electrospun fibers. Then C2C12 myoblasts were cultured on the electrospun fibrous scaffolds, on which cellular elongation and a subsequent myogenic differentiation were observed.[98] Zhao *et al.* used chitosan-grafted polyaniline with oxidized dextran as the crosslinker to prepare conductive hydrogels and found that mesenchymal stem cells and C2C12 cells cultured on the hydrogel had faster proliferation rates.[99] Borriello *et al.* mixed polyaniline short fibers with PCL to prepare electrospun fibers. Mesenchymal stem cells were cultured onto the nanofiber scaffolds. These PCL/polyaniline electrospun fibrous scaffolds were found to promote the differentiation of mesenchymal stem cells into the cardiac phenotype.[100]

Poly(3,4-ethylenedioxythiophene) (PEDOT) is a derivative of polythiophene, which contains an additional dioxyalkylene bridging group that tends to lower the band gap, leading to superior conductivity.[101] McKeon-Fischer *et al.* mixed PEDOT with PCL solution, and added multi-walled carbon nanotubes into the solution for the electrospinning process. Skeletal muscle cells cultured on the fabricated scaffolds displayed an elongated morphology.[102] Niu *et al.* coated PEDOT on a PLLA microfibrous network, on which fibroblasts were cultured under electrical stimulation. The PLLA/PEDOT scaffolds were found to provide a favorable environment for the proliferation of fibroblasts.[103] Pires *et al.* blended PEDOT with polystyrene sulfonate (PSS) to prepare films. The films promoted the elongation of neural stem cells and the subsequent differentiation into neurons.[104] Srivastava *et al.* cultured embryonic stem cells on PEDOT/PSS films and found that the neural differentiation was enhanced.[105]

22.5.2 3D Printing of Conductive Polymers for Applications in Tissue Engineering

In recent years, the developments of conductive polymers combined with 3D printing techniques have drawn more attention than ever.[106,107] However, few research had been done regarding biomedical applications. Hamedi *et al.* used PEDOT/PSS to fabricate channels *via* 3D printing to serve as promising neural probes.[108] Mire *et al.* conducted extrusion printing and inkjet printing separately to deposit PEDOT/PSS polymers and found that extrusion printing offered lower printing resolution, yet they had better electrical characteristics.[109] Harman *et al.* compared the cytotoxicity of PEDOT/PSS and

PEDOT/dextran sulfate (DS), concluding that the latter had better cytocompatibility. In addition, PEDOT/DS could be fabricated into scaffolds by either extrusion printing or inkjet printing. These scaffolds could be used in tissue engineering to promote tissue repair in the future.[110] Runge *et al.* fabricated polypropylene fumarate scaffolds through 3D printing with polypyrrole, and cultured osteoblasts on the scaffolds to examine if they supported bone regeneration. The alkaline phosphate activity of the cells was observed on the scaffolds, demonstrating that the polypyrrole-modified polypropylene fumarate scaffold was suitable for applications in bone regeneration.[111] There have been only a few reports or research work so far on the topic of fabricating scaffolds for tissue engineering through 3D printing of conductive polymers. Given the capability to promote the differentiation of mesenchymal stem cells or muscle cells as well as the regeneration of bones and nerves, there is a lot of potential yet to be discovered.

22.5.3 Piezoelectric Materials for Applications in Tissue Engineering

Piezoelectricity refers to the effect that converts mechanical energy into electric energy in a reversible way. The effect was first discovered in the non-centrosymmetric crystals of inorganic materials. On the other hand, the piezoelectricity of polymers results from the strengths of the dipole moments of the functional groups on the polymer chains, where external stress causes the amount of electric charges to change, leading to measured electric potentials. Currently, some common piezoelectric materials include polyvinylidene fluoride (PVDF) and poly(vinylidenefluoride-*co*-trifluoroethylene) (PVDF-TrFE). In recent years, PLLA was also discovered to be slightly piezoelectric. The chemical structures of these polymers are shown in Figure 22.7. Among them, both PVDF and PLLA must be stretched to attain piezoelectricity. After being stretched, PVDF changed from α phase to β phase, each with a distinctive conformation, and an increase in the dipole moment was observed.[112] The stretching of PLLA induced the transformation of α-crystalline into β-crystalline, resulting in the formation of dipole moments.[113] The effect of stretching PVDF is illustrated in Figure 22.8. In contrast, since the conformation of PVDF-TrFE leads to large remnant polarization and strong piezoelectric activity, a stretching process is unnecessary.[114] Piezoelectric materials are currently used in transducers, sensors, and actuators.[115,116]

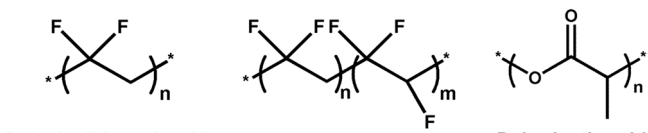

Figure 22.7 Chemical structures of some common piezoelectric polymers.

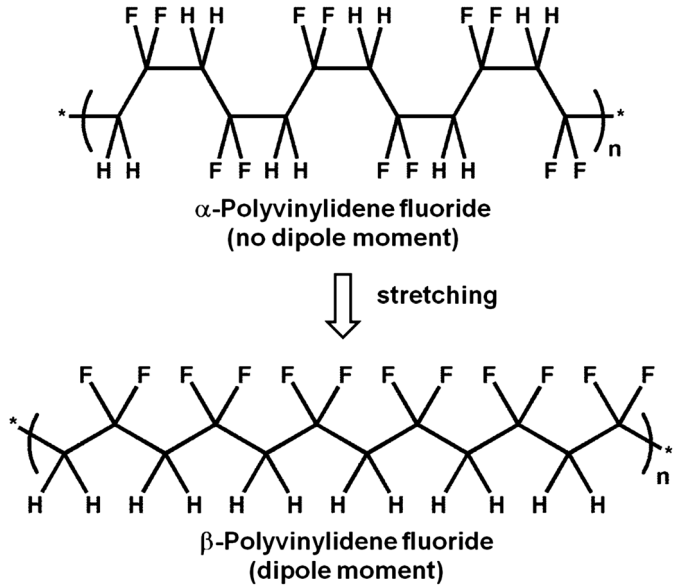

Figure 22.8 After being stretched, PVDF changed from α phase to β phase, resulting in the piezoelectric effect.

Yasuda *et al.* reported that human bones exhibited piezoelectric properties. This was due to the fact that bones contain collagen, of which the triple helix conformation was altered under external stress, consequently causing the direction of the dipole to change and leading to piezoelectricity.[117,118] Other tissues containing collagen, such as ligaments,[119] cartilage,[120] and dentin,[121] are also known to be piezoelectric. Aebischer *et al.* employed α- and β-phase PVDF to fabricate nerve guidance channels and separately implanted them into the bodies of mice to repair a 4-mm-wide gap sciatic nerve injury. The results indicated that nerve guidance channels consisting of β-phase PVDF enhanced nerve regeneration.[122] In addition, neuroblastoma cells cultured on piezoelectric substrates made of β-phase PVDF were shown to exhibit greater outgrowths and neurite lengths.[123] Arinzeh *et al.* used PVDF-TrFE to fabricate 3D electrospun fibrous scaffolds and cultured neural stem/progenitor cells on the piezoelectric scaffolds, and found out that the material promoted the differentiation of the cells.[124] Guo *et al.* prepared PVDF/PU scaffolds *via* electrospinning. Because of the stretching during the electrospinning process, the conformation of PVDF changed from the nonpiezoelectric α-phase into the piezoelectric β-phase. Co-electrospinning with PU contributed to improved elasticity. The fibroblasts cultured on the PVDF/PU scaffolds showed enhanced migration, adhesion, and secretion. Therefore, these scaffolds have potential for wound healing applications.[125] Damaraju *et al.* cultured mesenchymal stem cells onto the electrospun fibrous scaffolds made of β-phase PVDF. The scaffolds were capable of supporting osteogenic differentiation.[126] Fukada *et al.* made use of PLLA of which the

piezoelectricity and high strength are comparable to those of human bones. The material was implanted into the tibiae of cats to promote fracture healing. Compared with scaffolds composed of polyethylene (PE), those made of the piezoelectric β-crystalline PLLA were shown to enhance bone formation after four weeks due to the piezoelectric currents generated by the mechanical strains caused by the moving legs of the cats.[127]

22.5.4 3D Printing of Piezoelectric Materials for Applications in Tissue Engineering

Piezoelectric materials combined with 3D printing techniques are becoming more common for biomedical applications. Nonetheless, there have been only a few applications in tissue engineering. Pabst *et al.* fabricated actuators and sensors from PVDF-TrFE by 3D printing and demonstrated that they were promising for lab-on-a-chip applications.[128] Kim *et al.* incorporated barium titanate ($BaTiO_3$, BTO) nanoparticles into polyethylene glycol diacrylate to fabricate piezoelectric scaffolds with patterned microstructures *via* 3D printing. The composites might be used as sensors or for applications in tissue engineering in the future.[129] Marino *et al.* doped commercially available Ormo-Comp® photopolymer with piezoelectric BTO and conducted 3D printing to fabricate scaffolds for bone regeneration. Human SaOS-2 osteosarcoma cells were then cultured onto the scaffolds. The amount of type I collagen produced by SaOS-2 and the deposition of hydroxyapatite were both significantly greater. Therefore, the material was suitable for supporting bone regeneration.[130] The applications of piezoelectric materials combined with 3D printing techniques in tissue engineering developed so far are still limited and most of these materials are non-biodegradable. However, PLLA is both biodegradable and piezoelectric. Besides, PLLA has been frequently reported to promote the regeneration of bones, cartilage, and nerves.[131] Therefore, PLLA is suitable for the 3D printing of piezoelectric scaffolds. The fabricated scaffolds could enhance tissue regeneration owing to the piezoelectric currents generated by recurring external stress. The advantages of combining a distinctive smartness and 3D printing techniques, which include accuracy and customization, make the materials very promising for applications in tissue engineering.

22.6 Potential Clinical Applications of Smart Materials Combined with 3D Printing Techniques

Thus far, there have been only a few studies that have evaluated the potential of smart materials combined with 3D printing in terms of clinical use, with most concentrating on environment-sensitive 3D printed hydrogels. Chi *et al.* blended PEG dimethacrylate photo-responsive hydrogels with chondrocytes, and assessed the potential clinical applications in an *ex vivo* osteochondral defect model.[132] The results indicated that PEG dimethacrylate

photo-responsive hydrogels mixed with chondrocytes facilitated the repair of osteochondral defects. Cohen *et al.* blended alginate with $CaSO_4$ and loaded the hydrogel into a syringe, followed by direct printing onto osteochondral defects in a process named *in situ* orthopaedic repair printing.[133] Hsu *et al.* mixed thermo-responsive PU hydrogels with neural stem cells to perform 3D printing and the printed constructs were proven to promote central nervous system repair of zebrafish.[27] Since environment-sensitive hydrogels could be developed into bioinks for 3D bioprinting and affect cell behavior and differentiation, the materials show great potential for clinical applications in the future. Despite a lack of reports considering the potential clinical use of self-healing hydrogels, shape-memory polymers, and conductive polymers combined with 3D printing, these smart materials endowed printed scaffolds with smartness as well as influenced cell proliferation and differentiation. Therefore, the clinical applications of the materials might gradually come into focus in the medical field in the near future.

22.7 Conclusion

Currently, the combination of 3D printing and smart materials in the biomedical field is mainly involved in the fabrication of environment-responsive hydrogels. The reason is that 3D-printed hydrogels may provide a bio-mimicking 3D environment for cells to grow. However, apart from smart hydrogels, shape-memory, conductive, and piezoelectric materials have been reported in the biomedical field to add even more functions to the prepared scaffolds. For instance, shape-memory materials deform in response to the environment, which is seen as an analog to human cardiac muscles or skeletal muscles that contract when stimulated by signals. Thus, shape-memory materials combined with 3D printing and other biofabrications could be used as biomimetic actuators, or they could serve as scaffolds in tissue engineering for minimally invasive surgeries. The electrical stimulations that arise from conductive and piezoelectric materials have been reported to have a lot of potential in the repair of bones, muscles and nerves. Therefore, customized artificial scaffolds for bones, nerve guidance conduits, or artificial scaffolds for muscles fabricated by 3D printing may facilitate tissue regeneration. In the future, the combined use of 3D printing/biofabrication techniques and smart materials can help tissue engineering overcome the technical barriers and attain more breakthroughs to develop more biomimetic and multifunctional smart scaffolds for applications in the field.

References

1. J. M. Jani, M. Leary, A. Subic and M. A. Gibson, *Mater. Des.*, 2014, **56**, 1078.
2. I. Y. Galaev and B. Mattiasson, *Trends Biotechnol.*, 1999, **17**, 335.
3. F. Ganji, S. Vasheghani-Farahani and E. Vasheghani-Farahani, *Iran. Polym. J.*, 2010, **19**, 375.

4. Z. Zhang, T. Chao and S. Jiang, *J. Phys. Chem. B*, 2008, **112**, 5327.
5. K. M. Park, S. Y. Lee, Y. K. Joung, J. S. Na, M. C. Lee and K. D. Park, *Acta Biomater.*, 2009, **5**, 1956.
6. S. D. Bruck, *J. Biomed. Mater. Res.*, 1973, **7**, 387.
7. S. A. Hutchens, R. S. Benson, B. R. Evans, H. M. O'Neill and C. J. Rawn, *Biomaterials*, 2006, **27**, 4661.
8. J. A. Yang, J. Yeom, B. W. Hwang, A. S. Hoffman and S. K. Hahn, *Prog. Polym. Sci.*, 2014, **39**, 1973.
9. E. S. Gil and S. M. Hudson, *Prog. Polym. Sci.*, 2004, **29**, 1173.
10. J. Hu, H. Meng, G. Li and S. I. Ibekwe, *Smart Mater. Struct.*, 2012, **21**, 053001.
11. D. Schmaljohann, *Adv. Drug Delivery Rev.*, 2006, **58**, 1655.
12. T. C. Tseng, L. Tao, F. Y. Hsieh, Y. Wei, I. M. Chiu and S. H. Hsu, *Adv. Mater.*, 2015, **27**, 3518.
13. N. A. Peppasa, P. Buresa, W. Leobandunga and H. Ichikawa, *Eur. J. Pharm. Biopharm.*, 2000, **50**, 27.
14. Y. Qiu and K. Park, *Adv. Drug Delivery Rev.*, 2012, **64**, 49.
15. H. Meng and J. Hu, *J. Intell. Mater. Syst. Struct.*, 2010, **21**, 859.
16. B. Duan, L. A. Hockaday, K. H. Kang and J. T. Butcher, *J. Biomed. Mater. Res., Part A*, 2013, **101**, 1255.
17. A. I. Van Den Bulcke, B. Bogdanov, N. De Rooze, E. H. Schacht, M. Cornelissen and H. Berghmans, *Biomacromolecules*, 2000, **1**, 31.
18. T. Billiet, E. Gevaert, T. De Schryver, M. Cornelissen and P. Dubruel, *Biomaterials*, 2014, **35**, 49.
19. L. E. Bertassoni, M. Cecconi, V. Manoharan, M. Nikkhah, J. Hjortnaes, A. L. Cristino, G. Barabaschi, D. Demarchi, M. R. Dokmeci, Y. Yang and A. Khademhosseini, *Lab Chip*, 2014, **14**, 2202.
20. K. Yuea, G. T. Santiago, M. M. Alvarez, A. Tamayol, N. Annabi and A. Khademhosseini, *Biomaterials*, 2015, **73**, 254.
21. D. B. Kolesky, R. L. Truby, A. S. Gladman, T. A. Busbee, K. A. Homan and J. A. Lewis, *Adv. Mater.*, 2014, **26**, 3124.
22. C. Xu, W. Chai, Y. Huang and R. R. Markwald, *Biotechnol. Bioeng.*, 2012, **109**, 3152.
23. Y. Yu, Y. Zhang, J. A. Martin and I. T. Ozbolat, *J. Biomech. Eng.*, 2013, **135**, 91011.
24. S. H. Hsu, K. C. Hung, Y. Y. Lin, C. H. Su, H. Y. Yeh, U. S. Jeng, C. Y. Lu, S. A. Dai, W. E. Fu and J. C. Lin, *J. Mater. Chem. B*, 2014, **2**, 5083.
25. C. W. Ou, C. H. Su, U. S. Jeng and S. H. Hsu, *ACS Appl. Mater. Interfaces*, 2014, **6**, 5685.
26. Y. C. Tsai, S. Li, S. G. Hu, W. C. Chang, U. S. Jeng and S. H. Hsu, *ACS Appl. Mater. Interfaces*, 2015, **7**, 27613.
27. F. Y. Hsieh, H. H. Lin and S. H. Hsu, *Biomaterials*, 2015, **71**, 48.
28. A. P. Zhang, X. Qu, P. Soman, K. C. Hribar, J. W. Lee, S. Chen and S. He, *Adv. Mater.*, 2012, **24**, 4266.
29. R. A. Barry, R. F. Shepherd, J. N. Hanson, R. G. Nuzzo, P. Wiltzius and J. A. Lewis, *Adv. Mater.*, 2009, **21**, 2407.

30. H. Shepherd, S. T. Parker, R. F. Shepherd, M. U. Gillette, J. A. Lewis and R. G. Nuzzo, *Adv. Funct. Mater.*, 2011, **21**, 47.
31. D. H. Martin, G. Peter, L. Christoph, V. D. Z. Sybrand and S. S. Ulrich, *Adv. Mater.*, 2010, **22**, 5424.
32. Z. Rao, M. Inoue, M. Matsuda and T. Taguchi, *Colloids Surf., B*, 2011, **82**, 196.
33. Y. Chen, A. M. Kushner, G. A. Williams and Z. Guan, *Nat. Chem.*, 2012, **4**, 467.
34. T. C. Tseng, L. Tao, F. Y. Hsieh, Y. Wei, I. M. Chiu and S. H. Hsu, *Adv. Mater.*, 2015, **27**, 3518.
35. Y. Zhang, L. Tao, S. Li and Y. Wei, *Biomacromolecules*, 2011, **12**, 2894.
36. B. Yang, Y. Zhang, X. Zhang, L. Tao, S. Li and Y. Wei, *Polym. Chem.*, 2012, **3**, 3235.
37. E. J. Fleet, Y. Zhang, S. A. Hayes and P. J. Smith, *J. Mater. Chem. A*, 2015, **3**, 2283.
38. C. B. Highley, C. B. Rodell and J. A. Burdick, *Adv. Mater.*, 2015, **27**, 5075.
39. M. Behl, M. Y. Razzaq and A. Lendlein, *Adv. Mater.*, 2010, **22**, 3388.
40. W. M. Huang, C. L. Song, Y. Q. Fu, C. C. Wang, Y. Zhao, H. Purnawali, H. B. Lu, C. Tang, Z. Ding and J. L. Zhang, *Adv. Drug Delivery Rev.*, 2013, **65**, 515.
41. A. Lendlein and S. Kelch, *Angew. Chem., Int. Ed.*, 2002, **41**, 2034.
42. D. Ratna and J. Karger-Kocsis, *J. Mater. Sci.*, 2008, **43**, 254.
43. C. Liu, H. Qin and P. Mather, *J. Mater. Chem.*, 2007, **17**, 1543.
44. C. M. Yakacki, R. Shandas, C. Lanning, B. Rech, A. Eckstein and K. Gall, *Biomaterials*, 2007, **28**, 2255.
45. P. Rychter, E. Pamula, A. Orchel, U. Posadowska, M. Krok-Borkowicz, A. Kaps, N. Smigiel-Gac, A. Smola, J. Kasperczyk, W. Prochwicz and P. Dobrzynski, *J. Biomed. Mater. Res., Part A*, 2015, **103**, 3503.
46. A. Metcalfe, A. Desfaits, I. Salazkin, L. H. Yahia, W. M. Sokolowski and J. Raymond, *Biomaterials*, 2003, **24**, 491.
47. M. F. Metzger, T. S. Wilson, D. Schumann, D. L. Matthews and D. J. Maitland, *Biomed. Microdevices*, 2002, **4**, 89.
48. A. U. Daniels, M. K. Chang, K. P. Andriano and J. Heller, *J. Appl. Biomater.*, 1990, **1**, 57.
49. X. Lu, W. Cai and L. Zhao, *Mater. Sci. Forum*, 2005, **475–479**, 2399.
50. X. Zhang, X. Lu, Z. Wang, J. Wang and Z. Sun, *J. Biomater. Sci., Polym. Ed.*, 2013, **24**, 1057.
51. M. Radjabian, M. H. Kish and N. Mohammadi, *J. Polym. Res.*, 2012, **19**, 9870.
52. E. D. Rodriguez, X. Luo and P. T. Mather, *ACS Appl. Mater. Interfaces*, 2011, **3**, 152.
53. T. Hirai, H. Maruyama, T. Suzuki and S. Hayashi, *J. Appl. Polym. Sci.*, 1992, **45**, 1849.
54. T. Hirai, H. Maruyama, T. Suzuki and S. Hayashi, *J. Appl. Polym. Sci.*, 1992, **45**, 1449.

55. M. Bothe, K. Y. Mya, E. M. J. Lin, C. C. Yeo, X. Lu, C. He and T. Pretsch, *Soft Matter*, 2012, **8**, 965.
56. T. Sauter, K. Lützow, M. Schossig, H. Kosmella, T. Weigel, K. Kratz and A. Lendlein, *Adv. Eng. Mater.*, 2012, **14**, 818.
57. S. H. Hsu, C. T. Hsieh and Y. M. Sun, *J. Mater. Chem. B*, 2015, **3**, 9089.
58. L. Xue, S. Dai and Z. Li, *Biomaterials*, 2010, **31**, 8132.
59. Q. Zhang and J. Feng, *Sol. Energy Mater. Sol. Cells*, 2013, **117**, 259.
60. S. Chen, F. Mo, F. J. Stadler, S. Chen, Z. Ge and H. Zhuo, *J. Mater. Chem. B*, 2015, **3**, 6645.
61. X. Xiao, D. Kong, X. Qiu, W. Zhang, Y. Liu, S. Zhang, F. Zhang, Y. Hu and J. Leng, *Sci. Rep.*, 2015, **5**, 14137.
62. L. Wang, L. Cao, J. Shansky, Z. Wang, D. Mooney and H. Vandenburgh, *Mol. Ther.*, 2014, **22**, 1441.
63. O. Guillaume, A. Daly, K. Lennon, J. Gansau, S. F. Buckley and C. T. Buckley, *Acta Biomater.*, 2014, **10**, 1985.
64. K. M. Lee, H. Koerner, R. A. Vaia, T. J. Bunning and T. J. White, *Soft Matter*, 2011, **7**, 4318.
65. D. Iqbal and M. H. Samiullah, *Materials*, 2013, **6**, 116.
66. A. Lendlein, H. Jiang, O. Jünger and R. Langer, *Nature*, 2005, **434**, 879.
67. G. Li, Q. Yan, H. Xia and Y. Zhao, *ACS Appl. Mater. Interfaces*, 2015, **7**, 12067.
68. H. Chen, Y. Li, Y. Liu, T. Gong, L. Wang and S. Zhou, *Polym. Chem.*, 2014, **5**, 5168.
69. Y. Li, D. Liu, W. Wang, Y. Liu and S. Zhou, *ACS Appl. Mater. Interfaces*, 2015, **7**, 12988.
70. S. Tibbits, S. Linor, D. Dikovsky and S. Hirsch, *Archit. Des.*, 2013, **84**, 116.
71. Q. Zhang, D. Yan, K. Zhang and G. Hu, *Sci. Rep.*, 2015, **5**, 8936.
72. Y. Yang, Y. Chen, Y. Wei and Y. Li, *Int. J. Adv. Manuf. Technol.*, 2016, **84**, 2079.
73. K. Yu, A. Ritchie, Y. Mao, M. L. Dunn and H. J. Qi, *Procedia IUTAM*, 2015, **12**, 193.
74. Q. Ge, H. J. Qi and M. L. Dunn, *Appl. Phys. Lett.*, 2013, **103**, 131901.
75. A. Balasubramanian, R. Morhard and C. J. Bettinger, *Adv. Funct. Mater.*, 2013, **23**, 4832.
76. A. Balasubramanian, R. Morhard and C. J. Bettinger, *Adv. Funct. Mater.*, 2014, **24**, 4860.
77. N. Roy, R. Sengupta and A. K. Bhowmick, *Prog. Polym. Sci.*, 2012, **37**, 781.
78. H. Pang, L. Xu, D. X. Yan and Z. M. Li, *Prog. Polym. Sci.*, 2014, **39**, 1908.
79. Y. Du, S. Z. Shen, K. Cai and P. S. Casey, *Prog. Polym. Sci.*, 2012, **37**, 820.
80. M. Jaymand, M. Hatamzadeh and Y. Omidi, *Prog. Polym. Sci.*, 2015, **47**, 26.
81. J. Y. Wong, R. Langer and D. E. Ingber, *Proc. Natl. Acad. Sci. U. S. A.*, 1994, **91**, 3201.
82. C. E. Schmidt, V. R. Shastri, J. P. Vacanti and R. Langer, *Proc. Natl. Acad. Sci. U. S. A.*, 1997, **94**, 8948.

83. P. R. Bidez 3rd, S. Li, A. G. Macdiarmid, E. C. Venancio, Y. Wei and P. I. Lelkes, *J. Biomater. Sci., Polym. Ed.*, 2006, **17**, 199.
84. A. Kotwal and C. E. Schmidt, *Biomaterials*, 2001, **22**, 1055.
85. N. Takei and M. Akai, *Arch. Orthop. Trauma Surg.*, 1993, **112**, 159.
86. R. Goldman and S. Pollack, *Bioelectromagnetics*, 1996, **17**, 450.
87. N. K. Guimard, N. Gomez and C. E. Schmidt, *Prog. Polym. Sci.*, 2007, **32**, 876.
88. X. Wang, X. Gu, C. Yuan, S. Chen, P. Zhang, T. Zhang, J. Yao, F. Chen and G. Chen, *J. Biomed. Mater. Res., Part A*, 2004, **68**, 411.
89. G. Shi, M. Rouabhia, Z. Wang, L. H. Dao and Z. Zhang, *Biomaterials*, 2004, **25**, 2477.
90. J. Serra Moreno, S. Panero, S. Materazzi, A. Martinelli, M. G. Sabbieti, D. Agas and G. Materazzi, *J. Biomed. Mater. Res., Part A*, 2009, **88**, 832.
91. N. Gomez, J. Y. Lee, J. D. Nickels and C. E. Schmidt, *Adv. Funct. Mater.*, 2007, **17**, 1645.
92. T. Sudwilai, J. J. Ng, C. Boonkrai, N. Israsena, S. Chuangchote and P. Supaphol, *J. Biomater. Sci., Polym. Ed.*, 2014, **25**, 1240.
93. D. Kai, M. P. Prabhakaran, G. Jin and S. Ramakrishna, *J. Biomed. Mater. Res., Part A*, 2011, **99**, 376.
94. S. J. Chen, D. Y. Wang, C. W. Yuan, X. D. Wang, P. Y. Zhang and X. S. Gu, *J. Mater. Sci. Lett.*, 2000, **19**, 2157.
95. R. Balint, N. J. Cassidy and S. H. Cartmell, *Acta Biomater.*, 2014, **10**, 2341.
96. P. Humpolicek, V. Kasparkova, P. Saha and J. Stejskal, *Synth. Met.*, 2012, **162**, 722.
97. C. H. Wang, Y. Q. Dong, K. Sengothi, K. L. Tan and E. T. Kang, *Synth. Met.*, 1999, **102**, 1313.
98. L. Wang, Y. Wu, B. Guo and P. X. Ma, *ACS Nano*, 2015, **9**, 9167.
99. X. Zhao, P. Li, B. Guo and P. X. Ma, *Acta Biomater.*, 2015, **26**, 236.
100. A. Borriello, V. Guarino, L. Schiavo, M. A. Alvarez-Perez and L. Ambrosio, *J. Mater. Sci.: Mater. Med.*, 2011, **22**, 1053.
101. C. A. Thomas, K. Zong, P. Schottland and J. R. Reynolds, *Adv. Mater.*, 2000, **12**, 222.
102. K. D. McKeon-Fischer, D. P. Browe, R. M. Olabisi and J. W. Freeman, *J. Biomed. Mater. Res., Part A*, 2015, **103**, 3633.
103. X. Niu, M. Rouabhia, N. Chiffot, M. W. King and Z. Zhang, *J. Biomed. Mater. Res., Part A*, 2015, **103**, 2635.
104. F. Pires, Q. Ferreira, C. A. Rodrigues, J. Morgado and F. C. Ferreira, *Biochim. Biophys. Acta*, 2015, **1850**, 1158.
105. N. Srivastava, V. Venugopalan, M. S. Divya, V. A. Rasheed, J. James and K. S. Narayan, *Tissue Eng., Part A*, 2013, **19**, 1984.
106. J. T. Kim, S. K. Seol, J. Pyo, J. S. Lee, J. H. Je and G. Margaritondo, *Adv. Mater.*, 2011, **23**, 1968.
107. N. Aydemir, J. Parcell, C. Laslau, M. Nieuwoudt, D. E. Williams and J. Travas-Sejdic, *Macromol. Rapid Commun.*, 2013, **34**, 1296.
108. M. Hamedi, R. Forchheimer and O. Inganäs, *Nat. Mater.*, 2007, **6**, 357.
109. C. A. Mire, A. Agrawal, G. G. Wallace, P. Calvert and M. In Het Panhuis, *J. Mater. Chem.*, 2011, **21**, 2671.

110. D. G. Harman, R. Gorkin 3rd, L. Stevens, B. Thompson, K. Wagner, B. Weng, J. H. Chung, M. In Het Panhuis and G. G. Wallace, *Acta Biomater.*, 2015, **14**, 33.
111. M. B. Runge, M. Dadsetan, J. Baltrusaitis and M. J. Yaszemski, *J. Biol. Regul. Homeostatic Agents*, 2011, **25**, S15.
112. K. C. Satyanarayana and K. Bolton, *Polymer*, 2012, **53**, 2927.
113. S. J. Lee, A. P. Arun and K. J. Kim, *Mater. Lett.*, 2015, **148**, 58.
114. H. Ohigashi, K. Koga, M. Suzuki, T. Nakanishi, K. Kimura and N. Hashimoto, *Ferroelectrics*, 1984, **60**, 263.
115. A. Kholkin, N. Amdursky, I. Bdikin, E. Gazit and G. Rosenman, *ACS Nano*, 2010, **4**, 610.
116. L. J. Romasanta, M. A. Lopez-Manchado and R. Verdejo, *Prog. Polym. Sci.*, 2015, **51**, 188.
117. I. Yasuda, *J. Jpn. Orthop. Surg. Soc.*, 1954, **28**, 267.
118. E. Fukada and I. Yasuda, *J. Phys. Soc. Jpn.*, 1957, **12**, 1158.
119. S. B. Lang, *Nature*, 1966, **212**, 704.
120. M. H. Shamos and L. S. Lavine, *Nature*, 1967, **213**, 267.
121. A. R. Liboff and M. H. Shamos, *J. Dent. Res.*, 1971, **50**, 516.
122. P. Aebischer, R. F. Valentini, P. Dario, C. Domenici, V. Guénard, S. R. Winn and P. M. Galletti, *ASAIO Trans.*, 1987, **33**, 456.
123. R. F. Valentini, T. G. Vargo, J. A. Gardella Jr and P. Aebischer, *Biomaterials*, 1992, **13**, 183.
124. Y. S. Lee and T. L. Arinzeh, *Tissue Eng., Part A*, 2012, **18**, 2063.
125. H. F. Guo, Z. S. Li, S. W. Dong, W. J. Chen, L. Deng, Y. F. Wang and D. J. Ying, *Colloids Surf., B*, 2012, **96**, 29.
126. S. M. Damaraju, S. Wu, M. Jaffe and T. L. Arinzeh, *Biomed. Mater.*, 2013, **8**, 045007.
127. Y. Ikada, Y. Shikinami, Y. Hara, M. Tagawa and E. Fukada, *J. Biomed. Mater. Res.*, 1996, **30**, 553.
128. O. Pabst, J. Perelaer, E. Beckert, U. S. Schubert, R. Eberhardt and A. Tünnermann, *Org. Electron.*, 2013, **14**, 3423.
129. K. Kim, W. Zhu, X. Qu, C. Aaronson, W. R. McCall, S. Chen and D. J. Sirbuly, *ACS Nano*, 2014, **8**, 9799.
130. A. Marino, J. Barsotti, G. de Vito, C. Filippeschi, B. Mazzolai, V. Piazza, M. Labardi, V. Mattoli and G. Ciofani, *ACS Appl. Mater. Interfaces*, 2015, **7**, 25574.
131. I. Armentano, N. Bitinis, E. Fortunati, S. Mattioli, N. Rescignano, R. Verdejo, M. A. Lopez-Manchado and J. M. Kenny, *Prog. Polym. Sci.*, 2013, **38**, 1720.
132. X. Cui, K. Breitenkamp, M. G. Finn, M. Lotz and D. D. D'Lima, *Tissue Eng., Part A*, 2012, **18**, 1304.
133. D. L. Cohen, J. I. Lipton, L. J. Bonassar and H. Lipson, *Biofabrication*, 2010, **2**, 035004.

CHAPTER 23

Smart Materials-Originated Microfluidic Systems for Tissue Engineering

ASHLYN T. YOUNG[a] AND MICHAEL A. DANIELE*[a,b]

[a]Joint Department of Biomedical Engineering, NC State University and University of North Carolina, 911 Oval Dr., Chapel Hill, Raleigh, NC 27695, USA; [b]Department of Electrical & Computer Engineering, NC State University, 890 Oval Dr., Raleigh, NC 27695, USA
*E-mail: mdaniel6@ncsu.edu

23.1 Introduction

Stimuli-responsive materials are significant in tissue engineering due to their ability to change in response to the environment, allowing instantaneous formation of biocompatible and complex structures. As scaffolds, smart materials offer the ability to crosslink in a controlled and quick manner, therefore minimizing the risk of contamination and long exposures to room-temperature environments where experiments are often facilitated. The concentration and configuration of polymers allow for fine-tuning desirable features in scaffolds, offering the ability to design a biomimetic environment for cells to thrive.

Microfluidics are also a popular platform for cellular assays due to minimal solution requirements, user-friendly control, and high throughput qualities. Many microfluidics can be rapidly prototyped to compare and

Smart Materials No. 25
Smart Materials for Tissue Engineering: Applications
Edited by Qun Wang

Published by the Royal Society of Chemistry, www.rsc.org

determine the optimal geometry for the desired application. Due to these benefits, microfluidic platforms are increasingly used in tissue engineering for controlled cell culture and tissue constructs. In partnership with smart materials, microfluidics can be used to create dynamic, hybrid materials for mimicking extracellular matrices to create biomimetic scaffolds. The hydrodynamic focusing capabilities of microfluidic devices allow for unique structures, such as fibers and droplets, to be formed and used as tissue implants or three-dimensional cell research. Additionally, smart materials can be locally controlled as pumps and valves in microchannels for precise fluid-flow control. Entire channels can even be produced from smart materials and lined with endothelial cells to mimic vascular systems. The techniques and methods for tissue engineering utilizing microfluidics and smart materials will be discussed, along with the cell types used and specific benefits of each technique.

23.2 Chemically-Reactive Smart Materials in Microfluidics for Tissue Engineering

A popular substrate for the crosslinking hydrogel scaffolds is chemically-responsive materials, polymerizing upon exposure to an external solution. Some of the benefits of this method include rapid response, minimal bench top equipment, and non-exposure to stimuli that can be harmful for cells, such as ultra violet radiation. Additionally, microfluidics offer a platform by which small volumes of co-reactive materials can interact, utilizing flow and geometry to create unique structures. A variety of microfluidic devices, chemically-reactive smart materials, and cell types will be discussed in relation to practical applications in tissue engineering.

23.2.1 Microfiber Fabrication Using Chemically-Responsive Smart Materials

Microfluidic-formed microfibers as a platform for tissue engineering is an emerging topic due to the ability to rapidly form micro-sized, cell-laden vessels. Microvessels have a wide variety of applications, including cell studies, organ-on-chip devices, and *in vivo* vessel replacements.

Microvessels come in many orientations, with or without a lumen. Microvessels without a lumen can be fabricated for cell capture[1–3] or to observe cell affinity with controlled protein release.[4] Figure 23.1(a) and (b) displays solid microfibers laden with cells. Targeted cell types are trapped within the vessel during fabrication, allowing for single cell handing and observation. Microvessels with a lumen can alternatively be used for co-culture with continuous core flow, as displayed in Figure 23.1(e).[5] In all forms, microvessels are unique in that they can be fabricated meters at a time, producing high throughput groups of similar species.[6] Figure 23.1(c) demonstrates a high throughput method to create many microstrands simultaneously though the

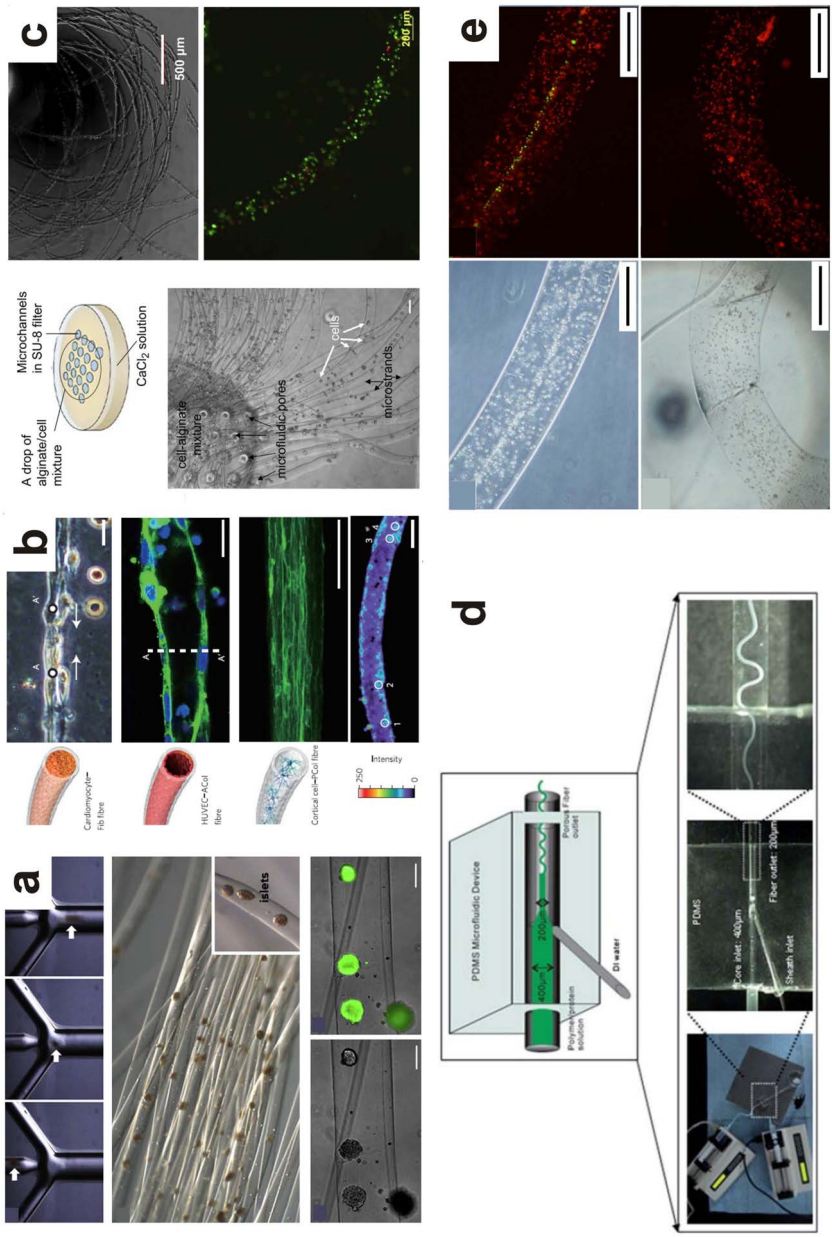

Figure 23.1 Microfluidic devices can be used to create cell-laden microvessels from chemically-responsive materials. (a) Pancreatic islets were seeded into a microvessel using collagen alginate and $CaCl_2$. Reprinted from *Biomaterials*, Vol. 33 Issue 34, Yesl Jun, Min Jun Kim, Yong Hwa Hwang, Eun Ae Jeon, Ah Ran Kang, Sang-Hoon Lee, Dong Yun Lee, Microfluidics-generated pancreatic islet microfibers for enhanced immunoprotection, pages 8122–8130. Copyright 2013, with permission from Elsevier.[2] (b) Micro-fibers were engineered using different cell types and geometries with the same device. Reproduced with permission. Reprinted by permission from Macmillan Publishers Ltd: *Nature Materials*,[1] copyright 2013. (c) Multiple alginate microfibers were produced simultaneously, seeded with mouse embryonic stem cells. Reproduced with permission. Reprinted from *Biomaterials*, Vol. 32 Issue 20, Nurazhani Abdul Raof, Michael R. Padgen, Alison R. Gracias, Magnus Bergkvist, Yubing Xie, One-dimensional self-assembly of mouse embryonic stem cells using an array of hydrogel microstrands, pages 4498–4505, Copyright 2011, with permission from Elsevier.[6] (d) A coaxial microfluidic device was used to create an amphiphilic ABA tri-block copolymer microfiber. Reproduced from ref. 4 with permission from the PCCP Owner Societies. (e) Microfibers encase mouse fibroblast cells, imaged with phase microscopy and fluorescence microscopy. Scale bars represent 500 μm. Reprinted from *Biochemical Engineering Journal*, Vol. 49 Issue 1, Takayuki Takei, Naoya Kishihara, Shinji Sakai, Koei Kawakami, Novel technique to control inner and outer diameter of calcium–alginate hydrogel hollow microfibers, and immobilization of mammalian cells, pages 143–147. Copyright 2010, with permission from Elsevier.[5]

use of microchannels in a filter. Additionally, through altering flow rates and patterns, complex structures can be produced with numerous cell types.[7] The rapid fabrication and tunable features of microvessels are facilitated by the use and incorporation of stimuli-responsive polymers. In particular, many fabrication techniques involve the coaxial microfluidic flow of a hydrogel that polymerizes upon contact with a biocompatible chemical, such as $CaCl_2$. Coaxial microfluidic flow for microfiber fabrication is diagramed in Figure 23.1(d), where an amphiphilic ABA triblock copolymer is used to form a 200 μm fiber.

The geometry and size of a microvessel allow for studies that look at very specific interactions between cells, and the role of single cell types in an organ system. For example, microfibers have been used to culture and observe the interactions between hepatocytes and other cell types. Co-flowing microfluidic systems have been used to create alginate hydrogel fibers housing hepatic cells.[8] Alginate gelatin was used to capture hepatocytes between 3T3 fibroblasts. Polymerized with a $CaCl_2$ sheath, alginate acted as a scaffold allowing 3T3 fibroblasts to orient around hepatocytes, creating an organoid upon enzymatic removal. The fabrication process and cell orientation of the hepatocytes and 3T3 fibroblasts is displayed in Figure 23.2(a). This group demonstrated the use of smart hydrogel materials in microfluidics for the culture and formation of a biomimetic micro-organoid. Similarly, fabricated chitosan microfibers were embedded with hepatoma cells as a potential method for liver tissue engineering.[5,9] Solid, pure chitosan fibers were fabricated using a co-axial microfluidic channel with chitosan in contact with crosslink-inducing sodium triphosphate pentabasic (STP) as the outer sheath layer. Diagramed in Figure 23.2(b), post-fabrication Hep2 hepatoma cells were seeded into a micro-device containing fibers, and self-aggregated into spheroids on top of the microfibers. The spheroid orientation and liver function displayed by the Hep2 cells confirmed the possible application of chitosan fibers in liver tissue engineering. As an alternative to STP polymerization, it was also demonstrated by the same group that chitosan–alginate can be used as a substrate for Hep2 growth, polymerized with $CaCl_2$.[10] Cells were both encapsulated within fibers and seeded onto the fiber surface, displaying a high viability and adherence. Cells are observed to have better viability within the chitosan–alginate fiber as compared to the pure alginate fiber in Figure 23.2(c).

Microfluidic devices used for fabricating microvessels are often simple, optically transparent coaxial structures, allowing a layered flow.[1,3–5,10–12] Alternatively, more complex devices allow the creation of concentration gradients and high-throughput parallel fabrication.[6,13] Some devices include external controls for digitally tuning fiber design, allowing structures and cell types to be ordered to fit a specific application.[7,14] Kang *et al.* created a digitally tunable device that mimicked the silk spinning techniques of a spider.[14] Valves were pneumatically controlled to precisely choose the sample type and order for the final fiber. A spool was used to rotate the final cell-laden fibers, allowing the formation of twisted fibers for co-culture of different cell types.

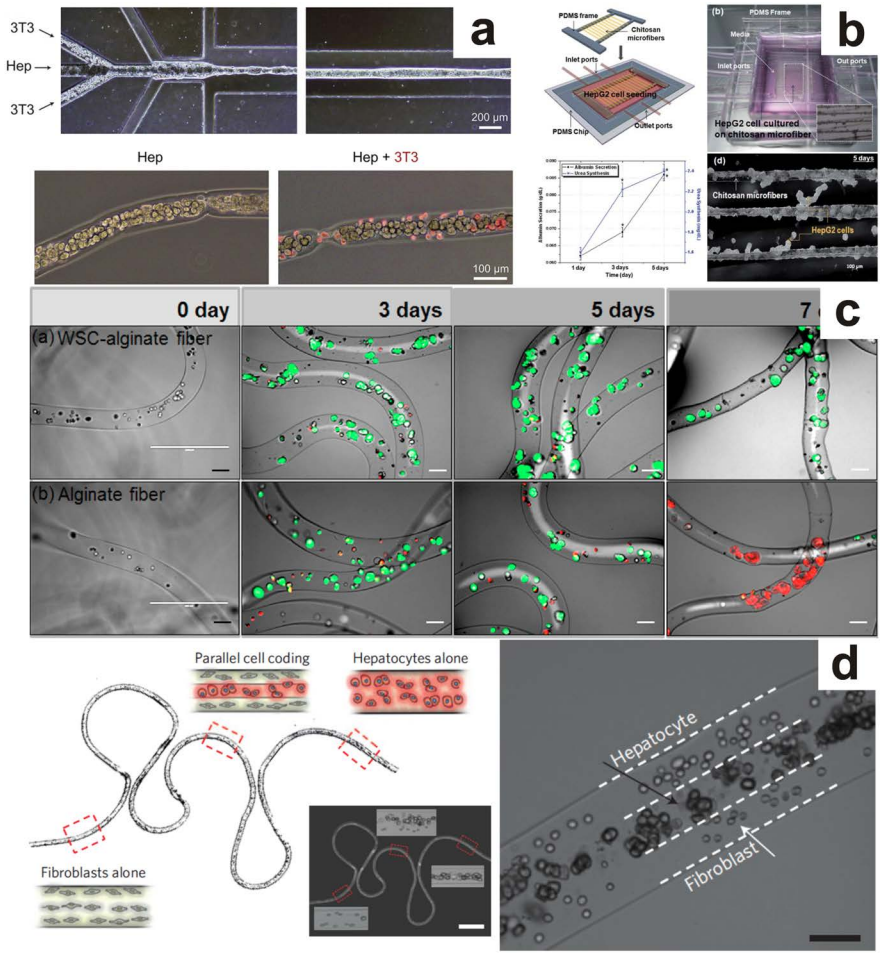

Figure 23.2 Hepatocytes can be seeded around or inside microfibers to function as a bioartificial liver. (a) Mouse hepatocytes were surrounded by mouse feeder cells to create a liver organoid. Reprinted from *Biomaterials*, Vol. 33 Issue 33, Masumi Yamada, Rie Utoh, Kazuo Ohashi, Kohei Tatsumi, Masayuki Yamato, Teruo Okano, Minoru Seki, Controlled formation of heterotypic hepatic micro-organoids in anisotropic hydrogel microfibers for long-term preservation of liver-specific functions, pages 8304–8315, Copyright 2012, with permission from Elsevier.[8] (b) Hepatocytes grew on top of chitosan microfibers wound around a PDMS frame. Reproduced from ref. 9 with permission from the PCCP Owner Societies. (c) Hepatocytes cultured on chitosan–alginate were compared to those cultured on calcium–alginate through using a live–dead stain. Reprinted with permission from Lee, Bo Ram, *et al.*, "Microfluidic wet spinning of chitosan–alginate microfibers and encapsulation of HepG2 cells in fibers." *Biomicrofluidics* 5.2 (2011): 022 208. Copyright 2011, AIP Publishing LLC.[10] (d) Through using a digitally-tunable microfluidic device, hepatocytes were seeded within a fibroblast sheath. Reprinted by permission from Macmillan Publishers Ltd: *Nature Materials*,[14] copyright 2011.

When coded serially, segments of different solutions can be deliberately ordered, while parallel coding allows for numerous fibers to orient side-by-side. Serial fibers can be created to have spindles, joints, and segments with varying material properties and size, and parallel fibers can be used to create grooves for cell adhesion. The parallel techniques were used to create a fiber organoid, with fibroblasts encasing hepatocyte cells as displayed in Figure 23.2(d), as well as culture neurons on top of grooved fibers to observe adhesion and orientation along the fiber. The serial technique was used to observe neutrophil migration along a fiber, by alternating fiber sections with and without neutrophils. These devices display the expansive variability and user control permitted in tissue engineering through the use of microfluidic devices.

23.2.2 Microvessel Network Fabrication and Application Using Chemically-Responsive Smart Materials

An alternative to microfluidic fabrication of long vessels, channels can be created within a smart polymer to allow the flow and interaction of cell-laden solutions. Microfluidic devices are traditionally fabricated using soft lithography, etching, or hot embossing to create permanent, durable channels in plastics or polymers. The downside of this approach in tissue engineering is that cells are unable to interact between channels, cannot infiltrate the device material, and are often restricted to planar movement. To combat these issues, smart polymers can be used to create permeable and porous channels of variable thickness for cells to communicate and travel through. Xu *et al.* designed and created a microvessel network by 3D-printing "hurdles" onto a surface.[15] The hurdles were composed of biocompatible alginate, gelatin, and fibrin, crosslinked with $CaCl_2$. Co-culture adipose-derived stem cells' and hepatocytes' motility and orientation around and on top of the hurdles were observed. Morphological changes and interactions were also noted, suggesting 3D printing biocompatible responsive polymers as a promising approach to tissue engineering. Fluid flow within the channels and hepatocyte proliferation around the hydrogel can be observed in Figure 23.3(a).

Similarly, Mu *et al.* created a 3D vascular network using a collagen/alginate hydrogel to mimic a nephron.[48] A liquid mold in partnership with polydimethylsiloxane (PDMS) barriers was used to create the hydrogel channels, crosslinked with $CaCl_2$. A cell solution was introduced to the channels, allowing passive diffusion between a channel containing human umbilical vein endothelial cells (HUVECs) and a channel containing Madin–Darby canine kidney (MDCK) cells. The endothelial-lined channel mimicked a vessel, while the MDCK-lined channel mimicked a tubule, therefore accurately representing the structure of a nephron. Dye was introduced inside one channel, and perfusion was observed into the other channel and quantified. The hydrogel microchannels facilitate a biomimetic environment for passive transfer of molecules between channels with tunable perfusable properties. HUVECs seeded within a molded hydrogel channel is demonstrated in Figure 23.3(b).

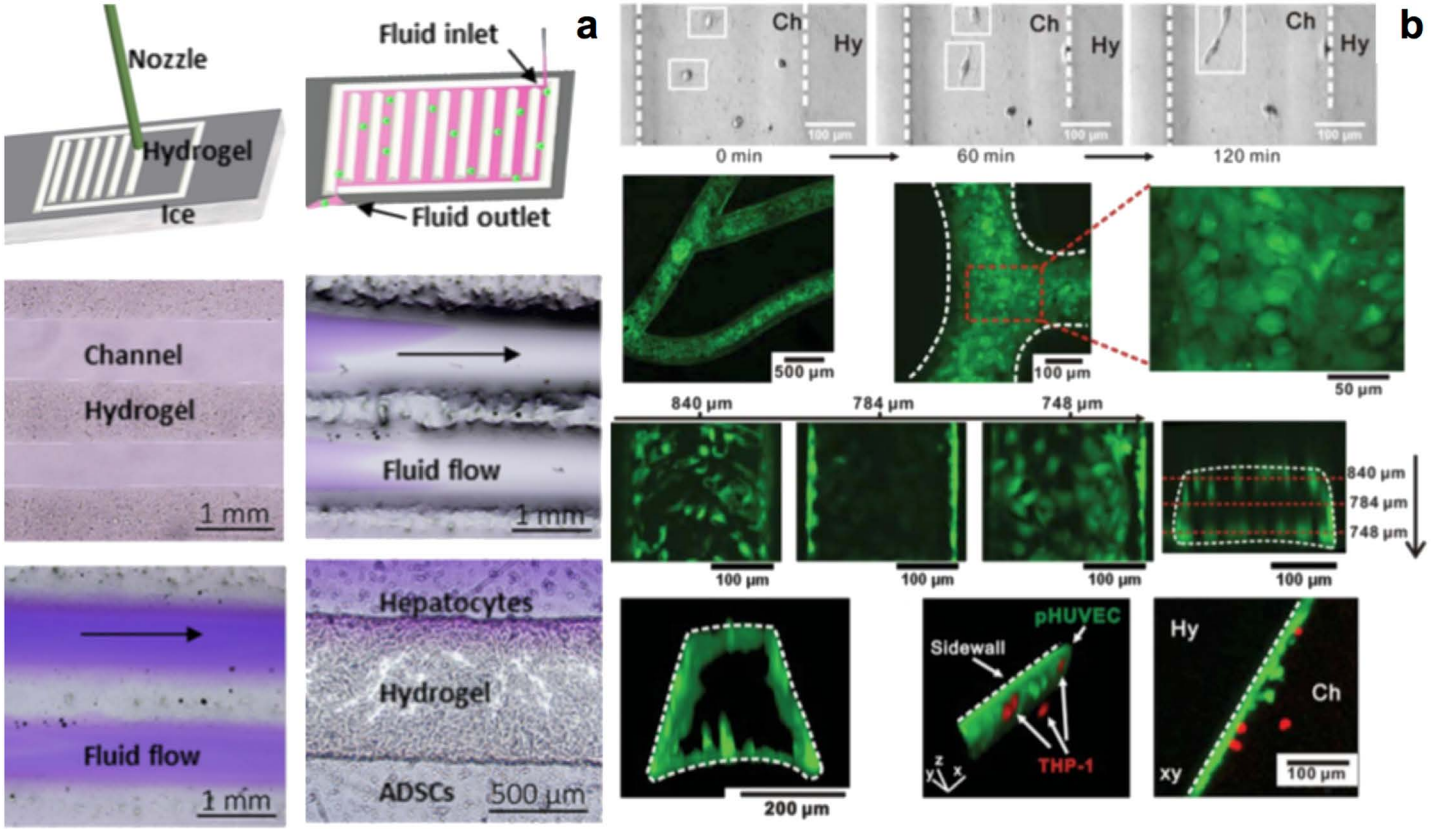

Figure 23.3 Microchannels can be formed in smart materials to create biomimetic microvasculature. (a) Alginate/gelatin/fibrin hurdles were created between parallel microchannels and seeded with hepatocytes and adipose-derived stem cells. Reprinted from *Biotechnology & Bioengineering*, Vol. 12 Issue 8, Yufan Xu and Xiaohong Wang, Fluid and cell behaviors along a 3D printed alginate/gelatin/fibrin channel, pages 1683–1695. Copyright 2015 with permission from John Wiley and Sons.[15] © 2015 Wiley Periodicals, Inc. (b) HUVECs were seeded into molded hydrogel microchannels. Reproduced from ref. 48 with permission from the PCCP Owner Societies.

23.2.3 Microsphere Fabrication in a Microfluidic Device Using Chemically-Responsive Materials

It is well recognized that cells represent *in vivo* activity more closely when cultured in three-dimensions in comparison to a two-dimensional planar culture.[16] *In vivo* cells are seldom restricted to a planar environment, therefore cellular interactions and morphologies are best studied in three-dimensions. Three-dimensional cultures require scaffold material that is representative of the extracellular matrix (ECM), allowing cells to self-orient and receive the proper nutrients from their surroundings. Smart materials make great three-dimensional scaffolds due to their tunable properties and rapid response to environmental conditions. Hydrogels can be engineered to have porosity similar to the ECM found in the desired organ system, as well as rapid crosslinking to maintain short-term cell exposure to stressful or room-temperature environments.

Microspheres are a commonly used platform for three-dimensional cell studies. Microspheres are a valuable tool for single cell encapsulation, as well as the study and isolation of cell spheroids. Commonly fabricated from hydrogels, microspheres allow the self-orientation of small amounts of cells within a restricted environment. This permits the study of specific cell secretions, interactions, and morphologies. Traditionally, microspheres are fabricated through emulsion and manually forming droplets from syringes. These methods do not create uniform structures, therefore reducing the repeatability of experiments. Additionally, these methods require manual handing of microspheres post-production to observe single spheres. As an alternative, microfluidic devices can be used to fabricate uniform microspheres that are linearly spaced and easily imaged post-production.

Fabrication of chemically reactive hydrogels within a microfluidic device is often performed using two immiscible solutions.[17] Many groups form microspheres with a three-channel laminar flow design. The three channels will converge, with the outer two channels containing oil with a crosslinker solution and the inner channel containing the microsphere solution. The oil channels will "pinch" the middle channel into a single sphere and diameter can be controlled *via* flow rates. The spheres are crosslinked upon the introduction of reacting chemicals. This technique is described in Figure 23.4(a). Headen *et al.* fabricated four-arm PEGMAL microspheres to encapsulate mesenchymal stem cells. The four-arm PEGMAL material functionalizes at a physiological pH, and crosslinks when exposed to dithiothreitol (DTT). Cell-laden PEGMAL is pinched by oil with DTT emulsions, forming a sphere that quickly crosslinks. The tunable properties offered in this method allow a robust system by which cells can be captured and studied. Similarly, Hung *et al.* compared solvent extraction and evaporation from two different emulsion-based microfluidic designs.[18] The solvent extraction design is particularly interesting, combining droplets of water and poly(lactide-*co*-glycolide) (PLGA)–dimethyl sulfoxide (DMSO). When exposed to water, the DMSO is immediately extracted, creating a miniature bioreactor forming

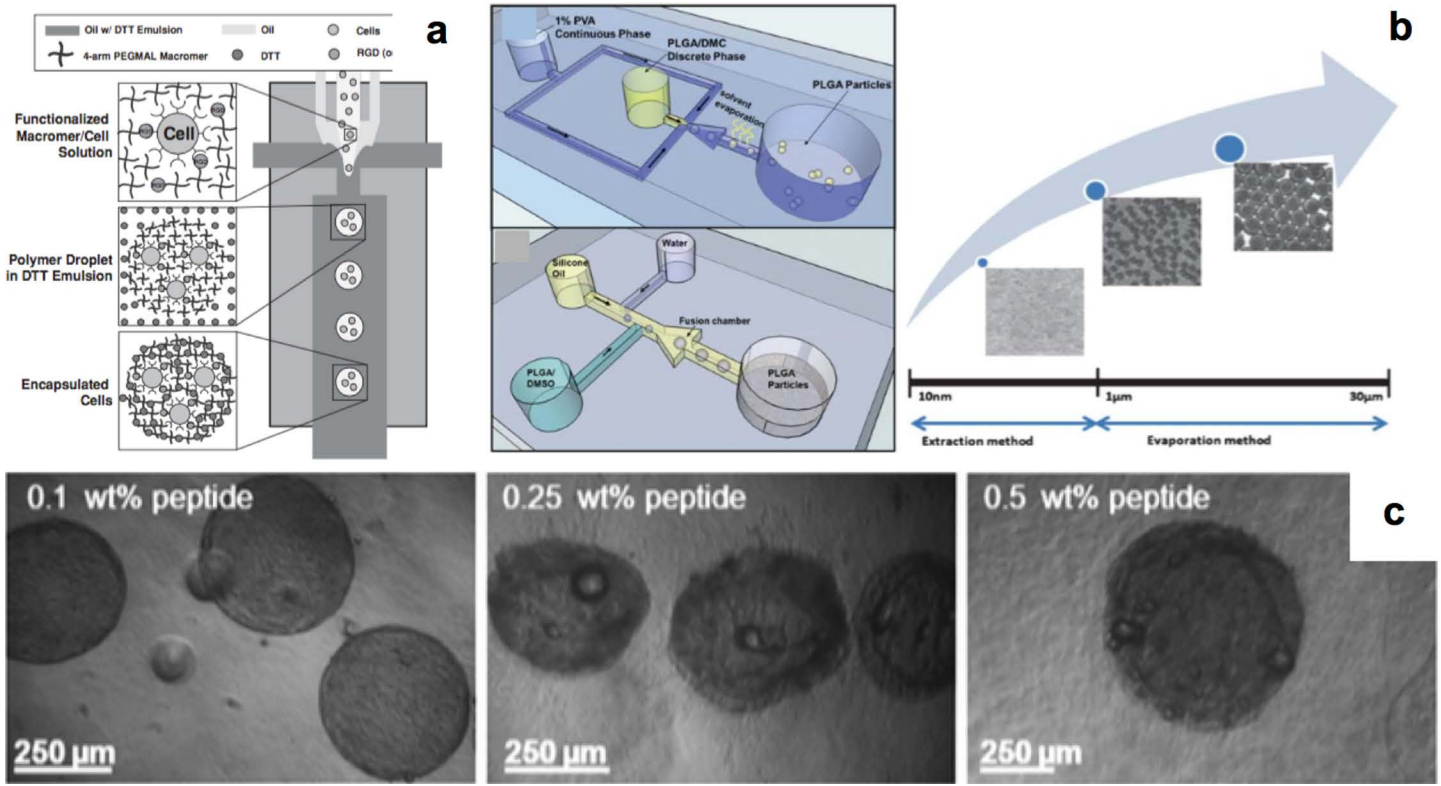

Figure 23.4 Cell-laden microdroplets and microparticles can be created using smart materials in a microfluidic device. (a) A four-arm PEGMAL macromer is pinched into cell-encapsulating microspheres using a three-channel microfluidic device. Reprinted from *Advanced Materials*, Vol. 26 Issue 19, Devon M. Headen, Guillaume Aubry, Hang Lu, and Andrés J. García, Microfluidic-Based Generation of Size-Controlled, Biofunctionalized Synthetic Polymer Microgels for Cell Encapsulation, pages 3003–3008, Copyright 2014 with permission from John Wiley and Sons.[17] © 2014 WILEY-VCH Verlag GmbH & Co. KGaA, Weinheim. (b) Solvent extraction and solvent evaporation polymerization methods were tested and compared. Reproduced from ref. 18 with permission from the PCCP Owner Societies. (c) Xanthan–K2(QL)6K2 microcapsules were created in a microfluidic device with three peptide concentrations, imaged with bright field microscopy. Reprinted with permission from Mendes, Ana C., *et al.*, "Microfluidic fabrication of self-assembled peptide–polysaccharide microcapsules as 3D environments for cell culture." *Biomacromolecules* 13.12 (2012): 4039–4048. Copyright 2012 American Chemical Society.[19]

PLGA particles. The non-toxicity of the solvents used in this method preserve the biocompatible integrity of the method. Modifying the polymer composition changes the degradation rate, making PLGA particles a viable candidate for degradable scaffolding in tissue engineering. Comparison between the extraction and evaporation methods is shown in Figure 23.4(b), with the evaporation method resulting in larger microspheres.

Microfluidic devices facilitate high-throughput fabrication of uniform microspheres with controllable size, microsphere-material-determining porosity and structure of the final product. Many hydrogels possess an uncontrollable "randomness" in structure at the nano-level that can have negative effects on the macroscale function. Mendes *et al.* suggested a method to combat this variability by microencapsulating a self-assembled peptide to ensure uniform and predictable assembly at the nanoscale.[19] They chose a K2(QL)6K2 peptide along with xanthum gum used as the self-assembly "trigger". By changing the ratio of peptide to polysaccharide, different properties could be observed in the microsphere. As shown in Figure 23.4(c), chondrocyte cells were encapsulated in the microspheres to examine long-term culture capabilities, demonstrating that the cells maintained viability for over 21 days. Self-assembled peptides are presented as a great tool for precise control of structure, shape, and performance of micro particles in partnership with tissue engineering.

23.3 Photo-Responsive Smart Materials in Microfluidics for Tissue Engineering

Smart materials that respond to environmental light sources offer a variety of benefits unattainable with the previously discussed chemically-responsive hydrogels. They do not require supplementary solutions, therefore additional channels and collection chambers to facilitate reactions are not necessary. Microfluidic devices are commonly fabricated from an optically transparent material, such as PDMS or acrylic, to allow the imaging and analysis of intra-channel components. This feature also allows an external light source to enter a channel, therefore facilitating a light-induced response to whatever material is inside the device. Additionally, many light sources are minimally harmful to cells when at low intensity, making light-responsive smart materials suitable for tissue engineering. Photo-responsive smart materials, and their application for tissue engineering using smart materials, will be further discussed in regards to microfibers, microvessel networks, microspheres, and channel valves.

23.3.1 Microfiber Fabrication and Applications Using Photo-Responsive Smart Materials

As discussed previously regarding chemically-responsive smart materials, microfibers are a powerful tool in mimicking microvessels *in vitro* and can be rapidly and uniformly fabricated using a microfluidic device. As opposed

to the methods previously discussed, photo-responsive materials facilitate the controlled polymerization of fibers in-channel with simplified additional reagents. Rather than using alginate as the fiber bulk, photo-polymerization allows the use of gelatin-based hydrogels. Gelatin is more representative of ECM in comparison to alginate due to the more randomized and textured microsurface. The cell affinity for microgrooved alginate fibers was experimentally compared to microgrooved methacrylamide-modified gelatin (GelMA).[20] The GelMA material was photopolymerized after flowing through a patterned microdevice into an ethanol or saline bath, while the alginate material flowed through the same device, but into $CaCl_2$ for polymerization. Through analyzing cell orientation and viability, it was determined that GelMA possessed desirable cell response with minimally intensive fabrication. Cells were seeded inside and on top of the fibers, displaying cell alignment along the grooved surfaces as well as successful cell encapsulation. Cell alignment and co-culture can be seen in Figure 23.5(a). The biocompatibility and cellular response in GelMA were experimentally proven to be superior to those of alginate due to the porosity and surface roughness offered. Additionally, the fiber strength and processing ease suggested GelMA as a promising scaffold for tissue engineering.

Rather than using pure GelMA, polymers can be tailored to display ideal characteristics through adjusting ratios and introducing new components. Daniele *et al.* demonstrated the creation of a bio/synthetic interpenetrating network ($BioSIN_x$) containing four-arm poly(ethylene glycol) (PEG) and GelMA.[21] When exposed to ultra-violet light, the network crosslinks to create a highly cyto-compatible scaffold with lessened gelatin dissolution when compared to other gelatin and hydrogel scaffold materials. A microfiber, microtubule, coaxial microfiber, and triaxial microfiber fabricated from the $BioSIN_x$ are displayed in Figure 23.5(b). The un-crosslinked $BioSIN_x$ material was introduced to a hydrodynamic-focusing microfluidic device to create microfibers.[22] The microdevice utilized a chevron-shaped wall structure to allow for passive and uniform hydrodynamic focusing of the $BioSIN_x$ material, as demonstrated in Figure 23.5(c). Adjusting the flow rates and number of channels into the microfluidic device allows the dynamic, controlled creation of hollow tubes of varying shapes, dimensions, and layers. Endothelial cells remained viable when entrapped in the lumen of the vessel.[21] This method can be used to create bio-similar blood or lymph vessels, seeded with various cell types and perfused with media to facilitate cellular interaction and orientation along the vessel.

23.3.2 Microvessel Network Fabrication and Application Using Photo-Responsive Smart Materials

One of the greatest benefits of using a photo-responsive material is the control offered in exposing devices to light. Rather than attempting to precisely control flow of solutions, light sources can be focused and directed to polymerize the desired area. This is especially useful when fabricating layered devices, as displayed by Hasan *et al.*[23] A multilayered blood-vessel was

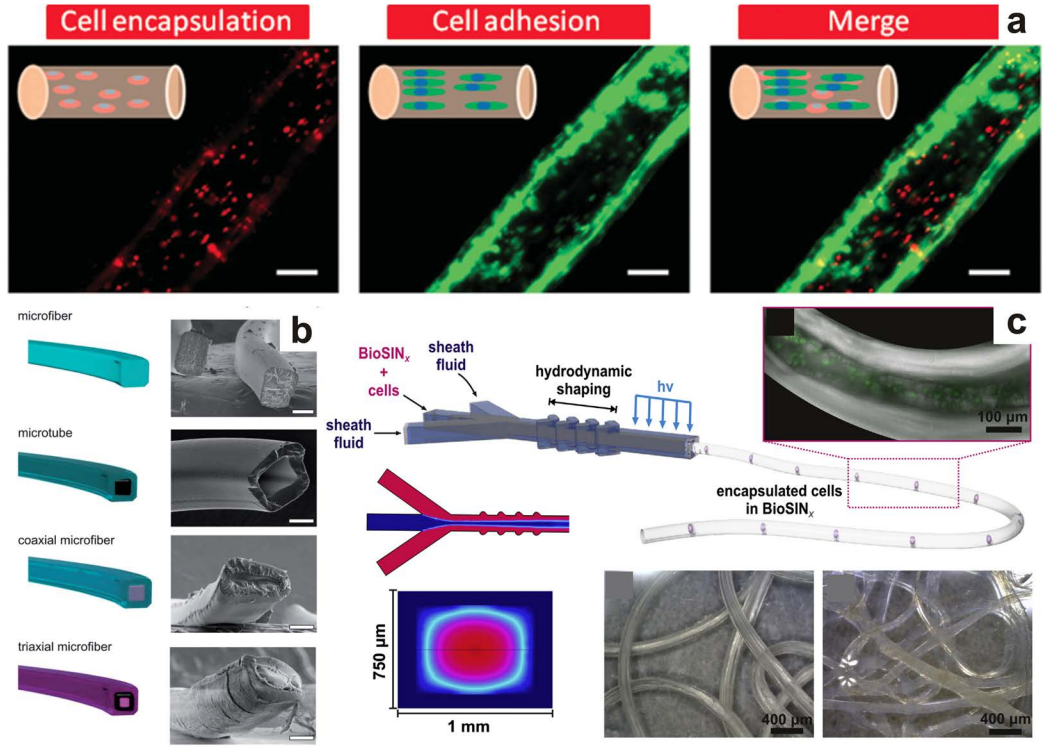

Figure 23.5 Photo-responsive polymers were used within microfluidic devices to make cell-laden microfibers. (a) HUVECs and myoblasts were seeded onto and inside GelMA microfibers, photopolymerized within a microfluidic device. Reprinted from *Advanced Functional Materials*, Vol. 25 Issue 15, Xuetao Shi, Serge Ostrovidov, Yihua Zhao, Xiaobin Liang, Motohiro Kasuya, Kazue Kurihara, Ken Nakajima, Hojae Bae, Hongkai Wu, and Ali Khademhosseini, Microfluidic Spinning of Cell-Responsive Grooved Microfibers, pages 2250–2259, Copyright 2015, with permission from John Wiley and Sons.[20] © 2015 WILEY-VCH Verlag GmbH & Co. KGaA, Weinheim. (b) Microfibers with varying geometries and layers were fabricated using a hydrodynamic shaping microfluidic device. Reproduced from ref. 22 with permission from the PCCP Owner Societies. (c) Cells were encapsulated into a bio/synthetic interpenetrating network microfiber using a hydrodynamic shaping microfluidic device. Reprinted from *Biomaterials*, Vol. 25 Issue 6, Michael A. Daniele, André A. Adams, Jawad Naciri, Stella H. North, Frances S. Ligler, Interpenetrating networks based on gelatin methacrylamide and PEG formed using concurrent thiol click chemistries for hydrogel tissue engineering scaffolds, pages 1845–1856, Copyright 2014, with permission from Elsevier.[21]

created in a PDMS mold through the use of concentric needles. The procedural steps are outlined in Figure 23.6(a). Each cell type was introduced and polymerized step-wise to create an ordered layer of fibroblasts, smooth muscles cells, and endothelial cells. GelMA was used as the crosslinked scaffold, allowing tunable mechanical properties and dependable cell viability. The lumen of the device is determined from the needle diameter for the precise control of size and repeatability. Fabricating microfluidic channels by photopolymerizing GelMA around a needle is a well-defined method for quick experimental analysis of smart materials in tissue engineering, as displayed in Figure 23.6(c).[24]

Another useful biocompatible photo-reactive material for creating microchannels is poly(ethylene glycol) diacrylate (PEGDA).[25] PEGDA is a well-understood perfusable material that supports high cell viability when used as a scaffold, providing a platform for 3D tissue engineering. Signaling gradients can be facilitated within the PEGDA scaffold, creating a dynamic environment for tissue fabrication, demonstrated in Figure 23.6(d) with toluidine blue. Cell motility, as well as controlled exposure can be utilized in single cell and co-culture studies with an easily tunable slow-release polymer, such as PEGDA. An alternative to slow release, polymers can be engineered to have a controlled release of substances. Chueh *et al.* demonstrated a method to pattern co-cultured devices by utilizing a light-directed release of calcium in a microfluidic device.[26] By selectively applying UV light, certain segments of a microchannel could be polymerized while the rest remained in solution. This method allows for location control of cell types, such as MC3T3 cells and HUVECs, to observe interactions and motility. Figure 23.6(b) outlines the steps required to obtain an endothelial cell and osteocyte co-culture. Additionally, by selectively and rapidly directing polymerization within a channel, flow can be directed and altered during experimentation without requiring expensive and complex external equipment.

23.3.3 Microparticle Fabrication in a Microfluidic Device Using Photo-Responsive Smart Materials

A popular method for tissue engineering, demonstrated throughout this discussion, is to create a cell-laden scaffold, seeded either before or after polymerization, and to allow the cells to self-orient within the scaffold. Although an effective way to create macro-sized groups of tissues, Lin *et al.* argues that this method prevents effective control of the entire tissue structure, specifically considering inner properties.[27] Rather than performing bulk tissue engineering, this team suggests the creation and organization of cell-encapsulated microbeads, allowing precise control of the microbead structure, and using them to create a larger assembly. An optically switched dielectrophoretic force (ODEP) was used to assemble alginate microbeads laden with articular chondrocytes from 18–24 month steers, within a microfluidic device.[27] Groups of cells captured within microbeads are displayed in Figure 23.7(b), demonstrating viability within the alginate structures. ODEP forces

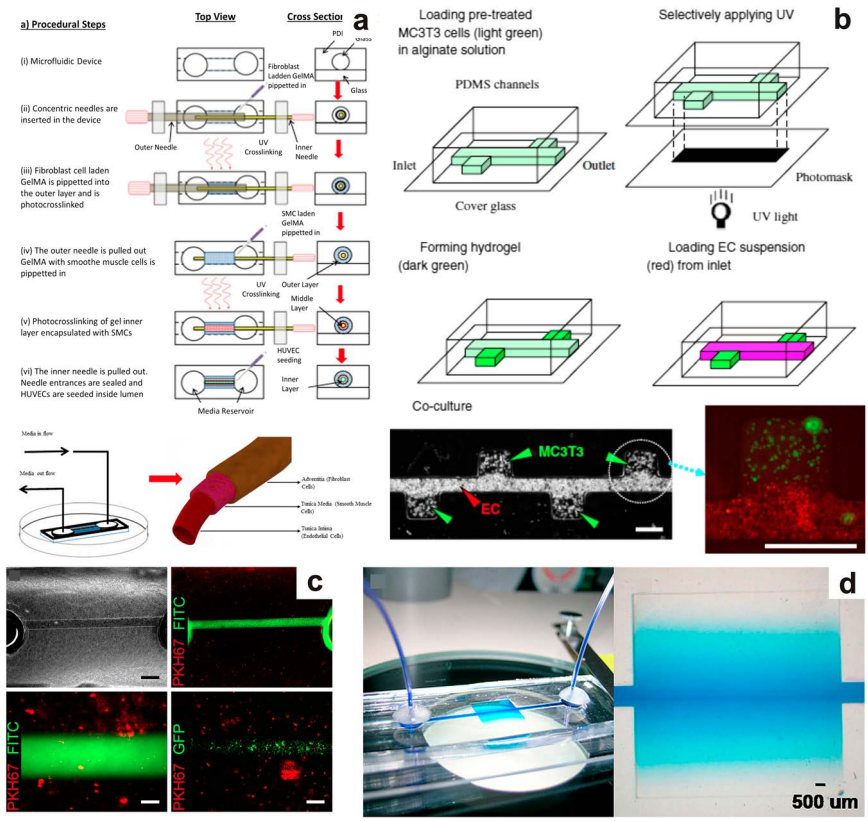

Figure 23.6 Microchannels with varying properties and controlled fluid flow can be produced using photo-responsive hydrogels. (a) A tri-layered vessel was created by UV-polymerizing concentric layers containing different cell types using needles of varying sizes. Reprinted from *Biomedical Microdevices*, A multilayered microfluidic blood vessel-like structure, Vol. 17 Issue 5, 2015, pages 1–13, Anwarul Hasan, Arghya Paul, Adnan Memic, and Ali Khademhosseini. © Springer Science + Business Media New York 2015. With permission of Springer.[23] (b) Channels were patterned by selectively applying UV to alginate, trapping endothelial and osteoblast cells. Reprinted from *Biomedical Microdevices*, Patterning alginate hydrogels using light-directed release of caged calcium in a microfluidic device, Vol. 12 Issue 1, 2009, pages 145–151, Bor-han Chueh, Ying Zheng, Yu-suke Torisawa, Amy Y. Hsiao, Chunxi Ge, Susan Hsiong, Nathaniel Huebsch, Renny Franceschi, David J. Mooney, and Shuichi Takayama. © Springer Science + Business Media, LLC 2009. With permission of Springer.[26] (c) Fibroblasts were seeded and imaged in GelMA microchannels, polymerized with UV light. Reprinted from *Biomaterials*, Vol. 31 Issue 21, Jason W. Nichol, Sandeep T. Koshy, Hojae Bae, Chang M. Hwang, Seda Yamanlar, Ali Khademhosseini, Cell-laden microengineered gelatin methacrylate hydrogels, pages 5536–5544, Copyright 2010, with permission from Elsevier.[24] (d) A multilayered microfluidic device was perfused with toluidine blue to display diffusion properties. Reprinted from *Biomaterials*, Vol. 31 Issue 21, Michael P. Cuchiara, Alicia C. B. Allen, Theodore M. Chen, Jordan S. Miller, Jennifer L. West, Multilayer microfluidic PEGDA hydrogels, pages 5491–5497, Copyright 2010, with permission from Elsevier.[25]

were created by sandwiching a pillar array between a glass substrate coated with photoconductive material and an indium–tin–oxide glass substrate. A 10 V AC voltage was applied between the top and bottom glass substrates to create an electric field, and microbeads were organized using a digital projector and mask. Different microbead organization patterns created using this technique are demonstrated in Figure 23.7(a). Microbeads were created using a micro-vibrator, polymerized in $CaCl_2$. This method allows for the precise control of bulk tissue microstructure through microbead assembly through a bottom-up assembly approach.

As an alternative to emulsion-based particle production, stop-flow lithography can be used to create microparticles within a microchannel. This allows for the formation of particles with unique geometry, as well as varying properties and sizes. Stop-flow lithography is performed by introducing a mask to the area of a channel exposed to a light source. The mask allows the exposure and therefore polymerization of the particle, while leaving the rest of the channel in solution. This is done by seizing flow while the light source is turned on, allowing the crosslinking of particles, and then the flow continues to move on to an unpolymerized portion.[28–35] This method can be used to create magnetic particles for separation from solutions[28,31] as well as particles with varying opacity.[29] Stop-flow lithography is used to create microbeads in Figure 23.7(c), and microparticles with a height gradient in Figure 23.7(d). Magnetic particles fabricated using stop-flow lithography are imaged in Figure 23.7(e), engineered in varying shapes and sizes for specific applications. It was demonstrated that by controlling the oxygen concentration in the device, colloidal disks as small as 0.8 μm could be created, appropriate to flow through endothelial lined microvasculature.[35] This technique, modeled in Figure 23.7(f), could be used to test molecule effect on vasculature with controlled and precisely engineered microparticles. Stop-flow lithography formed microparticles have been engineered to carry oxygen, similar to red blood cells.[34] The microparticles were created with UV-crosslinkable per-fluorocarbon oil-in-water nanoemulsions embedded in PEGDA. The nanoemulsions are capable of facilitating oxygen transport, making them a platform by which to deliver oxygen to engineered tissue *in vitro*. Oxygen-carrying particle size and oil volume fractions are compared in Figure 23.7(g), demonstrating that a larger percentage of oil in the particle results in larger particles. Microparticles produced using stop-flow lithography have also been demonstrated as viable platforms for cell culture.[33] PEGDA-based microparticles were patterned with different substrates to compare cell-adhesive surfaces on a single particle. Breast cancer cells are imaged at different time points to display the effects of a poly-L-lysine coating in Figure 23.7(h).

Beyond cell capture and experimentation, microdroplets have also been used as valves within a microfluidic device. Jadhav *et al.* demonstrated the fabrication and testing of photoresponsive microvalves made of poly(*N*-isopropylacrylamide) and polypyrrole nanoparticles controlled with a near

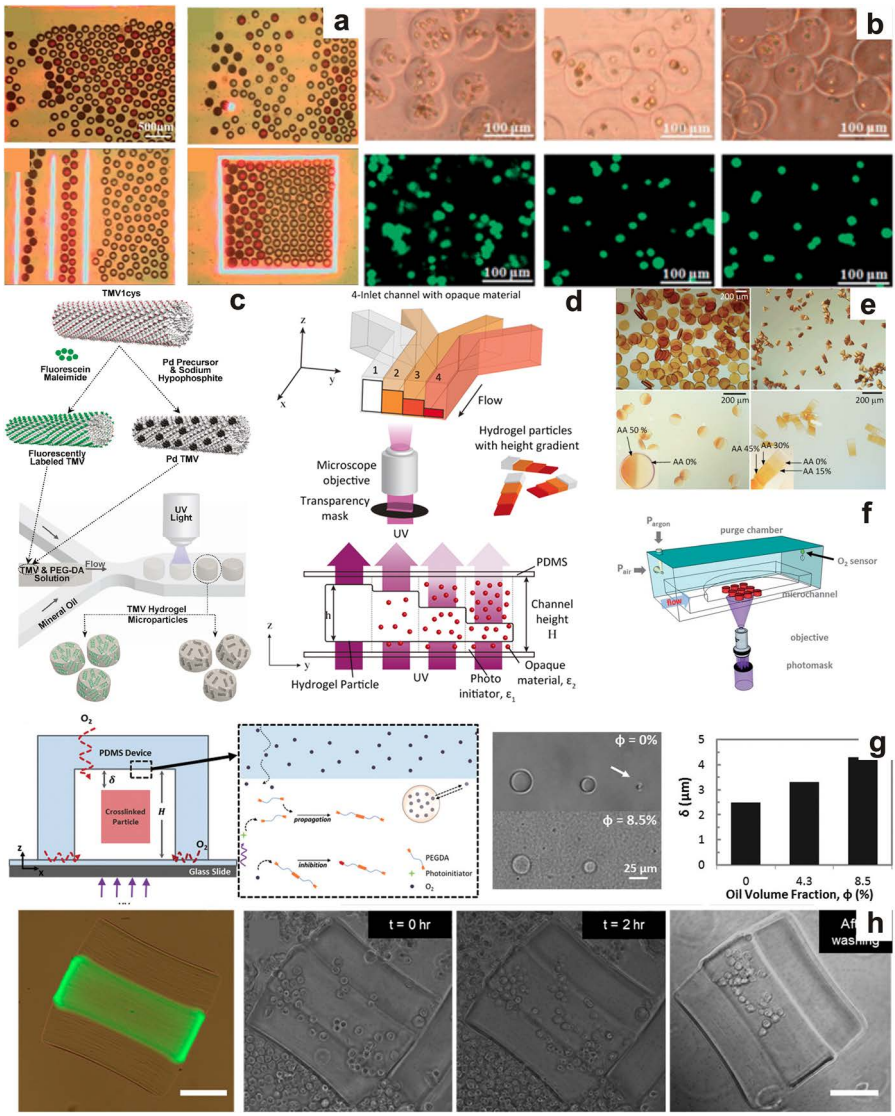

Figure 23.7 Photo-responsive microparticles were fabricated and patterned using stop-flow lithography and selective light exposure. (a), (b) An optically switched dielectrophoretic force was used to manipulate and assemble cell-laden microbeads. Reproduced from ref. 27 with permission from the PCCP Owner Societies. (c) Stop-flow photolithography within a microfluidic device was used to create PEG-DA hydrogels. Reprinted with permission from Lewis, Christina L., *et al.*, "Microfluidic fabrication of hydrogel microparticles containing functionalized viral nanotemplates." *Langmuir* 26.16 (2010): 13436–13441. Copyright 2010 American Chemical Society.[31] (d) Stop-flow lithography was used within a microfluidic device to create opaque hydrogel particles with a height gradient. Reprinted with permission from Suh, Su Kyung, *et al.*, "Using stop-flow lithography to produce opaque microparticles: Synthesis and modeling." *Langmuir* 27.22 (2011): 13 813–13 819. Copyright 2011 American Chemical

infrared (NIR) laser.[36] Trapped microgels in PDMS shrink when exposed to NIR, allowing cell solution to flow through the channel. The shrunken microgels remained trapped in the device, allowing flow to escape above the particle, while the expanded microgels blocked all flow. The device was tested with A549 epithelial cells to observe pulsed drug treatment. A quick response was observed and the device was displayed to maintain pulsatile and laminar flow within a microchannel. The pulsatile flow is especially useful for *in vitro* vessel systems to mimic the types of flow found in the human body. This method could also be used for in-device cell culture, remotely controlling the introduction and removal of media and other solutions.

23.4 Thermo-Responsive Smart Materials in Microfluidics for Tissue Engineering

Thermo-responsive smart materials are valuable tools for tissue engineering due to their ability to change geometry or operation when transferred from physiological temperature to room temperature. This provides a valuable tool for on-chip cell culture and cellular release from activated surfaces. Hydrogel and polymer orientation and surface properties can be greatly modified with a temperature change of just a few degrees Celsius, providing the precise control required for tissue engineering. Additionally, small volume requirements in microfluidics facilitate a rapid temperature change and hydrogel response prevents the extended exposure of cells to undesirable environments. The use of thermo-responsive smart materials is also displayed in microvalves and pumps, which are an avenue to avoid the use of large and invasive exterior equipment while still possessing precise control of fluid flow and transfer within microchannels. These applications will be discussed, as well as current and possible applications in tissue engineering, smart materials, and microfluidics.

Society.[29] (e) Magnetic particles of varying geometries were produced using stop-flow lithography in a microfluidic channel. Reprinted with permission from Suh, Su Kyung, *et al.*, "Synthesis of nonspherical superparamagnetic particles: *in situ* coprecipitation of magnetic nanoparticles in microgels prepared by stop-flow lithography." *Journal of the American Chemical Society* 134.17 (2012): 7337–7343. Copyright 2012 American Chemical Society.[28] (f) Colloidal disks were fabricated in a microfluidic channel using oxygen-controlled flow lithography. Reproduced from ref. 35 with permission from the PCCP Owner Societies. (g) Stop-flow lithography within a microfluidic device was used to create oxygen-carrying microparticles. Reproduced from ref. 34 with permission from the PCCP Owner Societies. (h) Anisotropic particles were photo-polymerized in a microfluidic channel, coated with a poly-L-lysine-coated middle channel, and breast cancer cells grew on top of the particles, imaged at three timepoints. Reprinted with permission from Bong, Ki Wan, *et al.*, "Synthesis of Cell-Adhesive Anisotropic Multifunctional Particles by Stop Flow Lithography and Streptavidin–Biotin Interactions." *Langmuir* 31.48 (2015): 13 165–13 171. Copyright 2015 American Chemical Society.[33]

23.4.1 Microchannels Utilizing Thermally-Responsive Smart Materials

As previously examined, microfluidics are a great platform for creating vessel-like microchannels. The ability to create masks with very small features allows for the repeatable fabrication of micro-sized channels for small volumes of fluid flow. Additionally, small channels and the surrounding matrix can be fabricated out of biomimetic polymers suitable for cell infiltration. The polymers chosen are specifically engineered for the cell types and application, utilizing hybrid, dynamic hydrogels to create the most suitable end-result. Many of these polymers and hydrogels respond to temperature changes to facilitate a cellular response, or form the proper geometry. As an example, Park *et al.* created a cylindrical microchannel with micro-pores formed by leaching sucrose crystals.[37] Micropores are an important feature when imitating the extracellular matrix in engineered tissue structures. They allow for cellular infiltration into the matrix and proper chemical exchange between cells. The protocol for micropore fabrication in agarose is diagramed in Figure 23.8(a). Sucrose, agarose, and cells were mixed and rapidly cooled in a PDMS mold with a needle inserted to create the capillary channel. Micropores were created through dissolving sucrose with rapid cooling, and sucrose concentrations determined micro-pore distributions in the gel. A HepG2 cell line was seeded into the scaffold, displaying high cell viability and diffusion of biomolecules. These features are especially important for cell studies in order to observe signaling molecules secreted from cells, as well as cellular responses to treatments and materials.

It is a common technique to use a needle or mask to create microchannels due to the repeatability and economical benefits.[37,38] An alternative to this method is 3D printing, offering more dynamic geometry and allowing phase changes between different hydrogels. Lee *et al.* utilized 3D printing of a collagen and cell-gelatin matrix to create a vascular channel.[39] Collagen layers were printed around a cell-gelatin, which liquefied with a change in temperature and was rotated every fifteen minutes to allow cellular adhesion on all walls of the vessel. After sufficient cell culture, the liquefied gelatin was perfused out of the channel and replaced with cell media. Different densities of HUVECs were tested, and the outer collagen matrix was also seeded with endothelial cells. Whenever cells are seeded into a device, it is important to operate around 37 °C, a proper cell culture temperature condition. The gelatin used in this vascular network liquefied at 37 °C, allowing for seeding and proliferation of cells at a biologically stable temperature. HUVECs displayed angiogenic properties in the collagen matrix of the microvessel, as well as biomimetic gene expression to display the potential of 3D printed vascular networks in vascular tissue engineering. Cell adhesion and orientation within the bioprinted channels is displayed in Figure 23.8(b).

Along with using the thermo-responsive properties of smart materials for hydrogel polymerization or hydrogel properties, they can also be used as a method of capturing and releasing cells in a microchannel. When performing

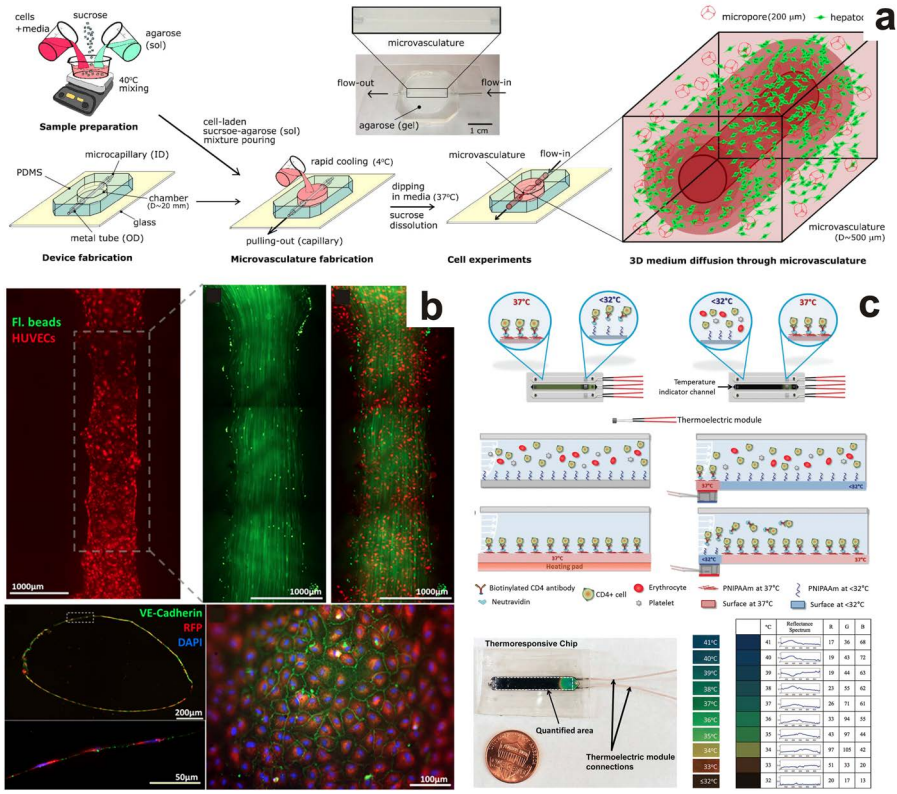

Figure 23.8 Microchannels were fabricated on-chip utilizing thermo-responsive materials. (a) Microporous hydrogel channels were fabricated by dissolving sucrose in a channel polymerized around a capillary, and seeded with hepatic cells. Reproduced with permission. Reprinted from *Biotechnology & Bioengineering*, Vol. 106 Issue 1, Jae Hong Park, Bong Geun Chung, Won Gu Lee, Jinseok Kim, Mark D. Brigham, Jae-sool Shim, Seunghwan Lee, Chang Mo Hwang, Naside Gozde Durmus, Utkan Demirci, and Ali Khademhosseini, Microporous cell-laden hydrogels for engineered tissue constructs, pages 138–148. Copyright 2010 with permission from John Wiley and Sons.[37] © 2010 Wiley Periodicals, Inc. (b) Bioprinted channels were seeded with endothelial cells and imaged over time. Reprinted from *Biomaterials*, Vol. 35 Issue 28, Vivian K. Lee, Diana Y. Kim, Haygan Ngo, Young Lee, Lan Seo, Seung-Schik Yoo, Peter A. Vincent, Guohao Dai, Creating perfused functional vascular channels using 3D bio-printing technology, pages 8092–8102. Copyright 2014, with permission from Elsevier.[39] (c) Cells were captured and released using a smart interface thermo-responsive material within a microchannel. Reprinted from *Advanced Healthcare Materials*, Vol. 1 Issue 5, Umut Atakan Gurkan, Savas Tasoglu, Derya Akkaynak, Oguzhan Avci, Sebnem Unluisler, Serli Canikyan, Noah MacCallum, and Utkan Demirci, Smart Interface Materials Integrated with Microfluidics for On-Demand Local Capture and Release of Cells, pages 661–668, Copyright 2012 with permission from John Wiley and Sons.[41] © 2012 WILEY-VCH Verlag GmbH & Co. KGaA, Weinheim.

on-chip cell culture, it is important to consider the method by which cells will be harvested or passaged after proper growth. Trypsin is commonly used for cell release from cultured surfaces, a detriment to some cell surface proteins. This cell damage can affect experimentation and tissue growth if trypsinization is used as a cell detachment method for many passages. As an alternative, poly(*N*-isopropylacrylamide) (PNIPAAm) is a thermo-responsive smart material that has been coated in microchannels for chemical-free cell release.[40] When the temperature is lowered below 32 °C, PNIPAAm becomes hydrophilic, therefore releasing cells bound to the surface. PNIPAAm was permanently bound to PDMS microchannels, and cultured with fibroblast cells. The cells detached at room temperature, allowing passaging after three days of culture without a dramatic or damaging temperature change. Higher cell viability was observed when compared to tripsinized cells, presenting PNIPAAm surface modification as a platform for on-chip cell-based assays. Similarly, Gurkan *et al.* utilized PNIPAAm in conjunction with CD4 lymphocyte antibodies. This method facilitated the capture and release of lymphocytes from unprocessed human whole blood without cell damage or non-specific antibody binding.[41] Microchannel surfaces etched into polymethyl-methacrylate (PMMA) were coated with PNIPAAm, sealed to form closed channels, and treated with biotinylated anti-CD4 antibody. Whole blood was manually pumped through microchannels at 37 °C. CD4-positive lymphocytes attached to the microchannel surface, while additional blood components flowed to the channel outlet. Additional cells were washed away with PBS, followed by the introduction of red blood cell lysis solution. The final bound CD4-positive cells were locally released by the introduction of cooling modules to the chip surface. Released cells were washed into the outlet channel, collected, and counted to determine viability. The user-controlled local capture and release of specific cell types was demonstrated using PNIPAAm and proven as an appropriate method for cell assays on a micro-chip. Figure 23.8(c) outlines the capture and release mechanics of cells within a microfluidic channel using a thermo-responsive material.

23.4.2 Thermo-Responsive Microdroplet Fabrication in a Microfluidic Device

Thermo-responsive materials also have a practical application for tissue engineering in droplet form. It has been demonstrated that human cells can be captured and selectively delivered through the use of thermo-responsive microcapsules.[42] Agarose and gelatin were combined in microcapsule form. Agarose is a stable solid from 30 °C to 60 °C, while gelatin becomes liquid when heated above 35 °C. This difference in state at similar temperatures allows for the gelatin to melt when at 37 °C, releasing cellular components through pores in the microdroplets. Fibroblasts and HUVECs were proven to remain viable and proliferate in this system, as well as escape when exposed to a biologically relevant temperature. Fibroblast release from agarose–gelatin–fibrin microparticles is displayed in Figure 23.9(a).

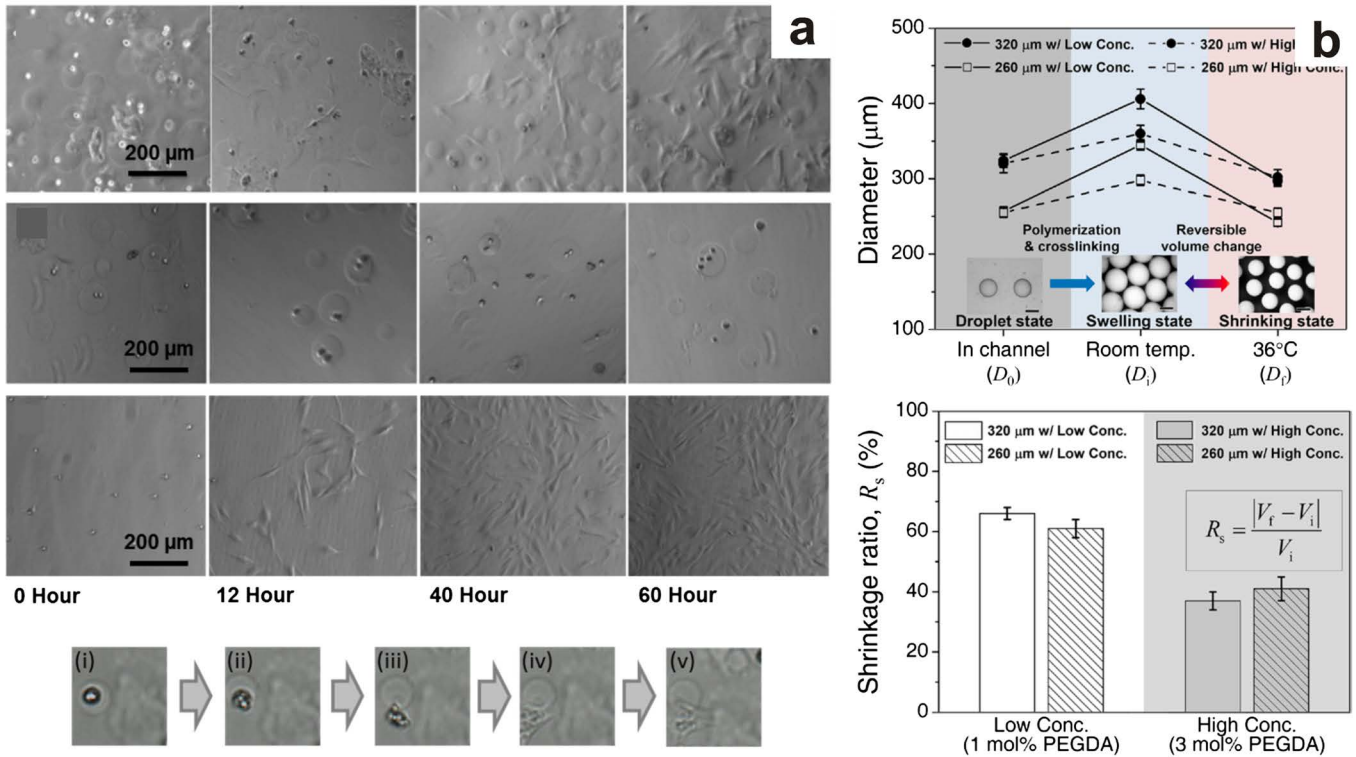

Figure 23.9 Microparticles can be fabricated within a microfluidic device to respond to physiological temperatures. (a) Human fibroblast cells are released from agarose–gelatin–fibrin microparticles when at 37 °C, and compared to agarose-only controls, and non-encapsulated fibroblasts over a 60 hour time period. Reprinted from *Journal of Functional Biomaterials*, Vol. 6 Issue 2, Wing Cheung Mak, Kim Olesen, Petter Sivlér, Chyan-Jang Lee, I. Moreno-Jimenez, Joel Edin, David Courtman, Mårten Skog, and May Griffith, Controlled delivery of human cells by temperature responsive microcapsules, pages 429–453. Copyright 2015, with permission from the Multidisciplinary Digital Publishing Institute. All rights reserved.[42] (b) Microdroplets fabricated in a microfluidic device shrink when at physiological temperature and swell when at room temperature. Reprinted from *Journal of Micromechanics and Microengineering*, Vol. 24 Issue 8, Kyoung Duck Seo and Dong Sung Kim, Microfluidic synthesis of thermo-responsive poly (*N*-isopropylacrylamide)–poly (ethylene glycol) diacrylate microhydrogels as chemo-embolic microspheres, page 085 001, Copyright 2014 IOP Publishing. Reproduced with permission. All rights reserved.[43]

The released fibroblasts are compared to agarose-only controls and non-encapsulated fibroblasts at different time points. Thermo-responsive hydrogels can be used in controlled cell release in *in vivo* models, as well as *in vitro* biomimetic models. Although this method did not utilize microfluidic devices in droplet production, it is a viable technique for uniform production and precise control, as discussed previously. Seo *et al.* displayed this method through creating thermo-responsive hydrogel droplets using microfluidics.[43] A hydro-dynamic focusing microfluidic device was utilized to create thermo-responsive poly(*N*-isopropylacrylamide)–poly(ethylene glycol) (PNIPAAm–PEGDA) hydrogel spheres. UV irradiation was used to polymerize the microspheres, and the crosslinker concentration was changed to determine the ratio of sphere diameter to temperature. The diameter of the spheres decreased when at higher temperatures, displaying an approximate 300 μm diameter at 36 °C compared to a 400 μm diameter at room temperature, as described in Figure 23.9(b). Remaining at biological temperature limits, droplet swelling under a temperature drop suggests a possible application in cellular release for in-chip cell culture and co-culture assays. Additionally, the materials used were tested in an animal model to display biocompatibility as well as the ability to release trapped molecules.

23.4.3 Thermo-Responsive Microvalves and Pumps in Microfluidic Devices

Thermo-responsive materials are ideal for use as microvalves and pumps due to their ability to rapidly and predictably deform and change shape in response to a temperature change. Fluid flow can be directed and pushed through the use of responsive hydrogel strips. Electroactive valves have been displayed as a reliable and effective method to pump liquids through a microfluidic device.[44] Kwon *et al.* uses an electroactive valve as a micropump within a microfluidic device for biomedical applications. The device mechanics are diagramed and described in Figure 23.10(a). The microfluidic device was fabricated from PDMS with a responsive strip made from hydrogel and crosslinking agents 4-hydroxybutyl acrylate (4-HBA), 2,2-dimethoxy-2-phenylacetophenone (DMPA), ethylene glycol dimethacrylate (EGDMA), and acrylic acid (AA). The responsive hydrogel strip was manipulated toward the inlet or outlet due to the presence of electrodes on either side, acting as a pump. The pumping capabilities of this design was accredited to an asymmetrical design and bending motion. Anti-cancer drug effects on human cancer cells were observed in the device with controlled pumping of Adriamycin to a 96-well plate containing MCF-breast cancer cells. Low energy consumption and high durability were also demonstrated through long-term device testing. This proposed device provides a system for delivering solutions to cells cultured on-chip without requiring complex external equipment and additional tubing and connections. As an alternative to drug delivery, the same group demonstrated the use of electroactive valves in cell sorting.[45] A symmetric, forked microfluidic channel was used in partnership with a hydrogel strip, facilitating sorting of mouse

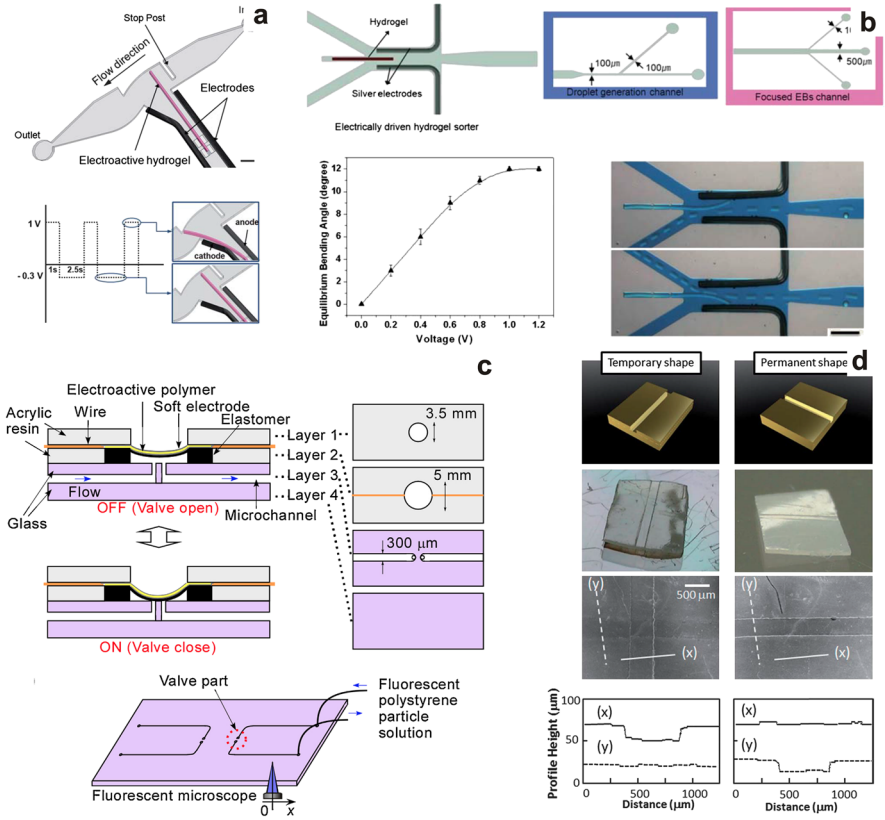

Figure 23.10 Thermo-responsive materials can be used as valves and pumps within microfluidic devices for on-chip cell culture. (a) A thermo-responsive strip is used to pump fluid through a microfluidic device. Reproduced from ref. 44 with permission from the PCCP Owner Societies. (b) A thermo-responsive strip is used to sort mouse embryoid bodies in a microfluidic device. Reproduced from ref. 45 with permission from the PCCP Owner Societies. (c) An electroactive polymer is used as a valve in a microfluidic device. Reprinted from Sensors and Actuators B: Chemical, Vol. 184, Yo Tanaka, Tomohiro Fujikawa, Yutaka Kazoe, and Takehiko Kitamori, An active valve incorporated into a microchip using a high strain electroactive polymer, Pages 163–169, Copyright 2013, with permission from Elsevier.[46] (d) A shape-memory polymer can be used as a pump or valve to direct fluid flow in a microfluidic channel. Reproduced from ref. 47 with permission from the PCCP Owner Societies.

embryoid bodies (mEBs) according to size. A hydrogel-4-HBA strip was incorporated into a straight channel, with a silver electrode on either side of the strip, as diagramed in Figure 23.10(b). The device operated at low driving voltages to prevent bubbles, and in cell media for cell survival. The mEBs flowed linearly in a channel, monitored using video inspection for the manual operation of the hydrogel strip. Depending on size, cells were directed to a “small”

or "large" cell collection chamber by user discretion. A 1 V-applied voltage, causing the strip to bend when the voltage was on, allowed cell flow into the selected channel. The cells were sorted without damage, maintaining pluripotency and differentiating into three germ layers following sorting. Tanaka *et al.* presented another method for cell sorting, using a microchannel etched in glass, an electroactive polymer film, and carbon electrodes.[46] Figure 23.10(c) diagrams a voltage applied to the polymer film, deforming it downwards to create a stop valve on the chip and preventing flow from continuing through the channel. This four-layer device allowed for precise control of fluid flow in a microfluidic channel, with a response time similar to that of a piezoelectric actuator valve. The dynamic, durable nature of electroactive valves allows for customizable and biocompatible platforms by which to manipulate, sort, and provide media for cells in a microfluidic channel.

Rather than including just one thermo-responsive biomaterial component in a microfluidic, entire channels and surrounding structures can be fabricated from smart materials to create a bulk response. Ebara *et al.* demonstrated a shape-memory polymer that deforms under a temperature stimulus, and can return back to its original shape when the temperature is returned back to the original temperature.[47] Shape-memory poly(3-caprolactone) (PCL) is formed against silicone molds to create permanent and temporary channel geometries as a method for flow control. Channel shapes and dimensions are shown in Figure 23.10(d). The shape-memory polymer could return to the original shape with a recovery of almost 100%, making the device reliable and reusable. When the polymer device was placed on a hot plate, fluid would flow from one side to the other due to the gradual closing of the channel along with heat transfer. The device could also be utilized as a microvalve with localized heating, causing the opening or closing of a particular part of the channel. PCL can be engineered to operate at physiological temperatures, making it a possible platform for on-chip cell assays. Additionally, the use of a single polymer simplifies the fabrication process, in comparison to a device with many different components, making shape-material biomaterials a desirable platform for microfluidic control.

23.5 Conclusions

The use of microfluidics for tissue and cell culture is an area of increasing interest in the field of tissue engineering. This is due to precise control capabilities, minimal solution requirements, and rapid fabrication techniques. Through introducing smart materials to tissue engineering in microfluidics, incredibly complex and dynamic materials can be created at a micro-level. Cellular interactions can be magnified to specifically observe processes that are otherwise clouded by confounding factors. Extremely small physiological features can also be mimicked, such as vasculature or lymph systems, to create realistic organ-on-chip systems for drug discovery and biomolecular research. Furthermore, on-chip cell-culture can be achieved through the use of cell-releasing materials and in-chip actuators and pumps. The applications

and techniques utilizing smart materials in microfluidic devices for tissue engineering will continue to flourish as new materials, device geometries, and possible tissue constructs are discovered.

23.5.1 Clinical Potential and Applications

The clinical potential of smart materials-based microfluidic systems is expansive, with applications ranging from replacement organs to drug development. The major benefit of combining smart materials and microfluidics is the increased precision of both material synthesis and microscale control. For example, microfluidic systems provide for manipulation of single cells within a well-defined scaffold, providing a platform for bottom-up tissue engineering. Specifically, cell-laden fibers and organoids can be organized, stacked, and weaved together to create a more complex tissue with possible applications in organ transplantation or organ augmentation. Additionally, different cell types can be placed in close proximity to facilitate controlled cell interactions, similar to those found in human organ systems. This deliberate placement would be highly user intensive or unattainable without the aid of microfluidic systems and smart materials. Traditional fabrication techniques do not provide the same level of heterogeneous material control.

Perhaps one of the most enticing potential applications for the integration of smart materials and microfluidic systems is the creation of vasculature. Stimuli-responsive properties and microscale manipulation are the hallmarks of smart materials and microfluidics, respectively. These properties are direct analogs to the required characteristics of both healthy vasculature and any engineered blood vessel. Scientists have recognized these similarities and are approaching this issue through the methods described previously by reproducing vasculature with smart materials and microfluidics. Engineers currently are constrained by nutrient diffusion limits; however, the capability to generate large vascular networks will enable the expansion of engineered tissue volumes and lead to new clinical uses for engineered tissue, including transplantation.

Another application of microfluidics in tissue engineering that has gained great traction in the scientific community is organ-on-chip devices. These devices are designed to mimic human organ systems, with translational potential in the pharmaceutical industry. Rather than relying on mouse models or homogeneous cell culture, organ-on-chip devices offer a platform for dynamic analysis of drug interactions with microscale organ systems. Multiple cell types can be intricately co-cultured to recapitulate an organ, displaying functionality similar to *in vivo* conditions. When run in parallel, high throughput candidate selection and drug screening may be achieved. Smart materials are especially valuable in this application due to the ability to control cell location, co-culture interactions, and flow spontaneously with an environmental stimulus. The need for external pneumatic controls can even be omitted through the use of environmentally responsive pumps incorporated within a channel, similar to vascular valves.

Ultimately, the combination of stimuli-responsive materials and microfluidic controls provides unique possibilities to mimic *in vivo* anatomy and function, which can lead to new applications in regenerative medicine and pharmacoengineering.

References

1. H. Onoe, T. Okitsu, A. Itou, M. Kato-Negishi, R. Gojo, D. Kiriya, K. Sato, S. Miura, S. Iwanaga, K. Kuribayashi-Shigetomi, Y. T. Matsunaga, Y. Shimoyama and S. Takeuchi, *Nat. Mater.*, 2013, **12**, 584–590.
2. Y. Jun, M. J. Kim, Y. H. Hwang, E. A. Jeon, A. R. Kang, S.-H. Lee and D. Y. Lee, *Biomaterials*, 2013, **34**, 8122–8130.
3. S. Mazzitelli, L. Capretto, D. Carugo, X. Zhang, R. Piva and C. Nastruzzi, *Lab Chip*, 2011, **11**, 1776–1785.
4. M. Marimuthu, S. Kim and J. An, *Soft Matter*, 2010, **6**, 2200–2207.
5. T. Takei, N. Kishihara, S. Sakai and K. Kawakami, *Biochem. Eng. J.*, 2010, **49**, 143–147.
6. N. A. Raof, M. R. Padgen, A. R. Gracias, M. Bergkvist and Y. Xie, *Biomaterials*, 2011, **32**, 4498–4505.
7. Y. Cheng, F. Zheng, J. Lu, L. Shang, Z. Xie, Y. Zhao, Y. Chen and Z. Gu, *Adv. Mater.*, 2014, **26**, 5184–5190.
8. M. Yamada, R. Utoh, K. Ohashi, K. Tatsumi, M. Yamato, T. Okano and M. Seki, *Biomaterials*, 2012, **33**, 8304–8315.
9. K. H. Lee, S. J. Shin, C.-B. Kim, J. K. Kim, Y. W. Cho, B. G. Chung and S.-H. Lee, *Lab Chip*, 2010, **10**, 1328–1334.
10. B. R. Lee, K. H. Lee, E. Kang, D.-S. Kim and S.-H. Lee, *Biomicrofluidics*, 2011, **5**, 022208.
11. M. Yamada, S. Sugaya, Y. Naganuma and M. Seki, *Soft Matter*, 2012, **8**, 3122–3130.
12. S. Ghorbanian, M. A. Qasaimeh, M. Akbari, A. Tamayol and D. Juncker, *Biomed. Microdevices*, 2014, **16**, 387–395.
13. E. Kang, S.-J. Shin, K. H. Lee and S.-H. Lee, *Lab Chip*, 2010, **10**, 1856–1861.
14. E. Kang, G. S. Jeong, Y. Y. Choi, K. H. Lee, A. Khademhosseini and S.-H. Lee, *Nat. Mater.*, 2011, **10**, 877–883.
15. Y. Xu and X. Wang, *Biotechnol. Bioeng.*, 2015, **112**, 1683–1695.
16. A. Abbott, *Nature*, 2003, **424**, 870–872.
17. D. M. Headen, G. Aubry, H. Lu and A. J. García, *Adv. Mater.*, 2014, **26**, 3003–3008.
18. L.-H. Hung, S.-Y. Teh, J. Jester and A. P. Lee, *Lab Chip*, 2010, **10**, 1820–1825.
19. A. C. Mendes, E. T. Baran, P. Lisboa, R. L. Reis and H. S. Azevedo, *Biomacromolecules*, 2012, **13**, 4039–4048.
20. X. Shi, S. Ostrovidov, Y. Zhao, X. Liang, M. Kasuya, K. Kurihara, K. Nakajima, H. Bae, H. Wu and A. Khademhosseini, *Adv. Funct. Mater.*, 2015, **25**, 2250–2259.
21. M. A. Daniele, A. A. Adams, J. Naciri, S. H. North and F. S. Ligler, *Biomaterials*, 2014, **35**, 1845–1856.

22. M. A. Daniele, K. Radom, F. S. Ligler and A. A. Adams, *RSC Adv.*, 2014, **4**, 23440–23446.
23. A. Hasan, A. Paul, A. Memic and A. Khademhosseini, *Biomed. Microdevices*, 2015, **17**, 1–13.
24. J. W. Nichol, S. T. Koshy, H. Bae, C. M. Hwang, S. Yamanlar and A. Khademhosseini, *Biomaterials*, 2010, **31**, 5536–5544.
25. M. P. Cuchiara, A. C. B. Allen, T. M. Chen, J. S. Miller and J. L. West, *Biomaterials*, 2010, **31**, 5491–5497.
26. B.-h. Chueh, Y. Zheng, Y.-s. Torisawa, A. Hsiao, C. Ge, S. Hsiong, N. Huebsch, R. Franceschi, D. Mooney and S. Takayama, *Biomed. Microdevices*, 2010, **12**, 145–151.
27. Y.-H. Lin, Y.-W. Yang, Y.-D. Chen, S.-S. Wang, Y.-H. Chang and M.-H. Wu, *Lab Chip*, 2012, **12**, 1164–1173.
28. S. K. Suh, K. Yuet, D. K. Hwang, K. W. Bong, P. S. Doyle and T. A. Hatton, *J. Am. Chem. Soc.*, 2012, **134**, 7337–7343.
29. S. K. Suh, K. W. Bong, T. A. Hatton and P. S. Doyle, *Langmuir*, 2011, **27**, 13813–13819.
30. R. L. Srinivas, S. D. Johnson and P. S. Doyle, *Anal. Chem.*, 2013, **85**, 12099–12107.
31. C. L. Lewis, Y. Lin, C. X. Yang, A. K. Manocchi, K. P. Yuet, P. S. Doyle and H. Yi, *Langmuir*, 2010, **26**, 13436–13441.
32. H. Lee, S. G. Lee and P. S. Doyle, *Lab Chip*, 2015, **15**, 3047–3055.
33. K. W. Bong, J. J. Kim, H. Cho, E. Lim, P. S. Doyle and D. Irimia, *Langmuir*, 2015, **31**, 13165–13171.
34. H. Z. An, E. R. Safai, H. B. Eral and P. S. Doyle, *Lab Chip*, 2013, **13**, 4765–4774.
35. H. Z. An, H. B. Eral, L. Chen, M. B. Chen and P. S. Doyle, *Soft Matter*, 2014, **10**, 7595–7605.
36. A. D. Jadhav, B. Yan, R.-C. Luo, L. Wei, X. Zhen, C.-H. Chen and P. Shi, *Biomicrofluidics*, 2015, **9**, 034114.
37. J. H. Park, B. G. Chung, W. G. Lee, J. Kim, M. D. Brigham, J. Shim, S. Lee, C. Hwang, N. G. Durmus, U. Demirci and A. Khademhosseini, *Biotechnol. Bioeng.*, 2010, **106**, 138–148.
38. J. Borenstein, M. Tupper, P. Mack, E. Weinberg, A. Khalil, J. Hsiao and G. García-Cardeña, *Biomed. Microdevices*, 2010, **12**, 71–79.
39. V. K. Lee, D. Y. Kim, H. Ngo, Y. Lee, L. Seo, S.-S. Yoo, P. A. Vincent and G. Dai, *Biomaterials*, 2014, **35**, 8092–8102.
40. D. Ma, H. Chen, Z. Li and Q. He, *Biomicrofluidics*, 2010, **4**, 044107.
41. U. A. Gurkan, S. Tasoglu, D. Akkaynak, O. Avci, S. Unluisler, S. Canikyan, N. Maccallum and U. Demirci, *Adv. Healthcare Mater.*, 2012, **1**, 661–668.
42. W. C. Mak, K. Olesen, P. Sivler, C. J. Lee, I. Moreno-Jimenez, J. Edin, D. Courtman, M. Skog and M. Griffith, *J. Funct. Biomater.*, 2015, **6**, 439–453.
43. K. D. Seo and D. S. Kim, *J. Micromech. Microeng.*, 2014, **24**, 085001.
44. G. H. Kwon, G. S. Jeong, J. Y. Park, J. H. Moon and S.-H. Lee, *Lab Chip*, 2011, **11**, 2910–2915.

45. G. H. Kwon, Y. Y. Choi, J. Y. Park, D. H. Woo, K. B. Lee, J. H. Kim and S.-H. Lee, *Lab Chip*, 2010, **10**, 1604–1610.
46. Y. Tanaka, T. Fujikawa, Y. Kazoe and T. Kitamori, *Sens. Actuators, B*, 2013, **184**, 163–169.
47. M. Ebara, K. Uto, N. Idota, J. M. Hoffman and T. Aoyagi, *Soft Matter*, 2013, **9**, 3074–3080.
48. X. Mu, W. Zheng, L. Xiao, W. Zhang and X. Jiang, *Lab Chip*, 2013, **13**, 1612–1618.

Subject Index

AcN-(KLDL) 3-CNH2, 207
active scaffolds
  biomolecular delivery, biomaterials for, 173–8
  biosensing, biomaterials for, 179–82
  limitations, 182–4
acute wounds, 258, 259
α-cyclodextrin (α-CD), 81
adamantane, 71, 81
adipose-derived mesenchymal stem cells (ASCs), 476
adipose-derived regenerative cells (ADRCs), 305–7
ADRCs *see* adipose-derived regenerative cells (ADRCs)
ADSCs *see* encapsulated adipose-derived stem cells (ADSCs)
adult neural stem cells (aNSCs), 394, 399
AFM *see* atomic force microscopy (AFM)
aggrecan, 78
alginate, 51–2, 201, 620
alginate-based wound dressings, 262
alginate poly-L-lysine (PLL), 158
5-aminolevulinic acid (5-ALA), 487
AMP cathelicidin LL-37, 45
anisotropic morphology/topography, 318–19
antimicrobial properties, thermo-responsive materials with, 271–2
Arg-Gly-Asp (RGD) motif, 43
arginine-glycine-aspartic acid (RGD) peptide, 5, 419, 420, 492, 498
arterial TEVGs, 248
arteries, cardiovascular structures, 232
arthritis, 198
articular cartilage (AC), 194–5, 217
aryl oxalate ester-containing polymers, 267
atomic force microscopy (AFM), 301–2
  silicon nanowires (SiNWs), 445–6
azobenzene-polymers, 493

bacterial enzyme-responsive materials for infection control, 277–9
BALB/3T3/*v-src* cells, 427
barium titanate ($BaTiO_3$, BTO) nanoparticles, 635
BDNF *see* brain-derived neurotrophic factor
Binachi method, 332
bioactive-agent-releasing matrices, 209–11
bioactive glasses (BG), 9, 73
bioactive molecules, 117
biocompatibility, 40, 115–16, 171, 197
  of polyaniline, 112–13, 116
  of polypyrrole, 115
biodegradability, 116–17, 171
biodegradable polymers, 42–3, 240–43
biodegradation, 197
bio-electrospraying, 584

bioinert materials, 172
biological applications, shape-memory materials, 625–7
biological-based scaffold, heart valve tissue engineering, 246–7
biologic materials
  extracellular matrix, 52–4
    cell infiltration on, 57–8
    degradation of, 55–7
    modulation of the immune response, 54–5
  future challenges for translation of, 59–60
  polysaccharide-based materials, 51–2
  protein-based materials, 48–50
  structure, 40–41
biomaterials
  for biomolecular delivery, 173–8
  for biosensing, 179–82
biomer, 240
biomimetic nanofibrous matrix, 262
biomolecular delivery, biomaterials for, 173
  nucleic acids, 176–8
  peptides and proteins, 173–5
  small molecules, 176
biomolecules, 262–3
bioresorbable electronics, 459–62, 464
bioresorbable polymers, 172
biosensing, biomaterials for, 179
  extracellular conditions, biomaterial constructs to report, 179–81
  monitor intracellular expression, biomaterial constructs to, 181–2
biostable synthetic polymers, 239–40
bio/synthetic interpenetrating network (BioSIN$_x$), 653
biosynthetic materials, 45–7
biphasic calcium phosphate (BCP), 73, 563
bis(acrylamide), gelation of, 487
blend electrospinning, 578
blood–brain barrier (BBB), 520
  functional delivery systems for, 399–400
blood vessel regeneration, magnetic cell therapy for, 316–17
BMPs *see* bone morphogenetic proteins (BMPs)
BMP-scaffold systems, 174
bone and cartilage
  multifunctional scaffolds, applications of, 2–3
    hybrid polymer/inorganic materials, 11–13
    hybrid synthetic/natural polymers, 13–15
    inorganic materials, 9–11
    natural polymers, 3–6
    synthetic polymers, 6–9
bone marrow-derived mesenchymal stem cells (MSCs), 263
bone marrow mesenchymal stem cells (BMSCs), 73
bone marrow stromal cells (BMSCs), 6, 10–11
bone morphogenetic protein 2 (BMP-2), 4–5, 9, 10–13, 15, 498, 546
  chemical structures, 7
  DNA plasmid, 176
  growth factor, 569
bone morphogenetic protein 4 (BMP-4), 148
bone morphogenetic protein 7 (BMP-7), 6
  growth factor, 569
bone morphogenetic proteins (BMPs), 42, 173–4
  signaling, 336
bone tissue engineering, 124–7
bone tissue engineering, multi-functional biomaterials for, 169–70

active scaffolds, 173–84
clinical applications of, 184–5
passive biomaterials for mechanical support, 170–72
bone tissue regeneration
electrospinning for, 577–82
selective laser sintering for, 574–7
bone, tissue repair and regeneration, 73–5
boronic ester-based polymers, 268
bovine serum albumin (BSA_{488}), 493
brain-derived neurotrophic factor (BDNF), 121
brown adipose derived stem cells (BADSCs), 80

Caco-2 cell line, 334
calcium metaphosphate (CMP), 42
calcium peroxide, 148
camphorsulfonic acid (CPSA), 129
cAMP signaling *see* intracellular cyclic AMP (cAMP) signaling
Ca-P/PHBV nanocomposite, 575–7
electrospinning, 575–7
carbon delivery vehicles, 511
carbon nanofiber (CNF), 132
carbon nanotubes (CNTs), 114, 446–51
Carbopol®, 512
cardiac cells, three-dimensional cultures of, 291
cardiac patch, 291
cardiac tissue engineering, 129–32
cardiomyocytes, magneto-mechanical stimuli effects, 312–14
cardiovascular disease (CVD)
multifunctional scaffolds, applications of, 21
surface coatings to enhance endothelialization, 22–4
tissue engineered, 24–5
tissue repair and regeneration, 80–82
cardiovascular tissue engineering
clinical motivation, 230–31
clinical potentials and applications of, 248–9
decellularized vascular scaffolds, 235–6
heart valve tissue engineering, 245–8
magnetic-responsive materials applications *see* magnetic-responsive materials applications
myocardial tissue engineering, 243–5
natural polymeric biomaterials, 236–9
polymeric scaffold, 239–43
vascular neotissue formation and TEVG remodeling, 231–4
cartilage tissue engineering, 196
bioactive-agent-releasing matrices, 209–11
for cartilage repair, 196–8
creation and development of, 195
dynamic loading, 211–13
matrix metalloproteinase response, 213
natural polymers *see* natural polymers
overview of, 193–6
pH-responsive systems, 204–7
physicochemical and biological properties of, 197
research, 196–7
self-assembling peptides, 207–9
shape-memory systems, 213–16
synthetic polymers *see* synthetic polymers
thermo-responsive matrices, 202–4
cartilage, tissue repair and regeneration, 75–8
catheters, 58

CBC stem cells *see* crypt-based columnar (CBC) stem cells
cell adhesion and detachment, materials for modulating, 411–12
cell-based tissue engineering, 559
cell behaviors, 155
cell culture, modulating
  applications and clinical perspectives
    cell segregation, 432–3
    cell-sheet engineering, 428–30
    3D culture, 430–32
  mechanical actuation, 424–6
  microfluidic, 422–4
  repositioning of cells, 426–8
cell differentiation
  stiffness-induced, 495
  stress stiffening/relaxation-induced, 495–496
  by *in vivo* gelation, 476–7
cell electrospraying, 584
cell encapsulation, smart biomaterials for, 144–5
  direct cell phenotype, 155–9
  foreign body reaction, 152–5
  injectable smart biomaterials, 160–61
  native microenvironment, 145–8
  overcome suffocation, 148–50
  shape memory polymers (SMPs), 162
  vascularization, 150–51
cell graft–host integration, 546–7
cell infiltration, on extracellular matrix, 57–8
cells, 332–4
cell segregation, 432–3
cell-sheet engineering, 428–30, 433
cell therapy, 291, 309, 314
  for blood vessel regeneration, 316–17
  for heart regeneration, 315–16
cell transplantation
  central nervous system *see* central nervous system (CNS)
cellulose, 415–16
cellulose nanocrystals (CNCs), 629
central nervous system (CNS) cell transplantation
  clinical potential and applications of smart materials, 548
  development of biomaterials, 535–42
  history of, 530–31
  localization and migration of cells and injury, 545
  objectives and challenges for modern, 531–5
  optimal cell graft–host integration, 546–7
  protecting cells during, 542–4
  regulating grafted cell differentiation *in vivo,* 545–6
  stimulating transplanted neural cells, 547–8
ceramics, 42, 172
cerium oxide nanoparticle (CONP)-composite hydrogel, 149
channelrhodopsin (ChR2), 459
chemical environment, 345–9
chemically-reactive smart materials
  microfiber fabrication, 643–8
  microsphere fabrication in microfluidic device, 650–52
  microvessel network fabrication and application, 648–9
  see also photo-responsive smart materials; thermo-responsive smart materials
chemotactism, 536
chemotherapeutic agents, 331–2
CH-GP-HEC *see* chitosan-β-glycerophosphate-hydroxyethyl cellulose
chitosan, 52, 199–200, 238, 416
  cell adhesion and detachment from, 418
  pH-responsiveness, 417
chitosan/β-glycerol phosphate (β-GP), tissue repair and regeneration, 73, 80, 104, 388

chitosan-β-glycerophosphate-hydroxyethyl cellulose (CH-GP-HEC), 210
chitosan-poly (acrylic acid) (chi-PAA) hydrogel, 498–9
Chol-PEG-Chol, 622–3
chondroitin-4-sulfate crosslinked with ethylene diglycidyl ether, 454
chronic wounds, 258, 259, 264
clinical translation, extracellular matrix, 58–9
CNF *see* carbon nanofiber
CNT-GelMA scaffolds, 132, 133
CNTs *see* carbon nanotubes
coaxial electrospraying, of nanofibrous cell-laden scaffolds, 584–7
coaxial microfluidic flow, 646
collagen, 49–50, 198, 341
  hydrogel, 609–10
  scaffolds, 236–7
collagen (Type I), 24
colorectal cancer (CRC), 331
commercial anti-adhesion agent, 271
common injectable hydrogels, 161
composite/hybridization, for multifunctional tissue engineering scaffolds, 571–3
composite hydrogel, 148, 160
concanavalin (Con A), 518
conductive materials, for tissue engineering
  advantages of, 132
  biocompatibility, 115–16
  biodegradability, 116–17
  bone tissue engineering, 124–7
  cardiac tissue engineering, 129–32
  conductive polymers, 112–13
  modification of, 117–18
  muscle tissue engineering, 127–9
  nerve regeneration, 394–9
  nerve tissue engineering, 118–24
  novel conductive nanomaterials, 114–15
  overview of, 110–11
  piezoelectric polymeric materials, 113–14
  self-assembled conductive hydrogels, 115
conductive polymers, 45
  applications, 631–2
    piezoelectric, 633–5
  chemical structures of, 630
  polyaniline, 112–13
  polypyrrole, 112
  polythiophene derivatives, 113
  3D printing of, 632–3
    of piezoelectric materials, 635
conductive scaffolds, 117
co-polymers, 172
co-precipitated chondroitin-6-sulfate (C-6-S), 538
core–shell structure, PDLLA nanofiber, 579–80
CorMatrix ®, 235
CPAs *see* cryoprotectant agents
CRC *see* colorectal cancer (CRC)
CRDTEGE-ARG SVIDRC peptide, 70
cryoprotectant agents (CPAs), 194–5
crypt-based columnar (CBC) stem cells, 334, 338
crypts of Lieberkühn, 330
crypt-villus junction, 335
curcumin-PPS microspheres, 265
β-cyclodextrin (β-CD), 71–2, 81
cyclosporin A, 536
cytokines, 262
cytoplasmic nanoparticles, 299

decellularized vascular scaffolds, 235–6
degradable hydrogels, 619–22
degradable synthetic scaffolds, heart valve tissue engineering, 247–8
degradation, ROS-responsive materials *via*, 265–8

dendrimers, 511
deprotonation, 204
DEX *see* dexamethasone (DEX)
dexamethasone (DEX), 13, 15, 276
diblock copolypeptide hydrogels (DCH), 541
dielectrophoresis (DEP), 603
Diels–Alder reaction, 420
2-(diethylaminoethyl) methyl methacrylate (DEAEMA), 390
3-(4,5-dimethoxy-2-nitrophenyl)-2-butyl (DMNPB), 492
2-(dimethylamino) ethyl methacrylate (DMAEMA), 390
2,5-dioxopyrrolidin-1-yl 4-(4-(1-((4-(4-formylbenzamido) butanoyl)oxy) ethyl)-2-methoxy-5-nitrophenoxy)butanoate (NHS-*o*NB-CHO), 493
direct cell phenotype, 155–9
directionally-oriented collagen-based scaffold, 318
dodecylbenzenesulfonate-doped polypyrrole (PPy-DBS) film, 485
doped nHAp, 181
dorsal root ganglion (DRG), 120
Doxil®, 510
DRG *see* dorsal root ganglion
drug delivery systems, 262
drug-eluting stents (DES), 21, 28

ECM *see* extracellular matrix
EGF *see* epidermal growth factor (EGF)
EHS tumor *see* Engelbreth–Holm–Swarm (EHS) tumor
elastin, 50, 237–8
elastin-like synthetic peptides (ELPs), 425–6
electrical stimulation, 111
  of neurons, 547
electrical-stimuli-responsive biomaterials, nerve regeneration, 394–9
electric field-responsive drug delivery systems, 523–5
electro-active microfluidic system, 600–604
electroactive polymers (EAPs), 523–4
electroactive shape memory polymers, 17
electroactive valves, 664
electrochemical materials, 484–5
  regulating fate of stem cells, 485
electro-magnetic fields, effects on cells, 317–18
electronic drug delivery devices, 524
electrophysiological activity, 461
electro-responsiveness, 417–22
electrospinning, 567–8, 588
  for bone tissue regeneration, 577–82
  Ca-P/PHBV nanocomposite, 575–7
  of nanofibrous cell-laden scaffolds, 582–7
electrospun fibers, 146
electrospun multicomponent scaffolds, for bone tissue regeneration, 577–82
electrospun scaffold, 240
embedded CONPs, 148
embryonic stem cells, 24, 560
encapsulated adipose-derived stem cells (ADSCs), 160–61
encapsulating donor cells, 160
encapsulating growth factors, 150
endocytosis, of magnetic nanoparticles, 296–7
endothelial cells
  dysfunction, 299
  magnetic targeting of, 316–17
  morphological re-arrangement of, 309
endothelial cell-sheet, 430
endothelial cells (ECs) *versus* SMCs, 21–2
endothelialization, surface coatings to enhance, 22–4
endothelial nitric oxide synthase (eNOS), 299

endothelial progenitor cells (EPCs), 315
Engelbreth–Holm–Swarm (EHS) tumor, 343
engineered gel, 150–51
eNOS *see* endothelial nitric oxide synthase (eNOS)
enteroendocrine cells, 331
environment-responsive hydrogels, 618–19
  for clinical applications, 636
  in 3D printing, 619–22
enzymatically degradable microfluidic system, 608–10
enzyme-responsive biomaterials, nerve regeneration, 393–4
enzyme-responsive injectable hydrogels, 70–71
enzyme-responsive materials in wound healing, 273–9
enzyme-sensitive fibrinogen, 499
EPCs *see* endothelial progenitor cells (EPCs)
EphB/EphrinB interaction, 338
epicardial patches, 245
epidermal growth factor (EGF), 261, 337, 345
epithelial cell proliferation, 348
ethylenediaminetetraacetic acid (EDTA), cell adhesion, 412, 413
externally drug delivery systems (DDSs), applications
  electric field-responsive, 523–5
  light-responsive, 521–3
  magnetic-field-responsive, 520–21
extracellular conditions, biomaterial constructs to report, 179–81
extracellular matrix (ECM), 52–8, 117, 118, 145–6, 148, 195, 232, 233, 235, 329, 337, 451
  bone, 2
  cell adhesion, 411–12
  cell infiltration on, 57–8
  clinical translation of, 58–9
  decellularization, 52–3
  de-cellularized, 563
  degradation of, 55–7
  functionalization of synthetic polymer materials with, 55
  modulation of the immune response, 54–5
  role in tissue regeneration process, 562
  self-assembly, 54
  solubilization, 53–4
  structure of, 53
ex vivo culture, 343

fate of stem cells, regulating
  electrochemical materials, 484–5
  photo-activatable materials, 487–91
  photo-cleavable materials, 492–3
  photo-responsive materials, 486–7
  pH-sensitive materials, 498–9
  piezoelectric materials, 484–6
  thermosensitive materials, 475–6
  thixotropic materials *see* thixotropic materials
feasible sterilization methods, 171
Fenton's reaction, ROS-responsive materials *via* mediation of, 268–9
FGF-1 *see* fibroblast growth factor 1 (FGF-1)
Fgf10, 346
fibrin, 201, 238
fibrin-based scaffold, 238
fibrin polymer spray, 263
fibroblast growth factor 1 (FGF-1), 148
fibrocartilage, 217
fibronectin, 50, 200–201, 420
fibrotic scarring, 309
field-effect transistor (FET), monitoring electrophysiological activity, 455–7
“first generation” scaffolds, 171

flexible micro- and nanoelectronics
for biological activity, 454
bioresorbable electronics, 459–62
field-effect transistor (FET), 455–7
clinical applications of, 465–6
stimulation of excitable tissues, 462–5
flow activated cell sorting (FACS), 432
fluid flow control, 423
fluorescein diacetate (FDA), 99
focused ion-beam (FIB) lithography, silicon nanowires (SiNWs), 445
foreign body reaction, 152–5
Förster resonance energy transfer (FRET), 267
four-dimensional (4D) printing, 629
FRET *see* Förster resonance energy transfer (FRET)
functional cardiac tissue generation, 309–14
functionalization of scaffolds, 173
functional TEVG, 248

β-galactosidase-responsive hydrogel, 274
β-glucuronidase (β-GUS), 277
gas foaming technique, 564
Gαs protein, 303
gastrin, 349
gastrointestinal (GI) tract, 330
gelatin, 237, 619–20
gelatin methacrylate (GelMA), 620
hydrogels, 115
gel–sol transitions
PEO-PLLA copolymer, 69
PEO-PLLA-PEO, 68–9
gel-to-sol transition, 70–71
gemcitabine, 521
gene therapy in biomaterials, 280–81
GFs *see* growth factors (GFs)
GI tract *see* gastrointestinal (GI) tract
glucan-like peptide-2 (GLP-2), 345
glucose-oxidase-based glucose systems, 517
glucose-responsive drug delivery systems, 517–19
glucose-responsive insulin delivery systems, 517, 519
glycosaminoglycans (GAG), 45
glycosyl-nucleosylfluorinated compounds, 75
gold–cadmium alloys, 625
gold nanoparticle (AuNP), 399
theranostics, 588
gold nanowire (Alg–NW) nanocomposite, 462–3
GORE® PROPATEN® Vascular Graft, 239
graphene, 114–15, 397, 399
grooved methacrylamide-modified gelatin (GelMA) microfibers, 604–6
growth factors (GFs), 319–20
growth hormone (GH) binds cellular GH receptors, 345
GtneHPA hydrogels, 395, 399

Hanks' buffered saline solution (HBSS), 348
hASCs, 484, 485, 498
HBSS *see* Hanks' buffered saline solution (HBSS)
heart attacks, 290–91
heart regeneration
biomaterial construction principles for, 243–4
magnetic cell therapy for, 315–16
heart valves, 232
heart valve tissue engineering, 245–6
biological-based scaffold, 246–7
degradable synthetic scaffolds, 247–8
hemostasis, 259, 260
heparin, auto-regulation, 71
hepatocyte cells (HepG2), 430–31
hepatocyte growth factor (HGF), 345

hepatocytes, 647
herpes simplex virus type 1 peptide (gH625), 399
hESCs-derived cardiac progenitor cells, 499–500
HGF *see* hepatocyte growth factor (HGF)
high-affinity immunoglobulin E (IgE) receptors, 303–4
high porosity, 171
HM *see* hollow microsphere (HM)
hNSCs *see* human neural stem cells
hollow microsphere (HM), 269
homopolymer, 172
horseradish peroxidases (HRP), 394
hTESI *see* human TESI (hTESI)
human bone marrow stromal cells (hBMSC), 11
human ISCs culture, 349, 352
human mesenchymal stem cells (hMSCs), 20, 127, 394, 484, 493–4
  EMF-triggered neuronal differentiation, 398
human neural progenitors (hNPCs), 485, 486
human neural stem cells (hNSCs), 124
  neural differentiation of, 125
human postnatal organoids, 342
human TESI (hTESI), 342–3
human umbilical vein endothelial cells (HUVECs), 432
hyaluronan, 198
hyaluronic acid (HA), 22, 51, 198–9
  ester groups, 334
hyaluronic acid-*g*-chitosan-*g*-poly(*N*-isopropylacrylamide) (HA-CPN), 73
hybrid polymer/inorganic materials, 11–13
hybrid synthetic/natural polymers, 13–15
hydrogel injection, for cardiovascular tissue engineering, 244
hydrogels, 146, 510–11, 616–18
  environment-responsive hydrogels, 618–19
    in 3D printing, 619–22
  self-healing *see* self-healing hydrogels
hydrophilic, 203, 208
hydrophobicity, 203, 208
hydroxyapatite (HA), 6, 9–12, 42, 563
hydroxyapatite (HA)/β-tricalcium phosphate (TCP), 11
hydroxypropyl cellulose, 416
hypoxia tolerance, 148

IAP activity *see* intestinal alkaline phosphatase (IAP) activity
IGFs *see* insulin-like growth factor (IGFs)
IKVAV, 158
Ilizarov limb-lengthening, 185
immunogenicity, smart materials, 433
implantable devices
  for monitoring neuronal activity, 460
  for *in vivo* recordings, 458–9
induced pluripotent stem cells (iPSCs), 305–7, 314
inflammation, 259–61
inflammation reduction, thermo-responsive materials for, 271
injectable biohybrid matrix, 161
injectable biomaterials, myocardial tissue engineering, 244–5
injectable hydrogels, 160
injectable smart biomaterials, 160–61
injectable smart materials, for tissue repair and regeneration
  bone, 73–5
  cardiovascular disease, 80–82
  cartilage, 75–8
  skeletal muscle and tendon, 82
  skin, 78–80
injectable supramolecular hydrogels, 71–2, 79

injectable thermosensitive hydrogel, 78, 80, 82
inorganic materials, 9–11
inorganic semiconductors, 442–6
insulin-like growth factor (IGFs), 345
intestinal alkaline phosphatase (IAP) activity, 343
intestinal microbiota homeostasis, 331
intestinal stem cells (ISCs), 332, 334
  intestinal tissue engineering (TE) with, 329–32, 334–40
intestinal stem cell tissue engineering (ISC TE), 343–4, 353
  chemical factors in, 350–51
intestinal subepithelial myofibroblasts (ISEMF), 342
intestinal tissue engineering (TE) with intestinal stem cells, 329–32, 334–40
  cells, 332–4
  environmental factors, 340–49
intracellular cyclic AMP (cAMP) signaling, 303
intramolecular hydrogen bonds, 270
in vitro culture, 343
in vivo gelation, cell differentiation by, 476–7
in vivo ligament healing, 111
ion-triggered shape memory hydrogel, 162
iPSCs *see* induced pluripotent stem cells (iPSCs)
ISCs *see* intestinal stem cells (ISCs)
ISC TE *see* intestinal stem cell tissue engineering (ISC TE)
ISEMF *see* intestinal subepithelial myofibroblasts (ISEMF)
isoleucine–lysine–valine–alanine–valine (IKVAV), 392

keratinocytes, 261

localization of cells, 545
LCST *see* lower critical solution temperature
leaching/solvent casting process, 563–4
left ventricular ejection fraction (LVEF), 476
left ventricular shortening fraction (LVSF), 476
leucine rich-extracellular domain (LGR5), 335
  expression, 343
LGR5 *see* leucine rich-extracellular domain (LGR5)
light-responsive drug delivery systems, 521–3
light-responsive microfluidic system, 604–6
light-sensitive liposomes, 523
light-sensitive polymers, 522
lipopolysaccharide-stimulated macrophages, 267
liposome gels, 622
liposomes, 509–10
living cells, 170
localized gene delivery, 151
long-term cell encapsulation, 150
lower critical solution temperature (LCST), 202–3
  PNIPAAm, 412–13
  poly(ethylene glycol) (PEG), 414–15
lower critical solution temperature (LCST) thermosensitive hydrogels, 476

macrophages, 260
  for tissue remodeling, 54–5
Madin–Darby canine kidney (MDCK) cells, 648
MagBICE *see* magnetic bifunctional cell engager (MagBICE)
magnesium (Mg) alloys, 41
magnetic alginate microfibers (MAMs), 607–8
magnetically-enhanced cell engraftment, 315
magnetically-responsive polymer scaffold, 300–302

magnetic bifunctional cell engager (MagBICE), 316
magnetic cell therapy, 314
  for blood vessel regeneration, 316–17
  for heart regeneration, 315–16
magnetic electrospinning of nanofibers, 607
magnetic-field-responsive drug delivery systems, 520–21
magnetic force-based tissue engineering (Mag-TE), 296, 307, 310
magnetic force bioreactors, 292–5
magnetic nanoparticles (MNPs), 291–300
magnetic NPs (MNPs), 520–21
magnetic-responsive materials
  applications, 290–92, 320–21
    anisotropic morphology/ topography, 318–19
    cell therapy, 314–17
    electro-magnetic fields effects on cells, 317–18
    functional cardiac tissue generation, 309–14
    mechanical cues application *via* magnetic force, 292–305
    remote controlled release scaffold, 319–20
    vascularization, 305–10
magnetite-cationic liposomes (MCLs), 296
magnetite nanoparticles
  dynamic aggregation of, 426–7
  in repositioning of cells, 426–8
magneto-mechanical cues
  applied *via* magnetic particles, 292–300
  applied *via* magnetic scaffolds, 300–302
  cellular response to mechanical stress, 302–5
magneto-responsive microfluidic system, 607–8
Mag-TE *see* magnetic force-based tissue engineering (Mag-TE)
marrow mesenchymal stem cells (BMSCs), 13
Matrigel, 343, 346, 348
matrix metalloproteinase-responsive materials in wound healing, 273–4
matrix metalloproteinases (MMPs), 261, 274
matrix metalloproteinase-sensitive peptides, 213
matrix metalloproteinase (MMP)-sensitive peptides, 70–71
maturation, 261
MCLs *see* magnetite-cationic liposomes (MCLs)
mechanical actuation, microfluidics, 424–6
mechanical environment, 340–44
mechanical heart valves, 245
mechanical strain, 313
mechanical support, passive biomaterials for, 170–72
16-mercapto hexadecanoic acid (MHA), 418
mesenchymal stem cells (MSCs), 11, 151, 185, 334
mesoporous bioactive glasses (MBG), 11
mesoporous silica nanoparticles, 268
messenger RNA (mRNA), 281
metal delivery vehicles, 511
metalloproteinase (MMP)-responsive peptide, 81
methacrylamide chitosan, 392–3
methacrylamide-modified gelatin (GelMA), 653
methoxypoly(ethylene glycol)-*graft*-chitosan, 263
methylcellulose, 415–16
methylcellulose (MC), 388
MI *see* myocardial infarction (MI)
microdroplet fabrication, in microfluidic devices, 662–4
microfiber
  fabrication, 643–8
    and applications, 652–3

microfluidic cell culture, 422–4
microfluidic system
  electro-active, 600–604
  enzymatically degradable, 608–10
  light-responsive, 604–6
  magneto-responsive, 607–8
  pH-sensitive, 599–600
  thermo-responsive, 597–9
micro/nanoparticle systems with pH-responsive properties, 272
microparticle, fabrication in a microfluidic device, 655–9
micropores, 660–61
microRNA (miRNA) for wound healing applications, 281
microscale photodiode array, 464
microsphere, fabrication in a microfluidic device, 650–52
microthread electrodes (MTEs), 458
microvalves, in microfluidic devices, 664–6
microvessel network, fabrication and application, 648–9, 653–5
migration of cells, 545
mixing-induced two-component hydrogels (MITCH), 543
MMP-degradable PEG hydrogel (M-PEG), 272
MNPs *see* magnetic nanoparticles (MNPs)
monitor intracellular expression, biomaterial constructs to, 181–2
monodomain gel, 147
mouse TESI (mTESI), 342–3
M-PEG *see* MMP-degradable PEG hydrogel (M-PEG)
mRNA *see* messenger RNA (mRNA)
MSCs *see* mesenchymal stem cells (MSCs)
mTESI *see* mouse TESI (mTESI)
mucin (mucus glycoprotein) secretion, 331
multi-functional biomaterials for bone tissue engineering, 169–70
  active scaffolds, 173–84
  clinical applications of, 184–5
  passive biomaterials for mechanical support, 170–72
multifunctional polyoxalate-based micelles, 267
multifunctional scaffolds, applications of
  bone and cartilage, 2–3
    clinical potential and applications, 27–8
    hybrid polymer/inorganic materials, 11–13
    hybrid synthetic/natural polymers, 13–15
    inorganic materials, 9–11
    natural polymers, 3–6
    synthetic polymers, 6–9
  cardiovascular diseases, 21
    surface coatings to enhance endotheliali-zation, 22–4
    tissue engineered, 24–5
  clinical potential and, 26–8
  muscle, 15–17
  neural tissue engineering, 25–6
  skin tissue engineering, 17–20
multifunctional tissue engineering scaffolds
  composite/hybridization approaches, 571–2
  electrospinning, for bone tissue regeneration, 577–82
  requirements in tissue regeneration, 569–71
  selective laser sintering, for bone tissue regeneration, 574–7
  theranostic-embedded, for cancer patients, 587–9
multiple-responsive drug delivery systems, 519–20
multi-source multi-power (MSMP) electrospinning, 580–82
multi-walled carbon nanotubes (MWCNTs), 127, 172, 446, 450
murine islet transplant model, 151

muscle, 15–17
muscle–tendon junction (MTJ), 17
muscle tissue engineering, 127–9
musculoskeletal repair, 58
musculoskeletal tissue engineering, 185
myocardial infarction (MI), 291
myocardial tissue engineering, 243–5

nanocomposite hydrogel, 75
nanofibrous cell-laden, for regeneration of complex body tissues, 582–7
nanogels, 519
nanohydroxyapatite (nHAp), 73, 477
nanomaterial building blocks
  and their interfaces with cells and tissues, 441–2
    carbon-based materials, 446–51
    inorganic semiconductors, 442–6
    plymers, 451–4
nanoparticles (NPs), 507–8
  safety in cells, 297–300
nano-scale materials, 172
nanostructured polymers, 451–4
  synthesis and bio-interface, 453
Nap-FFGEY peptide, 72
native microenvironment, 145–8
native tissue regeneration process, complexity in, 568–9
native valvular interstitial cells (VICs), 159
natural *in vivo* cellular microenvironment, 155
natural polymeric biomaterials, 236–9
natural polymers, 3–6
  alginate, 201
  chitosan, 199–200
  collagen, 198
  fibronectin, 200–201
  hyaluronic acid, 198–9
natural polysaccharides, 262
nerve growth factor (NGF), 120–21
nerve tissue engineering, 118–24
neural stem cells (NSCs)
  differentiation, 399
  growth, 397
neural stem progenitor cells (NSPCs), 531–4
neural tissue engineering, 25–6
Neuromaix, 400
neurotransmitter stimulation, of neurons, 547
“neutral competition model”, 339
neutrophils, 260
NGF *see* nerve growth factor
NICD *see* Notch intracellular domain (NICD)
NIPAA m/AAc/NA S/HEMA-PTMC hydrogel, 477
N-isopropylacrylamide, 70
nitric oxide (NO), production of, 299, 300
Noggin (Nog), 336–7
non-degradable hydrogels, 622
non-degradable polymeric scaffolds, 239
non-obese diabetic/severe combined immunodeficiency (NOD/SCID) gamma chain-deficient mice, 342
Notch intracellular domain (NICD), 335
Notch signaling, 335, 338
novel biomaterials, 145
novel conductive nanomaterials, 114–15
nucleic acids, 176–8

obstructive coronary artery disease, 316
O-carboxymethyl chitosan (*O*-CMC), 160
O-CMC *see O*-carboxymethyl chitosan (*O*-CMC)
oligo(poly(ethylene glycol) fumarate) (OPF), 210

oligo(ethylene glycol) methacrylate (OEGMA), 414
o-nitrobenzyl (*o*NB) moieties, 493
OPF *see* oligo(poly(ethylene glycol) fumarate)
optically switched dielectrophoretic force (ODEP), 655, 657
optimal cell graft–host integration, 546–7
organoids, 346, 352
osteoarthritis (OA), 194
osteoconductive scaffolds, 171
osteoinductive scaffolds, 171
oxidative stress, 148
oxygen, 149
  sufficient generation of, 148

P(DMAEMA) *see* poly((2-dimethyl amino)ethyl methacrylate)
P(NIPAAm-*co*-VI) *see* poly(*N*-isopropylacrylamide-*co*-vinylimidazole)
paclitaxel, 28
Paneth cells, 335, 338–9
  adjacent, 337
PANI *see* polyaniline
passive biomaterials for mechanical support, 170–72
patch-forming scaffolds, 245
PCBMA-based zwitterionic hydrogel, 154
PCL *see* poly(ε-caprolactone) (PCL)
PCL/PA Ni/pSi composite, 102–3
PDGF *see* platelet-derived growth factor (PDGF)
PDMAEMA content *see* poly(dimethylaminoethyl methacrylate) (PDMAEMA) content
PEDOT *see* poly(3,4-ethylenedioxythiophene)
PEG-*g*-PLGA *see* poly(DL-lactic acid-*co*-glycolic acid)-poly (ethylene glycol)
PEGMAL microspheres, 650
PEG–PCL–PEG copolymer, 74
PEGylation, 510
PEO–PLLA copolymer, gel–sol transitions, 69
PEO–PLLA–PEO copolymer, gel–sol transitions, 68–9
PEO–PPO –PEO triblock copolymer, 73
peptide amphiphiles (PAs), 208
peptide-based supramolecular hydrogels, 78
peptides, 173–5, 204
Perimaix, 400
PGA *see* poly(glycolic acid) (PGA)
PGA fiber scaffolds *see* polyglycolic acid (PGA) fiber scaffolds
PGS *see* poly(glycerol-sebacate) (PGS)
PHA *see* polyhydroxyalkanoates (PHA)
PHEMA *see* poly(2-hydroxyethyl methacrylate)
pHEMA microperiodic scaffolds, 622
phenylboronic acid (PBA), 518
  glucose-responsive nanogels, 519
photo-activatable materials, 487–91
  and their regulation for fate of stem cells, 492
photo-cleavable materials, 492–3
photodiode array, 464
photopolymerization, 392
photo-responsive applications, shape-memory materials, 628
photo-responsive biomaterials, nerve regeneration, 392–3
photo-responsive miR-148b, 184
photo-responsive smart materials, 486–7
  microfiber fabrication and applications, 652–3
  microparticle fabrication in a microfluidic device, 655–9
  microvessel network fabrication and application, 653–5
  and their regulation for fate of stem cells, 492
PHPMA *see* poly(2-hydroxypropyl methacrylate) (PHPMA)
pH-reporting scaffold, 181

pH-responsive biomaterials, nerve regeneration, 390–91
pH-responsive drug delivery systems, 512–15
pH-responsive hydrogels, 182, 618–19
pH-responsive injectable hydrogels, 69–70
pH-responsive materials for wound healing, 272–3
pH-responsiveness, 417
pH-responsive systems, 204–7
pH-responsive valves, 423–4
pH-sensitive materials, 498–9
pH-sensitive microfluidic system, 599–600
pH-sensitive polymers, 618–19, 628–9
piezoelectricity, 633
piezoelectric materials, 484–6
piezoelectric polymers, 113–14
  chemical structures, 634
plasmid transfection, 176
plasmin-degradable PEG hydrogel (P-PEG) mimicking ECM, 272
platelet-derived growth factor (PDGF), 6, 261, 277, 345
platelet-derived growth factor receptor (PDGFα), 293
platelet-released chemokines, 260
platelet-responsive materials in wound healing, 279–80
PLGA *see* poly(lactic-*co*-glycolic acid) (PLGA)
PLGA/PCL/HA nanocomposite, 13
PLGA-PEG-PLGA, 210
PLGA-PLL nanoparticles *see* poly-(lactic-*co*-glycolic) acidpoly-L-lysine (PLGA-PLL) nanoparticles
PLGA/TCP scaffolds, 12
PLGA/VEGF microspheres, 348
PLL *see* alginate poly-L-lysine (PLL)
PLLA/PEDOT scaffolds, 632
Pluronic F127, 620
PNIPAAm *see* poly(*N*-isopropylacryl-amide) (PNIPAAm)
PNIPAAm–AA hydrogel, 499
PNIPA M-*co*-ALA *see* poly(*N*-isopropy-lacrylamide)-*co*-allylamine (PNIPA M-*co*-ALA) nanogels
POEGMA-CNC nanocomposite hydrogels, 161
poly((2-dimethyl amino)ethyl methacrylate) (P(DMAEMA)), 204
poly(2-hydroxyethyl methacrylate) (PHEMA), 115, 539
poly(2-hydroxypropyl methacrylate) (pHPMA), 270
poly(3,4-ethylenedioxythiophene) (PEDOT), 113, 116
poly(3-hydroxybutyrate) (PHB), 626
poly(acrylic acid) (PAA), 512–13, 599
poly(β-amino ester) (PBAE), 9
poly(D,L-lactic acid) (PDLLA), 121
  nanofiber
    core–shell structure, 579–80
    fabrication, 581
poly(D,L-lactide-*co*-ε-caprolactone) (PDLCL), 120
poly(diethylaminoethyl methacrylate) (PDEAEM), 390
poly(ε-caprolactone) (PCL), 117, 242–3, 562, 626
poly(ether-urethane urea), 240
poly(ethylene glycol) (PEG), 392, 414–15
  lower critical solution temperature of, 414–15
poly(glycerol-sebacate) (PGS), 129, 243
poly(glycolic acid) (PGA), 241–2
poly(L-lactic acid) (PLLA), 121, 242
  nerve regeneration, 388
poly(lactic-*co*-glycolic acid) (PLGA)
  microsphere, 268
  nanoparticles, 262
poly(lactide-*co*-ethylene oxide-*co*-fumarate) (PLEOF), 75
poly(L-lactic acid) (PLLA), 215
poly(MEO_2MA-*co*-OEGMA) (PMO), 414–15
poly(*N,N′*-diethyl-aminoethyl meth-acrylate) (PDEAEM), 512, 514

poly(*N*-isopropylacrylamide) (PNIPAAm), 68, 73, 80, 81, 203, 209–10, 270, 412–13, 516–17, 522, 597–9, 662
  actuator, 424–6
  cell segregation, 432–3
  copolymerization of, 390
  3D cell culture, 430–32
  lower critical solution temperature, 412–13
  microfluidic cell culture, 423–4
  nerve regeneration, 384, 388
  pH-responsiveness, 417
poly(*N*-isopropylacrylamide-*co*-vinylimidazole) (P(NIPAAm-*co*-VI)), 210
poly(*N*-vinyl caprolactam) (PVCL), 517
poly(propylene sulfide) (PPS), 264, 265
poly(propyleneoxide) (PPO), 390
poly(styrene-*b*-isobutylene-*b*-styrene) (SIBS), 117
poly(vinylidene fluoride) (PVDF), 113, 114, 127
poly(vinylidene fluoride trifluoroethylene) (PVDF-TrFE), 486
β-poly(vinylidene fluoride) (β-PVDF), 485
poly(lactic-*co*-glycolic) acidpoly-L-lysine (PLGA-PLL) nanoparticles, 280
polyacrylate amides (PA-A), 623
polyacrylic acid (PAAc), 69
polyaniline, 632
polyaniline (PANI), 102, 112–13, 121
polyaniline and polypropylene (PA–PP) blends, 396
poly(lactic acid) (PLA)-based MNPs, 297, 300
poly(ethylene glycol)-*block*-poly(L-alanine) (PEG-L-PA), 477
poly(ethylene glycol)-*b*-polycaprolactone-(dodecanedioic acid)-polycaprolactone-poly(ethylene glycol) (PVL–PEG–PVL), 81
poly butyric acid, 201–2
poly(dimethylsiloxane) (PDMS)-CaO_2 disk, 148
poly(*N*-isopropylacrylamide)-*co*-allylamine (PNIPA M-*co*-ALA) nanogels, 272
poly(ε-caprolactone) (PCL)/collagen fibers, 17
poly(dimethylaminoethyl methacrylate) (PDMAEMA) content, 272
poly(ethylene glycol) (PEG)-diacrylate, 487
poly(ethylene glycol) (PEG)-diacrylate (PEGDA), 622
poly(ethylene glycol) diacrylate (PEGDA), 655, 657
poly(ethylene glycol) (PEG) dimethacrylate
  for clinical applications, 636–7
polyelectrolytes, 512
polyesters, 240–41
poly(polyethylene glycol citrate-*co*-*N*-isopropylacrylamide) (PPCN) gel, 271
polyglycolic acid (PGA) fiber scaffolds, 212, 340
poly(ethylene glycol) (PEG)-grafted PLGA (PLGA-*g*-PEG), 74
poly(L-glutamic acid)-graft-tetraaniline/ poly(L-lysine)-*graft*-tetreaniline, 8
poly(vinyl alcohol) (PVA) hydrogel, 629
polyhydroxyalkanoates (PHA), 45–7, 243
poly(ε-caprolactone)-2-hydroxylethyl methacrylate (PCL-HEMA), 81
polylactic acid (PLA) composites, 44
polylactide with chondroitin sulfate-doped PPy (PLA–PPy), 484
poly-L-lactic acid (PLLA), 341, 626, 629, 633–5
  with collagen fibers, 17
polymeric delivery systems, 262
polymeric scaffold
  biodegradable synthetic polymers, 240–43
  biostable synthetic polymers, 239–40

polymer micelles, 271
polymersomes, 508–9
poly(oligoethylene glycol) methacrylate (POEGMA), 517
poly(lactic-*co*-glycolic acid) (PLGA) nanofibers, 180
poly(vinyl alcohol) (PVA) nanofibers, 607
poly(L-glutmate-*co*-*N*-3-L-glutamylphenylboronic acid) (PGGA) nanogel, 519
polyoxalate-based materials, 267
poly(lactic-*co*-glycolic acid) (PLGA) particles, 652
poly-(1,4-phenyleneacetone dimethylene thioketal) (PPADT), 265
poly(L-lactic acid)-Pluronic L35-poly(L-lactic acid), 80
poly(3,4-ethylenedioxythiophene):poly(4-styrene sulfonate) (PSS), 126–7
poly(DL-lactic acid-*co*-glycolic acid)-poly (ethylene glycol) (PEG-*g*-PLGA), 208
poly(ethylene glycol)–poly(L-alanine-*co*-L-phenyl alanine), 75
poly(lactic-*co*-glycolic acid) (PLGA) poly-L-lysine, 400
poly(vinyl alcohol) (PVA) polymers, 626
poly(α-caprolactone-*co*-lactide)–poly (ethylene glycol)–poly(α-caprolactone-*co*-lactide), 70
poly(ethylene glycol)–poly(L-alanine) (PEG–L-PA), 388, 389
poly(3,4-ethylenedioxythiophene) (PEDOT)/polystyrene sulfonate (PSS), 632–3
poly(3,4-ethylenedioxythiophene)/PSS polymers, 632–3
polypyrrole (PPy), 112, 454, 631–2
poly(organophosphazene)–RGD, 477
polysaccharide-based materials, 51–2
polysaccharide hydrogel, 620
poly(lactic-*co*-glycolic acid) (PLGA) scaffolds, 562
poly(L-lactic acid-*co*-ε-caprolactone)/silk fibroin (PLCL-SF), 121
polytetrafluoroethylene (PTFE), 127, 201–2, 239
polythiophene derivatives, 113
poly(vinylidene fluoride) (PVDF)-trifluoroethylene (PVDF-TrFE), 124, 127
poly(ester urethane)urea elastomers (PEUUs), 44, 240
polyurethane (PU), 201–2, 240, 626–7
  hydrogel, 620–21
polyvinylidene fluoride (PVDF), 633–4
pore structure control, 95
porosity, 40
porous silicon (pSi)
  cell attachment and differentiation on, 97
  pore structure control, 95
  shapes and forms, 91–5
  as “smart” biomaterial, 101
  surface chemistry, 95–6
porous silicon/polycaprolactone (pSi/PCL) composites
  advantages of composites as implants, 97–101
  clinical potential aplication, 103–5
  as “smart” biomaterial, 101–3
positively charged polymer, 420
postnatal organoids, 342
PPADT *see* poly-(1,4-phenyleneacetone dimethylene thioketal) (PPADT)
PPCN gel *see* poly(polyethylene glycol citrate-*co*-*N*-isopropylacrylamide) (PPCN) gel
PPS *see* poly(propylene sulfide) (PPS)
PPy-coated poly(lactic-*co*-glycolic acid) (PPy-PLGA), 120
PPy-functionalized graphene (PPy-G), 121

PPy-G *see* PPy-functionalized graphene
PPy-PLGA *see* PPy-coated poly(lactic-*co*-glycolic acid)
primary neural stem cells (pNSC), 541
proliferation, 261
Pro–Phe–Ser–Ser–Thr–Lys–Thr–Cys (PFSSTKTC), 493
propylacrylic acid, 70
protein-based materials, 48–50
proteins, 171, 173–5
protonation, 204
PTFE *see* polytetrafluoroethylene
pumps in microfluidic devices, 664–6
purmorphamine, 176
PVDF *see* poly(vinylidene fluoride)
PVI-AN hydrogel, 162
pyridine, 629

RADA 16, 158
RADA16-II peptides, 392
RADA16-I peptides, 392
RAD16-I (RADARADARADARADA-PuraMatrix™) hydrogel, 207
reactive hydroxyl radicals, 268
reactive oxygen species (ROS), 299
reactive oxygen species (ROS)-responsive materials for inflammation treatment, 263–9
regulating grafted cell differentiation *in vivo,* 545–6
remodeling, 261
remote controlled release scaffold, 319–20
repositioning of cells, 426–8
responsive short peptides, 391–2
resveratrol (RSV), 97
retinal ganglion cells (RGCs), 121
reversible isomers, 493–4
RGCs *see* retinal ganglion cells
Rho-associated protein kinase (ROCK), 338
RNA moieties, 177
ROCK *see* Rho-associated protein kinase (ROCK)
ROS *see* reactive oxygen species (ROS)
R-spondin family proteins, 335
rTIMP-3, 70, 71, 274, 276
runt-related transcription factor 2 (RUNX2), 177
RUNX2 *see* runt-related transcription factor 2 (RUNX2)

SAP *see* self-assembling peptide (SAP)
SBS *see* short bowel syndrome (SBS)
scaffold-based technologies, 281–2
scaffold-based tissue engineering, 562
scaffold manufacture technologies
  additive manufacture, 565–6
  for fibrous scaffolds, 566–8
scaffold-mediated delivery, 173
scaffolds, 169–71
SDF-1α *see* stromal cell-derived factor-1α (SDF-1α)
selective laser sintering (SLS), 565–6
  for bone tissue regeneration, 574–7
self-assembled conductive hydrogels, 115
self-assembled monolayers (SAMs), 418–20, 492
self-assembling biomaterials, nerve regeneration, 391–2
self-assembling peptide (SAP), 78, 158, 207–9, 392
self-healing gels, 623
self-healing hydrogels, 622–3
  in 3D printing, 623–5
self-regulated drug delivery systems (DDSs), applications
  glucose-responsive, 517–19
  multiple-responsive, 519–20
  pH-responsive polymers, 512–15
  temperature-responsive polymers, 515–17
semiconductor nanowires, advantage of, 455

semi-interpenetrating polymer network (sIPN), 81
serotonergic replacement therapy (5HT1A/7 and 5HT2 agonists), 463
shape-memory effect, 625
shape-memory materials, 625
  applications
    photo-responsive, 628
    polymers, in 3D printing, 629–30
    thermo-responsive, 627–8
    see also conductive polymers
shape-memory poly(3-caprolactone) (PCL), 666
shape memory polymers (SMPs), 162, 625
  in 3D printing, 629–30
shape-memory systems, 213–16
shear-thinning hydrogel (STG), 82
short bowel syndrome (SBS), 332
SIBS *see* poly(styrene-*b*-isobutylene-*b*-styrene) (SIBS)
silicon delivery vehicles, 511
silicon nanowires (SiNWs)
  biocompatibility of, 446
  FETs, monitoring electrophysiological activity, 455–7
  interfaces, 445
  morphology and surface topography of, 442–4
silk fibroin, 239
silk fibroin proteins, 48
silver (Ag)-NP-based nanogels, 519
Si nanomembrane electrode, 461
single-walled carbon nanotubes (SWCNT), 446–51
  chemical vapor deposition (CVD) for, 447–9
  conductivity, 449
sirolimus (rapamycin), 28
SIS *see* small intestinal submucosa (SIS)
skeletal muscle, tissue repair and regeneration, 82
skin tissue engineering, 17–20
skin, tissue repair and regeneration, 78–80
skin wound healing, 261
small intestinal submucosa (SIS), 235
small molecules, 176
smart biomaterials for cell encapsulation, 144–5
  direct cell phenotype, 155–9
  foreign body reaction, 152–5
  injectable smart biomaterials, 160–61
  native microenvironment, 145–8
  overcome suffocation, 148–50
  shape memory polymers (SMPs), 162
  vascularization, 150–51
smart biomaterials systems, 282
smart drug delivery vehicles, 507–8
  dendrimers, 511
  hydrogels, 510–11
  liposomes, 509–10
  other delivery vehicles, 511–12
  polymersomes, 508–9
smart matrices (scaffolds)
  bioactive-agent-releasing matrices, 209–11
  pH-responsive systems, 204–7
  self-assembling peptides, 207–9
  thermo-responsive matrices, 202–4
smart polymers, 616
  chemical and physical crosslinking, 616–17
SMCs *see* smooth muscle cells (SMCs)
smooth muscle cells (SMCs), 232, 233, 331, 334
  ECs *versus,* 21–2
SMO–PCLA–PEG–PCLA–SMO copolymer, 70
SMPs *see* shape memory polymers (SMPs)

sodium bicarbonate, 272
sodium-glucose linked transporter (SGLT-1) TESI localization, 343
soft lithography, 648
solid peroxide, 148
sol-to-gel transition, 70
solubility switch, ROS-responsive materials *via*, 264–5
solvent casting/particulate leaching technique, 566
spherical nanoparticles, 274
sphingosine 1-phosphate receptor 3 (S1PR) agonist, 282
SPION *see* superparamagnetic iron oxide nanoparticles (SPION)
spiropyran polymers, 493
S1PR agonist *see* sphingosine 1-phosphate receptor 3 (S1PR) agonist
stem cells, 155, 330–31, 352, 560
  delivery, 281–2
  differentiation of, 474
stem cell therapy, 499
  in wound repair, 263
stent thrombosis (LST), 21
stiffness-induced cell differentiation, 494–5
stimuli-responsive biomaterials, nerve regeneration, 383–4
  conductive, electrical-stimuli-responsive biomaterials, 394–9
  enzyme-responsive biomaterials, 393–4
  photo-responsive biomaterials, 392–3
  pH-responsive biomaterials, 390–91
  self-assembling biomaterials, 391–2
  temperature-responsive biomaterials, 384–90
stimuli-responsive injectable polymeric hydrogels, 68–71
stop-flow lithography, 657
stromal cell-derived factor-1 (SDF-1), 454
stromal cell-derived factor-1α (SDF-1α), 267
sufficient generation of oxygen, 148
sufficient mechanical properties, 171
suffocation, 148–50
sulfamethazine oligomers (SMOs), 70
sulfated glycosaminoglycan, 212
superparamagnetic iron oxide nanoparticles (SPION), 296
supramolecular biomaterials, 147
supramolecular interactions, reversibility of, 147
surface coatings to enhance endothelialization, 22–4
surface-enhanced Raman scattering (SERS), 588–9
surface-grafted chitosan, 172
surface plasmon resonance (SPR) absorption, 588
surface topography, 197
synthetic materials, 41–5
synthetic polymers, 6–9
  poly butyric acid, 201–2
  polytetrafluoroethylene, 201–2
  polyurethane, 201–2

T-cell factor (Tcf)/β-catenin transcription, 335
TCP *see* tissue culture plates (TCP)
teflon *see* polytetrafluoroethylene
TEHV *see* tissue engineered heart valve (TEHV)
temperature-responsive biomaterials, nerve regeneration, 384–90
temperature-responsive drug delivery systems, 515–17
temperature-responsive injectable hydrogels, 68–9
temperature-responsive materials for wound healing, 270–72
temperature-responsive self-assembly, 391
temperature-sensitive hydrogels, 80
temporomandibular joint disorders, 217

tendon, tissue repair and regeneration, 82
TESI *see* tissue-engineered small intestine (TESI)
2,2,6,6-tetramethylpiperidine-*N*-oxyl (TEMPO) moieties, 272
TEVG, 237, 248
  remodeling, 231–4
theranostic-embedded scaffolds for cancer patients, 587–9
theranostics, 588
thermally hydrocarbonized porous silicon (THCPSi) microparticles, 97
thermally induced phase separation (TIPS), 565
thermoplastic polymer, 202
thermo-responsive applications, shape-memory materials, 627–8
thermo-responsive hydrogels, 618
thermo-responsive materials, 270
thermo-responsive matrices, 202–4
thermo-responsive microfluidic system, 597–9
thermo-responsive polymer solutions, 271
thermo-responsive smart materials, 659
  microchannels utilizing, 660–62
  microdroplet fabrication in microfluidic device, 662–4
  microvalves and pumps in microfluidic devices, 664–6
thermo-responsive technology, 428
thermo-sensitive hydrogels, 78
thermosensitive materials, 475–6
  and their regulation for fate of stem cells., 478–83
thermosensitive polymers, 515–17
thioketal-based materials, 265–7
thioketal nanoparticles (TKNs), 266
thixotropic materials, 494–5
  stiffness-induced cell differentiation, 495
  stress stiffening/relaxation-induced cell differentiation, 495–8
  and their regulation for fate of stem cells, 496–7
  viscoelasticity of, 494
3D graphene foams (3D-GF), 115
thrombin, 71
thromboxane A2 (TXA2), 259–60
TiO_2 nanotube arrays, 22
tissue culture plates (TCP), 124
tissue engineered cardiovascular diseases, 24–5
tissue engineered heart valve (TEHV), 245
tissue-engineered small intestine (TESI), 332, 333, 340–42, 347, 348
tissue engineering materials, 562
tissue regeneration process, 560–62
  growth factors, 560–61
  requirements for multiple functions of scaffolds in, 569–71
titanium (Ti), 172
TKNs *see* thioketal nanoparticles (TKNs)
tonsil-derived mesenchymal stem cells (TMSCs), 388
toxicity, smart materials, 433
transform growth factor-β (TGF-β), 209
transglutaminases, 393–4
TREK-1 ion channels, 293, 296
tricalcium phosphate (TCP), 9, 563
trypsin, cell adhesion, 412, 413
TXA2 *see* thromboxane A2 (TXA2)
type I collagen, 236

upper critical solution temperature (UCST), 203

vancomycin (VCM), 97
vapor–liquid–solid growth, 442
vascular endothelial growth factor (VEGF), 15, 261, 277, 430
vascular grafts, 429–30

vascularization, 150–51
    vessel structure formation, 305
    vessel structure organization, induction of, 305–10
vascularized bone flaps, 185
vascular neotissue formation, 231–4
vascular scaffolds, 237
vascular smooth muscle cells (VSMCs), 316
VEGF *see* vascular endothelial growth factor (VEGF)
VEGF-releasing hydrogel, 151
veins, cardiovascular structures, 232
vessel structure organization, induction of, 305–10
VICs *see* native valvular interstitial cells (VICs)
VSMCs *see* vascular smooth muscle cells (VSMCs)

water-in-oil-in-water double emulsion, 268
water-soluble fullerene biomaterial, 149
Wnt ligand binding, 335
Wnt signaling, 337–9
wound dressings, 262
    temperature-responsive materials as, 270–71
wound healing, smart materials for, 18, 258–9, 342
    advances in immunotherapy, 282
    current methods and material applications in, 262–3
    gene therapy in biomaterials, 280–81
    stages, 259–61
    stem cell delivery, 281–2
    stimuli-responsive materials for, 263–80
wound repair, stem cell therapy in, 263

xyloglucan, 389–90

zwitterionic PCBMA hydrogel, 154